RPP-ENV-58782, Rev. 0

Performance Assessment of Waste Management Area C, Hanford Site, Washington

Author Name:
S. Mehta, M. W. Kozak, N. Hasan, R. Khaleel, D. Morgans – INTERA, Inc.
W. J. McMahon – CH2M HILL Plateau Remediation Company; B. Sun – Ramboll Environ, Inc.
M. P. Bergeron, J. G. Field, K. M. Singleton – Washington River Protection Solutions, LLC
M. P. Connelly – TecGeo, Inc.
Richland, WA 99352
U.S. Department of Energy Contract DE-AC27-08RV14800

EDT/ECN: DRCF UC: N/A
Cost Center: N/A Charge Code: N/A
B&R Code: N/A Total Pages: 1,029

Key Words: Performance Assessment, Waste Management Area C, PA, WMA C, single-shell tank, STOMP, process-level model, GoldSim, system-level model, modeling codes, vadose zone, groundwater, unsaturated flow, vadose zone flow, groundwater flow, contaminant transport, radiological dose, sensitivity analysis, uncertainty analysis, DOE Order 435.1, tank farm closure

Abstract: This document provides the DOE O 435.1, Radioactive Waste Management performance assessment analysis for Waste Management Area C. The performance assessment is required by DOE O 435.1 for closing U.S. Department of Energy-operated facilities that will manage radioactive waste generated during departmental activities as low-level waste. The fundamental objective of this performance assessment is to support the closure of tanks and ancillary equipment within Waste Management Area C that will contain residual levels of radioactive wastes left at closure.

TRADEMARK DISCLAIMER. Reference herein to any specific commercial product, process, or service by trade name, trademark, manufacturer, or otherwise, does not necessarily constitute or imply its endorsement, recommendation, or favoring by the United States Government or any agency thereof or its contractors or subcontractors.

DATE:
Oct 04, 2016
HANFORD RELEASE

APPROVED
By Lana Perry at 11:25 am, Oct 04, 2016

Release Approval Date Release Stamp

Approved For Public Release

RPP-ENV-58782
Revision 0

Performance Assessment of Waste Management Area C, Hanford Site, Washington

S. Mehta
M. W. Kozak
N. Hasan
R. Khaleel
D. L. Morgans
INTERA, Inc.

W. J. McMahon
CH2M HILL Plateau Remediation Company

B. Sun
Ramboll Environ, Inc.

M. P. Bergeron
J. G. Field
K. M. Singleton
Washington River Protection Solutions, LLC

M. P. Connelly
TecGeo, Inc.

Date Published
September 2016

Prepared for the U.S. Department of Energy
Office of River Protection

Contract No. DE-AC27-08RV14800

Approved for public release; distribution unlimited

Version History

Version	Date	Author	Change Description
Draft A	30-Sept-2015	S. Mehta et. al	Initial Draft for DOE-ORP Review
Draft B	30-Dec-2015	S. Mehta et. al	Updates to Draft A in response to review comments provided by DOE-ORP and WRPS
Rev. 0	30-Sep-2015	S. Mehta et. al	Updates to Draft B in response to review comments provided by DOE-HQ through the Low-Level Waste Disposal Facility Federal Review Group (LFRG).

EXECUTIVE SUMMARY

The U.S. Department of Energy, Office of River Protection (DOE-ORP) is pursuing closure on the single-shell tank (SST) Waste Management Area (WMA) C under Federal requirements and forthcoming State-approved closure plans and permits in accordance with the Hanford Federal Facility Agreement and Consent Order (HFFACO) (Ecology et al. 1989), Action Plan, Appendix I. Waste Management Area C is located in the 200 East Area of the Central Plateau at the Hanford Site in southcentral Washington (Figure ES-1) and is one of 12 tank farms grouped into 7 WMAs (A-AX, B-BX-BY, C, S-SX, T, TX-TY, and U) containing 149 SSTs and ancillary equipment built from 1943 to 1964 (see Figure ES-2).

This document provides the DOE O 435.1, Radioactive Waste Management performance assessment (PA) analysis for WMA C. The PA is required by DOE O 435.1 for closing U.S. Department of Energy (DOE)-operated facilities that will manage radioactive waste generated during departmental activities as low-level waste. The fundamental objective of this PA is to support the closure of tanks and ancillary equipment within WMA C that will contain residual levels of radioactive wastes left at closure.

Waste Management Area C is located in the east central portion of the 200 East Area in land that is designated to be Industrial-Exclusive. In general, the WMA C boundary is represented by the fenceline surrounding the 241-C Tank Farm (C Farm) (Figure ES-3). The WMA C facility contains twelve 100-series tanks and four 200-series tanks (see Figure ES-3). The 100-series tanks are 23 m (75 ft) in diameter, have a 5-m (15-ft) operating depth, and have an operating capacity of 2,006,000 L (530,000 gal) each. The 200-series tanks are 6 m (20 ft) in diameter with a 7.32-m (24-ft) operating depth and an operating capacity of 208,000 L (55,000 gal) each. The tanks sit below grade with at least 2 m (7 ft) of soil cover to provide shielding from radiation exposure to operating personnel. Tank pits are located on top of the tanks and provide access to the tanks, pumps, and associated monitoring equipment. To support the transfer and storage of waste within WMA C SSTs, there is a complex waste transfer system of pipelines (transfer lines), diversion boxes, vaults, valve pits, and other miscellaneous structures. These miscellaneous features of the tank farm are referred to in this document by the general term "ancillary equipment and components."

Closure of the individual SSTs and WMA C in its entirety occurs in three major steps: 1) SST waste retrieval, 2) filling the tanks with grout for stabilization, and 3) surface cover barrier placement. The final state of a tank farm that is considered in the PA is therefore a set of grouted tanks with associated ancillary equipment containing residual wastes that remain at the end of retrieval, covered by a modified Resource Conservation and Recovery Act of 1976 (RCRA) Subtitle C surface cover, residing in the native geological setting.

Figure ES-1. Hanford Site and its Location in Washington State.

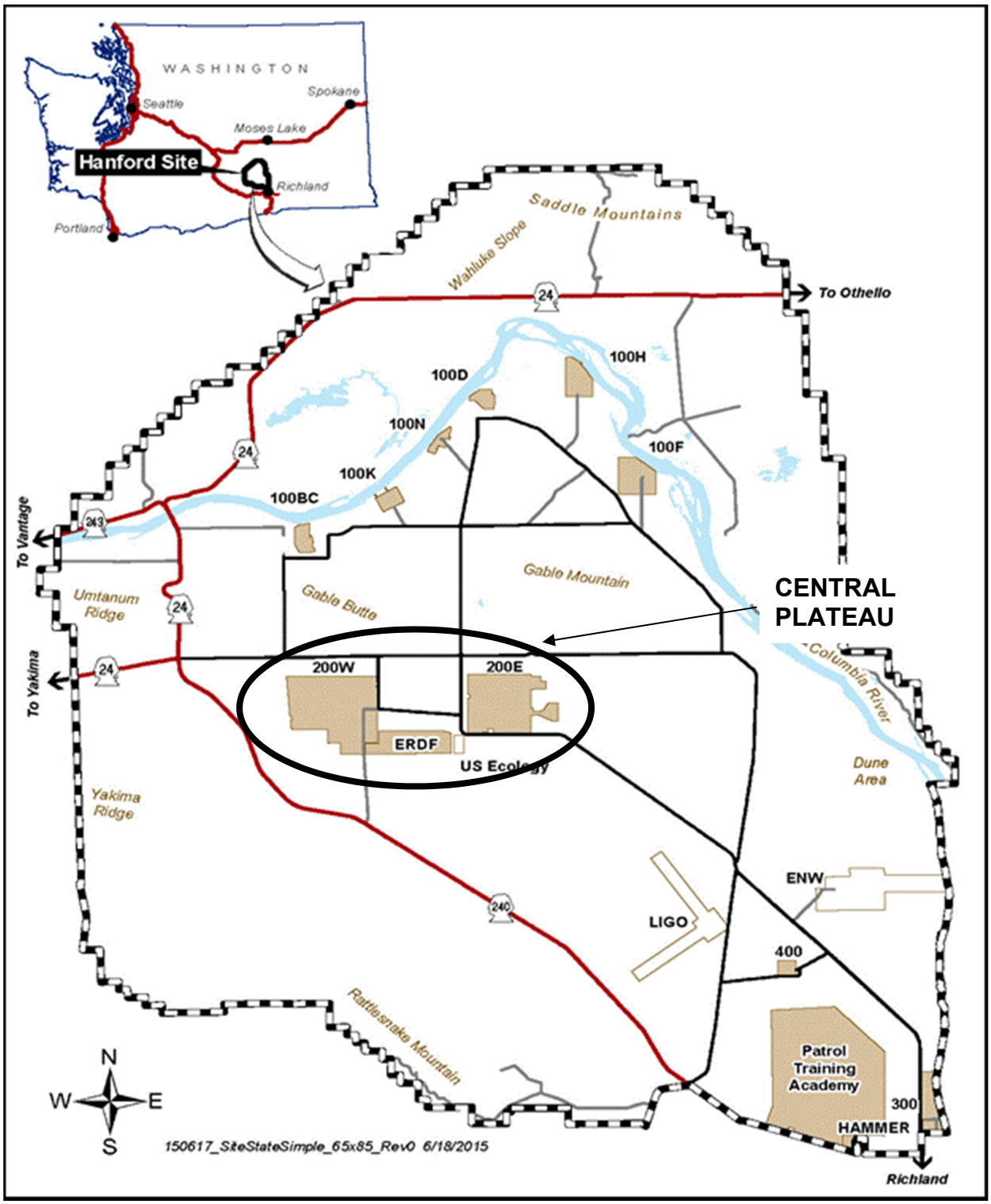

ENW = Energy Northwest
ERDF = Environmental Restoration Disposal Facility
HAMMER = Volpentest Hazardous Materials Management and Emergency Response (HAMMER) Federal Training Center
LIGO = Laser Interferometer Gravitational Wave Observatory

Figure ES-2. Hanford Site Tank Farms.

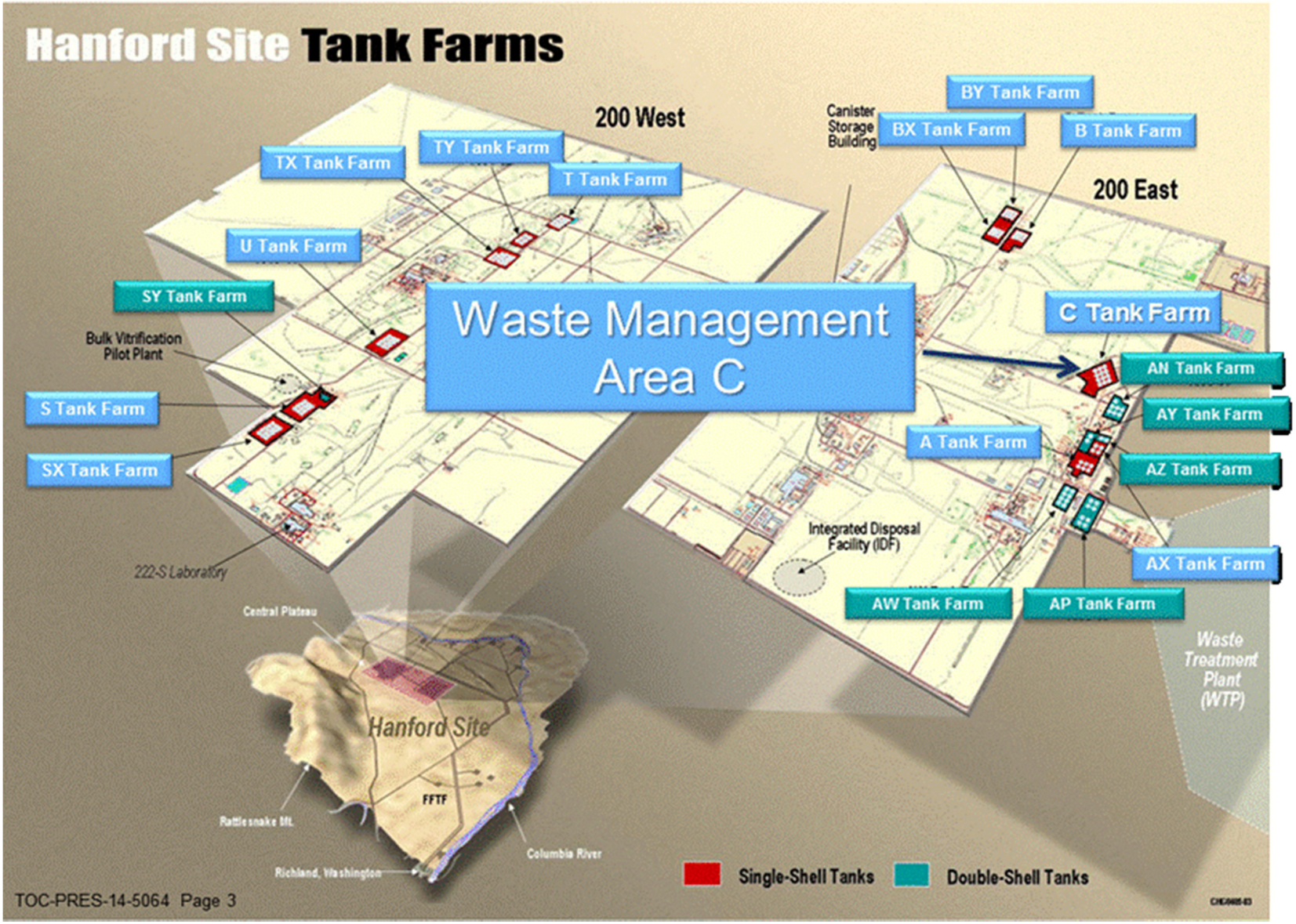

Figure ES-3. Location of Facilities at Waste Management Area C and Surrounding Area.

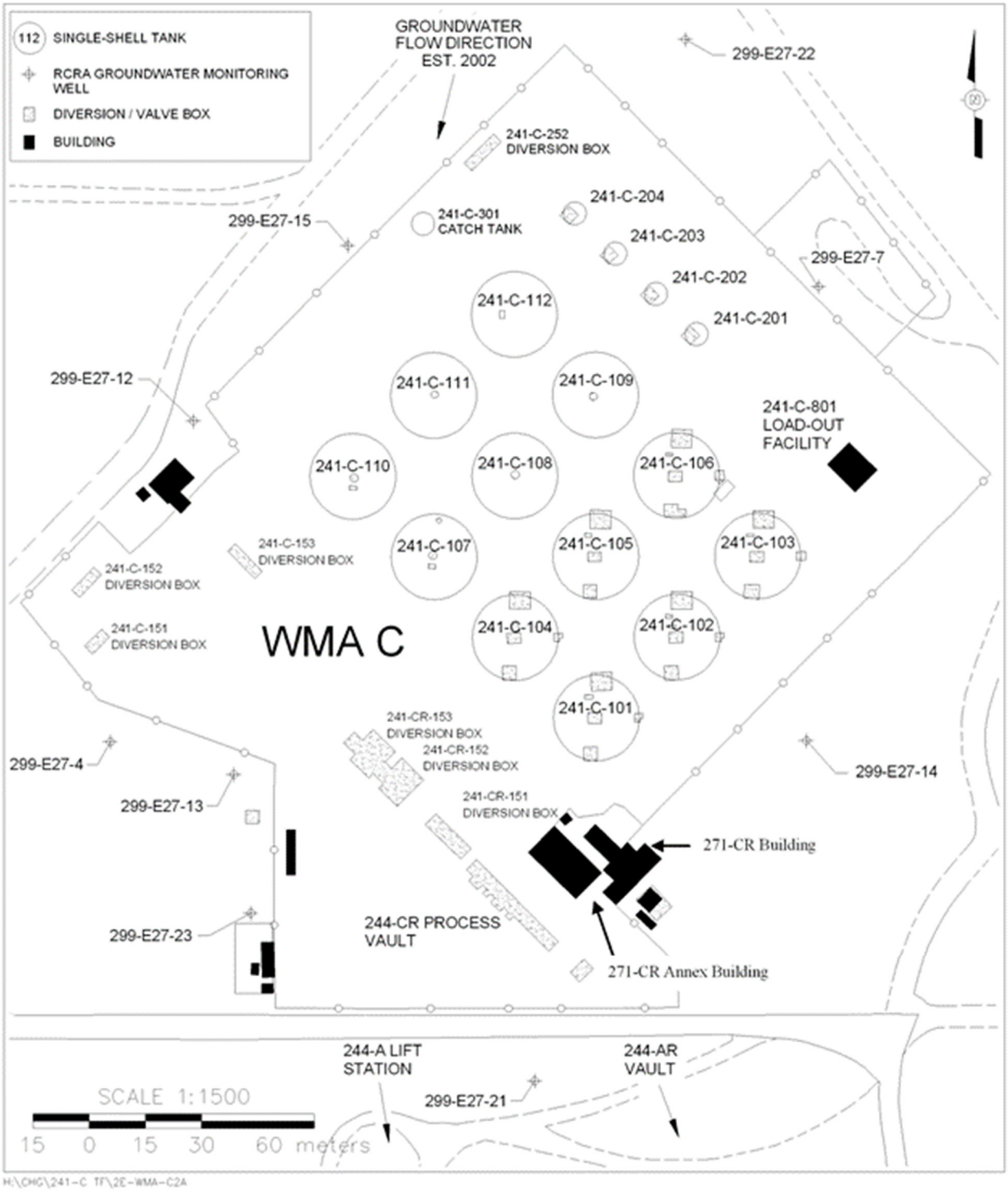

RCRA = Resource Conservation and Recovery Act of 1976 WMA = Waste Management Area

The safety concept for this system is composed of a set of safety functions of manmade as well as natural components that act together to provide the long-term performance of a closed facility

required in closure regulations. The safety functions represent multiple and redundant barriers, so that the loss of one or some of the safety functions continues to result in adequate performance of the overall system. A schematic depiction of these safety functions for the closed WMA C is provided in Figure ES-4. The manmade components of the system that influence contaminant migration include a closure surface barrier, and the distribution of waste in the subsurface tanks and ancillary equipment. The natural components of the system that influence contaminant migration are the several underlying, nearly-horizontal stratigraphic layers within the vadose zone and the unconfined aquifer.

The WMA C PA has been structured to evaluate the behavior of the closed tank farm under a variety of potential future conditions. An analysis case has been defined in which the safety functions evolve in an expected manner without unusual behavior or unanticipated disruption; this is termed the "base case." The base case is the main analysis used to compare against the performance objectives, but is not the sole analysis for such comparisons. In addition, a set of deterministic sensitivity analyses have been conducted that show the effects when the safety functions are degraded compared to their expected behavior as defined in the base case. The specific safety functions examined in this way relate to the various physical components of the disposal system that included model evaluations of groundwater impacts with the following:

- Higher than expected infiltration rates; these may be the result of a number of potential effects, ranging from unexpectedly poor performance of the cover, through changes in land use with irrigation on top of the facility

- Changes in the effectiveness of the tanks and infill grout to act as barriers, by assuming that the hydraulic conductivity of the tanks increases at times earlier than expected

- Changes in the leachability of the residual wastes, by assuming that the material would dissolve instantly and completely upon contact with water

- Bounding inventories for unretrieved tanks

- Alternative conceptualizations of the stratigraphy of the vadose zone

- Alternative assumptions about dilution in the aquifer.

In addition to these deterministic analyses of the effect of the safety functions, a probabilistic analysis of the base case was conducted to show the effects of parameter uncertainty on the performance of the system. A number of parameters were assigned probability density functions, the PA was run probabilistically, and uncertainty estimates in dose were evaluated.

Consequently, the PA includes a base case representing the expected behavior of the disposal system, alternative cases representing degraded safety functions, and uncertainty analyses that represent the effects of parameter uncertainty. These three elements of the PA represent the uncertainties in the post-closure performance of the closed WMA C that will support closure decisions.

Figure ES-4. A Schematic Depiction of the Safety Functions for a Closed Waste Management Area C.

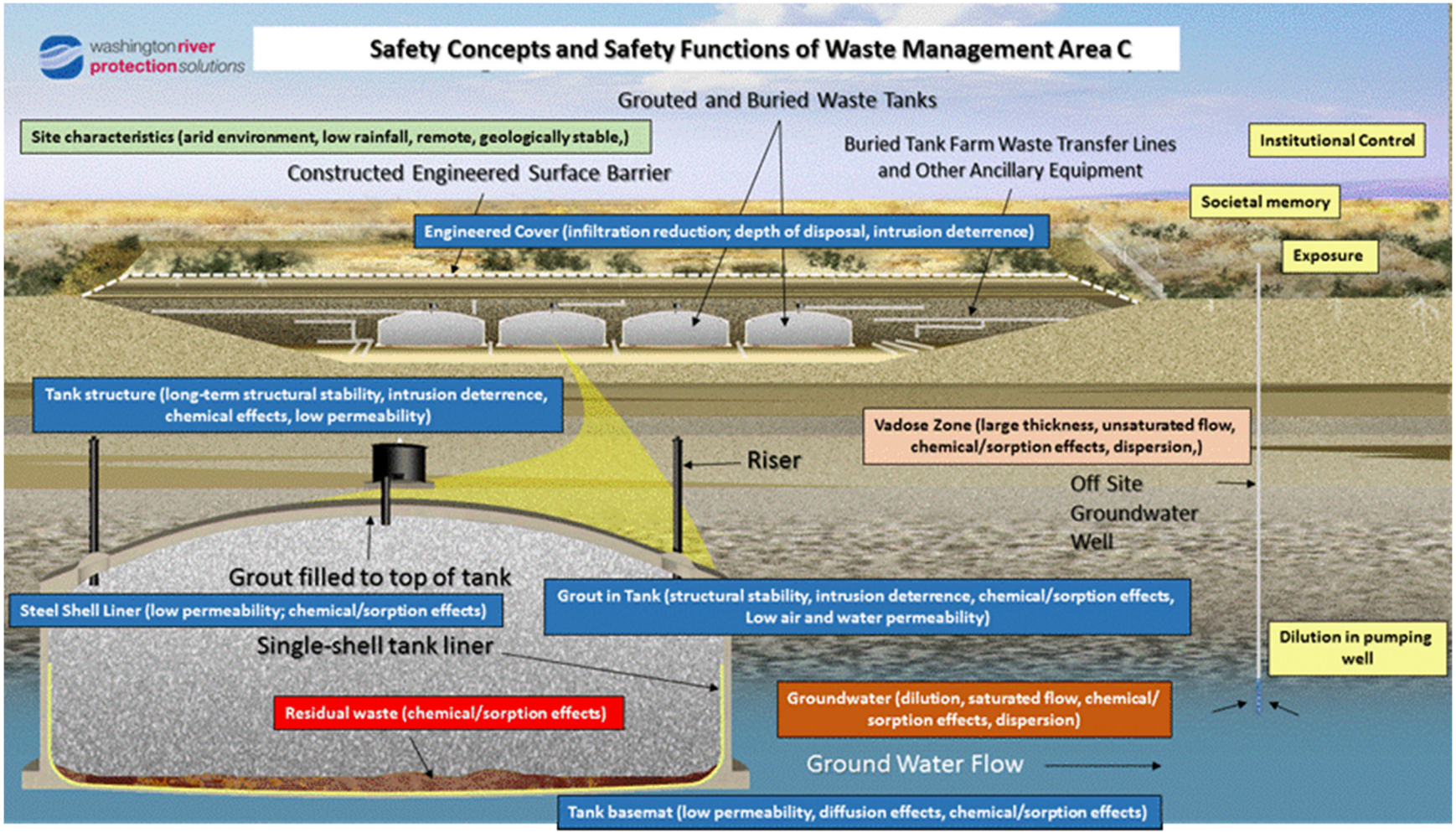

A closure date of year 2020 has been assumed for the WMA C PA. In the post-closure assessment, four time periods have been considered: (1) a 100-year institutional control period when the engineered surface cover works to its design capability, resulting in effectively 0.5 mm/yr recharge rate under the base of surface cover system; (2) a 400-year post-institutional control period (from 100 years to 500 years after closure) within which the surface cover remains intact; (3) the time period from 500 years after closure up to the DOE O 435.1-defined compliance time period of 1,000 years after closure, during which the surface cover barrier function is assumed to be fully degraded at the start of the time period (assuming a design life of 500 years after closure); and (4) the post-compliance period (beyond 1,000 years after closure) up to 10,000 years after closure for the purpose of evaluating uncertainty and sensitivity on dose estimates.

Residual inventory estimates used in this PA were determined based on information and conditions as of September 2014. Inventory estimates were developed for 1) residuals in retrieved tanks with post-retrieval sampling, 2) residuals in retrieved tanks without post-retrieval sampling, 3) residuals in tanks undergoing retrieval and 4) post-retrieval residual inventory estimates for ancillary equipment, including C-301 catch tank, 244-CR vault tanks, and sumps, pits, diversion boxes, and waste transfer pipelines. All radionuclides left in tanks and ancillary equipment at WMA C at closure with half-lives greater than 3 years and non-negligible inventories were included in the PA. In addition, few radionuclides were included that are decay progeny of radionuclides in the inventory to complete the decay chain. A total of 43 radionuclides are evaluated in the WMA C PA.

Radiological contaminant releases from the grout inside the tanks and 244-CR vault are controlled by diffusion processes while the grout is assumed to remain intact. In the base case, the tank structure and infill grout placed into the tanks were assumed to be intact for the entire period of analysis. This assumption is supported by an evaluation of the degradation rate of cementitious materials at Hanford. Because all waste transfer lines will likely be disposed in place without the emplacement of infill grout within individual pipelines, the PA considered contaminant release from wastes within the pipelines using a combination of advection and diffusion release mechanisms.

The various pathways of possible exposure evaluated in the WMA C PA are illustrated in Figure ES-5. The major pathways for contamination entering the environment are the groundwater pathway, the air pathway, and an inadvertent intruder pathway (through drill cuttings brought to the surface). The groundwater pathway evaluates the effect of moisture from rain and snowfall entering the subsurface, contacting waste, and carrying dissolved contaminants through the vadose zone to the unconfined aquifer. Therefore, a primary focus of the PA is estimating the groundwater dose to a hypothetical member of the public (i.e., receptor) who:

- Consumes contaminated groundwater, leafy vegetables, and produce that were irrigated with contaminated groundwater, and

- Consumes milk and meat from animals that in turn consume contaminated water and fodder that was irrigated with contaminated groundwater (Figure ES-5).

Figure ES-5. Overview of the Dose Calculations for Exposure Along the Groundwater Pathway and Air Pathway for the Waste Management Area C Performance Assessment.

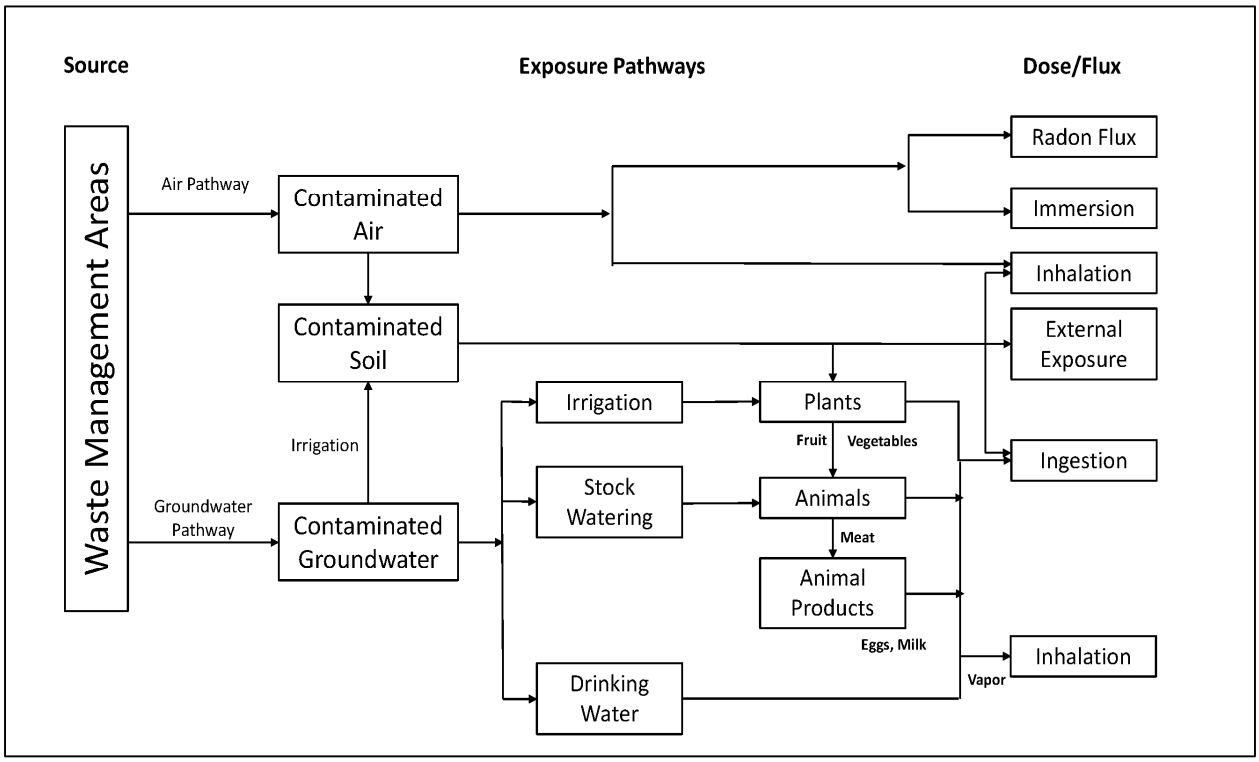

WMA = Waste Management Area

During the compliance and post-compliance periods, the receptor is assumed to reside 100 m downgradient of the WMA C fenceline. The surface water pathway is not a possible exposure pathway for the disposal facility because surface water is not present near WMA C, and is too limited on the Hanford Site Central Plateau in quantity to be used domestically.

All-pathway dose calculations have been performed by evaluating the long-term release of radionuclides from the closed WMA C along the groundwater and atmospheric pathways. The groundwater pathway analysis is the most complex and included the following.

(a) An initial three-dimensional screening analysis to identify radionuclides that cannot provide calculable groundwater contamination over the duration of the simulation and thus can be screened out from further calculations. Using conservative recharge rates and hydraulic properties it was determined that radionuclides with a $K_d > 0.1$ mL/g require no detailed analysis for the 1,000-year compliance time frame, and radionuclides with a $K_d > 1.5$ mL/g require no detailed analysis for the 10,000-year post-compliance period. As a result of the screening, radionuclides with $K_d > 1.5$ mL/g are excluded from further consideration in the groundwater pathway calculations.

(b) A three-dimensional flow and transport analysis for the base case with the parameter values set at their expected values. This involved determining the appropriate boundary conditions under steady-state conditions that are expected in the future. No breakthrough

of contaminant was observed within the 1,000-year compliance time period at the 100-m downgradient compliance location in the saturated zone. The first breakthrough of non-retarded contaminants occurred after 1,500 years after closure.

(c) One-dimensional abstraction models for performing uncertainty analyses and multiple parameter sensitivity analyses. For the uncertainty analysis, including evaluation of the coupled effects of uncertainty in source term, engineered system, and natural system, a PA abstraction model was developed. A full uncertainty analysis using the Monte Carlo sampling methodology was undertaken by developing stochastic inputs and performing multi-realization simulations. Uncertainties in the dose estimates are calculated for the compliance and post-compliance time periods.

(d) A suite of sensitivity analyses to evaluate the performance of the system when the safety functions are degraded compared to their expected behavior.

The PA results of the all-pathways, atmospheric, radon flux, inadvertent intruder, and groundwater (water resources) protection analyses are shown in Table ES-1 for the compliance and post-compliance periods. Only the peak values of the effective dose equivalent or peak concentrations are compared to the standards. Releases to groundwater and air were evaluated against performance objectives for the all-pathways analysis required by DOE O 435.1. The all-pathways analysis combines the groundwater pathway analysis and the air pathway analysis for the base case, as discussed in Section 6.

As illustrated in Figure ES-6, the peak dose for the all-pathways analysis in the compliance period is associated with the air pathway, with the peak dose of 4×10^{-3} mrem/yr dominated by tritium resulting from upward gaseous diffusive flux from the residual waste. The peak calculated dose occurs in the institutional control period, between 10 and 20 years after closure. This peak dose occurs during the period of institutional control, and cannot, strictly speaking, be regarded as a dose to a member of the public. Instead, the dose during this time period would represent a potential dose to a worker at the compliance boundary. This calculated dose does not consider the active monitoring measures that are anticipated during institutional control. The all-pathways dose remains low, approximately 4×10^{-5} mrem/yr, for about 800 years after closure, but shows a rapid increase near the end of the compliance time period due to breakthrough of ^{99}Tc at 100 m downgradient of the facility along the groundwater pathway. The peak dose within the sensitivity/uncertainty analysis time period (1,000 to 10,000 years after closure) occurs at about 1,500 years after closure, and results primarily from a peak in ^{99}Tc groundwater concentration at 100 m downgradient of the facility. The peak total dose within the sensitivity/uncertainty analysis time period is 0.1 mrem/yr. The peak dose remains over two orders of magnitude below the performance objective of 25 mrem/yr during the sensitivity/uncertainty analysis period.

Table ES-1. Comparison of Performance Objectives and Measures with the Waste Management Area C Performance Assessment Results for the Compliance and Post-Compliance Periods.

Performance Objective and/or Measure	Standard	Performance Assessment Results	
		Compliance Period (2020–3020)[a]	Post-Compliance Period (3020–12020)[a]
All Pathways (DOE O 435.1 Chg 1)	25 mrem/yr EDE	4E-3 mrem/yr	0.17 mrem/yr
Atmospheric (40 CFR 61, Subpart H)	10 mrem/yr EDE	4E-3 mrem/yr	2E-5 mrem/yr
Atmospheric (40 CFR 61, Subpart Q)	20 $pCi.m^{-2}.s^{-1}$ radon flux (at surface of disposal facility)	2E-4 $pCi.m^{-2}.s^{-1}$	7E-3 $pCi.m^{-2}.s^{-1}$
Acute Inadvertent Intruder (DOE O 435.1 Chg 1)	500 mrem EDE[b]	36 mrem	11.1 mrem
Chronic Inadvertent Intruder (DOE O 435.1 Chg 1)	100 mrem/yr EDE[b]	8.2 mrem/yr [f]	7E-02 mrem/yr[g]
Groundwater Protection (water resources) (40 CFR 141)	Beta-gamma dose equivalent ≤ 4 mrem/yr	5E-4 mrem/yr	0.13 mrem/yr[c]
	Gross alpha activity concentration (excluding radon and uranium) ≤ 15 pCi/L	0 pCi/L	1E-10 pCi/L[d]
	Combined Ra-226 and Ra-228 concentration ≤ 5 pCi/L	0 pCi/L	7E-7 pCi/L[d]
	Uranium concentration ≤ 30 µg/L	0 µg/L	0.05 µg /L[d]
	Sr-90 concentration ≤ 8 pCi/L[e]	Not applicable	Not applicable
	H-3 concentration ≤ 20,000 pCi/L	0 pCi/L	1E-10 pCi/L[d]

[a] Compliance at 100 m downgradient of Waste Management Area C except for inadvertent intruder scenarios.

[b] Not applicable for post-compliance time period.

[c] Beta-gamma dose equivalent ≤ 4 mrem/yr (based on Federal MCL) and calculated as (C_{Peak}/MCL) × 4 mrem/yr. For Tc-99, which contributes almost the entire dose, C_{Peak} = 30 pCi/L and MCL = 900 pCi/L, so the equivalent dose is calculated to be 0.1 mrem/yr.

[d] Concentrations less than 1E-10 pCi/L are essentially zero.

[e] Not applicable; Sr-90 was screened out during evaluation of the groundwater pathway due to its relatively short half-life and its low mobility in the subsurface.

[f] Peak dose based on assumed inadvertent intrusion into a waste transfer line at 100 years following loss of institutional control using a rural pasture exposure scenario. Peak dose occurs at 100 years after closure.

[g] Peak dose based on assumed inadvertent intrusion into a waste transfer line after 1,000 years following loss of institutional control using a suburban garden exposure scenario. Peak dose occurs at 1,000 years after closure.

EDE = effective dose equivalent MCL = maximum contaminant level

References:

40 CFR 61, "National Emission Standards for Hazardous Air Pollutants," Subpart H—National Emission Standards for Emissions of Radionuclides Other Than Radon From Department of Energy Facilities, Code of Federal Regulations, as amended.

40 CFR 61, "National Emission Standards for Hazardous Air Pollutants," Subpart Q—National Emission Standards for Radon Emissions From Department of Energy Facilities, Code of Federal Regulations, as amended.

40 CFR 141, "National Primary Drinking Water Regulations," Code of Federal Regulations, as amended.

DOE O 435.1, 2001, Radioactive Waste Management, Change 1, U.S. Department of Energy, Washington, D.C.

Figure ES-6. All-Pathways Dose Results for Base Case that Includes Air and Groundwater Pathway Contributions at the Maximum Point of Concentration. The DOE O 435.1 compliance time (1,000 years) is shown as a vertical blue dashed line, and the compliance dose (25 mrem/yr) is shown as the black horizontal dashed line. Note the logarithmic vertical axis.

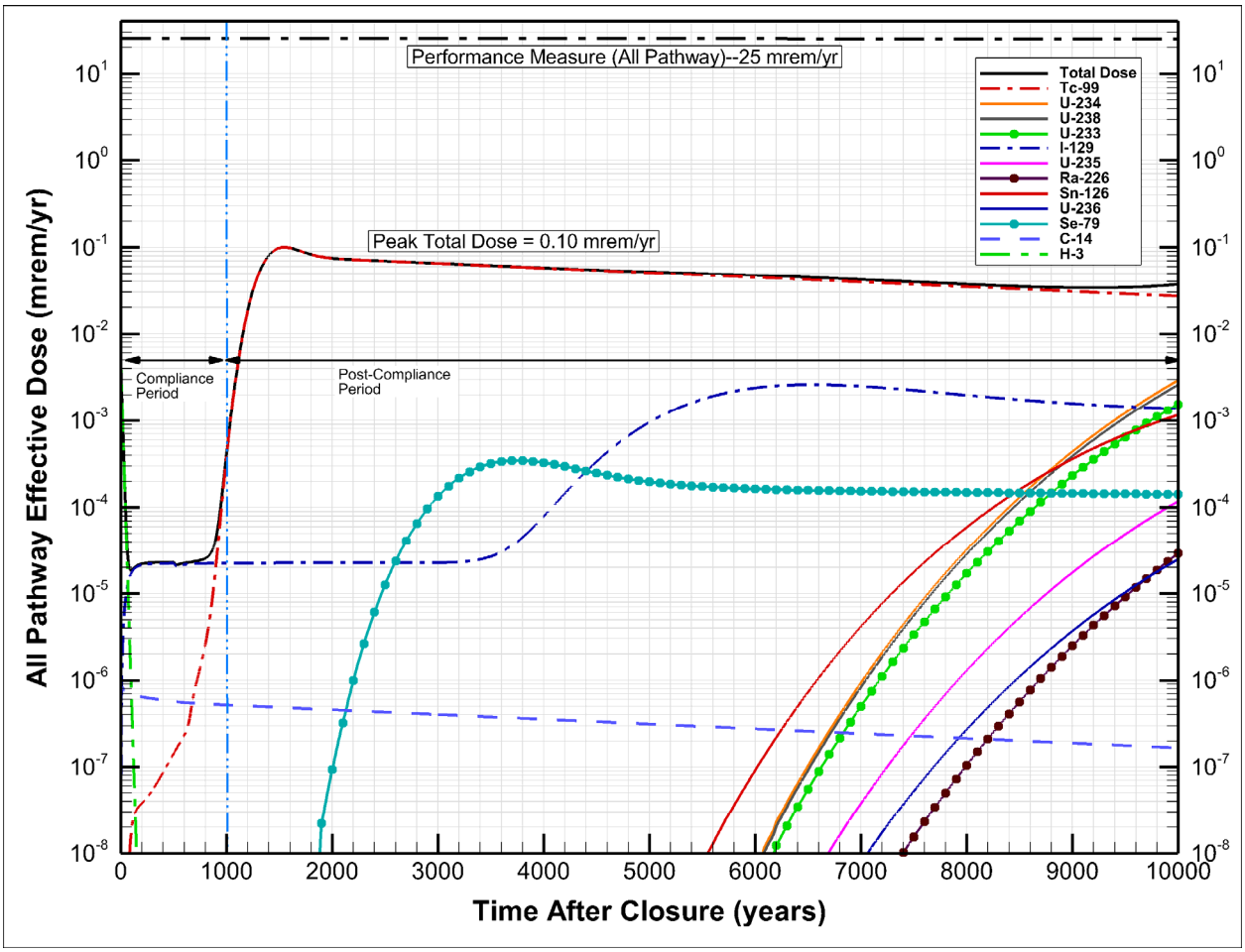

Reference: DOE O 435.1, 2001, Radioactive Waste Management, U.S. Department of Energy, Washington, D.C.

In the uncertainty analysis performed with the system-level model based on GoldSim©[1] (see Figure ES-7, the highest calculated groundwater dose in the compliance period was about 0.07 mrem/yr, and the highest calculated peak dose in the sensitivity/uncertainty analysis period was 2.5 mrem/yr, as discussed in Section 10.6. The most influential parameters that affect the peak dose in the groundwater pathway are the vadose zone hydraulic properties and Darcy flux in the saturated zone (see Section 8.1.4.4 for details).

[1] GoldSim© simulation software is copyrighted by GoldSim Technology Group LLC of Issaquah, Washington (see http://www.goldsim.com).

Figure ES-7. Results of Uncertainty Analysis Based on 300 Realizations of System Model Based on GoldSim© (a) Groundwater Pathway Dose Results and (b) All-Pathways Dose Results.

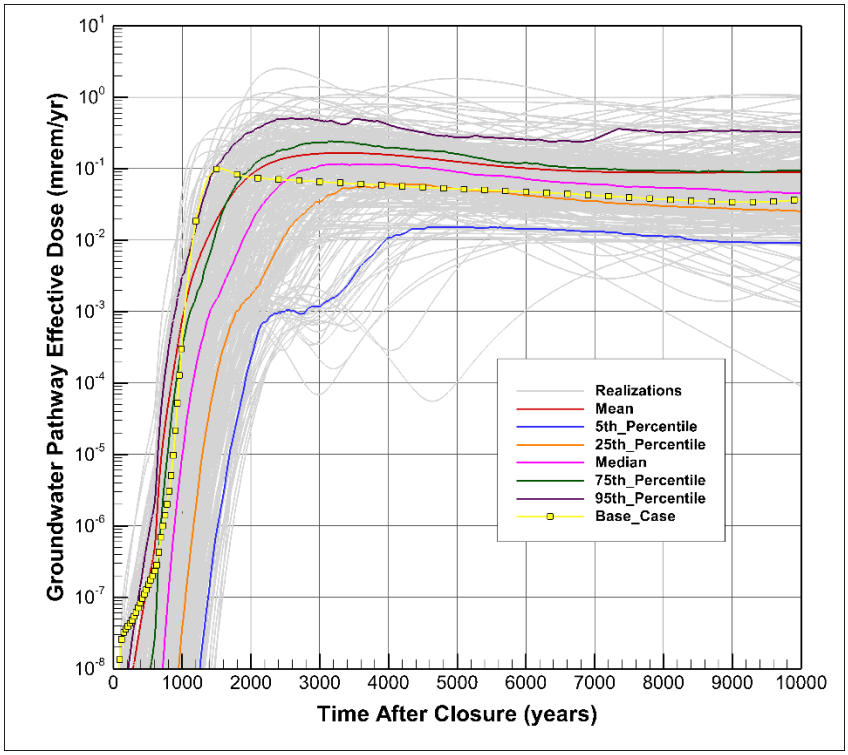

(a)

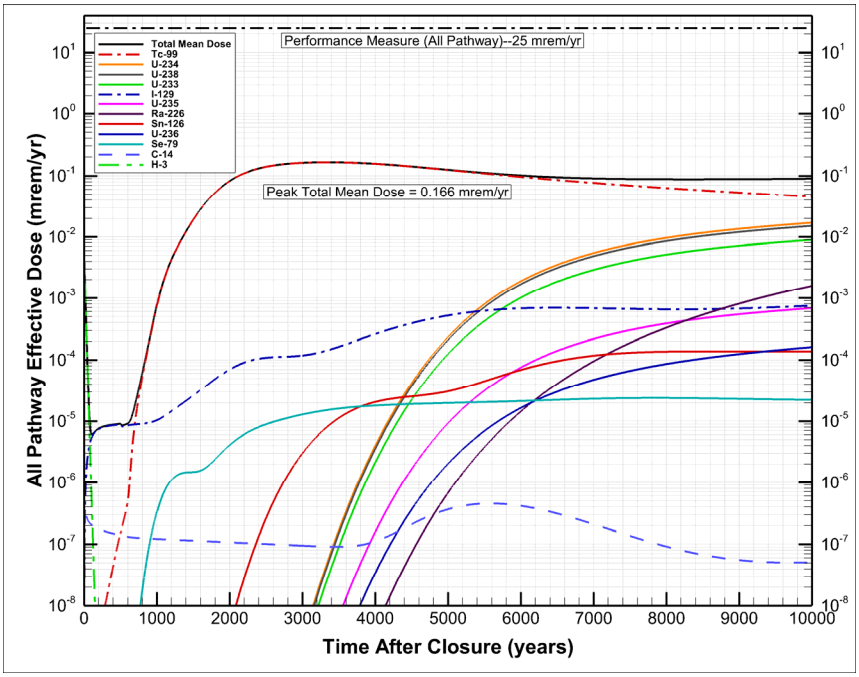

(b)

GoldSim© simulation software is copyrighted by GoldSim Technology Group LLC of Issaquah, Washington (see http://www.goldsim.com).

Among the sensitivity cases with degraded safety functions, the maximum deviation from the base case was a factor of 4.8 higher than the base case, which occurred for the sensitivity case which assumed the bounding ^{99}Tc inventory in the unretrieved tanks. For this case, there is no change in the time dependence of the results compared to the base case; the peak occurs in the sensitivity/uncertainty time period, and the concentration in the compliance time period is small. This case represents an assumption that no further retrieval of ^{99}Tc from tanks will be possible.

In the parameter uncertainty analysis, for the entire range of input parameters, even including the extreme of the sampled inputs, the disposal system met the performance objectives. A summary of these results show the robustness of the PA to uncertainties in the input parameters used in the model.

For the air pathway, only the radionuclides ^{14}C, ^{3}H, and ^{129}I are considered as they are the only volatile radionuclides considered for air pathway dose calculations. Potential releases into the gaseous pathway were evaluated and compared to the DOE O 435.1 performance objective of 10 mrem/yr for doses from airborne contamination. The results of the analyses were orders of magnitude below the performance objective, as shown in Table ES-1.

Releases of radon from the facility were evaluated and compared to the 20 pCi/m^2/s radon flux performance objective in DOE O 435.1. The inventory of ^{226}Ra (the parent of ^{222}Rn) in WMA C residual waste is small, and initial radon fluxes are very low compared to the performance objectives. Ingrowth of ^{226}Ra from decay of the ^{238}U decay chain leads to increasing radon fluxes at longer times. However, the fluxes remain many orders of magnitude below the performance objective at all times, as presented in Section 10.3.

Doses associated with hypothetical inadvertent human intrusion were calculated for all sources in WMA C (see Section 9.0) and compared to the acute and chronic performance measures in DOE O 435.1. However, the calculated doses do not take account of the likelihood of intrusion into the various sources, and there are significant differences between them. The tank domes were constructed of reinforced concrete, which are still in good condition and will likely provide a very substantial barrier to a drilling intrusion. Furthermore, upon closure the tanks will be filled with grout, which will add a second, very significant barrier to drilling intrusion. As a result of these barriers, intrusion into grouted tanks is not regarded as a credible event, as the tank domes and infill grout form very substantial and long-lasting barriers to the intrusion. Consequently, while the potential doses from intrusion into a tank are the highest calculated, the likelihood of occurrence of intrusion into a tank is regarded as very small. As a result, the intrusion analyses for tanks should be regarded as informational, and should not be compared to the performance measures.

By contrast, barriers are much less robust or nonexistent for pipelines and other ancillary equipment, and as a result the primary potential for intrusion is considered to be into ancillary equipment. The most likely intrusion event for ancillary equipment would be intrusion into one of the waste transfer lines within the area of WMA C (see Section 9). Doses resulting from this type of intrusion event were used for comparison with performance measures for acute and chronic exposure.

The PA results indicate that the performance objectives and measures for the all-pathways dose, the air pathway dose, the radon flux, and groundwater protection are met for both the 1,000-year compliance time period (2020 to 3020) and the post-compliance period (3020 to 12020). For all of the sensitivity analyses and uncertainty analyses evaluated, the disposal system met the performance objectives. This result demonstrates the robustness of the PA to alternative assumptions with respect to the behavior of the safety functions and input parameters.

Calculated doses for the acute and chronic exposure scenarios from a potential intrusion into a waste transfer pipeline remain below the DOE O 435.1 performance measure for the time period evaluated beyond 100 years after closure. The acute scenario dose is dominated by ^{137}Cs and ^{239}Pu, while chronic scenario doses are dominated by ^{90}Sr, ^{137}Cs and ^{239}Pu. The total dose generally shows a steep decline compared to the timescales evaluated in the PA due to short half-lives of ^{90}Sr and ^{137}Cs, but becomes stable once long-lived ^{239}Pu becomes the dominant dose contributor. The dominant exposure conditions for the assessment were from the acute scenario, which had higher doses than the chronic exposure scenario at 100 years after closure. At longer times (greater than about 500 years after closure), the acute scenario also produced higher calculated doses for the intrusion into waste transfer pipelines, mainly because long-lived ^{239}Pu plays a more important role in the dose calculation.

TABLE OF CONTENTS

1.0 INTRODUCTION 1-1

1.1 GENERAL APPROACH 1-2

1.1.1 Waste Management Area C Performance Assessment Scoping Process 1-8

1.1.2 Model Development and Implementation Process 1-10

1.2 REGULATORY CONTEXT 1-12

1.2.1 National Environmental Policy Act of 1969 1-13

1.2.2 Hanford Federal Facility Agreement and Consent Order 1-13

1.2.3 Resource Conservation and Recovery Act of 1976/Hazardous Waste Management Act 1-14

1.2.4 Atomic Energy Act of 1954 1-14

1.2.5 Comprehensive Environmental Response, Compensation, and Liability Act of 1980 1-15

1.3 GENERAL FACILITY DESCRIPTION 1-15

1.4 A SAFETY CONCEPT AND SAFETY FUNCTIONS FOR CLOSED WASTE MANAGEMENT AREA C 1-19

1.5 LAND USE AND INSTITUTIONAL CONTROL ASSUMPTIONS 1-22

1.6 WASTE MANAGEMENT AREA C HISTORY AND PLAN FOR CLOSURE 1-26

1.6.1 History 1-26

1.6.2 Closure 1-29

1.7 PREVIOUS PERFORMANCE ASSESSMENTS AND OVERLAPPING ANALYSES 1-30

1.7.1 Single-Shell Tank Performance Assessment 1-31

1.7.2 Tank Closure and Waste Management Environmental Impact Statement Analysis of Waste Management Area C 1-31

1.7.3 Waste Management Area C Pipeline Feasibility Study 1-32

1.8 SUMMARY OF KEY ASSESSMENT ASSUMPTIONS 1-33

2.0 ASSESSMENT CONTEXT 2-1

2.1 PUBLIC PROTECTION PERFORMANCE OBJECTIVES AND MEASURES 2-3

2.2 POINT OF ASSESSMENT AND TIMING ASSUMPTIONS 2-3

2.3 ASSESSMENT PERIOD 2-5

2.4 MODELING APPROACH 2-5

2.4.1 Source Term Release 2-5

2.4.2 Contaminant Fate and Transport along the Groundwater Pathway 2-7
2.4.3 Contaminant Fate and Transport along the Air Pathway 2-8
2.4.4 Exposure and Dose Analysis for Comparison with Performance Objectives 2-9

2.5 HYPOTHETICAL INADVERTENT INTRUSION 2-9

2.6 REASONABLE EFFORTS TO MINIMIZE RELEASES 2-12

3.0 SITE AND FACILITY CHARACTERISTICS 3-1

3.1 SITE CHARACTERISTICS 3-1

3.1.1 Geography and Demography 3-1
3.1.2 Meteorology and Climatology 3-15
3.1.3 Ecology 3-22
3.1.4 Geology, Seismology, and Volcanology 3-28
3.1.5 Hydrology 3-52
3.1.6 Geochemical Properties 3-83
3.1.7 Natural Resources 3-84
3.1.8 Natural Background Radiation 3-85
3.1.9 Waste Management Area C Site Characterization 3-86

3.2 WASTE MANAGEMENT AREA C PRINCIPAL FACILITY DESIGN FEATURES 3-101

3.2.1 Facility Description 3-104
3.2.2 Tank Residual Waste Inventory 3-119

4.0 SCREENING APPROACHES 4-1

4.1 SCREENING BASED ON INVENTORY-RELATED INFORMATION 4-1

4.2 SUMMARY OF RADIONUCLIDE SCREENING 4-2

5.0 WASTE CHARACTERISTICS 5-1

6.0 ANALYSIS OF PERFORMANCE 6-1

6.1 OVERVIEW OF ANALYSIS 6-1

6.2 CONCEPTUAL MODEL OF FACILITY PERFORMANCE 6-3

6.2.1 Source Term and Engineered Features 6-9
6.2.2 Radionculide Transport 6-29
6.2.3 Exposure Pathways and Scenarios 6-42

6.3 MATHEMATICAL MODELS 6-43

6.3.1 Source Term and Engineered Features 6-44
6.3.2 Radionuclide Transport 6-76
6.3.3 Exposure and Dose Analysis 6-134

6.4 MODEL VALIDATION 6-158
6.4.1 Basis for Recharge Estimates Used for Land Surface Boundary Condition 6-158
6.4.2 Basis for Source-Term Model Development and Implementation 6-159
6.4.3 Basis for Vadose Zone Model Development 6-160
6.4.4 Comparison of Vadose Zone Modeling Results with Measured Data in Vicinity of Waste Management Area C 6-162
6.4.5 Comparison of Vadose Zone Model with Tank Closure and Waste Management Environmental Impact Statement Model for Alternative 2B 6-163
6.4.6 Basis for Saturated Zone Model Development 6-164
6.4.7 Verification of Air Pathway Modeling Approach 6-165

7.0 RESULTS OF ANALYSIS 7-1

7.1 SOURCE TERM 7-1

7.2 ENVIRONMENTAL TRANSPORT OF RADIONUCLIDES 7-6

7.2.1 Groundwater Transport of Radionuclides 7-6
7.2.2 Air Transport of Radionuclides 7-29

7.3 DOSE ANALYSIS 7-35

7.3.1 All-Pathways Dose 7-37
7.3.2 Air Pathway Dose 7-39

8.0 UNCERTAINTY AND SENSITIVITY ANALYSIS 8-1

8.1 UNCERTAINTY ANALYSIS 8-1

8.1.1 Methodology for Propagation of Uncertainty 8-2
8.1.2 Rationale for Assigning Probability Distributions 8-2
8.1.3 Parameter Uncertainty Distributions 8-5
8.1.4 Development of Vadose Zone Flow Fields and Propagation of Uncertainty 8-35
8.1.5 Results of Uncertainty Analyses 8-50
8.1.6 Statistical Stability 8-65

8.2 SENSITIVITY ANALYSIS FOR THE GROUNDWATER PATHWAY 8-66

8.2.1 Surface Barrier Flow Sensitivity Analyses 8-70
8.2.2 Aquifer Dilution Sensitivity Analyses 8-72
8.2.3 Vadose Zone Flow and Dispersion Sensitivity Analyses 8-73
8.2.4 Inventory Sensitivity Analyses 8-83
8.2.5 Grout Flow Sensitivity Analyses 8-84
8.2.6 Waste Form Sensitivity Analysis 8-88
8.2.7 Tank Flow Sensitivity Analyses 8-100
8.2.8 Evaluation of Long-Term Peak Dose 8-102

9.0 INADVERTENT INTRUDER ANALYSIS 9-1

9.1 CONSIDERATION OF THE PROBABILITY OF INTRUSION 9-3

9.2 ACUTE EXPOSURE SCENARIOS 9-6

9.2.1 Radionuclide Concentration in Drill Cuttings 9-8
9.2.2 Acute Well Driller Scenario – Incidental Soil Ingestion 9-9
9.2.3 Acute Well Driller Scenario – Inhalation of Soil Particulates 9-9
9.2.4 Acute Well Driller Scenario – External Exposure 9-10

9.3 CHRONIC SCENARIOS 9-10

9.3.1 Chronic Rural Pasture Scenario 9-11
9.3.2 Chronic Suburban Garden Scenario 9-17
9.3.3 Chronic Commercial Farm Scenario 9-21

9.4 INTRUDER ANALYSIS RESULTS 9-24

9.4.1 Acute Exposure Dose 9-24
9.4.2 Chronic Exposure Dose 9-25

9.5 INTRUDER SENSITIVITY/UNCERTAINTY ANALYSIS 9-27

10.0 PERFORMANCE EVALUATION AND INTERPRETATION OF RESULTS 10-1

10.1 ALL PATHWAYS ANALYSIS 10-1

10.2 AIR PATHWAY ANALYSIS 10-2

10.3 RADON FLUX 10-2

10.4 INADVERTENT HUMAN INTRUSION 10-3

10.5 GROUNDWATER RESOURCE PROTECTION 10-4

10.6 SENSITIVITY AND UNCERTAINTY ANALYSES FOR THE GROUNDWATER PATHWAY 10-6

10.7 USE OF PERFORMANCE ASSESSMENT RESULTS 10-8

10.8 FUTURE WORK 10-9

11.0 QUALITY ASSURANCE 11-1

11.1 ENVIRONMENTAL MODEL LIFECYCLE QUALITY ASSURANCE PROCESS 11-1

11.2 CONTROLLED SOFTWARE USE 11-2

11.2.1 Subsurface Transport Over Multiple Phases 11-3
11.2.2 GoldSim© 11-4
11.2.3 Other Hanford Site Tank Waste Management Software Tools 11-4

11.3 MODEL DOCUMENTATION, CONTROL, AND PRESERVATION 11-7

12.0 PREPARERS 12-1

13.0 REFERENCES 13-1

LIST OF APPENDICES

A Key Assumptions in the Performance Assessment ..... A-i

B Basis for Development of Vadose Zone Hydraulic Properties at Waste Management Area C ..... B-i

C Technical Basis for Waste Management Area C Unconfined Aquifer Conceptual Model: Field Data and Related Investigations ..... C-i

D Flow and Contaminant Transport Numerical Model for the Waste Management Area C Performance Assessment ..... D-i

E Validation of the Air-Pathway Modeling Approach ..... E-i

F Development of Heterogeneous Media Model and Comparison to Base Case Model Results for Waste Management Area C Performance Assessment ..... F-i

G Comparison of Selected Model Results for Alternative 2B from the Tank Closure and Waste Management Environmental Impact Statement for Waste Management Area C with Equivalent Results Using the Waste Management Area C Performance Assessment Base Case Model ..... G-i

H List of Features, Events and Processes Applied to Waste Management Area C ..... H-i

I Results of Flow-Fields Developed in the Vadose Zone for the Purpose of Uncertainty Analysis ..... I-i

LIST OF FIGURES

Figure 1-1. Hanford Site Tank Farms. 1-4

Figure 1-2. The Components of the Appendix I Performance Assessment. 1-5

Figure 1-3. Use of Subsurface Transport Over Multiple Phases and GoldSim© in the Evaluation of Parts of the Performance Assessment. 1-11

Figure 1-4. Hanford Site and its Location in Washington State. 1-17

Figure 1-5. Location Map of Waste Management Area C and Surrounding Area. 1-18

Figure 1-6. Location Map of Unplanned Release Sites of Waste Management Area C. 1-19

Figure 1-7. A Schematic Depiction of the Safety Functions for a Closed Waste Management Area C. 1-24

Figure 1-8. Hanford Site, Showing Land-Use Designations Including the Hanford Reach National Monument. 1-25

Figure 1-9. Photographs Showing Different Stages of the Historical Construction of Tanks and Selected Ancillary Equipment in Waste Management Area C. 1-27

Figure 2-1. Schematic Overview of the Model Approach for the Waste Management Area C Performance Assessment. 2-6

Figure 2-2. Complimentary Use of Process-Level and System-Level Models for Groundwater Pathway in the Waste Management Area C Performance Assessment. 2-7

Figure 3-1. U.S. Department of Energy's Hanford Site and Surrounding Area. 3-3

Figure 3-2. Facilities in the 200 East and 200 West Areas. 3-4

Figure 3-3. Waste Management Area C Tanks and Associated Infrastructure. 3-5

Figure 3-4. Generalized Land Use of the Hanford Site and Adjacent Areas. 3-7

Figure 3-5. Population Centers with Estimated Population within 80 kilometers (50 miles) of the Hanford Meteorological Station. 3-9

Figure 3-6. Hanford Meteorological Monitoring Network Wind Roses in 2010 at the 9.1-meter (30-foot) Level. 3-17

Figure 3-7. Hanford Meteorological Monitoring Network Wind Roses from 1982 to 2006 at the 9.1-meter (30-foot) Level. 3-20

Figure 3-8. Precipitation Reconstruction for Past 100,000 Years Based on Pollen Data. 3-23

Figure 3-9. Temperature Reconstruction for Past 100,000 Years Based on Pollen Data. 3-24

Figure 3-10. Extent of Area Burned During Recent Fires at the Hanford Site. 3-26

Figure 3-11. Vegetation Communities in and near 200 East Area. 3-27

Figure 3-12. Habitat Areas within a 500 Foot Perimeter of Waste Management Area C. 3-29

Figure 3-13. Geologic Elements of the Pasco Basin Portion of the Columbia Basin, Washington. 3-31

Figure 3-14. Geologic Setting of the Columbia Basin and Pasco Basin. 3-32

Figure 3-15. Flood in the South of the Hanford Site, Washington, between 18,000 to 13,000 Years Ago. 3-35

Figure 3-16. Geologic and Geomorphic Map of the 200 Areas and Vicinity. 3-36

Figure 3-17. Generalized Stratigraphy of the Hanford Site Including the Central Plateau. 3-38

Figure 3-18. Cross-Section Running through the Central Plateau of the Hanford Site. 3-39

Figure 3-19. Fence Diagram of Sediment Overlying the Columbia River Basalt Group in the Central Plateau, Hanford Site. 3-40

Figure 3-20. Isopach Map of the Ice Age Flood Deposits (Hanford Formation). 3-44

Figure 3-21. Typical Type II Clastic Injection Dike Exposed in a Wall of the Environmental Restoration Disposal Facility Excavation Exposed during Construction. 3-45

Figure 3-22. Topography of the 200 Areas Central Plateau in Meters above Mean Sea Level. 3-46

Figure 3-23. Historical Earthquake Activity of the Columbia Basin, Washington, and Surrounding Areas. 3-49

Figure 3-24. Earthquake Swarm Areas in the Vicinity of the Hanford Site. 3-50

Figure 3-25. Surface Water Features including Rivers, Ponds, Major Springs, and Ephemeral Streams on the Hanford Site, Washington. 3-53

Figure 3-26. Flood Area for the Probable Maximum Flood on the Hanford Site, Washington, as Determined by the Upper Limit of Precipitation and Maximum Runoff. 3-57

Figure 3-27. Extent of Probable Maximum Flood in Cold Creek Area, Hanford Site, Washington, delineated using the U.S. Army Corps of Engineers' HEC-2 Water Surface Profiles Model. 3-58

Figure 3-28. Recharge Dependence on Surface Conditions. 3-61

Figure 3-29. Recharge Dependence on Surface Conditions. 3-63

Figure 3-30. Examples of Anthropogenic Recharge in the 200 Area. (Photographs a – c are from DOE/ORP-2008-01 Appendix K, Photographs d and e are Archive Photos). 3-64

Figure 3-31. Hydrogeologic Units Present at the Water Table in June 1998. 3-71

Figure 3-32. Discharge History for the 216-B Pond System and Gable Mountain Pond. 3-72

Figure 3-33. Discharge History for the 216-T Pond and 216-U Pond. 3-74

Figure 3-34a. Hind Cast Water Table Map of the Hanford Site, January 1944. 3-75

Figure 3-34b. Water Table Elevations for June 1987. 3-75

Figure 3-34c. Water Table Elevations for 2013 3-75

Figure 3-35. Groundwater Contamination for 2013 which Originated within the Central Plateau along with Central Plateau Groundwater Interest Areas. 3-80

Figure 3-36. Waste Management Area C Tanks, Infrastructure, and Associated Unplanned Releases. 3-87

Figure 3-37. Fence Diagram Showing Cross-Sections through Waste Management Areas A AX and C. 3-88

Figure 3-38. Fence Diagram of Alternative Geologic Models to be Used in Waste Management Area C. 3-90

Figure 3-39. Vadose Zone and Groundwater Monitoring Network for Waste Management Area C. 3-91

Figure 3-40a. Completed Phase 2 RCRA Facility Investigation Characterization Locations. 3-93

Figure 3-40b. Completed Transitional (Phase 1.5) Characterization Locations. 3-94

Figure 3-41. Moisture Content (% Vol) Measurements in Vadose Zone at Waste Management Area C. 3-97

Figure 3-42. Three-Dimensional Perspective of Waste Management Area C Tanks and Drywells Showing Occurrence of Significant (>10 pCi/g) Cesium-137 Contamination in the Vadose Zone along with Technetium-99 at Borehole C4297. 3-98

Figure 3-43. Technetium-99 Concentrations in Waste Management Area C Wells from January 2006 through December 2014. 3-102

Figure 3-44. Cyanide Concentrations in Waste Management Area C Wells from January 2006 through December 2014. 3-103

Figure 3-45. Waste Management Area C Tanks and Associated Tank Infrastructure. 3-109

Figure 3-46. Corner of Tank Floor with Tank Sides for the C-100 and C-200 Series Tanks. 3-110

Figure 3-47. 244-CR Process Tank Vault Waste pH, Temperature, and Volume Estimates in 2005. 3-113

Figure 3-48. Conceptual Model of Tank Filled with Cementitious Grout. 3-114

Figure 3-49. Conceptual Model of Cementitious Grouted Tank Aging. 3-115

Figure 3-50. Generic Modified RCRA C Baseline Design from DOE/RL-93-33. 3-117

Figure 5-1. Photographs of As-Received, Post-Final Retrieval Residual Waste Samples from Tanks 241-C-103, 241-C-106, 241-C-202, and 241-C-203. 5-3

Figure 5-2. Low- and High-Magnification Electron Micrographs of Typical Solids Present in Unleached Tank 241-C-103 Residual Waste. 5-6

Figure 5-3. Electron Micrograph (top) and Multi-Element Energy Dispersive Spectroscopy Map (bottom) for an Aggregate of U-Na-C-O-P ± H and Fe Oxide/Hydroxide Particles Present in Sequential-Leached Water Extraction Sample of Tank 241-C-203 Residual Waste. 5-7

Figure 5-4. Uranium Concentrations in Tank 241-C-202 Single-Pass Flow-Through Leachates as a Function of the Total Volume of Leachate that has Contacted the Waste in Terms of Leachate/Solid (Initial) Weight Ratio. 5-8

Figure 5-5. Technetium-99 Concentration in Tank 241-C-202 Single-Pass Flow-Through Leachates as a Function of the Total Volume of Leachate that has Contacted the Waste in Terms of Leachate/Solid (Initial) Weight Ratio. 5-9

Figure 5-6. Chromium Concentration in Tank 241-C-202 Single-Pass Flow-Through Leachates as a Function of the Total Volume of Leachate that has Contacted the Waste in Terms of Leachate/Solid (Initial) Weight Ratio. 5-10

Figure 6-1. Overview of the Dose Calculations for Exposure Along the Groundwater Pathway and Air Pathway for the Waste Management Area C Performance Assessment. 6-5

Figure 6-2. Schematic Conceptual Representation of Waste Management Area C and Contaminant Migration into the Environment along the Various Pathways Evaluated in the Performance Assessment. 6-6

Figure 6-3. Conceptual Model of the Waste Management Area C Site Showing Stratigraphy. 6-7

Figure 6-4. Aerial View of Waste Management Area C Showing Surface Features and the Surrounding Area. 6-8

Figure 6-5. Computer-Aided Modeling Results Showing Distribution of Residual Waste for a Retrieved Tank. 6-11

Figure 6-6. Conceptual Model of Tank after Site Closure. 6-12

Figure 6-7. Engineered Structure at the Base of the C-100-Series Tank. 6-15

Figure 6-8. C-100-Series Tank Corner Features. 6-16

Figure 6-9. C-200-Series Tank Cross-Section. 6-17

Figure 6-10. Schematic of the 244-CR Process Tank Vault in Waste Management Area C. 6-18

Figure 6-11. Location of Active and Existing Pipelines Along with New and Existing Facilities for Waste Fractionization Operations (1961 to 1978). 6-20

Figure 6-12. Carbonation Process Acting on the Buried Tank Wall. 6-21

Figure 6-13. Demolition of (a) Pool 1 Monolith and (b) Pool 2 Monolith after Only 5 Days after the Capping Layer had been Poured. 6-24

Figure 6-14. Evaluation of 55-inch Diameter Reinforced Concrete Dome Plug from Tank 214-C-107. 6-25

Figure 6-15. Evaluation of Sidewall Concrete Core from Tank 241-A-106. 6-26

Figure 6-16. Surface Conditions In and Around Waste Management Area C during the Construction and Operations Period. 6-34

Figure 6-17. Inferred Surface Conditions In and Around Waste Management Area C during the Post-Closure Period. 6-35

Figure 6-18. Conceptualization of Air Pathway Diffusive Release from the Tank to the Surface. 6-41

Figure 6-19. Technetium-99 Concentration in Single-Pass Flow-Through Leachates for (a) Tank 241-C-103, (b) Tank 241-C-202, and (c) Tank 241-C-203 as a Function of the Total Volume of Leachate that has Contacted the Waste in Terms of Leachate Solution to Solid (Initial) Weight Ratio. 6-46

Figure 6-20. Fractional Release of Technetium-99 for Single-Pass Flow-Through Experiments from Tank 241-C-103 Along with the Estimate of the First-Order Reaction Rate Constant of 8E-04 day^{-1}. 6-49

Figure 6-21. Fractional Release of Technetium-99 for Single-Pass Flow-Through Experiments from Tank 241-C-202 Along with the Estimate of the First-Order Reaction Rate Constant of 6E-04 day^{-1}. 6-50

Figure 6-22. Fractional Release of Technetium-99 for Single-Pass Flow-Through Experiments from Tank 241-C-203 Along with the Estimate of the First-Order Reaction Rate Constant of 5E-04 day^{-1}. 6-51

Figure 6-23. Simulated Versus Observed Effluent Concentrations of Technetium-99 (µg/L) from the Single-Pass Flow-Through Experiments Conducted on Tanks 241-C-103 and 241-C-202 Residual Waste. 6-52

Figure 6-24. Uranium and Total Inorganic Carbon Concentrations (A) and the Paragenetic Sequence of Uranium Phases Present in the Waste (B) as a Function of Reaction Progress for the $Ca(OH)^2$ Saturated Water Scenario. 6-54

Figure 6-25. Uranium and Total Inorganic Carbon concentrations (A) and the Paragenetic Sequence of Uranium Phases Present in the Waste (B) as a Function of Reaction Progress for the $CaCO^3$ Saturated Water Scenario. 6-55

Figure 6-26. Uranium Solubility Model Implemented with Solubility Limits Varying with Time. 6-56

Figure 6-27. Comparison of Initially Imposed Uranium Solubility Limit of 1×10^{-4} M to the Observed Concentrations during the Single-Pass Flow-Through Conducted on 241-C-202 Tank Residual. 6-57

Figure 6-28. Diffusive Pathway for Transport of Non-Volatile Contaminants to the Near-Field Environment. 6-58

Figure 6-29. Set-Up of the Diffusive Half-Cell Experiment Contacting Contaminant-Spiked Sediment (or Concrete) Sample with the Non-Spiked Sediment (or Concrete) Sample. 6-59

Figure 6-30. Technetium-99 Concentration Profiles in Concrete from Sediment-Concrete Half-Cell Experiments Conducted on (A) 4% Sediment Moisture, Carbonated Monoliths, (B) 4% Sediment Moisture, Non-Carbonated Monoliths, (C) 7% Sediment Moisture, Carbonated Monoliths, (D) 7% Sediment Moisture, Non-Carbonated Monoliths, (E) 15% Sediment Moisture, Carbonated Monoliths, and (F) 15% Sediment Moisture, Non-Carbonated Monoliths. 6-62

Figure 6-31. Effective Diffusion Coefficient of Technetium-99 in Concrete Based on Experiments Conducted Using Sediment-Concrete Half-Cells. 6-63

Figure 6-32. Porosity-Permeability Relationship as a Function of Hydration and Water-to-Cement Ratio. 6-67

Figure 6-33. Soil-Moisture Characteristics Curves for the Grout Hydraulic Properties Evaluated. 6-68

Figure 6-34. Two-Dimensional Cross Section Model to Evaluate the Flow Through the Tanks along with the Flow-Field at Long Time Representing near Steady-State Conditions. 6-69

Figure 6-35. Simulated Vertical Darcy Flux and Volumetric Moisture Content for the Tank Node and Backfill Node over a Large Time Scale. 6-70

Figure 6-36. The Interpolated Numerical Three-Dimensional Post-Closure Alternative I Hydrogeologic Model. 6-81

Figure 6-37. Plan View of Waste Management Area C Performance Assessment Model Domain Showing the Horizontal Distribution and Surface Type of the Irregularly-Spaced Calculation Nodes. 6-85

Figure 6-38. Diagram of the Interpolated Numerical Three-Dimensional Post-Closure Alternative I Hydrogeologic Model. 6-87

Figure 6-39. The Interpolated Numerical Three-Dimensional Post-Closure Alternative II Hydrogeologic Model. 6-88

Figure 6-40. Diagram of the Interpolated Numerical Three-Dimensional Post-Closure Alternative II Hydrogeologic Model. 6-89

Figure 6-41. Hindcast Water Table Map of the Hanford Site, January 1944. 6-94

Figure 6-42. Waste Management Area C Three-Dimensional Model Subsurface Transport Over Multiple Phases (STOMP©)-Based Model Node Locations. ... 6-103

Figure 6-43. Three-Dimensional Subsurface Transport Over Multiple Phases (STOMP©)-Based Model Node Locations for Waste Management Area C along with Location of Cross-Section Lines. 6-104

Figure 6-44. Northwest-Southeast Trending Geologic Cross-Sections Through the Tank Farm Using Information from Three Dimensional Subsurface Transport Over Multiple Phases (STOMP©)-Based Model. 6-105

Figure 6-45. Moisture Content Distribution below Tank 241-C-105 at Various Times during (a) Surface Barrier Design Time Period of 500 years Following Closure and (b) Post-Surface Barrier Design Time Period. 6-108

Figure 6-46. Vertical Darcy Flux Distribution below Tank 241-C-105 at Various Times..... 6-109

Figure 6-47. Representative Hydrostratigraphic Column for (a) 100-Series and (b) 200-Series Tanks. 6-110

Figure 6-48. Representative Flow Field Applied Under 100-Series Tank for the Base Case (Intact Tank Condition). 6-114

Figure 6-49. Representative Flow Field Applied Under 200-Series Tank for the Base Case (Intact Tank Condition). 6-115

Figure 6-50. Representative Flow Field Applied for Degraded Tank Conditions for (a) 100-Series Tank and (b) 200-Series Tank. 6-116

Figure 6-51. Implementation of Aquifer Pathway for a Given Source Area Along with Points of Evaluation of Concentrations. 6-117

Figure 6-52. Vertical Darcy Flux Extracted from Three-Dimensional Subsurface Transport Over Multiple Phases (STOMP©)-Based Model Nodes Located below Tanks 241-C-105, 241-C-112, and 241-C-201 along with Their Location in Waste Management Area C. 6-118

Figure 6-53. Comparison between Three-Dimensional Subsurface Transport Over Multiple Phases (STOMP©) Based Model Prediction and GoldSim©-Based One-Dimensional Abstraction Model Prediction for Nodes Located in H1 Gravelly Sand Unit. 6-119

Figure 6-54. Comparison between Three-Dimensional Subsurface Transport Over Multiple Phases (STOMP©)-Based Model Prediction and GoldSim©-Based One-Dimensional Abstraction Model Prediction for Nodes Located in H2 Sand Unit and H3 Gravelly Sand Unit. 6-120

Figure 6-55. Comparison Between Three-Dimensional Subsurface Transport Over Multiple Phases (STOMP©)-Based Model Prediction and GoldSim©-Based One-Dimensional Abstraction Model Prediction in the Saturated Zone at 100 m Distance from the Waste Management Area C Fenceline. 6-121

Figure 6-56. Atmospheric Transport Pathway from a Source to the Receptor Located at the Point of Calculation Along the Centerline of the Gas Plume. 6-125

Figure 6-57. A Schematic of Gaseous Plume Movement Based on Gaussian Distribution in the Horizontal and Vertical Direction. 6-126

Figure 6-58. Comparison of Measured Tortuosity (i.e., Ratio of Diffusion Coefficient in Soil [D_{ef}] to that in Free Air [D_0]) with Fitted Tortuosity Models. 6-128

Figure 6-59. Burrow and Root Density with Depth in Various Northwestern Semiarid Sites. 6-135

Figure 6-60. Location of Sisson and Lu Field Injection Site in 200 East Area. 6-161

Figure 6-61. Simulated Average Moisture Contents for Different Stratigraphic Units Using Equivalent Homogeneous Medium Model. 6-163

Figure 6-62. Comparison of Simulated (Blue) and Observed (Circle) Moisture Content for Hanford H2 Sand-Dominated Unit. 6-164

Figure 6-63. Central Plateau Groundwater Model Calibration Results in the Vicinity of Waste Management Area C. 6-166

Figure 7-1. Release Rate of Technetium-99 (pCi/yr) from Each Source. 7-3

Figure 7-2. Comparison of Dissolved Concentration of Technetium-99 (pCi/L) in the Residual Waste and Tank Bottom for Tank 241-C-105. 7-4

Figure 7-3. Release Rate of Uranium-238 (pCi/yr) from Representative Source Terms. 7-5

Figure 7-4. Comparison of Dissolved Concentration of Uranium-238 (pCi/L) in the Residual Waste and Tank Bottom for Tank 241-C-105. 7-5

Figure 7-5. Release Rate of Total Uranium (g/yr) from Representative Sources. 7-6

Figure 7-6. First-Arrival Time (in Calendar Year) of Radionuclides for Various K_d Values Based on Screening Analysis Using Subsurface Transport Over Multiple Phases. 7-7

Figure 7-7. Moisture Content in the Vadose Zone at Tank 241-C-105 in Waste Management Area C for Four Times of Interest: (a) Pre-Hanford Steady State, (b) Waste Management Area C Closure, (c) 100 Years after Closure, and (d) At 1,000 Years. 7-11

Figure 7-8. Moisture Content in the Vadose Zone in Waste Management Area C between Tanks 241-C-105, 241-C-106, 241-C-108, and 241-C-109 for Four Times of Interest: (a) Pre-Hanford Steady State, (b) Waste Management Area C Closure, (c) 100 Years after Closure, and (d) At 1,000 Years. 7-12

Figure 7-9. Darcy Flux in the Vadose Zone at Tank 241-C-105 in Waste Management Area C for Four Times of Interest: (a) Pre-Hanford Steady State, (b) Waste Management Area C at Closure, (c) 100 Years after Closure, and (d) At 1,000 Years after Closure. 7-14

Figure 7-10. Darcy Flux in the Vadose Zone in Waste Management Area C between Tanks 241-C-105, 241-C-106, 241-C-108, and 241-C-109 for Four Times of Interest: (a) Pre-Hanford Steady State, (b) Waste Management Area C at Closure, (c) 100 Years after Closure, and (d) At 1,000 Years after Closure. 7-15

Figure 7-11. Points of Calculation 100 Meters Downgradient of Waste Management Area C. 7-16

Figure 7-12. Extent of Transport of Technetium-99 (K_d = 0 mL/g) in the Vadose Zone at the End of the 1,000-Year Compliance Period. 7-19

Figure 7-13. Extent of Transport of Iodine-129 (K_d = 0.2 mL/g for Sand-Dominated Units) in the Vadose Zone at the End of the 1,000-Year Compliance Period. 7-20

Figure 7-14. Extent of Transport of Uranium-238 (K_d = 0.6 mL/g for Sand-Dominated Units) in the Vadose Zone at the End of the 1,000-Year Compliance Period. 7-21

Figure 7-15. Maximum Groundwater Concentration of Technetium-99 at All Points of Calculation 100 Meters Downgradient from Waste Management Area C. 7-24

Figure 7-16. Groundwater Concentration of Technetium-99 from Each Source at Point of Calculation 4. 7-25

Figure 7-17. Maximum Groundwater Concentration of Iodine-129 at All Points of Calculation 100 Meters Downgradient from Waste Management Area C. 7-26

Figure 7-18. Groundwater Concentration of Iodine-129 from Each Source at Point of Calculation 4. 7-27

Figure 7-19. Maximum Predicted Groundwater Concentration of Uranium-238 at All Points of Calculation 100 Meters Downgradient from Waste Management Area C. 7-28

Figure 7-20. Groundwater Concentration of Uranium-238 According to Each Source at Point of Calculation 3 Where the Maximum Concentration Occurs 100 Meters Downgradient from Waste Management Area C. 7-29

Figure 7-21. Maximum Calculated Groundwater Concentration at 100 Meters Downgradient from Waste Management Area C. 7-30

Figure 7-22. Extent of Technetium-99 Plume in Groundwater 500 Years after Closure at the End of the Surface Barrier Design Life. 7-31

Figure 7-23. Extent of Technetium-99 Plume in Groundwater 1,000 Years after Closure at the End of the Compliance Time Frame. 7-32

Figure 7-24. Extent of Technetium-99 Plume in Groundwater 1,570 Years after Closure at the Time of the Maximum Concentration at the Point of Compliance. 7-33

Figure 7-25. Technetium 99 Concentration Breakthrough Curves in Groundwater after Closure at Different Points of Calculation and Downgradient Locations. 7-34

Figure 7-26. Results and Regression Lines Associated with the Vadose Leachate Flux to Groundwater for the Base Case Evaluation of Technetium-99. 7-36

Figure 7-27. Air Concentration for Volatiles at Receptor Location in pCi/L. 7-37

Figure 7-28. Radon Flux at Surface of Waste Management Area C. 7-38

Figure 7-29. Groundwater Pathway Dose (mrem/yr) as a Function of Time for All Points of Calculation at the 100 Meters Compliance Distance. 7-39

Figure 7-30. All-Pathways Dose Results that Includes Air and Groundwater Pathway Contributions at the Maximum Point of Concentration. 7-40

Figure 7-31. Results of the Groundwater Pathway Dose Analysis at the Maximum Point of Concentration. 7-41

Figure 7-32. Results of the Air Pathway Dose Analysis. 7-43

Figure 8-1. Cumulative Distribution Function of Normalized Inventory of Technetium-99 for Retrieved Tanks, and the Average Cumulative Distribution Function. 8-12

Figure 8-2. Cumulative Distribution Function of Normalized Inventory of Various Analytes for the Retrieved Tanks along with the Average Cumulative Distribution Function. 8-15

Figure 8-3. Cumulative Distribution Function of Normalized Residual Volume for the Retrieved Tanks along with the Average Cumulative Distribution Function. 8-25

Figure 8-4. Fitted Log-Normal Distribution to the Saturated Hydraulic Conductivity Dataset Used for H2 Unit. 8-26

Figure 8-5. Fitted Log-Normal Distribution to the van Genuchten "Alpha" Parameter Dataset Used for H2 Unit. 8-27

Figure 8-6. Fitted Log-Normal Distribution to the van Genuchten "*n*" Parameter Dataset Used for H2 Unit. 8-27

Figure 8-7. 200 Realizations of Unsaturated Hydraulic Conductivity as a Function of Matric Potential for H2 Unit. Red line indicates the Composite curve used in the Base Case. 8-28

Figure 8-8. 200 Realizations of Soil-Moisture as a Function of Matric Potential for H2 Unit. Red line indicates the Composite curve used in the Base Case. 8-29

Figure 8-9. Fitted Log-Normal Distribution to the Saturated Hydraulic Conductivity Dataset Used for H1/H3 Units. 8-31

Figure 8-10. Fitted Log-Normal Distribution to the van Genuchten "Alpha" Parameter Dataset Used for H1/H3 Units. 8-32

Figure 8-11. Fitted Log-Normal Distribution to the van Genuchten "*n*" Parameter Dataset Used for H1/H3 Units. 8-32

Figure 8-12. 200 Realizations of Unsaturated Hydraulic Conductivity as a Function of Matric Potential for H1/H3 Units. Red line indicates the Composite curve used in the Base Case. 8-33

Figure 8-13. 200 Realizations of Soil-Moisture as a Function of Matric Potential for H1/H3 Units. Red line indicates the Composite curve used in the Base Case. 8-35

Figure 8-14. Cumulative Distribution Function of Pore Water Velocity from 200 Realizations for the H2 Unit. 8-39

Figure 8-15. Cumulative Distribution Function of Pore Water Velocity from 200 Realizations for the H1/H3 Unit. 8-40

Figure 8-16. Cumulative Distribution Function of Pore Water Velocity from 200 Realizations for the Backfill Unit. 8-41

Figure 8-17. Normalized Darcy Flux for H1 Unit (Node 66) for 100-Series Representative Column during (a) Early Post-Closure Period (b) Late Post-Closure Period. 8-45

Figure 8-18. Normalized Darcy Flux for H2 and H3 Units for 100-Series Representative Column during (a) Early Post-Closure Period (b) Late Post-Closure Period. 8-46

Figure 8-19. Normalized Moisture Content for H1 Unit (Node 66) for 100-Series Representative Column during (a) Early Post-Closure Period (b) Late Post-Closure Period. 8-47

Figure 8-20. Normalized Moisture Content for H2 and H3 Units for 100-Series Representative Column during (a) Early Post-Closure Period (b) Late Post-Closure Period. 8-48

Figure 8-21. Comparison between Darcy Flux Calculated Using Regression Equation and that Obtained from Three-Dimensional Subsurface Transport Over Multiple Phases Based Model Simulation for the 5th Percentile Hydraulic Property Case for (a) H1 Unit under 100-Series Tank (Node 66); (b) H2 Unit under 100-Series Tank (Node 47); (c) H1 Unit under 200-Series Tank (Node 66); and (d) H2 Unit under 200-Series Tank (Node 43). 8-53

Figure 8-22. All-Pathway Mean Dose Calculation Results Based on 300 Realizations. 8-57

Figure 8-23. Uncertainty in Groundwater Pathway Dose Based on 300 Realizations. 8-58

Figure 8-24. Selected Realizations for Groundwater Pathway Dose Analysis. 8-59

Figure 8-25. Scatter Plots of Selected Uncertain Parameters Against Groundwater Pathway Dose at 3,400 Years after Closure. 8-64

Figure 8-26. Peak Dose Values from Groundwater Pathway for 300 Realizations. 8-65

Figure 8-27. Scatter Plots of Selected Uncertain Parameters Against Peak Dose for Groundwater Pathway for 300 Realizations. 8-67

Figure 8-28. Uncertainty in Atmospheric Pathway Dose Based on 300 Realizations. 8-69

Figure 8-29. Scatter Plot of Selected Uncertain Parameters Against the Atmospheric Pathway Dose at Early Time Period (2 Years after Closure). 8-72

Figure 8-30. Scatter Plots of Selected Uncertain Parameters Against the Atmospheric Pathway Dose at Intermediate Time Period (100 Years after Closure). 8-74

Figure 8-31. Scatter Plots of Selected Uncertain Parameters Against the Atmospheric Pathway Dose at Late Time Period (1,000 Years after Closure). 8-75

Figure 8-32. Statistical Stability Analysis with Different Number of Realizations, Comparing (a) Mean, (b) Median, and (c) 95th Percentile Values of the Groundwater Pathway Dose. 8-76

Figure 8-33. Confidence Limits on the Mean Effective Groundwater Pathway Dose. 8-79

Figure 8-34. Recharge (Net Infiltration) Sensitivity Analysis Results of the Technetium-99 Concentration in Groundwater for the Minimum (inf01) Post-Design Life Value. 8-85

Figure 8-35. Recharge (Net Infiltration) Sensitivity Analysis Results of the Technetium-99 Concentration in Groundwater for the Maximum (inf02) Post-Design Life Value. 8-86

Figure 8-36. Comparison of Recharge (Net Infiltration) Sensitivity Analysis Results of the Technetium-99 Concentration in Groundwater for the Base Case, Minimum (inf01), and Maximum (inf02) Post-Design Life Values. 8-87

Figure 8-37. Aquifer Property Sensitivity Analysis Results of the Technetium-99 Concentration in Groundwater for the 5th Percentile (gwp01) Hydraulic Conductivity Values. 8-89

Figure 8-38. Aquifer Property Sensitivity Analysis Results of the Technetium-99 Concentration in Groundwater for the 95th Percentile (gwp03) Hydraulic Conductivity Values. 8-90

Figure 8-39. Comparison of the Aquifer Property Sensitivity Analysis Results of the Technetium-99 Concentration in Groundwater for the Base Case, 5th Percentile (gwp01), and 95th Percentile (gwp03) Hydraulic Conductivity Values at Point of Calculation 4. 8-91

Figure 8-40. Vadose Zone Property Sensitivity Analysis Results of the Technetium-99 Concentration in Groundwater for the 5th (vzp01) Percentile Hydraulic Parameter Values. 8-92

Figure 8-41. Vadose Zone Property Sensitivity Analysis Results of the Technetium-99 Concentration in Groundwater for the Median (vzp02) Percentile Hydraulic Parameter Values. 8-93

Figure 8-42. Vadose Zone Property Sensitivity Analysis Results of the Technetium-99 Concentration in Groundwater for the 95th (vzp03) Percentile Hydraulic Parameter Values. 8-94

Figure 8-43. Comparison of Vadose Zone Property Sensitivity Analysis Results of the Technetium-99 Concentration in Groundwater for the Base Case, 5th (vzp01), Median (vzp02), and 95th Percentile (vzp03) Hydraulic Parameter Values. 8-95

Figure 8-44. Alternative Geologic Model Evaluation Results of the Technetium-99 Concentration in Groundwater for the Alternative Geologic Model (vzp04) Geologic Conceptualization. 8-97

Figure 8-45. Alternative Geologic Model Evaluation Results of the Technetium-99 Concentration in Groundwater for the Hypothesized Clastic Dike (vzp05) Geologic Conceptualization. 8-98

Figure 8-46. Comparison of the Results of the Technetium-99 Concentration in Groundwater for the Alternative Geologic Model (vzp04) and the Hypothesized Clastic Dike (vzp05) Geologic Conceptualizations. 8-99

Figure 8-47. Comparison of Base Case and INV1 Case (a) Technetium-99 Concentration at 100 meter Boundary (b) Technetium-99 Release to Vadose Zone from Tank 241-C-105. 8-101

Figure 8-48. Comparison of Base Case and GRT1, GRT2, GRT3, GRT4 Case (a) Technetium-99 Concentration at 100 meter Boundary (b) Technetium-99 Release to Vadose Zone from Tank 241-C-105. 8-103

Figure 8-49. Comparison of Base Case and RLS1 Case (a) Technetium-99 Concentration at 100 meter Boundary (b) Technetium-99 Release to Vadose Zone from Tank 241-C-105. 8-104

Figure 8-50. Comparison of Base Case and RLS1 Case for Uranium-238 Concentration at 100 meter Boundary. 8-106

Figure 8-51. Comparison of Base Case and DIF1, DIF2, DIF3 Case (a) Technetium-99 Concentration at 100 meter Boundary (b) Technetium-99 Release to Vadose Zone from Tank 241-C-105. 8-108

Figure 8-52. Sensitivity Case Showing the Results of Peak Groundwater Pathway Dose Calculations. 8-109

Figure 9-1. Sequence of Events Necessary for Inadvertent Human Intrusion at Waste Management Area C. 9-5

Figure 9-2. Exposure Pathways Considered in the Inadvertent Intruder Acute Well Driller Scenario. 9-7

Figure 9-3. Exposure Pathways Considered for the Inadvertent Intruder Chronic Rural Pasture Exposure Scenario. 9-12

Figure 9-4. Exposure Pathways Considered in the Inadvertent Intruder Chronic Suburban Garden Exposure Scenario. 9-17

Figure 9-5. Exposure Pathways Considered for the Inadvertent Intruder Chronic Commercial Farm Exposure Scenario. 9-22

Figure 9-6. Effective Dose for the Well Driller Acute Exposure Scenario. 9-27

Figure 9-7. Effective Dose for the Well Driller Acute Exposure Scenario for (a) Tank 241-C-301 and (b) Pipeline Residual Waste. 9-28

Figure 9-8. Effective Dose for the Rural Pasture Chronic Exposure Scenario. 9-29

Figure 9-9. Effective Dose for the Rural Pasture Chronic Exposure Scenario for (a) Tank 241-C-301 and (b) Pipeline Residual Waste. 9-30

Figure 9-10. Effective Dose for the Suburban Garden Chronic Exposure Scenario. 9-31

Figure 9-11. Effective Dose for the Suburban Garden Chronic Exposure Scenario for (a) Tank 241-C-301 and (b) Pipeline Residual Waste. 9-32

Figure 9-12. Effective Dose for the Commercial Farm Chronic Exposure Scenario. 9-33

Figure 9-13. Effective Dose for the Commercial Farm Chronic Exposure Scenario for (a) Tank 241-C-301 and (b) Pipeline Residual Waste. 9-34

Figure 9-14. Effective Dose for All Three Chronic Exposure Scenarios for (a) Tank 241-C-301 and (b) Pipeline Residual Waste. 9-35

Figure 9-15. Effective Dose for All Three Chronic Exposure Scenarios for a Fully Plugged Cascade Pipeline. 9-36

Figure 11-1. Lifecycle Quality for Environmental Models. 11-5

LIST OF TABLES

Table 1-1. Data Packages Produced as a Part of the Waste Management Area C Performance Assessment Scoping Process. 1-10

Table 1-2. List of Safety Functions for the Performance Assessment of Waste Management Area C. 1-20

Table 2-1. Exposure Scenarios, Performance Objectives and Measures, and Points of Assessment for the Waste Management Area C Performance Assessment. 2-4

Table 3-1. Monthly and Average Annual Temperatures at Hanford Meteorological Station since 2000 (°C). 3-18

Table 3-2. Monthly and Average Annual Precipitation at Hanford Meteorological Station since 2000 (cm). 3-19

Table 3-3. Summary Statistics for Volumetric Moisture Content in the Lithologic Units Underlying Waste Management Area C. 3-96

Table 3-4. Operating Period and Capacities for Waste Management Area C Facilities Included in the Performance Assessment. 3-105

Table 3-5. Single-Shell Tank Retrieval Status at Waste Management Area C as of May 31, 2014. 3-111

Table 3-6. Summary of Design Criteria for the Modified RCRA C Barrier. 3-118

Table 3-7. Standard Best-Basis Inventory Constituents. 3-122

Table 3-8. Primary Chemical Constituents. 3-123

Table 3-9. Primary Radiological Constituents. 3-123

Table 3-10. Waste Types Received into 241-C 100-Series Tanks (1956 through 1978). 3-124

Table 3-11. Waste Types in C-200 Series Tanks. 3-125

Table 3-12. Current Waste Types in 241-C Farm Tanks. 3-125

Table 3-13a. 241-C Tank Farm Residual Inventory Estimates for Retrieved Tanks with Post-Retrieval Sampling. 3-127

Table 3-13b. 241-C Tank Farm Residual Inventory Estimates for Retrieved Tanks with Post-Retrieval Sampling. 3-131

Table 3-14a. 241-C Tank Farm Residual Inventory Estimates for Tanks Undergoing Retrieval. 3-133

Table 3-14b. 241-C Tank Farm Residual Inventory Estimates for Tanks Undergoing Retrieval. 3-135

Table 3-15a. 241-C Tank Farm Residual Inventory Estimates for Ancillary Equipment. 3-136

Table 3-15b. 241-C Tank Farm Residual Inventory Estimates for Ancillary Equipment. 3-138

Table 3-16a. 241-C Tank Farm Residual Inventory 95% Confidence Interval Estimates for Retrieved Tanks with Post-Retrieval Sampling. 3-139

Table 3-16b. 241-C Tank Farm Residual Inventory 95% Confidence Interval Estimates for Retrieved Tanks with Post-Retrieval Sampling. 3-142

Table 3-17a. 241-C Tank Farm Residual Inventory Lower Bound and Upper Bound Estimates for Tanks Undergoing Retrieval. 3-144

Table 3-17b. 241-C Tank Farm Residual Inventory Lower Bound and Upper Bound Estimates for Tanks Undergoing Retrieval. 3-146

Table 3-18. Inventory Uncertainties. 3-148

Table 3-19. 241-C Tank Farm Post-Retrieval Waste Volume Estimates (cubic feet). 3-149

Table 3-20. 241-C Tank Farm Post-Retrieval Waste Volume Estimates (cubic feet). 3-150

Table 3-21. Sample-Based Template Waste Type Groups for 241-C Tank Farm. 3-151

Table 3-22. Comparison of Hanford Tank Waste Operations Simulator Pre-Retrieval Concentration Estimates for Tank 241-C-103 Residuals with Post-Retrieval Sample Results. 3-152

Table 4-1. List of Radionuclides Considered for the Performance Assessment. 4-3

Table 4-2. List of Radionuclides Screened from the Performance Assessment with the Rationale for their Elimination. 4-5

Table 4-3. Estimated Inventory of Radionuclides (in Curies) at Closure of Waste Management Area C (Decay Corrected to January 1, 2020) Used in the Performance Assessment Calculation. 4-7

Table 5-1. Average Composition (µg/g dry weight) for Selected Elements, Primary Contaminants of Interest, and Anions in Bulk Residual Waste from Some Waste Management Area C Tanks. 5-4

Table 5-2. Solid Phases Identified in Tank Residual Waste Samples. 5-5

Table 5-3. Percentages of Total Uranium and Technetium-99 Leached from Tanks 241-C-202, 241-C-203, and 241-C-103 Residual Wastes during the Single-Pass Flow-Through Experiments. 5-11

Table 6-1. Characteristics of Concrete Cores from Aboveground Structures at the Hanford Site. 6-27

Table 6-2. Bounding Depth of Carbonation for Buried Concrete Calculated For Different Exposure Times Under Hanford-Specific Conditions. 6-28

Table 6-3. Timeline Considered for Representing the Evolution of Waste Management Area C. 6-32

Table 6-4. Characterisitics of Concrete Specimens Used in Sediment-Concrete Half-Cell Experiments Along with Derived Effective Diffusion Coefficient of Technetium-99 for the Concrete. 6-61

Table 6-5. K_d Values (mL/g) for Grout/Concrete Used for Waste Management Area C Performance Assessment. 6-64

Table 6-6. Base Case Recharge Rate (Net Infiltration) Estimates for Surface Conditions during the Pre-Construction, Operational, and Post-Closure Periods. 6-90

Table 6-7. Composite van Genuchten-Mualem Parameters for Various Strata at the Waste Management Area C Site Used in the Base Case Evaluations of Alternative Geologic Models I and II. 6-91

Table 6-8. Effective Bulk Density ($E[\rho_b]$, g/cm^3) Estimates for Various Strata at Waste Management Area C Used in the Base Case Evaluations of Alternative Geologic Models I and II. 6-92

Table 6-9. Macrodispersity Estimates for Various Strata at Waste Management Area C Used in the Base Case Evaluations of Alternative Geologic Models I and II. 6-92

Table 6-10. Base Case Soil Hydraulic Properties for Aquifer Soil Type Used for Base Case at Waste Management Area C. 6-95

Table 6-11. Distribution Coefficients (K_d) Values Used to Approximate the Transport of the Radionuclides in the Base Case. 6-97

Table 6-12. Summary of Key Elements and Base Case Parameters Associated with Site-Specific Model Components for Waste Management Area C (The basis for the elements and parameter selection provided in the individual model components sections). 6-99

Table 6-13. Maximum Net Infiltration (Recharge) Estimates Developed for the Uncertainty Analysis for Pre-Construction Period, Operational Period, and Post-Closure of Waste Management Area C (Section 8.1.4.1). 6-101

Table 6-14. van Genuchten-Mualem Parameters Associated with the Maximum Pore Water Velocity Based on the Cumulative Distribution Functions in Section 8.1.4. 6-101

Table 6-15. Hydrostratigraphic Unit Thickness Under the Tanks Taken From the Three-Dimensional Subsurface Transport Over Multiple Phases (STOMP©)-Based Model. 6-106

Table 6-16. Vertical Grid Discretization and Flow Field for the System-Level Model. 6-111

Table 6-17. Henry's Law Constants. 6-123

Table 6-18. Diffusion Coefficients in Air at 20 °C and 1 Atm. 6-127

Table 6-19. Best Estimate K_d (mL/g) for Grout Material. 6-129

Table 6-20. Wind Speed Observed Above the Hanford Site and Corresponding Pasquill Class for a Moderate Solar Radiation. 6-131

Table 6-21. Maximum Penetration Depths for Biota at the Hanford Site. 6-134

Table 6-22. Scenario-Dependent Exposure Parameters for the All-Pathways Reference Person Scenario. 6-137

Table 6-23. Bioconcentration Factors for the All-Pathways Reference Person Scenario. 6-139

Table 6-24. Radionuclide-Specific Shielding Factors. 6-141

Table 6-25. Radionuclide-Specific Dose Conversion Factors. 6-144

Table 6-26. Parameters Used to Calculate the Tritium Concentration in Crops. 6-147

Table 6-27. Parameters for Tritium Concentration Calculation in Animal Products. 6-148

Table 6-28. Summary of Intake Rates for All-Pathways Reference Person. 6-149

Table 6-29. Dose-Specific Parameters for the Atmospheric Pathway. 6-155

Table 7-1. First-Arrival Time (in Calendar Year) of Radionuclides for Various K_d Values Based on Screening Analysis Using Subsurface Transport Over Multiple Phases. 7-8

Table 7-2. Radionuclides that Arrive at the Water Table within the 1,000-Year Compliance and 10,000-Year Sensitivity and Uncertainty Time Frame Based on the Screening Analysis Conducted Using Subsurface Transport Over Multiple Phases. 7-9

Table 7-3. Summary of Base Case Peak Groundwater Concentrations and Arrival Times for Selected Radionuclides. 7-18

Table 7-4. Summary of Base Case Peak Groundwater Concentrations and Arrival Times for Selected Radionuclides. 7-22

Table 7-5. Summary of Peak Doses (mrem/yr) for the Groundwater Pathway and the Time of Occurrence for All Radionuclides Giving Nonzero Doses in the Base Case Analysis. 7-42

Table 8-1. Main Uses of Several Common Distribution Functions..... 8-4

Table 8-2. Guidance for Selection of Probability Distribution Function Considering the Data Constraints. 8-6

Table 8-3. Spatial and Temporal Uncertainty in Recharge Rates Considered for Waste Management Area C..... 8-10

Table 8-4. Uncertainty Distributions Developed for H1/H3 Hydraulic Properties. 8-30

Table 8-5. Uncertainty Distributions Developed for Backfill Hydraulic Properties. 8-36

Table 8-6. Uncertainty in K_d Values (mL/g) for Sand As a Triangular Distribution. 8-37

Table 8-7. van Genuchten-Mualem Parameters Corresponding to the Percentiles Selected from the Vertical Pore Water Velocity Cumulative Distribution Functions. 8-43

Table 8-8. Recharge Rate Used in Scaling Flow Field. 8-44

Table 8-9. Example of Normalized Darcy Flux at Calendar Year 2300 from Selected Three-Dimensional STOMP©-Based Model Nodes under Tank 241-C-105 Using 5th Percentile Hydraulic Property..... 8-44

Table 8-10. Regression Equations for Scaling Darcy Flux for 100-Series Tank..... 8-49

Table 8-11. Regression Equations for Scaling Darcy Flux for 200-Series Tank..... 8-49

Table 8-12. Regression Equations for Scaling Volumetric Moisture Content. 8-50

Table 8-13. Uncertain Parameters Important to Groundwater Pathway at (a) End of Compliance Time Period (1,000 Years after Closure) and (b) Time of Peak Dose (about 3,400 Years after Closure). 8-63

Table 8-14. Uncertain Parameters Important to Atmospheric Pathway Dose at Various Times. 8-71

Table 8-15. Summary of Sensitivity Cases..... 8-80

Table 8-16. Recharge Sensitivity Evaluation..... 8-83

Table 8-17. Aquifer Property Sensitivity Evaluation. 8-88

Table 8-18. Vadose Zone Sensitivity Evaluation. 8-96

Table 8-19. Inventory Estimate Sensitivity Evaluation. 8-100

Table 8-20. Grout Flow Safety Function Sensitivity Evaluation. 8-102

Table 8-21. Residual Chemistry Safety Function. 8-105

Table 8-22. Tank Flow Safety Function Sensitivity Evaluation. 8-107

Table 9-1. Descriptions of the Inadvertent Intruder Scenarios Evaluated in the Waste Management Area C Performance Assessment. 9-2

Table 9-2. Parameters Common to the Inadvertent Intruder Scenarios. 9-3

Table 9-3. Exposure Parameters for the Acute Well Driller Exposure Scenario. 9-8

Table 9-4. Exposure Parameters for the Chronic Rural Pasture Exposure Scenario. 9-13

Table 9-5. Exposure Parameters for the Chronic Suburban Garden Exposure Scenario. 9-18

Table 9-6. Exposure Parameters for the Chronic Commercial Farm Exposure Scenario. 9-23

Table 9-7. Peak Effective Dose for the Inadvertent Intruder Scenarios for All Residual Waste Sources. 9-25

Table 9-8. Relative Fraction of Pathway Contributions to the Inadvertent Intruder Dose for Pipeline at 100 Years After Closure. 9-26

Table 10-1. Summary of All-Pathways Analysis Results for the Base Case. 10-2

Table 10-2. Summary of Results for the Air Pathway. 10-3

Table 10-3. Summary of Radon Flux Analyses. 10-3

Table 10-4. Summary of Inadvertent Human Intrusion Analyses for Intrusion into Ancillary Equipment. 10-4

Table 10-5. Comparison of Peak Groundwater Pathway Results to Groundwater Protection Criteria. 10-5

Table 10-6. Summary of Maximum Results from Sensitivity Cases. 10-7

Table 10-7. Summary of Relevant Results from the Probabilistic Uncertainty Analysis of Groundwater Pathway. 10-8

LIST OF TERMS

Acronym or Abbreviation

1-D	one-dimensional
2-D	two-dimensional
3-D	three-dimensional
AEA	Atomic Energy Act of 1954
ALARA	As Low As Reasonably Achievable
ARAR	Applicable or relevant and appropriate requirement
ASR	alkali-silica reaction
BBI	Best-Basis Inventory
bgs	below ground surface
BP	before present
BRA	Baseline Risk Assessment
CA	composite analysis
CAD	computer-aided design
CCMS	camera/CAD modeling system
CCU	Cold Creek unit
CDF	cumulative distribution function
CERCLA	Comprehensive Environmental Response, Compensation, and Liability Act of 1980
CFR	Code of Federal Regulations
CHPRC	CH2M HILL Plateau Remediation Company
CMS	corrective measures study
COPC	constituent of potential concern
CPGWM	Central Plateau Groundwater Model

CRBG	Columbia River Basalt Group
C-S-H	calcium silicate hydrate
D&D	Demolition and Decommissioning
DAS	Disposal Authorization Statement
DCF	dose conversion factor
DDI	distilled de-ionized
DI	deionized
DKPRO	Radioactive Decay (DK) and Processing (PRO) code
DOE	U.S. Department of Energy
DOE-ORP	U.S. Department of Energy, Office of River Protection
DNFSB	Defense Nuclear Facilities Safety Board
DQO	data quality objectives
DWS	drinking water standard
Ecology	State of Washington Department of Ecology
EDS	energy dispersive spectroscopy
EHM	equivalent homogeneous media
EIS	Environmental Impact Statement
EMCF	Environmental Model Calculation File
EMMA	Environmental Model Management Archive
EMSL	Environmental and Molecular Sciences Laboratory
EPA	U.S. Environmental Protection Agency
ERDF	Environmental Restoration Disposal Facility
ETF	Effluent Treatment Facility
FEPs	Features, Events, and Processes

FFTF	Fast Flux Test Facility
FLTF	Field Lysimeter Test Facility
FR	Federal Register
H3/CCu/RF	H3, CCU and Ringold Formation
HCP	Final Hanford Comprehensive Land-Use Plan
HDW	Hanford Defined Waste (Model)
HEIS	Hanford Environmental Information System
Hf	Hanford formation
HFFACO	Hanford Federal Facility Agreement and Consent Order
HFSUWG	Hanford Future Site Uses Working Group
HISI	Hanford Information Systems Inventory
HLAN	Hanford local area network
HLW	high-level waste
HMS	Hanford Meteorological Station
HSU	hydrostratigraphic unit
HTWOS	Hanford Tank Waste Operations Simulator
HWIS	Hanford Well Information System
HWMA	Hazardous Waste Management Act
ICRP	International Commission on Radiological Protection
IDF	Integrated Disposal Facility
ILAW	immobilized low-activity waste
IPA	Appendix I Performance Assessment
K-U-T	potassium, uranium, thorium
LANL	Los Alamos National Laboratory

LERF	Liquid Effluent Retention Facility
LFRG	Low-Level Waste Disposal Facility Federal Review Group
LHS	Latin hypercube sampling
LIGO	Laser Interferometer Gravitational Wave Observatory
LLW	low-level waste
MCL	maximum contaminant level
MMI	Modified Mercalli Intensity (scale)
NAVD88	North American Vertical Datum of 1988
NCRP	National Council on Radiation Protection
NEPA	National Environmental Policy Act of 1969
NRC	U.S. Nuclear Regulatory Commission
NRIZ	normal residential intrusion zone
OECD	Organisation for Economic Co-operation and Development
OFM	Office of Financial Management
ORIGEN2	Oak Ridge Isotope Generation and Depletion Code 2
OU	operable unit
PA	performance assessment
PFP	Plutonium Finishing Plant
PHB	Prototype Hanford Barrier
PNNL	Pacific Northwest National Laboratory
PoCal	Point of Calculation
PUREX	Plutonium Uranium Extraction (facility)
RCA	RCRA Closure Analysis
RCC	Retrieval Completion Certification

RCRA	Resource Conservation and Recovery Act of 1976
RCW	Revised Code of Washington
REDOX	Reduction-Oxidation (facility)
RETC	RETention Curve
RFI	RCRA facility investigation
RI/FS	remedial investigation/feasibility study
ROD	Record of Decision
RPPDF	River Protection Project Disposal Facility
RSD	relative standard deviation
SALDS	State-Approved Land Disposal Site
SD	standard deviation
SEM	scanning electron microscopy
SGE	Surface Geophysical Exploration
SI	saturation index
SNF	spent nuclear fuel
SPFT	single-pass flow-through
SST	single-shell tank
SSTIP	Single-Shell Tank Integrity Project
SST PA	DOE/ORP-2005-01, Initial Single-Shell Tank System Performance Assessment for the Hanford Site
STOMP	Subsurface Transport Over Multiple Phases (computer code)
TC&WM	Tank Closure and Waste Management
TEDF	Treated Effluent Disposal Facility
TIC	Total inorganic carbon
TOC	Total organic carbon

TSD	treatment, storage and disposal
TWINS	Tank Waste Information Network System
TWRS	Tank Waste Remediation System
UCL	upper confidence limit
UPR	unplanned release
USACE	U.S. Army Corps of Engineers
UST	underground storage tank
WAC	Washington Administrative Code
WIR	waste incidental to reprocessing
WMA	Waste Management Area
WRPS	Washington River Protection Solutions, LLC
WTP	Waste Treatment Plant

Waste Types

1C	First cycle $BiPO_4$ decontamination waste
1CFeCN	Ferrocyanide sludge from in-plant scavenging of T-Plant 1C waste (without coating waste)
2C	Second cycle $BiPO_4$ decontamination waste
AR	Water washed PUREX sludge (1967-1976)
$BiPO_4$	bismuth phosphate
BL	B Plant strontium processing wastes and miscellaneous wastes
BNW	research waste from Battelle Northwest
CW	cladding (coating) waste from Plutonium Uranium Extraction (PUREX) or Reduction Oxidation (REDOX) Plants
CWP1	PUREX aluminum cladding waste (1956-1960)

CWP2	PUREX aluminum cladding waste (1961-1972)
CWR1	Reduction-Oxidation (S Plant) aluminum cladding waste
CWZr1	PUREX/REDOX zirconium cladding waste (1968-1972)
HS	201-C Hot Semiworks waste (1961-1968)
IX	cesium denuded waste from ion exchange process in B Plant
MW1	$BiPO_4$ Metal Waste (1944-1949)
OWW3	PUREX organic wash waste (1968-1972)
PFeCN	Ferrocyanide sludge from tributyl phosphate (TBP) in-plant scavenged supernate and co-disposed TBP sludge
PSN	PUREX high-level waste (HLW) supernate
PSS	PUREX Sludge Supernate derived from washing PUREX HLW sludges in 244-AR Vault or 241-A and 241-AX tanks
RSN	REDOX HLW Supernate
SRR	Strontium recovery waste (1969-1985)
TBP	tributyl phosphate
TBP (UR)	Tributyl phosphate/Uranium Recovery Waste (1952-1957)
TFeCN	Ferrocyanide waste from 244-CR vault treatment of TBP waste
TH	Thorium process waste from PUREX Plant
TH1	Thoria process waste (1966)
TH2	Thoria process waste (1970)

1.0 INTRODUCTION

The U.S. Department of Energy, Office of River Protection (DOE-ORP) is pursuing closure on the single-shell tank (SST) Waste Management Area (WMA) C under Federal requirements and forthcoming State-approved closure plans and permits in accordance with the Hanford Federal Facility Agreement and Consent Order (HFFACO) (Ecology et al. 1989), Action Plan, Appendix I. Waste Management Area C is located in the 200 East Area of the Central Plateau at Hanford and is one of 12 tank farms grouped into 7 WMAs (A-AX, B-BX-BY, C, S-SX, T, TX-TY, and U) containing 149 SSTs and ancillary equipment built from 1943 to 1964 (see Figure 1-1).

This document provides the DOE O 435.1, Radioactive Waste Management performance assessment (PA) (see section 1.1 for PA definition) analysis for WMA C. The PA is required by DOE O 435.1 for closing U.S. Department of Energy (DOE)-operated facilities that will manage generated radioactive waste as low-level waste (LLW) which was produced during departmental activities. The fundamental objective of this PA is to support the closure of tanks and ancillary equipment within WMA C that will contain residual levels of radioactive wastes left at closure.

The potential radiological dose to receptors from releases from a closed facility like WMA C is typically evaluated with a PA that examines the following: 1) the release of radionuclides from that facility, 2) the transport of those radionuclides through the environment, and 3) the exposure to humans to environmental concentration levels of constituents of potential concern (COPCs) that are released. In addition, the analysis also evaluates the exposure to potential receptors who inadvertently intrude into the residual waste left in the facility.

The PA process provides the technical basis for subsequent decision documents to demonstrate compliance with the performance objectives outlined in DOE G 435.1-1, Implementation Guide for Use with DOE M 435.1-1, Radioactive Waste Management Manual, Chapter IV – Low-Level Waste Requirements. The WMA C PA project made use of an inter-agency scoping process during the development/planning phases of the PA effort, which resulted in a collaborative understanding of the WMA C PA modeling approaches and assumptions.

This document follows as much as possible the general outline and content guidelines that are identified in the Draft Radioactive Waste Management Disposal Authorization Statement Technical Basis Documentation (DOE-STD-XXX) and those presented in the June 2014 working session. The purpose of this section, Section 1 Introduction, is to provide a general overview of the PA process for WMA C including high-level assumptions, the relationship of this PA with previous PA documents, and background information on the WMA C facility and regulatory requirements. This information is presented in the following subsections:

- General Approach (Section 1.1)
- Regulatory Context (Section 1.2)
- General Facility Description (Section 1.3)

- A Safety Concept and Safety Functions for Closed Waste Management Area C (Section 1.4)
- Land Use and Institutional Control Assumptions (Section 1.5)
- Waste Management Area C History and Plan for Closure (Section 1.6)
- Previous Performance Assessments and Overlapping Analyses (Section 1.7)
- Summary of Key Assessment Assumptions (Section 1.8).

The remainder of the document is comprised of the following sections:

- Assessment Context (Section 2)
- Site and Facility Characteristics (Section 3)
- Screening Approaches (Section 4)
- Waste Characteristics (Section 5)
- Analysis of Performance (Section 6)
- Results of Analysis (Section 7)
- Uncertainty and Sensitivity Analysis (Section 8)
- Inadvertent Intruder Analysis (Section 9)
- Performance Evaluation and Interpretation of Results (Section 10)
- Quality Assurance (Section 11)
- Preparers (Section 12)
- References (Section 13).

Additional information supporting this document is contained in Appendices A through H.

1.1 GENERAL APPROACH

A Performance Assessment assesses the long-term fate and transport of contamination in the environment and provides DOE with a reasonable assurance that in this case, the residual radioactive waste left in tanks and ancillary equipment within the closed WMA C will meet defined performance objectives and measures for the protection of human health and the environment into the future.

This PA will satisfy part of the requirements outlined in Appendix I of the HFFACO. Appendix I of the HFFACO Action Plan contains language that broadened the scope of a "performance assessment." Section 2.5 of HFFACO Action Plan Appendix I states:

> "Ecology, as the lead agency for SST system closure, EPA, and DOE have elected to develop and maintain as part of the SST system closure plan <u>one performance assessment</u> for the purposes of evaluating whether SST system closure conditions are protective of human health and the environment for <u>all contaminants of</u>

> concern, both radiological and nonradiological. DOE intends that this performance assessment (PA) will document by reference relevant performance requirements defined by RCRA, HWMA, Clean Water Act, Safe Drinking Water Act, and the Atomic Energy Act of 1954 (AEA) and any other performance requirements that might be ARARs under CERCLA. The PA is of larger scope than a risk assessment required solely for nonradiological contaminants. The PA is expected to provide a single source of information that DOE can use to satisfy potentially duplicative functional and/or documentation requirements. A PA will be developed for each WMA and will incorporate the latest information available. These PAs will be approved by Ecology and DOE pursuant to their respective authorities. For Ecology approval means incorporation by reference, into the Site-Wide Permit through the closure plans.
>
> As individual components are retrieved or characterized, or other component closure activities are completed, the resulting component characterization information will be incorporated into the WMA PA to determine its relative risk compared to the entire WMA performance. In doing this, the Parties will be able to make interim closure decisions for individual components. Initially, the WMA PA will be based on assumptions and available data describing component characterization information. As each WMA proceeds toward closure, its respective PA will be updated to address all pertinent new results and findings – and will, as a minimum, incorporate the following results as they become available: actual volumes of tank waste residuals left after retrieval, results of leak investigations, new geologic and ancillary equipment waste characterization information, and the results of new barrier and tank residual stabilization and fill performance studies and tests. Final WMA closure decisions will be made after all components are retrieved and/or characterized, and all other component closure activities have been completed and a final WMA PA is completed."

Note: Underlining is added to emphasize key points in the scope of the HFFACO Action Plan Appendix I "performance assessment."

To distinguish between the two terms and avoid confusion, the term "performance assessment" will be used in this document in the following manner:

- The broadened scope of the HFFACO Action Plan Appendix I analysis, which includes non-radiological contaminants, will be referred to as the "Appendix I Performance Assessment" (IPA)

- The simpler "performance assessment" (PA) will refer solely to the DOE O 435.1 definition of performance assessment for radionuclides.

Appendix I of the HFFACO Action Plan describes the waste retrieval and closure process that is to be implemented for the Hanford Site SST system. The four components of the IPA are illustrated in Figure 1-2.

Figure 1-1. Hanford Site Tank Farms.

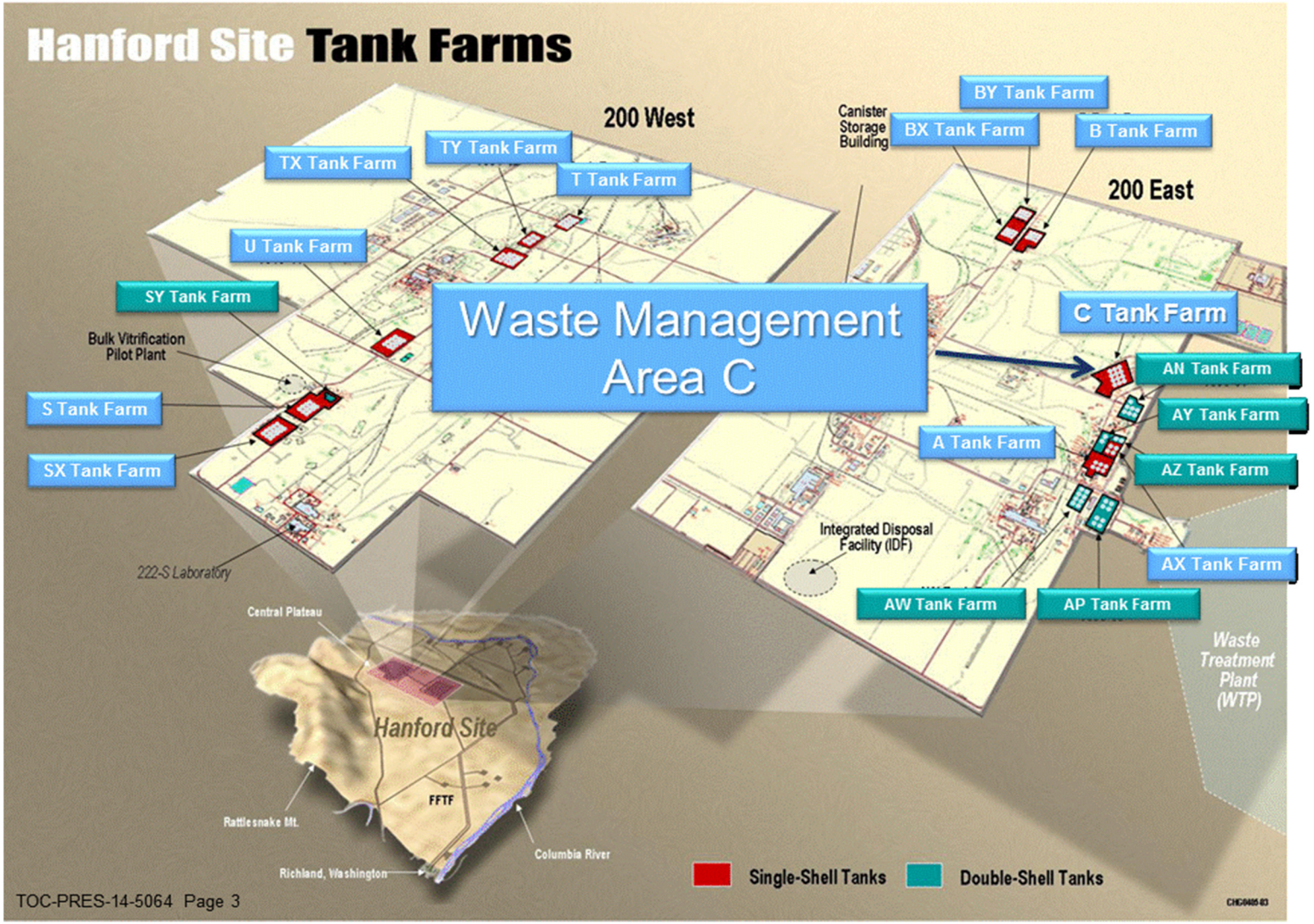

FFTF = Fast Flux Test Facility

Reference: TOC-PRES-14-5064-VA, "Waste Management Area C Performance Assessment (PA) Current Status."

Figure 1-2. The Components of the Appendix I Performance Assessment.

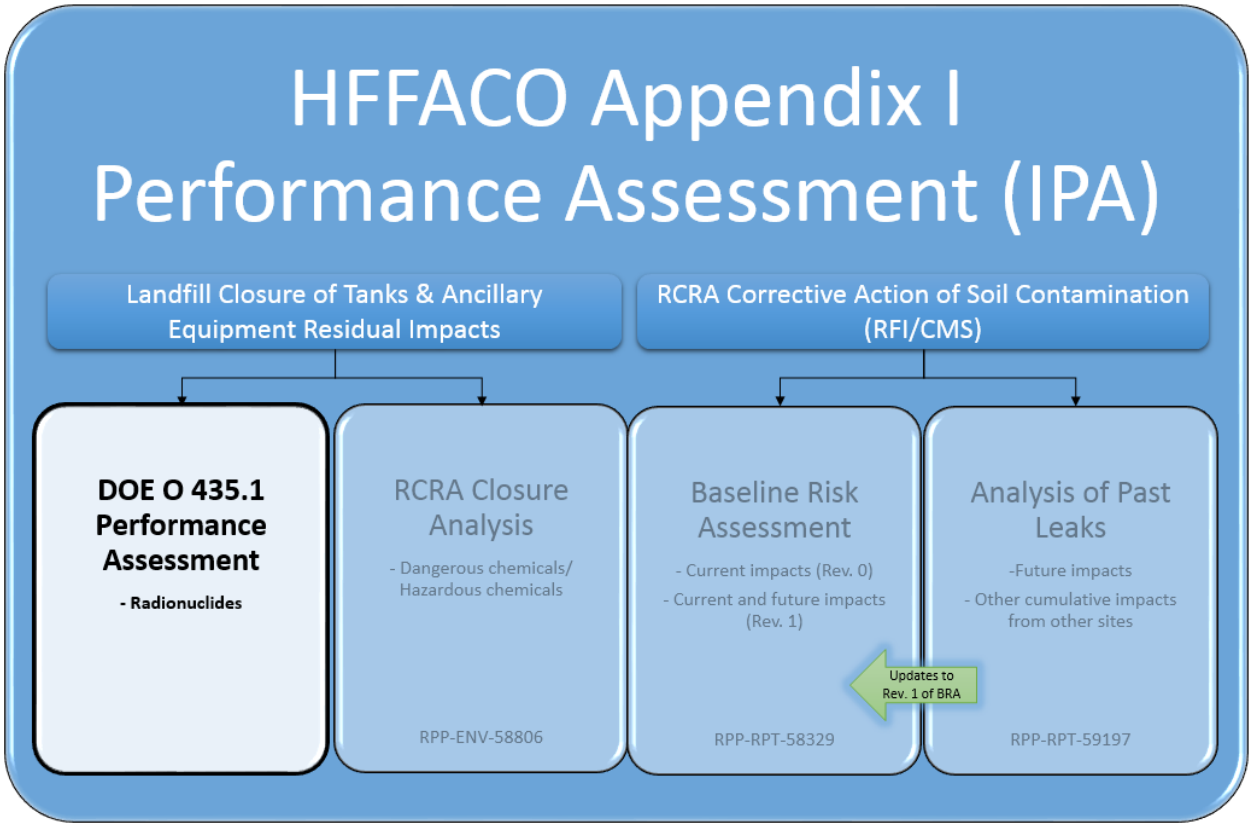

BRA = Baseline Risk Assessment
HFFACO = Hanford Federal Facility Agreement and Consent Order
RCRA = Resource Conservation and Recovery Act of 1976
RFI/CMS = RCRA facility investigation/corrective measures study

References:
DOE O 435.1, Radioactive Waste Management.
RPP-ENV-58806, "RCRA Closure Analysis of Tank Waste Residuals Impacts at Waste Management Area C, Hanford Site, Washington."
RPP-RPT-59197, "Analysis of Past Tank Waste Leaks and Losses in the Vicinity of Waste Management Area C at the Hanford Site, Southeast Washington."
RPP-RPT-58329, "Baseline Risk Assessment for Waste Management Area C."

Closure decisions for the Hanford Site SST system soils will be made through the Resource Conservation and Recovery Act of 1976 (RCRA) corrective action process. The RCRA corrective action component of the IPA is documented in RPP-RPT-58339, "Phase 2 RCRA Facility Investigation Report for Waste Management Area C," Draft A and will contain 1) a baseline risk assessment and 2) an analysis of past leaks.

- **Baseline Risk Assessment** – An evaluation of impacts to human and ecological receptors from both non-radiological and radiological contaminants in soils at WMA C under current condition, in the absence of actions to control or mitigate releases. Following guidance for RCRA Facility Investigation (RFI) and Corrective Measures Studies (CMS), a baseline risk assessment is completed at contaminated waste sites prior to remediation

activities to establish a need for action. Guidance for the conduct of human health and ecological risk assessments are summarized in Sections 3.0 and 4.0 of the initial version of the baseline risk assessment (RPP-RPT-58329, "Baseline Risk Assessment for Waste Management Area C") that was prepared to support an RFI for WMA C (RPP-RPT-58339, Draft A). Revision 1 of this document will address both current and future impacts to human health and the environment.

- **Analysis of Past Leaks** – An evaluation of future impacts to human and ecological receptors from both non-radiological and radiological contaminants in soils at the closed WMA C. This evaluation of future impacts will support updates to the anticipated Revision 1 of the baseline risk assessment (RPP-RPT-58329).

The evaluation of residual waste in tanks and ancillary equipment in support of decisions for closure at WMA C is documented in two documents: 1) a RCRA Closure Analysis, and 2) a DOE O 435.1 PA.

- **RCRA Closure Analysis (RCA)** – An evaluation of hazardous chemicals and dangerous waste residual contaminants in tanks and ancillary equipment at a closed WMA C. This component of the IPA is documented in a companion report, RPP-ENV-58806, "RCRA Closure Analysis of Tank Waste Residuals Impacts at Waste Management Area C, Hanford Site, Washington."

- **DOE O 435.1 PA** – An evaluation of radioactive residual waste contaminants in tanks and ancillary equipment at the closed WMA C. This component of the IPA is the sole focus of this current document.

This PA is limited to analyses of radiological impacts of residual wastes in tanks and ancillary equipment left in the closed WMA C under DOE O 435.1. The types of analysis in the PA required by DOE O 435.1 along with their performance objectives are given in Chapter IV – Low-Level Waste Requirements of DOE M 435.1-1, Radioactive Waste Management Manual and are briefly summarized below.

- **Performance Objective Analyses.** These analyses determine if characteristics of the closed WMA C that control radionuclide releases to the surrounding environment are sufficient to satisfy long-term (1,000 years post-closure) period objectives. Prescribed objectives include dose to humans from groundwater and air contamination (all-pathways 25 mrem/yr limit and a 10 mrem/yr atmospheric release limit) and a radon flux limit (20 pCi/m^2/s). Of these, the groundwater pathway is the most complex, requiring numerical simulations for radionuclide release from the closed WMA C and transport to a downgradient aquifer well. In contrast, the atmospheric release and radon flux analyses can be completed with simpler numerical solutions or semi-analytic solutions, essentially as bounding calculations.

- **Performance Measures Analyses.** These analyses establish two kinds of criteria for WMA C. Criteria 1 includes radionuclide-specific concentration limits quantified with respect to dose limit for inadvertent intruders that receive dose after exhuming waste.

These analyses estimate dose from a set of algebraic equations that calculates the intensity and duration of exposure to the intruder. Criteria 2 includes an analysis that presumes a cause-and-effect relationship between inventory remaining in tanks and ancillary equipment and groundwater contamination levels after release from WMA C and employs the groundwater pathways analyses used for the all-pathways analysis.

- **Other Analyses.** Other analyses include sensitivity/uncertainty, As Low As Reasonably Achievable (ALARA), and biota analyses. Sensitivity and uncertainty analyses are completed to determine plausible ranges of environmental contamination resulting from uncertainty in parameter values and processes considered in the PA and to identify the most important parameters that influence the dose/risk at a designated point of calculation (PoCal). Both deterministic and probabilistic approaches require numerical simulations. The goal of ALARA analysis is attainment of lowest practical dose level after taking into account health and non-health (societal, environmental, technical, economic, and public policy) considerations and showing that closure at WMA C is being conducted in a manner than maintains ALARA releases of radionuclides to the public and the environment. The biota analysis is a calculation of dose to humans through contact with contaminated biota.

The WMA C PA presents a comprehensive, systematic analysis of the long-term impacts of a closed LLW facility in a semi-arid, near-surface environment. In addition to the specific analyses included in the PA itself, the PA will be used to support decisions related to waste incidental to reprocessing (WIR) that will be left at closure within tanks and ancillary equipment. DOE M 435.1-1 Chapter IIB.(2)(a)2. is the second criteria for the WIR evaluation process. This criterion states that such wastes "(w)ill be managed to meet safety requirements comparable to the performance objectives set out in 10 CFR 61 Subpart C, *Performance Objectives*." This PA will be the primary tool used to demonstrate that Title 10, Code of Federal Regulations (CFR), Part 61, "Licensing Requirements for Land Disposal of Radioactive Waste" (10 CFR 61), Subpart C—Performance Objectives, § 61.41, Protection of the General Population from Releases of Radioactivity and § 61.42, Protection of individuals from inadvertent intrusion are met. Further, the PA will be used to develop the site-specific factors related to 10 CFR 61, Subpart D—Technical Requirements for Land Disposal Facilities, § 61.55, Waste classification Class C comparison.

Closure of WMA C will require a WIR determination of the tank residuals, a DOE O 435.1 Tier I Closure Authorization/II Closure Plan submittal, and RCRA Tier 1, 2, and 3 closure plans which will be submitted as permit modifications to the Hanford Sitewide RCRA Permit (WA7 89000 8967, "Hanford Facility Resource Conservation and Recovery Act Permit, Dangerous Waste Portion Revision 8C for the Treatment, Storage, and Disposal of Dangerous Waste") for hazardous waste remaining in the tanks along with soils.

The WIR determination and the decision to landfill close the tanks will be made in accordance with DOE O 435.1 and implemented through DOE M 435.1-1 Administrative Change 2, Section I.2.F.(18) and II.B.(2), which requires consultation and coordination with the Office of Environmental Management through the evaluation process. In practice, this will require the Site Manager to submit the decision document (WIR Decision Evaluation and the DOE O 435.1

Tier I and II Closure Plans) through the Deputy Assistant Secretary for Site Restoration to the Secretary of Energy for approval. The closure of the tanks will also follow a process similar to that governed by the Ronald W. Reagan National Defense Authorization Act for Fiscal Year 2005, Section 3116, which will include consultation with the U.S. Nuclear Regulatory Commission (NRC). This PA report may be updated to incorporate substantive comments received during the NRC consultation. The finalized WMA C PA will form the technical basis for the WIR determination.

In addition, in accordance with the HFFACO, the IPA will be developed to evaluate whether SST system closure conditions are protective of human health and the environment for all contaminants of concern, both radiological and non-radiological. The IPA will include the documents outlined in Figure 1-2 to satisfy relevant DOE O 435.1, RCRA and Comprehensive Environmental Response, Compensation, and Liability Act of 1980 (CERCLA) performance requirements.

The decision to remediate the contaminated soil and groundwater underneath the tank farms will be made in accordance with DOE M 435.1-1 Administrative Change 2 Sections II.U.(2) and I.2.F(5), which require the Site Manager to submit the decision document, such as the Record of Decision (ROD), or any other document that serves as the authorization to dispose, to the Deputy Assistant Secretary for Site Restoration for approval.

Related assessment activities (e.g., safety assessments, risk assessments, engineering evaluations, and cost/design studies) are being evaluated in other documents related to WMA C. Although occupational doses to workers are an important area of concern for facility retrieval and closure operations, they are addressed by regulations and guidance that differ from those used in a long-term human health and environmental impacts analysis. Additionally, this document excludes the potential impacts of chemical toxicity of radiological constituents and non-radiological hazardous constituents that may be present in the residual waste left in a closed WMA C because this is part of the RCRA analysis.

1.1.1 Waste Management Area C Performance Assessment Scoping Process

The foundation of the WMA C IPA was established in a scoping process that was conducted with regulatory agencies and stakeholders between 2009 and 2011. As a part of the scoping process, a series of working sessions were conducted that addressed the following technical topic areas:

- Residual Inventory (Detailed conceptual models and data related to residual waste inventories left in WMA C tanks and ancillary equipment at closure) (May 5-7, 2009)
- Assessment Context/General Conceptual Models (September 1-3, 2009)
- Soil Inventory (Detailed conceptual models and data on waste inventories released to the environment from historical releases during operations) (October 27-29, 2009)

- Engineered System #1 (Detailed conceptual models and data on natural recharge and waste release) (January 26-28, 2010)

- Natural System (Detailed conceptual models and data on vadose zone and groundwater flow and transport) (May 25-27, 2010)

- Engineered System #2 (Continuation discussion of detailed conceptual models, data, and characteristics of the engineered systems) (July 27-29, 2010)

- Exposure Scenarios (Detailed conceptual models and data on human health exposure scenarios) (September 28-30, 2010)

- Vadose Zone and Groundwater Flow and Transport Modeling (Use of numerical and system-level codes and models to support the PA) (January 25-27, 2011)

- Ecological Risk Assessment (Detailed conceptual models and data related to ecosystem risk assessments) (May 17-19, 2011).

Regulatory agency members who participated in the scoping process included representatives from DOE, U.S. Environmental Protection Agency (EPA), NRC, and the State of Washington Department of Ecology (Ecology) as well as their contractors. Other participants in the working sessions include representatives of the tribal nations, representatives of the Hanford Advisory Board, other stakeholders groups, and members of the public.

The results of the WMA C IPA scoping process have been documented in a series of data package reports that were produced in the 2009 to 2011 scoping time frame. These data packages document the outcomes of working sessions held with relevant regulatory agencies and stakeholders. The purpose of these working sessions was to solicit input from the working session participants, and to obtain a common understanding concerning the scope, methods, and data to be used in the HFFACO Appendix I PA for WMA C among the participants. The listing of the current versions of each data package produced in each of the working sessions is summarized in Table 1-1. Following each working session, Ecology provided comments on each data package. Following the comment resolution, the data packages were revised incorporating those comments. Both the comments and resolution to those comments are provided as an appendix to each data package.

Between the development of these data packages and today, updated information has become available for some of the inputs, and new conceptualizations and interpretations of data have been developed. In addition, stakeholders have expressed ideas and concerns that have led to the development of additional conceptual models and sensitivity analysis cases.

Specific areas in which deviations or updates from the prior data packages occurred include the following:

- Tank inventories have been updated for retrieved tanks based on sampling of waste residuals after completion of the retrieval process

- Data on the contaminant-specific release behavior of waste residuals has been used to develop empirical approaches from modeling dissolution of the tank residuals

- Data and modeling have been conducted on degradation of the engineered barrier system to provide an improved basis for the analysis

- Two alternative models of the site stratigraphy have been implemented based on collaboration with stakeholders

- Vadose zone flow properties have been updated to better represent site-specific data

- Aquifer flow properties have been updated to reflect new data and interpretations.

Table 1-1. Data Packages Produced as a Part of the Waste Management Area C Performance Assessment Scoping Process.

Working Session Topical Area	Report Number (Year Published)	Current Revision No.	Title
Residual Inventory	RPP-RPT-42323 (2015)	3	Hanford C-Farm Tank and Ancillary Equipment Residual Waste Inventory Estimates
Assessment Context	RPP-RPT-41918 (2010)	0	Assessment Context for Performance Assessment for Waste in C Tank Farm Facilities after Closure
Soil Inventory	RPP-RPT-42294 (2016)	2	Hanford Waste Management Area C Soil Contamination Inventory Estimates
Engineered System #1	RPP-RPT-44042 (2010)	0	Recharge and Waste Release within Engineered System in Waste Management Area C
Engineered System #2	RPP-RPT-46879 (2011)	2	Corrosion and Structural Degradation within Engineered System in Waste Management Area C
Natural System	RPP-RPT-46088 (2010)	1	Flow and Transport in the Natural System at Waste Management Area C
Exposure Scenarios	RPP-RPT-47479 (2011)	1	Exposure Scenarios for the Waste Management Area C Performance Assessment
Numerical Codes	RPP-RPT-48490 (2011)	1	Technical Approach and Scope for Flow and Contaminant Transport Analysis in the Initial Performance Assessment of Waste Management Area C
Ecosystem Risk	RPP-RPT-49425 (2011)	1	Ecological Risk Assessment Approach for Hanford Waste Management Area C

1.1.2 Model Development and Implementation Process

The WMA C PA effort is supported by a variety of modeling approaches, directed at various specific parts of the analysis, as shown in Figure 1-3. These include process-level models that address particular flow and transport mechanisms specific in the groundwater pathway analysis

and an integrative system-level model that summarizes the entire system, from 1) contaminant release from the residual waste and environmental transport through the groundwater pathway, 2) volatile contaminant releases from the residual waste and environmental transport through the air pathways, and 3) direct contact with residual wastes in the inadvertent intruder analysis. The system-level model uses the results of these analyses in subsequent evaluations of exposure pathways and dose. While the modeling that supports the PA considers a wide range of processes contributing to contaminant transport and exposure pathways, the primary technical approach is focused on the groundwater pathway, which includes release of contaminants from the residual waste, transport through the tank structure and porous media at the site (including consideration of air, water, and solid phases of engineered media such as grout and environmental media such as unsaturated and saturated soils), and exposure of contaminants by humans using contaminated groundwater.

Figure 1-3. Use of Subsurface Transport Over Multiple Phases and GoldSim© in the Evaluation of Parts of the Performance Assessment.

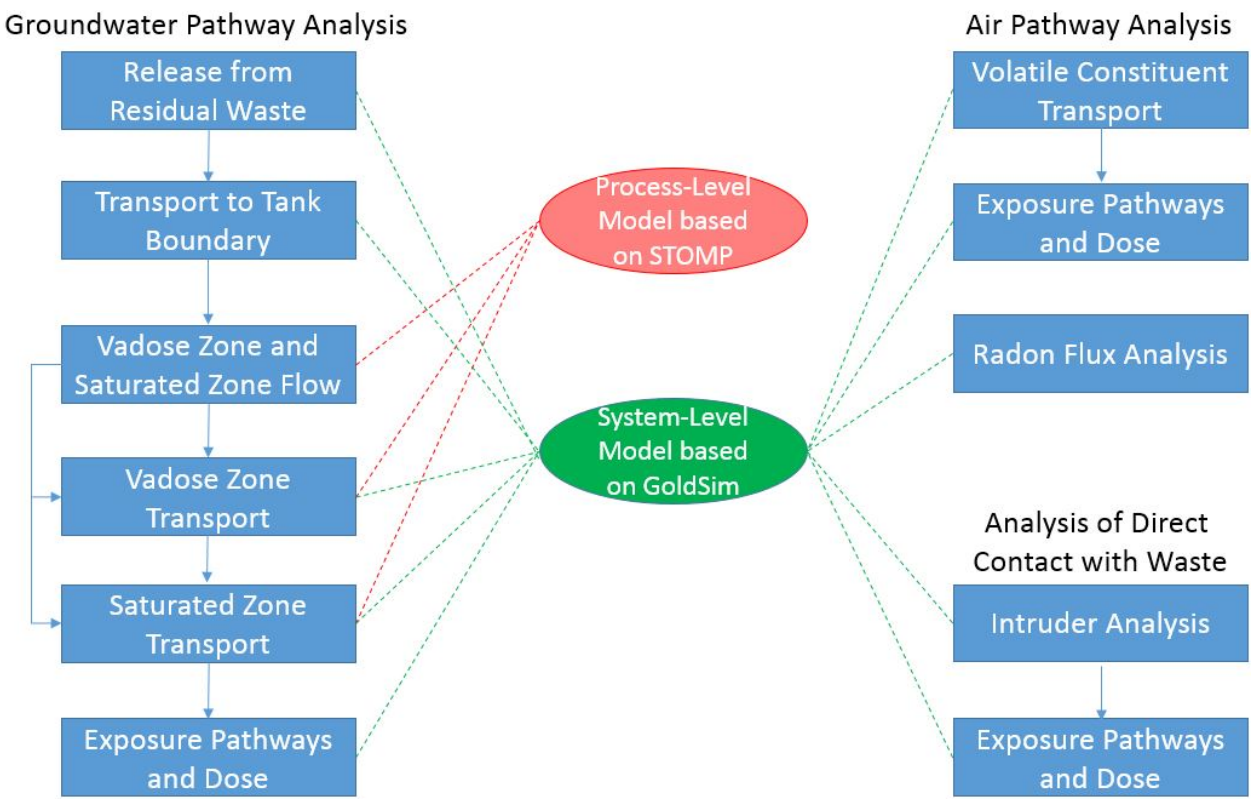

GoldSim© simulation software is copyrighted by GoldSim Technology Group LLC of Issaquah, Washington (see http://www.goldsim.com).
Subsurface Transport Over Multiple Phases (STOMP©) is copyrighted by Battelle Memorial Institute, 1996.

The groundwater pathway analysis in this PA is focused solely on the local-scale impacts at WMA C, not on a regional scale, owing to the regulatory requirements it addresses. The groundwater impacts are evaluated at 100 m (328 ft) downgradient of WMA C, as stipulated in DOE O 435.1.

As shown in Figure 1-3, the PA model analysis makes use of a combination of process and systems models. The Subsurface Transport Over Multiple Phases (STOMP©)[1] simulator process-based code is used in the analysis of post-closure flow for both the unsaturated and saturated flow systems. These groundwater flow analyses are used in subsequent groundwater transport analyses in both STOMP© and GoldSim©[2]. The STOMP©-based process models are used deterministically to examine a range of model parameters through sensitivity analyses, whereas the GoldSim©-based system-level model is used to perform uncertainty analyses and additional sensitivity analyses to support the basis for comparisons with performance objectives under DOE O 435.1. The scope of the uncertainty analysis and sensitivity analysis cases are developed and justified on a formal approach based on the combined use of safety functions that are linked to a formal review of Features, Events, and Processes (FEPs) (see discussion of this topical area in Appendix H). These approaches have been combined with the approaches presented and developed in the 2009 – 2011 Working Sessions to produce a suite of sensitivity and uncertainty analyses that represent the basis for comparisons with performance objectives and measures. The approach establishes the safety concept for the closed WMA C facility, and leads to the identification of specific analyses that query the robustness of the disposal system.

1.2 REGULATORY CONTEXT

The regulatory context for tank farm closure, including requirements for the protection of human health and the environment, is complex and regulated by multiple agencies, DOE, Ecology, and EPA. The primary laws and regulations which govern cleanup and closure processes include the following:

- National Environmental Policy Act of 1969 (NEPA)
- HFFACO
- RCRA/Hazardous Waste Management Act (HWMA) (Revised Code of Washington [RCW] 70.105, “Hazardous Waste Management”)
- Atomic Energy Act of 1954 (AEA)
- CERCLA.

In concert, these laws and regulations provide the overarching guidelines for the cleanup and closure processes. NEPA provides the decision-making structure for Federal agencies. The HFFACO describes closure activities, which are driven by both the requirements of 1) the AEA, as amended, regulating the radioactive portion of mixed waste and 2) RCRA/HWMA as implemented through Washington Administrative Code (WAC) 173-303, “Dangerous Waste

[1] Battelle Memorial Institute (Battelle) retains copyright on all versions, revisions, and operational modes of the Subsurface Transport Over Multiple Phases (STOMP©) software simulator, as permitted by the U.S. Department of Energy. STOMP© is used here under a limited government use license.

[2] GoldSim© simulation software is copyrighted by GoldSim Technology Group LLC of Issaquah, Washington (see http://www.goldsim.com).

Regulations," regulating the nonradioactive dangerous portion of mixed waste. It should be noted that the various laws and regulations for closure create redundant and possibly conflicting administrative requirements. The HFFACO, in part, was established to address these issues and to also identify the need for a single IPA that will be approved by Ecology and by DOE pursuant to their authorities under RCRA and the AEA, respectively, and to ensure the actions taken for WMA closure are protective of human health for all contaminants of concern, both radiological and non-radiological.

1.2.1 National Environmental Policy Act of 1969

In December 2012, DOE published a NEPA environmental impact statement (EIS) for the closure of Hanford Site tanks: DOE/EIS-0391, "Final Tank Closure and Waste Management Environmental Impact Statement for the Hanford Site, Richland, Washington" (TC&WM EIS). The TC&WM EIS in part analyzes SST system closure alternatives, including clean, landfill, and hybrid clean/landfill closure. The summary to the TC&WM EIS states:

> "For closure of the SSTs, DOE prefers landfill closure…which may require soil removal or treatment of the vadose zone. Decisions on the extent of soil removal or treatment, if needed, will be made on the tank farm– or waste management area–basis through the RCRA closure permitting process."

The DOE issued the TC&WM EIS ROD in December 2013 (78 FR 75913, "Record of Decision: Final Tank Closure and Waste Management Environmental Impact Statement for the Hanford Site, Richland, Washington"). The ROD stated "The tanks will be grouted and contaminated soils may be removed. The SSTs will be landfill-closed, which means they will be stabilized and an engineered modified RCRA Subtitle C barrier put in place followed by post-closure care." The Basis for the Decision states, "DOE has determined landfill closure of the SST system, which would include corrective/mitigation actions that may require soil removal or treatment of the vadose zone, is a more appropriate approach for SST system closure than clean closure."

1.2.2 Hanford Federal Facility Agreement and Consent Order

The HFFACO, signed by DOE, Ecology, and EPA on May 15, 1989, is an enforceable agreement that requires DOE to clean up and dispose of radioactive and hazardous waste at the Hanford Site and close facilities that have been used to treat, store, or dispose of such waste. The HFFACO establishes work requirements (milestones), methods for resolving problems, and an action plan for cleanup that addresses priority activities. The HFFACO also recognizes the applicability of RCRA and its amendments to the Hanford Site. It incorporates a regulatory strategy that specifically places SST activities, including waste retrieval, facility cleanup, remediation, waste disposal, and closure under the HWMA.

An integrated regulatory closure process entitled "Single-Shell Tank System Waste Retrieval and Closure Process" has been developed in the HFFACO Action Plan Appendix I by DOE, in conjunction with Ecology and EPA, to streamline regulatory approval for Hanford Site tank farm closure. This integrated regulatory process uses the existing HFFACO process, action plan, and milestones; completes the HWMA closure process as negotiated by DOE and Ecology; and also

recognizes that SST WMA closure and other waste site cleanup activities via compliance with Federal and State requirements need integration[3]. The process also integrates the applicable requirements of the above regulations consistent with DOE M 435.1-1 and the AEA. The agency responsible for the closure of all SST WMAs is DOE.

The HFFACO Action Plan, Appendix I, Section 2.5 establishes the need for a single IPA that will be approved by Ecology and by DOE pursuant to their authorities under RCRA and the AEA, respectively, and to ensure the actions taken for WMA closure will be protective of human health for all contaminants of concern, both radiological and non-radiological. This PA being developed per DOE O 435.1 will also undergo extensive internal DOE review and be reviewed by the NRC under a consultation agreement. Furthermore, the RCRA Closure Analysis, a separate document, will undergo extensive review by both DOE and Ecology.

1.2.3 Resource Conservation and Recovery Act of 1976/ Hazardous Waste Management Act

The HFFACO Appendix I, Section 2.5 designates Ecology as the lead regulatory agency for SST closure. Ecology regulates the SSTs as dangerous waste storage and treatment units under the HWMA (RCW 70.105) and WAC 173-303, which implement RCRA.

The decision under the ROD for the TC&M EIS is that the SST system will be landfill closed under the WAC regulations. Following the ROD, and in accordance with WAC 173-303-610, "Closure and Post-Closure" and WAC 173-303-640, "Tank Systems," DOE submitted DOE/ORP-2014-02, Clean Closure Practicability Demonstration for Single-Shell Tanks to Ecology via Letter 14-ECD-0030, "Transmittal of Clean Closure Practicability Demonstration for the Single-Shell Tanks DOE/ORP-2014-02," which demonstrated that clean closure of any portion of the SST system is impracticable. DOE will close the WMAs and perform closure and post-closure care in accordance with applicable landfill closure and post-closure requirements set forth in WAC 173-303-610 and WAC 173-303-665, "Landfills" subsection (6) "Closure and post-closure care."

1.2.4 Atomic Energy Act of 1954

Under its authority of the AEA, DOE regulates the closure of its facilities containing radioactive materials. The primary mechanism for this regulation is DOE O 435.1 and the associated documents (particularly DOE M 435.1-1).

Where information regarding treatment, management, and disposal of the radioactive source, byproduct material, special nuclear material (as defined by the AEA) and/or the radionuclide component of mixed waste has been incorporated into the Hanford Site-Wide RCRA Permit, it is not incorporated for the purpose of regulating the radiation hazards of such components under the authority of this closure plan or RCW 70.105.

[3] For the purpose of this document and HFFACO Appendix I, the terms "integrate" and "integration" mean "to coordinate for the purposes of efficiency and effectiveness." Such terms have no effect on respective agency authority, requirements, or responsibilities (see page I-1 of HFFACO Action Plan).

1.2.5 Comprehensive Environmental Response, Compensation, and Liability Act of 1980

Under Appendix I of HFFACO (Ecology et al. 1989), closure decisions for SST system soils will be made through the RCRA corrective action process pursuant to Agreement Milestones M-45-55 through M-45-62 and its established process for the development of interim measures where appropriate, RCRA RFI/CMS work plans, remedial field investigations, and corrective measures studies. Ecology will also seek the involvement of EPA for the purpose of ensuring the work is consistent with future CERCLA remedial decisions, and to provide EPA and DOE a basis to evaluate the need for additional work that might be required if the closure activities were conducted under CERCLA remedial action authority. Note that the SST WMAs will be closed in close coordination with other closure and cleanup activities of the Hanford Site Central Plateau, including the CERCLA evaluations being conducted for the BP-5 and PO-1 groundwater operable units.

1.3 GENERAL FACILITY DESCRIPTION

The Hanford Site, a facility in the DOE nuclear waste complex, encompasses ~1,500 km^2 (~586 mi^2) northwest of the city of Richland along the Columbia River in southeastern Washington State, as shown in Figure 1-4. The Federal government acquired the Site in 1943 for the production of plutonium. Production of special nuclear materials continued until the 1980s. Since the 1990s, DOE has focused on environmental remediation of the Hanford Site.

Waste Management Area C (WMA C or the 241-C Tank Farm [C Farm]), part of the SST system, is located in the Central Plateau (see Figure 1-4), near the eastern edge of the 200 East Area. One of the first tank farms built, it was constructed in 1944 and 1945.

The WMA C facility contains twelve 100-series tanks and four 200-series tanks (see Figure 1-5). The 100-series tanks are 23 m (75 ft) in diameter, with a maximum 5 m (16-ft) depth and 2,006,000 L (530,000 gal) design capacity. The 200-series tanks are 6 m (20 ft) in diameter with a maximum 7 m (24-ft) depth and 208,000 L (55,000 gal) design capacity. Only tanks 241-C-101 (C-101) through 241-C-106 (C-106) have concrete pits. The other 100-series tanks are equipped with centrally located salt well pump pits. The tanks sit below grade with at least 2 m (7 ft) of soil cover to provide shielding from radiation exposure to operating personnel. Tank pits are located on top of the tanks and provide access to the tanks, pumps, and associated monitoring equipment.

The SSTs were constructed in place with 0.95-cm (0.375-in.)-thick carbon steel (ASTM A283 Grade C) lining the bottom and 0.64-cm (0.25-in.)-thick carbon steel lining the sides of a reinforced-concrete shell. The tanks have concave bottoms (center of tanks lower than the perimeter) and a curving intersection of the sides and bottom, where the carbon steel plate is 0.8 cm (0.3125 in.) thick. The inlet and outlet lines are located near the top of the liners. There are four inlet lines on each tank, which are also known as nozzles. Pipelines from the diversion boxes to tanks C-101, 241-C-104 (C-104), 241-C-107 (C-107), 241-C-108 (C-108), 241-C-110 (C-110), and 241-C-111 (C-111) are supported by concrete viaducts. At ~3 m (9 ft 10 in.) from the tank wall, the viaduct surface steps down and the void space between the pipes and the

viaduct surface is grouted. At this point, the viaduct begins fanning out from 0.8 m (2 ft 8 in.) wide to 2.2 m (7 ft 4 in.) wide to support the spread placement of the fill lines through the tank wall. Tanks C-101, C-104, C-107, and C-110 each have one outlet line to the next tank in series. Tanks 241-C-102 (C-102), 241-C-105 (C-105), C-108, and C-111 each have one additional inlet line and one outlet line. Tanks 241-C-103 (C-103), C-106, 241-C-109 (C-109), and 241-C-112 (C-112) each have one additional inlet line from the previous tank in the series. The lines connecting each tank are also referred to as "cascade" lines since they allowed transfer of fluids between tanks using gravity flow.

To support the transfer and storage of waste within WMA C SSTs, there is a complex waste transfer system of pipelines (transfer lines), diversion boxes, vaults, valve pits, and other miscellaneous structures. These miscellaneous features of the tank farm are referred to in this document by the general term "ancillary equipment and components."

The 244-CR Process Tank Vault (244-CR vault) is located south of the tanks. The vault is a two-level, multi-cell, reinforced-concrete structure constructed below grade, which contains four underground tanks along with overhead piping and equipment. Two tanks (TK-CR-001 and TK-CR-011) have a capacity of 170,343 L (45,000 gal) each. The other two tanks (TK-CR-002 and TK-CR-003) have capacities of 55,645 L (14,700 gal) each. These sets of ancillary equipment and components are included in the DOE O 435.1 PA.

Fourteen unplanned releases (UPRs) have occurred within or near WMA C (Figure 1-6). The largest ones are associated with leaks in pipelines or diversion boxes, with releases from inlet/outlet ports of the SSTs, or with leaks from the SSTs. RPP-PLAN-39114, "Phase 2 RCRA Facility Investigation/Corrective Measures Study Work Plan for Waste Management Area C" provides more detail on these UPR sites. Impacts from the UPRs are not considered under the scope of this DOE O 435.1 PA. Potential and future impacts from the UPRs will be addressed through the RCRA Corrective Action process.

In the ROD issued December 13, 2013 (78 FR 75913), the preferred closure alternative for the tanks is Alternative 2B. Under this alternative, the tanks would be retrieved to 99% of the original inventory and filled with grout. The grout under consideration is formed from cement, fly ash, fine aggregate, sodium bentonite clay, and water to create a free-flowing material that can be used to fill the tanks after waste retrieval is completed. The grout hardens in the tanks to form a monolithic cementitious material inside the tanks. For long-term performance, the grout provides several benefits: it provides structural stability to the tank, it chemically conditions the interior of the tanks to a high pH environment, it provides a low permeability layer to limit contact of water with the residual wastes, and it provides a barrier to potential inadvertent human intrusion.

The specific formulation of the grout has not yet been established. DOE/EIS-0391 (2012) assumed the fill material for the tanks will be similar to the cold-cap grout formulation developed by the U.S. Army Corps of Engineers (USACE) for the Hanford Grout Vault Program. This formulation has low-hydration heat and is free-flowing, self-leveling, and designed to generate little or no free water during curing.

Figure 1-4. Hanford Site and its Location in Washington State.

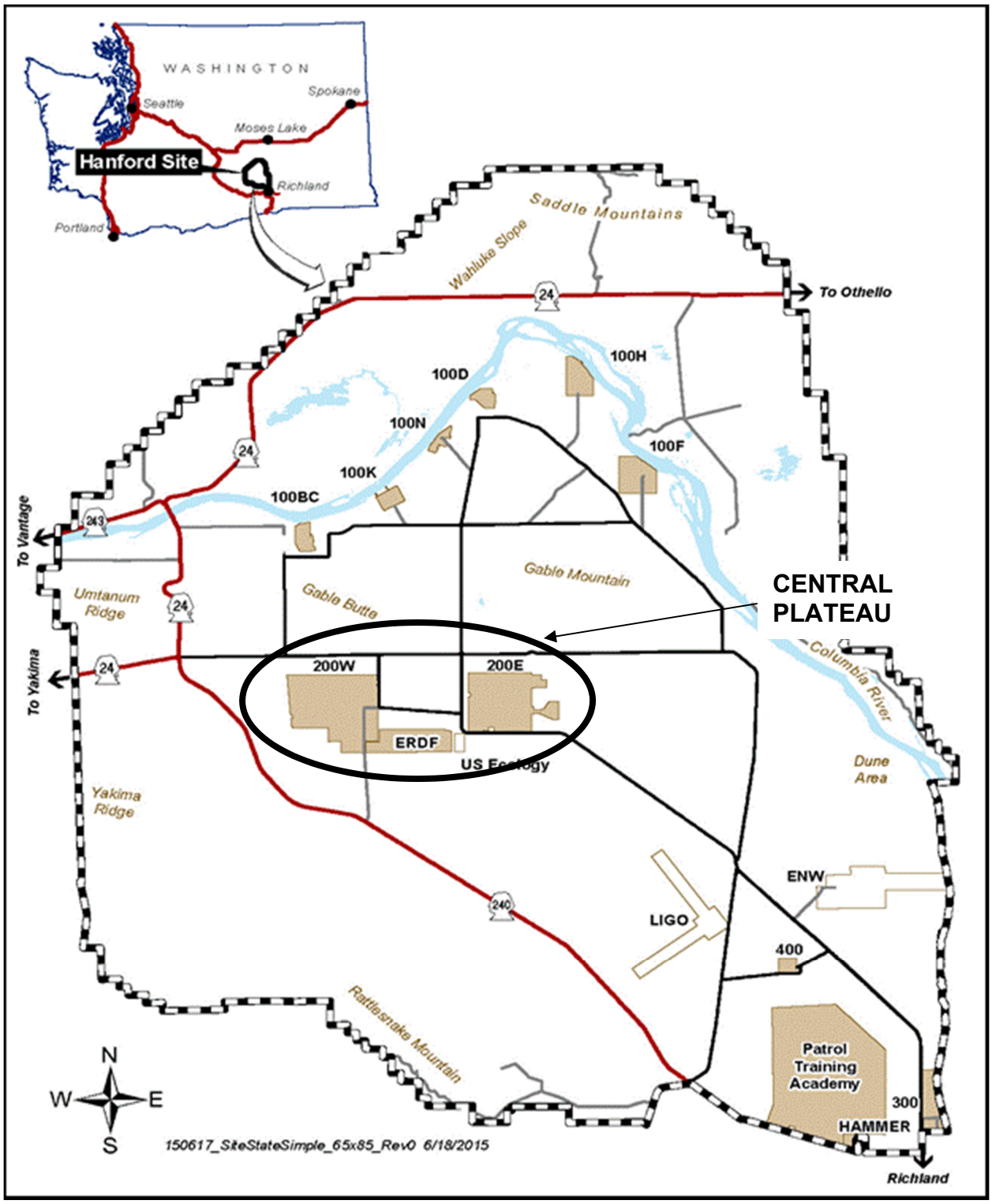

ENW = Energy Northwest Columbia Generating Station LIGO = Laser Interferometer Gravitational Wave Observatory
ERDF = Environmental Restoration Disposal Facility

Figure 1-5. Location Map of Waste Management Area C and Surrounding Area.

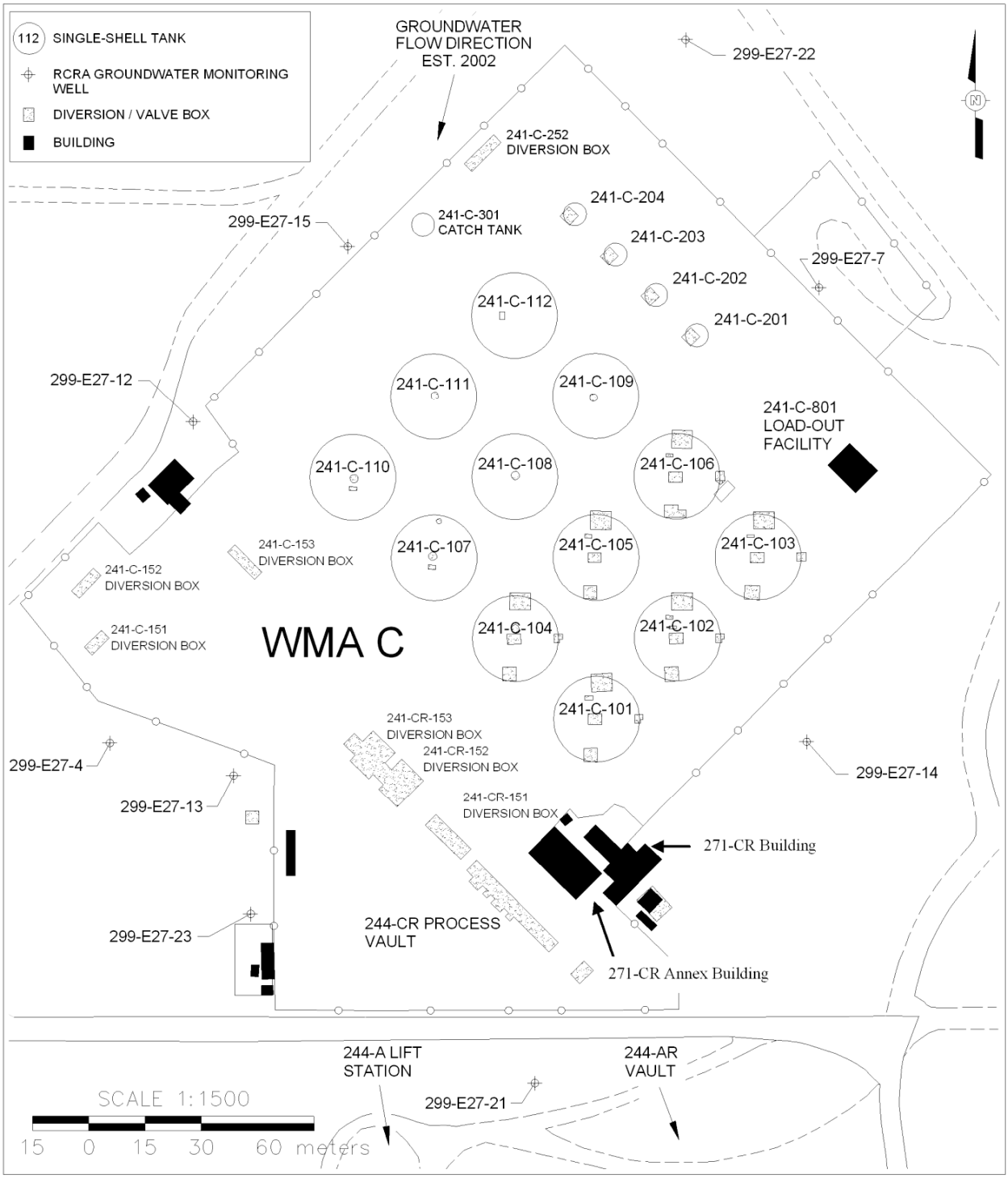

RCRA = Resource Conservation and Recovery Act of 1976 WMA = Waste Management Area

Figure 1-6. Location Map of Unplanned Release Sites of Waste Management Area C.

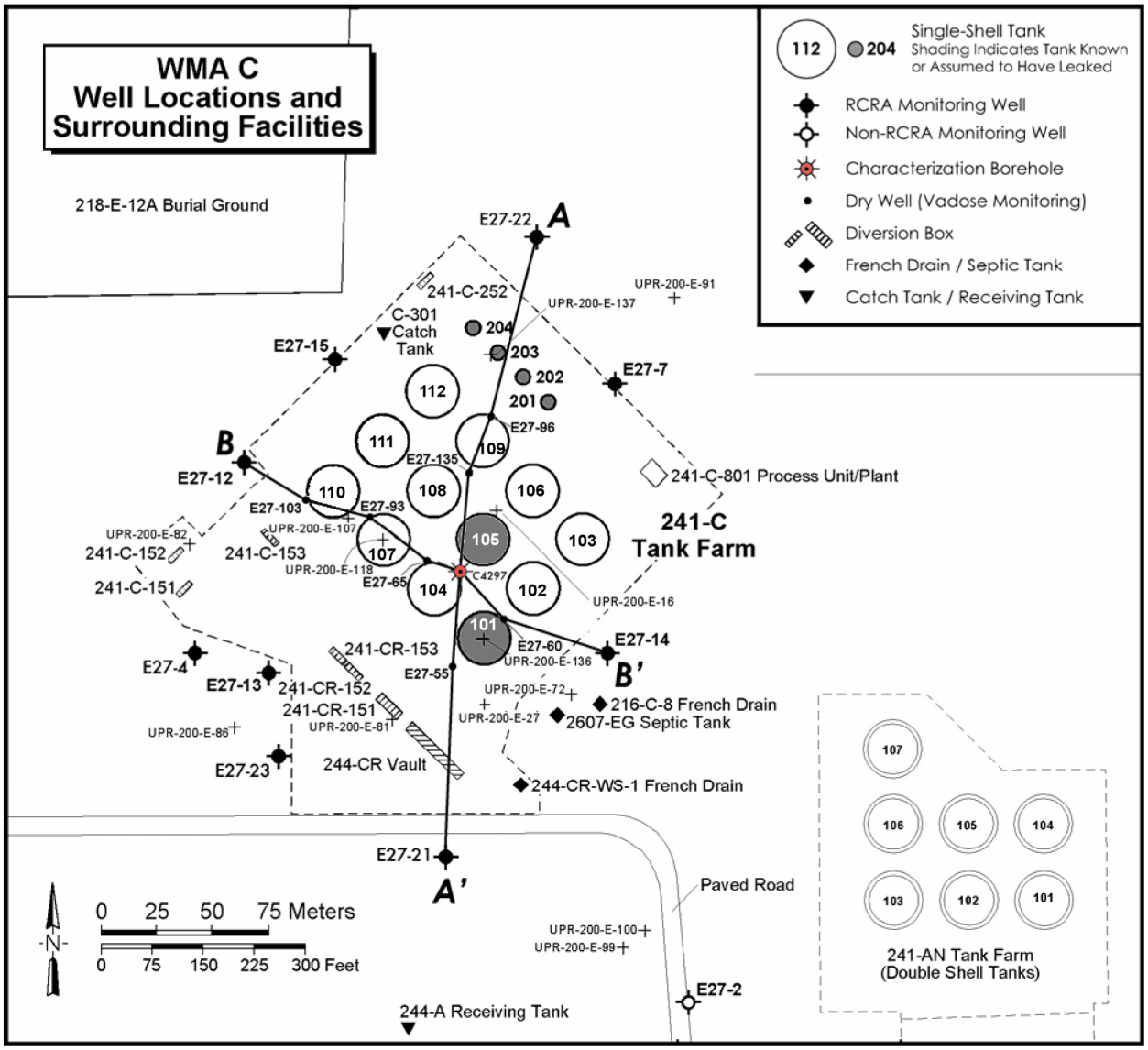

RCRA = Resource Conservation and Recovery Act of 1976 WMA = Waste Management Area

1.4 A SAFETY CONCEPT AND SAFETY FUNCTIONS FOR CLOSED WASTE MANAGEMENT AREA C

The safety concept for tank closure is composed of a set of safety functions that act together to provide the long-term performance of a closed facility required in closure regulations. The safety functions represent multiple and redundant barriers, so that the loss of one or some of the safety functions continues to result in adequate performance of the overall system. A set of safety functions for WMA C are shown in Table 1-2. A schematic depiction of these safety functions for the closed WMA C is provided in Figure 1-7. The goal of the PA is to evaluate these safety functions, to provide reasonable assurance of performance even when some of the safety functions are lost or degraded through time or disruptive events.

Table 1-2. List of Safety Functions for the Performance Assessment of Waste Management Area C. (2 sheets)

I1	Institutional control	By rule, it is assumed that control of the site will be retained for 100 years. A strong potential exists that the U.S. government will retain control of the site for a much more extended period of time.
I2	Societal memory	Societal memory is represented by records, deed restrictions, and other passive controls that would warn someone that additional care should be taken in the area. For a member of the public to come onsite to experience exposures to contamination from WMA C, records that the Hanford Site existed would need to be forgotten or ignored.
I3	Exposure point	By rule, it is assumed a post-closure well is established 100 m downgradient at the point of highest exposure. It is highly unlikely that groundwater exposure will occur at this location, and potential wells in other locations would produce much lower impacts to a member of the public. Furthermore, the 100 m boundary for WMA C lies under the A Complex, and does not represent a realistic exposure point. Exposures are more likely to occur further downgradient.
EB1	RCRA cover (permeability)	The final design cover has not yet been established, but is believed to be able to produce very low initial flow rates. Over some period of time this function may deteriorate.
EB2	Steel shell (permeability)	The function of the carbon steel shell to limit flow through the tank is not currently explicitly accounted for in the performance assessment. It is assumed to be permeable at all times. The shell is part of the overall assessment of low flow through the tank for long periods of time. Its potential eventual failure is considered as part of the generic barrier failure cases.
EB3	Steel shell (chemical)	The carbon steel shell will corrode over a period of time, leaving behind corrosion products of (primarily) iron oxides. These corrosion products are highly sorptive and tend to produce reducing conditions that are highly advantageous for limiting solubilities of key radionuclides, particularly technetium-99. This safety function is currently assumed to have no effect on system performance.
EB4	Steel shell (structural)	The steel shell provides structural support preventing short term subsidence of the closed facility.
EB5	Grout in tank (permeability)	The grout acts to limit water flow through the facility, making contaminant releases dominated by diffusion from the waste.
EB6	Grout in tank (chemical)	The grout acts to condition the chemistry of the waste residuals, with sorption characteristics of high pH environments.
EB7	Grout in tank (chemical)	The grout provides a passive and high pH environment for steel corrosion. This safety function is not included in the assessment since the steel shell is assumed to be permeable at all times.
EB8	Grout in tank (structural)	The grout provides structural support preventing subsidence of the closed facility.
EB9	Tank base mat (permeability)	The tank pad, if intact, will provide a flow-limiting layer.
EB10	Tank base mat (chemical)	The concrete pad is anticipated to continue to provide a high pH environment, with associated sorption, for an extended time in the future.

Table 1-2. List of Safety Functions for the Performance Assessment of Waste Management Area C. (2 sheets)

WF1	Residual waste (chemical)	The residual waste is recalcitrant by nature, providing limitations to the amount and contaminant release rate upon contact with water.
VZ1	Water flow through vadose zone	The rate of water flow through the soil is slow, leading to long transport times in the vadose zone.
VZ2	Sorption on vadose zone soils	Vadose zone soils sorb some of the constituents of potential concern, delaying their arrival at the water table. However, a number of key contaminants are not believed to sorb significantly.
VZ3	Dispersion in vadose zone	Dispersion results in spreading contaminants in the vadose zone, and thereby decreasing concentrations.
VZ4	Anisotropy in vadose zone	Anisotropy may increase mixing and dispersion in the vadose zone, thereby decreasing concentrations.
SZ1	Water flow in saturated zone	Advective groundwater flow in the saturated zone leads to contaminant dilution.
SZ2	Sorption on saturated zone soils	Saturated zone soils sorb some of the constituents of potential concern, delaying their arrival at the point of compliance. A number of key contaminants are not believed to sorb significantly.
SZ3	Dispersion in saturated zone	Spreading of the plume in the saturated zone, adding dilution to the contaminant plume and lowering concentrations.
SZ4	Dilution in well	Dilution is caused by mixing at a groundwater well extracting groundwater where it is usable and accessible by a member of the public. This safety function is omitted from the performance assessment to make it compatible with the groundwater protection requirements.

RCRA = Resource Conservation and Recovery Act of 1976 WMA = Waste Management Area

A significant part of the safety concept lies in the land ownership of the Central Plateau by DOE. It is noteworthy that all of the technical calculations that are presented in the WMA C PA are predicated on the loss of the first two safety functions: loss of institutional control of the Central Plateau by DOE, followed by loss of societal memory that the Hanford Site existed. If either or both of these safety functions remain in place, the radiological impacts of releases or residual wastes from WMA C are very low and greatly delayed in time, as shown in the TC&WM EIS analyses for tank residual wastes. In the assessment context of PAs conducted under DOE O 435.1, both of these safety functions are assumed to lose functionality completely after the institutional control period of 100 years.

DOE O 435.1 introduces another administrative safety function into the analysis: the point of compliance. If the first two safety functions (institutional control and societal memory) are lost, DOE O 435.1 requires an assumption that a groundwater well is installed 100 m (328 ft) from the disposal facility fenceline in the location of peak concentration. This assumption means that relatively little credit is given for delay and dilution in the groundwater aquifer. Furthermore, since the PA evaluates impacts from groundwater use at 100 m (328 ft) downgradient of the facility fenceline, potential impacts inferred from this analysis would reflect larger potential

impacts and provide an additional margin of safety than would be realized by either individuals potentially using groundwater further downgradient or individuals not using groundwater at all.

The remaining parts of the safety concept involve the use of the engineering, environmental, and hydrogeological setting to provide multiple and redundant barriers to the release and migration of residual wastes from tanks and ancillary equipment. The barriers can be divided into one of three types: structural safety functions, hydrological safety functions, and chemical safety functions. The safety concept calls for backfilling the tanks with grout, leading to a highly stable underground structural matrix. The resulting monolith of grout contained in the tank can be assumed to maintain its ability to support the soil overburden for very long periods of time. Discussion of the potential longevity of the tank structure and the emplaced grout is provided in Section 6.2.1.2 (Evaluation of Tank Stability). The hydrological safety functions are features and processes taking place in the vadose zone and unconfined aquifer that reduce the concentration of a contaminant at a PoCal, such as dispersion, adsorption, natural attenuation, and dilution with clean surrounding water. The chemical safety functions are intended to decrease the solubility and increase the sorption of key contaminants, and to provide a stable and passive chemical environment for the engineered barriers.

As discussed above, the purpose of the PA is to evaluate the safety concept in order to provide reasonable assurance of its performance. Confidence in the overall safety concept is enhanced if there is reasonable assurance of performance even in the event that one or more of the safety functions are lost or are degraded in time. It is therefore reasonable to ask which FEPs might affect a particular safety function in a way that might degrade its function, or to cause the safety function to act differently than expected.

This approach can then be used to identify a set of sensitivity analyses that can be used to explore the implications of the loss of safety functions, while at the same time exploring the implications of aggregated FEPs that might affect the safety function in similar ways. The structure of the PA for WMA C will therefore be to identify sensitivity cases and alternative models for the safety functions shown in Table 1-2, and to examine outcomes when the safety function behaves differently than expected, is degraded compared to a base case, or is lost entirely. Particular attention will be given to any FEPs identified that might affect multiple safety functions simultaneously.

1.5 LAND USE AND INSTITUTIONAL CONTROL ASSUMPTIONS

In September 1999, DOE issued the Final Hanford Comprehensive Land-Use Plan (HCP) EIS (DOE/EIS-0222-F, “Final Hanford Comprehensive Land-Use Plan Environmental Impact Statement”). The HCP EIS analyzed the impacts of alternatives for implementing a land-use plan for DOE’s Hanford Site for at least the next 50-year planning period and lasting for as long as DOE retains legal control of some portion of the real estate. In November 1999 DOE issued its ROD establishing the HCP, which consisted of four key elements:

- A land-use map that addressed the Hanford Site as five geographic areas,

- A set of nine land-use designations that define the permissible uses for each area of the site,
- The land-use policies, and
- The implementing procedures that would govern the review and approval of future land uses.

These elements were reaffirmed in the HCP EIS Supplement Analysis (DOE/EIS-0222-SA-02, "Supplement Analysis of the Hanford Comprehensive Land-Use Plan Environmental Impact Statement") and in the amended ROD (73 FR 55824, "Amended Record of Decision for the Hanford Comprehensive Land-Use Plan Environmental Impact Statement").

The Central Plateau was designated Industrial-Exclusive by the HCP EIS to allow for continued waste management operations within the Central Plateau geographic area. The definition of Industrial-Exclusive includes treatment, storage, and disposal of all appropriate categories of wastes and related management activities. Figure 1-8 shows the Industrial-Exclusive area established by the HCP EIS within the Central Plateau.

As stated in Section 3.3.2.3.3 of the Final HCP EIS: "This [Industrial-Exclusive] designation would … allow expansion of existing facilities or development of new compatible facilities. Designating the Central Plateau as Industrial-Exclusive would be consistent with the Working Group's recommendations, current DOE management practice, other governments' recommendations, and many public stakeholder values throughout the region."

DOE/RL-2001-41, Sitewide Institutional Controls Plan for Hanford CERCLA Response Actions describes institutional controls for the current Hanford Site CERCLA response actions. This Plan originally was developed to fulfill the requirement for submittal of a Sitewide plan that describes how the DOE Richland Operations Office will implement and maintain the operable unit-specific institutional controls specified in CERCLA decision documents.

This plan includes specific discussion about each of the five categories of institutional controls including warning notices, entry restrictions, fencing, land use management, and groundwater use management on the Hanford Site for CERCLA-based remedial actions.

For all of the operational areas (i.e., including the 100, 200, and 300 Areas), this plan states: "Land use is managed according to the comprehensive land-use plan as described in DOE/EIS-0222-F and DOE/EIS-0222-SA-01and [*sic*] in compliance with DOE orders and cleanup end states as established in CERCLA decision documents."

Despite the designation of the Central Plateau, including WMA C, the assumption under DOE O 435.1 is that control of the site and institutional records (e.g., deed restrictions) associated with its designation as Industrial-Exclusive are lost or otherwise not implemented beginning 100 years after facility closure. Such events are a necessary precursor to the types of exposure scenarios and the exposure location assumed in the PA. Such assumptions do not represent an administrative intention by DOE to release the site from its Industrial-Exclusive designation, but are only assumptions made as a basis for PA under DOE O 435.1.

Figure 1-7. A Schematic Depiction of the Safety Functions for a Closed Waste Management Area C.

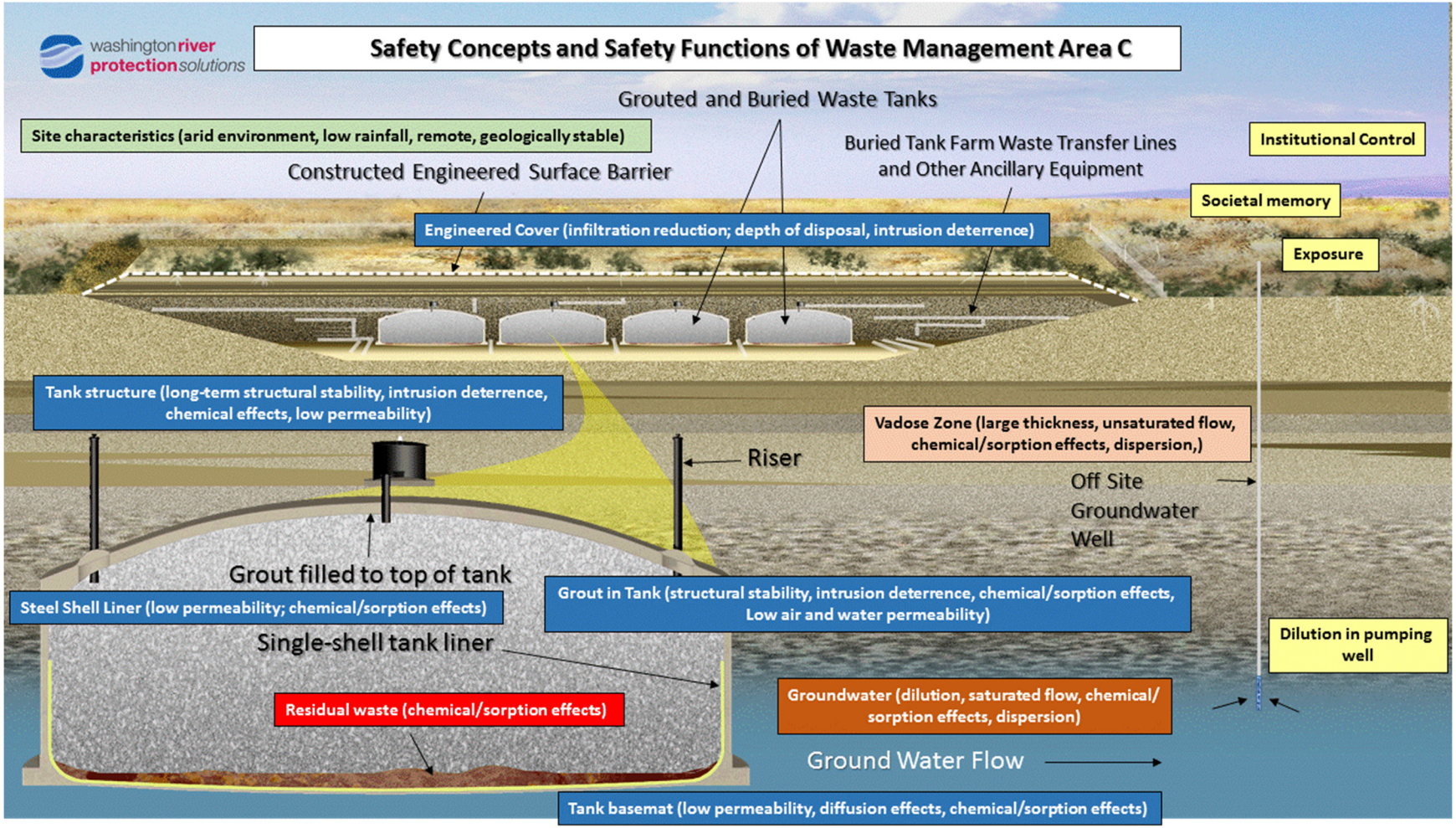

Figure 1-8. Hanford Site, Showing Land-Use Designations Including the Hanford Reach National Monument.

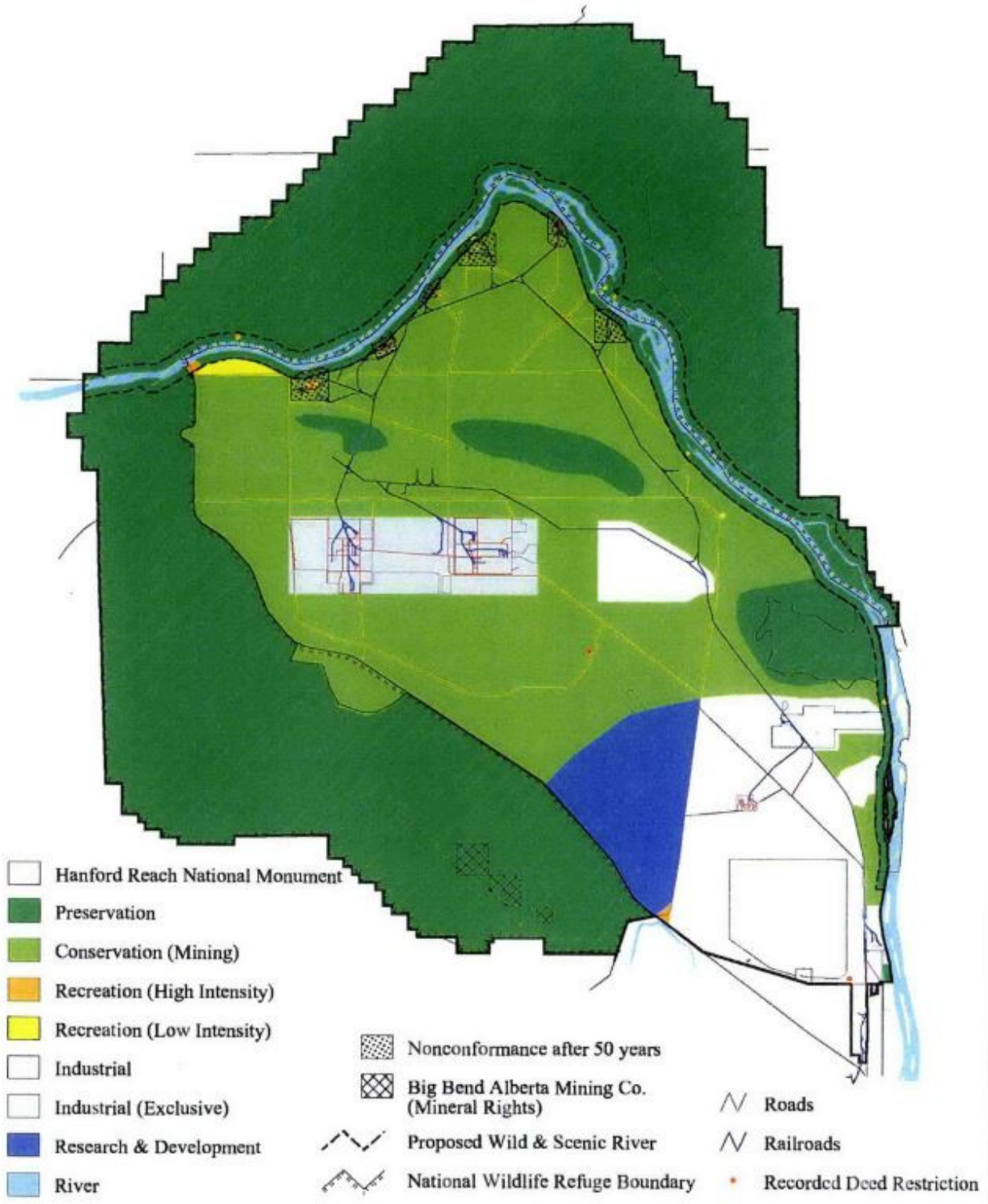

1.6 WASTE MANAGEMENT AREA C HISTORY AND PLAN FOR CLOSURE

1.6.1 History

In this section, a summary is provided of the facility history with an emphasis on those features that are important to the PA. However, this section can only provide a summary of the available information because of the long operating history of the site.

This tank farm was constructed from 1944 to 1945 and originally consisted of twelve 100-series tanks, four 200-series tanks, catch tank 241-C-301 (C-301 catch tank), four diversion boxes (241-C-151, 241-C-152, 241-C-153, 241-C-252) and interconnecting pipelines (Appendix D of RPP-7494, "Historical Vadose Zone Contamination from A, AX, and C Tank Farm Operations"). Construction of the tank farm is shown through a series of photographs (Figure 1-9). On February 10, 1945, the constructed facilities at WMA C were turned over to operations (HW-7-1388-DEL, "Hanford Engineer Works Monthly Report February 1945," page 16). However, the tanks were not utilized until March 1946 starting with the receipt of waste into the 100-series tanks and receipt of waste in the 200-series tanks in September 1947.

New facilities were constructed in WMA C in 1951 and 1952 to allow removal of the stored metal waste in tanks C-101 through C-106 as well as C-201 through C-204. New pump pits, sluice pits, and heel pits were constructed atop these 100-series SSTs for installing waste retrieval equipment through tank risers. The 244-CR vault was installed for acidification, dissolution of solids, and blending the retrieved metal waste slurries. Diversion boxes 241-CR-151, 241-CR-152, and 241-CR-153 along with concrete-encased pipelines were installed for transferring metal wastes from the SSTs to the 244-CR vault. A control room, the 271-CR building, was also constructed for operation of the 244-CR vault equipment. In 1962, building 241-C-801 was constructed to enable the recovery of ^{137}Cs. Finally, from the 1970s through the 1990s additional pipelines and facilities were installed to support interim stabilization.

The tanks received wastes from the various chemical separations processes conducted at the Hanford Site. For a number of reasons, essentially all of the very high-activity waste streams generated during plutonium recovery operations at the Hanford Site prior to 1980 have been reprocessed. Often, these high-activity waste streams were reprocessed multiple times by physical, chemical, and thermal means. In many cases, reprocessed high-activity waste streams were commingled with lower activity wastes to produce the materials stored in the tanks. An extended summary of the waste processing activities that contributed to wastes in the tank farm is provided in Appendix B of DOE/ORP-2005-01, Initial Single-Shell Tank System Performance Assessment for the Hanford Site (SST PA).

Figure 1-9. Photographs Showing Different Stages of the Historical Construction of Tanks and Selected Ancillary Equipment in Waste Management Area C.

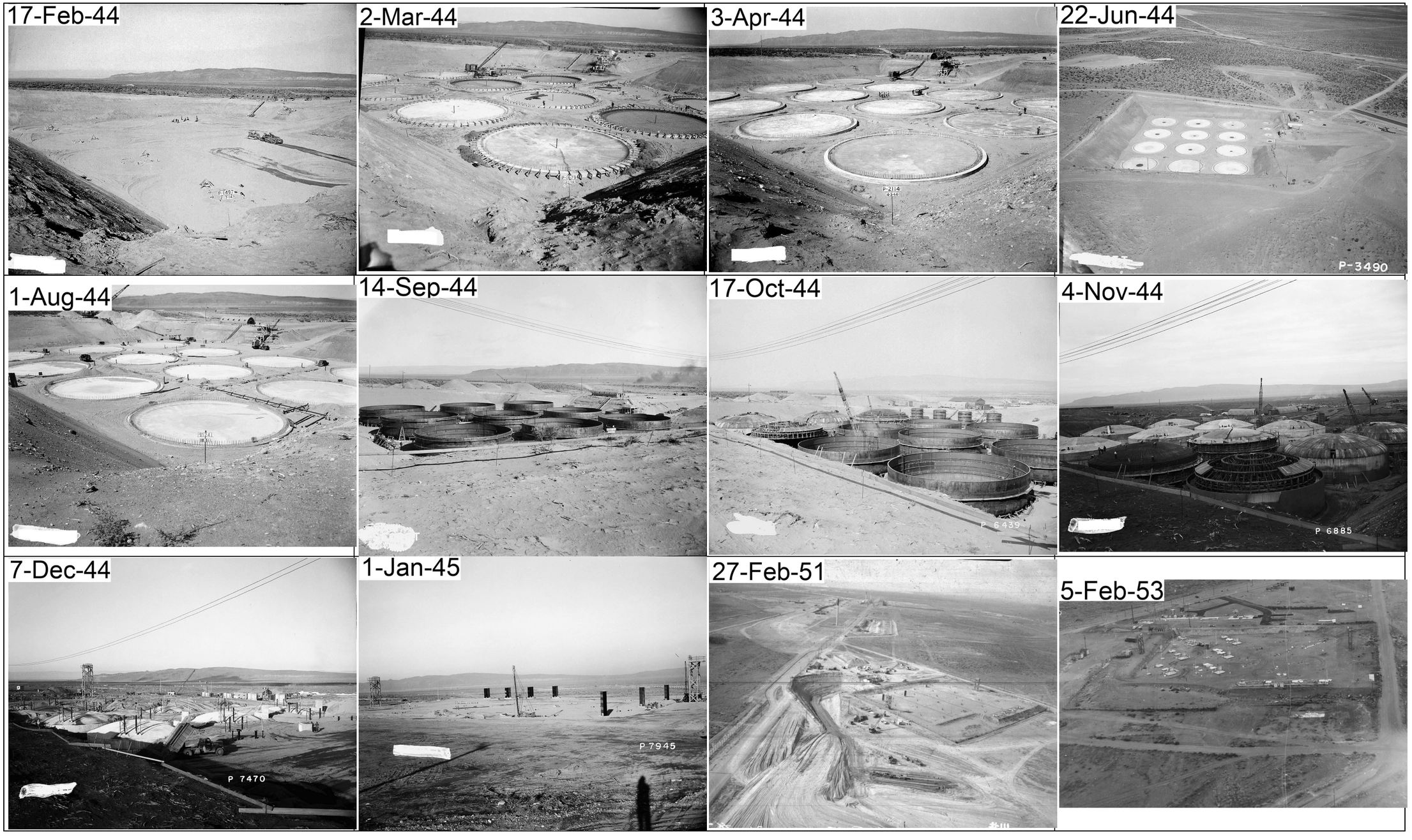

Waste retrieval activities have been ongoing since 2003. As of September 1, 2014, waste has been retrieved from 13 SSTs in C Farm (C-101, C-103, C-104, C-106, C-107, C-108, C-109, C-110, C-112, 241-C-201 [C-201], 241-C-202 [C-202], 241-C-203 [C-203], and 241-C-204 [C-204]). Waste retrieval is completed for 13 of the 16 tanks. A practicability request to forego a third technology has been submitted for tank C-102 (RPP-RPT-58676, "Practicability Evaluation Request to Forego a Third Retrieval Technology for Tank 241-C-102") and is under review, and tank C-106 is undergoing a HFFACO (Ecology et al. 1989) Appendix H Attachment 2 "Exception to Retrieval Criteria for Single-Shell Tanks" process that will "indicate the reason DOE does not believe the retrieval criteria can met" (RPP-20658, "Basis for Exception to the Hanford Federal Facility Agreement and Consent Order Waste Retrieval Criteria for Single-Shell Tank 241-C-106"). Residual tank waste constituents and/or hard heel constituents after retrieval were sampled and analyzed. Tank C-203 was not sampled, and tanks C-101, C-107 and C-112 sample results are not yet available. As of September 30, 2014, waste has been partially retrieved and waste retrieval operations are ongoing for SSTs C-102, C-105 and C-111.

1.6.2 Closure

Closure of the individual SSTs and WMA C in its entirety occurs in three major steps as identified in RPP-RPT-41918, "Assessment Context for Performance Assessment for Waste in C Tank Farm Facilities after Closure": 1) SST waste retrieval, 2) tank filling for stabilization, and 3) surface barrier placement. A general description of these steps follows.

1. For landfill closure of WMA C to occur, DOE must retrieve as much waste as technically possible (Ecology et al. 1989). The DOE should meet the performance objectives for the disposal of Class C LLW provided in 10 CFR 61, Subpart C. In addition, because the tank waste residual is mixed waste, it has to meet Washington State dangerous waste requirements for closure (WAC 173-303). In the HFFACO Appendix I (Ecology et al. 1989) entitled, "SST System Waste Retrieval and Closure Process," closure permits will be incorporated into the Hanford Site-Wide Permit (WA7 89000 8967).

2. The next closure action process after Ecology and DOE Headquarters approval would be to fill the tanks with grout to stabilize and immobilize the residual waste to prevent further long-term degradation of the SSTs, and to discourage intruder access as required for a near-surface disposal facility. As discussed in Section 1.3, the specific formulation of the grout has not yet been established, but the TC&WM EIS assumed the fill material for the tanks will be similar to the cold-cap grout formulation developed by USACE for the Hanford Grout Vault Program. This formulation has low-hydration heat and is free-flowing, self-leveling, and designed to generate little or no free water during curing. This assumption has been adopted for the purposes of this PA.

3. The final closure activity would be placement of an engineered surface cover. This surface cover will provide a barrier to infiltration and intrusion. The specific design of the closure cover has not been finalized, but it is likely to be based on the Modified RCRA Subtitle C Barrier concept (RPP-RPT-49701, "Waste Management Area C Closure – Conceptual Design Report").

1.7 PREVIOUS PERFORMANCE ASSESSMENTS AND OVERLAPPING ANALYSES

Over the years, numerous PAs relating to various disposal activities at the Hanford Site, meeting the requirements of DOE O 435.1, have been completed, including:

- WHC-EP-0645, "Performance Assessment for the Disposal of Low-Level Waste in the 200 West Area Burial Grounds"
- BHI-00169, "Environmental Restoration Disposal Facility Performance Assessment"
- WHC-SD-WM-TI-730, "Performance Assessment for the Disposal of Low-Level Waste in the 200 East Area Burial Grounds"
- WHC-SD-WM-EE-004, "Performance Assessment of Grouted Double-Shell Tank Waste Disposal at Hanford"
- PNNL-11800, "Composite Analysis for Low-Level Waste Disposal in the 200 Area Plateau of the Hanford Site"
- DOE/ORP-2000-24, Hanford Immobilized Low-Activity Waste Performance Assessment: 2001 Version.

These assessments do not directly pertain to WMA C, but represent a broad base of knowledge and activities for other facilities at Hanford and regionally relevant issues. At several sites, the nature and behavior of the general geological setting is expected to be similar.

A number of documents dealing with assessments for closing tank farms with specific relevance to WMA C have been issued. Early PAs relevant to WMA C include:

- DOE/ORP-2003-11, "Preliminary Performance Assessment for Waste Management Area C at the Hanford Site, Washington"
- RPP-13774, "Single-Shell Tank System Closure Plan."

These older assessments were updated with current information in recent assessments that include:

- DOE/ORP-2005-01, "Initial Single-Shell Tank System Performance Assessment for the Hanford Site"
- DOE/EIS-0391, "Final Tank Closure and Waste Management Environmental Impact Statement for the Hanford Site, Richland, Washington"
- RPP-PLAN-47559, "Single-Shell Tank Waste Management Area C Pipeline Feasibility Evaluation."

These more recent assessments provide relevant information to the IPA and are briefly summarized in the following sections.

1.7.1 Single-Shell Tank Performance Assessment

The SST PA (DOE/ORP-2005-01), that met the requirements of the DOE O 435.1, presented an analysis of the long-term impacts of residual wastes assumed to remain after retrieval of tank wastes and closure of the SST farms. The SST PA was intended to be a comprehensive evaluation of closure of all SST WMAs at Hanford, and included WMA C in its scope, but was not exclusively focused on it.

The reference case set of parameters and engineering assumptions evaluated in the SST PA was selected to represent a best estimate of the closed facility performance at WMA C. The SST PA also examined a range of values for parameters to support defining the expected performance range of each barrier or feature. To estimate the robustness of the selected set of barriers, alternative conceptualizations were analyzed using variations on the reference case design to establish the level of performance degradation that might occur. Additionally in the SST PA, residual tank waste impacts on groundwater, air resources, and the inadvertent intruder were shown to be limited and well below most important performance objectives for the reference case used in the analysis.

1.7.2 Tank Closure and Waste Management Environmental Impact Statement Analysis of Waste Management Area C

The HCP EIS and subsequent supplemental analysis (DOE/EIS-0222-F; DOE/EIS-0222-SA-01, "Hanford Comprehensive Land-Use Plan Environmental Impact Statement Supplement Analysis") and RODs [64 FR 61615, "Record of Decision: Hanford Comprehensive Land-Use Plan Environmental Impact Statement (HCP EIS)"; 73 FR 55824] designated a 5,064-hectare (12,513-acre) area within the Central Plateau of Hanford as Industrial-Exclusive. This area, which includes the 200 East and 200 West Areas, includes WMA C. The Industrial-Exclusive designation preserves DOE control of continuing remediation activities and use of the existing compatible infrastructure required to support activities such as radioactive and mixed waste treatment, storage, and disposal. Further, under this designation, DOE continues its Federal waste disposal mission. The Industrial-Exclusive designation also allows for the expansion of existing facilities or the development of new compatible facilities in support of ongoing missions.

The TC&WM EIS (DOE/EIS-0391) included in its scope an evaluation of residual wastes in WMA C. The EIS also included an evaluation of waste sources in the tank farm, including past tank leaks, retrieval leaks from the tanks, and UPRs from within the WMA C fenceline. In Federal Register notice 78 FR 75913, DOE issued the first in a series of RODs announcing its preferred alternative (Alternative 2B) for wastes contained in underground radioactive waste storage tanks evaluated in the Final TC&WM EIS, DOE/EIS-0391 (2012). Decisions announced in this ROD pertain to each of the three main areas analyzed in the EIS, i.e., tank closure, decommissioning of the Fast Flux Test Facility (FFTF), and waste management. This ROD amends the 1997 Tank Waste Remediation System (TWRS) ROD (62 FR 8693, "Record of

Decision for the Tank Waste Remediation System, Hanford Site, Richland, WA," February 26, 1997).

As a part of the ROD issued December 13, 2013 (78 FR 75913) arising from the TC&WM EIS, the preferred closure alternative for the SST WMAs was Alternative 2B. This ROD includes retrieval of 99% of the waste volume currently stored in Hanford's 177 underground storage tanks, landfill closure of the SST farm systems, and operation and maintenance of the tank farms. Tank Closure Alternative 2B considers vitrification treatment of waste from the Hanford 200 East and 200 West Area tank farms in accordance with the TWRS EIS ROD and supplemental analyses.

The end state of the tanks evaluated under Alternative 2B assumes that the individual WMAs of the SST waste system would be closed as landfill units under the requirements of WAC 173-303 and DOE O 435.1, as applicable, or decommissioned under DOE O 430.1B, Real Property Asset Management. The tanks and selected ancillary equipment would be filled with grout to immobilize residual waste, prevent long-term degradation of the tanks, and discourage inadvertent intruder access. Under Alternative 2B, removal and replacement of the top 4.5 m (15 ft) of soil was considered for the 241-BX and 241-SX Tank Farms, but no such actions are under consideration for WMA C. The ROD states that decisions on the extent of soil removal or treatment would be made on a tank farm or WMA basis through the RCRA closure permitting process. The closed tank system would be covered with an engineered Modified RCRA Subtitle C Barrier, followed by post-closure care for 100 years.

The details of the basis for the impacts analyses from WMA C for Alternative 2B within the TC&WM EIS are provided in Appendix F. Because of the importance of the TC&WM EIS in establishing the ROD for landfill closure of WMA C and other SST WMAs, the PA effort evaluated a specific sensitivity case using the current base case numerical model developed for the WMA C PA with the same residual inventories, recharge, and waste release models used for the WMA C model developed for the EIS. A comparison of results of this sensitivity case with comparable results for the WMA C-specific model used in the TC&WM EIS analysis is also described and provided in Appendix G.

1.7.3 Waste Management Area C Pipeline Feasibility Study

Revision 1 of RPP-PLAN-47559 provided an initial scoping analysis of the post-closure consequences of residual wastes in ancillary equipment. This analysis did not consider residual wastes in tanks. These analyses resulted in the following general conclusions:

- For the inadvertent drilling intrusion scenario, a total acute dose to the intruding receptor was well below the generally accepted performance objective for inadvertent intrusion (500 mrem for acute exposure) at closed LLW facilities under DOE O 435.1

- For groundwater, a peak chronic total dose to the receptor was well below the drinking water standard of 4 mrem/yr

- For key non-radiological contaminants assumed to be left behind in waste pipelines, human health and environmental impacts via the groundwater pathway were well below groundwater cleanup level.

1.8 SUMMARY OF KEY ASSESSMENT ASSUMPTIONS

This assessment has been structured as a series of sensitivity and uncertainty analyses intended to evaluate the effect of a wide range of assumptions on site evolution and alternative concepts regarding the physical behavior of the site. The alternative analyses include sensitivity cases that evaluate conditions well outside the range of the base case analysis. In all cases the calculations produced results that are below the performance measures. Therefore, none of the assumptions listed in this section are key assumptions to compliance, and there are no specific design variables that must be met in order to meet the regulatory goals of DOE O 435.1.

An extended list of key assumptions used in the PA are presented in Appendix A. Specific key assumptions are presented here that specifically relate to potential decisions regarding design features and closure of the facility.

- It has been assumed that the landfill closure of WMA C occurs in 2020, consistent with planning assumptions in the TC&WM EIS. The results of the PA are not significantly affected by alternative assumptions about closure timing.

- The engineered cover for WMA C is not yet designed, but is assumed to be similar to the Modified RCRA Subtitle C Barrier that limits infiltration through the waste primarily by evapotranspiration processes (i.e., surface barrier) based on the work done for the Hanford Prototype barrier (DOE/ORP-2008-01, RCRA Facility Investigation Report for Hanford Single-Shell Tank Waste Management Areas, Appendix C). These processes are not modeled directly, but those processes have been studied through field measurements, tracer studies, and numerical models to estimate net infiltration (PNNL-14744, "Recharge Data Package for the 2005 Integrated Disposal Facility Performance Assessment"; PNNL-14960, "200-BP-1 Prototype Hanford Barrier Annual Monitoring Report for Fiscal Year 2004"; "Multiple-Year Water Balance of Soil Covers in a Semiarid Setting" [Fayer and Gee 2006]). Instead, the recommended net infiltration rates from those reports are applied to the area under the engineered cover and are varied spatially and temporally as appropriate according to the estimated or assumed time-dependent performance of a surface barrier.

- The specific formulation of the grout has not yet been established, and site-specific measurements of the chemical influence of the grout have not been performed. The chemical effect of the grout is represented by contaminant-specific distributions of distribution coefficients (K_d), which have been developed from international literature on sorption of radionuclides on cementitious materials. These values are generally consistent with, or more conservative than, comparable values used for the facility-specific grout at the Savannah River F and H tank farm PAs [WSRC-STI-2007-00369, "Hydraulic and Physical Properties of Tank Grouts and Base

Mat Surrogate Concrete for FTF Closure" and WSRC-STI-2007-00607, "Chemical Degradation Assessment of Cementitious Materials for the HLW Tank Closure Project (U)"].

- Inventories of contaminants in retrieved tanks are based on post-retrieval sampling and measurements. It is assumed that the sampling results are representative of the entire waste residuals. Inventories for tanks that have not yet completed retrieval use the best estimates of post-retrieval conditions available at this time. These data have been estimated as of September 30, 2014. Additional sensitivity cases executed based on alternative inventories in the 2009 to 2011 working sessions.

2.0 ASSESSMENT CONTEXT

The scope of the PA must be considered within the framework of the HFFACO (Ecology et al., 1989). Appendix I of the HFFACO contains language that broadened the scope of the PA. This definition by the regulatory agencies in Section 2.5 of Appendix I states:

> "Ecology, as the lead agency for SST system closure, EPA, and DOE have elected to develop and maintain as part of the SST system closure plan <u>one performance assessment</u> for the purposes of evaluating whether SST system closure conditions are protective of human health and the environment for <u>all contaminants of concern</u>, both radiological and non-radiological. DOE intends that this performance assessment (PA) will document by reference relevant performance requirements defined by RCRA, HWMA, *Clean Water Act*, *Safe Drinking Water Act*, and the *Atomic Energy Act of 1954* (AEA) and any other performance requirements that might be ARARs *[applicable or relevant and appropriate requirements]* under CERCLA. <u>The PA is of larger scope than a risk assessment</u> required solely for nonradiological contaminants. The PA is expected to provide a single source of information that DOE can use to satisfy potentially duplicative functional and/or documentation requirements. <u>A PA will be developed for each WMA</u> and will incorporate the latest information available. These PAs will be approved by Ecology and DOE pursuant to their respective authorities. For Ecology approval means incorporation by reference, into the Site-Wide Permit through the closure plans.
>
> As <u>individual components are retrieved or characterized</u>, or other component closure activities are completed, <u>the resulting component characterization information will be incorporated into the WMA PA</u> to <u>determine its relative risk compared to the entire WMA performance.</u> In doing this, the Parties will be able to make interim closure decisions for individual components. Initially, the WMAPA *[sic]* will be based on assumptions and available data describing component characterization information. As each WMA proceeds toward closure, its respective PA will be updated to address all pertinent new results and findings – and will, as a minimum, incorporate the following results as they become available: actual volumes of tank waste residuals left after retrieval, results of leak investigations, new geologic and ancillary equipment waste characterization information, and the results of new barrier and tank residual stabilization and fill performance studies and tests. <u>Final WMA closure decisions</u> will be made after <u>all components</u> are <u>retrieved and/or characterized</u>, and all other component <u>closure activities have been completed</u> and <u>a final WMA PA is completed.</u>"

Note: Underlining is added to emphasize key points in the scope of the HFFACO Appendix I PA.

Based on the regulatory requirements outlined above, the closure "performance assessment" as it is defined in HFFACO Appendix I will contain three major components, and is a broader

analysis than "performance assessment" as it is defined in DOE O 435.1. It is therefore important to distinguish between the two to avoid confusion about the term "performance assessment." For the purposes of this report, the term "Appendix I performance assessment" (IPA) will be used to refer to the HFFACO Appendix I analysis, whereas when the simpler term "performance assessment" (PA) is used, it will refer solely to the DOE M 435.1-1 definition of "performance assessment."

The three major components of the IPA include: (1) a baseline risk assessment that evaluates human and ecological risks for current environmental contamination conditions, (2) an assessment of a closed WMA C driven by the regulatory requirements of HFFACO Appendix I for hazardous constituents, and (3) a long-term PA on the fate and transport of radionuclide tank residuals in a closed WMA C driven by the regulatory requirements of DOE O 435.1. This third component of the IPA is the topic of this report, and will be supplemented by additional documents that detail the results of other two analysis components.

The baseline risk assessment, which is the first component of the IPA, presents the risks and hazard impacts from releases of radionuclides and hazardous substances to the environment from current contamination in the absence of any actions to control or mitigate these releases. Under either the CERCLA or RCRA Corrective Action processes, a baseline risk assessment is completed at contaminated waste sites prior to remediation activities to establish a need for action. A baseline risk assessment is also used by Ecology to determine cleanup levels and assess the performance of remedial actions against the Model Toxics Control Act (RCW 70.105D, "Hazardous Waste Cleanup — Model Toxics Control Act") cleanup levels (see WAC 173-340-740, "Unrestricted Land Use Soil Cleanup Standards"; WAC 173-340-745, "Soil Cleanup Standards for Industrial Properties"; and WAC 173-340-747, "Deriving Soil Concentrations for Groundwater Protection"). An initial version of the baseline risk assessment has been prepared (RPP-RPT-58329) to support the RCRA Facility Investigation of WMA C (RPP-RPT-58339). As this version of the baseline risk assessment is updated, it will be supplemented by results of an analysis of past leaks and releases at WMA C that will include a scoping analysis and forward projection of the potential radiological and hazardous chemical impacts from past leaks and releases into the future.

The second component of the WMA C IPA will be an initial assessment of long-term impacts of hazardous chemical constituents within the residual wastes in tanks and ancillary equipment left in a closed WMA C. This component of the IPA will be documented in a companion report to this current PA.

The third component of the IPA for WMA C is the PA required for radioactive constituents of the residual wastes in tanks and ancillary equipment in a closed WMA C under DOE O 435.1. This component is the sole focus of this report.

As identified in Section 1, this PA satisfies a part of the IPA requirements outlined in Appendix I of the HFFACO Action Plan. The PA is limited to the analyses of impacts from radiological waste constituents from residual wastes in tanks and ancillary equipment, which are anticipated to be left in WMA C after closure, and is expected to satisfy those requirements under DOE O 435.1.

This section on Assessment Context includes a description of performance objectives and performance measures along with the timing and locations for points of assessment. It is comprised of the following subsections:

- Public Protection Performance Objectives and Measures (Section 2.1)
- Point of Assessment Timing and Assumptions (Section 2.2)
- Assessment Period (Section 2.3)
- Modeling Approach (Section 2.4)
- Hypothetical Inadvertent Intrusion (Section 2.5)
- Reasonable Efforts To Minimize Releases (Section 2.6).

2.1 PUBLIC PROTECTION PERFORMANCE OBJECTIVES AND MEASURES

An extended discussion of the full set of HFFACO Appendix I regulatory requirements and other elements of the assessment context is presented in RPP-RPT-41918. The performance objectives under HFFACO Appendix I comprise a combination of DOE O 435.1, RCRA closure requirements, and Ecology requirements. For the current report, which is focused on the requirements of DOE O 435.1, a subset of these regulatory requirements is applicable. This subset of the overall requirements is shown in Table 2-1.

2.2 POINT OF ASSESSMENT AND TIMING ASSUMPTIONS

As previously identified, the TC&WM EIS ROD for landfill closure of SSTs was published in the Federal Register on December 13, 2013. For the landfill closure of WMA C, site closure is assumed to occur at year 2020, at which time the tanks are assumed to be filled with grout and covered with a final closure cover. The point of assessment and timing assumptions are consistent with the requirements of DOE O 435.1 and HFFACO. It is assumed for the purposes of this PA that institutional control and societal memory are retained for 100 years after the year of closure, based on the standard DOE O 435.1 requirement for inadvertent human intrusion. The point of assessment for all-pathways (i.e., combined doses for the groundwater and air pathways) and groundwater protection analyses is 100 m (328 ft) from the downgradient fenceline of WMA C per DOE G 435.1-1, Chapter IV – Low Level Waste Requirements. In order to ensure consistency in the assessment, hazardous chemicals will also be evaluated at this point in the companion report that addresses these requirements.

The concentrations used for comparison with the performance measures for water resource protection are the peak concentrations in groundwater at that distance from the facility, calculated across a spatial plane at 100 m (328 ft) downgradient of the facility fenceline. These concentrations are strictly applicable solely to the Ecology water resources performance objectives. Doses calculated for the all-pathways (i.e., combined groundwater and air pathways) performance objective apply to a point of exposure at which people might be exposed (i.e., at the wellhead of a pumping well) at 100 m downgradient of the facility fenceline. For consistency and simplicity, the peak concentrations in groundwater calculated for comparison with water resource protection are used as the concentration in the all-pathways analyses. Since taking

account of the well will only have a potential to dilute the groundwater concentrations, using peak groundwater concentrations would give similar or higher dose calculations compared to using wellhead concentrations.

Table 2-1. Exposure Scenarios, Performance Objectives and Measures, and Points of Assessment for the Waste Management Area C Performance Assessment.

Exposure Scenario	Performance Objective and Measures	Point of Assessment	
		Operational and Active Institutional Control Periods [a]	Post-Institutional Control Period
All-pathways [b]	25 mrem/yr [c]	Facility boundary	100 m (328 ft) [d]
Air pathway [b]	10 mrem/yr [c]	Facility boundary	100 m (328 ft) [d]
Radon [b]	20 pCi/m^2/s	Flux rate at facility surface	Flux rate at facility surface
	0.5 pCi/L [e]	Facility boundary	100 m (328 ft) [d]
Water resources	Washington Department of Ecology requirements on concentrations of radionuclides	At the source and 100 m (328 ft) [d]	100 m (328 ft) [d]
Intruder [b]	100 mrem/yr Chronic [c, f]	Not applicable	Facility
	500 mrem Acute [c, f]	Not applicable	Facility

[a] The active institutional control period includes final closure.
[b] Chapter IV – Low-Level Waste Requirements of DOE M 435.1-1, Radioactive Waste Management Manual.
[c] Excluding radon in air.
[d] The point of highest projected dose or concentration beyond a 100 m (328 ft) buffer zone surrounding the disposed waste. Additionally, concentrations found in tank residuals will be compared against the standard Model Toxics Control Act three-phase model.
[e] Alternative radon Performance Objective.
[f] Performance Measure.

Comparison with the radon performance objective has been evaluated using the surface flux criterion in Table 2-1, applied at the top of the disposal cover.

The intruder protection objective has been applied consistent with DOE O 435.1 principles and guidance. The facility has been evaluated for credible exposure situations, taking account of the facility design and local construction and drilling practices. The closed facility is assumed to remain under institutional control for a period of 100 years after closure, at which time control and memory of the facility is assumed to be lost, and potential inadvertent human intrusion can occur.

2.3 ASSESSMENT PERIOD

The DOE O 435.1 compliance time period for a PA is 1,000 years after closure. Longer time frames (10,000 years) are included in the analysis per NRC draft guidance[1] (NUREG-1854, NRC Staff Guidance for Activities Related to U.S. Department of Energy Waste Determinations – Draft Final Report for Interim Use, Section 4.1.1.1) and as a sensitivity and uncertainty analysis component per DOE O 435.1 to provide information to decision makers about potential long-term doses, but doses after 1,000 years need not be directly compared with performance objectives and measures of the DOE Order. The closed facility is assumed to remain under institutional control for a period of 100 years after closure, at which time control and memory of the facility is assumed to be lost. This assumption is applied primarily for the purpose of comparison with the performance measures related to inadvertent human intrusion in DOE O 435.1, and does not represent a DOE intent to release the facility in the future (see DOE P 454.1, Use of Institutional Controls).

2.4 MODELING APPROACH

This section provides an overview of the modeling approach for evaluation of 1) source-term release; 2) contaminant fate and transport along the groundwater pathway; 3) contaminant fate and transport along the air pathway; and 4) exposure and dose analysis. A schematic representation of this overall modeling approach is provided in Figure 2-1.

2.4.1 Source Term Release

For source-term release in the PA effort, contaminant release for the residual wastes and subsequent contaminant release for the grouted tank and ancillary equipment to the surrounding environment was performed using a system-level model based on GoldSim© using its contaminant transport module (see Figure 2-1). The source term considers processes associated with release of contaminants from residual waste into the natural environment. Separate source terms are considered for each of the twelve 100-series tanks, four 200-series tanks, C-301 catch tank, 244-CR vault, and pipelines, resulting in 19 separate source terms. The inventory used in the source term model includes the current estimate of the inventory and residual volume (see Section 3.2). Source terms for pits and diversion boxes are not explicitly considered but are incorporated as part of the pipeline source term.

Both mineral phase solubility-limited and matrix degradation rate-limited processes are considered for release of contaminant from the waste. These conceptual models are based on observations made through multi-year leaching tests and identification of mineral phases as

[1] On March 26, 2015, NRC issued a proposed revision to 10 CFR Part 61 and associated guidance on treatment of timeframes in performance assessment (80 FR 16082, "Low-Level Radioactive Waste Disposal"; NUREG-2175, Guidance for Conducting Technical Analyses for 10 CFR Part 61 – Draft Report for Comment). At this time these regulatory changes and associated guidance are in the public comment period, and are not completed. Consequently, they are not addressed in this report.

presented in Section 5. The following release mechanisms are considered based on experimental results:

- a matrix-degradation-rate-based release of ^{99}Tc, and
- solubility-controlled releases of uranium.

Figure 2-1. Schematically Overview of the Model Approach for the Waste Management Area C Performance Assessment.

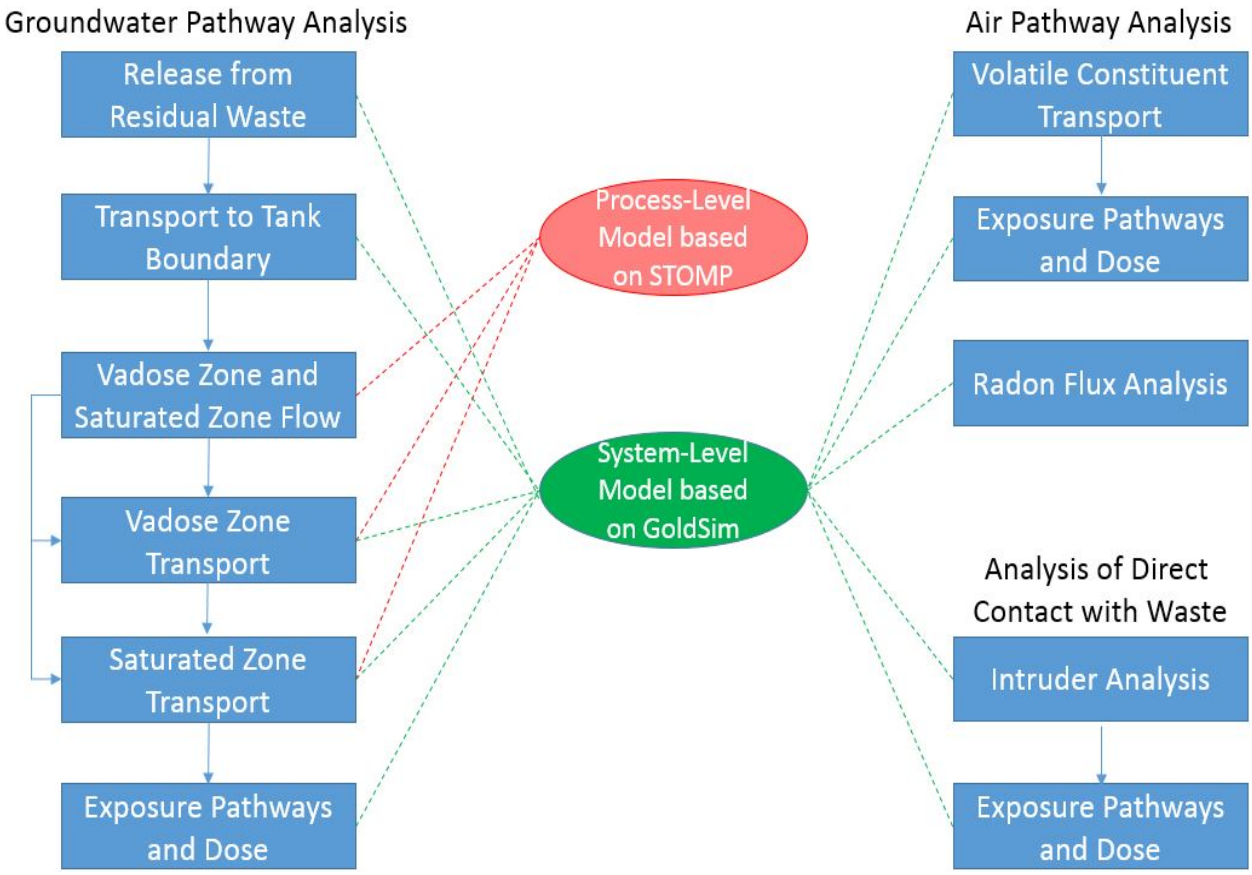

GoldSim© simulation software is copyrighted by GoldSim Technology Group LLC of Issaquah, Washington (see http://www.goldsim.com).
Subsurface Transport Over Multiple Phases (STOMP©) is copyrighted by Battelle Memorial Institute, 1996.

The source term processes that are considered in the post-closure period include releases of contaminants from residual waste, and their transport to the underlying vadose zone via either diffusion or advection out of the tank structures filled with grout and ancillary equipment.

The specific details of the conceptual and mathematical models of the source term release from the waste residuals into the surrounding environment as implemented in the system model based on GoldSim© are discussed in Sections 6.2.1 and 6.3.1, respectively.

2.4.2 Contaminant Fate and Transport along the Groundwater Pathway

For simulating contaminant fate and transport along groundwater, the PA is being conducted using complementary approaches, including both deterministic and probabilistic approaches (see Figure 2-2). Deterministic analyses use detailed representations of the geological system that are implemented in STOMP©, so that influences of relevant features and processes on water flow and radionuclide transport in groundwater can be evaluated. However, the model for evaluating flow requires significant computational time, limiting its ability to fully address parameter uncertainties using Monte Carlo analyses. As a result, the deterministic analyses are augmented using probabilistic analyses for an abstracted model of the groundwater system. The abstracted model, implemented in GoldSim©, will use probability density functions to represent the uncertainty in input parameters and demonstrate their influence on contaminant transport predictions. Consistency between the probabilistic GoldSim©-based system model and the physically-based STOMP© model is achieved through an abstraction process, in which the STOMP© flow fields are used as inputs to the GoldSim©-based model. This approach assures consistency between the flow field calculated using STOMP© and the flow field needed by GoldSim©.

Figure 2-2. Complimentary Use of Process-Level and System-Level Models for Groundwater Pathway in the Waste Management Area C Performance Assessment.

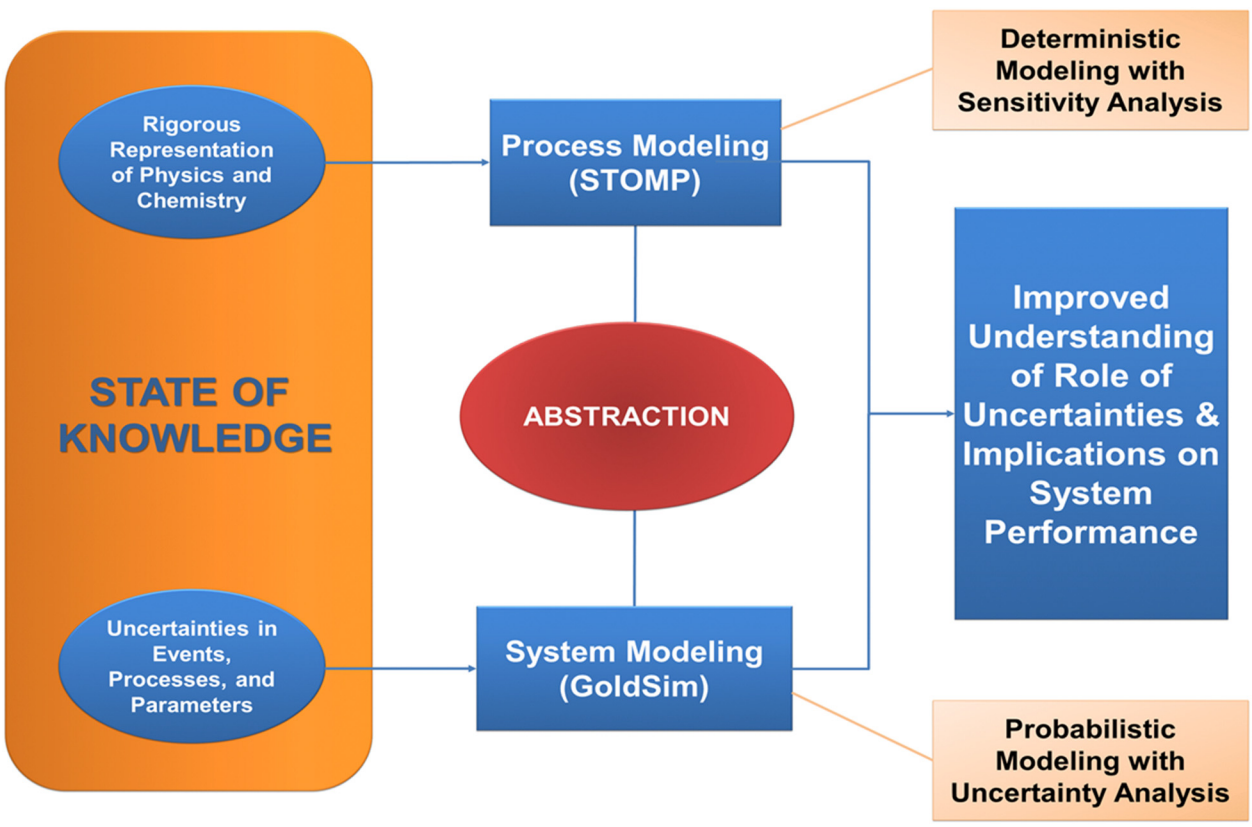

GoldSim© simulation software is copyrighted by GoldSim Technology Group LLC of Issaquah, Washington (see http://www.goldsim.com).
Subsurface Transport Over Multiple Phases (STOMP©) is copyrighted by Battelle Memorial Institute, 1996.

The abstraction approach assures that, for a specific set of input parameters for flow, the flow field in both models is consistent, differing only in the discretization of the two models. This approach is extended to support probabilistic analyses as follows. A set of STOMP© analyses are conducted for a discrete set of combinations of input parameters, selected to span the range of values in the input parameters. The outputs from these flow analyses are used to construct a response surface representation of the flow for the full range of input parameters. This response surface is constructed by interpolating between the STOMP©-calculated flow rates to give an approximation to the flow field for the full range of input parameters. The response surface is then used in the probabilistic analyses by sampling the input parameters, and using the response surface to represent the flow field for the sampled input parameters.

2.4.3 Contaminant Fate and Transport along the Air Pathway

For simulating contaminant fate and transport along the air pathway, the PA evaluates gases and vapors that could travel upward from the residual inventory within tanks and ancillary equipment through the surface barrier to the ground surface using the system-level model based on GoldSim© (see Figure 2-1). The principal mechanism by which nuclides migrate from the waste to the ground surface is gaseous diffusion. For tanks, in which the residual waste is predominantly on the bottom of the tank, this means that the gases are transported through the tank infill grout, the tank dome, the soil overburden, and the surface barrier. For pipelines, the diffusion would occur through the soil overburden and the surface barrier.

Releases to the atmospheric pathway and groundwater pathway begin at the start of the simulation. The partitioning of inventory into the aqueous and gaseous phase occurs within the source-term model (in the residual waste layer). The mass partitioned into the aqueous phase is then available for transport to the underlying vadose zone, while the partitioned fraction in the gas phase is available for upward transport to the atmosphere. Although diffusive path length for the gas phase can vary based on lateral movement, in order to maximize the flux, only the shortest vertical upward path length is considered. In addition, to maximize the upward transport through the gas phase, the downward flow of water above the residual waste location is not modeled. Any physical effect of surface barrier on gaseous flux is also ignored.

Of the radionuclides contained in residual inventory at closure (Section 3), four could potentially originate as gas:

- Carbon-14 as CO_2 gas
- Hydrogen-3 (tritium) as H_2 gas
- Iodine-129 as I_2 gas
- Radon-222 as radon gas.

A separate calculation, specific for radon using the GoldSim© system model, is used for comparisons with the performance objective of 20 $pCi/m^{-2}/s^{-1}$ for radon flux at the surface of the disposal facility.

The specific details of the conceptual and mathematical models of the contaminant fate and transport along the air pathway as implemented in the system model based on GoldSim© are discussed in Sections 6.2.2 and 6.3.2.5, respectively.

2.4.4 Exposure and Dose Analysis for Comparison with Performance Objectives

For the exposure and dose analysis performed, the PA effort examined the combined doses from the groundwater and air pathways dose that resulted in the all-pathways doses using the system-level model based on GoldSim© (see Figure 2-1).

To meet the DOE O 435.1 requirements, an all-pathways farmer scenario is implemented to calculate the total effective dose equivalent for comparison to the performance objective of 25 mrem, which is the total effective dose equivalent in a year from all exposure pathways, excluding the dose from radon and progeny in air. In this scenario, calculations are performed based on predicted radionuclide transport through the groundwater pathway and atmospheric pathway, and exposure at the point of contact.

For the groundwater pathway part of the all-pathways dose analysis, the assessment assumes the individual who receives dose is a Representative Person ("ICRP Publication 101a: Assessing Dose of the Representative Person for the Purpose of the Radiation Protection of the Public" [ICRP 2006]) who resides near the WMA C tank farm and draws contaminated water from a well downgradient of WMA C. The all-pathways Representative Person is assumed to use the water to drink, irrigate crops, and water livestock. The conceptual and mathematical models for the specific implementation of the dose analysis for the groundwater pathway in the system-level model based on GoldSim© is described in Sections 6.2.3 and 6.3.3.1, respectively.

For the atmospheric transport pathway, the following three exposure routes are considered for the receptor residing 100 m (328 ft) downgradient of the facility fenceline:

- Air immersion
- Inhalation of dust
- External exposure to radiation from the contaminated ground surface.

Calculation of the dose of the air pathway for purposes of comparison with the all-pathways and air pathway performance objectives considers the effects of releases of tritium, ^{14}C, and ^{129}I and specifically excludes the effects of radon and its progeny in air.

The conceptual and mathematical models for the specific implementation for the air pathway of the dose analysis in the system-level model based on GoldSim© are described in Sections 6.2.3 and 6.3.3.2, respectively.

2.5 HYPOTHETICAL INADVERTENT INTRUSION

To meet the DOE O 435.1 requirements, a hypothetical inadvertent intruder scenario is implemented to calculate the total effective dose equivalent for comparison to the performance

measure of 500 mrem for acute exposure and 100 mrem/yr for chronic exposures. These calculations have been implemented in the system-level model based on GoldSim© (see Figure 2-1).

Calculation in the PA takes account of the potential for future human actions resulting in inadvertent intrusion into WMA C after the assumed 100-year period of institutional control.

Protection of inadvertent intruders may be accomplished through one of several strategies. The combination of strategies is intended to ensure that adequate protection of the inadvertent intruder is achieved ("Safety assessment for near-surface disposal of low- and intermediate-level radioactive waste" [Kozak 2010]). These strategies are

- Depth of disposal,
- Institutional controls,
- Control of waste concentrations, and
- Intruder barriers.

The combination of these strategies is used to minimize the likelihood of an intrusion event occurring, or to minimize the consequences of the intrusion event should it occur. The end state of WMA C contains features that support all four of these strategies for protection of the inadvertent intruder.

Controlling the depth of disposal has long been a key parameter for evaluating intrusion scenarios. The NRC, in its development of its regulation for near-surface disposal (10 CFR 61) examined a number of alternative ways in which an inadvertent human intruder might disrupt a waste trench (NUREG/CR-4370, Update of Part 61 Impacts Analysis Methodology). An underlying concept in the NRC analyses is that the number of potential types of intrusion activities that could result in an inadvertent human intrusion decreases quickly with depth, and that therefore the likelihood of an intrusion event decreases with depth. In the requirements for disposal of Class C waste established in 10 CFR 61.55, this concept was made explicit: Class C waste "must be disposed of so that the top of the waste is a minimum of 5 meters below the top surface of the cover or must be disposed of with intruder barriers that are designed to protect against an inadvertent intrusion for a least 500 years." [10 CFR 61, Subpart D, § 61.52, Land disposal facility operation and disposal site closure, subsection (a)(2)].

This concept was also made explicit in international guidance by the Nuclear Energy Agency of the Organisation for Economic Co-operation and Development (OECD) ("Shallow Land Disposal of Radioactive Waste: Reference Levels for Acceptance of Long-Lived Radionuclides" [NEA 1987]), who introduced the concept of the "normal residential intrusion zone (NRIZ)," which represented the depth of a foundation of a residential home. This zone was stated nominally to be about 3 m (10 ft) deep, but which could vary according to site-specific considerations. This approach was intended to account, to a certain extent, for the effect introduced by differing depths for excavating foundations in different locations.

The current conceptual design of the Modified RCRA Subtitle C Barrier is based on DOE/RL-93-33, Focused Feasibility Study of Engineered Barriers for Waste Management Units

in the 200 Areas. The modified RCRA Subtitle C Barrier design described by DOE/RL-93-33 provides 1.7 m (5.6 ft) of depth in its basic design. However, on page 3-10 of DOE/RL-93-33, it is noted that to meet Class C depth of disposal requirements, "the thicknesses of one or more of the barrier layers (e.g., grading fill [Layer 8] or topsoil [Layers 1 and/or 2]) could be modified (i.e., increased) to conform to" a 5 m (16.4 ft) depth. Therefore, consistent with these design considerations, for the purposes of this PA, it is assumed that the modified RCRA Subtitle C barrier is designed to provide at least 5 m (16.4 ft) depth to the top-most waste zone in the closed configuration.

The closed tank farm has several additional features that will act to deter intrusion. The tank dome materials are reinforced concrete and exhibit only minor degradation (see RPP-RPT-50934, "Inspection and Test Report for the Removed 241-C-107 Dome Concrete" and RPP-RPT-58254, "Concrete Core Testing Report for the Single-Shell Tank 241-A-106 Sidewall Coring Project"), so they retain substantial strength to resist an intrusion event. Similarly, the infill grout that will be added to the tanks in the closure process will have substantial structural strength and the ability to resist intrusion. These features of the system make intrusion into tank residuals very unlikely. Furthermore, intrusion into ancillary equipment would produce similar or greater consequences to intrusion into tank waste. Consequently, the primary focus for intrusion into WMA C considers an intrusion event into ancillary equipment. Intrusion into tank wastes will be considered only as a sensitivity analysis for comparison with intrusion into ancillary equipment.

Based on these considerations, the following approach is taken to evaluating inadvertent human intrusion.

- The only credible intrusion event is a drilling event. Depth of disposal together with concrete and grout intrusion barriers limit the types of events that may be considered credible.

- The intrusion is assumed to be into the ancillary equipment rather than a tank. This type of event is more credible than a tank intrusion, since the tank dome and grout form a substantial intruder protection barrier.

- The driller is assumed to penetrate a 7.6-cm (3-in.)-diameter waste transfer pipeline that is assumed to be 5% full of waste.

- The drilling event is assumed to occur any time after 100 years post-closure.

- The acute exposure to the driller is calculated using assumptions about the duration of the drilling based on present day drilling methods at the Hanford Site.

The conceptual and calculational models for the specific implementation for the acute and chronic hypothetical inadvertent intruder scenarios in the system-level model based on GoldSim© are described in Section 9.2 and 9.3, respectively.

2.6 REASONABLE EFFORTS TO MINIMIZE RELEASES

DOE O 458.1, Radiation Protection of the Public and the Environment requires the application of a graded approach to consider optimization of the disposal system to keep doses to members of the public ALARA. A feature of DOE O 435.1 compared to earlier DOE Orders is the removal of specific performance objectives for ALARA based on the view that, for disposal, ALARA is a process to reduce potential doses to the public that is not amenable to numerical criteria to limit releases (National Council on Radiation Protection [NCRP] Report No. 152, "Performance Assessment of Near-Surface Facilities for Disposal of Low-Level Radioactive Waste"). Since numerical ALARA is not directly applicable to post-closure conditions of a closed disposal facility, the evaluation should instead address whether reasonable efforts have been made to minimize post-closure releases from the facility.

For WMA C, the process to minimize releases to the extent practicable is an intrinsic part of the retrieval and closure processes. The established retrieval criteria for SSTs are as defined in the HFFACO, Milestone M-045-00:

> "Closure will follow retrieval of as much tank waste as technically possible, with tank waste residues not to exceed *[10.2 m^3]* 360 cubic feet (cu. ft.) in each of the 100 series tanks, *[0.8 m^3]* 30 cu. ft. in each of the 200 series tanks, or the limit of waste retrieval technology capability, whichever is less. If the DOE believes that waste retrieval to these levels is not possible for a tank, then DOE will submit a detailed explanation to EPA and Ecology explaining why these levels cannot be achieved, and specifying the quantities of waste that the DOE proposes to leave in the tank. The request will be approved or disapproved by EPA and Ecology on a tank-by-tank basis."

When DOE completes retrieval of waste from a tank, DOE provides documentation to Ecology, known as a Retrieval Completion Certification (RCC), that DOE has completed retrieval of that tank. The RCC describes the technological approaches used to remove waste to the extent practicable. Therefore, the efforts to minimize releases from the closed facility using retrieval of waste are extensively documented and go through a regulatory review and approval process.

In addition to retrieval, releases from the facility can be minimized using design and closure methods. Alternative methods for closing the SSTs were evaluated as part of the scope of the TC&WM EIS (DOE/EIS-0391). Under the Tank Closure Alternatives, DOE evaluated each of the primary tank closure components, specifically, storage, retrieval, treatment, and disposal of tank waste and closure of the SST system. The TC&WM EIS considered a number of alternative options for retrieval, treatment, and closure of the SSTs. Specifically for residual wastes, these alternatives considered several possible approaches for SST closure, with an associated range of implications for long-term releases from the closed WMA C, as follows.

- Alternative 1: No action alternative.

- Alternative 2a: Retrieval of 99% of waste from the SSTs. The SST system would not be closed.

- Alternatives 2b, 3, and 6c: Retrieval of 99% of waste from the SSTs. Landfill closure of all SSTs under RCRA with the SSTs covered with an engineered, modified RCRA Subtitle C barrier designed to provide 500-year protection. Under these alternatives, contaminated soil would be removed down to 4.6 m (15 ft) at the 241-BX and 241-SX Tank Farms and replaced with clean soil from onsite sources. The 4.6-m (15-ft) depth would allow removal of some of the ancillary equipment prior to closure.

- Alternative 4: Retrieval of 99.9% of the waste from the SSTs. Selective clean closure of 241-BX and 241-SX Tank Farms, which means the tanks, ancillary equipment, and contaminated soil would be removed, and the remaining tank farms (including WMA C) would be closed as landfills and covered with an engineered, modified RCRA Subtitle C barrier.

- Alternative 5: Retrieval of 90% of the waste from the SSTs. The SST system would be closed as a landfill and covered with an engineered Hanford barrier, a multi-layer barrier designed to provide 1,000-year protection.

- Alternatives 6a and 6b: Retrieval of 99.9% of the waste from the SSTs. The SST system would be clean closed. Here, clean closure meant the removal or remediation of all hazardous waste such that further regulatory control under RCRA is not necessary.

Alternative 2b was selected as the preferred option in a ROD resulting from the EIS consideration of these options (78 FR 75913). By evaluating these alternatives, DOE has demonstrated reasonable efforts to minimize releases associated with the end state of WMA C.

This page intentionally left blank.

3.0 SITE AND FACILITY CHARACTERISTICS

This section provides descriptive information relevant to the WMA C site, environment, and facility to provide the basis for a conceptual model of how radionuclides and hazardous chemicals may be released following closure of the WMA. The organization of this section was taken from Performance Assessment Annotated Outline for Chapter Four given in DOE-STD-XXX, Radioactive Waste Management Disposal Authorization Statement Technical Basis Documentation Technical Standard. It is comparable to the information found in Chapter 3 "Physical Characteristics of the Study Area" in the more recent remedial investigations/feasibility studies (RI/FSs) (e.g., DOE/RL-2010-97, Remedial Investigation/ Feasibility Study for the 100-KR-1, 100-KR-2, and 100-KR-4 Operable Units, Draft A).

The assessment of radionuclide and hazardous chemical transport from WMA C and the resulting human exposure from release of those contaminants into the environment requires careful consideration of factors affecting transport processes and the potential for exposure. Topographic features and hydrogeologic characteristics strongly affect the fate and transport of contaminants potentially released from the closed site. Projected land use and population distributions affect the estimation of impacts from human exposure. Facility features control how contaminants would be released and the rate at which they are released from the facility. The waste inventory, concentration, volume, and form affect the magnitude and rate of constituent releases from the source term. Each of these topics is discussed in the following sections.

3.1 SITE CHARACTERISTICS

The relevant natural and demographic characteristics and data for WMA C and the surrounding area are given in this section. The purpose of this information is to provide basis for the site conceptual model and method of analysis in sufficient detail to support the PA required by HFFACO (Ecology et al. 1989) Appendix I Section 2.5. Detailed information on the topics given in this section can be found in the data packages produced for the WMA C PA scoping session meetings that took place from May 2009 through May of 2011, as well as new characterization documents that have been released since the end of the scoping sessions. References to the detailed information are provided in the summary descriptions. A listing of the scoping sessions and associated data packages are given in the Introduction and Appendix A.

3.1.1 Geography and Demography

This section describes the geography and demography of the Hanford Site, including a description of the use of adjacent lands, the current population database, the socioeconomics of the area, past and planned DOE activities, and the results of an investigation of future uses conducted for inclusion in the "Final Hanford Comprehensive Land-Use Plan Environmental Impact Statement" and associated ROD (DOE/EIS-0222-F, 64 FR 61615). Additional detailed information on the geography and demography of the site can be found in Revision 18 of PNNL-6415, "Hanford Site National Environmental Policy Act (NEPA) Characterization."

3.1.1.1 Site Location

3.1.1.1.1 Hanford Site. The Hanford Site encompasses ~1,517 km² (~586 mi^2) in Benton, Franklin, and Grant Counties, located in south-central Washington State (Figure 3-1) within the semi-arid Pasco Basin of the Columbia Plateau. Nearby towns are Richland (40 km [25 mi] to the southeast) and Yakima (80 km [50 mi] to the west), with the nearby major metropolitan areas being Spokane (201 km [125 mi] to the northeast), Seattle (241 km [150 mi] to the northwest) and Portland, Oregon (~400 km [~250 mi] downstream on the Columbia River). The Hanford Site stretches ~48 km (~30 mi) north to south and ~38 km (~24 mi) east to west, immediately north-northwest of the confluence of the Yakima and Columbia Rivers, the Cities of Kennewick, Pasco, and Richland (the Tri-Cities), and the City of West Richland.

The Columbia River flows eastward through the northern part of the Hanford Site and then turns south, forming part of the eastern Site boundary. This section of the river is known as the Hanford Reach and is a free-flowing section of the Columbia River, ~82 km (~51 mi) long. It is named after a large northward bend in the river's otherwise southbound course. It is the only section of the Columbia River in the U.S. that is neither tidal nor part of a reservoir. The following seven dams are upstream of the Hanford Site and are listed from closest to furthest from Hanford: Priest Rapids, Wanapum, Rocky Island, Rocky Reach, Wells, Chief Joseph, and Grand Coulee. Other important rivers near the Hanford Site are the Yakima River to the south and southwest and the Snake River to the east. The Cascade Mountains, which are ~160 km (100 mi) to the west, have an important effect on the climate of the area.

The Yakima River runs near the southern boundary of the Hanford Site, joining the Columbia River at the City of Richland. Rattlesnake Mountain, Yakima Ridge, and Umtanum Ridge form the southwestern and western boundaries of the Site, and Saddle Mountain forms its northern boundary. The plateau of the central portion of the Hanford Site is punctuated by two small east-west ridges, Gable Butte and Gable Mountain. Lands adjoining the Hanford Site to the west, north, and east are principally range and agricultural areas.

3.1.1.1.2 Waste Management Area C. Waste Management Area C is one of 12 SST farms that were built from 1943 to 1962 and designed to store and transfer mixed waste generated as a part of Hanford Site operations. A complete description of WMA C is given in Section 3.2 Facility Design and Operational Features. It is located within the Hanford Site in the east central portion of the 200 East Area (Figures 3-1 and 3-2). The WMA C boundary is represented by the fenceline surrounding C Farm (Figure 3-3), which encloses an area of ~3.4 hectares (~8.5 acres). In Figure 3-3, the waste transfer pipelines emanating out of the diversion boxes have been color coded to the diversion box, thereby allow the reader to follow the pipelines and associated connections. Waste Management Area C is located 11.3 km (7 mi) west of the Columbia River, with the groundwater gradient toward the Columbia River.

Figure 3-1. U.S. Department of Energy's Hanford Site and Surrounding Area.

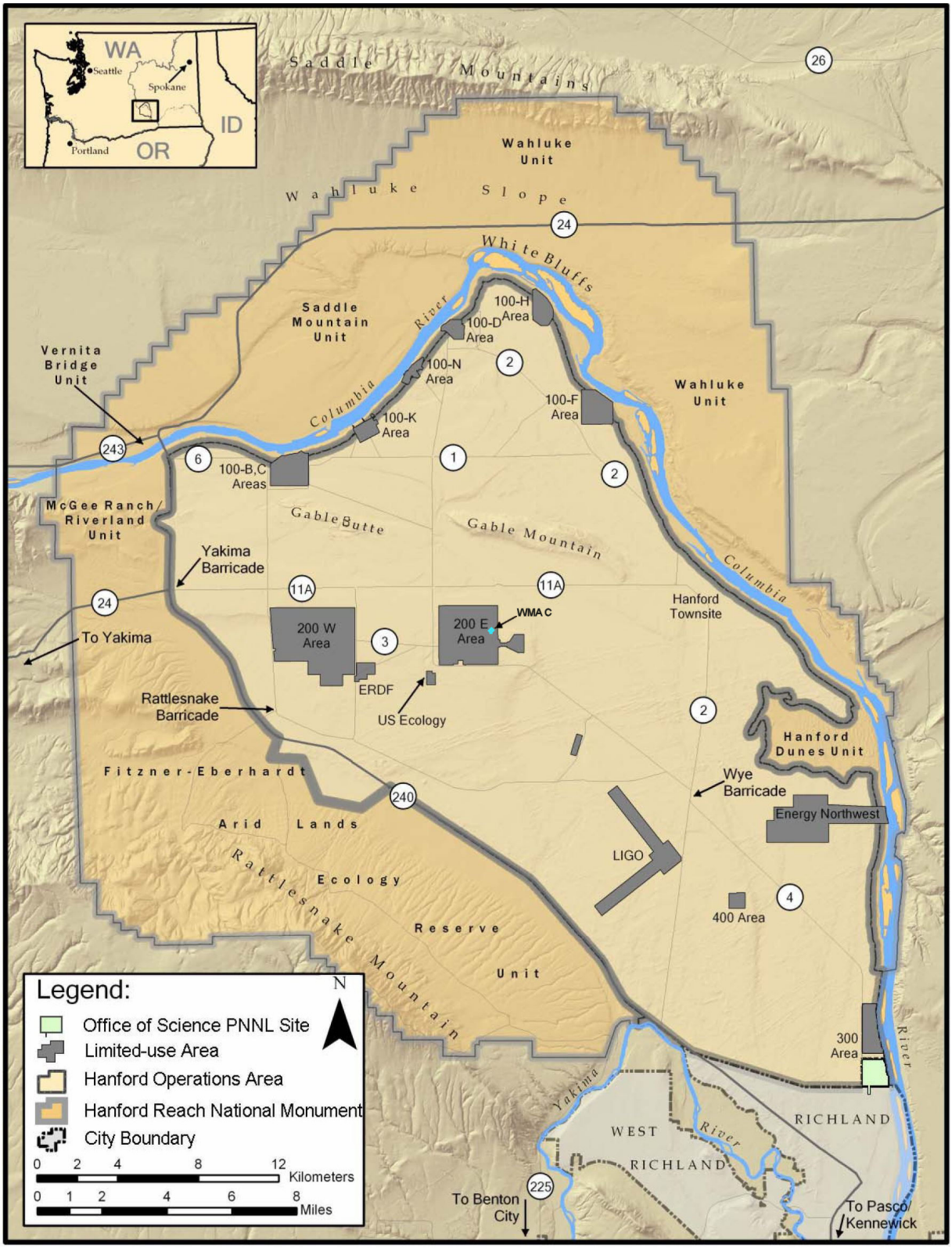

ERDF = Environmental Restoration Disposal Facility
LIGO = Laser Interferometer Gravitational Wave Observatory
PNNL = Pacific Northwest National Laboratory
WMA = Waste Management Area

Figure 3-2. Facilities in the 200 East and 200 West Areas.

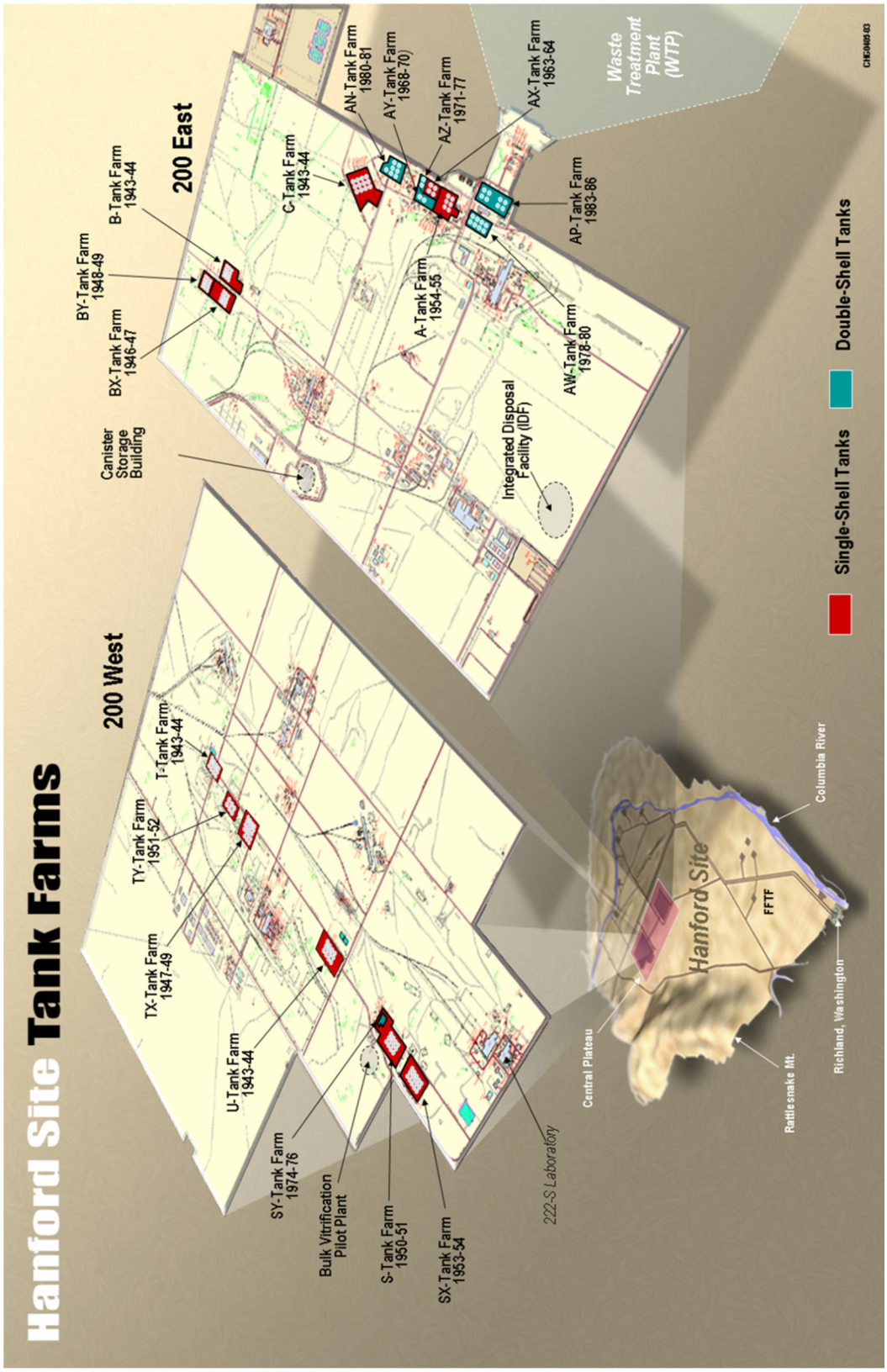

FFTF = Fast Flux Test Facility

Figure 3-3. Waste Management Area C Tanks and Associated Infrastructure.

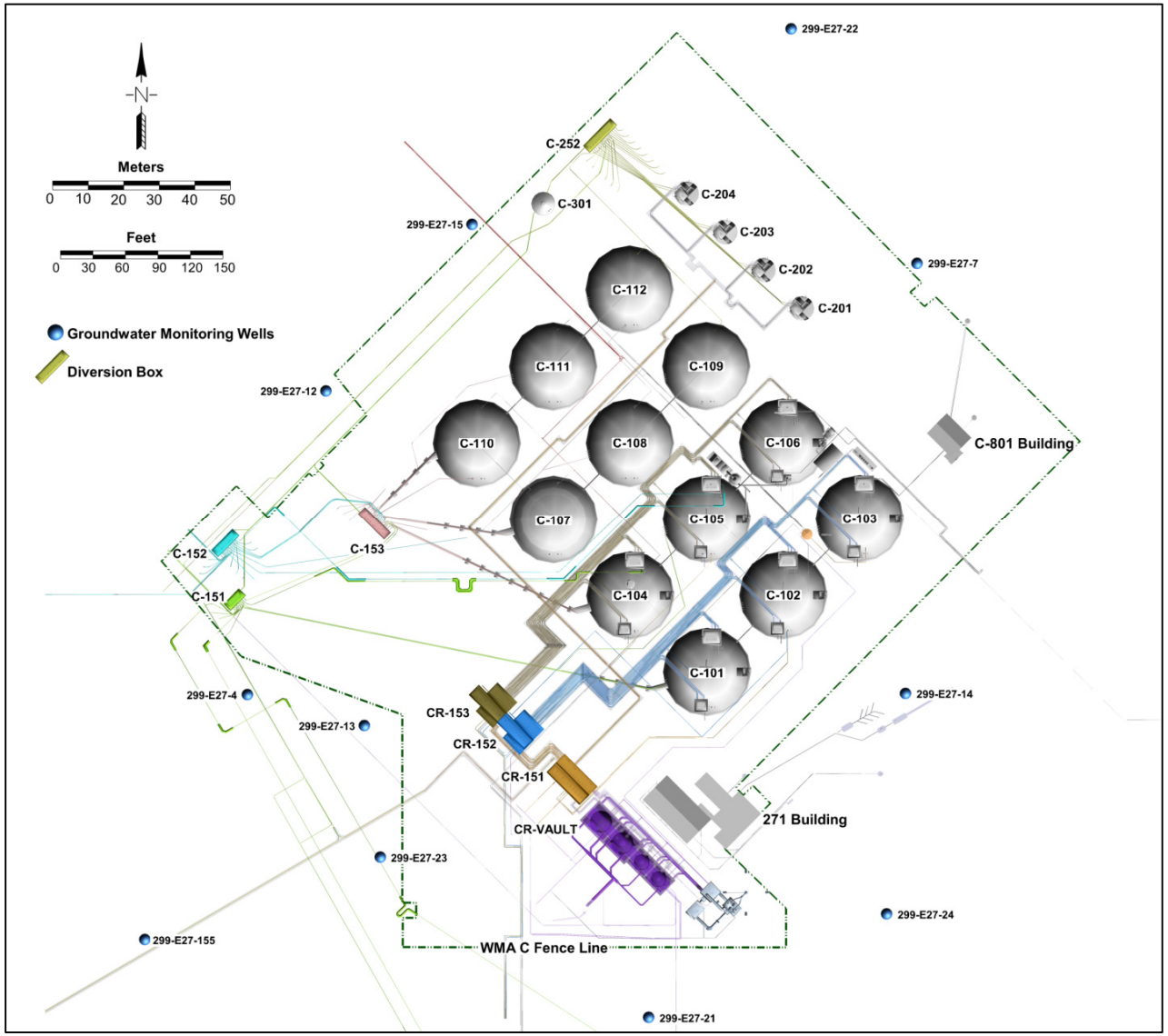

WMA = Waste Management Area

3.1.1.2 Site Description

3.1.1.2.1 Hanford Site Description. The Hanford Site is a relatively undeveloped area of shrub-steppe (a drought-resistant, shrub and grassland ecosystem) that contains a rich diversity of plant and animal species. This area has been protected from disturbance, except for fire, over the past 60 years. This protection has allowed plant species and communities that have been displaced by agriculture and development in other parts of the Columbia Basin to thrive at the Hanford Site.

In the past, the Hanford Site was a U.S. Government defense materials production site that included nuclear reactor operation; uranium and plutonium processing; the storage and processing of spent nuclear fuel (SNF); and the management of radioactive and hazardous chemical wastes. The current mission at Hanford includes managing waste products, cleaning up the site, researching new ideas and technologies for waste disposal and cleanup, and reducing the size of the site [PNNL-20548, "Hanford Site Environmental Report for Calendar Year 2010 (Including Some Early 2011 Information)," page v.]. Present Hanford programs are diversified and include the management of radioactive waste, cleanup of waste sites and soil and groundwater contaminated by past waste releases, stabilization and storage of SNF, research into renewable energy and waste disposal technologies, cleanup of contamination, and stabilization and storage of plutonium.

Hanford is owned and used primarily by DOE, but portions of it are owned, leased, or administered by other Government agencies. Public access to the Site is limited to travel on the Route 4 and Route 10 access roads as far as the Wye Barricade, State Routes 24 and 240, and the Columbia River. By restriction of access, the public is shielded from portions of the Site formerly used for the production of nuclear materials and currently used for waste storage and disposal. Only ~6% of the land area has been disturbed and is actively used, leaving mostly vacant land with widely scattered facilities (Revision 17 of PNNL-6415, page 4.144). Figure 3-4 shows the generalized land use at Hanford as developed in the "Final Hanford Comprehensive Land-Use Plan Environmental Impact Statement" (DOE/EIS-0222-F, 64 FR 61615) and modified by the designation of the Hanford Reach National Monument (65 FR 37253, "Establishment of the Hanford Reach National Monument").

In June 2000, a Presidential proclamation (65 FR 37253) established the 78,914-hectare (195,000-acre) Hanford Reach National Monument to protect the nation's only un-impounded stretch of the Columbia River above Bonneville Dam and the largest remnant of the shrub-steppe ecosystem that once blanketed the Columbia River Basin. In 2003, DOE and the U.S. Fish and Wildlife Service began management of the monument. The U.S. Fish and Wildlife Service administered three major management units of the monument totaling ~668 km² (~258 mi^2). These included (1) the Fitzner/Eberhardt Arid Lands Ecology Reserve Unit, a 310-km² (120-mi^2) tract of land in the southwestern portion of the Hanford Site; (2) the Saddle Mountain Unit, a 129-km² (50-mi^2) tract of land located north-northwest of the Columbia River and generally south and east of State Highway 24; and (3) the Wahluke Unit, an 225-km² (87-mi^2) tract of land located north and east of both the Columbia River and the Saddle Mountain Unit.

Figure 3-4. Generalized Land Use of the Hanford Site and Adjacent Areas.

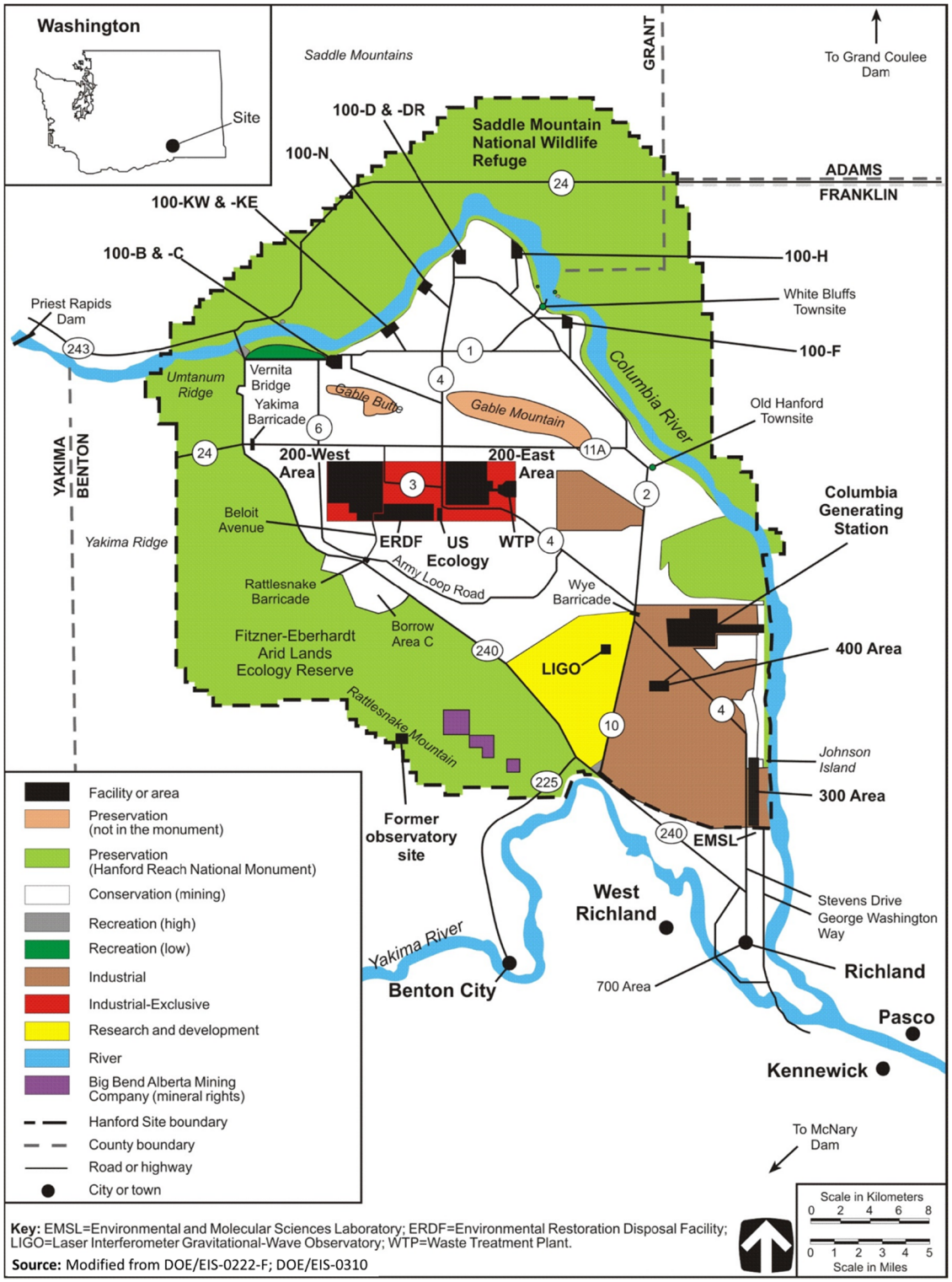

References:

DOE/EIS-0222-F, "Final Hanford Comprehensive Land-Use Plan Environmental Impact Statement."

DOE/EIS-0310, "Final Programmatic Environmental Impact Statement for Accomplishing Expanded Civilian Nuclear Energy Research and Development and Isotope Production Missions in the United States, Including the Role of the Fast Flux Test Facility."

3.1.1.2.2 Waste Management Area C. This section provides a summary description of WMA C (Section 3.2 provides a complete detailed description of the WMA). Waste Management Area C is one of 12 tank farms that make up the SST system. The Hanford Site SST system consists of 149 underground SSTs and processing equipment, and was designed and constructed between 1940 and 1964 to transport and store radioactive and hazardous chemical wastes generated from reprocessing spent nuclear fuel. One of the first tank farms built, WMA C was constructed in 1944 and 1945.

The WMA C contains twelve 100-series tanks and four 200-series tanks (see Figure 3-4). The 100-series tanks are 23 m (75 ft) in diameter, have a 5-m (15-ft) operating depth, and have an operating capacity of 2,006,000 L (530,000 gal) each. The 200-series tanks are 6 m (20 ft) in diameter with a 7.32-m (24-ft) operating depth and an operating capacity of 208,000 L (55,000 gal) each. Other specific details of these tanks are provided in Sections 1.3 and 3.2. The transfer and storage of waste within WMA C SSTs was supported by a complex waste transfer system of pipelines (waste transfer lines), diversion boxes, vaults, valve pits, and other miscellaneous structures.

Additionally, 14 UPRs have occurred within or near to WMA C. The largest ones are associated with releases from pipelines or diversion boxes, with releases from inlet/outlet ports of the SSTs, or with leaks from the SSTs. RPP-PLAN-39114 and RPP-RPT-58339 provide more detail on these UPR sites. Evaluation of these UPRs is outside the scope of the current PA analysis; but rather, will be addressed through the RCRA Corrective Action process.

3.1.1.3 Population Distribution. Demographic data are used within a performance assessment to help set the exposure scenarios for assessing dose/risk and to select dosimetry parameters. The population data for Washington is for April 1, 2014 from Office of Financial Management (OFM) April 1 Official Population Estimates (State of Washington Office of Financial Management, Queried 05/17/2015, [April 1 official population estimates], http://www.ofm.wa.gov/pop/april1/default.asp). The population data for Oregon are from the Population Research Center at Portland State University, which provides the official post-census estimate of population numbers for Oregon and are used to disburse State revenues to Oregon counties and cities. The estimates were published April 15, 2014 for the July 1, 2013 populations (Portland State University College of Urban & Public Affairs: Population Research Center, Queried 05/17/2015, [Population Estimates and Reports], http://www.pdx.edu/prc/population-reports-estimates).

The major population centers within an 80-km (50-mi) radius of the Hanford Site are shown in Figure 3-5, along with their estimated 2013 to 2014 populations. The 80-km (50-mi) radius is centered on the Hanford Meteorological Station (HMS), located ~1.7 km (~1.0 mi) east of WMA T in the 200 West Area, and 6.6 km (4.1 mi) west of WMA C. Portions of Benton, Franklin, Adams, Grant, Kittitas, Yakima, Klickitat, and Walla Walla Counties in Washington, and Morrow and Umatilla Counties in Oregon, lie within the 80-km (50-mi) radius. Most of the people reside in the counties of Benton and Franklin, which are two of the fastest growing counties in Washington with rates of growth during the 2000s of 23% and 58%, respectively. From 2010 to April 1, 2014, Benton and Franklin counties continue to be the fastest-growing counties in the State with rates of growth of 6.5% and 10.8%, respectively.

Figure 3-5. Population Centers with Estimated Population within 80 kilometers (50 miles) of the Hanford Meteorological Station.

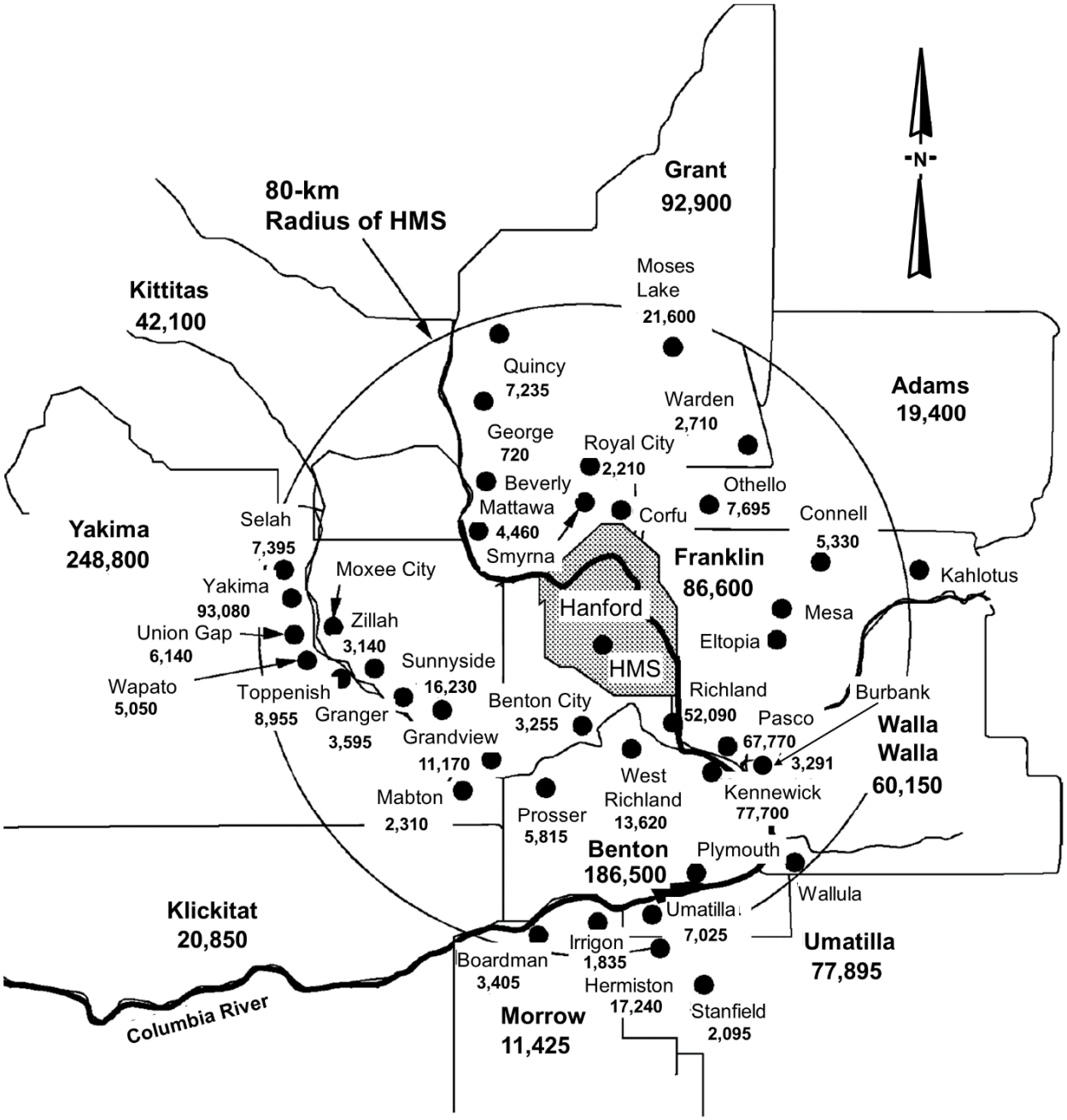

Note: If population not listed, less than 1,000
Data: Washington State April 2014, Oregon July 2013
HMS = Hanford Meteorological Station

The largest population center within the 80-km (50-mi) radius of the site is the Tri-Cities (i.e., Richland, Kennewick, and Pasco), located ~40 km (~25 mi) to the southeast of HMS for Richland, and 56 km (35 mi) to the southeast of HMS for Kennewick and Pasco. Other major population centers include Moses Lake, 64 km (40 mi) to the north-northeast of HMS; Yakima,

69 km (43 mi) to the west of HMS; and Umatilla, 75 km (47 mi) to the south-southeast of HMS. The Washington cities of Ellensburg and Walla Walla lie just beyond the 80-km (50-mi) radius.

In 2010, ~586,500 people resided within 80 km (50 mi) of the HMS (PNNL-20631, "Hanford Site Regional Population-2010 Census"). This total represents an increase in population of 29% from 1990 to 2000 and 21% from 2000 to 2010 (PNNL-20631). Because WMA C's location is near the center of the Hanford Site, the resident population within 16 km (10 mi) is estimated to be only 15, and 13,000 within 32 km (20 mi) (PNNL-20631). About 186,000 people, located mostly to the southwest and the southeast, live between 32 and 48 km (20 and 30 mi) from WMA C (PNNL-20631). The population has grown since 2010.

3.1.1.4 Uses of Adjacent Lands. This section describes the socioeconomics of the region, historical use of the land, and the expected future use of the land.

3.1.1.4.1 Socioeconomics. The principal driving forces of the Tri-Cities' economy since the early 1970s are: 1) DOE and its contractors operating the Hanford Site; 2) Energy Northwest (formerly the Washington Public Power Supply System) which operates a nuclear power plant just north of Richland; and 3) the agricultural community, including a substantial food-processing component. Although DOE activities, agriculture and food processing are the dominant industries, there has been a substantial rise in the number of visitors to the Tri-Cities over the last several years resulting in tourism playing an increasing role in helping to diversify and stabilize the area's economy. Overall tourism expenditures for 2011 were $393 million, up from $299 million in 2005. The socioeconomics of the area surrounding the Hanford Site are more fully described in Section 4.7 of PNNL-6415.

The land use classification around the Hanford Site varies from urban to rural. Most of the land south of the Hanford Site is urban, including the Tri-Cities, while much of the land to the north and east is irrigated crop land. Most of the irrigation water comes from the Bureau of Reclamation Columbia Basin Project, which uses the water behind Grand Coulee Dam (e.g., Roosevelt and Banks Reservoirs) as the primary water source. The water is transported via canals to the areas north and east of the Columbia River. The land to the west of the Hanford Site is used for irrigated agriculture near the Yakima River and dry-land farming at the higher elevations. The Columbia River is used by the cities of Richland, Pasco, and Kennewick for drinking water. It is used to transport numerous grains and other agricultural-related commodities by barge and similar means. It is also used for recreation and hydroelectric power production for the western United States.

Additionally, the Hanford Reach contains islands, riffles, gravel bars, oxbow ponds, and backwater sloughs that support some of the most productive salmon spawning areas in the Northwest, including the largest remaining stock of wild fall chinook salmon in the Columbia Basin. The loss of other spawning grounds on the Columbia and its tributaries has increased the importance of the Hanford Reach's fisheries.

3.1.1.4.2 Early Historical Use of the Land. In prehistoric and early historic times, American Indians of various tribal affiliations heavily populated the Hanford Reach, and some of their descendants still live in the region. Present-day tribal members retain traditional secular and

religious ties to the region, and many have knowledge of the ceremonies and lifestyles of their culture. The Washani, or Seven Drums religion, which has ancient roots, is still practiced by many American Indians. Native plant and animal foods, some of which can be found at Hanford, are used in ceremonies performed by tribal members (DOE/EIS-0310, "Final Programmatic Environmental Impact Statement for Accomplishing Expanded Civilian Nuclear Energy Research and Development and Isotope Production Missions in the United States, Including the Role of the Fast Flux Test Facility," pages 3-125).

Significant non-Indian settlement of the region began relatively late. In 1888, small irrigation companies and farmer cooperatives began to develop irrigation systems in the Columbia Basin. The agricultural economy of the region saw upswings and downswings, from agricultural price increases during World Wars I and II, drought during the 1920s, and the Great Depression during the 1930s. While, principally, non-Indian farmers lived on the adjacent private lands, members of the Wanapum Band continued to reside on portions of the future Hanford Site that remained in Federal ownership. In 1942, ~19,000 people lived in Benton and Franklin counties. Pasco was the largest population center, with ~3,900 people (WHC-MR-0293, "Legend and Legacy: Fifty Years of Defense Production at the Hanford Site"). The City of Richland had a population of ~200 people (Drummers and Dreamers [Relander 1956]).

In the early 1940s, almost all of the land that would at some time be considered part of the Hanford Site was being used for crops or grazing. More than 88% (~152,971 hectares [378,000 acres]) was sagebrush range land interspersed with volcanic outcroppings, where some 18,000 to 20,000 sheep grazed during winter and spring. Some 11% (almost 19,830 hectares [49,000 acres]) was farmland, much of it irrigable but not all under cultivation. Less than 1% (less than 809 hectares [2,000 acres]) consisted of town plots, right of ways, school sites, cemeteries, and similarly used land, most of it in or near the three small communities of Richland, Hanford, and White Bluffs (United States Army in World War II, Special Studies -- Manhattan: The Army and the Atomic Bomb [Jones 1985]).

3.1.1.4.3 Past and Present U.S. Department of Energy Activities at the Hanford Site. In 1943, the Hanford Engineer Works was established as one of the three original Manhattan Project sites and USACE began construction of the Hanford Site to produce plutonium for national defense. It was the first nuclear production facility in the world. The region was selected because of its remoteness and because it had abundant electrical power from Grand Coulee Dam (located ~230 mi [~370 km] upstream from the old Hanford town site), a functional railroad, clean water from the Columbia River, and available sand and gravel for construction. The USACE divided the site into a number of operational areas which are briefly summarized below (for more information on the description of each operational area, please see PNNL-6415, Revision 18 or DOE/EIS-0391).

- **100 Areas:** These areas of the Site are situated along the shore of the Columbia River in the northern portion of the Site and contain nine retired nuclear reactors. The irradiated fuel produced in the 100 Areas reactors was transported by rail to the 200 Areas.

- **200 Areas:** Fuel reprocessing, plutonium and uranium separation, plutonium finishing, and waste management including treatment, storage, and disposal activities, have been

conducted in the 200 Areas. Waste from the research and development activities and fuel fabrication activities in the 300 Area, reactor operation programs conducted in the 100 Areas, and FFTF in the 400 Area is sent to the 200 Areas for storage and disposal. Waste management activities are scheduled to continue until the mid-21st century. Waste management facilities are located in the 200 Areas, which are surrounded by security fencing. The following major facilities, many of which are inactive, are located in the 200 Areas (Figure 3-2):

- Burial trenches, burial grounds, low-level waste burial grounds

- 18 underground storage tank farm areas including the 241-A, 241-AN, 241-AP, 241-AW, 241-AX, 241-AY, 241-AZ, 241-B, 241-BX, 241-BY, 241-C, 241-S, 241-SX, 241-SY, 241-T, 241-TX, 241-TY, and 241-U Tank Farms

- Very large fuel processing and recovery facilities including the B, T, U, and Z Plants, and the Reduction-Oxidation (REDOX) and Plutonium Uranium Extraction (PUREX) facilities

- Tank wastewater evaporator facilities (242-A, 242-S, and 242-T Evaporators)

- Office and warehouse buildings.

Between and just south of the 200 East and West Areas is the Environmental Restoration Disposal Facility (ERDF) (Figures 3-1 and 3-4). This facility is a trench system and will hold most of the contaminated soil and materials from facility decontamination and decommissioning and Hanford Site remediation. Washington State leases a 3.9-km^2 (1.5-mi^2) parcel located between the 200 West and 200 East Areas, which, in turn, subleases a portion of this land to U.S. Ecology, Inc., a private company, for the disposal of commercially-generated low-level radioactive waste.

- **300 Area:** This area of the Site is located just north of Richland and was the location of nuclear fuel fabrication and research and development activities.

- **400 Area:** This area of the Site is located northwest of the 300 Area. It is the location of FFTF, a 400-megawatt thermal, liquid-metal (sodium)-cooled nuclear research and test reactor owned by DOE. The facility, which operated for ~10 years, has been shut down since 1993 and is currently being deactivated.

- **600 Area:** This area of the Site includes the Hanford Reach National Monument and all the land not included in the 100, 200, 300, and 400 Areas. The Hanford Reach National Monument, established in 2000 (65 FR 37253), totals 792.6 km^2 (306 mi^2) and includes Fitzner-Eberhardt Arid Lands Ecology Reserve Unit, Saddle Mountain Wildlife Refuge Unit, McGee Ranch/Riverlands Unit, and land 0.40 km (0.25 mi) inland from the mean high-water mark on the south and west shores of the 82-km (51-mi)-long Hanford Reach of the Columbia River. It also includes the Federally-owned islands in the Hanford Reach and the sand dune area northwest of the Energy Northwest site. This designation

establishes the protection and management of the land encompassing the monument. A separate memorandum allows for the incorporation of additional Hanford Site lands into the monument as the land is remediated.

- **Former 700 Area:** This area of the Site was the original location for administrative activities for the Hanford Site and was located where the Federal Building is located today (DOE/RL-97-02, National Register of Historic Places Multiple Property Documentation Form - Historic, Archaeological and Traditional Cultural Properties of the Hanford Site, Washington). It is no longer part of the Hanford Site.

- **Former 1100 Area:** This area of the Site was the location of general stores and transportation maintenance facilities for the Hanford Site. The 1100 Area was located between the 300 Area and the city of Richland, encompassing an area of ~311 hectares (~768 acres). In September 1996, the 1100 Area was declared remediated and EPA issued a delisting of this area of the Site from the National Priorities List (DOE/RL-96-16, Screening Assessment and Requirements for a Comprehensive Assessment: Columbia River Comprehensive Impact Assessment). Most of the 1100 Area has been incorporated into the city of Richland and is no longer a part of the Hanford Site (DOE/RL-88-30, Hanford Site Waste Management Units Report).

For more than 40 years, the primary mission at Hanford was associated with the production of nuclear materials for national defense. Land management and development practices at the Hanford Site were driven by resource needs for nuclear production, chemical processing, waste management, and research and development activities. The DOE developed infrastructure and facility complexes to accomplish this work, but large tracts of land used as protective buffer zones for safety and security purposes remained undisturbed. These buffer zones preserved a biological and cultural resource setting unique in the Columbia Basin region.

In the late 1980s, the primary DOE mission changed from defense materials production to environmental restoration. In 1989, DOE entered into the HFFACO (Tri-Party Agreement) with EPA and Ecology (Ecology et al. 1989).

The Hanford Site encompasses more than 2,963 waste management units and contaminated groundwater plumes that have been grouped into 75 operable units (OUs). Each OU has common characteristics such as geography, waste content, type of facility, and relationship to contaminant plumes. The grouping into designated OUs allows for economies of scale to reduce the cost and number of characterization investigations and remedial actions required to complete environmental cleanup (WHC-EP-0216, “Preliminary Operable Units Designation Project”).

3.1.1.4.4 Future Hanford Land Use. In 1992, DOE, EPA, and Ecology gathered a group of stakeholders (Hanford Future Site Uses Working Group [HFSUWG]) to study potential future uses for the Hanford Site land. This HFSUWG issued a summary (“The Future for Hanford: Uses and Cleanup, Summary of the Final Report of the Hanford Future Site Uses Working Group” [HFSUWG 1992a]) and a detailed report (“The Future for Hanford: Uses and Cleanup, The Final Report of the Hanford Future Site Uses Working Group” [HFSUWG 1992b]) of its findings. The “Final Hanford Comprehensive Land-Use Plan Environmental Impact Statement”

(DOE/EIS-0222-F) is heavily based on the work of the HFSUWG. However, DOE land use planning extends for only 50 years instead of the 100 years forecast by the HFSUWG. HFSUWG (1992a) contains the following statement about near-term use of the 200 Areas, called the Central Plateau in the report:

> "The presence of many different types of radionuclides and hazardous constituents in various volumes, forms and combinations throughout the site poses a key challenge to the Hanford cleanup. To facilitate cleanup of the rest of the site, wastes from throughout the Hanford site should be concentrated in the Central Plateau. … Waste storage, treatment, and disposal activities in the Central Plateau should be concentrated within this area as well, whenever feasible, to minimize the amount of land devoted to, or contaminated by, waste management activities. This principle of minimizing land used for waste management should specifically be considered in imminent near-term decisions about utilizing additional uncontaminated Central Plateau lands for permanent disposal of *[sic]* grout."

The report continues on the subject of future use options (HFSUWG 1992a):

> "In general, the Working Group desires that the overall cleanup criteria for the Central Plateau should enable general usage of the land and groundwater for other than waste management activities in the horizon of 100 years from the decommissioning of waste management facilities and closure of waste disposal areas."

Based on conversations of the HFSUWG, they could not agree on a definition of "general use." For the "foreseeable future," the HFSUWG developed options involving waste treatment, storage, and disposal of DOE low-level radioactive waste. The differences among the options are whether offsite waste (radioactive and/or hazardous) would be allowed to be disposed of on the Hanford Site. Finally, the report states (HFSUWG 1992a):

> "The working group identified a single cleanup scenario for the Central Plateau. This scenario assumes that future uses of the surface, subsurface, and groundwater in and immediately surrounding the 200 West and 200 East Areas would be exclusive. Surrounding the exclusive area would be a temporary surface and subsurface exclusive buffer zone composed of at least the rest of the Central Plateau. As the risks from the waste management activities decrease, it is expected that the buffer zone would shrink commensurately."

For nearer-term land use planning, the ROD (64 FR 61615) for the "Final Hanford Comprehensive Land-Use Plan Environmental Impact Statement" (DOE/EIS-0222-F) identifies near-term land uses for the Hanford Site. The ROD prescribes the use in the 200 Areas as exclusively industrial (primarily waste management) with much of the surrounding land having the use of preservation or conservation. The Hanford Reach National Monument was established along the Columbia River corridor as well as in lands at the northern and western edges of the Site (65 FR 37253). For further discussion of Hanford land uses, the reader is referred to DOE/EIS-0222-F and DOE/RL-2009-10, Hanford Site Cleanup Completion Framework.

3.1.2 Meteorology and Climatology

The climate of the Pasco Basin, where the Hanford Site is located, can be classified as either mid-latitude semiarid or mid-latitude desert, depending on which climatological classification system is being used. Large diurnal temperature variations are common, resulting from intense solar heating and night-time cooling. Summers are warm and dry with abundant sunshine. Daytime high temperatures in June, July, and August can exceed 40 °C (104 °F). Winters are cool with occasional precipitation that makes up ~44% of the yearly total. During the winter, outbreaks of cold air associated with modified arctic air masses can reach the area and cause temperatures to drop below –18 °C (0.4 °F). Overcast skies and fog occur during the fall and winter months.

The region's climate is greatly influenced by the Pacific Ocean and the Cascade Mountain Range to the west, and other mountain ranges to the north and east. The Pacific Ocean moderates temperatures throughout the Pacific Northwest, and the Cascade Range generates a rain shadow that limits rain and snowfall in the eastern half of Washington State. The Cascade Range also serves as a source of cold air drainage, which has a considerable effect on the wind regime on the Hanford Site. Mountain ranges to the north and east of the region shield the area from the severe winter storms and frigid air masses that move southward across Canada.

3.1.2.1 Current Data. Climatological data for the Hanford Site are compiled at the HMS, which is located on the Central Plateau, just outside the northeast corner of the 200 West Area and ~4 km (~2.5 mi) west of the 200 East Area. To characterize meteorological differences accurately across the Hanford Site, the HMS operates a network that currently contains 30 monitoring stations (Figure 3-6). Data are collected and processed at each station, and information is transmitted to the HMS every 15 minutes. This monitoring network has been in full operation since the early 1980s. Data from the HMS capture the general climatic conditions for the region and describe the specific climate of the Central Plateau. Meteorological measurements have been made at the HMS since late 1944. Before the HMS was established, local meteorological observations were made at the old Hanford town site (1912 through late 1943) and in Richland (1943 to 1944) (PNNL-6415). Meteorological data collected at the HMS are considered to be representative of conditions at WMA C.

3.1.2.2 Temperature and Humidity. Daily and monthly averages and extremes of temperature, dew point temperature, and relative humidity for 1945 through 2004 are reported in PNNL-15160, "Hanford Site Climatological Summary 2004 with Historical Data." From 1945 through 2010, the record maximum temperature was 45 °C (113.0 °F) recorded in August 1961, July 2002, and July 2006. The record minimum temperature was -30.6 °C (-23.1 °F) in February 1950. Normal monthly average temperatures ranged from a low of -0.2 °C (31.6 °F) in December to a high of 24.6 °C (76.3 °F) in July. During winter, the highest monthly average temperature at the HMS was 6.9 °C (44.4 °F) in February 1991, and the record lowest was -11.1 °C (12.0 °F) in January 1950. During summer, the record maximum monthly average temperature was 27.9 °C (82.2 °F) in July 1985, and the record minimum was 17.2 °C (63.0 °F) in June 1953. Table 3-1 provides the average monthly temperatures for the last 13 years along with average annual temperature. The bottom two rows provide the average annual temperature from 1947 to 2013, and the normal temperature which is a 30-year average from 1980 to 2010.

The normal annual relative humidity at the HMS is 54%. Humidity is highest during winter, averaging ~76%, and lowest during summer, averaging ~36%.

3.1.2.3 Precipitation. Average annual precipitation at the HMS is 17 cm (6.7 in.). During 1995, the wettest year on record, 31.3 cm (12.3 in.) of precipitation was measured; during 1976, the driest year, only 7.6 cm (3 in.) was measured. The wettest season on record was the winter of 1996-1997 with 14.1 cm (5.6 in.) of precipitation; the driest season was the summer of 1973, when only 0.1 cm (0.04 in.) of precipitation was measured. Most precipitation occurs during the late autumn and winter, with more than half of the annual amount occurring from November through February. Days with greater than 1.3 cm (0.51 in.) precipitation occur on average less than one time each year. Table 3-2 provides the monthly and average annual precipitation at HMS since 2000. The bottom two lines provide the average yearly precipitation since 1947 and normal precipitation, which is a 30-year average from 1980 to 2010.

Average snowfall ranges from 0.25 cm (0.1 in.) during October to a maximum of 13.2 cm (5.2 in.) during December and decreases to 1.3 cm (0.5 in.) during March. The record monthly snowfall of 59.4 cm (23.4 in.) occurred during January 1950. The seasonal record snowfall of 142.5 cm (56.1 in.) occurred during the winter of 1992-1993. Snowfall accounts for ~38% of all precipitation from December through February.

3.1.2.4 Wind. On the Hanford Site, the prevailing wind direction is from the northwest all year long. The secondary wind direction is from the southwest. Summaries of wind directions indicate that winds from the northwestern quadrant occur most often during winter and summer. During spring and fall, the frequency of southwesterly winds increases, with a corresponding decrease in the northwesterly flow. Monthly average wind speeds are lowest during winter months, averaging ~3 m/s (~7 mi/hr), and highest during summer, averaging ~4 m/s (~9 mi/hr). Wind speeds well above average are usually associated with southwesterly winds. However, summertime drainage winds are generally northwesterly and frequently exceed 13 m/s (29 mi/hr). These winds are most prevalent over the northern portion of the Hanford Site. Figure 3-6 shows the 2010 wind roses (i.e., diagrams showing direction and frequencies of wind) measured at a height of 9 m (30 ft) for the 30 meteorological monitoring stations located at and around the Hanford Site. Figure 3-7 provides wind roses for the same stations from 1982 to 2006 (PNNL-6415).

The monthly and annual prevailing wind directions, average speeds, and peak gusts are summarized in Tables 5.1 through 5.4 of PNNL-15160. The annual average wind speed for meteorological records kept from year 1945 to 2004 is calculated to be ~3.4 m/s (7.6 mi/hr) at 15.2 m (50 ft) above the ground. During 2010, the average wind speed was 3.6 m/s (8.1 mi/hr), which was 0.2 m/s (0.4 mi/hr) above normal (PNNL-20548).

Figure 3-6. Hanford Meteorological Monitoring Network Wind Roses in 2010 at the 9.1-meter (30-foot) Level.

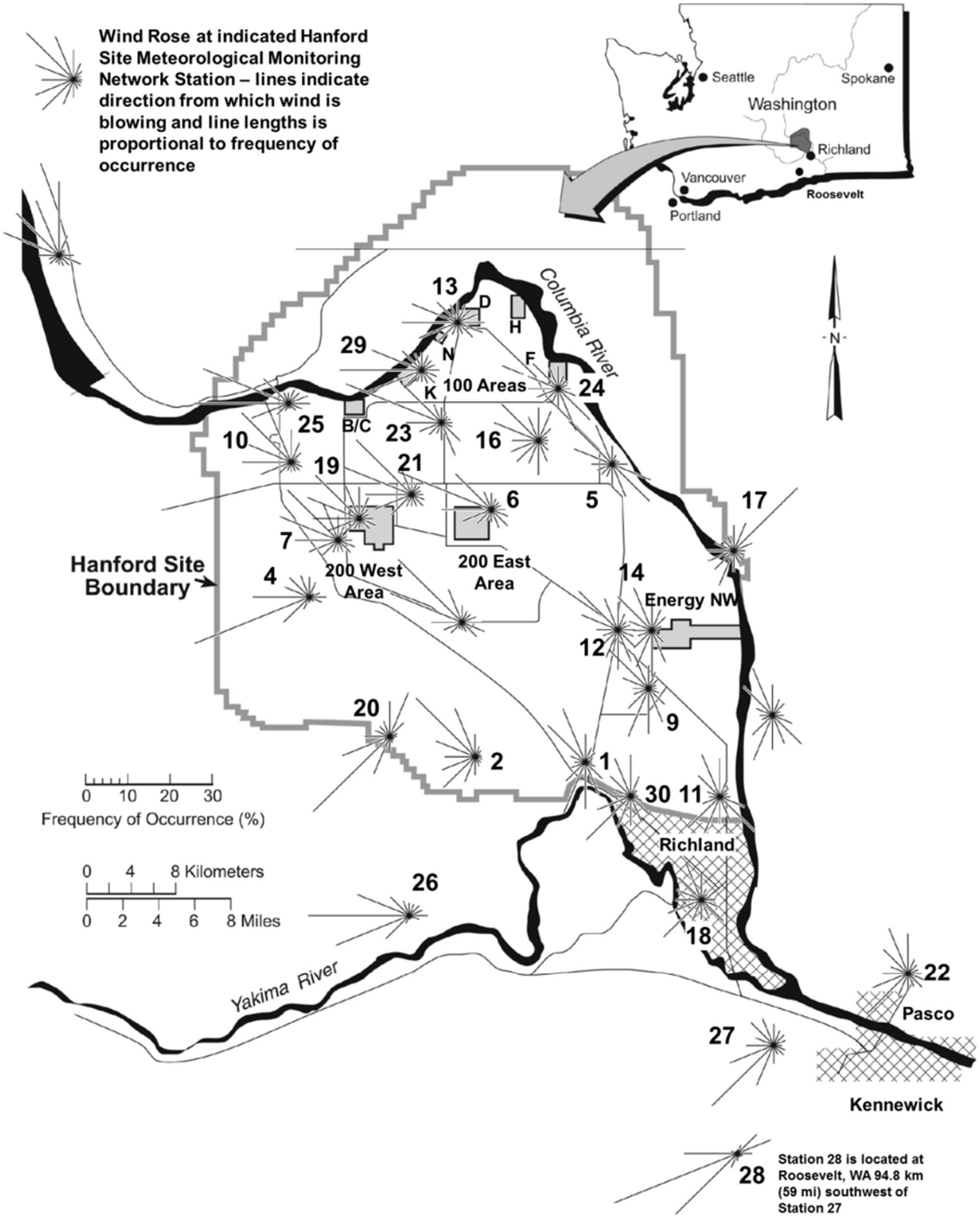

Adapted from PNNL-20548, "Hanford Site Environmental Report for Calendar Year 2010 (Including Some Early 2011 Information)."

Table 3-1. Monthly and Average Annual Temperatures at Hanford Meteorological Station since 2000 (°C).

YEAR	JAN	FEB	MAR	APR	MAY	JUN	JUL	AUG	SEP	OCT	NOV	DEC	ANNUAL
2000	0.5	3.7	7.1	13.0	16.2	21.1	24.2	23.3	17.6	11.2	1.1	-1.2	11.4
2001	0.8	2.1	8.2	10.8	17.6	19.2	24.4	25.4	20.6	11.9	6.0	1.6	12.4
2002	3.1	3.6	5.8	11.8	15.6	22.0	26.4	24.2	19.1	10.2	5.0	2.9	12.4
2003	3.3	4.4	9.4	11.2	16.2	22.5	26.8	24.7	20.7	14.1	3.2	0.5	13.1
2004	-1.6	2.8	9.8	12.7	16.4	21.3	26.4	25.5	18.3	12.5	4.3	2.2	12.6
2005	-1.1	3.2	9.4	12.0	17.9	20.3	25.3	24.8	18.4	12.4	3.5	-2.6	11.9
2006	3.6	2.3	7.2	11.2	17.0	21.3	26.7	23.8	19.3	11.3	4.4	-1.7	12.2
2007	-1.8	3.2	8.6	11.3	17.3	20.3	27.2	23.3	18.7	10.8	4.0	0.4	11.9
2008	-2.7	4.8	6.3	9.3	17.6	20.1	25.1	23.7	18.9	11.3	5.7	-3.9	11.3
2009	-0.7	1.7	5.5	10.9	16.8	21.9	26.5	24.6	20.2	10.1	5.0	-4.1	11.6
2010	3.3	5.6	8.3	11.8	14.4	19.4	24.8	23.7	18.8	12.3	2.6	0.9	12.2
2011	0.9	1.7	6.7	9.1	14.0	19.4	23.0	24.7	20.8	12.3	3.6	-0.7	11.3
2012	0.2	3.2	7.6	12.7	16.2	18.9	25.6	25.4	19.7	11.6	5.6	2.4	12.4
2013	-1.2	3.9	7.9	12.0	17.3	21.0	27.1	25.4	20.7	11.4	3.6	-2.8	12.2
AVERAGE	-0.4	3.2	7.4	11.6	16.6	20.7	24.9	24.0	19.1	11.7	4.5	0.1	11.9
NORMAL	0.8	3.4	8.1	11.9	16.7	20.9	25.1	24.3	19.1	11.7	4.7	-0.5	12.2

[1] Normal is a 30-year average from 1980 to 2010.

Table 3-2. Monthly and Average Annual Precipitation at Hanford Meteorological Station since 2000 (cm).

YEAR	JAN	FEB	MAR	APR	MAY	JUN	JUL	AUG	SEP	OCT	NOV	DEC	ANNUAL
2000	2.77	2.84	2.39	1.45	1.96	0.64	1.17	Trace	1.42	1.45	2.74	1.70	20.52
2001	0.74	1.07	1.70	2.11	0.20	3.23	0.13	0.20	0.33	0.94	4.24	2.03	16.92
2002	1.07	1.70	0.48	0.74	0.41	1.65	0.41	0.03	Trace	0.30	0.97	5.99	13.74
2003	4.75	2.08	0.66	5.66	0.20	Trace	0.00	1.17	0.61	0.18	0.38	4.98	20.68
2004	5.38	2.34	0.91	0.53	2.26	2.08	0.08	2.41	0.36	2.18	0.74	0.94	20.22
2005	2.36	0.10	0.79	0.66	2.01	0.15	0.23	0.15	1.68	0.74	2.26	5.11	16.23
2006	3.00	1.04	0.61	3.30	1.45	3.38	Trace	Trace	0.53	1.93	1.80	4.45	21.49
2007	0.36	1.93	1.88	0.66	0.76	1.14	0.18	0.81	1.45	0.53	2.87	1.35	13.92
2008	3.25	1.40	0.51	0.20	1.42	0.99	Trace	1.22	0.10	0.56	1.88	2.41	13.94
2009	2.92	1.63	2.03	0.99	0.46	0.41	Trace	0.10	0.15	1.98	1.42	1.80	13.89
2010	3.15	1.42	0.51	1.50	3.38	2.92	1.17	0.33	2.41	1.57	2.90	4.62	25.88
2011	1.35	0.08	2.21	0.64	3.10	0.99	0.30	Trace	0.13	1.96	0.30	0.25	11.30
2012	2.77	1.70	1.63	1.55	0.56	3.84	0.38	Trace	0.08	1.05	0.80	1.41	8.18
2013	0.41	0.23	0.99	0.76	4.06	3.45	0.03	0.61	1.07	0.97	0.91	0.18	13.67
AVERAGE	2.36	1.57	1.27	1.19	1.37	1.42	0.51	0.58	0.76	1.37	2.18	2.62	17.22
NORMAL[1]	2.39	1.78	1.45	1.40	1.30	1.30	0.58	0.46	0.79	1.24	2.41	3.05	18.14

[1] Normal is a 30 year average from 1980 to 2010.

Figure 3-7. Hanford Meteorological Monitoring Network Wind Roses from 1982 to 2006 at the 9.1-meter (30-foot) Level.

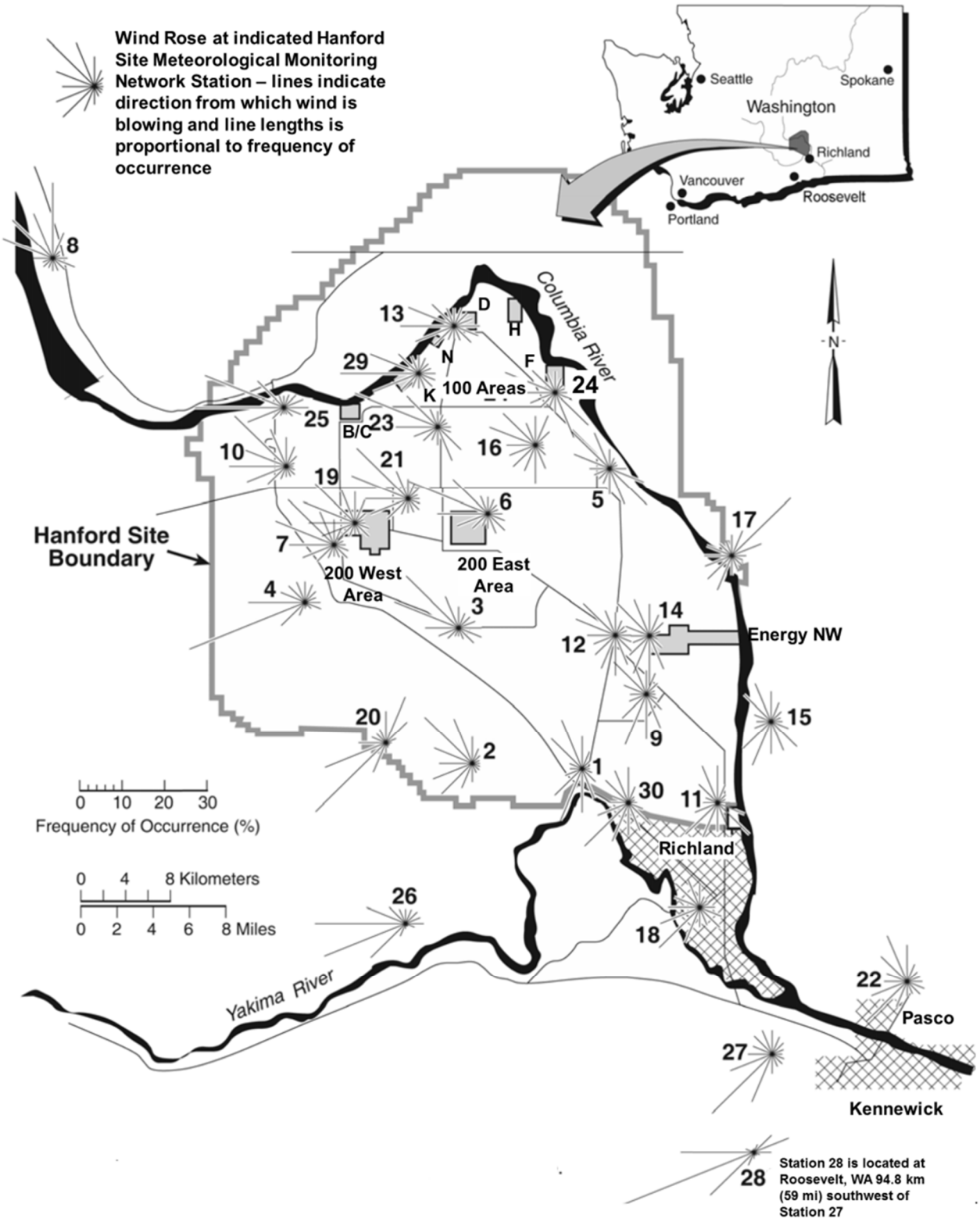

Adapted from PNNL-6415, "Hanford Site National Environmental Policy Act (NEPA) Characterization."

3.1.2.5 Severe Weather. Concerns about severe weather usually center on hurricanes, tornadoes, and thunderstorms. Fortunately, the occurrence of hurricanes and tornadoes is infrequent and their scale is generally small in the northwestern portion of the United States. According to the records of the HMS and the National Severe Storms Forecast Center database, only 24 separate tornados have occurred between 1916 and 1994 within 160 km (99 mi) of the Hanford Site. Only one of these tornadoes was observed within the boundaries of the Hanford Site itself (at the extreme western edge), and no damage resulted. The estimated probability of a tornado striking a point at the Hanford Site is 9.6×10^{-6}/yr. Hurricanes do not reach the interior of the Pacific Northwest.

Severe winds are associated with thunderstorms or the passage of strong cold fronts. The average occurrence of thunderstorms in the vicinity of the HMS is 10 per year. They are most frequent during the summer; however, they have occurred in every month. High speed winds at the Site are more commonly associated with strong cold frontal passages. In rare cases, intense low pressure systems can generate winds of near-hurricane force. The greatest peak wind gust was 130 km/hr (81 mi/hr), recorded at 15 m (49 ft) above ground level at the HMS. Extrapolations based on 35 years of observation indicate a return period of ~200 years for a peak gust in excess of 145 km/hr (90 mi/hr) at 15 m (49 ft) above ground level.

3.1.2.6 Climate Change. In Global Climate Change Impacts in the United States: A State of Knowledge Report from the U.S. Global Change Research Program, Karl et al. (2009) projects that the in Pacific Northwest, regionally averaged temperatures are expected to increase 1.7 to 5.6 °C (3 to 10 °F) during this century. They also noted that temperatures rose 0.83 °C (1.5 °F) over the past century and some areas saw increases up to 2.2 °C (4.0 °F). Karl et al. (2009) also suggests that winter precipitation will increase and summer precipitation will decrease. Most of the concern is with snowpack because it dominates water storage for irrigation and hydro system functioning. Scenarios of future climate for the Pacific Northwest, Climate Impacts Group (Mote et al. 2008) stated that the best estimate of future temperature change in the Pacific Northwest is 0.28 °C (0.5 °F) per decade until about 2050. Mote et al. (2008) estimated precipitation changes would range from -10% to +20% by the year 2080. They also noted that warming will be greater in summer than in the other seasons.

For an analysis of recharge in the 200 East Area, PNNL-13033, "Recharge Data Package for the Immobilized Low-Activity Waste 2001 Performance Assessment" represented future climate conditions by scaling the current temperature and precipitation data to match paleoclimate observations derived from pollen data. "Vegetation and climate change in northwest America during the past 125 kyr" (Whitlock and Bartlein 1997) described a 125,000-year paleoclimate record constructed from the pollen record in cores taken from Carp Lake, near Goldendale, Washington. Carp Lake is located ~175 km (~109 mi) southwest of the Hanford Site, at an elevation of 714 m (2,343 ft). Similar pollen records at the Hanford Site were eliminated during the glacial flooding 13,000 years ago. Thus, Carp Lake provides a proxy for paleoclimate information relevant to the Hanford Site. BHI-00144, "Long-term Climate Change Effects Task for the Hanford Site Permanent Isolation Barrier Development Program: Final Report" described the Carp Lake pollen interpretation relative to precipitation and temperature. For the entire Holocene (i.e., the last 10,000 years), the data suggest that annual temperatures and precipitation ranged from 0 to 2.8 °C (0 to 5 °F) warmer and 0 to 50% drier compared to modern

climate. During the glacial period prior to the Holocene, annual temperatures ranged from 0.2 °C (0.36 °F) warmer to 2.5 °C (4.5 °F) cooler and precipitation ranged from 75 to 128% of modern levels. In summary, for the last 100,000 years, annual precipitation ranged from 50 to 128% of modern levels and annual temperatures ranged from -2.5 to 2.8 °C (-4.5 to 5 °F) of modern levels. These ranges appear to bracket the latest estimates for precipitation and temperature changes in the Pacific Northwest. Figures 3-8 and 3-9 illustrate the pollen-derived precipitation and temperature records, respectively.

3.1.3 Ecology

This section summarizes the ecology of the Hanford Site (PNNL-6415, Section 4.5; DOE/EIS-0391, Section 3.7), highlighting the 200 Areas where WMA C is located. The information in this section emphasizes plant and animal activities that may affect exposure pathways. The primary impact would be through roots penetrating and animals burrowing through surface barriers into a disposal facility. Secondarily, the types of plants and animals and their density can affect net recharge to groundwater, which is greatly influenced by surface vegetation and burrowing. PNNL-6415 details both the terrestrial and aquatic ecology of the Hanford Site and presents extensive listings of plant and animal species, but this section considers only terrestrial ecological effects because WMA C is not located near significant aquatic ecological systems.

The Hanford Site consists of primarily undeveloped land. Chemical processing facilities, nuclear reactors that have been shut down, and supporting facilities occupy only ~6% of the site. Most of the Hanford Site has not experienced tillage or agricultural grazing since the early 1940s.

The Hanford Site is characterized as a shrub-steppe ecosystem that is adapted to the mid-latitude semiarid climate of the region. These ecosystems are typically dominated by a shrub overstory with a grass understory. In the early 1800s, dominant plants in the area were big sagebrush (*Artemisia tridentata*) and an understory consisting of perennial Sandberg's bluegrass (*Poa sandbergii*) and bluebunch wheatgrass (*Pseudoregneria spicata*). Other species included threetip sagebrush, bitterbrush, gray rabbitbrush, spiny hopsage, needle and thread grass, Indian rice grass, and prairie June grass.

With the advent of settlement, livestock grazing and agricultural production contributed to colonization by non-native vegetation species that currently dominate portions of the landscape. Although agriculture and livestock production were the primary subsistence activities at the turn of the century, these activities ceased when the Hanford Site was designated in 1943. No farming has occurred on the Hanford Site since the government took control of the site.

Figure 3-8. Precipitation Reconstruction for Past 100,000 Years Based on Pollen Data.

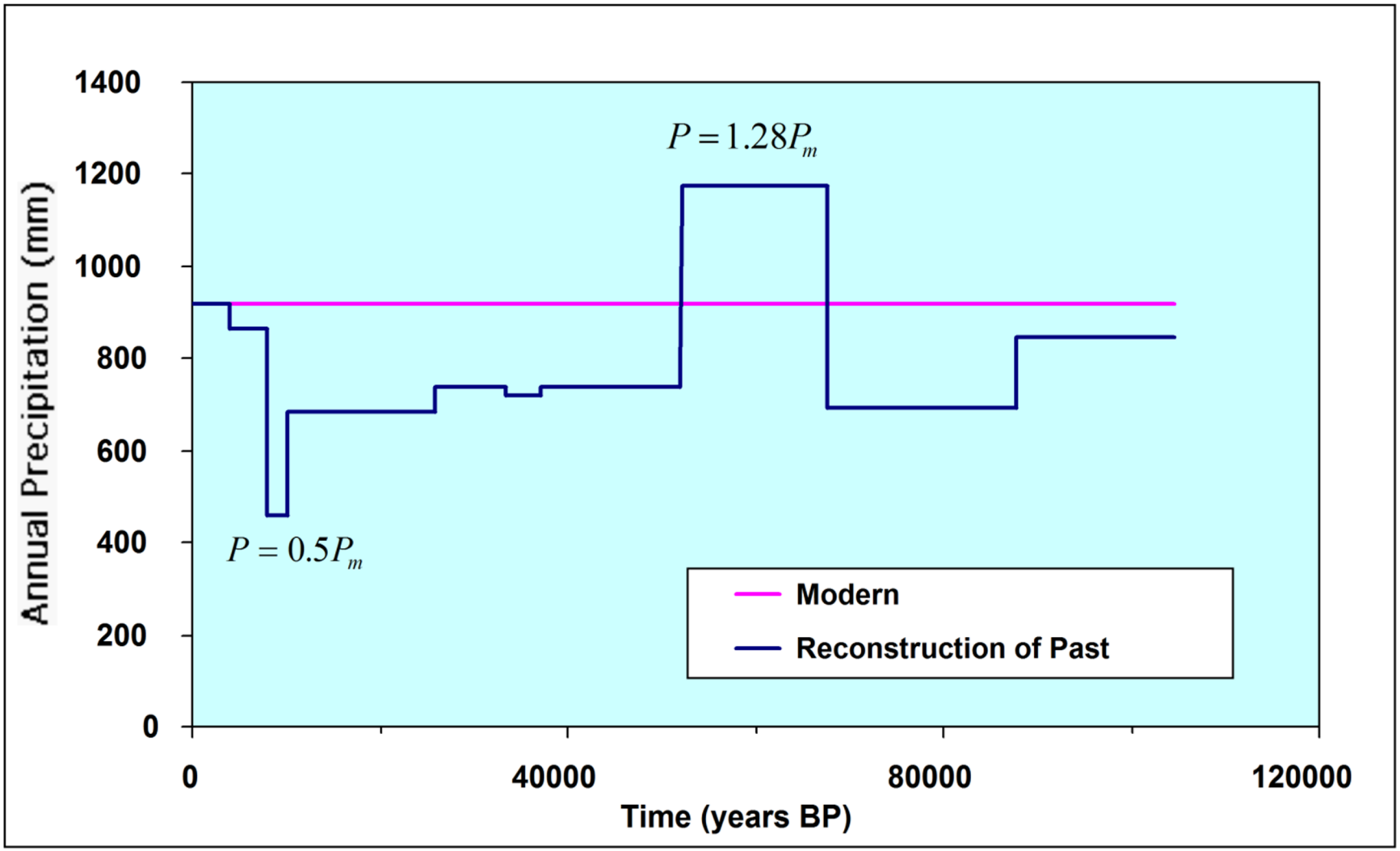

BP = before present

Figure 3-9. Temperature Reconstruction for Past 100,000 Years Based on Pollen Data.

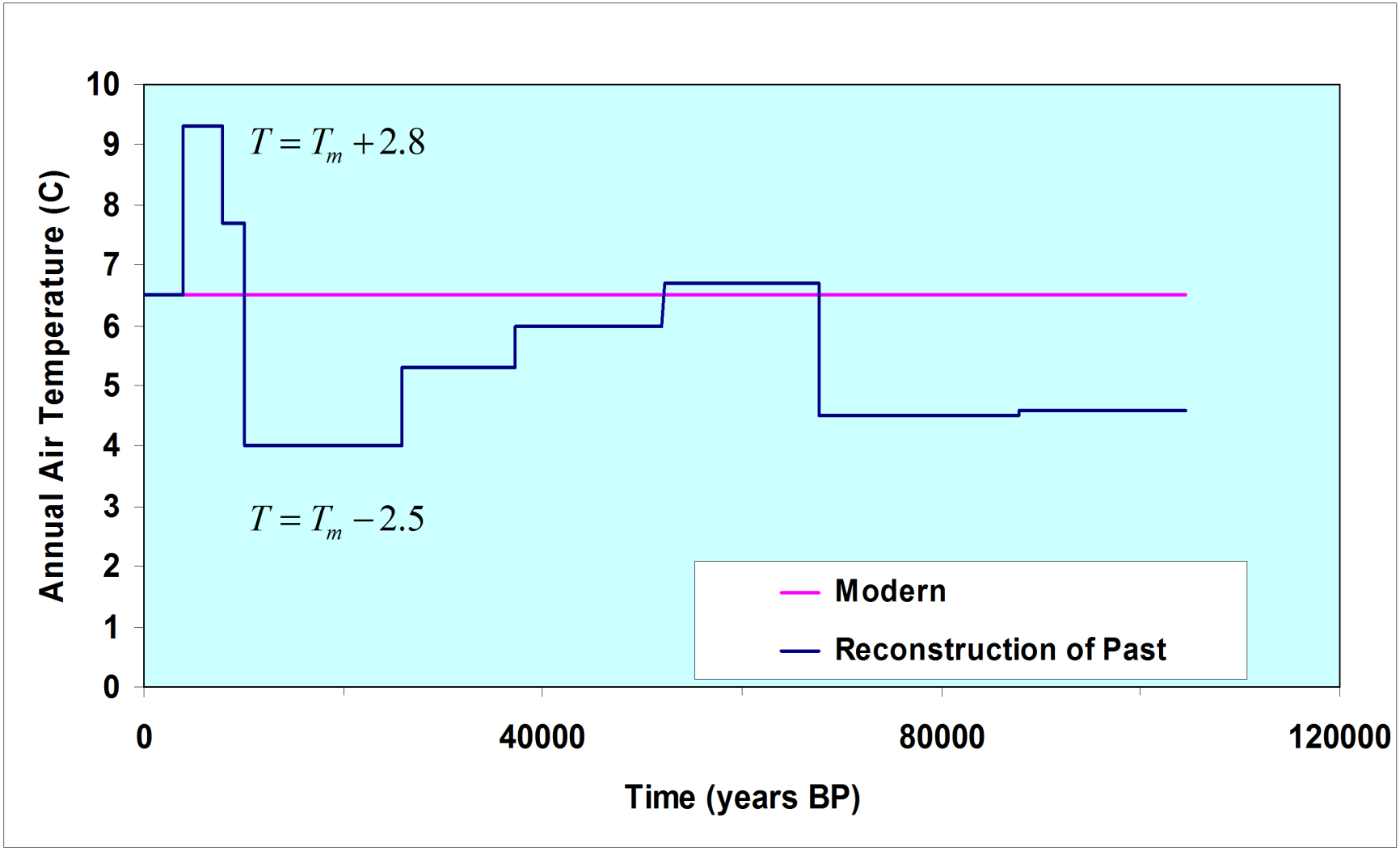

BP = before present

The dominant non-native species, cheat grass, is an aggressive colonizer and has become well established across the Site. Over the past decade, several knapweed species also have become persistent invasive species in areas not dominated by shrubs. Range fires that historically burned through the area during the dry summers eliminated fire-intolerant species (e.g., big sagebrush) and allowed more opportunistic and fire-resistant species to establish. Of the 590 species of vascular plants recorded for the Hanford Site, ~20% are non-native. Wildfires are frequent on the Hanford Site. Several of the more recent fires are shown on Figure 3-10 and are described on page 3-7 of DOE/EIS-0391. Vegetation loss due to fires and firefighting activities exposed the soil to erosion by subsequent wind and rain, and can enhance recharge by removing vegetation from evapotranspiration barriers placed over the site.

Figure 3-11 illustrates vegetation and land cover in and around the 200 East Area following the 24 Command (June/July 2000) and Wautoma Fires (August 2007). Most of the 200 Areas were not directly impacted by either fire (see Figure 3-10). Undisturbed portions of the 200 Areas are characterized by the following communities: big sagebrush/bunchgrass-cheat grass, cheat grass-bluegrass, crested wheatgrass-bunchgrass-cheat grass, and gray rabbit brush/cheat grass-bluegrass. The former two communities are prominent in the 200 East Area, while the latter two are more common in the 200 West Area. Most of the waste disposal and storage sites are covered by non-native vegetation or are kept in a vegetation-free condition by the controlled application of approved herbicides because plants could potentially accumulate waste constituents. Where vegetation is present, it aids in stabilizing surface soil, controlling soil moisture, or displacing more-invasive, deep-rooted species like Russian thistle (PNNL-6415, page 4.98). Due to the disturbed nature of most of the 200 Areas, wildlife use is limited; however, surveys have recorded the badger, coyote, Great Basin pocket mouse, mule deer, long-billed curlew, killdeer, horned lark, Say's phoebe, American robin, American kestrel, western meadowlark, and common raven [PNNL-14133, "Blanket Biological Review for General Maintenance Activities Within Active Burial Grounds, 200 E and 200 W Areas, ECR #2002-200-034," page 3; PNNL-14233, "Biological Review of the Hanford Solid Waste EIS – Borrow Area C (600 Area), Stockpile and Conveyance Road Area (600 Area), Environmental Restoration Disposal Facility (ERDF) (600 Area), Central Waste Complex (CWC) Expansion (200 West), 218-W-5 Expansion Area (200 West), New Waste Processing Facility (200 West), Undeveloped Portion of 218-W-4C (200 West), Western Half & Northeastern Corner of 218-W-6 (200 West), Disposal Facility Near Plutonium-Uranium Extraction (PUREX) Facility (200 East), ECR #2002-600-012b," pages 9, 10; PNNL-16620, "Ecological Data in Support of the Tank Closure and Waste Management Environmental Impact Statement Part 2: Results of Spring 2007 Field Surveys"].

All WMAs in the tank farm system are actively managed to prevent vegetation, insects, and wildlife from using the WMA as habitat, including WMA C. Herbicides and pesticides are used on a regular basis and fences are placed around the perimeter to keep larger animals out. Without a source of food within the WMA, smaller animals are less likely to enter. Figure 3-12 provides the size of the habitat areas within 152 m (500 ft) of WMA C.

Figure 3-10. Extent of Area Burned During Recent Fires at the Hanford Site.

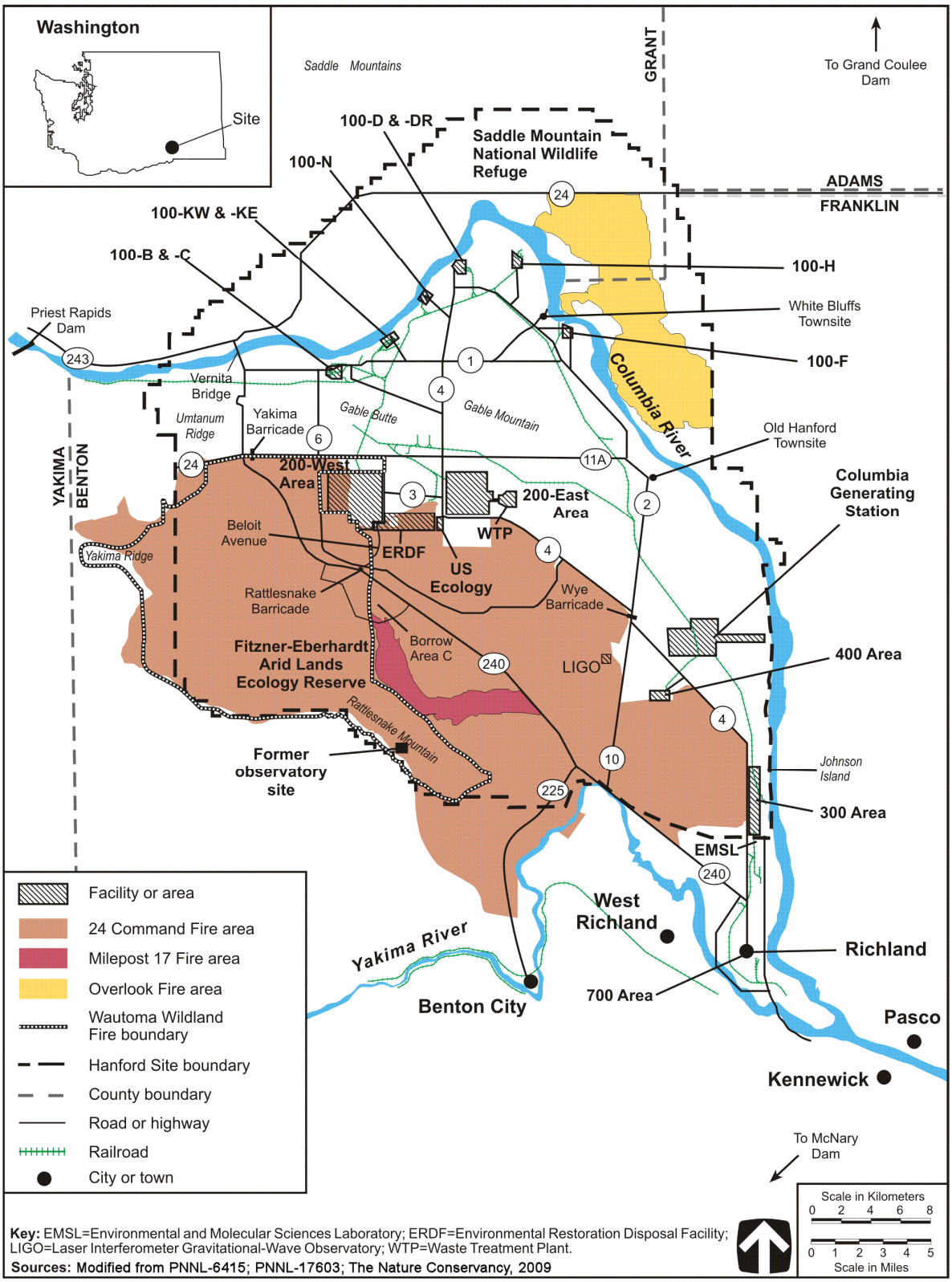

Source: DOE/EIS-0391, "Final Tank Closure and Waste Management Environmental Impact Statement for the Hanford Site, Richland, Washington."

Figure 3-11. Vegetation Communities in and near 200 East Area.

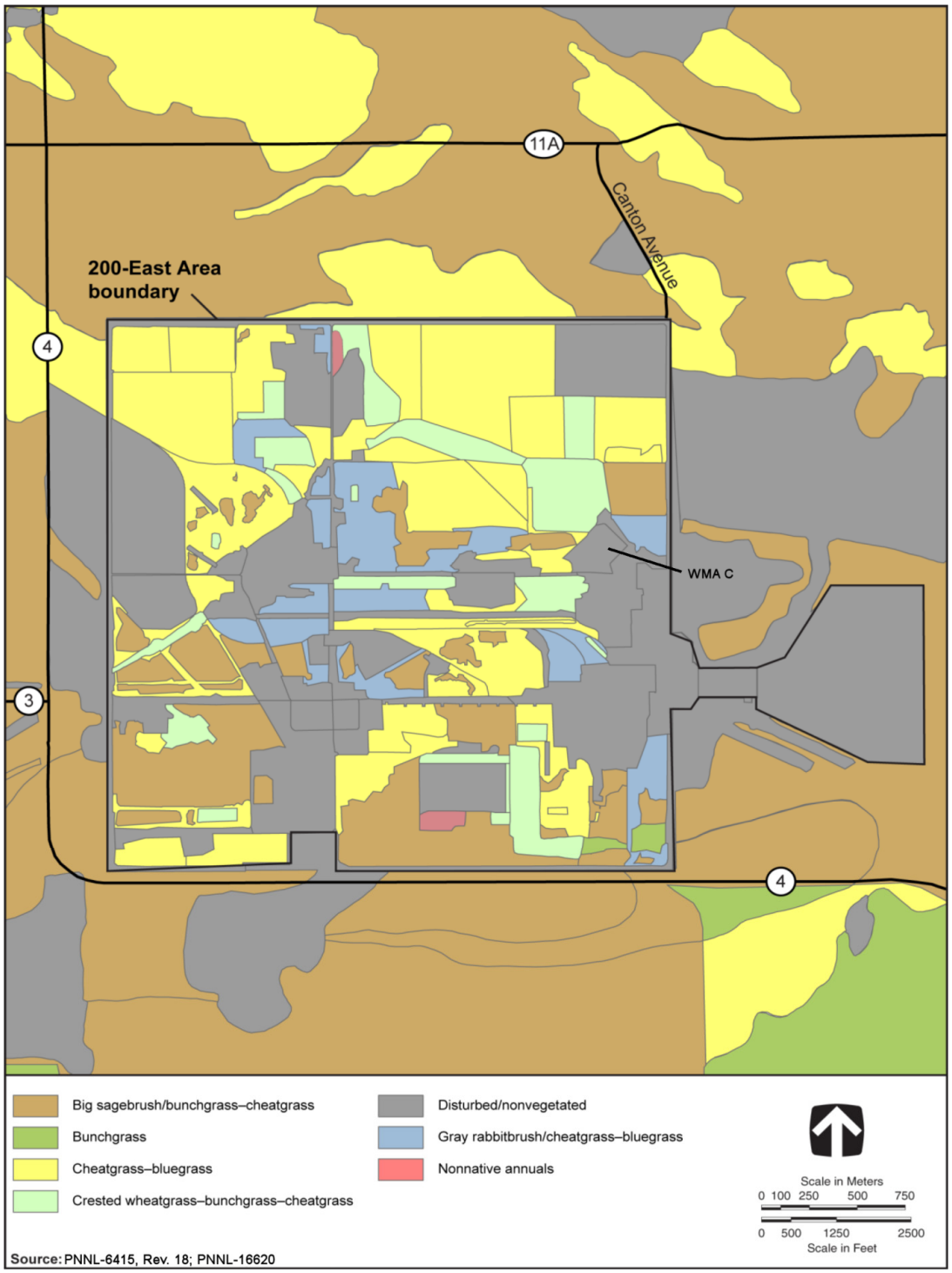

Modified from DOE/EIS-0391, "Final Tank Closure and Waste Management Environmental Impact Statement for the Hanford Site, Richland, Washington."

References:

PNNL-6415, "Hanford Site National Environmental Policy Act (NEPA) Characterization."
PNNL-16620, "Ecological Data in Support of the Tank Closure and Waste Management Environmental Impact Statement Part 2: Results of Spring 2007 Field Surveys."

3.1.4 Geology, Seismology, and Volcanology

Since the Hanford Site started operating in the early 1940s, a large volume of information on the geology, seismology, and volcanology of the Site has been collected and evaluated. Over the last several years, the following two data packages have been prepared to describe the geology, hydrology, and geochemistry of the SST system and WMA C:

1) RPP-RPT-46088, "Flow and Transport in the Natural System at Waste Management Area C"

2) PNNL-15955, "Geology Data Package for the Single-Shell Tank Waste Management Areas at the Hanford Site."

Most of the data included in the geologic data package were collected by (or used by) several projects between about 1980 and the present. Those projects include the Basalt Waste Isolation Project, the Skagit Hanford Nuclear Project, the Washington Public Power Supply System safety analysis, several PAs, and numerous regulatory-driven geologic and hydrologic characterizations, assessments, and monitoring projects.

The technical aspects of all of these projects, and thus the data, interpretations of the data, and conclusions, have been overseen by one or more regulatory agencies and stakeholder groups including the NRC, the National Academy of Science, the Defense Nuclear Facilities Safety Board (DNFSB), the EPA, the U.S. Geological Survey, the Washington State Departments of Ecology and Health, the Oregon Department of Energy, and the Yakama, Nez Perce, and Wanapum Indian Nations and the Confederated Tribes of the Umatilla Reservation. The high level of oversight has helped ensure a rigorous understanding of bounding geologic, seismic, and volcanic risks.

This section provides a summary of the data in the two data packages, highlighting those aspects that are important to developing the conceptual model describing transport of contaminants away from the waste facility to a receptor. This section will focus on the regional and Hanford Site geologic framework. The geology of WMA C is discussed in Section 3.1.9 Waste Management Area C Site Characterization.

3.1.4.1 Regional Geologic Framework. The Hanford Site (Figure 3-13) lies within the Columbia Plateau, a broad plain situated between the Cascade Range to the west and the Rocky Mountains to the east, and is underlain by the Miocene Columbia River Basalt Group (CRBG) (Figure 3-14). The northern Oregon and Washington portion of the Columbia Plateau is often called the Columbia Basin because it forms a lowland surrounded on all sides by mountains. The low-relief plains of the Central Plains physiographic region and anticlinal ridges of the Yakima Folds region dominate the physiographic setting of the Hanford Site. In the central and western parts of the Columbia Basin and Pasco Basin where the Hanford Site is located, the basalt is underlain predominantly by Tertiary continental sedimentary rocks and overlain by late Tertiary and Quaternary fluvial and glacio-fluvial deposits. All these were folded and faulted during the Cenozoic Era to form the current landscape of the region.

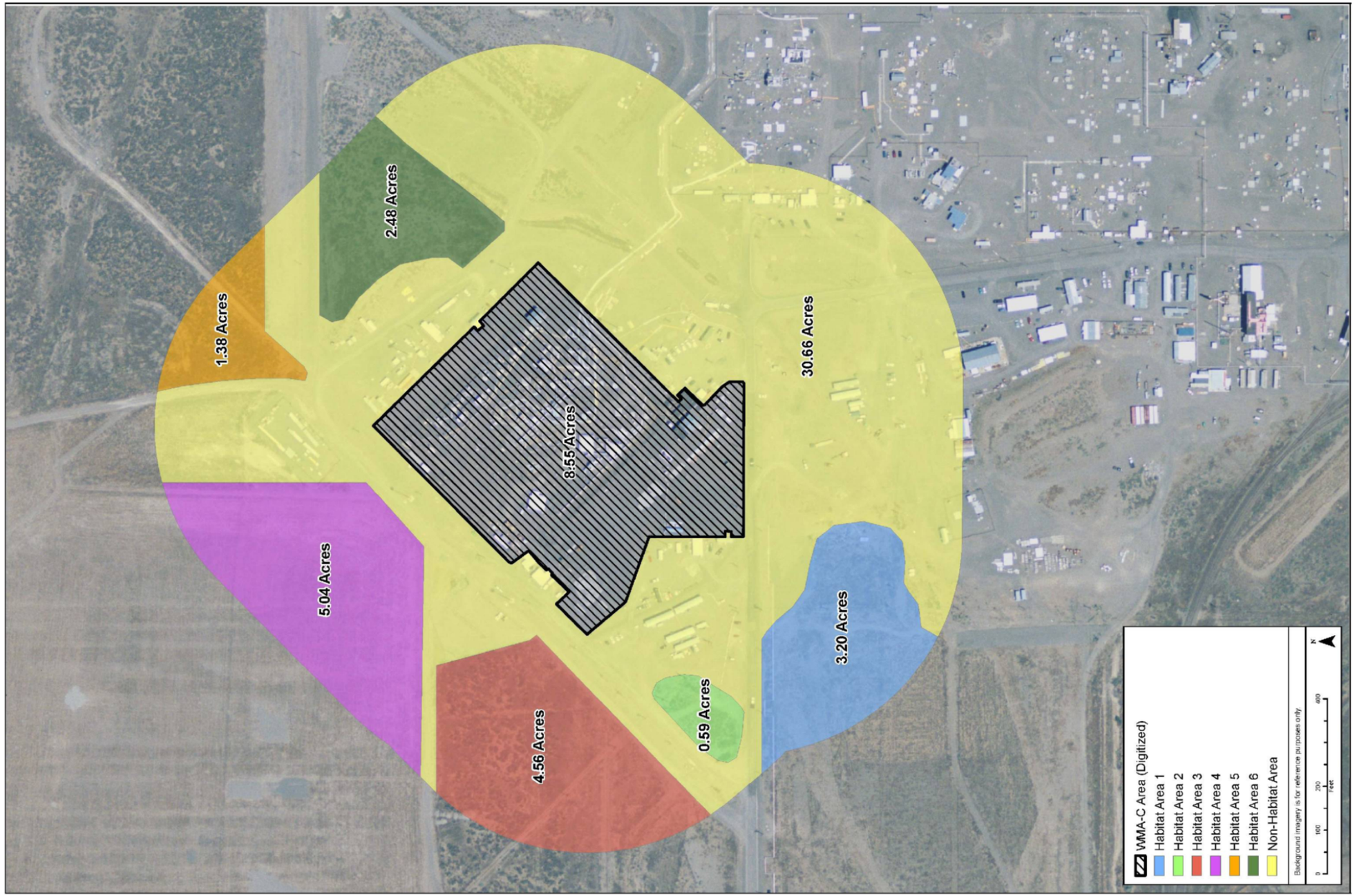

Figure 3-12. Habitat Areas within a 500 Foot Perimeter of Waste Management Area C.

WMA = Waste Management Area

Figure 3-13. Geologic Elements of the Pasco Basin Portion of the Columbia Basin, Washington.

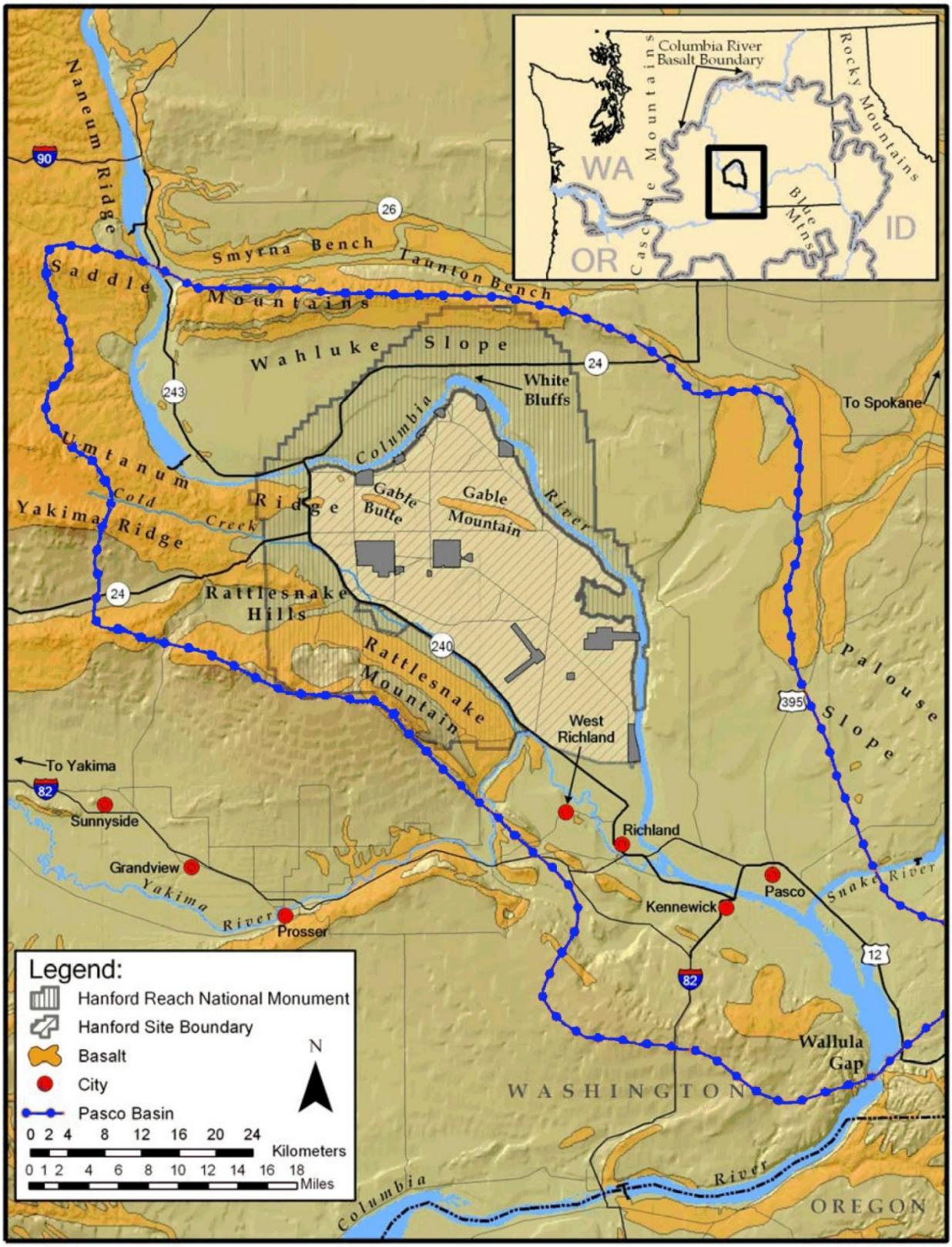

Figure 3-14. Geologic Setting of the Columbia Basin and Pasco Basin.

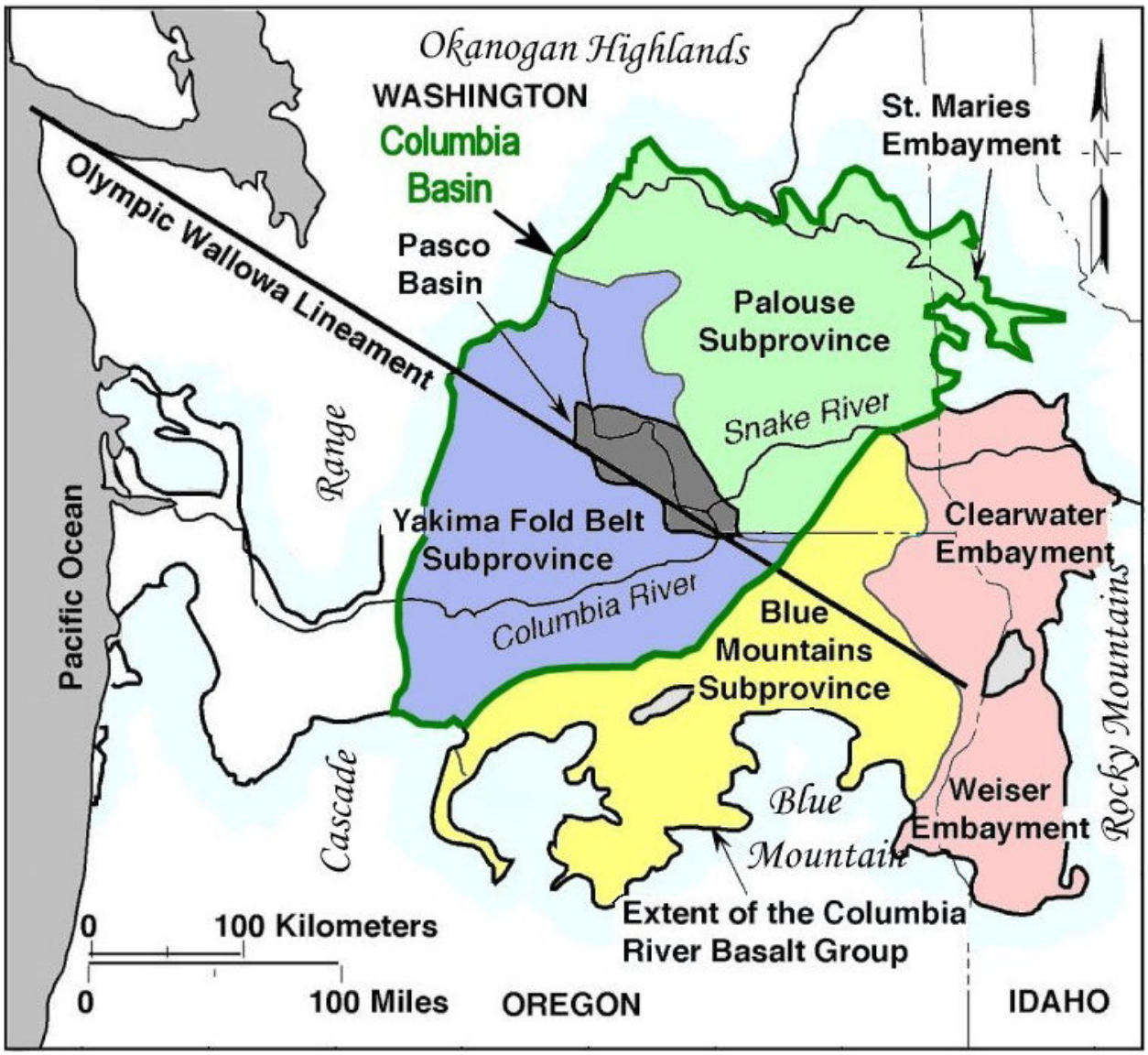

The Columbia Basin is a structurally and topographically low area surrounded by mountains ranging in age from the late Mesozoic to recent (Figure 3-14). The Columbia Basin is composed of two fundamental sub-provinces, the Palouse Slope and the Yakima Fold Belt (Figure 3-14). The Palouse Slope is a stable, undeformed area overlying the old continental craton that dips westward toward the Hanford Site. The Yakima Fold Belt is a series of anticlinal ridges and synclinal valleys in the western and central parts of the Columbia Basin. The edge of the old continental craton lies at the junction of these two structural sub-provinces and is currently marked by the Ice Harbor dike swarm of the CRBG east of the Hanford Site. The Blue Mountains sub-province of the Columbia River flood-basalt province is a northeast trending anticlinorium that extends 250 km from the Oregon Cascades to Idaho and forms the southern border of the Columbia Basin and the southern part of the Columbia Plateau.

3.1.4.1.1 Lava Flows. Lava flows erupted over a period of time from 17 to 6 million years ago. Under the Hanford Site, basaltic lava deposits (CRBG) are over 4 km (13,000 ft) thick ("Volcanism and Tectonism in the Columbia River Flood-Basalt Province," page 386, plate 1 [Reidel and Hooper 1989]), spreading over portions of Idaho, Oregon, and Washington. The Columbia Basin encloses the CRBG. A depression in the lower part of the Columbia Basin is referred to as the Pasco Basin (Figure 3-14). The Pasco Basin is bounded by the Saddle Mountains to the north, Naneum Ridge to the west, Rattlesnake Hills to the south, and the Palouse Slope to the east, generally the area north of where the Snake River flows into the Columbia River. Geographically, the ridges surrounding the Hanford Site and vicinity define the Pasco Basin, which contains Ringold Formation sediment from the ancestral Columbia River and sediment deposited by the Ice Age floods.

3.1.4.1.2 Crustal Folding. During and after the eruption of the lava flows, the Earth's tectonic forces buckled and folded the basalt in the western Columbia Basin into generally east-west trending, long, narrow ridges (anticlines), and intervening valleys (synclines). Collectively, this is identified as the Yakima Fold Belt.

3.1.4.1.3 Ancestral Columbia River Deposits. The ancestral Columbia River repeatedly changed its course over the past 15 million years, depositing gravel, sand, silt, and clay (RHO-BWI-ST-14, "Subsurface Geology of the Cold Creek Syncline," "Chapter 2 – Suprabasalt Sediments of the Cold Creek Syncline Area"; "Paleodrainage of the Columbia River System on the Columbia Plateau of Washington State – A Summary" [Fecht et al. 1987]; DOE/RW-0164, Consultation Draft Site Characterization Plan Reference Repository Location, Hanford Site, Washington; "Late Cenozoic Structure and Stratigraphy of South-Central Washington" [Reidel et al. 1994]; Open File Report 96-8, "The Miocene to Pliocene Ringold Formation and Associated Deposits of the Ancestral Columbia River System, South-Central Washington and North-Central Oregon"). Uplifting basalt ridges diverted the course of the Columbia River from a southerly direction (toward Goldendale) to an easterly direction (toward Wallula Gap) and left behind the Ringold Formation (Fecht et al. 1987). Later regional uplift associated with the Cascade Mountains caused the river to cut through its own earlier deposits (the Ringold Formation), exposing the White Bluffs. Within the Hanford Reach, the Columbia River continues to erode the White Bluffs. Groundwater seepage from irrigation along the bluffs makes them unstable. Consequently, the White Bluffs are land sliding and sloughing into the Columbia River along much of the shoreline (Fecht et al. 1987).

3.1.4.1.4 Ice Age Floods. During the Pleistocene, cataclysmic floods inundated the Pasco Basin several times when ice dams failed on the Clark Fork River that created Glacial Lake Missoula ("Quaternary Geology of the Columbia Plateau" [Baker et al. 1991]). The Ice Age floods began as early as 2.5 million years ago ("Long History of Pre-Wisconsin, Ice Age Cataclysmic Floods: Evidence from Southeastern Washington State" [Bjornstad et al. 2001]) with the most recent occurring 18,000 to 13,000 years ago. Current interpretations suggest as many as 40 flooding events occurred as ice dams holding back glacial Lake Missoula repeatedly formed and broke. In addition to larger major flood episodes, there were probably numerous smaller individual flood events. Deciphering the history of cataclysmic flooding in the Pasco Basin is complicated, not only because of floods from multiple sources but also because the paths of Missoula floodwaters migrated and changed course with the advance and retreat of the Cordilleran Ice Sheet.

Along with sedimentological evidence for cataclysmic flooding in the Pasco Basin, high-water marks and faint strandlines occur along the basin margins. Temporary lakes were created when flood waters were hydraulically dammed, resulting in the formation of the short-lived Lake Lewis behind Wallula Gap. High water mark elevations for Lake Lewis (Figure 3-15), inferred from ice-rafted erratics on ridges, range from 370 to 385 m (1,214 to 1,263 ft) above sea level.

The sediment deposited by the cataclysmic flood waters has been informally called the Hanford formation because the best exposures and most complete deposits are found there. The coarse-grained flood facies (gravel-dominated facies of DOE/RL-2002-39, Standardized Stratigraphic Nomenclature for Post-Ringold-Formation Sediments Within the Central Pasco Basin) is generally confined to relatively narrow tracts within or near flood channel ways. The plane-laminated sand facies (sand-dominated facies of DOE/RL-2002-39), on the other hand, occurs as a broad sheet over most of the central basin.

3.1.4.2 Hanford Site Geologic Framework. The previous section provided the regional geologic framework. This section provides a summary of the geologic structure and stratigraphy unique to the Hanford Site. Please see the geologic data packages for more complete descriptions.

3.1.4.2.1 Geologic Structure. The Cold Creek syncline (Figure 3-16) lies between the Umtanum Ridge-Gable Mountain uplift and the Yakima Ridge uplift and is an asymmetric and relatively flat-bottomed structure. The Cold Creek syncline began developing during the eruption of the CRBG and has continued to subside since that time. The 200 Areas lie on the northern flank, and the bedrock dips gently (approximately 5°) to the south. The deepest parts of the Cold Creek syncline, the Wye Barricade depression and the Cold Creek depression, are ~12 km (~7.5 mi) southeast of the 200 Areas and southwest of the 200 West Area, respectively (Figure 3-16).

The Wahluke syncline north of Gable Mountain is the principal structural unit that contains the 100 Areas. The Wahluke syncline is an asymmetric and relatively flat-bottomed structure similar to the Cold Creek syncline. The northern limb dips gently (approximately 5°) to the south. The steepest limb is adjacent to the Umtanum Ridge-Gable Mountain structure.

The 200 East Area is located on the eastern part of the Cold Creek bar, which is along the northern flank of the Cold Creek syncline (Figure 3-16). Another deep structural low, the Wye Barricade depression, developed along the Cold Creek syncline southeast of the 200 East Area. The May Junction fault is a normal fault that marks the western boundary of the depression.

The 200 East Area sits at the southern end of a series of secondary doubly plunging anticlines and synclines that are associated with the Umtanum Ridge-Gable Mountain anticlinal structure. Waste Management Areas A, AX, B-BX-BY, and C in the 200 East Area lie near the southern flank of the closest secondary anticline. A fault was recently detected during drilling of seismic test boreholes at the Waste Treatment Plant. The fault caused some displacement in the Pomona Basalt that lies beneath the Elephant Mountain Member but is not thought to have caused any displacement in younger basalts or overlying sediments (PNNL-16407, “Geology of the Waste Treatment Plant Seismic Boreholes”).

Figure 3-15. Flood in the South of the Hanford Site, Washington, between 18,000 to 13,000 Years Ago.

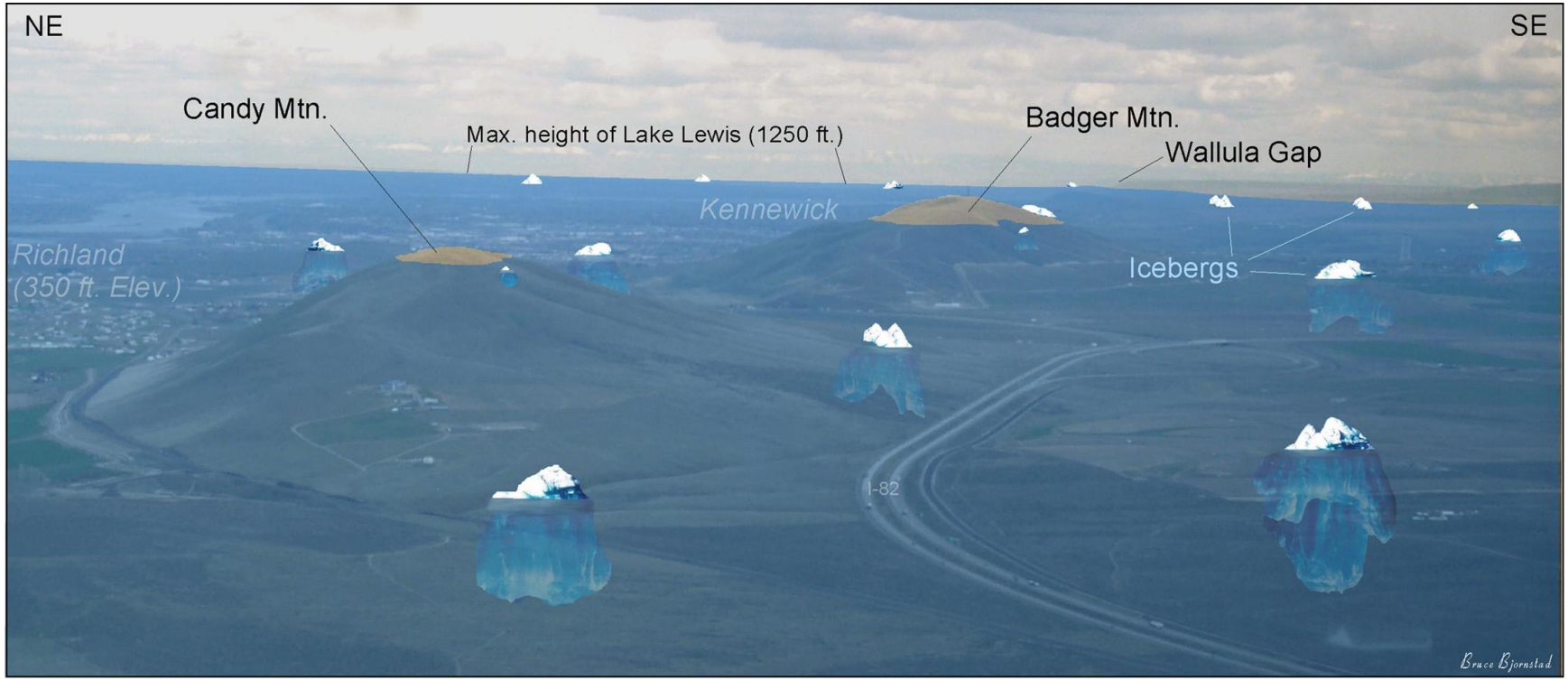

Figure 3-16. Geologic and Geomorphic Map of the 200 Areas and Vicinity.

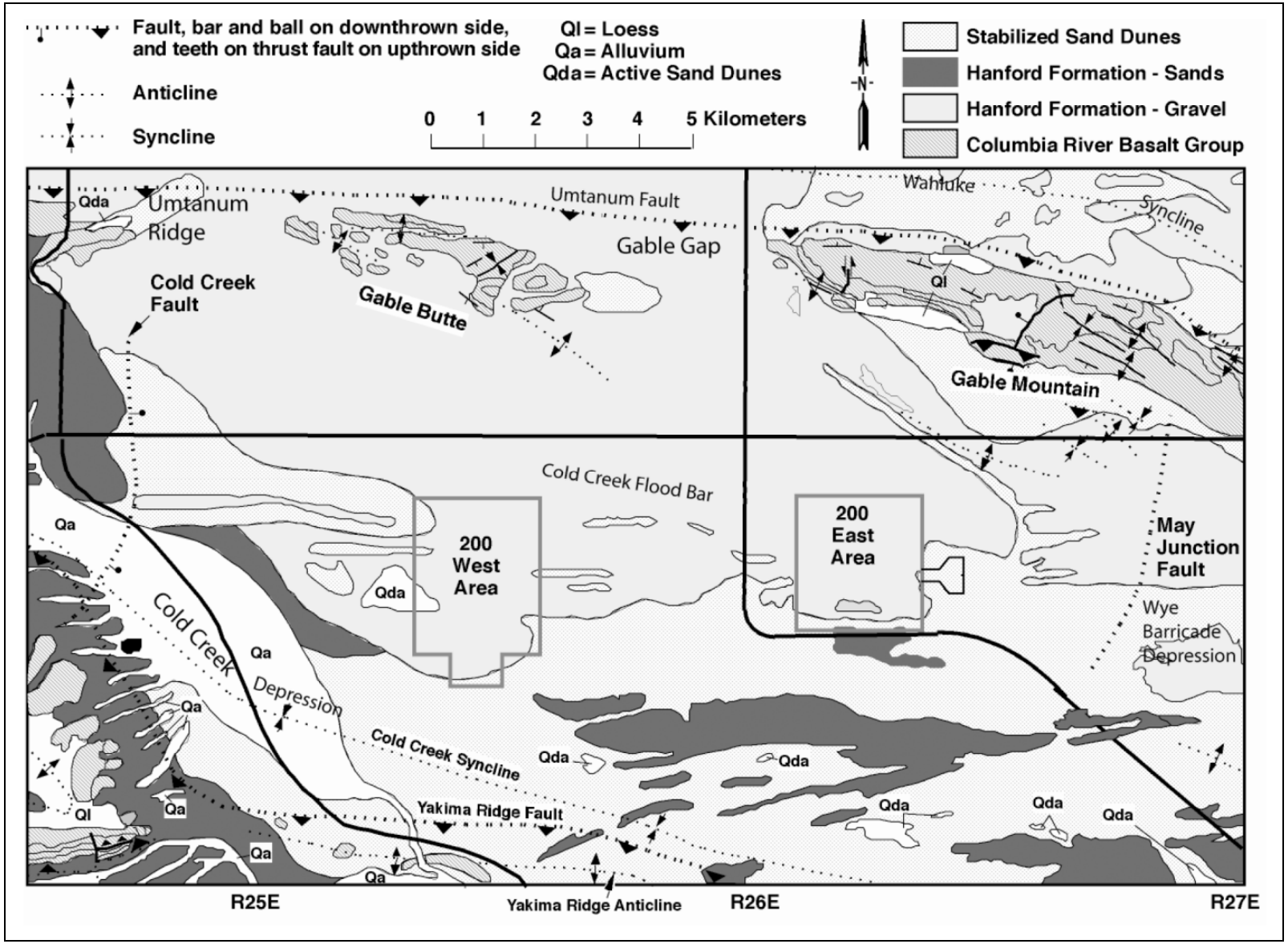

3.1.4.2.2 Stratigraphy. The generalized stratigraphy of the Pasco Basin and Hanford Site is shown in Figure 3-17. The principal rocks exposed at the surface of the surrounding ridges are the CRBG and intercalated sedimentary rocks of the Ellensburg Formation. In the low-lying basins and valleys, these are overlain by younger sedimentary rocks of the Ringold Formation, Cold Creek unit (CCU), and the Pleistocene cataclysmic flood deposits of the Hanford formation. Figure 3-18 provides an approximate west to east cross section through the Hanford Site.

Columbia River Basalt Group and Ellensburg Formation: The Elephant Mountain Member is the uppermost basalt flow beneath the 200 Areas and much of the Hanford Site. Where folds and faults have formed basalt ridges, other flows from the Saddle Mountains, Wanapum, and Grande Ronde Formations are exposed.

The Ellensburg Formation is intercalated with and overlies the CRBG in the Pasco Basin and includes epiclastic and volcaniclastic sedimentary rocks ("Stratigraphic and Lithologic Variations in the Columbia River Basalt" [Waters 1961]; USGS Bulletin 1457-G, "Revisions in stratigraphic nomenclature of the Columbia River Basalt Group"). The upper Ellensburg Formation consists of sand and gravel marking mainstream deposits and sand, silt, and clay overbank deposits that are sandwiched between basalt flows. Along with the more permeable basalt flow bottoms and flow tops, these sediments form the uppermost confined basalt aquifer system beneath the Hanford Site. The upper, younger Ellensburg Formation interbedded with the Saddle Mountains Basalt (as noted on Figure 3-17 as part of the CRBG) reflects changes in river courses, with sediments from the Columbia River becoming dominant as developing anticlinal ridges pushed the Columbia River east and basalt flows pushed the Clearwater-Salmon system to the south. Relatively few boreholes in the 200 Areas penetrate the Ellensburg Formation. Those boreholes that do penetrate the Ellensburg Formation generally find tuffaceous siltstones and sandstones, with conglomerates marking ancient main river channels. The Ellensburg stratigraphy of the Hanford Site has been discussed in more detail in Fecht et al. (1987).

The uppermost basalt flow beneath the Central Plateau is the Elephant Mountain Member (RHO-BWI-ST-14, "Chapter 3 – Wanapum and Saddle Mountains Basalts of the Cold Creek Syncline Area"). The top of basalt surface dips to the southwest beneath the 200 West Area and to the south-southwest beneath the 200 East Area. Low-amplitude secondary folds such as the one to the northeast of the 200 East Area may occur throughout the area and have probably not been fully identified. Between the 200 East Area and Gable Gap to the north, the Elephant Mountain has been eroded to expose underlying basalt flows. There is also a suspected window eroded through the Elephant Mountain near the northeast corner of the 200 East Area.

Post-Columbia River Basalt Sediments: The Hanford Site and tank farms are situated on a sequence of Ringold Formation, CCU, and Hanford formation sediments overlying the CRBG (Figure 3-19). The upper Miocene to middle Pliocene record of the Columbia River system in the Columbia Basin is represented by the upper Ellensburg and Ringold Formations. Except for local deposits (e.g., the CCU), there is a hiatus (erosion or lack of sedimentation) in the stratigraphic record between the end of the Ringold Formation deposition (3.4 Ma) and the beginning of Pleistocene (1.6 Ma) time (DOE/RW-0164, DOE/RL-2002-39).

Figure 3-17. Generalized Stratigraphy of the Hanford Site Including the Central Plateau.

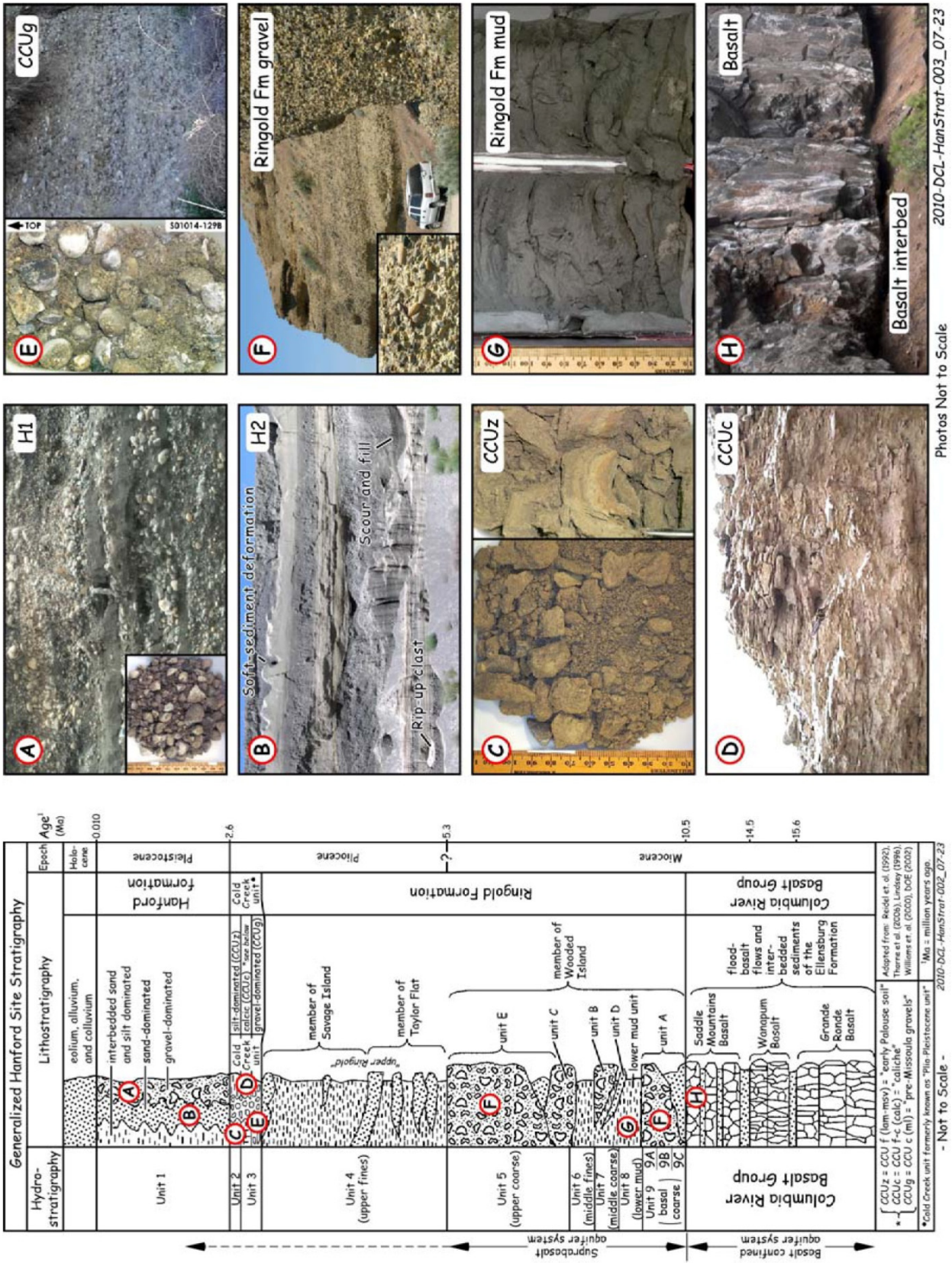

Figure 3-18. Cross-Section Running through the Central Plateau of the Hanford Site.

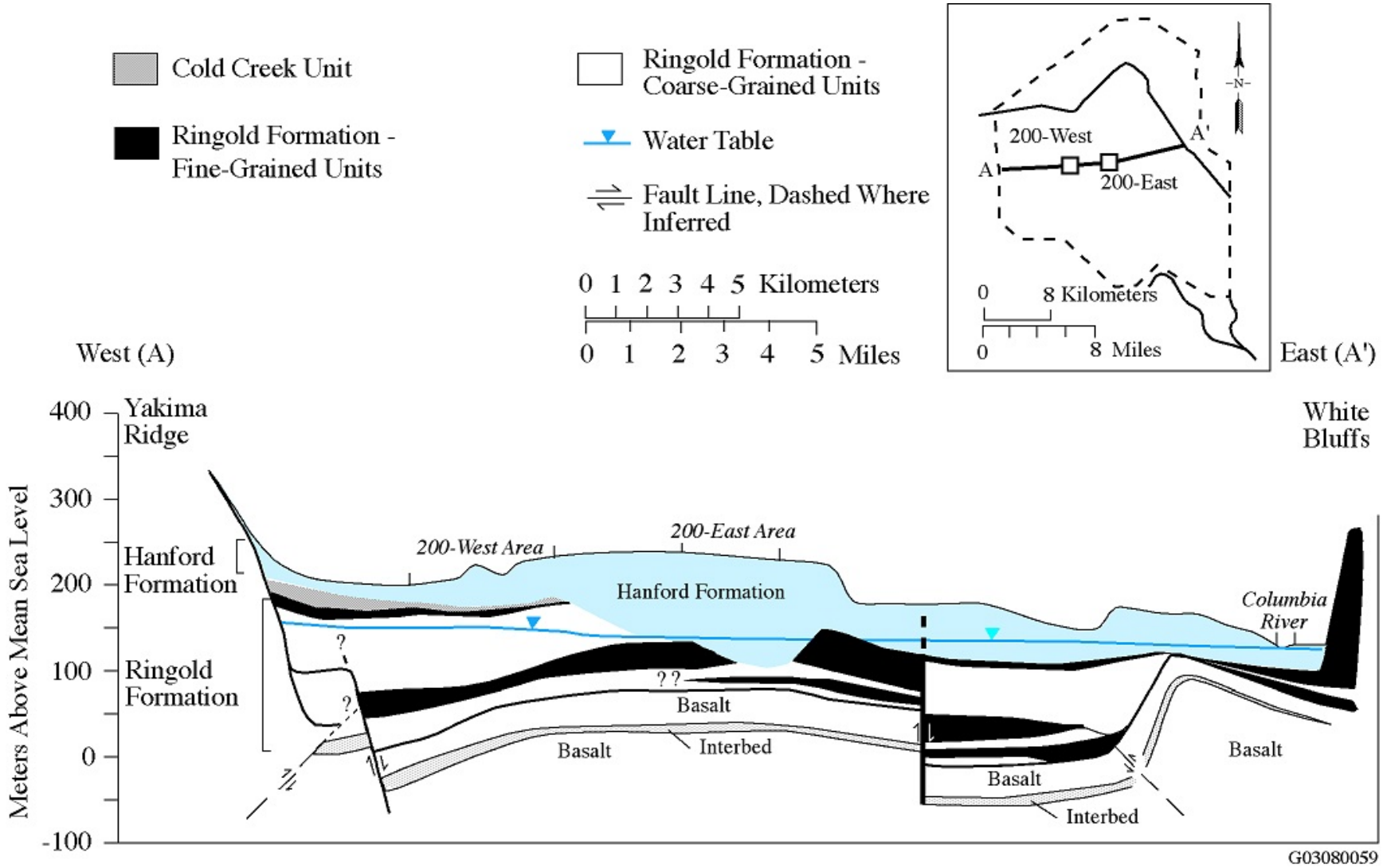

Figure 3-19. Fence Diagram of Sediment Overlying the Columbia River Basalt Group in the Central Plateau, Hanford Site.

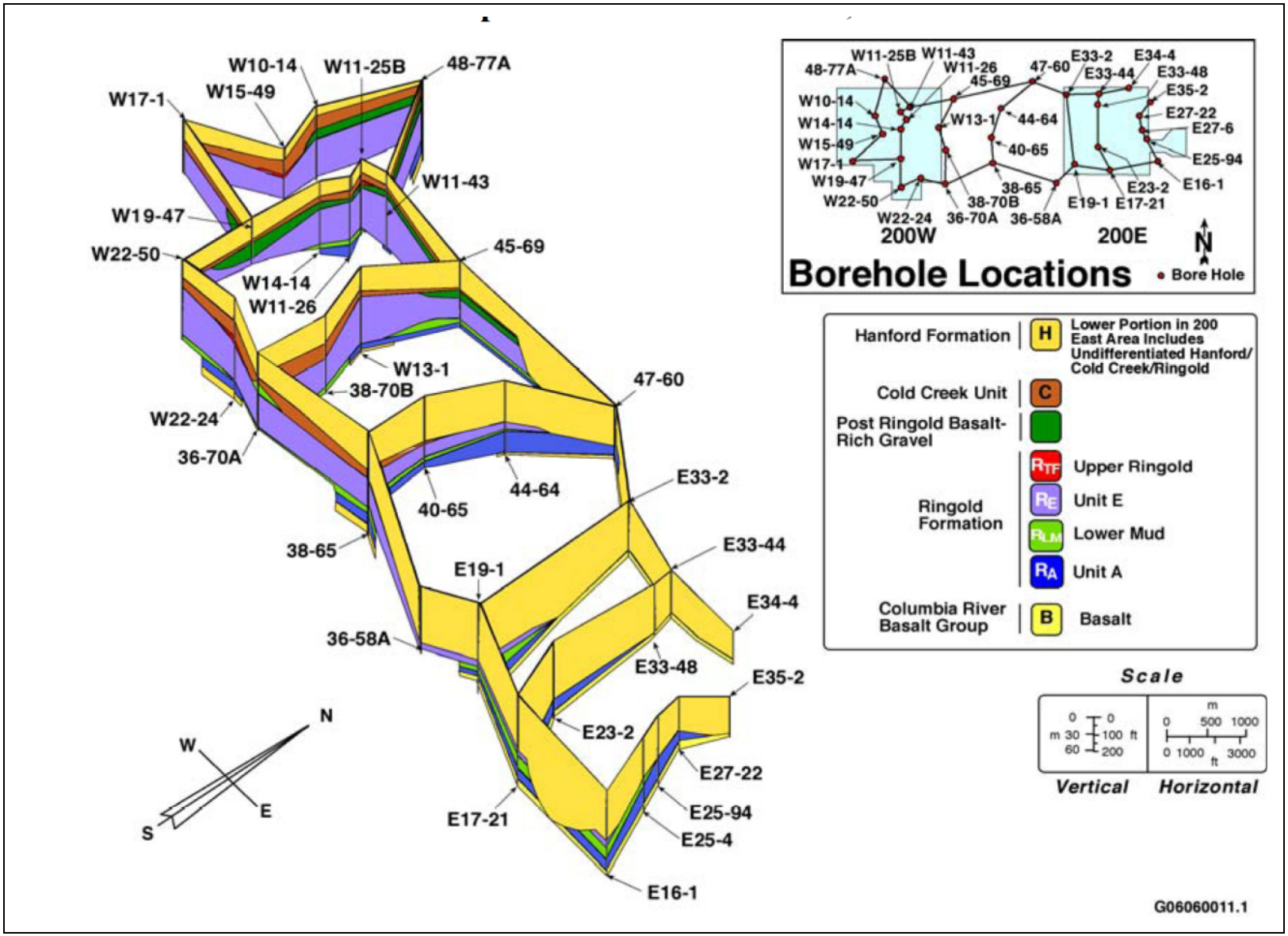

Ringold Formation: The Ringold Formation at the Hanford Site is up to 185 m (607 ft) thick in the deepest part of the Cold Creek syncline south of the 200 West Area and 170 m (558 ft) thick in the western Wahluke syncline near the 100 B Area. The Ringold Formation pinches out against the Gable Mountain, Yakima Ridge, Saddle Mountains, and Rattlesnake Mountain anticlines. It is largely absent in the northern and northeastern parts of the 200 East Area. It consists of semi-indurated clay, silt, pedo-genically altered sediment, fine- to coarse-grained sand, and granule to cobble gravel. Ringold Formation strata typically are below the water table on the Hanford Site, and the textural variations influence groundwater flow.

In the Pasco Basin, the lower half of the Ringold Formation, the member of Wooded Island, is the main unconfined aquifer under the Hanford Site and contains five separate stratigraphic intervals dominated by the fluvial gravel facies. These gravels, designated units A, B, C, D, and E, are separated by intervals containing deposits typical of the overbank and lacustrine facies (WHC-SD-EN-EE-004, "Revised Stratigraphy for the Ringold Formation, Hanford Site, South-Central Washington"). In the 200 Areas, only fluvial gravel units A and E occur. Between these two gravel units in many places is the lowermost of the fine-grained.

The upper part of the Ringold Formation, informally called the member of Taylor Flat (BHI-00184, "Miocene- to Pliocene-Aged Suprabasalt Sediments of the Hanford Site, South-Central Washington") consists of the sequence of fluvial sands, overbank deposits, and lacustrine sediments overlying unit E. This corresponds to the upper unit as originally defined by "Ringold Formation of Pleistocene Age in Type Locality, the White Bluffs, Washington" (Newcomb 1958) along the White Bluffs in the eastern Pasco Basin. The fluvial sand facies is the principal facies of the upper part under the tank farms at the Hanford Site.

Cold Creek Unit: The CCU (DOE-RL-2002-39) includes all material underlying the Hanford formation, overlying the Ringold Formation in the vicinity of the 200 West Area, and may extend over most of the central Pasco Basin. The CCU distinguishes itself from the Hanford and Ringold formations because it was formed when the Ringold Formation was eroding and relatively little was being deposited at the Hanford Site. This subunit is found locally in the Cold Creek syncline in the subsurface.

The CCU is laterally discontinuous and overlies the tilted and truncated Ringold Formation in an unconformable relationship in the western Cold Creek syncline in the vicinity of the 200 West Area (DOE/RL-2002-39). To the east, the pre-Missoula gravels replace the calcrete and silt-dominated subunits of the CCU. The CCU appears to be correlative to other side stream alluvial, eolian, and pedogenic deposits found near the base of the ridges bounding the Pasco Basin on the north, west, and south. These sedimentary deposits are inferred to have a late Pliocene to early Pleistocene age on the basis of stratigraphic position and magnetic polarity of interfingering loess units (DOE/RW-0164).

Distribution of the CCU depends in part on erosion and weathering of the underlying Ringold Formation and post-depositional erosion by the Ice Age floods ("Buried carbonate paleosols developed in Pliocene-Pleistocene deposits of the Pasco Basin, south-central Washington, U.S.A." [Slate 1996]). The thickness of the Cold Creek deposit ranges from 0 to 20 m (0 to 66 ft). Locally the CCU contains very hard rock that formed as precipitation evaporated and left

behind minerals forming what geologists call caliche or hardpan. This layer can influence contaminant migration by slowing its rate of downward movement and potentially diverting contaminants laterally (Slate 1996). However, CCU as described above is largely absent from the 200 East Area.

Hanford formation: The Hanford formation is the informal name given to all glacio-fluvial deposits from cataclysmic Ice Age floods found in the Pasco Basin (RHO-BWI-ST-4, "Geologic Studies of the Columbia Plateau: A Status Report"). Sources for floodwaters included glacial Lake Missoula, and ice-margin lakes that formed around the margins of the Columbia Plateau and Lake Bonneville (Baker et al. 1991). On average, interglacial conditions lasting ~50,000 years have been separated by major glacial advances, also averaging ~50,000 years. To date, Ice Age flood deposits from only four of the major glacial events that occurred between 1 million and 13,000 years ago are identified within the Pasco Basin (Baker et al. 1991; Open File Report 94-8, "Geologic Map of the Richland 1:100,000 Quadrangle, Washington"). Evidence to support the other major glacial cycles in the Pasco Basin either are masked or have been destroyed by subsequent Ice Age floods.

When the Ice Age floodwaters entered the Pasco Basin, they quickly became impounded behind Wallula Gap, which was too restrictive for the volume of water involved. Floodwaters formed temporary lakes with shorelines up to 381 m (1,250 ft) in elevation. The lakes lasted not more than a few days ("Magnitudes and implications of peak discharges from glacial Lake Missoula" [O'Connor and Baker 1992]). The deposits that were left after the floodwater receded, known as the Hanford formation, blanket low-lying areas over most of the Hanford Site. These Ice Age floods created Cold Creek bar (Figure 3-20), a giant, streamlined deposit of gravel, sand, and silt that extends for 19.3 km (12 mi) downstream of Umtanum Ridge. Gravel-dominated deposits, laid down under the strongest flood currents, are generally restricted to the north side of the bar. At the south end of the bar, where flood currents were gentler, interbedded sand and silt deposits were laid down. In between these two areas deposits of predominantly sand accumulated, which includes the area beneath C Farm.

The Hanford formation consists of mostly unconsolidated sediments that cover grain sizes from pebble to boulder gravel, fine- to coarse-grained sand, silty sand, and silt. The formation is further subdivided into gravel-, sand-, and silt-dominated facies, which transition into one another laterally with distance from the main, high-energy, flood channels. Beneath much of the Hanford Site the Hanford formation has been locally subdivided into several informal subunits. WHC-SD-EN-TI-290, "Geologic Setting of the Low-Level Burial Grounds" subdivides the Hanford formation in the 200 East and West Areas into three basic units: H1, H2, and H3. H1 is described as consisting of a gravel facies-dominated interval in the upper part of the formation throughout much of the 200 East and West Areas. Unit H2 is described as a predominantly sand facies-dominated unit, which increases in predominance within the formation from north to south across the same area. The H3 unit is generally described as a mixed sand and gravel facies unit found comprising the lower part of the formation in much of the 200 East Area, and possibly locally in the 200 West Area.

Furthermore, PNNL-19702, "Hydrogeologic Model for the Gable Gap Area, Hanford Site" identified five paleochannels (A through E) running through the Central Plateau that are filled

with coarse-grained, highly permeable flood deposits of the Hanford formation. These paleochannels may have initially formed during Ringold time, and if so, were further deepened during cataclysmic flooding which removed all Ringold-age deposits from the channel. Paleochannel D, which has a remnant of Ringold Formation along its east side, might be an example of a Ringold-age channel that was cut deeper during Ice Age flooding. Paleochannel D runs from the northwest corner through to the southeast corner of 200 East Area.

Holocene Surficial Deposits: Holocene surficial deposits consist of silt, sand, and gravel that form a thin layer across much of the Hanford Site. These sediments were deposited by a combination of eolian and alluvial processes.

Tank Farm Backfill: The shallowest sediments found within the confines of the tank farm are described primarily as basaltic pebble-cobble gravel with a sand and silt matrix. This material is commonly brown in color and contains construction debris, including nails, wood, and cement. These strata are interpreted to be tank farm backfill, which is consistent with previous interpretations of area geology (ARH-LD-132, "Geology of the 241-C Tank Farm"). Moisture logs collected in many of the tank farm leak detection borings show increased moisture ~12 to 13 m (40 to 42 ft) below ground surface (bgs). This is interpreted to be moisture accumulating above the compacted base of the original tank farm excavation. No soil has developed over the backfill and the vegetation within the WMA is controlled through herbicides.

3.1.4.2.3 Clastic Dikes. Clastic dikes are found in the Hanford formation and locally in other sedimentary units (RHO-BWI-C-64, "Clastic Dikes Of The Pasco Basin, Southeastern Washington, Final Report"; BHI-00230, "Geologic Field Inspection of the Sedimentary Sequence at the Environmental Restoration Disposal Facility"; BHI-01103, "Clastic Injection Dikes of the Pasco Basin and Vicinity – Geologic Atlas Series"). Clastic dikes (Figure 3-21) are vertical to sub-horizontal fissures filled by multiple layers of unconsolidated sand, silt, clay, and minor gravel aligned parallel to sub-parallel to dike walls. Clastic dikes range in vertical extent from 0.3 m to 55 m (1 ft to 180 ft). In cross-section, clastic dikes range from 1 millimeter to 1.8 m (0.04 in. to 5.91 ft) in thickness, and in plan view clastic dikes extend up to 100 m (328 ft) along strike. Clastic dikes form a branching pattern that in plan view forms polygons many feet across. Where the dikes intersect the ground surface, a feature known as patterned ground is observed. Patterned ground features are most abundant when Hanford formation sand-dominated and silt-dominated facies are at or near ground surface. BHI-01103 summarizes the location at Hanford where clastic dikes have been identified. Clastic dikes are inferred to be present beneath the SST farms, and at least locally, they cross-cut the Plio-Pleistocene boundary (WHC-EP-0698, "Groundwater Impact Assessment Report for the 216-U-14 Ditch"). BHI-01103 did not identify any clastic dikes in the vicinity of WMA C.

3.1.4.2.4 200 Areas Topography. Figure 3-22 shows the 200 Areas and the WMAs in a perspective view (note that the vertical to horizontal exaggeration in this figure is 5:1). The 200 Areas Central Plateau contains a topographic high in between the 200 East and 200 West Areas with gently dipping sides, except in the northwest corner of the 200 West Area. The WMAs were always located downhill from the waste-generating facilities to allow gravity flow in the pipelines from the facilities to the tanks. The relative flatness of the WMAs means that the final topography will be determined by the surface cover and grading of the surrounding soil.

Figure 3-20. Isopach Map of the Ice Age Flood Deposits (Hanford Formation).

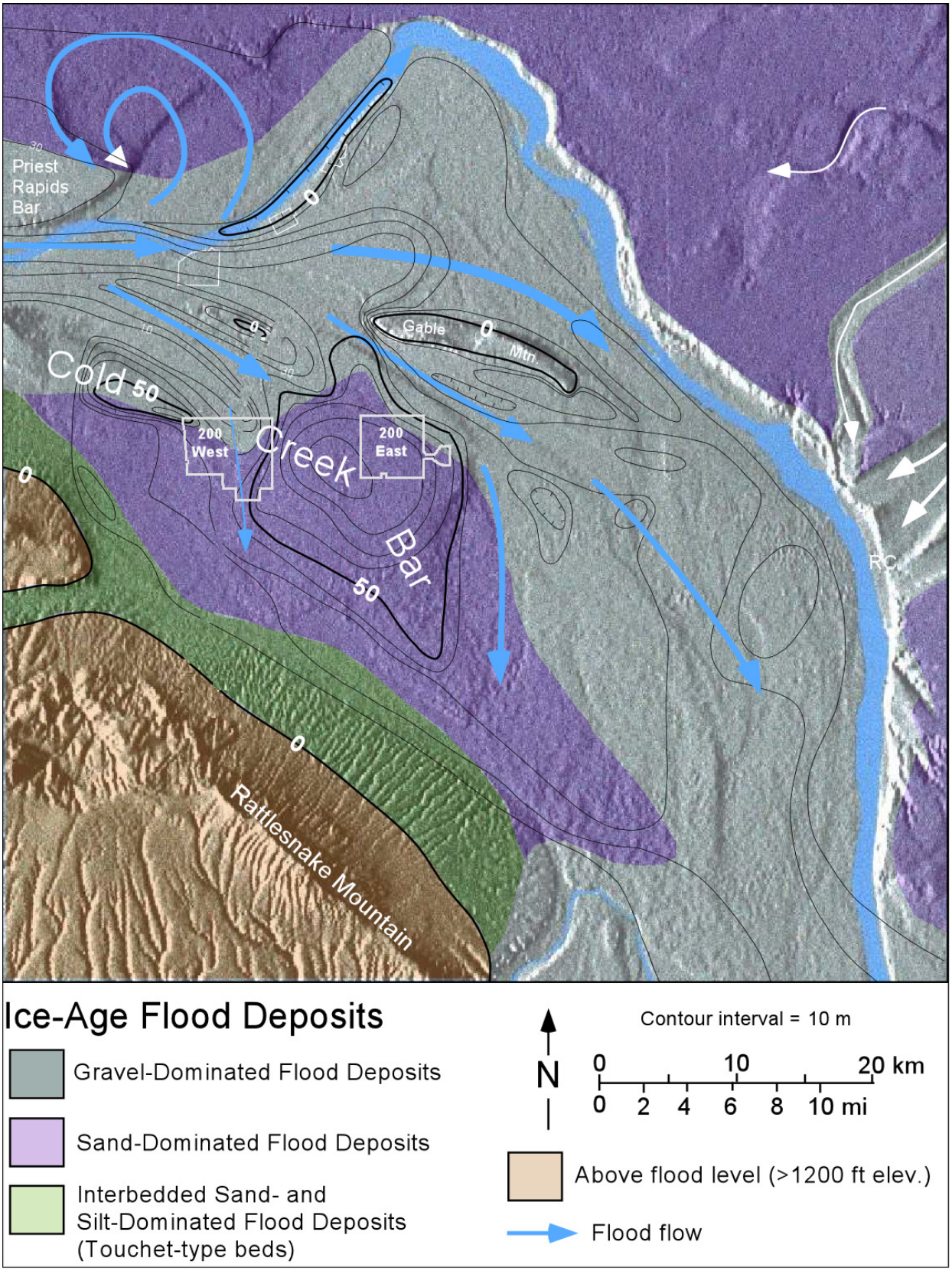

Figure 3-21. Typical Type II Clastic Injection Dike Exposed in a Wall of the Environmental Restoration Disposal Facility Excavation Exposed during Construction. The facility is located on the 200 Area Pleistocene Glacio-fluvial Flood Bar in the central Hanford Site.

Source: BHI-01103, "Clastic Injection Dikes of the Pasco Basin and Vicinity – Geologic Atlas Series."

Figure 3-22. Topography of the 200 Areas Central Plateau in Meters above Mean Sea Level.

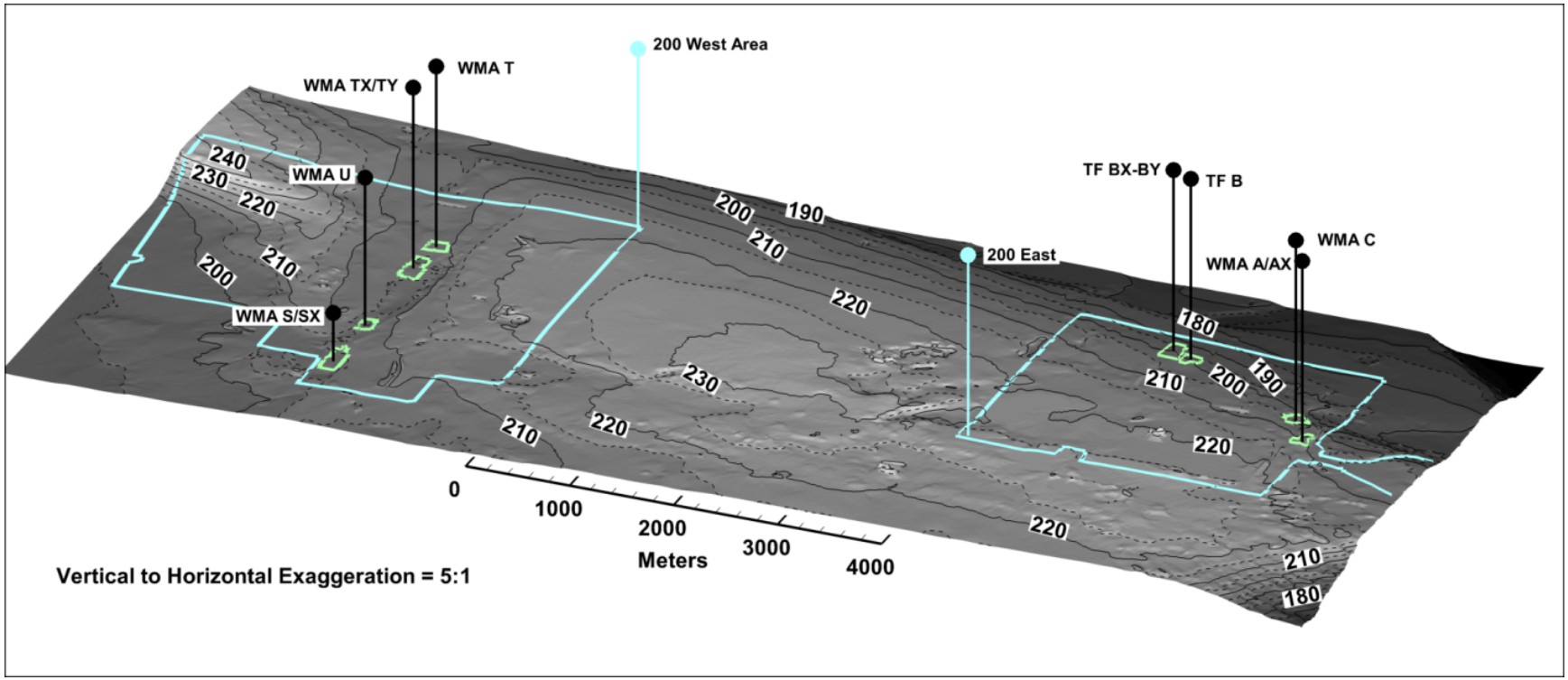

WMA = Waste Management Area

3.1.4.2.5 Surface Soils. The Holocene deposits and exposed Hanford formation sediments have experienced soil development and evolved into identifiable soil types. BNWL-243, "Soil Survey Hanford Project in Benton County Washington" describes 15 different surface soil types on the Hanford Site, varying from sand to silty and sandy loam. Various classifications, including land use, are also given in BNWL-243. These soil types control the flux of water reaching the water table (i.e., recharge) (PNNL-13033). The soils found in the Central Plateau in and around the 200 Areas are Quincy Sand (formally known as Rupert Sand), Burbank Loamy Sand, and Ephrata Sandy Loam. BNWL-243 described these types of soil as follows.

- **Quincy Sand (formally known as Rupert Sand).** This mapping unit represents one of the most extensive soils on the Hanford Site. The surface is a brown to grayish-brown coarse sand, which grades to a dark grayish-brown sand at ~1 m (~36 in.). Rupert soils developed under grass, sagebrush, and hopsage in coarse sandy alluvial deposits, which were mantled by wind-blown sand. Relief characteristically consists of hummocky terraces and dune-like ridges. This soil may be correlated as Quincy Sand, which was not separated here. Active sand dunes are present. Some dune areas are separated; however, many small dunes, blow-outs, and associated small areas of Ephrata and Burbank soils are included.

- **Burbank Loamy Sand.** This is a dark-colored (surface is very dark grayish-brown; subsoil is dark grayish-brown), coarse-textured soil which is underlain by gravel. The surface soil is usually 0.41 m (~16 in.) thick but can be 0.76 m (30 in.) thick. The gravel content of the subsoil may range from 20 to 80% by volume.

- **Ephrata Sandy Loam.** The surface of this soil is dark colored with subsoil that is dark grayish-brown and medium-textured. It is underlain by gravelly material that may extend for many feet.

- **Esquatzel Silt Loam.** This soil is not found within the 200 Areas Central Plateau, but rather to the south of the 200 West Area. It is mentioned here because it is a possible source for borrow material needed for the Modified RCRA Subtitle C Barrier (D&D-25575, "Silt Borrow Source Field Investigation Report"). It is deep dark-brown soil formed in recent alluvium and is derived from loess and lake sediment. The subsoil grades to dark grayish-brown in many areas, but color and texture of the subsoil are variable because of the stratified nature of the alluvial deposits.

Since the end of the Pleistocene, the main geologic process at the Hanford Site has been wind. After the last Missoula flood drained from the Pasco Basin, winds moved the loose, unconsolidated material until vegetation was able to stabilize it. Stabilized sand dunes cover much of the Pasco Basin, but there are areas, such as along the Hanford Reach National Monument, where active sand dunes remain.

3.1.4.3 Seismology. The historic record of earthquakes in the Pacific Northwest dates from about 1840. The early part of this record is based on newspaper reports of human perception of shaking and structural damage as classified using the Modified Mercalli Intensity (MMI) scale; the early record is probably incomplete because the region was sparsely populated. The

historical record appears to be complete since 1905 for MMI V and since 1890 for MMI VI ("Earthquake Recurrence Rate Estimates for Eastern Washington and the Hanford Site," CONF-8910192--18 [Rohay 1989]). Seismograph networks did not start providing earthquake locations and magnitudes of earthquakes in the Pacific Northwest until about 1960. A comprehensive network of seismic stations that provides accurate locating information for most earthquakes of magnitude greater than 2.5 on the Richter scale was installed in eastern Washington during 1969. Currently, measured seismic activity for the Hanford Site is reported quarterly and annually (e.g., PNNL-20302, "First Quarter Hanford Seismic Report for Fiscal Year 2011"). Figure 3-23 provides summaries of known events at and around the Hanford Site between 1890 and 2005 (PNNL-6415).

Three horizontal layers of stratigraphy related to seismicity exist at the Hanford Site and vicinity including the CRBG, the pre-basalt sediments, and the crystalline basement. About 75% of Hanford Site earthquake events originate in the CRBG layer. The pre-basalt sedimentary layer has been the origin of 8% of the events, and the crystalline basement has been the origin of 17% of these events (Revision 5-C of RPP-13033, "Tank Farms Documented Safety Analysis").

The most frequent seismic occurrences at the Hanford Site are earthquake swarms (Figure 3-24) that consist of multiple small energy events that fall within a small energy range and are constrained temporally (weeks to months) and spatially (5 to 10 km [3 to 6 mi] in length). Swarms tend to reoccur in particular locations, ~90% of individual earthquakes are at Richter scale magnitudes of 2 or less, and 70% to 80% of them occur at depths less than 4 km (2.5 mi) bgs.

Larger isolated earthquakes also occur nearby (DOE/RW-0164). The largest single event earthquake recorded near the Hanford Site occurred in Milton-Freewater, Oregon, located ~80 km (50 mi) away in 1936 at a Richter magnitude of 5.75 and a maximum MMI of VII. The two next largest nearby earthquakes occurred north of the Hanford Site in 1917 and 1973 near Othello, Washington, ~48 km (30 mi) north of the 200 Areas with magnitudes above 4 on the Richter scale and MMI of V. The 1973 earthquake occurred ~1 km (0.6 mi) bgs. Since 1973, 80 small earthquakes (2.5 to 4.3 magnitudes) have been recorded within a radius of 90 km (56 mi) of the Hanford Site Central Plateau, the closest being a magnitude 3.3 event with the epicenter 8 km (5 mi) north of the 200 Areas. Earthquake depths vary for isolated events and have been estimated as deep as 30 km (~19 mi).

Greater magnitude earthquakes have been recorded at greater distances from the Hanford Site at the edges of the Columbia Plateau, along the coastal subduction zones to the west and in the Rocky Mountains to the east. The Columbia Plateau, which is made up of thick and extensive sequences of flood basalt layers in the Columbia River Group, extends well beyond the Hanford Site covering parts of eastern Washington, eastern Oregon, and Idaho. Notable events in these areas are the 2001 "Nisqually earthquake" in the Puget Sound (6.8 magnitude), an approximate magnitude 6.8 to 7.4 earthquake in north-central Washington in 1872 near Lake Chelan, the 1959 Hebgen Lake earthquake (7.5 magnitude) in western Montana, and the 1983 Borah Peak earthquake in eastern Idaho (7.3 magnitude).

Figure 3-23. Historical Earthquake Activity of the Columbia Basin, Washington, and Surrounding Areas.

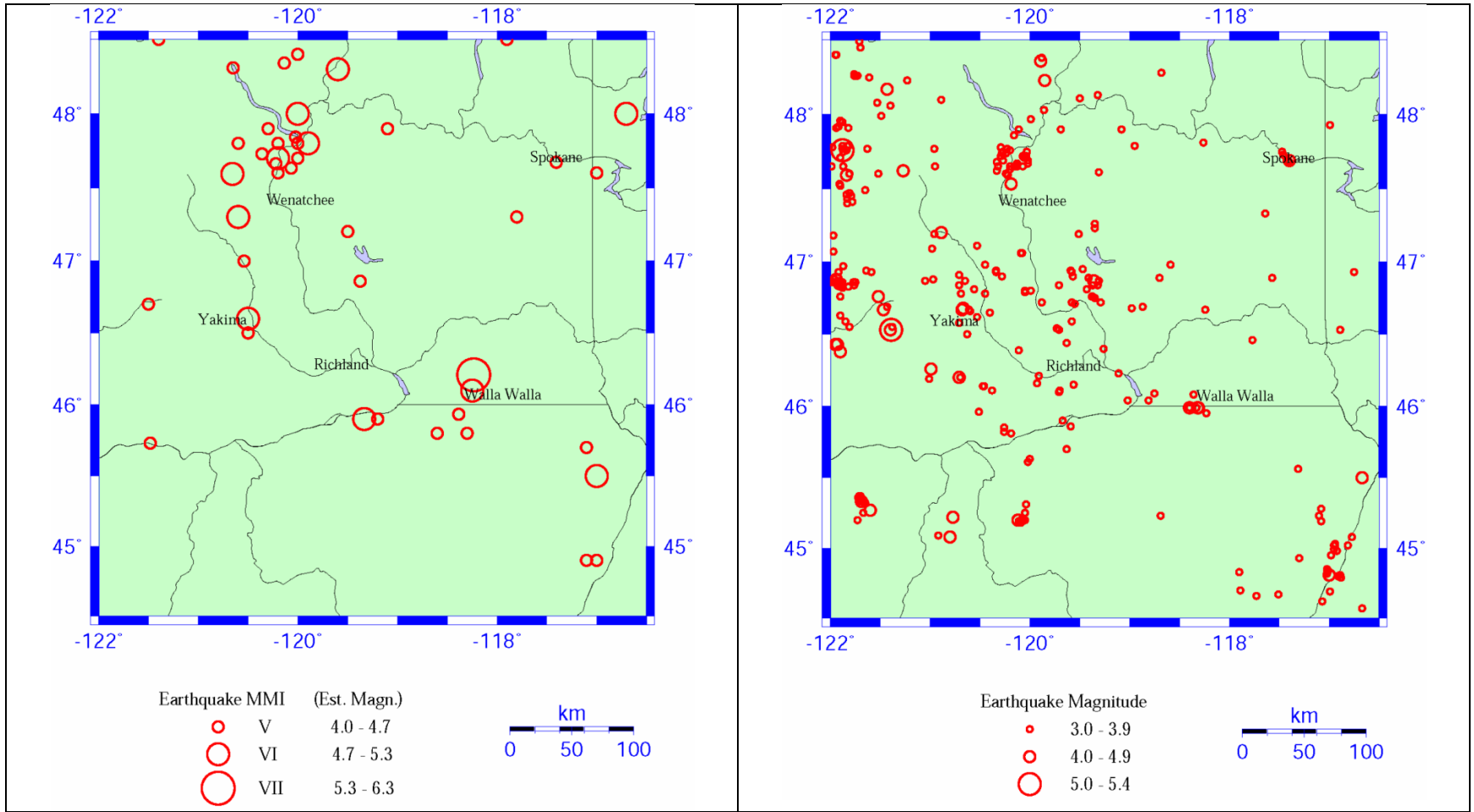

Left: *Historical Earthquake Activity of the Columbia Basin, Washington, and Surrounding Areas. All earthquakes between 1890 and 1970 with a Modified Mercalli Intensity (MMI) V or larger and/or a magnitude 4 or larger are shown ("Earthquake Recurrence Rate Estimates for Eastern Washington and the Hanford Site," CONF-8910192--18 [Rohay 1989]).*

Right: *Earthquake Activity of the Columbia Basin, Washington, and Surrounding Areas as Measured by Seismographs. All earthquakes between 1970 and 2005 with Richter magnitudes of 3 or larger are shown (Northern California Earthquake Data Center, Queried 09/2005, [Advanced National Seismic System (ANSS) Catalog Search], http://www.quake.geo.berkeley.edu/anss/catalog-search.html).*

Source: PNNL-6415, "Hanford Site National Environmental Policy Act (NEPA) Characterization."

Figure 3-24. Earthquake Swarm Areas in the Vicinity of the Hanford Site.

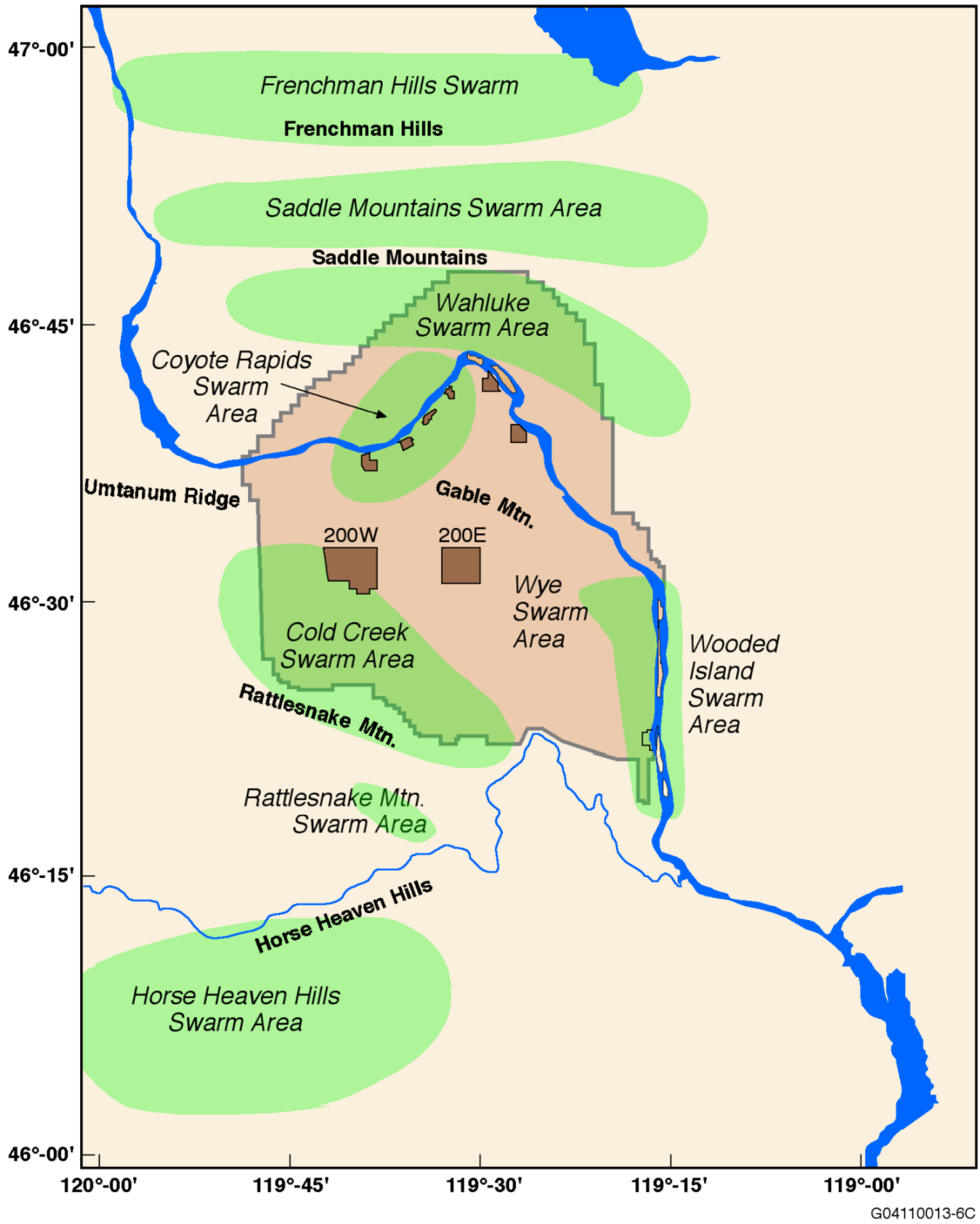

The gross pattern of seismic activity around the Hanford Site is consistent with our understanding of regional tectonic characteristics of the Northwest. That is, the flood basalts form a large and relatively competent block of rock that is surrounded by numerous complex zones of active faults where large-scale stresses, imposed primarily by the ongoing subduction of the Pacific and Juan de Fuca Plates underneath the North American Plate, are mostly relieved. Consequently, relatively minimal stress relief occurs in the Columbia Plateau and earthquake energy is correspondingly small. This means that potential ground motion that accompanies these earthquakes is also relatively small.

Relative movement is commonly quantified as some fraction of gravitational acceleration (g) and has been usually correlated with earthquake magnitude. For the range of earthquake magnitudes suggested by data summarized above for the Hanford Site (<3 to 6), peak accelerations between <0.0017 and 0.18 g are proposed. The associated range of motion is generally imperceptible compared to clearly felt movement that can result in minimal building damage. A probabilistic seismic hazard analysis (WHC-SD-W236A-TI-002, "Probabilistic Seismic Hazard Analysis, DOE Hanford Site, Washington") estimated that a 0.1 g horizontal acceleration would occur every 500 years and a 0.2 g acceleration would occur every 2,500 years.

3.1.4.4 Volcanology. Two types of volcanic hazards have affected the Hanford Site in the past 20 million years. The hazards were (1) continental flood basalt volcanism that produced the CRBG and (2) volcanism associated with the Cascade Range. Several volcanoes in the Cascade Range are currently considered to be active, but activity associated with flood basalt volcanism has ceased.

The flood basalt volcanism that produced the CRBG occurred between 17 and 6 million years ago. Most of the lava was extruded during the first 2 to 2.5 million years of the 11-million-year volcanic episode. Volcanic activity has not recurred during the last 6 million years, suggesting that the tectonic processes that created the episode have ceased. The recurrence of CRBG volcanism is not considered to be a credible volcanic hazard (DOE/RW-0164).

Volcanism in the Cascade Range was active throughout the Pleistocene Epoch and has remained active through the Holocene Epoch. The eruption history of the current Holocene Epoch best characterizes the most likely types of activity in the next 100 years. Many of the volcanoes have been active in the last 10,000 years, including Mount Mazama (Crater Lake) and Mount Hood in Oregon; and Mount Saint Helens, Mount Adams, and Mount Rainier in Washington. The Hanford Site is 150 km (~93 mi) from Mount Adams, 175 km (109 mi) from Mount Rainier, and 200 km (124 mi) from Mount Saint Helens, the three closest active volcanoes. At these distances, the deposition of tephra (ash) is the only potential hazard. Mount Saint Helens has been considerably more active throughout the Holocene Epoch than Mount Rainier or Mount Adams, which is the least active of the three. WHC-SD-GN-ER-30038, "Volcano Ashfall Loads for the Hanford Site," concludes that the Hanford Site is sufficiently distant from the Cascade Range volcanoes that hazards from lava flows, pyroclastic flows and surges, landslides, lahars, and ballistic projectiles are below a probability of concern.

3.1.4.5 Subsurface Subsidence and Liquefaction. Field and laboratory studies that have been completed at many of the tank farm sites are summarized in WHC-SD-GN-ER-30009, "Bibliography and Summary of Geotechnical Studies at the Hanford Site." These studies reveal

that there are no areas of potential surface or subsurface subsidence, uplift, or collapse at the Hanford Site, with the minor exceptions of the Cold Creek and Wye Barricade depressions, neither of which are close to WMA C. With the exception of the loose superficial wind-deposited silt and sand in some locations, the in-place soils are competent and form good foundations.

Liquefaction is the sudden decrease of shearing resistance of a cohesionless soil, caused by the collapse of the structure by shock or strain, and is associated with a sudden but temporary increase of the pore fluid pressure. Saturated or near-saturated soil (sediments) are required for liquefaction to occur. The average volumetric moisture content at WMA C is less than 10% (see Section 3.1.9.2.2). Therefore, liquefaction of soils beneath the tank farms would not be a credible hazard because the water table is greater than 65 m (213 ft) bgs.

3.1.5 Hydrology

This section presents the summary of the hydrology/hydrogeology (water and soil characteristics) of the Hanford Site, focusing on surface water, recharge, characteristics of the unsaturated zone or vadose zone and the saturated zone or groundwater. Due to waste disposal operations at the Hanford Site, the hydrology of the Site has been studied and monitored in detail. Therefore, the information presented in this section will primarily be a summation of previous work highlighting those characteristics that affect the WMA C PA. For additional detail, see the following references.

- PNNL-20548, "Hanford Site Environmental Report for Calendar Year 2010 (Including Some Early 2011 Information)" provides the overview of the characterization and monitoring activities conducted at the Hanford Site during the calendar year.

- DOE/RL-2013-22, Hanford Site Groundwater Monitoring Report for 2012. This document describes the groundwater monitoring activities during the fiscal year.

- Revision 18 of PNNL-6415, "Hanford Site National Environmental Policy Act (NEPA) Characterization" provides a standardized description of the Hanford Site environment.

- DOE/ORP-2008-01, RCRA Facility Investigation Report for the Hanford Single-Shell Tank Waste Management Areas. This document describes the Phase 1 vadose zone characterization efforts at the SST farms.

These overview documents will contain references to site-specific documents that describe the hydrology for a particular waste site (e.g., WMA C). A summary of the hydrology for WMA C is given in Section 3.1.9 Waste Management Area C Site Characterization.

3.1.5.1 Surface Water. Surface water at the Hanford Site includes the Columbia River, Columbia Riverbank seepage, springs, and ponds. Intermittent surface streams, such as Cold Creek, may also contain water after large precipitation or snowmelt events. In addition, the Yakima River flows along a short section of the southern boundary of the Hanford Site (Figure 3-25), and there is surface water associated with irrigation east and north of the Site.

Figure 3-25. Surface Water Features including Rivers, Ponds, Major Springs, and Ephemeral Streams on the Hanford Site, Washington.

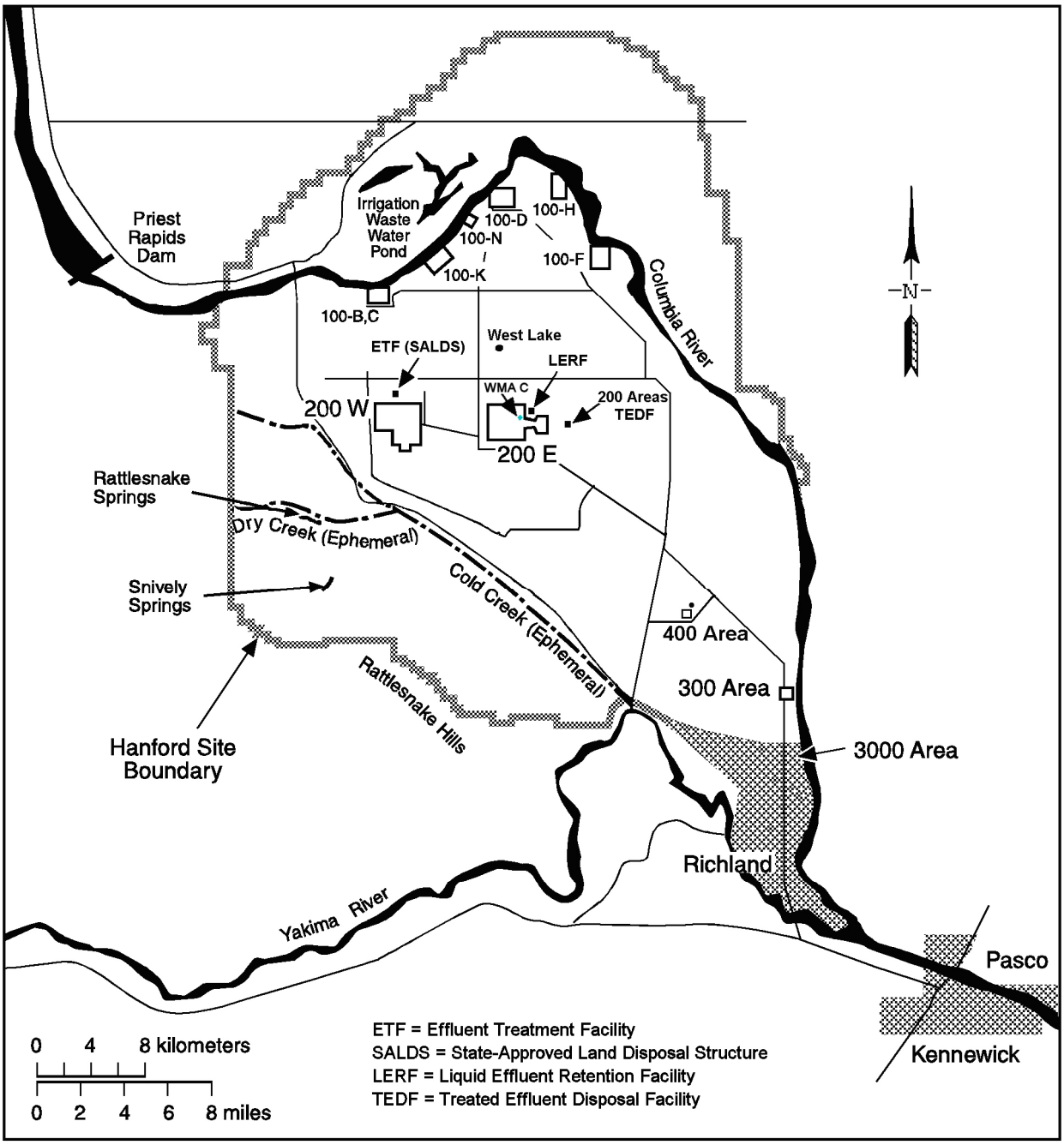

S9508017.4

3.1.5.1.1 Columbia River. The Columbia River is the second largest river in the contiguous United States in terms of total flow and is the dominant surface-water body on the Hanford Site. The original selection of the Hanford Site for plutonium production and processing was based, in part, on the occurrence of abundant water provided by the Columbia River. The existence of the Hanford Site has precluded development of this section of the river. Waste left at WMA C

following closure could impact the Columbia River through the groundwater pathway. Waste Management Area C is located ~11.2 km (7 mi) from the Columbia River.

The Columbia River originates in the mountains of eastern British Columbia, Canada, and drains an area of ~680,000 km^2 (262,480 mi^2) enroute to the Pacific Ocean. Columbia River flow at the U.S. Geological Survey gauging station, located just west of the Hanford Site boundary (located downstream of Priest Rapids Dam), has been measured during a 90-year period from 1917 to 2007. Daily average flows during this period ranged from 570 to 19,540 m^3/s (20,000 to 690,000 ft^3/s). The lowest and highest flows occurred before the construction of upstream dams. During the 10-year period from 1997 through 2006, the average flow rate was also ~3,300 m^3/s (116,500 ft^3/s). The river elevation is ~121 m (396 ft) near the 100 B and C areas and ~105 m (343 ft) at the 300 Area.

The Columbia River flows through the northern part and along the eastern border of the Hanford Site with these areas of the Hanford Site draining into the Columbia River. Except for the Columbia River estuary, the only unimpounded stretch of the river in the United States is the Hanford Reach, which extends from Priest Rapids Dam (located upstream of the Site) downstream ~82 km (51 mi) to the northern upstream extent of Lake Wallula (formed by McNary Dam), which begins above Richland. The Hanford Reach of the Columbia River was recently incorporated into the land area established as the Hanford Reach National Monument.

Flows in the Hanford Reach are directly affected by releases from Priest Rapids Dam; however, Priest Rapids operates as a run-of-the-river dam rather than a storage dam. Flows are controlled to generate power and promote salmon egg and embryo survival. Several drains and intakes are also present along the Hanford Reach, including irrigation outfalls from the Columbia Basin Irrigation Project, intakes at the Columbia Generating Station operated by Energy Northwest, and Hanford Site intakes for onsite water use.

The State of Washington has promulgated water quality standards for the Columbia River, WAC 173-201A, "Water Quality Standards for Surface Waters of the State of Washington." The Hanford Reach of the Columbia River has been designated as Class A (Excellent). This designation requires that the water be usable for substantially all needs, including drinking water, recreation, and wildlife. The DOE has conducted routine water-quality monitoring of the Columbia River since 1958.

3.1.5.1.2 Yakima River. The Yakima River, which follows a small length of the southwest boundary of the Hanford Site, has much lower flows than the Columbia River. The average flow, based on nearly 72 years of daily flow records (U.S. Geological Survey, Queried 09/2015, [USGS Water Data for the Nation], http://waterdata.usgs.gov/nwis/nwis), is ~100 m^3/s (3,530 ft^3/s), with an average monthly maximum of ~500 m^3/s (17,550 ft^3/s), and minimum of 4.7 m^3/s (165 ft^3/s). The Yakima River System drains surface runoff from approximately one-third of the Hanford Site. Contaminant plumes in groundwater that originate from the Hanford Site do not reach the Yakima River and, because the elevation of the river surface is higher than the adjacent water table (based on well water-level measurements), groundwater is expected to flow from the Yakima River into the aquifer underlying the Site rather than from the

aquifer into the river (PNL-10195, "Three-Dimensional Conceptual Model for the Hanford Site Unconfined Aquifer System: FY 1994 Status Report").

3.1.5.1.3 Springs and Streams. Springs are found on the slopes of Rattlesnake Hills (Figure 3-25) along the western edge of the Site (DOE/RW-0164). An alkaline spring is located at the east end of Umtanum Ridge ("Biodiversity Inventory and Analysis of the Hanford Site, 1997 Annual Report" [The Nature Conservancy 1998]). Rattlesnake and Snively Springs form small surface streams (Figure 3-25). Water is discharged from Rattlesnake Springs and flows in Dry Creek for ~2.6 km (1.6 mi) before disappearing into the ground. Cold Creek and its tributary, Dry Creek, are ephemeral streams within the Yakima River drainage system in the southwestern portion of the Site. These streams drain areas to the west of the Site and cross the southwestern part of the Site toward the Yakima River. When surface flow occurs, it infiltrates rapidly and disappears into the surface sediments in the western part of the Site. The quality of water in these springs and streams varies depending on the source; they are upgradient of Hanford waste and plumes of contaminated groundwater found on the Hanford Site.

3.1.5.1.4 Flooding. Columbia River flow is regulated by three upstream dams in Canada and by seven upstream dams in the United States. The Hanford Reach, ~80 km (50 mi) long, extends from Priest Rapids Dam to just north of the 300 Area. Flow through the Hanford Reach fluctuates significantly and is controlled at Priest Rapids Dam. The three dams with the largest reservoirs upstream from the Hanford Site are the Mica and Hugh Keenleyside Dams in Canada and the Grand Coulee Dam in the United States. The controlled flow of the Columbia River caused by these dams results in a lower flood hazard for high-probability floods (e.g., 100-year floods); however, dam-failure scenarios are significant potential contributors that result in high flood flows.

The probable maximum flood for the Columbia River downstream of Priest Rapids Dam has been calculated to be 40,000 m^3/s (1.4 million ft^3/s) (Figure 3-26) and is greater than the 500 year flood. This flood would inundate parts of the 100 Area adjacent to the Columbia River, but the central portion of the Hanford Site would remain unaffected [DOE/RW-0070, Nuclear Waste Policy Act (Section 112), Environmental Assessment, Reference Repository Location, Hanford Site, Washington]. The USACE has derived the Standard Project Flood with both regulated and unregulated peak discharges given for the Columbia River downstream of Priest Rapids Dam ("Water Control Manual for McNary Lock and Dam, Columbia River, Oregon and Washington" [USACE 1989]). The regulated Standard Project Flood for this part of the river is given as 15,200 m^3/s (536,800 ft^3/s) and the 100 year regulated flood as 12,400 m^3/s (438,000 ft^3/s). Impacts to the Hanford Site are negligible and would be less than the probable maximum flood.

The USACE evaluated a number of scenarios on the effects of failures of Grand Coulee Dam, assuming flow conditions on the order of 11,325 m^3/s (400,000 ft^3/s). The discharge resulting from a 50% breach at the outfall of Grand Coulee Dam was determined to be 595,000 m^3/s (21 million ft^3/s). In addition to the areas inundated by the probable maximum flood, the remainder of the 100 Area, the 300 Area, and nearly all of Richland would be flooded (DOE/RW-0070) as shown in Figure 3-26. No determinations were made for breaches greater than 50% of Grand Coulee Dam, for failures of dams upstream, or for associated failures

downstream of Grand Coulee. Based on a 1951 USACE study (USACE 1951, "Artificial Flood Possibilities on the Columbia River"), the 50% breach scenario was believed to represent the largest realistically conceivable flow resulting from either a natural or human-induced breach (DOE/RW-0070). It was also assumed that a scenario such as the 50% breach would occur only as the result of direct explosive detonation, and not because of a natural event such as an earthquake, and that even a 50% breach under these conditions would indicate an emergency situation in which there might be other overriding major concerns.

A flood scenario of a 50% breach of Grand Coulee Dam results in a flood level of ~143.3 m (470 ft) above mean sea level at Columbia River mile 365; this low point is the closest flood route to the 200 Areas Plateau. River mile 365 is ~45.7 m (150 ft) below the ground surface of the lowest elevation tank farm. The 50% breach of the Grand Coulee Dam would not impact the 200 East and 200 West areas or the land within the 600 Area (i.e., between the 200 East and 200 West areas) occupied by tank farm facilities. Therefore, this scenario bounds all other Columbia River flood scenarios. UCRL-21069, "Probabilistic Flood Hazard Assessment for the N Reactor, Hanford, Washington" provides a detailed hazard assessment of other flood scenarios.

The Yakima River is ~19.3 km (12 mi) south of and greater than 61 m (200 ft) in elevation below the 200 East and 200 West areas. The Yakima River is not a flood hazard for the tank farm facilities. During 1980, a flood risk analysis of Cold Creek was conducted as part of the characterization of a basaltic geologic repository for high-level radioactive waste. In lieu of 100- and 500-year floodplain studies, a probable maximum flood evaluation was performed based on a large rainfall or combined rainfall/snowmelt event in the Cold Creek and Dry Creek watershed (RHO-BWI-C-120/PNL-4219, "Flood Risk Analysis of Cold Creek near the Hanford Site") (Figure 3-27). The probable maximum flood discharge rate for the lower Cold Creek Valley was 2,265 m^3/s (80,000 ft^3/s) compared to 564 m^3/s (19,900 ft^3/s) for the 100 year flood. Modeling indicated that State Route 240, along the Hanford Site's southwestern and western areas, would not be usable. Based on this information, flooding of WMA C would not be a credible scenario.

3.1.5.1.5 Columbia Riverbank Springs. During the early 1980s, researchers identified 115 springs along the Benton County shoreline of the Hanford Reach (PNL-5289, "Investigation of Ground-Water Seepage from the Hanford Shoreline of the Columbia River"). Seepage occurs both below the river surface and on the exposed riverbank, particularly at low river stage. Riverbank springs flow intermittently, apparently influenced primarily by changes in river level. In many areas, water flows from the river into the aquifer at high river stage and then returns to the river at low river stage. This "bank storage" phenomenon has been modeled numerically for the 100 H Area (PNNL-13674, "Zone of Interaction Between Hanford Site Groundwater and Adjacent Columbia River: Progress Report for the Groundwater/River Interface Task Science and Technology Groundwater/Vadose Zone Integration Project"). In areas of contaminated groundwater, riverbank springs are also generally contaminated. The concentrations in seeping water along the riverbank may be lower than groundwater; however, the mixing between river water and the contaminated aquifer contributed to the fluctuating bank storage phenomenon.

Figure 3-26. Flood Area for the Probable Maximum Flood on the Hanford Site, Washington, as Determined by the Upper Limit of Precipitation and Maximum Runoff.

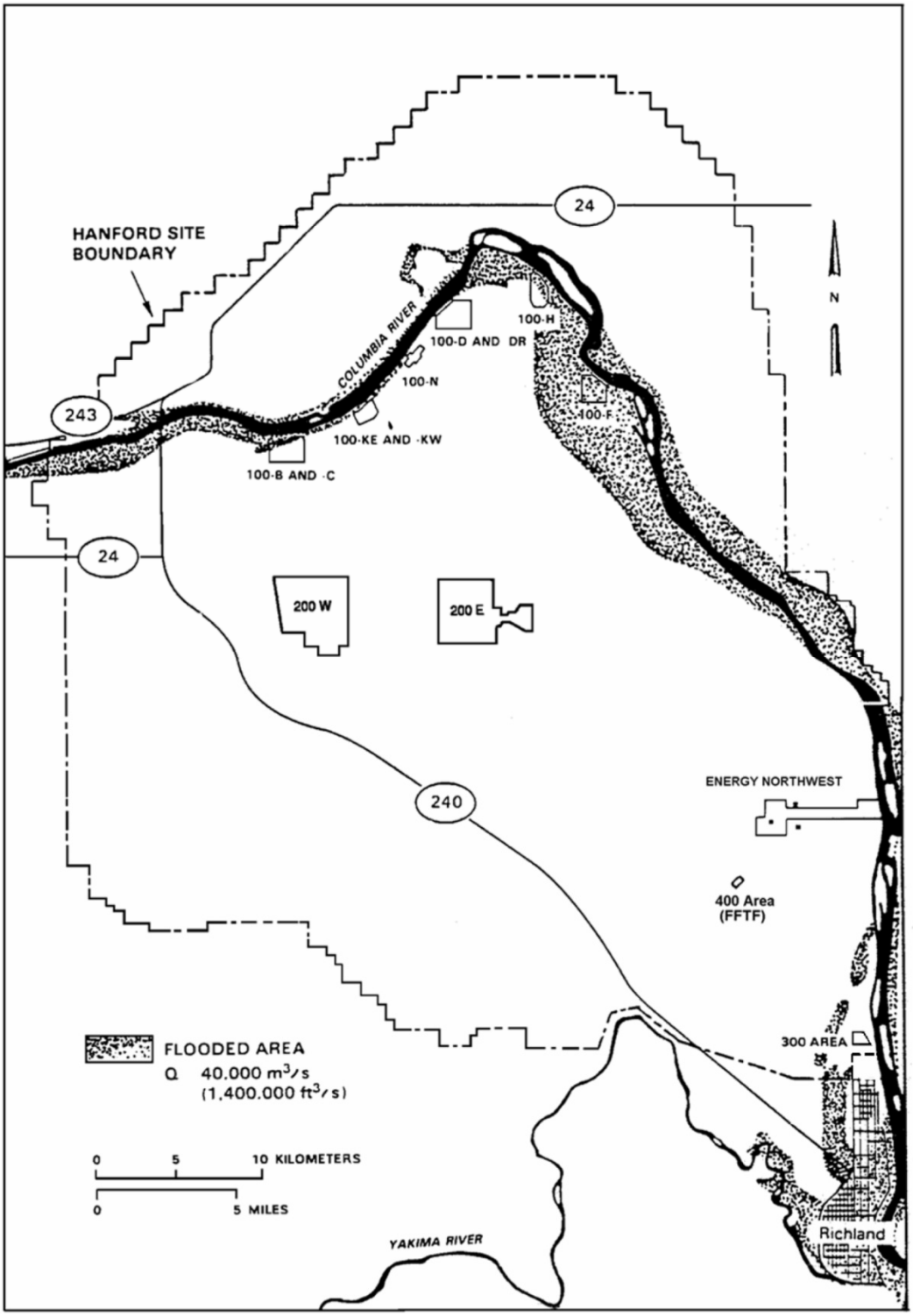

Reference: DOE/RW-0070, Nuclear Waste Policy Act (Section 112), Environmental Assessment, Reference Repository Location, Hanford Site, Washington.

FFTF = Fast Flux Test Facility

Figure 3-27. Extent of Probable Maximum Flood in Cold Creek Area, Hanford Site, Washington, delineated using the U.S. Army Corps of Engineers' HEC-2 Water Surface Profiles Model.

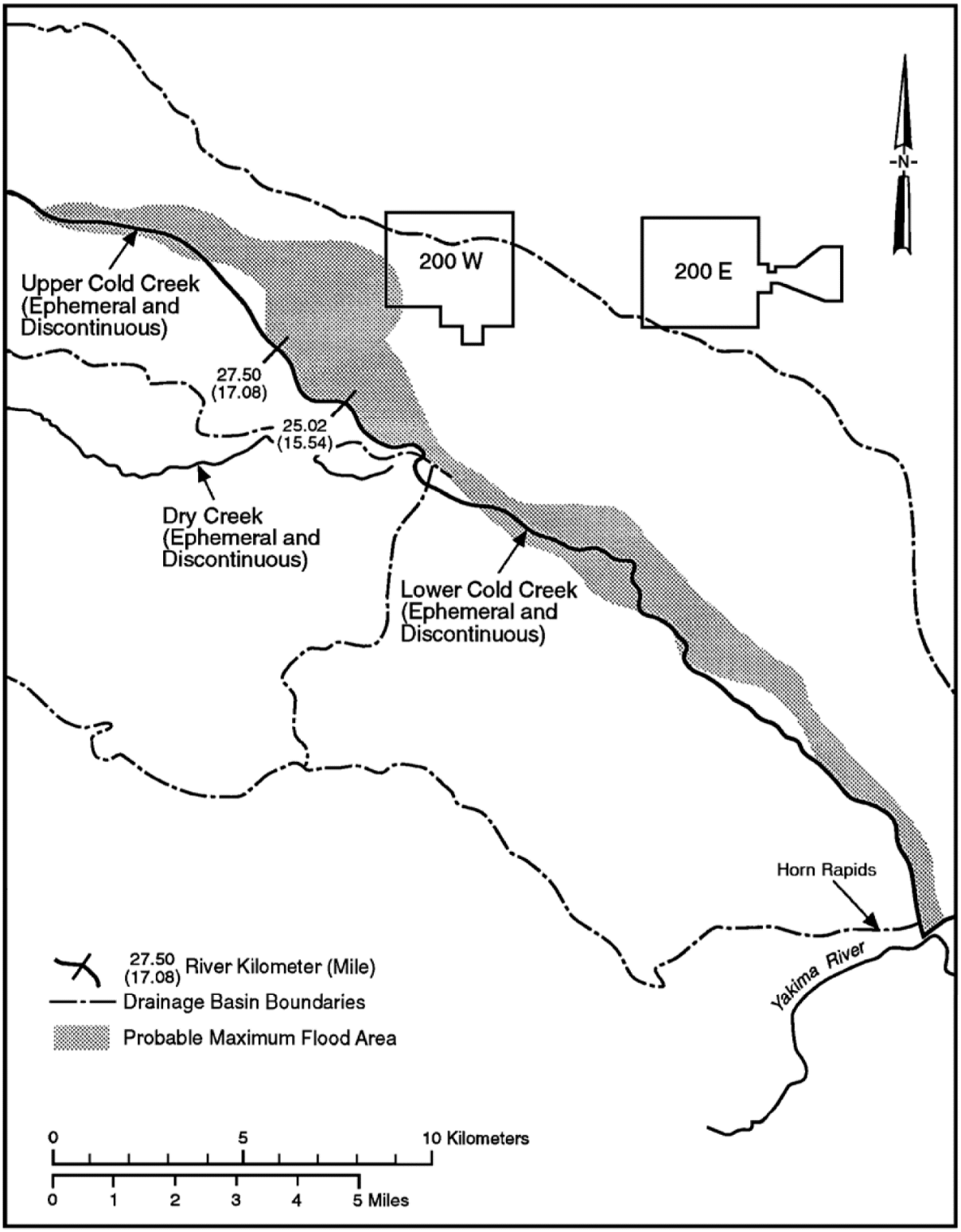

Reference: RHO-BWI-C-120/PNL-4219, "Flood Risk Analysis of Cold Creek near the Hanford Site."

Contamination historically has been detected in near-shore samples downstream from riverbank springs (PNNL-20548). Riverbank springs are monitored for radionuclides at each of the 100 Areas, the Hanford town site, and the 300 Area. Detected radionuclides include ^{90}Sr, ^{99}Tc, ^{129}I, ^{234}U, ^{235}U, and ^{238}U, and tritium, as well as arsenic, chromium, chloride, fluoride, nitrate, and sulfate. Metals and anions (chloride, fluoride, nitrate, and sulfate) were detected in spring water from samples collected in 2005. Concentrations of volatile organic compounds were near or below their detection limits in all samples. Trichloroethylene was detected (1.4 µg/L [0.19 oz/gal]) in one sample from the 300 Area and was the only analyte detected at all shoreline spring sampling locations. Trichloroethylene has been consistently detected at low concentrations in the 300 Area shoreline spring water (PNNL-20548).

3.1.5.1.6 Non-Riverine Surface Water. The occurrence of non-riverine surface water on the Hanford Site is shown in Figure 3-25. These surface water bodies include West Lake and the 200 Areas Treated Effluent Disposal Facility (TEDF) disposal ponds (see next section). West Lake is located north of the 200 East Area and 5 km (3 mi) north-northwest of WMA C, and is a natural feature recharged from groundwater (ARH-CD-775, "Geohydrologic Study of the West Lake Basin"; PNL-7662, "An Evaluation of the Chemical, Radiological, and Ecological Conditions of West Lake on the Hanford Site"). West Lake is the only natural pond at the Hanford Site. West Lake has not received direct effluent discharges from Site facilities; rather, its existence is caused by the intersection of the elevated water table with the land surface in the topographically low area. Water levels of West Lake fluctuate with water table elevation, which is influenced by wastewater discharges in the 200 Areas. The water level and size of the lake has been decreasing over the past several years because of reduced wastewater discharge.

Several naturally-occurring vernal ponds, which are not depicted on Figure 3-25, are located near Gable Mountain and Gable Butte (The Nature Conservancy 1998). The formation of these ponds in any particular year depends on the amount and temporal distribution of precipitation and snowmelt events. The vernal ponds range in size from ~6.1 m by 6.1 m to 45.73 m by 30.5 m (20 ft by 20 ft to 150 ft by 100 ft), and were found in three clusters. Approximately ten were documented at the eastern end of Umtanum Ridge, seven were observed in the central part of Gable Butte, and three were found at the eastern end of Gable Mountain.

3.1.5.1.7 Disposal Ponds. The TEDF in the 200 Areas consists of two disposal ponds. These ponds are each 0.02 km^2 (0.008 mi^2) in size and receive industrial wastewater permitted in accordance with WAC 173-216, "State Waste Discharge Permit Program." The wastewater percolates into the ground from the disposal ponds. Current disposal ponds (i.e., 200 Area TEDF) have an artificial influence on net contributions to the water table. Since these ponds are located between the WMAs and the Columbia River, they could impact the groundwater flow path. However, the disposal activities within the 200 Areas are not expected to exist after current operations end, so their long-term influence is not considered in this WMA C PA.

Historical Site activities discharged contaminated effluent to liquid waste sites, which caused the groundwater table to rise on the Central Plateau (DOE/RL-2001-54, Central Plateau Ecological Evaluation) creating artificial ponds and wetlands. In 1995, these management practices ceased, eliminating all man-made wetlands, with the exception of a small wetland identified in the 200 East Area during the 2001 Ecological Compliance Assessment Program survey.

3.1.5.2 Recharge. Two types of recharge, natural and anthropogenic, occur at the Hanford Site. Natural recharge occurs as the result of the process of water from rain, snow, and other sources moving downward through the soil and reaching the top of the groundwater aquifer. Anthropogenic recharge occurs as a result of water and/or liquids applied to the surface and/or subsurface by human activities. Examples of anthropogenic recharge would include intentional releases of waters and/or wastes into ponds, ditches, and/or cribs; the uncontrolled release of water from testing of fire hydrants; the use of water to wash down, excavate, and/or decontaminate equipment or facilities; the collection of water in low-lying areas with improper drainage control (i.e., ponding of snow melt or precipitation in tank farm areas); water recharge down man-made preferential pathways (i.e., unsealed wells or boreholes); or the unintentional or unplanned loss of waters and/or waste fluids or liquids from tanks and/or water and waste transfer pipelines.

3.1.5.2.1 Runoff. Total estimated precipitation over the Pasco Basin is ~9×10^8 m^3 (~3.2×10^{10} ft^3) annually (DOE/RW-0164). This was calculated by multiplying the average annual precipitation averaged over the Pasco Basin by the 4,900 km^2 (1,900 mi^2) basin area. Precipitation varies both spatially and temporally with higher amounts generally falling at higher elevations. As noted in Section 3.1.2.3, annual precipitation measured at the HMS has varied from 6.8 to 31.3 cm (2.7 to 12.3 in.) since 1947. Most precipitation occurs during the late autumn and winter, with more than half of the annual amount occurring from November through February. Mean annual runoff from the Pasco Basin is estimated at <3.1×10^7 m^3/yr (<1.1×10^9 ft^3/yr), or ~3% of the total precipitation (DOE/RW-0164). Most of the remaining precipitation is lost through evapotranspiration. However, some precipitation that infiltrates the soil is not lost to evaporation or transpiration and eventually recharges the groundwater flow system.

3.1.5.2.2 Natural Recharge. The recharge rate at a specific location is determined by the soil, plant, and weather conditions that control the water balance at that location. The water balance describes the storage and movement of water in and out of the soil, which is the upper part of the unsaturated zone that experiences soil-forming processes and encompasses the evaporation and plant root zone. Water arrives at the soil surface in the form of precipitation, either as rain or snow. Plant water uptake and evaporation, both of which are influenced by weather conditions, remove water stored in the soil and return it to the atmosphere. Deep drainage is the movement of stored water downward below the root zone. Once water is below the root zone, gravity continues to draw the water downward until it eventually recharges the water table.

"Variations in Recharge at the Hanford Site" (Gee et al. 1992) and "Estimating Recharge Rates for a Groundwater Model Using a GIS" (Fayer et al. 1996) estimate that recharge rates from precipitation across the Hanford Site range from near zero to over 100 mm/year (3.94 in./yr). Recharge is variable both spatially and temporally. It is greatest in areas where coarse-textured soils bare of deep-rooted vegetation exist and in years with rapid snowmelt events and precipitation during cool months. The magnitude of recharge at a particular location is influenced by five main factors: climate, soils, vegetation, topography, and springs and streams. Events such as the fire that burned vegetation from a large portion of the Hanford Site during the summer of 2000 also affect recharge rates. Fayer et al. (1996) used several types of field data and computer modeling to estimate the areal distribution of mean recharge rates for the soil and vegetation conditions at the Hanford Site, including any disturbance by Hanford Site operations.

Figure 3-28 shows how the recharge rate is affected by both the presence and type of plants. Shrubs with deep root systems tend to produce lower recharge rates because the deep roots can access a greater volume of soil and thus more stored water. In contrast, grasses with shallow root systems tend to produce higher recharge rates because the roots can access only a smaller volume of soil (and, thus, less stored water). In addition to rooting depth differences, shrubs tend to be active for a much greater portion of the year than grasses. Having a longer period of activity gives the shrubs a greater likelihood of finding and extracting soil water. Without any plants, water is removed only via evaporation from the soil surface. Annual changes in weather and plant activity ensure that recharge is never absolutely constant. However, the impacts from annual plant and weather changes on recharge are muted when recharge is measured below the root zone and averaged over decades. The result is a recharge rate that appears to be fairly constant.

Figure 3-28. Recharge Dependence on Surface Conditions.

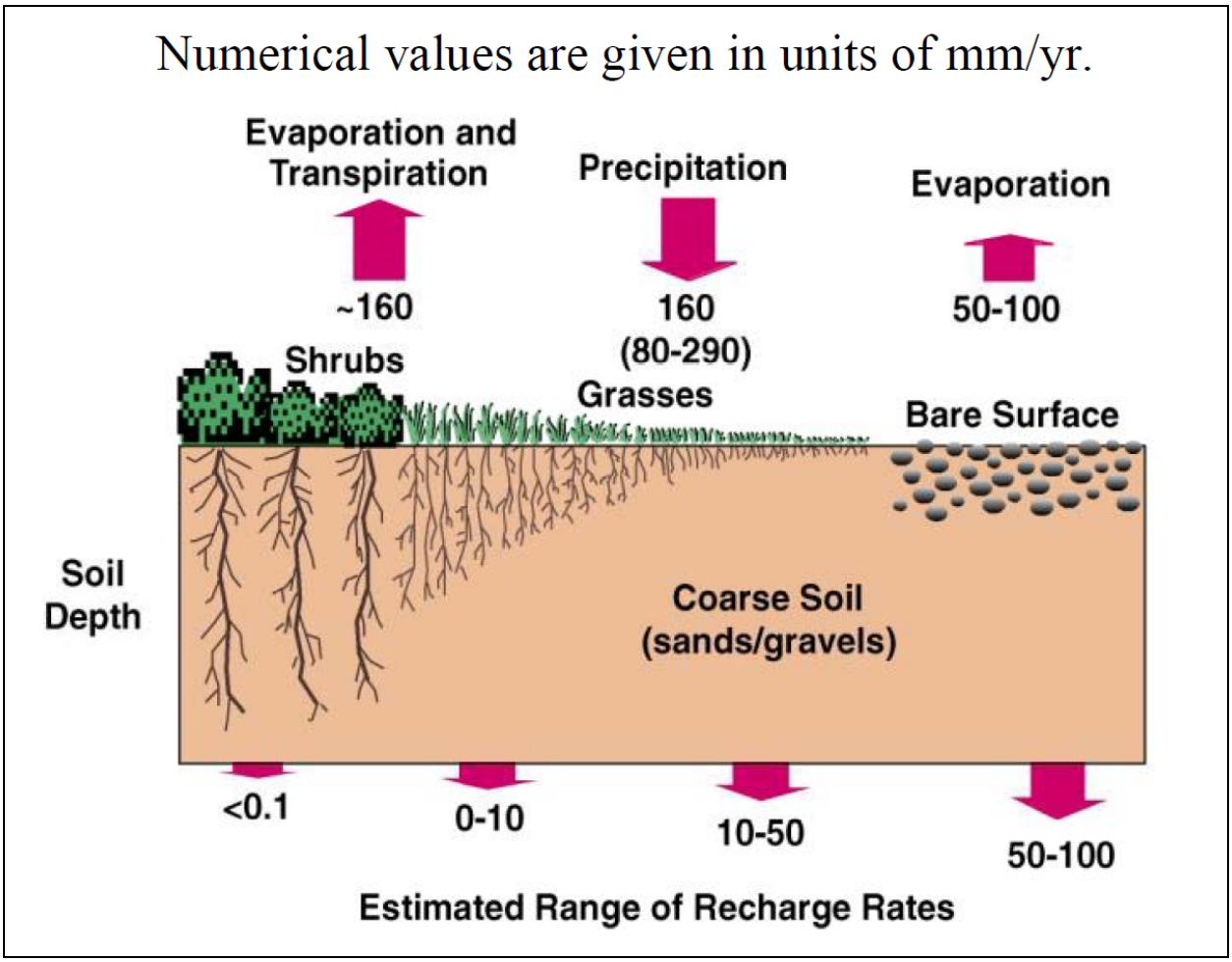

Measurements of recharge on the Hanford Site for over 20 years for a variety of precipitation rates, soil, and vegetation conditions, including conditions representative of evapotranspiration barrier, have been made at the Field Lysimeter Test Facility (FLTF) (PNNL-16688, "Recharge Data Package for Hanford Single-Shell Tank Waste Management Areas"). The site is located

close to the 200 West Area eastern fence and within a few hundred of the HMS. Figure 3-29 is a cut-away drawing of a key lysimeter facility in operation at the Hanford Site. The FLTF contains 18 large lysimeters (surface areas of 2.3 and 3.1 m^2 [24.8 and 33.4 ft^2]; depth from 1.5 to 3.0 m [4.9 to 9.8 ft]) and 6 smaller lysimeters (surface area is 0.07 m^2 [0.75 ft^2]; depth 3.0 m [9.8 ft]).

Treatments include variations of material types and thicknesses, the presence of vegetation, and the use of irrigation to mimic the increased precipitation of a possible future climate. Data from this facility include drainage, water content, matric potential, temperature, and vegetation observations. Challenges for the measurement technique include impacts on recharge (the act of measuring can affect the measurement), difficulty of replicating natural soil conditions in a container, cost of establishing measurement facilities, and length of time needed to gather enough data to get a reasonable estimate of the recharge rate.

3.1.5.2.3 Anthropogenic Recharge. Over and above natural recharge, human activities within the tank farms can provide additional recharge. This occurs because of manmade sources (e.g., leaking waterlines, waste lines, or tanks, testing of fire hydrants, excavation with water), preferential pathways (unsealed abandoned wells or poorly capped boreholes), and improper drainage control (ponding of precipitation at tank farms). Figure 3-30 provides examples of a number of these conditions.

The amount of anthropogenic recharge due to pipeline leaks and improper drainage is extremely difficult to quantify. For example, if a waterline developed a small leak on the order of a quart per minute, this would lead to an additional volume of ~49,000 L (~130,000 gal) released per year. That is equivalent to increasing the natural recharge over the ~3.24-hectare (8-acre) WMA C by 15%. Additionally, the records do not indicate when and how much water was applied during operations [Figure 3-30(d)] or how often ponding occurred on WMA C [Figure 3-30(e)]. Scoping calculations examining the potential effects of anthropogenic recharge on the release and transport of contaminants in past tank waste leaks and losses from WMA C facilities are evaluated and described in RPP-RPT-59197, "Analysis of Past Tank Waste Leaks and Losses in the Vicinity of Waste Management Area C at the Hanford Site, Southeast Washington."

However, for future conditions, anthropogenic recharge is not expected to be a factor in release from the WMAs because in the late 1990s and early 2000s two major efforts took place to eliminate anthropogenic recharge within Hanford's SST System. The first effort was interim stabilization of the SSTs by removing pumpable liquids from the SSTs to mitigate potential future leaks from them. Furthermore, these tanks will be filled with grout prior to the placement of a recharge barrier. The second effort was to apply interim measures to reduce/stop additional recharge in the tank farms. Surface water controls have been constructed to reduce surface water run-on from major meteorological events and from breaks in waterlines. Also, waterlines that were determined unnecessary have been isolated, cut, and capped. Waterlines that were found to be necessary for continued operations have been leak tested and any lines found to be leaking were replaced (DOE/ORP-2008-01). Once retrieval operations cease, the remaining waterlines are expected to be taken out of service.

Figure 3-29. Recharge Dependence on Surface Conditions.

Data collection at the FLTF began in November 1987. Three separate lysimeter designs are included in the facility.

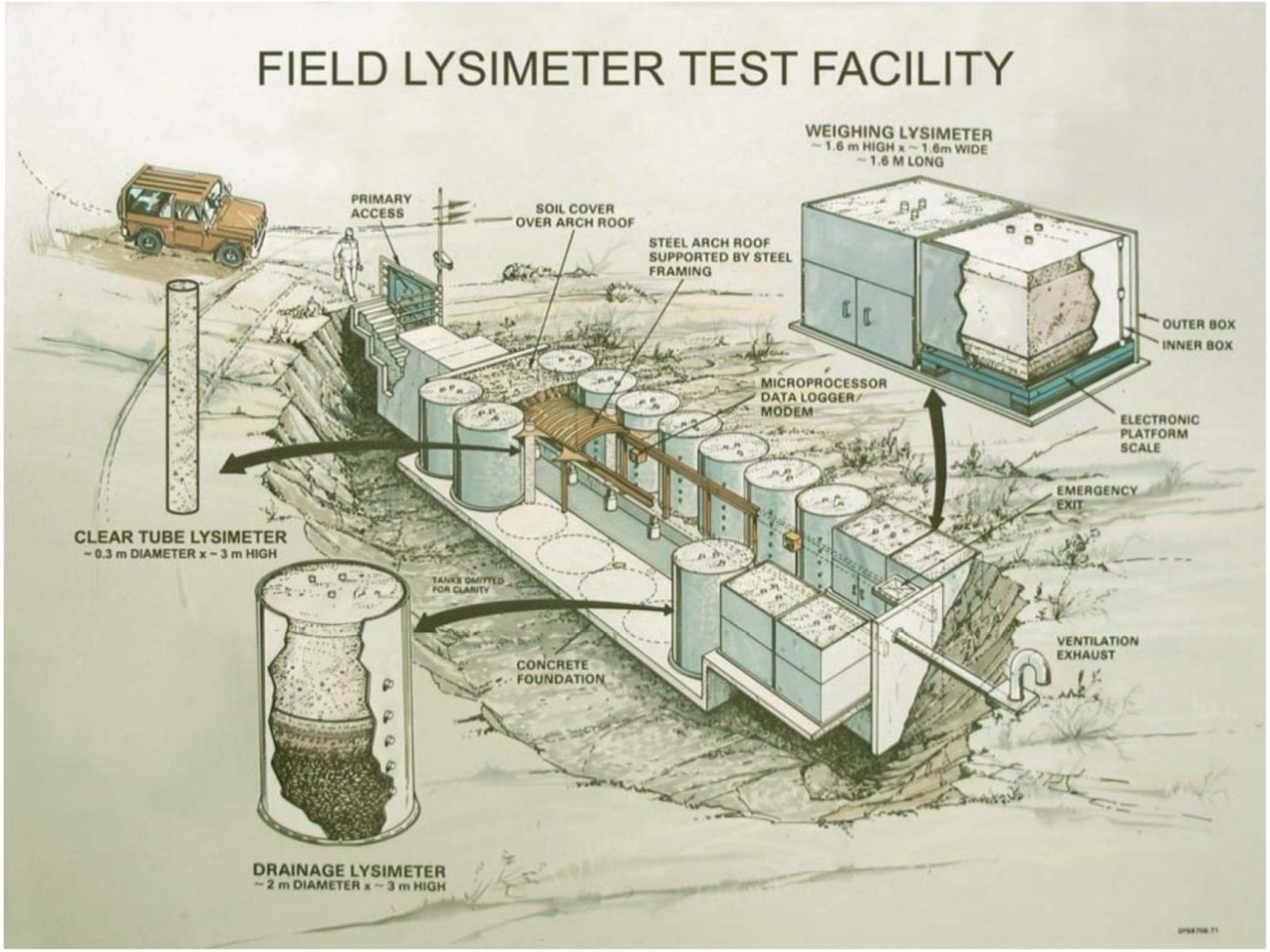

FLTF = Field Lysimeter Test Facility

Figure 3-30. Examples of Anthropogenic Recharge in the 200 Area. (Photographs a – c are from DOE/ORP-2008-01 Appendix K, Photographs d and e are Archive Photos).

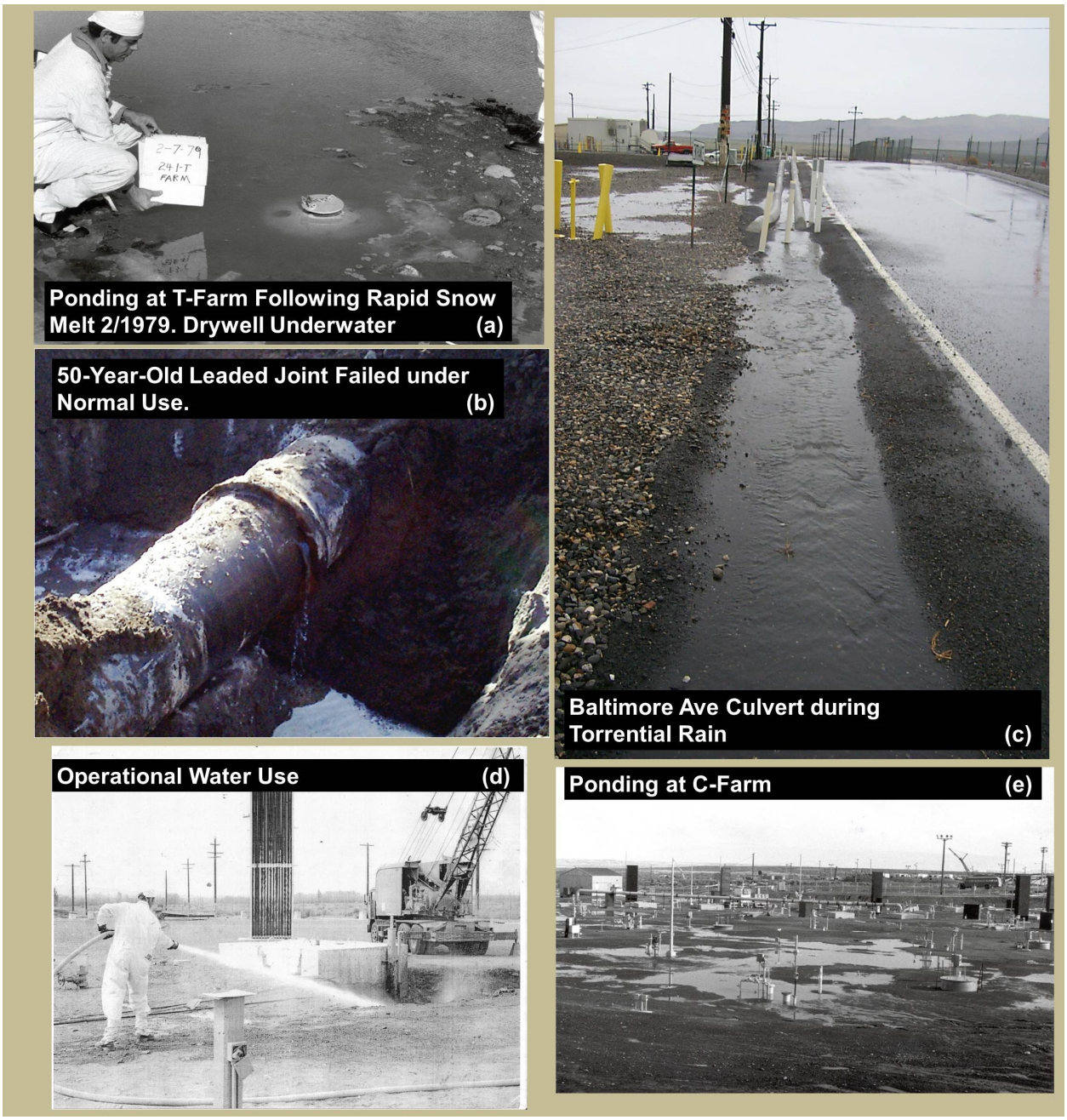

Reference: DOE/ORP-2008-01, RCRA Facility Investigation Report for Hanford Single-Shell Tank Waste Management Areas.

3.1.5.3 Vadose Zone. The vadose zone is that part of the geologic media which extends from the earth's surface to the water table. At the Hanford Site, the thickness of the vadose zone ranges from 0 m (0 ft) near the Columbia River to greater than 100 m (328 ft) under parts of the Central Plateau (PNNL-13080, "Hanford Site Groundwater Monitoring: Setting, Sources, and Methods"). Unconsolidated glacio-fluvial sands and gravels of the Hanford formation make up most of the vadose zone (Figure 3-17). In some areas, such as most of the 200 West Area and in

some of the 100 Areas, the fluvial-lacustrine sediments of the Ringold Formation make up the lower part of the vadose zone. The CCU also makes up part of the vadose zone. The integrated knowledge obtained from previous and ongoing studies provides a good conceptual understanding of the geologic, hydraulic, and geochemical environment and its controls on the distribution and movement of contaminants within the vadose zone (PNNL-14702, "Vadose Zone Hydrogeology Data Package for Hanford Assessments"). Figure 3-19 provides a fence diagram of sediment overlying the Columbia River Basalt Group in the Central Plateau. In the 200 East Area around WMA C, the undifferentiated low Hanford gravels (H3), CCU, Ringold formation would replace the CCU and upper Ringold and Ringold E shown in this figure.

The primary features relevant to the vadose zone flow and transport include the hydrogeologic materials (and their physical, hydraulic, and geochemical properties), subsurface conditions (e.g., fluid statics and thermal conditions), and fluid properties. Other features relevant to the vadose zone conceptual model, such as climate and weather statistics, terrestrial ecology, and projected land use were given in the previous sections.

3.1.5.3.1 Hydrostratigraphy. The vadose zone stratigraphy influences the movement of liquid through the soil column. The vadose zone beneath the 200 East Area can be subdivided into six principal hydrostratigraphic units (HSUs), including three units within the Hanford formation, a fluvial gravel facies of the CCU (equivalent to the Pre-Missoula Gravels of "Appendix 2R - Stratigraphic Investigation of the Skagit/Hanford Nuclear Project," in Skagit/Hanford Nuclear Project, Preliminary Safety Analysis Report [Webster and Crosby 1982] and WHC-SD-ER-TI-003, "Geology and Hydrology of the Hanford Site: A Standardized Text for Use in Westinghouse Hanford Company Documents and Reports"), and two units belonging to the Ringold Formation (WHC-SD-EN-TI-012, "Geologic Setting of the 200 East Area: An Update"; WHC-SD-EN-TI-019, "Hydrogeologic Model for the 200 East Groundwater Aggregate Area"; PNNL-12261, "Revised Hydrogeology for the Suprabasalt Aquifer System, 200-East Area and Vicinity, Hanford Site, Washington"; DOE/RL-2002-39).

The Hanford formation units include (1) an upper gravel-dominated facies, (2) a sand-dominated facies, and (3) a lower gravel-dominated facies. Over most of the 200 East Area, the Hanford sand-dominated facies lies between the upper and lower gravel-dominated facies (WHC-SD-EN-TI-012, WHC-SD-EN-TI-019, DOE/RL-2002-39). Based on borehole samples, the upper and lower gravel-dominated facies appear to have similar physical and chemical properties. The Ringold Formation in the 200 East Area is, for the most part, eroded away in the northern half of the 200 East Area. Here, the Hanford formation lies directly on top of basalt bedrock. With the dropping water table, basalt crops out above the water table and, thus, is unsaturated beneath the northeastern portion of the 200 East Area. Underneath WMA C, the top of the unconfined aquifer lies within a unit composed of undifferentiated gravels from the lower Hanford formation gravels (H3), the CCU, and the Ringold formation.

The vadose zone stratigraphy influences the potential for spreading of liquid within the soil column. Where conditions are favorable, lateral spreading of liquid effluent and/or local perched water zones may develop. Lateral spreading can occur along any strata with contrasting hydraulic conductivity. Where low-permeability layers within the Hanford formation have been documented, they are thin (0.5 m [1.6 ft] or less) and laterally discontinuous. Low-permeability

layers within the sand-dominated facies of the Hanford formation are generally thicker and more continuous than those in the gravel-dominated facies. Some paleosols and facies changes (i.e., the contact between fine-grained and coarser-grained facies) may be fairly continuous over the range of 100 m (328 ft) or so, with some lateral spreading of crib effluent noted on that same scale. Lateral spreading can delay the arrival of contaminants at the water table but may cause mixing of the subsurface plume at one site with that of an adjacent site. Spreading may also require increasing the area of surface barriers to cover wider plumes.

Clastic dikes have also been observed in the Hanford formation beneath the 200 East Area. Their most important feature is their potential to either enhance or inhibit vertical and lateral movement of contaminants in the subsurface, depending on textural relationships (BHI-01103). For example, the vertically-oriented clay skins within clastic dikes may locally form an impediment to lateral flow. This could then cause ponding (perching) of the water and eventual breakthrough to underlying strata.

Sublinear channel-cut scour and fill features occur within the Hanford formation and may act as preferential pathways in the horizontal direction. Other types of heterogeneity are associated with stratigraphic pinch-out or offlapping/onlapping of facies.

3.1.5.3.2 Hydraulic and Transport Properties. Accurate predictions of flow and transport in the vadose zone require a detailed characterization of the hydrologic properties and their variability, as well as estimates of transport parameters such as dispersivity. In particular, data that are essential for quantifying the water storage and flow properties of unsaturated soil include the soil moisture characteristics (i.e., soil moisture content versus pressure head, and unsaturated hydraulic conductivity versus pressure head relations) for sediment in various geologic units.

Data on particle-size distribution, moisture retention, and saturated hydraulic conductivity (K_s) have been cataloged for over 284 samples from throughout the Hanford Site, including 12 locations in the 200 East and West Areas (WHC-EP-0883, “Variability and Scaling of Hydraulic Properties for 200 Area Soils, Hanford Site”; “Evaluation of van Genuchten-Mualem Relationships to Estimate Unsaturated Hydraulic Conductivity at Low Water Contents” [Khaleel et al. 1995]; “Correcting Laboratory-Measured Moisture Retention Data for Gravels” [Khaleel and Relyea 1997]; PNNL-13672, “A Catalog of Vadose Zone Hydraulic Properties for the Hanford Site”; WMP-17524, “Vadose Zone Hydraulic Property Letter Reports”; and “On the Hydraulic Properties of Coarse-Textured Sediments at Intermediate Water Contents” [Khaleel and Heller 2003]). Laboratory analyses of the hydraulic properties of samples collected at Hanford have been performed at a number of different laboratories using techniques similar to those described by Methods of Soil Analysis, Part 1—Physical and Mineralogical Methods (Klute 1986).

Macrodispersivity estimates for non-reactive species have been estimated using the “Three-dimensional stochastic analysis of macrodispersion in aquifers” (Gelhar and Axness 1983) equation where the longitudinal macrodispersivity depends on the mean pressure head. HNF-4769, “Far-Field Hydrology Data Package for Immobilized Low-Activity Tank Waste Performance Assessment” estimated a longitudinal macrodispersivity of ~1 m (~3 ft) for the sand-dominated facies of the Hanford formation in the 200 East Area. The transverse

dispersivities have been estimated as one tenth of the longitudinal values ("A Critical Review of Data on Field-Scale Dispersion in Aquifers" [Gelhar et al. 1992]). Based on a survey of literature, Stochastic Subsurface Hydrology (Gelhar 1993) examined the longitudinal vadose zone dispersivities as a function of the scale of the experiment, and found an increase of dispersivity with an increase in scale.

3.1.5.3.3 Vadose Zone Contamination. The Hanford Site has more than 800 past-practice liquid-disposal facilities. Mixed radioactive liquid waste was discharged to the vadose zone through reverse (injection) wells, French drains, cribs, ponds, trenches, and ditches. From 1944 through the late 1980s, 1.5 to 1.7 billion m^3 (396 to 449 billion gal) of effluent were disposed to the soils (PNNL-SA-32152, "A Short History of Plutonium Production and Nuclear Waste Generation, Storage, and Release at the Hanford Site"). Most effluent was released in the 200 Areas. The largest groundwater contaminant plumes emanating from the 200 Areas are those of tritium and nitrate. The major source for both was discharges from chemical processing of irradiated nuclear fuel rods.

Also present are ^{99}Tc and ^{129}I that, like tritium and nitrate, are mobile in both the vadose zone and groundwater. The major sources of ^{99}Tc and ^{129}I were discharges to liquid disposal facilities. Vadose zone sources for these contaminants remain beneath many past-practice disposal facilities. However, other than physical sampling and laboratory analysis, few direct ways exist to monitor tritium, nitrate, ^{99}Tc, and ^{129}I in the vadose zone.

Approximately 280 UPRs in the 200 Areas also contributed contaminants to the vadose zone (DOE/RL-96-81, Waste Site Grouping for 200 Areas Soil Investigations). Many of these were associated with tank farm operations, and have contributed significant contamination to the vadose zone. Over the past 15 years, a significant effort has been implemented to better understand and quantify vadose zone contamination in and around the WMAs. These investigations have focused on developing a better understanding of major releases and of the potential impacts on groundwater quality. These efforts have integrated information from a number of different DOE and Hanford Site projects and have focused on evaluating the past release events that contribute the bulk of subsurface contamination.

The information sources used for the SST WMA-level vadose zone investigations included baseline spectral gamma logging of the ~750 shallow monitoring boreholes (referred to as drywells) within each of the seven WMAs, as well as assessments of the historical gross gamma logging data from each WMA. "Gross gamma logging" refers to logs in which gamma activity is measured without regard to energy level. The gross gamma log simply reports the total gamma activity as a function of depth. Drywell gross gamma logging data were used as part of the tank farm leak detection program until 1994. "Spectral gamma logging" refers to logs in which energy spectra are collected in the borehole. In a spectral gamma log, individual gamma photons are counted as a function of energy level. This allows radionuclides to be identified and quantified on the basis of gamma activity at specific energy levels. From 1995 to 2000, spectral gamma logging was performed in the existing drywell network to develop a baseline understanding of subsurface contamination conditions in each of the SST WMAs. Results of the baseline spectral gamma logging project are summarized in a series of 12 reports (one for each SST farm). In 2000, DOE/RL-99-36, Phase 1 RCRA Facility Investigation/Corrective Measures

Study Work Plan for Single-Shell Tank Waste Management Areas was issued to collect vadose zone characterization data in the single-shell WMAs, and characterization data related to this work plan was collected from 2000 to 2008.

Vadose zone characterization efforts have included drilling, sampling, and soil analysis in multiple SST WMAs, coupled with review of historical process records and gamma logging data. The information collected during this time is provided in DOE/ORP-2008-01. Since the issuance of this report, a Phase 2 vadose characterization program was initiated at WMA C to collect additional vadose zone data (RPP-PLAN-39114). The results of the vadose zone sampling at WMA C are documented in RPP-RPT-58339.

In 2007, a process was started (RPP-32681, "Process to Assess Tank Farm Leaks in Support of Retrieval and Closure Planning") to re-assess SST leak volumes based on a synthesis of available information, including vadose zone borehole drilling and sampling data from DOE/ORP-2008-01, gamma-ray logging data, and historical information. In Table 3-3 of HNF-EP-0182, "Waste Tank Summary Report for Month Ending August 31, 2005," Rev. 209, 67 tanks were classified as "confirmed or suspected" of having leaked contaminated liquid to the vadose zone. These classifications were assigned based largely on data and priorities from the period of tank farm operations. As a result of the re-assessment process, the most recent "Waste Tank Summary Report for Month Ending May 31, 2014" (HNF-EP-0182, Rev. 317, Table 3-2) has 64 tanks classified "confirmed or suspected" of having leaked. The re-assessment has added one new tank to the list (C-105) and removed five tanks (241-A-103, C-110, C-111, 241-SX-104, 241-SX-110) from the list. Vadose zone inventory estimates based on the revised leak volumes are being developed. Presently, inventory estimates are available for WMA C (RPP-RPT-42294, "Hanford Waste Management Area C Soil Contamination Inventory Estimates," Rev. 2), 241-B Tank Farm (RPP-RPT-49089, "Hanford B-Farm Leak Inventory Assessments Report"), WMA U (RPP-RPT-50097, "Hanford 241-U Farm Leak Inventory Assessment Report"), 241-TX Tank Farm (RPP-RPT-50870, "Hanford 241-TX Farm Leak Inventory Assessment Report"), and WMA T (RPP-RPT-55084, "Hanford 241-T Farm Leak Inventory Assessment Report"). Uncertainties in leak volume estimates are addressed as part of the inventory estimates.

3.1.5.4 Groundwater. This section describes the relevant characteristics of the groundwater hydrology, which has been studied and monitored in detail because of the waste disposal operations at the site. The hydrology characteristics of the Hanford Site are important to the definition of potential pathways for the WMA C contaminants to the public and the estimation of the magnitudes of the environmental impacts. Evaluating this pathway requires information about the types of aquifers, depth to the water table, and regional flow paths toward surface water discharge points. Surface water flow represents an exposure pathway for both human health and the environment.

The discussion focuses on the geohydrology of the 200 Areas but also includes information on the Hanford Site in general, highlighting those aspects that were important to the modeling of the post-closure system performance. This information was summarized largely from material

presented in PNNL-6415, DOE/RL-2014-32, Hanford Site Groundwater Monitoring Report for 2013 and PNNL-20548, as follows.

- "Hanford Site Environmental Report for Calendar Year 2010 (Including Some Early 2011 Information)" (PNNL-20548) provides the overview of the characterization and monitoring activities conducted at the Hanford Site during the calendar year.

- Hanford Site Groundwater Monitoring Report for 2014 (DOE/RL-2014-32) describes the groundwater monitoring activities during the fiscal year.

- "Hanford Site National Environmental Policy Act (NEPA) Characterization" (PNNL-6415) provides a standardized description of the Hanford Site environment.

Groundwater beneath the Hanford Site is found in both an upper unconfined aquifer system and deeper basalt-confined aquifers. The unconfined aquifer system is also referred to as the suprabasalt aquifer system because it is within the sediments that overlie the basalt bedrock. Portions of the suprabasalt aquifer system are locally confined. However, because the entire suprabasalt aquifer system is interconnected on a site-wide scale, it is referred to in this report as the Hanford unconfined aquifer system.

3.1.5.4.1 Basalt-Confined Aquifer System. The upper basalt-confined aquifer groundwater system occurs within basalt fractures and joints, interflow contacts, and sedimentary interbeds within the upper Saddle Mountains Basalt. The thickest and most widespread sedimentary unit in this system is the Rattlesnake Ridge interbed, which is present beneath much of the Hanford Site. Groundwater also occurs within the Levey interbed, which is present only in the southern portion of the Site. A small interflow zone occurs within the Elephant Mountain Member of the upper Saddle Mountains Basalt and may be significant to the lateral transmission of water. The upper basalt-confined aquifer system is confined by the dense, low-permeability interior portions of the overlying basalt flows and in some places by silt and clay units of the lower Ringold Formation that overlie the basalt. Approximately 50 wells screened in the upper basalt-confined aquifer have been sampled or had water levels measured in recent years.

The horizontal hydraulic conductivities of most of these basalt-confined aquifers fall in the range of 10^{-10} to 10^{-4} m/s (3×10^{-10} to 3×10^{-4} ft/s). Saturated but relatively impermeable dense interior sections of the basalt flows have horizontal hydraulic conductivities ranging from 10^{-15} to 10^{-9} m/s (3×10^{-15} to 3×10^{-9} ft/s), about five orders of magnitude lower than some of the confined aquifers that lie between these basalt flows (DOE/RW-0164). Hydraulic-head information indicates that groundwater in the basalt-confined aquifers generally flows toward the Columbia River and, in some places, toward areas of enhanced vertical inter-aquifer flow within the unconfined aquifer system (PNNL-16346, "Hanford Site Groundwater Monitoring for Fiscal Year 2006"; DOE/RW-0164; SD-BWI-TI-335, "Fresh-Water Potentiometric Map and Inferred Flow Direction of Ground Water Within the Mabton Interbed, Hanford Site, Washington State -- January 1987").

The DOE monitors groundwater quality in the upper basalt-confined aquifer system because of the potential for downward migration of contaminants from the overlying unconfined aquifer in

areas where confining units are absent or fractured. The upper basalt-confined aquifer system is not affected by contamination as much as the unconfined aquifer. Contamination found in the upper basalt-confined aquifer system is most likely to occur in areas where the confining units have been eroded away or were never deposited, and where past disposal of large amounts of wastewater resulted in downward hydraulic gradients.

Researchers have identified areas of intercommunication between the contaminated unconfined aquifer and the upper basalt-confined aquifer by geochemical signatures and the presence of nitrate and tritium in groundwater in some basalt-confined wells near the 200 East Area (PNL-10817, "Hydrochemistry and Hydrogeologic Conditions within the Hanford Site Upper Basalt Confined Aquifer System"). However, groundwater monitoring data do not indicate that contamination has migrated into the upper basalt-confined aquifer. Because of poor seals in wells constructed prior to implementation of WAC 173-160, "Minimum Standards for Construction and Maintenance of Wells," intercommunication between aquifers has permitted groundwater flow from the unconfined aquifer to the underlying confined aquifer in the past, increasing the potential to spread contamination. Section 2.14.2 of DOE/RL-2008-01 further discusses communication between the upper basalt-confined aquifer system and the overlying aquifers. The small amount of contamination detected in the upper basalt-confined aquifer is attributed to areas where confining units of basalt have been partially removed by erosion or are absent, or where wells provided a pathway for migration. The basalt-confined aquifer system would not provide a pathway for contaminants from WMA C to the accessible environment.

3.1.5.4.2 Unconfined Aquifer System. The base of the uppermost aquifer system is defined as the top of the uppermost basalt flow, with the top of the system being the water table. This aquifer system is bounded laterally by anticlinal basalt ridges and is ~152 m (500 ft) thick near the center of the Pasco Basin. Within the Hanford Site, this uppermost aquifer system lies at depths ranging from less than 0.3 m (1 ft) below the ground surface near West Lake and the Columbia and Yakima Rivers, to more than 107 m (350 ft) in the central portion of the Cold Creek syncline. Groundwater in the unconfined aquifer at the Hanford Site generally flows from recharge areas in the elevated region near the western boundary of the Hanford Site toward the Columbia River on the eastern and northern boundaries. The Columbia River is the primary discharge area for the unconfined aquifer. The Yakima River borders the Hanford Site on the southwest and is generally regarded as a source of recharge.

The unconfined aquifer system underlying the Hanford Site exists within sediments deposited on top of the Columbia River Basalts. It is composed primarily of the Ringold Formation and overlying Hanford formation. Figure 3-31 is a hydrogeologic map of the units present at the water table surface in June 1998, which represents the top of the unconfined aquifer just prior to the start of active remediation. In the 200 West Area, the water table occurs almost entirely in the Ringold Unit E gravels, while in the 200 East Area, it occurs primarily in the Hanford formation and in the Ringold Unit A gravels (Figure 3-18). Along the southern edge of the 200 East Area, the water table is in the Ringold Unit E gravels. The upper Ringold facies were eroded in most of the 200 East Area by the ancestral Columbia River and, in some places, by the Missoula floods that subsequently deposited Hanford gravels and sands on what was left of the Ringold Formation (DOE/RL-2002-39). Because the Hanford formation and possibly the CCU sand and gravel deposits are much more permeable than the Ringold gravels, the water table is relatively flat in the 200 East Area, but groundwater flow velocities are higher.

Figure 3-31. Hydrogeologic Units Present at the Water Table in June 1998.

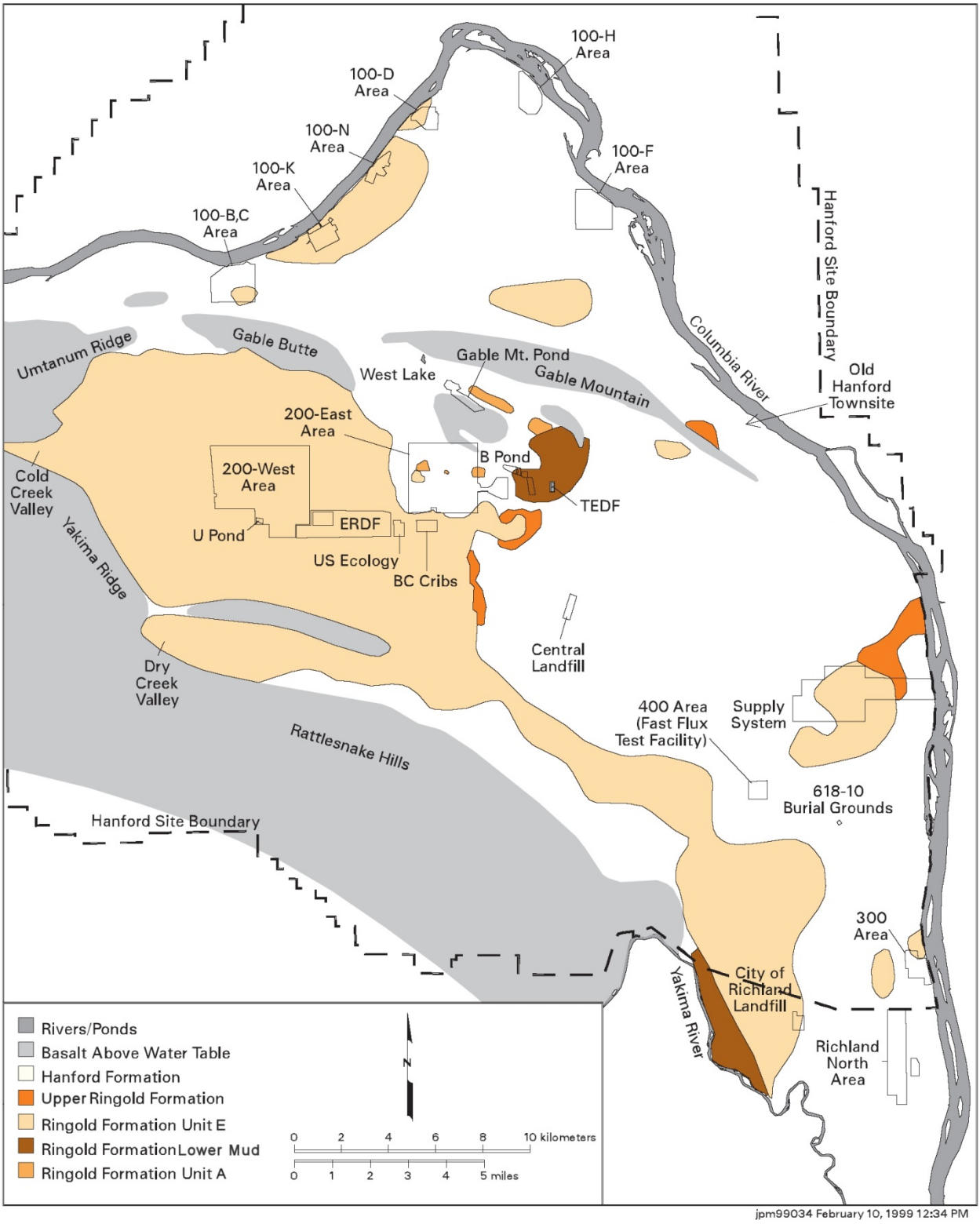

Source: WCH-520, "Performance Assessment for the Environmental Restoration Disposal Facility, Hanford Site, Washington."

ERDF = Environmental Restoration Disposal Facility TEDF = Treated Effluent Disposal Facility

The hydrology of the 200 Areas has been strongly influenced by the discharge of large quantities of wastewater to the ground. Between 1944 and the mid-1990s, an estimated 1.68×10^{12} L (4.44×10^{11} gal) of liquid was discharged to disposal ponds, trenches, and cribs. Wastewater discharge has decreased since 1984 and currently only contributes a volume of recharge in the same range as the estimated natural recharge from precipitation. The largest volumes of discharge around the 200 East Area were to the 216-B Pond system, the 216-A-25 (Gable Mountain) pond system, and several of the PUREX cribs in the southeast corner of 200 East Area. Figure 3-32 shows the liquid discharge history for the two ponds. The Gable Mountain Pond is estimated to have received ~293 billion L (77 billion gal) of effluent, while the 216-B Pond to have received ~256 billion L (68 billion gal) of effluent. In the 200 West Area, the largest volumes of discharge were to the 216-T Pond system and the 216-U-10 Pond (Figure 3-33). The 216-T Pond system is estimated to have received ~424 billion L (112 billion gal) of effluent (WHC-EP-0815, "Groundwater Impact Assessment Report for the 216-T-4-2 Ditch"), while the 216-U Pond to have received ~158 billion L (41.7 billion gal) of effluent (WHC-EP-0707, "216-U-10 Pond and 216-Z-19 Ditch Characterization Studies").

Figure 3-32. Discharge History for the 216-B Pond System and Gable Mountain Pond.

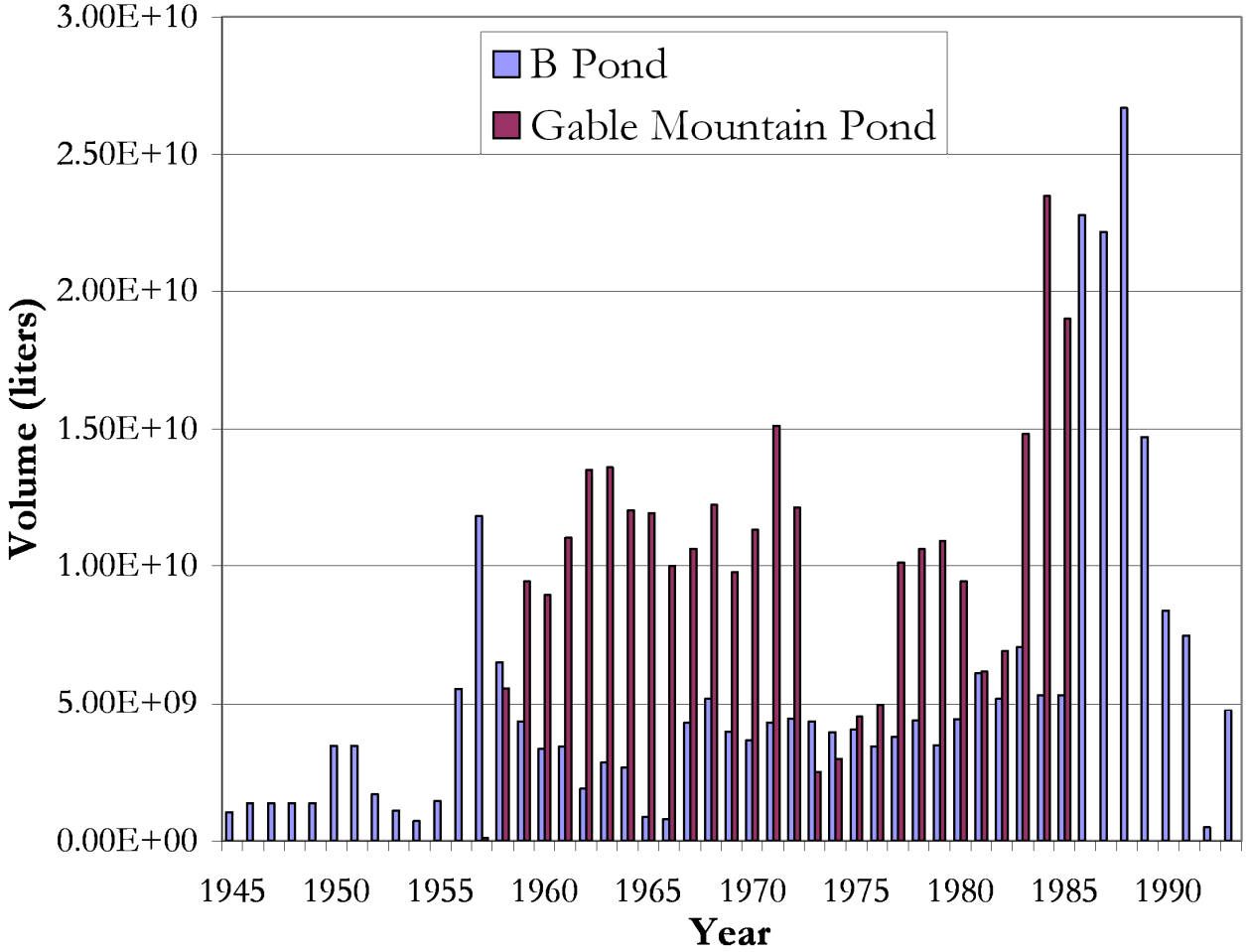

Figure 3-34 shows a series of water table elevation maps for the time periods representing pre-operational conditions, operational conditions, and present day conditions for the Hanford

Site. The first water table map (Figure 3-34a) is a hind cast map of water table elevations (ERDA-1538, "Final Environmental Impact Statement, Waste Management Operations, Hanford Reservation, Richland, Washington") prior to the start of significant Hanford Site wastewater discharges. This water map includes the effects of limited irrigation near the former towns of White Bluff and Hanford, but not the effects of extensive irrigation now common in Cold and Dry Creeks. The 1944 water table contours indicate that groundwater flow is easterly toward the Columbia River with a relatively uniform hydraulic gradient (~1.5 m/km [5 ft/mi]). Regional groundwater flow was generally toward the east-northeast, while flow north of Gable Mountain was more to the north.

The pre-Manhattan Project water table in the 200 West Area and 200 East Area was ~123 m (404 ft) and 120 m (394 ft) above sea level, respectively (BNWL-B-360, "Selected Water Table Contour Maps and Well Hydrographs for the Hanford Reservation, 1944-1973"). In the 200 West Area, the water table elevation increased rapidly from 1949 to 1956, but appeared to stabilize between the late 1960s and the late 1980s. Water levels began to decline in the late 1980s when wastewater discharges in the 200 West Area were reduced. In the 200 East Area, the water table elevation increased rapidly from 1954 to 1963. The water table declined somewhat in the late 1960s and early 1970s, but then increased again in the early 1980s before beginning a final decline throughout the 1990s when wastewater discharges in the 200 East Area were reduced.

During operations, water levels in the uppermost and unconfined aquifer rose as much as 26 m (85 ft) and 9 m (30 ft) beneath the 200 West Area and 200 East Area, respectively, because of artificial recharge caused by liquid waste disposed from the mid-1940s to 1995. Figure 3-34b shows water table mounding present in the 200 Areas for June 1987. The volume of water that was discharged to the ground at the 200 West Area was actually less than that discharged at the 200 East Area. However, the lower hydraulic conductivity of the aquifer near the 200 West Area inhibited groundwater movement in this area, resulting in a higher groundwater mound.

Presently, groundwater in the unconfined aquifer generally flows from upland areas in the west toward the regional discharge area north and east along the Columbia River (Figure 3-34c). Steep hydraulic gradients occur in the western, eastern, and northern regions of the Site. Shallow gradients occur southeast of 100-FR and in a broad arc extending from west of 100-BC toward the southeast between Gable Butte and Gable Mountain (Gable Gap), through the 200 East Area and into the central portion of the Site. The reduction of wastewater discharges has caused water levels to drop significantly; however, a residual groundwater mound beneath the 200 West Area is still present today as shown by the curved water table contours near this area. Additionally, small groundwater mounds exist near the 200 Area TEDF and State-Approved Land Disposal Site wastewater disposal sites.

Comparing the approximate rate of water table decline in the 200 East Area with that in the 200 West Area shows that the rate of decline is three to four times faster in the 200 West Area. This is probably due, in part, to the greater increase in water level at U Pond than at B Pond. Also, the water table gradient is extremely flat in the 200 East Area, whereas the gradient is steeper beneath the 200 West Area. This indicates that a small increment of water table decline must be spread out over a much larger area in the 200 East Area than in the 200 West Area.

Figure 3-33. Discharge History for the 216-T Pond and 216-U Pond.

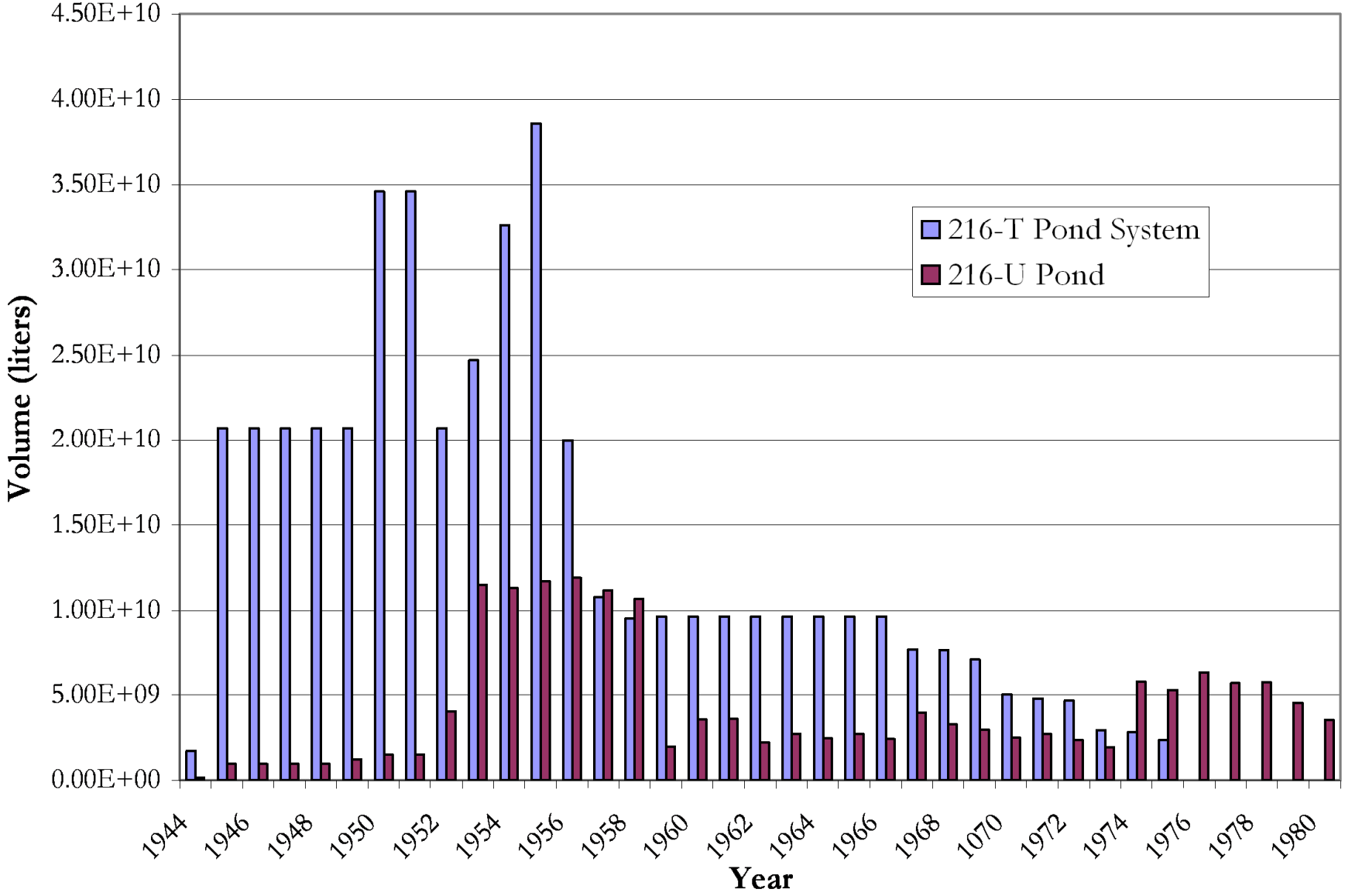

Figure 3-34a. Hind Cast Water Table Map of the Hanford Site, January 1944.

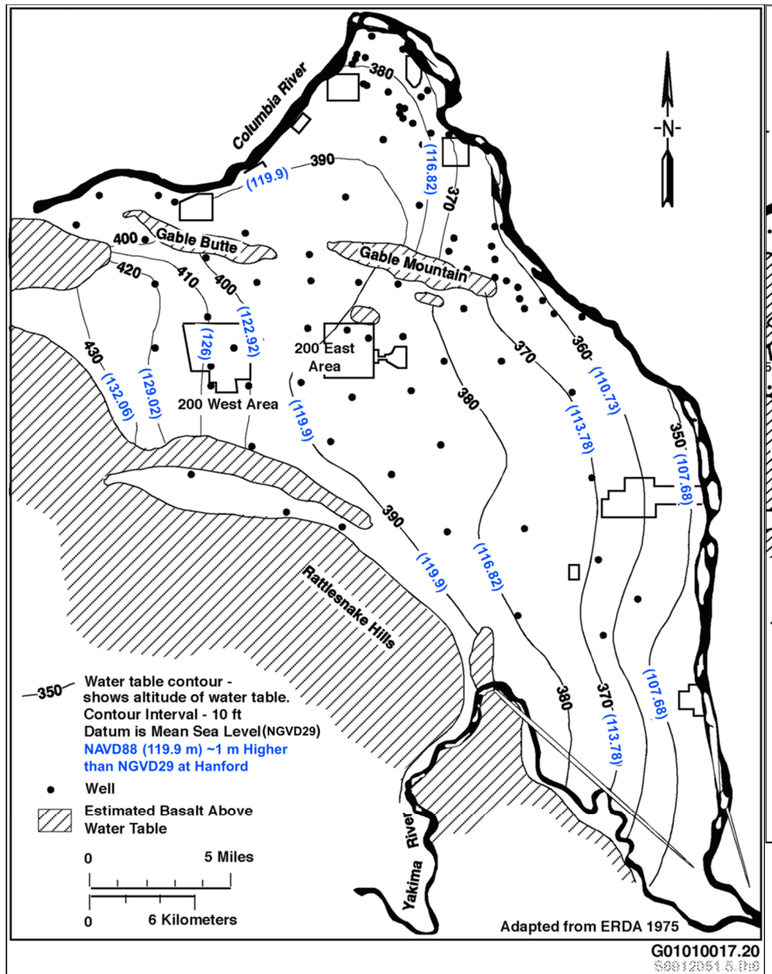

ERDA 1975 refers to ERDA-1538, "Final Environmental Impact Statement, Waste Management Operations, Hanford Reservation, Richland, Washington."

Figure 3-34b. Water Table Elevations for June 1987.

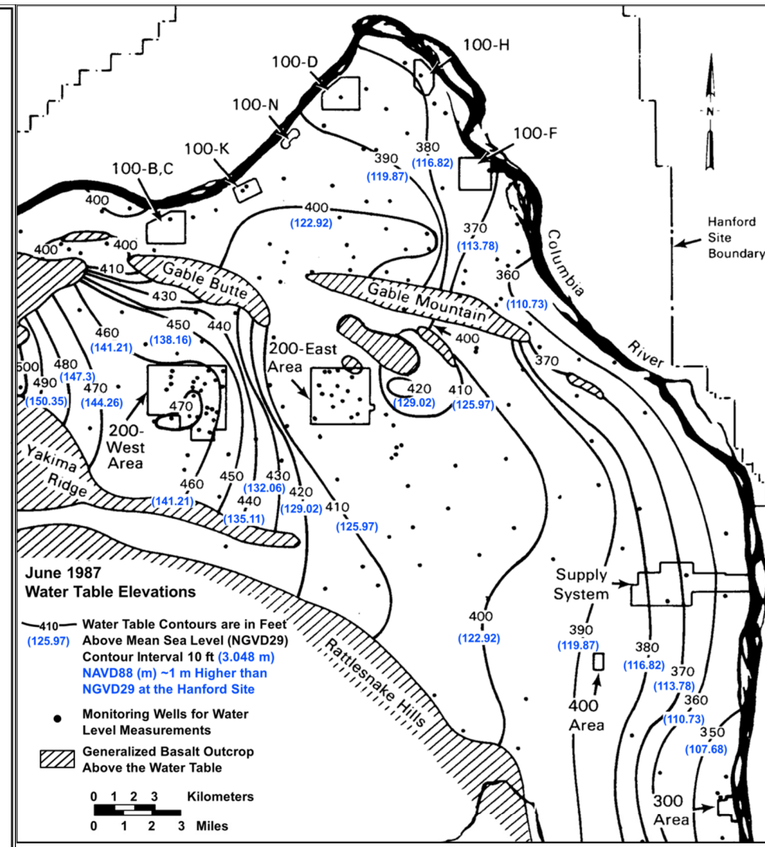

Reference: PNL-6464, "Environmental Monitoring at Hanford for 1987."

Figure 3-34c. Water Table Elevations for 2013.

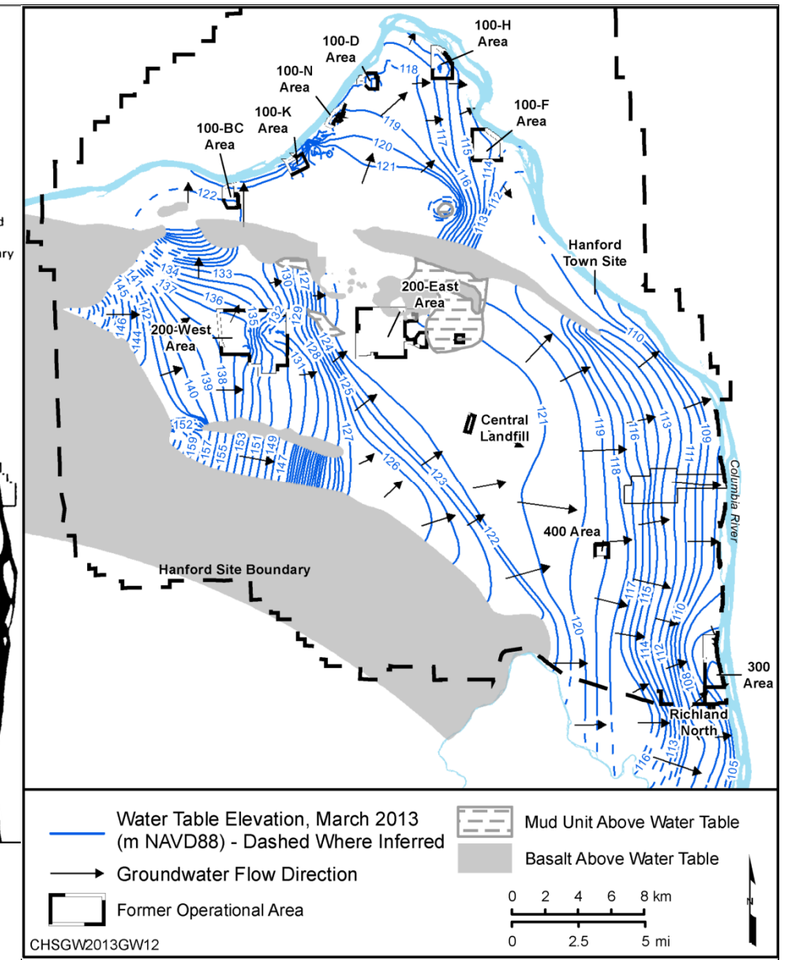

Source: DOE/RL-2014-32, Hanford Site Groundwater Monitoring Report for 2013.

The groundwater mounds drastically changed the flow direction causing radial flow from the discharge areas, and, in some areas, resulted in a complete reversal of flow direction. Until about 1980, the edge of the mounds migrated outward from the sources. Groundwater levels have declined over most of the Hanford Site since 1984 because of decreased wastewater discharges (DOE/RL-2014-32), and since 1996, when all non-permitted discharges to the ground ceased, groundwater flow has begun to return to pre-Hanford Site conditions.

The dominant source of water in the unconfined aquifer beneath the 200 East Area and vicinity is inflow of groundwater from upgradient areas to the west. Formerly, the direction of groundwater flow diverged beneath the 200 East Area in the general vicinity of WMA C and the B Complex (WMA B-BX-BY and nearby Cribs), with some water flowing toward the north through Gable Gap and some flowing southeast. The flow direction changed during 2011; since then, flow has been toward the south and southeast across much of the 200 East Area. This change in flow directions is important because contaminant plumes located in the northwest corner of the 200 East Area located near and under the B Complex could flow under WMA C.

A limited amount of hydraulic property data is available from testing of wells. Hydraulic test results from wells on the Hanford Site have been compiled for the Hanford Groundwater Monitoring Project and for environmental restoration efforts (BNWL-1709, "Collection and Analysis of Pump Test Data for Transmissivity Values"; PNL-8337, "Summary and Evaluation of Available Hydraulic Property Data for the Hanford Site Unconfined Aquifer System"; PNL-10835, "Comparison of Constant-Rate Pumping Test and Slug Interference Test Results at the Hanford Site B Pond Multilevel Test Facility"; PNNL-13342, "Analysis of the Hydrologic Response Associated with Shutdown and Restart of the 200-ZP-1 Pump-and-Treat System"; PNNL-13378, "Results of Detailed Hydrologic Characterization Tests – Fiscal Year 1999"; PNNL-13514, "Results of Detailed Hydrologic Characterization Tests – Fiscal Year 2000"; PNNL-14058, "Prototype Database and User's Guide of Saturated Zone Hydraulic Properties for the Hanford Site"; PNNL-14113, "Results of Detailed Hydrologic Characterization Tests – Fiscal Year 2001"; WHC-SD-EN-TI-014, "Hydrogeologic Model for the 200 West Groundwater Aggregate Area"; and WHC-SD-EN-TI-019). Most hydraulic tests were conducted within the upper 15 m (49 ft) of the aquifer, and many were open to more than one geologic unit. In some cases, changes in water table elevation may have significantly changed the unconfined aquifer transmissivity at a well since the time of the hydraulic test. Few hydraulic tests within the Hanford Site unconfined aquifer system have yielded accurate estimates of aquifer-specific yield.

Horizontal hydraulic conductivities of sand and gravel facies within the Ringold Formation generally range from ~1 to 100 m/day (3 to 328 ft/day), compared to 10 to 7,000 m/day (33 to 23,000 ft/day) for the Hanford formation and the coarse-grained multi-lithic facies of the CCU (pre-Missoula gravels) (DOE/RW-0164; PNNL-13641, "Uncertainty Analysis Framework – Hanford Site-Wide Groundwater Flow and Transport Model"; PNNL-14058; PNNL-14656, "Borehole Data Package for Four CY 2003 RCRA Wells 299-E27-4, 299-E27-21, 299-E27-22, and 299-E27-23 at Single-Shell Tank, Waste Management Area C, Hanford Site, Washington"; PNNL-14804, "Results of Detailed Hydrologic Characterization Tests – Fiscal Year 2003"; WHC-SD-EN-TI-019). Because the Ringold Formation sediments are more consolidated and partially cemented, they are ~10 to 100 times less permeable than the sediments of the overlying Hanford formation. Before wastewater disposal operations at the Hanford Site, the uppermost

aquifer was mainly within the Ringold Formation, and the water table extended into the Hanford formation at only a few locations ("Geology and Ground-Water Characteristics of the Hanford Reservation of the U.S. Atomic Energy Commission, Washington" [Newcomb et al. 1972]). However, wastewater discharges raised the water table elevation across the site. The general increase in groundwater elevation caused the unconfined aquifer to extend upward into the Hanford formation over a larger area, particularly near the 200 East Area. This resulted in an increase in groundwater velocity because of both the greater volume of groundwater and the higher permeability of the newly-saturated Hanford formation sediments.

3.1.5.4.3 Existing Groundwater Contamination. When the Hanford Site was operating, spent fuel reprocessing, isotope recovery operations, and associated waste management activities occurred within the 200 East and 200 West Areas located in the central portion of the Site. Waste disposal within the 200 Areas began with startup of plutonium-separation operations in late 1944 (WHC-MR-0521, "The Plutonium Production Story at the Hanford Site: Processes and Facilities History"). Three separations processes were used. The earliest was the bismuth-phosphate process, which was used between 1944 and 1956 at T Plant in the 200 West Area (200-ZP groundwater interest area), and between 1945 and 1952 at B Plant in the 200 East Area (200-BP). The REDOX process was used between 1952 and 1967 at the REDOX Plant in the 200 West Area (200-UP). Finally, the PUREX process was used from 1956 to 1972, and again from 1983 to 1989 at the PUREX Plant in the 200 East Area (200-PO).

Beginning in 1949, the product from the separations plants was further processed at the Plutonium Finishing Plant (PFP) (200-ZP), which operated until 1989. Other chemical processes performed in the 200 Areas included uranium recovery, using the tributyl phosphate process at U Plant (200-UP) between 1952 and 1957, and radionuclide recovery by various methods at B Plant (200-BP) between 1963 and 1983 [PNL-SA-23121 S, "Hanford Technical Exchange Program: Process Chemistry at Hanford (Genesis of Hanford Wastes)"]. Each chemical processing facility generated multiple waste streams and used multiple waste sites for waste management and disposal.

Additionally, the 200 Areas contain seven SST WMAs: A-AX, B-BX-BY, and C within the 200 East Area and S-SX, T, TX-TY, and U within the 200 West Area. Unplanned releases (e.g., tank liner leaks or releases from cascade lines or spare ports) have contaminated the vadose zone and some of this contamination has migrated downward to the groundwater (e.g., PNNL-11810, "Results of Phase I Groundwater Quality Assessment for Single-Shell Tank Waste Management Areas S-SX at the Hanford Site"). Migration through the vadose zone may have been facilitated in the past by additions of water from various sources, most notably nearby wastewater ditches and cribs, water supply pipeline leaks, and rainfall/snowmelt runoff events. Nitrate, chromium and ^{99}Tc from many of the tank farms, as well as uranium specifically from WMA B-BX-BY, form substantial groundwater plumes. These plumes generally are expanding in areal extent and exhibit increasing constituent concentrations indicating that contaminants continue to enter the groundwater from the vadose zone.

The intentional disposal of waste streams to ponds, ditches, and cribs, combined with the UPRs from the WMAs has resulted in a complex mixture of soil and groundwater contamination that complicates the process of interpreting specific contaminant sources for specific plumes.

Groundwater monitoring is/has been performed on a regular basis to evaluate levels of contamination, movement of groundwater plumes, and changes to the unconfined/confined aquifers. Each year an annual groundwater monitoring report is issued with the most recent being DOE/RL-2014-32. This annual report provides monitoring results for the AEA, as required by DOE Orders; for RCRA treatment, storage, and disposal (TSD) units; and for CERCLA groundwater OUs.

The annual report divides the Central Plateau into four geographical groundwater interest areas (200-BP-5, 200-PO-1, 200-UP-1, and 200-ZP-1). These groundwater interest areas encompass groundwater contamination from the 200 East and 200 West Areas and regions into which this contamination has migrated beyond the Central Plateau (Figure 3-35). WMA C falls within the 200-BP-5 OU, which also contains WMA B-BX-BY.

Groundwater contaminant plumes of tritium, nitrate, and ^{129}I formed when the waste discharged to ponds and cribs reached the aquifer. These contaminants form regional plumes originating on the Central Plateau (Figure 3-35). The tritium and nitrate plumes have decreased in area over the years as a result of radioactive decay (tritium only) and dispersion; the area of ^{129}I has remained stable. A large carbon tetrachloride plume originated in the 200 West Area. Other groundwater contaminants in the Central Plateau include ^{99}Tc, uranium, ^{90}Sr, trichloroethene, cyanide, and other dangerous waste constituents.

The unconfined aquifer within the 200 East Area boundary is the primary aquifer impacted by past waste disposal operations and is associated with the suprabasalt sediment of the Ringold Formation, CCU, and Hanford formation (Figure 3-17). The greatest concentration/activity of nitrate, ^{99}Tc, and uranium is in the 200-BP-5 OU area within the northwest portion of the 200 East Area, also referred to as the B Complex (e.g., 241-B-BX-BY single-shell underground storage tank [UST] area "Waste Management Area B-BX-BY" and adjacent liquid waste sites). These plumes extend both to the northwest and southeast within an ancestral Columbia River paleochannel that incised semi-consolidated gravels and cohesive fluvial-lacustrine Ringold deposits. With the groundwater flow in the vicinity of the B Complex changing flow direction from northwest through Gable Gap to the southeast toward the Columbia River and through the paleochannel, contaminant plumes in the vicinity of the B Complex could intersect contaminant plumes originating at WMA C in the near future.

Below is a summary description for existing groundwater contamination in the 200-BP-5 groundwater interest area taken from DOE/RL-2014-32 (the reader is referred to that document for more information) for the following contaminants:

- Tritium
- ^{129}I
- Nitrate
- ^{99}Tc
- Uranium
- Cyanide.

Figure 3-35. Groundwater Contamination for 2013 which Originated within the Central Plateau along with Central Plateau Groundwater Interest Areas.

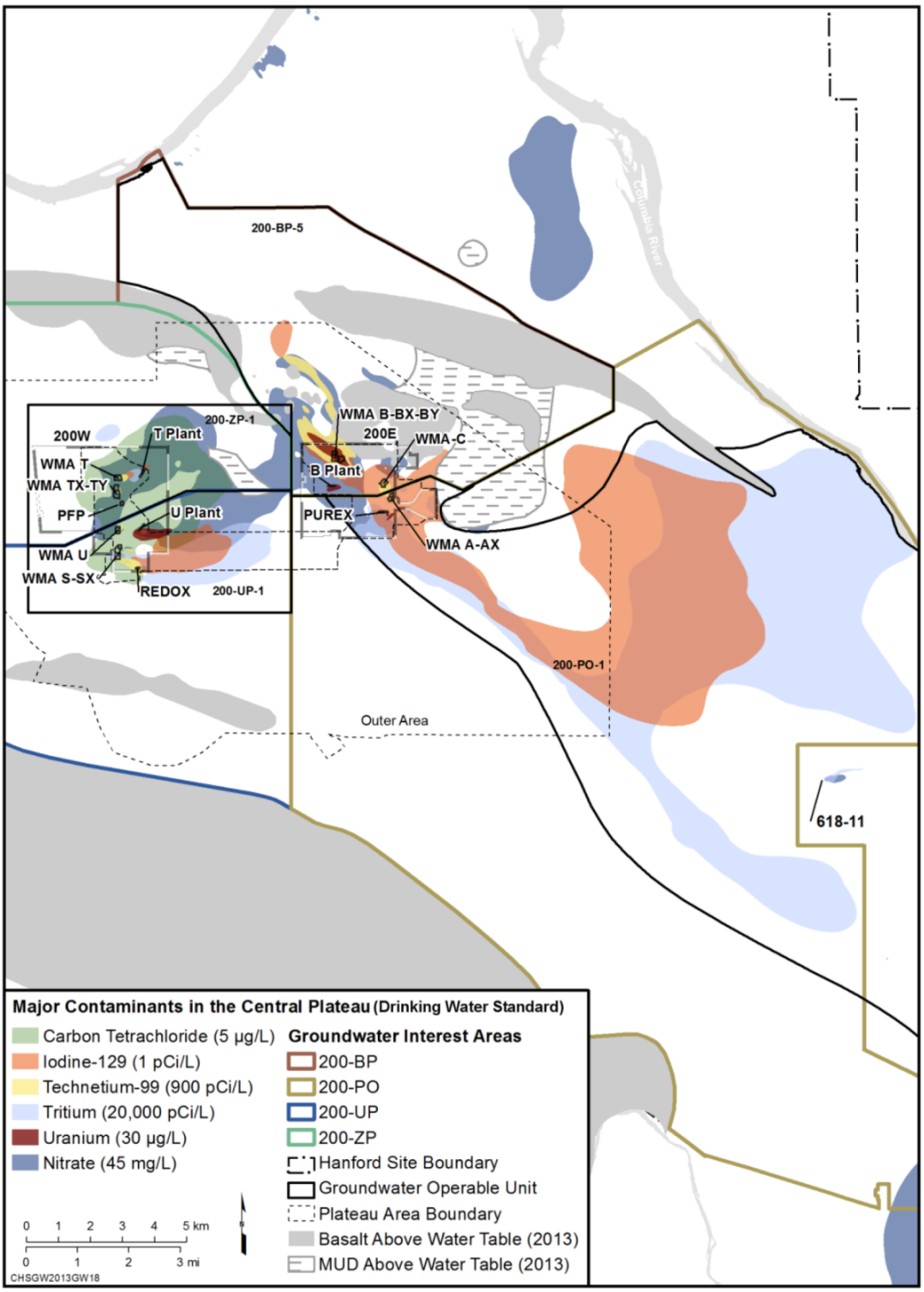

Source: DOE/RL-2014-32, Hanford Site Groundwater Monitoring Report for 2013.

PFP = Plutonium Finishing Plant
PUREX = Plutonium Uranium Extraction (facility)
REDOX = Reduction-Oxidation (facility)
WMA = Waste Management Area

Tritium

The major sources of tritium within the 200-BP-5 groundwater interest area were the 216-B-50 and 216-B-57 cribs located north and northwest of 241-BY Tank Farm (BY Farm), 216-BX-102 UPR from SST 241-BX-102 (BX-102), 216-B-3 pond just east of the 200 East Area and the 216-B-12 Crib ~750 m (2,460 ft) south-southwest of WMA B-BX-BY. However, at 216-B-12 crib, the source could also be from the 200-PO sources (DOE/RL-2014-32). The size of the tritium plume in the upper part of the unconfined aquifer within 200-BP has decreased since 2003. The decline is attributed with radioactive decay, dispersion, and possibly diminishing levels of drainage from the vadose zone at certain locations. The maximum tritium levels near the 216-B-50 and 216-B-57 cribs are ~22,000 pCi/L; at the BX-102 site, the maximum tritium levels are on the order of 25,000; at the 216-B-12 crib, the levels range from 94,000 pCi/L to 150,000 pCi/L and finally at the 216-B-3 pond the maximum levels observed are ~42,000 pCi/L. While tritium is found in the unconfined aquifer underneath WMA C at levels below the drinking water standard (DWS), no known sources for the tritium are suspected to have originated from WMA C.

Iodine-129

There are three sources of iodine in southeast 200 East Area (216-A-10 Crib vicinity, 216-A-29 Ditch, and B Pond) that were contributors to the widespread distribution of ^{129}I within the 200 East Area and Gable Gap. Other potential sources of ^{129}I to groundwater include the BY Cribs, 241-BX-102 UPR, and the 216-B-8 Crib. Overall ^{129}I activity in 2013 within the 200-BP-5 groundwater interest area ranged from ~7 pCi/L near WMA C (299-E27-22 [Figure 3-4]) to less than 1 pCi/L at wells in the northern part of Gable Gap. The northwest plume extent reflects the primary flow path in the late 1980s when discharges to Gable Mountain Pond were terminated. Although WMA C is not considered a source for ^{129}I, all 12 groundwater monitoring wells at WMA C had ^{129}I levels exceeding DWS. The levels at WMA C ranged from 2.5 to 7.5 pCi/L. Iodine-129 levels detected near WMA C have been relatively consistent over the past two decades.

Nitrate

The most extensive plume in 2013 within the 200-BP-5 groundwater interest area is the nitrate (Figure 3-35). Nitrate sources have been identified as: BY Cribs (located just to the north of BY Farm), 216-B-7A&B Cribs, 216-B-8 Crib, SST 241-BX-102 UPR, releases with 241-B Tank Farm (B Farm) (part of WMA B-BX-BY), 216-B-12 Crib, 216-B-5 Injection Well, 216-B-2-2 Ditch, WMA C, Gable Mountain Pond, and Gable Gap. The highest nitrate levels observed in 2013 were at B Farm with a level of close to 1,700 mg/L (0.23 oz/gal), followed by the BY Cribs at ~1,400 mg/L (0.19 oz/gal). Contaminant levels drop off to ~300 to 800 mg/L (0.04 oz/gal to 0.11 oz/gal) at 241-BX-102 UPR and 216-B-7A&B Cribs. Waste Management Area C is the source of nitrate found at monitoring wells around WMA C. A total of three wells had nitrate levels above the DWS (45 mg/L [0.006 oz/gal]). The highest level observed was 110 mg/L (0.015 oz/gal) at well 299-E27-14 (Figure 3-4) on the east side of the tank farm. The contaminant level has been fairly constant at well 299-E27-14 for the past several years. The other two wells at WMA C with levels above the DWS are 299-E27-21 (~46 mg/L [0.006 oz/gal]) and 299-E-27-24 (70 mg/L [0.009 oz/gal]).

Technetium-99

Technetium-99 sources have been identified at BY Cribs, 216-B-7A&B Cribs, 216-B-8 Crib, 241-BX-102 UPR, releases with B Farm (WMA B-BX-BY), WMA C and Gable Gap. Three general plume areas are present within the 200-BP-5 groundwater interest area (Figure 3-35); one area north of 200 East, one near WMA B-BX-BY, and one near WMA C. The largest of the three plumes is near WMA B-BX-BY and sources include the BY Cribs, 216-B-7A&B Cribs, 216-B-8 Crib, 241-BX-102 UPR, and releases associated with the B Farm. The greatest ^{99}Tc activity in the 200-BP-5 groundwater interest area in 2013 occurred at well 299-E33-18, with a maximum activity of 36,000 pCi/L. The ratio of ^{99}Tc to nitrate in groundwater is potentially useful for evaluating source contributions. The ^{99}Tc-to-nitrate ratio associated with this area indicates a potentially different source than the other high activity wells in this area, due to the greater ^{99}Tc activity and lower nitrate concentration. This is consistent with the type of waste released; metal waste from tank BX-102.

Technetium-99 in the 200-BP-5 groundwater interest area is primarily from liquid waste associated with the BY Cribs, which received a mean inventory of 128.6 Ci of ^{99}Tc (Appendix C of RPP-26744, "Hanford Soil Inventory Model, Rev. 1"). Prior to the 2011 groundwater flow reversal, ^{99}Tc activity beneath the BY Cribs exceeded 30,000 pCi/L in all three wells located within the BY Cribs footprint. The increased activity was the result of minimal groundwater flow between 2006 and 2011 and continuous ^{99}Tc infiltration into the aquifer at an average activity of ~3.8 µCi/L based on RPP-26744. Since 2011 this concentrated ^{99}Tc plume has migrated and expanded to the southeast as a result of the groundwater flow reversal in this area.

Uranium

Uranium found in the 200-BP-5 groundwater interest area primarily originated from large disposal inventories to the 216-B-12 Crib and the 241-BX-102 UPR. The uranium inventory disposed to these sites exceeded 10,000 kg, which is at least an order of magnitude greater than other waste sites within the 200-BP-5 groundwater interest area. Rough order of magnitude calculations indicated that 1,050 kg (2,310 lbs) of water-extractable uranium may reside in the Cold Creek silt-dominated unit ~3 m (10 ft) above the aquifer. The estimate was based on sample results from three boreholes in an east-west orientation within the perched water zone. The highest concentration of uranium observed in the unconfined aquifer in 2013 was 3,330 µg/L (4.4×10^{-4} oz/gal) (DWS is 30 µg/L [4.4×10^{-6} oz/gal]) at well 299-E33-18 (~80 m [262 ft] due east of 241-BX Tank Farm). At WMA C, uranium has leaked from the SSTs and/or pipelines. RPP-35484, "Field Investigation Report for Waste Management Areas C and A-AX" reported ^{236}U in vadose zone samples taken from well 299-E27-7 as an indication of irradiated fuel fission product being released to the soil. However, it is not clear as to the source of uranium in the groundwater. It may be from WMA C or may be the result of slightly contaminated groundwater flowing into the area around WMA C. There are no clear trends over the last 6 years in the groundwater data for uranium and the concentrations found in groundwater wells bounding WMA C are 3 to 10 times less than the DWS (i.e., ~2 to 11 µg/L [2.7×10^{-7} to 1.5×10^{-6} oz/gal]).

Cyanide

Cyanide found in the 200-BP-5 interest area originated from disposal of tributyl phosphate wastes scavenged for ^{137}Cs. After scavenging was completed, the tank supernate, including the remaining dissolved ferrocyanide compounds, was discharged to the BY Cribs at the B Complex. In the late 1990s, cyanide concentrations began to increase in the groundwater beneath the BY Cribs along with nitrate and ^{99}Tc. In addition, low concentrations of cyanide detected in the vicinity of WMA C are attributed to historical releases of ferrocyanide-containing waste at that facility.

As of 2013, cyanide is the only dangerous waste constituent determined as impacting groundwater from C Farm. More specifically, cyanide only exceeded the detection limit in three wells in 2013 (299-E27-14, 299-E27-23, and 299-E27-24 [Figure 3-4]). The concentrations were significantly less than the 200 µg/L (2.7×10^{-5} oz/gal) DWS. By the end of 2013 the cyanide concentrations in two of the wells were below the detection limit. The highest concentration, 13.9 µg/L (1.9×10^{-6} oz/gal), in 2013 was in well 299-E27-24, which is screened across the bottom of the aquifer. During 2013 the cyanide concentration in this well ranged between 8.64 and 13.9 µg/L (1.2×10^{-6} oz/gal and 1.9×10^{-6} oz/gal).

3.1.5.4.4 Groundwater Travel Times. Travel time of water through the unconfined aquifer from the 200 East Area to the Columbia River has been estimated to be in the range of 10 to 30 years (Open File Report 87-222, "Subsurface Transport of Radionuclides in Shallow Deposits of the Hanford Nuclear Reservation, Washington – Review of Selected Previous Work and Suggestions for Further Study"; PNL-6328, "Estimation of Ground-Water Travel Time at the Hanford Site: Description, Past Work, and Future Needs"). This is because of large volumes of recharge from wastewater that were disposed in the 200 Areas between 1944 and the mid-1990s, and the relatively high permeability of Hanford formation sediments, which are below the water table between the 200 East Area and the Columbia River. Analysis of the tritium plume in DOE/RL-2009-85, Remedial Investigation Report for the 200-PO-1 Groundwater Operable Unit estimated a travel time of 33 years. It further states that this estimate is likely to be conservative (i.e., overstates the groundwater contamination migration rates compared to current conditions) because of the past groundwater mounding in the Central Plateau.

3.1.6 Geochemical Properties

The Hanford formation sediment in the 200 Areas consists of glacio-fluvial materials deposited by cataclysmic Ice Age floods. The mineralogy of this sediment is highly variable, depending on grain size. Gravel-dominated sediment tends to have a high abundance of lithic fragments (mostly basaltic, with some plutonic, metamorphic, and detrital caliche fragments) (DOE/RL-2002-39). Finer-grained facies have proportionally less lithic fragments and more quartz, feldspar, and mica grains. Microprobe analysis of the sand and finer-grained fraction indicates dominance by quartz (18 to 67.1% by weight), plagioclase (5.1 to 41.5%) and microcline (1.8 to 30.1%) (RHO-ST-23, "Geology Of The Separation Areas, Hanford Site, South-Central Washington"; PNL-8889, "Solid-Waste Leach Characteristics and Contaminant-Sediment Interactions, Volume 1: Batch Leach and Adsorption Tests and Sediment Characterization"; PNNL-14202, "Mineralogical and Bulk-Rock Geochemical Signatures of

Ringold and Hanford Formation Sediments"). Other common minerals include amphiboles up to 36.6%, pyroxenes up to 27.5%, mica (biotite/illite) up to 13.1%, and calcite up to 6.5% by weight. Smectite clays represent a few weight percent of the bulk sand fraction (3.3 to 5% [PNL-8889]) and generally dominate the clay fraction (RHO-ST-23). PNNL-14586, "Geologic Data Package for 2005 Integrated Disposal Facility Waste Performance Assessment" reported chlorite concentrations generally <3% by weight except for one sample that had 8% by weight of chlorite.

Hanford formation sediment is typified as having low organic carbon content, generally <0.1% by weight (PNL-8889), and low-to-moderate cation exchange capacity (2.6 to 7.8 milli-equivalents per 100 g [3.53 oz] [PNL-8889]). The sediment has a slightly basic pH when wetted (PNL-8889 found the pH of saturation extract ranging from 7.66 to 8.17). Small amounts of detrital calcium carbonate (calcite) are common and can act as a weak buffer.

Empirical bulk distribution coefficient (K_d) data for Hanford formation and Ringold Formation sediments are fairly abundant for dilute waste solutions and groundwater (PNNL-13895, "Hanford Contaminant Distribution Coefficient Database and Users Guide"). Fewer K_d data are available for the CCU sediments, or for high ionic strength waste solutions with slightly acidic to slightly basic pH values. A relatively small amount of K_d data exists for the combined high ionic-strength/highly-basic tank liquors for many common radionuclides. These distribution coefficient (K_d) data have been well tabulated [PNNL-13895; PNNL-11800; PNL-7297, "Hanford Waste-Form Release and Sediment Interaction – A Status Report with Rationale and Recommendations for Additional Studies"; PNNL-13037, "Geochemical Data Package for the Hanford Immobilized Low-Activity Tank Waste Performance Assessment (ILAW PA)," Rev. 1; PNNL-11485, "Radionuclide Adsorption Distribution Coefficients Measured in Hanford Sediments for the Low Level Waste Performance Assessment Project"; PNNL-11965, "Effects of Aging Quartz Sand and Hanford Site Sediment with Sodium Hydroxide on Radionuclide Sorption Coefficients and Sediment Physical and Hydrological Properties: Final Report for Subtask 2a"; and PNNL-13037, "Geochemical Data Package for the 2005 Hanford Integrated Disposal Facility Performance Assessment," Rev. 2]. In most instances, adsorption appears to be the controlling geochemical process, but neutralization of acid waste by the alkaline sediment and neutralization of basic tank waste can cause precipitation of some contaminant species within the sediment pores. Outside the zone of pH neutralization, adsorption is considered to be the dominant contaminant retardation process in the vadose zone.

3.1.7 Natural Resources

The following section discusses the natural geologic and water resources on the Hanford Site. The Central Plateau of the Hanford Site has no important natural resources.

3.1.7.1 Geologic Resources. Geologic resources at the Hanford Site are very limited. Hanford Site mineral resources include sand, gravel, silt, clay, and aggregate. Historically, these resources were extracted at several quarries or pits at the Hanford Site and used for road construction and maintenance, and waste burial activities. No major mining operations exist in the Hanford Site area. Oil and gas exploration have occurred; however, no economically viable accumulations were found.

3.1.7.2 Water Resources. The Columbia River is used as a source of both drinking water and industrial water for several Site facilities (PNNL-20548). The water systems of Richland, Pasco, and Kennewick withdrew a large portion of the 48.8 billion L (12.9 billion gal) used during 2006 from the Columbia River. Each city operates its own supply and treatment system, located downgradient and downriver of the Site. The Richland water supply system derives ~82% of its water directly from the Columbia River, while the remainder is split between a well field in north Richland (that is recharged from the river) and groundwater wells.

The City of Richland's total water usage during 2006 was 20.1 billion L (5.3 billion gal). The Kennewick system uses two wells and the Columbia River for its water supplies. These wells serve as the sole source of water between November and March and can provide ~40% of the total maximum supply of 94.6 billion L/day (25 million gal/day). Total 2006 usage in Kennewick was 13.4 billion L (3.5 billion gal). A significant number of Kennewick's residents (~22,000 residential customers) draw irrigation water from the Kennewick Irrigation District, which has the Yakima River as its source. The City of Pasco system also draws from the Columbia River for its water needs. During 2006, Pasco consumed 15.5 billion L (4.1 billion gal). Energy Northwest operates the Columbia Generating Station northeast of the 400 Area. Energy Northwest uses Columbia River water for both potable and process/cooling water applications.

3.1.8 Natural Background Radiation

The Hanford Site has an extensive monitoring program. Studies have been directed at determining background levels of possible contaminants in the soil (DOE/RL-92-94, Hanford Site Background: Part 1, Soil Background for Nonradioactive Analytes; DOE/RL-95-55, Hanford Site Background: Evaluation of Existing Soil Radionuclide Data; DOE/RL-96-12, Hanford Site Background: Part 2, Soil Background for Radionuclides) and in the groundwater (WHC-EP-0595, "Westinghouse Hanford Company Operational Groundwater Status Report, 1990-1992"). Also, reports are issued annually covering general environmental conditions (PNNL-6415) and groundwater monitoring (DOE/RL-2014-32).

Low concentrations of some longer-lived radionuclides such as isotopes of cesium, plutonium, potassium, strontium, and uranium are detectable that are associated with particulate matter that accumulated in riverbed sediments (PNNL-20548). The levels were similar to those measured in previous years. No discernible increase in concentration could be attributed to current Hanford Site operations. DOE/RL-91-45, Hanford Site Risk Assessment Methodology, summarizes all the measurements taken to determine radionuclide background levels at the Hanford Site (see Appendix B, Section B.2.8).

Recent annual Hanford Site environmental reports (e.g., PNNL-20548) estimate that the total annual dose from Hanford Site operations in 2010 to a hypothetical maximally-exposed individual at an offsite location was ~0.18 mrem. The air-pathway annual dose was 0.053 mrem (excluding radon) and 0.067 mrem (including radon). These radiation exposures are small compared to other natural and human-produced sources that are estimated to contribute ~365 mrem annual dose to individuals living near the Hanford Site (NCRP Report No. 93, "Ionizing Radiation Exposure of the Population of the United States").

3.1.9 Waste Management Area C Site Characterization

The previous sections provided summary information on the Hanford Site characteristics. This section provides a brief summary of the characterization of the vadose zone and unconfined aquifer in and around WMA C, including contamination in both the vadose zone and unconfined aquifer. Since the late 1990s there has been an extensive effort to characterize the vadose zone and unconfined aquifer around WMA C. These efforts are described in numerous documents including, but not limited to, DOE/ORP-2008-01 Appendix L; DOE/RL-2014-32; GJO-98-39-TAR/GJO-HAN-18, "Hanford Tank Farms Vadose Zone: C Tank Farm Report"; GJO-98-39-TARA/GJO-HAN-18, "Hanford Tank Farms Vadose Zone: Addendum to the C Tank Farm Report"; RPP-PLAN-39114; RPP-RPT-56356, "Development of Alternative Digital Geologic Models of Waste Management Area C"; and RPP-RPT-58339. For more detailed information, please refer to the characterization documents.

The principal driver for site characterization at WMA C is a number of confirmed or suspected waste loss events which occurred in WMA C (labeled as UPRs in Figure 3-36) during its operational history. These included suspected tank leaks and known waste losses from waste transfer piping systems. The current understanding of contaminant occurrences and environmental conditions at WMA C is described in RPP-ENV-33418, "Hanford C-Farm Leak Inventory Assessments Report" and DOE/ORP-2008-01. The primary contamination zones currently identified in WMA C include a localized high ^{137}Cs activity zone near the bottom of the southwest part of tank C-105 and three UPRs near waste transfer pipelines and diversion boxes in the southwest part of WMA C. Sampling at groundwater wells 299-E27-21 and 299-E27-23 along the southern boundary (Figure 3-36) of WMA C had results for ^{99}Tc at concentrations greater than 25 times the DWS of 900 pCi/L.

3.1.9.1 Geology. The geology of WMA C is summarized from the information provided in DOE/ORP-2008-01, RPP-RPT-46088, and RPP-RPT-56356. A generalized fence diagram through WMAs A-AX and C is shown in Figure 3-37.

Six stratigraphic units lie within WMAs A-AX and C. From oldest to youngest, the primary geologic units are:

- Columbia River Basalt Group
- Undifferentiated Hanford lower gravelly sequence (H3 unit)/Cold Creek/Ringold formations
- Hanford formation – sand sequence (H2 unit)
- Hanford formation – upper gravelly sequence (H1 unit)
- Backfill
- Recent deposits.

Figure 3-36. Waste Management Area C Tanks, Infrastructure, and Associated Unplanned Releases.

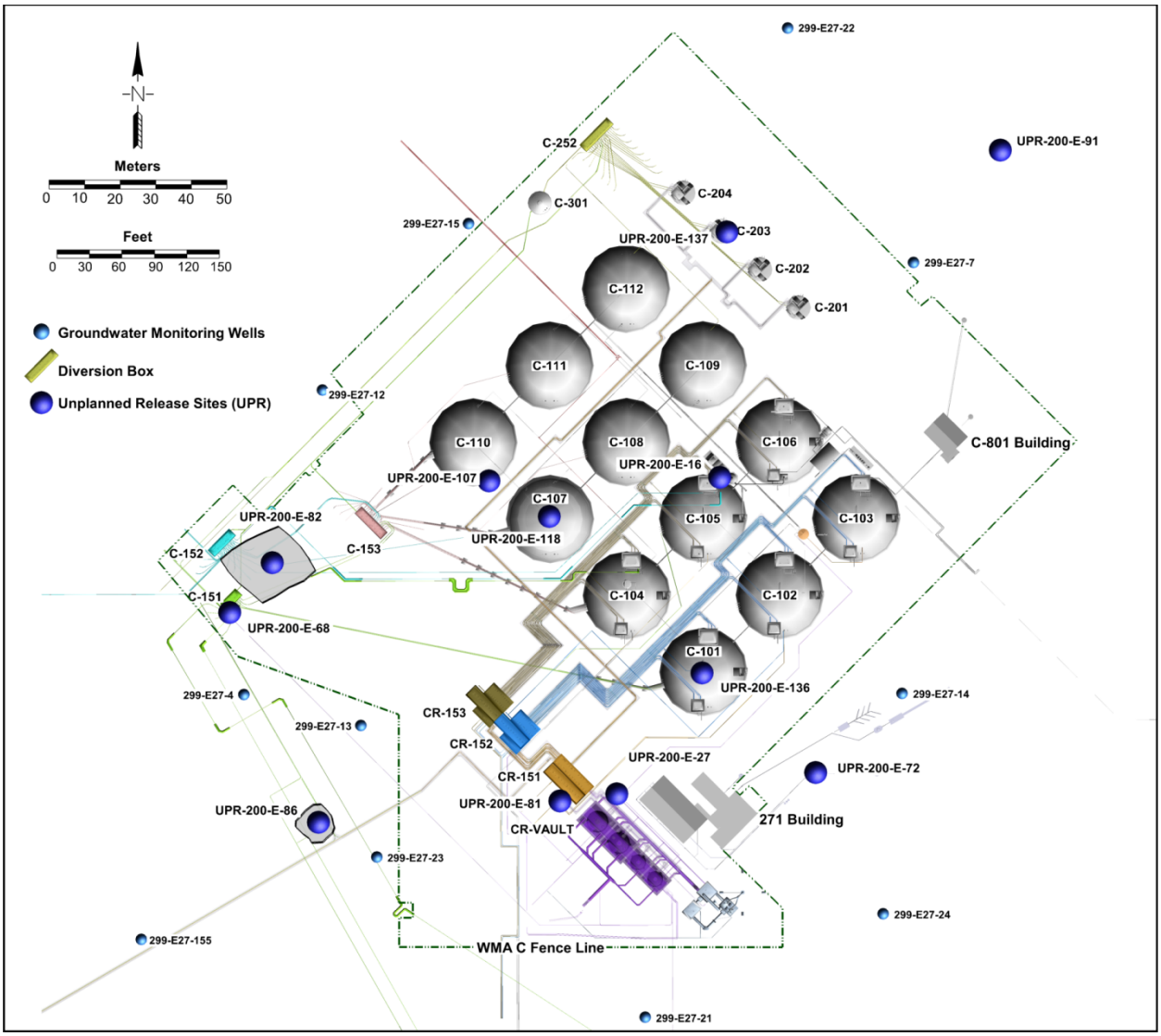

WMA = Waste Management Area

The general characteristics of these units are described in more detail in Section 3.1.4, RPP-RPT-46088 and RPP-RPT-56356. At WMA C, it is not possible to separate out the Ringold Formation, CCU and the lower gravely sequence of the Hanford formation (H3). In the vicinity of WMA C, this unit is referred to as undifferentiated H3, CCU and Ringold Formation ($H_3/CC_u/RF$). The SSTs at WMA C were emplaced in an excavation of the Hanford formation sediments of the upper, gravel-dominated (H1) unit. This excavation may also locally intercept the upper portions of the sand-dominated Hanford (H2) unit. Once the tanks were built, the excavation was backfilled with reworked sediments of the upper, gravel-dominated (H1) unit. The water table or the unconfined aquifer's surface lies ~60 m (~200 ft) below the bottom of the tank farms excavations within the undifferentiated $H_3/CC_u/RF$.

Figure 3-37. Fence Diagram Showing Cross-Sections through Waste Management Areas A-AX and C.

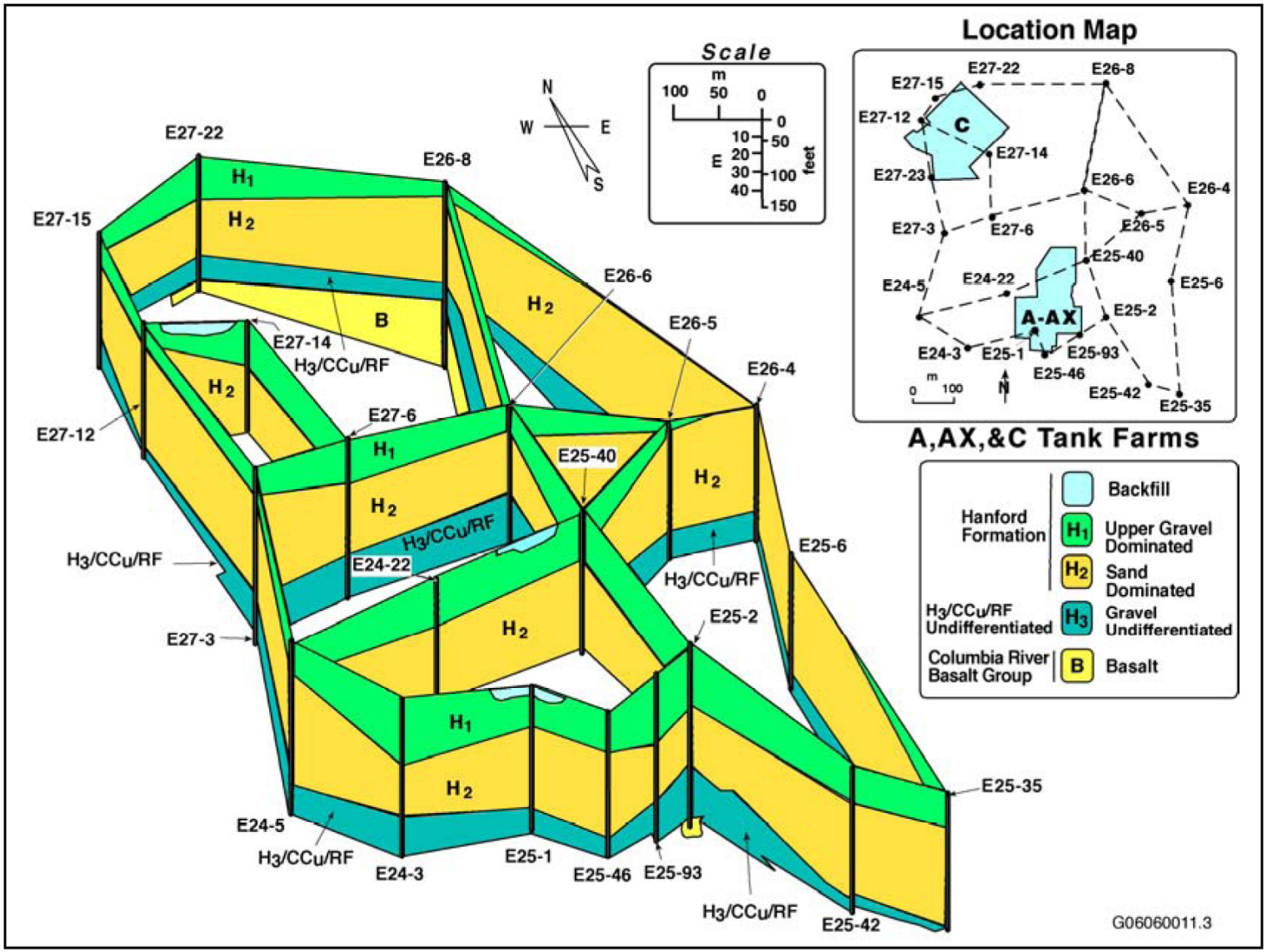

Source: RPP-RPT-46088, "Flow and Transport in the Natural System at Waste Management Area C."

The geologic strata underlying WMA C was characterized in conjunction with soil sampling and borehole logging for radionuclides and hazardous waste constituents as part of the Phase 1 and 2 RCRA Facility Investigations at WMA C. The borehole and geologic logging was used to identify the elevations of tops of the geologic units in the vicinity of WMA C. Specifically potassium, uranium, thorium (K-U-T) data from geophysical logs were used to map the tops of the different geologic units at WMA C (RPP-RPT-56356). Two alternative geologic models were developed based on this data.

Additional conceptual models are being developed with detailed heterogeneous representations of the geologic framework at WMA C. One is a facies-based model based primarily on a geostatistical analysis of the K-U-T data collected in selected direct push boreholes within WMA C; the other is based on geostatistical evaluations of volumetric moisture content measured in multiple direct push boreholes and drywells within WMA C.

The major difference between the two existing developed alternative models is whether or not a sandy gravel facies is to include a silt layer identified at the bottom of the H2 subunit in the vicinity of WMA C. The K-U-T data (i.e., a lower gross gamma and potassium count) indicates that there is a coarsening of the sand at the bottom of the H2 turning more into a sandy gravel. Underlying this sandy gravel facies is a silt unit with a strong potassium peak and occasional strong natural uranium peak. The difficulty in making this determination is that there are few direct pushes or drywells that are at a sufficient depth to obtain both good geophysical logs and geologic logs (with drill cuttings). The drill cuttings from some of the nearby groundwater wells indicated that there was definite fining of the sands along with some silt found at the vertical location as indicated by the K-U-T data in the geophysical logs, but a competent silt layer was not observed. Alternative Geologic Model I does not include the sandy gravel and underlying silt unit with the H2 unit, while Alternative Geologic Model II does include them. The existence of these layers could cause increased lateral movement in the vadose zone. A series of fence diagrams showing the differences between the two models within WMA C is given in RPP-RPT-56356. The fence diagram for both these models running southwest to northeast through the center of WMA C is given in Figure 3-38.

3.1.9.2 Hydrology. Following is an overview of the hydrology of the vadose zone and uppermost, unconfined aquifer beneath WMA C. More detailed information supporting this section can be found in DOE/ORP-2008-01, RPP-RPT-46088, and RPP-RPT-58339.

3.1.9.2.1 Vadose Zone – Monitoring and Characterization Activities. Waste Management Area C has 70 drywell monitoring boreholes (see Figure 3-39) available for leak detection monitoring and to provide access for limited vadose zone characterization (e.g., geophysical logging). These drywells were drilled from 1944 to 1982. In 1997, C Farm drywells were logged using a high-resolution spectral gamma logging system. This effort was part of the baseline characterization for WMA C. Results are documented in GJO-98-39-TAR/ GJO-HAN-18 and its associated addendum GJO-98-39-TARA/GJO-HAN-18. The depth ranges for most of these drywells is between 30.5 and 45.7 m bgs (100 and 150 ft bgs). The deepest drywell in WMA C is 47.2 m bgs (155 ft bgs) (30-00-03), and the maximum logged depth is 43.6 m bgs (143 ft bgs) (30-04-08).

Figure 3-38. Fence Diagram of Alternative Geologic Models to be Used in Waste Management Area C.

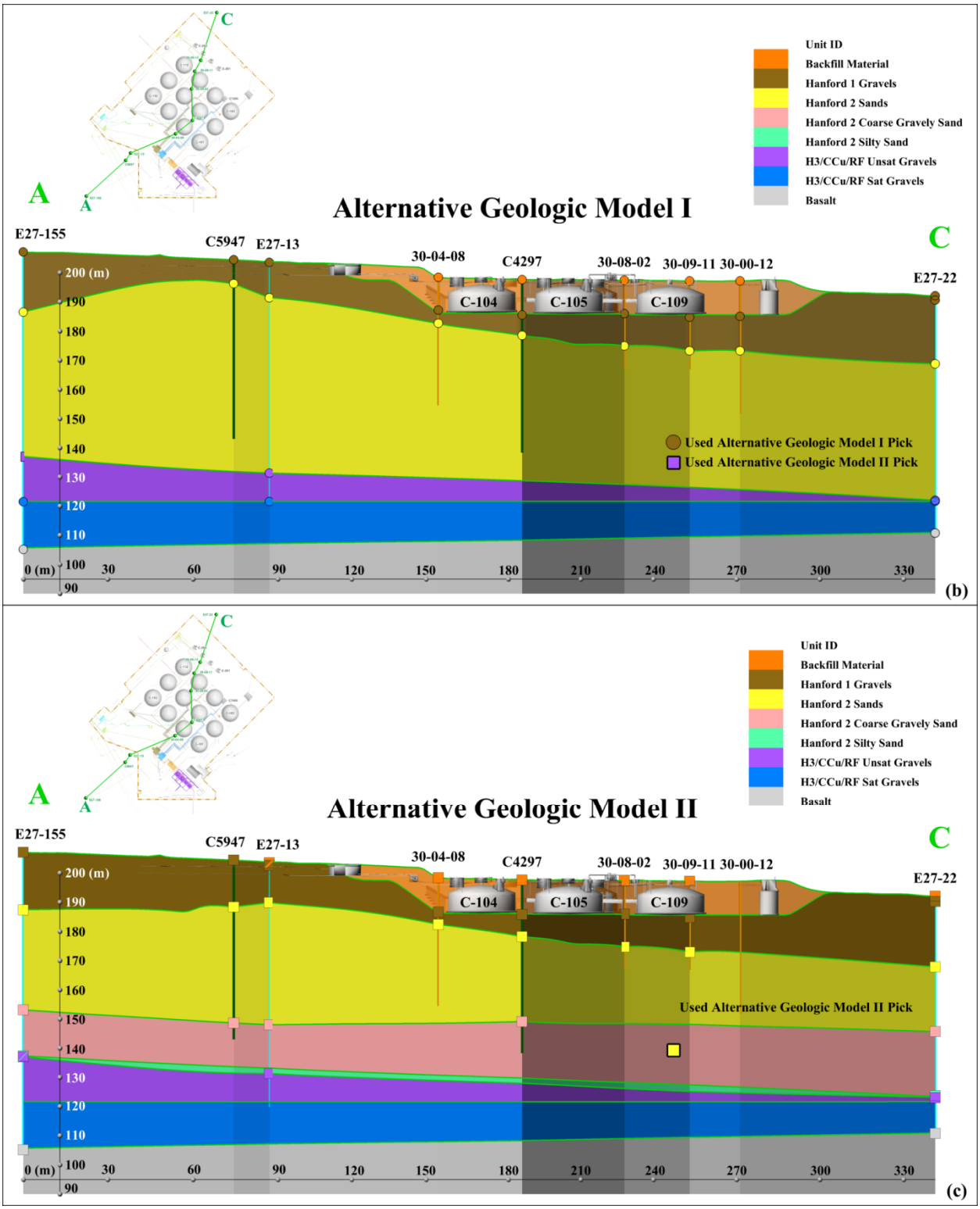

H3/CCu/RF = undifferentiated H3, Cold Creek Unit and Ringold Formation

Figure 3-39. Vadose Zone and Groundwater Monitoring Network for Waste Management Area C.

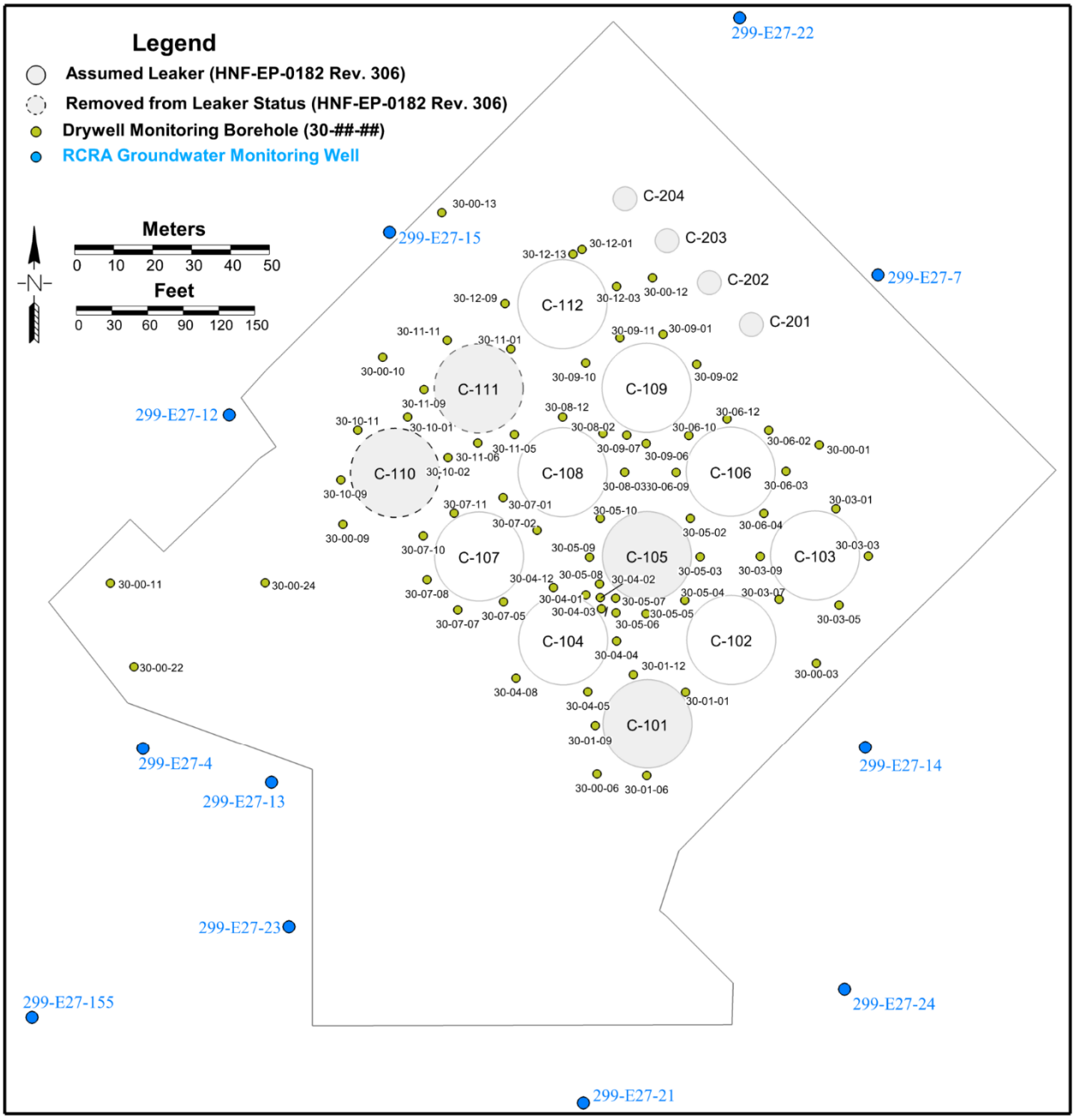

Reference: HNF-EP-0182, "Waste Tank Summary Report for Month Ending September 30, 2013," Rev. 306.

RCRA = Resource Conservation and Recovery Act of 1976

The major gamma-emitting contaminants associated with WMA C are ^{137}Cs and ^{60}Co with lesser amounts of ^{154}Eu. These contaminants are located mostly in and around areas of confirmed or suspected tank and pipeline leaks. Although most of the drywells are deeper than the surrounding contamination, some zones of contamination extend deeper than nearby drywells.

Consequently, the maximum depth of vadose zone contamination is not known in some areas of WMA C.

Since 2004, extensive vadose characterization activities have been conducted at WMA C in support of the RCRA corrective action. The characterization was divided into two phases. The first phase concentrated on characterizing an area of high ^{137}Cs concentrations observed in drywells at the depth of the base of tank C-105 below the cascade line running between tanks C-104 and C-105 and the pipeline leak known as UPR-200-E-82 close to the 241-C-152 diversion box. The characterization borehole drilled next to tank C-105 was the deepest characterization within WMA C at 59.9 m (196.5 ft) bgs at the time. Results from soil sampling show the greatest concentration of ^{99}Tc (8.4 pCi/g) and nitrate (20 µg/g [2.7×10^{-6} oz/gal]) at 41.1 to 47.2 m bgs (~135 to 155 ft bgs). Slant direct pushes underneath UPR-200-E-82 found ^{99}Tc (28.6 pCi/g) and nitrate (19.7 µg/g [2.6×10^{-6} oz/gal]) centered below the pipeline leak at 23.5 m bgs (77 ft bgs). Complete results of the first phase of characterization are documented in DOE/ORP-2008-01 Appendix L.

The second phase started in 2008 and characterization data was collected per the work plan (RPP-PLAN-39114). For Phase 2, site characterization data was collected at the 23 sites identified in Figure 3-40a. Each characterization site was given a letter map designation. The site characterization activities for Phase 2 included the following:

a. Soil collection and analysis through direct push boreholes technology

b. Geophysical logging at drywell boreholes and groundwater monitoring wells

c. Surface Geophysical Exploration

d. Tissue sampling for ecological risk assessment

e. Possible sampling of vadose zone during the installation of any new groundwater wells within ~30 m (~100 ft) of WMA C.

RPP-PLAN-39114 provides a complete description of what was to be collected at each of these sites. During the preparation of the work plan for the Phase 2 characterization, a transitional characterization (Phase 1.5) effort was undertaken and vadose zone characterization took place at two past UPR sites (UPR-200-E-81 and UPR-200-E-86) (Figure 3-40b). This transitional characterization effort was called “near-term characterization” and focused on the deployment of hydraulically-driven direct push technology to push boreholes (i.e., Phase 1.5) for geophysical logging, placement of deep electrodes, and collection of soil samples. The results of both the transitional characterization and the Phase 2 characterization efforts are given in RPP-RPT-58339.

3.1.9.2.2 Vadose Zone – Moisture Content. Moisture content data from both neutron logging and laboratory analyses were collected during both Phase 1 and 2 characterization efforts of the RCRA Facility Investigation. A statistical summary of this moisture content data is provided here. The reader is referred to Appendix B for additional detailed information about this moisture content data and its use in the PA model development process.

Figure 3-40a. Completed Phase 2 RCRA Facility Investigation Characterization Locations.

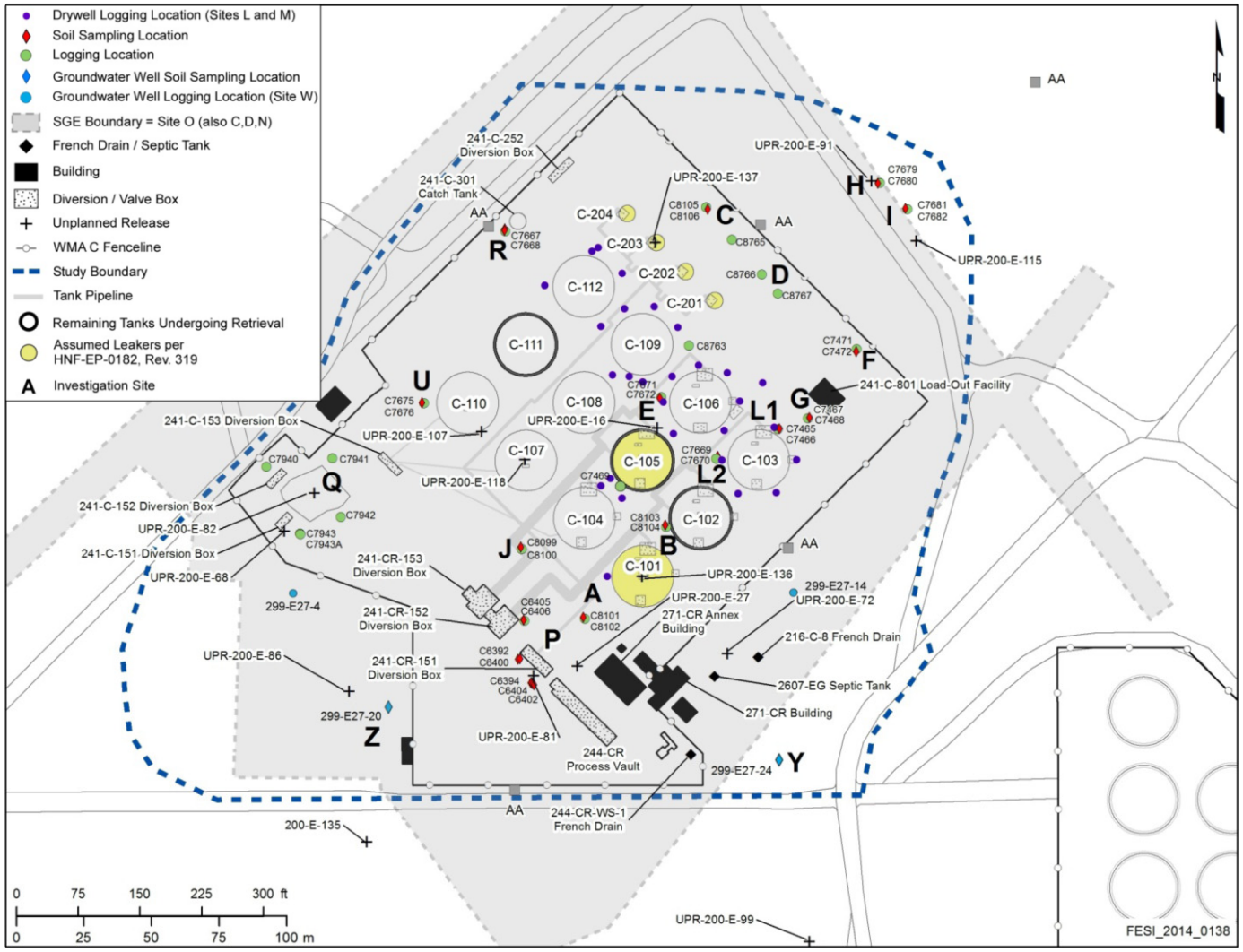

Reference: HNF-EP-0182, "Waste Tank Summary Report for Month Ending July 31, 2014," Rev. 319.

RCRA = Resource Conservation and Recovery Act of 1976, 42 USC 6901, et seq.
SGE = Surface Geophysical Exploration
WMA = Waste Management Area

Figure 3-40b. Completed Transitional (Phase 1.5) Characterization Locations.

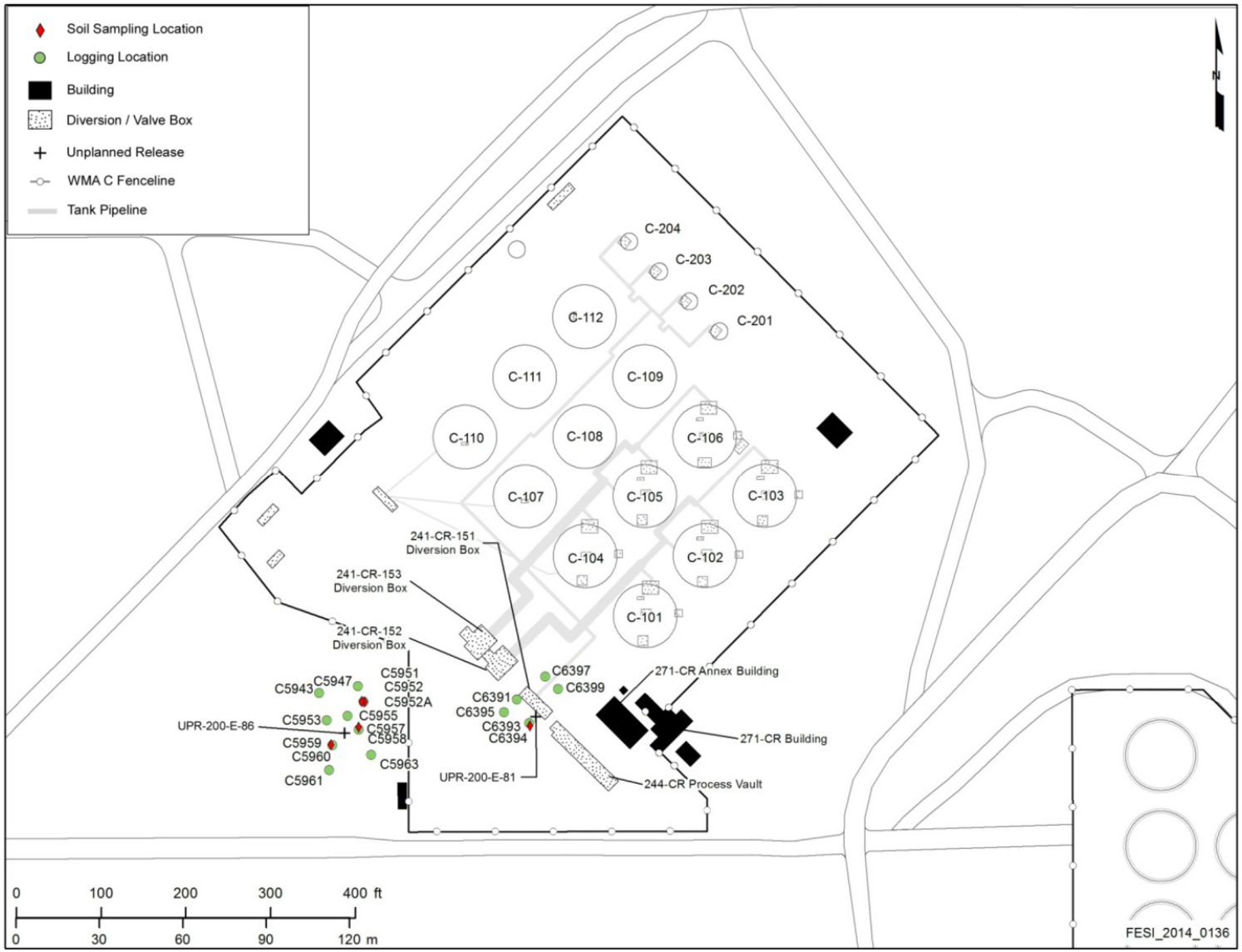

WMA = Waste Management Area

The neutron logging data came from two drywells and 63 direct push boreholes. Laboratory measured moisture content (weight % converted to volumetric moisture content) came from one groundwater well (299-E27-22) and one characterization borehole (C4297).

The spacing for the neutron logging of moisture content varied from 0.05 m to 0.15 m (~0.15 ft to 0.5 ft). The spacing on the laboratory samples was greater. A total 32,912 measurements were made and moisture content ranged from 0.11 to 30.64 volumetric percent, with a mean of 5.69, and a median of 5.09. Furthermore, the formations were identified in each well/borehole/direct push and a statistical analysis of volumetric moisture content data was run for each formation (Table 3-3). The locations for the moisture content measurements are shown in Figure 3-41.

3.1.9.2.3 Vadose Zone – Contamination. Figure 3-42 provides a visualization of the vadose zone contamination beneath WMA C as represented by ^{137}Cs data and the ^{99}Tc at borehole C4297. This figure is a three-dimensional (3-D) perspective of WMA C providing locations of tanks and associated drywells. Tanks considered to be leakers are based on information in HNF-EP-0182, "Waste Tank Summary Report for Month Ending February 28, 2015," Rev. 326. For ^{137}Cs each drywell is represented with a single vertical line. Shaded rings around the drywells indicate the level of vadose zone contamination based on spectral gamma logging results. Only the more significant soil contamination zones (i.e., ^{137}Cs contamination levels greater than 10 pCi/g) are shown.

Spectral gamma logging data provided in Figure 3-42 indicate the presence of contamination in the region between tanks C-104 and C-105. The most concentrated contamination occurs at drywell 30-05-07 on the southwest side of tank C-105 (Figure 3-42), where two high ^{137}Cs concentration zones occur at and below the tank bottom (DOE/ORP-2008-01). Also shown on Figure 3-42 are sample locations showing where the more mobile ^{99}Tc was found in characterization borehole C4297. In addition to the high ^{137}Cs at tank C-105, evidence from the historical record indicates that three unplanned near-surface release events (UPR-200-E-81, UPR-200-E-82, UPR-200-E-86) occurred on the southwest side of C Farm (Figure 3-36). These events are known to have made relatively significant contributions to vadose zone contamination (RPP-14430, "Subsurface Conditions Description of the C and A-AX Waste Management Area").

The UPR-200-E-81 event occurred near the 241-CR-151 diversion box and involved the loss of ~140,000 L (~36,000 gal) of waste. The UPR-200-E-82 event occurred near the 241-C-152 diversion box and involved the loss of ~10,000 L (~2,600 gal) of waste. The UPR-200-E-86 event occurred in a pipeline break near the southwest corner of C Farm and involved the loss of ~66,000 L (~17,400 gal) of waste. Other UPRs occurred within or near to WMA C (RPP-ENV-33418) and are the subject of further characterization efforts at WMA C (RPP-PLAN-39114). These other UPRs are also shown on Figure 3-36. The Phase 2 RCRA Facility Investigation (RPP-RPT-58339) found low levels of contaminants related to tank waste. However, the contaminant concentrations levels found in the soil are so low that the areas in which they are found are not considered to be the sources for the groundwater contamination at WMA C.

Table 3-3. Summary Statistics for Volumetric Moisture Content in the Lithologic Units Underlying Waste Management Area C.

Unit	Count of Wells	Count of Measurements	Minimum (Vol %)	Maximum (Vol %)	Average (Vol %)	Median (Vol %)	Mode (Vol %)	Standard Deviation	Variance
Backfill	52	4,052	0.11	30.61	8.09	7.48	6.20	3.71	13.75
H1	66	7,977	0.13	30.64	5.88	4.72	3.26	3.67	13.47
H2	64	20,876	1.06	26.32	5.15	4.96	4.89	1.82	3.30
H3	1	7	5.54	7.09	6.18	6.01	Too Few	0.65	0.43
Waste Management Area C	67	32,912	0.11	30.64	5.69	5.09	4.89	2.82	7.95

Figure 3-41. Moisture Content (% Vol) Measurements in Vadose Zone at Waste Management Area C.

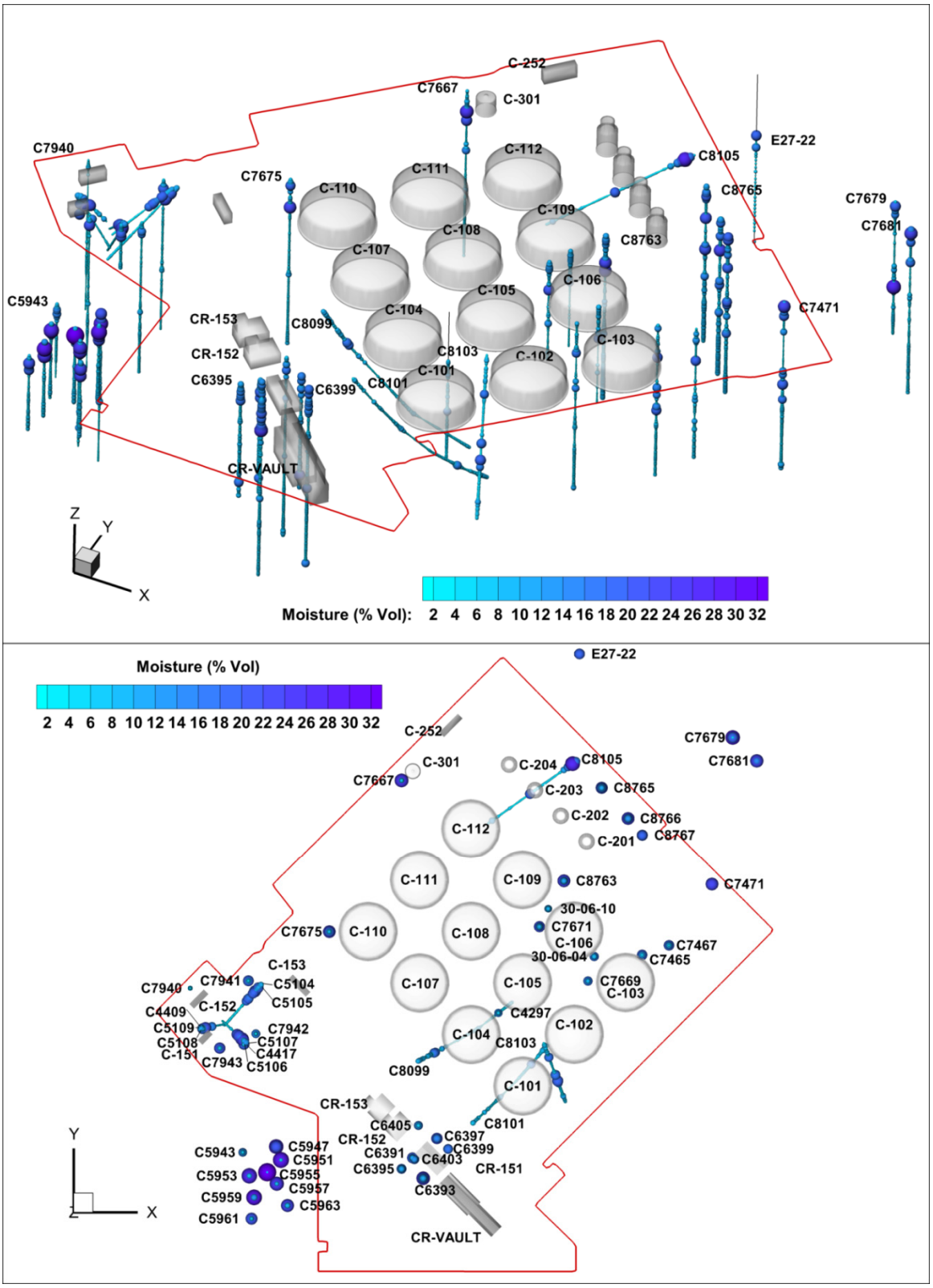

Figure 3-42. Three-Dimensional Perspective of Waste Management Area C Tanks and Drywells Showing Occurrence of Significant (>10 pCi/g) Cesium-137 Contamination in the Vadose Zone along with Technetium-99 at Borehole C4297.

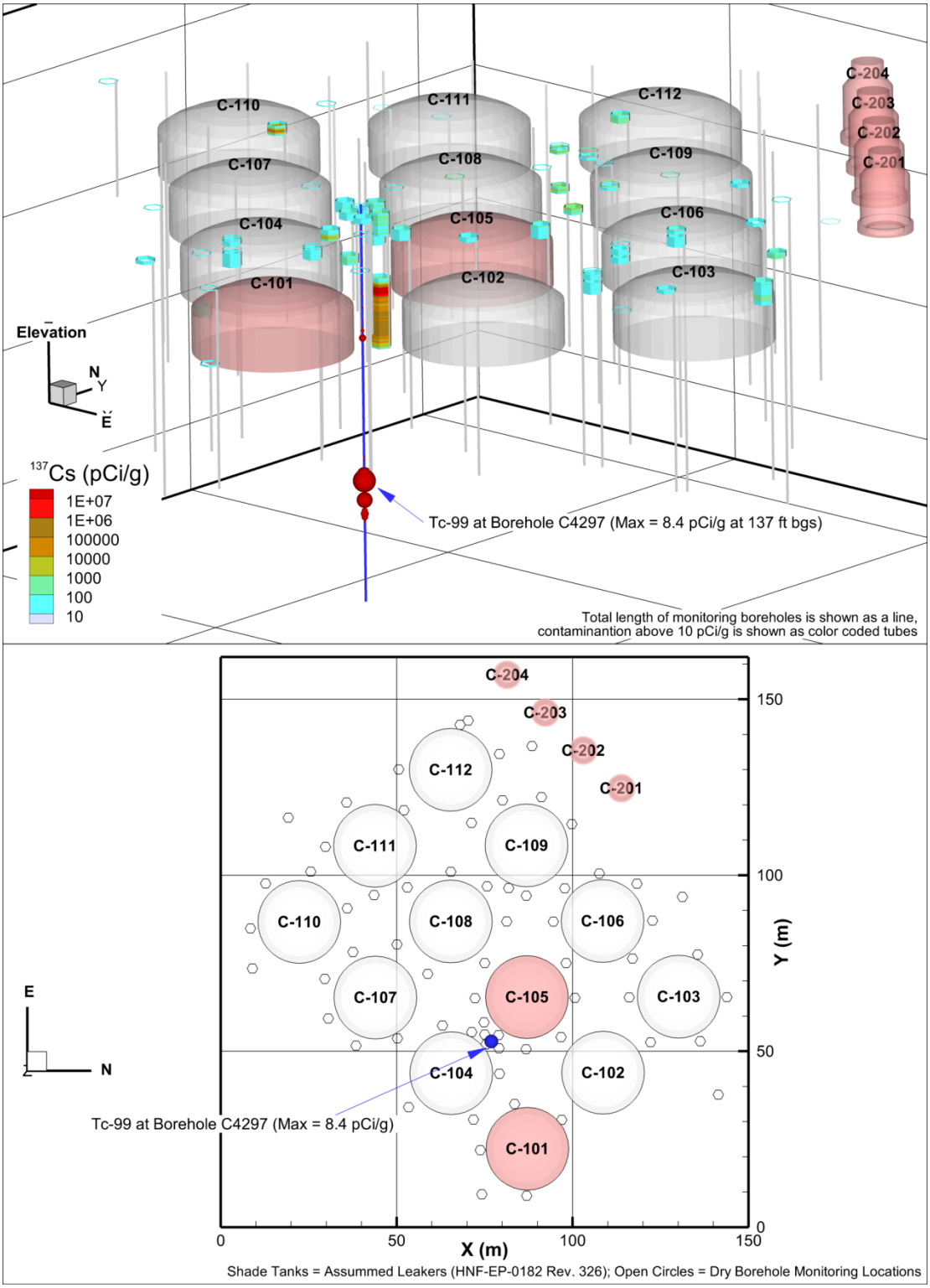

Reference: HNF-EP-0182, "Waste Tank Summary Report for Month Ending February 28, 2015," Rev. 326.

3.1.9.2.4 Unconfined Aquifer – Monitoring. Quarterly groundwater monitoring was initiated at WMA C in 1992 in accordance with WHC-SD-EN-AP-012, "Interim-Status Groundwater Monitoring Plan for the Single-Shell Tanks." The initial well network consisted of five wells: 299-E27-7, 299-E27-12, 299-E27-13, 299-E27-14, and 299-E27-15 (Figure 3-39). These wells were used for quarterly groundwater monitoring beginning in March 1992 and continued until the Fall of 1993. In the Spring of 1994, semi-annual sampling began for indicator parameter evaluation. Monthly sampling began in June 1998 to prepare for sluicing at tank C-106. The monthly sampling was scaled back to bi-monthly in 2000 and then returned to quarterly sampling in 2001. In 2001, a new monitoring plan, PNNL-13024, "RCRA Groundwater Monitoring Plan for Single-Shell Tank Waste Management Area C at the Hanford Site," was initiated and required additional wells to ensure adequate monitoring network coverage for WMA C. Wells 299-E27-4, 299-E27-21, 299-E27-22, and 299-E27-23 (Figure 3-39) were subsequently added to the network.

In 2009, WMA C was placed in assessment monitoring because of the exceedance of the critical mean for the indicator parameter specific conductance. In addition, the dangerous constituent cyanide has been found in groundwater beneath WMA C, albeit at levels much lower than the DWS. To meet quarterly RCRA assessment requirements, a new monitoring plan (DOE/RL-2009-77, Groundwater Quality Assessment Plan for the Single-Shell Tank Waste Management Area C) was developed which superseded PNNL-13024. Currently, assessment monitoring is being completed in accordance with DOE/RL-2009-77. Three wells (299-E27-24, 299-E27-25, and 299-E27-155; see Figure 3-39) were added to the network per DOE/RL-2009-77. Well 299-E27-25 is not shown on Figure 3-39; it is located ~170 m (~550 ft) northeast of the northeast fenceline of WMA C. The network now is composed of 12 WMA C monitoring network wells.

In addition to meeting the quarterly assessment requirements, quarterly monitoring is also done to meet the requirements of External letter 04-TPD-083, "Agreement on Content of Tank Waste Retrieval Work Plans," in which quarterly groundwater monitoring sample results are to be provided to Ecology during tank retrievals. To meet the sampling requirements, the groundwater monitoring analyses include RCRA and AEA constituents from the following: anions, cyanide, metals, ^{99}Tc, gross beta, total uranium, and low-level gamma scan. The most recent quarterly monitoring report is SGW-58561, "WMA C Quarterly October Through December 2014 Quarterly Groundwater Monitoring Report."

3.1.9.2.5 Unconfined Aquifer – Groundwater Flow Conditions. The water table or potentiometric surface lies ~60 m (~200 ft) below the bottom of the tank farm excavations within the undifferentiated $H_3/CC_u/RF$. The aquifer materials consist dominantly of sandy gravel or silty sandy gravel. The water table elevation beneath WMA C is ~122 m (400 ft) NGVD88 with ~77 m (255 ft) of vadose zone. The aquifer thickness, based on the top of basalt at 108 m (355 ft), is ~13.4 m (44 ft). Hydraulic conductivity values reported for the aquifer in this area vary considerably, ranging from 0.04 (silt lenses within the sandy gravel) to 6,900 m/day (1.6 in. to 22,600 ft). Additional hydraulic property data from aquifer testing at wells near WMA C is provided in RPP-RPT-46088.

Currently, the general groundwater flow direction in the unconfined aquifer beneath WMA C is to the south/southeast. The water table is very flat overall, with an estimated hydraulic gradient between 1×10^{-5} to 2×10^{-5} m/m; the estimated groundwater flow velocity ranges from 0.2 to 0.4 m/day (0.7 to 1.3 ft/day) (RPP-RPT-46088). Those hydraulic gradient estimates are also consistent with those recently reported in SGW-54165, "Evaluation of the Unconfined Aquifer Hydraulic Gradient Beneath the 200 East Area, Hanford Site" for the unconfined aquifer near the Integrated Disposal Facility (IDF) and PUREX cribs. Also coincident with the flow change are decreasing concentrations of other contaminants in monitoring wells west of C Farm, indicating a change in flow direction. These observations and other interpretations discussed in SGW-58561 provide sufficient evidence for the determination of a south to southeast flow direction at WMA C.

The discharge of large volumes of wastewater in the early 1950s to B Pond raised the water table in the vicinity of WMAs C and A-AX as much as 4.9 m (16 ft) above the pre-Hanford Site operations level (PNNL-14548, "Hanford Site Groundwater Monitoring for Fiscal Year 2003"). The corresponding flow direction underneath WMA C at this time was toward the southwest (DOE/ORP-2008-01 Appendix H). Water levels began to decline in the late 1980s when wastewater discharges were reduced. The decline has become even more pronounced since other effluent discharges throughout the 200 Areas ceased in 1995. Water levels are expected to continue declining within the region surrounding WMAs A-AX and C, with the flow direction changing to the southeast. With the change in flow direction, contamination originating in the B Complex in the northwest corner of 200 East may flow underneath WMA C in the not too distant future.

3.1.9.2.6 Unconfined Aquifer – Contamination. Observations of elevated concentrations of nitrate, sulfate, and ^{99}Tc appear to be associated with past releases from WMA C because these constituents are much higher in the downgradient wells compared to upgradient wells, and they exceed their respective groundwater DWSs. Additionally, cyanide, which is a dangerous waste constituent, is also found in the aquifer at levels above the detection limit, but well below the DWS of 200 µg/L (2.7×10^{-5} oz/gal). The measured cyanide concentration was 13.9 µg/L (1.9×10^{-6} oz/gal) in December 2013 at well 299-E27-14. Only ^{99}Tc and cyanide are discussed further in this section. Technetium-99 exceeded the DWS by a factor of almost 30 and cyanide is a dangerous waste constituent. For discussions and interpretations of the overall trends of other constituents in monitoring wells in the vicinity of WMA C, the reader is referred to SGW-58561.

In December 2014, ^{99}Tc had concentrations exceeding the 900 pCi/L DWS in 7 of the 11 monitoring wells surrounding WMA C (Figure 3-43). However in 2006, only 4 of the 11 wells exceeded the DWS. Three of these wells (299-E27-4, 299-E27-13, and 299-E27-23) are located just outside the south-central region of WMA C (Figure 3-39). The other well that exceeded the DWS is 299-E27-14, located east of WMA C. Two new wells (299-E27-155 and 299-E27-4) placed to the south and east of WMA C after 2006 also showed ^{99}Tc concentrations above the DWS when they were installed. The ^{99}Tc in the groundwater in that region appears to be centered on well 299-E27-23 with the trend in that well increasing from ~5,000 pCi/L in late 2006 to ~26,000 pCi/L by April 2012. Since then, the trend at the well has been decreasing, falling to ~3,400 pCi/L by December 2014. This decline is associated with changes in the flow

direction to the east and southeast. The resulting change in flow direction and sampling in downgradient wells (299-E27-21 and 299-E27-24) from 299-E27-23 show ^{99}Tc increasing in these wells, indicating plume movement to the east-southeast. Finally, at well 299-E27-14, ^{99}Tc values ranged between 1,500 and 2,600 pCi/L from 2006 to late 2012. However, in early 2013 they started increasing, peaking in June of 2013 at 10,700 pCi/L and decreasing since then; they had decreased to 6,200 pCi/L by December 2014. It is believed the ^{99}Tc found at well 299-E27-14 is from a different source than ^{99}Tc found in the south-central region of WMA C.

The specific source of ^{99}Tc in the groundwater at WMA C has not been identified.

The dangerous waste constituent cyanide was detected at four WMA C wells in December 2014 at concentrations far below the 200 µg/L DWS. A possible reason for the increased number of wells with detectable cyanide between June and December is that the detection limit for cyanide decreased from 4 to 1.67 µg/L (5.3×10^{-7} oz/gal to 2.2×10^{-7} oz/gal). Three of the four wells (299-E27-7, 299-E27-14, and 299-E27-23) with detected cyanide were reported with concentrations between 3 and 4 µg/L (4.0×10^{-7} oz/gal to 5.3×10^{-7} oz/gal). The other well (299-E27-4) was detected with 7.9 µg/L (1.1×10^{-6} oz/gal). Concentrations at well 299-E27-4 are generally near the detection level but were higher in December of 2009, 2011, and 2014 (10.4, 7.98, and 7.9 µg/L [1.39×10^{-6} oz/gal, 1.06×10^{-6} oz/gal and 1.07×10^{-6} oz/gal], respectively). Remnant levels of low cyanide concentrations appear to be present sporadically beneath the eastern and western portions of the C Farm facility, while more persistent concentrations exist to the southeast (wells 299-E27-14 and 299-E27-24) as can be seen in Figure 3-44. However, cyanide concentrations have appeared to diminish beneath C Farm. The highest cyanide concentration in December 2014 was 7.9 µg/L (1.1×10^{-6} oz/gal) at well 299-E27-4. As discussed in DOE/RL-2009-77, the source is likely be related to past releases from WMA C, but a specific source within WMA C has not been identified.

3.2 WASTE MANAGEMENT AREA C PRINCIPAL FACILITY DESIGN FEATURES

Waste Management Area C is part of the Hanford Site SST system consisting of 149 underground SSTs and processing equipment designed and constructed between 1940 and 1964 to transport and store radioactive and hazardous chemical wastes generated from irradiated nuclear fuel processing. The tanks, designed to store waste, vary in size from 190,000 to 3,800,000 L (50,000 gal to 1,000,000 gal) and contain a variety of solid and liquid waste. In addition to the tanks, a large amount of ancillary equipment associated with the system exists and, although not designed to store wastes, the ancillary equipment is contaminated through contact with the waste. Waste was routed to the tanks through a network of underground waste transfer piping, with interconnections provided in concrete pits that allowed changes to the routing through instrumentation. Processing vaults used during waste handling operations, evaporators used to reduce the waste stored in the system, and other miscellaneous structures used for a variety of waste handling operations are also included in the system. The SST system was taken out of service in 1980 and no additional waste has been added to the tanks.

Figure 3-43. Technetium-99 Concentrations in Waste Management Area C Wells from January 2006 through December 2014.

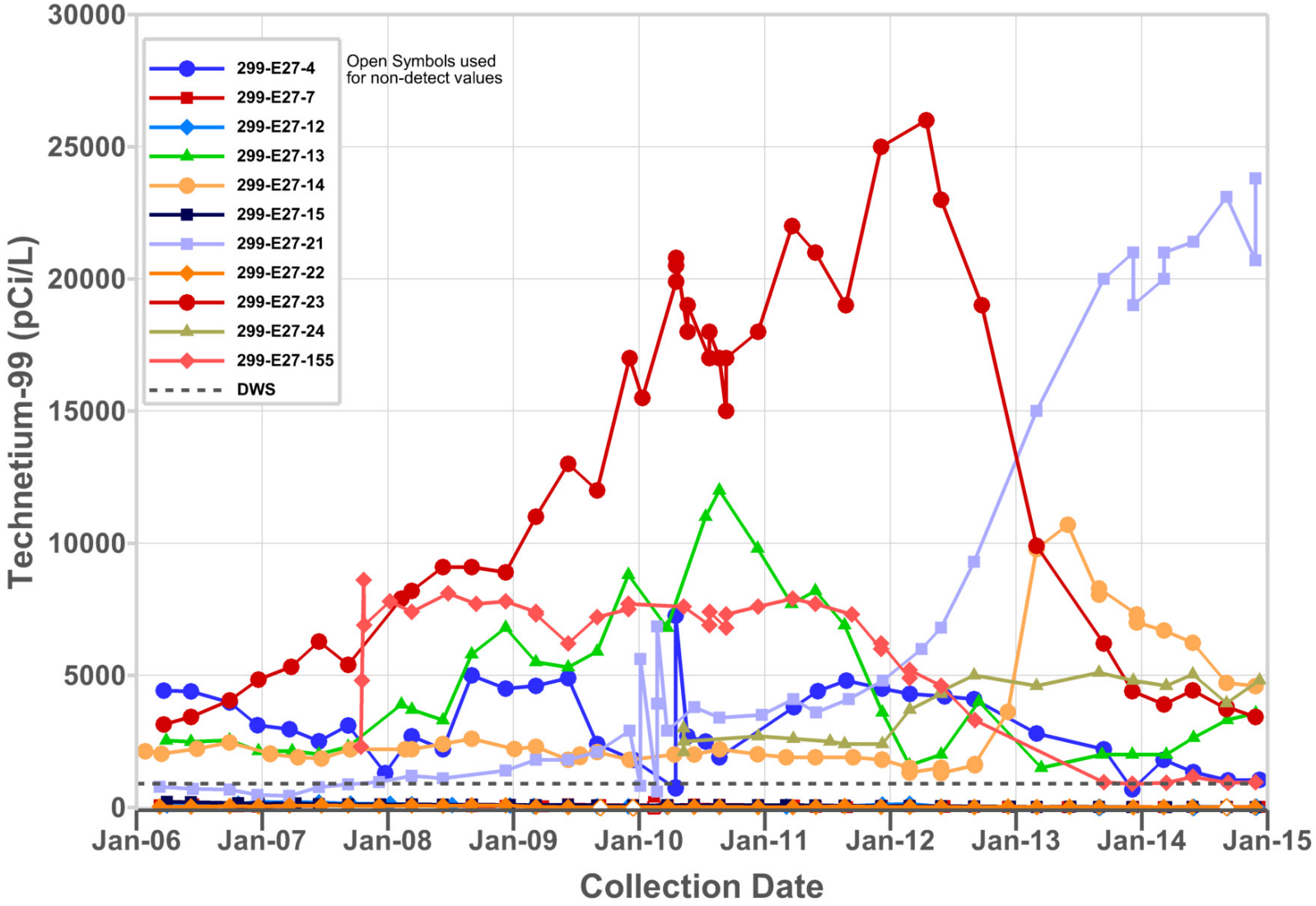

Figure 3-44. Cyanide Concentrations in Waste Management Area C Wells from January 2006 through December 2014.

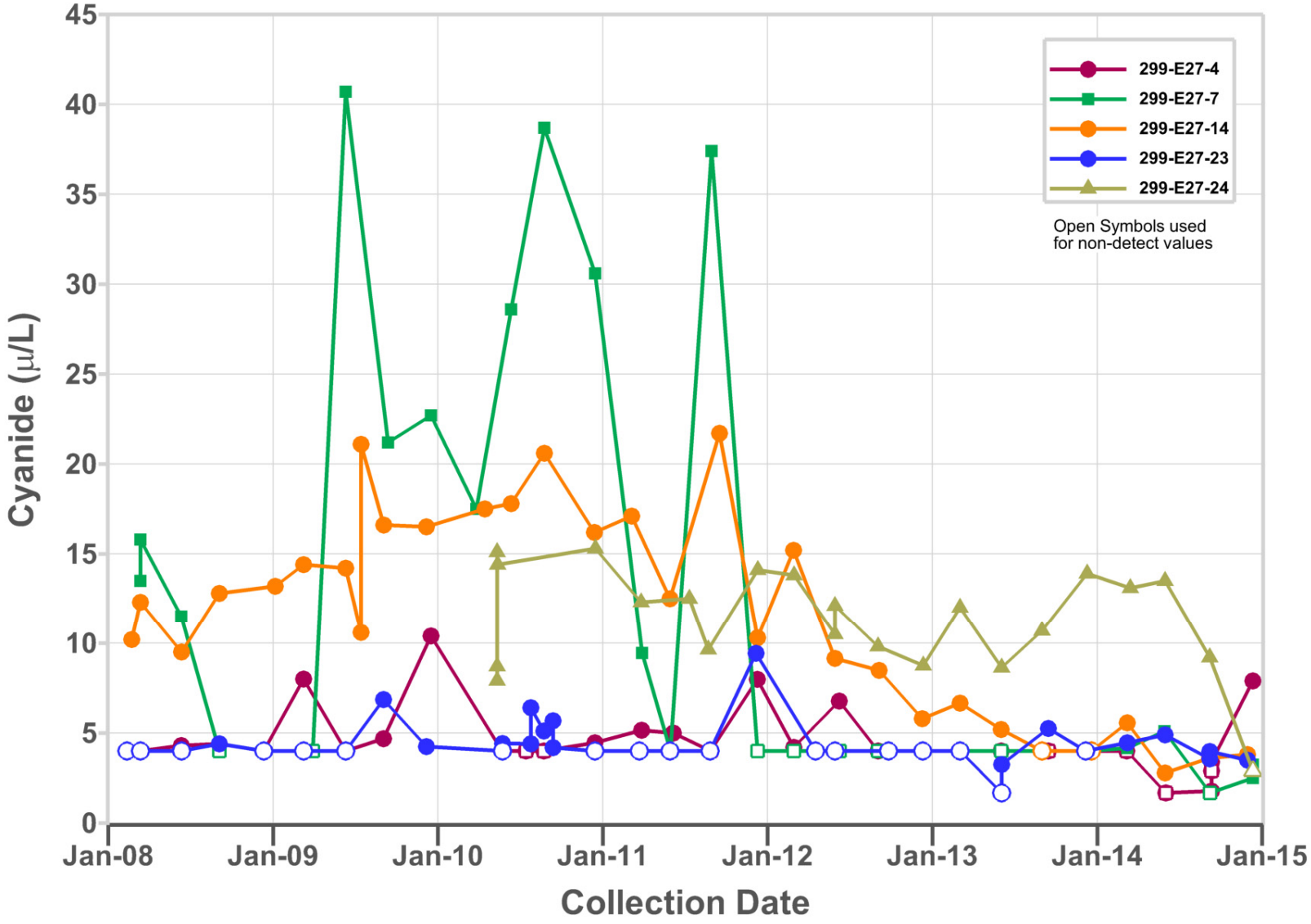

For the landfill closure[1] of WMA C, site closure is assumed to occur at year 2020, at which time the tanks are assumed to be filled with grout and covered with a final closure cover. This section provides site-specific information for WMA C. It is a summary from the most recent documents that describe present conditions, geology and hydrology, subsurface contamination, and source terms. The list of these documents and what they contain is given in Appendix A. The majority of these documents were produced to support the working sessions for the WMA C PA that took place from February 2009 to May 2011. In addition to the data packages, several other documents have been produced after the working sessions that provide updated information on WMA C facility characteristics.

3.2.1 Facility Description

Waste Management Area C is located in the east central portion of the 200 East Area (Figure 3-4) in land that is designated to be Industrial-Exclusive. Waste Management Area C is one of seven WMAs (A-AX, B-BX-BY, C, S-SX, T, TX-TY, and U) containing 149 SSTs built from 1943 to 1964 (Figure 3-2). In general, the WMA C boundary is represented by the fenceline surrounding the C Farm (Figure 3-3). Waste Management Area C contains twelve 100-Series SSTs and four 200-Series SSTs that were constructed in 1943 to 1944 along with associated ancillary equipment (i.e., diversion boxes, pipes). It was placed in service in 1946, and used to store and transfer waste until the mid-1980s. Additional ancillary equipment (244-CR vault and CR diversion boxes) were added in the early 1950s. Because of its long operational history, C Farm received waste generated by essentially all of the Hanford Site major chemical processing operations including bismuth phosphate fuel processing, uranium recovery, PUREX fuel processing, Hot Semiworks Facility pilot plant operations, fission product recovery, and tank farm interim stabilization and isolation activities.

Fifteen of the 16 WMA C SSTs were interim stabilized between 1981 and 2003 (HNF-SD-RE-TI-178, "Single-Shell Tank Interim Stabilization Record"). The interim stabilization process removed as much pumpable liquid as practicable. "Practicable" means pumping was continued until the pump rate was less than 0.19 L/min (0.05 gpm). Only tank C-106 was not interim stabilized. This tank went directly to retrieval. The waste in the WMA C tanks is currently in the process of being retrieved and transferred to Hanford's double-shell tanks. However, not all waste can be retrieved and estimates of the inventory of radionuclides and hazardous chemicals remaining in the tank residuals after closure are given in Section 3.2.2.

3.2.1.1 Infrastructure. This section summarizes the information given in the following data packages produced for the working sessions: RPP-RPT-44042, "Recharge and Waste Release within Engineered System in Waste Management Area C" and RPP-RPT-46879, "Corrosion and Structural Degradation within Engineered System in Waste Management Area C." Table 3-4 lists the WMA C infrastructure components that were included in the WMA C PA. Inventories of radionuclides and hazardous chemicals remaining in these components are provided in Section 3.2.2.

[1] 78 FR 75913, "Record of Decision: Final Tank Closure and Waste Management Environmental Impact Statement for the Hanford Site, Richland, Washington" (December 13, 2013).

Table 3-4. Operating Period and Capacities for Waste Management Area C Facilities Included in the Performance Assessment.*

Facility	Interim Stabilized	Constructed	Operating Capacity (gal)
Single-Shell Tanks			
241-C-101	1983	1943 to 1944	530,000
241-C-102	1995	1943 to 1944	
241-C-103	2003	1943 to 1944	
241-C-104	1989	1943 to 1944	
241-C-105	1995	1943 to 1944	
241-C-106	N/A	1943 to 1944	
241-C-107	1995	1943 to 1944	
241-C-108	1984	1943 to 1944	
241-C-109	1983	1943 to 1944	
241-C-110	1995	1943 to 1944	
241-C-111	1984	1943 to 1944	
241-C-112	1990	1943 to 1944	
241-C-201	1982	1943 to 1944	55,000
241-C-202	1981	1943 to 1944	
241-C-203	1982	1943 to 1944	
241-C-204	1982	1943 to 1944	
Miscellaneous Underground Storage Tanks			
Facility	**Removed From Service**	**Constructed**	**Operating Capacity (gal)**
241-C-301 catch tank	1988	1946	36,000
244-CR-001 vault tank**	1988 (244-CR Process Tank Vault)	1946	40,000
244-CR-002 vault tank**		1946	15,000
244-CR-003 vault tank**		1946	15,000
244-CR-011 vault tank**		1946	40,000
Underground Waste Transfer Lines			
241-C tank farm pipelines	N/A	1943 to 1944	~26,700
241-C-151	1985	1946	N/A
241-C-152	1985	1946	N/A
241-C-153	1985	1946	N/A
241-C-252	1985	1946	N/A
241-CR-151	1985	1952	N/A
241-CR-152	1985	1952	N/A
241-CR-153	1985	1952	N/A

* Data on the facilities are from DOE-RL-88-30, Hanford Site Waste Management Units Report; RPP-15043, "Single-Shell Tank System Description"; RPP-PLAN-47559, Single-Shell Tank Waste Management Area C Pipeline Feasibility Evaluation."

** Capacity estimates for tanks associated with the 244-CR Process Tank Vault are from HNF-EP-0182, "Waste Tank Summary Report for Month Ending February 29, 2016," Rev. 338.

N/A = not applicable

3.2.1.1.1 Single-Shell Tanks. The 241-C Tank Farm (C Farm, i.e., WMA C) contains 12 first-generation, reinforced-concrete tanks with carbon steel liners covering the sides and bottoms. The 100-series tanks are 23 m (75 ft) in diameter, with a maximum 5-m (16-ft) depth and 2,006,000-L (530,000-gal) design capacity. The 200-series tanks are 6 m (20 ft) in diameter with a maximum 7-m (24-ft) depth and 208,000-L (55,000-gal) design capacity. Typical tank configuration and dimensions are shown in Figure 3-45. The 100-series tanks sit below grade with at least 2 m (7 ft) of soil cover to provide shielding from radiation exposure to operating personnel. Tank pits are located on top of the 100-series tanks and provide access to the tank, pumps, and monitoring equipment.

The SSTs were constructed in place with carbon steel (ASTM A283/A283M-03, "Standard Specification for Low and Intermediate Tensile Strength Carbon Steel Plates") lining the bottom and sides of a reinforced concrete shell. The tanks have concave bottoms (i.e., center of tanks lower than the perimeter) and a curving intersection of the sides and bottom (Figure 3-46). The inlet and outlet lines are located near the top of the liners (Figure 3-45). The tanks are arranged in four rows of three tanks. The tanks in each row are piped together so that when the first tank fills, it overflows (cascades) into the second tank, and the second into the third. The four smaller 200-series tanks are piped to diversion box 241-C-252 (Figure 3-45). For additional history of types of waste that went into WMA C, please see RPP-RPT-44042.

The HFFACO Appendix H requires that tanks C-103 and C-106 be retrieved to less than 10.2 m^3 (360 ft^3) for 100-series SSTs and 0.85 m^3 (30 ft^3) for 200-series SSTs or the limit of technology, whichever is lower. The thresholds of 10.2 m^3 (360 ft^3) and 0.85 m^3 (30 ft^3) were the average calculated residual volume left in each of the 100-series and 200-series SSTs, respectively, after 99% of the waste is retrieved. The C Farm will be the first tank farm at Hanford to be completely retrieved. The limits of technology that govern the retrieval process for tanks C-101, C-102, C-104, C-105, C-107, C-108, C-109, C-110, C-111, C-112 are provided in the Consent Decree in Washington v. DOE, Case No. CV-08-5085-RMP (E.D. Wa. October 25, 2010). Table 3-5 provides the current status of retrieval operations at WMA C as of February 28, 2015.

3.2.1.1.2 Ancillary Equipment. To support the transfer and storage of waste within the WMA C SSTs, a complex waste transfer system of pipelines (waste transfer lines), diversion boxes, vaults, valve pits, and other miscellaneous structures exists. Collectively, these are referred to as ancillary equipment, as shown in Figure 3-36. Multiple levels of piping were installed over time in WMA C. A time line of piping installations is described in (RPP-7494). It is estimated that there are ~11 km (~7 mi) of waste transfer piping in C Farm (RPP-PLAN-47559). Estimated total volume of piping is given in Table 3-4; estimated volume of residuals remaining in pipes after closure is 5,962 L (1,575 gal) (RPP-PLAN-47559).

The 244-CR vault is located south of the tanks. The vault is a two-level, multi-cell, reinforced-concrete structure constructed below grade (DOE/RL-92-04, PUREX Source Aggregate Area Management Study Report), which contains four underground tanks along with overhead piping and equipment. This reference estimated a capacity of 170,343 L (45,000 gal) each for two tanks (TK-CR-001 and TK-CR-011) and a capacity of 55,494 L (14,700 gal) each for the other two tanks (TK-CR-002 and TK-CR-003). HNF-EP-0182 currently lists the capacities of TK-CR-001 and TK-CR-011 as 151,400 L (40,000 gal) each and the capacities of

TK-CR-002 and TK-CR-003 as 56,775 L (15,000 gal) each. This vault and associated diversion boxes 241-CR-151, 241-CR-152, and 241-CR-153 were constructed in 1951 and ceased operating in 1988. Figure 3-47 shows the waste pH, temperature, and volume estimates in 2005. Approximately 98% of the liquid volume in the cells was removed in early 2010 (RPP-RPT-45845, "Completion of Pumpable Liquid Removal from 244-CR Vault"). In addition to the tanks in the 244-CR vault, a catch tank C-301 exists that was used to catch waste from the diversion boxes.

The routing of liquid waste from the operations buildings to the tank farms was accomplished using underground transfer lines, diversion boxes, and valve pits. The diversion boxes housed jumpers (remote pipeline connectors) where waste could be routed from one transfer line to another. The diversion boxes are below-ground, reinforced-concrete boxes that were designed to contain any waste that leaked from the high-level waste (HLW) transfer line connections. Per INDC-356-VOL3, "Construction Hanford Engineer Works U.S. Contract Number W-7412-ENG-1 Du Pont Project 9536 History of the Project Volume III" (page 923), the interior surfaces of diversion boxes were coated with a chemically resistant paint. If waste leaked into a diversion box, it generally drained by gravity to nearby catch tanks where any spilled waste was stored and then pumped to SSTs (DOE/RL-92-04). The seven diversion boxes located within WMA C are labeled (241-) C-151, C-152, C-153, C-252, CR-151, CR-152, and CR-153 on Figure 3-36.

3.2.1.2 Closure. The TC&WM EIS ROD (78 FR 75913) was published on December 13, 2013. It states the following:

> "SST closure operations include filling the tanks and ancillary equipment with grout to immobilize the residual waste. Disposal of contaminated equipment and soil will occur on site. The tanks will be grouted and contaminated soil may be removed. The SSTs will be landfill-closed, which means they will be stabilized, and an engineered modified RCRA Subtitle C barrier put in place followed by post-closure care."

Waste Management Area C closure is anticipated to occur during the next decade (i.e., ~2020), at which time the tanks will be filled with grout and covered with a final closure cover. Although tank leaks and soil releases have been identified in C Farm, for a nominal modeling case it is assumed that at the time of closure the C Farm tank liners will be intact. This is because tank C-105 is the only C Farm tank currently assumed to have a breach in the liner, with ~40% probability (RPP-ASMT-46452, "Tank 241-C-105 Leak Assessment Completion Report"). There are several other sources of releases near this tank and a liner breach for this tank is not confirmed. Other releases were assessed to have occurred high on the tank wall or to be cascade line or spare inlet releases (tanks C-101, C-104, C-108 and C-110). Liquid level decreases in tank C-111 and in the C-200-series tanks were assessed to be caused by evaporation with no apparent releases to the soil (RPP-ENV-33418). Drywell and leak detection monitoring to date in the vicinity of tanks retrieved showed no evidence of leakage during retrieval (RPP-RPT-58386, "Retrieval Data Report for Single-Shell Tank 241-C-101"; RPP-RPT-33060, "Retrieval Data Report for Single-Shell Tank 241-C-103"; RPP-RPT-54072, "Retrieval Data Report for Single-Shell Tank 241-C-104"; RPP-20577, "Stage II Retrieval Data Report for

Single-Shell Tank 241-C-106"; RPP-RPT-58295, "Retrieval Data Report for Single-Shell Tank 241-C-107"; RPP-RPT-55896, "Retrieval Data Report for Single-Shell Tank 241-C-108"; RPP-RPT-55284, "Retrieval Data Report for Single-Shell Tank 241-C-109"; RPP-RPT-56796, "Retrieval Data Report for Single-Shell Tank 241-C-110"; RPP-RPT-58490, "Retrieval Data Report for Single-Shell Tank 241-C-112"; RPP-RPT-26475, "Retrieval Data Report for Single-Shell Tank 241-C-203"; RPP-RPT-29095, "Retrieval Data Report for Single-Shell Tank 241-C-202"; RPP-RPT-30181, "Retrieval Data Report for Single-Shell Tank 241-C-201"; RPP-RPT-34062, "Retrieval Data Report for Single-Shell Tank 241-C-204"), indicating that the waste containment appears to be intact for these tanks. In addition, operational high resolution resistivity monitoring data to date, in the vicinity of the remaining tanks undergoing retrieval (C-102, C-105, and C-111), shows no evidence of waste losses during the retrieval process (e-mail from A. R. Olander to J. G. Field, "RE: WMA C PA - Editing" (Olander, A. R., 2016-05-03); e-mail from A. R. Olander to M. P. Bergeron, "RE: WMA C PA - Editing" (Olander, A. R., 2016-08-18)). Recent summary information on depth gamma and moisture measurements made in dry wells near tank C-102 (HGLP-MBL-018, "241-C-102 Tank Waste Retrieval Project Final Report of Drywell Monitoring Data") before and after retrieval supports this general conclusion. The monitoring data results collected during retrieval of tank C-105 call into question the hypothesis of a possible breach in the liner of tank C-105.

While the tanks most likely will be filled with grout following retrieval of the waste in the tanks, the final closure cover may be delayed because of the proximity to nearby single-shell and double-shell tanks just to the east and southeast of WMA C. With the presence of grout in tanks and the possible use of a suitable interim cover over the tank farm, the delay in placement of final closure cover is not expected to have a significant adverse impact on the potential contaminant releases to the groundwater pathway from the tank farm after closure. This section summarizes information provided in RPP-RPT-44042 and RPP-RPT-46879.

3.2.1.2.1 Stabilization of Tank and Selected Components with Grout Fill. After the retrieval of the residual waste, the SSTs and some of the ancillary equipment and components (i.e., C-301 catch tank, 244-CR vault, and diversion boxes but not pipelines) within WMA C will be filled with grout. Grout is a material formed from cement, fly ash, fine aggregate, sodium bentonite clay, and water to create a free-flowing material that can be used to fill the tanks after waste retrieval is completed. The grout hardens in the tanks to stabilize the residual waste and provide structural stability for landfill closure of the tank farms.

The closure plan approach to fill the tanks will provide a high quality grout throughout the tank (DOE/EIS-0391, 2012). Although the final formulation of the grout has not been developed, it is assumed the grout would be similar to the cold-cap grout formulation developed by USACE for the Hanford Grout Vault Program. This formulation exhibits a low-hydration heat and is free-flowing, self-leveling, and designed to generate little or no free water during curing (DOE/EIS-0391 Appendix E). Figure 3-48 shows the conceptual model of an SST shortly after the emplacement of the grout, while Figure 3-49 shows the conceptual model of an aged tank system. The modified RCRA C barrier is not shown in either of these figures.

Figure 3-45. Waste Management Area C Tanks and Associated Tank Infrastructure.

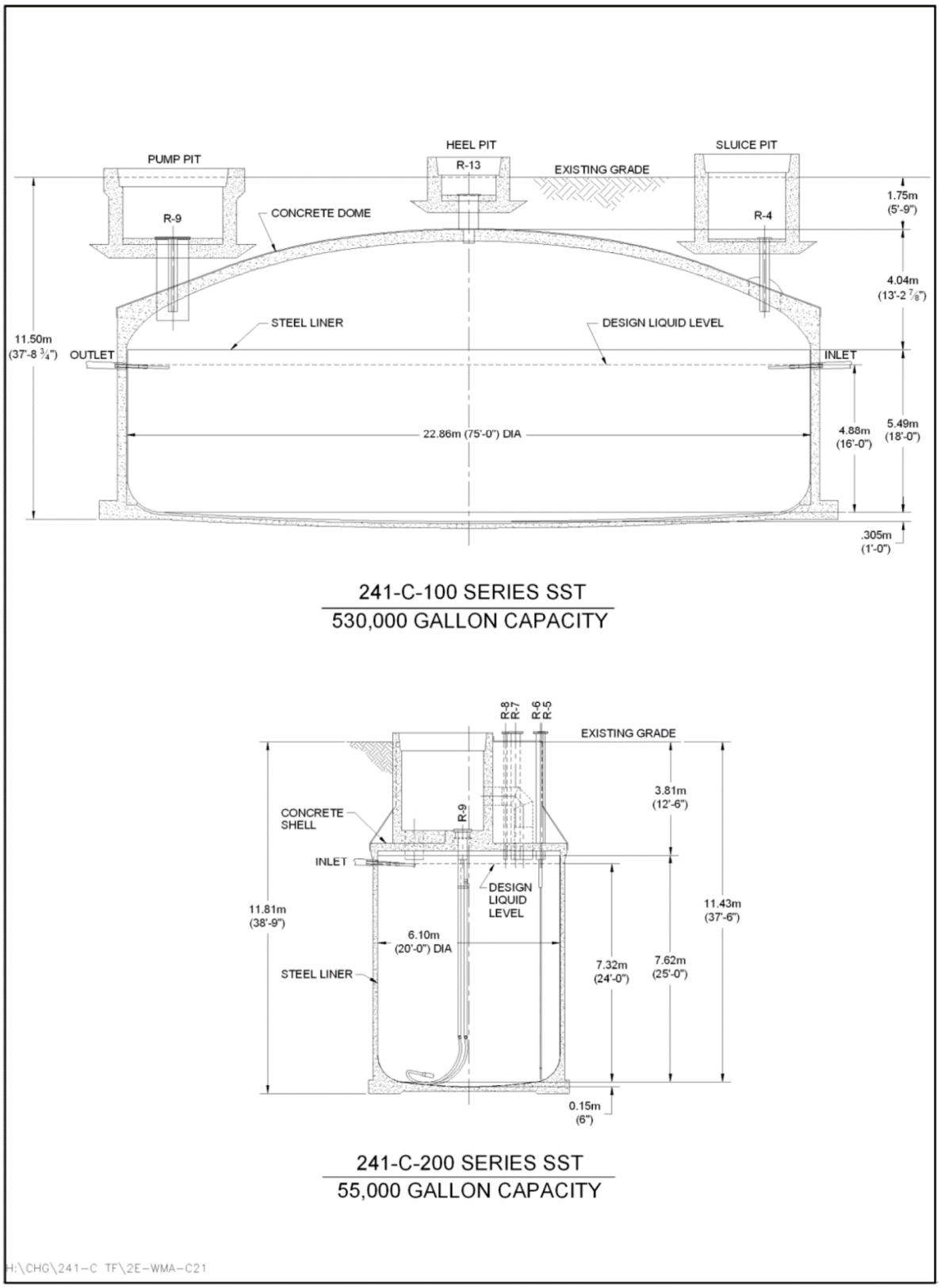

SST = single-shell tank

Figure 3-46. Corner of Tank Floor with Tank Sides for the C-100 and C-200 Series Tanks.

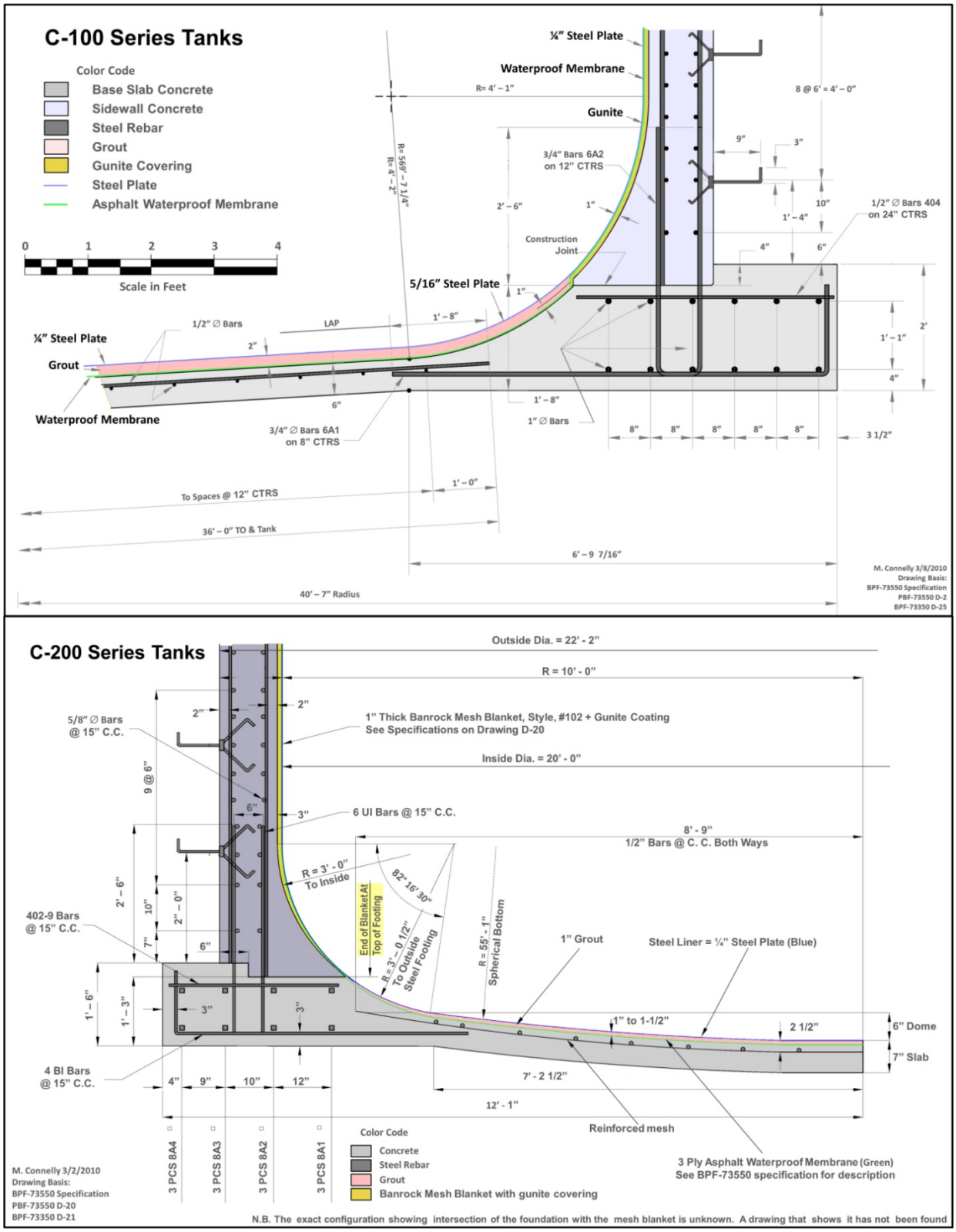

Reference: BPF-73550, "Specifications For Construction of Composite Storage Tanks Bldg. No. 241 Hanford Engineer Works Project 9536."

Table 3-5. Single-Shell Tank Retrieval Status at Waste Management Area C as of May 31, 2014.[a] (2 sheets)

Tank Number	Status	Comments	Nominal Volume of Remaining Waste[b]	Reference
241-C-101	Complete	Declared "Retrieved to Limit of First and Second Retrieval Technologies," September 25, 2013	5.0 kgal	RPP-CALC-56434, "Post-Retrieval Camera/CAD Modeling System Waste Volume Estimate for Tank 241-C-101"
241-C-102	Ongoing	Retrieval in progress – retrieval initiated April 27, 2014	51.7 kgal	HNF-EP-0182, "Waste Tank Summary Report for Month Ending February 28, 2015," Rev. 326 Note 10
241-C-103	Complete	Declared "Retrieval Completed," August 23, 2006	2.5 kgal	RPP-RPT-33060, "Retrieval Data Report for Single-Shell Tank 241-C-103"
241-C-104	Complete	Declared "Retrieval Completed," August 17, 2012	1.9 kgal	RPP-CALC-54284, "Post-Hard Heel Retrieval Camera/CAD Modeling System Waste Volume Estimate for Tank 241-C-104"
241-C-105	Ongoing	Retrieval in progress – retrieval initiated June 11, 2014	131.3 kgal	HNF-EP-0182 Rev. 326 Note 13
241-C-106	Complete	Declared "Retrieval Completed," December 31, 2003	2.8 kgal	RPP-20577, "Stage II Retrieval Data Report for Single-Shell Tank 241-C-106"
241-C-107	Complete	Declared "Retrieved to Limit of Third Retrieval Technology," September 30, 2014	10.7 kgal	RPP-CALC-59985, "Post-Retrieval Camera/CAD Modeling System Waste Volume Estimate for Tank 241-C-107"
241-C-108	Complete	Declared "Retrieved to Limit of Modified Sluicing Technology," March 22, 2012	3.4 kgal	RPP-CALC-54266, "Post-Hard Heel Retrieval Camera/CAD Modeling System Waste Volume Estimate for Tank 241-C-108"
241-C-109	Complete	Declared "Retrieved to Limit of Modified Sluicing Technology," September 12, 2012	2.0 kgal	RPP-CALC-54759, "Post-Hard Heel Retrieval Camera/CAD Modeling System Waste Volume Estimate for Tank 241-C-109"
241-C-110	Complete	Declared "Retrieval Completed," October 30, 2013	1.8 kgal	RPP-CALC-56399, "Post-Hard Heel Retrieval Camera/CAD Modeling System Waste Volume Estimate for Tank 241-C-110"
241-C-111	Ongoing	Retrieval in progress – retrieval initiated September 14, 2010	32.8 kgal	HNF-EP-0182 Rev. 326 Note 19
241-C-112	Ongoing	Declared "Retrieval Completed," May 29, 2014	12.7 kgal	RPP-CALC-56856, "Estimated Waste Volume Remaining in Single Shell Tank 241-C-112 after Hard Heel Retrieval"

Table 3-5. Single-Shell Tank Retrieval Status at Waste Management Area C as of May 31, 2014.[a] (2 sheets)

Tank Number	Status	Comments	Nominal Volume of Remaining Waste[b]	Reference
241-C-201	Complete	Declared "Retrieval Completed," March 23, 2006	0.14 kgal	RPP-29441, "Post-Retrieval Waste Volume Determination for Single-Shell Tank 241-C-201"
241-C-202	Complete	Declared "Retrieval Completed," August 11, 2005	0.15 kgal	RPP-RPT-29095, "Retrieval Data Report for Single-Shell Tank 241-C-202"
241-C-203	Complete	Declared "Retrieval Completed," March 24, 2005	0.14 kgal	RPP-RPT-26475, "Retrieval Data Report for Single Shell Tank 241-C-203"
241-C-204	Complete	Declared "Retrieval Completed," December 11, 2006	0.14 kgal	RPP-RPT-34062, "Retrieval Data Report for Single-Shell Tank 241-C-204"

[a] Status taken from HNF-EP-0182, Rev 326.

[b] Nominal volume of waste inventory is the best estimate of residual volume. Retrieval Data Reports also provide 95% upper confidence level volume as the bounding estimate of remaining waste.

Figure 3-47. 244-CR Process Tank Vault Waste pH, Temperature, and Volume Estimates in 2005.

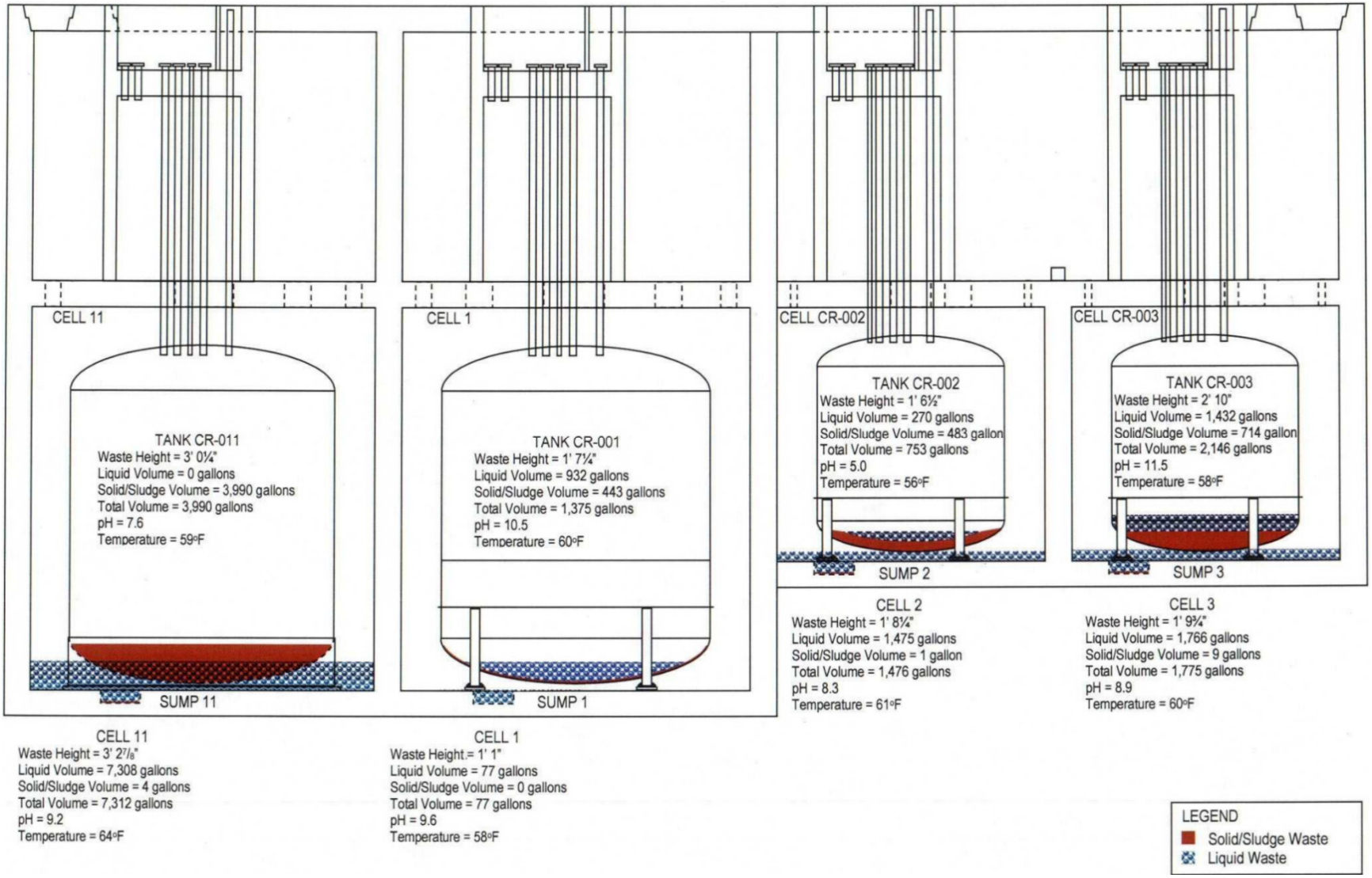

Source: RPP-RPT-24257, "244-CR Vault Liquid Level Assessment and Video Inspection Completion Report."

Figure 3-48. Conceptual Model of Tank Filled with Cementitious Grout.

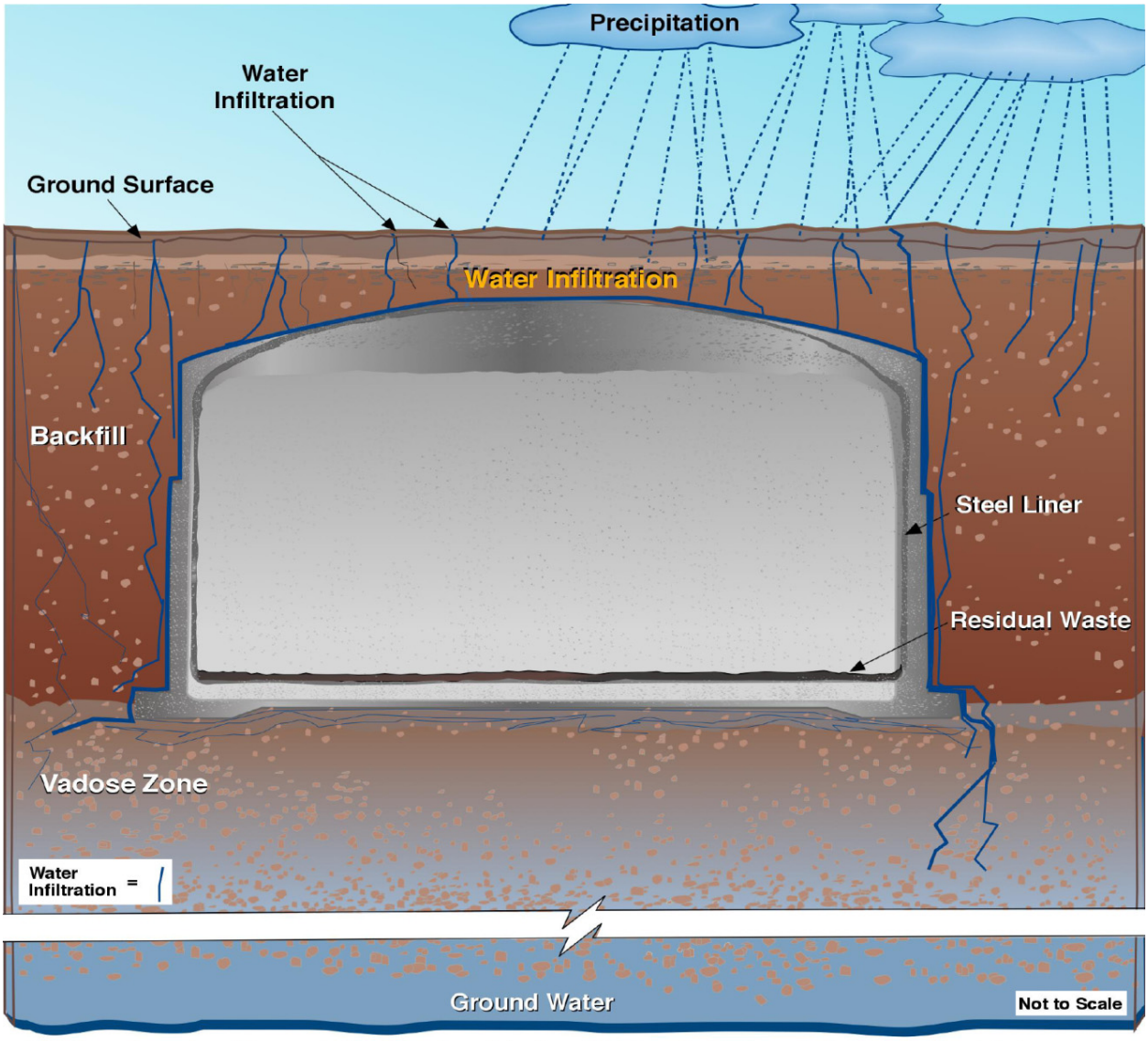

This is a schematic to illustrate infiltration of precipitation which is typically through slow gravitational drainage.

Pacific Northwest National Laboratory (PNNL) has conducted numerous studies to understand release of ^{99}Tc, chromium, and uranium from residual waste left in the WMA C SSTs (C-103, C-104, C-106, C-108, C-202, C-203, and C-204) after closure using distilled water, as well as water in equilibrium with a young grout and an aged grout. The results of these studies are given in Section 5.0 of this document.

3.2.1.2.2 Use of Modified RCRA Subtitle C Barrier. After the tank and ancillary equipment have been grouted, the closure plan approach would be to place an engineered modified RCRA Subtitle C barrier over the site. DOE/RL-93-33 provides the conceptual design criteria, regulatory requirements, technical guidance, and the conceptual baseline design of the modified RCRA Subtitle C barrier. The surface cover does not currently exist, but the expected performance of the barrier comes from lysimeter studies, tracer tests, and computer simulations

(PNNL-14744) as well as monitoring of the 200-BP-1 Prototype Hanford Barrier (PNNL-18845, "200-BP-1 Prototype Hanford Barrier – 15 Years of Performance Monitoring").

Figure 3-49. Conceptual Model of Cementitious Grouted Tank Aging.

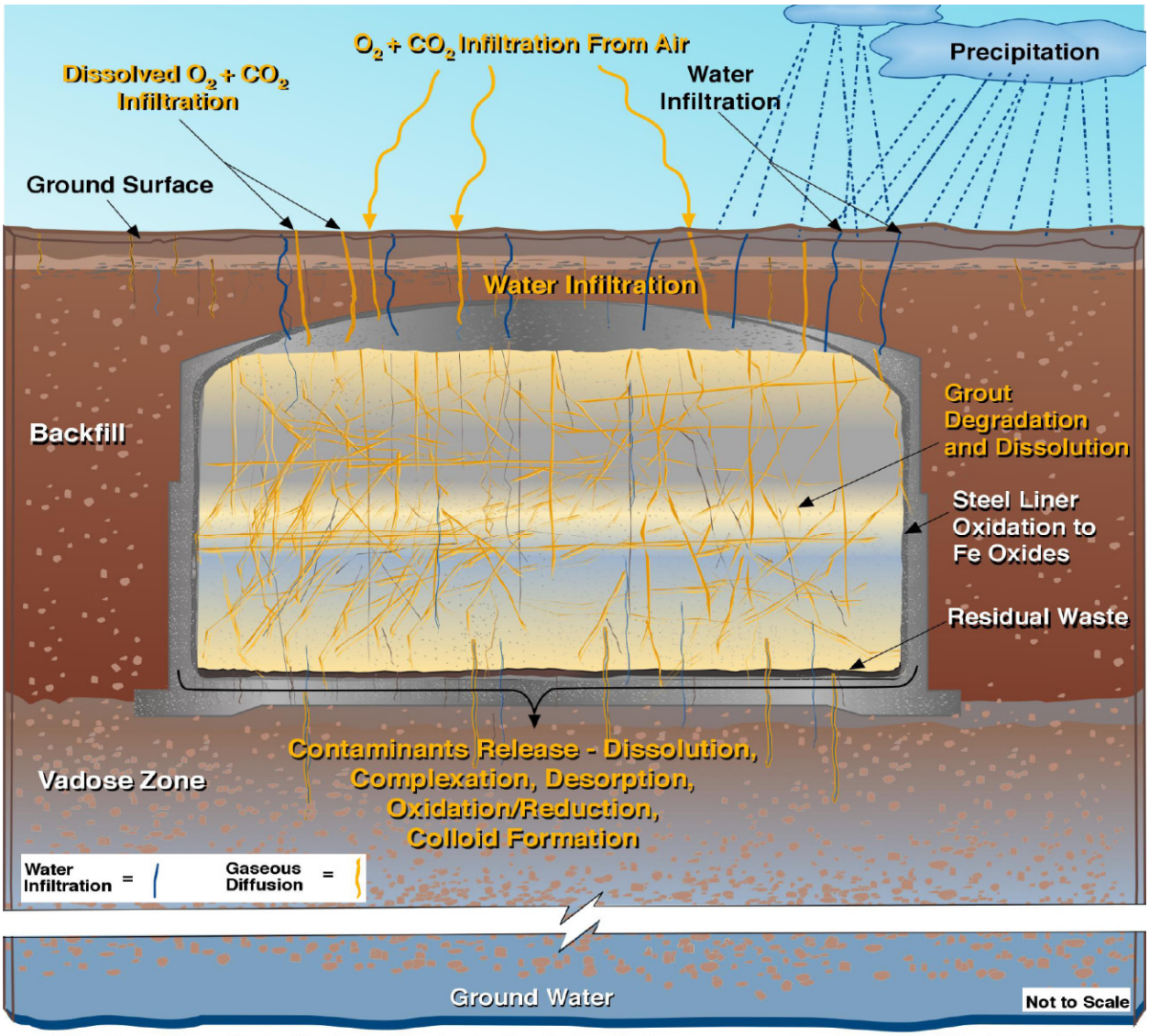

This is a schematic to illustrate the physical and chemical processes acting on grouted tank over time

The modified RCRA Subtitle C barrier generally consists of a layer of clay, geo-membrane material, and sand and gravel. This RCRA-compliant barrier will be modified by the addition of ~4.6 m (15 ft) of soil to provide shielding from radioactive material and to deter intrusion. The cover includes a vegetated surface layer of fine-grained soils to retain moisture and encourage evapotranspiration, thereby minimizing infiltration and vadose zone transport of contaminants to groundwater. It is expected that thickness of the top layer of the barrier will be increased to provide additional defense-in-depth against direct contact exposure from a basement excavation over the site. Prior to cover construction, specific closure cover designs will be evaluated and the most appropriate closure cover design will be selected for construction.

Figure 3-50 provides the generic modified RCRA Subtitle C barrier baseline design from DOE/RL-93-33. The expected performance of this design configuration is used in building the fate and transport model. The performance of the barrier with regard to recharge comes from the upper one meter of the barrier which contains the silt loam layer. This layer collects and holds the precipitation that falls over the site during the winter months; then during the summer months, evapotranspiration takes place that removes the stored precipitation from an assumed silt loam layer.

For a degraded surface barrier, a range of potential recharge rates may result. PNNL-14744 investigated the possibility of the most likely natural failure mechanisms (i.e., bioturbation of the silt loam layer, wind erosion, and accretion of windblown sand). With appropriate design considerations, PNNL-14744 argues that the failure possibility of these natural systems is quite low, and the emplaced silt-loam soils will continue to perform for as long as they remain in place. Based on these arguments, PNNL-14744 concluded that the long-term effectiveness of the surface barrier would continue to limit recharge rates to less than 0.1 mm/yr for thousands of years.

These arguments are further supported by the monitoring of the Hanford Barrier documented in PNNL-18845, which reports 15 years of data collection on the following:

- water-balance monitoring, consisting of precipitation, runoff, soil moisture storage, and drainage measurements with evapotranspiration calculated by difference
- stability monitoring, consisting of asphalt-layer-settlement, basalt-side-slope-stability, and surface-elevation measurements
- vegetation dynamics
- animal use.

The 200-BP-1 Prototype Hanford Barrier was installed in 1994 over the 216-B-57 Crib. Based on monitoring of the Prototype Hanford Barrier, it is expected that the barrier will continue to perform even after fires have burned off the vegetation (PNNL-18934, “The Effects of Fire on the Function of the 200-BP-1 Engineered Surface Barrier”) and extreme precipitation events (PNNL-14143, “The Hanford Site 1000-Year Cap Design Test”). The lessons learned from the Prototype Hanford Barrier indicate that the cover design for the WMA C barrier will be very robust and will be able to continue to perform as designed for very long time frames, but to address potential uncertainties, cases are considered that address increased infiltration/recharge that could occur as a result of a variety of changes that may happen in the far future.

The modified RCRA-compliant closure cover being considered for WMA C will be designed to meet or exceed the regulatory requirements for applications at Category 1 LLW and Category 3 LLW (NRC Class C waste) facilities (see DOE/RL-93-93 for complete listing of regulatory requirements. The basis for cover design criteria is summarized in Table 3-6 (DOE/RL-93-33, Table 2-5).

Figure 3-50. Generic Modified RCRA C Baseline Design from DOE/RL-93-33.

Modified RCRA C Barrier

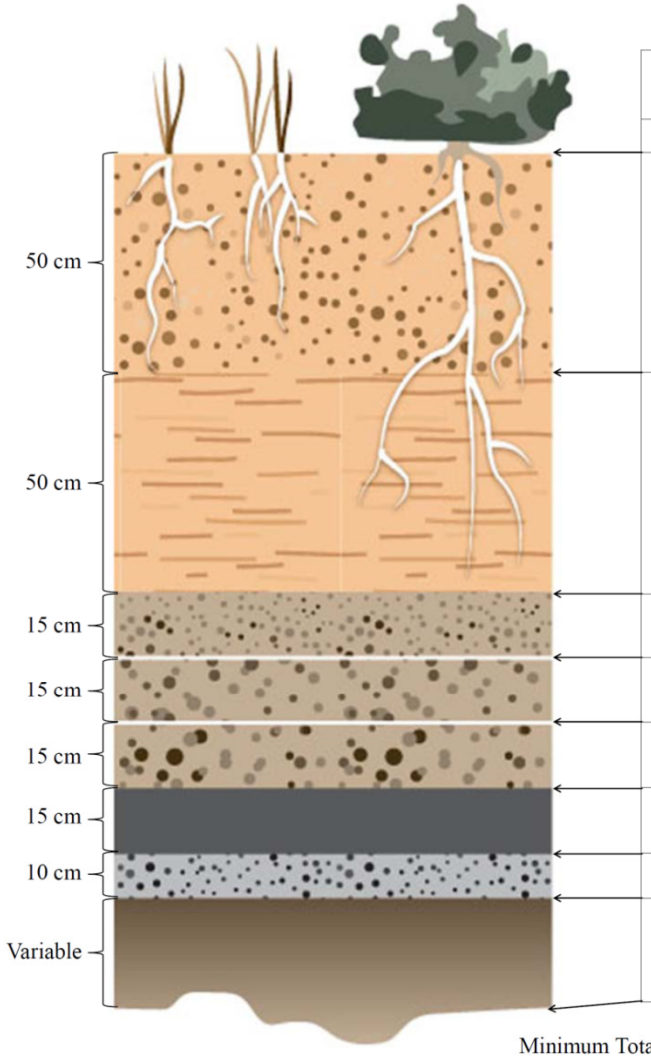

Layer Number	Thickness cm (in)	Layer Description	Function
0	N/A	Cover Vegetation	Mixed perennial grasses to enhance transpiration
1	50 (20)	Silt loam with pea gravel admix	The topsoil material was identified for optimal water retention properties and should provide a good rooting medium for cover vegetation. The pea gravel is designed to minimize wind erosion of the silt loam without significantly affecting its moisture retention capabilities. (thickness may be increased to provided for protection against inadvertent intruder [DOE/RL-93-93 *Focused Feasibility Study of Engineered Barriers for Waste Management Units in the 200 Area*])
2	50 (20)	Compacted topsoil	Same as Layer 1. Layer 2 provides a supplemental soil moisture storage capacity. Compaction of this layer is intended to retard the rate of infiltration of soil moisture. The extended residence time of moisture in Layer 2 will increase the amount of moisture removed by evapotranspiration. (thickness may be increased to provided for protection against inadvertent intruder [DOE/RL-93-93])
3	15 (6)	Sand Filter	This layer is part of a two-layer graded filter designed to prevent the migration of topsoil particles into Layer 5.
4	15 (6)	Gravel Filter	Same as Layer 3.
5	15 (6)	Lateral drainage aggregate	The lateral drainage layer will intercept and divert moisture along a 2% slope to the margin of the cover for collection and/or discharge.
6	15 (6)	Asphaltic concrete with spray applied asphalt coating	This layer will function as a hydrologic barrier and as a biointrusion barrier.
7	10 (4)	Asphalt base course	The function of the material in this layer is to provide a stable base for placing and supporting the asphalt layer.
8	Variable	Grading Fill	This layer will provide a smooth, level subgrade for construction of the overlying layers. (thickness may be increased to provided for protection against inadvertent intruder [DOE/RL-93-93])

Minimum Total Thickness = 1.7 m

Reference: DOE/RL-93-33, Focused Feasibility Study of Engineered Barriers for Waste Management Units in the 200 Areas.

RCRA = Resource Conservation and Recovery Act of 1976, 42 USC 6901, et seq.

Table 3-6. Summary of Design Criteria for the Modified RCRA C Barrier*.

1	Minimize moisture infiltration through the cover.
2	Design a multilayer cover of materials that are resistant to natural degradation processes.
3	Design a durable cover that needs minimal maintenance during its design life.
4	Design a cover with a functional life of 500 years.
5	Prevent plants from accessing and mobilizing contamination (i.e., prevent root penetration into the waste zone).
6	Prevent burrowing animals from accessing and mobilizing contamination.
7	Ensure that the top of the waste is at least 5 m (16 ft) below final grade or include appropriate design provisions to limit inadvertent human intrusion.
8	Facilitate drainage and minimize surface erosion by wind and water.
9	Design the low-permeability layer of the cover to have a permeability less than or equal to any natural subsoil present.
10	Design the cover to prevent the migration and accumulation of topsoil material within the lateral drainage layer (i.e., clogging of the lateral drainage layer).
11	For frost protection, the lateral drainage layer and the low-permeability asphalt layer must be located at least 0.76 m (2.5 ft) below final grade.

RCRA = Resource Conservation and Recovery Act of 1976, 42 USC 6901, et seq.

* Reference: Table 2-5 DOE/RL-93-33, Focused Feasibility Study of Engineered Barriers for Waste Management Units in the 200 Areas.

Erosion Protection. Water and wind erosion surface cover material can impact the integrity of a surface cover. The low precipitation, the low intensity of precipitation events, the absence of surface run-on features at the Hanford Site, and stability monitoring (PNNL-18845) all support the assumption that water erosion will not be a significant factor at WMA C barrier. Wind erosion, however, has been observed at the Hanford Site, primarily in exposed sandy areas and in the sand dunes to the southeast of WMA C.

DOE/RL-99-11, 200-BP-1 Prototype Barrier Treatability Test Report evaluated the potential for wind erosion for surface barriers. DOE/RL-99-11 calculated that the worst-case potential erosion rate would be to lose 15 cm (6 in.) of silt loam in 500 years. The analysis method was derived for agricultural soils and did not consider the benefits of the pea gravel admix. Extensive wind tunnel studies performed at the Hanford Site show that a mixture of fine-grained soil and pea gravel significantly reduced erosion due to wind forces. Soil/pea gravel armoring can reduce erosion rates from 96.5% to more than 99% at wind speeds of 72, 90 and 108 km/hr (45, 56, and 67 mi/hr) (PNL-8478, “Soil Erosion Rates Caused by Wind and Saltating Sand Stresses in Wind Tunnel”; WHC-EP-0673, “Permanent Isolation Surface Barrier Development Plan”). With the lower reduction value (96%), the wind erosion potential would be 15 cm (6 in.) in 12,500 years. The experience at the Prototype Hanford Barrier (“Quest for the Perfect Cap” [Wing and Gee 1994]) suggests that wind erosion will be negligible within months after the barrier surface is vegetated. Therefore, for all intents and purposes, wind erosion of the silt loam should be minor and is assumed to be so for the WMA C vegetated, closure surface barrier.

The engineered cover system surface will be seeded and fertilized to promote plant growth. Vegetation will minimize erosion and accelerate removal of water from the water storage layer through transpiration. Long-term considerations include periods of drought or fire so erosion and hydrologic modeling studies have assumed a poor stand of vegetation. The vegetation will consist of local plant species based on vegetation studies performed for Hanford disturbed areas.

Post-Closure Inadvertent Intrusion Protection. DOE/RL-93-33 included design criteria 4 and 7 listed in Table 3-6 as part of the design of the Modified RCRA Subtitle C Barrier to meet the requirements of 10 CFR 61.42 and 10 CFR 61.52 for the protection of the inadvertent intruder. Additionally, to further deter the inadvertent intrusion of humans into the waste, a marker system will be used to warn future generations of the dangers of the buried waste. Permanent markers that identify the potential exposure hazards will be installed at all corner boundaries of the closed facility. The DOE is expected to maintain active control of the Hanford Site (using fences, patrols, alarms, and monitoring instruments). Site information will be provided on an Internet website, U.S. Geological Survey maps, libraries, and other information repositories that would be readily available to the public. Land-use restrictions and institutional controls will be placed on the closed WMA C facility and its adjacent buffer zone to permanently preclude development until unacceptable risk no longer remains at the site.

The closed WMA C facility will clearly delineate the boundaries of the surface barrier by providing a distinct contrast with the surrounding terrain. The side slopes are engineered structures that will point to an obvious anthropogenic origin. These distinct side slopes in combination with warning signs are intended to minimize the risk of human intrusion.

As discussed above, the WMA C engineered surface cover system also contains a bio-intrusion layer consisting of gravel. The function of this layer is to prevent small burrowing animals and rodents from penetrating the underlying cover components and the waste material. Barrier studies at Hanford have shown that a thin layer of gravel is effective in preventing animals and rodents from penetrating underlying waste materials (WHC-EP-0673). The bio-intrusion material will consist of gravel screened from the local available alluvium at the Hanford Site. The alluvium gravels at the Hanford Site are composed of granite, quartz, and other durable minerals that make it ideally suited for long-term applications.

3.2.2 Tank Residual Waste Inventory

This section summarizes residual waste inventory information and describes the methods and assumptions used to estimate the inventories and concentrations of radionuclides and chemicals in residual waste in the WMA C SSTs and ancillary equipment at closure. The ancillary equipment includes the C-301 catch tank, the 244-CR vault, diversion boxes and pits, and waste transfer pipelines associated with WMA C.

The following topics are discussed in this section:

- Major waste types

- Updated waste inventory estimates for tanks and ancillary equipment
    - Retrieved tanks with post-retrieval sampling
    - Retrieved tanks without post-retrieval sampling
    - Tanks undergoing retrieval
    - Ancillary Equipment including C-301 catch tank, the 244-CR vault, waste transfer pipelines, pits and diversion boxes
- Inventory uncertainties.

Tank waste inventories for the 25 chemicals and 46 radionuclides are tracked using a Best-Basis Inventory (BBI) process. A listing of these constituents is provided in Table 3-7. Available analytical data are evaluated to identify which data best represent the waste concentrations in a tank. When analytical data are not available for a chemical or radionuclide, waste concentrations are estimated based on waste process information. Waste volume estimates in the BBI are based on waste-level measurements and/or waste transfer information. In addition to standard chemical and radionuclide BBI inventory estimates, after sampling tank residuals, inventories were developed for primary and secondary constituents in RPP-23403, "Single-Shell Tank Component Closure Data Quality Objectives."

As of September, 2014, waste was retrieved from 13 of 16 SSTs in C Farm (C-101, C-103, C-104, C-106, C-107, C-108, C-109, C-110, C-112, C-201, C-202, C-203, and C-204) and was in progress for the remaining 3 tanks (C-102, C-105 and C-111). Only BBI inventory estimates based on pre-retrieval samples and model estimates are currently available for the three unretrieved tanks (i.e., C-102, C-105, and C-111). After waste is retrieved, residual waste is sampled for constituents specified in RPP-23403. Tables 3-8 and 3-9 show primary chemical and radionuclide constituents in RPP-23403.

3.2.2.1 Waste Inventory Assumptions. Key enabling assumptions for current residual inventory estimates for C Farm SSTs and ancillary equipment include the following.

a. For tanks retrieved, the retrieval volumes and inventories documented in applicable retrieval data reports or residual inventory reports are the assumed inventories in WMA C SSTs at closure (see RPP-RPT-42323, "Hanford C-Farm Tank and Ancillary Equipment Residual Waste Inventory Estimates").

b. Radionuclides were decayed to January 1, 2020. Therefore, the radionuclide values presented differ from the 2014 BBI values, which are decayed to January 1, 2008 (see RPP-RPT-42323).

c. For tanks not yet retrieved (i.e., C-102, C-105, and C-111), it was assumed that, for a lower bound estimate, the minimum volume remaining would be 10 kL (360 ft^3). This is the threshold goal for 100-series SSTs specified in the HFFACO.

d. The Hanford Tank Waste Operations Simulator (HTWOS) model is assumed to provide a minimum estimate for threshold residual waste inventory estimates for tanks not yet retrieved (i.e., C-102, C-105, and C-111). This is because HTWOS assumes soluble constituents are mobilized during the retrieval process and largely removed when waste is retrieved to the threshold goal. The HTWOS assumptions are located in HNF-SD-WM-SP-012, "Tank Farm Contractor Operation and Utilization Plan."

e. The current BBI inventory is assumed to provide an upper bound estimate for tanks not yet retrieved (i.e., C-102, C-105, and C-111). These upper bound estimates presented for the tanks not yet retrieved reflect conditions in WMA C as of September 1, 2014.

f. Waste concentrations in ancillary equipment are assumed to be represented by the average concentration of waste in WMA C tanks that have been retrieved.

This simplifying assumption is made because:

- Little analytical data is available for waste in ancillary equipment,
- Ancillary equipment was flushed, mobilizing soluble constituents similar to retrieval,
- Ancillary equipment received waste to or from many of the tanks in a farm, and
- Process history of waste types and volumes received by different ancillary equipment has not been developed and estimates would be highly uncertain.

g. It is assumed that waste in the C-301 catch tank and 244-CR vault will be retrieved prior to closure (no specific goals or limits have been established for these facilities). Retrieval of 90% of the waste was assumed for these facilities. The average residual concentrations for WMA C tanks retrieved to date was assumed for these facilities.

h. It was assumed that the waste was or will be flushed from pits and diversion boxes and the primary residual waste remaining at closure will be limited to waste adsorbed to concrete surfaces with waste penetration to a depth of 0.04 cm (0.0157 in.) (RPP-15043, "Single-Shell Tank System Description").

i. It was assumed that the majority of waste transfer pipelines are 5% full of waste except for a plugged line and cascade lines which are assumed to be full. The technical basis for these assumptions and the associated pipeline lengths and estimated waste volumes are given in RPP-PLAN-47559.

Table 3-7. Standard Best-Basis Inventory Constituents.

Chemicals		Radionuclides		
Al	Na	^{3}H	^{134}Cs	^{234}U
Bi	Ni	^{14}C	^{137}Cs	^{235}U
Ca	NO_2	^{59}Ni	^{137m}Ba	^{236}U
Cl	NO_3	^{60}Co	^{151}Sm	^{237}Np
CO_3	Oxalate	^{63}Ni	^{152}Eu	^{238}Pu
Cr	Pb	^{79}Se	^{154}Eu	^{238}U
F	PO_4	^{90}Sr	^{155}Eu	^{239}Pu
Fe	Si	^{90}Y	^{226}Ra	^{240}Pu
Hg	SO_4	^{93}Zr	^{227}Ac	^{241}Am
K	Sr	^{93m}Nb	^{228}Ra	^{241}Pu
La	Total organic carbon	^{99}Tc	^{229}Th	^{242}Cm
Mn	U-TOTAL	^{106}Ru	^{231}Pa	^{242}Pu
	Zr	^{113m}Cd	^{232}Th	^{243}Am
		^{125}Sb	^{232}U	^{243}Cm
		^{126}Sn	^{233}U	^{244}Cm
		^{129}I		

3.2.2.2 Major Waste Types. The residual waste in WMA C at closure will be contained in tanks, vaults, pits/boxes, and waste transfer pipelines. The waste originally stored in these tanks and ancillary equipment consisted of supernate and sludge from the processing of irradiated uranium fuel. Supernate is free-standing liquid from the waste processing operations and sludge is precipitate from the supernate.

Tables 3-10 and 3-11 show waste types and processes that generated wastes transferred to C Farm. These processes and the waste types generated are discussed in HNF-SD-WM-TI-740, "Standard Inventories of Chemicals and Radionuclides in Hanford Tank Wastes." Table 3-12 shows the principal types of sludge remaining in the C Farm tanks and ancillary equipment. The waste consists of a large array of chemicals and radionuclides. Process knowledge-based waste type composition estimates based on reactor fuel irradiation records and process plant records are provided in RPP-19822, "Hanford Defined Waste Model – Revision 5.0."

3.2.2.3 Residual Waste Inventory Estimates. Residual inventory estimates used in this PA were determined based on information and conditions as of September 2014. Inventory estimates were developed for 1) residuals in retrieved tanks with post-retrieval sampling, 2) residuals in retrieved tanks without post-retrieval sampling, 3) residuals in tanks undergoing retrieval and 4) post-retrieval residual inventory estimates for ancillary equipment, including:

C-301 catch tank, 244-CR vault tanks, and sumps, pits, diversion boxes, and waste transfer pipelines. These inventory estimates are reported in Tables 3-13, 3-14, 3-15, 3-16, and 3-17.

Table 3-8. Primary Chemical Constituents.

Inorganic Constituents			
Acetate – $C_2H_3O_2^-$	Chromium – Cr	Iron – Fe	pH
Aluminum – Al	Cobalt – Co	Lead – Pb	Selenium – Se
Ammonium – NH_4^+	Copper – Cu	Manganese – Mn	Silver – Ag
Antimony – Sb	Cyanide – CN^-	Mercury – Hg	Strontium – Sr
Arsenic – As	Ferrocyanide – $Fe(CN)_6^{4-}$	Nickel – Ni	Thallium – Tl
Barium – Ba	Fluoride – F^-	Nitrate – NO_3^-	Uranium – U
Beryllium – Be	Formate – CHO_2^-	Nitrite – NO_2^-	Vanadium – V
Cadmium – Cd	Glycolate – $C_2H_3O_3^-$	Oxalate – $C_2O_4^{2-}$	Zinc – Zn
Organic Constituents			
1,1,2-Trichloroethylene	4-Methyl-2-pentanone (MIBK)	m-Xylene	Polychlorinated biphenyls
2-Butanone (MEK)	Xylenes (Mixed isomers of o-, m-, and p-)	p-Xylene	
2-Propanone (Acetone)	o-Xylene	Tributyl phosphate	

Reference: RPP-23403, "Single-Shell Tank Component Closure Data Quality Objectives."

Table 3-9. Primary Radiological Constituents.

Cesium 137 – ^{137}Cs	Technetium 99 – ^{99}Tc	Plutonium 238 – ^{238}Pu
Cobalt 60 – ^{60}Co	Antimony 125 – ^{125}Sb	Plutonium 239/240 – $^{239/240}Pu$
Europium 152 – ^{152}Eu	Seleniium 79 – ^{79}Se	Plutonium 241 – ^{241}Pu
Europium 154 – ^{154}Eu	Tin 126 – ^{126}Sn	Americium241 – ^{241}Am
Europium 155 – ^{155}Eu	Uranium 233 – ^{233}U	Curium 242 – ^{242}Cm
Carbon 14 – ^{14}C	Uranium 234 – ^{234}U	Curium 243 – ^{243}Cm
Tritium – ^{3}H	Uranium 235 – ^{235}U	Curium 244 – ^{244}Cm
Iodine 129 – ^{129}I	Uranium 236 – ^{236}U	Thorium 228 – ^{228}Th
Nickel 63 – ^{63}Ni	Uranium 238 – ^{238}U	Thorium 230 – ^{230}Th
Strontium 90 – ^{90}Sr	Neptunium 237 – ^{237}Np	Thorium 232 – ^{232}Th

Reference: RPP-23403, "Single-Shell Tank Component Closure Data Quality Objectives," Rev. 5.

Table 3-10. Waste Types Received into 241-C 100-Series Tanks (1956 through 1978).

Year	C-101	C-102	C-103	C-104	C-105	C-106	C-107	C-108	C-109	C-110	C-111	C-112
1956	TFeCN			CW	CW					OWW	OWW	TFeCN
1957			PSN	CW	CW	PSN/ OWW		TFeCN	TFeCN		CW/ TFeCN	TFeCN
1958				CW	CW							
1959					CW				CW		CW	
1960	CW	CW	CW		CW			CW			CW	CW
1961		CW					CW	CW			CW	HS
1962		CW					CW		HS		HS	HS
1963	PSN	CW	PSN		PSN	PSN					HS	
1964	PSN	CW					HS		HS		HS	
1965		CW	PSN				HS	HS	HS			
1966		TH/CW	PSN				BNW/HS		HS			
1967		CW					HS					
1968		CW/OWW			PSN							
1969		OWW		OWW	PSN	PSS						
1970			IX	TH/OWW/PSN	PSN/RSN	PSS	IX	OWW/IX	IX	IX		IX
1971			IX	CW/OWW	PSS	PSS						
1972			CW/OWW	CW/OWW	PSS					IX		
1973			Misc	Misc	PSS		Misc	Misc				
1974			Misc	Misc	PSS	BL						
1975			Misc	Misc	PSS	BL						
1976			Misc	Misc	PSS	BL						
1977						BL						
1978						BL						

Definitions:

Colors in table are used to highlight each waste type

BL B Plant strontium processing wastes and miscellaneous wastes

CW Cladding (coating) waste from Plutonium Uranium Extraction (PUREX) or Reduction-Oxidation (REDOX) Plants

HS 201-C Hot Semiworks waste

IX Cesium denuded waste from ion exchange process in B Plant

Misc Sources may include research waste from Battelle Northwest (i.e., BNW) which is now Pacific Northwest National Laboratory, reactor decontamination waste, etc.

OWW Organic Wash Waste from PUREX Plant

PSN PUREX high-level waste (HLW) supernate

PSS PUREX Sludge Supernate derived from washing PUREX HLW sludges in 244-AR Vault or 241-A and 241-AX tanks

RSN REDOX HLW Supernate

TFeCN Ferrocyanide waste from 244-CR vault treatment of tributyl phosphate waste

TH Thorium process waste from PUREX Plant

Table 3-11. Waste Types in C-200 Series Tanks.

Waste Type	241-C-201	241-C-202	241-C-203	241-C-204
Metal Waste – Addition from B Plant	November 1947 – December 1948			
Metal Waste Supernate – Removal to 241-C-106	December 1953			
Metal Waste Supernate – Removal to 241-C-104	None	None	None	7,000 gallons 11/1954
Metal Waste Sluicing to 244-CR Process Tank Vault	2/15/1954 – 3/17/1954	1/9/1954 – 1/14/1954	1/15/1954 – 1/28/1954	1/1955 – 2/1955
Hot Semiworks – PUREX process waste (5/1955 – 3/1956) Process equipment and facility flushes for modifications	5/1955 – 11/1955	11/1955 – 5/1956	12/1955 – 11/1956 4/1956 – 11/1956	12/1955 – 11/1956 4/1956 – 11/1956
Supernate Removal			1/1970 – 3/1970	
Supernate Removal	4/1970 – 6/1970			
Supernate Removal				7/1977
Supernate Removal	10/1980			

Table 3-12. Current Waste Types in 241-C Farm Tanks.

Waste Type	Description	Tanks
AR	Water washed PUREX sludge (1967-1976)	C-103,1 06
BL	B Plant Low activity waste (1963-1972)	C-106
1C	First cycle $BiPO_4$ coating waste (1944-1956)	C-107, 109, 110, 111, 112
CWP1	PUREX aluminum cladding waste (1956-1960)	C-101, 102, 103, 104, 105, 106, 111, 112
CWP2	PUREX aluminum cladding waste (1961-1972)	C-102, 104, 107, 112
CWZr1	PUREX/REDOX zirconium cladding waste (1968-1972)	C-102, 104
HS	Hot Semiworks waste (1961-1968)	C-111, 112, 201, 202, 203, 204
MW1	$BiPO_4$ Metal Waste (1944-1949)	C-102
OWW3	PUREX organic wash waste (1968-1972)	C-104
SRR	Strontium recovery waste (1969-1985)	C-107
TBP (UR)	Tributyl phosphate /Uranium Recovery Waste (1952-1957)	C-101, 102, 105, 106
TFeCN	Ferrocyanide sludge (1955-1958)	C-111, 112
TH1	Thoria process waste (1966)	C-102
TH2	Thoria process waste (1970)	C-104

$BiPO_4$ = bismuth phosphate
PUREX = Plutonium-Uranium Extraction (facility)
REDOX = Reduction-Oxidation (S Plant)

Inventory estimates for other constituents for which analytical results are available are reported in Appendix D of RPP-RPT-42323. These include primary analytes in RPP-23403 shown in Tables 3-8 and 3-9 and secondary constituents in the data quality objectives (DQO) document (RPP-23403). Additional discussion and details for current residual inventory estimates are provided in RPP-RPT-42323.

Concentrations for BBI constituents for the SSTs were calculated by dividing the inventories by associated volumes shown in the respective residual inventory tables (Tables 3-13 and 3-14). This calculation provides average concentrations for sludge, interstitial liquids and supernate and for multiple waste types in a tank. Where available, concentrations are based on analytical results. As of September 2014, analytical results were obtained for 10 of the 13 SSTs retrieved for constituents shown in Tables 3-8 and 3-9.

3.2.2.3.1 Retrieved Tanks with Post-Retrieval Sampling. Inventory estimates for the 10 SSTs (C-103, C-104, C-106, C-108, C-109, C-110, C-201, C-202, C-203, and C-204) for which retrieval operations have been completed and post-retrieval samples have been obtained are based on the BBI. As of September 2014, waste volume estimates were completed using a camera/computer-aided design (CAD) modeling system (CCMS) and post-retrieval residual sampling and analysis was completed for these 10 SSTs. In addition to standard chemical and radionuclide BBI inventory estimates, inventories were developed for many other constituents after sampling tank residuals.

The base case inventory for these tanks is the average BBI estimate and the upper bound inventory is the upper 95% confidence interval for the mean inventory. These inventories are provided in Tables 3-13 and 3-16.

Average and upper limit concentrations for these tanks for constituents specified in RPP-23403 are shown in Appendix D of RPP-RPT-42323.

3.2.2.3.2 Retrieved Tanks without Post-Retrieval Sampling. Inventory estimates for the three SSTs (C-101, C-107 and C-112) for which retrieval operations have been completed, but post-retrieval samples have not been obtained, are also based on the BBI and CCMS estimates. However, the basis for waste composition estimates for these tanks varies. For tanks C-101 and C-107 the BBI inventory estimates are based on pre-retrieval sample results, sample-based templates and process knowledge. For tank C-112, the BBI inventory estimates are based on in-process transfer samples representative of the C1 waste type and sample and process knowledge templates. Statistical uncertainties were not estimated for inventories based on process knowledge.

The base case inventory for retrieved tanks without post-retrieval sampling is the average BBI estimate. Because many of the constituents are not sample based, an upper bound inventory could not be estimated for many constituents for these tanks. It is believed that the concentration and inventories of soluble constituents will be lower than those currently estimated by the BBI. Inventory estimates for these tanks will be adjusted as needed, after post-retrieval sampling and analyses are completed. The inventories for tanks in this category are provided in Table 3-13; average waste concentrations are shown in Appendix B of RPP-RPT-42323.

Table 3-13a. 241-C Tank Farm Residual Inventory Estimates for Retrieved Tanks with Post-Retrieval Sampling. (sheet 1 of 2)

Tanks Retrieved (BBI average)[a]	241-C-101[b]	241-C-103	241-C-104	241-C-106	241-C-107[b]	241-C-108	241-C-109	241-C-110	241-C-112[b]	241-C-201	241-C-202	241-C-203	241-C-204
Residual Volume (kL [kgal])	18.9(4.99)	9.57(2.53)	7.2(1.9)	10.49(2.77)	53(14)	12.9(3.4)	7.6(2.0)	8(2.1)	48(12.7)	0.6(0.16)	0.6(0.16)	0.5(0.13)	0.5(0.13)
Total Radionuclides (Ci)[c]	7.30E+03	1.47E+04	1.43E+04	1.00E+05	6.37E+04	2.67E+03	4.75E+03	5.28E+03	1.92E+03	4.10E+02	7.25E+02	3.50E+02	2.33E+02
^{106}Ru	9.11E-20	1.72E-16	2.14E-10	8.59E-10	8.85E-17	7.01E-17	4.86E-17	1.38E-17	6.52E-17	2.82E-11	2.87E-11	2.35E-11	2.20E-11
^{113m}Cd	1.47E-03	1.49E-02	5.11E-02	2.13E+00	2.50E-03	1.97E-03	1.37E-03	3.89E-04	1.84E-03	5.77E-04	5.88E-04	4.80E-04	4.50E-04
^{125}Sb	9.36E-07	6.96E-07	9.60E-01	3.62E-03	1.31E-06	1.04E-06	7.20E-07	2.04E-07	9.70E-07	5.39E-05	5.49E-05	4.50E-05	4.21E-05
^{126}Sn	5.13E-04	5.27E-05	8.81E-03	1.76E+00	4.94E-04	3.91E-04	2.71E-04	2.38E-02	3.65E-04	1.10E-04	1.13E-04	9.21E-05	8.61E-05
^{129}I	5.55E-05	3.00E-03	4.84E-04	6.31E-04	4.07E-02	3.81E-05	2.65E-05	2.65E-04	3.57E-05	4.57E-07	7.35E-06	1.47E-05	3.57E-07
^{134}Cs	2.01E-09	3.78E-09	7.18E-06	1.54E-05	2.59E-10	2.05E-10	1.42E-10	4.04E-11	1.92E-10	4.13E-08	4.22E-08	3.46E-08	3.22E-08
^{137}Cs	3.61E+02	6.07E+02	6.22E+02	1.00E+03	2.32E+03	8.57E+01	4.31E+01	2.02E+01	7.66E+02	7.01E+00	6.18E+00	9.10E+00	4.13E+00
^{137m}Ba	3.22E+02	5.41E+02	5.54E+02	8.95E+02	2.06E+03	7.59E+01	3.84E+01	1.80E+01	6.80E+02	6.25E+00	5.51E+00	8.09E+00	3.67E+00
^{14}C	2.76E-03	6.99E-03	3.08E-03	8.21E-03	2.16E-02	8.18E-03	7.65E-04	1.51E-03	1.60E-02	7.64E-04	2.03E-04	1.66E-04	1.88E-04
^{151}Sm	4.00E+00	4.30E-01	3.17E+03	7.82E+03	1.04E+04	6.66E+00	4.65E+00	1.32E+00	6.25E+00	2.39E+01	2.43E+01	1.99E+01	1.86E+01
^{152}Eu	6.38E-05	2.58E-05	3.54E-02	2.02E+00	1.35E-04	1.07E-04	7.41E-05	2.11E-05	1.00E-04	2.10E-03	2.14E-03	1.75E-03	1.64E-03
^{154}Eu	2.77E-03	1.41E+00	1.57E+00	2.25E+01	5.70E-03	4.52E-03	3.13E-03	8.89E-04	4.22E-03	9.42E-02	9.61E-02	1.50E-02	5.62E-02
^{155}Eu	4.69E-04	4.37E-01	2.29E-01	7.65E+00	8.66E-04	6.84E-04	4.74E-04	1.35E-04	6.39E-04	1.45E-02	1.48E-02	1.81E-02	1.13E-02
^{226}Ra	5.90E-07	1.54E-08	3.24E-07	5.13E-04	5.95E-07	4.73E-07	3.26E-07	9.27E-08	4.40E-07	1.00E-09	1.02E-09	8.40E-10	7.86E-10
^{227}Ac	1.58E-06	6.39E-08	1.11E-05	1.74E-03	6.20E-06	7.78E-07	3.40E-06	9.62E-07	4.57E-06	3.45E-09	3.51E-09	2.87E-09	2.69E-09
^{228}Ra	2.64E-13	4.70E-05	8.73E-04	1.32E-04	9.70E-04	3.70E-06	2.06E-12	5.85E-13	2.78E-12	9.51E-07	9.70E-07	4.48E-07	3.35E-06
^{229}Th	1.33E-10	2.60E-11	8.56E-08	1.91E-05	1.89E-09	1.50E-09	1.04E-09	2.95E-10	1.40E-09	1.18E-11	1.20E-11	9.81E-12	9.17E-12
^{230}Th[d]	—	—	—	9.38E-04	—	—	—	—	—	—	—	—	—
^{231}Pa	2.48E-08	1.66E-07	7.47E-05	2.53E-03	3.83E-05	3.02E-05	2.10E-05	5.96E-06	2.82E-05	6.79E-09	6.93E-09	5.67E-09	5.30E-09
^{232}Th	1.12E-12	1.99E-04	3.70E-03	5.60E-04	4.11E-03	1.57E-05	8.72E-12	2.48E-12	1.18E-11	4.03E-06	4.11E-06	1.90E-06	1.42E-05
^{232}U	1.75E-06	4.29E-06	3.53E-02	4.87E-04	2.20E-06	4.50E-07	9.94E-08	1.91E-08	4.50E-07	2.25E-06	2.00E-06	6.60E-06	4.93E-06
^{233}U	1.71E-07	5.85E-03	2.18E+00	1.82E-03	2.15E-07	4.10E-08	9.69E-09	1.86E-09	4.39E-08	1.14E-05	1.02E-05	3.37E-05	2.51E-05
^{234}U	1.69E-01	1.36E-02	4.17E-01	9.40E-04	2.07E-01	3.25E-02	9.35E-03	2.64E-03	4.23E-02	3.65E-02	3.52E-02	1.13E-01	8.27E-02
^{235}U	7.54E-03	7.10E-04	1.98E-02	3.86E-05	9.24E-03	1.82E-03	4.01E-04	1.14E-04	1.89E-03	1.48E-03	1.42E-03	4.79E-03	3.42E-03
^{236}U	1.93E-03	3.74E-04	4.85E-03	1.73E-05	2.31E-03	2.85E-04	9.61E-05	2.93E-05	4.73E-04	5.23E-04	3.52E-04	8.33E-04	5.13E-04
^{237}Np	3.45E-04	1.35E-02	7.97E-02	5.41E-02	2.08E-04	2.17E-05	6.46E-04	1.09E-03	1.54E-04	3.42E-03	2.90E-03	2.70E-05	2.16E-02
^{238}Pu	1.13E-01	1.30E+00	5.89E-01	2.38E+00	8.05E-01	4.37E-03	1.56E-02	1.56E-02	3.59E-02	4.42E-01	3.99E-01	1.36E-02	2.76E-04

Table 3-13a. 241-C Tank Farm Residual Inventory Estimates for Retrieved Tanks with Post-Retrieval Sampling. (sheet 2 of 2)

Tanks Retrieved (BBI average)[a]	241-C-101	241-C-103	241-C-104	241-C-106	241-C-107	241-C-108	241-C-109	241-C-110	241-C-112	241-C-201	241-C-202	241-C-203	241-C-204
^{238}U	1.72E-01	1.64E-02	4.39E-01	9.02E-04	2.11E-01	4.03E-02	9.53E-03	2.59E-03	4.32E-02	3.69E-02	3.28E-02	1.09E-01	8.13E-02
^{239}Pu	1.83E+01	4.99E+00	5.15E+00	1.67E+01	1.30E+02	6.68E-01	4.01E-01	1.17E+00	5.79E+00	1.58E+01	1.43E+01	4.86E-01	9.84E-03
^{240}Pu	1.96E+00	1.04E+00	1.55E+00	3.57E+00	1.42E+01	7.27E-02	4.36E-02	1.27E-01	6.29E-01	3.40E+00	3.08E+00	1.05E-01	2.12E-03
^{241}Am	9.91E+00	4.83E+00	8.46E+00	6.38E+01	3.70E+02	9.46E-01	3.71E-01	4.94E-02	9.42E-01	2.46E+00	1.21E+00	3.16E-02	3.16E-03
^{241}Pu	1.54E+00	1.80E+00	1.14E+01	1.84E+01	1.10E+01	7.91E-02	5.09E-01	3.58E-01	4.91E-01	8.36E+00	7.52E+00	2.58E-01	5.21E-03
^{242}Cm	2.23E-03	5.73E-05	3.13E-02	1.45E-01	6.09E-02	1.59E-04	6.17E-05	8.75E-06	1.54E-04	8.30E-02	4.01E-02	1.04E-03	1.04E-04
^{242}Pu	2.70E-05	3.24E-05	1.97E-02	4.16E-04	1.97E-04	1.01E-06	6.07E-07	1.77E-06	8.76E-06	1.60E-04	1.45E-04	4.94E-06	9.98E-08
^{243}Am	1.43E-03	3.70E-05	5.25E-03	3.05E-03	3.86E-02	9.78E-05	3.91E-05	5.54E-06	9.72E-05	9.76E-04	4.71E-04	1.22E-05	1.22E-06
^{243}Cm	1.86E-05	7.66E-07	3.64E-03	5.55E-02	5.02E-04	1.50E-06	5.09E-07	7.22E-08	1.26E-06	3.10E-03	1.50E-03	3.88E-05	3.87E-06
^{244}Cm	3.32E-04	1.52E-05	6.69E-02	7.39E-01	8.95E-03	2.96E-05	9.09E-06	1.29E-06	2.25E-05	5.55E-02	2.68E-02	6.95E-04	6.95E-05
^{3}H	2.45E-02	3.98E-03	9.32E-03	4.17E-03	1.44E-02	1.94E-02	3.51E-03	1.80E-03	1.06E-02	1.57E-04	1.60E-04	1.31E-04	1.13E-04
^{59}Ni	7.23E-04	1.12E-01	8.64E-02	1.05E+01	1.18E-03	9.30E-04	6.46E-04	1.83E-04	8.69E-04	4.07E-03	4.16E-03	3.40E-03	3.18E-03
^{60}Co	1.76E-04	1.83E-02	4.66E-01	2.23E+00	9.14E-04	7.22E-04	5.02E-04	1.42E-04	6.75E-04	2.37E-03	2.44E-03	2.15E-03	1.86E-03
^{63}Ni	5.53E-02	1.86E+01	9.95E+01	6.53E+01	1.46E-01	2.80E+00	8.78E-01	4.08E-01	1.08E-01	8.33E-01	2.00E-01	5.54E-02	1.46E-02
^{79}Se	2.80E-04	2.64E-05	8.56E-03	9.57E-03	2.70E-04	1.62E-03	1.48E-04	4.21E-05	1.99E-04	5.49E-05	5.61E-05	4.58E-05	4.29E-05
^{90}Sr	3.29E+03	6.78E+03	4.89E+03	4.50E+04	2.42E+04	1.25E+03	2.33E+03	2.62E+03	2.28E+02	1.71E+02	3.31E+02	1.56E+02	1.03E+02
^{90}Y	3.29E+03	6.78E+03	4.89E+03	4.50E+04	2.42E+04	1.25E+03	2.33E+03	2.62E+03	2.28E+02	1.71E+02	3.31E+02	1.56E+02	1.03E+02
^{93m}Nb	1.83E-05	3.69E-04	3.16E-02	5.92E+00	8.45E-02	4.80E-02	4.64E-02	1.32E-02	6.26E-02	7.46E-04	7.64E-04	6.26E-04	5.84E-04
^{93}Zr	3.35E-05	7.03E-04	6.24E-02	1.04E+01	1.55E-01	1.22E-01	8.45E-02	2.41E-02	1.14E-01	1.46E-03	1.49E-03	1.22E-03	1.14E-03
^{99}Tc	4.34E-02	4.48E-02	3.04E-01	1.64E-01	2.14E+00	4.87E-02	8.77E-03	4.46E-02	1.69E+00	2.63E-03	2.50E-03	2.32E-03	3.18E-03

Source: RPP-RPT-42323, "Hanford C-Farm Tank and Ancillary Equipment Residual Waste Inventory Estimates."

[a] September 1, 2014 Best-Basis Inventory (BBI), includes tank 241-C-106 for which retrieval completion is under review. Note: for less than detect values; BBI mean uses less than detect values or process knowledge estimate, whichever is lower.

[b] Inventories estimated without post-retrieval sampling.

[c] Radionuclides are decayed to January 1, 2020 for 241-C Tank Farm closure assessments.

[d] Thorium-230 is not a standard BBI constituent but is included for Performance Assessment modeling estimates. Only the tank 241-C-106 nominal inventory based on analytical results is presented. Concentrations for other tanks sampled were below detection limits.

Table 3-13b. 241-C Tank Farm Residual Inventory Estimates for Retrieved Tanks with Post-Retrieval Sampling.

Tanks Retrieved (BBI average)[a]	241-C-101[b]	241-C-103	241-C-104	241-C-106	241-C-107[b]	241-C-108	241-C-109	241-C-110	241-C-112[b]	241-C-201	241-C-202	241-C-203	241-C-204
Residual Volume (kL [kgal])	18.9 [4.99]	9.57 [2.53]	7.2 [1.9]	10.49 [2.77]	53 [14]	12.9 [3.4]	7.6 [2.0]	8 [2.1]	48 [12.7]	0.6 [0.16]	0.6 [0.16]	0.5 [0.13]	0.5 [0.13]
Total Chemicals (kg)	2.00E+04	4.15E+03	4.79E+03	1.90E+03	2.74E+04	9.05E+03	4.97E+03	4.87E+03	2.64E+04	4.55E+02	3.96E+02	5.08E+02	4.57E+02
Al	7.93E+01	3.63E+03	1.14E+03	3.82E+02	1.98E+03	3.47E+03	2.15E+03	1.29E+03	3.32E+02	4.11E+00	8.48E+00	0.00E+00	5.88E+00
Bi	2.23E+01	9.49E-05	2.91E+00	2.94E+00	1.02E+03	7.56E+01	1.98E+00	3.63E+01	1.32E+03	6.10E-01	6.34E-01	1.29E+00	0.00E+00
Ca	1.15E+02	2.17E+01	1.35E+01	1.18E+02	5.04E+01	2.40E+01	1.56E+01	5.84E+00	6.44E+01	6.76E+00	7.12E+00	2.02E+00	5.90E-01
Cl	6.17E+01	1.94E-01	5.95E-01	6.14E+00	5.99E+01	9.01E-02	6.46E-02	6.26E-01	7.86E+01	2.93E-01	2.87E-01	5.86E-02	5.58E-03
Cr	7.23E+00	2.38E+00	3.06E+00	3.78E+00	5.54E+01	6.31E-01	1.76E-01	1.12E+00	5.78E+01	1.22E+01	9.09E+00	2.60E+00	1.36E+00
F	3.46E+01	1.62E-01	1.54E+01	5.43E-01	6.05E+02	1.21E+02	9.68E+01	1.38E+02	7.09E+02	2.69E+00	2.26E+00	1.64E+00	8.05E-03
Fe	8.77E+02	1.19E+02	3.24E+02	2.07E+02	4.37E+03	2.82E+02	9.28E+01	1.90E+02	7.02E+02	1.10E+02	8.70E+01	1.28E+01	3.21E+01
Hg	2.98E+00	1.06E+00	1.35E+00	1.93E+00	3.78E+00	2.03E-02	1.84E-02	1.07E-01	2.63E-02	1.07E-01	2.87E-01	2.23E-03	1.47E-01
K	8.68E+00	3.60E+00	1.31E+00	1.77E+01	2.58E+01	2.74E+00	2.61E-01	4.46E-01	2.21E+01	8.91E-01	9.09E-01	1.83E+00	2.02E+00
La	1.56E+00	1.82E-01	2.34E-02	2.44E+00	1.03E+01	1.32E-02	1.20E-01	9.98E-03	1.18E-01	0.00E+00	0.00E+00	0.00E+00	0.00E+00
Mn	7.14E+00	4.42E+00	4.29E+01	5.49E+02	1.93E+02	4.08E+00	5.63E-01	7.61E-01	6.52E+00	1.90E+01	1.69E+01	5.13E-01	2.39E-01
Na	4.80E+03	9.60E+01	1.15E+03	1.88E+02	6.13E+03	3.27E+03	1.30E+03	1.20E+03	6.90E+03	4.91E+01	4.58E+01	5.59E+01	3.33E+01
Ni	3.27E+00	4.58E+00	6.00E+00	3.02E+01	9.86E+01	7.45E+01	1.33E+01	4.13E-01	1.46E+00	6.15E+00	7.28E+00	2.04E-01	8.01E-01
NO_2	5.64E+02	4.82E-01	5.06E+00	4.14E+01	2.15E+03	5.78E+00	3.83E+00	2.74E+00	6.75E+02	5.27E-01	4.52E-01	9.94E-01	3.13E-02
NO_3	8.20E+03	8.71E-01	9.38E+00	3.48E+01	3.59E+03	9.16E+00	4.52E+00	6.73E+00	8.76E+03	1.35E+00	1.25E+00	3.76E+00	2.22E-02
Pb	2.07E+01	8.50E+00	6.48E+00	2.56E+01	3.62E+02	1.71E+01	5.39E+00	5.62E+00	1.36E+01	6.25E+00	5.84E+00	3.07E+00	1.02E+00
PO_4	3.79E+03	2.99E+01	4.28E+01	9.00E+01	4.74E+03	1.18E+03	9.82E+02	1.40E+03	4.83E+03	5.46E+01	3.46E+01	7.24E+01	7.96E+01
Si	2.40E+01	1.27E+02	1.31E+02	1.60E+01	1.02E+02	8.78E+01	2.79E+01	2.05E+01	4.28E+02	6.99E+00	8.60E+00	2.01E+00	7.33E+00
SO_4	7.71E+02	2.16E+00	1.15E+00	3.90E+00	5.17E+02	2.93E+00	2.86E+00	7.46E+00	9.32E+02	3.66E+00	4.01E-01	6.58E-01	1.28E-02
Sr	2.34E+01	2.41E+00	9.35E-01	1.83E+00	1.71E+01	1.97E+01	4.91E-01	5.63E+01	1.00E+01	9.09E-01	1.22E+00	2.30E-01	3.67E-01
Total Inorganic Carbon as CO_3	6.57E+01	1.68E+01	4.77E+02	7.58E+01	6.45E+02	2.77E+02	2.03E+02	4.89E+02	4.12E+02	3.36E+01	3.43E+01	1.50E+01	1.41E+01
Total Organic Carbon	3.00E+01	1.25E+01	6.53E+01	9.07E+01	4.16E+01	3.96E+00	3.38E+01	1.20E+01	3.66E+01	2.43E+01	2.48E+01	4.47E+00	3.54E+01
UTOTAL	5.16E+02	4.91E+01	1.32E+03	2.70E+00	6.32E+02	1.21E+02	2.86E+01	5.49E+00	1.29E+02	1.11E+02	9.88E+01	3.26E+02	2.43E+02
Zr	3.79E-01	1.33E+01	2.49E+01	2.79E+00	2.80E+00	5.98E-01	7.05E+00	3.62E-01	9.53E+00	1.02E-02	9.45E-02	1.05E-01	0.00E+00

Source: RPP-RPT-42323, "Hanford C-Farm Tank and Ancillary Equipment Residual Waste Inventory Estimates."

[a] September 1, 2014 Best-Basis Inventory (BBI), includes tank 241-C-106 for which retrieval completion is under review. 95% Confidence Interval = Mean + 2 × Standard Deviation (Closure mean for tanks with closure reports, BBI mean for tanks 241-C-101, 241-C-107 and 241-C-112: no closure report). Difference between closure mean and BBI mean: Closure mean uses less than detect values in inventory estimates; BBI mean uses less than detect values or process knowledge estimate, whichever is lower. As a result, closure means may be higher than BBI means for some constituents.

[b] Inventories estimated without post-retrieval sampling.

Table 3-14a. 241-C Tank Farm Residual Inventory Estimates for Tanks Undergoing Retrieval. (2 sheets)

Base Case for Tanks not Retrieved [a]	**241-C-102**	**241-C-105**	**241-C-111**
Residual Volume (kL [kgal])	10.2 [2.69]	48.0 [12.7]	132 [34.9]
Total Radionuclides (Ci) [b]	9.19E+02	6.74E+04	6.24E+05
^{106}Ru	1.71E-13	6.76E-16	7.13E-10
^{113m}Cd	1.78E-02	5.85E-02	5.99E-02
^{125}Sb	1.27E-05	2.89E-06	1.37E-03
^{126}Sn	1.83E-04	2.93E-04	6.72E-03
^{129}I	2.56E-03	8.93E-03	1.41E-02
^{134}Cs	1.54E-07	1.52E-08	1.42E-06
^{137}Cs	8.07E+01	5.07E+03	7.14E+03
^{137m}Ba	8.07E+01	4.52E+03	6.36E+03
^{14}C	9.88E-04	4.85E-02	1.04E-01
^{151}Sm	9.72E-01	2.36E+00	6.39E+02
^{152}Eu	1.26E-04	1.12E-04	5.38E-02
^{154}Eu	1.36E-01	4.67E-03	2.41E+00
^{155}Eu	2.62E-02	6.07E-04	3.70E-01
^{226}Ra	2.88E-07	1.59E-07	4.51E-06
^{227}Ac	1.93E-02	5.16E-07	1.82E-05
^{228}Ra	3.64E-01	2.36E-13	6.54E-12
^{229}Th	1.06E-02	1.25E-10	3.56E-09
^{231}Pa	2.12E-03	6.56E-07	4.99E-05
^{232}Th	2.29E-02	9.98E-13	2.77E-11
^{232}U	2.83E-02	8.61E-06	2.22E-05
^{233}U	2.17E+00	5.01E-07	4.80E-05
^{234}U	1.13E-01	2.38E-01	7.74E-01
^{235}U	4.27E-03	1.02E-02	3.37E-02
^{236}U	1.43E-03	5.16E-03	1.32E-02
^{237}Np	5.16E-05	1.93E-04	3.32E-03
^{238}Pu	1.48E+00	7.48E-01	1.70E+00
^{238}U	9.78E-02	2.44E-01	7.88E-01
^{239}Pu	6.49E+01	5.27E+01	9.45E+01

Table 3-14a. 241-C Tank Farm Residual Inventory Estimates for Tanks Undergoing Retrieval. (2 sheets)

Base Case for Tanks not Retrieved [a]	241-C-102	241-C-105	241-C-111
^{240}Pu	1.55E+01	1.04E+01	1.85E+01
^{241}Am	2.12E+01	2.83E+01	8.32E+01
^{241}Pu	4.87E+01	1.75E+01	3.54E+01
^{242}Cm	1.15E-03	1.01E-03	6.21E-02
^{242}Pu	9.00E-04	3.13E-04	6.54E-04
^{243}Am	7.93E-04	6.71E-04	1.15E-02
^{243}Cm	6.22E-05	9.09E-06	1.82E-03
^{244}Cm	1.28E-03	1.56E-04	3.26E-02
^{3}H	2.15E-05	4.08E+00	2.58E+00
^{59}Ni	1.62E-01	4.40E-01	1.40E+00
^{60}Co	2.14E-01	6.82E-01	1.03E-01
^{63}Ni	1.36E+01	3.61E+01	1.13E+02
^{79}Se	1.60E-06	1.51E-04	3.53E-03
^{90}Sr	2.94E+02	2.88E+04	3.05E+05
^{90}Y	2.94E+02	2.88E+04	3.05E+05
^{93m}Nb	1.10E-02	1.45E-03	9.78E-02
^{93}Zr	4.22E-03	2.76E-03	1.81E-01
^{99}Tc	3.56E-03	7.81E+00	2.19E+00

Source: RPP-RPT-42323, "Hanford C-Farm Tank and Ancillary Equipment Residual Waste Inventory Estimates."

[a] Includes tanks 241-C-102, 241-C-105 and 241-C-111 for which retrieval is in progress as of September 1, 2014. Note: Based on retrieval results for other tanks and in-process results for these tanks, it appears that the retrieval goal of 360 ft^3 or less will not be met for these tanks. The base case reflects the assumed retrieval end state based on retrieval performance to date.

[b] Radionuclides are decayed to January 1, 2020 for 241-C Tank Farm closure assessments.

3.2.2.3.3 Tanks Undergoing Retrieval. Future residual waste volumes are unknown for the three SSTs for which retrieval is in progress (C-102, C-105 and C-111); therefore, lower and upper bound residual inventories were estimated for these tanks (C-102, C-105, and C-111). These inventories are provided in Table 3-17.

The lower bound residual waste volume was assumed to be 10.2 m^3 (360 ft^3) (the retrieval threshold goal) because it appears likely that more than 10.2 m^3 (360 ft^3) of residual waste will be left in these tanks after retrieval.

Table 3-14b. 241-C Tank Farm Residual Inventory Estimates for Tanks Undergoing Retrieval.

Base Case for Tanks not Retrieved*	241-C-102	241-C-105	241-C-111
Residual Volume (kL [kgal])	10.2 [2.69]	48.0 [12.7]	132 [34.9]
Total Chemicals (kg)	7.51E+03	2.76E+04	8.34E+04
Al	5.29E+03	1.49E+04	1.60E+04
Bi	4.53E+01	3.57E+01	1.55E+03
Ca	1.22E+02	1.90E+02	2.20E+03
Cl	2.62E-03	2.98E+01	2.21E+02
Cr	1.13E+01	3.70E+01	7.33E+01
F	6.06E-03	7.90E+01	8.07E+02
Fe	3.37E+02	3.92E+02	7.53E+03
Hg	7.55E-02	5.02E-01	4.69E+01
K	7.85E+00	8.26E+01	1.87E+02
La	2.26E+00	2.62E-01	5.68E+01
Mn	2.86E+01	1.82E+02	4.68E+01
Na	4.30E+02	3.66E+03	1.03E+04
Ni	1.20E+02	1.59E+02	2.65E+03
NO_2	2.78E-02	6.46E+02	5.50E+03
NO_3	9.54E-02	7.81E+02	1.47E+04
Pb	2.84E+01	3.45E+01	7.65E+02
PO_4	6.12E+01	5.77E+02	1.20E+04
Si	5.49E+02	2.97E+03	1.42E+03
SO_4	7.21E+00	2.80E+02	1.26E+03
Sr	2.38E+00	1.37E+01	3.58E+01
Total Inorganic Carbon as CO_3	5.80E+01	1.26E+03	3.47E+03
Total Organic Carbon	2.18E+01	4.14E+02	1.46E+02
UTOTAL	2.93E+02	7.32E+02	2.36E+03
Zr	9.46E+01	1.56E+01	3.02E+01

Source: RPP-RPT-42323, "Hanford C-Farm Tank and Ancillary Equipment Residual Waste Inventory Estimates."

* Includes tanks 241-C-102, 241-C-105 and 241-C-111 for which retrieval is in progress as of September 1, 2014. Note: Based on retrieval results for other tanks and in-process results for these tanks, it appears that the retrieval goal of 360 ft^3 or less will not be met for these tanks. The base case reflects the assumed retrieval end state based on retrieval performance to date.

Table 3-15a. 241-C Tank Farm Residual Inventory Estimates for Ancillary Equipment. (2 sheets)

Ancillary Equipment	Catch Tank 241-C-301 [a]	244-CR Process Tank Vault [a]	Pits [b]	Diversion Boxes [b]	Pipelines [b]
Residual Volume (kL [kgal])	4.0 [1.06]	4.1 [1.08]	0.1 [0.03]	0.2 [0.06]	6.1 [1.6]
Total Radionuclides (Ci) [b]	7.04E+03	7.22E+03	2.13E+02	4.13E+02	1.07E+04
^{106}Ru	1.19E-10	1.22E-10	3.60E-12	6.98E-12	1.80E-10
^{113m}Cd	8.63E-02	8.85E-02	2.61E-03	5.06E-03	1.31E-01
^{125}Sb	5.36E-02	5.50E-02	1.62E-03	3.15E-03	8.12E-02
^{126}Sn	6.91E-02	7.08E-02	2.09E-03	4.05E-03	1.05E-01
^{129}I	2.09E-04	2.15E-04	6.34E-06	1.23E-05	3.17E-04
^{134}Cs	1.10E-06	1.12E-06	3.32E-08	6.43E-08	1.66E-06
^{137}Cs	1.23E+02	1.26E+02	3.74E+00	7.24E+00	1.87E+02
^{137m}Ba	1.10E+02	1.13E+02	3.33E+00	6.46E+00	1.67E+02
^{14}C	2.07E-03	2.12E-03	6.28E-05	1.22E-04	3.14E-03
^{151}Sm	5.38E+02	5.51E+02	1.63E+01	3.16E+01	8.15E+02
^{152}Eu	8.45E-02	8.66E-02	2.56E-03	4.96E-03	1.28E-01
^{154}Eu	1.19E+00	1.22E+00	3.60E-02	6.98E-02	1.80E+00
^{155}Eu	3.66E-01	3.75E-01	1.11E-02	2.15E-02	5.54E-01
^{226}Ra	1.96E-05	2.01E-05	5.94E-07	1.15E-06	2.97E-05
^{227}Ac	6.72E-05	6.89E-05	2.04E-06	3.94E-06	1.02E-04
^{228}Ra	5.99E-05	6.14E-05	1.82E-06	3.52E-06	9.08E-05
^{229}Th	7.32E-07	7.51E-07	2.22E-08	4.30E-08	1.11E-06
^{231}Pa	1.03E-04	1.06E-04	3.12E-06	6.04E-06	1.56E-04
^{232}Th	2.54E-04	2.60E-04	7.69E-06	1.49E-05	3.85E-04
^{232}U	1.99E-03	2.04E-03	6.04E-05	1.17E-04	3.02E-03
^{233}U	1.21E-01	1.25E-01	3.68E-03	7.13E-03	1.84E-01
^{234}U	2.30E-01	2.35E-01	6.96E-03	1.35E-02	3.48E-01
^{235}U	9.72E-03	9.96E-03	2.94E-04	5.70E-04	1.47E-02
^{236}U	1.96E-03	2.01E-03	5.94E-05	1.15E-04	2.97E-03
^{237}Np	2.87E-02	2.94E-02	8.68E-04	1.68E-03	4.34E-02
^{238}Pu	7.52E-01	7.71E-01	2.28E-02	4.41E-02	1.14E+00
^{238}U	2.26E-01	2.31E-01	6.83E-03	1.32E-02	3.42E-01

Table 3-15a. 241-C Tank Farm Residual Inventory Estimates for Ancillary Equipment. (2 sheets)

Ancillary Equipment	Catch Tank 241-C-301 [a]	244-CR Process Tank Vault [a]	Pits [b]	Diversion Boxes [b]	Pipelines [b]
^{239}Pu	2.17E+01	2.22E+01	6.57E-01	1.27E+00	3.28E+01
^{240}Pu	4.68E+00	4.79E+00	1.42E-01	2.74E-01	7.08E+00
^{241}Am	5.63E+00	5.77E+00	1.70E-01	3.30E-01	8.52E+00
^{241}Pu	1.23E+01	1.26E+01	3.71E-01	7.19E-01	1.86E+01
^{242}Cm	9.02E-02	9.25E-02	2.73E-03	5.29E-03	1.37E-01
^{242}Pu	1.32E-03	1.35E-03	3.99E-05	7.74E-05	2.00E-03
^{243}Am	1.39E-03	1.43E-03	4.21E-05	8.16E-05	2.11E-03
^{243}Cm	5.41E-03	5.55E-03	1.64E-04	3.17E-04	8.19E-03
^{244}Cm	8.74E-02	8.96E-02	2.65E-03	5.13E-03	1.32E-01
^{3}H	2.13E-03	2.18E-03	6.44E-05	1.25E-04	3.22E-03
^{59}Ni	4.21E-01	4.31E-01	1.27E-02	2.47E-02	6.37E-01
^{60}Co	1.18E-01	1.21E-01	3.58E-03	6.93E-03	1.79E-01
^{63}Ni	9.69E+00	9.93E+00	2.93E-01	5.69E-01	1.47E+01
^{79}Se	1.05E-03	1.07E-03	3.17E-05	6.14E-05	1.58E-03
^{90}Sr	3.11E+03	3.18E+03	9.40E+01	1.82E+02	4.70E+03
^{90}Y	3.11E+03	3.18E+03	9.40E+01	1.82E+02	4.70E+03
^{93m}Nb	2.34E-01	2.40E-01	7.08E-03	1.37E-02	3.54E-01
^{93}Zr	4.13E-01	4.24E-01	1.25E-02	2.43E-02	6.26E-01
^{99}Tc	3.70E-02	3.80E-02	1.12E-03	2.17E-03	5.61E-02

Source: RPP-RPT-42323, "Hanford C-Farm Tank and Ancillary Equipment Residual Waste Inventory Estimates."

[a] Assumes 90% retrieval for C-301 catch tank and 244-CR vault. Note: Current volumes and inventories for these tanks are 10 times the values shown in this table.

[b] Estimated waste volumes and inventories at closure for pits, diversion boxes and waste transfer pipelines.

Note: Radionuclides are decayed to January 1, 2020 for 241-C Tank Farm closure assessments.

The HTWOS model was used to estimate residual inventories for the lower bound if tanks are retrieved to the threshold goal of 10.2 m^3 (360 ft^3). The HTWOS model simulates retrieval operations considering the mobility and composition of waste and retrieval fluids to estimate the waste residual inventories after retrieval. As such, it provides a more rigorous approach to estimate residual inventories compared to estimates based on simple percentage of waste currently in the tanks and differentiates between soluble and insoluble constituents. However, if only a portion of the waste is retrieved and if soluble constituents are not washed from the waste,

the inventories of soluble and insoluble constituents may be much different than that predicted by the HTWOS model.

Table 3-15b. 241-C Tank Farm Residual Inventory Estimates for Ancillary Equipment.

Ancillary Equipment	Catch Tank 241-C-301 [a]	244-CR Process Tank Vault [a]	Pits [b]	Diversion Boxes [b]	Pipelines [b]
Residual Volume (kL [kgal])	4.0 [1.06]	4.1 [1.08]	0.1 [0.03]	0.2 [0.06]	6.1 [1.6]
Total Chemicals (kg)	2.64E+03	2.70E+03	7.98E+01	1.55E+02	3.99E+03
Al	5.28E+02	5.41E+02	1.60E+01	3.10E+01	7.99E+02
Bi	6.40E+00	6.56E+00	1.94E-01	3.75E-01	9.69E+00
Ca	1.94E+01	1.98E+01	5.86E-01	1.14E+00	2.93E+01
Cl	7.51E-01	7.70E-01	2.27E-02	4.40E-02	1.14E+00
Cr	1.79E+01	1.83E+01	5.41E-01	1.05E+00	2.70E+01
F	2.12E+01	2.18E+01	6.43E-01	1.25E+00	3.22E+01
Fe	2.21E+02	2.27E+02	6.70E+00	1.30E+01	3.35E+02
Hg	5.82E-01	5.96E-01	1.76E-02	3.41E-02	8.81E-01
K	5.30E+00	5.43E+00	1.60E-01	3.11E-01	8.02E+00
La	1.09E-01	1.12E-01	3.31E-03	6.40E-03	1.65E-01
Mn	4.82E+01	4.94E+01	1.46E+00	2.83E+00	7.30E+01
Na	4.40E+02	4.51E+02	1.33E+01	2.58E+01	6.65E+02
Ni	1.45E+01	1.48E+01	4.38E-01	8.49E-01	2.19E+01
NO_2	3.87E+00	3.97E+00	1.17E-01	2.27E-01	5.86E+00
NO_3	7.50E+00	7.69E+00	2.27E-01	4.40E-01	1.14E+01
Pb	1.41E+01	1.45E+01	4.28E-01	8.28E-01	2.14E+01
PO_4	3.46E+02	3.55E+02	1.05E+01	2.03E+01	5.24E+02
Si	3.63E+01	3.72E+01	1.10E+00	2.13E+00	5.49E+01
SO_4	4.16E+00	4.27E+00	1.26E-01	2.44E-01	6.30E+00
Sr	5.57E+00	5.71E+00	1.69E-01	3.27E-01	8.43E+00
Total Inorganic Carbon as CO_3	1.42E+02	1.46E+02	4.31E+00	8.35E+00	2.16E+02
Total Organic Carbon	7.47E+01	7.66E+01	2.26E+00	4.38E+00	1.13E+02
UTOTAL	6.76E+02	6.93E+02	2.05E+01	3.97E+01	1.02E+03
Zr	2.61E+00	2.67E+00	7.89E-02	1.53E-01	3.95E+00

Source: RPP-RPT-42323, "Hanford C-Farm Tank and Ancillary Equipment Residual Waste Inventory Estimates."

[a] Assumes 90% retrieval for C-301 catch tank and 244-CR vault. Note: Current volumes and inventories for these tanks are 10 times the values shown in this table.

[b] Estimated waste volumes and inventories at closure for pits, diversion boxes and waste transfer pipelines.

Table 3-16a. 241-C Tank Farm Residual Inventory 95% Confidence Interval Estimates for Retrieved Tanks with Post-Retrieval Sampling. (3 sheets)

Tanks Retrieved (95% Confidence Interval with post-retrieval residual data)[a]										
	241-C-103	**241-C-104**	**241-C-106**	**241-C-108**	**241-C-109**	**241-C-110**	**241-C-201**	**241-C-202**	**241-C-203**	**241-C-204**
^{106}Ru	—[b]	—[b]	—[b]	—[b]	—[b]	—[b]	—[b]	—[b]	—[b]	—[b]
^{113m}Cd	—	—	—	—	—	—	—	—	—	—
^{125}Sb	—[b]	—[b]	—[b]	—[b]	—[b]	—[b]	—[b]	—[b]	—[b]	—[b]
^{126}Sn	—	1.68E-02	—	—[b]	—[b]	3.53E-02	—	—	—	—
^{129}I	3.81E-03	—[b]	—[b]	—[b]	—[b]	—[b]	—[b]	9.64E-06	3.84E-05	—[b]
^{134}Cs	2.08E-06	—	—[b]	—	—	—	—	—	—	—
^{137}Cs	7.40E+02	1.14E+03	1.35E+03	1.07E+02	5.55E+01	3.18E+01	9.13E+00	7.18E+00	1.09E+01	5.16E+00
^{137m}Ba	6.60E+02	9.99E+02	1.20E+03	9.52E+01	4.91E+01	2.83E+01	8.14E+00	6.40E+00	9.70E+00	4.60E+00
^{14}C	—[b]	4.64E-03	—[b]	—[b]	—[b]	—[b]	1.38E-03	—[b]	—[b]	—[b]
^{151}Sm	—	—	—	—	—	—	—	—	—	—
^{152}Eu	—[b]	—[b]	—[b]	—[b]	—[b]	—[b]	—[b]	—[b]	—[b]	—[b]
^{154}Eu	1.89E+00	—[b]	—[b]	—[b]	—[b]	—[b]	—[b]	—[b]	—[b]	—[b]
^{155}Eu	—[b]	—[b]	—[b]	—[b]	—[b]	—[b]	—[b]	—[b]	—[b]	—[b]
^{226}Ra	—	—[b]	—	—	—	—	—	—	—	—
^{227}Ac	—	—	—	—	—	—	—	—	—	—
^{228}Ra	—	—	—	—	—	—	—	—	—	—
^{229}Th	—	—	—	—	—	—	—	—	—	—
^{231}Pa	—	—[b]	—[b]	—[b]	—[b]	—[b]	—	—	—	—

Table 3-16a. 241-C Tank Farm Residual Inventory 95% Confidence Interval Estimates for Retrieved Tanks with Post-Retrieval Sampling. (3 sheets)

	Tanks Retrieved (95% Confidence Interval with post-retrieval residual data)[a]									
	241-C-103	**241-C-104**	**241-C-106**	**241-C-108**	**241-C-109**	**241-C-110**	**241-C-201**	**241-C-202**	**241-C-203**	**241-C-204**
^{230}Th[c]	—[b]	—[b]	1.45E-03	—[b]	—[b]	—[b]	—[b]	—[b]	—[b]	—[b]
^{232}Th	2.36E-04	7.21E-03	7.68E-04	1.99E-05	1.32E-05	—	7.76E-06	7.75E-06	4.27E-06	2.52E-05
^{232}U	—	—	—	—	—	—	—	—	—	—
^{233}U	6.95E-03	—[b]	2.36E-03	—[b]	—[b]	—[b]	2.03E-07	—[b]	—[b]	—[b]
^{234}U	1.84E-02	6.08E-01	1.21E-03	4.72E-02	—[b]	3.80E-03	4.27E-04	4.44E-02	1.41E-01	1.07E-01
^{235}U	8.69E-04	2.99E-02	5.16E-05	2.20E-03	5.93E-04	1.53E-04	6.22E-09	1.75E-03	5.67E-03	4.26E-03
^{236}U	4.58E-04	7.30E-03	2.40E-05	5.12E-04	1.75E-04	3.72E-05	1.12E-07	4.90E-04	1.06E-03	6.57E-04
^{237}Np	2.52E+01	—[b]	1.03E-01	—[b]	—[b]	1.43E-03	7.33E+00	5.02E+00	—[b]	5.61E+01
^{238}Pu	2.19E+00	1.06E+00	—[b]	4.85E-03	2.12E-02	2.20E-02	—[b]	—[b]	—[b]	—[b]
^{238}U	2.01E-02	8.57E-01	1.30E-03	4.97E-02	1.41E-02	—	2.30E-08	4.00E-02	1.29E-01	1.01E-01
^{239}Pu	7.26E+00	9.01E+00	2.24E+01	7.83E-01	6.03E-01	1.69E+00	2.76E+01	1.63E+01	7.34E-01	1.23E-02
^{240}Pu	1.57E+00	2.71E+00	4.83E+00	8.52E-02	6.56E-02	1.85E-01	5.95E+00	3.52E+00	1.58E-01	2.64E-03
^{241}Am	6.90E+00	1.67E+01	8.13E+01	1.18E+00	4.41E-01	6.67E-02	4.06E+00	1.39E+00	4.16E-02	3.93E-03
^{241}Pu	3.08E+00	1.90E+01	2.04E+01	6.63E-02	6.05E-01	4.62E-01	1.10E+01	7.10E+00	3.71E-01	6.17E-03
^{242}Cm	—[b]	5.86E-02	—	—[b]	—[b]	—[b]	—	—[b]	—[b]	—[b]
^{242}Pu	—	3.54E-02	—	1.18E-06	—[b]	2.57E-06	—	—	—	—
^{243}Am	—	—	—	—	—	—	—	—	—	—
^{243}Cm	5.32E-02	8.10E-03	6.30E-01	—[b]	—[b]	—[b]	2.92E-02	—[b]	—[b]	2.41E-05
^{244}Cm	1.06E+00	1.48E-01	1.20E+01	—[b]	—[b]	—[b]	5.57E-01	—[b]	—[b]	4.78E-04

Table 3-16a. 241-C Tank Farm Residual Inventory 95% Confidence Interval Estimates for Retrieved Tanks with Post-Retrieval Sampling. (3 sheets)

Tanks Retrieved (95% Confidence Interval with post-retrieval residual data)[a]										
	241-C-103	**241-C-104**	**241-C-106**	**241-C-108**	**241-C-109**	**241-C-110**	**241-C-201**	**241-C-202**	**241-C-203**	**241-C-204**
^{3}H	—[b]	—[b]	—[b]	—[b]	—[b]	2.46E-03	—[b]	—[b]	—[b]	—[b]
^{59}Ni	—[b]	—[b]	—[b]	—[b]	—[b]	—[b]	—[b]	—[b]	—[b]	—[b]
^{60}Co	—[b]	—[b]	—[b]	—[b]	—[b]	—[b]	—[b]	—[b]	—[b]	—[b]
^{63}Ni	2.26E+01	2.60E+02	8.78E+01	3.69E+00	1.08E+00	5.38E-01	1.27E+00	2.40E-01	6.90E-02	1.86E-02
^{79}Se	—[b]	—[b]	—[b]	2.15E-03	—[b]	—[b]	—[b]	—[b]	—[b]	—[b]
^{90}Sr	9.73E+03	9.74E+03	5.75E+04	1.77E+03	2.99E+03	3.69E+03	2.30E+02	3.60E+02	2.11E+00	1.29E+02
^{90}Y	9.73E+03	9.74E+03	5.75E+04	1.77E+03	2.99E+03	3.69E+03	2.30E+02	3.60E+02	2.11E+00	1.29E+02
^{93m}Nb	—	—	—	—	—	—	—	—	—	—
^{93}Zr	—	—	—	—	—	—	—	—	—	—
^{99}Tc	5.37E-02	4.65E-01	2.22E-01	6.12E-02	1.10E-02	7.08E-02	4.78E-03	3.88E-03	3.97E-03	4.03E-03

Source: RPP-RPT-42323, "Hanford C-Farm Tank and Ancillary Equipment Residual Waste Inventory Estimates."

[a] Analytical data as of September 1, 2014, Best-Basis Inventory (BBI) constituents only, includes tank 241-C-106 for which retrieval completion is under review. 95% confidence interval = Mean + 2 × Standard Deviation (Closure mean for tanks with closure reports, BBI mean for C-101, C-107 and C-112: no closure report). 95% confidence intervals are not included for constituents with concentrations below analytical detection limits.

[b] Concentration less than analytical detection limit.

[c] Thorium-230 is not a standard BBI constituent, but is included for Performance Assessment model estimates. Radionuclides are decayed to January 1, 2020 for 241-C Tank Farm closure assessments.

Table 3-16b. 241-C Tank Farm Residual Inventory 95% Confidence Interval Estimates for Retrieved Tanks with Post-Retrieval Sampling. (2 sheets)

Tanks Retrieved (Best-Basis Inventory, 95% Confidence Intervals for Single-Shell Tanks with post-retrieval residual data)[a]										
	241-C-103	**241-C-104**	**241-C-106**	**241-C-108**	**241-C-109**	**241-C-110**	**241-C-201**	**241-C-202**	**241-C-203**	**241-C-204**
Al	4.34E+03	1.80E+03	4.89E+02	4.17E+03	2.94E+03	1.74E+03	5.50E+00	9.28E+00	—[b]	5.88E+00
Bi	—[b]	4.35E+00	—[b]	—[b]	2.49E+00	4.72E+01	1.08E+00	1.03E+00	1.52E+00	—[b]
Ca	2.65E+01	2.39E+01	1.53E+02	2.86E+01	2.26E+01	7.49E+00	1.02E+01	7.86E+00	2.45E+00	5.90E-01
Cl	4.97E-01	9.06E-01	—[b]	—[b]	—[b]	—[b]	6.15E-01	5.86E-01	7.36E-02	6.98E-03
Cr	3.02E+00	4.45E+00	4.85E+00	7.98E-01	2.45E-01	1.61E+00	2.52E+01	9.94E+00	3.70E+00	1.36E+00
F	2.02E-01	3.01E+01	—[b]	1.60E+02	1.20E+02	1.84E+02	4.97E+00	2.84E+00	2.20E+00	8.05E-03
Fe	1.62E+02	4.83E+02	2.65E+02	3.71E+02	1.41E+02	2.68E+02	2.01E+02	9.99E+01	1.90E+01	3.21E+01
Hg	1.71E+00	1.95E+00	2.86E+00	2.49E-02	3.03E-02	1.64E-01	1.53E-01	3.34E-01	2.98E-03	1.47E-01
K	4.46E+00	1.82E+00	—[b]	—	—[b]	6.73E-01	—[b]	—[b]	—[b]	—[b]
La	2.51E-01	—[b]	3.12E+00	—[b]	1.78E-01	—[b]	—[b]	—[b]	—[b]	—[b]
Mn	5.44E+00	8.90E+01	7.11E+02	6.73E+00	9.34E-01	1.04E+00	3.91E+01	1.86E+01	7.02E-01	2.39E-01
Na	1.14E+02	1.60E+03	2.43E+02	3.97E+03	1.91E+03	1.56E+03	7.03E+01	5.75E+01	6.64E+01	3.33E+01
Ni	5.60E+00	1.10E+01	3.99E+01	8.99E+01	1.97E+01	5.38E-01	1.28E+01	8.05E+00	3.01E-01	8.01E-01
NO_2	6.13E-01	7.81E+00	—[b]	6.85E+00	4.49E+00	—[b]	8.86E-01	6.63E-01	2.98E+00	3.12E-02
NO_3	1.10E+00	1.30E+01	—[b]	1.15E+01	5.79E+00	1.33E+01	2.11E+00	1.73E+00	—[b]	2.23E-02
Pb	1.08E+01	9.91E+00	3.31E+01	2.26E+01	6.39E+00	7.32E+00	8.93E+00	6.45E+00	4.00E+00	1.02E+00
PO_4	4.81E-01	7.52E+01	—[b]	1.68E+03	1.49E+03	1.82E+03	—	—	—	7.96E+01
Si	1.53E+02	1.82E+02	2.07E+01	1.49E+02	5.12E+01	2.76E+01	1.14E+01	1.00E+01	2.90E+00	7.33E+00

Table 3-16b. 241-C Tank Farm Residual Inventory 95% Confidence Interval Estimates for Retrieved Tanks with Post-Retrieval Sampling. (2 sheets)

Tanks Retrieved (Best-Basis Inventory, 95% Confidence Intervals for Single-Shell Tanks with post-retrieval residual data)[a]										
	241-C-103	**241-C-104**	**241-C-106**	**241-C-108**	**241-C-109**	**241-C-110**	**241-C-201**	**241-C-202**	**241-C-203**	**241-C-204**
SO_4	2.27E-01	1.60E+00	—[b]	3.54E+00	3.62E+00	9.33E+00	5.41E+00	4.41E-01	1.98E+00	1.28E-02
Sr	3.16E+00	1.46E+00	2.34E+00	2.61E+01	7.52E-01	8.94E+01	1.68E+00	1.33E+00	2.78E-01	3.67E-01
TIC as CO_3	—	—	—	—	—	—	—	—	—	—
TOC	—	—	—	—	—	—	—	—	—	—
UTOTAL	6.03E+01	1.99E+03	—[b]	1.48E+02	4.24E+01	7.51E+00	2.12E+02	1.54E+02	3.70E+02	3.04E+02
Zr	1.65E+01	5.55E+01	3.60E+00	7.57E-01	—	4.63E-01	2.19E-02	1.08E-01	1.25E-01	—[b]

Source: RPP-RPT-42323, "Hanford C-Farm Tank and Ancillary Equipment Residual Waste Inventory Estimates."

[a] September 1, 2014 Best-Basis Inventory (BBI), includes tank 241-C-106 for which retrieval completion is under review.
95% Confidence Interval = Mean + 2 × Standard Deviation (Closure mean for tanks with closure reports, BBI mean for C-101, C-107 and C-112: no closure report).
95% confidence intervals were not calculated for constituents with concentrations below analytical detection limits.

[b] Concentration less than analytical detection limit.

TIC = Total inorganic carbon TOC = Total organic carbon

Table 3-17a. 241-C Tank Farm Residual Inventory Lower Bound and Upper Bound Estimates for Tanks Undergoing Retrieval. (2 sheets)

	BBI – Upper Bound Estimate for Tanks not Retrieved as of September 1, 2014 [a]			HTWOS – Lower Bound Estimate for Tanks not Retrieved (assumes 360 ft^3 in tanks after retrieval) [a]		
	241-C-102	**241-C-105**	**241-C-111**	**241-C-102**	**241-C-105**	**241-C-111**
Residual Volume (kL [kgal])	405 [107]	500 [132]	132 [34.9]	10.2 [2.69]	10.2 [2.69]	10.2 [2.69]
Total Radionuclides (Ci)[b]	2.75E+04	7.02E+05	6.24E+05	9.19E+02	2.28E+04	1.39E+05
^{106}Ru	1.13E-12	7.04E-15	7.13E-10	1.71E-13	2.33E-16	1.63E-10
^{113m}Cd	3.24E-01	6.10E-01	5.99E-02	1.78E-02	1.30E-02	1.22E-02
^{125}Sb	2.27E-04	3.01E-05	1.37E-03	1.27E-05	8.84E-07	3.12E-04
^{126}Sn	3.54E-03	3.05E-03	6.72E-03	1.83E-04	7.72E-05	1.53E-03
^{129}I	7.89E-02	9.30E-02	1.41E-02	2.56E-03	2.72E-07	1.75E-08
^{134}Cs	1.09E-05	1.58E-07	1.42E-06	1.54E-07	4.81E-09	2.02E-12
^{137}Cs	6.08E+03	5.29E+04	7.14E+03	8.07E+01	1.52E+03	8.40E-03
^{137m}Ba	5.43E+03	4.71E+04	6.36E+03	8.07E+01	1.52E+03	8.40E-03
^{14}C	4.89E-01	5.05E-01	1.04E-01	9.88E-04	5.54E-04	1.31E-07
^{151}Sm	1.73E+01	2.46E+01	6.39E+02	9.72E-01	8.14E-01	1.46E+02
^{152}Eu	2.24E-03	1.16E-03	5.38E-02	1.26E-04	3.85E-05	1.23E-02
^{154}Eu	2.42E+00	4.86E-02	2.41E+00	1.36E-01	1.60E-03	5.50E-01
^{155}Eu	4.66E-01	6.32E-03	3.70E-01	2.62E-02	2.09E-04	8.45E-02
^{226}Ra	5.21E-06	1.66E-06	4.51E-06	2.88E-07	5.46E-08	1.03E-06
^{227}Ac	2.90E-01	5.38E-06	1.82E-05	1.93E-02	4.89E-07	1.91E-05
^{228}Ra	9.63E-02	2.45E-12	6.54E-12	3.64E-01	5.17E-12	1.14E-10
^{229}Th	1.90E-01	1.30E-09	3.56E-09	1.06E-02	4.06E-11	8.12E-10
^{231}Pa	3.77E-02	6.83E-06	4.99E-05	2.12E-03	2.23E-07	1.07E-05
^{232}Th	4.08E-01	1.04E-11	2.77E-11	2.29E-02	3.25E-13	7.14E-12
^{232}U	5.10E-01	8.97E-05	2.22E-05	2.83E-02	2.80E-06	5.06E-06
^{233}U	3.91E+01	5.22E-06	4.80E-05	2.17E+00	1.63E-07	1.10E-05
^{234}U	2.04E+00	2.48E+00	7.74E-01	1.13E-01	7.77E-02	1.77E-01
^{235}U	7.68E-02	1.06E-01	3.37E-02	4.27E-03	3.33E-03	7.70E-03
^{236}U	2.58E-02	5.37E-02	1.32E-02	1.43E-03	1.68E-03	3.02E-03
^{237}Np	9.45E-04	2.01E-03	3.32E-03	5.16E-05	6.30E-05	7.58E-04

Table 3-17a. 241-C Tank Farm Residual Inventory Lower Bound and Upper Bound Estimates for Tanks Undergoing Retrieval. (2 sheets)

	BBI – Upper Bound Estimate for Tanks not Retrieved as of September 1, 2014 [a]			HTWOS – Lower Bound Estimate for Tanks not Retrieved (assumes 360 ft^3 in tanks after retrieval) [a]		
	241-C-102	241-C-105	241-C-111	241-C-102	241-C-105	241-C-111
^{238}Pu	2.64E+01	7.79E+00	1.70E+00	1.48E+00	2.58E-01	3.89E-01
^{238}U	1.76E+00	2.54E+00	7.88E-01	9.78E-02	7.97E-02	1.80E-01
^{239}Pu	1.16E+03	5.49E+02	9.45E+01	6.49E+01	1.81E+01	2.16E+01
^{240}Pu	2.77E+02	1.08E+02	1.85E+01	1.55E+01	3.57E+00	4.21E+00
^{241}Am	3.50E+02	2.95E+02	8.32E+01	2.12E+01	1.00E+01	1.94E+01
^{241}Pu	8.68E+02	1.82E+02	3.54E+01	4.87E+01	6.01E+00	8.06E+00
^{242}Cm	2.09E-02	1.06E-02	6.21E-02	1.15E-03	3.50E-04	1.41E-02
^{242}Pu	1.60E-02	3.26E-03	6.54E-04	9.00E-04	1.08E-04	1.49E-04
^{243}Am	1.47E-02	6.99E-03	1.15E-02	7.93E-04	5.83E-05	2.62E-03
^{243}Cm	1.13E-03	9.47E-05	1.82E-03	6.22E-05	3.14E-06	4.13E-04
^{244}Cm	2.34E-02	1.62E-03	3.26E-02	1.28E-03	5.36E-05	7.39E-03
^{3}H	5.00E+00	4.25E+01	2.58E+00	2.15E-05	1.24E-04	3.22E-06
^{59}Ni	2.93E+00	4.58E+00	1.40E+00	1.62E-01	1.51E-01	3.20E-01
^{60}Co	3.90E+00	7.10E+00	1.03E-01	2.14E-01	2.27E-01	2.35E-02
^{63}Ni	2.46E+02	3.76E+02	1.13E+02	1.36E+01	1.24E+01	2.57E+01
^{79}Se	2.03E-03	1.57E-03	3.53E-03	1.60E-06	4.59E-09	4.80E-09
^{90}Sr	6.47E+03	3.00E+05	3.05E+05	2.94E+02	9.86E+03	6.95E+04
^{90}Y	6.47E+03	3.00E+05	3.05E+05	2.94E+02	9.86E+03	6.95E+04
^{93m}Nb	3.89E-02	1.51E-02	9.78E-02	1.10E-02	2.41E-03	1.04E-01
^{93}Zr	7.82E-02	2.88E-02	1.81E-01	4.22E-03	9.39E-04	3.90E-02
^{99}Tc	3.02E-01	8.14E+01	2.19E+00	3.56E-03	9.43E-01	5.49E-02

Source: RPP-RPT-42323, "Hanford C-Farm Tank and Ancillary Equipment Residual Waste Inventory Estimates."

[a] Inventory estimates based on retrievals through September 1, 2014 for tanks 241-C-102, 241-C-105, and 241-C-111. These would be the residual inventories if no additional waste was retrieved from these tanks after September 1, 2014. Note: Based on retrieval results for other tanks and in-process results for these tanks, it appears that the retrieval goal of 360 ft^3 or less will not be met for these tanks. The base case reflects the assumed retrieval end state based on retrieval performance to date.

[b] Radionuclides are decayed to January 1, 2020 for 241-C Tank Farm closure assessments.

BBI = Best-Basis Inventory HTWOS = Hanford Tank Waste Operations Simulator

Table 3-17b. 241-C Tank Farm Residual Inventory Lower Bound and Upper Bound Estimates for Tanks Undergoing Retrieval.

	BBI – Upper Bound Estimate for Tanks not Retrieved as of September 1, 2014 [a]			HTWOS – Lower Bound Estimate for Tanks not Retrieved (assumes 360 ft^3 in tanks after retrieval) [a]		
	241-C-102	**241-C-105**	**241-C-111**	**241-C-102**	**241-C-105**	**241-C-111**
Residual Volume (kL [kgal])	405 [107]	500 [132]	132 [34.9]	10.2 [2.69]	10.2 [2.69]	10.2 [2.69]
Total Chemicals (kg)	2.28E+05	2.86E+05	8.34E+04	7.51E+03	7.55E+03	1.017E+04
Al	9.45E+04	1.55E+05	1.60E+04	5.29E+03	5.14E+03	3.51E+03
Bi	8.23E+02	3.72E+02	1.55E+03	4.53E+01	1.09E+01	3.52E+02
Ca	2.25E+03	1.98E+03	2.20E+03	1.22E+02	6.49E+01	5.02E+02
Cl	6.09E+02	3.10E+02	2.21E+02	2.62E-03	9.07E-04	2.76E-04
Cr	2.19E+02	3.85E+02	7.33E+01	1.13E+01	2.42E+00	1.25E+01
F	1.41E+03	8.23E+02	8.07E+02	6.06E-03	2.41E-03	1.01E-03
Fe	5.98E+03	4.08E+03	7.53E+03	3.37E+02	1.35E+02	1.72E+03
Hg	2.06E+00	5.23E+00	4.69E+01	7.55E-02	1.53E-05	5.83E-05
K	4.08E+02	8.60E+02	1.87E+02	7.85E+00	1.86E+01	9.32E+00
La	4.01E+01	2.73E+00	5.68E+01	2.26E+00	9.05E-02	1.30E+01
Mn	5.10E+02	1.90E+03	4.68E+01	2.86E+01	6.22E+01	1.06E+01
Na	3.60E+04	3.81E+04	1.03E+04	4.30E+02	5.80E+02	2.42E+02
Ni	2.18E+03	1.66E+03	2.65E+03	1.20E+02	5.47E+01	6.05E+02
NO_2	6.46E+03	6.73E+03	5.50E+03	2.78E-02	1.97E-02	6.86E-03
NO_3	2.22E+04	8.14E+03	1.47E+04	9.54E-02	2.38E-02	1.83E-02
Pb	5.47E+02	3.59E+02	7.65E+02	2.84E+01	9.07E+00	1.75E+02
PO_4	5.58E+03	6.01E+03	1.20E+04	6.12E+01	1.76E-02	1.37E+03
Si	1.20E+04	3.09E+04	1.42E+03	5.49E+02	1.02E+03	1.83E+02
SO_4	2.45E+03	2.92E+03	1.26E+03	7.21E+00	8.55E-03	1.57E-03
Sr	5.24E+01	1.43E+02	3.58E+01	2.38E+00	4.59E+00	7.49E+00
TIC as CO_3	2.57E+04	1.31E+04	3.47E+03	5.80E+01	1.18E+02	7.91E+02
TOC	6.32E+02	4.31E+03	1.46E+02	2.18E+01	8.78E+01	2.05E+01
UTOTAL	5.27E+03	7.63E+03	2.36E+03	2.93E+02	2.39E+02	5.38E+02
Zr	1.75E+03	1.62E+02	3.02E+01	9.46E+01	5.29E+00	6.49E+00

Source: RPP-RPT-42323, "Hanford C-Farm Tank and Ancillary Equipment Residual Waste Inventory Estimates."

[a] Inventory estimates based on retrievals through September 1, 2014 for tanks 241-C-102, 241-C-105, and 241-C-111. These would be the residual inventories if no additional waste was retrieved from these tanks after September 1, 2014. Note: Based on retrieval results for other tanks and in-process results for these tanks, it appears that the retrieval goal of 360 ft^3 or less will not be met for these tanks. The base case reflects the assumed retrieval end state based on retrieval performance to date.

BBI = Best-Basis Inventory
HTWOS = Hanford Tank Waste Operations Simulator
TIC = Total inorganic carbon
TOC = Total organic carbon

The upper bound inventory was the BBI inventory on September 1, 2014 for each tank; this would be the residual inventory if no additional waste can be retrieved from these tanks. The BBI waste volumes and concentrations were used to calculate upper bound inventories for these tanks.

A base case estimate for the volume and concentration of residual waste that will remain after retrieval was also made based on characteristics of the waste and retrieval performance to date for these tanks. Base case estimates are presented in Table 3-14 and discussed in Section 3.2.2.4.3.

3.2.2.3.4 Residual Inventory Estimates for Ancillary Equipment. Because little information is available for waste in catch tanks and waste transfer pipelines, it was assumed that the composition of waste in pipelines and catch tanks is the same as the average composition of waste in the BBI for retrieved and sampled C Farm SSTs. Waste volumes for C-301 catch tank and the 244-CR vault were based on measurements. However, the amount of waste remaining in pits, diversion boxes and pipelines is unknown. Based on operations information, most of the waste has been flushed from the pits, diversion boxes, and pipelines. Hence, the residual waste volume is expected to be small compared to catch tank and SST post-retrieval residuals. A volume estimate for pits and diversion boxes was developed based on the surface area of pits and diversion boxes in C Farm. A volume estimate for pipelines was developed based on the length and size of pipelines in C Farm.

The inventory estimates for the ancillary equipment are provided in Table 3-15. RPP-RPT-42323 Appendix C-3 shows average waste concentrations for retrieved and sampled tanks.

3.2.2.4 Inventory Uncertainty. Table 3-18 shows different sources of uncertainties that must be considered for inventory estimates for retrieved and non-retrieved tanks and different types of ancillary equipment. The following sections address inventory uncertainties.

3.2.2.4.1 Inventory Estimates for Retrieved Tanks with Post-Retrieval Sample Analyses. The primary sources of uncertainty for retrieved tanks with post-retrieval samples and analysis are analytical uncertainty and residual waste volume uncertainty. Post-retrieval samples were collected in accordance with the SST Component Closure DQO (RPP-23403). Samples were collected at multiple locations in the residual waste in an attempt to provide a representative sample. Analytical uncertainty estimates are determined for each constituent and sample analyzed considering precision and accuracy of samples based on variability between primary and duplicate samples, and other quality controls specified in the DQO and sampling and analysis plan. Differences between sample results from two or more locations provide a measure of spatial variability and representativeness of the tank samples.

The median sample-based relative standard deviation (RSD) for the 10 tanks sampled was ~0.17. Radionuclides and chemical constituents with low concentrations tend to have higher RSDs than those with high concentrations. The RSDs by constituent for C Farm tanks are included in applicable Retrieval Data Reports and in Appendix D.1 and D.2 of RPP-RPT-42323. Based on tank sample data and sample analytical reports, mean concentrations, RSDs of the mean and

95% upper confidence limit (UCL) values were calculated for the constituents in each waste phase. As shown in Appendix D.1, for some constituents analytical results were below detection levels for the method used. Nominal concentration estimates for these constituents are based on the detection limit or other estimates, whichever is lower. Upper bound inventories (Table 3-16) were not calculated for constituents with concentrations lower than analytical detection limits.

Table 3-18. Inventory Uncertainties.

Facility	Uncertainties
Retrieved tanks with post-retrieval sample analyses	• Analytical uncertainties. • Waste volume measurement uncertainties.
Retrieved tanks without post-retrieval analyses	• Pre-retrieval analytical sample uncertainties. • Process knowledge uncertainty for constituents without sample analysis. • Uncertainty in waste composition changes after retrieval. • Waste volume measurement uncertainties.
Tanks undergoing retrieval	• Uncertainty in waste volume that will be retrieved. • Pre-retrieval analytical sample uncertainties. • Process knowledge uncertainty for constituents without sample analysis. • Uncertainty in waste composition changes after retrieval.
Catch Tank 241-C-301 and 244-CR Process Tank Vault	• Waste volume measurement uncertainties. • Uncertainty in waste volume that will be retrieved. • Limited sample data, inventories based on average composition of residual tank waste samples.
Pits, Diversion Boxes, and Waste Transfer Pipelines	• Uncertainty in waste volume remaining in waste transfer pipelines. • Uncertainty in the number and length of waste transfer pipelines. • No sample data and limited process knowledge data. Inventories based on the average composition of residual tank waste samples.

Waste volume measurements for retrieved tanks were performed using a CCMS. In-tank videos of SSTs were recorded following retrieval. The videos document the location of residual solids and liquid waste remaining in the tank. Using CAD 3-D software, a 3-D model of the SST was built, and video of the tank waste was reviewed. Knowledge of tank construction, plate lengths and heights, the size of debris in the tanks, and other measurable features were used as a guide to estimate the area and height of waste remaining in a tank. Based on CCMS estimates of sand piles with known volumes, a regression line was calculated to determine uncertainty for CCMS measurements. The regression equation was changed over time as additional data was obtained. Uncertainty equations and requirements for CCMS are specified in RPP-23403. Tables 3-19 and 3-20 and Appendix D of RPP-RPT-42323 show volume uncertainty estimates for tanks retrieved to date.

3.2.2.4.2 Inventory Estimates for Retrieved Tanks without Post-Retrieval Sample Analyses. For tanks without post-retrieval analysis or for which analysis is in progress (C-101, C-107), current inventory estimates are based on pre-retrieval sample results, sample-based templates, or process knowledge. Sample results after bulk retrieval are included in the BBI for tank C-112; however, the closure inventory report and retrieval data report with the complete set

of inventories and analytical results for constituents specified in the DQO was not available as of September 1, 2014.

Table 3-19. 241-C Tank Farm Post-Retrieval Waste Volume Estimates (cubic feet).

Component	241-C-103[a]	241-C-106[b]	241-C-201[c]	241-C-202[d]	241-C-203[e]	241-C-204[f]
In dish bottom	266	348	10.7	8.5	13.4	9.6
In tank equipment	3.6	4.8	3.4	6.1	0	3.4
On stiffener rings and walls	68.4	17	5.1	5.1	5.1	5.3
Total	338	370	19.2	19.7	18.5	18.3
95% upper confidence limit	351[g]	466[h]	20.5	20.9	19.9	19.6

[a] RPP-RPT-33060, "Retrieval Data Report for Single-Shell Tank 241-C-103."

[b] RPP-20577, "Stage II Retrieval Data Report for Single-Shell Tank 241-C-106," and RPP-19866, "Calculation for the Post-Retrieval Waste Volume Determination for Tank 241-C-106."

[c] RPP-RPT-30181, "Retrieval Data Report for Single-Shell Tank 241-C-201."

[d] RPP-RPT-29095, "Retrieval Data Report for Single-Shell Tank 241-C-202."

[e] RPP-RPT-26475, "Retrieval Data Report for Single-Shell Tank 241-C-203."

[f] RPP-RPT-34062, "Retrieval Data Report for Single-Shell Tank 241-C-204."

[g] In accordance with RPP-23403, "Single-Shell Tank Component Closure Data Quality Objectives," Rev. 3, 1.04 × dish bottom volume + 0.85 + Equip + Rings + Wall.

[h] In accordance with RPP-13889, "Tank 241-C-106 Component Closure Action Data Quality Objectives."

For tanks C-101 and C-107, current BBI concentration estimates take no credit for soluble analytes that may have been washed out of the waste during retrieval processes. However, because the volume of waste remaining in these tanks was well above the retrieval goal of 10.2 m^3 (360 ft^3), it is unknown what portion of the soluble analytes were removed. Pre-retrieval sample results were not available for many of the constituents specified in the BBI and sample-based templates or process knowledge estimates were developed to fill these gaps.

Sample-based template values were developed from a review of sample data for tanks with similar process histories and at least one waste layer from the same waste process (i.e., same waste type). Table 3-21 lists waste type groupings for waste transferred to C Farm tanks. The decision to include tank data in a template was based on tank transfer records indicating the expected waste type and depth in a tank and a comparison with expected analytical concentrations for a given waste type, and is documented in each update of the BBI for that tank. Although sample-based template RSDs fall between 0 and 1.0, template RSDs can be much larger (as large as 17.0 for uranium; most values are 5.0 or lower). These results have large uncertainties because some are based on tank averages which have large variability with few data points. Waste type templates and uncertainties are described in RPP-8847, "Best-Basis Inventory Template Compositions of Common Tank Waste Layers."

Table 3-20. 241-C Tank Farm Post-Retrieval Waste Volume Estimates (cubic feet).

Component	241-C-101[a]	241-C-104[b]	241-C-108[c]	241-C-109[d]	241-C-110[e]	241-C-112[f]
In dish bottom	511	190	305	192	224	1,657
In tank equipment	0	0	0	1.9	0	0
On stiffener rings and walls	156	26.6	91.9	35.7	13.4	42.9
Total	667	217	397	230	237	1,700
Total Residual Volume[g]	767	254	456	267	281	1,700

[a] RPP-CALC-56434, "Post-Retrieval Camera/CAD Modeling System Waste Volume Estimate for Tank 241-C-101."
[b] RPP-CALC-54284, "Post-Hard Heel Retrieval Camera/CAD Modeling System Waste Volume Estimate for Tank 241-C-104."
[c] RPP-CALC-54266, "Post-Hard Heel Retrieval Camera/CAD Modeling System Waste Volume Estimate for Tank 241-C-108."
[d] RPP-CALC-54759, "Post-Hard Heel Retrieval Camera/CAD Modeling System Waste Volume Estimate for Tank 241-C-109."
[e] RPP-CALC-56399, "Post-Hard Heel Retrieval Camera/CAD Modeling System Waste Volume Estimate for Tank 241-C-110."
[f] RPP-CALC-56856, "Estimated Waste Volume Remaining in Single Shell Tank 241-C-112 after Hard Heel Retrieval."
[g] In accordance with RPP-23403, "Single-Shell Tank Component Closure Data Quality Objectives," Rev. 5, 1.195 × dish bottom volume + 0.27 + Equip + Rings + Wall.

Due to the uncertainty associated with modeling, process knowledge model results are generally only used in the BBI in the absence of analytical data or waste sample-based templates for a given waste type. The process knowledge results are model results from the Hanford Defined Waste Model (HDW) Rev. 5. In the 1990s, Steve Agnew of the Los Alamos National Laboratory developed the HDW model (WHC-SD-WM-TI-632, "Hanford Defined Wastes: Chemical and Radionuclide Compositions"). The HDW Rev. 4 uses radionuclide fuel production output from the Oak Ridge Isotope Generation and Depletion Code 2 (ORIGEN2) model (RPP-13489, "Activity of Fuel Batches Processed Through Hanford Separations Plants, 1944 Through 1989"), then models fuel transfers through various processing steps to estimate waste types and composition for each Hanford tank through 1994. In 2004, the ORIGEN2 and HDW models were updated and with new data and methods (RPP-19822, Rev. 0-A). The scope of HDW Rev. 5 was limited to estimating waste type compositions, because sample data and volume measurements appeared to provide better estimates for distribution of the waste types between the tanks and the volume of waste in the tanks. The uncertainty in HDW waste type composition estimates has not been quantified. RPP-26744 shows the range of variability for different waste types and constituents based on reactor production variability as a function of time. Although this is only one of several potential sources of uncertainty, variability ranges by over an order of magnitude for some constituents.

3.2.2.4.3 Inventory Estimates for Tanks Undergoing Retrieval. The basis for a base case estimate for post-retrieval residual inventories varies for each of the three tanks remaining to be

retrieved (C-102, C-105 and C-111). The largest uncertainty is how much waste can be retrieved and the extent to which soluble analytes (such as ^{99}Tc) will be removed.

Table 3-21. Sample-Based Template Waste Type Groups for 241-C Tank Farm.

Waste Type Group	Common Factors to Group
1C, 2C, 1CFeCN	Bismuth phosphate-bearing waste generated by decontamination of the bismuth phosphate process plutonium product.
CWP1, CWP2, CWR1	Wastes generated by the decladding of aluminum clad reactor fuel.
TBP, PFeCN, **TFeCN**	Wastes resulting from the retrieval of metal waste for uranium recovery (typically high fission product waste).

Note: Bold text for waste types in 241-C Tank Farm.

1C = First cycle bismuth phosphate decontamination waste
1CFeCN = Ferrocyanide sludge from in-plant scavenging of T-Plant 1C waste (without coating waste)
2C = Second cycle bismuth phosphate decontamination waste
CWR1 = Reduction-Oxidation (S Plant) aluminum cladding waste
PFeCN = Ferrocyanide sludge from tributyl phosphate (TBP) in-plant scavenged supernate and co-disposed TBP sludge

Base Case Estimate of Inventory. For purposes of modeling, the following subjective base case estimates were made for each of the three tanks based on retrieval results to-date and based on remaining waste properties. Details for these estimates are provided in RPP-RPT-42323.

Tank C-102: The initial waste retrieval performance information shows that for tank C-102, through August 2014 waste removal has been tracking as for other similar waste type tanks for which retrievals were completed to below 10.2 m^3 (360 ft^3). Therefore, achieving a final waste volume of 10.2 m^3 (360 ft^3) and using HTWOS model estimates for the residual inventory seems to be a reasonable assumption for this tank.

Tank C-105: Initial waste retrieval performance information for tank C-105 indicates that equipment and waste characteristics limit the performance of the designated retrieval technology (Mobile Arm Retrieval System [MARS]-Vacuum [V]) and that other waste retrieval technologies (e.g., sluicing), or equipment modifications would be required to remove additional waste from the tank. Application of sluicing (particularly hot water sluicing) is expected to result in additional retrieval from tank C-105. The waste types and waste transfer history for tank C-105 are unique but there are some similarities to other C Farm tanks. In an effort to establish a residual waste volume that would be plausible, it is assumed that the quantity of waste remaining in tank C-105 will be similar to the quantity remaining in tank C-112, ~1,700 ft^3, 48 kL (~12,700 gal) (the maximum quantity remaining in any of the C Farm tanks retrieved as of September 2014).

Tank C-111: Waste retrieval performance data indicates that it will be difficult to remove any additional waste from tank C-111. The waste physical characteristics are such that negligible waste was removed during modified sluicing. Additional waste retrieval technologies, caustic and water dissolution, are planned. However, because of the hard, low-permeability waste layer

remaining in tank C-111, little or none of the remaining waste may be removed by waste retrieval operations. Therefore, the BBI provides a reasonable volume estimate for tank C-111.

Lower-bound Estimates of Inventory. As a lower bound, the HTWOS inventory estimates were used for tanks remaining to be retrieved. The HTWOS estimate assumes the retrieval goal of 10.2 m^3 (360 ft^3) will be met. It also factors in wash/leach processes to estimate the composition of residuals after retrieval.

A general idea of how well HTWOS predicts tank waste residual inventories can be shown by comparing the 2002 HTWOS residual concentration estimates for tank C-103 with post-retrieval measurements for the tank (Table 3-22). On average, the HTWOS overestimated the measured chemical values for concentrations greater than 10^{-3} g/L (1.34×10^{-4} oz/gal) by a factor of ~3 and underestimated measured radionuclide concentrations > 10^{-7} Ci/L by a factor of ~0.7. In general, the HTWOS estimates were closer to measured values for constituents with higher concentrations.

Table 3-22. Comparison of Hanford Tank Waste Operations Simulator Pre-Retrieval Concentration Estimates for Tank 241-C-103 Residuals with Post-Retrieval Sample Results. (2 sheets)

Constituent	Units	HTWOS 2002 Residual Waste Estimate	2014 Residual Data	Ratio of HTWOS 2002/ 2014 Residuals
Al	g/L	2.45E+01	3.79E+02	6.47E-02
Ca	g/L	4.68E-01	2.27E+00	2.06E-01
Cl	g/L	8.22E-02	2.03E-02	4.05E+00
Cr	g/L	1.23E-01	2.49E-01	4.93E-01
F	g/L	1.29E-01	1.69E-02	7.64E+00
Fe	g/L	2.00E+00	1.24E+01	1.61E-01
Hg	g/L	2.52E-02	1.11E-01	2.27E-01
K	g/L	8.22E-02	3.76E-01	2.19E-01
La	g/L	2.59E-02	1.90E-02	1.36E+00
Mn	g/L	5.98E-02	4.62E-01	1.30E-01
Na	g/L	3.26E+00	1.00E+01	3.25E-01
Ni	g/L	5.48E-01	4.79E-01	1.15E+00
NO_2	g/L	1.99E+00	5.04E-02	3.96E+01
NO_3	g/L	1.94E-01	9.10E-02	2.13E+00
Pb	g/L	8.01E-02	8.88E-01	9.02E-02
PO_4	g/L	3.95E-01	3.12E+00	1.27E-01
Si	g/L	4.46E+00	1.33E+01	3.36E-01

Table 3-22. Comparison of Hanford Tank Waste Operations Simulator Pre-Retrieval Concentration Estimates for Tank 241-C-103 Residuals with Post-Retrieval Sample Results. (2 sheets)

Constituent	Units	HTWOS 2002 Residual Waste Estimate	2014 Residual Data	Ratio of HTWOS 2002/ 2014 Residuals
SO_4	g/L	3.27E-01	2.26E-01	1.45E+00
Sr	g/L	3.99E-03	2.52E-01	1.58E-02
TIC as CO_3	g/L	3.27E+00	1.76E+00	1.86E+00
TOC	g/L	1.03E+00	1.31E+00	7.91E-01
Zr	g/L	1.45E+00	1.39E+00	1.04E+00
^{137}Cs	Ci/L	9.55E-03	6.35E-02	1.50E-01
^{14}C	Ci/L	5.94E-07	7.30E-07	8.14E-01
^{154}Eu	Ci/L	2.13E-04	1.47E-04	1.45E+00
^{155}Eu	Ci/L	3.69E-05	4.57E-05	8.07E-01
^{234}U	Ci/L	2.71E-07	1.42E-06	1.91E-01
^{238}Pu	Ci/L	1.02E-05	1.36E-04	7.50E-02
^{238}U	Ci/L	2.78E-07	1.71E-06	1.62E-01
^{241}Am	Ci/L	5.46E-04	5.04E-04	1.08E+00
^{241}Pu	Ci/L	2.60E-04	1.88E-04	1.38E+00
^{60}Co	Ci/L	1.06E-05	1.91E-06	5.56E+00
^{63}Ni	Ci/L	4.93E-04	1.94E-03	2.54E-01
^{90}Sr	Ci/L	3.43E-01	7.08E-01	4.84E-01
^{99}Tc	Ci/L	4.20E-06	4.68E-06	8.97E-01

HTWOS = Hanford Tank Waste Operations Simulator
TIC = Total inorganic carbon
TOC = Total organic carbon

For all tanks retrieved, the HTWOS concentration estimates for total chemicals (kg/L) were a factor of 1.8 times higher than post-retrieval measurements for tank C-106 and 0 to 10 times lower for other tanks. The HTWOS concentration estimates for total radionuclides (Ci/L) were 2 to 35 times lower than post-retrieval measurements.

Upper-bound Estimates of Inventory. The BBI, showing the current inventories for these tanks, provides the best available information for an upper-bound estimate. This would be the residual waste volume if no additional waste can be retrieved from the tanks. The BBI waste concentrations for these tanks are based on pre-retrieval measurements and pre-retrieval process knowledge. Current BBI concentration estimates take no credit for soluble analytes that may have been washed out of the waste during retrieval processes to-date.

3.2.2.4.4 Residual Inventory in Ancillary Equipment.

Residual Inventory Volume in Catch Tank 241-C-301 and 244-CR Process Tank Vault. For the base case an assumption was made that 90% of the waste will be retrieved from these tanks. Whether more or less waste is retrieved is unknown. Therefore, as an upper bound it should be assumed that no retrieval occurs and the current waste volume will remain at closure.

Although the C-301 tank was sampled, few sample data were obtained. An estimate of waste types and contents could be made based on waste transfer sources, but the correlation of sources to residual waste remaining in C-301 would be highly speculative. Furthermore, some or all of the waste may have been diluted for transfer. Therefore, a simplifying assumption was made that the composition of waste in tank C-301 and in the 244-CR vault tanks and sumps is similar to the average composition of residual waste samples from the C Farm SSTs. Although there is high uncertainty in this assumption, if the waste was more dilute than tank waste, the actual composition should be lower. Nevertheless, it is recommended that improved characterization of the C-301 catch tank and the 244-CR vault should be included in the PA maintenance plan.

Residual Inventory Volume in Pits, Diversion Boxes and Waste Transfer Pipelines. Sources of volume uncertainty include the number and length of pits, diversion boxes and waste transfer pipelines. For pits and pipelines, another uncertainty is the thickness of waste adsorbed and whether any other residual waste remains in the tank. The volume of waste expected to be in the pits and diversion boxes is very small compared to the pipelines, and as a result, uncertainty in the waste inventory is of negligible importance for the PA. As a result, no uncertainty evaluations are recommended. For the waste pipelines base case, the volume is from RPP-PLAN-47559 and assumes all pipelines are only 5% full except for a plugged line and cascade lines, which are assumed to be completely full. Studies suggest that the pipelines may be less than 5% full; however, it is possible that some pipelines contain more waste.

Waste Composition (Same as Catch Tank 241-C-301 and 244-CR Process Tank Vault). The waste composition was assumed to be similar to post-retrieval tank residuals because, like a retrieved tank, the pits, diversion boxes and pipelines are flushed. It could be argued that the waste, especially in plugged pipelines, is more similar to waste in tanks before retrieval than after. However, post-retrieval residual waste compositions were assumed given the relatively small length of plugged lines compared to unplugged lines, uncertainty in assumptions about the applicability of pre- or post-retrieval average waste composition for pipelines, and the fact that analytical data for many of the closure DQO constituents is only available for post-retrieved tanks.

4.0 SCREENING APPROACHES

Radiological COPCs were identified for the PA effort using two types of screening evaluations: 1) one evaluation that considered inventory-related information including radionuclide half-lives, the in-growth of constituents from chain decay, and activity level, and 2) another evaluation that considered information on the groundwater pathway including travel times to the accessible environment and constituent-specific mobility. These evaluations and their results are described in the following sections.

4.1 SCREENING BASED ON INVENTORY-RELATED INFORMATION

The approach for identifying specific radionuclides subject to additional analysis in the PA is based on an evaluation of inventory-related information as outlined below.

- The first step in the evaluation was to identify all radionuclides in the BBI for WMA C tank inventory information within the official Tank Waste Information Network System (TWINS). The BBI contained inventory estimates for 46 radionuclides.

- The second step in the evaluation examined radioactive decay. The BBI list contains some very short-lived radionuclides (half-lives less than three years), such as ^{90}Y, ^{106}Ru, ^{125}Sb, ^{134}Cs, ^{137m}Ba, and ^{242}Cm. These six radionuclides were removed because either they were assumed to decay to negligible concentrations (^{106}Ru, ^{125}Sb, ^{134}Cs, ^{242}Cm) or their parents were already included in the PA calculations (^{90}Y, ^{137m}Ba). When the parent was included in the PA calculations, the contribution of the progeny was also included in the dose calculation for the parent.

- An additional evaluation was conducted to identify any supplemental radionuclides that were not included in the BBI estimates for retrieved tanks, but may be of interest for the PA evaluations. For this, the residual inventory estimates for retrieved tanks were obtained from RPP-RPT-42323, Table D-1. Radionuclides identified in RPP-RPT-42323, Table D-1 were eliminated because they had half-lives less than three years and are not directly related to Hanford Site operations or are non-detects. This led to assumption of zero initial mass of ^{228}Th (naturally occurring with half-life of 1.91 years) and ^{230}Th (naturally occurring/non-detect). Only the tank C-106 nominal inventory for ^{230}Th was above the detection limit and was included.

- The next step was to include radionuclides needed to complete the uranium decay chain to calculate radon flux. This step identified ^{222}Rn along with intermediate parent ^{230}Th that forms during the decay from ^{234}U. In addition, ^{210}Pb was identified as it is the decay product of ^{222}Rn. The initial mass of all three radionuclides (^{230}Th, ^{222}Rn, and ^{210}Pb) is assumed to be zero at closure (except for ^{230}Th for tank C-106).

- The next step in the screening evaluation was to ensure that the daughter radionuclides that are part of the decay chain are included and tracked in PA calculations. Necessary radionuclide data (atomic weights, decay rates, and daughter products stoichiometry)

needed for this evaluation were obtained from "ICRP Publication 107: Nuclear Decay Data for Dosimetric Calculations" (International Commission on Radiological Protection [ICRP] 2008). This source of information was consistent with the information in DOE's Derived Concentration Technical Standard (DOE-STD-1196-2011). Progeny radionuclides with a half-life of less than two years are assumed to be in secular equilibrium with their parent, which yielded a reduced number of species but still accounted for the radiological effects of the progeny.

Additional screening was performed using the 3-D flow and transport STOMP© model to determine the maximum K_d value of radionuclides in the WMA C tank residuals that are capable of reaching the water table in 1,000 and 10,000 years. Methodology used in that screening analysis is presented in Section 6.3.2.3, and results are provided in Section 7.2.1.

The results of this overall screening process identified a total of 43 radionuclides to be included in the more detailed PA analysis.

4.2 SUMMARY OF RADIONUCLIDE SCREENING

The final set of 43 radionuclides are presented in Table 4-1. The list of radionuclides screened out of the PA analysis with a rational for their elimination is provided in Table 4-2.

The initial inventory estimates are decay corrected to the assumed closure date of January 1, 2020. Furthermore, the residual inventory of pits is not considered due to very small estimated residual volume, which is a factor of 50 smaller than the pipeline estimate. The final base case estimate of inventory for radionuclides considered in the PA is presented in Table 4-3.

Table 4-1. List of Radionuclides Considered for the Performance Assessment. (2 sheets)

Number	Species ID	Description	Atomic Weight	Half-life	Daughter1	Stoichiometry 1	Daughter2	Stoichiometry 2
1	Ac227	Actinium-227	227.028	21.772 yr				
2	Am241	Americium-241	241.057	432.2 yr	Np237	1		
3	Am243	Americium-243	243.061	7,370 yr	Pu239	1		
4	C14	Carbon-14	14.0032	5,700 yr				
5	Cd113m	Cadmium-113	112.904	14.1 yr				
6	Cm243	Curium-243	243.061	29.1 yr	Pu239	0.9976	Am243	0.0024
7	Cm244	Curium-244	244.063	18.1 yr	Pu240	1		
8	Co60	Cobalt-60	59.9338	5.2713 yr				
9	Cs137	Cesium-137	136.907	30.167 yr				
10	Eu152	Europium-152	151.922	13.537 yr				
11	Eu154	Europium-154	153.923	8.593 yr				
12	Eu155	Europium-155	154.923	4.7611 yr				
13	H3	Hydrogen-3	3.01605	12.32 yr				
14	I129	Iodine-129	128.905	1.57E+7 yr				
15	Nb93m	Niobium-93	92.9064	16.13 yr				
16	Ni59	Nickel-59	58.9343	1.01E+5 yr				
17	Ni63	Nickel-63	62.9297	100.1 yr				
18	Np237	Neptunium-237	237.048	2.144E+6 yr	U233	1		
19	Pa231	Protactinium-231	231.036	32,760 yr	Ac227	1		
20	Pb210	Lead-210	209.984	22.2 yr				
21	Pu238	Plutonium-238	238.05	87.7 yr	U234	1		
22	Pu239	Plutonium-239	239.052	24,110 yr	U235	1		
23	Pu240	Plutonium-240	240.054	6,564 yr	U236	1		

Table 4-1. List of Radionuclides Considered for the Performance Assessment. (2 sheets)

Number	Species ID	Description	Atomic Weight	Half-life	Daughter1	Stoichiometry 1	Daughter2	Stoichiometry 2
24	Pu241	Plutonium-241	241.057	14.35 yr	Am241	0.99998	Np237	2.45E-05
25	Pu242	Plutonium-242	242.059	3.75E+5 yr	U238	1		
26	Ra226	Radium-226	226.025	1,600 yr	Rn222	1		
27	Ra228	Radium-228	228.031	5.75 yr				
28	Rn222	Radon-222	222.018	3.8235 day	Pb210	0.9998		
29	Se79	Selenium-79	78.9185	2.95E+5 yr				
30	Sm151	Samarium-151	150.92	90 yr				
31	Sn126	Tin-126	125.908	2.3E+5 yr				
32	Sr90	Strontium-90	89.9077	28.79 yr				
33	Tc99	Technetium-99	98.9063	2.111E+5 yr				
34	Th229	Thorium-229	229.032	7340 yr				
35	Th230	Thorium-230	230.033	75,380 yr	Ra226	1		
36	Th232	Thorium-232	232.038	1.405E+10 yr	Ra228	1		
37	U232	Uranium-232	232.037	68.9 yr				
38	U233	Uranium-233	233.04	1.592E+5 yr	Th229	1		
39	U234	Uranium-234	234.041	2.455E+5 yr	Th230	1		
40	U235	Uranium-235	235.044	7.04E+8 yr	Pa231	1		
41	U236	Uranium-236	236.046	2.342E+7 yr	Th232	1		
42	U238	Uranium-238	238.051	4.468E+9 yr	U234	1		
43	Zr93	Zirconium-93	92.9065	1.53E+6 yr	Nb93m	0.975		

Table 4-2. List of Radionuclides Screened from the Performance Assessment with the Rationale for their Elimination.

Species ID	Description	Half-life	Exclusion
^{125}Sb	Antimony-125	2.759 yr	Half-life less than 3 years
^{137m}Ba	Barium-137m*	2.552 m	
^{134}Cs	Cesium-134	2.065 yr	
^{242}Cm	Curium-242	162.8 d	
^{106}Ru	Ruthenium-106	373.59 d	
^{228}Th	Thorium-228	1.91 yr	
^{90}Y	Yttrium-90*	64.1 hr	

* ^{90}Y and ^{137m}Ba are included through the evaluation of their parents ^{90}Sr and ^{137}Cs, respectively.

This page intentionally left blank.

Table 4-3. Estimated Inventory of Radionuclides (in Curies) at Closure of Waste Management Area C (Decay Corrected to January 1, 2020) Used in the Performance Assessment Calculation.

Tank/ Equipment	Ac-227	Am-241	Am-243	C-14	Cd-113m	Cm-243	Cm-244	Co-60	Cs-137	Eu-152	Eu-154	Eu-155	H-3	I-129	Nb-93m	Ni-59	Ni-63	Np-237	Pa-231	Pb-210	Pu-238	Pu-239
241-C-101	1.58E-06	9.91E+00	1.43E-03	2.76E-03	1.47E-03	1.86E-05	3.32E-04	1.76E-04	3.61E+02	6.38E-05	2.77E-03	4.69E-04	2.45E-02	5.55E-05	1.83E-05	7.23E-04	5.53E-02	3.45E-04	2.48E-08	0.00E+00	1.13E-01	1.83E+01
241-C-102	1.93E-02	2.12E+01	7.93E-04	9.88E-04	1.78E-02	6.22E-05	1.28E-03	2.14E-01	8.07E+01	1.26E-04	1.36E-01	2.62E-02	2.15E-05	2.56E-03	1.10E-02	1.62E-01	1.36E+01	5.16E-05	2.12E-03	0.00E+00	1.48E+00	6.49E+01
241-C-103	6.39E-08	4.83E+00	3.70E-05	6.99E-03	1.49E-02	7.66E-07	1.52E-05	1.83E-02	6.07E+02	2.58E-05	1.41E+00	4.37E-01	3.98E-03	3.00E-03	3.69E-04	1.12E-01	1.86E+01	1.35E-02	1.66E-07	0.00E+00	1.30E+00	4.99E+00
241-C-104	1.11E-05	8.46E+00	5.25E-03	3.08E-03	5.11E-02	3.64E-03	6.69E-02	4.66E-01	6.22E+02	3.54E-02	1.57E+00	2.29E-01	9.32E-03	4.84E-04	3.16E-02	8.64E-02	9.95E+01	7.97E-02	7.47E-05	0.00E+00	5.89E-01	5.15E+00
241-C-105	5.17E-07	2.84E+01	6.73E-04	4.86E-02	5.87E-02	9.11E-06	1.56E-04	6.83E-01	5.08E+03	1.12E-04	4.68E-03	6.08E-04	4.08E+00	8.95E-03	1.45E-03	4.41E-01	3.61E+01	1.93E-04	6.57E-07	0.00E+00	7.50E-01	5.28E+01
241-C-106	1.74E-03	6.38E+01	3.05E-03	8.21E-03	2.13E+00	5.55E-02	7.39E-01	2.23E+00	1.00E+03	2.02E+00	2.25E+01	7.65E+00	4.17E-03	6.31E-04	5.92E+00	1.05E+01	6.53E+01	5.41E-02	2.53E-03	0.00E+00	2.38E+00	1.67E+01
241-C-107	6.20E-06	3.70E+02	3.86E-02	2.16E-02	2.50E-03	5.02E-04	8.95E-03	9.14E-04	2.32E+03	1.35E-04	5.70E-03	8.66E-04	1.44E-02	4.07E-02	8.45E-02	1.18E-03	1.46E-01	2.08E-04	3.83E-05	0.00E+00	8.05E-01	1.30E+02
241-C-108	7.78E-07	9.46E-01	9.78E-05	8.18E-03	1.97E-03	1.50E-06	2.96E-05	7.22E-04	8.57E+01	1.07E-04	4.52E-03	6.84E-04	1.94E-02	3.81E-05	4.80E-02	9.30E-04	2.80E+00	2.17E-05	3.02E-05	0.00E+00	4.37E-03	6.68E-01
241-C-109	3.40E-06	3.71E-01	3.91E-05	7.65E-04	1.37E-03	5.09E-07	9.09E-06	5.02E-04	4.31E+01	7.41E-05	3.13E-03	4.74E-04	3.51E-03	2.65E-05	4.64E-02	6.46E-04	8.78E-01	6.46E-04	2.10E-05	0.00E+00	1.56E-02	4.01E-01
241-C-110	9.62E-07	4.94E-02	5.54E-06	1.51E-03	3.89E-04	7.22E-08	1.29E-06	1.42E-04	2.02E+01	2.11E-05	8.89E-04	1.35E-04	1.80E-03	2.65E-04	1.32E-02	1.83E-04	4.08E-01	1.09E-03	5.96E-06	0.00E+00	1.56E-02	1.17E+00
241-C-111	1.82E-05	8.32E+01	1.15E-02	1.04E-01	5.99E-02	1.82E-03	3.26E-02	1.03E-01	7.14E+03	5.38E-02	2.41E+00	3.70E-01	2.58E+00	1.41E-02	9.78E-02	1.40E+00	1.13E+02	3.32E-03	4.99E-05	0.00E+00	1.70E+00	9.45E+01
241-C-112	4.57E-06	9.42E-01	9.72E-05	1.60E-02	1.84E-03	1.26E-06	2.25E-05	6.75E-04	7.66E+02	1.00E-04	4.22E-03	6.39E-04	1.06E-02	3.57E-05	6.26E-02	8.69E-04	1.08E-01	1.54E-04	2.82E-05	0.00E+00	3.59E-02	5.79E+00
241-C-201	3.45E-09	2.46E+00	9.76E-04	7.64E-04	5.77E-04	3.10E-03	5.55E-02	2.37E-03	7.01E+00	2.10E-03	9.42E-02	1.45E-02	1.57E-04	4.57E-07	7.46E-04	4.07E-03	8.33E-01	3.42E-03	6.79E-09	0.00E+00	4.42E-01	1.58E+01
241-C-202	3.51E-09	1.21E+00	4.71E-04	2.03E-04	5.88E-04	1.50E-03	2.68E-02	2.44E-03	6.18E+00	2.14E-03	9.61E-02	1.48E-02	1.60E-04	7.35E-06	7.64E-04	4.16E-03	2.00E-01	2.90E-03	6.93E-09	0.00E+00	3.99E-01	1.43E+01
241-C-203	2.87E-09	3.16E-02	1.22E-05	1.66E-04	4.80E-04	3.88E-05	6.95E-04	2.15E-03	9.10E+00	1.75E-03	1.50E-02	1.81E-02	1.31E-04	1.47E-05	6.26E-04	3.40E-03	5.54E-02	2.70E-05	5.67E-09	0.00E+00	1.36E-02	4.86E-01
241-C-204	2.69E-09	3.16E-03	1.22E-06	1.88E-04	4.50E-04	3.87E-06	6.95E-05	1.86E-03	4.13E+00	1.64E-03	5.62E-02	1.13E-02	1.13E-04	3.57E-07	5.84E-04	3.18E-03	1.46E-02	2.16E-02	5.30E-09	0.00E+00	2.76E-04	9.84E-03
C-301	6.62E-05	5.54E+00	1.37E-03	2.04E-03	8.49E-02	5.33E-03	8.60E-02	1.16E-01	1.21E+02	8.31E-02	1.17E+00	3.60E-01	2.09E-03	2.06E-04	2.30E-01	4.14E-01	9.54E+00	2.82E-02	1.01E-04	0.00E+00	7.40E-01	2.13E+01
CR-Vault	1.20E-04	1.01E+01	2.49E-03	3.71E-03	1.54E-01	9.68E-03	1.56E-01	2.11E-01	2.21E+02	1.51E-01	2.13E+00	6.54E-01	3.80E-03	3.75E-04	4.18E-01	7.52E-01	1.73E+01	5.13E-02	1.84E-04	0.00E+00	1.34E+00	3.88E+01
Pipelines	1.02E-04	8.52E+00	2.11E-03	3.14E-03	1.31E-01	8.19E-03	1.32E-01	1.79E-01	1.87E+02	1.28E-01	1.80E+00	5.54E-01	3.22E-03	3.17E-04	3.54E-01	6.37E-01	1.47E+01	4.34E-02	1.56E-04	0.00E+00	1.14E+00	3.28E+01

Tank/ Equipment	Pu-240	Pu-241	Pu-242	Ra-226	Ra-228	Rn-222	Se-79	Sm-151	Sn-126	Sr-90	Tc-99	Th-229	Th-230	Th-232	U-232	U-233	U-234	U-235	U-236	U-238	Zr-93
241-C-101	1.96E+00	1.54E+00	2.70E-05	5.90E-07	2.64E-13	0.00E+00	2.80E-04	4.00E+00	5.13E-04	3.29E+03	4.34E-02	1.33E-10	0.00E+00	1.12E-12	1.75E-06	1.71E-07	1.69E-01	7.54E-03	1.93E-03	1.72E-01	3.35E-05
241-C-102	1.55E+01	4.87E+01	9.00E-04	2.88E-07	3.64E-01	0.00E+00	1.60E-06	9.72E-01	1.83E-04	2.94E+02	3.56E-03	1.06E-02	0.00E+00	2.29E-02	2.83E-02	2.17E+00	1.13E-01	4.27E-03	1.43E-03	9.78E-02	4.22E-03
241-C-103	1.04E+00	1.80E+00	3.24E-05	1.54E-08	4.70E-05	0.00E+00	2.64E-05	4.30E-01	5.27E-05	6.78E+03	4.48E-02	2.60E-11	0.00E+00	1.99E-04	4.29E-06	5.85E-03	1.36E-02	7.10E-04	3.74E-04	1.64E-02	7.03E-04
241-C-104	1.55E+00	1.14E+01	1.97E-02	3.24E-07	8.73E-04	0.00E+00	8.56E-03	3.17E+03	8.81E-03	4.89E+03	3.04E-01	8.56E-08	0.00E+00	3.70E-03	3.53E-02	2.18E+00	4.17E-01	1.98E-02	4.85E-03	4.39E-01	6.24E-02
241-C-105	1.04E+01	1.75E+01	3.14E-04	1.60E-07	2.36E-13	0.00E+00	1.51E-04	2.37E+00	2.93E-04	2.89E+04	7.83E+00	1.25E-10	0.00E+00	1.00E-12	8.62E-06	5.02E-07	2.39E-01	1.02E-02	5.17E-03	2.44E-01	2.77E-03
241-C-106	3.57E+00	1.84E+01	4.16E-04	5.13E-04	1.32E-04	0.00E+00	9.57E-03	7.82E+03	1.76E+00	4.50E+04	1.64E-01	1.91E-05	9.38E-04	5.60E-04	4.87E-04	1.82E-03	9.40E-04	3.86E-05	1.73E-05	9.02E-04	1.04E+01
241-C-107	1.42E+01	1.10E+01	1.97E-04	5.95E-07	9.70E-04	0.00E+00	2.70E-04	1.04E+04	4.94E-04	2.42E+04	2.14E+00	1.89E-09	0.00E+00	4.11E-03	2.20E-06	2.15E-07	2.07E-01	9.24E-03	2.31E-03	2.11E-01	1.55E-01
241-C-108	7.27E-02	7.91E-02	1.01E-06	4.73E-07	3.70E-06	0.00E+00	1.62E-03	6.66E+00	3.91E-04	1.25E+03	4.87E-02	1.50E-09	0.00E+00	1.57E-05	4.50E-07	4.10E-08	3.25E-02	1.82E-03	2.85E-04	4.03E-02	1.22E-01
241-C-109	4.36E-02	5.09E-01	6.07E-07	3.26E-07	2.06E-12	0.00E+00	1.48E-04	4.65E+00	2.71E-04	2.33E+03	8.77E-03	1.04E-09	0.00E+00	8.72E-12	9.94E-08	9.69E-09	9.35E-03	4.01E-04	9.61E-05	9.53E-03	8.45E-02
241-C-110	1.27E-01	3.58E-01	1.77E-06	9.27E-08	5.85E-13	0.00E+00	4.21E-05	1.32E+00	2.38E-02	2.62E+03	4.46E-02	2.95E-10	0.00E+00	2.48E-12	1.91E-08	1.86E-09	2.64E-03	1.14E-04	2.93E-05	2.59E-03	2.41E-02
241-C-111	1.85E+01	3.54E+01	6.54E-04	4.51E-06	6.54E-12	0.00E+00	3.53E-03	6.39E+02	6.72E-03	3.05E+05	2.19E+00	3.56E-09	0.00E+00	2.77E-11	2.22E-05	4.80E-05	7.74E-01	3.37E-02	1.32E-02	7.88E-01	1.81E-01
241-C-112	6.29E-01	4.91E-01	8.76E-06	4.40E-07	2.78E-12	0.00E+00	1.99E-04	6.25E+00	3.65E-04	2.28E+02	1.69E+00	1.40E-09	0.00E+00	1.18E-11	4.50E-07	4.39E-08	4.23E-02	1.89E-03	4.73E-04	4.32E-02	1.14E-01
241-C-201	3.40E+00	8.36E+00	1.60E-04	1.00E-09	9.51E-07	0.00E+00	5.49E-05	2.39E+01	1.10E-04	1.71E+02	2.63E-03	1.18E-11	0.00E+00	4.03E-06	2.25E-06	1.14E-05	3.65E-02	1.48E-03	5.23E-04	3.69E-02	1.46E-03
241-C-202	3.08E+00	7.52E+00	1.45E-04	1.02E-09	9.70E-07	0.00E+00	5.61E-05	2.43E+01	1.13E-04	3.31E+02	2.50E-03	1.20E-11	0.00E+00	4.11E-06	2.00E-06	1.02E-05	3.52E-02	1.42E-03	3.52E-04	3.28E-02	1.49E-03
241-C-203	1.05E-01	2.58E-01	4.94E-06	8.40E-10	4.48E-07	0.00E+00	4.58E-05	1.99E+01	9.21E-05	1.56E+02	2.32E-03	9.81E-12	0.00E+00	1.90E-06	6.60E-06	3.37E-05	1.13E-01	4.79E-03	8.33E-04	1.09E-01	1.22E-03
241-C-204	2.12E-03	5.21E-03	9.98E-08	7.86E-10	3.35E-06	0.00E+00	4.29E-05	1.86E+01	8.61E-05	1.03E+02	3.18E-03	9.17E-12	0.00E+00	1.42E-05	4.93E-06	2.51E-05	8.27E-02	3.42E-03	5.13E-04	8.13E-02	1.14E-03
C-301	4.60E+00	1.21E+01	1.30E-03	1.93E-05	5.90E-05	0.00E+00	1.03E-03	5.29E+02	6.80E-02	3.06E+03	3.64E-02	7.21E-07	0.00E+00	2.50E-04	1.96E-03	1.20E-01	2.26E-01	9.56E-03	1.93E-03	2.22E-01	4.07E-01
CR-Vault	8.36E+00	2.19E+01	2.36E-03	3.51E-05	1.07E-04	0.00E+00	1.87E-03	9.62E+02	1.24E-01	5.55E+03	6.62E-02	1.31E-06	0.00E+00	4.54E-04	3.57E-03	2.17E-01	4.11E-01	1.74E-02	3.51E-03	4.04E-01	7.39E-01
Pipelines	7.08E+00	1.86E+01	2.00E-03	2.97E-05	9.08E-05	0.00E+00	1.58E-03	8.15E+02	1.05E-01	4.70E+03	5.61E-02	1.11E-06	0.00E+00	3.85E-04	3.02E-03	1.84E-01	3.48E-01	1.47E-02	2.97E-03	3.42E-01	6.26E-01

5.0 WASTE CHARACTERISTICS

The WMA C tanks and ancillary equipment received a wide range of waste streams produced from processing of spent nuclear fuel and selective extraction of isotopes of concern to support the Hanford operations. The wastes consist of a large array of chemicals and radionuclides and their inventory is estimated on a tank-by-tank basis. As of September 2014, waste has been retrieved from 13 of 16 SSTs in WMA C and is in progress for the remaining 3 tanks (C-102, C-105, and C-111). This section provides information related to the chemical and physical characteristics of the residual waste that are relevant to developing conceptual and mathematical models for source term release.

Following retrieval of tanks, post-retrieval sampling of the residual waste has been conducted for various constituents as indicated in Section 3.2.2 to estimate the residual inventory and volume. Table 3-12 summarizes the current waste types (primarily sludge) present in various WMA C tanks and Tables 3-13 through 3-15 provide residual inventory and residual volume estimates for the tanks and ancillary equipment. For the retrieved tanks that have undergone post-retrieval sampling, the density of sludge typically varies from ~1,550 to 2,000 kg/m^3 (96.8 to 124.9 lbs/ft^3) and the gravimetric moisture content varies from 20 to 40 wt.%.

As part of the waste characterization efforts, analytical methods are used to measure the chemical and radiological constituents in the waste sludge and to understand their composition, solid-phase characteristics, and the leachability of primary contaminants of interest. (e.g., PNNL-16738, "Hanford Tank 241-C-103 Residual Waste Contaminant Release Models and Supporting Data"; PNNL-15187, "Hanford Tank 241-C-106: Residual Waste Contaminant Release Model and Supporting Data," Rev. 1; PNNL-19425, "Hanford Site Tank 241-C-108 Residual Waste Contaminant Release Models and Supporting Data"; PNNL-14903, "Hanford Tanks 241-C-203 and 241-C-204: Residual Waste Contaminant Release Model and Supporting Data," Rev. 1; PNNL-16229, "Hanford Tanks 241-C-202 and 241-C-203: Residual Waste Contaminant Release Model and Supporting Data").

"Hanford tank residual waste – Contaminant source terms and release models" (Deutsch et al. 2011) summarized the characterization information of solid phases from four WMA C tank residuals (C-103, C-106, C-202, and C-203). Multiple samples of residual waste from each tank were received. The samples represent composite samples of solids collected from several locations in each storage tank. The photographs of the samples are shown in Figure 5-1. The yellowish color of the tank C-203 residual sample is due to presence of uranium at a concentration of ~50 wt.% while the color of the tank C-106 sample is likely due to presence of high manganese concentration resulting from oxalate reaction with the metals in the waste solids. Tank C-106 is the only tank from which waste was removed using oxalic acid.

The average reported composition (µg/g dry weight) for selected elements, primary contaminants of interest, and anions in bulk residual waste developed from laboratory analysis of selected tank waste residual samples used for waste release studies by Deutsch et al. (2011), are presented in Table 5-1. Concentrations of certain contaminants and elements differ by orders of magnitude, indicating large variability. For example, the uranium concentrations for adjacent tanks C-202 and C-203 are relatively high (207,000 and 505,000 µg/g [7,302 and 17,813 oz/ton],

respectively) while they are relatively low for tanks C-103 and C-106 (3,730 and 310 µg/g [132 and 11 oz/ton], respectively). On the other hand, the trend in aluminum concentrations is reversed, being relatively high for tanks C-103 and C-106 compared to tanks C-202 and C-203. The iron (Fe) concentration for tank C-202 is 122,000 µg/g (4,300 oz/ton) and for tank C-203 is 16,300 µg/g (575 oz/ton). These compositional differences between tanks are due to 1) the mixing of various types of waste disposed over the decades when they were in use, 2) the chemical reactions within the tanks from heating and evaporation, and 3) the effects of various waste retrieval methods (sluicing of wastes using tank supernates, groundwater, and/or oxalic acid). Additional information on average composition of selective constituents in waste residuals developed from inventory estimates in RPP-RPT-42323 is summarized in Tables 3-13 through 3-17.

The mineralogy of solid phases from the retrieved tanks has been summarized by Deutsch et al. (2011) and provided in Table 5-2. Gibbsite [$Al(OH)_3$] is a common mineral in tanks with high aluminum concentrations, while non-crystalline U–Na–C–O–P ± H phases are common in the uranium-rich residual wastes from tanks C-202 and C-203. Iron oxides/hydroxides have been identified in all residual waste samples studied to date. Figure 5-2 shows the electron micrograph of typical solids present in unleached tank C-103 residual waste.

Technetium was identified by scanning electron microscopy/energy dispersive spectroscopy (SEM/EDS) associated with iron oxide/hydroxide particles in tank C-103 residual waste at concentration from ~0.6 to 1.0 wt.%, providing direct evidence of technetium in solid phases. No iodine-containing phases could be identified, perhaps due to low mass concentrations. In tank C-106, due to leaching with oxalate, the manganese-bearing mineral phases are dominant; however, the presence of aluminum and iron-bearing mineral phases exists. The majority of the manganese occurs as Mn(II). Spectral analysis of tank C-106 samples indicate that uranium occurs primarily in the hexavalent oxidation state [U(VI)]; however, a small fraction may be present as U(IV). The majority of the chromium appears to be in the reduced trivalent [Cr(III)] oxidation state, while the iron is present in the oxidized trivalent [Fe(III)] state.

The residual waste in tanks C-202 and C-203 contains mostly amorphous solids of U-Na-C-O-P ± H and iron oxide/hydroxide as shown in Figure 5-3. No phases containing iodine or technetium were detected, most likely due to low concentration of these contaminants.

"Single-pass flow-through test elucidation of weathering behavior and evaluation of contaminant release models for Hanford tank residual radioactive waste" (Cantrell et al. 2013) evaluated contaminant release models for Hanford tank residuals using single-pass flow-through tests. This work provided an analysis of solid phases in the radioactive residual waste following leaching with three different leachates, namely the deionized (DI) water, $CaCO_3$ saturated solution, and 0.005 M $Ca(OH)_2$ solution which represented a range of possible water types contacting the residual waste. In general, the nature of the leachate did not have a large impact on the phases that were identified. For the tank C-103 samples, the only phase identified was gibbsite, regardless of the leachate used. In the tank C-202 samples, calcite was positively identified, while for tank C-203 samples, calcite and schoepite were positively identified. Besides these, some possible (tentative) phases identified for tanks C-202 and C-203 included hydroxylapatite, $CaUO_4$, soddyite, studtite, $Na_2U_2O_7.6H_2O$, and boltwoodite.

Figure 5-1. Photographs of As-Received, Post-Final Retrieval Residual Waste Samples from Tanks 241-C-103, 241-C-106, 241-C-202, and 241-C-203.

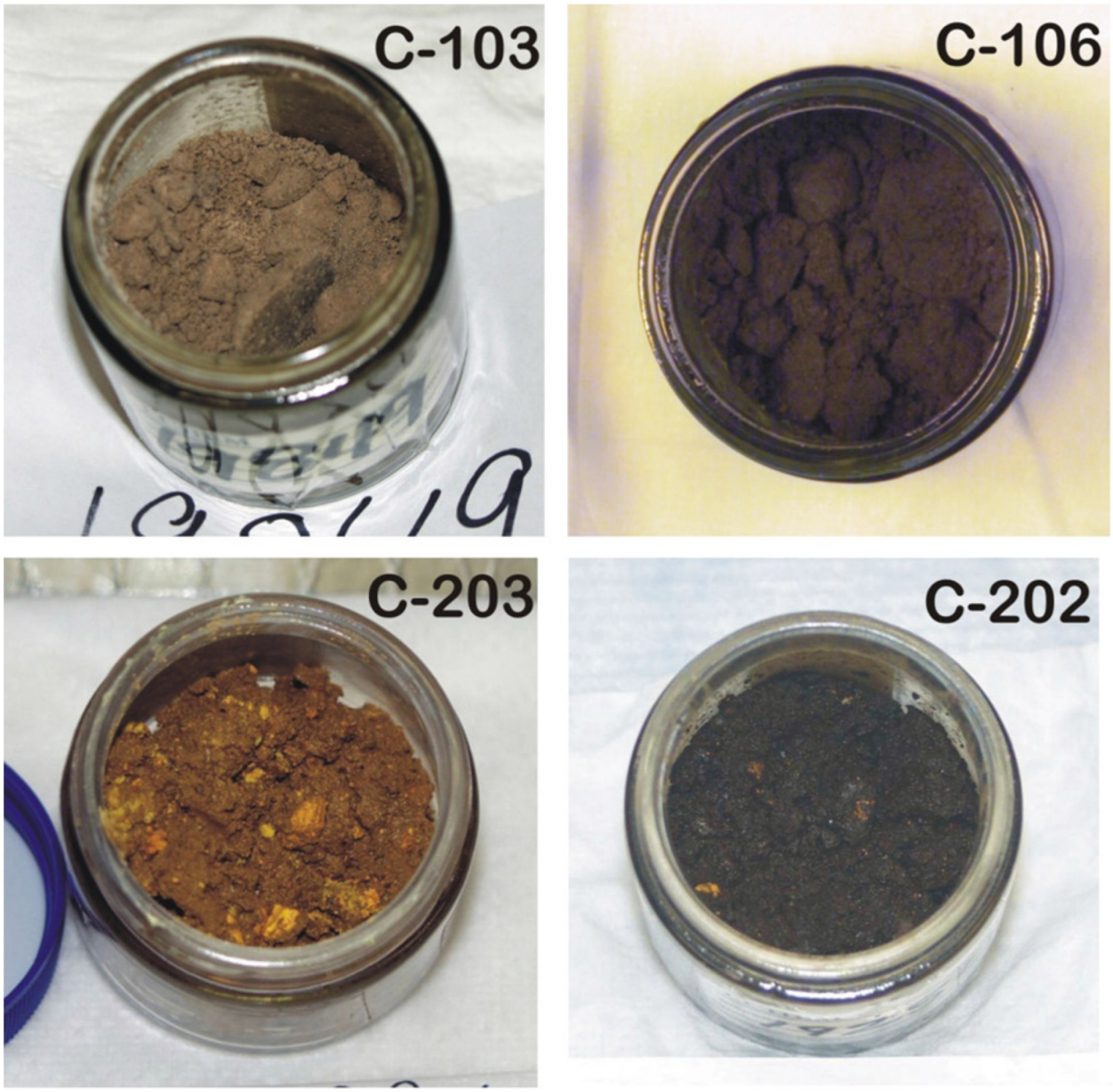

Source: "Hanford tank residual waste – Contaminant source terms and release models" (Deutsch et al. 2011).

Table 5-1. Average Composition (µg/g[a] dry weight) for Selected Elements, Primary Contaminants of Interest, and Anions in Bulk Residual Waste from Some Waste Management Area C Tanks.

Analyte	241-C-103 (µg/g dry wt.)	241-C-106 (µg/g dry wt.)	241-C-202 (µg/g dry wt.)	241-C-203 (µg/g dry wt.)
Al	136,000	81,699	13,600	<710
Ba	181	914	208	<142
Ca	616	46,490	14,500	3,140
Cr	193	(727)[a]	13,200	5,910
Fe	12,000	36,663	122,000	16,300
K	Below detection limit	8,526	<15,800	<355,000
Mg	-42	3,162	2,560	-729
Mn	470	108,069	25,700	956
Na	7,840	46,720	58,800	95,800
Ni	420	5,373	9,070	510
Pb	892	4,814	7,980	5,630
Si	9,070	(4,895)[a]	25,000	3,490
Sr	90.7	(493)[a]	1,510	409
^{238}U	3,730	310	207,000	505,000
^{239}Pu	8.02	27.7	435	18.2
^{237}Np	1.3	9.04	2.16	(0.0519)[a]
^{241}Am	0.053	2.05	0.449	0.014
^{99}Tc	0.231	1.14	0.149	(0.0947)[a]
^{129}I	(1.11E-5)[a]	Not available	Not available	Not available
F^-	(31)[a]	33	6,030	2,760
Cl^-	(5.4)[a]	87	161	201
NO_2^-	(59)[a]	<73	485	610
NO_3^-	(250)[a]	<70	3,540	4,840
CO_3^{2-}	Below detection limit	39,500	12,200	49,900
SO_4^{2-}	Below detection limit	<66	334	288
PO_4^{3-}	(66)[b]	<91	17,700	43,300
Oxalate	—	63,900	32,400	1,500

[a] 1 ug/g is equal to 0.0352 oz/ton.
[b] Value in parenthesis is the estimated quantification limit.

Modified from "Hanford tank residual waste – Contaminant source terms and release models" (Deutsch et al. 2011).

Table 5-2. Solid Phases Identified in Tank Residual Waste Samples.

Tank Number	Solid Phases		Comments
	Major	Minor/Trace	
241-C-103	Gibbsite [$Al(OH)_3$]; hematite (a-Fe_2O_3)	Two Fe oxide/hydroxides; cancrinite [$Na_6CaAl_6Si_6(CO_3)O_{24}$_$2H_2O$]; oxides of Ag ± Hg, U, Ca–P, Na–Ca–U, Si–Al–Mg–Na–Fe, Zr, and Th	Tc in three Fe oxide/hydroxide particles
241-C-106	Lindbergite ($MnC_2O_4.2H_2O$); whewellite ($CaC_2O_4.2H_2O$); gibbsite; böhmite [AlO(OH)]; dawsonite [$NaAlCO_3(OH)_2$]; hematite; rhodochrosite [$MnCO_3$]; possible Ag–Hg phase	Mn–Al–Fe–Na–P–Si–Ca–O ± C ± H; Mn–O–P ± Al ± C± H; Si–Al–Na–O ± C ±H; REE-rich oxide; Ca–Si–Al–O ± C ± H; Ag^0; Pb-containing phase	Tank leached with 0.9 M oxalic acid ($H_2C_2O_4$) during waste retrieval
241-C-202	Amorphous (non-crystalline) solids of either U Na–C–O–P ± H or Fe oxide/hydroxide	Trace amounts of Mn and Cr and sometimes Pb	No crystalline phases identified
241-C-203	Amorphous solids of primarily U Na–C–O–P ± H	Amorphous solids of Fe oxide/ hydroxide with trace amounts of Mn, Cr, Pb, and/or Cu	No crystalline phases identified; Similar to C-202

Modified from "Hanford tank residual waste – Contaminant source terms and release models" (Deutsch et al. 2011).

The general trends in uranium leachate concentrations for the C-103, C-202, and C-203 tank residual wastes used in Cantrell et al. (2013) were very similar. The results are presented for tank C-202 in Figure 5-4. The leached uranium concentration using DI water and $CaCO_3$ saturated solution are significantly higher than those in the 0.005 M $Ca(OH)_2$ leachates. This is attributed to the formation of Ca-rich precipitates (Ca phosphate and calcite) on the surfaces of the waste particles when using $Ca(OH)_2$ leachate, inhibiting dissolution of the underlying uranium phases in the waste. Since the tanks are planned to be grouted prior to the closure, the primary leachate is expected to be $Ca(OH)_2$ solution, which is likely to reduce the leaching of uranium.

To investigate this leaching behavior, thermodynamic equilibrium modeling was conducted to calculate the mineral saturation indices and to identify solid phases potentially in equilibrium with the leachate composition. The saturation index is defined as SI = log (Q/K_{sp}), where Q is the activity product and K_{sp} is the mineral solubility product at equilibrium at the temperature of interest. Minerals with SI values near zero (within ± 0.5) are generally considered to be at or near equilibrium, more positive values are considered supersaturated, and more negative values are considered undersaturated with respect to the solution composition. The SI calculated for the tank C-202 single-pass flow-through (SPFT) test effluents for the three leachates indicated that DI water and $CaCO_3$ saturated leachate give similar SI results while the $Ca(OH)_2$ leachate-based SI results are quite different. Results from DI water and $CaCO_3$ saturated leachates indicate that $NaUO_2PO_4.xH_2O$ is near equilibrium while Ca-containing phases (such as calcite and hydroxylapatite) were all undersaturated. The SI results for the $Ca(OH)_2$ leachates indicate all uranium-bearing phases to be highly undersaturated, but near saturation with respect to Ca-containing phases. Calcite was near saturation while hydroxylapatite and flourapatite were

consistently highly supersaturated. These results are consistent with the observed leaching behavior of uranium. It is hypothesized that precipitation of Ca-rich phases resulted in coatings on the waste particles that could have temporarily inhibited dissolution and attainment of equilibrium for any uranium phase in contact with $Ca(OH)_2$ leachate solutions.

Figure 5-2. Low- and High-Magnification Electron Micrographs of Typical Solids Present in Unleached Tank 241-C-103 Residual Waste.

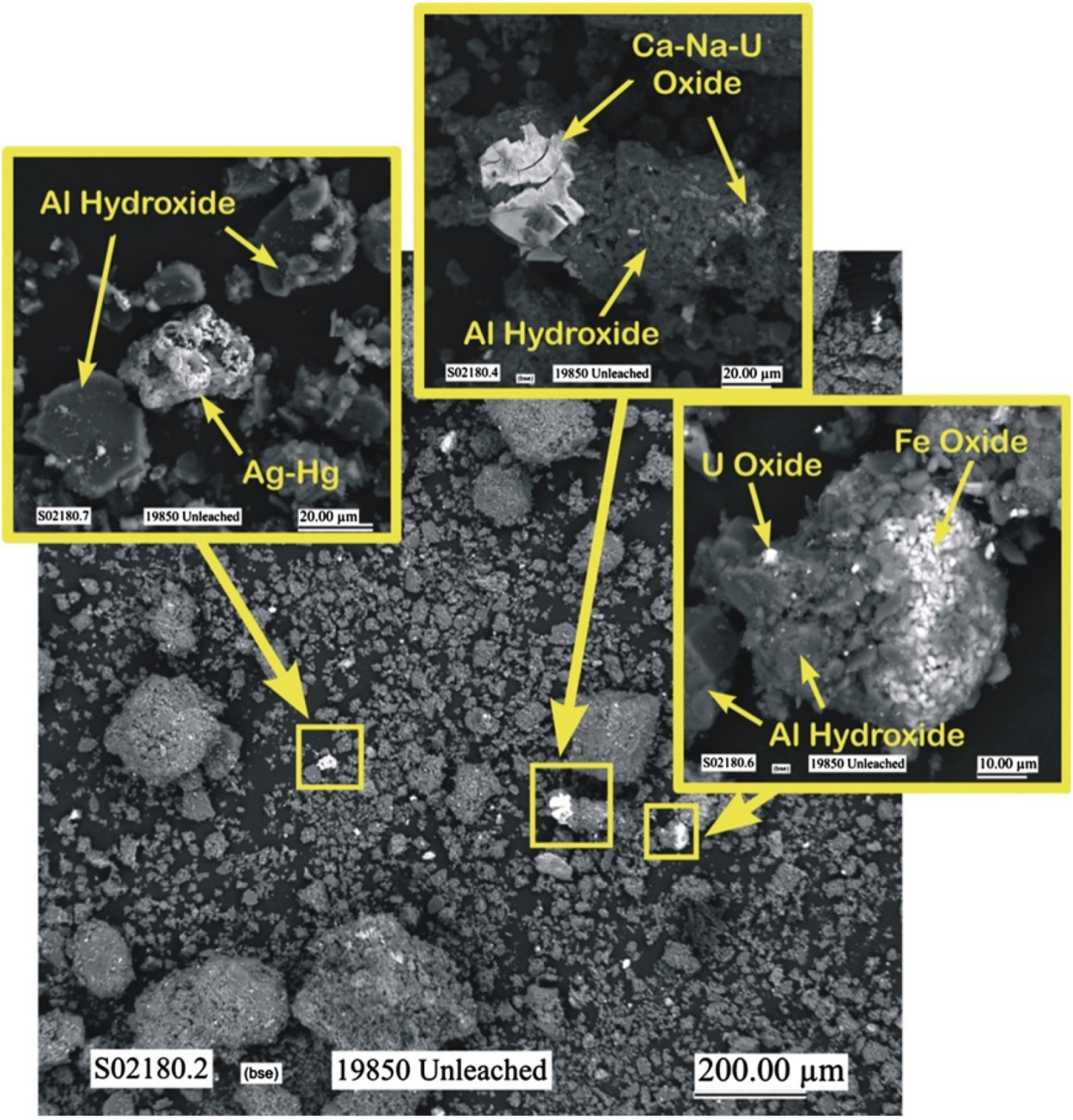

Reference: PNNL-16738, "Hanford Tank 241-C-103 Residual Waste Contaminant Release Models and Supporting Data."

Figure 5-3. Electron Micrograph (top) and Multi-Element Energy Dispersive Spectroscopy Map (bottom) for an Aggregate of U-Na-C-O-P ± H and Fe Oxide/Hydroxide Particles Present in Sequential-Leached Water Extraction Sample of Tank 241-C-203 Residual Waste.
(The large aggregate at the center of the colored element distribution map is the same large aggregate, but rotated 45 degree counterclockwise, shown in the electron micrograph).

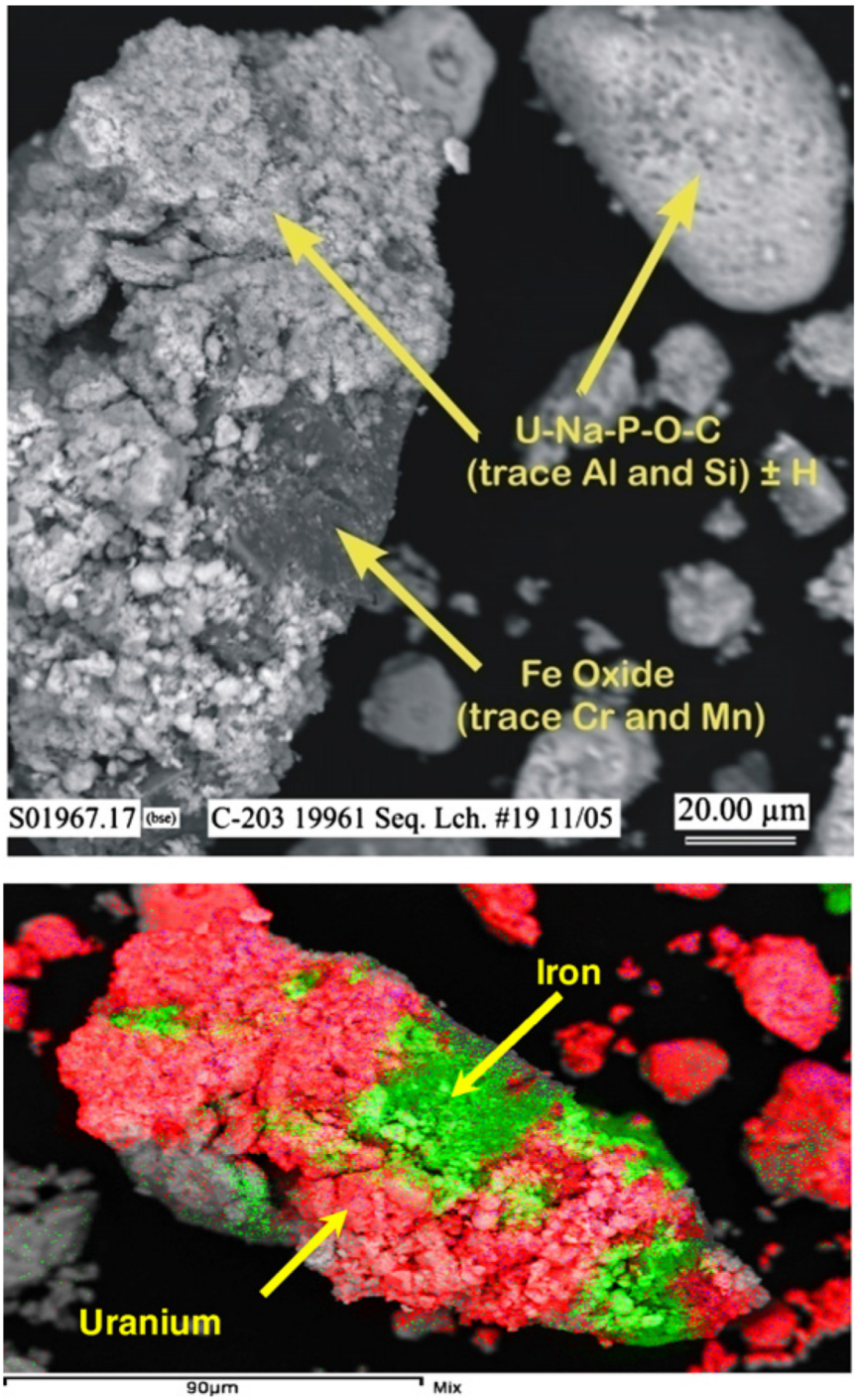

Reference: PNNL-16229, "Hanford Tanks 241-C-202 and 241-C-203: Residual Waste Contaminant Release Models and Supporting Data."

Figure 5-4. Uranium Concentrations in Tank 241-C-202 Single-Pass Flow-Through Leachates as a Function of the Total Volume of Leachate that has Contacted the Waste in Terms of Leachate/Solid (Initial) Weight Ratio.

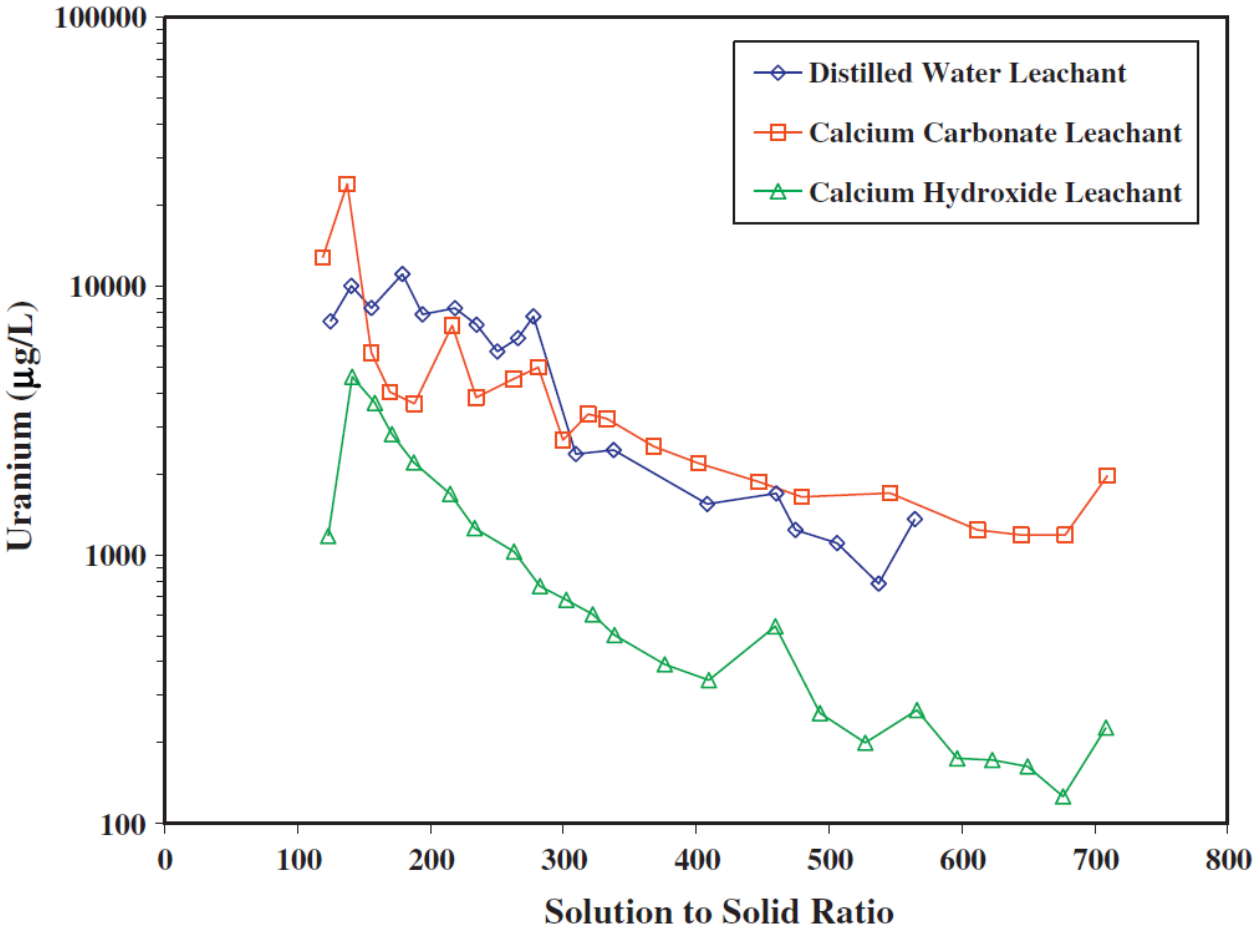

Reference: "Single-pass flow-through test elucidation of weathering behavior and evaluation of contaminant release models for Hanford tank residual radioactive waste" (Cantrell et al. 2013).

These results indicate that as long as the infiltrating water through the tank passes through the infill grout material, it will be conditioned to be similar to a dilute $Ca(OH)_2$ leachate solution and the uranium dissolution will remain inhibited. At some distant time in the future when the tank is assumed to be sufficiently degraded such that large open fractures develop that do not allow appreciable residence time for infiltrating waters to contact the grout material, the leachate would be similar to the $CaCO_3$ saturated water, and at that time, the uranium concentrations may increase when the residual waste is contacted.

Similar SPFT experiments, as indicated above to evaluate the uranium leaching, were conducted by Cantrell et al. (2013) to evaluate the leaching characteristics of ^{99}Tc and chromium from tank C-202. Figures 5-5 and 5-6 indicate the ^{99}Tc and chromium concentrations in tank C-202 SPFT leachates for the three leachate solutions as a function of solution to solid ratio. Figure 5-5 indicates that the ^{99}Tc concentrations in all three leachates are very similar, with concentrations dropping near exponentially with increasing solution to solid ratio. Results for tanks C-203 and C-103 are very similar to tank C-202, although the magnitudes of the concentrations vary as a

function of the residual inventory. The actual release mechanism for ^{99}Tc remains indeterminate; however, it is likely that ^{99}Tc is adsorbed onto and/or co-precipitated with iron oxides/hydroxides (Cantrell et al. 2013), and may slowly leach from dissolution of iron oxides/hydroxides mineral phases. This is consistent with the observation where technetium was identified by SEM/EDS associated with iron oxide/hydroxide particles in tank C-103 residual waste at concentration from ~0.6 to 1.0 wt.%.

Figure 5-5. Technetium-99 Concentration in Tank 241-C-202 Single-Pass Flow-Through Leachates as a Function of the Total Volume of Leachate that has Contacted the Waste in Terms of Leachate/Solid (Initial) Weight Ratio.

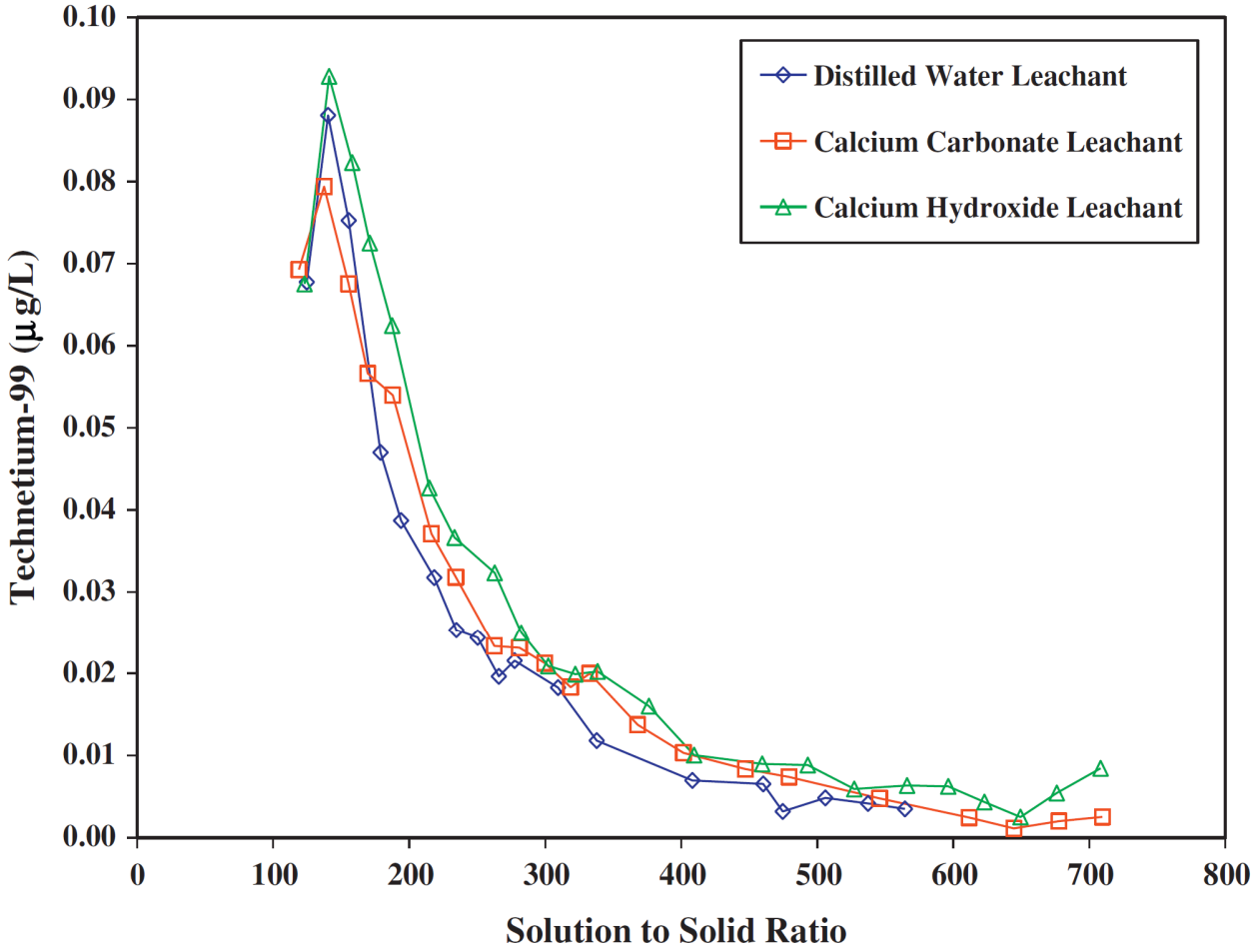

Reference: "Single-pass flow-through test elucidation of weathering behavior and evaluation of contaminant release models for Hanford tank residual radioactive waste" (Cantrell et al. 2013).

Chromium in the SPFT leachates for tank C-202 residual waste (Figure 5-6) shows relatively high release concentrations initially, with concentrations in the $Ca(OH)_2$ leachates being much higher than those of the DI water and $CaCO_3$ leachates. The relatively high concentrations of chromium in $Ca(OH)_2$ leachate were not found for tank C-203, and the reason for this difference is not readily apparent. The leachate concentrations from C-103 tank residual waste were below the detection limit of 5 ppb. These results indicate large variations in the chromium release characteristics, and perhaps reflect the variability in the chromium present in trivalent and

hexavalent oxidation states along with association with iron oxides/hydroxides. It is also possible that some chromate may also have been co-precipitated with phosphate in $NaUO_2PO_4.xH_2O$. As residual waste is leached with $Ca(OH)_2$ and portions of $NaUO_2PO_4.xH_2O$ are converted to $CaUO_4$, both PO_4 and CrO_4 are slowly released.

Figure 5-6. Chromium Concentration in Tank 241-C-202 Single-Pass Flow-Through Leachates as a Function of the Total Volume of Leachate that has Contacted the Waste in Terms of Leachate/Solid (Initial) Weight Ratio.

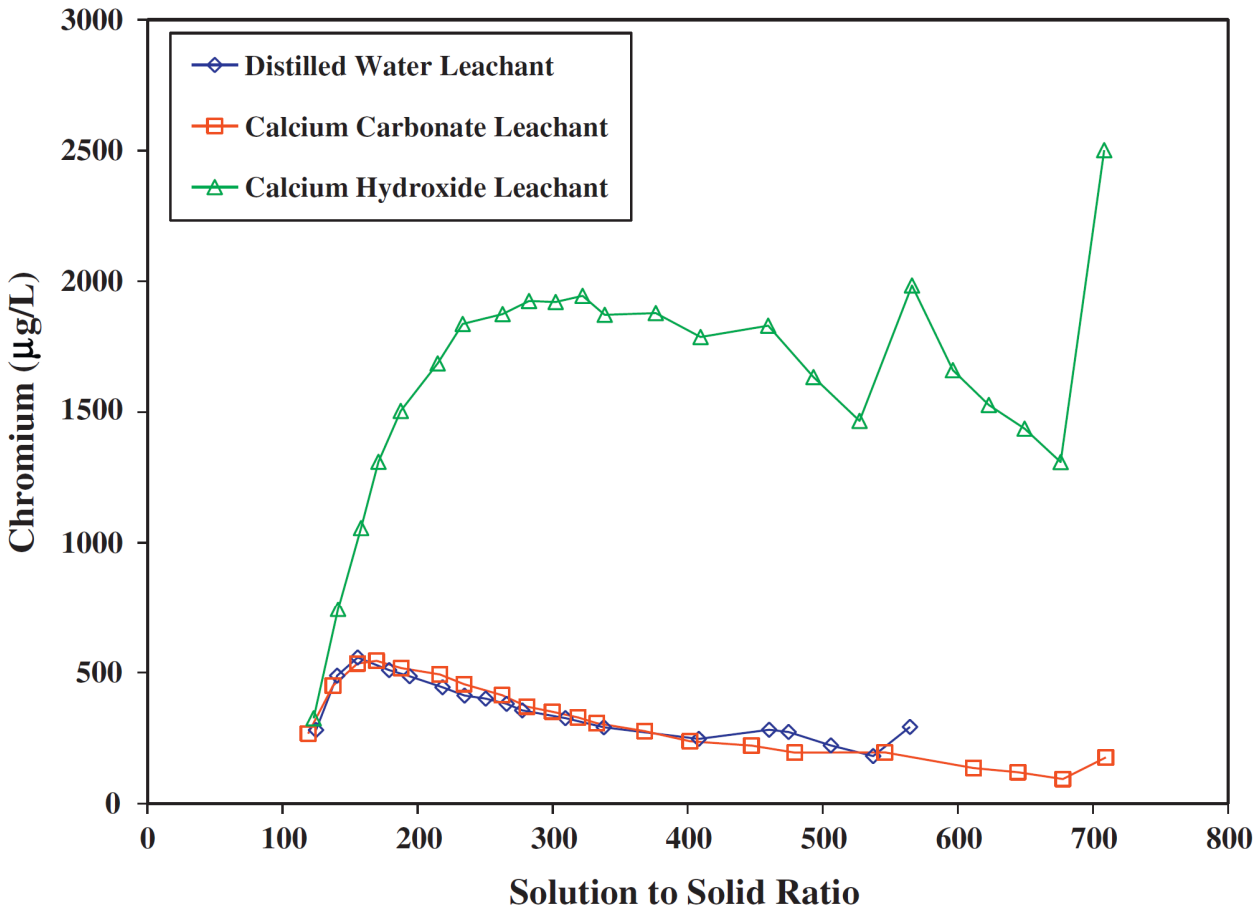

Reference: "Single-pass flow-through test elucidation of weathering behavior and evaluation of contaminant release models for Hanford tank residual radioactive waste" (Cantrell et al. 2013).

The total percentages of uranium and ^{99}Tc leached from the residual waste samples during the course of the SPFT experiments were calculated and are presented in Table 5-3. The percent uranium leached varies from 0.3% to 9.4%, while the percent ^{99}Tc leached ranges from 4.5% to 15%. The percentage of uranium leached varies by the leachate type, with greater amount leached using DI water and $CaCO_3$ saturated water and significantly less with the $Ca(OH)_2$ leachate. In contrast, the percentage of ^{99}Tc leached does not vary by the leachate type, but is influenced more by the particular sample.

Table 5-3. Percentages of Total Uranium and Technetium-99 Leached from Tanks 241-C-202, 241-C-203, and 241-C-103 Residual Wastes during the Single-Pass Flow-Through Experiments.

Tank	Leachate	Percent Uranium Leached	Percent Technetium-99 Leached
241-C-202	Deionized water	1.3	7.8
241-C-202	$CaCO_3$	1.7	8.3
241-C-202	$Ca(OH)_2$	0.3	9.0
241-C-203	Deionized water	2.5	6.2
241-C-203	$CaCO_3$	2.1	7.4
241-C-203	$Ca(OH)_2$	0.22	4.5
241-C-103	Deionized water	5.4	15
241-C-103	$CaCO_3$	9.4	15
241-C-103	$Ca(OH)_2$	3.5	12

Reference: "Single-pass flow-through test elucidation of weathering behavior and evaluation of contaminant release models for Hanford tank residual radioactive waste" (Cantrell et al. 2013).

This page intentionally left blank.

6.0 ANALYSIS OF PERFORMANCE

This PA provides an assessment of the long-term human health impacts following the closure of the WMA C facility in the 200 East Area of the Hanford Site. This section provides an overview of the methodology developed to assess the scenarios and pathways and describes the conceptual models of facility performance and the development and implementation of the mathematical models used to estimate the impacts from the proposed closure action. It also integrates the information presented in earlier sections that forms the basis for the conceptual and mathematical model of the WMA C facility following closure. The information related to the analysis and modeling approach is presented in the following subsections:

- 6.1 Overview of Analysis
- 6.2 Conceptual Model of Facility Performance
- 6.3 Mathematical Models
- 6.4 Model Validation.

6.1 OVERVIEW OF ANALYSIS

The method of analysis used to assess the long-term performance of WMA C is briefly described in this section, with more detailed information presented in later sections. The analysis incorporates key elements of the disposal system called *safety functions* that are deemed important in assessing the system performance. The safety concept of the closed tank farm is that various features of the closed facility have specific attributes that contribute to the ability of the system to meet performance objectives. These attributes are called *safety functions* in this PA. Safety functions are identified from basic understanding of the projected behavior of the system in the post-closure period. These safety functions and their behavior are used to identify specific analysis cases that show the robustness and defense-in-depth of the closed facility.

Facility performance is defined in terms of the onsite and offsite exposures and doses from radionuclides that may be inadvertently contacted and/or that might migrate from the disposal facility. All of the calculated exposures in the PA are hypothetical, and depend on a future member of the public engaging in activities on the Central Plateau without knowledge of the prior existence of the Hanford Site and its disposal activities. Exposure calculated in this way is higher and occurs at earlier times than potential exposures off the Hanford Site, and therefore provides a more stringent set of exposure conditions than potential offsite exposures.

The various pathways of potential exposure are illustrated in Figure 6-1. The most important exposure pathway for hydrologic transport is groundwater use for drinking water, irrigation, livestock watering, and biotic transport. In the groundwater pathway, the analysis is focused on meteoric water from rain and snowfall, which enters the subsurface, contacts contaminants that have diffused from the grouted residual waste, and carries these contaminants to the unconfined aquifer. The surface water pathway is omitted from this PA because surface water does not exist within the 100 m (328 ft) point of analysis distance from the WMA C boundary. Potential atmospheric exposures are included as a separate analysis; however, their impact is expected to be limited because only a few radionuclides (e.g., tritium, ^{14}C, ^{129}I, and ^{222}Rn) that are present in

the residual waste inventory can partition into the gas phase. As a result, the main focus of this PA is on evaluating the groundwater pathway.

The analysis of the groundwater pathway comprises evaluations directed at two different performance objectives. The first is an all-pathway dose contribution to a hypothetical receptor that consumes contaminated groundwater, leafy vegetables and produce that were irrigated with contaminated groundwater, and milk and meat from animals that consume contaminated water and pasture grass irrigated with contaminated groundwater. The second is a groundwater protection performance objective, which limits concentrations in groundwater, regardless of use or potential exposure by humans.

The strategy for the WMA C PA is to define and analyze both a base case and a suite of sensitivity and uncertainty cases. The base case is a single deterministic evaluation of future dose to the public as a result of the anticipated retrieval and closure actions taken at WMA C. It represents the scenario in which the safety functions behave as expected as the facility evolves into the future. The base case assumptions and parameters generally are based on best available information, but some parameter estimates related to future conditions may have a conservative bias. The results of the base case are used to evaluate compliance with the DOE O 435.1 all-pathways performance objectives. Additional sensitivity cases and uncertainty analyses were defined to explore the effect of uncertainties in the models, assumptions, and parameter ranges. The sensitivity cases were defined to evaluate the consequences associated with either the full or partial loss of a safety function. In this way, the PA is specifically structured to evaluate the key elements of the disposal system that contribute to its long-term safety. Uncertainty analyses were conducted to evaluate the effect of parameter uncertainty on potential exposures. The uncertainty analyses were undertaken using an abstraction model so that a large number of analyses can be performed within a limited time.

Confidence in the data, assumptions, and methods used in the analysis was developed through the following approaches.

- Many data were based on WMA C-specific site characterization, sampling, measurements and interpretations, including those for contaminant inventory, geology, hydrology and geochemistry. When data specific to WMA C were not available, data from nearby sites, such as vadose zone hydraulic property data and information developed from soil samples collected in the vicinity of the IDF or comparable conditions, as well as data reported in the literature, were used.

- Data were upscaled to represent field-scale processes using scientifically-accepted approaches that have been published in peer-reviewed journals. Upscaling techniques use information from small, core-scale measurements to develop parameters that are applicable to large, field-scale models.

- The process-based modeling software, STOMP© code (PNNL-12030, “STOMP Subsurface Transport Over Multiple Phases Version 2.0 Theory Guide”; Pacific Northwest National Laboratory, Queried 12/18/2015, [STOMP User Guide], http://stomp.pnnl.gov/user_guide/STOMP_guide.stm; PNNL-11216, “STOMP

Subsurface Transport Over Multiple Phases Application Guide"), has been benchmarked and deemed suitable for use in this PA. The STOMP© code is the pre-authorized modeling software at the Hanford Site for vadose zone and near-field groundwater modeling (Internal memorandum 1301789, "Modeling to Support Regulatory Decisionmaking at Hanford"). The STOMP© code has previously been qualified for simulation use at Hanford by CH2M HILL Plateau Remediation Company (CHPRC) (CHPRC-00269, "STOMP Requirements Traceability Matrix CHPRC Build 4").

- The system-level modeling software, GoldSim© ("GoldSim Contaminant Transport Module User's Guide" [GoldSim Technology Group 2014a]; "GoldSim Distributed Processing Module User's Guide" [GoldSim Technology Group 2014b]; "GoldSim Probabilistic Simulation Environment User's Guide" [GoldSim Technology Group 2014c]), has been deemed suitable based on its wide usage and acceptance in the various PAs across the DOE complex. GoldSim© was the principal code used for systems-level and uncertainty analysis modeling in this PA effort. The GoldSim© software is an example of additional simulation software that may be used at Hanford as long as DOE and Environmental Management software quality requirements are met.

- Sensitivity and uncertainty analyses were conducted to evaluate the effect of parameter uncertainties and alternative conceptual models on the overall performance of the system.

Results using the models and values are presented in Section 7.0 for the groundwater and air-pathway scenarios and in Section 8.0 for intruder scenarios. Section 9.0 also presents the comparison to performance objectives.

6.2 CONCEPTUAL MODEL OF FACILITY PERFORMANCE

The WMA C PA methodology uses conceptual models that are based on the physical system and expected contaminant migration pathways. Figure 6-2 provides a schematic representation of both WMA C at closure and the contaminant migration into the environment along the various pathways evaluated in this PA. The WMA C site is composed of both man-made and natural components. The man-made components of the system that influence contaminant migration include a closure surface barrier, the WMA C tanks, pipelines, and infrastructure, and the distribution of waste in those components. The natural components of the system that influence contaminant migration are a number of mostly horizontal to slightly dipping (to the northeast) stratigraphic layers within the saturated and unsaturated zones, net infiltration resulting from rainfall, and any antecedent moisture conditions (and contaminants) within WMA C or from adjacent sites. For the base case, Figure 6-3 illustrates the major stratigraphic units for the WMA C site that form a thick vadose zone ranging from 75 to 85 m (246 to 280 ft) thick. The water table is located within the undifferentiated Hanford formation and Cold Creek gravels with a predominantly south/southeastwardly groundwater flow.

Figure 6-4 shows an aerial view of WMA C, and surrounding disturbed, undisturbed, and resurfaced areas. Also shown is the location of A Complex, where the 100 m (328 ft) point of analysis downgradient of WMA C is located. This location represents the assumed location of a

hypothetical well that supplies water for drinking and irrigation in the all-pathway dose scenario calculations.

Several key safety functions and related FEPs characterize the conceptual models for release and transport of radionuclides in WMA C and are discussed in Appendix H (Safety Functions and Features, Events, and Processes) for the post-closure period. The conceptual models and relevant parameters for fate and transport modeling are developed for the following four time periods:

- Pre-operations and initial construction period (before 1945) representing the time when the tank farm ground remained undisturbed from the Hanford Manhattan Project mission

- Operations period representing tank farm construction, current, and immediate future conditions of the tank farm (1945 to 2020)

- Closure and post-closure period during the assumed design life of the intact surface barrier (2020 to 2520) when the tanks become grouted and radionuclides begin to diffuse out of the grout

- Post-closure period beyond assumed design life of the surface barrier (2520 to 12120) when the performance of the surface barrier is assumed to degrade.

A 1,000-year post-closure period is considered in the WMA C PA for the purpose of evaluating compliance with DOE O 435.1 performance objectives; a 10,000-year post-closure period is considered for the purpose of evaluating uncertainty in the results because of the slow travel time through the vadose zone under post-closure conditions. Peak concentrations for many of the radionuclides evaluated occur between 1,000 and 10,000 years.

In the WMA C PA analysis, net infiltration is controlled by the Modified RCRA Subtitle C barrier. This barrier has a design life of 500 years, and this time period is used in the base case. However, the surface barrier may potentially last longer or shorter than the design life, depending on how the site evolves in the post-closure period. Sensitivity analysis cases evaluate alternative future behavior patterns in the infiltration rate due to uncertainty in the design life. Contact of infiltrating water with the residual waste is also limited by the tank structure, by the grout infill, and by the tank shell. There is substantial uncertainty about how long the tank wall may last before physical and chemical degradation occurs and allows water to flow through it. However, the tank structure and infill grout together will form a low-permeability barrier to flow. Evaluations of the durability of this material and the longevity of its function to reduce water flow indicate very long lifetimes for the cementitious features of the tanks, such that they produce very low flow rates through the residual wastes for more than 10,000 years (see Section 6.2.1.2, Evaluation of Tank Stability). Under these conditions, releases from the residual wastes only occur by diffusion through the base mat and into the vadose zone below the tanks. Sensitivity analyses evaluate alternative conditions when advective releases occur at earlier times.

Figure 6-1. Overview of the Dose Calculations for Exposure Along the Groundwater Pathway and Air Pathway for the Waste Management Area C Performance Assessment.

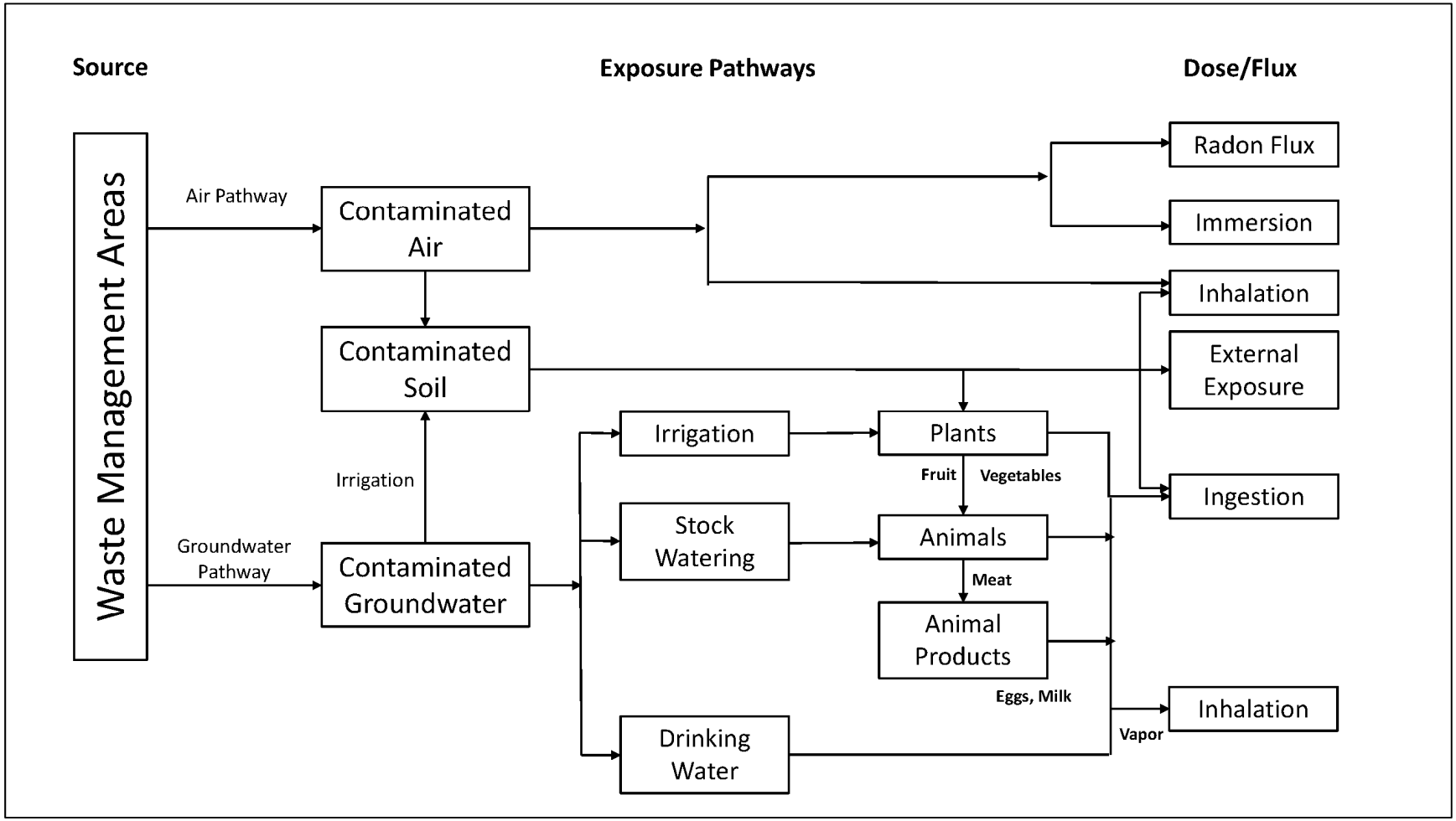

Figure 6-2. Schematic Conceptual Representation of Waste Management Area C and Contaminant Migration into the Environment along the Various Pathways Evaluated in the Performance Assessment.

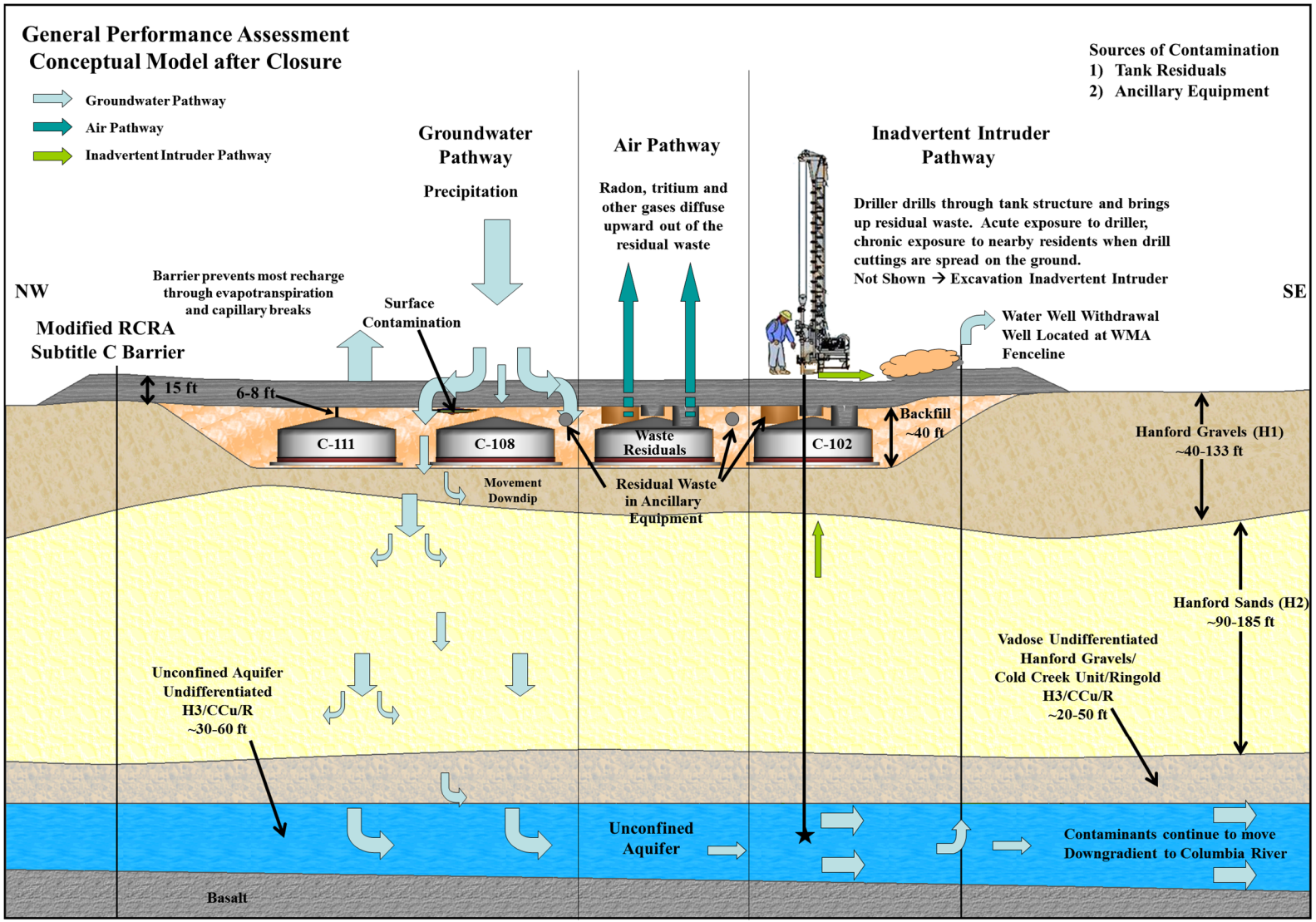

RCRA = Resource Conservation and Recovery Act of 1976 WMA = Waste Management Area

Figure 6-3. Conceptual Model of the Waste Management Area C Site Showing Stratigraphy.

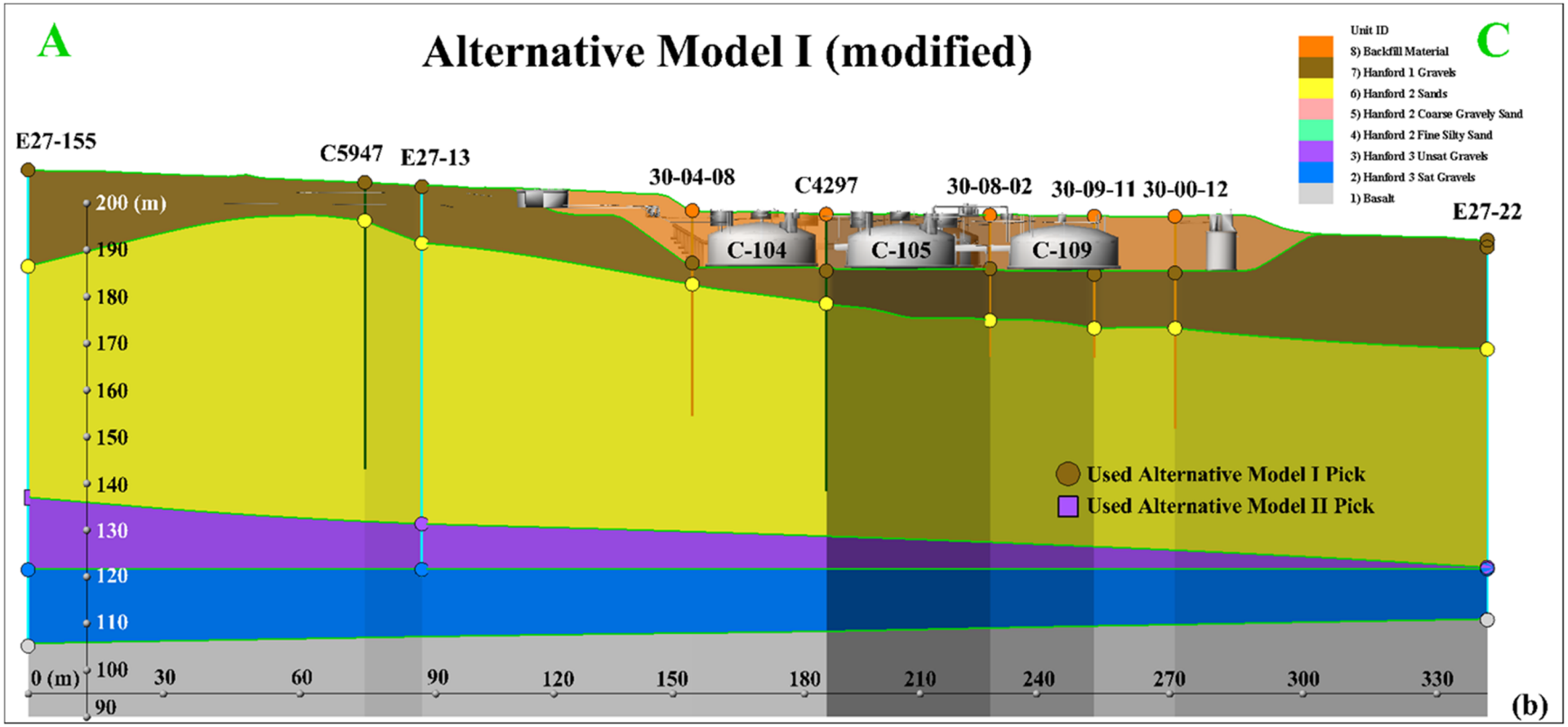

Figure 6-4. Aerial View of Waste Management Area C Showing Surface Features and the Surrounding Area.

WMA = Waste Management Area

For WMA C vadose zone modeling, small-scale laboratory measurements provide the basis for hydraulic properties used to predict the large, field-scale flow behavior (Appendix B). Each heterogeneous geologic unit is replaced by an equivalent homogeneous medium (EHM) with macroscopic flow properties. With each heterogeneous unit assigned its upscaled or effective hydraulic properties, the simulated flow fields predict the bulk or mean flow behavior at the field scale. Upscaling, in effect, accounts for the differences in scale between small, core-scale measurements and large, field-scale modeling. The radionuclides travel through the vadose zone until they reach the water table and the unconfined aquifer. The unconfined aquifer is also treated as an EHM, and an equivalent saturated hydraulic conductivity is estimated for the undifferentiated Hanford gravels and CCU sediments (Appendix C). In the final step of the analysis, the exposure scenario dose conversion factors are applied to the estimated groundwater concentrations at a 100 m (328 ft) downgradient location to determine total equivalent dose.

6.2.1 Source Term and Engineered Features

The source term considers processes associated with release of contaminants from residual waste into the natural environment. Separate source terms are considered for each of the twelve 100-series tanks, four 200-series tanks, C-301 catch tank, 244-CR vault, and pipelines, resulting in 19 separate source terms. The inventory used in the source term model includes the current estimate of the inventory and residual volume (Tables 3-13 through 3-15). Source terms for pits and diversion boxes are not explicitly considered but are incorporated as part of the pipeline source term.

Both mineral phase solubility-limited and matrix degradation rate-limited processes are considered for release of contaminant from the waste. These conceptual models are based on observations made through multi-year leaching tests and identification of mineral phases as presented in Section 5. The following release mechanisms are considered based on experimental results:

- a matrix-degradation-rate-based release of ^{99}Tc, and
- solubility-controlled releases of uranium.

The engineered features that are considered in the source term calculations are the tank structure, pipeline area,[1] infill grout material, and the emplaced surface cover at closure. The modified RCRA Subtitle C barrier reduces the net infiltration that will eventually percolate to the buried tank structures and ancillary equipment. The infill grout material provides not only structural stability to the tank configuration, but also provides a relatively impermeable barrier to flow leading to flow diversion around the tank, as long as the grout is not physically degraded. The infill grout material also controls the chemical conditions of the pore water that contacts the residual waste through mineral phase dissolution and precipitation (e.g., dissolution of portlandite and precipitation of calcite).

The source term processes that are considered in the post-closure period include releases of contaminants from residual waste, and their transport to the underlying vadose zone via either

[1] Individual pipelines are not treated as separate sources. Instead, the inventory associated with the pipeline source term is distributed uniformly over the area at WMA C that contains pipelines.

diffusion or advection. Conceptually, the key processes expected to affect contaminant releases from tank residuals include:

- Leaching of contaminants from the tank waste residual layer into the pore water associated with the tank residuals
- Diffusive transport of contaminants through the tank wall grout and concrete layer, along the tortuous continuous connections, to vadose zone soil outside the tank
- Ongoing chemical and physical degradation of the tank wall concrete and grout layer
- Ongoing dissolution and degradation of emplaced grout in the tank leading to eventual formation of cracks
- Once a sufficient number of cracks form in the engineered barriers, the potential exists for advective flow of water to begin to influence the source term.

Not all processes that are considered conceptually are included in the numerical models. Data from laboratory testing on the concrete samples provide a basis for the degradation of the concrete structure.

6.2.1.1 Conceptualization of Source Term. The distribution of residual waste volume within the retrieved tanks has been estimated by a variety of techniques that have involved video observations and computer/CAD modeling (e.g., RPP-CALC-54266, "Post-Hard Heel Retrieval Camera/CAD Modeling System Waste Volume Estimate for Tank 241-C-108"). The result of one such attempt is presented in Figure 6-5. The green and brown areas indicate the distribution of residual waste over the tank bottom while the blue area represents waste water remaining in the tank. Spatial distribution of residual waste volumes are estimated for the tank dish bottom, tank walls and stiffener rings, and in-tank equipment for the retrieved tanks, and are summarized in RPP-RPT-42323, Rev. 3. The estimates indicate that the majority of residual waste is located in the tank dish bottom (>80% for the 100-series tanks and >50% for the 200-series tanks), with minor amounts associated with the in-tank equipment.

For the purpose of developing a source release model for tanks and 244-CR vault, the residual waste volume is conceptualized to be present as a thin layer at the base of the tank (Figure 6-6). The estimated residual waste volume is assumed to be spread across the circular tank dish bottom area. The residual waste is conceptualized to be sludge-like, with a texture similar to a hardened paleosol. It is assumed to be fully saturated with a porosity of 40% based on evaluation of sludge waste phase from the retrieved tanks (TWINS, Queried 02/10/2014, [WMA C Tanks, wt% water in sludge/solid waste type], http://twins.pnl.gov/twins.htm). The variability associated with residual volume is considered in the uncertainty analysis.

While the tank is intact, it will divert any water that infiltrates through the surface cover. Therefore, the transport mechanism for release of contaminants from the residual tank waste to the underlying vadose zone is primarily diffusive. The dissolved concentration of contaminants in the residual waste pore volume is controlled by the waste characteristics, such as waste form

degradation and dissolution of solubility-controlling mineral phases. The presence of continuous water connections is assumed across the grout and concrete layers for the diffusive transport to occur in the aqueous phase.

Figure 6-5. Computer-Aided Modeling Results Showing Distribution of Residual Waste for a Retrieved Tank.

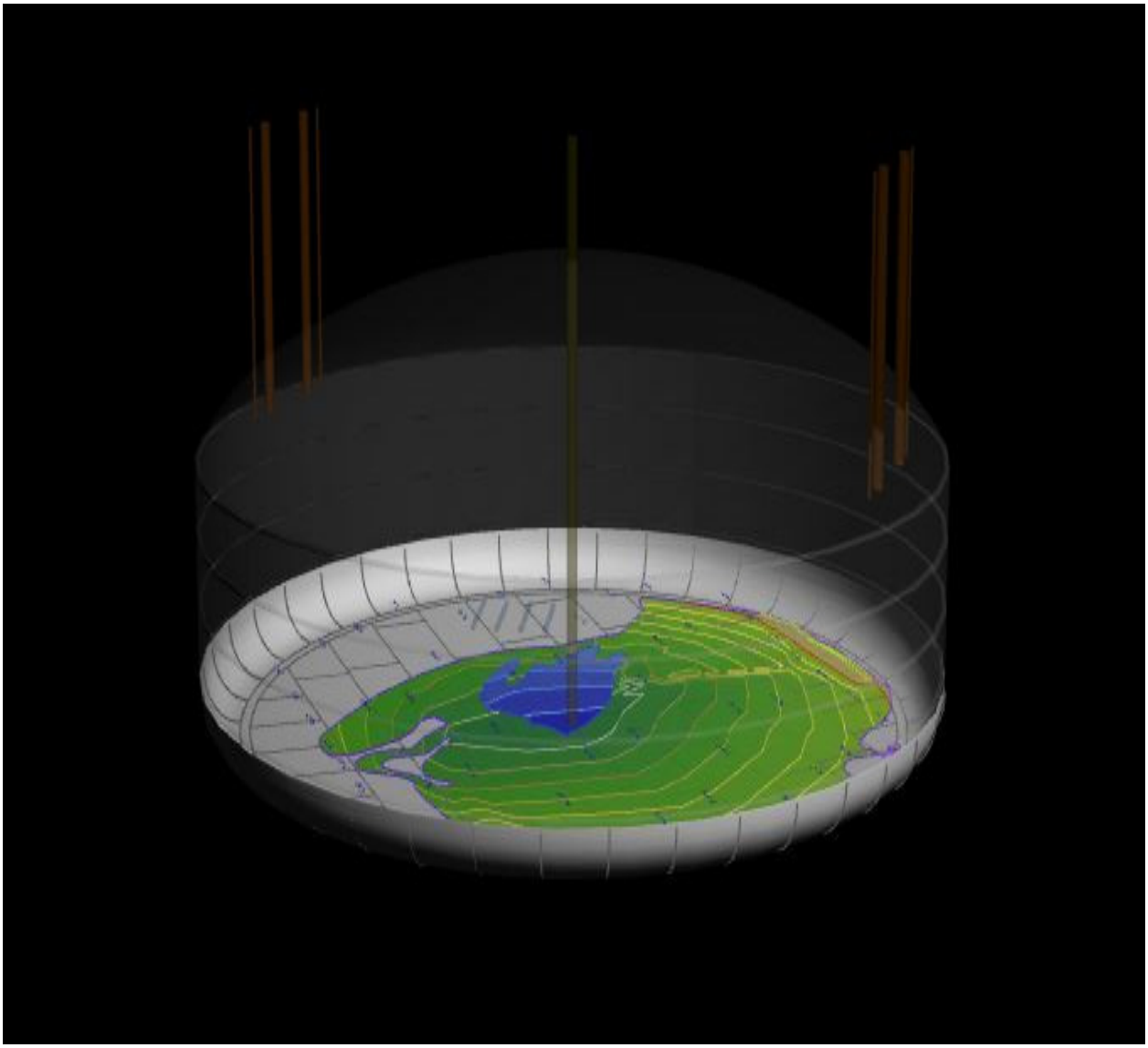

The source release model for the pipelines is quite different from the tanks. Instead of modeling discrete source terms, a single source area reflective of the approximate areal distribution of the waste transfer pipelines is considered. This is the assessed area of the tank farm where pipelines are generally present. The estimated residual inventory is uniformly spread over this area. Unlike tanks, the pipelines are assumed not to be filled with grout at closure, and due to limited information on the condition of the pipeline material, the pipeline walls are assumed to be absent (i.e., no structural integrity). Therefore, both advective and diffusive releases are considered from the pipelines. More details related to the source conceptualization are discussed below.

Only those aspects of the engineered features that are used in developing parameters for source term modeling are presented.

Figure 6-6. Conceptual Model of Tank after Site Closure.

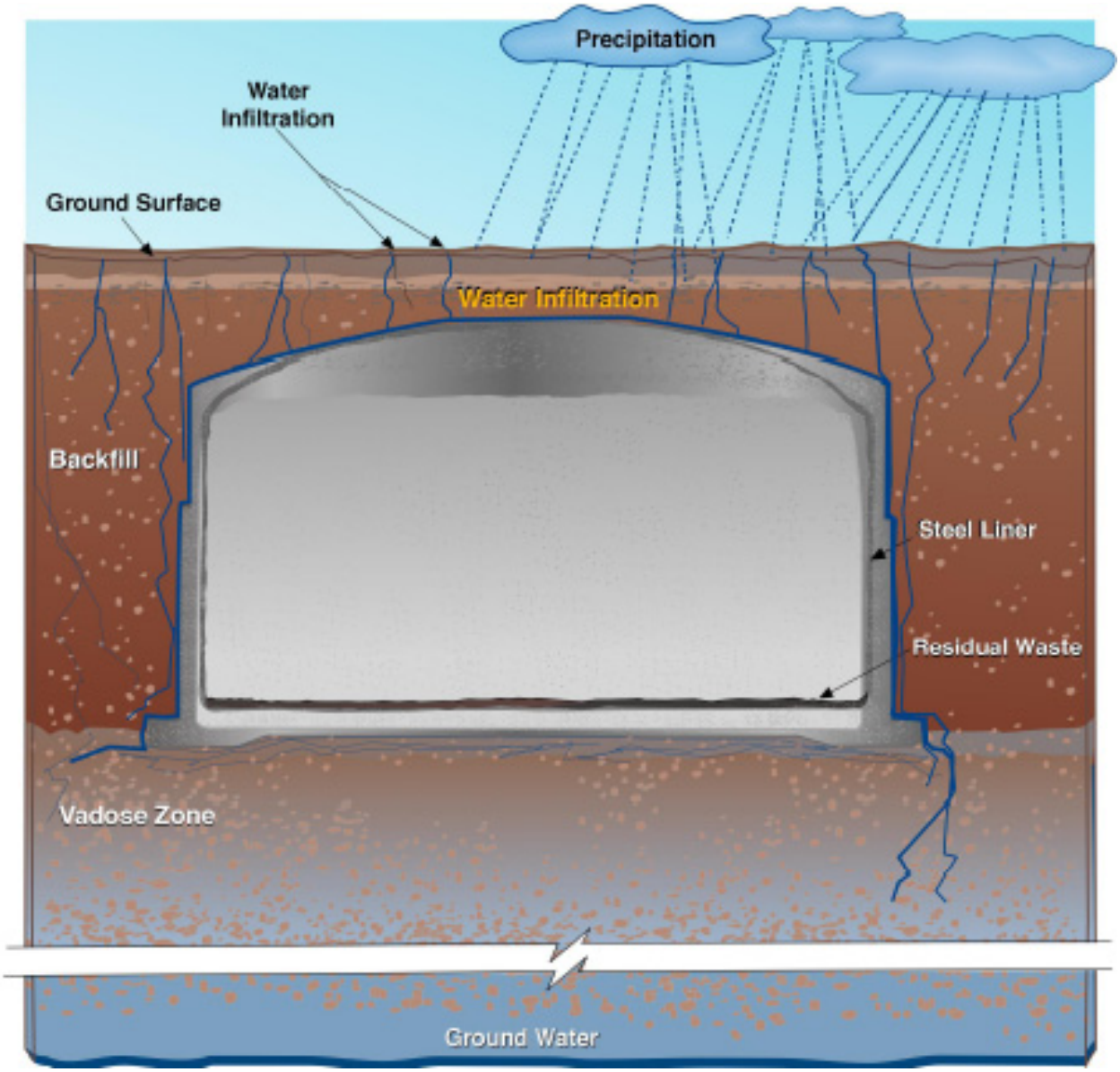

6.2.1.1.1 100-Series Tanks. The C-100-series tanks consist of a concrete base slab with a steel-plate lining. They have an inside diameter of 22.9 m (75 ft) and an internal height of 5.5 m (18 ft) from the bottom metal sheets to the top of the metal side plates, which is also the spring line for the dome. The tanks are buried underground with ~2.1 m (7 ft) of backfill over the top of the dome to provide shielding from radiation exposure. The details of the engineered structure at the base of the C-100-series tanks are shown in Figures 6-7 and 6-8. The structures were built by installing a reinforced-concrete base that is at least 0.15 m (6 in.) thick followed by 0.05 m (2 in.) of additional grout on top, over which carbon steel liner was emplaced. Following the

completion of the bottom of the tank, the sidewalls of the metal liner were welded together and the liner was encased in sidewall concrete ~0.3 m (1 ft) thick. A concrete dome ~0.38 m (1.25 ft) thick was erected on top of the tank with a 3-ply waterproof membrane applied to the top of the dome.

The carbon steel liner thickness varies, from 0.95 cm (0.375 in.) thick at the base of the tank to 0.64 cm (0.25 in.) thick along the sides. As shown in Figure 6-6, the residual waste layer is conceptualized to be located on top of the carbon steel liner. Although the carbon steel liner was designed to hold the waste in place and act as a barrier to transport of contaminants, the liner is assumed to be absent due to lack of information on its present condition. Recent studies related to characterization of the corrosion behavior of the carbon steel liner (WHC-EP-0772, "Characterization of the Corrosion Behavior of the Carbon Steel Liner in Hanford Site Single-Shell Tanks") determined several likely corrosion processes within the tank environment that could lead to degradation of steel. Some of the likely corrosion processes are pitting and crevice corrosion, stress corrosion cracking, general corrosion, and galvanic cell corrosion. These are discussed in more detail in RPP-RPT-46879. These processes lead to uncertainties regarding the state of the carbon steel liner; consequently, it is assumed to be absent in the model. As a result, the residual waste layer is conceptualized to overlie the 0.05-m (2-in.)-thick grout layer that is underlain by the 0.15-m (6-in.)-thick base slab concrete layer. The source term model represents the shortest possible vertical diffusive transport path length from residual waste layer to outside of the tank, which is the combined thickness of grout and base slab concrete layer of 0.2 m (8 in.). The diffusive area is taken to be the base area of the tank. The aqueous concentration of contaminants in the residual waste provide the upstream boundary concentration for diffusive transport with a zero concentration boundary being applied in the far-field (at the water table depth). The source term release calculations are performed using the system model.

6.2.1.1.2 200-Series Tanks. The details of the engineered structure at the base of the C-200-series tanks is presented in Figure 6-9. The 200-series tanks have an internal diameter of 6.1 m (20 ft) and an operating depth of 7.3 m (24 ft). Other than the difference in dimensions, the basic construction of the 200-series tanks is similar to the 100-series tanks. The 200-series tanks also have a base concrete slab over which a grout layer and a steel liner is present. The thickness of the base concrete slab is 0.15 m (6 in.), while the grout layer is 0.025 m (1 in.), leading to a combined thickness of 0.178 m (7 in.). Because the thickness differences are minor between the 100-series and 200-series tanks, a constant thickness of 0.2 m (8 in.) is applied to all the tanks for simplifying the diffusive transport calculations. Note that this thickness is conservative for diffusive release calculations as it ignores thickness of overlying steel liner (or steel corrosion products) and the residual waste (sludge) layer.

6.2.1.1.3 244-CR Process Tank Vault. The configuration of the 244-CR vault that is located in the southwest corner of the C Farm complex is shown in Figure 6-10 (with additional details shown in Figure 3-40). The vault is a two-level, underground, reinforced-concrete structure. The lower level consists of four cells, each equipped with a concrete sump. The exterior walls and dividing walls between the cells are 0.61 m (2 ft) thick, with each cell housing a steel tank. The cells housing tanks CR-011 and CR-001 are each 7.9 m (26 ft) long by 6.7 m (22 ft) wide. The cells housing tanks CR-002 and CR-003 are each 6.1 m (20 ft) long by 4.9 m (16 ft) wide.

Although the cells are distinct, for the purpose of source term modeling their inventory is assumed to be uniformly distributed over the rectangular footprint of the 244-CR vault of ~28-m (92-ft) length and 5.8-m (19-ft) width. The residual waste layer is conceptualized to be present over the grouted base of the tank, and the diffusive thickness is assumed to be 0.2 m (8 in.) to be consistent with the path lengths assumed for the 100-series and 200-series tanks.

6.2.1.1.4 Pipelines. An extensive network of transfer lines connects the various components of the tank farms. These pipelines carried a variety of process wastes, typically in a slurry form. The initial tank farm waste-transfer pipelines installed in 1944 to 1945 were direct-buried (not encased) pipelines, with some on concrete slabs. Typical burial depth was 1 m (3 ft). After 1947, all pipelines installed were either concrete encased or pipe-in-pipe encased. The primary pipe used was typically carbon or stainless steel. Figure 6-11 shows the areal extent of active and existing pipelines in WMA C during the 1961 to 1978 time period.

As discussed in RPP-PLAN-47559, ~11.2 km (7 mi) and 200 separate pipelines with different diameters and lengths comprise the abandoned pipelines in WMA C. Appendix A of RPP-PLAN-47559 compiles the information on various pipeline segments, indicating that the pipeline diameters typically vary from 0.05 m (2 in.) to 0.15 m (6 in.), with 0.076 m (3 in.) pipe diameter being the most common.

The residual pipeline inventory is based on the assumption of eight fully plugged cascade lines, one known plugged pipeline, and remaining pipelines assumed to be 5% full (RPP-PLAN-47559). Although the source inventory within the pipeline is spatially variable, for the purpose of the source release calculations the pipeline residual inventory is assumed uniformly distributed over a square area of side length 150 m (492 ft). This square area of areal extent 225,000 m^2 (0.09 mi^2) roughly coincides with the pipeline extent area shown in Figure 6-11. The contaminated thickness in the vertical direction is 0.076 m (3 in.), which is the most common pipeline diameter. The residual inventory is uniformly distributed within this volume mixed in with the bulk soil (backfill). Even though the pipeline material (carbon steel or stainless steel) or any pipe grout-fill (that may occur in the future) may act as a barrier, it is not considered in the model and the mass release from pipeline is both advective and diffusive.

6.2.1.1.5 Gas-Phase Diffusive Flux. While the infill grout is intact, upward gaseous diffusion of volatile contaminants is modeled from the residual waste layer towards the atmosphere. The air content within the infill grout is assumed to be 6% based on characterization information for possible Hanford grout (WSRC-TR-2005-00195, "Summary of Grout Development and Testing for Single Shell Tank Closure at Hanford"). Upward diffusive gas phase transport through the tank occurs along a 10-m (32.8-ft)-long pathway towards the land surface. This pathway is split into a lower 5-m (16.4-ft) thickness composed of infill grout material followed by another 5-m (16.4-ft) thickness of soil overburden. The porosity and saturation of the infill grout and soil overburden for the purpose of diffusive release calculations are fixed over time. The surface barrier that will be emplaced at closure over the tank farm will provide additional depth to the waste. For performing the air pathway calculations, this thickness is conservatively ignored.

Figure 6-7. Engineered Structure at the Base of the C-100-Series Tank.

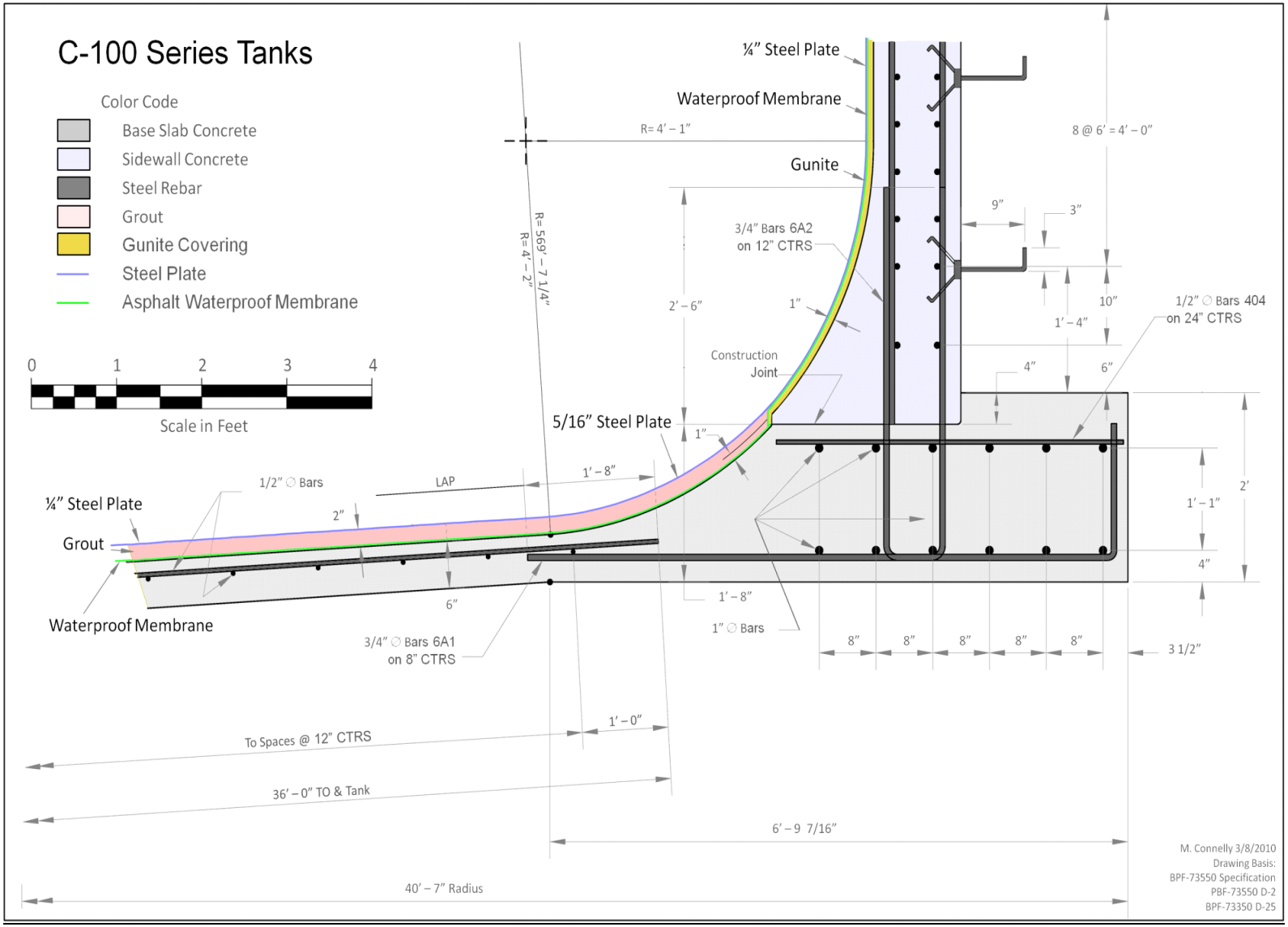

Reference: BPF-73550, "Specifications For Construction of Composite Storage Tanks Bldg. No. 241 Hanford Engineer Works Project 9536."

Figure 6-8. C-100-Series Tank Corner Features.

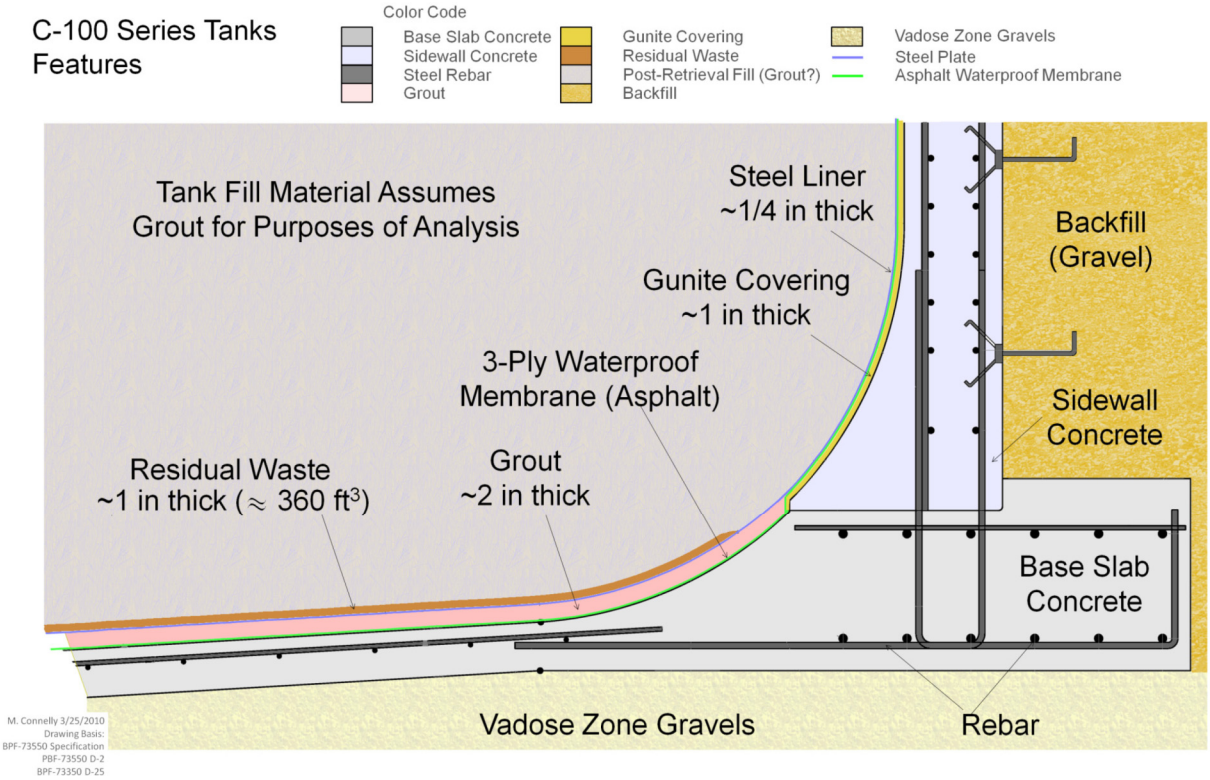

Reference: BPF-73550, "Specifications For Construction of Composite Storage Tanks Bldg. No. 241 Hanford Engineer Works Project 9536."

6.2.1.2 Evaluation of Tank Stability. At closure, the tanks will be filled in with grout to provide structural and chemical stability and low permeability. During the placement of grout, the tank structure itself acts as a form into which the grout is poured. If the placement is not significantly interrupted, and if the grout mixes meet the placement specifications, the result will be a large monolith of emplaced grout. The PA model calculations assume a 5-m (16.4-ft) thickness of the infill grout.

As the grout is not yet specified, reasonable assumptions are made about its likely composition and behavior. A possible tank fill is described in WSRC-TR-2005-00195 as consisting of three layers of grout: free flowing layer, structural stability layer, and a high compressive strength layer. The grout is anticipated to be formulated to meet the following core functions of the tank fill materials:

1. To confine residual waste through limitation of flow and through chemical stabilization of the residual material

2. To provide stability and minimize maintenance

3. To reduce potential for infiltration or inadvertent intrusion.

Figure 6-9. C-200-Series Tank Cross-Section.

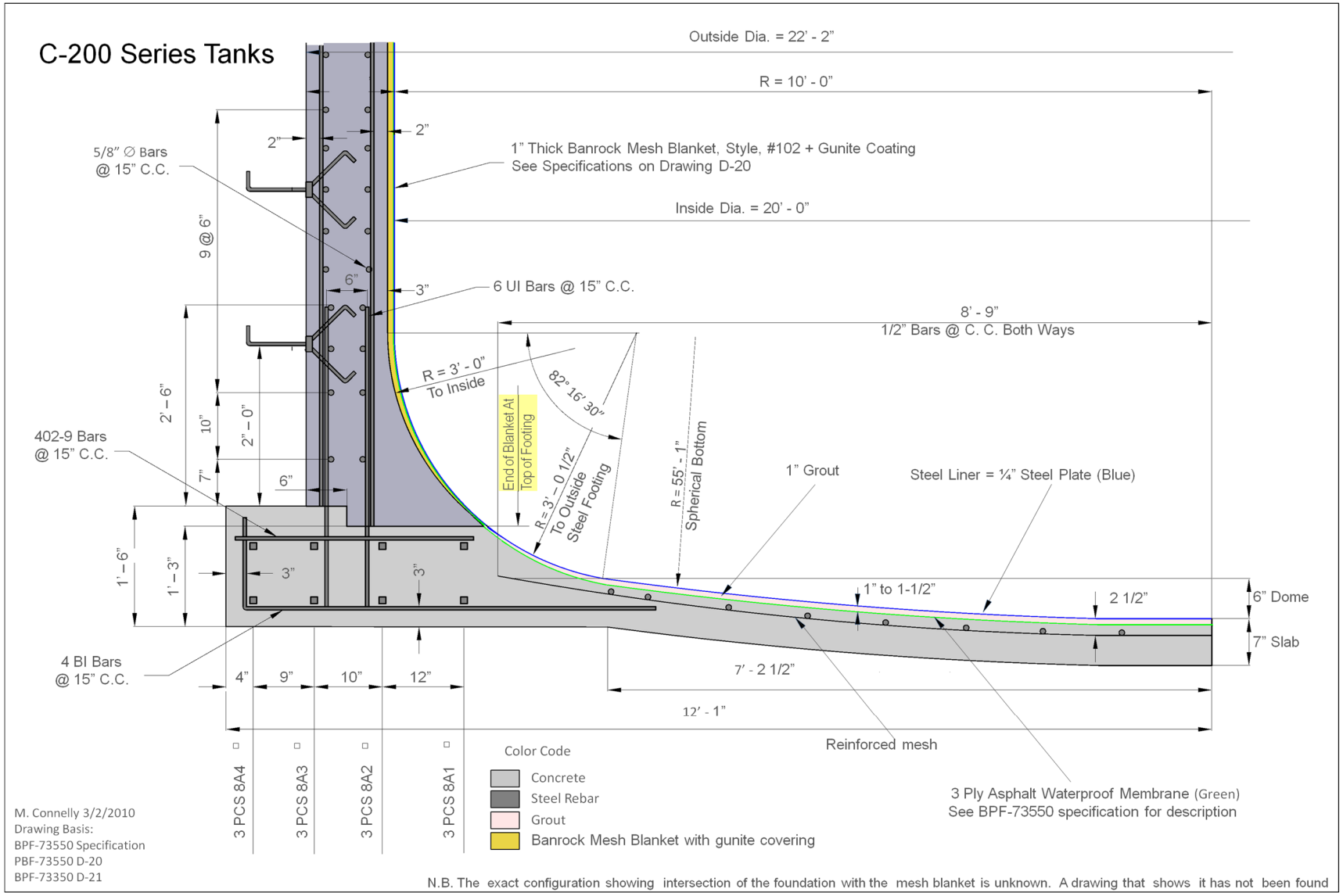

Reference: BPF-73550, "Specifications For Construction of Composite Storage Tanks Bldg. No. 241 Hanford Engineer Works Project 9536."

Figure 6-10. Schematic of the 244-CR Process Tank Vault in Waste Management Area C.

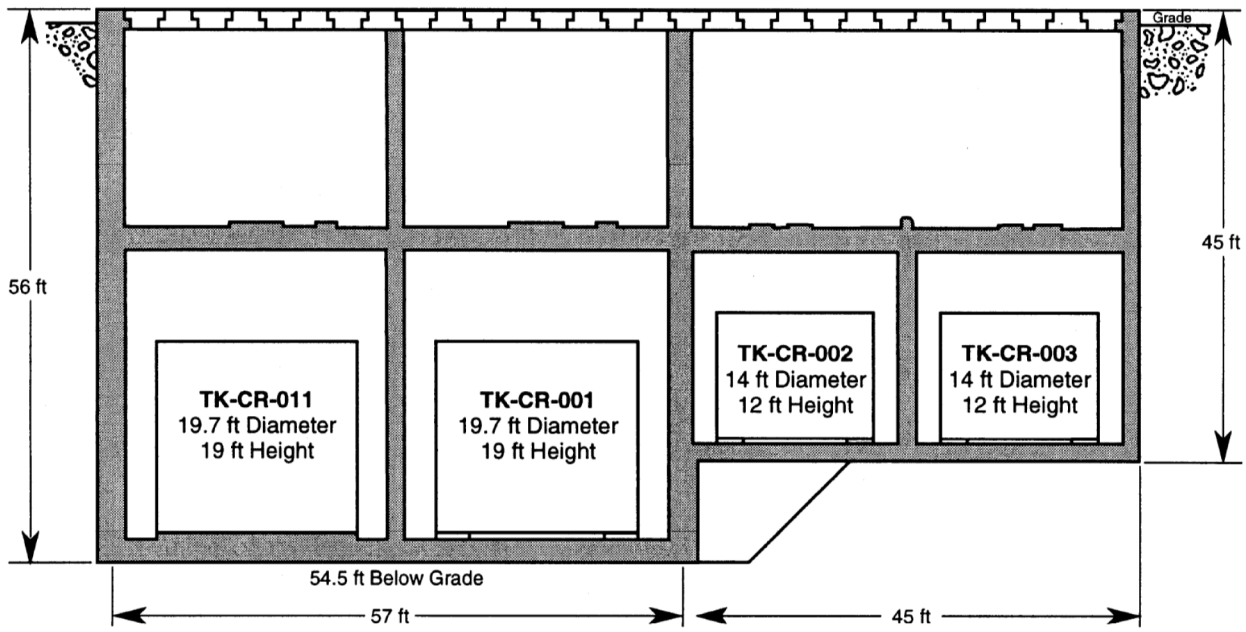

The exact composition of grout is currently unknown, but it is likely to provide a significant barrier to flow through the tank, thereby restricting the release from the residual waste to be diffusive controlled. Once the grout meets compressive strength to resist deformation, limited physical damage is expected since the tank structure is below ground and will be protected by lithostatic (overburden) pressure. Degradation due to freezing and thawing is not likely to be significant either, due to depth of the tanks and ancillary equipment being below the freeze zone (deeper than 0.61 m [24 in.]). In addition, the geochemical conditions in the Hanford vadose zone are favorable for preventing concrete degradation. The Hanford soil pore waters are alkaline and are at or near saturation with calcite; therefore, any meaningful decalcification (acid attack) is unlikely. The tank wall and grouted infill material is expected to undergo slow chemical and physical degradation. Therefore, the monolith is likely to remain an effective hydrologic barrier for a very long time as discussed in Section 6.2.1.2.3.

6.2.1.2.1 Grout Degradation. After closure, the tank concrete and grout is exposed to a combination of physical and chemical processes. Some processes may be beneficial (for example, continuing hydration and self-sealing of cracks), while others may create deleterious changes, such as shrinkage and thermal cracking. Although the geochemical conditions at the Hanford Site are favorable to preventing grout and concrete degradation, there are potential chemical degradation mechanisms that under certain conditions could lead to degradation of concrete forming the tank wall and the tank infill grout material. These key chemical degradation mechanisms are discussed and evaluated below along with the reasoning as to why these mechanisms are not carried forward into the numerical modeling.

Carbonation. Carbonation is the process where the CO_2 available in the soil-gas reacts with the calcium hydroxide in concrete to form calcium carbonate. This process is shown in Figure 6-12,

where the CO_2 (g) is supplied by gaseous diffusion through the soil column. The carbonation reaction front is defined as the interface where the $Ca(OH)_2$ actively reacts with CO_2 gas and where the pH transitions from >12 [reflecting $Ca(OH)_2$ equilibrated pore water] to pH of 9 (reflecting $CaCO_3$ equilibrated pore water). Carbonation of concrete is a slow and continuous process that progresses from the outer surface inwards but slows down with increasing diffusive length. Detailed studies have indicated that movement of a carbonation front is typically proportional to the square root of exposure time. Carbonation has two effects: it increases mechanical strength of concrete by reducing permeability and reducing porosity (calcite has higher molar volume than portlandite), but is also decreases alkalinity, which is essential for corrosion prevention of the steel liner and other reinforcement steel. Below a pH of 10, the steel's thin layer of surface passivation dissolves and corrosion is promoted. Depending on the amount of steel present and its role in maintaining structural integrity of the tank, the stability of the tank can be compromised. Unlike normal reinforced concrete where significant amounts of rebar are present, the WMA C SSTs have relatively little equipment (and therefore steel) incorporated into the grout.

The process of carbonation continues until all of the $Ca(OH)_2$ is dissolved. At this point, the dissolution chemistry is controlled by other hydrated calcium silicate and aluminate phases. When all of the $Ca(OH)_2$ has been leached away, other constituents become exposed to chemical decomposition. This decomposition eventually leaves behind silica and alumina compounds, which have little or no strength.

Sulfate attack. Sulfate attack represents a complex set of chemical and physical processes where the hydrated and unreacted phases in portland cement react with sulfate ions to form solid phases. This can lead to increased cracking due to formation of sulfate-bearing phases such as ettringite and gypsum, with considerable local expansion. Sulfate attack is typically managed by minimizing the reactive component (tricalcium aluminate) in the cement. The source of sulfate can be external (infiltrating water) or internal (from the concrete/cement itself). Delayed ettringite can form from an internal sulfate source such as sulfate present in the tank residuals. Although there may be some sulfate in the tank residuals, this amount is generally small (compared to the amount of grout infill) due to extensive washing and cleaning steps undertaken to remove the sludge. In addition, the grout is produced using low sulfate water with aggregate (fine sand) that is low in sulfate. The external source of sulfate is going to be slowly infiltrating waters, which have low sulfate content. Due to limited availability of sulfate, the impact from sulfate attack is not expected to be important for grout degradation in Hanford SSTs.

Alkali-aggregate Attack. The alkali-aggregate reaction occurs when aggregates containing reactive silica react with sodium and potassium oxides in the portland cement to form an alkali-silica gel. This gel can absorb water, which in turn can lead to expansion and cracking of the grout. In the mixes for Hanford tank fill, non-reactive quartz sand will likely be used. In addition, it is known that substitution of fly ash and blast furnace slag for some of the portland cement will mitigate the impact of the alkali-aggregate reactions. Finally, portland cements produced today intentionally have low amounts of alkali content to avoid alkali-aggregate reaction. Therefore, it appears unlikely that cracking due to alkali-aggregate reaction would occur in the Hanford SSTs.

Figure 6-11. Location of Active and Existing Pipelines Along with New and Existing Facilities for Waste Fractionization Operations (1961 to 1978).

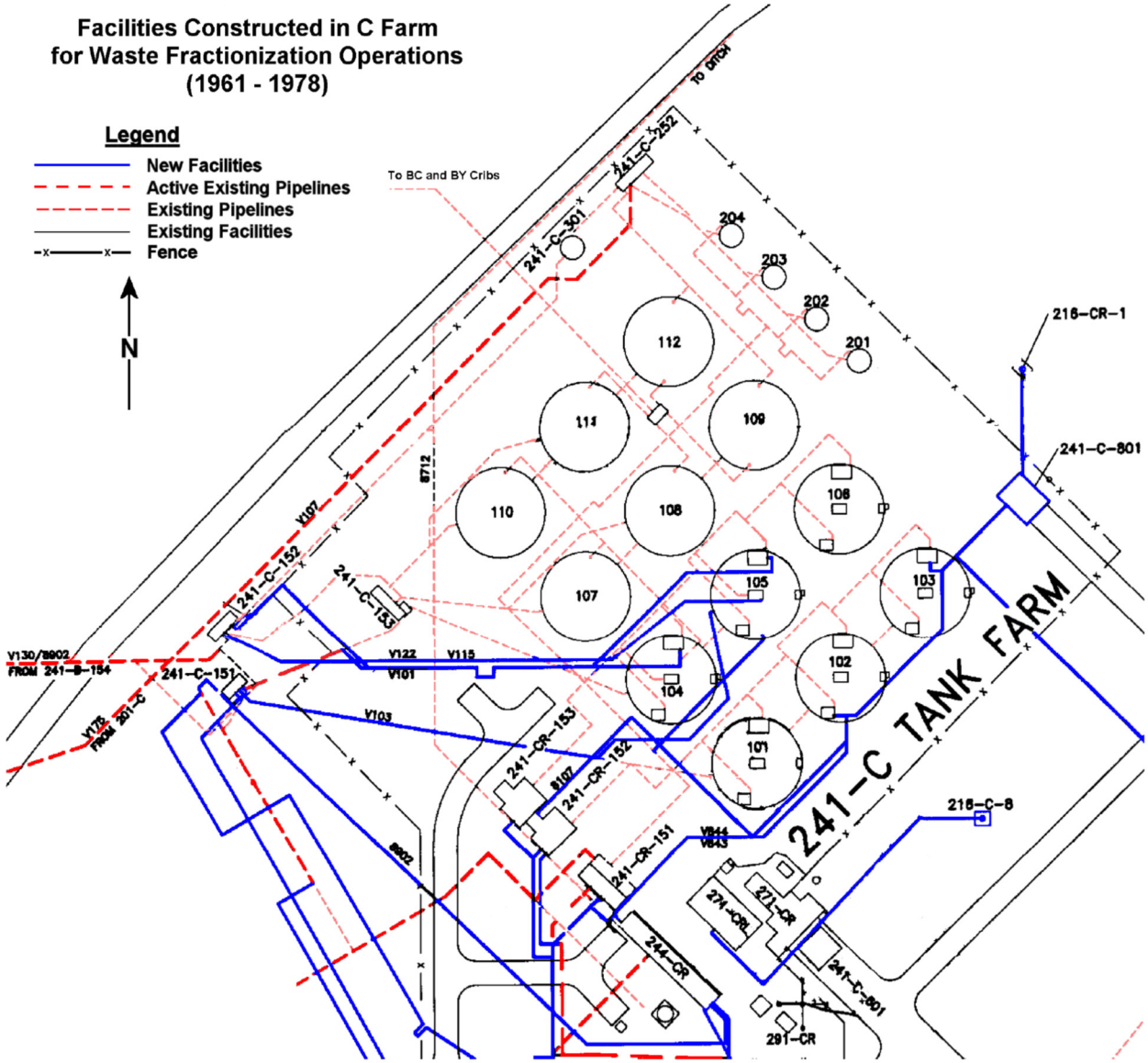

Acid Leaching (Decalcification). Acid leaching or decalcification refers to leaching of calcium ions (coupled with hydroxide ions) from pore solutions and dissolution of calcium hydroxide, C-S-H, and hydrated calcium aluminate phases in cementitious materials [WSRC-STI-2007-00607, "Chemical Degradation Assessment of Cementitious Materials for the HLW Tank Closure Project (U)"]. This form of degradation occurs when concrete is in contact with acidic water for long periods of time. The ultimate residue produced by decalcification consists of hydrous forms of silica (silica gel), alumina (alumina gel), and iron oxide. The rate of attack depends on the flow rate and the chemistry of water. Since ambient Hanford pore waters have high alkalinity and are at near saturation with calcite mineral phase, the process of decalcification is likely to be very slow, if it occurs at all.

Figure 6-12. Carbonation Process Acting on the Buried Tank Wall.

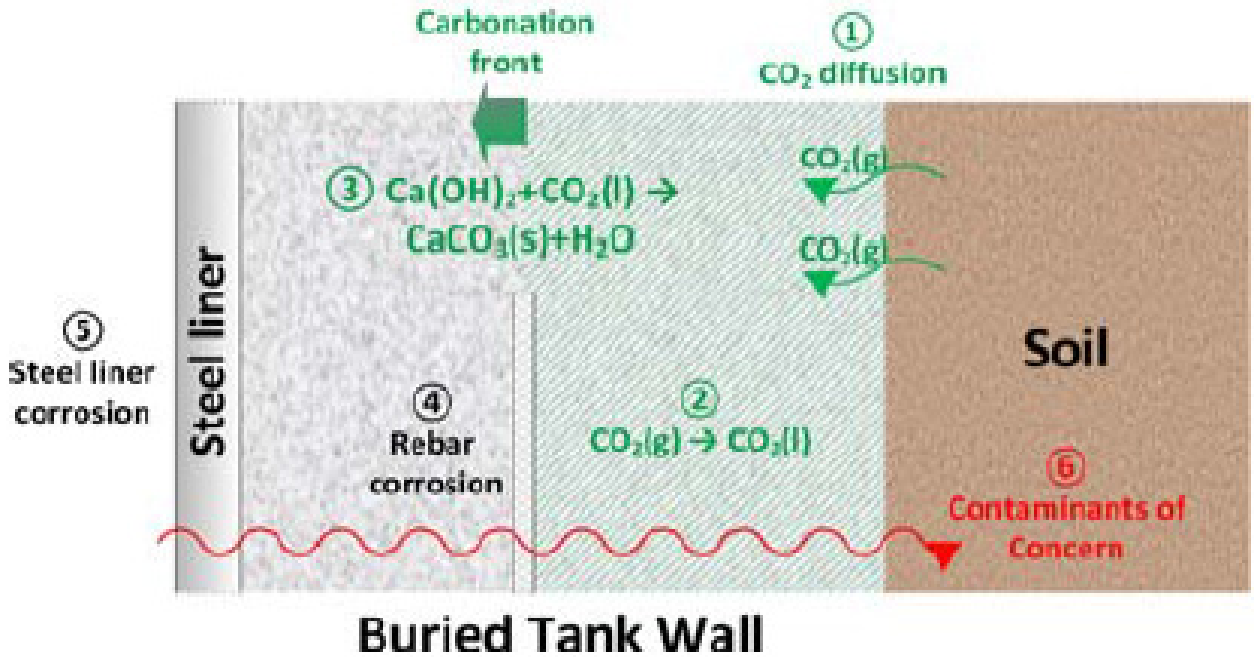

Current evaluations of chemical conditions inside the tank (based on residual waste chemistry) and outside the tank (based on pore water chemistry) indicate very benign conditions with regard to chemical degradation of concrete and tank-fill grout material. Consequently, the degradation due to chemical processes will progress at a very slow rate. Among the processes evaluated, carbonation was identified as the most likely chemical degradation mechanism, which will proceed naturally due to availability of CO_2 via gaseous diffusion.

6.2.1.2.2 Grout Monolith Stability. During scale-up testing for tank infill material, two monolith structures were created and tested for strength. The details are presented in WSRC-TR-2005-00195. Figure 6-13 shows the two monolith structures produced by placing three layers of grout into 4.6-m (15-ft)-diameter swimming pools during scale-up testing. These monoliths remained after the swimming pool structures were removed. The layered monoliths displayed significant strength, as demonstrated by the difficulty encountered in breaking them apart. In fact, the bulldozer and the heavy-duty forklift shown in the figure were unable to turn over the monoliths. Both monoliths were repeatedly lifted on one side and dropped without breaking. Eventually, the bulldozer was able to break the monoliths along horizontal planes by ramming the bulldozer blade at the level of the interfacial areas. These tests indicate substantial increase in strength even though these monoliths were in initial phase of curing (only 5 days after the capping grout had been poured, and about 8 total days since the pouring of the first stabilization layer). Compressive strength measurements confirmed this and indicate that significant strengthening likely continues to occur out to 90 days of curing.

6.2.1.2.3 Hanford Tank Concrete Evaluation. As part of the initiative to evaluate the structural integrity of the tanks (called Single-Shell Tank Integrity Project or SSTIP), a 1.4-m (55-in.)-diameter reinforced concrete dome “Plug” was removed from tank C-107 in December 2010. More recently, an 11.6-m (38-ft) sidewall concrete core was removed from

tank 241-A-106 (located in the WMA A-AX south of WMA C) in May 2014. Results from inspection, physical testing, and petrographic examination of the concrete cores are reported in RPP-RPT-50934 and RPP-RPT-58254. These analyses are very important in predicting the tank wall degradation because they provide direct empirical evidence on the state of concrete wall material after being left underground for 60 to 70 years. The results of analyses that are relevant for the PA are discussed below.

The 1.4-m (55-in.)-diameter concrete section ("Plug") removed from the center of the dome of tank C-107 is shown in Figure 6-14. It was removed using a combination of high-pressure water and garnet abrasive. Fourteen cores were taken from the concrete "Plug," each 10.7 cm (4.2 in.) in diameter. Of those 14 cores, 12 underwent mechanical testing and 2 underwent petrographic examination. No cracks or large air voids were found during the inspection process. Additionally, the protective asphaltic membrane and mortar layers that were laid out during the construction were found to be intact. The average compressive strength of all of the tested cores was about 55,158 kPa (8,000 psi), more than 2.5 times the original 28-day design strength specified at the time of construction. Based on the results of petrographic examination, the concrete represented by the cores was in good condition. No distress (cracking or excessive microcracking) was observed in either core. The concrete showed no evidence of chemical attack, significant alkali-aggregate reactions, or other deleterious mechanisms involving aggregates and/or paste constituents. The concrete in both cores exhibited good physical paste properties. Apart from localized softer paste at the immediate top surface, the paste in the cores was hard and dense through the depth of the concrete. Distribution of aggregates and other paste constituents was uniform. Macroscopically, the cores were well consolidated (no large voids). The cement was nearly completely hydrated. The depth of carbonation from the top surface of both cores was reported to be 1 to 2 mm (0.04 to 0.08 in.).

Sidewall coring of tank 241-A-106 was completed over two weeks in May 2014. Over 11.6 m (38 ft) of concrete core (8.4-cm [3.3-in.] diameter) was successfully removed to a depth approximately halfway through the tank footing. This tank was chosen due to its high heat load history and concerns over the thermal degradation of the concrete from heat exposure. The collected concrete cores are shown in Figure 6-15. Physical testing for structural integrity indicated favorable results, with values generally greater, and in many cases significantly greater, than expected. It is concluded that the effects of thermal degradation on the mechanical properties of the concrete appear to be negligible. No deficiencies were found with regard to the structural integrity of the tank. Petrographic analyses determined that the concrete is in overall good condition, with a minor amount of microcracking and minor evidence of deleterious mechanisms that do not appear to have significantly affected the overall quality and integrity of the concrete (RPP-RPT-58254). The concrete was composed of siliceous natural gravel coarse aggregate and natural sand fine aggregate uniformly distributed in a portland cement paste binder. The paste appeared to be of good quality, although some degree of paste alteration (leaching of calcium hydroxide from the paste) was observed, along with a small amount of secondary ettringite mineral, possibly from sulfate containing impurities in the paste. Only one crack and very few microcracks were observed in the examined core segments. A very minor degree of alkali-silica reaction (ASR) had occurred in the concrete; however, no deterioration (no associated cracks or microcracks) was observed. Given the age of the concrete and current degree of ASR, further reaction and/or associated expansion is deemed unlikely. The depth of

carbonation was found to be shallow and about 1 to 4 mm from outer surface in some core segments (RPP-RPT-58254).

Results of material properties tests of concrete cores from the haunch and wall of tank 241-SX-115 (SX-115) and 202-A PUREX Canyon Building have been evaluated and documented in RHO-RE-CR-2, "Strength and Elastic Properties Tests of Hanford Concrete Cores – 241-SX-115 Tank and 202-A Purex Canyon Building." Both structures were built in the 1953 to 1954 time frame using the same concrete mix design. Compression strength and tensile strength tests on concrete samples taken from tank SX-115 in year 1981 indicated a pattern of possible decreasing strength with depth, but all samples were above the design value (compressive strength of 20,680 kPa [3,000 psi]). Material property tests were conducted on 17 specimens from the 202-A PUREX Building under three temperature conditions: unheated, heated to 93.3 °C (200 °F), and heated to 93.3 °C (200 °F) and then cooled to ambient temperature. The rate of heating was set at 23.9 °C/day (75 °F/day) to determine if the heat-up rate was significant in affecting the strength. The compressive strength for samples tested after heating to 93.3 °C (200 °F) showed a small decline compared to the unheated samples. However, for samples that were heated to 93.3 °C (200 °F) and then allowed to cool to ambient temperature, some strength recovery was observed with values falling well within the range of strengths measured for the unheated concrete. The compressive strengths of the 202-A PUREX Building concrete specimens were in excess of 20,680 kPa (3,000 psi) design value in all cases.

Visual inspection of 37 concrete core samples from tank SX-115 and 17 concrete core samples from 202-A PUREX Building indicated that most of the samples had no visible signs of concrete deterioration. However, four tank farm cores and two PUREX Building cores were found to have visible cracks, ranging from ~5 to 25 cm (2 to 10 in.) in length, possibly from coring activities.

A number of tests have been performed to evaluate the strength and elastic properties of the Hanford Tank Farm concrete core materials for temperatures varying from 22.2 °C to 121.1 °C (72 °F to 250 °F) (RHO-RE-CR-2). These tests were conducted on 7.6 cm by 15.2 cm (3 in. by 6 in.) cylinders fabricated from core materials from the 241-A, 241-S, 241-T, and 241-U Tank Farms. The 241-A Tank Farm concrete compressive and tensile strengths were about 45% greater than those values obtained from tank SX-115 concrete; however, the elastic properties were essentially equal. This could be due to variations between concrete batches or the fact that SX-115 tank wall concrete was subjected to higher temperatures during tank farm operations than the dome concrete in the 241-A Tank Farm. In no case did compressive strength of any tank SX-115 specimen fall below 20,680 kPa (3,000 psi). The lowest strength measured was 26,372 kPa (3,825 psi).

These results indicate that the concrete walls within WMA C tanks are likely to be structurally stable and in relatively good condition. The elevated temperatures experienced due to heat generated from radioactive decay and chemical reactions within the tank are unlikely to cause any appreciable decline in strength of the concrete in the tank walls.

Figure 6-13. Demolition of (a) Pool 1 Monolith and (b) Pool 2 Monolith after Only 5 Days after the Capping Layer had been Poured.
Note that monolith from Pool 2 is in the foreground in (a). Also note the vertical crack in the Pool 2 monolith that occurred during the demolition.

(a)

(b)

Figure 6-14. Evaluation of 55-inch Diameter Reinforced Concrete Dome Plug from Tank 214-C-107.

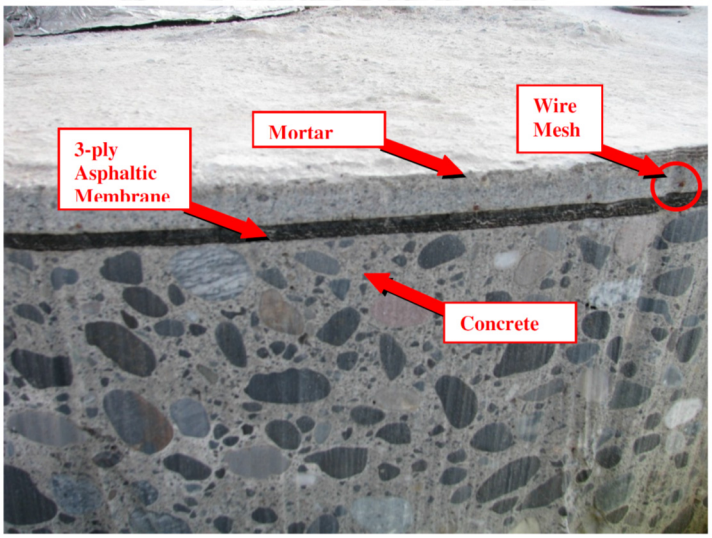

Figure 6-15. Evaluation of Sidewall Concrete Core from Tank 241-A-106.

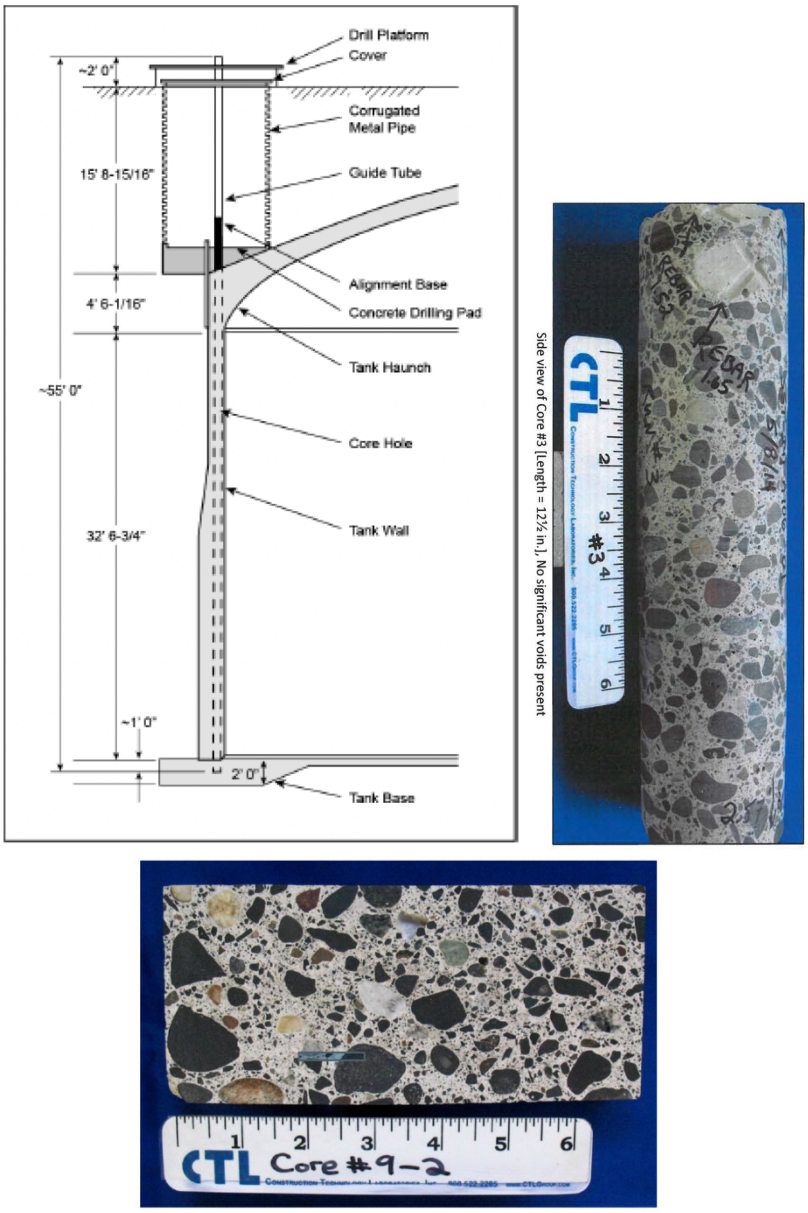

Aboveground Concrete Structure Evaluation. In addition to the concrete samples taken from SSTs, some information on chemical degradation is also available from concrete cores taken from aboveground concrete structures on the Hanford Site. PNNL-23841, "Radionuclide Migration through Sediment and Concrete: 16 Years of Investigations" summarizes the characteristics of three concrete cores from aboveground structures that have been exposed to Hanford weather for 14, 28, and 57 years. The characterization summary is presented in Table 6-1. A minor degree of microcracking is noticeable, along with a moderately tight paste-aggregate bond. Ettringite is observed in the void spaces. The depth of carbonation increases with increasing age of the concrete. In the oldest specimen (213J), the carbonation had extended ~50 mm (1.97 in.) into the concrete wall. Given the limited data, the rate of

carbonation of concrete at the Hanford Site can be estimated at ~0.3 to 0.9 mm (0.01 to 0.04 in.) per year. This carbonation rate provides an upper bound value that can be expected for a concrete under Hanford Site conditions.

Table 6-1. Characteristics of Concrete Cores from Aboveground Structures at the Hanford Site.

Characteristic	Field Lysimeter Test Facility Sample	622C Sample	213J Sample
Age	14	28	57
Carbonation Depth (mm)	1 – 10	2 – 8	48 – 53
Air Content (%)	4 – 5	2 – 4	1 – 2
Water/Cement Ratio	0.5 – 0.55	0.5 – 0.55	0.52 – 0.57
Secondary Deposits	Abundant ettringite lining voids	Ettringite lining voids	None in outer 50 mm – minor ettringite lining voids
Microcracks	Minor	Minor	Common in outer 50 mm
Steel	#4 ~103 mm cover	None	#4 ~80 mm cover
Unit Weight (pcf)	153	152	148
Aggregates	Well-graded siliceous gravel, 19 mm top size	Well-graded siliceous gravel, 23 mm top size	Well-graded siliceous gravel, 21 mm top size
Paste-Aggregate Bond	Moderately tight	Moderately tight	Moderately tight to moderately weak

Reference: PNNL-23841, "Radionuclide Migration through Sediment and Concrete: 16 Years of Investigations."

Observations of the cores for buried Hanford tanks indicate the carbonation depth ranges from 1 to 4 mm (0.04 to 0.16 in.). Considering about 60 to 70 years of burial time, the carbonation rates are calculated to be ~0.01 to 0.07 mm/yr (0.0004 to 0.0028 in./yr). For the aboveground concrete structure, the carbonation rate is expectedly much higher and calculated to be about 0.3 to 0.9 mm/yr (0.01 to 0.04 in.). However, the rate of carbonation would be affected by several factors, such as concrete composition, porosity, and the degree of exposure to weathering.

Simplifying carbonation as a sharp moving front, a simple analytical expression for the location x_c (mm) of the carbonation front when Relative Humidity exceeds 50% can be given as follows (Brown et al. 2013, "Modeling Carbonation of High-Level Waste Tank Integrity and Closure"):

$$x_c = A\sqrt{t}$$

where A is proportionality constant and a function of initial CO_2 concentration, effective diffusivity of CO_2, etc., while t is exposure time.

Experimental results have confirmed this non-linear relationship between the carbonation front and square root of exposure time. For the sake of simplicity, and in order to do a bounding

calculation, one can assume that the maximum depth of carbonation within the buried concrete tank structure is 10 mm (0.39 in.) (instead of the observed 1 to 4 mm [0.039 to 0.157 in.]). Next, considering 70 years of exposure time (burial time of SST in WMA C), the proportionality constant (*A*) can be calculated from the above equation to be 1.2 mm (0.05 in.) per square root of time in year. This Hanford Site-specific proportionality constant can then be used to calculate the depth of carbonation front as a function of time. Depths of carbonation front are calculated for arbitrary time periods in Table 6-2. Considering that a 0.2 m (8 in.) minimum thickness of concrete (and grout) layer exists at the base of the tank, the time for the carbonation front to propagate through this thickness will take over 20,000 years. The actual time frames would be even longer, since the observed depth of carbonation is 1 to 4 mm (0.039 to 0.157 in.) instead of assumed 10 mm (0.39 in.) for this calculation.

Table 6-2. Bounding Depth of Carbonation for Buried Concrete Calculated For Different Exposure Times Under Hanford-Specific Conditions.

Elapsed Time (yr)	Depth (mm)	Depth (inches)
1,000	37.8	1.5
5,000	84.5	3.3
10,000	119.5	4.7
20,000	169.0	6.7
50,000	267.3	10.5
100,000	378.0	14.9

The above calculated time does not include carbonation through the infill grout material, which will also have to undergo chemical degradation (likely carbonation) before tank integrity can be assumed to be lost. A simple calculation—using 5.5 m (18 ft) grout thickness in the tank, and assuming carbonation front propagating from both top and bottom directions, and assuming a bounding 0.1 mm/yr (0.004 in./yr) linear carbonation rate—shows that the grout will not be fully degraded for another 27,500 years. As a result, the total time for the carbonation front to move through both the concrete wall and the infill grout can easily exceed 50,000 years. Results from recent modeling conducted by Brown et al. (2013) under Hanford subsurface conditions (assuming 2.4% CO_2 in soil gas at 90% concrete saturations) indicates that the carbonation front propagation rate is < 0.1 mm/yr (0.004 in./yr).

The information presented above indicates that it is highly unlikely for the tank degradation to occur within the modeled time period of 10,000 years. As a result, the water entry in the tank is likely to be very slow or nonexistent altogether. For the purpose of the PA analysis, the infill grout is conceptualized to be located above the thin residual waste layer and separated from the grout/concrete layer at the base of the tank. While the infill grout is intact, no water can flow through the residual waste, and therefore the primary contaminant transport pathway is by diffusion through water in the pore spaces to the base of the tank and into the underlying vadose zone.

Natural Analogues. A way to gain insight into the longevity (durability) of grout, concrete, and mortar is through consideration of some of the well-studied ancient structures such as the Pantheon in Rome, Hadrian's Wall in Scotland, the Roman Aqueducts system, etc. Their durability is discussed in WSRC-TR-2005-00195. Such ancient structures that use pozzolanic materials in conjunction with hydrated lime [$Ca(OH)_2$] best simulate modern day concrete, grout, and mortar. Some of these ancient structures have existed for over 2,000 years despite being subjected to weather, abrasion, wars, and neglect. The longevity of these ancient structures, which is attributable to materials selection and placement techniques, suggests that the lifetimes for the grout monoliths within the protected, underground SSTs at Hanford could also extend into the thousands of years.

6.2.2 Radionuclide Transport

This section discusses the conceptual model of the projected transport of radionuclides from the source term through the environment to the points of exposure and identifies the mechanisms included in the analysis for groundwater, atmospheric, and biotic transport pathways.

6.2.2.1 Conceptual Model for Groundwater Pathway. This section provides an overview of major features that affect flow and transport of radionuclides within the vadose zone and saturated zone underlying WMA C. Estimates of radionuclide concentrations in environmental media are used to estimate doses to a hypothetical individual based on an assumed exposure scenario. Analysis of performance therefore requires estimates of (1) the inventory of radionuclides in the facility, (2) the release rates of these radionuclides from the tank and pipeline residual waste, and (3) the migration rates and concentrations of radionuclides released from the residual waste in environmental media (air, soil, and water).

The conceptual model of the groundwater pathway considers a diffusion-controlled release of radionuclides from the grouted tanks and ancillary equipment and an advection-controlled release from the pipelines, vertical transport through the vadose zone to the water table, and then transport laterally through the aquifer to a hypothetical well located 100 m (328 ft) downgradient. These features and processes reflect safety functions that serve as barriers to exposure in the context of defense in depth for protection of hypothetical receptors. The grouting of the tanks represents an engineered safety function or barrier to exposure, because one of the purposes of the grout is to limit the release of radionuclides from the tanks to the vadose zone. The modified RCRA Subtitle C barrier represents a hybrid barrier to exposure, because while it is an engineered structure it eventually evolves into part of the natural system. The vadose zone beneath WMA C can also be viewed as a natural barrier. Once contaminants enter the vadose zone, the low recharge (infiltration rate) controlled by the surface cover system, the thickness of the vadose zone between the base of the tanks and the unconfined aquifer, and the soil-contaminant interaction, prevent all but the least-reactive contaminants from reaching the unconfined aquifer for thousands of years. As leachate containing contaminants enters the aquifer from the vadose zone, it mixes with groundwater flowing within the saturated zone (aquifer) beneath WMA C to make concentrations of contaminants in groundwater more dilute. This dilution in concentration lowers the exposure point concentration and consequent dose to a receptor. Thus, the transport of radionuclides to the groundwater is a complicated process that depends on data and assumptions relevant to the following physical systems: (1) engineered

features of WMA C, (2) surface features of WMA C, (3) the vadose zone beneath WMA C, and (4) the saturated zone (groundwater) beneath WMA C.

First, this section describes the facility features important to modeling the release of contaminants from the source areas. This is followed by descriptions of the temporal evolution of the WMA C surface, the vadose zone stratigraphy, and the geochemical effects that impact radionuclide transport. Next is an overview discussing the basis for the saturated zone flow and transport used in the WMA C PA. The final section provides a detailed justification of important assumptions and simplifications of the vadose zone flow and transport model.

6.2.2.1.1 Waste Management Area C Facility Structures. Section 3 provides a description of WMA C and the planned surface engineered cover system. The physical system includes the closure barrier and the complex structures that make up the closed facility. The WMA C sources consist of twelve 2,006,000-L (530,000-gal) 100-series tanks, four 208,000-L (55,000-gal) 200-series tanks, a 136,000-L (36,000-gal) catch tank, a vault with two 57,000-L (15,000-gal) and two 151,000-L (40,000-gal) tanks, and an estimated 12.8 km (8 mi) of pipeline (RPP-50233, "Waste Management Area C Closure Conceptual Design Support Report"). RPP-RPT-49701 identifies the following four phases associated with the closure of WMA C.

- Facility Closure – All below-grade tanks and equipment are grouted to stabilize residual waste and void spaces.

- Demolition and Decommissioning (D&D) Activities – All above-grade facilities, equipment, utilities, and tank farm features are dispositioned, and all existing drywells and groundwater wells are decommissioned.

- Closure Cap Construction – The long-term surface barrier over the tank farm is constructed.

- Post-Closure Monitoring and Maintenance – Monitoring using a closure-related monitoring network continues as necessary to ensure the performance of the closure cap and to provide verification that the tank farm closure is satisfying the DOE O 435.1 performance objectives.

The grouting of the tanks and ancillary equipment is intended to stabilize these structures (prevent collapse) and to minimize the release of radionuclides by keeping the release controlled by diffusion processes. Contaminant releases from the grouted tanks and ancillary equipment are expected to remain diffusive, with no (or negligible) advection occurring through the tanks and ancillary equipment because sufficient degradation of the tank-wall and infill grout material is unlikely to occur within the simulated time period of 10,000 years. Chemical degradation rates are expected to be the same as carbonation rates, and it is estimated that for the carbonation front to propagate through the minimum wall thickness of a tank (~200 mm [~8 in.]), it will take ~30,000 years. This calculated time excludes grout material inside the tank, which will also have to undergo carbonation before tank integrity could be assumed to be lost.

6.2.2.1.2 Temporal Evolution of Waste Management Area C Surface. Net infiltration, deep percolation, and recharge of water are the major transport mechanisms for moving contaminants from the closed system to the groundwater. In arid and semiarid regions with thick vadose zones, such as the Hanford Site, long-term factors like climate change, changes in the annual precipitation rates, and changes in vegetation structure and community are necessary to influence the deep vertical water fluxes. In these regions, large seasonal fluctuations in soil water potential are generally contained within the upper few meters of soil, and the spatially and temporally varying moisture fluxes even out within the deep subsurface above the water table.

With expected changes to the land cover over time due to growth of vegetation, several time periods have been conceptualized (Table 6-3) to represent the changes in recharge rates and hydrologic conditions at WMA C. Each of these time periods is characterized by a different recharge rate that will be discussed in Section 6.3.2. Following is a discussion of two assumptions that pertain to recharge: (1) that net infiltration through the thick, heterogeneous vadose zone in the 200 Areas dampens the effect of discrete events, and therefore episodic precipitation events can be replaced by an average annual recharge rate; and (2) that impacts resulting from plausible climate change that may occur during the evaluation period do not adversely impact the performance of the surface or vadose zone as a barrier.

Multi-year evaluations of soil moisture content data collected from vegetated desert soils throughout the United States indicate that water potentials remain very low and relatively invariant below depths of 2 to 5 m (6.6 to 16.4 ft) ("Ecohydrological Control of Deep Drainage in Arid and Semiarid Regions" [Seyfried et al. 2005]). In response to intermittent years of elevated precipitation such as those caused by El Nino in the southwestern United States, the biomass usage of water by deep-rooted xeric vegetation increases, depleting the excess water, and no net increase in groundwater recharge occurs ("Global synthesis of groundwater recharge in semiarid and arid regions" [Scanlon et al. 2006], Analysis of Techniques for Estimating Potential Recharge and Shallow Unsaturated Zone Water Balance near Yucca Mountain, Nevada [Leary 1990]). Simulation results representing the impact of a 20-year period of temporally varying precipitation on a surface barrier and a clean, graveled surface indicate that the temporal variation in drainage can effectively be ignored, and that an average value can be used with little loss of accuracy (WHC-EP-0332, "Simulations of Infiltration of Meteoric Water and Contaminant Plume Movement in the Vadose Zone at Single-Shell Tank 241-T-106 at the Hanford Site," pp. 18-21).

The sensitivity-uncertainty period of analysis extends to 10,000 years. Therefore, impacts to the performance of the vadose zone as a barrier caused by climate change during the evaluation period are plausible. However, climate change is not likely to affect the performance of the vadose zone as a barrier appreciably. Recharge rates applied to the design and post-design periods of the modeling are likely to remain unchanged, even if the precipitation increases as a consequence of climate change. Long-term climate studies (see Section 3.1.2.6, Climate Change) indicate that for the last 10,000 years precipitation ranged from 0% to 50% less than current levels, and ranged between 75% and 128% of modern levels during the glacial period before the Holocene (PNNL-13033). The average annual precipitation (172.2 mm [6.78 in.]) at the Hanford Site for 1981 to 2010 is actually less than the lower end of the range typically associated with sagebrush-dominated ecosystems (200 to 500 mm/yr [7.87 to 19.69 in.],

U.S. Department of Agriculture, Natural Resources Conservation Service, Queried 12/18/2015, [Fact Sheets & Plant Guides/*Artemisia tridentata* ssp. tridentata], http://plants.usda.gov/plantguide/pdf/pg_artrt.pdf). Thus, the sagebrush community appears capable of exploiting any increases in soil moisture caused by increases in the annual precipitation consistent with or even in excess of the previous glacial period.

Table 6-3. Timeline Considered for Representing the Evolution of Waste Management Area C.

Phase	Conditions	Duration	Conceptual Half Cross Section of the Waste Management Area C Area
Pre-operations	Before construction of Waste Management Area C	Until steady-state moisture conditions are achieved for the year.	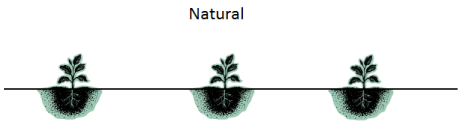
Construction and Operations	Current conditions	1945 to 2020	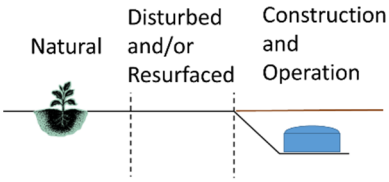
Early Post-Closure	Transition to conditions of restricted recharge due to modified RCRA C Subtitle C barrier	2020 to 2520	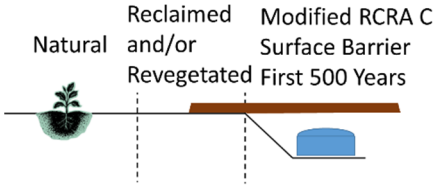
Late Post-Closure	Degraded surface barrier conditions	2520 to 12020 (end of sensitivity and uncertainty analysis evaluation period)	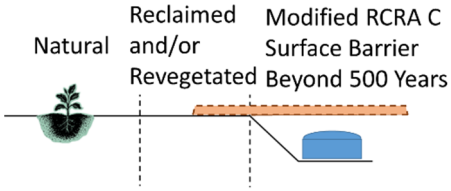

RCRA = Resource Conservation and Recovery Act of 1976

Pre-operations. Hydrologic conditions prior to the facility construction (1945) control the initial moisture content and the matric potential in the vadose zone. To estimate the initial conditions, a pre-operations phase is considered, which produces initial moisture conditions for subsequent temporal changes conceptualized at WMA C. A vegetation cover representative of natural conditions is assumed over the whole domain during this period.

Construction and Operations. The operations period (current condition) is considered to represent the WMA C construction phase along with operations until closure of the WMA. This period starts in 1945 and is assumed to end in 2020 when a surface barrier is placed over the

facility. A distinct recharge rate will be assigned to the following four different zones during this period (Figure 6-16):

- The undisturbed zone around the facility characterized by a native vegetation cover
- The disturbed zone around the facility that has scant, deep-rooted vegetation but extensive grass cover
- The resurfaced zone around the facility that has no vegetation cover
- The WMA A-AX zone that corresponds to the tank farm gravel backfill that is not covered by vegetation
- The WMA C zone that corresponds to the tank farm gravel backfill that is not covered by vegetation.

Early Post-Closure. At the end of the construction period, the early post-closure period is considered to represent the time when the modified RCRA C barrier functions according to its design specifications for 500 years according to DOE/RL-93-33. The closure barrier functions to limit the flow of infiltrating moisture into the system by its water storage capacity and built-in engineered capillary breaks. During this period, distinct recharge rates are assigned to five spatially distinct zones (Figure 6-17):

- The undisturbed zone, away from the WMA C surface barrier and the surrounding berm, characterized by an undisturbed native vegetation cover
- The disturbed zone, away from the WMA C surface barrier and the surrounding berm, characterized by an artificially-introduced vegetation cover attempting to reclaim the surface with native vegetation species
- The resurfaced zone, away from the WMA C surface barrier and the surrounding berm, characterized by an artificially-introduced vegetation cover attempting to reclaim the surface with native vegetation species
- The zone beneath the extent of the WMA A-AX surface barrier that is designed to minimize infiltration of meteoric waters
- The zone beneath the extent of the WMA C surface barrier that is designed to minimize infiltration of meteoric waters.

Figure 6-16. Surface Conditions In and Around Waste Management Area C during the Construction and Operations Period.

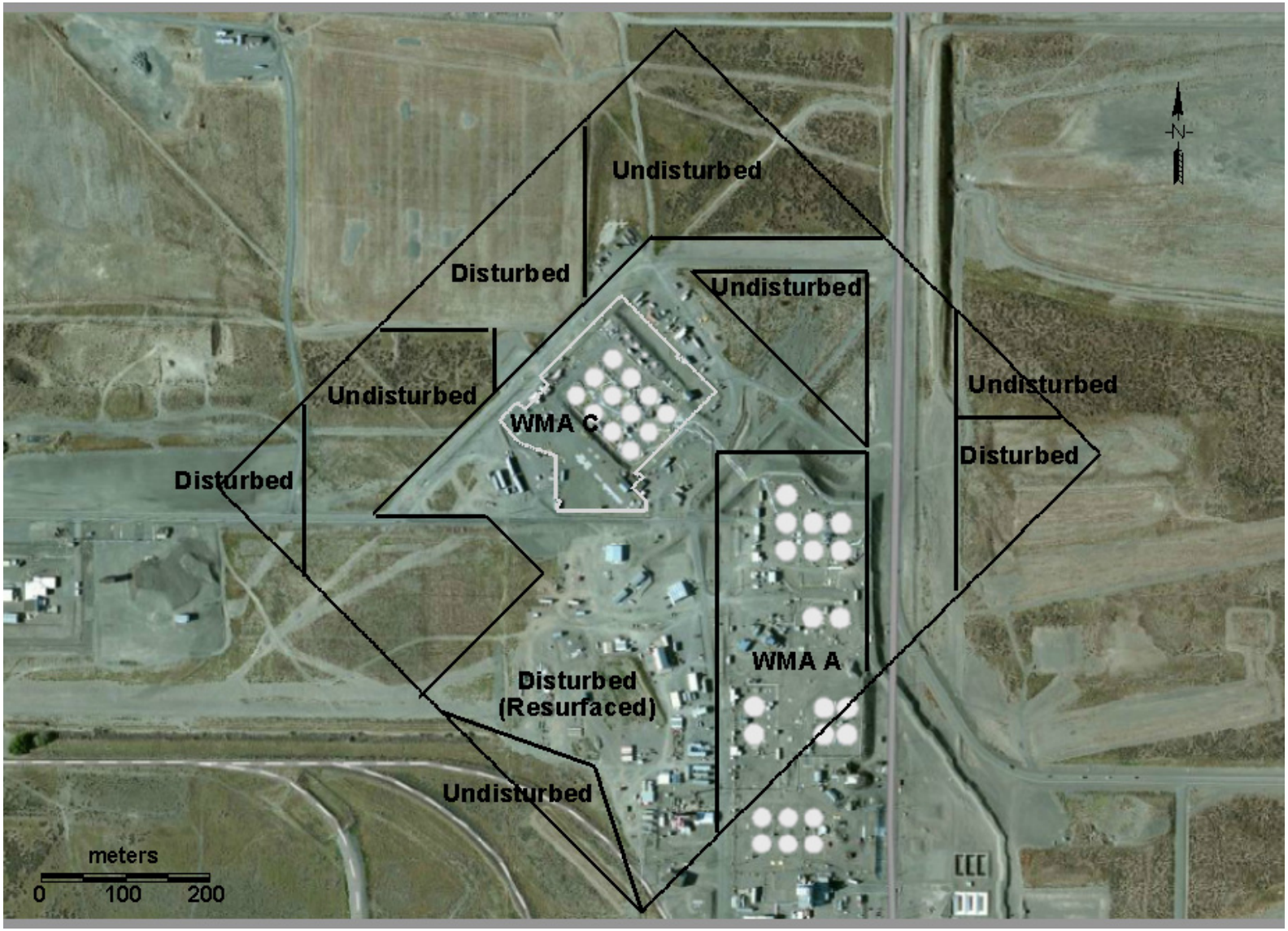

WMA = Waste Management Area

Figure 6-17. Inferred Surface Conditions In and Around Waste Management Area C during the Post-Closure Period.

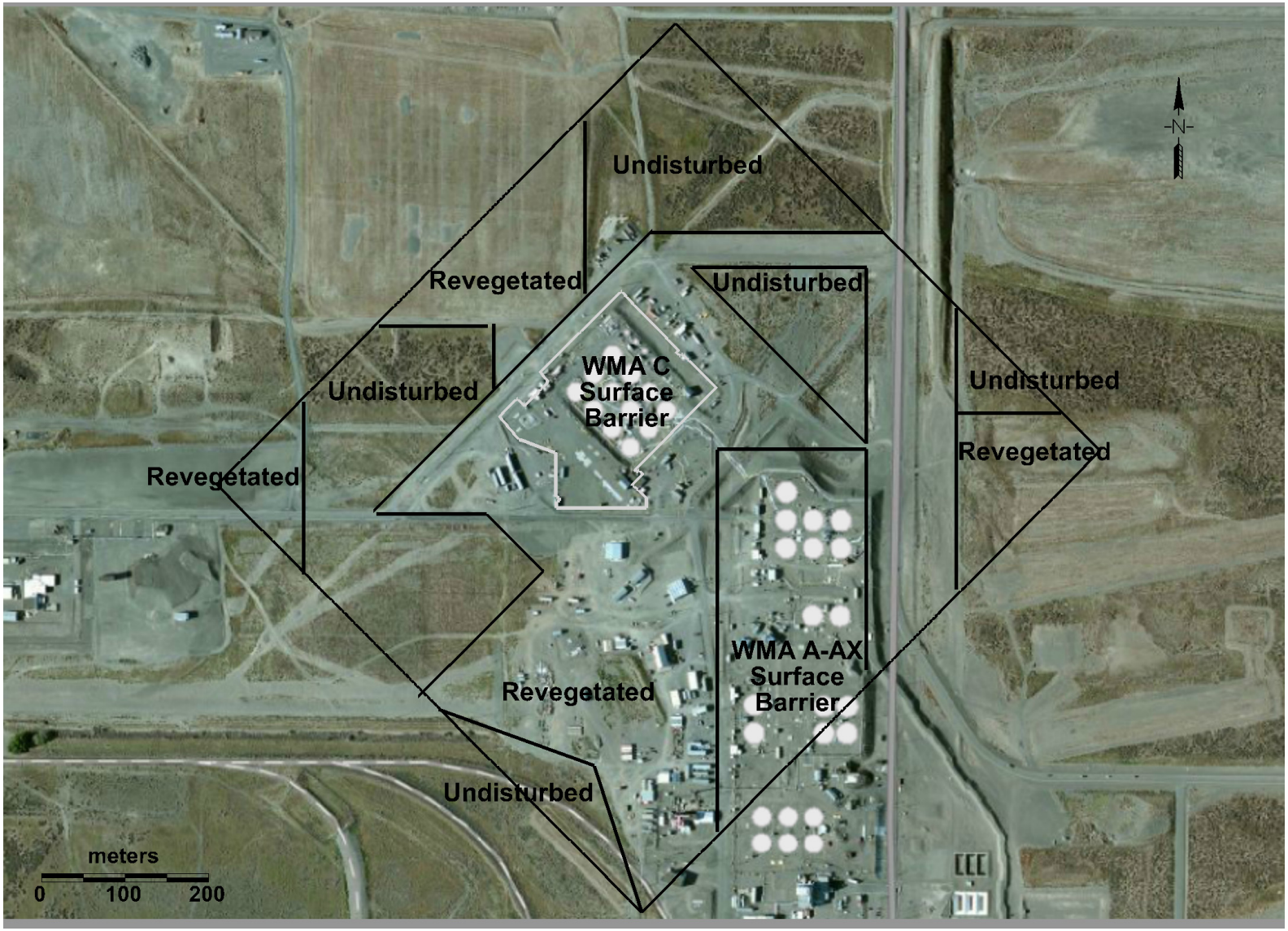

WMA = Waste Management Area

Late Post-Closure. Finally, a late post-closure period is considered to represent the functioning of a degraded surface barrier. This period will start at the end of its assumed design life expectancy of the surface barrier (year 2520) and will continue through the rest of the simulated time period. A distinct recharge rate will be assigned to three different zones during this period (Figure 6-17):

- The undisturbed, disturbed, and resurfaced zones away from the WMA C barrier characterized by undisturbed or reclaimed native vegetation cover
- The degraded WMA A-AX surface barrier fully covered with vegetation that has undergone reclaiming soil and ecological processes
- The degraded WMA C surface barrier fully covered with vegetation that has undergone reclaiming soil and ecological processes.

6.2.2.1.3 Vadose Zone Beneath Waste Management Area C. The vadose zone underlying WMA C consists of heterogeneous layers of sedimentary units that vary in thickness at different locations (see Section 3.1.9.1).

Conceptually, and for the purpose of simplification, each heterogeneous sedimentary unit is defined as an EHM having macroscopic flow properties as discussed in Appendix B. The porous media continuum assumption, an extended form of Darcy-Buckingham Law for vadose zone applications and the soil relative permeability/saturation/capillary pressure relations, provides the basis for vadose zone flow and transport modeling. In the model domain, the hydraulic properties describing flow and transport characteristics associated with each geologic layer are approximated by average up-scaled values. The upscaled hydraulic property values used in the flow and transport model for each EHM are derived from small- and micro-scale (sample) measurements (Appendix B). Each EHM unit thus possesses different flow and transport parameters (hydraulic conductivity, bulk density, and dispersivity). For each heterogeneous HSU having spatially variable hydraulic properties, moisture-dependent anisotropy represents the bulk behavior for the EHM ("Application of Stochastic Methods to Transient Flow and Transport in Heterogeneous Unsaturated Soils" [Polmann 1990]). The model thus describes the bulk (or mean) flow and contaminant transport behavior in the vadose zone that is applicable and appropriate to the evaluation and estimation of overall and eventual contaminant impacts to groundwater. Appendix B provides details on the approach for developing the effective (upscaled) flow and transport parameters for the vadose zone.

Features such as clastic dikes, sills, and tectonic structures can allow water and contaminants to bypass vadose zone continuum fate and transport processes. Clastic dikes (subvertical linear features composed of fine-textured sediments), discussed in Section 3.1.4.2.3, Clastic Dikes, do occur in the vadose zone, extend up to tens of meters in length, and crosscut the major layers. Within the Central Plateau, there is little evidence of enhanced transport in these preferential pathways in arid and semiarid climates with low-water flux in the vadose zone, particularly where soils are coarse-grained such as in Hanford formation sediments ("Influence of Clastic Dikes on Vertical Migration of Contaminants at the Hanford Site" [Murray et al. 2007]). While these features may form preferentially faster flow pathways under saturated conditions, under

unsaturated flow conditions these features tend to act as barriers to transport. Precipitation at arid sites is usually too low (in relation to saturated hydraulic conductivity) to invoke preferential flow. Much of the water in the dry soils is simply retained on grain surfaces by capillary forces and does not move along preferential pathways (Murray et al. 2007; "Hydrologic Mechanisms Governing Fluid Flow in a Partially Saturated, Fractured, Porous Medium" [Wang and Narasimhan 1985]).

6.2.2.1.4 Aquifer System Beneath Waste Management Area C. The integrated, saturated-unsaturated, 3-D WMA C PA model calculates concentrations of radionuclides in groundwater downgradient of the WMA C fenceline. For these calculations, flow and transport parameters need to be estimated for the unconfined aquifer because, as recharge containing contaminants enters the aquifer, the leachate mixes with groundwater and becomes more dilute. The flow and transport parameters needed for unconfined aquifer calculations are saturated hydraulic conductivity, specific storage, effective porosity, hydraulic gradient, depth to water table, and dispersivity.

A fundamental difference exists as to how the large-scale macroscopic parameters are derived for saturated media versus unsaturated media. First, in a highly heterogeneous flow domain such as WMA C exists a hierarchy of length scales that needs to be recognized (Appendix C, Figure C-1) and an increase in parameter estimates with an increase in flow domain is noticeable. The evolving heterogeneities at various length scales result in a scale dependence of effective parameters such as saturated hydraulic conductivity and dispersivity. For WMA C PA saturated media modeling, the flow domain of interest is the "Field Scale," which is shown on the right of Figure C-1. The unconfined aquifer is treated as an EHM, and an equivalent saturated hydraulic conductivity is estimated for the undifferentiated Hanford gravels (Appendix C).

For the large-time, large-scale PA modeling applications, the macro-scale parameterization for saturated media effective parameters depends on the configuration of the heterogeneous media, as well as the establishment and setup of the local boundary conditions. This is unlike the WMA C vadose zone parameterization wherein the effective parameters at the large and macro scale are derived from properties at the small and micro scale using upscaling methods. Instead, the effective parameterization for WMA C saturated media hydraulic conductivity, for example, is best achieved via a field-scale calibrated groundwater model, which accounts for appropriate local-scale boundary conditions, flow configuration, and history matching. Estimates of hydraulic properties are based on the groundwater flux in the aquifer around WMA C according to the Central Plateau groundwater model calibration reported in CP-47631, "Model Package Report: Central Plateau Groundwater Model Version 6.3.3." Flux is a rate measurement defined as the flow through a defined area. It is well suited for the PA because the emphasis of its evaluation is the contaminant mass conveyed through the aquifer to a PoCal aligned with the direction of groundwater flow. Thus, the hydraulic property values derived from the calibrated Central Plateau groundwater model fluxes are applied to the WMA C PA flow model domain.

6.2.2.1.5 Radionuclide Transport in the Environment. The geochemical and sorption conceptual model primarily concerns the movement and retardation of contaminants in the vadose zone. For the PA analysis, the empirical equilibrium sorption-based approach is assumed to approximate contaminant sorption during transport. The focus of the modeling is on far-field

transport, away from WMA C, with the bulk of the residence time of contaminants likely to be in the thick vadose zone. Concentration-dependent sorption/desorption of radionuclides, development of reaction fronts from dissolution and precipitation of mineral phases, and variable soil vapor pressures are possible at or very close to the tanks, vault, and pipelines. But away from these structures, due to mixing and continued buffering by mineral-water reactions, residual waste-derived water is expected to become similar to the ambient pore water within a short distance from the base of WMA C. The effluent concentrations from the base of the tank are likely to be so low that they cannot appreciably diminish the thick vadose zone's substantial capacity for sorption and buffering.

The use of the linear isotherm (constant K_d model) is assumed to be generally applicable when: (1) contaminants are present at low concentrations, (2) the geochemical environment being modeled is not affected by large spatial or temporal changes, and (3) the possible sorption sites occupied by the contaminant remain much less than the sorption capacity over the scale of transport. K_d values are chosen assuming low-salt, near-neutral waste chemistry. It is acknowledged that the K_d values used in fate and transport models are effective K_d values representing the effective combinations of processes contributing to the overall contaminant retardation and/or release behavior. The advantage of the empirical linear adsorption model or K_d approach is that it is easy to implement and generally deemed sufficient for modeling contaminant transport in the far-field through thick sediment column (DOE/RL-2011-50, Regulatory Basis and Implementation of a Graded Approach to Evaluation of Groundwater Protection).

6.2.2.1.6 Summary of Assumptions. The integrated, saturated-unsaturated, 3-D WMA C PA model calculates concentrations of radionuclides in groundwater downgradient of the WMA C fenceline. For the conceptual model, the following simplifying assumptions were made for the base case:

- WMA C closure occurs in 2020
- Release of radionuclides contained within the grouted residual waste is controlled by the process of diffusion, and remains diffusive with no advection occurring through the tank during the simulated time period of 10,000 years
- The impact of the varying size and shapes of waste material within the grouted tanks and ancillary equipment was ignored
- Moisture flow within the grouted tanks and ancillary equipment is negligible
- Episodic precipitation events and net infiltration through the thick, heterogeneous vadose zone in the 200 Areas can be approximated by an average annual recharge rate
- Impacts resulting from plausible climate change that may occur during the evaluation period do not adversely impact the performance of the surface or vadose zone as a barrier

- The modified RCRA Subtitle C barrier functions according to its design specifications for 500 years

- The impact of the closure barrier on moisture flow was approximated by an assumed recharge rate into the facility

- Flow in the vadose zone occurs in accordance with the porous media continuum assumption

- The hydrostratigraphy of the vadose zone is adequately represented by the delineation of equivalent homogeneous units for evaluating bulk (or mean) flow and contaminant transport

- Vadose zone hydraulic property values upscaled from small- and micro-scale (sample) measurements apply to the field scale for the equivalent homogeneous units

- The inclusion of moisture-dependent anisotropy functions allows the homogeneous HSUs to adequately approximate the effects of heterogeneity

- Features such as clastic dikes, sills, and tectonic structures that can allow water and contaminants to bypass vadose zone continuum fate and transport processes are not consequential to the analysis

- Effective parameterization for WMA C saturated media is best achieved via a field-scale calibrated groundwater model (Appendix C).

6.2.2.2 Conceptual Model for Air Pathway. Gases and vapors can potentially diffuse upward from the residual waste in the WMA C tanks and ancillary equipment to the ground surface. The principal mechanism by which contaminants migrate from the waste to the ground surface is gaseous diffusion along the air-filled pore spaces that are assumed to be continuous.

Of the contaminants contained in WMA C wastes at closure, four of them could potentially originate as gas from the residual wastes:

- Carbon-14 as CO_2 gas
- Hydrogen-3 as H_2 gas
- Iodine-129 as I_2 gas
- Radon-222 as radon gas.

Due to the small inventory of these radionuclides in the tank residuals, the dose contribution from the air pathway is expected to be small (relative to the groundwater pathway). Since tanks will be fully grouted at closure and the residual waste layer is conceptualized to be present near the base of the tank, it is assumed that grout will behave as a porous medium, and gases could slowly emanate and diffuse through the tortuous pathway along the gas-filled pore space. The

releases are driven by the partitioning of the radionuclides among the aqueous phase, solid phase, and gaseous phase, and therefore modeled by considering the following equilibrium coefficients:

- K_d for solid/water phase partitioning
- Henry's law constant (K_h) for air/water partitioning.

The atmospheric transport pathway calculations are conducted in two steps. The first step calculates the diffusive flux from the residual waste to the ground surface, while the second step calculates the transport in air to the receptor location. The details of each step are described below.

1. Gaseous fluxes emitted from each source term (tanks and ancillary equipment) are calculated by assuming a zero concentration boundary at the surface. This is conceptually equivalent to having a large enough wind speed near the ground surface of WMA C that the air parcel is renewed constantly, thereby maximizing the diffusive gradient.

   Upward diffusive gas phase transport through the SSTs, 244-CR vault, and C-301 catch tank is modeled to occur along a 10-m (32.8-ft)-long pathway towards the land surface. This pathway is split into a lower 5-m (16.4-ft) thickness composed of infill grout material, followed by another 5-m (16.4-ft) thickness of soil overburden (Figure 6-18). The diffusive area is the base area of each source term, consistent with the calculations described in Section 6.2.1. A surface barrier that will be emplaced at closure over the tank farm will provide additional diffusive pathway length to the surface but, for performing the air pathway calculations, this thickness is ignored. The diffusive length chosen is the minimum thickness over which gas-phase diffusion is likely to occur through the tortuous air-filled pore volume (defined by the air content). The 5-m (16.4-ft) thickness through the infill grout only considers the thickness up to the top of the steel liner, which is likely to remain as the minimum path length.

   The air content within the infill grout is assumed to be 6% based on characterization information for possible Hanford grout (WSRC-TR-2005-00195). The air content of the soil overburden is calculated by taking the difference in the backfill porosity and soil moisture content that varies as a function of time. The air content of the infill grout for the purpose of diffusive release calculations is fixed over time, even though studies have indicated that chemical transformation of initial grout material will likely cause porosity reduction over time due to increased molar volume of the newly formed mineral phases. The effective diffusion coefficient for each gas is calculated separately by taking its binary diffusion coefficient in free air, under atmospheric pressure of 1 atm and a temperature of 20 °C (68 °F), and multiplying by the gas tortuosity.

   The calculations consider equilibrium partitioning of contaminants among solid, water, and air phases. Assumed grout K_d values are applied for the 5-m (16.4-ft) diffusive pathway calculations within the infill tank grout material, while no sorption is assumed for the 5-m (16.4-ft) pathway length considered through the soil backfill material.

Figure 6-18. Conceptualization of Air Pathway Diffusive Release from the Tank to the Surface.

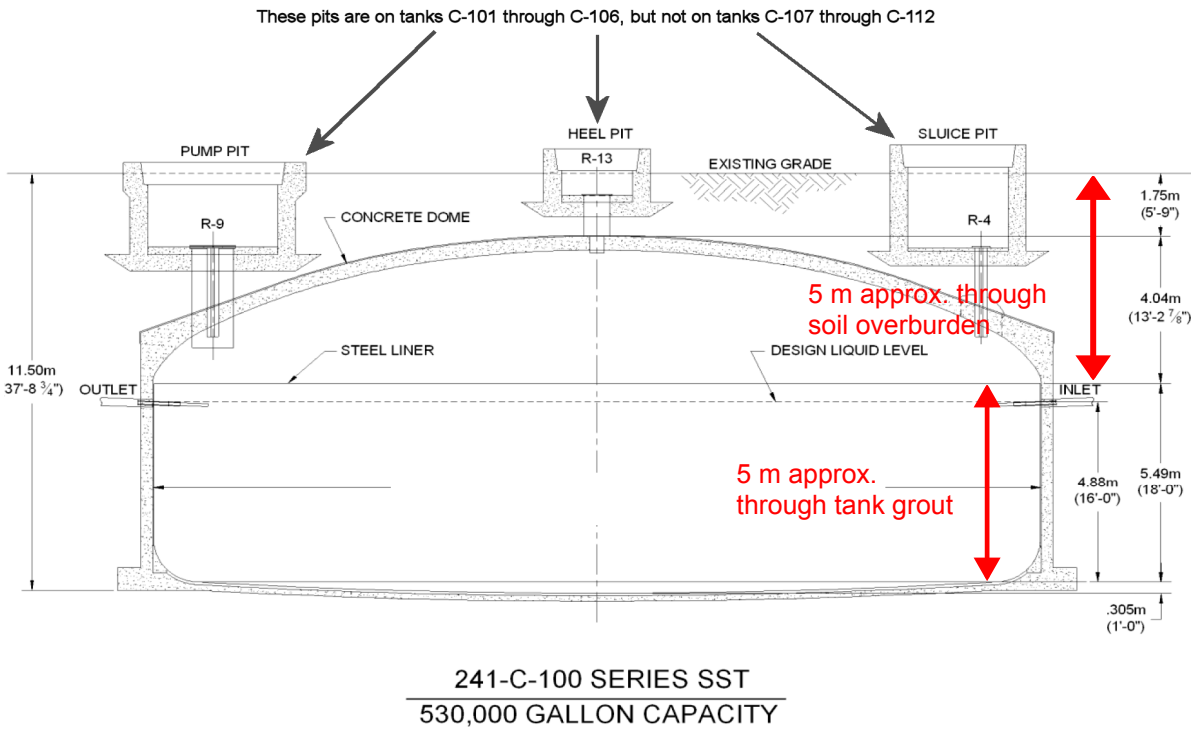

For the pipelines, the gas phase diffusive calculations are performed in a similar manner to that described above, except for consideration of the 5-m (16.4-ft) diffusive path length along the grout infill material. For pipeline analysis, only the 5-m (16.4-ft) diffusive path length along the soil overburden is considered.

2. The gas-phase diffusive mass flux arriving at the surface for each source area (twelve 100-series tanks, four 200-series tanks, CR-Vaults, C-301 catch tank, and the pipelines) is captured and then transported (except for radon), assuming advection and dispersion via wind movement to the receptor placed 100 m (328 ft) downwind from the WMA C fenceline. The air mixing height is assumed to be 2 m (6.6 ft). Horizontal air dispersion is considered along the transport pathway, which is based on the expected air turbulence in and around WMA C.

   The calculated air concentrations at the receptor location are used for evaluating air pathway dose, and are compared to the performance objective of 10 mrem/yr atmospheric release dose limit. On the other hand, the ^{222}Rn flux emanating at the surface from each source is compared to the performance objective of 20 pCi $m^{-2}s^{-1}$ atmospheric release flux limit.

6.2.3 Exposure Pathways and Scenarios

This section discusses the exposure scenarios that are developed to meet DOE O 435.1 PA requirements.

An exposure pathway can be described as the physical course that a COPC takes from the point of presence in a specific environmental media to a receptor. The route of exposure is the means by which a COPC enters a receptor. An exposure scenario includes data and exposure parameters that describe how exposure occurs. The receptor is assumed to reside 100 m (328 ft) downgradient of the facility fenceline.

To meet the DOE O 435.1 requirements, an all-pathways farmer scenario is implemented to calculate the total effective dose equivalent for comparison to the performance objective of 25 mrem, which is the total effective dose equivalent in a year from all exposure pathways, excluding the dose from radon and progeny in air. In this scenario, calculations are performed based on predicted radionuclide transport through the groundwater pathway and atmospheric pathway, and exposure at the point of contact.

For the groundwater transport pathway, the single family farmer is assumed to reside 100 m (328 ft) downgradient from the facility fenceline and draw contaminated water from a well. The receptor is an adult who is assumed to use the water to drink, irrigate crops, and water livestock. The receptor is assumed to receive dose from the following exposure routes:

- Ingestion of water
- Ingestion of fruits and vegetables grown on the farm
- Ingestion of beef raised on the farm
- Ingestion of milk from cows raised on fodder grown on the farm
- Ingestion of eggs from poultry fed with fodder grown on the farm
- Ingestion of poultry fed with fodder grown on the farm
- Incidental ingestion of contaminated soil
- Inhalation of contaminated soil (dust) in the air
- Inhalation of water vapor
- External exposure to radiation.

The equations associated with each exposure route are implemented in the system model. The exposure parameter values used in the equations, along with element-specific bioconcentration factors (transfer coefficients), are based on guidance provided in various guidance documents from EPA, National Council on Radiation Protection and Measurements, International Atomic Energy Agency, and International Commission on Radiological Protection. The dose conversion factors (effective dose coefficients) on a radionuclide basis are taken from DOE guidance documents (DOE-STD-1196-2011 and EPA-402-R-93-081, Federal Guidance Report No. 12, External Exposure to Radionuclides in Air, Water, and Soil), respectively.

For the atmospheric transport pathway, the following three exposure routes are considered for the receptor residing 100 m (328 ft) downgradient of the facility fenceline:

- Air immersion
- Inhalation of dust
- External exposure to radiation from the contaminated ground surface.

DOE M 435.1-1 Change (Chg) 1 IV.P.(2) states that the PA shall include an assessment of impacts calculated for a hypothetical person assumed to inadvertently intrude for a temporary period into the LLW disposal facility. Inadvertent intruder scenarios are discussed in detail in Section 9.

To evaluate protection of water resources, radionuclide concentration in groundwater 100 m (328 ft) downgradient from WMA C fenceline is compared to drinking water standards specified by Title 40, CFR, Part 141, "National Primary Drinking Water Regulations," Subpart G—National Primary Drinking Water Regulations: Maximum Contaminant Levels and Maximum Residual Disinfectant Levels, §141.66 Maximum contaminant levels for radionuclides (40 CFR 141.66) over the compliance period. Several separate comparisons are required to evaluate compliance with drinking water standards, as follows.

- Combined ^{226}Ra and ^{228}Ra – concentrations are added and the sum must be less than 5 pCi/L.

- Gross alpha activity (excluding radon and uranium) – the sum of concentrations for each radionuclide that decays by alpha particle emission must be less than 15 pCi/L.

- Beta and Gamma Emitters – the sum of all radionuclides that emit either a beta particle or gamma radiation must be less than 4 mrem/yr to the total body or any internal organ. The dose must be calculated assuming an individual who drinks 2 L/day (0.5 gal/day) of the contaminated water.

- Strontium-90 – concentrations must be less than 8 pCi/L.

- Tritium – concentrations must be less than 20,000 pCi/L.

- Total uranium (metal) – concentrations must be less than 30 µg/L (3.0×10^{-5} oz/ft^3).

6.3 MATHEMATICAL MODELS

This section presents development and implementation of mathematical models that are used to evaluate flow and radionuclide transport and long-term human health and environmental impacts. Mathematical models and their implementation into process-level or system-level models are described for the following components of the conceptual model of the closed WMA C facility including 1) source-term and engineered system (Section 6.3.1); 2) radionuclide

transport along the groundwater and atmospheric pathways (Section 6.3.2); and 3) exposure and dose analysis (Section 6.3.3).

6.3.1 Source Term and Engineered Features

The processes associated with the release of contaminants into the pore waters of the material in the tank and ancillary equipment, and their migration from the residual waste matrix through the surrounding engineered barriers, are denoted as the source term in this PA.

The experimental observation and conceptualizations related to each of these processes has been presented in Sections 5 and Section 6.2.1. The objective of this section is to present the mathematical description of the processes implemented for modeling the release of contaminants from the waste form (source) through the engineered features (tank) to the near-field just outside the tanks and ancillary equipment.

While the tank (and ancillary equipment) infill material remains intact, it is assumed that releases occur by diffusion through the base of the tank base mat, consisting of grout and concrete layers. For volatiles released from the residual wastes, it is assumed that their transport through the tank infill grout material and the soil overburden is controlled by upward diffusion.

Both mineral phase solubility-limited and matrix degradation rate-limited processes are considered for the key analytes. These have been studied in detail in the laboratory, and the laboratory results have been incorporated in the source term analysis. In particular, the following release models are used, which are based on empirical evidence:

- a matrix-degradation-rate-based release of ^{99}Tc
- solubility-controlled releases of uranium.

In the two subsections that follow, the empirical evidence for the release models for ^{99}Tc and uranium is established. Multi-year leaching studies have been conducted on tank residual samples focused on leaching behavior of key contaminants such as ^{99}Tc and uranium. Based on evaluation of the results, models based on solubility control or matrix degradation are implemented in the PA calculations for ^{99}Tc and isotopes of uranium, as discussed below. For all other radionuclides evaluated in this PA, conservative source-term calculations are performed whereby all of the radionuclides are assumed to be instantly and completely available in solution within the residual waste volume, and available for an immediate diffusive release.

The next two subsections discuss the basis for the diffusion coefficients for the aqueous and air pathways, and the basis for the sorption of contaminants in the grout/concrete layer. Finally, in the last subsection, the basis is presented for considering diffusive releases for the source term when the tank structure and infill grout material are intact.

6.3.1.1 Source Release Model for Technetium-99. The matrix-degradation-rate-based release model developed for ^{99}Tc is based on the results of the SPFT experiments conducted on C-103, C-202, and C-203 tank residual waste. The experimental setup and analyses results are presented in PNNL-20616, “Contaminant Release from Hanford Tank Residual Waste – Results

of Single-Pass Flow-Through Tests" and in Cantrell et al. 2013. These tests were conducted under low flow conditions (~0.1 mL/hr [0.06 in.^{3}/hr]) for a period of about six months with no stirring of residual waste in the solution. The initial solution-to-solid weight ratio is 120 (based on 0.06 L [0.016 gal] of initial solution in contact with 0.5 g [0.018 oz] sample), and the residence time of the solution in the reaction vessel was calculated to be 25 days. The initial concentrations of ^{99}Tc reported in the samples were: 0.23 µg/g (0.0081 oz/ton) for tank C-103, 0.23 µg/g (0.0081 oz/ton) for tank C-202, and 0.11 µg/g (0.0039 oz/ton) for tank C-203. Appendix A of PNNL-20616 provides the complete tabulation of the analytical results that are relevant to the PA for the three leachates—namely, deionized water, $CaCO_3$ saturated solution, and 0.005 M $Ca(OH)_2$ solution. The results of the leaching for the three tank residual waste samples are presented in Figure 6-19. The ^{99}Tc concentrations in all three leachates are very similar, with the concentrations appearing to drop off exponentially with increasing solution-to-solid ratio. The initial sample concentration was low because the leachate solutions contained no ^{99}Tc.

The results of the SPFT experiments were further analyzed to quantify the fractional leaching rate of ^{99}Tc using the 0.005 M $Ca(OH)_2$ solution, since it is expected that infill grout will condition the chemistry of incoming waters for a very long time period.

a) The results presented in Table A of PNNL-20616 in terms of solution-to-solid ratio are first converted to elapsed time (in days), based on 25 days of residence time in the reaction vessel being equivalent to 120 initial solution-to-solid ratio.

b) The initial concentration of ^{99}Tc in the residual waste sample is used, along with the mass of the sample, to estimate the initial ^{99}Tc mass (in terms of grams).

c) Based on reported ^{99}Tc concentrations (µg/L) in the effluent, the cumulative mass of ^{99}Tc leached is calculated and then converted to fraction of initial mass leached. From this, the fraction of mass remaining in the solid sample is calculated as a function of time.

d) An exponential trend line is fitted to the fraction remaining (as a function of time) and the rate constant is derived (in units of day^{-1}), which represents a first-order release rate from the solid to the solution. The trend line is fitted to the dataset following flushing of resident vessel volume (approximately 25 days) and while the concentrations are above the detection limit.

The fraction remaining for ^{99}Tc along with the fitted trend line results are presented in Figures 6-20 through 6-22. The results indicate that the first-order reaction rate constant defining the release of ^{99}Tc from the residual waste varies over a narrow range of 5×10^{-4} to 8×10^{-4} day^{-1}. This rate constant reflects the longer-term rate of release of ^{99}Tc following the initial release as noted by the early spike in concentration in Figure 6-19 (a-c). The percent ^{99}Tc leached from the various SPFT experiments varies from 4.5 to 15% (as noted in Table 5-3), and is influenced more by the particular sample type than by the type of the leachate.

Figure 6-19. Technetium-99 Concentration in Single-Pass Flow-Through Leachates for (a) Tank 241-C-103, (b) Tank 241-C-202, and (c) Tank 241-C-203 as a Function of the Total Volume of Leachate that has Contacted the Waste in Terms of Leachate Solution to Solid (Initial) Weight Ratio. (1 of 3 sheets)

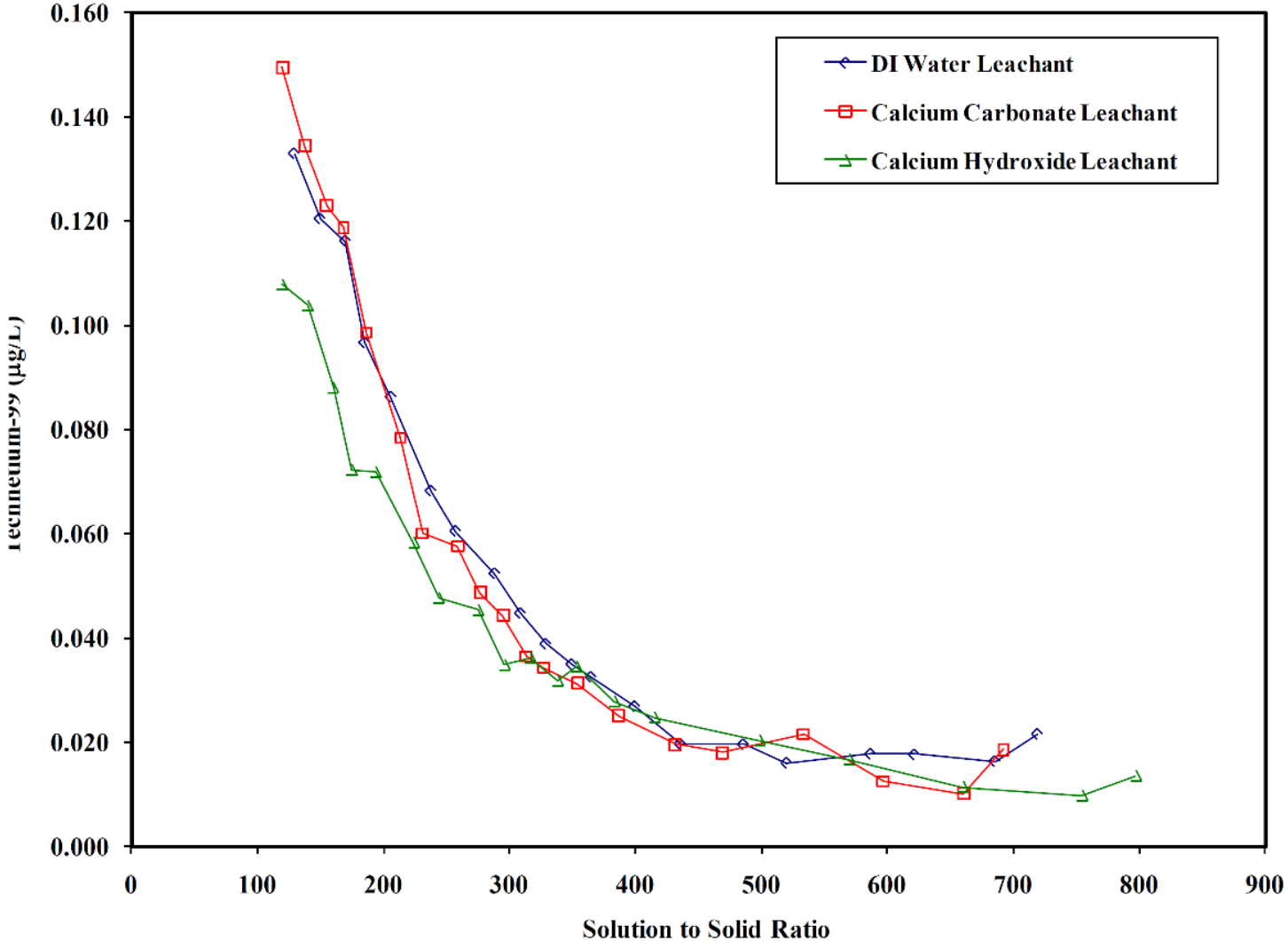

(a)

Figure 6-19. Technetium-99 Concentration in Single-Pass Flow-Through Leachates for (a) Tank 241-C-103, (b) Tank 241-C-202, and (c) Tank 241-C-203 as a Function of the Total Volume of Leachate that has Contacted the Waste in Terms of Leachate Solution to Solid (Initial) Weight Ratio. (2 of 3 sheets)

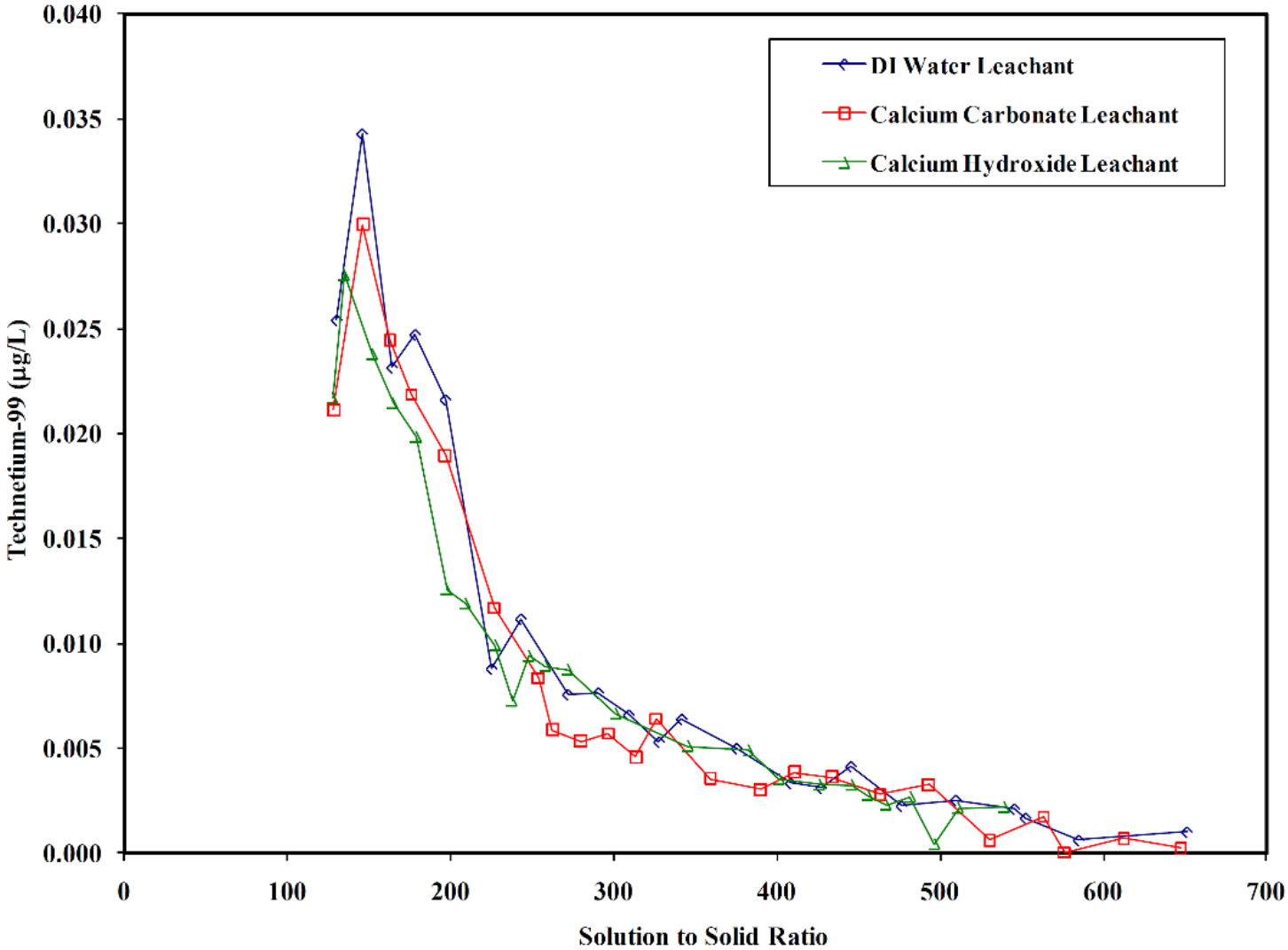

(b)

Figure 6-19. Technetium-99 Concentration in Single-Pass Flow-Through Leachates for (a) Tank 241-C-103, (b) Tank 241-C-202, and (c) Tank 241-C-203 as a Function of the Total Volume of Leachate that has Contacted the Waste in Terms of Leachate Solution to Solid (Initial) Weight Ratio. (3 of 3 sheets)

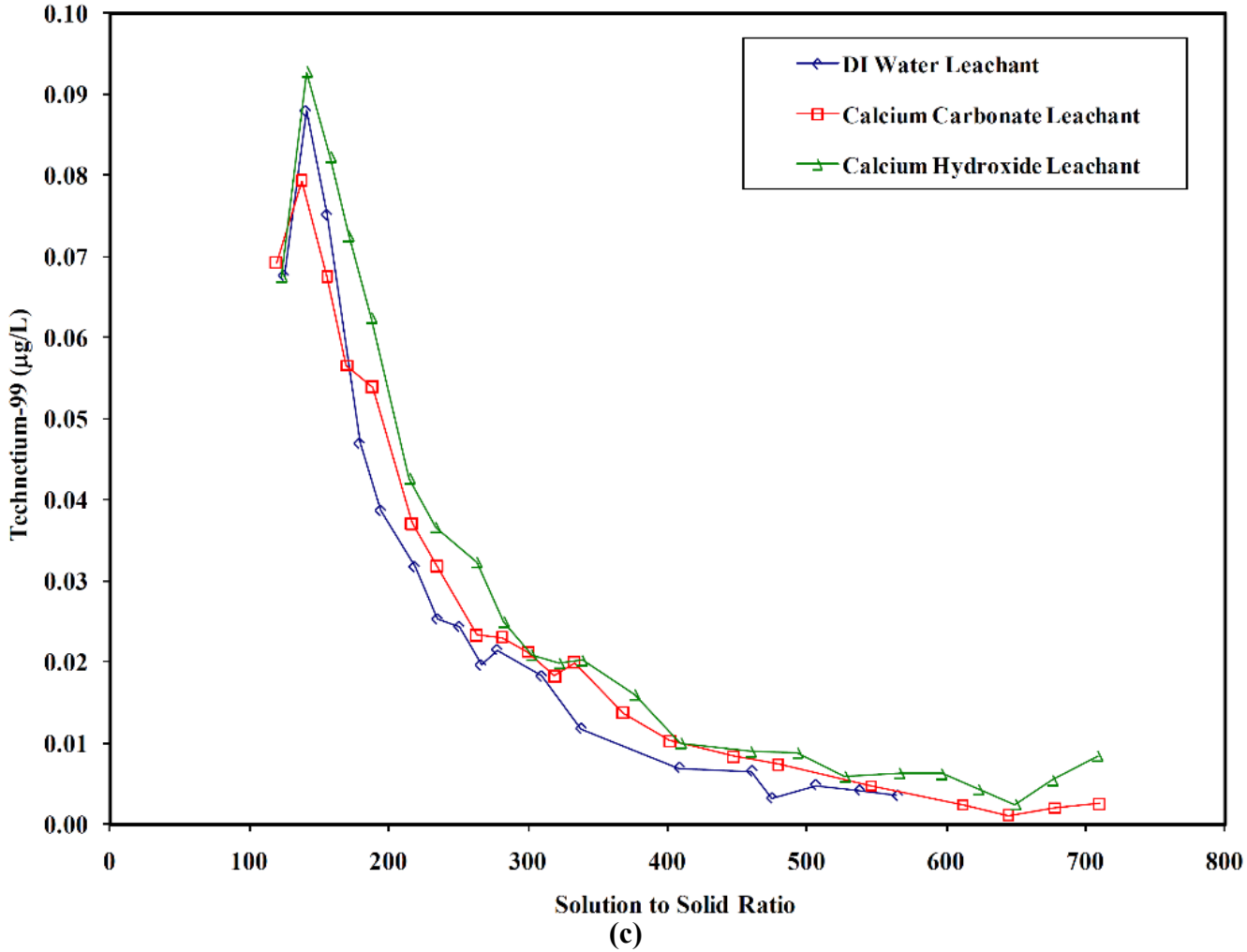

DI = deionized

Source: PNNL-20616, "Contaminant Release from Hanford Tank Residual Waste – Results of Single-Pass Flow-Through Tests."

Figure 6-20. Fractional Release of Technetium-99 for Single-Pass Flow-Through Experiments from Tank 241-C-103 Along with the Estimate of the First-Order Reaction Rate Constant of 8E-04 day^{-1}.

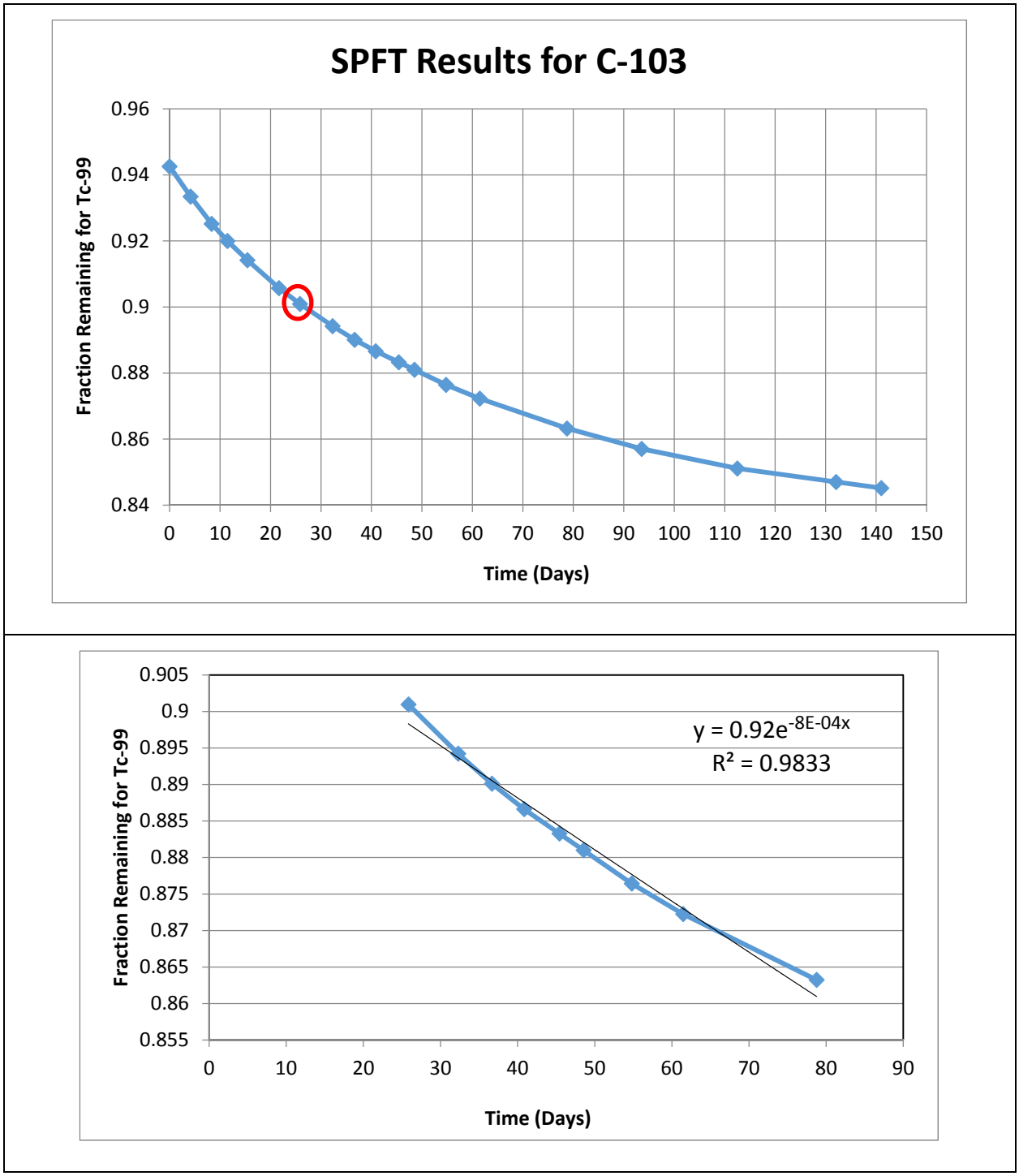

SPFT = Single-Pass Flow-Through

Figure 6-21. Fractional Release of Technetium-99 for Single-Pass Flow-Through Experiments from Tank 241-C-202 Along with the Estimate of the First-Order Reaction Rate Constant of 6E-04 day^{-1}.

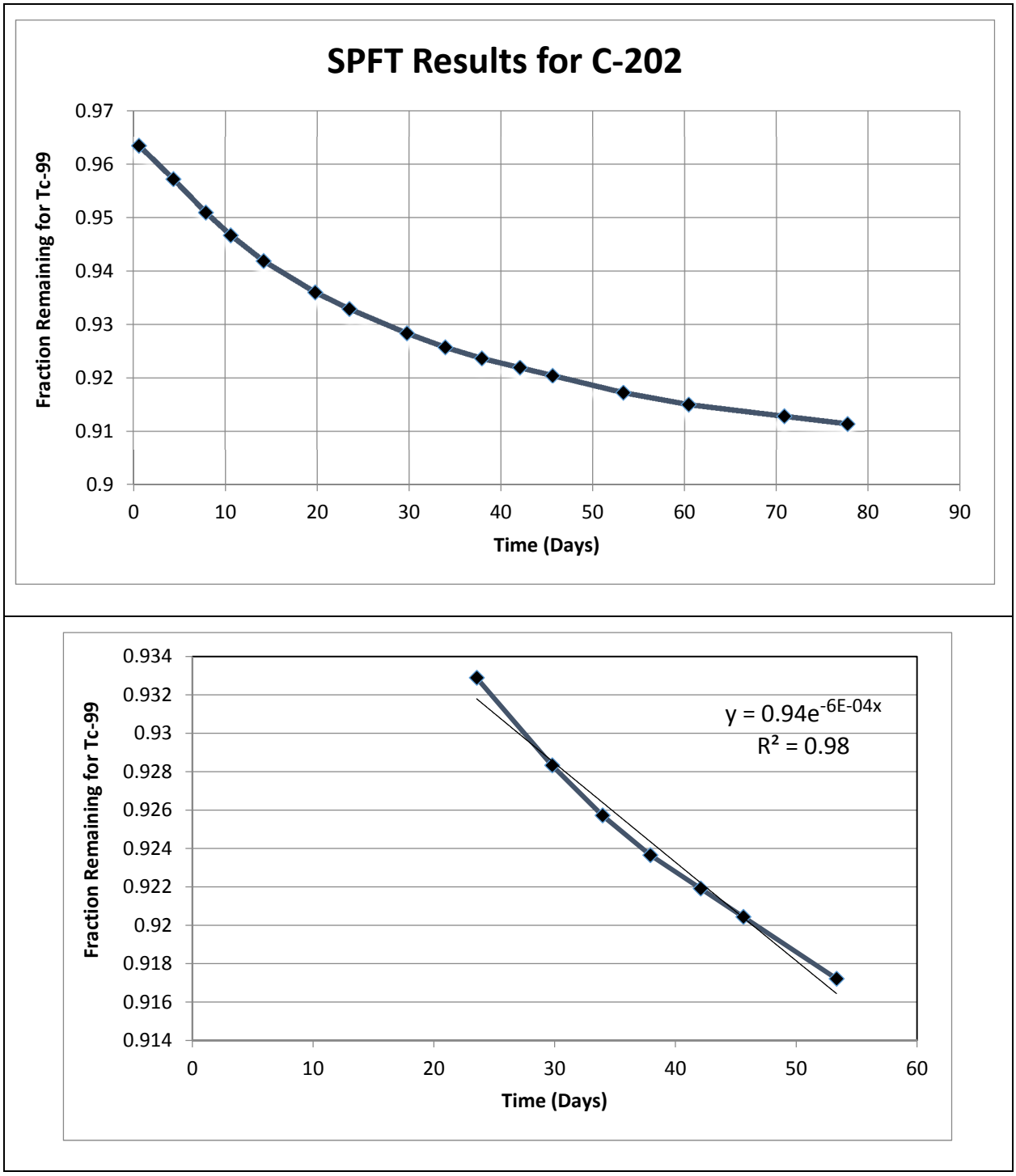

SPFT = Single-Pass Flow-Through

Figure 6-22. Fractional Release of Technetium-99 for Single-Pass Flow-Through Experiments from Tank 241-C-203 Along with the Estimate of the First-Order Reaction Rate Constant of 5E-04 day^{-1}.

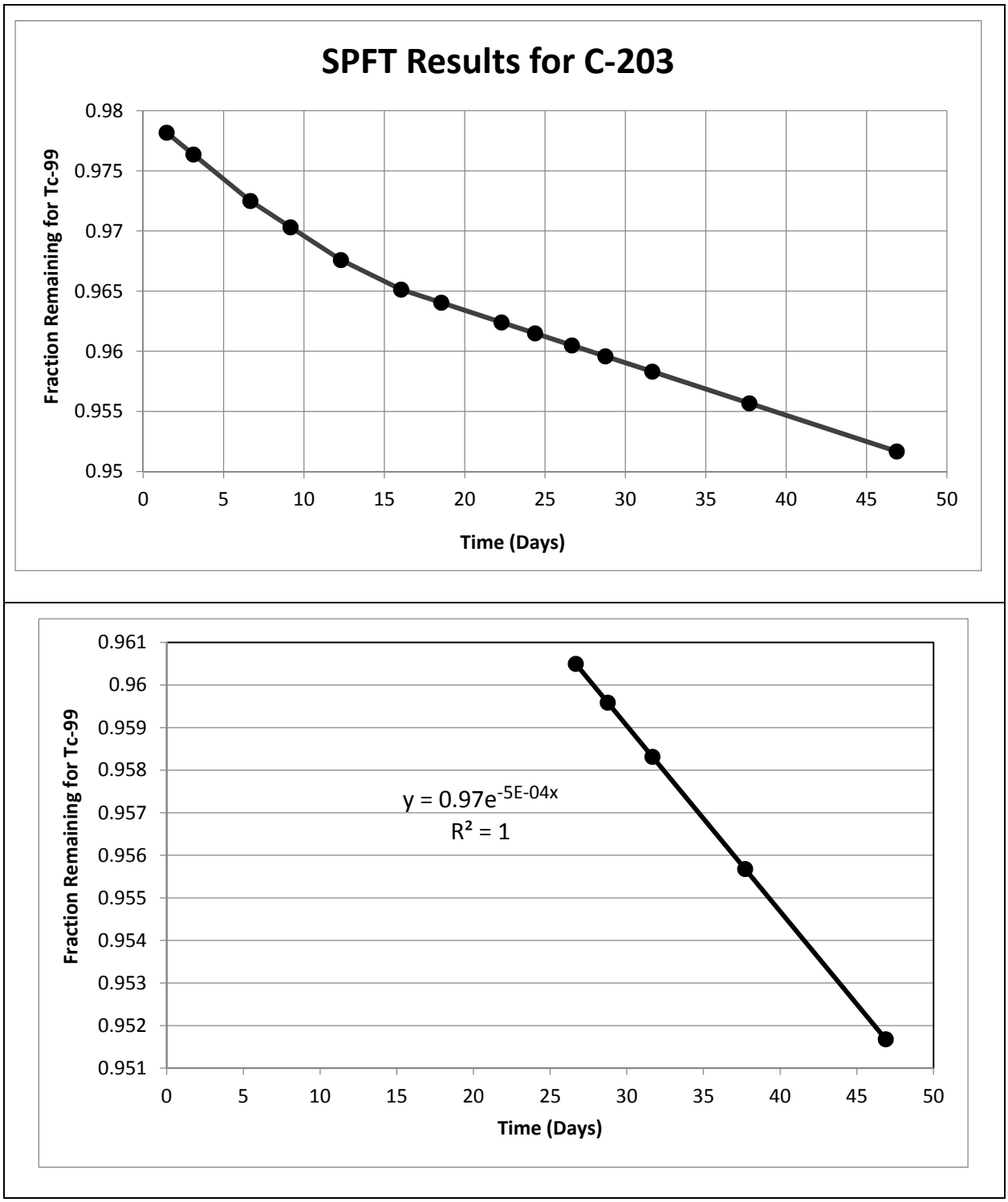

SPFT = Single-Pass Flow-Through

To make the source release model for ^{99}Tc consistent with the observations, an initial 6% fraction of the ^{99}Tc inventory is considered to be instantaneously available for release, while the remaining 94% fraction undergoes relatively slower release at the fractional rate of 6×10^{-4} day^{-1}. These estimates of parameters are implemented in the base case. The uncertainty in the initial release fraction and the fractional release rate is evaluated separately (see Section 8).

In order to evaluate the adequacy of the ^{99}Tc release model, a calculation is performed using the base case estimate parameters to simulate the release of ^{99}Tc from the SPFT experiments, which are then compared to the observed concentration in C-103 and C-202 tank effluents. The calculation setup is similar to the reactor vessel volume and flow rate used for doing the SPFT experiments. The results of the calculations are presented in Figure 6-23, indicating that the base case parameters capture the release of ^{99}Tc and lead to conservative dissolved concentrations for calculating the diffusive flux.

Figure 6-23. Simulated Versus Observed Effluent Concentrations of Technetium-99 (µg/L) from the Single-Pass Flow-Through Experiments Conducted on Tanks 241-C-103 and 241-C-202 Residual Waste. The simulated concentrations are based on best estimate release parameters from residual waste.

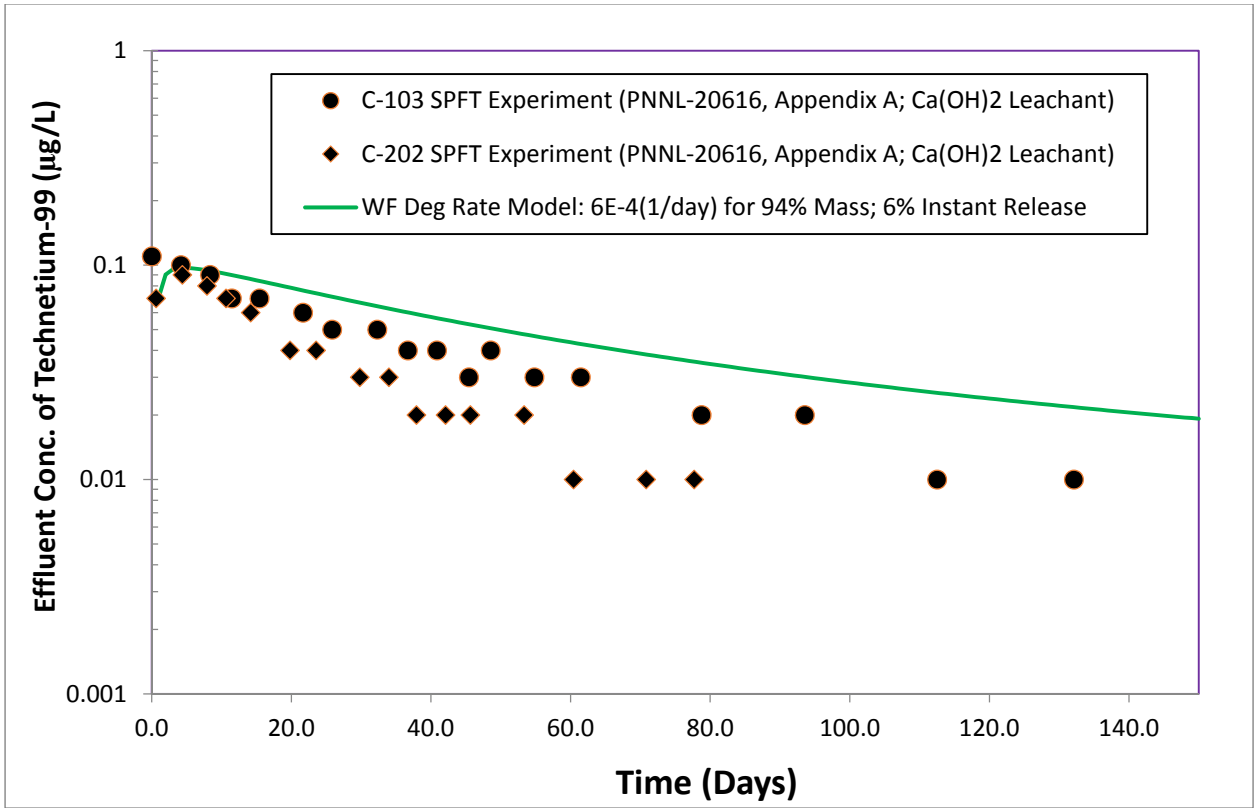

SPFT = Single-Pass Flow-Through

Reference: PNNL-20616, "Contaminant Release from Hanford Tank Residual Waste – Results of Single-Pass Flow-Through Tests."

6.3.1.2 Source Release Model for Uranium. As discussed in Section 5, laboratory leaching tests have been conducted on residual waste samples from various tanks. Cantrell et al. (2013) provided the analysis of residual waste following leaching with three different leachates—namely, DI (deionized) water, $CaCO_3$ saturated solution, and 0.005 M $Ca(OH)_2$ solution. These three leachates represent a range of possible water types contacting the residual waste. The $CaCO_3$ saturated solution was used to simulate a leachate produced by aged carbonate cement or a typical Hanford vadose zone pore water, 0.005 M $Ca(OH)_2$ solution was used to represent the likely influence of interaction of infiltrating vadose zone pore water with portlandite [$Ca(OH)_2$] in the grouted tanks, and the DI water was used as a baseline for the leach tests to evaluate the influence of waters that have not been altered by reactions with the $Ca(OH)_2$ and $CaCO_3$ leachates.

The general trends in uranium leachate concentrations for the C-103, C-202, and C-203 tank residual wastes are very similar. The results are presented for tank C-202 in Figure 5-4. The leached uranium concentration using DI water and $CaCO_3$ saturated solution are significantly higher than those in the 0.005 M $Ca(OH)_2$ leachates. This is attributed to forming Ca-rich precipitates (Ca phosphate and calcite) on the surfaces of the waste particles when using $Ca(OH)_2$ leachate, inhibiting dissolution of the underlying uranium phases in the waste. Since the tanks are planned to be grouted prior to closure, the primary leachate is expected to be $Ca(OH)_2$ saturated solution (Deutsch et al. 2011), which is likely to reduce the leaching of uranium.

To investigate this leaching behavior, thermodynamic equilibrium modeling was conducted. The saturation indices (SIs) calculated for the tank C-202 SPFT effluents for the three leachates indicated that DI water and $CaCO_3$ saturated leachate give similar SI results, while the $Ca(OH)_2$ leachate SI results are quite different. Results from DI water and $CaCO_3$ saturated leachates indicate that $NaUO_2PO_4.xH_2O$ is near equilibrium while Ca-containing phases (such as calcite and hydroxylapatite) were all undersaturated. The SI results for the $Ca(OH)_2$ leachates indicate all uranium-bearing phases to be highly undersaturated but are near-saturated or oversaturated with respect to Ca-containing phases. Calcite was near saturation, while hydroxylapatite and flourapatite were consistently highly oversaturated.

These results are consistent with the observed leaching behavior of uranium. It is hypothesized that precipitation of Ca-rich phases resulted in coatings on the waste particles that could have temporarily inhibited dissolution and attainment of equilibrium for any uranium phase in contact with $Ca(OH)_2$ leachate solutions.

These results indicate that as long as the infiltrating water though the tank passes through the infill grout material, it will be conditioned to be similar to a dilute $Ca(OH)_2$ leachate solution and the uranium dissolution will remain inhibited (Cantrell et al. 2013). At some distant time in the future when the tank is assumed to be sufficiently degraded such that large open fractures develop that do not allow appreciable residence time for infiltrating waters to contact and equilibrate with the grout material, the leachate would be similar to the $CaCO_3$ saturated water, and at that time the uranium concentrations may increase when the residual waste is contacted.

Reaction-path modeling was undertaken in "Thermodynamic Model for Uranium Release from Hanford Site Tank Residual Waste" (Cantrell et al. 2011) to evaluate the uranium release under the $Ca(OH)_2$ and $CaCO_3$ saturated waters by applying an infiltration rate of 1 mm/yr (0.039 in./yr) through the tank material over 10,000 years. The steel of the tank itself was assumed to have no impact on the hydrology or system chemistry, and the waste was assumed to be uniformly distributed at the bottom of the tank. The results of this reaction-path modeling are summarized below.

For $Ca(OH)_2$ saturated water, the tank was assumed to be filled with cementitious material (i.e., concrete or grout), and the composition of the simulated pore water was assumed to be 0.015 M $Ca(OH)_2$ and 1×10^{-5} M SI. The results of the reaction progress in terms of the uranium and total inorganic carbon (TIC) concentrations and the paragenetic sequence of uranium phases over the course of 10,000 years are shown in Figure 6-24. Initially, high uranium concentrations occur in solution (~3×10^{-4} M) because of high carbonate complexation of uranium, but decline rapidly and rebound somewhat as a small amount of andersonite [$Na_2CaUO_2(CO_3)_3.6H_2O$] first precipitates and then dissolves. As the reaction progress continues, $NaUO_2PO_4.xH_2O$ dissolved preferentially to $Na_2U_2O_7$(am). As carbonate continues to leach from the waste, uranium concentrations continue to decline until a plateau is reached at approximately 1×10^{-6} M. This occurs at the approximate point where $CaUO_4$ becomes the dominant phase. A dramatic reduction in uranium concentrations occurs when $Na_2UO_2O_7$ (am) dissolved completely, leaving $CaUO_4$ as the only phase to control uranium release concentrations. A reaction progress of 1.0 is equivalent to 1 mm/yr (0.039 in./yr) of flow for 10,000 years, and therefore represents 10,000 mm (394 in.) of flow.

Figure 6-24. Uranium and Total Inorganic Carbon Concentrations (A) and the Paragenetic Sequence of Uranium Phases Present in the Waste (B) as a Function of Reaction Progress for the $Ca(OH)_2$ Saturated Water Scenario. A reaction progress of 1 is equivalent to 10,000 years of infiltration at 1 mm/yr.

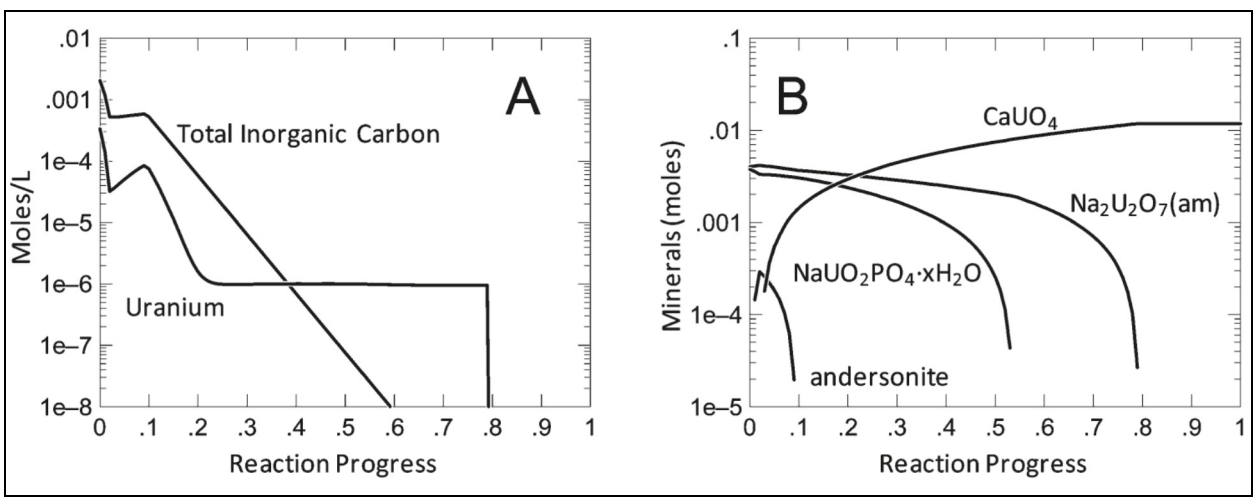

A similar reaction progress modeling calculation for the $CaCO_3$ saturated waters is shown in Figure 6-25. Initial high uranium concentrations in solution (~3×10^{-4} M) occur because of high carbonate complexation of uranium due to soluble Na_2CO_3 or cejkaite [$Na_4(UO_2)(CO_3)_3$]. As

very soluble carbonate phases dissolve, the uranium concentration of ~2.6×10^{-5} M is maintained primarily by dissolution of $NaUO_2PO_4.xH_2O$ and $Na_2U_2O_7$(am), although schoepite ($UO_3 \cdot 2H_2O$) also becomes important.

Figure 6-25. Uranium and Total Inorganic Carbon Concentrations (A) and the Paragenetic Sequence of Uranium Phases Present in the Waste (B) as a Function of Reaction Progress for the $CaCO_3$ Saturated Water Scenario. A reaction progress of 1 is equivalent to 10,000 years of infiltration at 1 mm/yr.

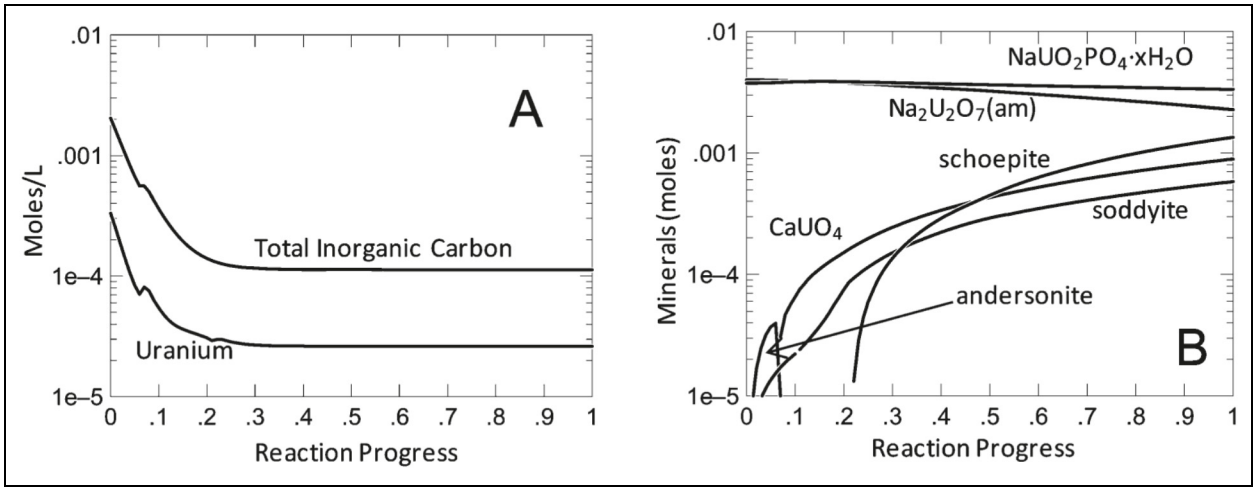

Over the course of these simulations, 2% of the uranium in the waste is calculated to be dissolved in the $Ca(OH)_2$ saturated water, compared to 6.4% for the $CaCO_3$ saturated water. This is attributed to the formation of relatively insoluble $CaUO_4$ phase under high Ca and high pH conditions.

The results of the reaction progress modeling are used to impose solubility limits for uranium. As a conservative calculation, it is assumed that the infill grout is not a barrier to flow through the tank, and the recharge rates imposed on the backfill material (0.5 mm/yr [0.019 in./yr] for the first 500 years and 3.5 mm/yr [0.138 in./yr] afterwards) are also the flow rates through the tanks, even though the rates are likely to be far lower due to lower permeability. Given these flow rates, it is calculated that in the 1,000-year post-closure compliance time period, a total of 2,000 mm (78.7 in.) of water would flow (0.5 mm/yr [0.019 in./yr] × 500 years + 3.5 mm/yr [0.138 in./yr] × 500 years). This is equivalent to a reaction progress of 0.2 presented in Figures 6-24 and 6-25. Using this information, the following solubility controls are imposed on the uranium concentrations for the base case, as shown in Figure 6-26.

- Apply solubility limit of 1×10^{-4} M for 1,000 years (equivalent to reaction progress of 0.2) based on the assumption that amorphous uranium mineral phases such as $Na_2U_2O_7$(am) control the solubility.

- After 1,000 years, apply the solubility limit of 1×10^{-6} M, assuming $CaUO_4$ as the solubility-controlling mineral phase under $Ca(OH)_2$ saturated conditions (infill grout saturated and intact-tank conditions).

- If and when the tank is assumed to be degraded such that flow rates are fast enough not to equilibrate with the infill grout material and rather are $CaCO_3$ saturated (vadose zone water), then apply a solubility limit of 1×10^{-4} M for 1,000 years. Beyond this time, apply solubility limit of 2×10^{-5} M based on the long-term uranium concentrations shown in Figure 6-25, assuming minimal influence of $Ca(OH)_2$ water.

Figure 6-26. Uranium Solubility Model Implemented with Solubility Limits Varying with Time. Reaction progress of 0.2 is equivalent to 1,000 years of flow under base case recharge conditions through the backfill material.

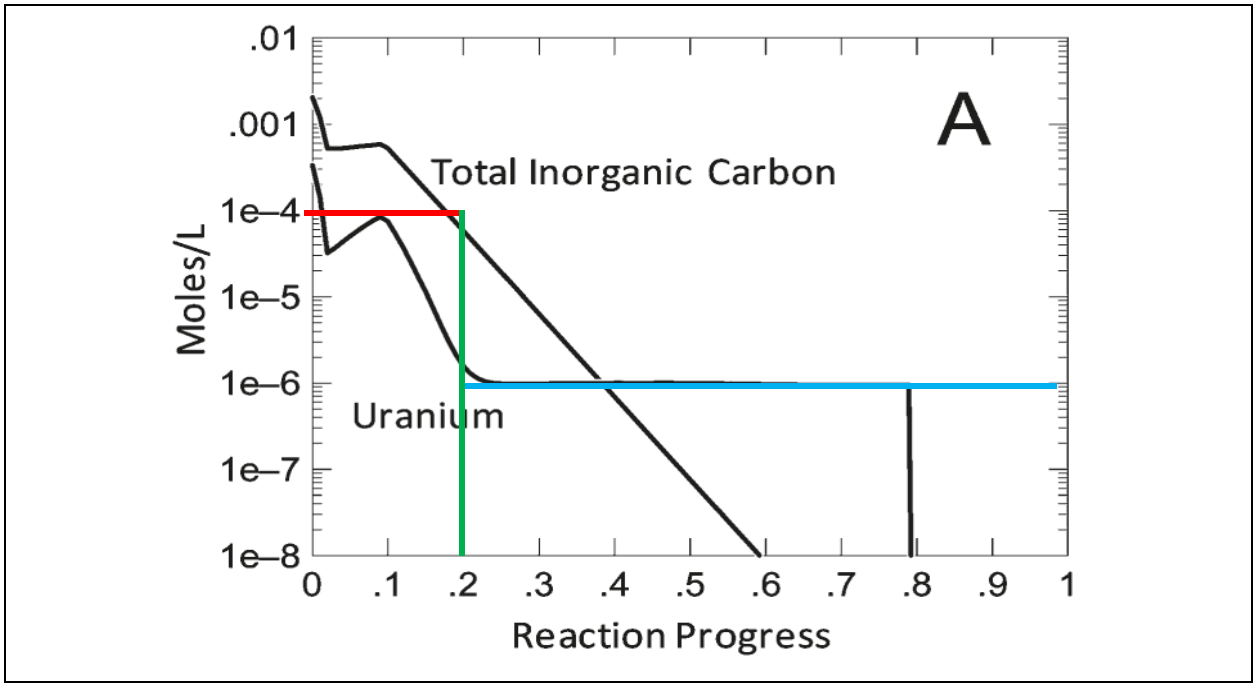

The reaction progress modeling calculations are performed under relatively static conditions. The SPFT tests discussed in Section 5 can be considered as analogous to column flow-through experiments. These are conducted under low flow conditions (~0.1 mL/hr [0.06 in.^{3}/hr]) for a period of about six months (at the sediment mass-to-solution ratio of 0.5 g [0.02 oz] to 0.06 L [3.66 in.^{3}]) with no stirring of the waste form in the solution. Even under these conditions, the application of the initial high solubility limit of 1×10^{-4} M is conservative for the 1,000-year time period. The SPFT test conducted on tank C-202 residuals (Figure 6-27) indicates that peak uranium concentrations for the $CaCO_3$ saturated water reached the solubility limit 1×10^{-4} M for a short duration at an early time, but later dropped to much lower numbers, and therefore represents a likely bounding uranium solubility value under all conditions at WMA C. This solubility limit is imposed for pipeline releases as well, where the releases are likely to be advectively dominated. This assumption is justified by the same logic about flow rates presented above.

6.3.1.3 Effective Diffusion Coefficient for Transport Through Tank Structure.

Observations of retrieved tanks show that the residual waste is primarily distributed on the tank

bottoms (see Section 5.2 of RPP-RPT-42323). Consequently, the residual waste is represented as a uniform layer at the base of the tank. Under the likely scenario, where tank wall integrity is maintained and the infill grout is not physically degraded (Section 6.2.1.2), the primary contaminant transport process will be diffusive. The shortest diffusive pathway for release to the near-field environment is through the base of the tank as presented in Figure 6-28. The diffusive thickness being considered is the 20 cm (8 in.) combined thickness of concrete and grout layer located at the base of the tank (ignoring the steel plate). The aqueous phase diffusive transport will occur along the water phase within the pore spaces of the grout and concrete layer. The effective diffusion coefficient (which includes effects of tortuosity), concentration gradient, and sorption behavior within the grout and concrete layer control the diffusive mass flux.

Figure 6-27. Comparison of Initially Imposed Uranium Solubility Limit of 1 × 10^{-4} M to the Observed Concentrations during the Single-Pass Flow-Through Conducted on 241-C-202 Tank Residual.

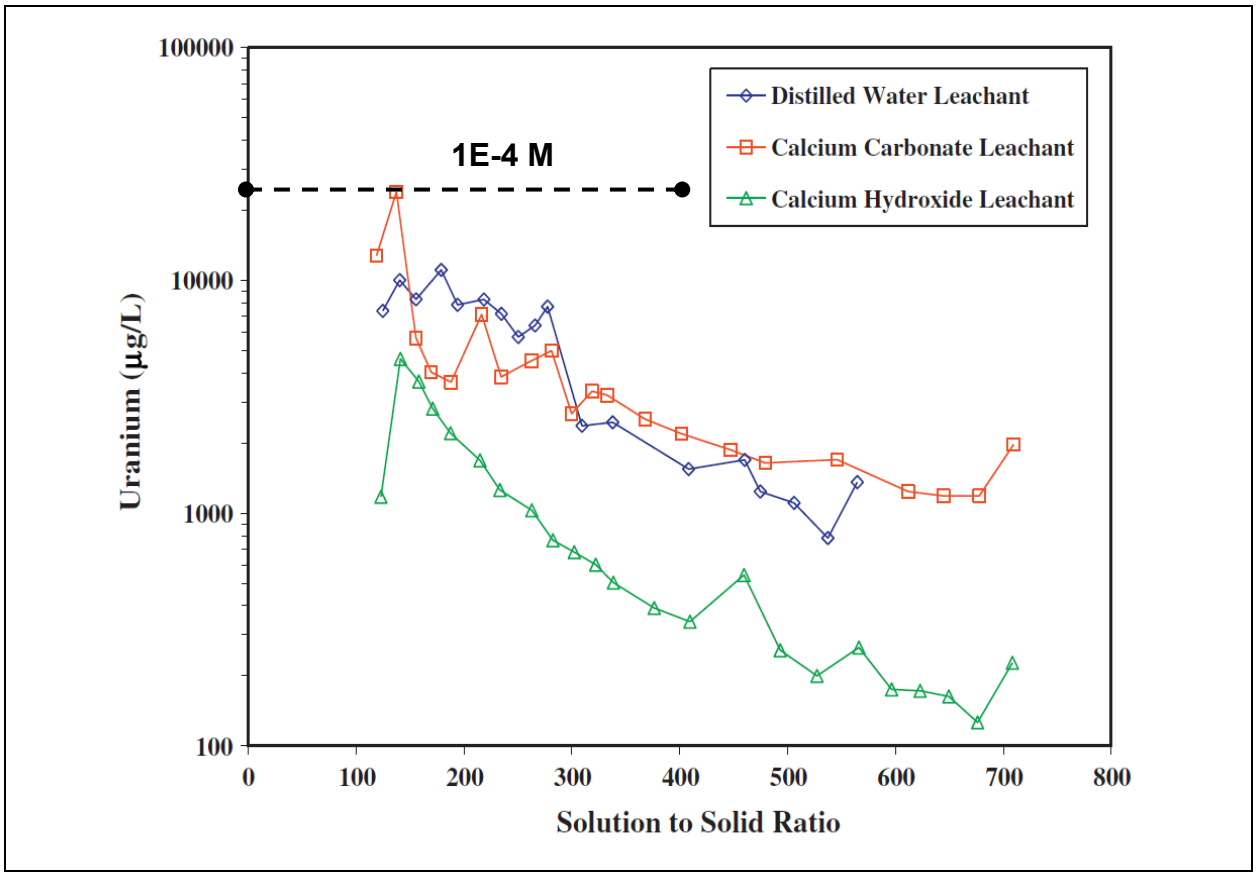

The effective diffusion coefficient of mobile contaminants (such as ^{99}Tc) through the combined grout and concrete base mat is considered a key parameter that controls the diffusive flux. Over the past decade, several experiments have been conducted to determine the effective diffusion coefficient through concrete for relatively mobile contaminants under unsaturated conditions. The results of various experiments are presented in PNNL-23841. Of particular interest are the sediment-concrete half-cell experiments conducted in Year 2008 (for a period of 351 days) with ^{99}Tc and stable iodine.

Figure 6-28. Diffusive Pathway for Transport of Non-Volatile Contaminants to the Near-Field Environment.

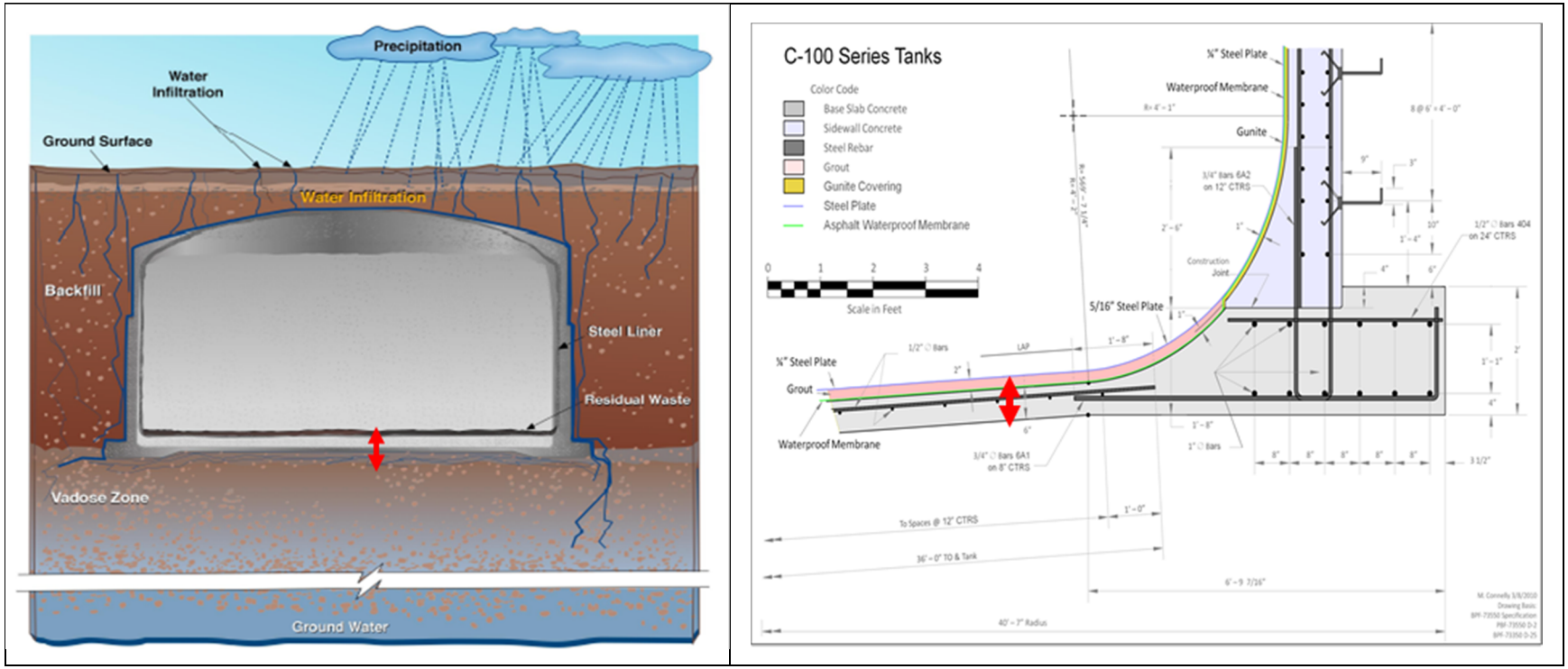

Laboratory-scale concrete mixtures were prepared by omitting coarse aggregates and using 40 to 60 mesh size sand instead. The concrete mix prepared consisted of mainly Type I/II sulfate resistant portland cement (27%), Class F fly ash (4%), sand (51%), and steel fiber (4%). The water-to-cement ratio was 0.5.

The experiments were conducted using cylindrical cells made of Schedule 40 PVC pipe (Figure 6-29). Caps were machined to fit into both ends of the PVC pipe and fitted with O-rings to minimize moisture loss during the test. For the sediment-concrete half-cells, the cell containing contaminant-spiked sediment was placed in contact with the non-spiked concrete monolith. The diffusion tests were run horizontally and undisturbed, with periodic rotation of the cell by 90 degrees. At the completion of the experiment, the concrete half-cells were sectioned parallel to the sediment-concrete interface. The concrete slices were then ground and two-to-one extracts (due to small sample size) by mass were performed on concrete fractions using the distilled deionized (DDI) water.

Figure 6-29. Set-Up of the Diffusive Half-Cell Experiment Contacting Contaminant-Spiked Sediment (or Concrete) Sample with the Non-Spiked Sediment (or Concrete) Sample.

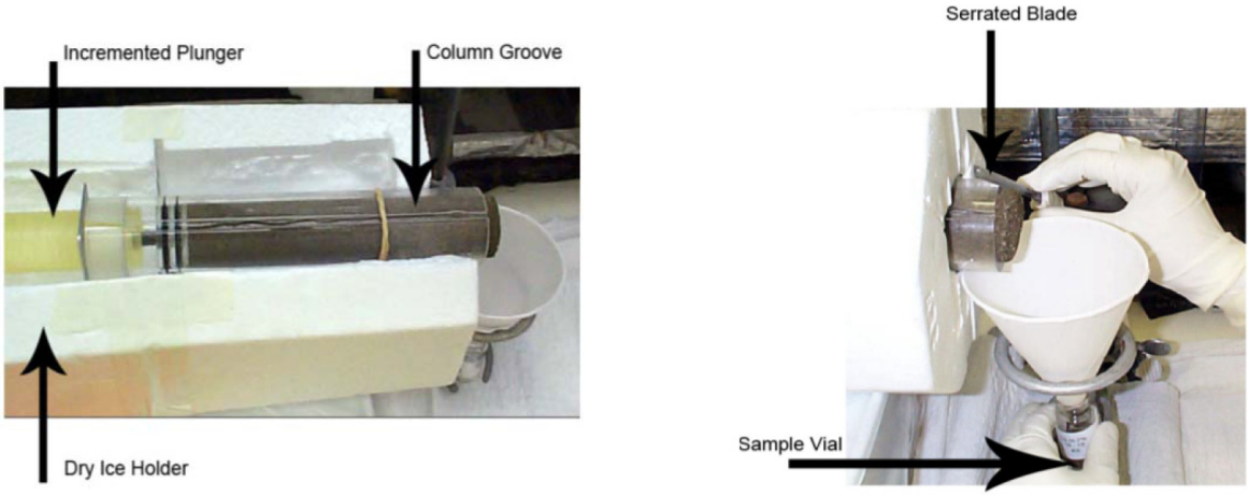

The concentration profiles developed in the concrete are analyzed by fitting the analytical solution to Fick's second law, with the assumption of zero concentration downstream boundary condition, and deriving a bulk diffusion coefficient for the media. This bulk diffusion coefficient implicitly incorporates the effects of porosity and tortuosity due to diffusion that primarily occurs along the water films in the concrete. For the purpose of modeling mass transport along the water (liquid) phase the effective diffusion coefficient in the water phase is needed (instead of bulk diffusion coefficient), which can be derived by multiplying bulk diffusion coefficient with the moisture content. Since the moisture content of the base mat concrete and grout material is not known and would likely change with time due to slow but steady physical and chemical degradation, the effective diffusion coefficient is chosen conservatively to be the same as the measured bulk diffusion coefficient for the purpose of source-term modeling. In other words, the reduction due to multiplying with moisture content is not applied for calculating the

diffusive flux. Note that the effective diffusion coefficient incorporates the effects of tortuosity resulting from transport along water films in the porous media.

Sediment-concrete diffusion experiments were initiated to investigate the effect of sediment moisture, concrete iron content, and concrete carbonation on the diffusivity of ^{99}Tc from sediment into concrete (PNNL-23841, Section 4.2.2). Sediment half-cell specimens were spiked with ^{99}Tc (4.2×10^{-4} mg ^{99}Tc/g sediment) to achieve a measurable diffusion profile in the concrete part of the half-cell. Hanford fine sand was used for the sediment half-cell. In these experiments, iron content was varied in the concrete specimens from 0% to 12%, sediment moisture content was varied (4%, 7%, or 15%), and half of the concrete monoliths were carbonated prior to preparing the half-cells. The characteristics of the concrete half-cells are listed in Table 6-4. Half-cell sampling was conducted at 351 days. Figure 6-30 presents the concentration profile developed in the concrete.

The calculated effective diffusion coefficients of ^{99}Tc derived from the experimental results are presented in Figure 6-31 and tabulated in Table 6-4. They range from 6.6×10^{-9} cm^2/s to 1.6×10^{-7} cm^2/s (1.0×10^{-7} in.^{2}/s to 2.5×10^{-6} in.^{2}/s), with a median value of ~3×10^{-8} cm^2/s (4.7×10^{-7} in.^{2}/s). No particular measurable trend exists to indicate whether the effective diffusion coefficient varies with moisture content of the sediment. The highest ^{99}Tc diffusivities were predominantly observed in the non-carbonated concrete cores contacting spiked sediments. A clear effect from the addition of iron was not observed. In general, the increased carbonation reduced diffusion coefficients.

Similar experiments, as described above, were performed using stable iodine in 2008, where the sediment half-cell specimens were spiked with stable iodine at concentrations of ~7 mg of iodine per gram (246.9 oz/ton) of sediment (PNNL-23841, Section 4.1.2). The concentration profiles developed in the concrete half-cells were evaluated and the effective diffusion coefficient was determined for iodine, which ranged from 1.4×10^{-8} cm^2/s to 9.7×10^{-8} cm^2/s (2.17×10^{-7} in.^{2}/s to 1.50×10^{-6} in.^{2}/s) with a median value of 2.6×10^{-8} cm^2/s (4.03×10^{-7} in.^{2}/s). The non-carbonated samples exhibited a larger depth of diffusion compared to the carbonated samples, similar to the observations made for ^{99}Tc. The range of effective diffusion coefficient (and the median value) for iodine in concrete is very similar to that for ^{99}Tc.

Experiments were also performed to assess the effect of fractures in the concrete on diffusion of ^{99}Tc and iodine. For this purpose, the concrete monoliths were wrapped in shrink-wrap (to prevent the formation of rubble), and the end of the flathead screwdriver was placed directly in the center of the core and stuck once. Each fractured concrete monolith had a single midline fracture that penetrated the length of the core. A set of sediment to fractured concrete diffusion half-cell experiments were conducted, by varying the iron content using both carbonated and non-carbonated concrete but keeping the moisture content in the sediment half-cell constant at 4%. The sediment half-cell specimens were spiked with ^{99}Tc at a concentration of 3.24×10^{-4} mg per gram (0.011 oz/ton) of sediment. The derived effective diffusion coefficient ranged from 1.9×10^{-9} cm^2/s to 2.5×10^{-8} cm^2/s (2.94×10^{-8} in.^{2}/s to 3.88×10^{-7} in.^{2}/s). Similar experiments conducted using stable iodine (spiked at 7 mg per gram [246.9 oz/ton] of sediment) resulted in effective diffusion coefficient that ranged from 4.7×10^{-9} cm^2/s to 8.4×10^{-8} cm^2/s (7.29×10^{-8} in.^{2}/s to 1.30×10^{-6} in.^{2}/s). These ranges are similar to the ranges calculated for diffusion in the unfractured concrete monolith.

Table 6-4. Characteristics of Concrete Specimens Used in Sediment-Concrete Half-Cell Experiments Along with Derived Bulk Diffusion Coefficient of Technetium-99 for the Concrete.*

Core ID	Length (cm)	Diameter (cm)	Surface Area (cm^2)	Volume (cm^3)	Weight (g)	Density (g/cm^3)	Iron (wt%)	Carbonated	Initial Sediment Moisture Content (%)	Technetium-99 Diffusivity (cm^2/s)
C-08-3-0-325	4.09	4.33	84.97	60.1	131.44	2.19	0	N	4	7.08E-08
C-08-3-0-329	4.32	4.33	88.13	63.53	139.5	2.2	0	N	7	6.55E-08
C-08-3-0-330	3.85	4.33	81.77	56.65	123.5	2.18	0	N	15	3.51E-08
C-08-3-0-332	4.33	4.32	88.09	63.48	139.65	2.2	0	Y	4	2.23E-08
C-08-3-0-333	4.35	4.33	88.57	64	140.79	2.2	0	Y	7	2.25E-08
C-08-3-0-334	4.07	4.32	84.56	59.67	130.55	2.19	0	Y	15	1.22E-08
C-08-3-4-350	3.84	4.32	81.43	56.28	127.25	2.26	4	N	4	3.21E-08
C-08-3-4-351	4	4.33	83.92	58.96	132.78	2.25	4	N	7	1.57E-07
C-08-3-4-353	4.01	4.33	83.99	59.04	133.38	2.26	4	N	15	3.09E-08
C-08-3-4-357	3.9	4.32	82.19	57.11	128.77	2.25	4	Y	4	3.09E-08
C-08-3-4-359	3.83	4.32	81.25	56.09	126.5	2.26	4	Y	7	1.07E-08
C-08-3-4-360	4.11	4.33	85.47	60.64	136.11	2.24	4	Y	15	3.26E-08
C-08-3-8-401	4.07	4.32	84.4	59.5	135.91	2.28	8	N	4	7.76E-09
C-08-3-8-402	3.81	4.32	81.02	55.84	127.31	2.28	8	N	7	2.85E-08
C-08-3-8-403	4	4.33	83.87	58.91	133.35	2.26	8	N	15	1.62E-08
C-08-3-8-404	4.05	4.33	84.61	59.71	133.69	2.24	8	Y	4	5.34E-08
C-08-3-8-405	3.86	4.33	81.77	56.65	126.96	2.24	8	Y	7	9.25E-09
C-08-3-8-406	3.94	4.33	83.08	58.05	130.61	2.25	8	Y	15	6.61E-09
C-08-3-12-425	4.33	4.27	87.54	62.88	143.44	2.28	12	N	4	1.07E-07
C-08-3-12-426	4.33	4.33	88.35	63.76	145.77	2.29	12	N	7	1.31E-08
C-08-3-12-427	4.33	4.22	86.94	62.23	141.71	2.28	12	N	15	8.21E-08
C-08-3-12-432	4.02	4.32	83.83	58.88	134.09	2.28	12	Y	4	4.6E-08
C-08-3-12-433	4.15	4.33	85.81	61.01	139.8	2.29	12	Y	7	6.95E-09
C-08-3-12-435	3.88	4.33	82.22	57.12	130.04	2.28	12	Y	15	7.09E-09

*Note: For the purpose of source-term calculations, the bulk diffusion coefficient is considered to be the same as effective diffusion coefficient.

Figure 6-30. Technetium-99 Concentration Profiles in Concrete from Sediment-Concrete Half-Cell Experiments Conducted on (A) 4% Sediment Moisture, Carbonated Monoliths, (B) 4% Sediment Moisture, Non-Carbonated Monoliths, (C) 7% Sediment Moisture, Carbonated Monoliths, (D) 7% Sediment Moisture, Non-Carbonated Monoliths, (E) 15% Sediment Moisture, Carbonated Monoliths, and (F) 15% Sediment Moisture, Non-Carbonated Monoliths.

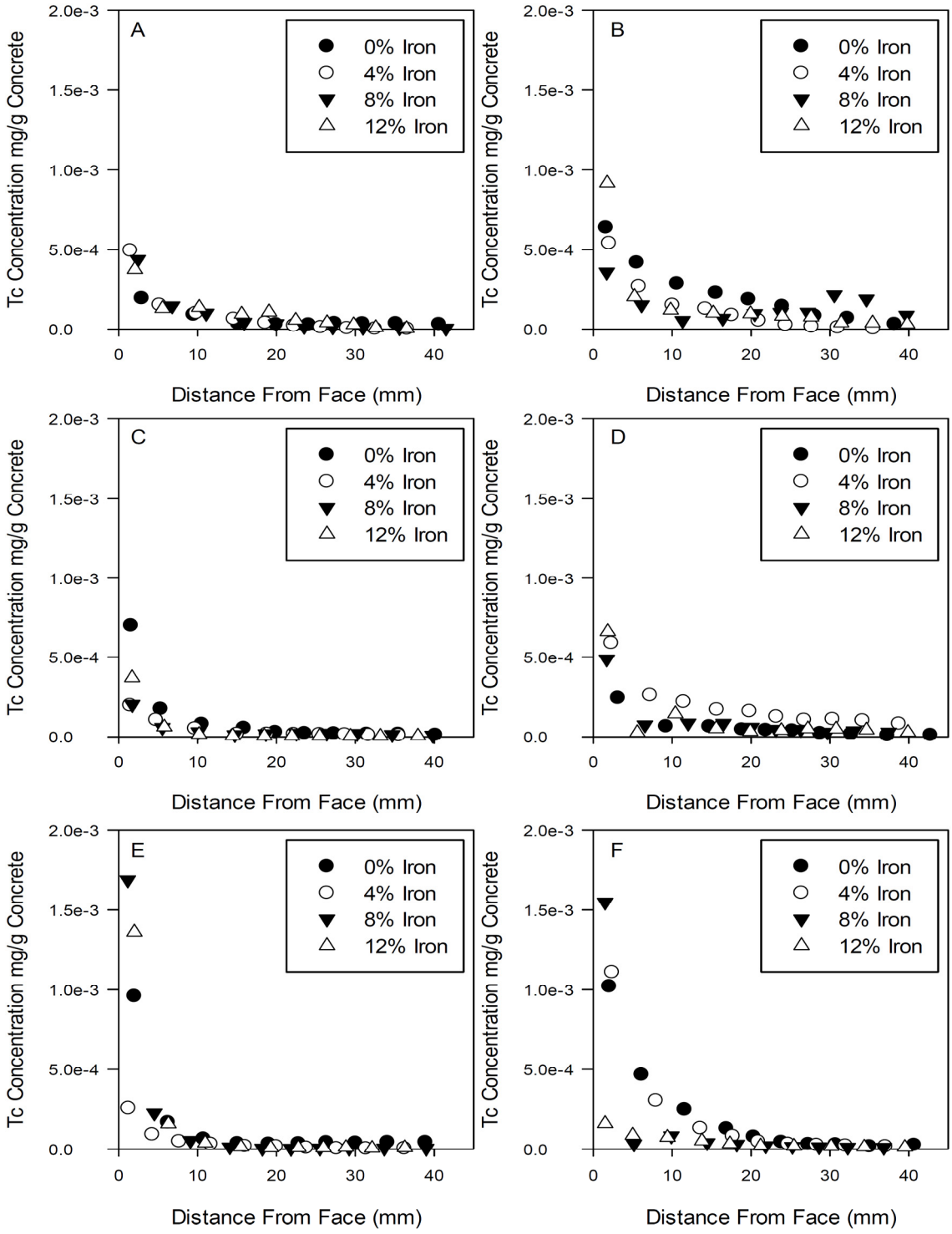

Figure 6-31. Effective Diffusion Coefficient of Technetium-99 in Concrete Based on Experiments Conducted Using Sediment-Concrete Half-Cells.

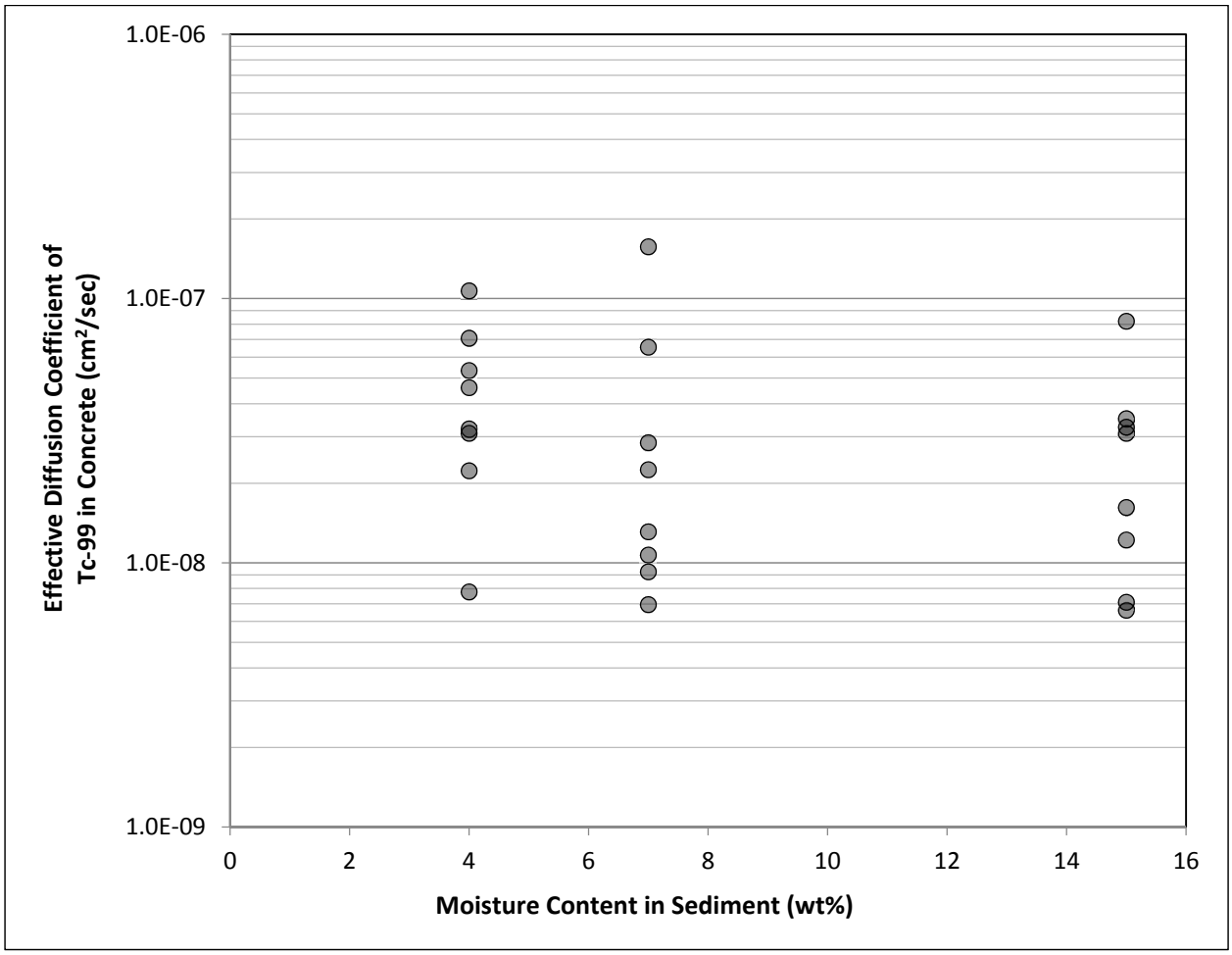

Reference: PNNL-23841, "Radionuclide Migration through Sediment and Concrete: 16 Years of Investigations."

For the purpose of the PA base case calculations, the experimental median value of 3×10^{-8} cm^2/s (4.65×10^{-7} in.^{2}/s) is chosen as the best estimate for the effective diffusion coefficient in concrete. This value is applied to all species diffusing through the concrete. Based on the range presented in Figure 6-31, an uncertainty range with a minimum and maximum value of 6×10^{-9} cm^2/s and 2×10^{-7} cm^2/s (9.30×10^{-8} in.^{2}/s and 3.10×10^{-6} in.^{2}/s) will be evaluated in Section 8 (Uncertainty Analysis).

6.3.1.4 Sorption of Contaminants to Grout and Concrete. A linear sorption isotherm (using a K_d approach) is considered for determining sorption within the grout and concrete layer for various contaminants as they undergo diffusive (and advective) transport through the tank. The K_d values are presented in Table 6-5 in terms of best estimate and the uncertainty range that are derived from relevant published literature for chemical conditions that are likely to exist within the grout/concrete layer within the tanks.

Table 6-5. K_d Values (mL/g) for Grout/Concrete Used for Waste Management Area C Performance Assessment.

Element	Best	Minimum	Maximum	Reference
Ac	1.00E+05	3.00E+03	3.30E+05	NAGRA NTB 02-20
Al	0.00E+00	0.00E+00	0.00E+00	No relevant information
Am	1.00E+03	2.00E+02	5.00E+03	SKB R-05-75
B	0.00E+00	0.00E+00	0.00E+00	No relevant information
C	2.00E+02	1.00E+02	4.00E+03	SKB R-05-75
Cd	4.00E+01	2.00E+00	8.00E+02	SKB R-05-75
Cm	1.00E+03	2.00E+02	5.00E+03	SKB R-05-75
CN	0.00E+00	0.00E+00	0.00E+00	No relevant information
Co	4.00E+01	4.00E+00	4.00E+02	SKB R-05-75
Cr	0.00E+00	0.00E+00	0.00E+00	No relevant information
Cs	1.00E+00	1.00E-01	1.00E+01	SKB R-05-75
Eu	5.00E+03	1.00E+03	2.50E+04	SKB R-05-75
F	0.00E+00	0.00E+00	0.00E+00	No relevant information
Fe	0.00E+00	0.00E+00	0.00E+00	No relevant information
H	1.00E-01	7.10E-02	1.40E-01	NAGRA NTB 02-20
Hg	0.00E+00	0.00E+00	0.00E+00	No relevant information
I	3.00E+00	3.00E-01	3.00E+01	SKB R-05-75
Mn	0.00E+00	0.00E+00	0.00E+00	No relevant information
Nb	5.00E+02	1.00E+02	2.50E+04	SKB R-05-75
Ni	4.00E+01	8.00E+00	2.00E+02	SKB R-05-75
NO_2	0.00E+00	0.00E+00	0.00E+00	No relevant information
NO_3	0.00E+00	0.00E+00	0.00E+00	No relevant information
Np	1.00E+02	7.10E+01	1.40E+02	NAGRA NTB 02-20
Pa	1.00E+02	7.10E+01	1.40E+02	NAGRA NTB 02-20
Pb	5.00E+02	3.60E+02	7.10E+02	NAGRA NTB 02-20
Pu	1.00E+02	7.14E+01	1.40E+02	NAGRA NTB 02-20
Ra	5.00E+01	5.00E+00	5.00E+02	SKB R-05-75
Rn	0.00E+00	0.00E+00	0.00E+00	No relevant information
Se	6.00E+00	1.00E-01	4.00E+02	SKB R-05-75
Sm	5.00E+03	1.00E+03	2.50E+04	SKB R-05-75
Sn	5.00E+02	2.50E+01	1.00E+04	SKB R-05-75
Sr	1.00E+00	5.00E-01	5.00E+01	SKB R-05-75
Tributyl phosphate	0.00E+00	0.00E+00	0.00E+00	No relevant information
Tc	1.00E+00	7.10E-01	1.40E+00	NAGRA NTB 02-20
Th	3.00E+04	1.00E+03	1.00E+06	NIROND-TR 2008-23 E
U	2.00E+03	1.40E+03	2.80E+03	NAGRA NTB 02-20
Zr	1.00E+04	3.00E+03	3.30E+04	NAGRA NTB 02-20

References:
NAGRA NTB 02-20, "Cementitious Near-Field Sorption Data Base for Performance Assessment of an ILW Repository in Opalinus Clay."
NIROND-TR 2008-23 E, "Review of sorption values for the cementitious near field of a near surface radioactive waste disposal facility, Project near surface disposal of category A waste at Dessel."
PSI Bericht Nr. 95-06, "Sorption Databases for the Cementitious Near-Field of a L/ILW Repository for Performance Assessment."
SKB Rapport R-05-75, "Assessment of uncertainty intervals for sorption coefficients SFR-1 uppföljning av SAFE."

Development of a sophisticated sorption model depends on the availability of complete sets of experimental data, including measurement of isotherm, and dependence on solid-to-liquid ratio under conditions that are applicable to the near-field environment. Presently the vast majority of sorption data on cementitious material are based on single-point measurements, and information on uptake mechanisms and uptake controlling phases in cement systems are lacking to a large extent (NAGRA NTB 02-20, "Cementitious Near-Field Sorption Data Base for Performance Assessment of an ILW Repository in Opalinus Clay"). Until studies are performed at the molecular level to discern uptake processes, sorption databases, in conjunction with scientific expertise, can be used to select site-specific sorption values.

As described below, selections for sorption values (K_d) have been made based on review of past reports that are focused on developing internally consistent cement sorption databases for cementitious near-field material (hardened cement paste) based on the composition of cement porewaters and stage of cement degradation.

- Conditions in the closed tank farm are expected to be moderately oxidizing, owing to the position of the waste in unsaturated conditions. Where data are available to differentiate between oxidizing and reducing conditions, K_d values under oxidizing conditions are preferentially selected, as it leads to lower K_d values relative to reducing conditions.

- Composition of the cementitious material (grout or concrete) may have different chemical compositions, and therefore differ in contaminant uptake mechanisms and cement phases. Due to lack of information, the differences in sorption between various types of cements and concrete are ignored.

- The selected K_d values are based on assumption of $Ca(OH)_2$ saturated waters contacting the waste, and therefore represent the so-called stage II of the chemical degradation of cementitious material. In this stage, chemical composition of the alkali-depleted cement pore water is controlled by the solubility of portlandite. The impact on K_d values during evolution of chemical conditions from stage I (higher alkali content and pH) to stage II is expected to be minor and incorporated within the uncertainty range.

- The reviews of SKB R-05-75, "Assessment of uncertainty intervals for sorption coefficients, SFR-1 uppföljning av SAFE" and NIROND-TR 2008-23 E, "Review of sorption values for the cementitious near field of a near surface radioactive waste disposal facility, Project near surface disposal of category A waste at Dessel" are more recent, and represent critical reviews and independent data from NAGRA NTB 02-20 and PSI Bericht Nr. 95-06, "Sorption Databases for the Cementitious Near-Field of a L/ILW Repository for Performance Assessment." Where appropriate values are available from these more recent references, they are preferred to the older ones.

- When K_d values are absent from these references, a value of zero has been assumed for the analyte since chemical equivalences between similar analytes have not been performed to justify nonzero K_d values. As necessary, chemical equivalences suggested by SKB R-05-75 may be used to update K_d values in future iterations of the PA modeling.

- When there was significant disagreement between literature sources, the lower (less sorptive) K_d value has been chosen. For example, K_d values under oxidizing conditions were selected over those measured under reducing conditions.

The K_d values were compared to values used in Savannah River F and H tank farm PAs (WSRC-STI-2007-00369, "Hydraulic and Physical Properties of Tank Grouts and Base Mat Surrogate Concrete for FTF Closure" and WSRC-STI-2007-00607). The values used for WMA C are generally consistent with or more conservative than comparable values used for the facility-specific grout used at Savannah River. When WMA C values are more conservative, it has been for one of the following two reasons.

- The grout used at Savannah River produces reducing conditions. In the absence of a specific grout formulation for WMA C, it has been assumed that oxidizing conditions will exist in the grout, which leads to lower (more conservative) K_d values for some radionuclides of interest.

- The disposal system at WMA C is very robust with respect to meeting performance objectives. As a result, when data were ambiguous or insufficient in any way, it was more efficient to make a conservative assumption about K_d than to spend resources to resolve the value in greater detail. So, for instance, when data are lacking for a contaminant it is assigned a value of zero.

6.3.1.5 Evaluation of Diffusive Release Assumption for Intact Tank Condition. Based on the tank infill grout and concrete degradation mechanisms discussed in Section 6.2.1.2, it was determined that tanks are not likely to be fully degraded within the modeled time period of 10,000 years. Due to the unlikely development of continuous fracture pathways within the infill grout over the 10,000 years, advective flow is likely to be very slow, to the extent that it is negligible. Therefore, the primary contaminant transport process will be diffusion (in the aqueous phase), where concentration differences across the grout and concrete tank base mat provide a gradient leading to diffusion. The predominance of diffusion with negligible amount of advection, if any, is based on the following reasoning.

1. The backfill material surrounding the tank structure will provide a preferential pathway for any water infiltrating through the surface cover. Due to large contrast in relative permeability (several orders of magnitude) between gravel-dominated backfill material and grout monolith inside the tank under ambient conditions, most of the infiltrating water will flow around and bypass the tank structure.

2. The capillary forces within the grout micropores are much larger than surrounding backfill soil. Therefore, initially when the grout is emplaced in the tank, the grout will wick water from the surrounding material and hold it in place, much like a clay lens within a sand body. With increasing degree of hydration over time that leads to formation of calcium silicate hydrate (C-S-H) gel, the amount of interconnected pore space is known to reduce, and some capillary pores will become discontinuous. This is likely to further reduce the permeability appreciably ("Relationships between permeability and pore structure of hardened cement paste" [Nyame and Illston 1981]) as shown in Figure 6-32.

Figure 6-32. Porosity-Permeability Relationship as a Function of Hydration and Water-to-Cement Ratio.

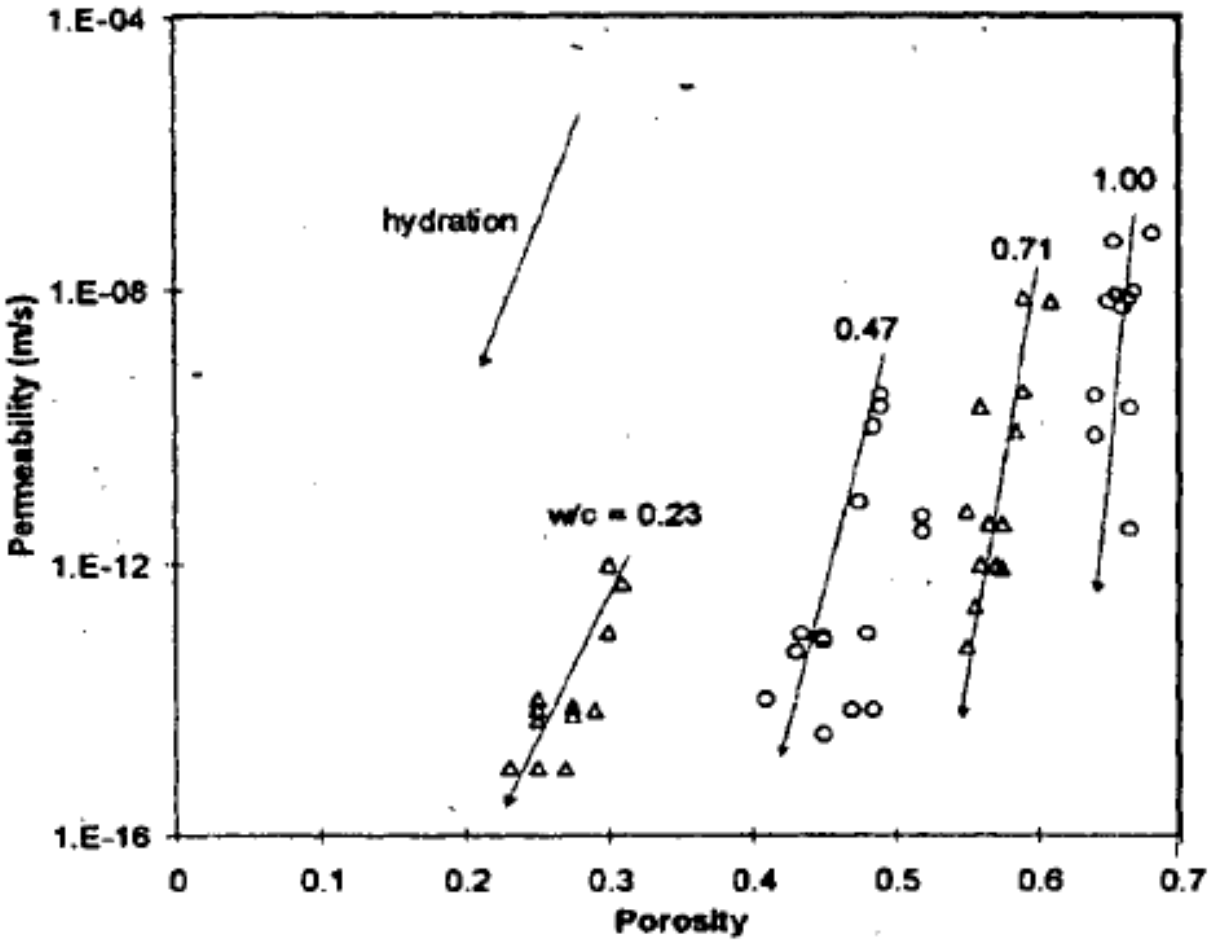

Reference: "Relationships between permeability and pore structure of hardened cement paste" (Nyame and Illston 1981).

A numerical simulation of flow around the grouted tank surrounded by backfill material was undertaken to evaluate the relative importance of advective flow. For this analysis, the tank was simplified by assuming that the concrete wall behaved identically to grout in hydraulic properties. The hydraulic properties assigned to the grout were chosen from WSRC-STI-2007-00369 that represented strong grout material. The corresponding characteristic curves are presented in Figure 6-33.

The numerical calculations were performed in a two-dimensional (2-D) vertical cross-section for a row of tanks under a 3.5 mm/yr (0.14 in./yr) constant recharge rate (same as the long-term post-closure recharge rate). The transient calculations were performed by setting the initial matric potential for the tank nodes to be -2,000 cm, representing conditions that are between fully saturated and near residual saturations. The 2-D cross-section, along with the long-term near steady-state flow field, is shown in Figure 6-34. The vertical Darcy flux in the backfill material is orders of magnitude higher than in the tank, consistent with the choice of parameters.

Figure 6-33. Soil-Moisture Characteristics Curves for the Grout Hydraulic Properties Evaluated.

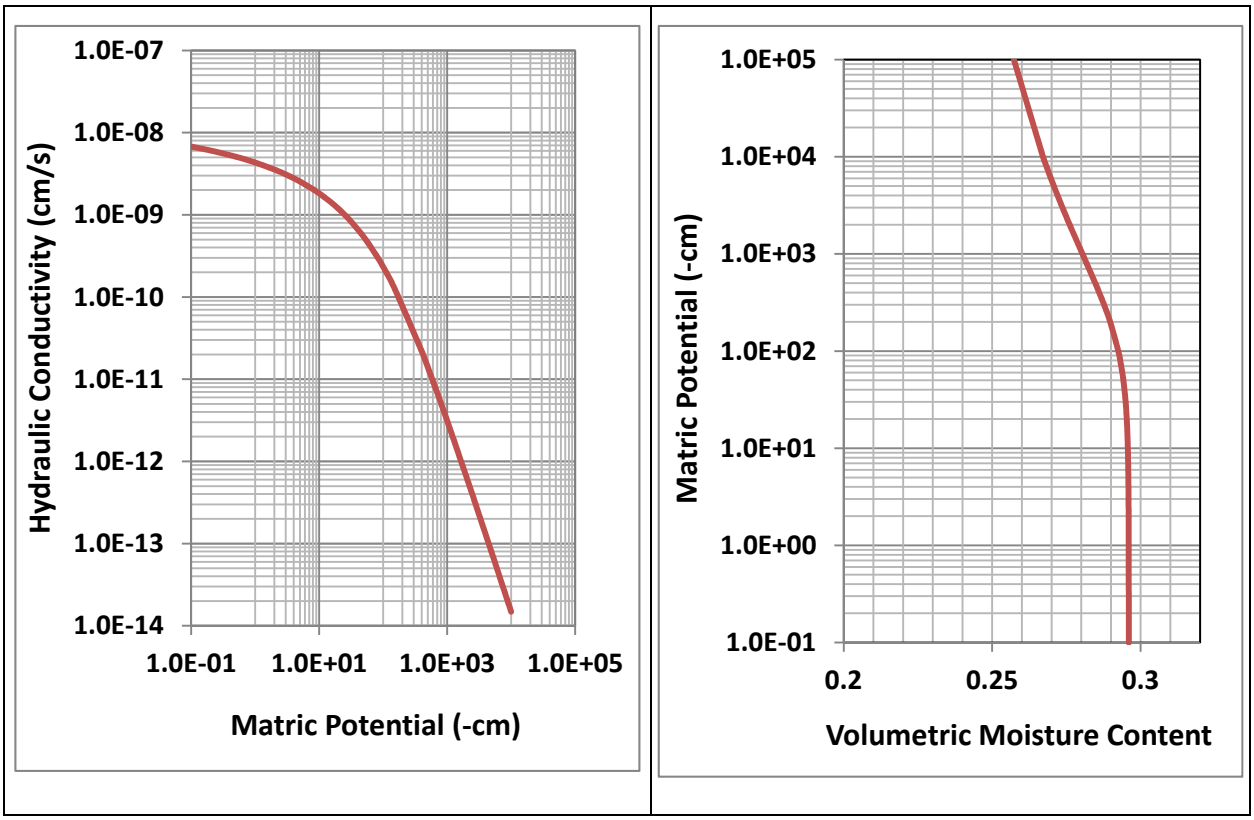

The transient conditions, showing the changing vertical Darcy flux and volumetric moisture content, are presented in Figure 6-35 for two selected nodes: one within the tank, and the other outside in the backfill. These results indicate that the vertical Darcy flux in the grout remains over three orders of magnitude lower than through the backfill. The Darcy flux in the grout is negligibly small for the first few thousand years, and gradually increases as the large capillary suction draws water in, eventually increasing the unsaturated hydraulic conductivity compared to the initial state.

To compare the relative importance of advection and diffusion, the dimensionless Peclet number (ratio of advective transport to diffusive transport rate) was calculated for the simulated results at 10,000 years. The characteristic length chosen was 1.25 m (4.1 ft), which is the vertical grid discretization over which the Darcy flux calculations are computed. The Peclet number for transport in the tank is approximately 0.1 while in the backfill it is about 2, indicating that transport through the tank is predominantly diffusion-controlled while transport through the backfill has a higher advective component. During the first 1,000 years, the Peclet number for the tank is close to zero due to negligibly small Darcy flux as shown in Figure 6-35, and increases gradually. Therefore, during the 10,000-year period, it is clear that diffusion dominates transport within the grouted tank; whereas in the backfill, both advection and diffusion play a role in transport.

Figure 6-34. Two-Dimensional Cross Section Model to Evaluate the Flow Through the Tanks along with the Flow-Field at Long Time Representing near Steady-State Conditions.

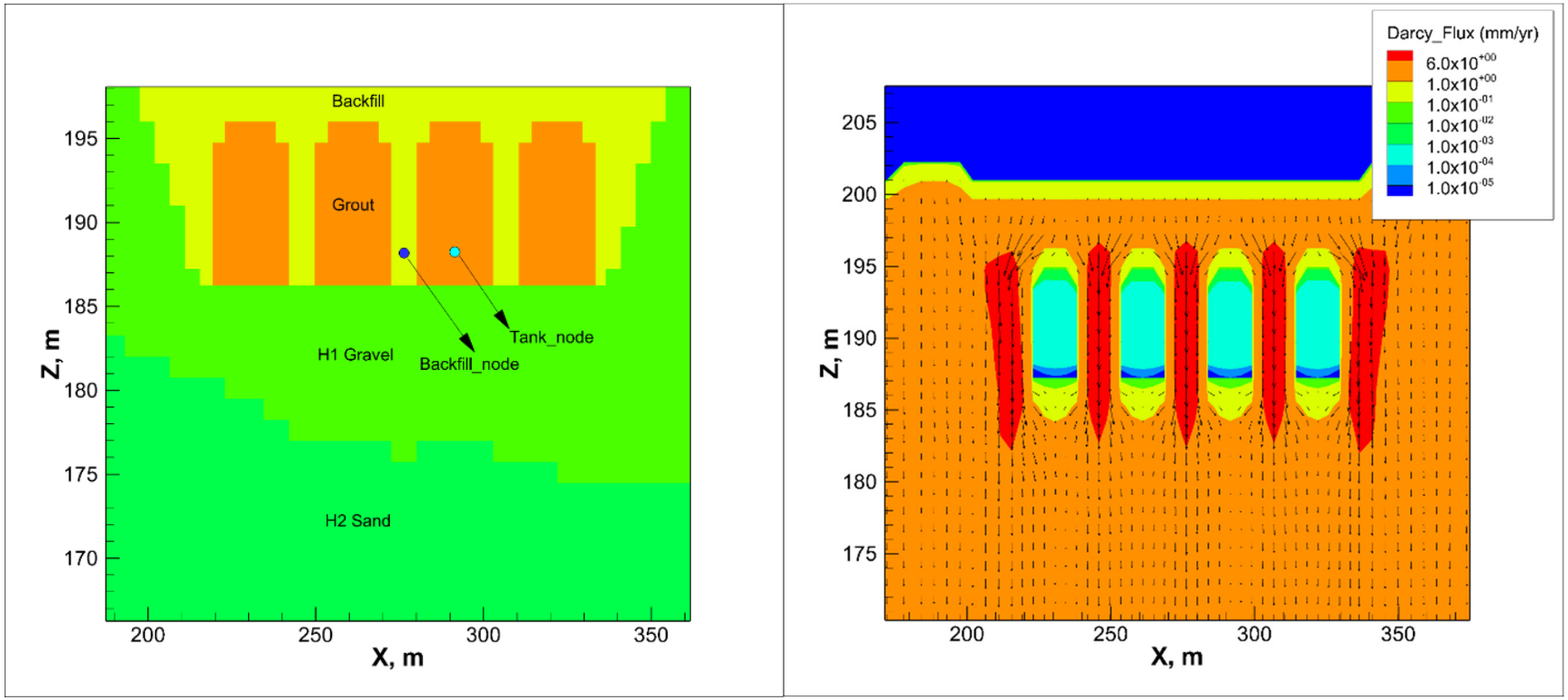

Figure 6-35. Simulated Vertical Darcy Flux and Volumetric Moisture Content for the Tank Node and Backfill Node over a Large Time Scale.

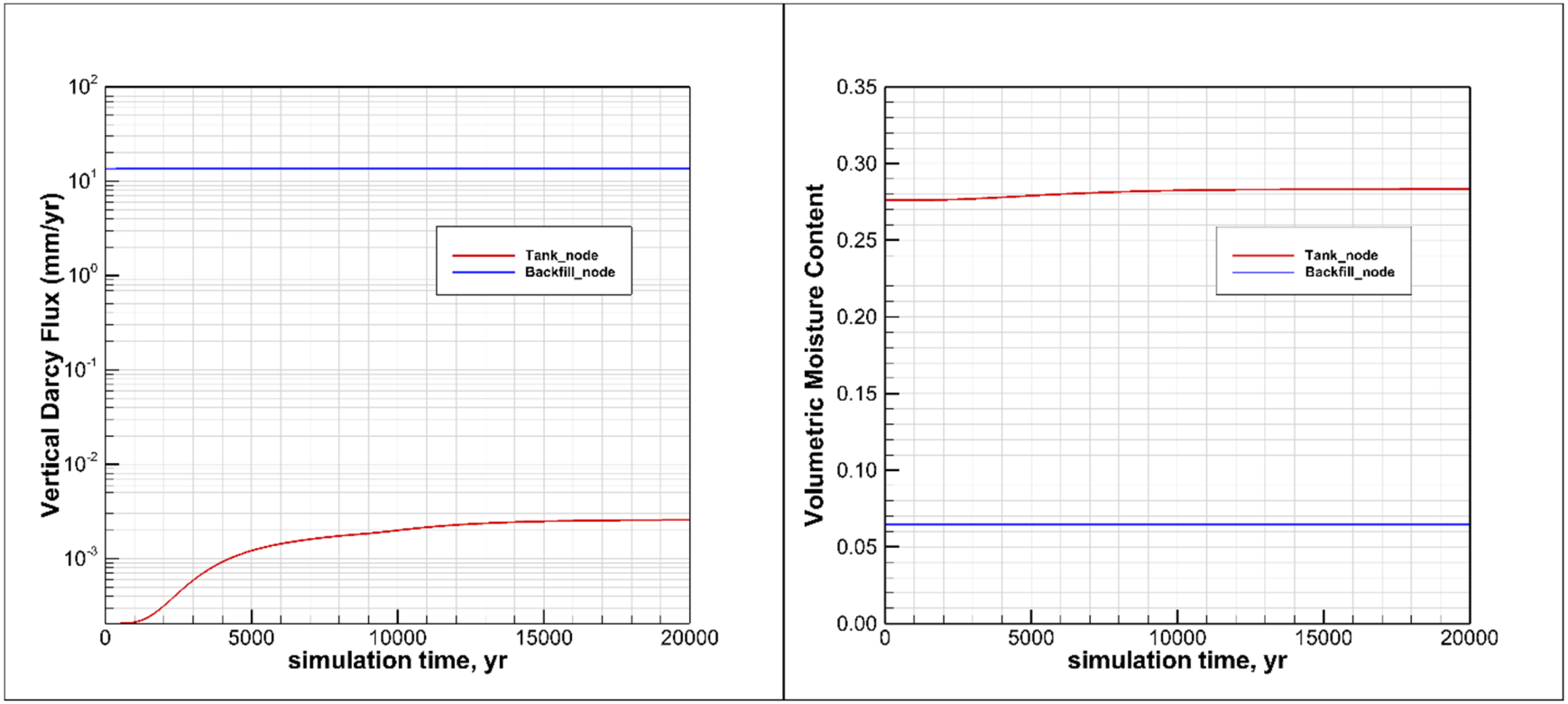

These analyses support the assumption of diffusion-dominated releases from an intact tank.

6.3.1.6 Parameters Used in Source Term Calculations. Following is the list of parameters used in developing source-term release calculations for the groundwater pathway.

Parameter	Value	Reference
Porosity of Residual Waste Layer	0.4	Assumed; based on evaluation of sludge waste phase from the retrieved tanks.
Saturation of Residual Waste Layer	1	Assumed fully saturated to maximize diffusive release
Residual Waste Volume	Variable by source	Section 3.1
Porosity of Concrete and Grout layer below the waste layer	0.11	SRNL-STI-2008-00421, Table 39
Porosity of in-fill Grout within the tank (at closure)	0.269	WSRC-STI-2007-00369, Table 29; Strong grout assumed.
Saturation of Concrete and Grout layer below the waste layer	1	Assumed to maximize diffusive release
Bulk Density of Concrete and Grout layer below the waste layer	2.41 g/cm^3 (151 lb/ft^3)	RPP-RPT-50934, p. C-3 (C-107 dome core density of 2.41 g/cm^3 [151 lb/ft^3])
Diffusive Length of Waste form layer	0 m (0 ft)	Assumed to maximize diffusive release
Diffusive Length of Concrete and Grout layer below the waste layer	0.203 m (8 in.)	Minimum diffusive thickness based on tank bottom geometry
Diffusive Area for source term release	410.4 m^2 (4,417.5 ft^2) for 100-Series Tanks; 29.2 m^2 (314.3 ft^2) for 200-Series Tanks and C-301 catch tank; 162.4 m^2 (1748.1 ft^2) for CR-Vaults; 22,500 m^2 (242,188.0 ft^2) for Pipelines	Base area for tanks based on circular geometry; area of CR-Vault is based on rectangular area with length of 28 m (92 ft) and average width of 5.8 m (19 ft); area of Pipeline assumed to be 150 m × 150 m (492 ft × 492 ft).
Effective Diffusion Coefficient through grout and concrete layer (incorporates effects of tortuosity)	3×10^{-8} cm^2/s (4.7×10^{-7} in.^{2}/s)	Section 6.3.1
Uranium solubility for intact tank conditions	1×10^{-4} M for 1,000 years; 1×10^{-6} M for time >1,000 years	Section 6.3.1

Parameter	Value	Reference
Uranium solubility for degraded tank conditions	1×10^{-4} M for 1,000 years; 2×10^{-5} M for time >1,000 years	Section 6.3.1
Technetium-99 release	6% of the waste inventory available for release instantaneously; remaining 94% waste form inventory made available based on first order fractional release rate of 6×10^{-4} day^{-1}.	Section 6.3.1
Contaminant K_d values for transport through the grout and concrete layer	Variable; See Table 6-5	Table 6-5
Release Type	Diffusive release from the tanks and CR-Vaults under intact conditions; Both advective and diffusive release for the Pipelines Both advective and diffusive release for tanks and CR-Vaults under degraded conditions	

References:
RPP-RPT-50934, "Inspection and Test Report for the Removed 241-C-107 Dome Concrete."
SRNL-STI-2008-00421, "Hydraulic and Physical Properties of Saltstone Grouts and Vault Concretes."
WSRC-STI-2007-00369, "Hydraulic and Physical Properties of Tank Grouts and Base Mat Surrogate Concrete for FTF Closure."

6.3.1.7 Source-Term Mathematical Model. The source-term model is implemented in GoldSim© using its Contaminant Transport Module. The Contaminant Transport Module allows the user to dynamically model mass transport using a compartment-based model of the system. The Contaminant Transport Module includes the following key features (GoldSim Technology Group 2014a).

- Radioactive decay chains can be simulated, taking account of ingrowth and decay.
- A large built-in database exists for radionuclide decay data (species, decay rates, and radioactive progeny) for over 1,300 radionuclides and their corresponding stable elements. The data is based on ICRP 2008.
- Specialized elements in GoldSim© called Source and Cells are available to model key release mechanisms from source term that include waste form degradation rate and solubility control.
- Both advective and diffusive transport mechanisms can be explicitly represented using the "Cell" pathway element, by specifying the flow rates for advective transport and the diffusion coefficient and geometric factors for diffusive transport. Media properties through which advection and diffusion occur also need to be specified.

- When multiple Cells are linked together via advective and diffusive mechanisms, the behavior of the Cell network is mathematically described using a coupled system of ordinary differential equations in time. A network of Cells is mathematically equivalent to a finite difference network of nodes. GoldSim© numerically solves the coupled system of equations to compute the contaminant mass present in each Cell and the mass fluxes between Cells as a function of time. The solution technique uses backwards-difference (fully implicit) algorithm for each cell-net and each species decay-chain family.

The basic mass balance equation for Cell *i* is as follows:

$$m'_{is} = -m_{is}\lambda_s + \sum_{p=1}^{NP_s} m_{ip}\lambda_p f_{ps} R_{sp}\left(\frac{A_s}{A_p}\right) + \sum_{c=1}^{NF_i} f_{cs} + S_{is} \qquad (6\text{-}1)$$

Where:

m'_{is} = rate of increase of mass of species s in Cell i (M/T)
m_{is} = mass of species s in Cell i (M)
λ_s = decay rate of species s (T^{-1})
NP_s = Number of direct parents for species s
f_{ps} = fraction of parent p which decays into species s
R_{sp} = stoichiometric ratio of moles of species s produced per mole of species p decayed
A_s = molecular (or atomic) weight of species s (M/mol)
A_p = molecular (or atomic) weight of species p (M/mol)
NF_i = number of mass flux links from/to Cell i
f_{cs} = influx rate of species s (into Cell i) through mass flux link c (M/T)
S_{is} = rate of direct input of species s to Cell i from external source (M/T).

The first term on the right-hand side in Equation 6-1 represents decay (or chemical reaction), the second term represents ingrowth, the third term represents mass transfer in or out of the Cell via mass flux links, and the fourth term represents the rate of direct input to the Cell from other sources.

Equation 6-1 couples in two ways to other mass balance equations: 1) through the ingrowth terms, which couple all species in a decay chain; and 2) through the mass flux terms, which couple all Cells that are connected by mass flux links. Representation of the mass flux terms (f_{cs}) is the most complex part of the above equation, and is described in detail below in terms of advective mass flux and diffusive mass flux.

Advective mass flux from Cell i to Cell j for species s is computed as follows:

$$f_{s,i\to j} = c_{ims}\, q \qquad (6\text{-}2)$$

Where:

q = the rate of advection of water for the mass flux link i to j (L^3/T)
c_{ims} = the total dissolved concentration of species s in medium m within Cell i (M/L^3).

Diffusive mass flux links are used to transport mass through a stagnant or slowly moving fluid via the process of molecular diffusion. Diffusive mass transport is proportional to a concentration difference, with mass diffusing from high concentration to low concentration. The constant of proportionality is referred to as the diffusive conductance:

Diffusive Mass Rate = (Diffusive Conductance) × (Concentration Difference)

In this equation, the Diffusive Mass Rate has dimensions of mass/time, the Diffusive Conductance has dimensions of volume/time, and the Concentration Difference has dimensions of mass/volume. Diffusive Conductance is a function of the properties of the species and fluids involved and the geometry of the diffusive process. For diffusion through a single fluid, the Diffusive Conductance for species s (D_s) is computed as:

$$D_s = \frac{(A\, d\, \tau\, \theta)}{L} \tag{6-3}$$

Where:

A = mean cross-sectional area of the connection (L^2)
d = free-water diffusivity of species s
τ = tortuosity of continuous liquid film in the porous medium
θ = moisture content (porosity times saturation)
L = diffusive length.

The diffusive flux f_s from pathway i to pathway j is computed as follows:

$$f_{s,i\rightarrow j} = D_s(C_{ims} - C_{jms}) \tag{6-4}$$

Where C_{ims} and C_{jms} are the dissolved concentrations of species s for medium m in Cell i and j.

The diffusion can occur in either direction, so the flux can be positive or negative. When media properties are changing for diffusive release calculation, such as when diffusion occurs between tank wall concrete layer and the surrounding soil, the diffusive conductance is calculated using a harmonic average of the physical properties of the two cell pathways as follows:

$$D_s = \frac{A}{\frac{L_i}{d_{msi}\theta_i\tau_{Pi}} + \frac{L_j}{d_{msj}\theta_j\tau_{Pj}}} \tag{6-5}$$

Where:

A = the area of the diffusive mass flux link (L^2)
L_i = diffusive length for the diffusive mass flux link in Cell i (L)
L_j = diffusive length for the diffusive mass flux link in Cell j (L)
d_{msi} = free-water diffusivity of species s for fluid m in Cell i (L^2/T)
d_{msj} = free-water diffusivity of species s for fluid m in Cell j (L^2/T)
τ_{Pi} = tortuosity for the porous medium for Cell i

τ_{Pj} = tortuosity for the porous medium for Cell j
θ_i = moisture content of porous media in Cell i
θ_j = moisture content of porous media in Cell j.

When mass enters a Cell, it is instantaneously partitioned among the media present in the Cell. The partitioning is controlled by the partition coefficients defined for each species in each medium, and the quantity of each medium present. In the absence of solubility limits, the concentration of the species s in medium m in Cell i is computed by GoldSim© as follows:

$$C_{ims} = \left(\frac{K_{mrs}}{\sum_{g=1}^{NM_i} K_{grs}.VM_{ig}}\right) m_{is} \tag{6-6}$$

Where:

C_{ims} = concentration of species s in medium m in Cell i ([M/L^3] for Fluids or [M/M] for Solids)
m_{is} = mass of species s in Cell i (M)
K_{mrs} = partition coefficient between medium m and Reference Fluid r for species s (L^3/L^3) for Fluids or (L^3/M) for Solids
K_{grs} = partition coefficient between medium g and Reference Fluid r for species s (L^3/L^3) for Fluids or (L^3/M) for Solids
VM_{ig} = quantity (volume or mass) of medium g in Cell i (L^3 for Fluids or M for Solids)
NM_i = the number of media in Cell i.

When a solubility constraint is applied for a species in a Cell, the Cell has a saturation capacity with respect to that species, which represents the maximum amount of species mass the Cell can contain before the species will start to precipitate out of solution. It is calculated as:

$$msat_{is} = sol_{sr} \sum_{g=1}^{NM_i} K_{grs}.VM_{ig} \tag{6-7}$$

Where:

$msat_{is}$ = saturation capacity for species s in Cell i (M)
sol_{sr} = solubility of species s in the Reference Fluid r (M/L^3)
K_{grs} = partition coefficient between medium g and Reference Fluid r for species s ([L^3/L^3] for Fluids or [L^3/M] for Solids)
VM_{ig} = quantity (volume or mass) of medium g in Cell i (L^3 for Fluids or M for Solids)
NM_i = the number of media in Cell i.

All or a portion of the mass within the Source can be specified to exist within the waste matrix, such that species that are bound in such a matrix are not released until the matrix itself degraded in some manner. Release of mass from the matrix is assumed to be congruent with the

degradation of the matrix. Degradation rates are specified by the user. The rate at which the waste is exposed for release is calculated as:

$$e_s(n,t) = M_s(t) \,.\, k_s(t) \,.\, I_s(n,t) \tag{6-8}$$

Where:

$e_s(n,t)$ = the exposure rate for species n in bound inventory s for the Source at time t (M/T)
$M_s(t)$ = fraction of unprotected but undegraded matrix (unitless)
$k_s(t)$ = fractional degradation rate of waste matrix for bound inventory s (1/T)
$I_s(n,t)$ = mass of species n in bound inventory s at time (M).

When applying a fractional degradation rate to the matrix (such as for release of ^{99}Tc), the fraction of undegraded matrix $M_s(t)$ can be determined by solving the following differential equation:

$$\frac{dM_s(t)}{dt} = h(t) - M_s(0) \,.\, k_s(t) \tag{6-9}$$

Where:

$h(t)$ = rate at which matrix is being unprotected (T^{-1})
$k_s(t)$ = rate at which unprotected matrix is being degraded (T^{-1}).

If $h(t)$ and $k_s(t)$ are constant, the solution to the above equation is:

$$M_s(t) = \frac{h}{k_s}(1 - e^{-k_s t}) + M_s(0)e^{-k_s t} \tag{6-10}$$

6.3.2 Radionuclide Transport

This section provides the detailed methods of analysis for the transport of radionuclides for the hydrologic (groundwater), atmospheric, and biotic transport pathways. The process-based modeling involved the use of STOMP©, and the system-level modeling involved the use of GoldSim© for the uncertainty analysis and certain sensitivity cases.

6.3.2.1 Process-Level Model Based on STOMP© Flow and Transport Simulator. The WMA C PA groundwater pathway modeling makes use of detailed process-level numerical models based on the STOMP© code, which was used to simulate 3-D flow and contaminant transport through the vadose zone and unconfined aquifer system. To calculate water flow, the STOMP©-based numerical model includes the assumption that the vadose zone and unconfined aquifer system can be represented and approximated by an equivalent porous continuum. The STOMP©-based numerical model solves a conservation of mass equation using a finite difference approximation to the matric potential form of the Richards' equation (Soil Physics,

6th edition [Jury and Horton 2004]) that calculates fluid flow entering, exiting, and accumulating within the finite numerical volumes as follows:

$$C(h)\frac{\partial h}{\partial t} = \frac{\partial}{\partial x}\left[K(h)\frac{\partial h}{\partial x}\right] + \frac{\partial}{\partial y}\left[K(h)\frac{\partial h}{\partial y}\right] + \frac{\partial}{\partial z}\left[K(h)(\frac{\partial h}{\partial z} + 1)\right] \pm S \qquad (6\text{-}11)$$

Where:

h	=	matric potential $h = h(x,y,z,t)$, t=time
$C(h) = d\theta/dh$	=	specific moisture capacity, C for a given h, and is equal to $d\theta/dh$, i.e., the inverse slope of the matric potential-moisture content, θ, relation (cm)
$K(h)$	=	the hydraulic conductivity (cm/s), which may be anisotropic and is dependent on matric potential
S	=	the amount of water added (source) or subtracted (sink) per unit volume through time (1/s).

Moisture content is a function of soil matric potential, and the soil matric potential-moisture retention relationship is described for each HSU using the following empirical relationship ("A Closed-form Equation for Predicting the Hydraulic Conductivity of Unsaturated Soils" [van Genuchten 1980]; EPA/600/2-91/065, The RETC Code for Quantifying the Hydraulic Functions of Unsaturated Soils):

$$\theta(h) = \theta_r + (\theta_s - \theta_r)\{1 + [\alpha h]^n\}^{-m} \qquad (6\text{-}12)$$

Where $\theta(h)$ is the moisture content, here expressed explicitly as a function of the soil matric potential, and the other terms are defined as follows:

θ_r	=	residual moisture content (dimensionless)
θ_s	=	saturated moisture content (dimensionless)
α	=	a fitting parameter (cm^{-1})
n	=	a fitting parameter (dimensionless)
m	=	$1 - 1/n$.

Combining the van Genuchten model with Mualem's (1976) model ("A New Model for Predicting the Hydraulic Conductivity of Unsaturated Porous Media") for unsaturated conductivity produces the following relationship for hydraulic conductivity and soil matric potential:

$$K(h) = \frac{K_s\{1-(\alpha h)^{mn}[1+(\alpha h)^n]^{-m}\}^2}{[1+(\alpha h)^n]^{ml}} \qquad (6\text{-}13)$$

Where $K(h)$ is the hydraulic conductivity (cm/s), which is, as expressed, dependent on the soil matric potential; K_s is the saturated hydraulic conductivity (cm/s); and l is a pore-connectivity parameter (dimensionless) that Mualem (1976) estimates to be about 0.5 for many soils and is assumed to equal 0.5 in this analysis.

Within the STOMP© code, tension-dependent anisotropy provides a framework for upscaling small-scale measurements to the effective (upscaled) properties for the large-scale vadose zone (Section 6.4 and Appendix B). Each heterogeneous geologic unit is represented in the model by an EHM with macroscopic flow and transport properties. With each heterogeneous unit assigned its upscaled or effective hydraulic properties, the simulated flow fields predict the bulk or mean flow behavior at the field scale. Upscaling, in effect, accounts for the differences in scale between small, core-scale measurements and large, field-scale modeling. Tension-dependent anisotropy provides a framework for upscaling small-scale measurements to the effective (upscaled) properties for the large-scale, macroscopic vadose zone. The stochastic model developed in Polmann (1990) is used to evaluate and apply tension-dependent anisotropy for the HSUs at WMA C. Details about the development of the Polmann stochastic tension-dependent anisotropy model and its application to the HSUs at WMA C are presented in Appendix B, Section B.3.2. Figures B-19 through B-21 in Appendix B illustrate the relationship between the matric potential and the resulting anisotropy.

Contaminant transport within the STOMP© code is described by the conventional advective-dispersive transport solution to the conservation of mass equation described in Soil Physics (6th edition [Jury and Horton 2004]) and applied to finite difference volumes:

$$\frac{\partial}{\partial t} M_c = \frac{\partial}{\partial x}\left(D_e \frac{\partial C_l}{\partial x}\right) + \frac{\partial}{\partial y}\left(D_e \frac{\partial C_l}{\partial y}\right) + \frac{\partial}{\partial z}\left(D_e \frac{\partial C_l}{\partial z}\right) - \frac{\partial}{\partial x}(J_x\, C_l) - \frac{\partial}{\partial y}(J_y\, C_l) - \frac{\partial}{\partial z}(J_z\, C_l) - M_c \frac{ln(2)}{t^{1/2}} \quad (6\text{-}14)$$

Where:

$\frac{\partial}{\partial t} M_c$ = the change in contaminant mass or activity present in the finite volume (g or Ci) through time and the mass or activity is calculated according to the equation ($\rho_b\, C_a + \theta\, C_l$)

ρ_b = soil bulk density (g/cm^3)

C_a = adsorbed solute concentration (g or Ci per g soil)

θ = moisture content (dimensionless), and as discussed previously, dependent on the soil matric potential

C_l = dissolved solute concentration (g or Ci per cm^3 water)

J_x, J_y, J_z = water or moisture flux (cm/s) along the x, y, and z directions, respectively

D_e = effective dispersion/diffusion coefficient (cm^2/s); note that the entire terms represent the flux of solutes that crosses the planes normal to the x, y, and z directions, respectively, because of diffusion and dispersion

$\frac{\partial C_l}{\partial\{x,y,z\}}$ = the change in dissolved solute concentration through space in the x, y, and z directions, respectively; note that the entire terms represent the flux of solutes that crosses the planes normal to the x, y, and z directions, respectively, because of diffusion and dispersion

$t^{1/2}$ = radioactive half-life(s), the entire term represents the mass of solute lost to radioactive decay.

In Equation 6-14, positive is used to indicate solute entering the finite volume, and negative is used to indicate what is exiting or lost to decay. The adsorbed and dissolved solute concentrations are related through an equilibrium linear sorption coefficient (K_d mL water per g

soil) formulation: $C_a = K_d C_l$. No temperature effects are considered for the vadose zone model (i.e., the model used is isothermal).

6.3.2.2 STOMP©-Based Process-Level Model Implementation of the Groundwater Pathway. This section describes the details of the implementation of the STOMP©-based process-level model used in the WMA C PA for evaluation of the groundwater pathway. The description presented in this section primarily addresses the development of the conceptual model components and base case parameters. The discussion includes the alternative geologic interpretations evaluated as part of the sensitivity analysis because those interpretations involve uncertainty in a conceptual model component. Parameter sensitivity and uncertainty are addressed in Section 8. DOE/RL-2011-50 contains the description of the generalized models, conditions, and parameters applicable to the Hanford Site vadose zone, which were refined and augmented for the WMA C PA evaluation.

The site-specific STOMP© model components for the WMA C PA evaluation are:

- Model domain and boundary conditions
- Hydrogeologic model
- Source term
- Recharge
- Vadose zone hydrogeology and fluid transport
- Groundwater domain and characteristics
- Geochemistry.

The model domain and boundary conditions are included in the list above to emphasize the fundamental nature of boundary conditions used in the modeling. The evaluation adopted modeling assumptions and parameter estimates for WMA C site-specific conditions to determine the impacts to groundwater resulting from post-retrieval residual waste remaining in tanks, ancillary equipment, and pipelines in accordance with DOE O 435.1 requirements.

The following subsections for the individual conceptual model components provide the basis, rationale, and references for the base case values. These parameters represent the values selected for use in the model from the ranges of plausible parameter values. These values may differ from parameter estimates for other Hanford Site modeling performed for different purposes or areas of the Hanford Site, or at different scales.

6.3.2.2.1 Model Domain and Boundary Conditions. The model domain and boundary conditions establish both a framework and limiting conditions for the numerical model. The model domain for flow and transport in the vadose zone is represented numerically in 3-D space, with one of the horizontal axes aligned in the general direction of groundwater flow. Aligning an axis with the general direction of groundwater flow allows concentrations to be calculated more easily downgradient of the waste sites. The numerical model adapts the physical elements of the conceptual model to a Cartesian grid, and also assigns numerical values to the parameters used in algorithms to represent the physical and geochemical systems and processes.

The WMA C model domain is 737.9 m (2,421 ft) northwest to southeast by 795.3 m (2,609 ft) southwest to northeast by 116 m (381 ft), vertically, extending about 12 m (39 ft) below the water table (Figure 6-36). The southwestern and northwestern boundaries of the model are 574656.09 m, 136454.41 m, and 575218.45 m, 137016.78 m, respectively (Lambert Coordinate system easting, NOAA Manual NOS NGS 5, "State Plane Coordinate System of 1983"). The southeastern and northeastern boundaries are 575177.86 m, 135932.64 m, and 575740.22 m, 136495.00 m, respectively. The vertical base elevation of the model is nominally 95 m (312 ft) (North American Vertical Datum of 1988 [NAVD88]), although the bottom and top of the model domain vary spatially according to the top of basalt elevation and surface relief, respectively (RPP-RPT-56356).

The horizontal node spacing varies between 3.0 and 20 m (9.8 and 65.6 ft) to optimize the discretization in the areas attempting to approximate the slopes associated with construction of WMA C and the 100-series tanks without overwhelming the available computational resources. Figure 6-37 shows the plan view distribution of the calculation nodes. The vertical spacing in the vadose zone ranged between 1 and 1.25 m (3.28 and 4.10 ft) except around the water table, where the spacing decreased to 0.5 m (1.6 ft) to capture the impact of the capillary fringe above the water table. The total number of nodes in the modeled rectangular prism equals 736,653. During the pre-operational phase, the number of active nodes equals 640,565 with 96,088 inactive. Inactive nodes represent space where no flow occurs, e.g., above ground surface, within basalt, or within intact tanks. During the operational and post-closure phases, the number of active nodes equals 637,543 with 99,110 inactive, the increase in inactive nodes attributed to the inactivation of the tank and ancillary equipment nodes within the WMA C excavation.

A specified-flux boundary condition was applied at the surface to simulate recharge. Recharge rates varied spatially and temporally along the upper boundary, depending on surface conditions, the presence of WMA C and other facilities, and the time of WMA C operations and surface conditions simulated (RPP-RPT-44042). The bottom boundary of the unsaturated (vadose) zone is the water table, and the bottom of the model (aquifer) was defined as a no-flow boundary condition. Boundary conditions at the sides of the model domain were assumed to be no flow in the vadose zone and prescribed flux and prescribed head in the aquifer on the upgradient and downgradient boundaries, respectively. The boundary condition in the aquifer on the upgradient boundary was assumed to be prescribed flux, calculated on the basis of the hydraulic conductivity and gradient, and independent of recharge. The prescribed flux boundary condition value includes a factor to account for the varying thickness of the unconfined aquifer and uneven surface of the underlying basalt. To account for the non-uniform aquifer thickness from the underlying basalt boundary, the nominal flux rate was calculated as the product of the hydraulic conductivity and gradient (base case values of 11,000 m/day [6.8 mi/day] and 2×10^{-5} m/m [6.6×10^{-5} ft/m], respectively; see the upcoming "Groundwater Domain and Characteristics" discussion and Appendix C for the basis of these parameter estimates), and was proportioned according to the ratio of the average aquifer cross-sectional area throughout the model domain (9,440 m^2 [2.3 acres]) and the aquifer area along the upgradient boundary (6,151 m^2 [1.5 acres]) where the prescribed flux is applied. The aquifer cross-sectional area refers to the area perpendicular to the direction of groundwater flow. The aquifer cross-sectional area varies from the northwest to southeast boundaries because of the uneven top of the basalt.

Figure 6-36. The Interpolated Numerical Three-Dimensional Post-Closure Alternative I Hydrogeologic Model.

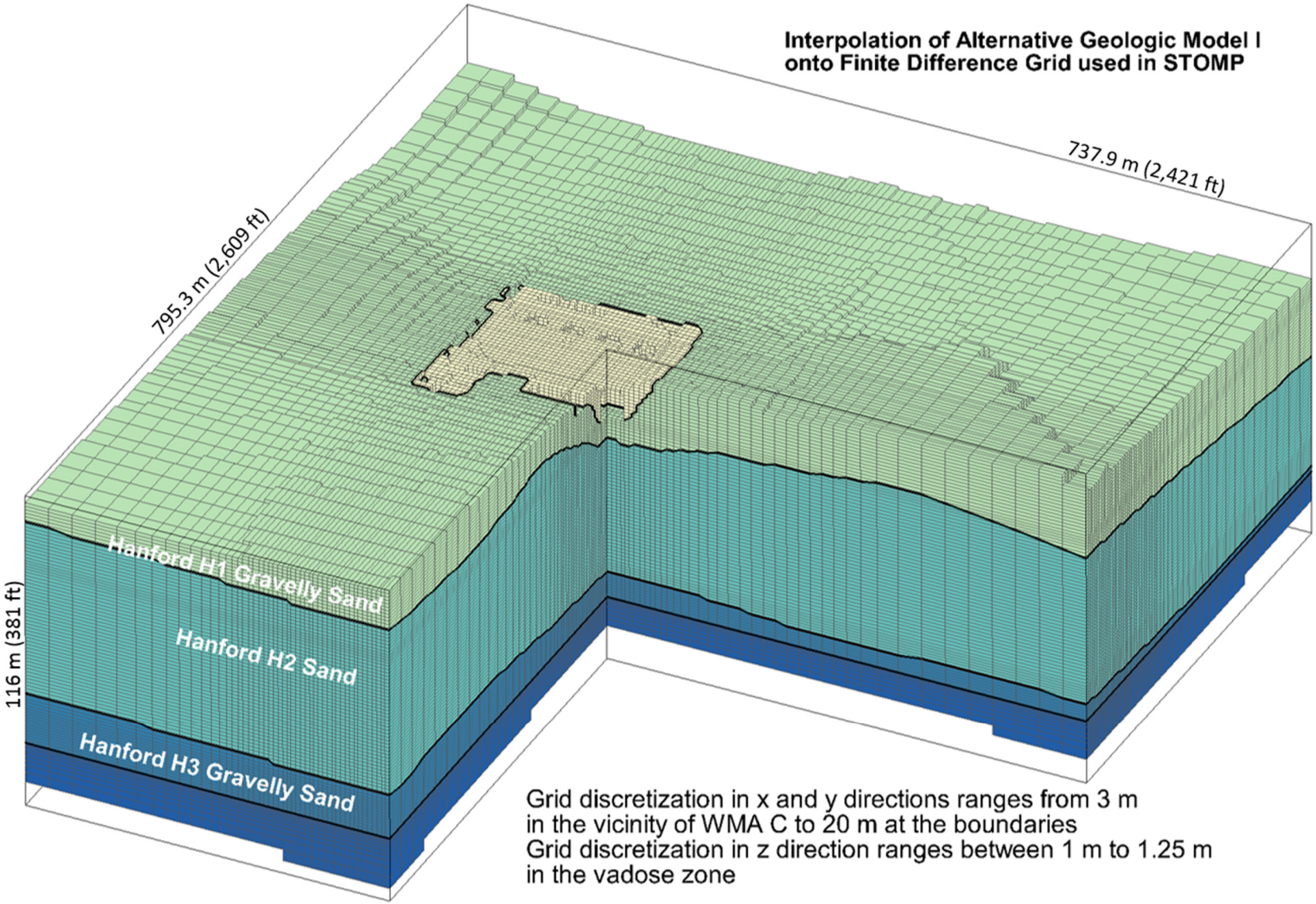

STOMP = Subsurface Transport Over Multiple Phases (computer code) WMA = Waste Management Area

Hydrogeologic Model. The hydrogeologic conceptual model developed for the WMA C PA (RPP-RPT-46088 and RPP-RPT-56356) provides the information basis and data necessary to prepare the 3-D geologic inputs used in the 3-D numerical model. Each node in the numerical model represents a unique set of horizontal (x and y) coordinates and vertical (z) elevation. A node is assigned the hydrogeologic properties associated with the HSU identified in the RPP-RPT-56356 geologic models as existing in the space represented by the node coordinates and elevation.

Figure 6-38 shows the geologic interpretation prepared by Washington River Protection Solutions, LLC (WRPS) staff and identified as Alternative Geologic Model I as interpolated onto the numerical grid used in the fate and transport model. Figure 6-38 shows some internal cross-sections of the geology to illustrate the shape and layering of the hydrogeologic units. Figures 6-39 and 6-40 show the geologic interpretation prepared with input from technical staff of the Nez Perce and identified as Alternative Geologic Model II. Alternative Geologic Model II includes the separation of the Hanford H2 sand unit into three distinct subunits: the Hanford H2 sand, the Hanford H2 gravelly sand, and the Hanford H2 fine or silty sand. Explanation of the basis and the development of the two geologic interpretations is presented in RPP-RPT-56356. The sensitivity analysis includes evaluation of a third alternative geologic model that is identical to Alternative Geologic Model I, except that a clastic dike is assumed to exist under tanks C-102, C-105, C-108, and C-111, and another is assumed to exist under tanks C-110, C-111, and C-112. These clastic dikes extend the length and width, respectively, of WMA C, and extend from the bottom of the WMA C excavation to the capillary fringe of the aquifer.

6.3.2.2.2 Source Term. The results from the source term release model implemented using GoldSim© provide the time varying release functions of residual waste inventory for all sources (tanks and ancillary equipment) as input to the STOMP©-based model. The nodes in the STOMP©-based model that define the base of tanks and ancillary equipment uniformly distribute the mass release provided by the GoldSim©-based source term for simulating the fate and transport through the vadose zone and saturated zone. The source term model calculations are described in Section 6.3.1 and use residual inventory information presented in Tables 3-13, 3-14, and 3-15, where the radionuclide inventory has been decayed to January 1, 2020.

6.3.2.2.3 Recharge. The magnitude of recharge for soils at the Hanford Site varies as a function of the soil type, condition of the vegetation cover, and soil integrity (e.g., disturbed versus undisturbed). The range of recharge values reported in RPP-RPT-44042 represents distinct populations of data based on lysimetry and isotopic measurements, and interpretation—and, in some instances, extrapolation—by Hanford Site subject matter experts. The natural background recharge rates represent a population for natural vegetated conditions. The range of values for operational conditions represents a population of recharge rates for vegetation-free disturbed soil.

The final design for the surface barrier for WMA C at closure has not been developed. The surface barrier is expected to function comparably to a modified RCRA Subtitle C barrier (Section 3.2.1.2.2), which PNNL-16688 indicates should function similarly to the Prototype Hanford Barrier. Summary of data collected over 13 years at the Prototype Hanford Barrier (PNNL-17176, "200-BP-1 Prototype Hanford Barrier Annual Monitoring Report for Fiscal

Years 2005 Through 2007"; DOE/RL-93-33) indicates that infiltration through the prototype is much less than 0.1 mm/yr (0.004 in./yr), and evaluations of the design using lysimeter data indicate that the barrier is capable of limiting recharge to this amount even with a complete lack of vegetation (Fayer and Gee 2006). However, for base case simulations involving WMA C PA with a functioning surface barrier, a base case recharge rate of 0.5 mm/yr (0.02 in./yr) is assumed, which is consistent with the drainage design specification in DOE/RL-93-33.

At the end of 500 years, the surface barrier performance is assumed to degrade to permit an infiltration rate of 3.5 mm/yr (0.14 in./yr) and maintain that infiltration rate for the remainder of the simulation for the base case. No quantifying data are available for specifying the performance of the barrier top after its design life, but the performance of the surface barrier in limiting recharge is not expected to diminish appreciably (PNNL-16688). According to PNNL-13033, not even the erosion of the silt loam layer and deposition of dune sand on the barrier is likely to alter the barrier performance significantly. The value of 3.5 mm/yr (0.14 in./yr) corresponds to the recharge in an undisturbed area, which indicates that native vegetation is assumed to reclaim the land.

Although the side slopes and berm are likely to function and perform differently than the surface of the barrier, they are included as part of the barrier surface. The impact of the side slopes on the overall recharge rate is expected to be relatively negligible. The sandy gravel/gravelly sand barrier side slope and berm are assumed eventually to resemble a Burbank loamy sand, and if that assumption is valid, then PNNL-16688 indicates that the long-term recharge rate for that soil type is 1.9 mm/yr (0.07 in./yr), which is less than the 3.5 mm/yr (0.14 in./yr) used in the analysis for the degraded barrier surface. Table 6-6 presents a summary of the base case recharge rates applied to the different surface types present within the WMA C model domain.

6.3.2.2.4 Vadose Zone Hydrogeology and Transport. The vadose zone hydrogeology and transport information presented here is a brief summary of the information presented in Appendix B. Appendix B includes detailed discussion and description of the data available and the methods used to develop the base case parameters, and sensitivity and uncertainty distributions and percentile values.

The flow and transport pathway process used for the WMA C vadose zone modeling is porous media continuum flow. The porous media continuum assumption and the soil relative permeability/saturation/capillary pressure relations provide the basis for vadose zone flow and transport modeling (PNNL-11216, PNNL-12030). The vadose zone at the Hanford Site is composed of sediments ranging in particle size associated with gravels to silts or clays. In the model domain, the hydraulic properties describing fluid transport characteristics associated with each geologic layer (also referred to as hydrostratigraphic units) are approximated by average upscaled values, with each unit having different flow and transport parameter values (hydraulic conductivity, bulk density, and dispersivity). The model describes bulk (or mean) flow and radionuclide transport behavior in the vadose zone, limiting the evaluation to estimating overall and eventual radionuclide impacts to groundwater. Porous media continuum transport in unsaturated media of this type is regarded as the fundamental process and feature for modeling contaminant fate and transport behavior in the vadose zone at the Hanford Site (DOE/RL-2011-50).

Table 6-7 lists the upscaled composite-fitted van Genuchten-Mualem (van Genuchten 1980, Mualem 1976, EPA/600/2-91/065) base case parameters for the various strata at the WMA C site. A stochastic model of variable moisture or tension-dependent anisotropy provides the framework for upscaling small-scale measurements to the effective (upscaled) properties for the large-scale vadose zone (Polmann 1990). The upscaling processes factor the inherent spatial variability that occurs on different scales in heterogeneous media into the field-scale parameter estimates ("Stochastic analysis of moisture plume dynamics of a field injection experiment" [Ye et al. 2005], "Estimation of effective unsaturated hydraulic conductivity tensor using spatial moments of observed moisture plume" [Yeh et al. 2005]). Specific upscaled flow parameters include moisture retention, and saturated and unsaturated hydraulic conductivity. Upscaled transport parameters include bulk density, diffusivity, sorption coefficients, and macrodispersivity. Detailed discussion of the Polmann (1990) model and the derivation of the upscaled parameters are presented in Appendix B.

Estimated unsaturated conductivities, based on saturated conductivity and the van Genuchten retention model, can differ by up to several orders of magnitude with measured conductivities at the dry end (e.g., Khaleel et al. 1995). Therefore, unlike the conventional approach, the unsaturated conductivities are not based on predictions using the measured retention curve and the measured saturated conductivity. Rather, the soil hydraulic properties are based on a simultaneous fit of moisture retention and unsaturated conductivity data, and all five unknown parameters θr, θs, α, n, and K_s, with m=1-1/n (van Genuchten 1980) were fitted to the data via a code named RETention Curve (RETC) (EPA/600/2-91/065). Thus, in order to obtain a better agreement with experimental data for the region of interest (i.e., relatively dry moisture regime), K_s is treated as a fitted parameter during the curve fitting process. This is considered appropriate because the WMA C PA predictions are needed for the relatively dry moisture regime observed in the field, rather than for the saturated or near-saturated regime. The pore size distribution factor, ℓ, was kept fixed at 0.5 during the simultaneous fitting.

For the Alternative Geologic Model II evaluation, the Hanford H2 gravel/coarse sand subunit was assumed to be more transmissive, and the Hanford H2 silty sand less transmissive, than the Hanford H2 sand. Therefore, as an initial estimate of these properties, the hydraulic properties associated with the 5th and 95th percentile realizations of unsaturated hydraulic conductivity curves developed for the Hanford H2 sand unit were considered representative of the Hanford H2 gravel/coarse sand and the Hanford H2 silty sand subunits, respectively.

The effective transport parameter (i.e., macrodispersivity, bulk density, and diffusivity) estimates used in the base case and sensitivity cases are presented. Because of natural variability, the transport parameters are all spatially variable. The purpose is similar to the upscaled flow parameters, to evaluate the effect of such variability on the large-scale transport process. Effective bulk density (ρ_b) estimates are needed to calculate retardation factors for different species. The average ρ_b, E[ρ_b] estimates for various strata at WMA C are presented in Table 6-8. These estimates are derived from bulk density sample values listed in Appendix B. Appendix B also provides a summary of the numerical simulation, stochastic theory, and 200 Areas experimental data that provide the basis for the base case estimates of macrodispersivity (Table B-11). The estimated values of macrodispersivity applicable to the scale of the WMA C PA model for the base case evaluation are shown in Table 6-9.

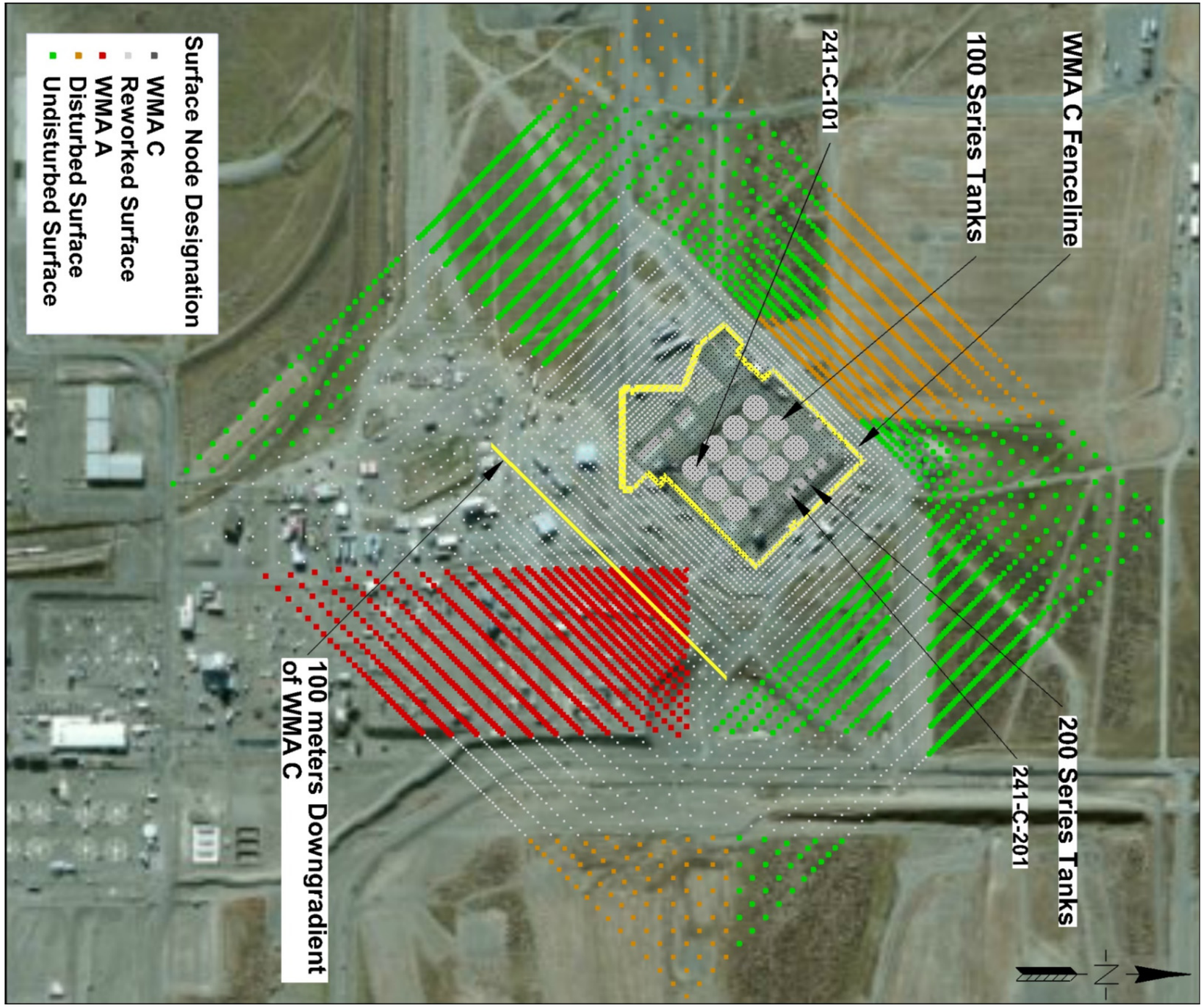

Figure 6-37. Plan View of Waste Management Area C Performance Assessment Model Domain Showing the Horizontal Distribution and Surface Type of the Irregularly-Spaced Calculation Nodes. The resolution increases in the area of Waste Management Area C.

WMA = Waste Management Area

Figure 6-38. Diagram of the Interpolated Numerical Three-Dimensional Post-Closure Alternative I Hydrogeologic Model.

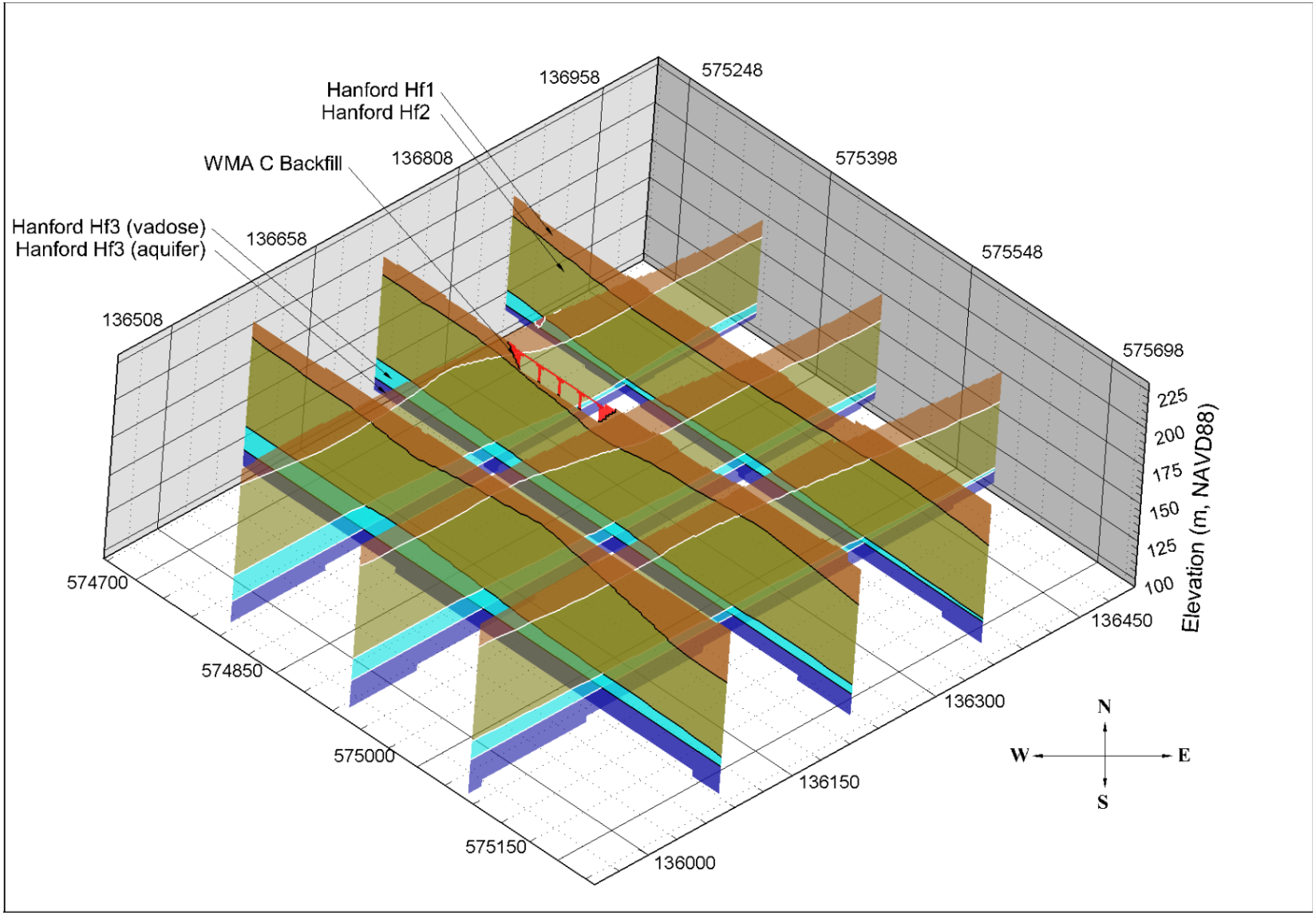

Hf = Hanford formation NAVD88 = North American Vertical Datum of 1988 WMA = Waste Management Area

Figure 6-39. The Interpolated Numerical Three-Dimensional Post-Closure Alternative II Hydrogeologic Model.

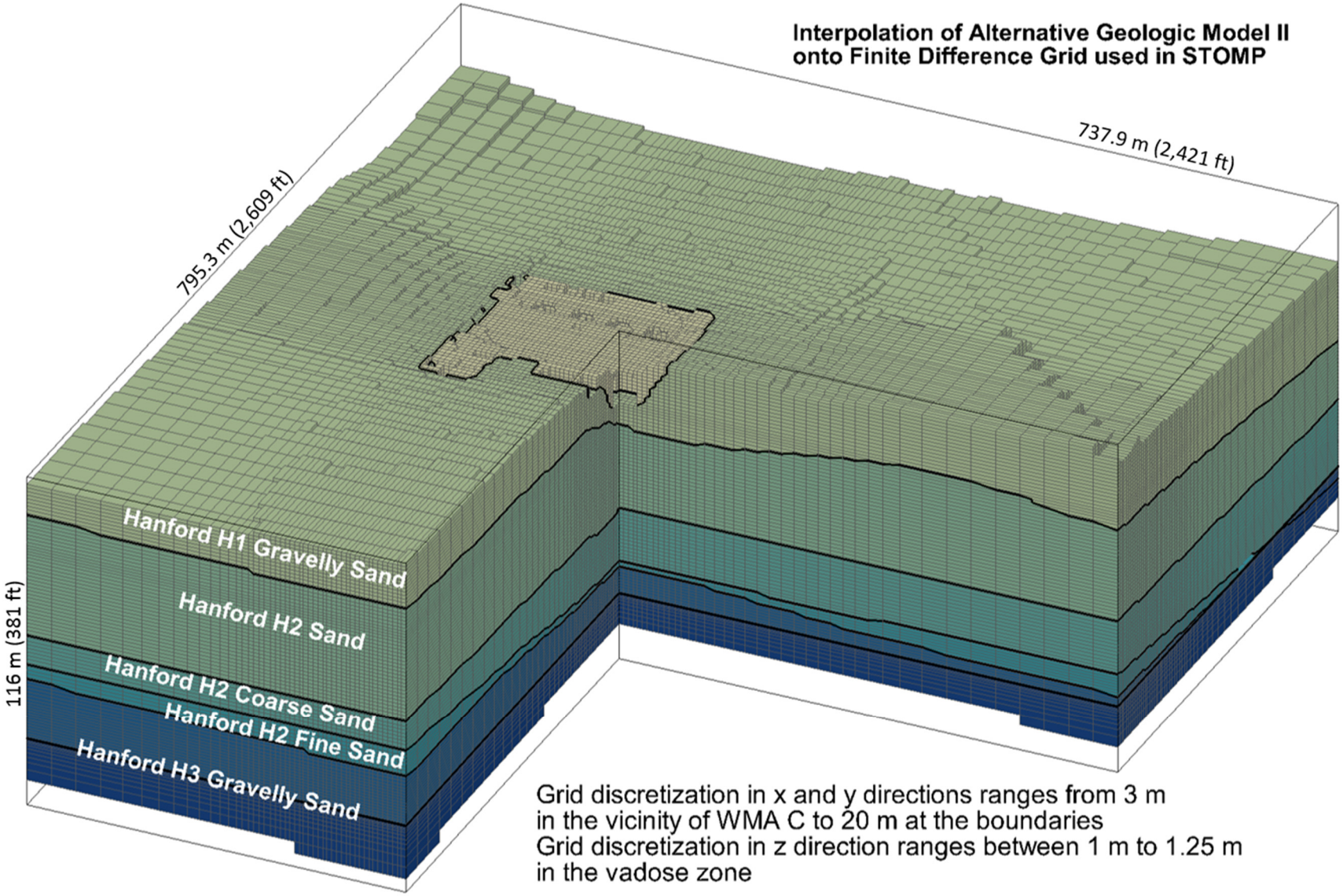

WMA = Waste Management Area

Figure 6-40. Diagram of the Interpolated Numerical Three-Dimensional Post-Closure Alternative II Hydrogeologic Model.

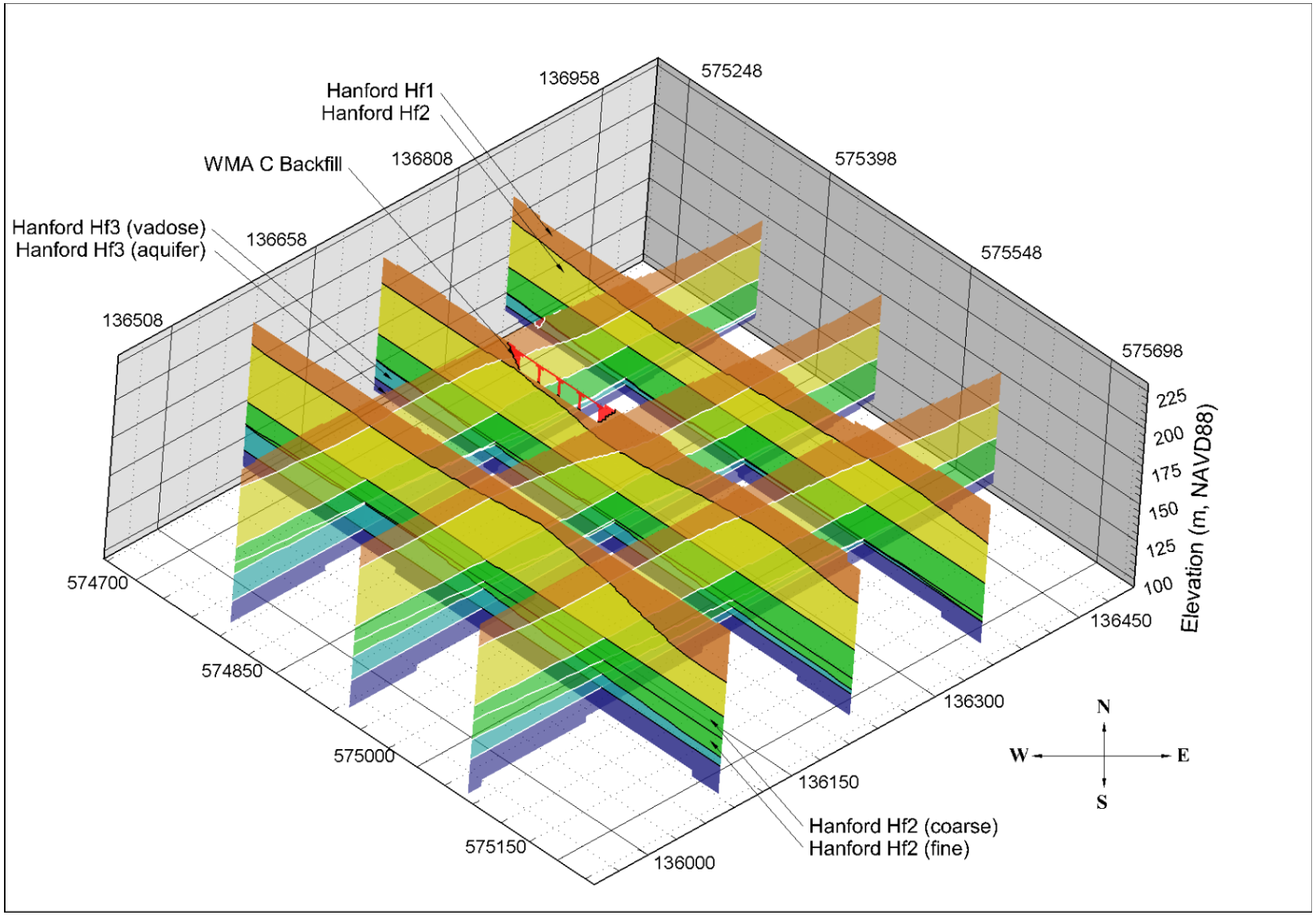

Hf = Hanford formation NAVD88 = North American Vertical Datum of 1988 WMA = Waste Management Area

Table 6-6. Base Case Recharge Rate (Net Infiltration) Estimates for Surface Conditions during the Pre-Construction, Operational, and Post-Closure Periods.

Period	Waste Management Area (WMA) C Region and Surface Condition	Base Case Value of Recharge Rate (mm/yr)
Pre-construction (before 1944)	Undisturbed region (Rupert sand with vegetation)	3.5
Operational period (1945 to 2020)	Undisturbed region (Rupert sand with vegetation)	3.5
	WMA C Surface region (Gravel without vegetation)	100
	WMA A Surface region (Gravel without vegetation)	100
	Disturbed revegetated region (Rupert sand with vegetation)	22
	Disturbed unrevegetated region (Rupert sand with no vegetation)	63
Early post-closure (2020 to 2520)	Undisturbed region (Rupert sand with vegetation)	3.5
	WMA C Surface region (Surface barrier with vegetation)	0.5
	WMA A Surface region (Surface barrier with vegetation beginning in 2050)	0.5
	Disturbed revegetated region (Rupert sand with vegetation beginning in 2050 with vegetation recovery completed in 2080)	3.5
	Disturbed unrevegetated region (Rupert sand with no vegetation until vegetation recovery begins in 2050 and completes in 2080)	3.5
Late post-closure (2520 to 3020 and beyond)	Undisturbed region (Rupert sand with vegetation)	3.5
	WMA C Surface region (Surface barrier with vegetation)	3.5
	WMA A Surface region (Degraded surface barrier with vegetation begins in 2550)	3.5
	Disturbed revegetated region (Rupert sand with vegetation recovery completed in 2080)	3.5
	Disturbed unrevegetated region (Rupert sand with vegetation recovery completed in 2080)	3.5

It is assumed that the effective, large-scale diffusion coefficients for all strata in the vadose zone at the WMA C site are a function of volumetric moisture content, θ, and can be expressed using the Millington-Quirk ("Permeability of Porous Solids" [Millington and Quirk 1961]) empirical relation:

$$D_e(\theta) = D_0 \frac{\theta^{10/3}}{\theta_s^2} \tag{6-15}$$

Where:

$D_e(\theta)$ = the effective diffusion coefficient of an ionic species

D_0 = the effective diffusion coefficient for the same species in free water
θ = the localized volumetric moisture content
θ_s = the localized volumetric moisture content at saturation.

Table 6-7. Composite van Genuchten-Mualem Parameters for Various Strata at the Waste Management Area C Site Used in the Base Case Evaluations of Alternative Geologic Models I and II.

Strata	Number of Samples	θ_s	θ_r	α (1/cm)	n	ℓ^c	Fitted K_s (cm/s)
Backfill (Gravelly)	10	0.138	0.010	0.021	1.374	0.5	5.60E-04
Hanford H1/H3 (Gravel-dominated)	15	0.171	0.011	0.036	1.491	0.5	7.70E-04
Hanford H2 (Sand-dominated)	44	0.315	0.039	0.063	2.047	0.5	4.15E-03
Hanford H2 – Gravel/coarse sand subunit*	not applicable	0.265	0.002	0.108	1.724	0.5	1.68E-02
Hanford H2 – Silty-sand subunit*	not applicable	0.354	0.029	0.040	1.633	0.5	1.79E-03

*Hydraulic properties of these units are only used in numerical model simulation of Alternative Geologic Model II. As an initial estimate of these properties, the hydraulic properties associated with the 5th and 95th percentile realizations of unsaturated hydraulic conductivity curves developed in the Uncertainty and Sensitivity Analysis for the Hanford H2 sand unit were considered to be representative of the Hanford H2 silty sand and the Hanford H2 gravel/coarse sand subunits, respectively.

The tortuosity formulation in the Millington-Quirk model is based on theoretical considerations absent from other empirical models, and accounts for the ranges of moisture contents present in the vadose zone around WMA C. The molecular diffusion coefficient for all species in pore water is assumed to be 2.5×10^{-5} cm^2/sec (6.98×10^{-4} in.^{2}/sec) (WHC-SD-WM-EE-004), which is consistent with, and representative of, values used in other Hanford PAs (WHC-EP-0645, BHI-00169, WHC-SD-WM-TI-730, WHC-SD-WM-EE-004, and DOE/ORP-2000-24).

6.3.2.2.5 Groundwater Domain and Characteristics. The groundwater in the aquifer system in the vicinity of WMA C has been studied extensively as part of the site characterization that is discussed in RPP-RPT-46088. The groundwater conceptual model for WMA C includes the uppermost unconfined aquifer system that exists within a channel eroded by the cataclysmic floods of the Pleistocene age. The base of the aquifer is the underlying basalt surface. The undifferentiated lower sands and gravels associated with the Hanford formation, CCU, and the Ringold Formation (Unit A) that comprise the aquifer sediments are simply categorized as saturated Hanford H3 sediments in the model. The thickness of the uppermost aquifer beneath WMA C is ~12 m (39 ft). The model results provided represent concentrations in the upper 5 m (16.4 ft) of the aquifer. The 5 m (16.4 ft) vertical interval corresponds to the well screen length of a conceptual groundwater monitoring well, and the basis for that delimiter to the groundwater concentrations calculation is presented in upcoming discussion regarding "Point of Calculation, Protectiveness Metric, and Time Frame Considerations."

Table 6-8. Effective Bulk Density ($E[\rho_b]$, g/cm^3) Estimates for Various Strata at Waste Management Area C Used in the Base Case Evaluations of Alternative Geologic Models I and II.

Strata	$E[\rho_b]$
Backfill (Gravelly)[1]	2.13
Hanford H1/H3 (Gravel-dominated)[1]	2.05
Hanford H2 (Sand-dominated)[2]	1.71
Hanford H2 – Gravel/coarse sand subunit[3]	1.83
Hanford H2 – Silty-sand subunit[3]	1.61

[1]See Appendix B.

[2]From Table 7 of RPP-20621, "Far-Field Hydrology Data Package for the Integrated Disposal Facility Performance Assessment," by taking the average of soil samples 7A through 35A.

[3]Effective bulk densities of these units are only used in numerical model simulation of Alternative Geologic Model II. The values are calculated based on particle density of 2.49 g/cm^3 and porosity equal to saturated moisture content presented in Table 6-7. The particle density of 2.49 g/cm^3 is derived from the bulk density of 1.71 g/cm^3 for Hanford H2 sand with porosity of 0.315 (Table 6-7).

Table 6-9. Macrodispersivity Estimates for Various Strata at Waste Management Area C Used in the Base Case Evaluations of Alternative Geologic Models I and II.

Strata	A_L (cm)	A_T (cm)
Backfill (Gravelly)	~20	2.0
Hanford H1/H3 (Gravel-dominated)	~20	2.0
Hanford H2 (Sand-dominated)	~25	2.5
Hanford H2 – Gravel/coarse sand subunit*	~25	2.5
Hanford H2 – Silty-sand subunit*	~25	2.5

*Macrodispersivities of these units are only used in numerical model simulation of Alternative Geologic Model II.

See Appendix B.

Groundwater flow beneath WMA C has been historically difficult to measure because the hydraulic gradient is very small and the hydraulic conductivity is very high in this region of the Hanford Site. In addition, the water table continues to recover from the operational liquid discharges at 216-B-3 Pond system and other large discharge sites in 200 East Area. The projected equilibrium state is expected to be similar to its pre-Hanford behavior (see Section 3 and Appendix C). As a result, the post-closure position of the water table and associated hydraulic gradient can only be evaluated through modeling. Consequently, the groundwater flux

in the aquifer beneath WMA C is calculated on the basis of the aquifer hydraulic properties, and the hydraulic gradient projected to exist in the future.

The hydraulic heads around WMA C are expected to continue declining slowly until they stabilize around 119.5 m (392 ft) within 100 years in the future (CP-47631). The gradient is generally expected to slope from northwest to southeast with a value of about 0.00002 m/m, which is close to the one observed prior to start of Hanford operations (Figure 6-41). Appreciable changes in hydraulic gradient are not expected in the future once the hydraulic heads stabilize. Thus, the hydraulic gradient is assumed to remain stable for the base case analysis.

Appendix C discusses the scale dependence of aquifer properties and indicates that field-scale calibrated groundwater models are the most appropriate approach for parameterization of the WMA C saturated media hydraulic conductivity. To date, the Central Plateau Groundwater Model (CPGWM, CP-47631) appears to be the most appropriate and applicable calibrated model to provide that parameterization. The CPGWM provides calibrated hydraulic conductivity estimates for the model layers and HSUs present within the aquifer in the vicinity of WMA C. Within the WMA C flow domain, the weighted average of hydraulic conductivity derived from the CPGWM is approximately 11,000 m/day (33,000 ft/day). Thus, the base case horizontal saturated hydraulic conductivity for the aquifer is estimated to be 11,000 m/day (33,000 ft/day). The CPGWM estimate of vertical anisotropy ratio of 0.1 is also incorporated in the WMA C base case. Table 6-10 presents a summary of the aquifer base case hydraulic parameters for the Hanford H3 – aquifer. The aquifer, identified as Hanford H3 – aquifer, is separated from that portion of the Hanford H3 above the water table, reflecting the distinctly different saturation conditions.

6.3.2.2.6 Sorption Characteristics. Linear K_d isotherm is a reasonable representation for modeling sorption of radionuclides on the sediments when released from tank residuals and ancillary equipment. The rationale for the use of a K_d-based approach for vadose zone units is presented in Section 6.2.2.1.5 and discussed in detail in DOE/RL-2011-50. The K_d values are chosen assuming low-salt, near-neutral waste chemistry in the vadose and saturated zone.

The basis for the K_d values used to approximate the transport of the contaminants and radionuclides are presented in Table 6-11, including the values lowered to account for the gravel content per the procedure described in PNNL-17154. PNNL-17154 indicates that K_d values are typically lower for materials that contain significant amounts of gravel (notably Backfill, Hanford H1, and Hanford H3) than those determined with <2-mm (0.08-in.)-size material. The gravel corrected values are not included in the table for the contaminants and radionuclides that the 3-D screening evaluation indicated would not arrive at the water table within 10,000 years.

6.3.2.2.7 Point of Calculation, Protectiveness Metric, and Time Frame Considerations. In accordance with risk assessment guidelines, the determination of soil contamination impacts to groundwater also requires the definition and rationale for (1) the PoCal, i.e., the place and points in the groundwater domain where modeled groundwater concentrations are to be assessed for potential impacts and protectiveness; (2) the protectiveness metric, i.e., the groundwater metric(s) to be used in the assessment of protectiveness at the PoCal, and; (3) the time frame considered applicable for the calculation of impacts to groundwater.

Figure 6-41. Hindcast Water Table Map of the Hanford Site, January 1944.

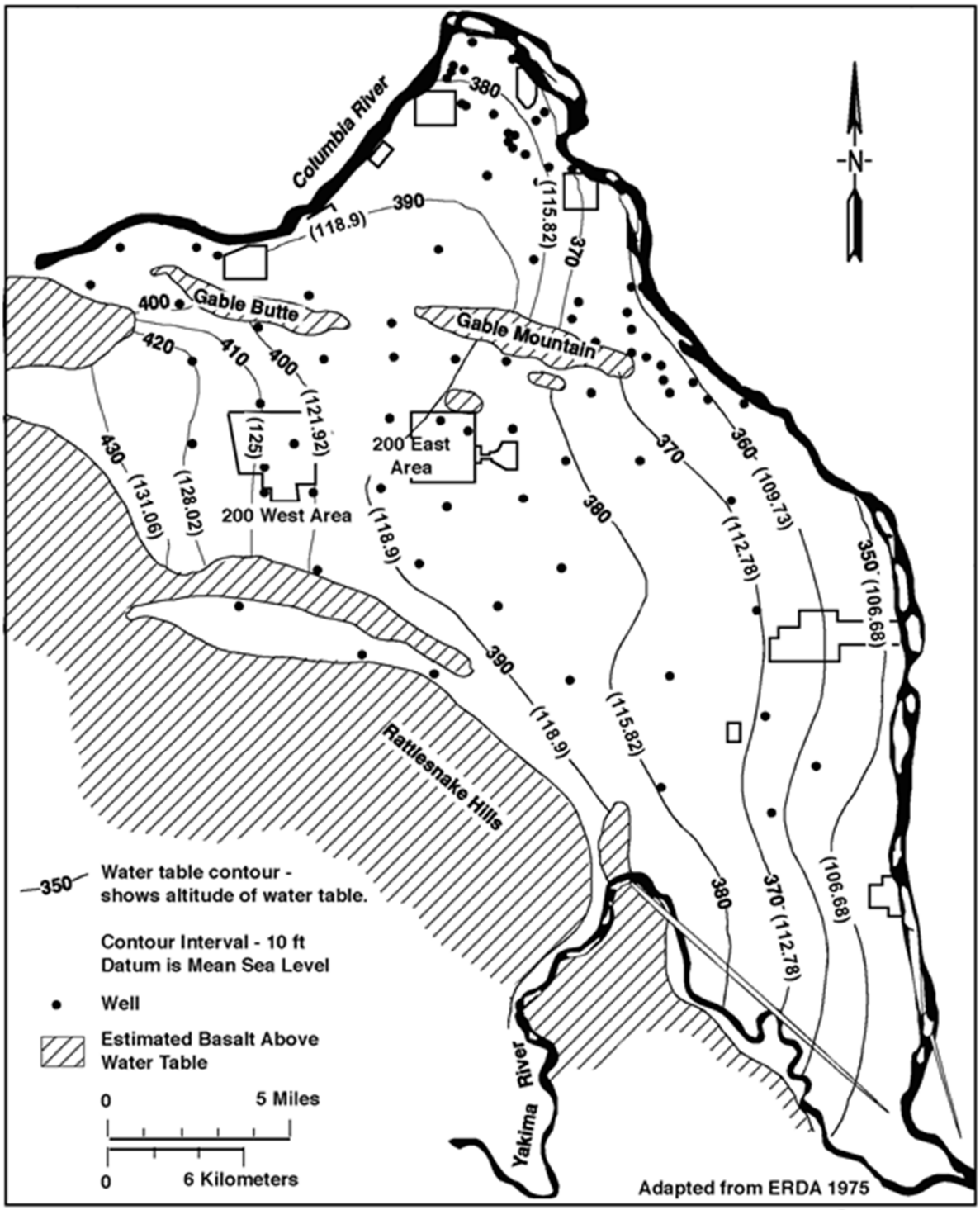

G01010017.20

ERDA 1975 = ERDA-1538, "Final Environmental Statement, Waste Management Operations, Hanford Reservation, Richland, Washington."

Source: WHC-SD-ER-TI-003, "Geology and Hydrology of the Hanford Site: A Standardized Text for Use in Westinghouse Hanford Company Documents and Reports."

Table 6-10. Base Case Soil Hydraulic Properties for Aquifer Soil Type Used for Base Case at Waste Management Area C.

Aquifer Soil Type	Total Porosity	Saturated Moisture Content	Horizontal Saturated Hydraulic Conductivity[a] (m/day)	Longitudinal Dispersivity[b] (m)	Aquifer Hydraulic Gradient (m/m)	Average Aquifer Water Flux ($m^3/day/m^2$)
Hanford H3 (aquifer)	0.20	0.20	11,000	10.5	0.00002	0.22

[a] Vertical Saturated Hydraulic Conductivity assumed equal to 1/10 of the Horizontal Saturated Hydraulic Conductivity.
[b] Transverse dispersivity assumed to be equal to 1/10 of the longitudinal dispersivity.

See Appendix C.

The PoCal for the groundwater impact analysis is 100 m (328 ft) downgradient from the WMA C fenceline. The PoCal is intended to effectively serve as the point where exposure point groundwater concentrations are evaluated in the model for the purpose of evaluating the achievement of the groundwater protection performance objectives. The PoCal for the protection of groundwater is related to "Point of Compliance" in Federal PA requirements (DOE M 435.1-1; DOE G 435.1-1, Chapter 4), which is described as follows:

> "The point of compliance shall correspond to the point of highest projected dose or concentration beyond a 100 meter buffer zone surrounding the disposed waste. A larger or smaller buffer zone may be used if adequate justification is provided."

The aquifer mixing zone extends into the upper 5 m (16.4 ft) of the aquifer for the purpose of the evaluations. DOE M 435.1-1 does not specify the level of protection required for water resources, and there are no applicable parameterization requirements or guidelines indicated in DOE G 435.1-1, Chapter 4. The format and content guide (DOE G 435.1-2, Implementation Guide for use with DOE M 435.1-1, Format and Content Guide for U.S. Department of Energy Low-Level Waste Disposal Facility Performance Assessments and Composite Analyses) indicates that the aquifer mixing must be consistent with State or local laws, regulations, or agreements. The Washington Administrative Code does specify a 5-m (16.4-ft) mixing zone in groundwater that is consistent with a 5-m (16.4-ft) vertical interval corresponding to a conceptual groundwater monitoring well with the 4.6-m (15-ft) well screen length (and mixing zone dimension) associated with State monitoring well descriptions (e.g., see Equation 747-4 in WAC 173-340-747).

The compliance time frame is defined as 1,000 years following closure of the facility (DOE M 435.1-1; DOE G 435.1-1, Chapter 4). The sensitivity-uncertainty analysis along with NRC guidance (NUREG-1854) extends the evaluation to 10,000 years, which is sufficient to evaluate the peak dose from all of the radionuclides that the screening analysis indicates may not impact groundwater within the compliance period. DOE M 435.1-1 and DOE G 435.1-1, Chapter 4 state that the sensitivity-uncertainty analysis time frame should include calculation of the maximum dose regardless of the time at which the maximum occurs, as a means of increasing confidence in the outcome of the modeling and increasing the understanding of the

models used. However, EPA-SAB-RAC-ADV-99-006, An SAB Advisory: Modeling of Radionuclide Releases from Disposal of Low Activity Mixed Waste warns that extending the modeling time frame beyond 10,000 years could make the results irrelevant and hinder public acceptance of the results because of the inherent scientific and social uncertainties associated with such an extended time frame. The 10,000-year time frame is sufficient to address uncertainty associated with radionuclides that impact groundwater during the compliance period (NUREG-1573, A Performance Assessment Methodology for Low-Level Radioactive Waste Disposal Facilities: Recommendations of NRC's Performance Assessment Working Group).

DOE G 435.1-1, Chapter 4 states that DOE LLW disposal facilities must comply with legally-applicable requirements for water resource protection. The protectiveness metric determined to be most appropriate for the evaluation of impacts to groundwater during the compliance period from the radionuclide and contaminant inventory in WMA C are the maximum contaminant levels (MCLs). Maximum concentration limits represent the "allowable concentrations" and/or "acceptable limits" of a radionuclide for minimizing further degradation of groundwater in accordance with the conditions identified in State and Federal anti-degradation goals (e.g., EPA/540/R-92/003, Guidance for Data Useability in Risk Assessment (Part A) Final; OSWER Directive 9841.00-6C, Alternate Concentration Limit Guidance, Part I, ACL Policy and Information Requirements, Interim Final; DOE/RL-2002-59, Hanford Site Groundwater Strategy Protection, Monitoring, and Remediation).

Defining the protection of groundwater in the context of vadose zone fate and transport requires consideration of the soil and groundwater media as a hybrid or coupled pathway. This pathway involves the determination of future concentrations in the groundwater medium that result from the transport of the radionuclide and contaminant inventory existing in the WMA C tank residuals. Per this working definition, protection of groundwater pathway is considered achieved if the radionuclide and contaminant levels in the WMA C tank residuals do not cause groundwater concentrations to exceed MCLs at the PoCal within 1,000 years after closure, which is assumed to begin in 2020. Table 6-12 provides a summary of key site-specific model elements and parameters used for the model components.

6.3.2.3 Groundwater Pathway Screening Analysis Methodology. The screening phase streamlines the PA modeling effort and computation time by distinguishing those contaminants and radionuclides that may impact groundwater during the specified compliance, and sensitivity and uncertainty analysis, time frames. The screening phase uses the 3-D model to determine the maximum K_d value of contaminants contained within the WMA C tank residuals that reach the water table within 1,000 and 10,000 years. According to the facility performance requirements in DOE O 435.1, performance objectives must be met for 1,000 years, and post-closure evaluations must extend out to 10,000 years to clarify long-term impacts.

The K_d screening threshold values are based on any non-zero radionuclide impact to groundwater. This threshold represents the first indication of a groundwater impact, i.e., leading edge of a groundwater plume arriving at the water table, rather than peak concentration, which arrives later than the leading edge. The groundwater arrival time screening criteria are only focused on whether there was any non-zero impact to groundwater within the time frames considered and are applied regardless of subsequent peak concentrations. The screening analysis

includes vadose zone hydraulic property values and recharge rates developed for the uncertainty analysis, which are discussed in Appendix B. In particular, the screening analysis applies the maximum recharge rates associated with each period for each surface type, assigns the vadose zone hydraulic properties that produce the fastest pore water velocity for each HSU (as determined for the uncertainty analysis), and executes an advection release function for the radionuclides. Results from the groundwater pathway screening analysis are presented in Section 7.2.1.1.

Table 6-11. Distribution Coefficients (K_d) Values Used to Approximate the Transport of the Radionuclides in the Base Case. (2 sheets)

Element or Contaminant	Base Case K_d (mL/g)				
	< 2mm Material	Backfill	Hanford H1/H3	Hanford H2	Reference
Ac	350	NM	NM	NM	PNNL-16663
Al	1,500	NM	NM	NM	RPP-RPT-46088
Am	600	NM	NM	NM	PNNL-17154
B	3	NM	NM	NM	RPP-RPT-46088
C	1	0.46	0.58	0.8	PNNL-17154
Cm	350	NM	NM	NM	PNNL-16663
CN	0	NM	NM	NM	RPP-RPT-46088
Co	0	0	0	0	PNNL-17154
Cr	0	0	0	0	PNNL-17154
Cs	100	NM	NM	NM	PNNL-17154
Eu	10	NM	NM	NM	PNNL-17154
F	0	0	0	0	PNNL-17154
Fe	25	NM	NM	NM	RPP-RPT-46088
H	0	0	0	0	PNNL-17154
Hg	52	NM	NM	NM	RPP-RPT-46088
I	0.2	0.09	0.12	0.16	PNNL-17154
Mn	65	NM	NM	NM	RPP-RPT-46088
Nb	0	0	0	0	PNNL-16663
Ni	3	1.4	1.7	2.4	PNNL-17154
NO_2	0	0	0	0	PNNL-17154
NO_3	0	0	0	0	PNNL-17154
Np	10	NM	NM	NM	PNNL-17154
Pa	300	NM	NM	NM	PNNL-17154

Table 6-11. Distribution Coefficients (K_d) Values Used to Approximate the Transport of the Radionuclides in the Base Case. (2 sheets)

Element or Contaminant	Base Case K_d (mL/g)				
	< 2mm Material	Backfill	Hanford H1/H3	Hanford H2	Reference
Pb	10	NM	NM	NM	PNNL-17154
Pu	600	NM	NM	NM	PNNL-17154
Ra	10	NM	NM	NM	PNNL-17154
Rn	0	0	0	0	No relevant information available
Se	0.1	0.05	0.06	0.08	PNNL-17154
Sm	10	NM	NM	NM	PNNL-17154
Sn	0.5	0.23	0.29	0.4	PNNL-17154
Sr	10	NM	NM	NM	PNNL-17154
TBP	1.89	NM	NM	NM	RPP-RPT-46088
Tc	0	0	0	0	PNNL-16663
Th	300	NM	NM	NM	PNNL-16663
U	0.6	0.28	0.35	0.48	RPP-RPT-46088
Zr	300	NM	NM	NM	PNNL-16663

NM = not included in the three-dimensional modeling because the results of screening indicated the element or contaminant does not arrive at the water table within 10,000 years.

References:
PNNL-16663, "Geochemical Processes Data Package for the Vadose Zone in the Single-Shell Tank Waste Management Areas at the Hanford Site."
PNNL-17154, "Geochemical Characterization Data Package for the Vadose Zone in the Single-Shell Tank Waste Management Areas at the Hanford Site."
RPP-RPT-46088, "Flow and Transport in the Natural System at Waste Management Area C."

As part of the uncertainty evaluation (Section 8.1.3.1), parametric distributions of recharge estimates were developed that identified maximum values for the different surface types and simulation periods. The maximum net infiltration rate present during the different simulation periods for each surface type (Table 6-13) is used for the screening evaluation. The maximum net infiltration rate during the operations time frame is assumed to be sufficient to account for any anthropogenic water sources and hypothetical leaks occurring during retrieval. Interim measures enacted during fiscal year 2002 included constructing surface water controls to reduce surface water run-on from major meteorological events and from breaks in waterlines; isolating, cutting, and capping unnecessary waterlines; and testing operating waterlines and replacing any lines found to be leaking (RPP-PLAN-39114). This provides almost 20 years of drainage before the surface barrier is emplaced, and contaminant releases from tank residuals are assumed not to occur. Long-term recharge after barrier failure is the only source of water expected to result in any significant transport of contaminant from the facility to groundwater. WMA C tank

residuals are not expected to contain appreciable quantities of liquid, and the retrieval operations are conducted in a manner to minimize uncontrolled retrieval leachate from escaping the tanks.

Table 6-12. Summary of Key Elements and Base Case Parameters Associated with Site-Specific Model Components for Waste Management Area C (The basis for the elements and parameter selection provided in the individual model components sections). (2 sheets)

Model Domain and Boundary Conditions	Rectangular Prism: 737.9 m (2,421 ft) × 795.3 m (2,609 ft) × 116 m (381 ft) Prescribed flux across the top (Recharge); no-flow along vertical side boundaries in the vadose zone; prescribed flux and head along the upgradient and downgradient vertical side boundaries in the aquifer, respectively; no-flow along the bottom of the model (aquifer). The prescribed volumetric water flux boundary condition is calculated to maintain mass conservation in the aquifer independent of recharge.

Geologic Setting	The Waste Management Area (WMA) C cross-section includes the following anthropogenic or natural units that occur from surface to groundwater (RPP-RPT-56356, "Development of Alternative Digital Geologic Models of Waste Management Area C"):
	• WMA C Backfill
	• Hanford H1 (gravel-dominated, generally identified as gravel or very coarse sand)
	• Hanford H2 Sand (sand-dominated facies generally identified as fining upward sequences of gravel, sandy/gravel to sand to very fine sand)
	• Hanford H3 (coarse-grained open framework gravel to sandy gravel; in the vicinity of WMA C is variously referred to in different references as undifferentiated H3 gravels, Cold Creek, or Ringold)
	• In Alternative Geologic Model II, the Hanford H2 Sand includes following two additional subunits
	  o Hanford H2 Coarse (gravel/coarse-grained facies that underlies the H2 fines)
	  o Hanford H2 Silty Sand – (a silty sand unit that is only observed in deep groundwater wells and a mappable unit may not be readily identified)

Groundwater Domain and Characteristics	WMA C post-closure water table elevation ~119.5 m NAVD88 and average hydraulic gradient ~0.00002 m/m Aquifer area along northwest cross-section boundary = 6,151 m^2 Aquifer area along southeast cross-section boundary = 13,998 m^2 Average aquifer area along all aquifer cross-sections = 9,440 m^2 Prescribed flux along northwest cross-section boundary (saturated K = 11,000 m/d); 11,000 m/d × 0.2000E-04 × 365.25 d/yr = 8.04E+01 m/yr; 8.04E+01 m/yr × 9,440 m^2 / 6,151 m^2 = 1.23E+02 m/yr Prescribed head along southeast cross-section boundary = 119.49 m Groundwater thickness is ~12 m (39 ft) in the aquifer; Groundwater concentrations evaluated for upper 5 m (16 ft) of the aquifer (rationale for aquifer depth presented in Section 6.3.2.2.9, Point of Calculation, Protectiveness Metric, and Time Frame Considerations) Aquifer Hydraulic Conductivity Horizontal to Vertical Anisotropy = **10:1** Aquifer Dispersivity Longitudinal to Transverse Anisotropy = **10:1** Appendix C identifies and describes the methods used to derive the aquifer properties and parameter values.

Table 6-12. Summary of Key Elements and Base Case Parameters Associated with Site-Specific Model Components for Waste Management Area C (The basis for the elements and parameter selection provided in the individual model components sections). (2 sheets)

Source Term/ Inventory	Table 3-13 "241-C Tank Farm Residual Inventory Estimates for Retrieved Tanks with Post-Retrieval Sampling," Table 3-14 "241-C Tank Farm Residual Inventory Estimates for Tanks Undergoing Retrieval," and Table 3-15 "241-C Tank Farm Residual Inventory Estimates for Ancillary Equipment" include tank, ancillary equipment, and pipeline-specific WMA C Base Case inventory estimates for the contaminants evaluated in this performance assessment (PA). Diffusion-controlled release occurs from the grouted tanks, and advection-controlled release occurs from the pipelines along with equilibrium sorption-desorption processes (i.e., K_d control).
Vadose Zone Hydrogeology and Fluid Transport	Table 6-7 "Composite van Genuchten-Mualem Parameters for Various Strata at the Waste Management Area C Site Used in the Base Case Evaluations of Alternative Geologic Models I and II" includes the hydrogeologic property estimates for WMA C PA models. Vadose Zone Hydraulic Conductivity Anisotropy allowed to vary as a function of the moisture content in accordance with the Polmann model ("Application of Stochastic Methods to Transient Flow and Transport in Heterogeneous Unsaturated Soils" [Polmann 1990]). Vadose Zone Dispersivity Longitudinal to Transverse Anisotropy = **10:1** Appendix B and Appendix D identify and describe the methods used to derive the properties and parameter values.
Recharge	Recharge varies spatially and temporally on the basis of surface conditions. Table 6-6 "Base Case Recharge Rate (Net Infiltration) Estimates for Surface Conditions during the Pre-Construction, Operational, and Post-Closure Periods" includes the base case recharge estimates applicable to the different surface conditions and periods evaluated in this PA.
Sorption Characteristics	K_d-control for radionuclide transport Table 6-11 "Distribution Coefficients (K_d) Values Used to Approximate the Transport of the Radionuclides in the Base Case" includes the base case distribution coefficient estimates applicable to the different radionuclides evaluated in this PA.

*Applies to all subfacies of this unit.

NAVD88 = North American Vertical Datum of 1988, National Geodetic Survey, U.S. Department of Commerce.
NP = Not present

As discussed in Section 8.1.4, uncertainty in the vadose zone hydraulic properties was addressed by randomly producing 200 combinations of van Genuchten-Mualem hydraulic parameter values for each HSU from the parameter distributions identified in Section 8.1.4. From these realizations, an empirical cumulative distribution function is calculated for the pore water velocity estimates, and the hydraulic parameter set corresponding to the maximum pore water

velocity occurring with a steady flux of 3.5 mm/yr (0.14 in./yr) is selected for the screening evaluation (Table 6-14).

Table 6-13. Maximum Net Infiltration (Recharge) Estimates Developed for the Uncertainty Analysis for Pre-Construction Period, Operational Period, and Post-Closure of Waste Management Area C (Section 8.1.4.1).

Surface Status	Pre-Construction (mm/yr)	Operational Period (mm/yr)	Post Closure	
			Until End of Barrier Design Life (500 yr after closure) (mm/yr)	After End of Barrier Design Life (mm/yr)
Waste Management Area C	5.2	140	1.0	5.2
Undisturbed	5.2	5.2	5.2	5.2
Disturbed	5.2	22	5.2	5.2
Reworked	5.2	63	5.2	5.2
Waste Management Area A	5.2	140	1.0	5.2

Table 6-14. van Genuchten-Mualem Parameters Associated with the Maximum Pore Water Velocity Based on the Cumulative Distribution Functions in Section 8.1.4.

Strata	θ_s	θ_r	α (1/cm)	n	Fitted K_s (cm/s)
Hanford H1 (gravelly sand)	0.100	0.0006	0.0190	1.789	5.07E-04
Hanford H2 (sand-dominated)	0.239	0.0006	0.0743	2.042	8.84E-03
Hanford H3 (gravelly sand)	0.100	0.0006	0.0190	1.789	5.07E-04
Aquifer	0.20	0.0006	0.0190	1.789	1.27*
Backfill	0.100	0.0003	0.0116	1.464	9.42E-05

*Value listed is 1/10 of the aquifer horizontal hydraulic conductivity.

For the purpose of the screening evaluation, the screening-phase model considers only the advective release of contaminants from the sediments. All of the contamination in the source area is available for advective transport, and the release occurs during a one-year span at closure and according to the equilibrium K_d. Results from the groundwater pathway screening analysis are presented in Section 7.2.1.1.

To complement the results of the screening analysis, an additional evaluation case was run to evaluate the peak doses for all 43 radiological COPCs beyond the 10,000-year post-closure time frame. The primary focus of this analysis is to evaluate the time and magnitude of peak doses

resulting from some selected constituents, like the uranium isotopes, that were found to be rising at the end of the 10,000-year period analysis, and other sorbed constituents that could potentially reach groundwater beyond the 10,000-year post-closure time frame. The specific assumptions of this evaluation case and its associated results are provided in Section 8.2.8 of this report.

6.3.2.4 Abstraction Approach for System-Level Modeling. The system model is implemented to reduce the computational time needed to carry out sensitivity and uncertainty analyses. The flow field for the vadose zone is derived from the 3-D STOMP©-based model calculations, abstracted to provide a close approximation to the full STOMP©-based solution. The objective of the system model is to evaluate the interaction of various submodels within the overall system. This is carried out by conducting transport analyses in one dimension (1-D) within the vadose zone and saturated zone for each source type (tank, ancillary equipment, and pipeline). This flow-field abstraction methodology was considered reasonable because of the EHM approach and upscaled flow parameters adopted in the STOMP©-based models. The reasonableness of the abstraction approach is demonstrated by comparing the results of the transport analysis conducted using the 1-D abstracted model to the full 3-D STOMP©-based model.

The flow field generated from the STOMP©-based model was evaluated by considering the following aspects of the flow field abstraction:

1. Variable HSU thickness within the model domain and its impact on flow velocity

2. Spatial and temporal variability in imposed recharge rates

3. Spatial and temporal variability in flow underneath the tank

4. Variable distances of tanks from the compliance location boundary.

The GoldSim©-based system model relies on the user to provide the moisture content, saturation, and Darcy flux as inputs; these flow-field related parameters were extracted from the STOMP©-based model. Figure 6-42 shows the STOMP©-based model node locations along with the extent of WMA C. For the abstraction of the flow field, the primary regions of interest were the ones underneath the various source locations within WMA C.

First, the approximate thicknesses of the HSUs were extracted from the STOMP©-based model under each of the twelve 100-series tank and four 200-series tank locations. Figure 6-43 shows the location of the nodes, along with the cross-section lines used in extracting the HSU thickness. Figure 6-44 shows the northwest-southeast trending geologic cross-sections through the tank farm area, while Table 6-15 summarizes the thicknesses of the HSUs directly underneath the tanks, along with the median values of the HSU thicknesses. The median value of the 100-series tanks is very similar to the HSU thickness below tank C-105. Similarly, median value for 200-series tanks is close to the thickness below tank C-203. Therefore, tanks C-105 and C-203 were selected as representative columns for the flow-field abstraction for the 100-series tanks and 200-series tanks, respectively.

Figure 6-42. Waste Management Area C Three-Dimensional Model Subsurface Transport Over Multiple Phases (STOMP©)-Based Model Node Locations.

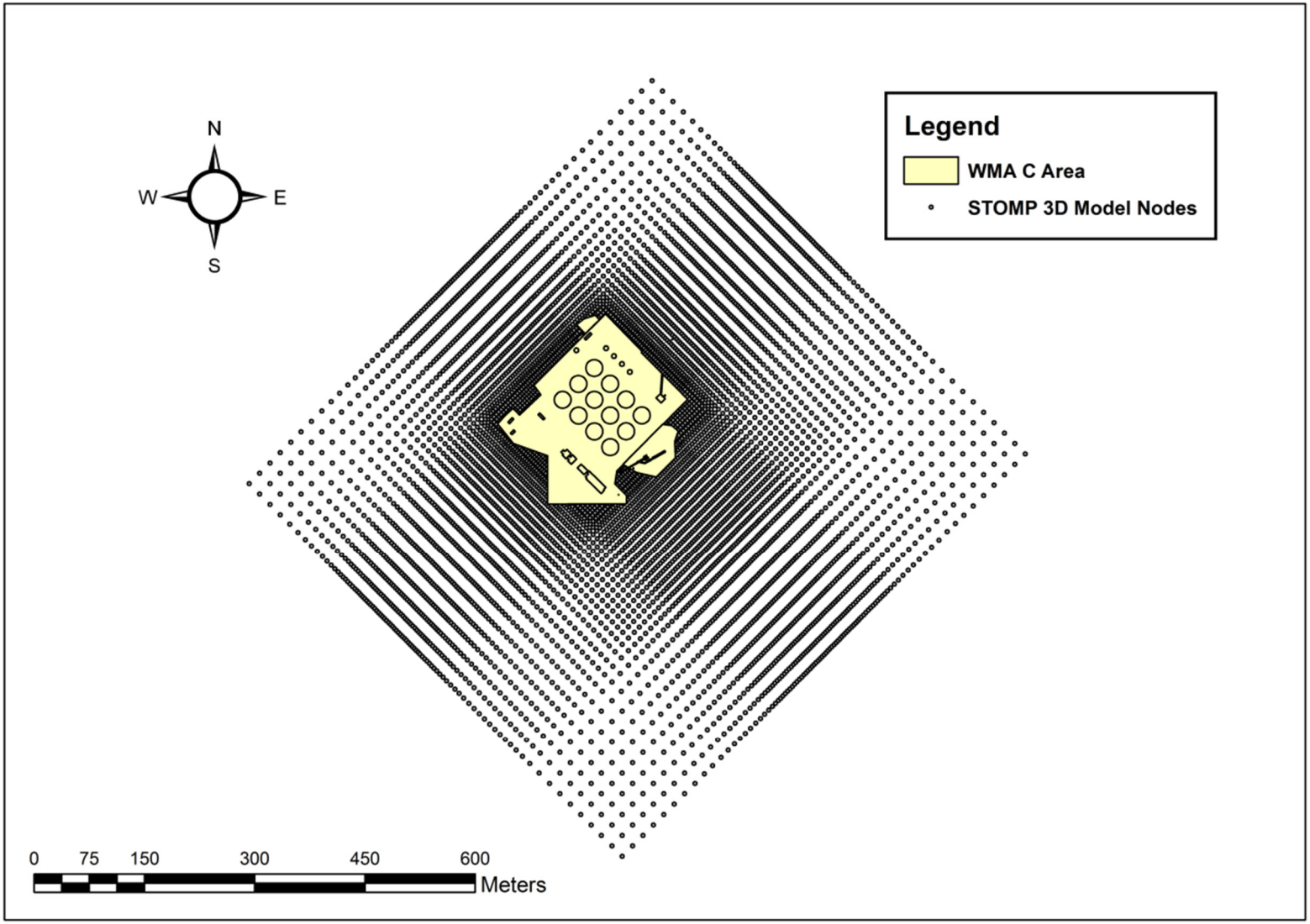

STOMP© 3D = Subsurface Transport Over Multiple Phases (code) three-dimensional WMA = Waste Management Area

Figure 6-43. Three-Dimensional Subsurface Transport Over Multiple Phases (STOMP©)-Based Model Node Locations for Waste Management Area C along with Location of Cross-Section Lines.

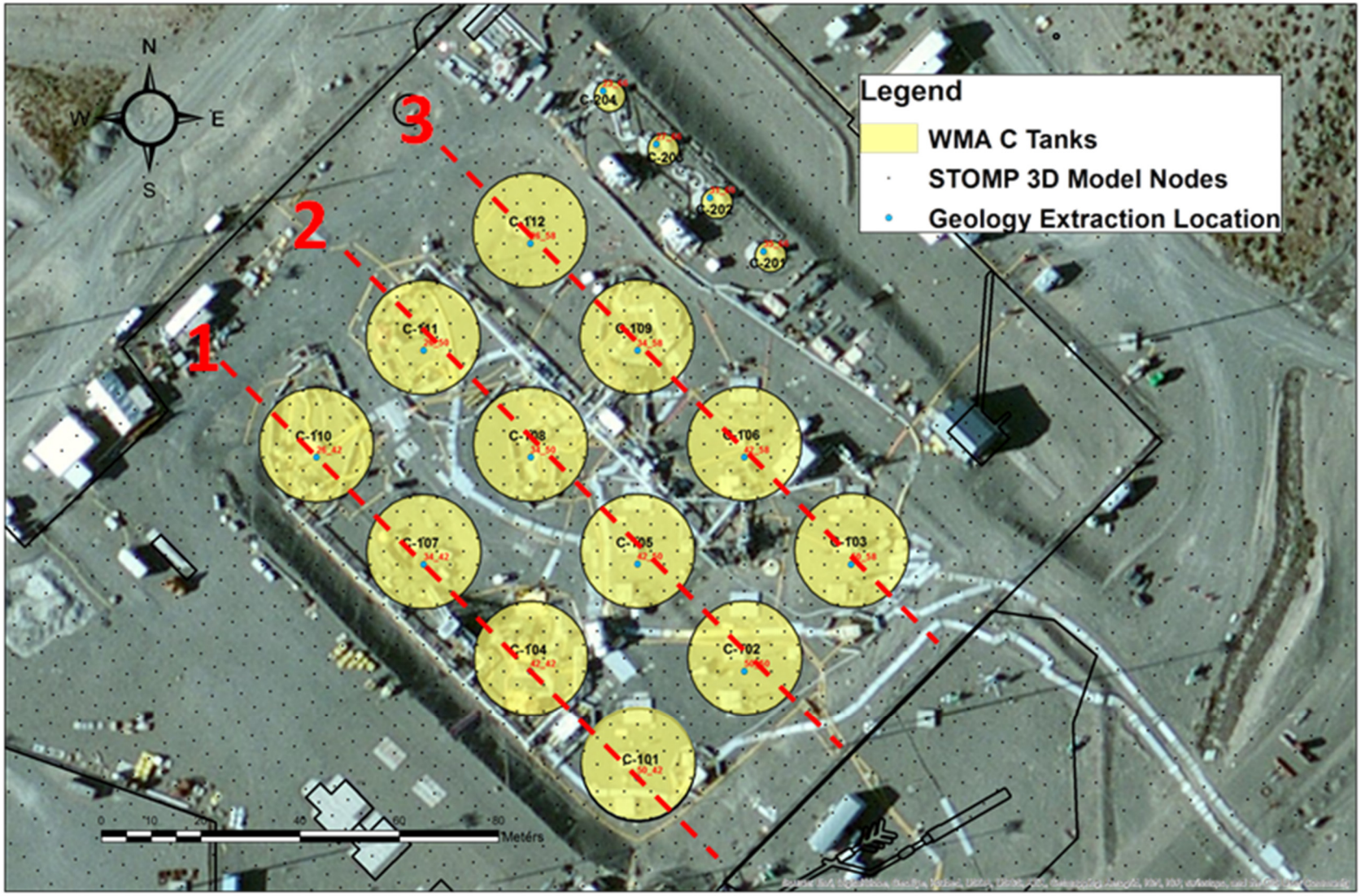

STOMP© 3D = Subsurface Transport Over Multiple Phases (code) three-dimensional WMA = Waste Management Area

Figure 6-44. Northwest-Southeast Trending Geologic Cross-Sections Through the Tank Farm Using Information from Three-Dimensional Subsurface Transport Over Multiple Phases (STOMP©)-Based Model.

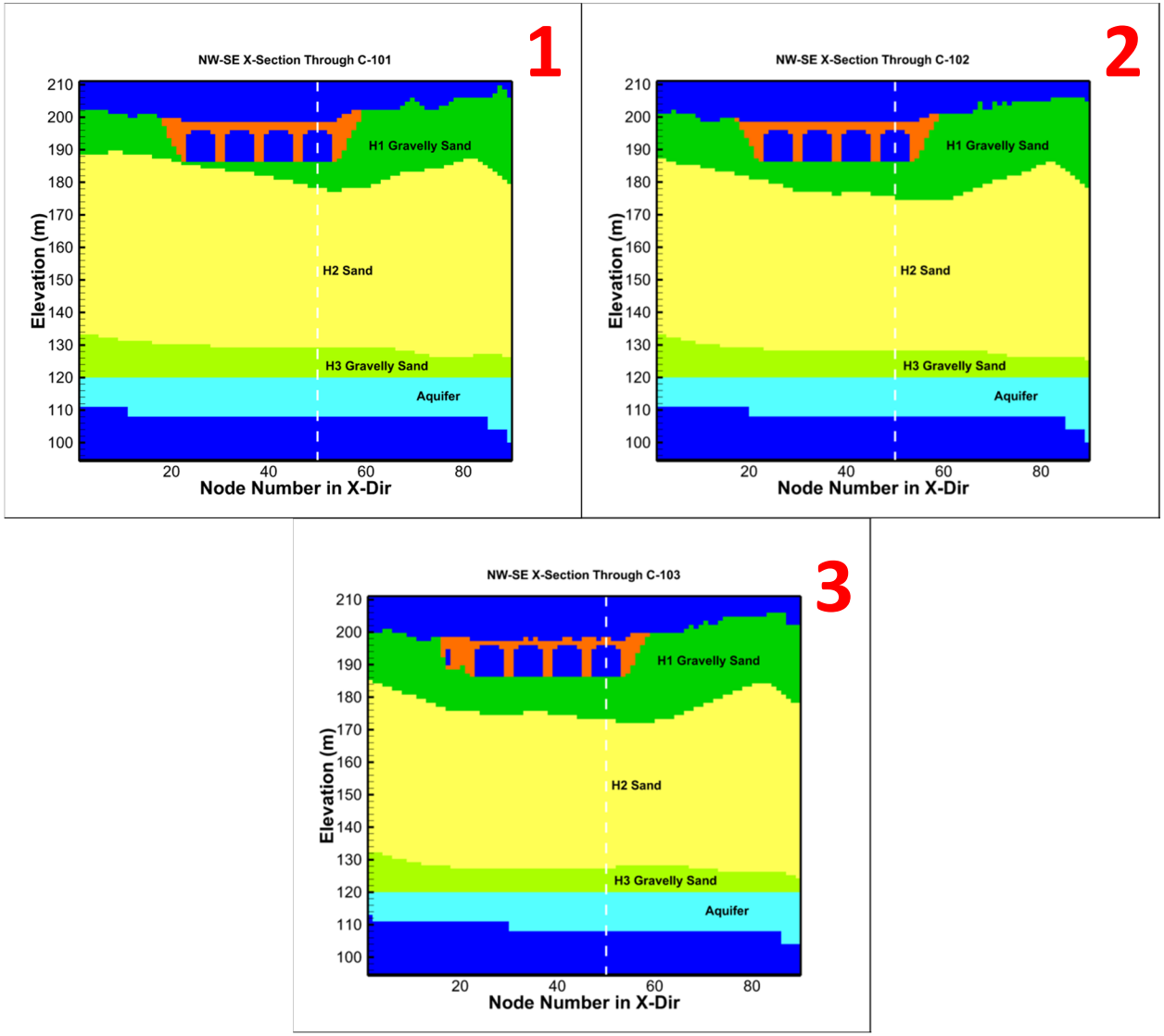

Table 6-15. Hydrostratigraphic Unit Thickness Under the Tanks Taken From the Three-Dimensional Subsurface Transport Over Multiple Phases (STOMP©)-Based Model.

Tank	STOMP_NODE (I_J)	H1 Gravelly Sand (m)	H2 Sand (m)	H3 Gravelly Sand (m)	Aquifer (m)
241-C-101	50_42	8.00	49.00	9.25	12.00
241-C-102	50_50	11.75	46.25	8.25	12.00
241-C-103	50_58	13.00	46.00	7.25	12.00
241-C-104	42_42	5.50	51.50	9.25	12.00
241-C-105	42_50	9.25	48.75	8.25	12.00
241-C-106	42_58	11.75	47.25	7.25	12.00
241-C-107	34_42	3.00	54.00	9.25	12.00
241-C-108	34_50	9.25	48.75	8.25	12.00
241-C-109	34_58	10.50	48.50	7.25	12.00
241-C-110	26_42	2.00	54.00	10.25	12.00
241-C-111	26_50	6.75	51.25	8.25	12.00
241-C-112	26_58	11.75	47.25	7.25	9.00
241-C-201	35_66	13.00	47.00	6.25	9.00
241-C-202	31_66	13.00	48.00	5.25	9.00
241-C-203	27_66	14.25	46.75	5.25	9.00
241-C-204	23_66	14.25	46.75	5.25	9.00
Median	100-Series Tank	9.2	48.7	8.2	12.0
Median	200-Series Tank	13.6	47.1	5.5	9.0

Subsurface Transport Over Multiple Phases (STOMP)© is copyrighted by Battelle Memorial Institute, 1996.

The flow-field abstractions were performed separately for the 100-series and 200-series tanks because (a) 100-series tanks are 22.9 m (75 ft) in diameter compared to 6.1 m (20 ft) in diameter for the 200-series tanks, which leads to different flow paths, and (b) the thickness of HSU below the 100-series tanks differs from the 200-series tanks.

Due to varying recharge conditions at the top boundary (see Section 6.3.2.2 for details), the moisture content and Darcy flux profiles within the soil column vary with depth and respond differently at different times as shown in Figures 6-45 and 6-46, respectively. While the surface barrier is effective (between years 2020 and 2520), moisture content and Darcy fluxes decrease with time as they respond to the change in the recharge rate from 100 mm/yr to 0.50 mm/yr (3.94 in./yr to 0.02 in./yr). After the barrier design period (year 2520 onwards), moisture content and Darcy fluxes equilibrate quickly to the change in recharge rate from 0.50 mm/yr to

3.5 mm/yr (0.02 in./yr to 0.14 in./yr). The flow-field abstraction process was implemented to capture these trends.

The representative hydrostratigraphic columns for the 100-series tanks and 200-series tanks are compared against the vertical discretization chosen for the system-level model in Figure 6-47. Also presented is the vertical discretization implemented in the STOMP©-based model. For the system-level model, finer discretization was chosen at shallow depths with increasingly coarser discretization at deeper depths. However, near the HSU contacts, finer discretization was used to capture the flow field at the interface. Coarser discretization was allowable in the deeper portion of the vadose zone (e.g., H3 gravelly sand) because the flow field did not change appreciably with depth.

The STOMP©-based model nodes that were used to represent the moisture content and Darcy flux for the grid cells in the system model are highlighted in brown color in Figure 6-47. For example, the H1 Gravelly Sand unit in the representative column for the 100-series tank has a total thickness of 9.25 m (30.3 ft) and is divided into three grid cells of 2 m, 3.5 m and 3.75 m (6.6 ft, 11.5 ft and 12.3 ft) thickness. The flow field (moisture content and Darcy flux) extracted from STOMP© model node 69 is applied in the first cell of this unit in the system-level abstraction model. Similarly, the flow field from STOMP© model node 66 and node 63 is applied to the second and third cell of this unit in the system model. The H2 Sand unit is the thickest HSU in the vertical profile. It is discretized into a 3.75-m (12.3-ft) grid cell at the top and 5-m (16.4-ft) grid cell at the bottom. The middle 40 m (131 ft) is discretized into 80 grid cells, each being 0.5 m (1.6 ft) in length to match the 0.25-m (0.82-ft) longitudinal dispersivity applied within the H2 Sand unit (the numerical dispersivity in GoldSim© cell is calculated to be equal to half the cell length). The top and bottom grid cells for the H2 Sand unit are assigned the flow field extracted from STOMP© nodes 61 and 24, respectively, while the middle 40-m (131-ft) length (consisting of 20 grid cells) is represented by the flow field from STOMP© node 47. A single flow field over the 40-m (131-ft) length is used, since the flow field varies little for the corresponding STOMP© nodes at depth. A similar discretization scheme is adopted for the 200-series tanks as shown in Figure 6-47. The details of the grid discretization are presented in Table 6-16.

Figure 6-48 provides an overview of how the moisture content and Darcy flux vary over time for the selected STOMP© nodes in relation to the location in the vertical direction in the system model under an intact 100-series tank. This flow field is applied to model the transport underneath the 100-series tank. The representative flow field underneath an intact 200-series tank is presented in Figure 6-49. In the early time period, the moisture content and Darcy flux decrease due to the decrease in recharge rate from 100 mm/yr to 0.50 mm/yr (3.94 in./yr to 0.02 in./yr) associated with the emplacement of the surface barrier. As the surface barrier is assumed to be degraded 500 years after closure, the recharge rate transitions from a barrier rate of 0.5 mm/yr (0.02 in./yr) to a natural background rate of 3.5 mm/yr (0.14 in./yr), and reaches steady state by year 3000. The STOMP© node 14 used to set the flow field for the grid cell at the base of the H3 Gravelly Sand unit shows high moisture content because it is located in the capillary fringe just above the water table.

Figure 6-45. Moisture Content Distribution below Tank 241-C-105 at Various Times during (a) Surface Barrier Design Time Period of 500 years Following Closure and (b) Post-Surface Barrier Design Time Period.

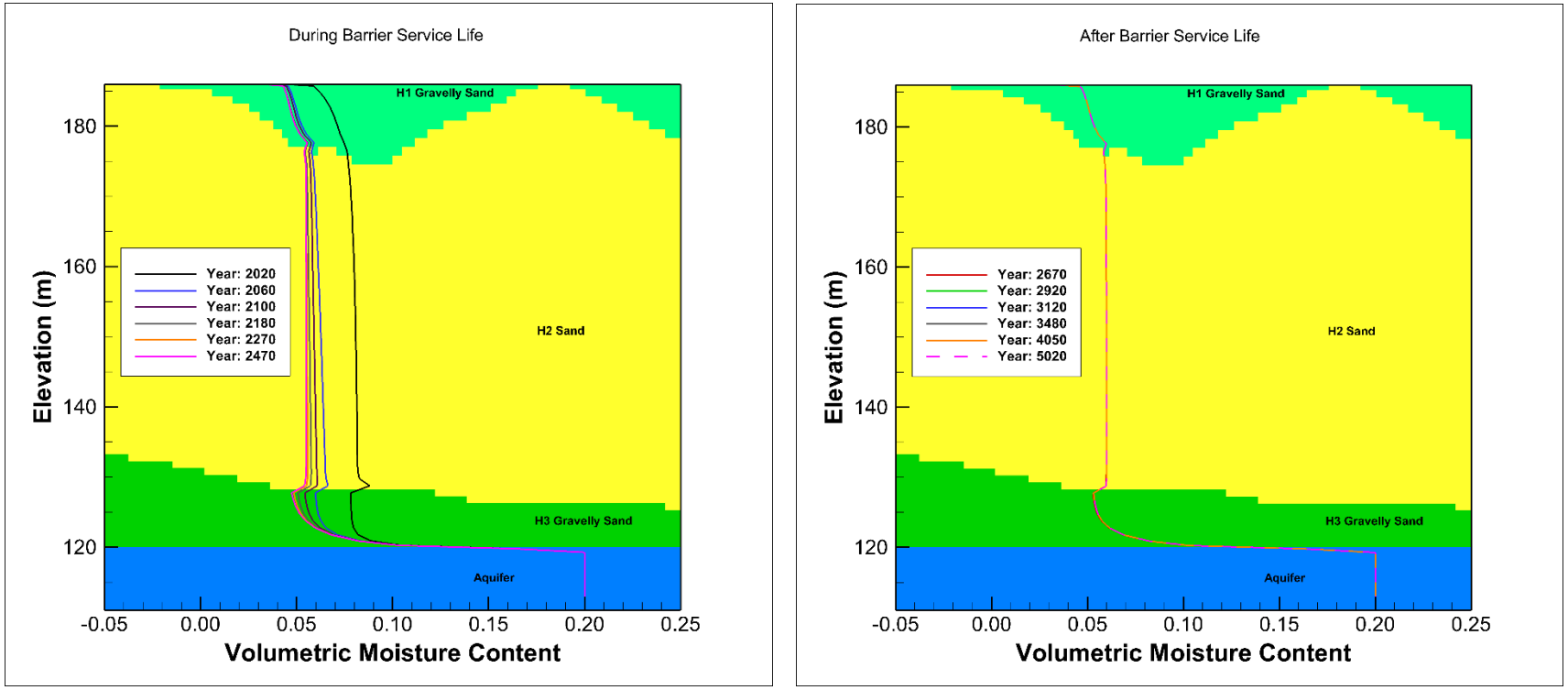

(a) (b)

Note: Barrier Service Life assumes intact surface cover leading to reduced net infiltration while Post-Barrier Service Life assumes degraded surface cover.

Figure 6-46. Vertical Darcy Flux Distribution below Tank 241-C-105 at Various Times.

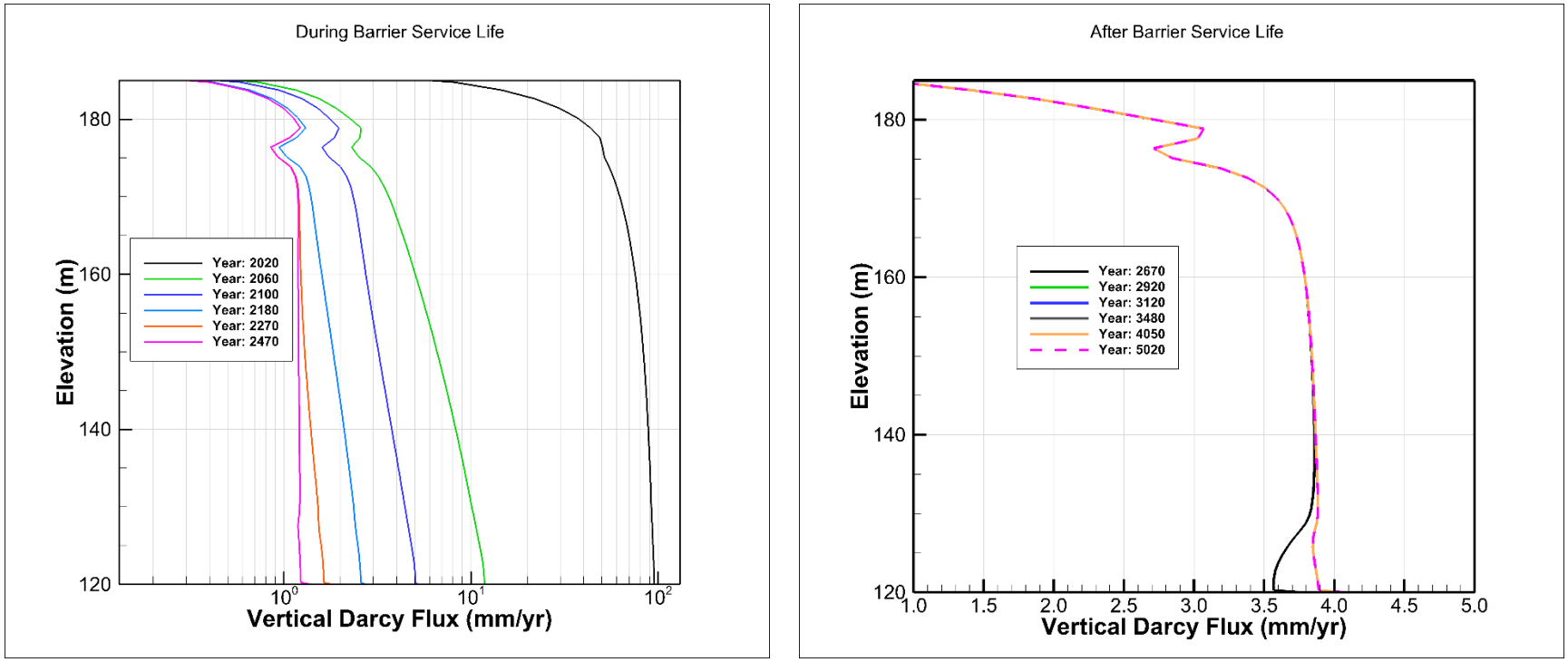

(a) (b)

Figure 6-47. Representative Hydrostratigraphic Column for (a) 100-Series and (b) 200-Series Tanks.

Hydrostratigraphy Below C-105	STOMP Node Elevation (m)	STOMP Node Numbers	STOMP Vertical Discretization (m)	GoldSim Vertical Discretization (m)
H1 Gravelly Sand	185.75	69	1.00	2 m
	184.75	68	1.00	
	183.75	67	1.00	3.5 m
	182.625	66	1.25	
	181.375	65	1.25	
	180.125	64	1.25	3.75 m
	178.875	63	1.25	
	177.625	62	1.25	
	176.375	61	1.25	3.75 m
	175.125	60	1.25	
	173.875	59	1.25	
H2 Sand	172.625	58	1.25	2 m (over 40 m thickness)
	171.375	57	1.25	
	170.125	56	1.25	
	168.875	55	1.25	
	167.625	54	1.25	
	166.375	53	1.25	
	165.125	52	1.25	
	163.875	51	1.25	
	162.625	50	1.25	
	161.375	49	1.25	
	160.125	48	1.25	
	158.875	47	1.25	
	157.625	46	1.25	
	156.375	45	1.25	
	155.125	44	1.25	
	153.875	43	1.25	
	152.625	42	1.25	
	151.375	41	1.25	
	150.125	40	1.25	
	148.875	39	1.25	
	147.625	38	1.25	
	146.375	37	1.25	
	145.125	36	1.25	
	143.875	35	1.25	
	142.625	34	1.25	
	141.375	33	1.25	
	140.125	32	1.25	
	138.875	31	1.25	
	137.625	30	1.25	
	136.375	29	1.25	
	135.125	28	1.25	
	133.875	27	1.25	
	132.75	26	1.00	5 m
	131.75	25	1.00	
	130.75	24	1.00	
	129.75	23	1.00	
	128.75	22	1.00	
H3 Gravelly Sand	127.75	21	1.00	7 m
	126.75	20	1.00	
	125.75	19	1.00	
	124.75	18	1.00	
	123.75	17	1.00	
	122.75	16	1.00	
	121.75	15	1.00	
	120.875	14	0.75	1.25 m
	120.25	13	0.50	
Aquifer	119.75	12	0.50	12 m
	119.25	11	0.50	
	118.625	10	0.75	
	117.75	9	1.00	
	116.625	8	1.25	
	115.25	7	1.50	
	113.75	6	1.50	
	112	5	2.00	
	109.5	4	3.00	
Inactive	106	3	4.00	
	102	2	4.00	
	97.5	1	5.00	

Node used in Flow-Field abstraction

(a)

Hydrostratigraphy Below C-203	STOMP Node Elevation (m)	STOMP Node Numbers	STOMP Vertical Discretization (m)	GoldSim Vertical Discretization (m)
H1 Gravelly Sand	185.75	69	1.00	2 m
	184.75	68	1.00	
	183.75	67	1.00	3.5 m
	182.625	66	1.25	
	181.375	65	1.25	
	180.125	64	1.25	8.75 m
	178.875	63	1.25	
	177.625	62	1.25	
	176.375	61	1.25	
	175.125	60	1.25	
	173.875	59	1.25	
	172.625	58	1.25	
H2 Sand	171.375	57	1.25	3.75 m
	170.125	56	1.25	
	168.875	55	1.25	
	167.625	54	1.25	2 m (over 40 m thickness)
	166.375	53	1.25	
	165.125	52	1.25	
	163.875	51	1.25	
	162.625	50	1.25	
	161.375	49	1.25	
	160.125	48	1.25	
	158.875	47	1.25	
	157.625	46	1.25	
	156.375	45	1.25	
	155.125	44	1.25	
	153.875	43	1.25	
	152.625	42	1.25	
	151.375	41	1.25	
	150.125	40	1.25	
	148.875	39	1.25	
	147.625	38	1.25	
	146.375	37	1.25	
	145.125	36	1.25	
	143.875	35	1.25	
	142.625	34	1.25	
	141.375	33	1.25	
	140.125	32	1.25	
	138.875	31	1.25	
	137.625	30	1.25	
	136.375	29	1.25	
	135.125	28	1.25	
	133.875	27	1.25	
	132.75	26	1.00	
	131.75	25	1.00	
	130.75	24	1.00	
	129.75	23	1.00	
	128.75	22	1.00	
	127.75	21	1.00	
	126.75	20	1.00	3
	125.75	19	1.00	
H3 Gravelly Sand	124.75	18	1.00	4
	123.75	17	1.00	
	122.75	16	1.00	
	121.75	15	1.00	
	120.875	14	0.75	1.25
	120.25	13	0.50	
Aquifer	119.75	12	0.50	9
	119.25	11	0.50	
	118.625	10	0.75	
	117.75	9	1.00	
	116.625	8	1.25	
	115.25	7	1.50	
	113.75	6	1.50	
	112	5	2.00	
Inactive	109.5	4	3.00	
	106	3	4.00	
	102	2	4.00	
	97.5	1	5.00	

Node used in Flow-Field abstraction

(b)

GoldSim© simulation software is copyrighted by GoldSim Technology Group LLC of Issaquah, Washington (see http://www.goldsim.com).
Subsurface Transport Over Multiple Phases (STOMP)© is copyrighted by Battelle Memorial Institute, 1996.

The above results are for the situation when the grout is structurally stable and provides a hydraulic barrier. However, a number of the sensitivity cases evaluate conditions where the effectiveness of grout as a hydraulic barrier is assumed to degrade at different times. Under degraded grout conditions, the grout is assumed to be highly fractured, and the infill material in the tank is assumed to behave like a porous material with hydraulic properties same as the

H2 Sand unit. The STOMP©-based model is run with the H2-sand hydraulic properties for the tank, and the flow field is calculated and abstracted in a manner similar to that described earlier for the intact tank. The flow field is calculated separately for the degraded tank conditions for the 100-series and 200-series tanks, as shown in Figure 6-50. One additional STOMP© node result (node 73) is extracted and added to the system model to represent the flow conditions inside the tank. In the sensitivity cases, when the tank degradation occurs, the flow field is switched from the intact tank flow field to the degraded tank flow field. As a result, the contaminants are released via advection at the time when the tank is degraded in addition to the ongoing diffusive release mechanism.

Table 6-16. Vertical Grid Discretization and Flow Field for the System-Level Model.

	Unit	Thickness (m)	Number of Grid Block Cells	Grid Discretization	Flow Field Discretization (Moisture Content and Vertical Darcy Flux)
100-Series Tanks	H1 Gravelly Sand	9.25	3	1 at 2 m, 1 at 3.5 m, 1 at 3.75 m	One flow field for each cell
	H2 Sand	48.75	22	1 at 3.75 m, 20 cells of 2 m thickness each for a total of 40 m 1 at 5 m	One flow field for the first cell. One flow field for the next 20 cells and One flow field for the remaining one cell
	H3 Gravelly Sand	8.25	2	1 at 7 m, 1 at 1.25 m.	One flow field for each cell
	Saturated Zone	12.00		Aquifer pathway	One flow field
200-Series Tanks	H1 Gravelly Sand	14.25	3	1 at 2 m, 1 at 3.5 m, 1 at 8.75 m	One flow field for each cell
	H2 Sand	46.75	22	1 at 3.75 m, 20 cells of 2 m thickness each for a total of 40 m 1 at 3 m	One flow field for the first cell. One flow field for the next 20 cells and One flow field for the remaining one cell
	H3 Gravelly Sand	5.50	2	1 at 4 m, 1 at 1.25 m.	One flow field per cell
	Saturated Zone	9.00		Aquifer pathway	One flow field

The flow field applied to pipeline releases is calculated separately. Vertical Darcy fluxes and volumetric moisture contents from the STOMP© nodes that fall within the pipeline source area (150 m by 150 m [492 ft by 492 ft]) but outside the tank footprint are averaged to calculate the pipeline flow-field. The representative hydrostratigraphic column for the 100-series tanks is applied to the pipeline source area. Advective flow occurs through the pipelines for all time periods. The hydraulic effect of the presence of buried pipelines in the vadose zone is not

modeled explicitly, and the areas occupied by the pipelines are modeled with hydraulic properties of soil backfill material.

The saturated zone is modeled as a 1-D aquifer, oriented along the primary flow direction using the aquifer pathway capability in GoldSim©. The volumetric flow rate through the aquifer is calculated based on the hydraulic gradient under steady-state conditions and saturated hydraulic conductivity consistent with the values used in the STOMP©-based model. The saturated zone thickness for the 100-series tanks is chosen to be 12 m (39.4 ft), while that for the 200-series tanks is chosen to be 9 m (29.5 ft) (Table 6-16).

The mass flux from the vadose zone for each source term (each of the 100- and 200-series tanks, the C-301 catch tank, the 244-CR vault, and pipelines) is calculated separately. Each source term is then transported to the aquifer, assuming that vertical mass transport in the vadose zone stays within the footprint of the source area, ignoring any lateral dispersion as shown in Figure 6-51. The aquifer pathway from each source area starts under its associated source in WMA C and extends to the PoCal, 100 m (328 ft) downgradient from the WMA C fenceline along the groundwater flow direction. The width of the aquifer pathway is taken to be the width of the source area. The length of the aquifer pathway varies depending on the location of the source area being modeled (tanks and ancillary equipment), relative to the PoCal 100 m (328 ft) downgradient from the WMA C fenceline along the groundwater flow path. As an example, the total length of the aquifer pathway from tank C-102 is ~144 m (472 ft), compared with ~174 m (571 ft) for tank C-105, and ~235 m (771 ft) for tank C-111. For the pipeline source, the aquifer pathway is assumed to begin at the center of the WMA C area leading to a total length of 175 m (574 ft). This length represents an average distance from all of the pipeline sources to the PoCal.

The mass loading on the aquifer pathway from the vadose zone occurs over the length of the source parallel to the flow path. For the tank sources, this is equivalent to the diameter of the tank. For the pipeline source, the source loading from the vadose zone to the aquifer is conservatively assumed to occur over the 75 m (246 ft) that represents the half-length of the pipeline source area along the flow path.

The average aquifer pathway concentrations at the 100 m (328 ft) downgradient boundary are calculated for each source separately, by assuming that the mass within the defined 1-D aquifer stream tube configuration does not laterally disperse. This 1-D approach tends to maximize the concentrations for a given source term, but it does not take account of overlapping plumes from lateral dispersion from other sources that are on parallel flow paths (Figure 6-51). To determine the maximum concentration, a separate calculation is performed. Since the highest concentrations were expected to occur along the centerline of the WMA C width, extended to the 100 m (328 ft) boundary, due to location of highest residual inventory tanks along the centerline, the calculated concentrations for the C-102, C-105, C-108 and C-111 tank sources at the 100 m (328 ft) boundary were combined. These four tanks fall along a single flow path (stream tube), since the flow direction is aligned with the orientation of these tanks. The amount of additional contaminant mass from lateral dispersion along adjacent flow paths is included by using an analytical solution (*Plume function* within GoldSim©) that calculates the concentration away from the centerline of the plume. Using this approach, the concentrations from surrounding aquifer pathways are calculated and added to the combined concentration for the aquifer pathway

that includes C-102, C-105, C-108, and C-111 tank sources. The two laterally adjacent and parallel aquifer pathways are (a) along the orientation of tanks C-101, C-104, C-107, and C-110, and (b) along the orientation of tanks C-103, C-106, C-109, and C-112. The primary groundwater flow path on which the 200-series tanks occur is deemed too far to influence the concentrations along the centerline, and therefore is not considered based on evaluation of STOMP© 3-D model results.

A spatial-variability study was undertaken to evaluate the adequacy of using one representative flow field for all of the 100-series tanks. For this purpose, the vertical Darcy fluxes from STOMP©-based model nodes located underneath intact tanks were compared. The vertical Darcy flux underneath tank C-105 (located near the center of the tank farm) was compared to that of tank C-112 (located at the northern edge of the tank farm). The vertical Darcy flux under a 200-series tank (C-201) located near tank C-112 was also compared. The comparison results are presented in Figure 6-52 for two nodes. Node 69 is located ~0.5 m (1.6 ft) below the base of the tank, while node 63 is located ~3 m (9.8 ft) below node 69. The results indicate that for node 69 the vertical Darcy flux for tank C-105 matches closely with that of tank C-112, and is quite different from that of tank C-201. For node 63, which is deeper, the differences among the three tanks are minor. The large difference observed for node 63 is attributed to its location near the base of the tank, where the amount of flow diversion around the tank is influenced by its diameter. The smaller diameter of tank C-201 (6.1 m [20 ft]) exhibits small flow diversion, and the Darcy flux under the tank is relatively high compared to the larger flow diversion observed for the larger-diameter (23 m [75 ft]) C-105 and C-112 tanks. These observations support the use of one representative flow field for all 100-series tanks and another for all 200-series tanks.

Confirmation of the abstraction modeling approach for evaluating system performance was undertaken by comparing the contaminant transport results to the STOMP©-based model results for the base case. Due to coarser vertical discretization employed in the 1-D abstraction model, the results from those nodes that are closest to the STOMP©-based model grid nodes are compared. The time-varying diffusive mass flux of ^{99}Tc calculated using the source term parameters for tank C-105 was applied as boundary conditions in both models. A comparison between the dissolved concentration of ^{99}Tc in the vadose zone using a STOMP© 3-D model and a GoldSim© 1-D model is presented for selected locations in the vadose zone (Figure 6-53 and Figure 6-54). There is a good match between the 3-D process model and 1-D abstraction model throughout the full thickness of the vadose zone under the tank (~66 m [217 ft]).

For the saturated zone, the groundwater concentration predicted by the STOMP©-based model (at the highest concentration PoCal) is compared to the GoldSim©-based abstraction model results at 100 m (328 ft) downgradient of the WMA C fenceline along the tank C-105 aquifer pathway (Figure 6-55). The first breakthrough times match well, but the 1-D model produces slightly higher concentrations following the peak. This result is expected, as the 1-D aquifer pathway does not allow lateral dispersion of the mass and assumes constant flow rate through the steam tube. Based on these results, the abstraction model was qualified as sufficiently accurate for its intended use in evaluating system performance.

Figure 6-48. Representative Flow Field Applied Under 100-Series Tank for the Base Case (Intact Tank Condition).

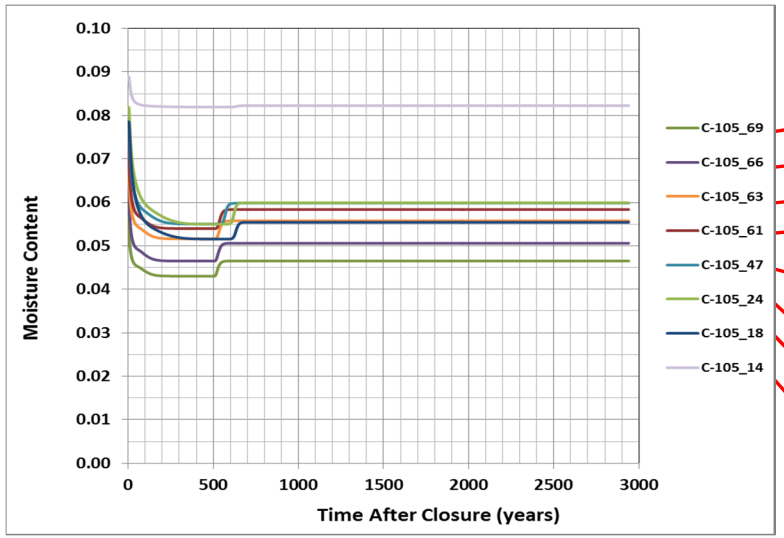

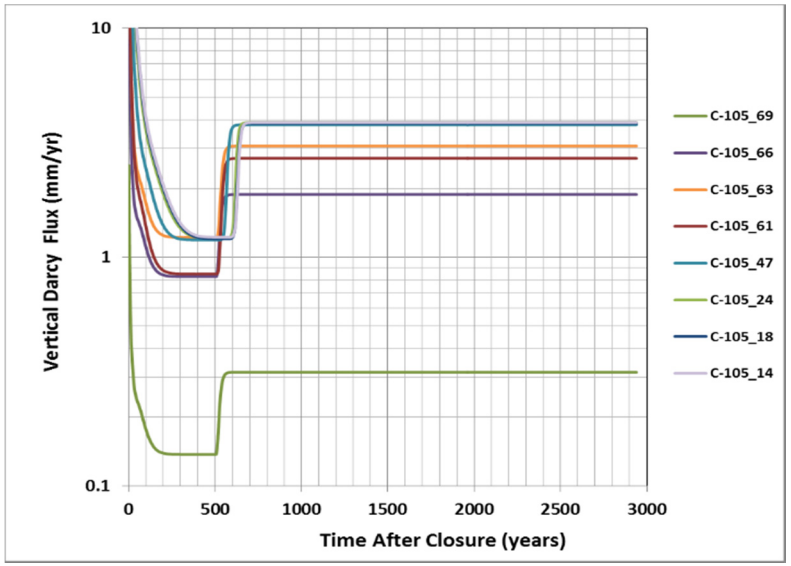

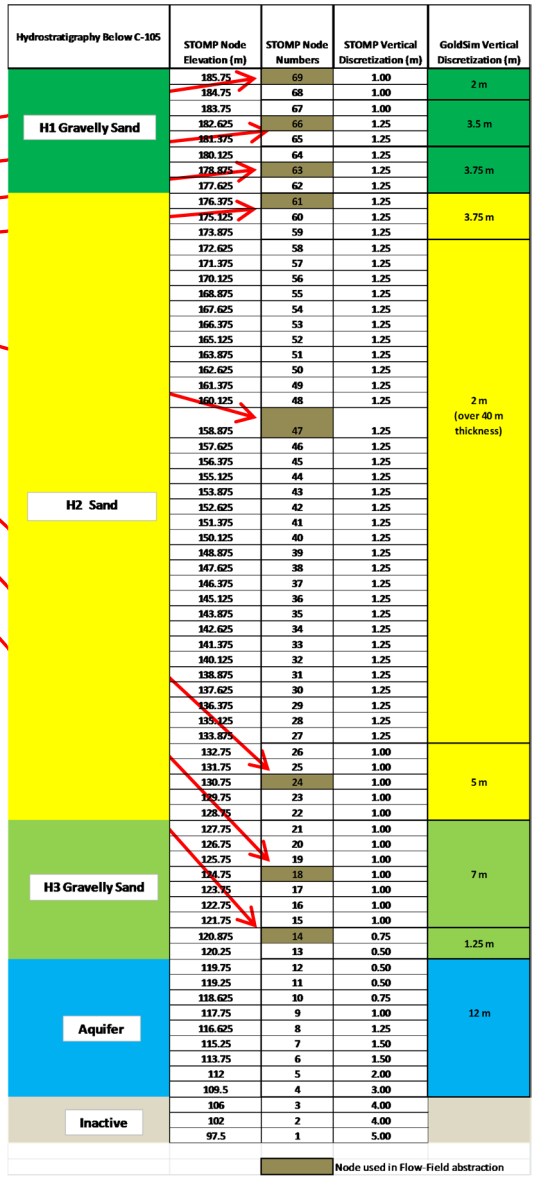

Hydrostratigraphy Below C-105	STOMP Node Elevation (m)	STOMP Node Numbers	STOMP Vertical Discretization (m)	GoldSim Vertical Discretization (m)
H1 Gravelly Sand	185.75	69	1.00	2 m
	184.75	68	1.00	
	183.75	67	1.00	3.5 m
	182.625	66	1.25	
	181.375	65	1.25	
	180.125	64	1.25	3.75 m
	178.875	63	1.25	
	177.625	62	1.25	
	176.375	61	1.25	3.75 m
	175.125	60	1.25	
	173.875	59	1.25	
H2 Sand	172.625	58	1.25	2 m (over 40 m thickness)
	171.375	57	1.25	
	170.125	56	1.25	
	168.875	55	1.25	
	167.625	54	1.25	
	166.375	53	1.25	
	165.125	52	1.25	
	163.875	51	1.25	
	162.625	50	1.25	
	161.375	49	1.25	
	160.125	48	1.25	
	158.875	47	1.25	
	157.625	46	1.25	
	156.375	45	1.25	
	155.125	44	1.25	
	153.875	43	1.25	
	152.625	42	1.25	
	151.375	41	1.25	
	150.125	40	1.25	
	148.875	39	1.25	
	147.625	38	1.25	
	146.375	37	1.25	
	145.125	36	1.25	
	143.875	35	1.25	
	142.625	34	1.25	
	141.375	33	1.25	
	140.125	32	1.25	
	138.875	31	1.25	
	137.625	30	1.25	
	136.375	29	1.25	
	135.125	28	1.25	
	133.875	27	1.25	
	132.75	26	1.00	5 m
	131.75	25	1.00	
	130.75	24	1.00	
	129.75	23	1.00	
	128.75	22	1.00	
H3 Gravelly Sand	127.75	21	1.00	7 m
	126.75	20	1.00	
	125.75	19	1.00	
	124.75	18	1.00	
	123.75	17	1.00	
	122.75	16	1.00	
	121.75	15	1.00	
	120.875	14	0.75	1.25 m
	120.25	13	0.50	
Aquifer	119.75	12	0.50	12 m
	119.25	11	0.50	
	118.625	10	0.75	
	117.75	9	1.00	
	116.625	8	1.25	
	115.25	7	1.50	
	113.75	6	1.50	
	112	5	2.00	
	109.5	4	3.00	
Inactive	106	3	4.00	
	102	2	4.00	
	97.5	1	5.00	

Subsurface Transport Over Multiple Phases (STOMP)© is copyrighted by Battelle Memorial Institute, 1996.
GoldSim© simulation software is copyrighted by GoldSim Technology Group LLC of Issaquah, Washington (see http://www.goldsim.com).

Figure 6-49. Representative Flow Field Applied Under 200-Series Tank for the Base Case (Intact Tank Condition).

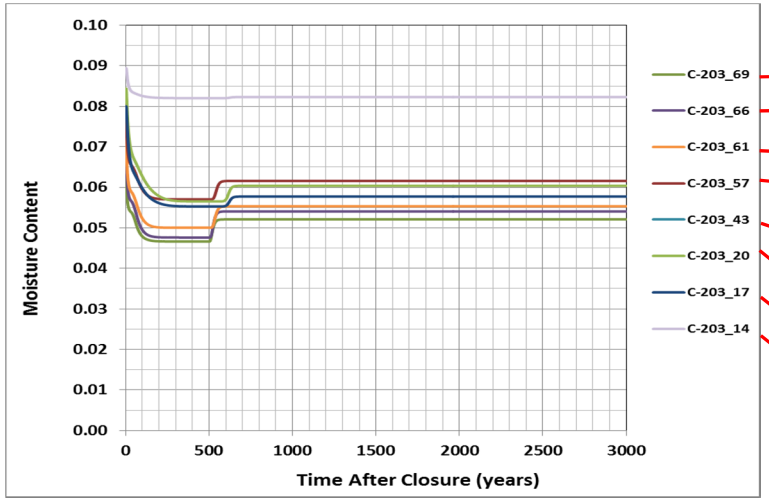

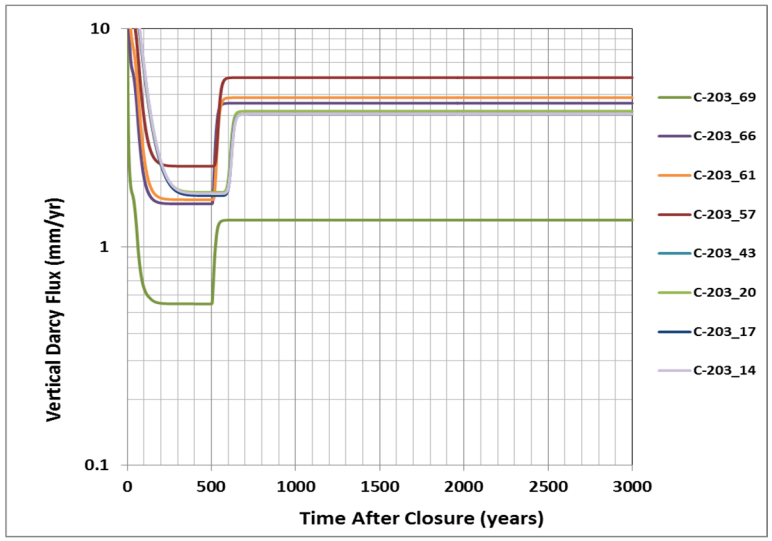

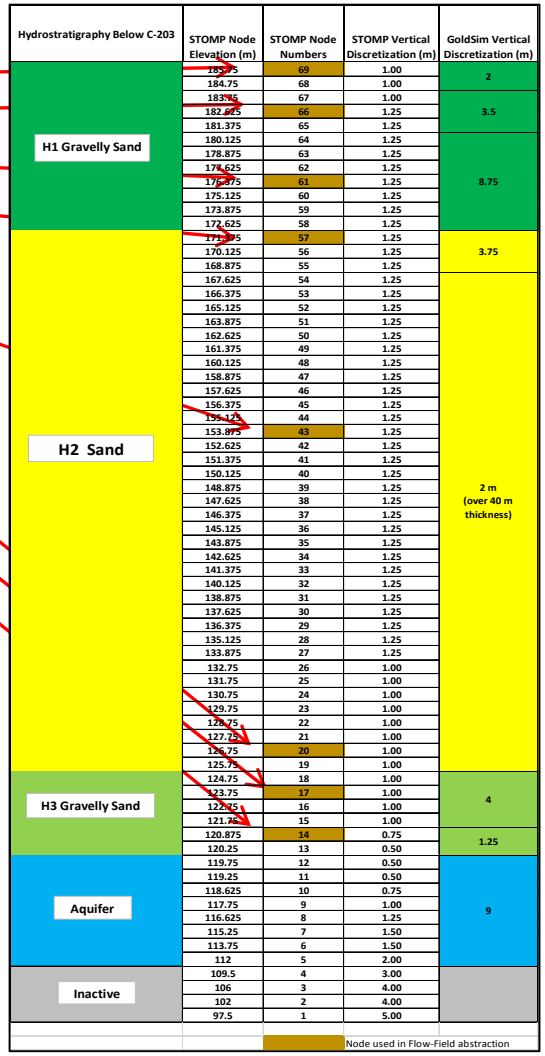

Hydrostratigraphy Below C-203	STOMP Node Elevation (m)	STOMP Node Numbers	STOMP Vertical Discretization (m)	GoldSim Vertical Discretization (m)
H1 Gravelly Sand	185.75	69	1.00	2
	184.75	68	1.00	
	183.75	67	1.00	
	182.625	66	1.25	3.5
	181.375	65	1.25	
	180.125	64	1.25	8.75
	178.875	63	1.25	
	177.625	62	1.25	
	176.375	61	1.25	
	175.125	60	1.25	
	173.875	59	1.25	
	172.625	58	1.25	
	171.375	57	1.25	
H2 Sand	170.125	56	1.25	3.75
	168.875	55	1.25	
	167.625	54	1.25	2 m (over 40 m thickness)
	166.375	53	1.25	
	165.125	52	1.25	
	163.875	51	1.25	
	162.625	50	1.25	
	161.375	49	1.25	
	160.125	48	1.25	
	158.875	47	1.25	
	157.625	46	1.25	
	156.375	45	1.25	
	155.125	44	1.25	
	153.875	43	1.25	
	152.625	42	1.25	
	151.375	41	1.25	
	150.125	40	1.25	
	148.875	39	1.25	
	147.625	38	1.25	
	146.375	37	1.25	
	145.125	36	1.25	
	143.875	35	1.25	
	142.625	34	1.25	
	141.375	33	1.25	
	140.125	32	1.25	
	138.875	31	1.25	
	137.625	30	1.25	
	136.375	29	1.25	
	135.125	28	1.25	
	133.875	27	1.25	
	132.75	26	1.00	
	131.75	25	1.00	
	130.75	24	1.00	
	129.75	23	1.00	
	128.75	22	1.00	
	127.75	21	1.00	
	126.75	20	1.00	
	125.75	19	1.00	
	124.75	18	1.00	
H3 Gravelly Sand	123.75	17	1.00	4
	122.75	16	1.00	
	121.75	15	1.00	
	120.875	14	0.75	1.25
	120.25	13	0.50	
Aquifer	119.75	12	0.50	9
	119.25	11	0.50	
	118.625	10	0.75	
	117.75	9	1.00	
	116.625	8	1.25	
	115.25	7	1.50	
	113.75	6	1.50	
	112	5	2.00	
Inactive	109.5	4	3.00	
	106	3	4.00	
	102	2	4.00	
	97.5	1	5.00	

Node used in Flow-Field abstraction

GoldSim© simulation software is copyrighted by GoldSim Technology Group LLC of Issaquah, Washington (see http://www.goldsim.com).
Subsurface Transport Over Multiple Phases (STOMP)© is copyrighted by Battelle Memorial Institute, 1996.

Figure 6-50. Representative Flow Field Applied For Degraded Tank Conditions for (a) 100-Series Tank and (b) 200-Series Tank.

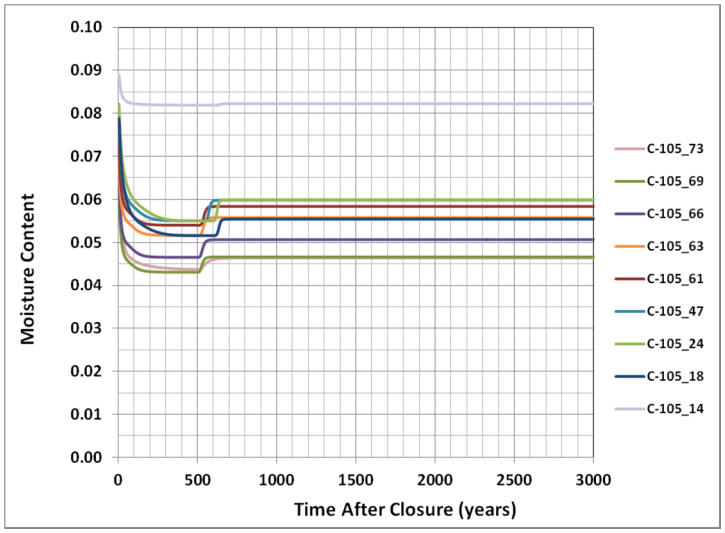

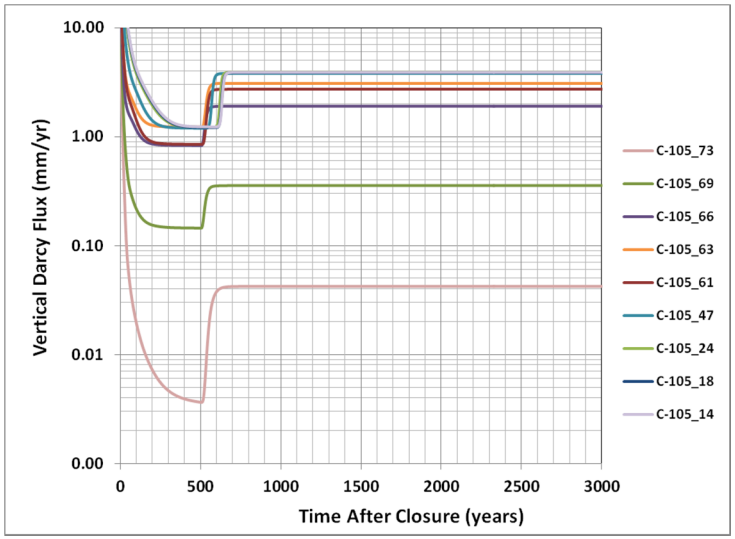

(a)

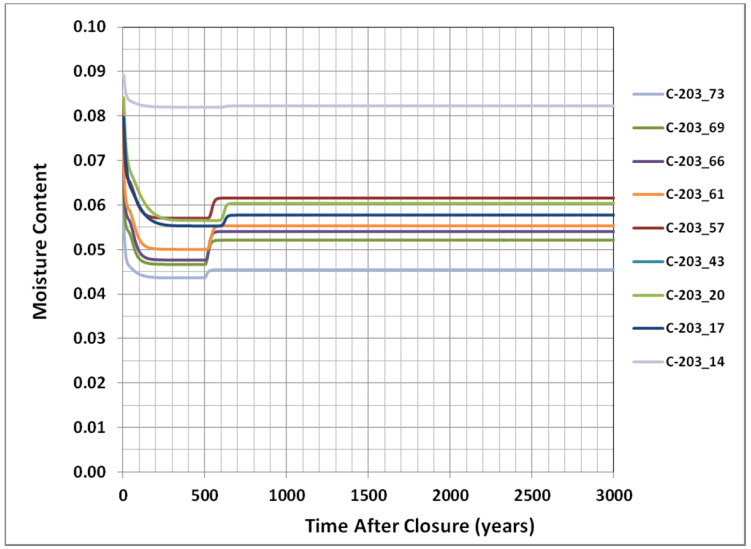

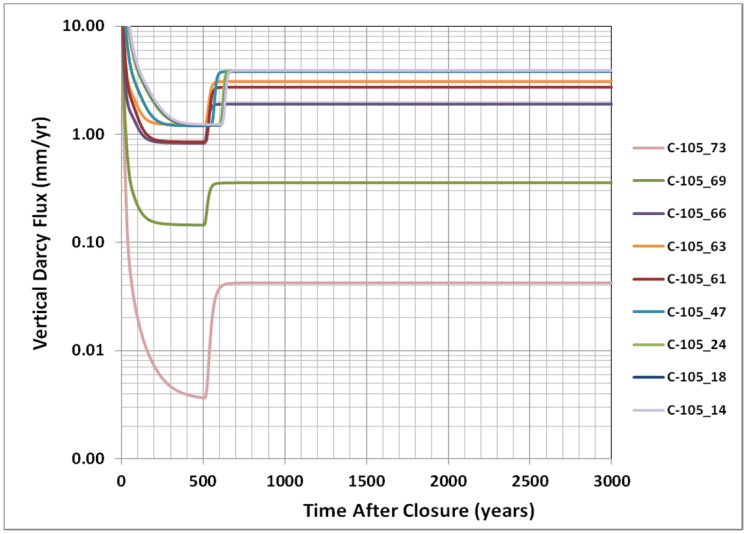

(b)

Figure 6-51. Implementation of Aquifer Pathway for a Given Source Area along with Points of Evaluation of Concentrations.

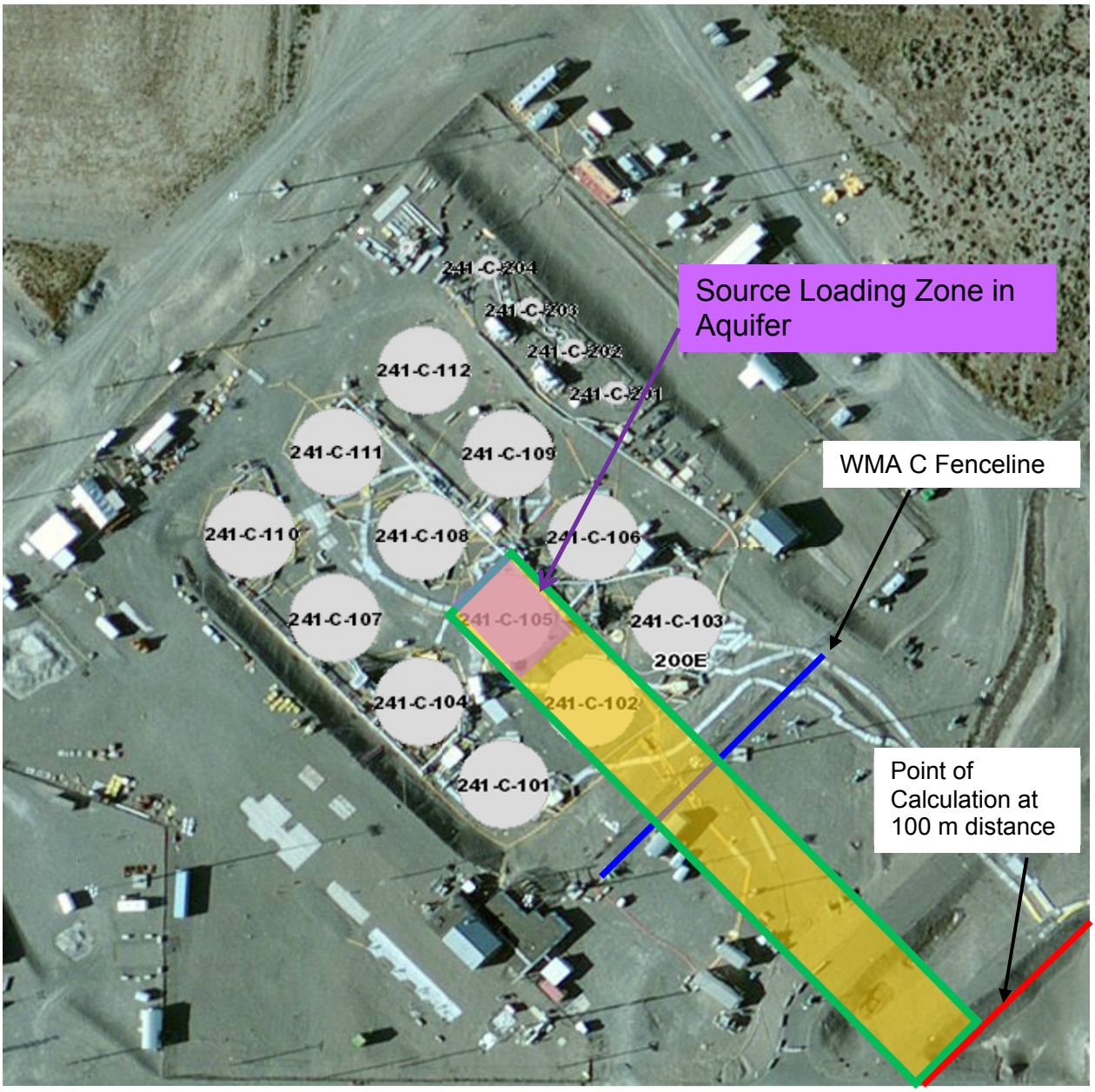

WMA = Waste Management Area

6.3.2.5 Atmospheric Transport Pathway. Gases and vapors could travel upward from the residual inventory within tanks and ancillary equipment through the surface barrier to the ground surface. The principal mechanism by which nuclides migrate from the waste to the ground surface is gaseous diffusion. For tanks, in which the residual waste is predominantly on the bottom of the tank, this means that the gases are transported through the tank infill grout, the tank dome, the soil overburden, and the surface barrier. For pipelines, the diffusion would occur through the soil overburden and the surface barrier.

Figure 6-52. Vertical Darcy Flux Extracted from Three-Dimensional Subsurface Transport Over Multiple Phases (STOMP©)-Based Model Nodes Located below Tanks 241-C-105, 241-C-112, and 241-C-201 along with Their Location in Waste Management Area C. Node 69 is located 0.5 m below the tank bottom while node 63 is located about 3 m below node 69.

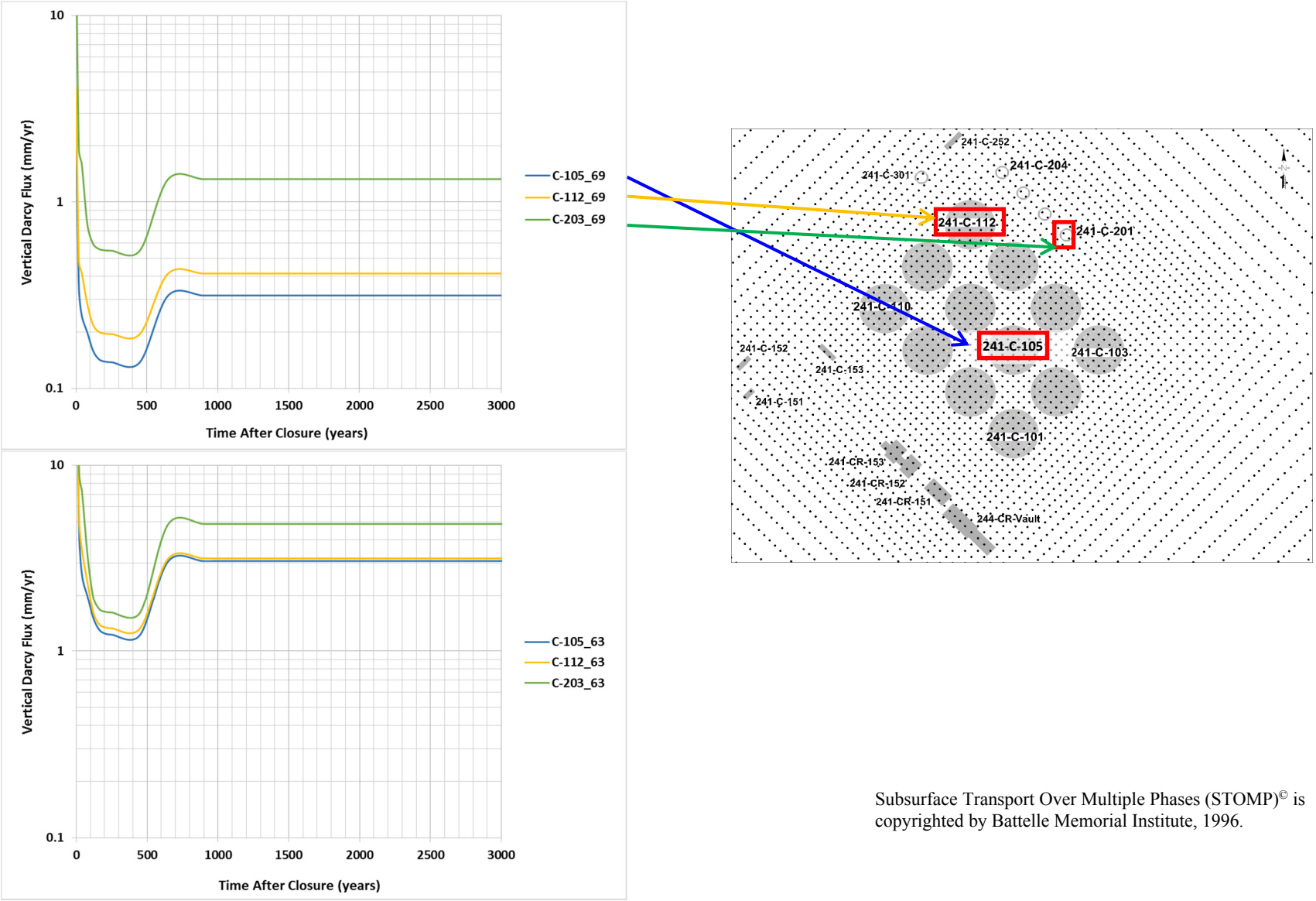

Subsurface Transport Over Multiple Phases (STOMP)© is copyrighted by Battelle Memorial Institute, 1996.

Figure 6-53. Comparison between Three-Dimensional Subsurface Transport Over Multiple Phases (STOMP©)-Based Model Prediction and GoldSim©-Based One-Dimensional Abstraction Model Prediction for Nodes Located in H1 Gravelly Sand Unit.

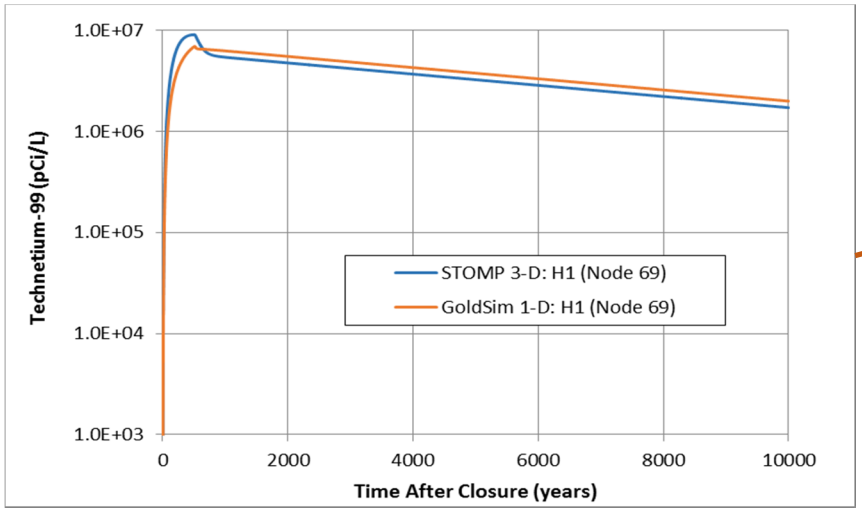

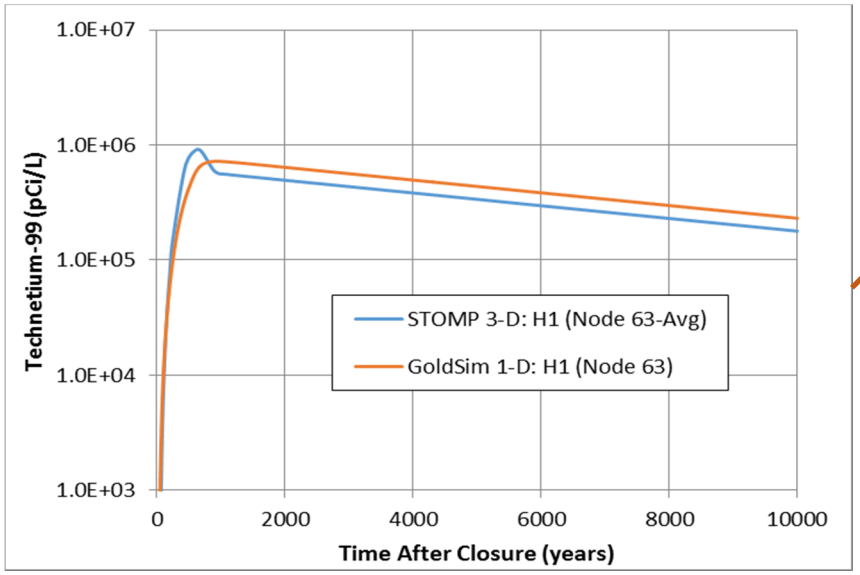

Hydrostratigraphy Below C-105	STOMP Node Elevation (m)	STOMP Node Numbers	STOMP Vertical Discretization (m)	GoldSim Vertical Discretization (m)
H1 Gravelly Sand	185.75	69	1.00	2 m
	184.75	68	1.00	
	183.75	67	1.00	3.5 m
	182.625	66	1.25	
	181.375	65	1.25	
	180.125	64	1.25	3.75 m
	178.875	63	1.25	
	177.625	62	1.25	
H2 Sand	176.375	61	1.25	3.75 m
	175.125	60	1.25	
	173.875	59	1.25	
	172.625	58	1.25	2 m (over 40 m thickness)
	171.375	57	1.25	
	170.125	56	1.25	
	168.875	55	1.25	
	167.625	54	1.25	
	166.375	53	1.25	
	165.125	52	1.25	
	163.875	51	1.25	
	162.625	50	1.25	
	161.375	49	1.25	
	160.125	48	1.25	
	158.875	47	1.25	
	157.625	46	1.25	
	156.375	45	1.25	
	155.125	44	1.25	
	153.875	43	1.25	
	152.625	42	1.25	
	151.375	41	1.25	
	150.125	40	1.25	
	148.875	39	1.25	
	147.625	38	1.25	
	146.375	37	1.25	
	145.125	36	1.25	
	143.875	35	1.25	
	142.625	34	1.25	
	141.375	33	1.25	
	140.125	32	1.25	
	138.875	31	1.25	
	137.625	30	1.25	
	136.375	29	1.25	
	135.125	28	1.25	
	133.875	27	1.25	
	132.75	26	1.00	5 m
	131.75	25	1.00	
	130.75	24	1.00	
	129.75	23	1.00	
	128.75	22	1.00	
H3 Gravelly Sand	127.75	21	1.00	7 m
	126.75	20	1.00	
	125.75	19	1.00	
	124.75	18	1.00	
	123.75	17	1.00	
	122.75	16	1.00	
	121.75	15	1.00	
	120.875	14	0.75	1.25 m
	120.25	13	0.50	
Aquifer	119.75	12	0.50	12 m
	119.25	11	0.50	
	118.625	10	0.75	
	117.75	9	1.00	
	116.625	8	1.25	
	115.25	7	1.50	
	113.75	6	1.50	
	112	5	2.00	
	109.5	4	3.00	
Inactive	106	3	4.00	
	102	2	4.00	
	97.5	1	5.00	

Node used in Flow-Field abstraction

GoldSim© simulation software is copyrighted by GoldSim Technology Group LLC of Issaquah, Washington (see http://www.goldsim.com).
Subsurface Transport Over Multiple Phases (STOMP)© is copyrighted by Battelle Memorial Institute, 1996.

Figure 6-54. Comparison between Three-Dimensional Subsurface Transport Over Multiple Phases (STOMP©)-Based Model Prediction and GoldSim©-Based One-Dimensional Abstraction Model Prediction for Nodes Located in H2 Sand Unit and H3 Gravelly Sand Unit.

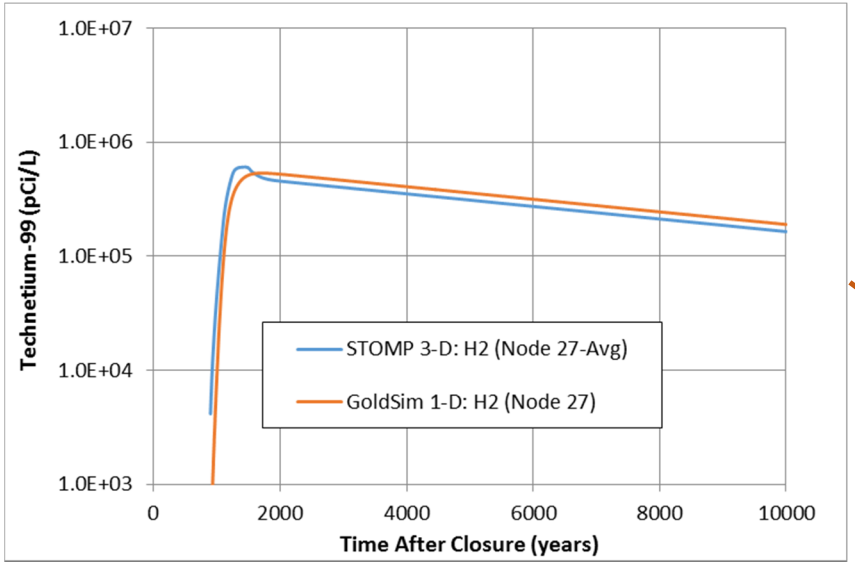

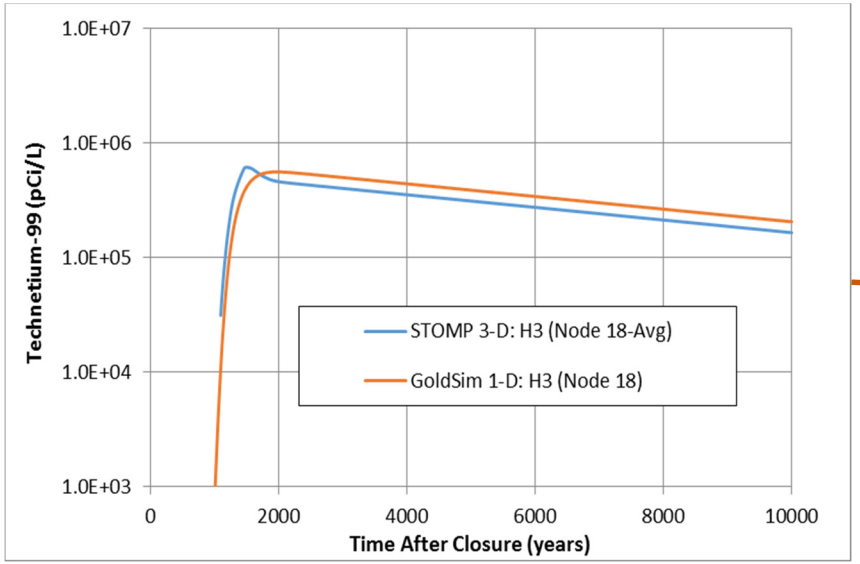

GoldSim© simulation software is copyrighted by GoldSim Technology Group LLC of Issaquah, Washington (see http://www.goldsim.com).

Subsurface Transport Over Multiple Phases (STOMP)© is copyrighted by Battelle Memorial Institute, 1996.

Hydrostratigraphy Below C-105	STOMP Node Elevation (m)	STOMP Node Numbers	STOMP Vertical Discretization (m)	GoldSim Vertical Discretization (m)
H1 Gravelly Sand	185.75	69	1.00	2 m
	184.75	68	1.00	
	183.75	67	1.00	3.5 m
	182.625	66	1.25	
	181.375	65	1.25	
	180.125	64	1.25	3.75 m
	178.875	63	1.25	
	177.625	62	1.25	
H2 Sand	176.375	61	1.25	3.75 m
	175.125	60	1.25	
	173.875	59	1.25	
	172.625	58	1.25	2 m (over 40 m thickness)
	171.375	57	1.25	
	170.125	56	1.25	
	168.875	55	1.25	
	167.625	54	1.25	
	166.375	53	1.25	
	165.125	52	1.25	
	163.875	51	1.25	
	162.625	50	1.25	
	161.375	49	1.25	
	160.125	48	1.25	
	158.875	47	1.25	
	157.625	46	1.25	
	156.375	45	1.25	
	155.125	44	1.25	
	153.875	43	1.25	
	152.625	42	1.25	
	151.375	41	1.25	
	150.125	40	1.25	
	148.875	39	1.25	
	147.625	38	1.25	
	146.375	37	1.25	
	145.125	36	1.25	
	143.875	35	1.25	
	142.625	34	1.25	
	141.375	33	1.25	
	140.125	32	1.25	
	138.875	31	1.25	
	137.625	30	1.25	
	136.375	29	1.25	
	135.125	28	1.25	
	133.875	27	1.25	
	132.75	26	1.00	5 m
	131.75	25	1.00	
	130.75	24	1.00	
	129.75	23	1.00	
	128.75	22	1.00	
H3 Gravelly Sand	127.75	21	1.00	7 m
	126.75	20	1.00	
	125.75	19	1.00	
	124.75	18	1.00	
	123.75	17	1.00	
	122.75	16	1.00	
	121.75	15	1.00	
	120.875	14	0.75	1.25 m
	120.25	13	0.50	
Aquifer	119.75	12	0.50	12 m
	119.25	11	0.50	
	118.625	10	0.75	
	117.75	9	1.00	
	116.625	8	1.25	
	115.25	7	1.50	
	113.75	6	1.50	
	112	5	2.00	
	109.5	4	3.00	
Inactive	106	3	4.00	
	102	2	4.00	
	97.5	1	5.00	

Node used in Flow-Field abstraction

Figure 6-55. Comparison Between Three-Dimensional Subsurface Transport Over Multiple Phases (STOMP©)-Based Model Prediction and GoldSim©-Based One-Dimensional Abstraction Model Prediction in the Saturated Zone at 100 m Distance from the Waste Management Area C Fenceline.

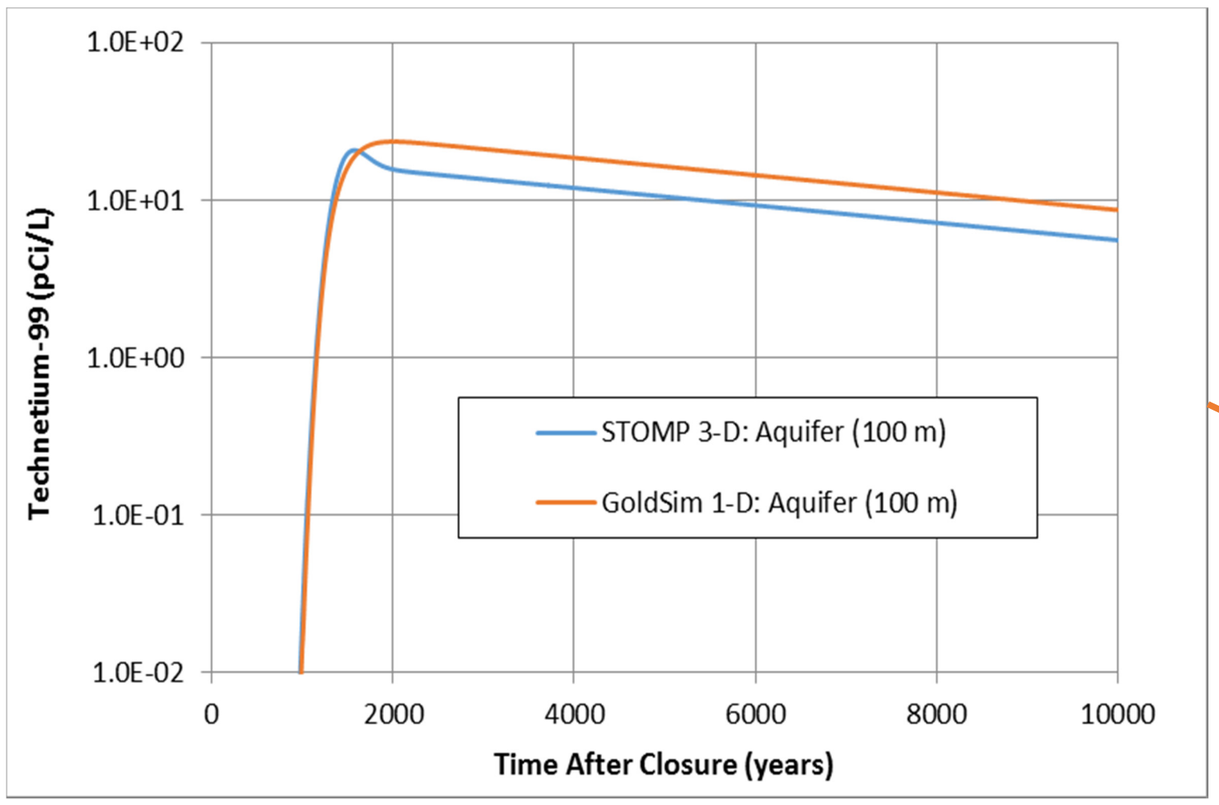

1-D = one-dimensional 3-D = three-dimensional

GoldSim© simulation software is copyrighted by GoldSim Technology Group LLC of Issaquah, Washington (see http://www.goldsim.com).
Subsurface Transport Over Multiple Phases (STOMP)© is copyrighted by Battelle Memorial Institute, 1996.

Releases to the atmospheric pathway and groundwater pathway begin at the start of the simulation. The partitioning of inventory into the aqueous and gaseous phase occurs within the source-term model (in the residual waste layer). The mass partitioned into the aqueous phase is then available for transport to the underlying vadose zone, while the partitioned fraction in the gas phase is available for upward transport to the atmosphere. Although diffusive path length for the gas phase can vary based on lateral movement, in order to maximize the flux, only the shortest vertical upward path length is considered. In addition, to maximize the upward transport through the gas phase, the downward flow of water above the residual waste location is not modeled. Any physical effect of surface barrier on gaseous flux is also ignored.

Of the radionuclides contained in residual inventory at closure (Section 3), four could potentially originate as gas:

- Carbon-14 as CO_2 gas
- Hydrogen-3 (tritium) as H_2 gas
- Iodine-129 as I_2 gas
- Radon-222 as radon gas.

These releases are driven by the partitioning of the radionuclides among the solid fraction of the porous medium (sorbed fraction), aqueous dissolved fraction (grout/water partitioning), and the gaseous fraction (air/water partitioning) by considering the following equilibrium coefficients:

- K_d representing grout-to-water partitioning

- Henry's law constant (K_h) for representing air-to-water partitioning (see Table 6-17 for the constant used for the constituents above).

Table 6-17. Henry's Law Constants.

Radionuclide	Gas Form	Aqueous-to-Gas Henry's Constant	Reference	Calculated Gas-to-Aqueous Dimensionless Henry's Constant at 20 °C
^{14}C	CO_2	4.5 (dimensionless)	Plummer et al. 2004	0.22
^{3}H	H_2	7.80E-4 (mol $atm^{-1}L^{-1}$)	Sander 1999	53.36
^{129}I	I_2	3.10E+0 (mol $atm^{-1}L^{-1}$)	Sander 1999	0.013
^{222}Rn	Rn	9.30E-3 (mol $atm^{-1}L^{-1}$)	Sander 1999	4.47

References:
"Transport of Carbon-14 in a Large Unsaturated Soil Column" (Plummer et al. 2004).
"Compilation of Henry's Law Constants for Inorganic and Organic Species of Potential Importance in Environmental Chemistry," Version 3 (Sander 1999).

The atmospheric transport pathway calculations are conducted in three steps, as follows.

1. First, a calculation is performed to compute the upward diffusive flux from each source term to the surface. A zero-concentration boundary condition at the surface is imposed

for purpose of calculating the gaseous flux. This is conceptually equivalent to having a large enough wind speed above WMA C such that the air parcel is renewed constantly, thereby maximizing the diffusive gradient.

For all sources except pipelines, while the infill grout is intact, upward gaseous diffusion of volatile contaminants is modeled from the residual waste layer towards the atmosphere. Upward diffusive gas phase transport through the tanks (or 244-CR vault) is modeled to occur along a 10-m (32.8-ft)-long pathway towards the land surface (Figure 6-18). This pathway is split into a lower 5-m (16.4-ft) thickness composed of infill grout material, followed by another 5 m thickness of soil overburden. For the pipeline source area, the diffusive length chosen is the pipeline diameter (0.076 m [3 in.]) and the 5-m (16.4-ft) thickness of the soil overburden.

A surface barrier that will be emplaced at closure over the tank farm will provide additional depth to the waste and therefore greater diffusive length. For the purpose of performing the air pathway calculations, this additional thickness is ignored.

For all grouted facilities, the air content within the infill grout is assumed to be 6% based on characterization information for possible Hanford grout (WSRC-TR-2005-00195). The porosity and saturation of the infill grout for the purpose of diffusive release calculations are fixed over time. Studies have indicated that chemical transformation of initial grout minerals will likely cause porosity reduction over time due to increased molar volume of the newly formed mineral phases. Fixing porosity maximizes diffusion.

2. Second, for each source area, the radionuclide transport in air along the downwind direction is performed using Gaussian plume dispersion methodology, where advection and dispersion occur via wind movement to the receptor placed 100 m (328 ft) downwind at the PoCal as conceptualized in Figure 6-56. As a continuous stream of gas (pollutants) is released into the steady wind in open atmosphere, the gas plume will travel with the mean wind speed. The plume will also spread out or disperse in the horizontal and vertical directions along the centerline. A schematic is presented in Figure 6-57 for a single source based on effective stack height (includes plume rise).

3. In order to evaluate the effect of commingling of gas plumes from different sources that could lead to increased concentration at the receptor location located 100 m (328 ft) downwind, a separate calculation is performed, where the upward diffusive flux emanating from various sources (described in Step 1) are combined into a point source, with the location near the approximate center point of the WMA C area. This is conceptually equivalent to a point source (i.e., stack source), but with the release rate (emission rate) equal to all the sources within the WMA C area. This point location is chosen to be the center of the pipeline area, which is 75 m (246 ft) from the WMA C fenceline. The total distance to the receptor is therefore 175 m (574 ft).

   The predominant wind direction in the 200 East Area is towards southeast as discussed in Section 3.1.2.4 (also see Figures 3-6 and 3-7), and therefore in the general direction of groundwater flow. The average annual wind speed of 3.4 m/s (11.2 ft/s) (average from

1944 to 2004) is applied to the pathway for transport. The air mixing height is assumed to be 2 m (6.6 ft). The calculated air concentrations at the receptor location are used for evaluating air-pathway dose.

Figure 6-56. Atmospheric Transport Pathway from a Source to the Receptor Located at the Point of Calculation Along the Centerline of the Gas Plume.

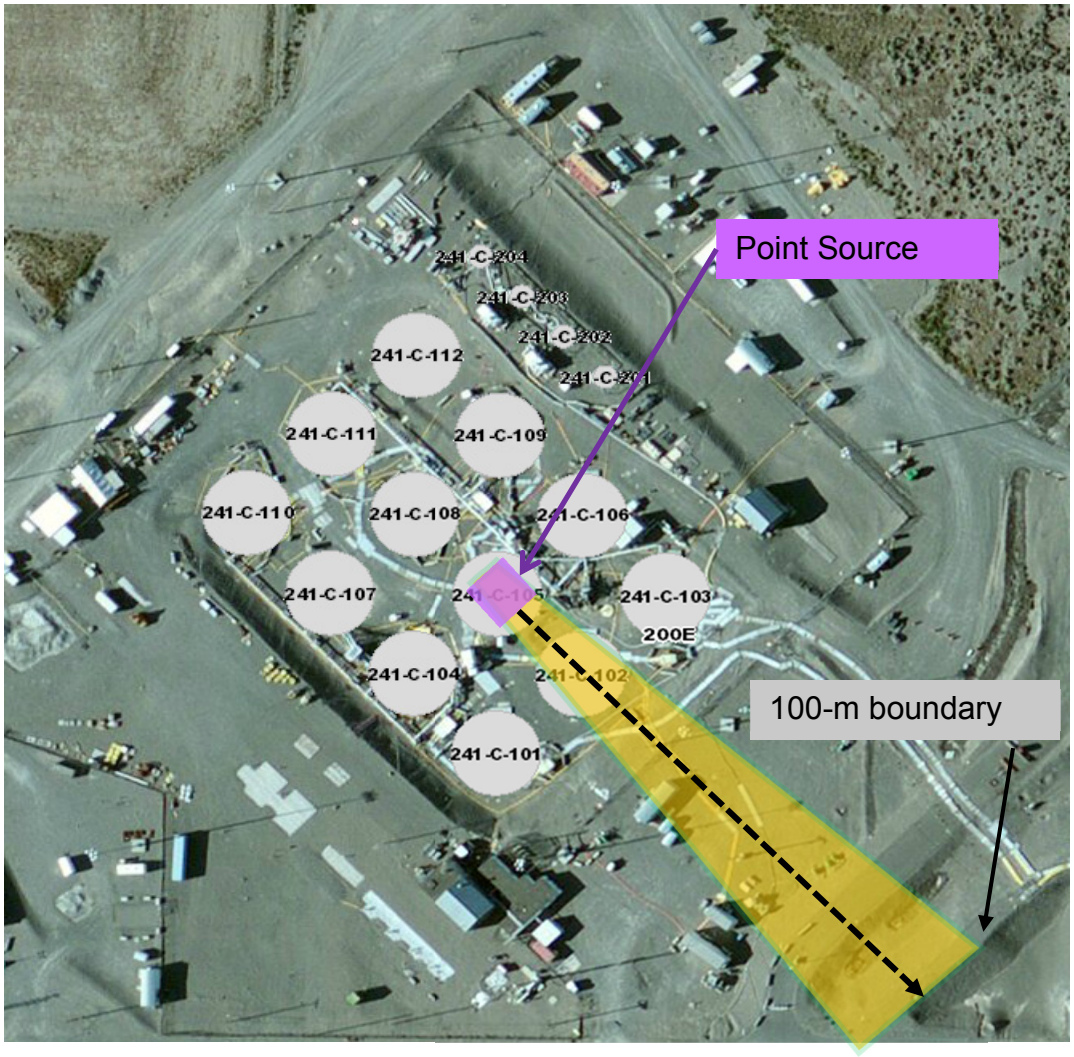

6.3.2.5.1 Mathematical Modeling of First Step. To calculate the diffusive flux emanating at the surface from a given source (buried tank or ancillary equipment), a 1-D model is developed using a finite-difference network of batch-reactor cells. The following transport equation (as per Fick's second law) is numerically solved using GoldSim© to compute the mass flux and concentration:

$$R_d \frac{\partial(\theta_a C)}{\partial t} = D_{ef} \frac{\partial^2 C}{\partial x^2} \tag{6-16}$$

Where:

$C(x,t)$	=	the air concentration (kg/m^3) in the pore network of a given gas at the distance x (m) from the residual waste layer and time t (s) from assumed closure at WMA C
D_{ef} (m^2/s)	=	the effective diffusion coefficient of a given gas through the tortuous air pathway of the porous medium
R_d	=	the retardation coefficient of a given gas due to partitioning among different phases (air, water and solids) of the porous medium
θ_a (-)	=	the air content (or air-filled porosity) of the porous medium.

Figure 6-57. A Schematic of Gaseous Plume Movement Based on Gaussian Distribution in the Horizontal and Vertical Direction.

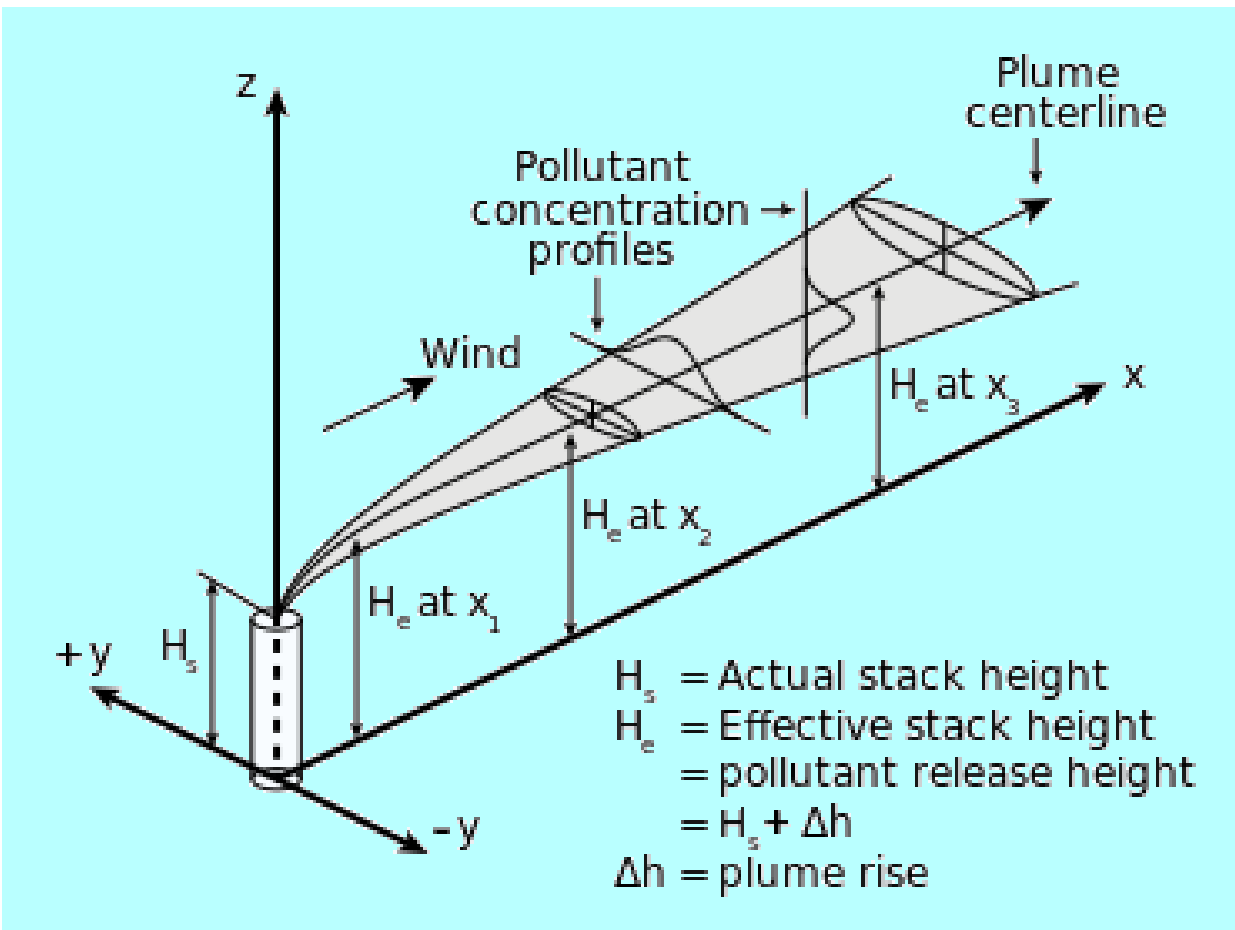

The diffusion coefficient for various gases of concern (CO_2, H_2, I_2, and radon) through the tortuous air pathway of the porous medium is calculated as follows:

$$D_{ef} = D_0 \tau \tag{6-17}$$

Where:

D_{ef} (m²/s) = the effective diffusion coefficient through the tortuous air pathway of the porous medium for a given gas

D_0 (m²/s) = the binary diffusion coefficient of the gas of concern in the air

τ = the tortuosity of the porous medium for air pathway.

An effective zero concentration boundary condition is imposed above WMA C to maximize the diffusive flux of gases. The diffusive area varies by the source geometry.

6.3.2.5.2 Diffusion Coefficients and Tortuosity. The binary diffusion coefficients of the different gases of concern in air have been calculated using the EPA methodology (United States Environmental Protection Agency, Queried 01/2012, [EPA On-line Tools for Site Assessment Calculation], https://www3.epa.gov/ceampubl/learn2model/part-two/onsite/estdiffusion.html) considering an atmospheric pressure of 1 atm and a temperature of 20 °C (68 °F). The calculated diffusion coefficients are reported in Table 6-18, together with the gas boiling point estimates used in the calculations. For radon, another reference has been considered (Radon and Its Decay Products in Indoor Air [Nazaroff and Nero 1988]) as EPA (2012) did not consider diffusion coefficient calculation for this gas.

Table 6-18. Diffusion Coefficients in Air at 20 °C and 1 Atm.

Radionuclide	Gas Form	Diffusion Coefficient in Air (cm^2s^{-1})	Reference	Boiling Point (°C) Used in EPA Calculations (Haynes and Lide 2011)
^{14}C	CO_2	0.160	EPA 2012 (average method)	-78.55
^{3}H	H_2	0.819	EPA 2012 (average method)	-252.76
^{129}I	I_2	0.0897	EPA 2012 (FSG/LaBas method)	184.45
^{222}Rn	Rn	0.11	Nazaroff and Nero (1988) cited in ANL/EAD-4	(-)

EPA = U.S. Environmental Protection Agency

References:
ANL/EAD-4, "User's Manual for RESRAD Version 6."
CRC Handbook of Chemistry and Physics, 92nd Edition (Haynes and Lide 2011).
Radon and Its Decay Products in Indoor Air (Nazaroff and Nero 1988).
United States Environmental Protection Agency, Queried 01/2012, [EPA On-line Tools for Site Assessment Calculation], https://www3.epa.gov/ceampubl/learn2model/part-two/onsite/estdiffusion.html.

"Simulating the Gas Diffusion Coefficient in Macropore Network Images: Influence of Soil Pore Morphology" (Liu et al. 2006) compiled data sets and presented the experimentally determined gas tortuosity (ratio of the effective diffusion coefficient in soil [D_{ef}] to that in free air [D_0]) as a function of the air-filled porosity (air content) for various soil types. They also provided the best fit lines and bounding estimates based on models presented by "Transport in porous media" (Millington and Quirk 1960) and Millington and Quirk (1961). The results from Liu et al. (2006) are reproduced in Figure 6-58.

Figure 6-58. Comparison of Measured Tortuosity (i.e., Ratio of Diffusion Coefficient in Soil [D_{ef}] to that in Free Air [D_0]) with Fitted Tortuosity Models.

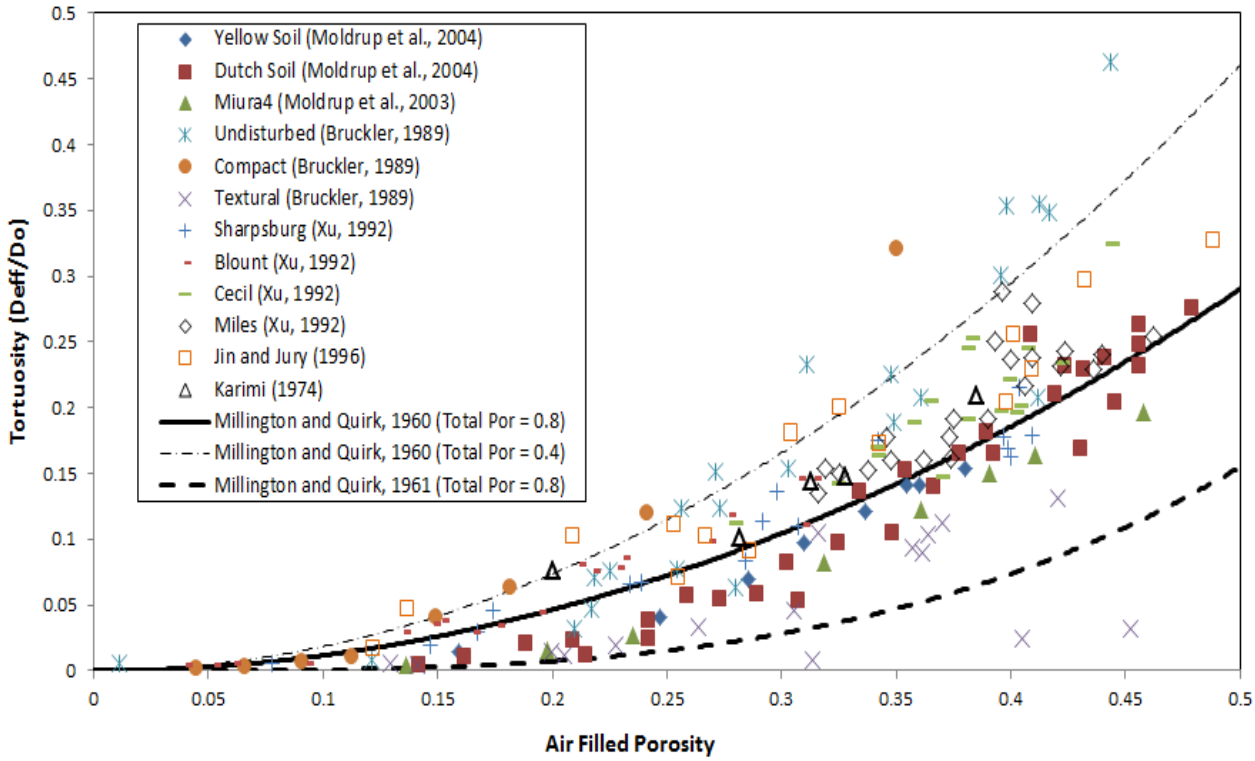

Source: "Simulating the Gas Diffusion Coefficient in Macropore Network Images: Influence of Soil Pore Morphology" (Liu et al. 2006).

References:
"Characterizing the Dependence of Gas Diffusion Coefficient on Soil Properties" (Jin and Jury 1996).
"Compaction Effect on the Gas Diffusion Coefficient in Soils" (Xu et al. 1992).
"Gas Diffusivity in Undisturbed Volcanic Ash Soils: Test of Soil-Water-Characteristic-Based Prediction Models" (Moldrup et al. 2003).
"Laboratory Estimation of Gas Diffusion Coefficient and Effective Porosity in Soils" (Bruckler et al. 1989).
"Permeability of Porous Solids" (Millington and Quirk 1961).
"Three-Porosity Model for Predicting the Gas Diffusion Coefficient in Undisturbed Soil" (Moldrup et al. 2004).
"Transport in porous media" (Millington and Quirk 1960).
"Vapor-phase Diffusion of Benzene in Soil" (Karimi et al. 1987).

Using the Millington and Quirk (1960) gas tortuosity equation below (Equation 6-18), Liu et al. (2006) found the best fit to the experimental data set by varying the value of the total porosity in the denominator and finally selecting a value of 0.8:

$$\tau = \frac{\theta_a^2}{\Phi^{2/3}} = \frac{(\phi - \theta_w)^2}{\Phi^{2/3}} \qquad (6\text{-}18)$$

Where:

τ = the tortuosity
θ_a = the air content (or air-filled porosity) of the porous medium
θ_w = the water content (or water-filled porosity) of the porous medium

ϕ = the total porosity (measured)
Φ = fitted total porosity; set equal to 0.8 for best fit (Liu et al. 2006).

The tortuosity in the infill grout material is calculated from first equality of Equation 6-18 using fixed value of θ_a (6%), while the second equality is used for calculating the tortuosity for the backfill material (soil overburden) where the θ_w (and hence tortuosity) varies as a function of time. Note that Liu et al. (2006) made an error in referencing the Millington and Quirk paper. They reversed a referenced paper's date ("1961" instead of correct date 1960) in the text and in the figure; the error is now corrected.

The solid surface within the tank and ancillary equipment (except for pipeline) is considered to be the infill grout. The grout-to-water partition coefficient (K_d) values applied are the same as those considered in Section 6.3.1.5 (and Table 6-5). These values are reported for conciseness in Table 6-19 for the relevant radionuclides. The K_d value for ^{222}Rn is set to zero because it is a noble gas, and unreactive with its surroundings.

Table 6-19. Best Estimate K_d (mL/g) for Grout Material.

Radionuclide	Best Estimated K_d for Grout (mL/g)
^{14}C	2.00E+02
^{3}H	1.00E-01
^{129}I	3.00E+00
^{222}Rn	0

Sorption on the backfill could be considered but is ignored since it is typically much smaller than on the grout and would lower the concentrations further.

6.3.2.5.3 Mathematical Modeling of Second Step. Once the gaseous diffusive flux from the source area is calculated, a plume dispersion model is applied using GoldSim© to evaluate the concentrations at the receptor (PoCal) using the double Gaussian plume equation of "The Estimation of the Dispersion of Windborne Material" (Pasquill 1961) as discussed in the CAP88-PC Version 4.0 User Guide (EPA 2014). This equation (which models the dispersion of a non-reactive gaseous pollutant from an emission point) is given below in a form that predicts the steady-state concentration as a point (*x, y, z*) located downwind from the source as shown in Figure 6-58:

$$C = \frac{Q}{2\,\pi\,u\,\sigma_y\sigma_z}\exp\left(-\frac{1}{2}\frac{y^2}{\sigma_y{}^2}\right)\left\{\exp\left(-\frac{1}{2}\frac{(z-H)^2}{\sigma_z{}^2}\right)+\exp\left(-\frac{1}{2}\frac{(z+H)^2}{\sigma_z{}^2}\right)\right\} \qquad (6\text{-}19)$$

Where:

C = steady-state concentration at x meters downwind, y meters crosswind, and z meters above ground (Ci/m^3)
Q = release rate (emission rate) from source (Ci/sec)
u = average wind speed at stack height (m/sec)

σ_y, σ_z = horizontal and vertical dispersion coefficient (spread parameters) (m)
z = vertical distance from ground level (m)
H = effective stack height (m) that includes physical stack height and plume rise.

In this model, the highest concentration occurs along the centerline of the plume. For the purpose of estimating the concentration in air at exposure location, the receptor is assumed to be located at the centerline (y = 0 m [0 ft]) of the plume. The effective stack height (H), which includes the plume rise, and the vertical distance from ground level (z) are each taken to be 2 m (assumed approximate height of the adult person). The above equation simplifies to:

$$C = \frac{Q}{2\,\pi\,u\,\sigma_y\sigma_z}\left\{1 + \exp\left(-\frac{1}{2}\frac{(z+H)^2}{{\sigma_z}^2}\right)\right\} \quad (6\text{-}20)$$

Where z + H = 4 m, and u (the average wind speed) is chosen to be 3.4 m/s.

6.3.2.5.4 Horizontal and Vertical Plume Dispersivity in Air. Horizontal and vertical dispersivities of the plume in air are required to calculate air concentrations downwind from WMA C, to simulate the effect of dispersion due to wind flow over a horizontal 1-D pathway.

EPA (2014) provides equations to calculate horizontal dispersion coefficient (σ_y) and vertical dispersion coefficient (σ_z) for dispersion calculations using the Gaussian plume model. In these equations, the dispersion coefficient is a function of the downwind distance, x, from a point source for different atmospheric turbulence classes under open-country conditions. These atmospheric turbulence classes are categorized according to the Pasquill classification (Pasquill 1961). This classification defines six stability classes named A, B, C, D, E, and F, with class A being the most turbulent and class F the most stable or least turbulent class. According to the wind speeds observed on the Hanford Site (Table 6-20), which usually range from 2.7 m/s (8.9 ft/s) during winter to 4 m/s (13.1 ft/s) during summer (monthly average), the most conservative (lowest dispersivity) Pasquill class for a moderate solar radiation above WMA C is Class C (i.e., "slightly unstable class"). The following equations are used to calculate the horizontal and vertical dispersion coefficient for Class C (EPA 2014):

$$\sigma_y = 0.11\,x\,(1 + 0.0001x)^{-½} \quad (6\text{-}21)$$

$$\sigma_z = 0.08\,x\,(1 + 0.0002x)^{-½} \quad (6\text{-}22)$$

where σ_y and σ_z are the horizontal and vertical dispersion coefficients (m) for Pasquill class C, and x is the downwind distance (m) from the point source.

The dispersion coefficient estimates for air transport to the fenceline vary by the distance of the source (tank and ancillary equipment) from the fenceline using the above equation. The air pathway calculations are performed for each source term (tank and ancillary equipment) separately, where the distance to the PoCal at 100 m (328 ft) boundary is calculated based on the location of the source.

Table 6-20. Wind Speed Observed Above the Hanford Site and Corresponding Pasquill Class for a Moderate Solar Radiation.

Season	Wind Speed*	Pasquill Class for a Moderate Solar Radiation
Winter	2.7 to 3.1 m/s	B
Summer	3.6 to 4 m/s	B-C
Summertime drainage winds	13 m/s	D

*See Section 3.1.2.4 for additional details.

Source: "The Estimation of the Dispersion of Windborne Material" (Pasquill 1961).

6.3.2.5.5 Radon Analysis. The modeling approach for calculating radon flux at the surface is slightly different than the approach for the other contaminants, because there is a different mechanism for emanation of radon from the waste into air. Radon-222 is produced from the alpha decay of ^{226}Ra in the waste. During the decay, by alpha recoil the produced ^{222}Rn atom (initially in the solid phase) has the potential to end up in either solid, liquid, or gas phase, with the amount in gas available for further diffusion to the ground surface. The fraction of ^{222}Rn in the gas phase over the total ^{222}Rn produced at any time is called the emanation coefficient, which is typically determined empirically for a given material. The emanation coefficient is highly variable from one material to another, and depends on a variety of specific features of the contaminated material, including the distribution of radium within the material particles, grain size and pore size distributions, and moisture content of the contaminated material ("A comprehensive review of radon emanation measurements for mineral, rock, soil, mill tailing and fly ash" [Sakoda et al. 2011]). Emanation coefficients have not been measured for residual wastes. For the purposes of this assessment, the residual wastes are assumed to have emanation properties comparable to soils. NCRP Report No. 103, "Control of Radon in Houses" has recommended a nominal emanation coefficient of about 0.2 for soils, and this value is adopted for this PA. The target emanation coefficient is implemented in the GoldSim© model as the fractional mass of radon produced in the residual waste that enters the gas phase.

A 1-D transport model is used to calculate diffusive flux of radon along with other volatile radionuclides. However, the radon flux analysis is conducted assuming there is no downward migration of the parent radionuclide ^{226}Ra. This assumption was made to keep the ^{226}Ra fixed in the residual waste, with a constant diffusion path for the duration of the analysis. The ^{222}Rn release rate from the ground surface is estimated using the diffusion equation (using Equation 6-16).

Radium-226 (half-life of 1,600 years) produces ^{222}Rn (half-life of 3.82 days) by radioactive decay. Radium-226 is produced by the radioactive decay of: ^{238}U (half-life of 4.47×10^9 years), ^{234}U (half-life of 2.45×10^5 years), ^{238}Pu (half-life of 87.7 years), and ^{230}Th (half-life of 7.54×10^4 years). Once the initial inventory of ^{226}Ra is depleted, it will be generated slowly, primarily from decay of ^{238}U and ^{234}U.

6.3.2.6 Biotic Pathway. In this section, an evaluation is presented of the potential for burrowing animals or deep-rooting plants to penetrate deeply enough to contact the residual waste left in tanks and ancillary equipment in its final closed configuration.

At closure, a modified RCRA Subtitle C barrier (Section 3.2.1.2.2) will be placed over the waste. The upper layer of this cover system is intended to mimic natural surface conditions to the extent possible. That is, natural vegetation will be planted on a soil layer intended to support growth of a stable ecology system that is the same as the surrounding conditions. The ambient ecological system is not totally pristine because colonization and agricultural practices have introduced additional nonnative species that will likely remain at the Hanford Site. Ecological conditions at the Hanford Site have been studied extensively since the start of Hanford Site operations, and numerous documents that describe and quantify local conditions have been completed. The most recent compilation (DOE/RL-2007-50, Central Plateau Ecological Risk Assessment Data Package Report) describes recent information and includes copies of significant previous summaries (e.g., DOE/RL-2001-54). The descriptions provided below are based on these and other documents.

The Hanford Site is a shrub-steppe ecosystem that is dominated by a shrub overstory with a grass understory. Because the climate is semi-arid, the dominant large shrub is big sagebrush (*Artemisia tridentate*) and the main grasses are Sandberg's bluegrass (*Poa Sandbergii*) and bluebunch wheatgrass (*Pseudoregneria spicata*). A ubiquitous nonnative species at the Hanford Site is cheatgrass, which often makes up a large fraction of the grasses. Less abundant plant species on the Central Plateau include threetip sagebrush, bitterbrush, gray rabbitbrush, spiny Hopsage, Indian ricegrass, and prairie June grass. Altogether, over 100 species of plants have been observed in the 200 Area on the Central Plateau. A survey of the 200 Area made prior to its construction showed the presence of big sagebrush and an understory of which approximately 90% was a mix of cheatgrass and Sandberg's bluegrass (PNNL-14233). The remaining 10% of the understory was a mix of cheatgrass and needle-and-thread grass.

Range fires can be expected to occur every few years. Observation has shown that regrowth vegetation is initially dominated by nonnative species, particularly cheatgrass and, to a lesser extent, Russian thistle. Native grasses and shrubs take longer to reestablish, particularly the big sagebrush, which must regenerate from seed. However, repopulation with sagebrush and other smaller shrubs such as gray rabbitbrush, which reestablishes itself more easily than big sagebrush, eventually happens because these species are abundant in undisturbed areas that have been burned many times.

A wide variety of mammals (about 40 species), birds (about 100 species), reptiles (about 10 species), and insects (hundreds) have been observed on the Central Plateau. Large mammals include elk (*Cervus elaphus*) and mule deer (*Odocoileus hemionus*). Smaller species include badgers (*Taxidea taxus*), coyotes (*Canis latrans*), blacktail jackrabbits (*Lepus californicus*), Townsend ground squirrels (*Spermophilus townsendii*), pocket mice (*Perognathus parvus*), and deer mice (*Peromyscus maniculatus*). Of these, the Great Basin pocket mice are the most abundant. The mammal most likely to burrow in the soil is the badger, which can dig several feet down in search of food (e.g., mice and squirrels).

Birds commonly found on the Central Plateau include passerine varieties, raptors, game birds, and nesting birds. Common passerine birds are starlings (*Sturnus vulgaris*), meadowlarks (*Sturnella neglecta*), black-billed magpies (*Pica pica*), and ravens (*Corvus corax*). Common raptors are the American kestrels (*Falco sparvarius*) and redtailed hawks (*Buteo jamaicensis*). Game birds include the mourning dove (*Zenaida macroura*), California quail (*Callipepla californica*), and Chukar partridge (*Alectoris chukar*). Nesting birds include burrowing owls (*Athene cunicularia*), sage sparrows (*Amphispiza belli*), loggerhead shrikes (*Lanius ludovicianus*), and long-billed curlews (*Numenius americanus*).

Abundant reptiles include gopher snakes (*Pituophis melanoleucus*) and sideblotched lizards (*Uta stansburiana*). Other less abundant species include sagebrush lizards (*Sceloporus graciosus*), horned toads (*Phryosoma douglassii*), western spadefoot toads (*Scaphiopus intermontana*), yellow-bellied racers (*Coluber constrictor*), Pacific rattlesnakes (*Crotalus viridis*), and striped whipsnakes (*Masticophis taeniatus*). Amphibians are not expected at the WMA C location. Common groups of insects include several species of darkling beetles, grasshoppers, butterflies, bees, and ants. Of these, the harvester ants, darkling beetles, solitary bees, and pocket gophers burrow below ground surface (WMP-20570, "Central Plateau Terrestrial Ecological Risk Assessment Data Quality Objectives Summary Report - Phase I").

The most likely means of plant and animal contact with buried waste is root penetration and burrowing habits. A summary of site-specific and generic data quantifying penetration depths for biota at the Hanford Site and similar semi-arid conditions is provided in WMP-20570. Most studies of biota at the Hanford Site catalog biota populations, record surface expression of biota, and measure contaminant uptake. However, a few studies have been completed to quantify penetration depths [PNL-5247, "Rooting Depth and Distributions of Deep-Rooted Plants in the 200 Area Control Zone of the Hanford Site"; RHO-SA-211, "Invasion of radioactive waste burial sites by the Great Basin Pocket Mouse (*Perognathus parvus*)"; DOE/RL-2001-54]. Measured maximum penetration depths at the Hanford Site are summarized in Table 6-21.

Two primary observations were made. First, the maximum likely depth is about 3 m (10 ft) bgs for both plant and animal behavior. Second, the frequency of roots and burrow depths are heavily skewed towards the surface (<1.5 m [5 ft] bgs), with only a few percent of penetration events reaching maximum depth. Soil sampling across Gable Mountain Pond and B Pond, two dried high-volume liquid discharge sites (DOE/RL-2001-54), yielded a large assortment of invertebrates that constructed burrows within a foot of the surface (several feet and 0.6 to 0.9 cm [2 to 3 ft], respectively). Deeper burrowing depths were associated with the harvester ants and solitary bees. Among mammals, badger burrows have been observed on a few occasions. One burrow in particular was found 1.2 m (4 ft) below a soil barrier (WHC-SA-1252-S, "Mammal Occurrence and Exclusion at the Hanford Site"). Offsite, badger burrows as deep as 3 m (10 ft) have been reported (The Mammals of North America [Hall 1981]).

Given the limited number of data collected at the Hanford Site, it is useful to compare these data with data collected at other semi-arid sites in the western United States. A collection of other site data is provided in INEEL/EXT-01-00273, "Biological Data to Support Operable Unit 7-13/14 Modeling of Plant and Animal Intrusion at Buried Waste Sites," and WMP-20570 (Appendix F). Badgers, squirrels, and mice are found at several sites with burrow penetration

depths similar to the Hanford Site (Figure 6-59). Plant data from other northern desert sites in Idaho and Wyoming include a common set of species (e.g., sagebrush and various grasses) with similar penetration depth profiles (Figure 6-59).

Table 6-21. Maximum Penetration Depths for Biota at the Hanford Site.

Species	Maximum Depth		Reference
	(cm)	(ft)	
Plants			
Antelope bitterbrush	300	9.8	PNL-5247, "Rooting Depth and Distributions of Deep-Rooted Plants in the 200 Area Control Zone of the Hanford Site"
Big sagebrush	200	6.6	PNL-5247
Spiny hopsage	195	6.5	PNL-5247
Russian thistle	172	5.6	PNL-5247
Mammals			
Great Basin pocket mouse	200	6.6	RHO-SA-211, "Invasion of radioactive waste burial sites by the Great Basin Pocket Mouse (*Perognathus parvus*)"
Soil Biota			
Harvester ants	270	8.8	PNL-2774, "Characterization of the Hanford 300 Area Burial Grounds Task IV - Biological Transport"

Source: WMP-20570, "Central Plateau Terrestrial Ecological Risk Assessment Data Quality Objectives Summary Report - Phase I," Table 2-1.

A modified RCRA Subtitle C barrier will be placed above WMA C that will be about 4.5 m (14.8 ft) in thickness (Figure 3-51). This cover will be placed above the interim compacted soil cover of ~0.6 m (2 ft). Thus, the minimum depth of intrusion needed to access the waste will be more than 5 m, which is below the observations of the biologically active zone, described above. The upper 0.9 m (3.0 ft) of the soil cover system is composed of an admixture of silt and gravels. This layer is intended to both reduce infiltration through the cover and enhance the resistance of the cover to burrowing animals and long-term wind erosion. In addition, an asphaltic concrete layer and asphaltic base course layer will be present at depth, which will further enhance resistance to burrowing animals and plants. Given the features of the surface barrier above WMA C, the likelihood of a biotic pathway to access the radionuclides from the waste is extremely small. As a result, the dose impact from this pathway is not considered in further analyses.

6.3.3 Exposure and Dose Analysis

The method for calculating doses from the radionuclide transport calculations discussed in previous sections is provided below. The dose calculation method for the all-pathway farmer scenario is discussed first, where contaminated groundwater is the pathway of contamination. This is followed by the air-pathway dose calculation methodology. Additional details are

presented in the supporting data package, RPP-ENV-58813, "Exposure Scenarios for Risk and Performance Assessments in Tank Farms at the Hanford Site, Washington."

Figure 6-59. Burrow and Root Density with Depth in Various Northwestern Semiarid Sites.

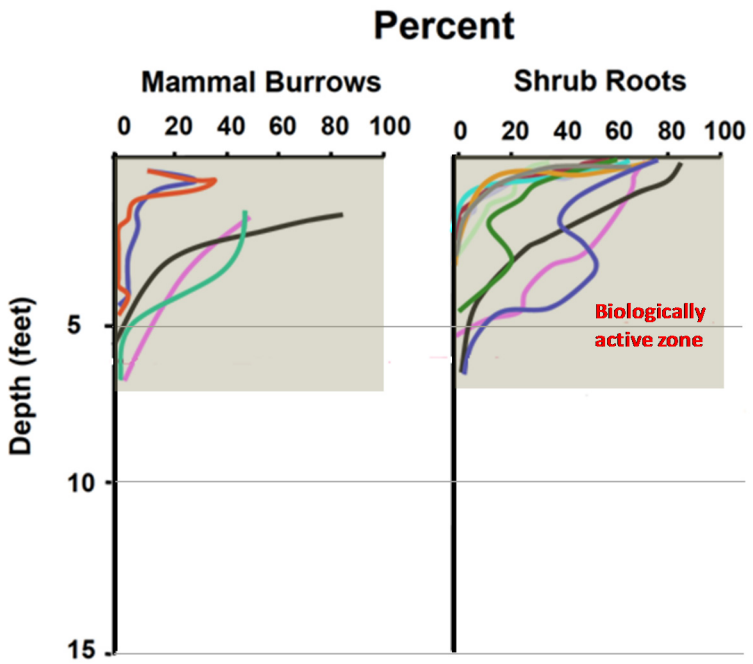

Adapted from Figure 2-3 of WMP-20570, "Central Plateau Terrestrial Ecological Risk Assessment Data Quality Objectives Summary Report – Phase I."

6.3.3.1 Groundwater Pathway Dose Analysis. For the all-pathways scenario, the individual who receives dose is a Representative Person who resides near the WMA C tank farm and draws contaminated water from a well downgradient of WMA C. The all-pathways Representative Person is assumed to use the water to drink, irrigate crops, and water livestock. The exposed Representative Person is assumed to receive dose by the exposure pathways shown in Figure 6-1.

Current DOE and ICRP guidance recommends the use of a Representative Person for describing the hypothetical member of the public for use in projecting future doses. The Representative Person is described as a person who is representative of the more highly exposed individuals in the population (see DOE O 458.1, ICRP 2006, and "ICRP Publication 103: The 2007 Recommendations of the International Commission on Radiological Protection" [ICRP 2007]). The concept of the Representative Person replaces the concept of an average member of the critical group used in older radiation protection guidance.

Internal doses to the Representative Person are calculated using the dose factors provided in DOE-STD-1196-2011, and external doses are calculated using dose factors in EPA-402-R-93-081. These dose factors represent effective dose coefficients calculated to a Reference Person in the manner of "ICRP Publication 72: Age-dependent Doses to the Members of the Public from Intake of Radionuclides - Part 5 Compilation of Ingestion and Inhalation Coefficients" (ICRP 1996). The Reference Person is a hypothetical aggregation of human (male

and female) physical and physiological characteristics arrived at by international consensus for the purpose of standardizing radiation dose calculations (DOE-STD-1196-2011; "Environmental Dosimetry" [Jannik 2014]).

The source of contamination for the all-pathways scenario is the portion of the inventory transported by groundwater to the well location, and drawn through the well. As noted in Section 1 (Table 1-2), dilution processes associated with drawing water through the well are not taken into account in the PA, and the concentrations used for the all-pathways scenario calculations are the maximum concentrations in groundwater at the PoCal. The contaminated water is the only source of exposure. The exposed individual is assumed to use the water to drink, shower, irrigate crops, and water livestock. Exposure occurs through the following pathways:

- Ingestion of water
- Ingestion of fruits and vegetables grown on the farm
- Ingestion of beef raised on the farm
- Ingestion of milk from cows raised on fodder grown on the farm
- Ingestion of eggs from poultry fed with fodder grown on the farm
- Ingestion of poultry fed with fodder grown on the farm
- Ingestion of contaminated soil
- Inhalation of contaminated soil in the air
- Inhalation of water vapor
- External exposure to radiation.

Equations and calculation methodologies for each exposure pathway are summarized below. They are described in detail in RPP-ENV-58813 and implemented in the system model using GoldSim©. The scenario-dependent exposure parameters for the all-pathways Representative Person scenario are summarized in Table 6-22. The element-specific factors (bioconcentration factors [transfer coefficients]) are provided in Table 6-23, the radionuclide-specific shielding factors are provided in Table 6-24, and the radionuclide-specific dose conversion factors are provided in Table 6-25 (see RPP-ENV-58813 for additional details).

Age- and gender-weighted intake rates are generally developed for a Representative Person in accordance with the recommendations described in DOE-STD-1196-2011. The 95th percentile intake rates were obtained from EPA/600/R-090/052F, "Exposure Factors Handbook: 2011 Edition, National Center for Environmental Assessment," based on available information. Even though mean intake rates were available, the 95th percentile values from the underlying distribution were chosen conservatively to maximize the likely exposure. Typically, the 95th percentile intake rates weighted by age and gender are calculated (Appendix P of RPP-ENV-58813). The exceptions to this approach were the indoor inhalation rate (taken directly from a reference source) and the soil ingestion rates (where simple age weighting is performed for children and adults).

Table 6-22. Scenario-Dependent Exposure Parameters for the All-Pathways Reference Person Scenario. (2 sheets)

Parameter	Notation	Value	Unit	Reference
Soil ingestion rate	IR_s	108.6	mg/day	EPA/600/P-95/052F
Exposure frequency	EF	350	days/yr	OSWER Directive 9285.6-03
Water ingestion rate	IR_w	2.66	L/day	EPA/600/P-95/052F; EPA, 06/18/2015
Crop ingestion rate (includes homegrown fruits and vegetables)	IR_c	272.33	kg/yr	EPA/600/P-95/052F; EPA, 06/18/2015
Beef ingestion rate	IR_b	101.9	kg/yr	EPA/600/P-95/052F; EPA, 06/18/2015
Water ingestion rate for beef	$IR_{w,b}$	53	L/day	EPA, 06/18/2015
Soil ingestion rate for beef	$IR_{s,b}$	0.39	kg/day	EPA, 06/18/2015
Fodder ingestion rate for beef	$IR_{fodder,b}$	11.77	kg/day	EPA, 06/18/2015
Milk ingestion rate	IR_m	311.3	L/yr	DOE-STD-1196-2011; EPA/600/P-95/052F; EPA, 06/18/2015
Water ingestion rate for dairy cattle	$IR_{w,d}$	92	L/day	EPA, 06/18/2015
Soil ingestion rate for dairy cattle	$IR_{s,d}$	0.41	kg/day	EPA, 06/18/2015
Fodder ingestion rate for dairy cattle	$IR_{fodder,d}$	16.9	kg/day	EPA, 06/18/2015
Egg ingestion rate	IR_e	40.5	kg/yr	DOE-STD-1196-2011; EPA/600/P-95/052F; EPA, 06/18/2015
Poultry ingestion rate	IR_p	99.4	kg/yr	DOE-STD-1196-2011; EPA/600/P-95/052F; EPA, 06/18/2015
Water ingestion rate for poultry	$IR_{w,p}$	1	L/day	EPA, 06/18/2015
Soil ingestion rate for poultry	$IR_{s,p}$	0.022	kg/day	EPA, 06/18/2015
Fodder ingestion rate for poultry	$IR_{fodder,p}$	0.2	kg/day	EPA, 06/18/2015
Inhalation rate – water vapor	INH_w	20	m^3/day	EPA/600/P-95/052F
Inhalation rate – indoors	INH_{in}	7,300	m^3/yr	NCRP Report No. 129
Mass loading factor	M	6.66E-05	g/m^3	NCRP Report No. 129
Fraction of time spent indoors	t_{in}	0.4	unitless	EPA, 06/18/2015
Inhalation rate – outdoors	INH_{out}	12,775	m^3/yr	NCRP Report No. 129
Fraction of time spent outdoors	t_{out}	0.486	unitless	EPA, 06/18/2015
Enrichment factor	E_f	0.7	unitless	NCRP Report No. 129
Transmission factor or shielding factor	ε	Isotope-specific 0.1 – 0.4	unitless	NCRP Report No. 129

Table 6-22. Scenario-Dependent Exposure Parameters for the All-Pathways Reference Person Scenario. (2 sheets)

Parameter	Notation	Value	Unit	Reference
Ratio of radionuclide concentrations in indoor versus outdoor air	I/O	0.3	unitless	NCRP Report No. 129
Andelman Volatilization Factor	K	0.5	L/m^3	EPA/540/R-92/003
Crop-soil bioconcentration factor through uptake	B_v	Element-specific	(pCi/kg fresh weight of crop)/ (pCi/kg dry weight of soil)	See Table 6-23 (for Vegetable, Fruit, and Grain)
Crop-soil bioconcentration factor from all resuspension/soil adhesion processes	B'_v	0.004	(pCi/kg fresh weight of crop)/ (pCi/kg dry weight of soil)	NCRP Report No. 129
Pasture-soil bioconcentration factor through uptake	B_p	Element-specific	(pCi/kg dry weight of fodder)/ (pCi/kg dry weight of soil)	See Table 6-23 (for Fodder and Grass)
Pasture-soil bioconcentration factor for all resuspension/soil adhesion processes	B'_p	0.1	(pCi/kg dry weight of fodder)/ (pCi/kg dry weight of soil)	NCRP Report No. 129
Fraction of locally-produced crops (fruits and vegetables) that is consumed	F_v	0.25	unitless	EPA/600/P-95/002Fa
Fraction of locally-produced animal products (beef, dairy, poultry, eggs) that is consumed	F_a	1	unitless	EPA/600/P-95/002Fa
Soil-water partition coefficient	K_d	Radionuclide-specific	mL/g	See Table 6-11
Soil volumetric water content – Theta W	θ_w	Soil-specific	mL water/cm^3 soil	—
Soil bulk density – Rho S	ρ_s	Soil-specific	g/cm^3	—
Unit conversion factor 1	CF	0.001	variable units	—
Unit conversion factor 2	CF_1	1,000	g/kg	1,000 g = 1 kg

References:
DOE-STD-1196-2011, Derived Concentration Technical Standard.
EPA/540/R-92/003, Guidance for Data Useability in Risk Assessment (Part A) Final, Office of Research and Development.
EPA/600/P-95/002Fa, Exposure Factors Handbook Volume 1: General Factors.
NCRP Report No. 129, "Recommended Screening Limits for Contaminated Surface Soil and Review of Factors Relevant to Site-Specific Studies."
OSWER Directive 9285.6-03, Risk Assessment Guidance for Superfund, Volume I: Human Health Evaluation Manual, Supplemental Guidance "Standard Default Exposure Factors."
United States Environmental Protection Agency, Queried 06/18/2015, [Preliminary Remediation Goals for Radionuclides], http://epa-prgs.ornl.gov/radionuclides/.

Table 6-23. Bioconcentration Factors for the All-Pathways Reference Person Scenario. (2 sheets)

Element	Bioconcentration Factors					
	Vegetables, Fruit, and Grain (B_v)	Fodder and Grass (B_p)	Milk (BCF_{milk})	Beef (BCF_{beef})	Poultry ($BCF_{poultry}$)	Egg (BCF_{egg})
	(pCi/kg fresh wgt of crop)/ (pCi/kg dry wgt of soil)	(pCi/kg dry wgt of fodder)/ (pCi/kg dry wgt of soil)	(day/L)	(day/kg)	(day/kg)	(day/kg)
Ac	1.00E-03[a]	4.00E-03[a]	2.00E-06[a]	2.00E-05[a]	4.00E-03[b]	2.00E-03[b]
Am	1.00E-03[a]	4.00E-03[a]	2.00E-06[a]	5.00E-05[a]	6.00E-03[b]	9.00E-03[b]
C	7.00E-01[b]	7.00E-01[b]	1.05E-02[c]	4.89E-02[c]	4.16E+00[c]	3.12E+00[c]
Cd	5.00E-01[a]	1.00E+00[a]	2.00E-03[a]	1.00E-03[a]	1.70E+00[d]	1.00E-01[b]
Cm	1.00E-03[a]	4.00E-03[a]	2.00E-06[a]	2.00E-05[a]	4.00E-03[b]	2.00E-03[b]
Co	8.00E-02[a]	2.00E+00[a]	2.00E-03[a]	3.00E-02[a]	9.70E-01[d]	3.30E-02[d]
Cs	4.00E-02[a]	2.00E-01[a]	1.00E-02[a]	5.00E-02[a]	2.70E+00[d]	4.00E-01[d]
Eu	2.00E-03[a]	5.00E-02[a]	6.00E-05[a]	2.00E-03[a]	4.00E-03[b]	7.00E-03[b]
H	2.86E+01[c]	2.86E+01[c]	3.36E+01[c]	3.36E+01[c]	3.36E+01[c]	3.36E+01[c]
I	2.00E-02[a]	1.00E-01[a]	1.00E-02[a]	4.00E-02[a]	8.70E-03[d]	2.40E+00[d]
Nb	1.00E-02[a]	1.00E-01[a]	2.00E-06[a]	1.00E-06[a]	3.00E-04[d]	1.00E-03[d]
Ni	5.00E-02[a]	1.00E+00[a]	2.00E-02[a]	5.00E-03[a]	1.00E-03[b]	1.00E-01[b]
Np	2.00E-02[a]	1.00E-01[a]	1.00E-05[a]	1.00E-03[a]	4.00E-03[b]	2.00E-03[b]
Pa	1.00E-02[a]	5.00E-02[a]	5.00E-06[a]	5.00E-06[a]	4.00E-03[b]	2.00E-03[b]
Pu	1.00E-03[a]	1.00E-03[a]	1.00E-06[a]	1.00E-04[a]	3.00E-03[b]	8.00E-03[b]
Ra	4.00E-02[a]	2.00E-01[a]	1.00E-03[a]	1.00E-03[a]	3.00E-02[b]	2.00E-05[b]
Rn	0.00E+00[e]	0.00E+00[e]	0.00E+00[e]	0.00E+00[e]	0.00E+00[e]	0.00E+00[e]
Se	1.00E-01[a]	5.00E-01[a]	1.00E-02[a]	1.00E-01[a]	9.70E+00[d]	1.60E+01[d]

Table 6-23. Bioconcentration Factors for the All-Pathways Reference Person Scenario. (2 sheets)

Element	Bioconcentration Factors					
	Vegetables, Fruit, and Grain (B_v)	Fodder and Grass (B_p)	Milk (BCF_{milk})	Beef (BCF_{beef})	Poultry ($BCF_{poultry}$)	Egg (BCF_{egg})
	(pCi/kg fresh wgt of crop)/ (pCi/kg dry wgt of soil)	(pCi/kg dry wgt of fodder)/ (pCi/kg dry wgt of soil)	(day/L)	(day/kg)	(day/kg)	(day/kg)
Sm	2.00E-03[a]	5.00E-02[a]	6.00E-05[a]	2.00E-03[a]	4.00E-03[b]	7.00E-03[b]
Sn	3.00E-01[a]	1.00E+00[a]	1.00E-03[a]	1.00E-02[a]	2.00E-01[b]	8.00E-01[b]
Sr	3.00E-01[a]	4.00E+00[a]	2.00E-03[a]	1.00E-02[a]	2.00E-02[d]	3.50E-01[d]
Tc	5.00E+00[a]	4.00E+01[a]	1.00E-03[a]	1.00E-04[a]	3.00E-02[b]	3.00E+00[b]
Th	1.00E-03[a]	1.00E-03[a]	5.00E-06[a]	1.00E-04[a]	4.00E-03[b]	2.00E-03[b]
U	2.00E-03[a]	1.00E-01[a]	4.00E-04[a]	8.00E-04[a]	1.20E+00[b]	9.90E-01[b]
Zr	1.00E-03[a]	5.00E-03[a]	6.00E-07[a]	1.00E-06[a]	6.00E-05[d]	2.00E-04[d]

[a]NCRP Report No. 129, "Recommended Screening Limits for Contaminated Surface Soil and Review of Factors Relevant to Site-Specific Studies," Appendix D.

[b]NUREG/CR-5512, Residential Radioactive Contamination From Decommissioning, Vol. 1, Technical Basis for Translating Contamination Levels to Annual Total Effective Dose Equivalent, Final Report.

[c]The units are dimensionless. Hydrogen values are calculated from Equations 6-26b and 6-28b using equilibrium model for tritium. For carbon, the value is based on derivation of equilibrium model for ^{14}C presented in Appendix O of RPP-ENV-58813, "Exposure Scenarios for Risk and Performance Assessments in Tank Farms at the Hanford Site, Washington."

[d]"Technical Reports Series No. 472, Handbook of Parameter Values for the Prediction of Radionuclide Transfer in Terrestrial and Freshwater Environments" (IAEA 2010), Tables 34 and 35.

[e]Not applicable (gas).

Table 6-24. Radionuclide-Specific Shielding Factors.

Radionuclide	Shielding Factor (ε) (unitless)	Radionuclide	Shielding Factor (ε) (unitless)
^{227}Ac	0.4	^{240}Pu	0.4
^{241}Am	0.2	^{241}Pu	0.4
^{243}Am	0.3	^{242}Pu	0.1
^{14}C	0.4	^{226}Ra	0.4
^{113m}Cd	0.3	^{228}Ra	0.4
^{243}Cm	0.4	^{222}Rn	0.4
^{244}Cm	0.1	^{79}Se	0.1
^{60}Co	0.4	^{151}Sm	0.1
^{137}Cs	0.3	^{126}Sn	0.3
^{152}Eu	0.4	^{90}Sr	0.3
^{154}Eu	0.4	^{99}Tc	0.2
^{155}Eu	0.3	^{229}Th	0.4
^{3}H	0.4	^{230}Th	0.3
^{129}I	0.1	^{232}Th	0.2
^{93m}Nb	0.1	^{232}U	0.3
^{59}Ni	0.4	^{233}U	0.4
^{63}Ni	0.4	^{234}U	0.2
^{237}Np	0.3	^{235}U	0.4
^{231}Pa	0.4	^{236}U	0.1
^{210}Pb	0.1	^{238}U	0.1
^{238}Pu	0.1	^{93}Zr	0.4
^{239}Pu	0.3	—	—

6.3.3.1.1 Equations to Calculate Soil Concentrations from Irrigation with Contaminated Water. When contaminated water is applied to soil, the contaminants are retained by the soil by two mechanisms: 1) sorption onto soil particles and 2) dissolved contaminants held in the water content in the soil. The following equation is used to calculate the concentration of contaminant sorbed on soil particles:

$$C_s = C_w \times K_d \times CF \tag{6-23}$$

Where:

C_s = radionuclide concentration in soil (pCi/g)
C_w = radionuclide concentration in irrigation water (pCi/L)
K_d = soil-water partition coefficient (mL/g)
CF = unit conversion factor of 0.001 (L/mL).

The following equation is used to calculate total radionuclide concentration in soil (i.e., sorbed plus dissolved plus vapor):

$$C_{stot} = C_w \times \left(K_d + \frac{\theta_w + \theta_a \times H'}{\rho_s}\right) \approx C_w \times \left(K_d + \frac{\theta_w}{\rho_s}\right) \times CF \qquad (6\text{-}24)$$

Where:

C_{stot} = total radionuclide concentration in surface soil layer (pCi/g)
θ_w = soil volumetric water content ([mL water]/[cm^3 soil])
θ_a = air-filled soil porosity (unitless)
H' = dimensionless Henry's Law constant (unitless)
ρ_s = soil dry bulk density (g/cm^3)
CF = unit conversion factor of 0.001 (L/mL).

The volatile radionuclide inventory in contaminated water used for irrigation is likely to be negligibly small, so $\theta_a \times H'$ can be ignored. The above equations are used whenever C_s and C_{stot} are used in the remainder of this section.

6.3.3.1.2 Equations to Calculate Tritium Concentrations in Crops (Fruits, Vegetables and Livestock Fodder). The tritium concentration in home-grown crops (fruits and vegetables) and livestock fodder is calculated separately using an equilibrium model. The crop and livestock fodder become contaminated as a result of root uptake of radionuclides in the contaminated soil and groundwater. A summary of the parameters used to calculate tritium in crops is provided in Table 6-26. The following equation is used to calculate tritium concentrations ($\boldsymbol{C_{c,t}}$; pCi/g fresh weight) in the crop using the equilibrium model:

$$C_{c,t} = \frac{C_w}{\rho_w} \times \frac{MW_{H20}}{2 \times AW_H} \times F_{H,C} \times \frac{I}{I+P} \times F_{C,I} \times CF \qquad (6\text{-}25)$$

The first term in the right-hand side of the equation expresses the water concentration in the unit of pCi/kg water. The second term is the ratio of the molecular weights of water and the atomic weight of hydrogen. This term is used to convert the hydrogen fractions ($F_{H,c}$) in the crop to water fractions. Since the hydrogen fractions include organically bound hydrogen as well as water, the crop concentration is a bounding value. The third term, which contains the total irrigation water amount (I) and total precipitation amount (P) during the irrigation period, adjusts the calculated concentration for the presence of uncontaminated water in the growing environment. The time-integration factor, $F_{C,I}$, is the factor that results from the time integral of the dose rate for tritium over the full year. For leafy vegetables, this factor value equals to 1. It is assumed that $F_{C,I} = 1$ for all crop types, as it would lead to a higher dose. The CF is the unit

conversion factor of 0.001 (kg/g). Using the parameter values given in Table 6-26, the tritium concentration in crops is calculated as:

$$C_{c,t} = 8.35 \times 10^{-4} \times C_w \quad \text{(6-26a)}$$

In the above equation the first term has units of liters of water per unit weight of crop. The above equation can be formulated in terms of C_{stot} instead of C_w by using the relationship presented in Equation 6-24. Considering soil K_d of 0 mL/g for tritium, soil dry bulk density of 2.05 g/cm^3 (Hanford H1 unit; Table 6-8), and soil moisture content of 0.06 (typical value), Equation 6-26a can be written as:

$$C_{c,t} = 28.56 \left(\frac{g_{soil}}{g_{crop}}\right) \times C_{stot} \quad \text{(6-26b)}$$

6.3.3.1.3 Equations to Calculate Tritium Concentrations in Animal Products (Beef, Milk, Poultry and Eggs). The tritium concentration in animal products (C_a) is also calculated separately using an equilibrium model. A summary of the parameters used to calculate tritium in animal products is provided in Table 6-27. The following equation is used to calculate tritium concentrations in animal products (pCi/g) using the equilibrium model given as:

$$C_{a,t} = \frac{C_w}{\rho_w} \times \frac{MW_{H2o}}{2 \times AW_H} \times F_{H,A} \times \frac{M_{W,C}}{M_{W,T}} \times F_{A,I} \times CF \quad \text{(6-27)}$$

The first two terms in this equilibrium model have the same functions as that in the model for calculating the tritium concentration in crops. The ratio of contaminated water mass ingested per day to total mass of water ingested per day is closer to 1.0 in the irrigation cases because the drinking water for the animals in the irrigated areas is most likely to be contaminated. Therefore, it is assumed that all the water ingested by the animal is contaminated and, subsequently, the ratio of contaminated water mass ingested per day to total mass of water ingested per day is equal to 1. The time-integration factor is the same as shown above for tritium concentration in crops. The CF is the unit conversion factor of 0.001 (kg/g). Using the parameter values given in Table 6-27, the tritium concentration in animal products is calculated as

$$C_{a,t} = 9.83 \times 10^{-4} \times C_w \quad \text{(6-28a)}$$

In the above equation the first term has units of Liters of water per unit weight of animal products. The above equation can be formulated in terms of C_{stot} instead of C_w by using the relationship presented in Equation 6-24. Considering soil K_d of 0 mL/g for tritium, soil dry bulk density of 2.05 g/cm^3 (Hanford H1 unit; Table 6-8), and soil moisture content of 0.06 (typical value), Equation 6-28a can be written as:

$$C_{c,t} = 33.62 \left(\frac{g_{soil}}{g_{animal\,product}}\right) \times C_{stot} \quad \text{(6-28b)}$$

Table 6-25. Radionuclide-Specific Dose Conversion Factors. (3 sheets)

Radionuclide	Inhalation (mrem/pCi)		Ingestion (mrem/pCi) (DCF_{ing})[b]	External Exposure (Groundwater Pathway) (mrem/yr)/(pCi/g) (DCF_{ext})[c]	External Exposure (Air Pathway) (mrem/yr)/(pCi/m^2) (DCF_{ext} for air pathway)[d]	Air Submersion (mrem/yr)/ (pCi/m^3) (DCF_{im})[e]
	(DCF_{inh})[a]	Lung Absorption Type[a]				
^{227}Ac	5.96E-01	F	1.45E-03	1.57E+00	4.52E-05	3.68E-03
^{241}Am	1.56E-01	M	8.81E-04	3.41E-02	3.21E-06	7.85E-05
^{243}Am	1.54E-01	M	8.73E-04	6.98E-01	2.53E-05	1.08E-03
^{14}C	8.21E-06	M	2.34E-06	1.05E-05	1.88E-09	3.04E-07
^{113m}Cd	4.33E-04	F	9.51E-05	5.06E-04	3.07E-08	1.08E-05
^{243}Cm	1.20E-01	M	6.66E-04	4.55E-01	1.46E-05	6.22E-04
^{244}Cm	1.01E-01	M	5.59E-04	9.83E-05	1.03E-07	4.67E-07
^{60}Co	4.14E-05	M	2.03E-05	1.27E+01	2.74E-04	1.39E-02
^{137}Cs	1.70E-05	F	4.92E-05	2.66E+00	6.46E-05	2.98E-03
^{152}Eu	3.67E-04	F	6.44E-06	5.47E+00	1.28E-04	6.28E-03
^{154}Eu	4.26E-04	F	9.66E-06	5.99E+00	1.39E-04	6.75E-03
^{155}Eu	5.11E-05	F	1.67E-06	1.42E-01	6.89E-06	2.53E-04
^{3}H	1.97E-07	M	7.77E-08	0.00E+00	0.00E+00	0.00E+00
^{129}I	1.50E-04	F	4.48E-04	1.01E-02	3.01E-06	3.34E-05
^{93m}Nb	2.26E-06	M	6.59E-07	8.12E-05	1.10E-07	3.55E-07
^{59}Ni	5.48E-07	M	2.95E-07	0.00E+00	0.00E+00	8.08E-08
^{63}Ni	2.01E-06	M	7.33E-07	0.00E+00	0.00E+00	0.00E+00
^{237}Np	8.51E-02	M	4.63E-04	8.57E-01	2.61E-05	1.18E-03
^{231}Pa	8.77E-01	F	2.07E-03	1.49E-01	4.75E-06	1.69E-04
^{210}Pb	4.48E-03	M	3.77E-03	4.76E-03	4.13E-07	3.57E-05

Table 6-25. Radionuclide-Specific Dose Conversion Factors. (3 sheets)

Radionuclide	Inhalation (mrem/pCi)		Ingestion (mrem/pCi) (DCF_{ing})[b]	External Exposure (Groundwater Pathway) (mrem/yr)/(pCi/g) (DCF_{ext})[c]	External Exposure (Air Pathway) (mrem/yr)/(pCi/m^2) (DCF_{ext} for air pathway)[d]	Air Submersion (mrem/yr)/ (pCi/m^3) (DCF_{im})[e]
	(DCF_{inh})[a]	Lung Absorption Type[a]				
^{238}Pu	1.72E-01	M	9.73E-04	1.18E-04	9.79E-08	3.92E-07
^{239}Pu	1.86E-01	M	1.07E-03	2.30E-04	4.29E-08	4.40E-07
^{240}Pu	1.86E-01	M	1.07E-03	1.14E-04	9.38E-08	3.84E-07
^{241}Pu	3.31E-03	M	1.93E-05	4.61E-06	2.25E-10	7.18E-09
^{242}Pu	1.77E-01	M	1.01E-03	9.99E-05	7.79E-08	7.51E-07
^{226}Ra	1.41E-02	M	1.68E-03	2.48E-02	1.94E-04	9.77E-03
^{228}Ra	1.14E-02	M	5.92E-03	1.26E+01	2.73E-04	1.47E-02
^{222}Rn	0.00E+00		0.00E+00	8.70E+00	0.00E+00	0.00E+00
^{79}Se	6.22E-06	F	1.73E-05	1.45E-05	2.42E-09	3.56E-07
^{151}Sm	3.64E-05	F	5.00E-07	7.68E-07	5.88E-10	3.09E-09
^{126}Sn	6.14E-04	S	2.36E-05	9.25E+00	2.29E-04	1.05E-02
^{90}Sr	1.45E-04	M	1.33E-04	1.92E-02	6.55E-07	1.04E-04
^{99}Tc	1.64E-05	M	3.33E-06	9.80E-05	9.11E-09	3.36E-06
^{229}Th	2.79E-01	S	2.25E-03	1.24E+00	3.70E-05	1.58E-03
^{230}Th	5.44E-02	S	9.36E-04	9.43E-04	8.76E-08	1.77E-06
^{232}Th	9.47E-02	S	1.03E-03	4.07E-04	6.44E-08	9.22E-07
^{232}U	3.19E-02	M	1.49E-03	7.96E+00	1.64E-04	1.00E-02
^{233}U	1.44E-02	M	2.23E-04	1.09E-03	8.36E-08	1.24E-06
^{234}U	1.41E-02	M	2.15E-04	3.13E-04	8.74E-08	7.17E-07
^{235}U	1.25E-02	M	2.03E-04	5.91E-01	1.94E-05	8.56E-04

Table 6-25. Radionuclide-Specific Dose Conversion Factors. (3 sheets)

Radionuclide	Inhalation (mrem/pCi)		Ingestion (mrem/pCi) (DCF_{ing})[b]	External Exposure (Groundwater Pathway) (mrem/yr)/(pCi/g) (DCF_{ext})[c]	External Exposure (Air Pathway) (mrem/yr)/(pCi/m^2) (DCF_{ext} for air pathway)[d]	Air Submersion (mrem/yr)/ (pCi/m^3) (DCF_{im})[e]
	(DCF_{inh})[a]	Lung Absorption Type[a]				
^{236}U	1.29E-02	M	2.02E-04	1.68E-04	7.59E-08	4.41E-07
^{238}U	1.16E-02	M	1.94E-04	8.89E-02	2.82E-06	2.04E-04
^{93}Zr	3.34E-05	M	3.70E-06	0.00E+00	0.00E+00	7.53E-11

[a]DOE-STD-1196-2011, Derived Concentration Technical Standard, Table A-2: Effective Dose Coefficients from Inhaled Air. The lung absorption type for particulate aerosols is taken from Table 4: Classification of Absorption Types for Particulates, by using recommended default absorption type, where F is fast, M is moderate, and S is slow absorption as defined in "ICRP Publication 66: Human Respiratory Tract Model for Radiological Protection" (ICRP 1994). Where default values are not indicated, then the highest value is selected among the absorption types for a given radionuclide.

[b]DOE-STD-1196-2011, Table A-1: Effective Dose Coefficients for Ingested Water.

[c]EPA-402-R-93-081, Federal Guidance Report No. 12, External Exposure to Radionuclides in Air, Water, and Soil, Table III.7. Dose Coefficients for Exposure to Soil Contaminated to an Infinite Depth; modified to include effects of progeny.

[d]EPA-402-R-93-081, Table III.3. Dose Coefficients for Exposure to Contaminated Ground Surface; modified to include effects of progeny.

[e]DOE-STD-1196-2011, Table A-3: Effective Dose Rate Coefficients from Air Submersion; modified to include effects of progeny.

DCF = dose conversion factor

Table 6-26. Parameters Used to Calculate the Tritium Concentration in Crops.

Parameter	Definition	Units	Input Value	Reference
$C_{c,t}$	Tritium concentration in crop	pCi/g fresh weight	Calculated	—
C_w	Tritium concentration in the irrigation water	pCi/L	Calculated	—
ρ_w	Density of water	kg/L	1	EPA/540/R-96/018
MW_{H2O}	Molecular weight of water	g	18.016	Calculated
AW_H	Atomic weight of hydrogen	g	1.008	Calculated
$F_{H,C}$	Mass fraction of hydrogen in crops (vegetable and fruit) that are locally produced	unitless	0.1	NUREG/CR-5512
$F_{C,I}$	Factor from time integral of tritium dose rate	unitless	1	NUREG/CR-5512
I	Total irrigation water applied during the irrigation period	cm	82.3	HNF-SD-WM-TI-707
P	Total precipitation during the irrigation period	cm	5.766	HNF-SD-WM-TI-707
CF	Unit conversion factor	kg/g	0.001	1 kg = 1,000 g

References:
EPA/540/R-96/018, Soil Screening Guidance: User's Guide, Second Edition, Publication 9355.4-23.
HNF-SD-WM-TI-707, "Exposure Scenarios and Unit Factors for the Hanford Tank Waste Performance Assessment."
NUREG/CR-5512, Residual Radioactive Contamination From Decommissioning, Vol. 1, Technical Basis for Translating Contamination Levels to Annual Total Effective Dose Equivalent, Final Report.

6.3.3.1.4 Dose Equations for the All-Pathways Representative Person. The dose equations that are presented in this section are for the all-pathways Representative Person. The equations are given for calculation of dose from a single radionuclide. To calculate total effective dose, it is necessary to sum the doses over all radionuclides at a particular time.

Age- and gender-weighted intake rates were developed for the all-pathways Representative Person in accordance with the recommendations described in DOE-STD-1196-2011 as described in RPP-ENV-58813. Table 6-28 presents a summary of the age- and gender-weighted intake rates used for the all-pathways Reference Person scenario.

6.3.3.1.5 Ingestion of Water. The following equation is used to calculate dose from ingestion of water (RPP-ENV-58813):

$$D_w = C_w \times IR_w \times EF \times DCF_{ing} \tag{6-29}$$

Where:

D_w = dose from drinking contaminated water (mrem/yr)
C_w = radionuclide concentration in water (pCi/L)

IR_w = water ingestion rate (L/day)
EF = exposure frequency (days/yr)
DCF_{ing} = ingestion dose conversion factor (mrem/pCi).

Table 6-27. Parameters for Tritium Concentration Calculation in Animal Products.

Parameter	Definition	Units	Input Value	Reference
$C_{a,t}$	Radionuclide concentration in animal products	pCi/g	Calculated	—
C_w	Radionuclide concentration in the irrigation water	pCi/L	Calculated	—
$F_{H,A}$	Mass fraction of hydrogen in animal products that are locally produced	unitless	0.11	NUREG/CR-5512
$F_{A,I}$	Factor from time integral of tritium dose rate	unitless	1	NUREG/CR-5512
$M_{W,C}$	Mass of contaminated water ingested daily by the animal	kg/day	$M_{W,C} = 1\ M_{W,T}$	Assumption
$M_{W,T}$	Total mass of contaminated water ingested daily by the animal	kg/day		
CF	Unit conversion factor	kg/g	0.001	1 kg = 1,000 g

Reference: NUREG/CR-5512, Residual Radioactive Contamination From Decommissioning, Vol. 1, Technical Basis for Translating Contamination Levels to Annual Total Effective Dose Equivalent, Final Report.

6.3.3.1.6 Ingestion of Homegrown Crops (Fruits and Vegetables). The following equations are used to calculate the concentration of contaminant in the crop (homegrown fruits and vegetables) and the dose from consumption of the crop (NCRP Report No. 129, "Recommended Screening Limits for Contaminated Surface Soil and Review of Factors Relevant to Site-Specific Factors"). The following equation is used to calculate the concentration of contaminant in the crop:

$$C_c = C_{stot} \times (B_v + B_v') \tag{6-30}$$

Where:

C_c = radionuclide concentration in crop (pCi/g)
C_{stot} = total radionuclide concentration in surface soil layer (pCi/g)
B_v = crop-soil bioconcentration factor through uptake $\left(\frac{\left(\frac{pCi}{kg\ fresh\ weight\ of\ crop}\right)}{\left(\frac{pCi}{kg\ dry\ weight\ of\ soil}\right)}\right)$
B_v' = crop-soil bioconcentration factor representing all resuspension-soil adhesion processes $\left(\frac{\left(\frac{pCi}{kg\ fresh\ weight\ of\ crop}\right)}{\left(\frac{pCi}{kg\ dry\ weight\ of\ soil}\right)}\right)$.

Table 6-28. Summary of Intake Rates for All-Pathways Reference Person.

Intake Parameter	Notation	Units	Value	Reference
Inhalation rate – indoor	INH_{in}	m^3/yr	7,300	NCRP Report No. 129
Soil ingestion rate*	IR_s	mg/day	108.6	EPA/540/R-92/003
Drinking water ingestion rate*	IR_w	L/day	2.66	EPA/600/R-090/052F
Crop ingestion rate (includes fruits and vegetables)*	IR_c	kg/year	272.3	
Beef ingestion rate*	IR_b	kg/year	101.9	
Milk ingestion rate*	IR_m	L/year	311.3	
Egg ingestion rate*	IR_e	kg/year	40.5	
Poultry ingestion rate*	IR_p	kg/year	99.4	

*See Appendix P of RPP-ENV-58813 for more details regarding the derivation of intake rates for a Reference Person. The intake rates are generally calculated based on age- and gender-weighted fraction provided in DOE-STD-1196-2011, Derived Concentration Technical Standard. Where information regarding mean and 95th percentile intake rates is available, the 95th percentile value is chosen and then weighted by age and gender. For soil ingestion rate, the rate published for children and adults is used with simple age weighting.

References:
EPA/540/R-92/003, Risk Assessment Guidance for Superfund: Volume I – Human Health Evaluation Manual (Part B, Development of Risk-based Preliminary Remediation Goals) Interim, Publication 9285.7-01B.
EPA/600/R-090/052F, Exposure Factors Handbook: 2011 Edition, National Center for Environmental Assessment.
NCRP Report No. 129, "Recommended Screening Limits for Contaminated Surface Soil and Review of Factors Relevant to Site-Specific Studies."
OSWER Directive 9200.1-120, "Human Health Evaluation Manual, Supplemental Guidance: Update of Standard Default Exposure Factors."

The following equation is used to calculate dose from consumption of homegrown fruits and vegetables:

$$D_c = C_c \times IR_c \times F_v \times CF_1 \times DCF_{ing} \tag{6-31}$$

Where:

D_c = dose from consumption of crop (homegrown fruits and vegetables) (mrem/yr)
IR_c = crop ingestion rate (kg/yr)
F_v = fraction of homegrown fruits and vegetables consumed (unitless)
CF_1 = unit conversion factor of 1,000 (g/kg)
DCF_{ing} = ingestion dose conversion factor (mrem/pCi).

6.3.3.1.7 Ingestion of Farm-Raised Beef. The following equations are used to calculate the concentration of contaminant in livestock fodder, the concentration of contaminant in beef, and the dose from consumption of the beef (NCRP Report No. 129).

The equation used to calculate the concentration of contaminant in livestock fodder is given by[2]

$$C_{fodder} = C_{stot} \times \left(B_p \times B'_p\right) \tag{6-32}$$

Where:

C_{fodder} = radionuclide concentration in livestock fodder (pCi/g)
C_{stot} = total radionuclide concentration in surface soil layer (pCi/g)
B_p = pasture-soil bioconcentration factor through uptake $\left(\frac{\left(\frac{pCi}{kg\ dry\ weight\ of\ fodder}\right)}{\left(\frac{pCi}{kg\ dry\ weight\ of\ soil}\right)}\right)$
B'_p = pasture-soil bioconcentration factor for all resuspension processes $\left(\frac{\left(\frac{pCi}{kg\ dry\ weight\ of\ fodder}\right)}{\left(\frac{pCi}{kg\ dry\ weight\ of\ soil}\right)}\right)$.

The following equation is used to calculate the concentration of contaminant in beef resulting from consumption of contaminated water, contaminated fodder, and contaminated soil:

$$C_b = \left(C_w \times IR_{w,b} + C_{fodder} \times IR_{fodder,b} \times CF_1 + C_{stot} \times IR_{s,b} \times CF_1\right) \times BCF_{beef} \tag{6-33}$$

Where:

C_b = radionuclide concentration in beef (pCi/kg)
C_w = radionuclide concentration in water (pCi/L)
$IR_{w,b}$ = ingestion rate of water for beef (L/day)
C_{fodder} = radionuclide concentration in livestock fodder (pCi/g)
$IR_{fodder,b}$ = ingestion rate of fodder for beef (kg/day)
CF_1 = unit conversion factor of 1,000 (g/kg)
C_{stot} = total radionuclide concentration in surface soil layer (pCi/g)
$IR_{s,b}$ = ingestion rate of soil for beef (kg/day)
BCF_{beef} = bioconcentration factor of radionuclides in beef (day/kg).

The equation used to calculate the dose from ingestion of farm-raised beef is given by

$$D_b = C_b \times IR_b \times F_a \times DCF_{ing} \tag{6-34}$$

Where:

D_b = dose from ingestion of beef (mrem/yr)
IR_b = beef ingestion rate (kg/yr)
F_a = fraction of farm-raised beef that is consumed (unitless)
DCF_{ing} = ingestion dose conversion factor (mrem/pCi).

[2] This equation is used for all food chain pathways that include consumption of livestock fodder.

6.3.3.1.8 Ingestion of Milk. This section describes the equations used to calculate the concentration of contaminant in milk and the dose from consumption of milk.

The following equation is used to calculate the concentration of contaminant in milk resulting from consumption of contaminated water, contaminated fodder, and contaminated soil by the dairy animal:

$$C_m = \left(C_w \times IR_{w,d} + C_{fodder} \times IR_{fodder,d} \times CF_1 + C_{stot} \times IR_{s,d} \times CF_1\right) \times BCF_{milk} \quad (6\text{-}35)$$

Where:

C_m = radionuclide concentration in milk (pCi/L)
C_w = radionuclide concentration in water (pCi/L)
$IR_{w,d}$ = ingestion rate of water by dairy cattle (L/day)
C_{fodder} = radionuclide concentration in livestock fodder (pCi/g)
$IR_{fodder,d}$ = ingestion rate of fodder by dairy cattle (kg/day)
CF_1 = unit conversion factor of 1,000 (g/kg)
C_{stot} = total radionuclide concentration in surface soil layer (pCi/g)
$IR_{s,d}$ = ingestion rate of soil by dairy cattle (kg/day)
BCF_{milk} = bioconcentration factor of radionuclides in milk (day/L).

The equation used to calculate the dose from ingestion of milk is given by

$$D_m = C_m \times IR_m \times F_a \times DCF_{ing} \quad (6\text{-}36)$$

Where:

D_m = dose from ingestion of milk (mrem/yr)
IR_m = milk ingestion rate (L/yr)
F_a = fraction of locally-produced milk that is consumed (unitless)
DCF_{ing} = ingestion dose conversion factor (mrem/pCi).

6.3.3.1.9 Ingestion of Eggs. This section describes the equations used to calculate the concentration of contaminant in eggs and the dose from consumption of eggs.

The equation used to calculate the concentration of contaminant in eggs resulting from consumption of contaminated water, contaminated fodder, and contaminated soil by the poultry is given as

$$C_e = \left(C_w \times IR_{w,p} + C_{fodder} \times IR_{fodder,p} \times CF_1 + C_{stot} \times IR_{s,p} \times CF_1\right) \times BCF_{egg} \quad (6\text{-}37)$$

Where:

C_e = radionuclide concentration in eggs (pCi/kg)
C_w = radionuclide concentration in water (pCi/L)

$IR_{w,p}$ = ingestion rate of water by poultry (L/day)
C_{fodder} = radionuclide concentration in livestock fodder (pCi/g)
$IR_{fodder,p}$ = ingestion rate of fodder by poultry (kg/day)
CF_1 = unit conversion factor of 1,000 (g/kg)
C_{stot} = total radionuclide concentration in surface soil layer (pCi/g)
$IR_{s,p}$ = ingestion rate of soil by poultry (kg/day)
BCF_{egg} = bioconcentration factor of radionuclides in eggs (day/kg).

The equation used to calculate the dose from ingestion of eggs:

$$D_e = C_e \times IR_e \times F_a \times DCF_{ing} \tag{6-38}$$

Where:

D_e = dose from consumption of eggs (mrem/yr)
IR_e = egg ingestion rate (kg/yr)
F_a = fraction of locally-produced eggs that are consumed (unitless)
DCF_{ing} = ingestion dose conversion factor (mrem/pCi).

6.3.3.1.10 Ingestion of Farm-Raised Poultry. This section describes the equations used to calculate the concentration of contaminant in poultry and the dose from consumption of poultry.

The following equation is used to calculate the concentration of contaminant in poultry:

$$C_p = \left(C_w \times IR_{w,p} + C_{fodder} \times IR_{fodder,p} \times CF_1 + C_{stot} \times IR_{s,p} \times CF_1\right) \times BCF_{poultry} \tag{6-39}$$

Where:

C_p = radionuclide concentration in poultry (pCi/kg)
C_w = radionuclide concentration in water (pCi/L)
$IR_{w,p}$ = ingestion rate of water by poultry (L/day)
C_{fodder} = radionuclide concentration in livestock fodder (pCi/g)
$IR_{fodder,p}$ = ingestion rate of fodder by poultry (kg/day)
CF_1 = unit conversion factor of 1,000 (g/kg)
C_{stot} = total radionuclide concentration in surface soil layer (pCi/g)
$IR_{s,p}$ = ingestion rate of soil by poultry (kg/day)
$BCF_{poultry}$ = bioconcentration factor of radionuclides in poultry (day/kg).

The following equation is used to calculate dose from ingestion of poultry:

$$D_p = C_p \times IR_p \times F_a \times DCF_{ing} \tag{6-40}$$

Where:

D_p = dose from ingestion of poultry (mrem/yr)

IR_p = ingestion rate of poultry (kg/yr)
F_a = fraction of locally-produced poultry that is consumed (unitless)
DCF_{ing} = dose conversion factor for ingestion (mrem/pCi).

6.3.3.1.11 Incidental Ingestion of Soil. The following equation is used to calculate the dose from incidental ingestion of soil:

$$D_s = C_s \times IR_s \times EF \times DCF_{ing} \times CF \quad (6\text{-}41)$$

Where:

D_s = dose from incidental ingestion of soil (mrem/yr)
IR_s = ingestion rate of soil (mg/day)
EF = exposure frequency (days/yr)
DCF_{ing} = ingestion dose conversion factor (mrem/pCi)
CF = unit conversion factor of 0.001 (g/mg).

6.3.3.1.12 Inhalation of Soil Particulates. The following equation is used to calculate the dose from inhalation of soil particulates:

$$D_{inh} = C_s \times E_f \times M \times \left(INH_{in} \times t_{in} \times \left(\frac{I}{O}\right) + INH_{out} \times t_{out}\right) \times DCF_{inh} \quad (6\text{-}42)$$

This equation assumes the concentration and mass loading factor are the same indoors and outdoors.

Where:

D_{inh} = dose from inhalation of soil (mrem/yr)
E_f = enrichment factor (unitless)
M = mass loading factor (g/m^3)
INH_{in} = indoor inhalation rate (m^3/yr)
t_{in} = fraction of time spent indoors (unitless)
I/O = ratio of radionuclide concentrations in indoor and outdoor air (unitless)
INH_{out} = outdoor inhalation rate (m^3/yr)
t_{out} = fraction of time spent outdoors (unitless)
DCF_{inh} = inhalation dose conversion factor (mrem/pCi).

And:

$$E_f = \frac{C_p}{C_s} \quad (6\text{-}43)$$

C_p = radionuclide concentration in airborne particles (pCi/g)
C_s = radionuclide concentration in soil (pCi/g).

6.3.3.1.13 Inhalation of Water Vapor. The following equation is used to calculate dose resulting from the inhalation of water vapor from showering or other household activities:

$$D_{inh_w} = C_w \times INH_w \times EF \times K \times DCF_{inh} \quad (6\text{-}44)$$

Where:

D_{inh_w} = dose resulting from inhalation of water vapor (mrem/yr)
C_w = radionuclide concentration in water (pCi/L)
INH_w = inhalation rate of water vapor (m^3/day)
EF = exposure frequency (days/yr)
K = Andelman volatilization factor (L/m^3)
DCF_{inh} = inhalation dose conversion factor for inhalation (mrem/pCi).

6.3.3.1.14 External Exposure. The following equation is used to calculate the dose from external exposure:

$$D_{ext} = C_{stot} \times (t_{in} \times \epsilon + t_{out}) \times DCF_{ext} \quad (6\text{-}45)$$

Where:

D_{ext} = dose from external exposure to soil (mrem/yr)
C_{stot} = total radionuclide concentration in soil (pCi/g)
t_{in} = fraction of time spent indoors (unitless)
ϵ = transmission or shielding factor (unitless)
t_{out} = fraction of time spent outdoors (unitless)
DCF_{ext} = dose conversion factor for external exposure ([mrem/yr]/[p/Ci/g]).

6.3.3.1.15 Total Effective Dose for All-Pathways Reference Person. The following equation is used to calculate the total effective dose from all groundwater pathways:

$$D_{total} = \sum_i^N D_i \quad (6\text{-}46)$$

Where:

D_{total} = total effective dose from all exposure pathways (mrem/yr)
D_i = total dose for the ith exposure pathway (mrem/yr)
N = number of exposure pathways.

6.3.3.2 Atmospheric-Pathway Dose Analysis. An atmospheric pathway scenario is considered in which an individual is exposed to radionuclides that are diffused to the surface from the wastes disposed at the WMA C tank farm and are transported 100 m downwind. Three exposure mechanisms are considered for the atmospheric pathway:

- Air immersion
- Inhalation

- External exposure to the contaminated ground surface.

External exposure results from a fraction of the waste in the air that settles on the ground via dry and wet depositions as they are transported by wind.

The exposed individual is assumed to encounter the same exposure conditions as the resident farmer (e.g., time spent indoors and outdoors). Inhalation of vapors from redeposition followed by resuspension and inhalation is considered. The dose-specific parameters for the atmospheric pathway are given in Table 6-29, and the dose conversion factors are summarized in Table 6-25.

Table 6-29. Dose-Specific Parameters for the Atmospheric Pathway.

Parameter	Notation	Value	Unit	Reference
Dry deposition rate for ^{129}I	V_d	0.035	m/s	EPA 2014
Dry deposition velocity for ^{14}C and ^{3}H	V_d	0	m/s	EPA 2014
Rainfall rate	RR	18.14*	cm/yr	Hanford.gov
Scavenging conversion factor	SCF	1.00E-07	yr/(cm s)	EPA 2014
Scavenging coefficient	SC	Calculated	s^{-1}	EPA 2014
Mixing layer height	H	2	m	Modeling assumption
Gamma shielding factor	GSF_o	1	(-)	PRGfR 2015
Inhalation rate when indoors	IR_{in}	7,300	m^3/yr	NCRP Report No. 129
Fraction of time spent indoors	t_{in}	0.4	(-)	PRGfR 2015; Based on 10 hr/day for 350 days/year
Inhalation rate when outdoors	IR_{out}	12,775	m^3/yr	NCRP Report No. 129
Fraction of time spent outdoors	t_{out}	0.4861	(-)	PRGfR 2015; Based on 12.167 hr/day for 350 days/year
Accumulation time	t_{accu}	3.15E+07	s	One-year time step

*Value given is 30-year average from 1981 to 2010.

References:
Hanford Site (Hanford.gov), Queried 07/2015, [Hanford Meteorological Station], http://www.hanford.gov/page.cfm/HMS.
NCRP Report No. 129, "Recommended Screening Limits for Contaminated Surface Soil and Review of Factors Relevant to Site-Specific Studies."

Preliminary Remediation Goals for Radionuclides (PRGfR), Queried 07/2015, [PRG User's Guide], http://epa-prgs.ornl.gov/radionuclides/prg_guide.html.
Radiation Risk Assessment Software: CAP-88 and CAP-88 PC (EPA 2014), Queried 07/2015, [CAP88-PC Version 4.0 User Guide], http://www.epa.gov/radiation/assessment/CAP88/index.html.

6.3.3.2.1 Deposition of Airborne Contaminants on the Ground Surface. Contaminants in the air can be deposited on the ground surface under both dry and wet conditions (rain or mist). The following equation is used to calculate the dry deposition rate:

$$Dep_d = C_{air} \times V_d \tag{6-47}$$

Where:

Dep_d = deposition rate for radionuclides under dry conditions (pCi/[m^2 sec])
C_{air} = radionuclide concentration in air (pCi/m^3)
V_d = velocity with which the dry deposition occurs (m/s).

The following equation is used to calculate wet deposition rate:

$$Dep_w = C_{air} \times SC \times H \tag{6-48}$$

And:

$$SC = RR \times SCF \tag{6-49}$$

Where:

Dep_w = deposition rate for radionuclides under wet conditions (pCi/[m^2 sec])
C_{air} = radionuclide concentration in air (pCi/m^3)
SC = scavenging coefficient (sec^{-1})
H = mixing layer height (m)
RR = rainfall rate (cm/yr)
SCF = scavenging conversion factor (yr/cm-sec).

The following equation is used to calculate the total deposition rate (pCi/[m^2 sec]):

$$TDep = Dep_d + Dep_w \tag{6-50}$$

Where:

$TDep$ = total deposition rate for radionuclides (pCi/[m^2 sec]).

6.3.3.2.2 Air Immersion Dose. An individual in the contaminated volume of air will receive external radiation exposure, primarily from gamma photon emitters in the surrounding air. The following equation is used to calculate the air immersion dose:

$$D_{im} = C_{air} \times t_{out} \times GSF_o \times DCF_{im} \tag{6-51}$$

Where:

D_{im} = dose from air immersion (mrem/yr)

C_{air} = radionuclide concentration in air (pCi/m^3)
t_{out} = fraction of time spent outdoors (unitless)
GSF_o = outdoor gamma shielding factor (unitless)
DCF_{im} = air immersion dose conversion factor $\left(\frac{(mrem/year)}{(pCi/m^3)}\right)$.

6.3.3.2.3 Inhalation Dose for Gaseous Radionuclides. In addition to the radiation dose received from air immersion, the exposed individual will receive a dose from inhalation of gaseous radionuclides in the air (tritium, ^{14}C, and ^{129}I). The following equation is used to calculate inhalation dose:

$$D_{inh} = C_{air} \times (INH_{in} \times t_{in} + INH_{out} \times t_{out}) \times DCF_{inh} \quad (6\text{-}52)$$

Where:

D_{inh} = dose from inhalation of gaseous radionuclides in air (mrem/yr)
C_{air} = radionuclide concentration in air (pCi/m^3)
INH_{in} = inhalation rate while indoors (m^3/yr)
t_{in} = fraction of time spent indoors (unitless)
INH_{out} = inhalation rate while outdoors (m^3/yr)
t_{out} = fraction of time spent outdoors (unitless)
DCF_{inh} = dose conversion factor for inhalation for each radionuclide (mrem/pCi).

6.3.3.2.4 External Exposure to Contaminated Soil. The final exposure considered for the atmospheric pathway is external exposure to radionuclides that have been redeposited on the ground. The radionuclide dose coefficients assume radionuclides are uniformly distributed on the ground to a depth that approximates a plane that is infinitely thick and infinitely horizontal. The following equation is used to calculate the radionuclide concentration that has accumulated on the ground surface:

$$C_{grd} = TDep \times t_{accu} \quad (6\text{-}53)$$

Where:

C_{grd} = radionuclide concentration on ground surface (pCi/m^2)
$TDep$ = total deposition rate (pCi/[m^2·sec])
t_{accu} = time interval over which the deposition has occurred (sec).

The following equation is used to calculate direct external exposure dose:

$$D_{ext} = C_{grd} \times (t_{in} \times \varepsilon + t_{out}) \times DCF_{ext} \quad (6\text{-}54)$$

Where:

D_{ext} = dose from the external exposure to contaminated ground surface (mrem/yr)
t_{in} = fraction of time spent indoors (unitless)

ε = transmission or shielding factor (unitless)
t_{out} = fraction of time spent outdoors (unitless)
DCF_{ext} = dose conversion factor for external exposure to contaminated ground surface ([mrem/yr]/[pCi/m^2]).

6.3.3.2.5 Total Effective Dose for Atmospheric Pathway. The following equation is used to calculate the total effective dose from all atmospheric pathways:

$$D_{total} = \sum_i^N D_i \tag{6-55}$$

Where:

D_{total} = total effective dose from all exposure pathways (mrem/yr)
N = number of exposure pathways
D_i = total dose for the ith exposure pathway (mrem/yr).

6.4 MODEL VALIDATION[3]

A substantial body of literature exists indicating the manner in which scientific validation of models is pursued (e.g., "Ground-Water Models: Validate or Invalidate" [Bredehoeft and Konikow 1993], "Validation of safety assessment models as a process of scientific and public confidence building" [Neuman 1992], "The Modeling Process and Model Validation" [Tsang 1991]). Because PA models cannot be tested over the spatial scales of interest and the long time periods for which the models make predictions, the customary definition of model validation (i.e., comparison of model estimates with actual data at the space-time scales of interest) is precluded (NUREG-1573; NUREG-1636, Regulatory Perspectives on Model Validation in High-Level Radioactive Waste Management Programs: A Joint NRC/SKI White Paper). Therefore, this section on model validation is viewed as a summary of the documented theoretical or scientific basis for each of the PA model components that have been developed and their suitability for supporting the PA decision-making. Below is presented a variety of topical discussions which serve as the basis of confidence building and model validation of WMA C PA process models and results.

6.4.1 Basis for Recharge Estimates Used for Land Surface Boundary Condition

Recharge rates have been estimated from studies conducted at the Hanford Site over the last 30 years. Recharge rates are available for natural and disturbed soils, for soils with and without vegetation, and for various plant communities. In addition, recharge has been estimated for surface covers with varying plant communities. These estimates are based on lysimeter records, tracer tests (chloride mass balance), and computer simulations to match field data. PNNL-16688 and PNNL-14702 provide primary sources of information on recharge estimates for the Hanford Site that are relevant to tank farms. The estimates used in the PA consider estimates of recharge

[3] In this section and in the context of WMA C PA modeling, the terms "confidence," "confidence building," "confidence enhancement," "validation," and "validation process" are used interchangeably.

made for the 200 Areas and for conditions at WMA C inferred from measurements made at the Field Lysimeter Test Facility (Section 3.1.5.2.2).

An extensive set of data exists for estimates of recharge for engineered barriers. For example, almost two decades of field-scale recharge studies have been conducted on an engineered Prototype Hanford Barrier (PHB) (a 5-m [16.4-ft] thick multilayered capillary barrier with 2 m [6.6 ft] of silt loam) that was constructed in the 200 East Area (north of WMA C) in August 1994. The barrier performance was monitored almost continuously for 15 years to document structural stability, erosion, and components of the water balance including precipitation, surface runoff, water storage, percolation out of the root zone, and evapotranspiration. The barrier recharge estimates used in the PA are supported by the PHB data (PNNL-18845).

Section 8.1.3.1 provides additional details related to developing the uncertainty distributions for the recharge estimates.

6.4.2 Basis for Source-Term Model Development and Implementation

The basis for the source-term model development and implementation is rooted in results of laboratory studies conducted of the tank waste residuals collected in a number of tanks following cessation of retrieval. As part of the waste characterization efforts, analytical methods are used to measure the chemical and radiological constituents in the waste sludge and to understand their composition, solid-phase characteristics, and the leachability of primary contaminants of interest. Several detailed characterization reports are available for various tank residuals (see Section 5).

Both mineral phase solubility-limited and matrix degradation rate-limited processes are considered for release of contaminant from the waste. These conceptual models are based on observations made through multi-year leaching tests and identification of mineral phases as presented in Section 5. Results from the flow-through and batch leach tests were used to develop both thermodynamic equilibrium and reaction progress models. Both empirical and process model-based information were used to develop the waste form release models for the PA (Section 6.2.1 provides additional details).

The effective diffusion coefficient of mobile contaminants (such as ^{99}Tc and ^{129}I) through the combined grout and concrete base mat is considered a key parameter that controls the diffusive flux. Over the past decade, several experiments have been conducted to determine the effective diffusion coefficient through concrete for relatively mobile contaminants under unsaturated conditions. The results of various experiments are presented in PNNL-23841 and summarized in Section 6.3.1.4. Of particular interest are the sediment-concrete half-cell experiments conducted in Year 2008 (for a period of 351 days) with ^{99}Tc and stable iodine. Sediment half-cell specimens were spiked with ^{99}Tc (or stable iodine) to achieve a measurable diffusion profile in the concrete part of the half-cell. In these experiments, iron content was varied in the concrete specimens from 0% to 12%, sediment moisture content was varied (4%, 7%, or 15%), and half of the concrete monoliths were carbonated prior to preparing the half-cells. The characteristics of the concrete half-cells are listed in Table 6-4. Half-cell sampling was conducted at 351 days. The effective diffusion coefficient through grout and concrete is based on evaluation of such experiments.

A linear sorption isotherm (using a K_d approach) is considered for determining sorption within the grout and concrete layer for various contaminants as they undergo diffusive (and advective) transport through the tank. The K_d values are presented in Table 6-7 in terms of best estimate and the uncertainty range that are derived from relevant published literature for chemical conditions that are likely to exist within the grout/concrete layer within the tanks.

6.4.3 Basis for Vadose Zone Model Development

The spatial extent of various HSUs within the WMA C model domain are based on an extensive borehole dataset discussed in Section 3.2.1. The geologic framework model for WMA C is derived from the information provided in RPP-RPT-56356 (Section 3.2.1). It should be noted that at the Hanford Site more than 3,000 boreholes have been logged (PNNL-13653, "A Catalog of Geologic Data for the Hanford Site") and primary HSU designations and extents are well established.

The vadose zone hydraulic properties for WMA C are derived from a set of laboratory (core-scale) experiments conducted on samples representative of Hanford H1, H2, and H3 units and backfill material. The methodology is discussed in detail in Appendix B (Section B.2). For WMA C vadose zone modeling, each heterogeneous geologic unit is replaced by an EHM with macroscopic flow properties. With each heterogeneous unit assigned its upscaled or effective hydraulic properties, the simulated flow fields predict the bulk or mean flow behavior at the field scale. The method of upscaling is discussed in Appendix B (Section B.3).

An independent evaluation of the vadose zone conceptual model and the EHM approximation was performed using the 200 East Area Sisson and Lu injection test site (Figure 6-60) moisture content database. The database at the nearby Sisson and Lu site therefore serves as a proxy for WMA C, and is an important resource in understanding large-scale moisture movement in imperfectly stratified heterogeneous media and a relatively dry moisture regime such as those existing at WMA C. Details of the Sisson and Lu site, field injections and the spatio-temporal distribution of observed moisture plume are described elsewhere ("Simulating field-scale moisture flow using a combined power-averaging and tensorial connectivity-tortuosity approach" [Zhang and Khaleel 2010]; Ye et al. 2005).

Two variations of EHM model for the heterogeneous Hanford sediments were explored based on the Sisson and Lu experiments. In the first method, the small-scale core measurements for hydraulic properties were used to predict the large-scale flow behavior at the Sisson and Lu site (Zhang and Khaleel 2010). The second method is based on an inverse approach which inverts the large-scale unsaturated properties using the temporal evolution of the moisture content distribution (Yeh et al. 2005). For both approaches, a moment analysis (Ye at al. 2005) was used to quantify the center of mass and the spread of the injected water for the observed and simulated moisture plumes. The first moments represent the mass center of the moisture plume in different directions at a given time. The second moments measure the spread of the plume about its mass centers. For the forward as well as the inverse EHM-based methods, spatial moments (first and second) of the simulated plume based on the effective hydraulic conductivities were in good agreement with those for the observed plume (Zhang and Khaleel 2010; Yeh et al. 2005).

Figure 6-60. Location of Sisson and Lu Field Injection Site in 200 East Area.

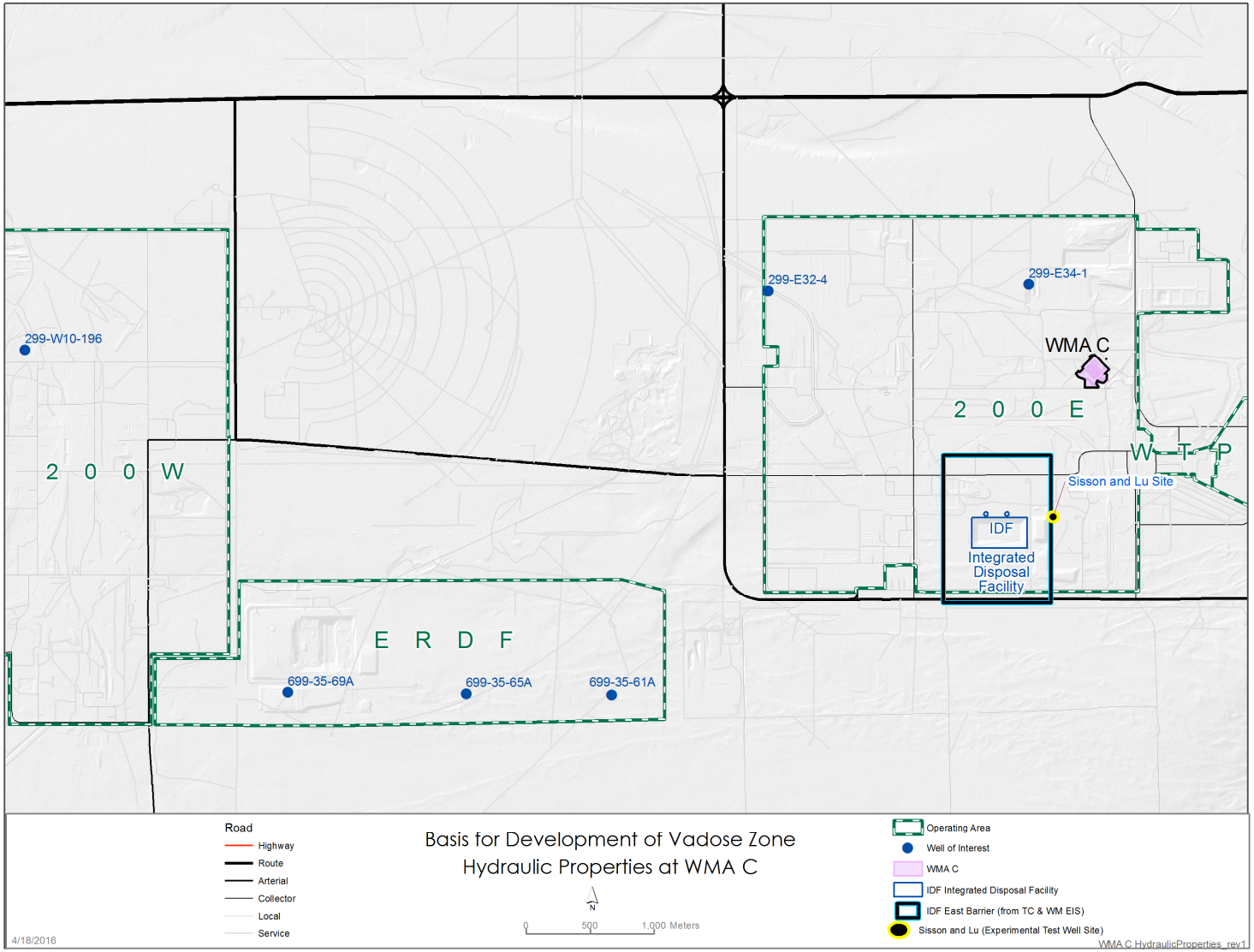

ERDF = Environmental Restoration Disposal Facility
TC&WM EIS = Tank Closure and Waste Management Environmental Impact Statement
WMA = Waste Management Area
WTP = Waste Treatment Plant

The Sisson and Lu site database also provided a framework for testing two heterogeneous modeling approaches based on combining soft (initial moisture content, bulk density and particle-size distribution) and hard (soil hydraulic properties) data ("Simulation of field injection experiments in heterogeneous unsaturated media using cokriging and artificial neural network" [Ye et al. 2007]; "A Markov chain model for characterizing medium heterogeneity and sediment layering structure" [Ye and Khaleel 2008]). The heterogeneous models do not invoke the EHM approximation. The use of both soft and hard data was valuable in reproducing the detailed moisture plume for the two heterogeneous models (i.e., the splitting of the moisture plume sandwiched within the coarse media between two fine layers at the Sisson and Lu site). However, the observed and simulated spatial moments (first and second) were not significantly different from those using the EHM-based models. Hence, models using both hard and soft data, in addition to honoring the observed first and second moments, were able to reproduce the splitting of the observed plume. On the other hand, the EHM-based modeling does not capture the detailed plume behavior, but honors the first and second moments of the observed moisture plume. With the WMA C PA simulations being conducted over a large flow domain and over a long time frame, the fact that the calculated moments for both the EHM and heterogeneous models are of similar magnitude is an important finding, and provides justification for use of EHM approximation for vadose zone modeling.

6.4.4 Comparison of Vadose Zone Modeling Results with Measured Data in Vicinity of Waste Management Area C

As part of WMA C site characterization, an extensive database of moisture content information is available for various HSUs. The moisture content database was developed as part of a direct push campaign conducted at WMA C in 2008, and understood as being long after the occurrence of past leaks and discharges at the farm. Figure 6-61 shows the simulated steady-state moisture profile for different stratigraphic units for the base case under long-term recharge conditions (3.5 mm/yr [0.14 in./yr]). The simulated volumetric moisture contents for different units vary within a narrow range of 4% and 7%. These values compare well with an extensive dataset of field observations where the average volumetric moisture content for the various HSUs vary from 5.1% to 6.2% (Appendix B, Table B-1). With moisture being the key driver for contaminant transport, the fact that the intermediate calculations for the simulated average moisture for different units is in overall agreement with field data enhances confidence in the PA modeling approach and calculations.

Figure 6-62 provides a comparison, for Hanford H2 unit, of the measured moisture profile (circles) for borehole C4297 that is located within WMA C and the simulated steady-state moisture profile (blue) from the base case. As indicated, for an expected long-term recharge estimate of 3.5 mm/yr (0.14 in./yr), the simulated H2 moisture profile, on the average, compares well with the measurements. As expected, the field-measured moisture contents are significantly impacted by small-scale heterogeneities and exhibit considerable variability (Figure 6-62). To the contrary, the PA simulations are based on upscaled or effective hydraulic properties; each heterogeneous formation is replaced by its homogeneous equivalent, and the upscaled or effective flow parameters are used to represent the EHM. This effectively results in a smoothing of the model estimates (Figure 6-3). Therefore, the variability of field-measured moisture contents, induced by media heterogeneities, is inherently larger in comparison to that based on

PA simulations using homogenized upscaled properties, and the ensemble average, embedded in EHM approximation, cannot capture the field-scale variability.

Figure 6-61. Simulated Average Moisture Contents for Different Stratigraphic Units Using Equivalent Homogeneous Medium Model.

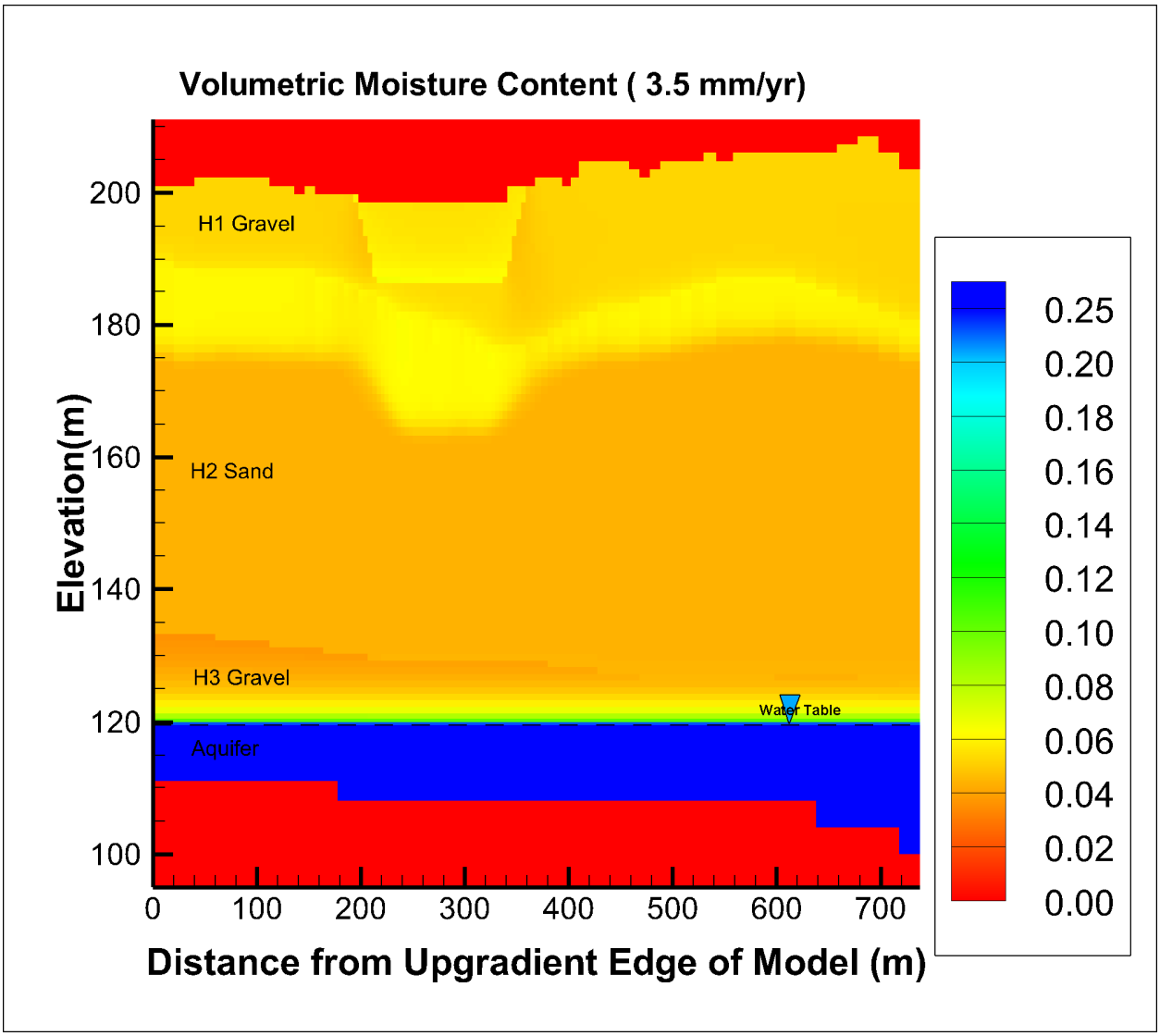

6.4.5 Comparison of Vadose Zone Model with Tank Closure and Waste Management Environmental Impact Statement Model for Alternative 2B

A comparison was performed to evaluate the vadose zone model developed for the WMA C PA against the TC&WM EIS model (DOE/EIS-0391) developed for WMA C. Due to varying inputs related to the residual waste inventory and waste release processes, direct comparison of results is not possible. Therefore, the residual waste inventory, waste release functions, and recharge rates were made consistent with the TC&WM EIS model by changing the inputs within the WMA C PA model (see Appendix G). The flux at the base of the vadose zone was compared

between the two models for ^{129}I. The time series releases of ^{129}I to the groundwater calculated in both models include two relative maxima and negligible difference between the two peak values are observed. The results of the comparison, provided in Appendix G, show that the two models are capable of producing consistent results indicating that the hydraulic properties used in the two models produce similar results.

Figure 6-62. Comparison of Simulated (Blue) and Observed (Circle) Moisture Content for Hanford H2 Sand-Dominated Unit.

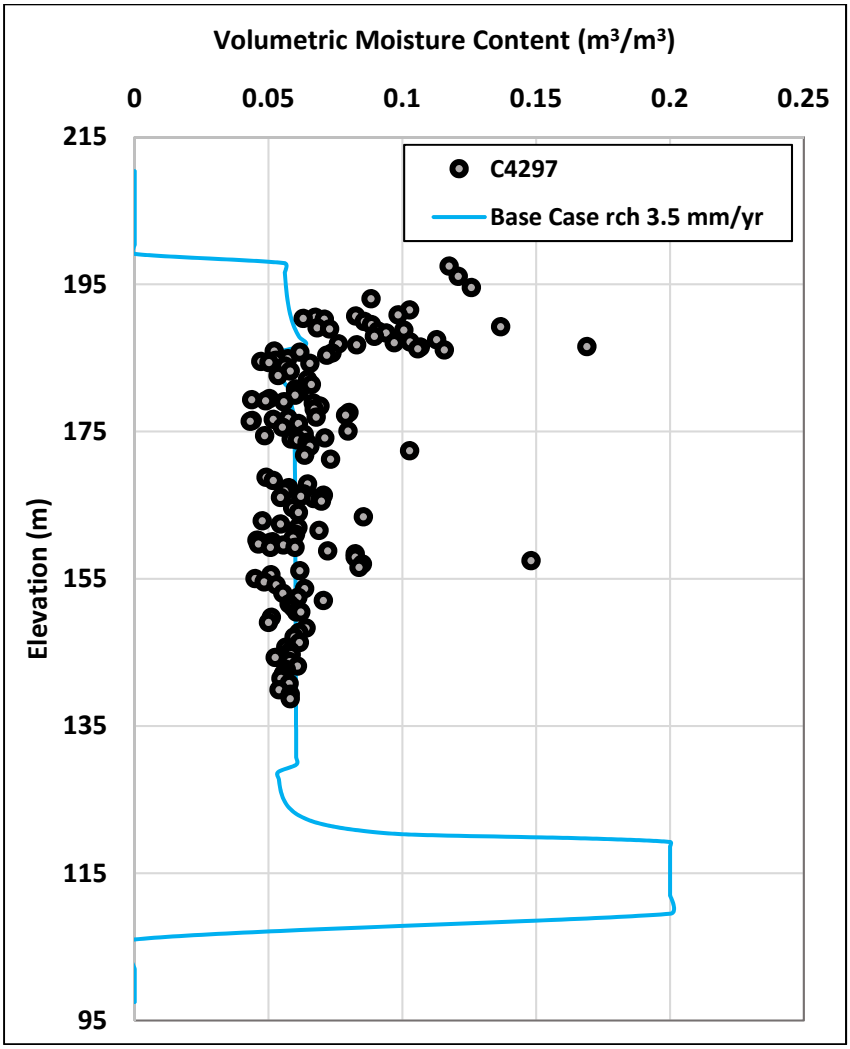

6.4.6 Basis for Saturated Zone Model Development

For the WMA C PA modeling, the unconfined aquifer is treated as an EHM, where effective parameters and appropriate boundary conditions derived from a regional scale groundwater flow model are used. The development of the model parameters is discussed in Appendix C. A calibrated CPGWM (CP-47631, Revision 2) serves as the basis for developing macro-scale parameters for the unconfined aquifer at WMA C. The development of CPGWM incorporates over 30 years of experience on development and application of groundwater models for the

Central Plateau [PNL-10886, "Development of a Three-Dimensional Ground-Water Model of the Hanford Site Unconfined Aquifer System: FY 1995 Status Report"; PNNL-13641; PNNL-14398, "Transient Inverse Calibration of the Site-Wide Groundwater Flow Model (ACM-2): FY 2003 Progress Report"; PNNL-14753, "Groundwater Data Package for Hanford Assessments"; PNNL-12261].

The CPGWM incorporates the large-scale geologic and hydrogeologic features and provides estimates of water levels, hydraulic gradients, and groundwater flows throughout the 200 West and 200 East Areas, for current and expected future groundwater conditions. Simulated water levels are compared to observed values for wells located upgradient (well 299-E27-15) and downgradient (well 299-E27-14) of WMA C (Figure 6-63). The observed heads and CPGWM-simulated heads, representing a time span of over 20 years, compare well, providing confidence in the predictive capabilities of the CPGWM as well as how the WMA C saturated media properties are parameterized and groundwater fluxes apportioned in the PA.

6.4.7 Verification of Air Pathway Modeling Approach

Among the radionuclides contained in the wastes in WMA C at closure, four of them can potentially emanate in gaseous form. These radionuclides are ^{14}C (as CO_2), ^{3}H (as H_2), ^{129}I (as I_2), and ^{222}Rn (as radon gas). However, radon is not included in the air pathway.

Appendix E provides verification of the air-pathway modeling approach by building confidence that diffusive flux can be adequately modeled to meet the PA performance requirements. The PA model methodology for air pathway calculations is compared to the modeling results generated using EPA CAP88-PC model-based results and those calculated from the recent Hanford Site NEPA Characterization Report (PNNL-6415) for a given receptor location and a given set of inputs. The comparison of results indicates that the WMA C PA model built for the air pathway calculation is valid for its intended purpose.

Figure 6-63. Central Plateau Groundwater Model Calibration Results in the Vicinity of Waste Management Area C.

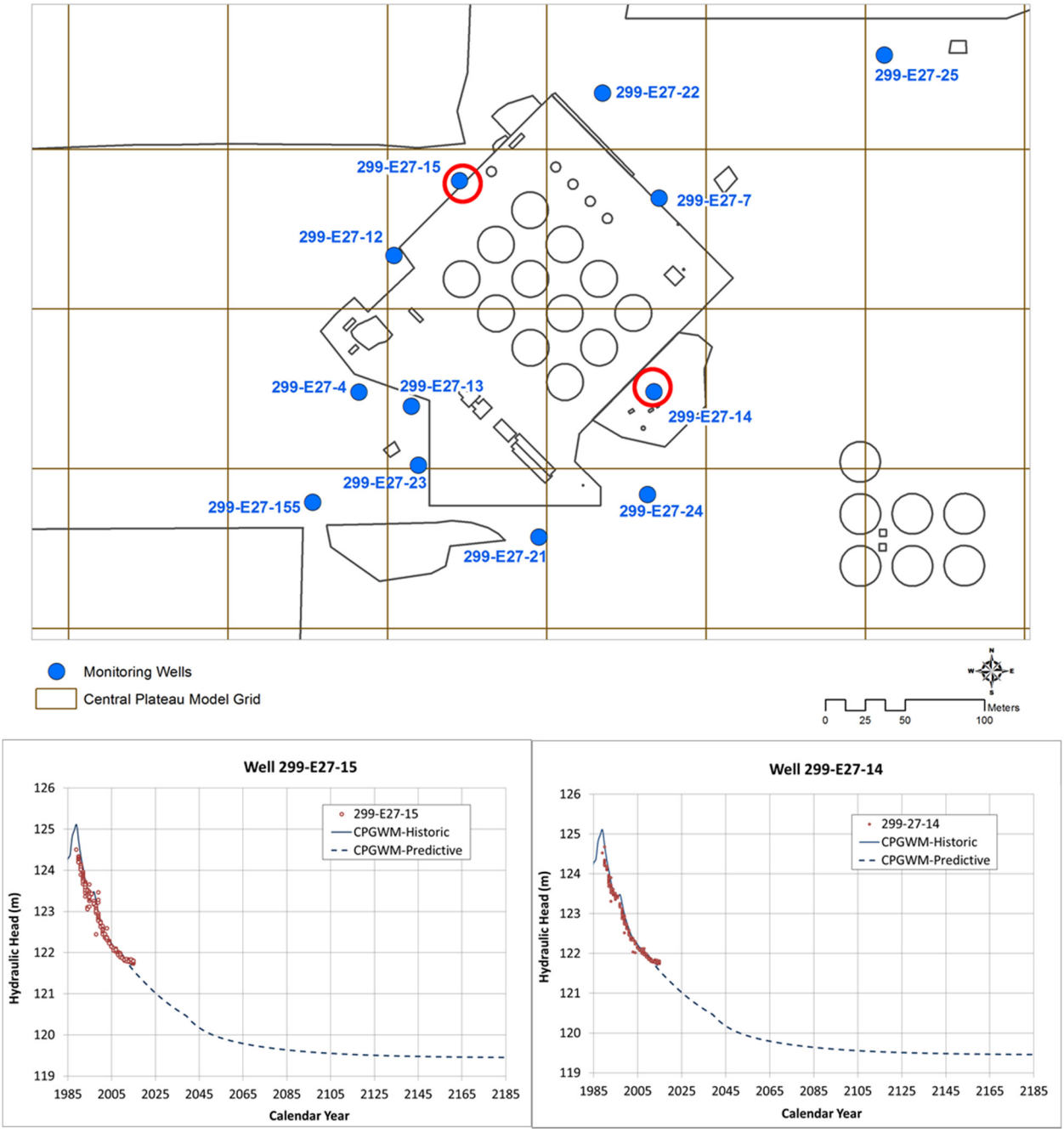

CPGWM = Central Plateau Groundwater Model

Reference: CP-47631, "Model Package Report: Central Plateau Groundwater Model Version 6.3.3."

7.0 RESULTS OF ANALYSIS

This section presents the results of the analyses described in Section 6.0 and discusses the (1) release of radionuclides from the source term (Section 7.1), and (2) environmental transport of radionuclides via the groundwater pathway (Section 7.2.1) and the air pathway including the radon analysis (Section 7.2.2). The results of the analyses conducted for each part of the modeling effort are summarized independently, leading to separate discussions of the groundwater and all-pathways dose presented in Section 7.3. Intermediate results are presented to illustrate the influence of each analysis step on the overall result. Results are provided for two time periods: compliance period (1,000 years) (2020 to 3020), and post-compliance period (up to 10,000 years from closure). Results are provided for the receptor located 100 m (328 ft) downgradient from WMA C. Intermediate results and doses are also projected out 10,000 years to identify peaks for some radionuclides that migrate slowly through the environment. The results from 1,000 to 10,000 years are given for completeness, but these are not part of the DOE O 435.1 compliance determination.

7.1 SOURCE TERM

The source term is defined as the rate of release from the facility as a function of time (NCRP Report 152). Since it is defined as a release from the facility, it includes a number of processes associated with mobilization of contaminants from the waste form and migration of the contaminants to the boundary of the facility. The boundary of the facility for WMA C source term is considered the outer boundary of the engineered features (i.e., the bottom of the tank base mat, or the outer surface of catch tanks, pipelines, and other ancillary equipment).

For the groundwater pathway, a total of 19 different sources for releases to groundwater are evaluated in the PA, which contribute to the overall source term. These sources consist of the twelve 100-series tanks, four 200-series tanks, C-301 catch tank, 244-CR vaults, and pipelines. The residual inventory and waste volume associated with each source is treated separately, resulting in an analysis of transport through groundwater for each source. Sources are added together to calculate the total impact as part of the groundwater analysis because plumes from different sources overlap in the groundwater analysis. This allows the impacts from each individual source to be placed in context to other sources, as well as the calculation of an individual source to the total impact of WMA C on the groundwater pathway.

For the situation when the tank concrete and infill grout are intact, the conceptual model is as follows. The intact concrete and grout cause any water in contact with residual wastes to be stagnant. As a result, the only driving force for migration of contaminants in residual wastes to the boundary of the engineered barriers is the chemical potential gradient between the waste and the tank surroundings. Therefore, mass release calculations are controlled by diffusion through the engineered structures (for tanks, the base mat) for all the sources except for the pipelines, which are considered advection-dominated because it is uncertain how much reliance can be placed on the waste transfer pipelines being intact. It is noteworthy that the conditions that produce a diffusion-dominated transport condition are not primarily based on, and indeed are not reliant on, an assumption that the base mat is intact. Instead, the diffusional release is caused

mainly by the infill grout, which limits water flow rates through the base mat. As discussed in Section 6.2.1.2 (Evaluation of Tank Stability), the infill grout is expected to be stable for long periods of time based on samples taken from C-107 tank dome and the sidewall of tank 241-A-106. As a result, this intact tank configuration with diffusional releases is the primary situation modeled in this PA, and is included in the base case analysis. Other conceptual models have been implemented in several of the sensitivity cases (see Section 8).

The base case release rate for ^{99}Tc from each of the sources in the source term is presented in Figure 7-1. An initial large release rate occurs for the pipeline source, and is attributable to the assumption that releases from the pipelines are dominated by advection. The sharp decline in the release rate is a reflection of source inventory depletion, and to a lesser extent of declining flow rate as the system responds to the placement of the cover. At closure (during emplacement of surface cover), the recharge rate changes from 100 mm/yr (3.9 in./yr) (operations time period) to the early Post-Closure recharge rate of 0.5 mm/yr (0.02 in./yr) (over 500 years). As a result, the vertical flow rate through the vadose zone adjusts slowly to the imposed boundary conditions. Nearly all of the ^{99}Tc inventory associated with the pipeline source term is released by approximately 100 years after closure (see Figure 7-1). In contrast, the release rate from grouted tanks increases gradually. This is partly attributable to an initial small release fraction (6%) of the ^{99}Tc inventory that is available for instantaneous release, while the rest of the inventory is made available gradually, reflecting waste form degradation process (see Section 6.3.1). However, the gradual release occurs over a relatively short time, and the primary control for the tank release rates is the diffusive transport through the tank base mat with associated sorption.

The magnitude of release rates for ^{99}Tc from each source is proportional to the chemical gradient as determined by the amount of residual inventory of ^{99}Tc within each source. Therefore, the release rate from tank C-105 is the highest since it has the highest residual inventory (7.83 Ci at closure). Releases from tank C-107, tank C-111, and tank C-112 have similar releases rates, as they have similar residual inventories of ^{99}Tc (~2 Ci each). The release rate from other sources is much smaller, owing to their smaller inventories.

The small rise in release rate noticeable at about 500 years is due to an increase in Darcy flux, when the surface barrier is assumed to transition to its degraded state and the recharge rate changes from 0.5 mm/yr (0.02 in./yr) to 3.5 mm/yr (0.14 in./yr). The diffusive release rate shows a slow gradual decline over the simulated time period, indicating that not all of the inventory of ^{99}Tc has been released by 10,000 years.

Figure 7-2 compares the concentration resulting from release of ^{99}Tc from the waste to that from the bottom of the tank base mat. There is a sharp initial spike in concentration due to the initial release fraction, followed by a gradual decrease in concentration. However, the concentrations exiting the tank base mat bottom show an initial increase reflecting the establishment of a steady concentration gradient through the base mat. The concentration then slowly decreases as the inventory is slowly depleted by diffusion.

Figure 7-1. Release Rate of Technetium-99 (pCi/yr) from Each Source.

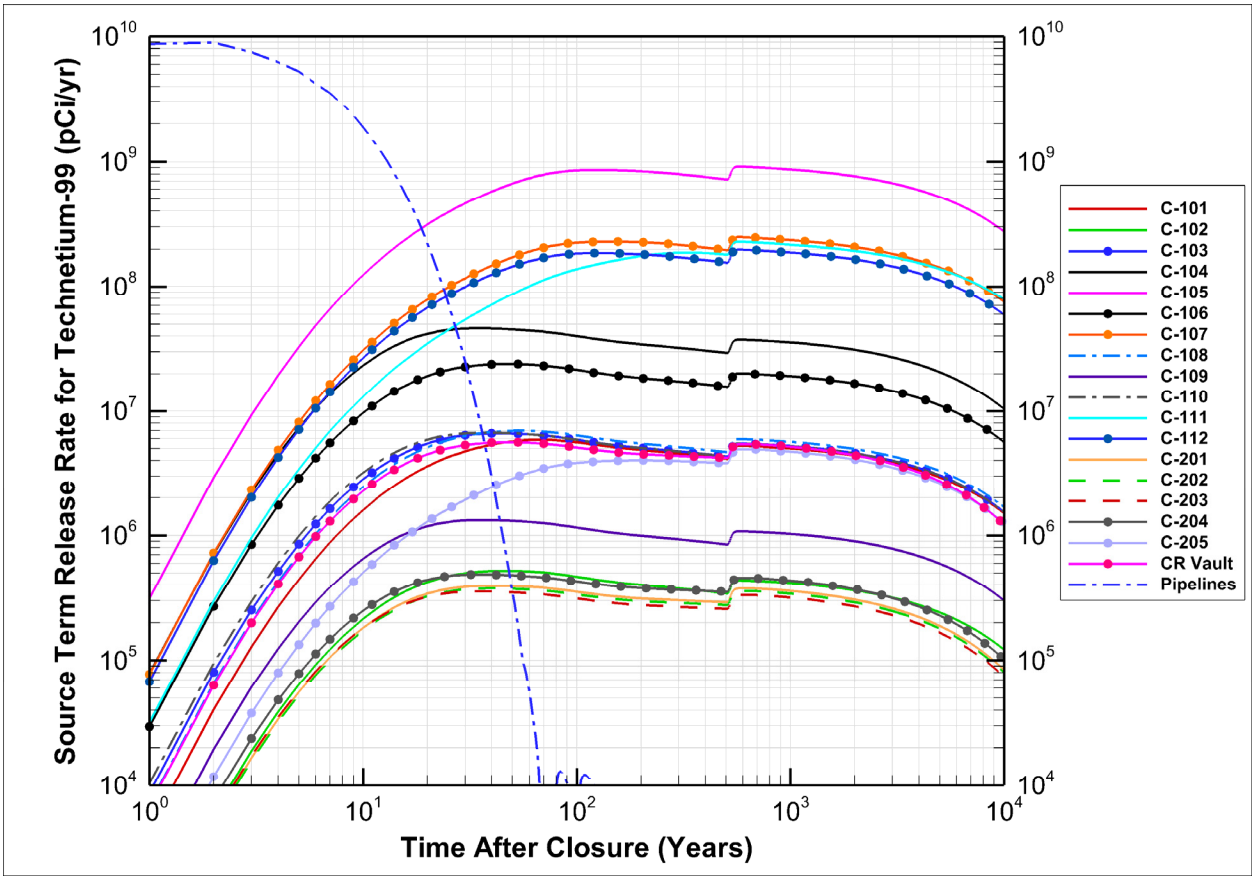

The release rate for ^{238}U from selected sources is presented in Figure 7-3; these sources illustrate representative behavior of the other sources in WMA C. The uranium solubility limits in the source cause the ^{238}U concentrations for several sources terms to be the same, and therefore only selected sources are presented in the figure. As discussed in Section 6.2.1, when the tank and infill grout are intact, the uranium solubility limit is set to 1×10^{-4} mol/L for the first 1,000 years and to 1×10^{-6} mol/L thereafter. Figure 7-4 presents two curves of the time-varying dissolved ^{238}U concentrations; one exiting the residual waste, and the other exiting out the bottom of the tank base mat for tank C-105. The general trends of these curves for tank C-105 provide a good example of the general shape of the similar curves for dissolved ^{238}U concentrations from other 100-series tanks. The concentrations released from the residual waste remain constant, consistent with the solubility limits, including the assumed step change at 1,000 years. This indicates that there is sufficient inventory of uranium retained in the tanks to maintain the solubility limit at the end of the simulation. The concentration leaving the tank remains at least an order of magnitude below the concentration leaving the residual waste, consistent with the sorption in the concrete and grout matrix.

The difference in release rates between tank C-105 and tank C-201 (Figure 7-3) are the result of different diffusive areas (tank bottom area). The release rate from the pipelines, as previously discussed, is primarily by advection, and therefore shows markedly different behavior. The pipeline release rate shows an initial decline, followed by increase at around 500 years and then

steep decline at around 700 years. The first 700 years reflect the transient effect of changing recharge as the system responds—first, to the addition of the closure cover, and second, to the assumed degradation of the cover function. The steep decline after 700 years is attributable to depletion of the pipeline inventory, such that dissolved concentrations drop below the solubility limit. The long-term gradual decline following the steep decline reflects the effect of near-field concentrations on advective and diffusive releases through the pipeline. As the released uranium mass moves slowly through the vadose zone, some backward diffusion occurs to the source inventory cell due to reversal of concentration gradient (for the pipeline). This mass then diffuses out of the inventory cell, resulting in a slowly declining release.

Figure 7-2. Comparison of Dissolved Concentration of Technetium-99 (pCi/L) in the Residual Waste and Tank Bottom for Tank 241-C-105.

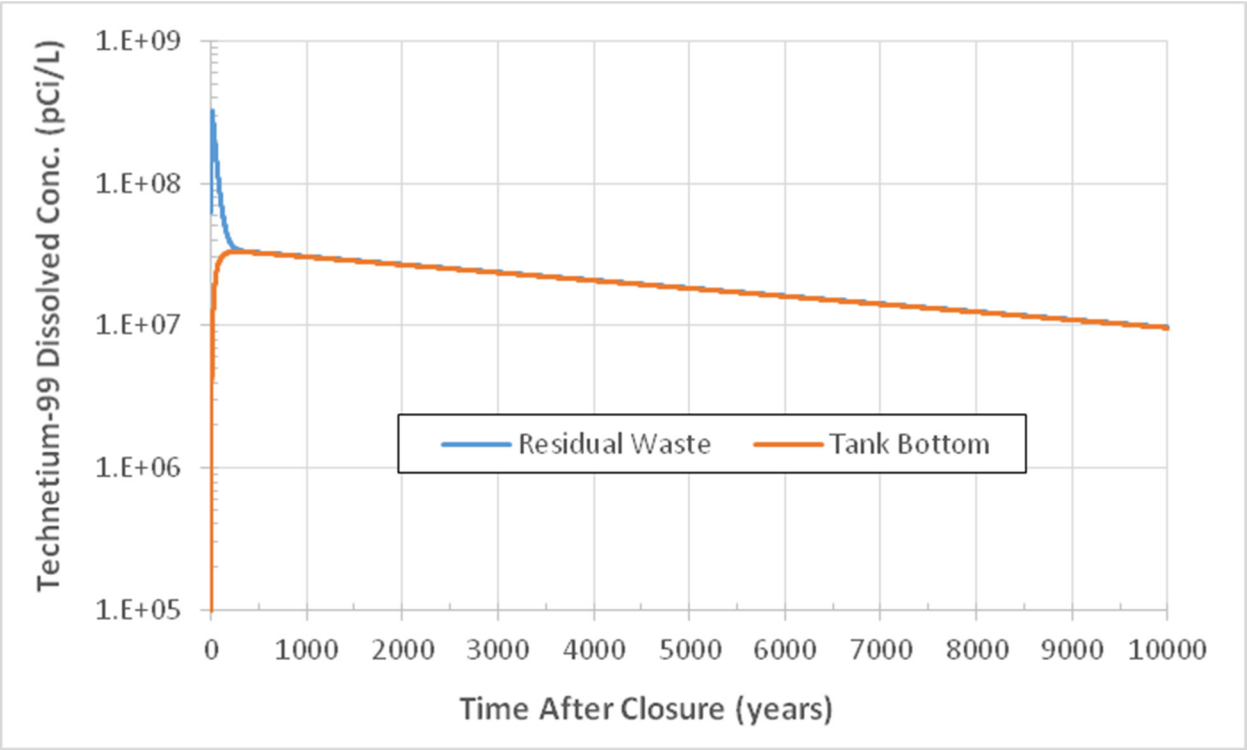

The release rates for uranium (total) from representative sources are presented in Figure 7-5. These exhibit similar behavior to the release rates for ^{238}U, as expected.

For all other analytes modeled, the releases are simpler, as no solubility limits or waste form degradation mechanisms are considered. For pipelines, the release is primarily by advection. For the remaining sources, where intact grouted tank conditions are assumed, the release mechanism is diffusion through the tank base mat. The effective diffusion coefficient for all of the analytes through the concrete and grout layer is 3×10^{-8} cm^2/s (4.7×10^{-8} in.^{2}/s) (based on the half-cell diffusion experiments conducted on ^{99}Tc). Differences in diffusion behavior are the result of different partition coefficients (K_d), so that different apparent diffusion coefficients are applied to each analyte.

Figure 7-3. Release Rate of Uranium-238 (pCi/yr) from Representative Source Terms.

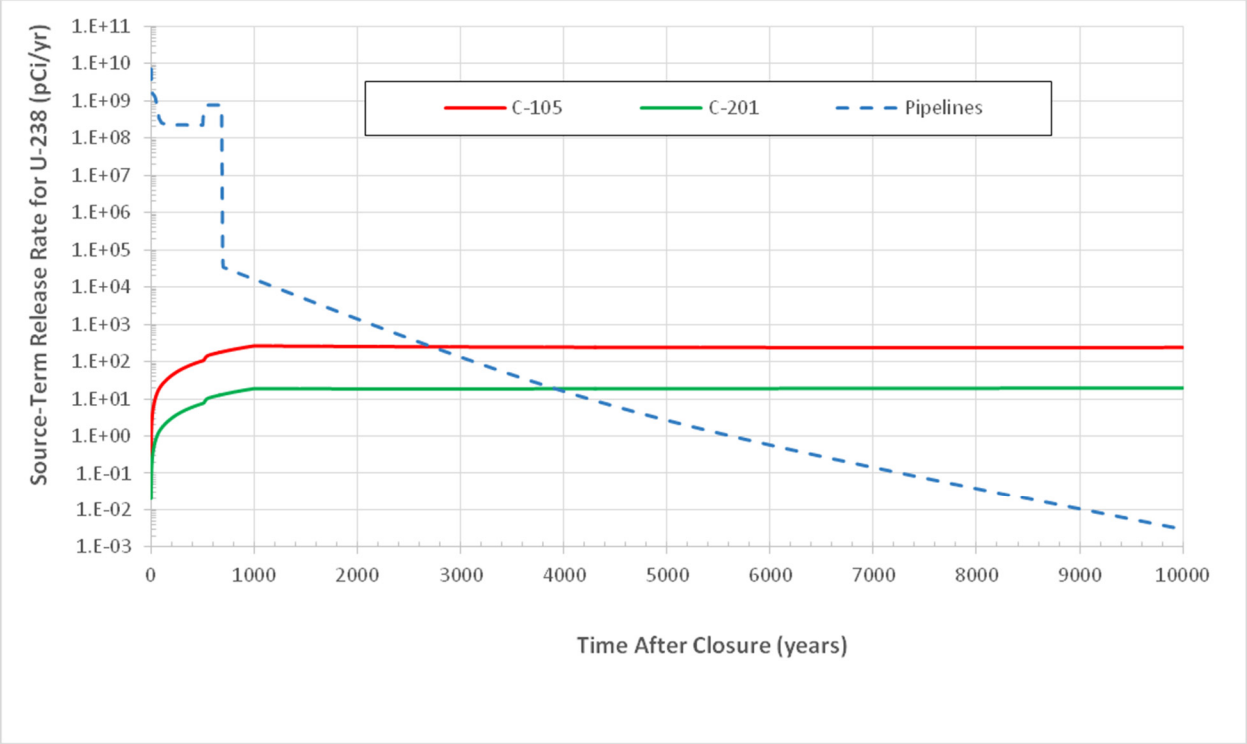

Figure 7-4. Comparison of Dissolved Concentration of Uranium-238 (pCi/L) in the Residual Waste and Tank Bottom for Tank 241-C-105.

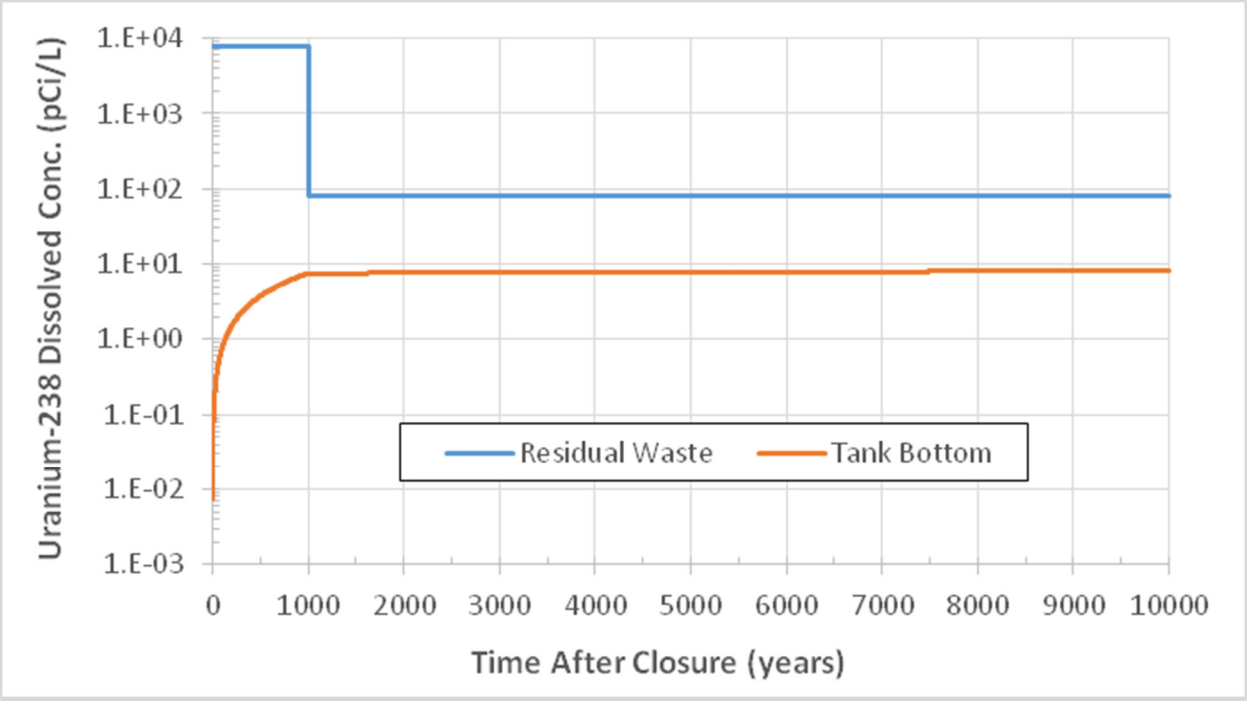

Figure 7-5. Release Rate of Total Uranium (g/yr) from Representative Sources.

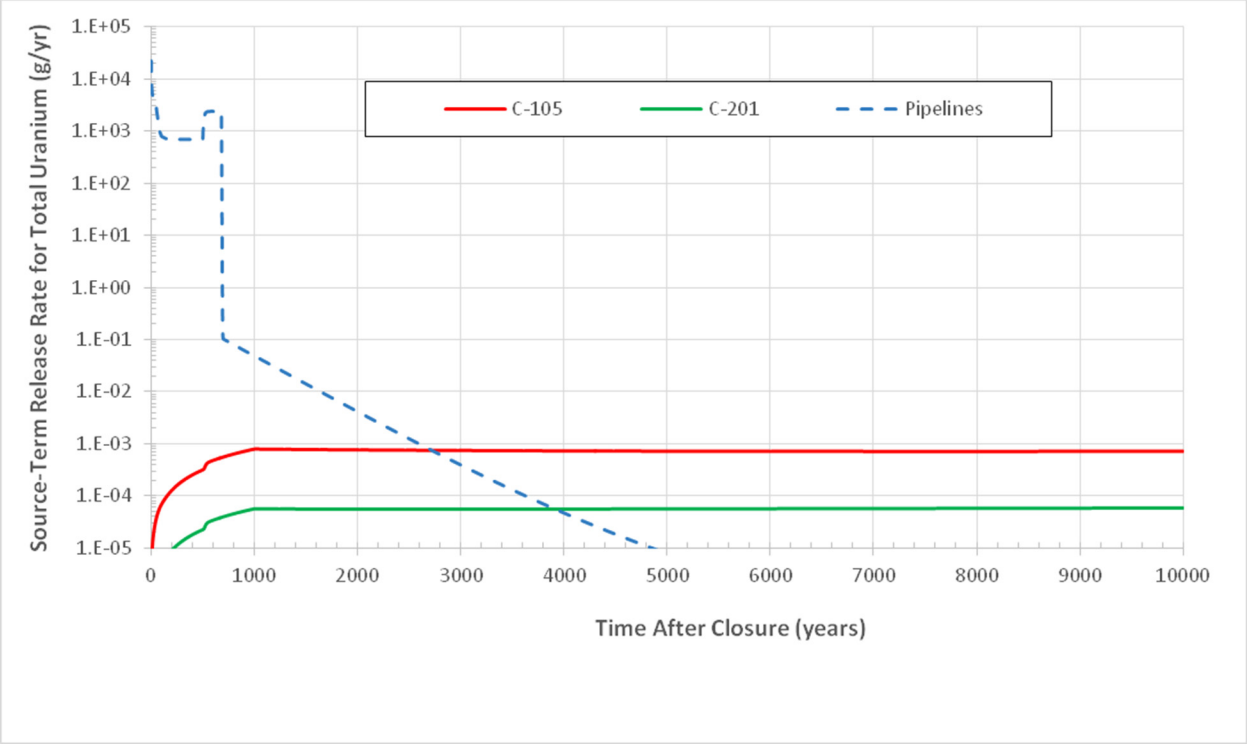

7.2 ENVIRONMENTAL TRANSPORT OF RADIONUCLIDES

This section presents the results of the analysis of the environmental transport of radionuclides for the groundwater pathway (Section 7.2.1) and the air pathway (Section 7.2.2). Tabular and graphical presentations of the summaries of the various transport calculations in water and air are presented. Discussions included in the air pathway results summarize the results of the transport of volatile radionuclides and transport analysis for radon.

7.2.1 Groundwater Transport of Radionuclides

This section presents the results of the analysis of the groundwater transport of radionuclides for the groundwater pathway, including its screening analysis. Tabular and graphical presentations of the summaries of the various transport calculations are presented. Discussions included in the air pathway results summarize the results of the volatile radionuclides and transport analysis for radon.

7.2.1.1 Result of Screening Analysis for Groundwater Pathway. The STOMP© 3-D groundwater flow and transport model was used to perform a screening analysis to identify those contaminants that are not sufficiently mobile to impact groundwater during the compliance and sensitivity/uncertainty analysis time frames. This screening step helps to streamline the PA, and to focus attention on the contaminants that affect performance.

The criterion chosen for screening is the first-arrival time of the contaminant. Hydraulic property selection was carried out to yield maximum transport rates. Maximum net infiltration rates were also assumed in the screening analysis. The screening evaluated an incremental range of K_d values between 0.1 mL/g and 2.5 mL/g (prior to gravel correction) to determine threshold values that reached the water table in 1,000 and 10,000 years. The use of screening methods is accepted by the EPA, and appropriate methods are outlined in EPA guidance (EPA/540/F-95/041, Soil Screening Guidance: Fact Sheet). This approach minimizes the number of contaminants eliminated from analysis. As a result, some contaminants may only arrive at the water table for particular sensitivity and uncertainty evaluations (i.e., evaluations that minimize the time of transport through the vadose zone). For the base case and many of the sensitivity cases, a number of the radionuclide contaminants not screened from further analysis may have no impact on the PA results because their transport to the water table requires more than 1,000 years (compliance time frame) or 10,000 years (the limit of the uncertainty/sensitivity analysis) for that particular case.

Results of the screening analysis are presented in Figure 7-6. The results show that the time of first arrival is a strong linear function of the K_d value. From this relationship, the first-arrival time for any radionuclide can be estimated accurately by using the trend equation shown on the figure. According to the screening model results, the minimum K_d value that produces an impact to groundwater within the 1,000-year compliance time frame is ~0.15 mL/g (without any gravel correction), and ~1.5 mL/g (without any gravel correction) within the 10,000-year compliance time frame.

Figure 7-6. First-Arrival Time (in Calendar Year) of Radionuclides for Various K_d Values Based on Screening Analysis Using Subsurface Transport Over Multiple Phases.

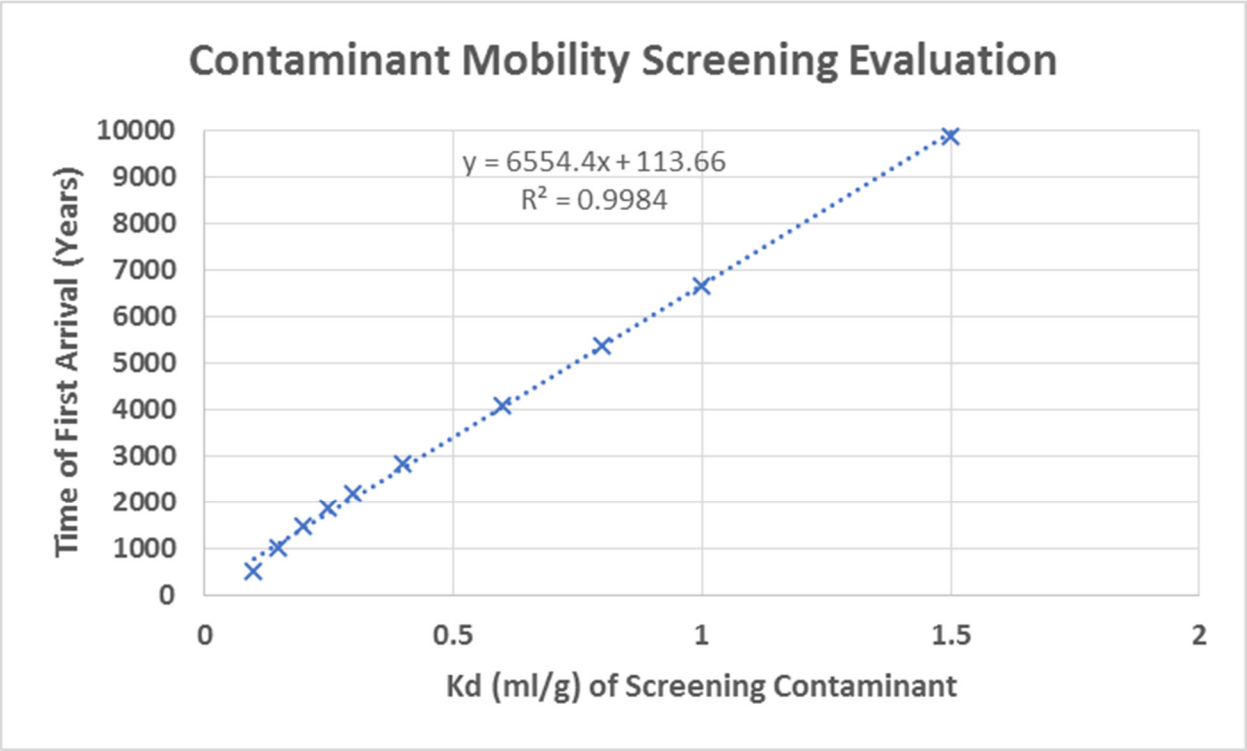

The first-arrival times for each of the representative K_d values used in the screening calculations using STOMP© are summarized in Table 7-1. The results of the screening analysis indicate that even when using parameter estimates biased to produce the greatest pore water velocity in the vadose zone: (1) contaminants with a $K_d > 0.15$ mL/g do not reach groundwater within the 1,000-year compliance time frame, and (2) radionuclides with a $K_d \geq 2.0$ mL/g do not reach groundwater within the 10,000-year post-compliance (i.e., uncertainty/sensitivity analysis) period (Table 7-1). While the actual K_d cutoff is likely only slightly greater than 1.5 mL/g, the screening evaluation did not include a representative contaminant with a K_d value between 1.5 mL/g and 2 mL/g (Table 6-11).

Table 7-1. First-Arrival Time (in Calendar Year) of Radionuclides for Various K_d Values Based on Screening Analysis Using Subsurface Transport Over Multiple Phases.

Contaminant K_d (material < 2 mm) (mL/g)	Calendar Year of First Arrival at Water Table	Time of Arrival, Post-Closure (Closure occurring in 2020) Years
0.10	2517.5	497.5
0.15	3022.5	1,002.5
0.20	3505	1,485
0.25	3900	1,880
0.30	4210	2,190
0.40	4840	2,820
0.60	6110	4,090
0.80	7390	5,370
1.0	8680	6,660
1.5	11900	9,880
2.0	>12020	>10,000
2.5	>12020	>10,000

Of the list of radionuclides in the WMA C residuals inventory and on the basis of the results of the screening phase, only seven (Table 7-2) are sufficiently mobile to arrive at groundwater during the compliance period, and three others (e.g., ^{129}I, ^{14}C, and the uranium isotopes) are sufficiently mobile to arrive at groundwater during the sensitivity/uncertainty analysis time frame. The other radionuclides in the WMA C residual inventory are not included in further groundwater impact analysis because they do not reach the water table within the evaluation time frames.

To complement the results of this screening analysis, an additional evaluation case was run to evaluate the peak doses for all 43 radiological COPCs beyond the 10,000-year post-closure time frame. The primary focus of this analysis is to evaluate the time and magnitude of peak doses resulting from some selected constituents, like the uranium isotopes (that were found to be rising at the end of the 10,000-year period analysis) and other sorbed constituents that could potentially

reach groundwater beyond the 10,000-year post-closure time frame. The specific assumptions of this evaluation case and its associated results are provided in Section 8.2.8 of this report.

Table 7-2. Radionuclides that Arrive at the Water Table within the 1,000-Year Compliance and 10,000-Year Sensitivity and Uncertainty Time Frame Based on the Screening Analysis Conducted Using Subsurface Transport Over Multiple Phases.

Radionuclides	K_d (material < 2 mm) (mL/g)	K_d (Backfill) (mL/g)	K_d (Hanford H1 and H3) (mL/g)	K_d (Hanford H2) (mL/g)
Radionuclides that may arrive at the water table within 1,000 years				
Co Isotopes	0	0	0	0
H Isotopes	0	0	0	0
Nb Isotopes	0	0	0	0
Rn Isotopes	0	0	0	0
Tc Isotopes	0	0	0	0
Se Isotopes	0.1	0.05	0.06	0.08
I Isotopes	0.2	0.09	0.12	0.16
Radionuclides that may arrive at the water table within 10,000 years				
Sn Isotopes	0.5	0.23	0.29	0.4
U Isotopes	0.6	0.28	0.35	0.48
C Isotopes	1	0.46	0.58	0.8

7.2.1.2 Results of Base Case Evaluation for Groundwater Pathway.

7.2.1.2.1 Flow Analysis. The moisture content in the vadose zone underneath WMA C changes in response to changes in the recharge imposed by the surface conditions. This includes an increase in moisture content that occurs during the operations period, and an eventual decrease in moisture content caused by the performance of the surface barrier. The moisture content is also influenced by the presence of the tank structures, which divert the water around the low permeability structures. For the base case, the tank structures are assumed to remain intact for the duration of the analysis.

The calculated moisture content profile at tank C-105 is presented in Figure 7-7(a-d) for the base case inputs for flow, for four times in the evolution of the facility. The pre-Hanford profile is shown in Figure 7-7(a). This profile provides a reference point for the subsequent behavior of the system in response to changes in the net infiltration rates. The range for the Hanford H2 Sands is from 0.059 to 0.060 for the pre-Hanford time period. The moisture content profile at the time of closure, when the surface barrier has just been constructed, is shown in Figure 7-7(b). This moisture profile is higher relative to the pre-Hanford profile, ranging from 0.076 to 0.088 in the Hanford H2 Sands, owing to the elevated net infiltration during the operational period. The response after 100 years to the construction of the surface barrier is shown in Figure 7-7(c). The

moisture content has decreased as the system responds to the lower recharge produced by the surface barrier; the range for the Hanford H2 Sands is from 0.056 to 0.061. In the base case analysis, the surface barrier is assumed to degrade after 500 years, leading to a return to a pre-Hanford recharge rate. As shown in Figure 7-7(d), by 1,000 years after closure the system has re-equilibrated to a steady-state moisture regime, with a moisture content profile similar to the pre-Hanford moisture content distribution shown in Figure 7-7(a).

Throughout this evolution, the changes in the moisture content profile are relatively small, despite the changes in net infiltration at the surface. These results are consistent with the hydraulic conductivity-moisture content relationships presented for the HSUs in Appendix B. The pre-Hanford and Hanford operations recharge rates, 3.5 mm/yr and 100 mm/yr (0.14 in./yr and 3.9 in./yr), respectively, translate to vertical unit gradient fluxes of 1.1×10^{-8} cm/s and 3.7×10^{-7} cm/s (4.3×10^{-9} in./s and 1.5×10^{-7} in./s), respectively. According to Figure B-13, the equilibrium matric potential values of Hanford H2 Sand for unsaturated hydraulic conductivity values of 1.1×10^{-8} cm/s and 3.7×10^{-7} cm/s (4.3×10^{-9} in./s and 1.5×10^{-7} in./s) are 190 cm and 90 cm (75 in. and 35 in.), respectively. According to Figure B-12, the equilibrium moisture content values of Hanford H2 Sand for matric potential values of 190 cm and 90 cm (75 in. and 35 in.) are ~0.061 and 0.085, respectively, which is consistent with the range of values indicated in Figure 7-7.

The calculated moisture content profile for a location between four 100-series tanks (C-105, C-106, C-108, and C-109) is presented in Figure 7-8. The pre-Hanford profile and range in Hanford H2 Sand moisture content shown in Figure 7-8(a) is almost identical to the profile shown in Figure 7-7(a) because the two locations are so close and the geology is essentially the same. Similar to Figure 7-7(a), Figure 7-8(a) provides a reference point for the subsequent behavior of the system in response to changes in the net infiltration rates. The moisture content profile at the time of closure shown in Figure 7-8(b) indicates that the moisture content, ranging from 0.083 to 0.089 in the Hanford H2 Sands, is elevated compared to both the pre-Hanford profile and the profile shown in Figure 7-7(b). The increase in moisture content compared to Figure 7-7(b) results from the tank umbrella effect that diverts infiltrating water from the tank domes to the area(s) surrounding the tanks. The response 100 years after closure is shown in Figure 7-8(c). It is almost identical to the response below tank C-105 shown in Figure 7-7(c) because with the surface barrier limiting net infiltration to 0.5 mm/yr (0.02 in./yr), the tank umbrella effect becomes inconsequential. By 1,000 years after closure the system has re-equilibrated to a steady-state moisture regime (Figure 7-8[d]). The moisture content profile appears very similar to the pre-Hanford moisture content profile shown in Figure 7-8(a), and Figure 7-7(a) and 7-7(d) below tank C-105.

Figure 7-7. Moisture Content in the Vadose Zone at Tank 241-C-105 in Waste Management Area C for Four Times of Interest: (a) Pre-Hanford Steady State, (b) Waste Management Area C Closure, (c) 100 Years after Closure, and (d) At 1,000 Years.

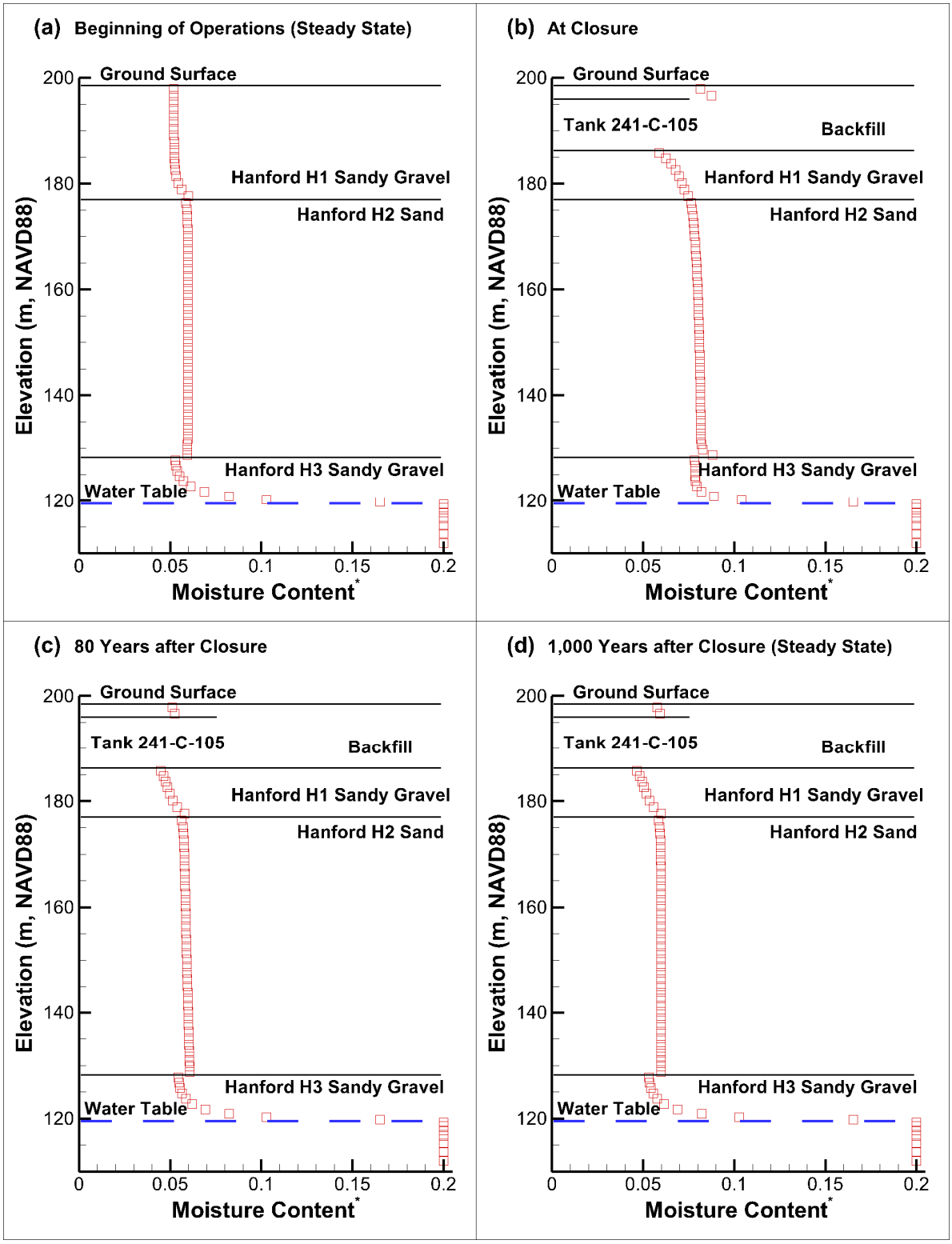

*The moisture content below the water table is equal to the porosity.

Figure 7-8. Moisture Content in the Vadose Zone in Waste Management Area C between Tanks 241-C-105, 241-C-106, 241-C-108, and 241-C-109 for Four Times of Interest: (a) Pre-Hanford Steady State, (b) Waste Management Area C Closure, (c) 100 Years after Closure, and (d) At 1,000 Years.

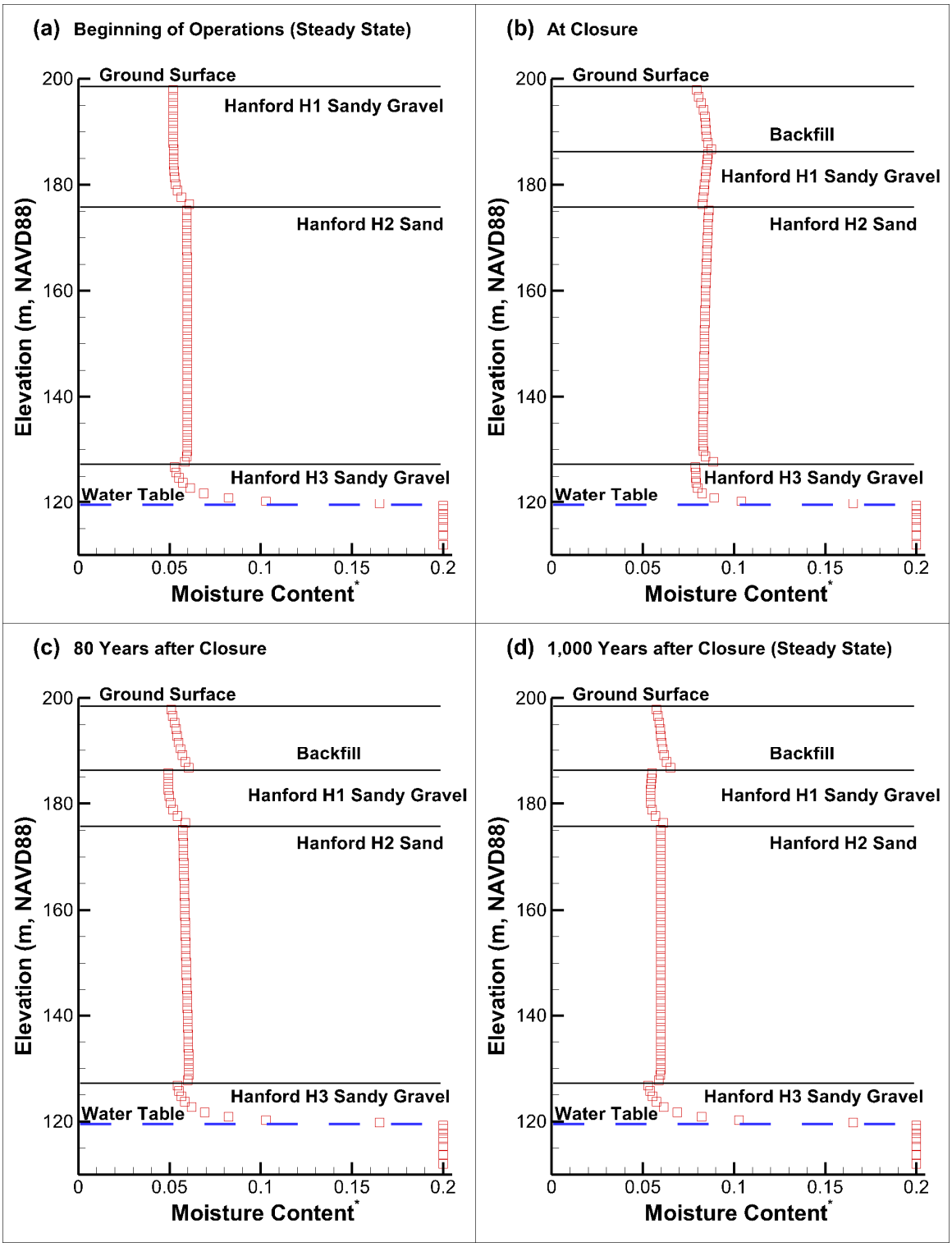

*The moisture content below the water table is equal to the porosity.

By contrast, the changes in the vertical Darcy flow rate or flux are more apparent than the changes in moisture content. Changes in the flux are going to be almost directly proportional to the changes in net infiltration, except where and how the tank shadow and umbrella effects influence the flow. The shadow effect of the tank appears most prominently immediately below the base and diminishes throughout the depth. Prior to construction of the tanks, the vertical velocity is essentially uniform, with only minor variations at the interfaces between soil units, as shown in Figure 7-9(a). For the remaining times, immediately below the tanks a shadow effect is observed, in which the velocity approaches zero, as shown in Figure 7-9(b-d). The shadow effect is strongest in the H1 layer, and remains throughout the simulation. The depth and extent of the shadow zone in the H2 layer is affected by the changing recharge on the system. The flux approaches the recharge rate imposed at the surface at the greater depths, increasing toward the value imposed at the surface (Figure 7-9[b] and [c]). The shape of the velocity profile shown in Figure 7-9(c) reflects the drainage of antecedent moisture once the surface barrier is added, indicating the velocity near the water table is the last to achieve steady state [compare Figure 7-9(c) and (d)].

Figure 7-9(d) shows the response to the degradation of the surface barrier, and the velocity profile in the H2 layer is similar to the pre-Hanford conditions shown in Figure 7-9(a). By 1,000 years post-closure, the moisture profile reaches a condition of nearly uniform downward flow, particularly in the Hanford H2 Sand, reflective of the 3.5 mm/yr (0.14 in./yr) recharge imposed in the modeling domain [see Figure 7-7(d)].

The consequences of the umbrella effect appear most prominently in the area between the tanks (Figure 7-10). Figure 7-10(a) indicates that the flux prior to tank farm construction is fairly uniform throughout the depth, similar to Figure 7-9(a). Once the tanks are present, the umbrella effect diverts and concentrates infiltrating water between them, and the flux in the backfill approaches almost twice the recharge rate imposed at the surface [Figure 7-10(b)]. At greater depths, the umbrella effect dissipates and the flux approaches the recharge rate imposed at the surface.

Figure 7-10(c) illustrates the transient conditions that occur after the surface barrier is emplaced. Eighty years is not sufficient to reach steady state as indicated by the non-uniform flux profile. The umbrella effect continues to concentrate water introduced during the operations period between the tanks while it drains, but the flux in the shallower depths, both near the surface and in the Hanford H1 Sandy Gravel, responds more quickly to changes in the recharge rate imposed at the surface. Throughout the Hanford H2 Sand, the flux is decreasing compared to the operation period [compare Figure 7-10(c) and (b)], but the flux has not achieved steady state, as indicated by the non-uniform profile. After 1,000 years [Figure 7-10(d)], the profile below the depths impacted by the umbrella effect appears fairly uniform, indicating that the system has achieved steady state.

Figure 7-9. Darcy Flux in the Vadose Zone at Tank 241-C-105 in Waste Management Area C for Four Times of Interest: (a) Pre-Hanford Steady State, (b) Waste Management Area C at Closure, (c) 100 Years after Closure, and (d) At 1,000 Years after Closure.

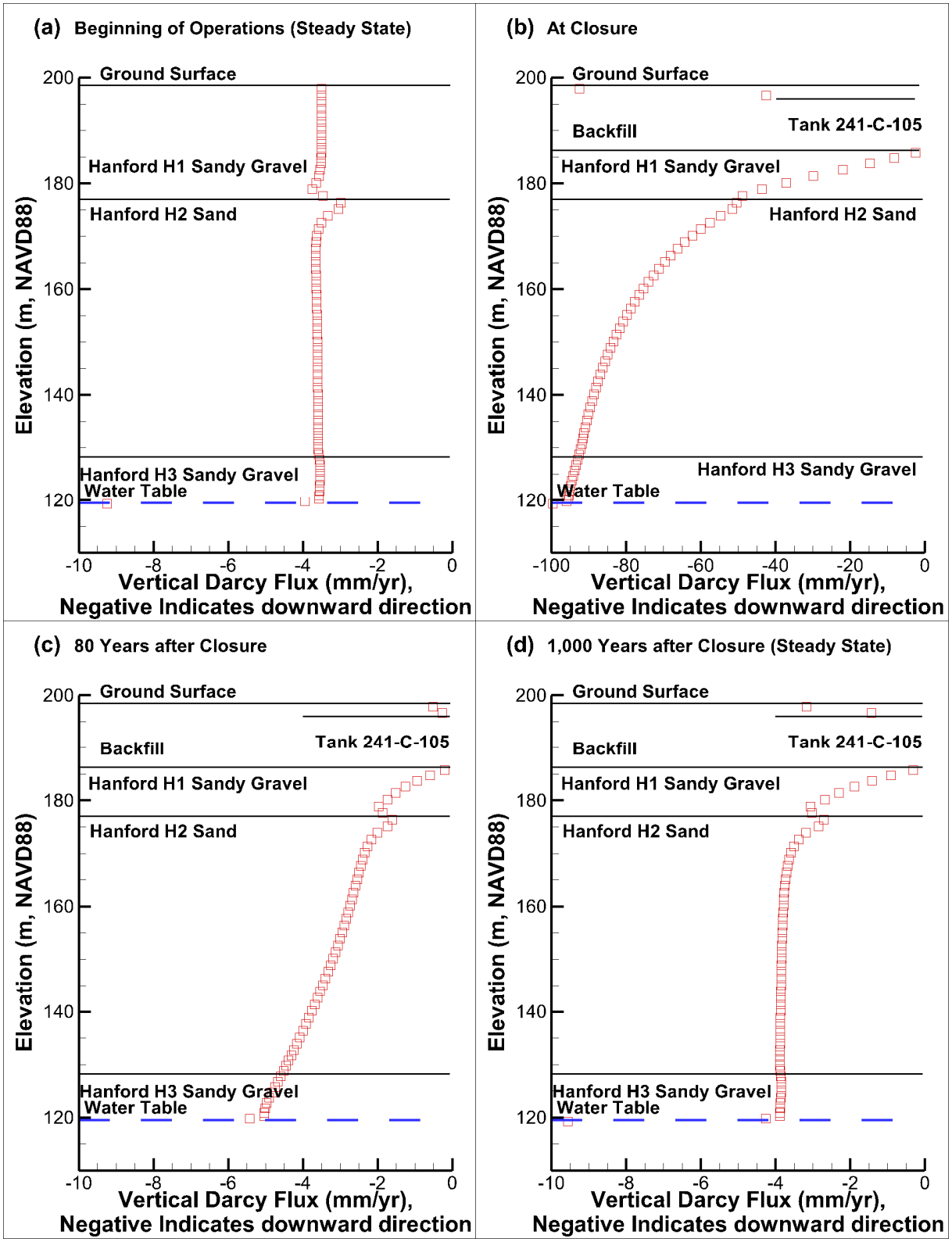

Figure 7-10. Darcy Flux in the Vadose Zone in Waste Management Area C between Tanks 241-C-105, 241-C-106, 241-C-108, and 241-C-109 for Four Times of Interest: (a) Pre-Hanford Steady State, (b) Waste Management Area C at Closure, (c) 100 Years after Closure, and (d) At 1,000 Years after Closure.

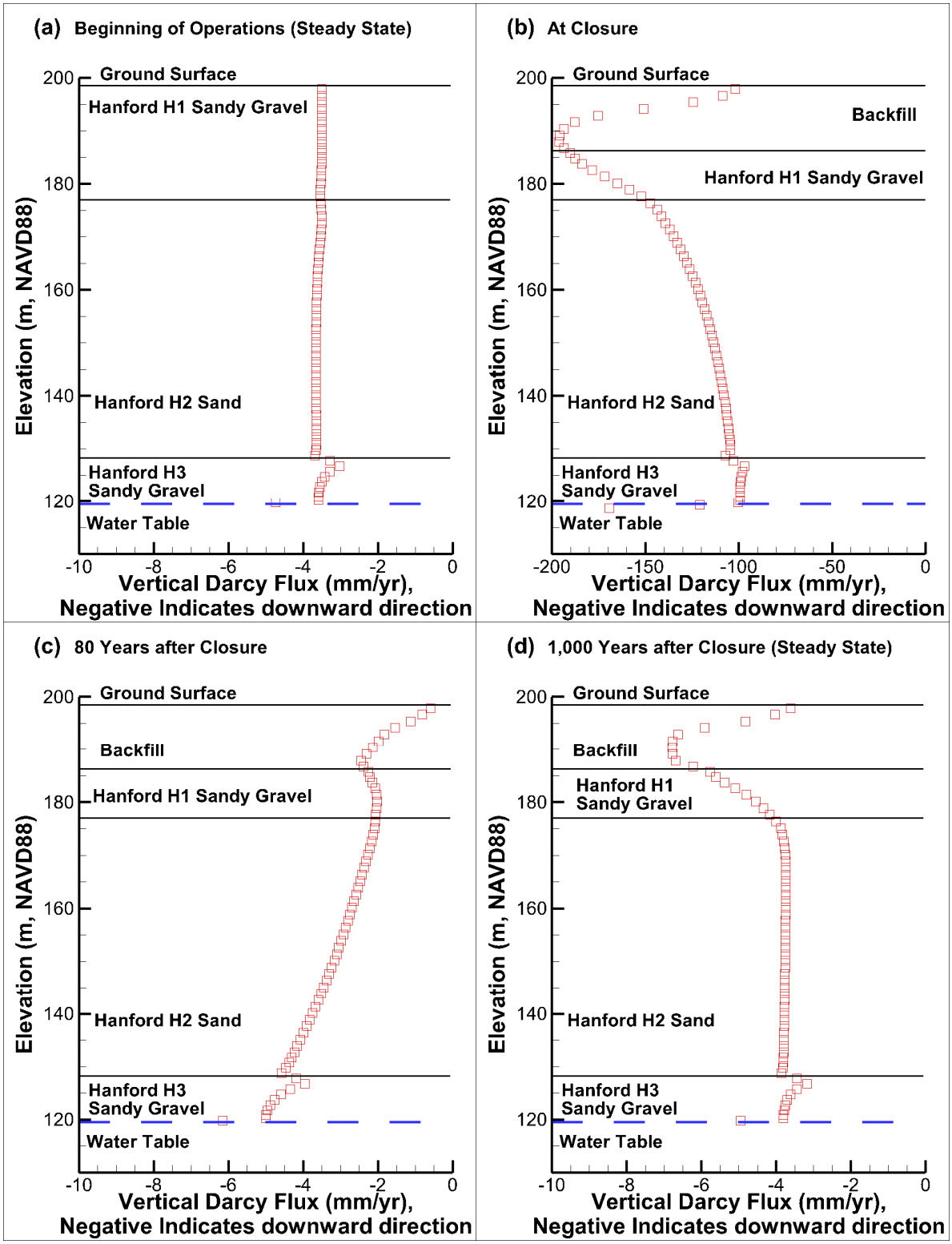

7.2.1.2.2 Transport Analysis. DOE M 435.1-1 requires that the WMA C PA includes calculations of the highest calculated concentration or dose, with an allowance for some volume averaging based on projected groundwater use, beyond a 100-m (328-ft) buffer zone surrounding WMA C. To determine the highest groundwater concentration, the modeling results indicate the average concentration in the aquifer within nine segments along the line perpendicular to, and 100 m (328 ft) beyond, the southeast edge of WMA C (Figure 7-11). The nine segments are ~30 m (98 ft) long (see Table D-11 in Appendix D), and aligned such that the centerlines of the plumes in the groundwater resulting from the residuals released from a single line of 100-series tanks parallel to the direction of groundwater flow (e.g., the centerline of the plumes resulting from the tank residuals in C-102, C-105, C-108, and C-111) intersect the perpendicular line within the same segment.

Figure 7-11. Points of Calculation 100 Meters Downgradient of Waste Management Area C.

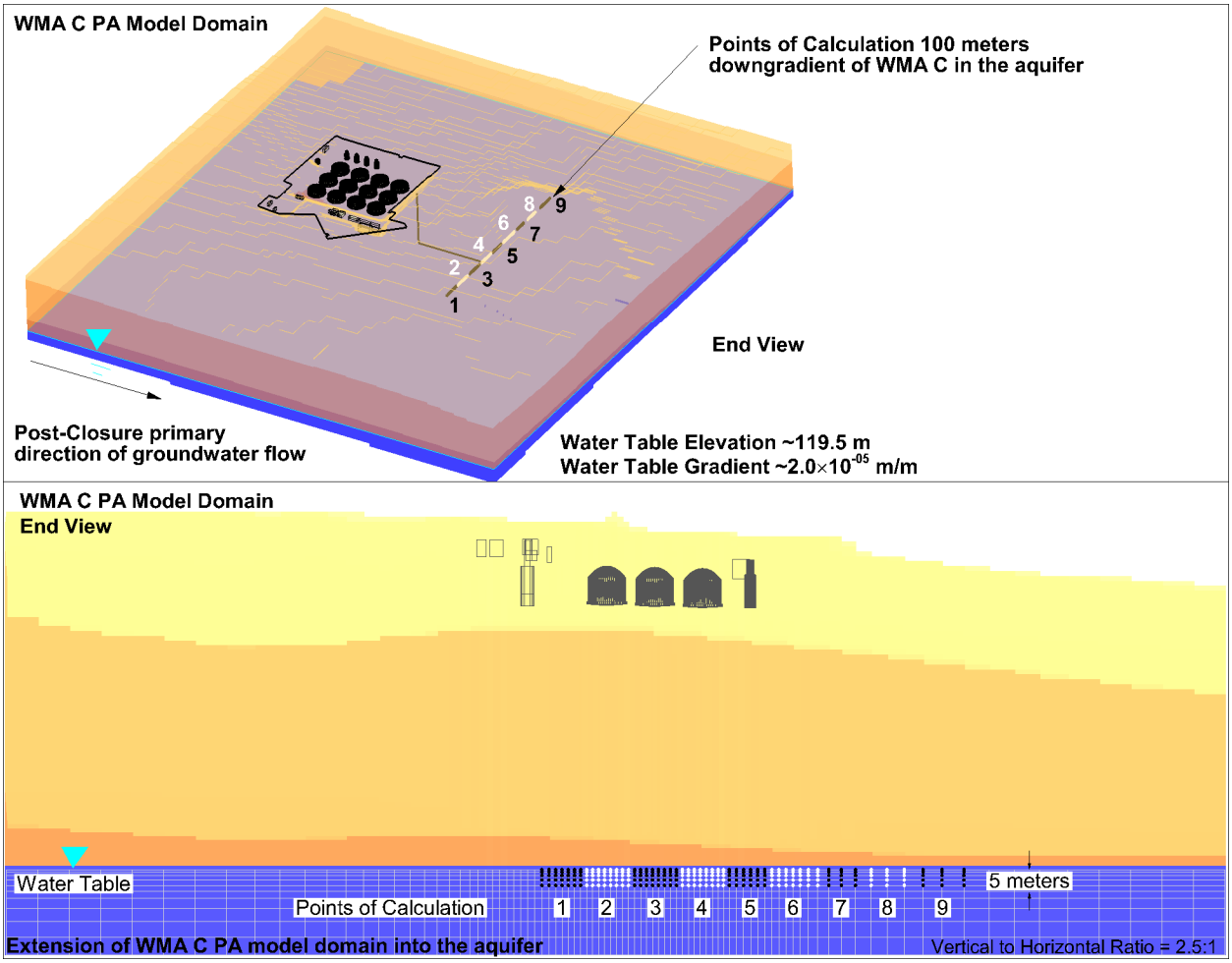

PA = Performance Assessment WMA = Waste Management Area

DOE M 435.1-1 does not specify the level of protection required for water resources and there are no applicable parameterization requirements or guidelines indicated in DOE G 435.1-1, Chapter 4. The DOE manual and guide state that the aquifer mixing must be consistent with

State or local laws, regulations, or agreements. EPA/540/R-95/128, Soil Screening Guidance: Technical Background Document and WAC 173-340-747 imply that the cross section width ought to equal the width of contamination entering the aquifer. Other PAs conducted at Hanford and other DOE facilities have used an aquifer mixing width equal to the width of the facility (e.g., WCH-520, "Performance Assessment for the Environmental Restoration Disposal Facility, Hanford Site, Washington"; WSRC-MS-2003-00582, "Performance Assessment/Composite Analysis Modeling to Support a Holistic Strategy for the Closure of F Area, a Large Nuclear Complex at the Savannah River Site"). As indicated previously, the width of the PoCal segments is sufficient to intercept the centerline of the plumes resulting from the tank residuals from a single line of 100-series tanks, which appears consistent with the intent of EPA/540/R-95/128 and WAC 173-340-747. The aquifer mixing zone extends into the upper 5 m (16.4 ft) of the aquifer on the basis of the 4.5 m (15 ft) well screen length (and mixing zone dimension) associated with state monitoring well descriptions (e.g., see Equation 747-4 in WAC 173-340-747).

Results of Base Case Evaluation for Groundwater Pathway for the Compliance Period 1,000 Years After Closure. The results of the base case modeling indicate that only contaminants with K_d values equal to zero reach the PoCals within the DOE O 435.1 compliance period of 1,000 years (Table 7-3). Among radionuclides, the only contaminant producing nonzero concentrations at 100 m from the WMA C fenceline in the compliance period is ^{99}Tc. Other mobile contaminants such as ^{3}H, ^{60}Co, and ^{93m}Nb decay to insignificant quantities before reaching the water table. The maximum concentration of ^{99}Tc in groundwater during this period is 0.1 pCi/L, which is a factor almost 4 orders of magnitude less than its MCL.

Concentration contours of ^{99}Tc in the vadose zone at 1,000 years are shown in Figure 7-12. Releases from the pipelines, vault, and tank residuals have reached the water table, but the center of the ^{99}Tc mass remains about halfway through the vadose zone above the water table. Immediately below WMA C, concentrations in groundwater are about 0.5 pCi/L.

Concentration contours of radionuclides with nonzero values of K_d are shown in Figure 7-13 (^{129}I, K_d = 0.2 mL/g) and Figure 7-14 (^{238}U, K_d = 0.6 mL/g) at 1,000 years. During the compliance period, both are contained within the Hanford H1 sandy gravel unit and upper H2 sandy unit, ~60 m (197 ft) above the water table (Figures 7-13 and 7-14). These contaminants do not reach the water table within 1,000 years.

Results of Base Case Evaluation for Groundwater Pathway for the Period Between 1,000 to 10,000 Years After Closure. As discussed in Section 6, the analysis approach evaluates the contribution of individual sources on the peak concentration in groundwater, and identifies at which PoCal that peak concentration occurs. The results are summarized in Table 7-3 and provide a comparison of simulation results with groundwater MCLs. Table 7-4 presents a summary of the results for the individual sources, identifying at which PoCal the peak concentration attributable to each source occurs.

Table 7-3. Summary of Base Case Peak Groundwater Concentrations and Arrival Times for Selected Radionuclides.

Radionuclide or Nonradiological Contaminant	Nominal K_d value (mL/g)	Maximum Concentration during Compliance Time Frame (pCi/L)	Point of Calculation where Maximum Concentration Occurs	Years after Closure of Maximum Concentration	Maximum Concentration during Sensitivity/Uncertainty Time Frame (pCi/L)	Point of Calculation where Maximum Concentration Occurs
Iodine-129	0.2	0	—	6,540	0.004	PoCal 4
Selenium-79	0.1	0	—	3,770	0.01	PoCal 5
Tin-126	0.5	0	—	10,000	0.05	PoCal 5
Technetium-99	0	0.1	PoCal 5	1,550	30	PoCal 4
Uranium-238	0.6	0	—	10,000	0.02	PoCal 3

Figure 7-12. Extent of Transport of Technetium-99 (K_d = 0 mL/g) in the Vadose Zone at the End of the 1,000-Year Compliance Period.

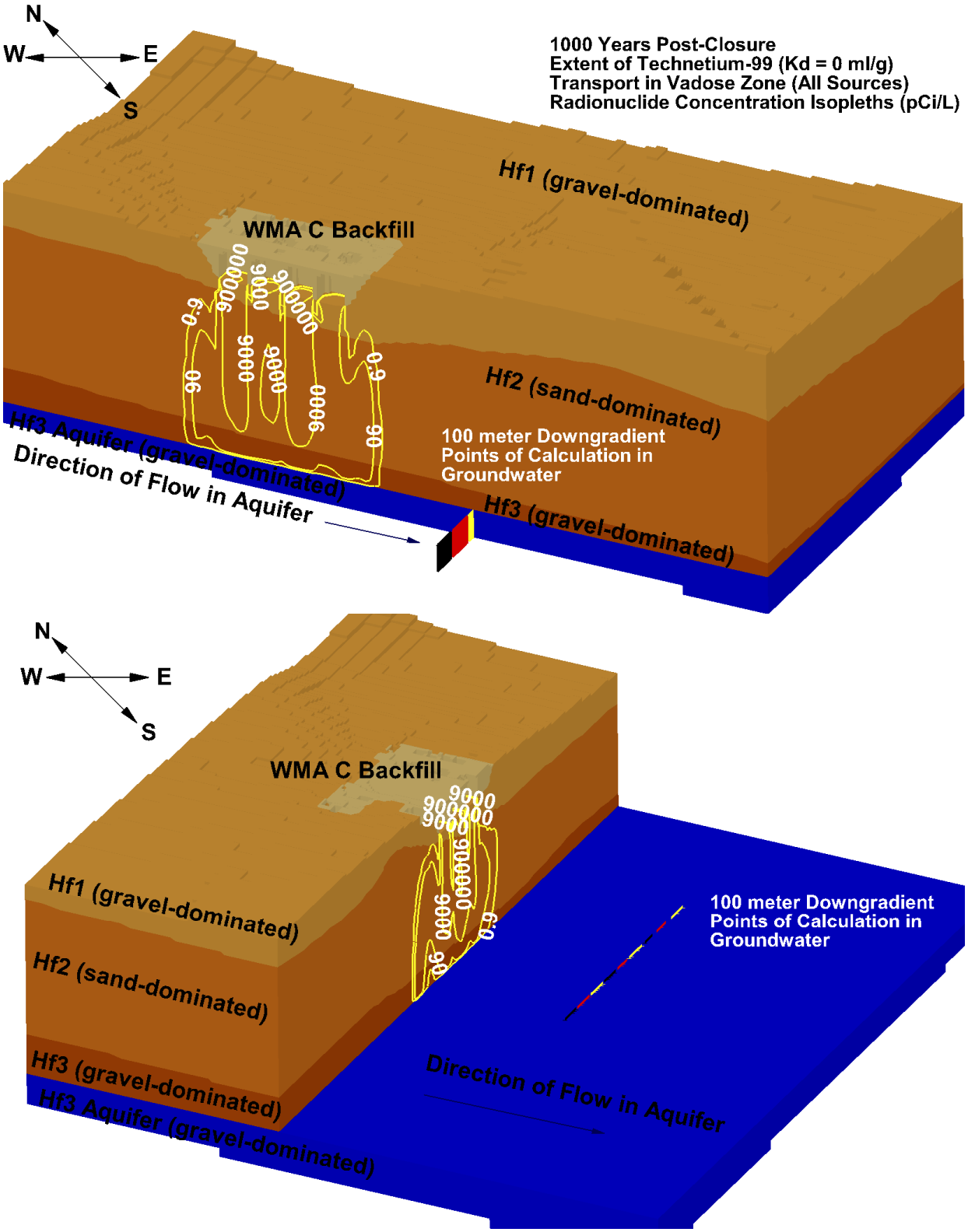

Hf = Hanford formation WMA = Waste Management Area

Figure 7-13. Extent of Transport of Iodine-129 (K_d = 0.2 mL/g for Sand-Dominated Units) in the Vadose Zone at the End of the 1,000-Year Compliance Period.

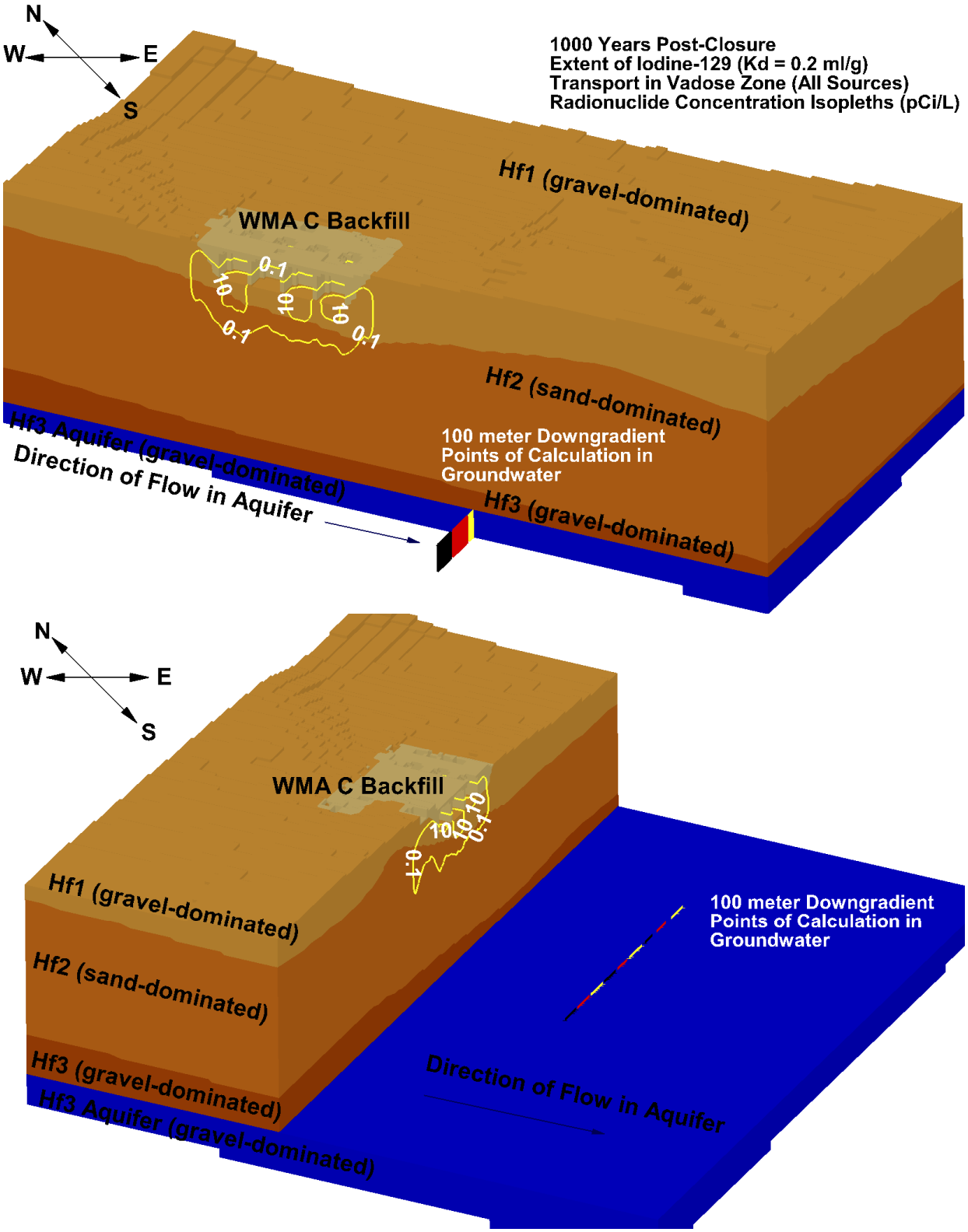

Hf = Hanford formation WMA = Waste Management Area

Figure 7-14. Extent of Transport of Uranium-238 (K_d = 0.6 mL/g for Sand-Dominated Units) in the Vadose Zone at the End of the 1,000-Year Compliance Period.

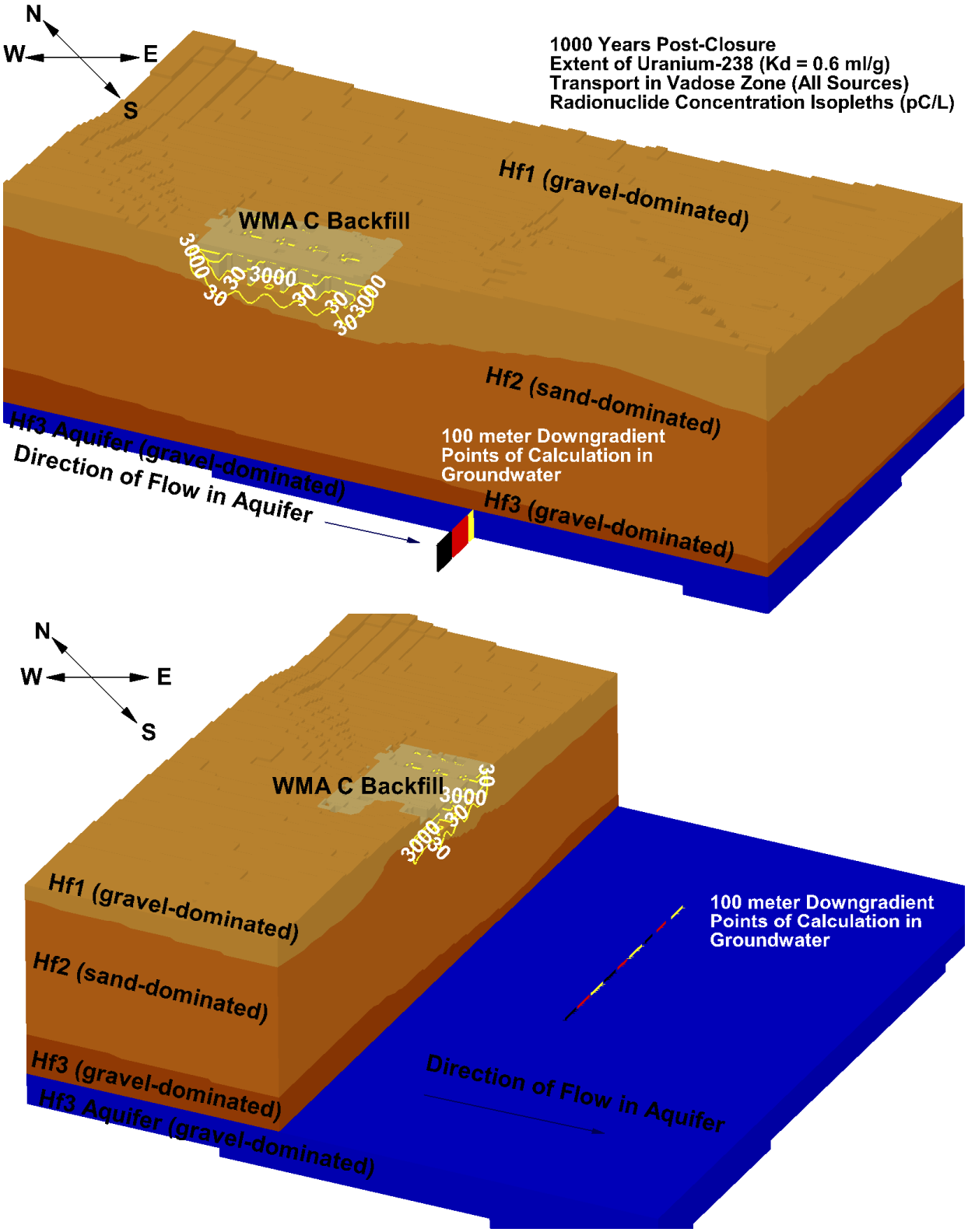

Hf = Hanford formation WMA = Waste Management Area

Table 7-4. Summary of Base Case Peak Groundwater Concentrations and Arrival Times for Selected Radionuclides. (2 sheets)

Source	Selenium-79			Technetium-99			Iodine-129		
	Years after Closure of Arrival	**Maximum Concentration (pCi/L)**	**PoCal**	**Years after Closure of Arrival**	**Maximum Concentration (pCi/L)**	**PoCal**	**Years after Closure of Arrival**	**Maximum Concentration (pCi/L)**	**PoCal**
241-C-101	4,100	0.0001	3	1,395	0.1	3	6,230	4E-6	3
241-C-102	4,520	0.0000007	4	1,495	0.01	4	6,840	0.0002	4
241-C-103	4,540	0.00001	5	1,500	0.1	5	6,860	0.0002	5
241-C-104	4,540	0.004	3	1,500	0.9	3	6,890	0.00003	3
241-C-105	4,800	0.00006	4	1,575	20	4	7,190	0.0006	4
241-C-106	4,750	0.004	5	1,555	0.5	5	7,170	0.00004	5
241-C-107	4,510	0.0001	3	1,505	5	3	6,760	0.003	3
241-C-108	4,480	0.0006	4	1,485	0.1	4	6,770	2E-6	4
241-C-109	5,040	0.00005	5	1,620	0.02	5	7,580	2E-6	5
241-C-110	4,970	0.00001	3	1,595	0.1	3	7,280	0.00001	3
241-C-111	4,500	0.001	5	1,485	4	5	6,580	0.0008	5
241-C-112	4,390	0.00007	6	1,460	4	6	6,570	2E-6	6
241-C-201	4,120	0.00002	6	1,420	0.008	6	6,250	3E-8	6
241-C-202	4,110	0.00002	7	1,415	0.008	7	6,230	5E-7	7
241-C-203	3,910	0.00002	7	1,370	0.007	7	5,940	1.00E-6	7
241-C-204	3,940	0.00002	7	1,370	0.01	7	5,970	3E-8	7
241-C-301	5,000	0.0004	6	1,630	0.08	6	7,340	0.00001	6
244 CR Vault	5,440	0.0005	1	1,630	0.1	1	7,710	0.00002	1
Pipelines	3,590	0.008	5	1,345	1	5	5,810	0.001	5
All	3,770	0.01	5	1,550	30	4	6,540	0.004	4

Table 7-4. Summary of Base Case Peak Groundwater Concentrations and Arrival Times for Selected Radionuclides. (2 sheets)

Source	Tin-126			Uranium-238					
	Years after Closure of Arrival	**Maximum Concentration (pCi/L)**	**PoCal**	**Years after Closure of Arrival**	**Maximum Concentration (pCi/L)**	**PoCal**			
241-C-101	10,000	5E-7	3	10,000	5E-8	3			
241-C-102	N/A	0	N/A	10,000	9E-9	4			
241-C-103	N/A	0	N/A	10,000	1E-8	5			
241-C-104	10,000	3E-6	3	10,000	1E-8	3			
241-C-105	N/A	0	N/A	10,000	3E-9	4			
241-C-106	10,000	0.0003	5	10,000	2E-9	5			
241-C-107	10,000	1E-7	3	10,000	1E-8	3			
241-C-108	N/A	0	N/A	10,000	1E-8	4			
241-C-109	N/A	0	N/A	10,000	1E-9	5			
241-C-110	10,000	7E-6	3	10,000	1E-8	4			
241-C-111	10,000	2E-6	5	10,000	2E-8	4			
241-C-112	N/A	0	N/A	10,000	2E-8	6			
241-C-201	N/A	0	N/A	10,000	2E-9	6			
241-C-202	N/A	0	N/A	10,000	2E-9	7			
241-C-203	N/A	0	N/A	10,000	6E-9	7			
241-C-204	N/A	0	N/A	10,000	6E-9	7			
241-C-301	10,000	4E-6	6	10,000	6E-11	6			
244 CR Vault	10,000	5E-6	1	10,000	4E-10	1			
Pipelines	10,000	0.04	3	10,000	0.02	3			
All	10,000	0.05	5	10,000	0.02	3			

N/A = not available

The evaluation of the peak PoCal for ^{99}Tc is shown in Figure 7-15; the peak concentration of ^{99}Tc is found to occur at PoCal 4. The contribution of individual sources within WMA C at PoCal 4 is shown in Figure 7-16. The peak contributor to the concentration of ^{99}Tc at all times is seen to be tank C-105. The peak concentration results predominantly from the combination of the tank C-105 releases and releases from the pipelines. Tank C-105 contains more than twice the amount of ^{99}Tc as any other WMA C source, and by itself the residual waste from tank C-105 produces a maximum concentration in groundwater of 21 pCi/L (note that the maximum concentration limit for ^{99}Tc is 900 pCi/L), which is more than five times the concentration that any other source contributes to the maximum.

Figure 7-15. Groundwater Concentration of Technetium-99 at All Points of Calculation 100 Meters Downgradient from Waste Management Area C.

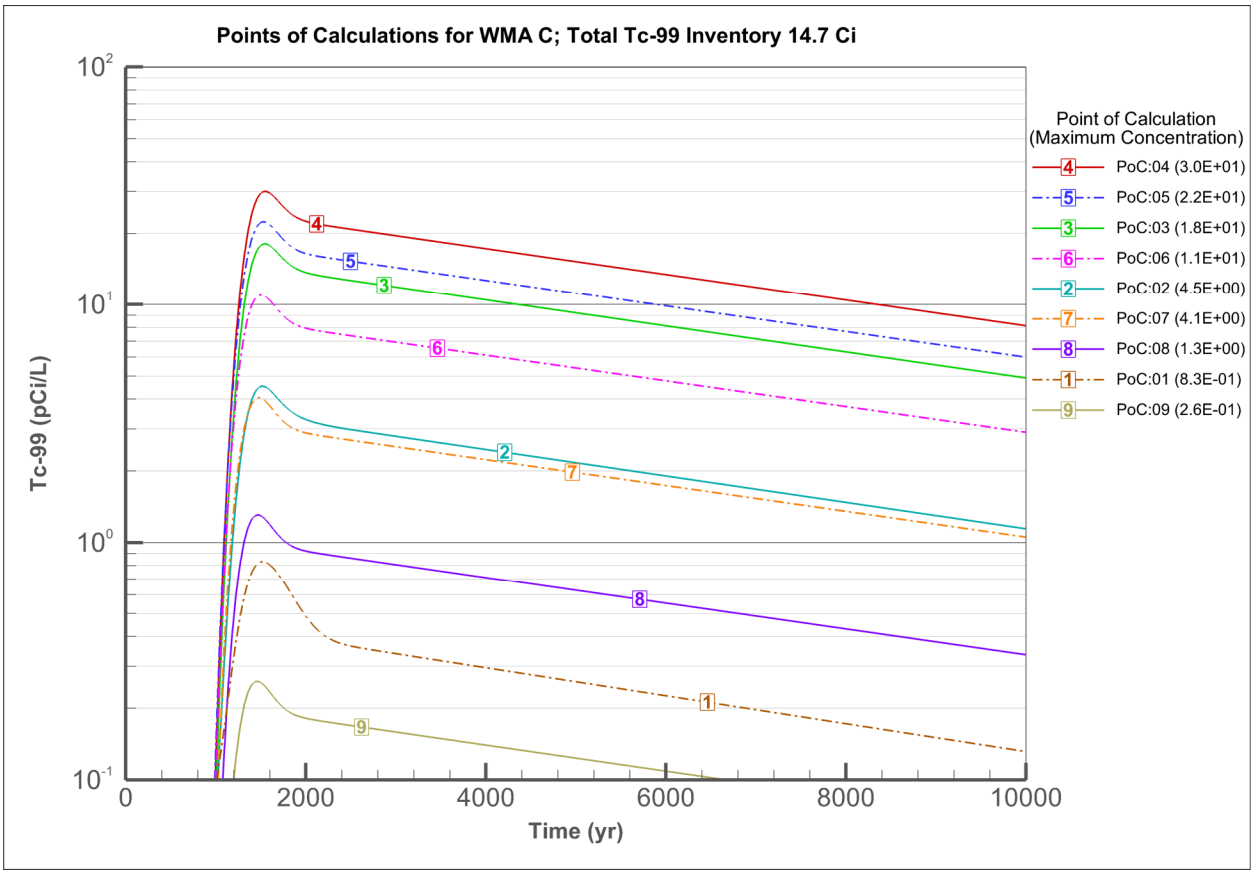

PoC = Point of Calculation WMA = Waste Management Area

The evaluation of the peak PoCal for ^{129}I is shown in Figure 7-17; the peak concentration of ^{129}I is found to occur at PoCal 4, although the peak at PoCal 3 is almost as large. The contribution of individual sources within WMA C at PoCal 4 is shown in Figure 7-18. The breakthrough curves for ^{129}I show the effect of slight retardation on contaminant transport through the vadose zone. First arrival does not occur until after 2,600 years after closure, and the peak concentration (0.004 pCi/L) occurs approximately 6,500 years after closure. The residual waste from tank C-107 is responsible for providing the largest contribution to the overall concentration, followed by that from the pipelines and tanks C-111 and C-105.

Figure 7-16. Groundwater Concentration of Technetium-99 from Each Source at Point of Calculation 4.

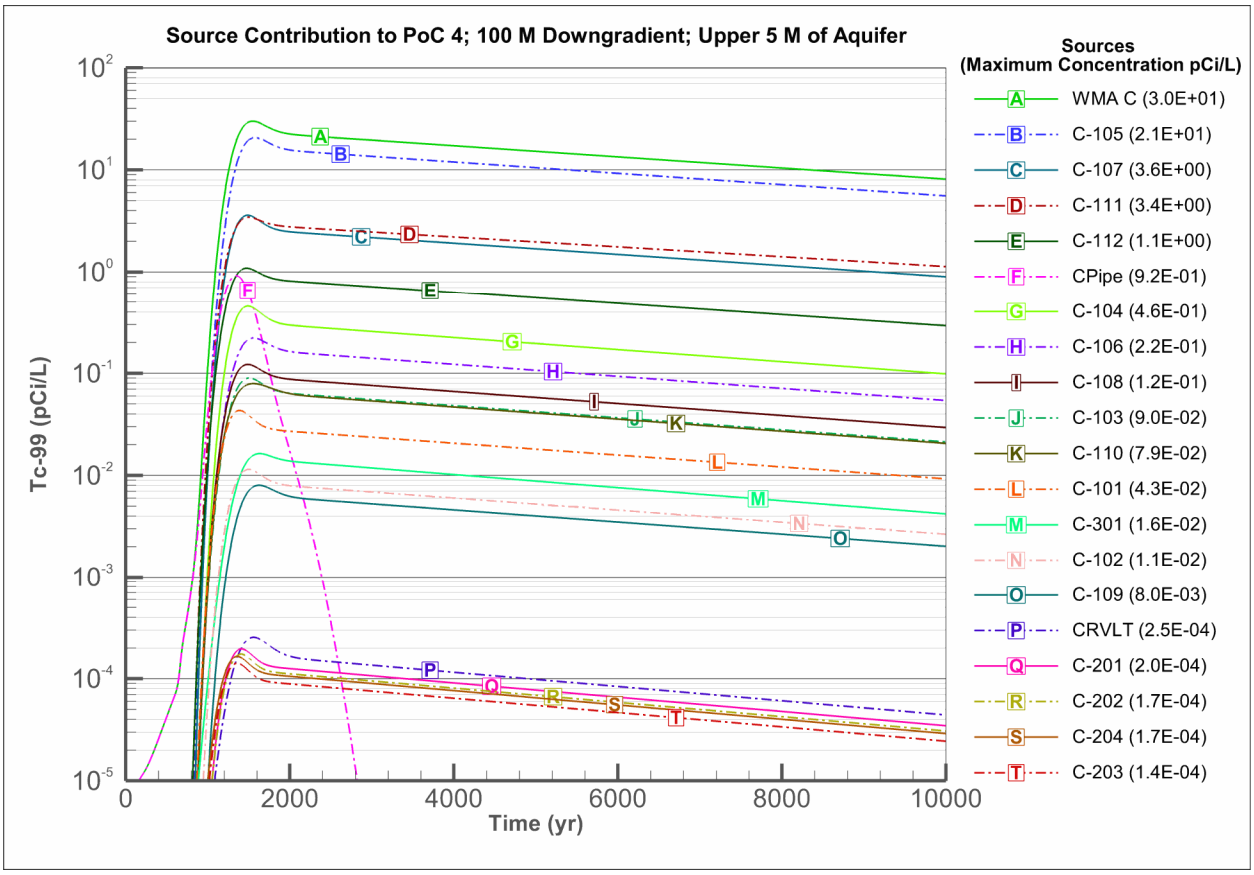

PoC = Point of Calculation WMA = Waste Management Area

The evaluation of the peak PoCal for ^{238}U is shown in Figure 7-19; the peak concentration of ^{238}U is found to occur at PoCal 3, although the peaks at PoCals 2, 4, 5, and 6 are almost as large. The contribution of individual sources within WMA C at PoCal 3 is shown in Figure 7-20. The breakthrough curves for ^{238}U show the effect of moderate retardation on contaminant transport through the vadose zone. First arrival does not occur until after 5,600 years after closure, and the maximum concentration (note the regulatory standard for ^{238}U is 15 pCi/L) occurs at the end of the sensitivity/uncertainty analysis time frame (10,000 years after closure). The trend in concentration is increasing at the end of the analysis time frame, indicating that it has yet to reach a peak. The residual waste from the pipelines is responsible for releases within 10,000 years, with all other sources negligible. This occurs because the release from the pipelines occurs by advection and is not retarded by sorption on cementitious material. By contrast, releases from the tanks and vault are influenced by sorption on the grout and are released by diffusion.

A summary of the peak concentrations at their respective peak PoCals is presented in Figure 7-21. During the sensitivity/uncertainty analysis period (1,000 to 10,000 years after closure), the primary radionuclides that break through at the PoCals include ^{99}Tc, ^{79}Se, ^{126}Sn, ^{129}I, and the uranium isotopes and their progeny. Concentrations of the simply decaying isotopes

and ^{238}U are shown in Figure 7-21, on both linear (upper) and log (upper) scales. The semi-log plot is needed since there are so many orders of magnitude difference among the contaminants. Technetium-99 is by far the contaminant with the largest impact on groundwater; the maximum concentration of ^{99}Tc in groundwater is 30 pCi/L, which occurs approximately 1,500 years after closure. The concentrations of ^{79}Se and ^{129}I reach their peaks within 10,000 years after closure, and then decline. Concentrations of ^{127}Sn, uranium, and the uranium progeny are on the rise at the end of the 10,000-year analysis period. The remaining radionuclides in the analysis did not reach the PoCals during the 10,000-year period because of decay, sorption, or a combination of the two.

Figure 7-17. Groundwater Concentration of Iodine-129 at All Points of Calculation 100 Meters Downgradient from Waste Management Area C.

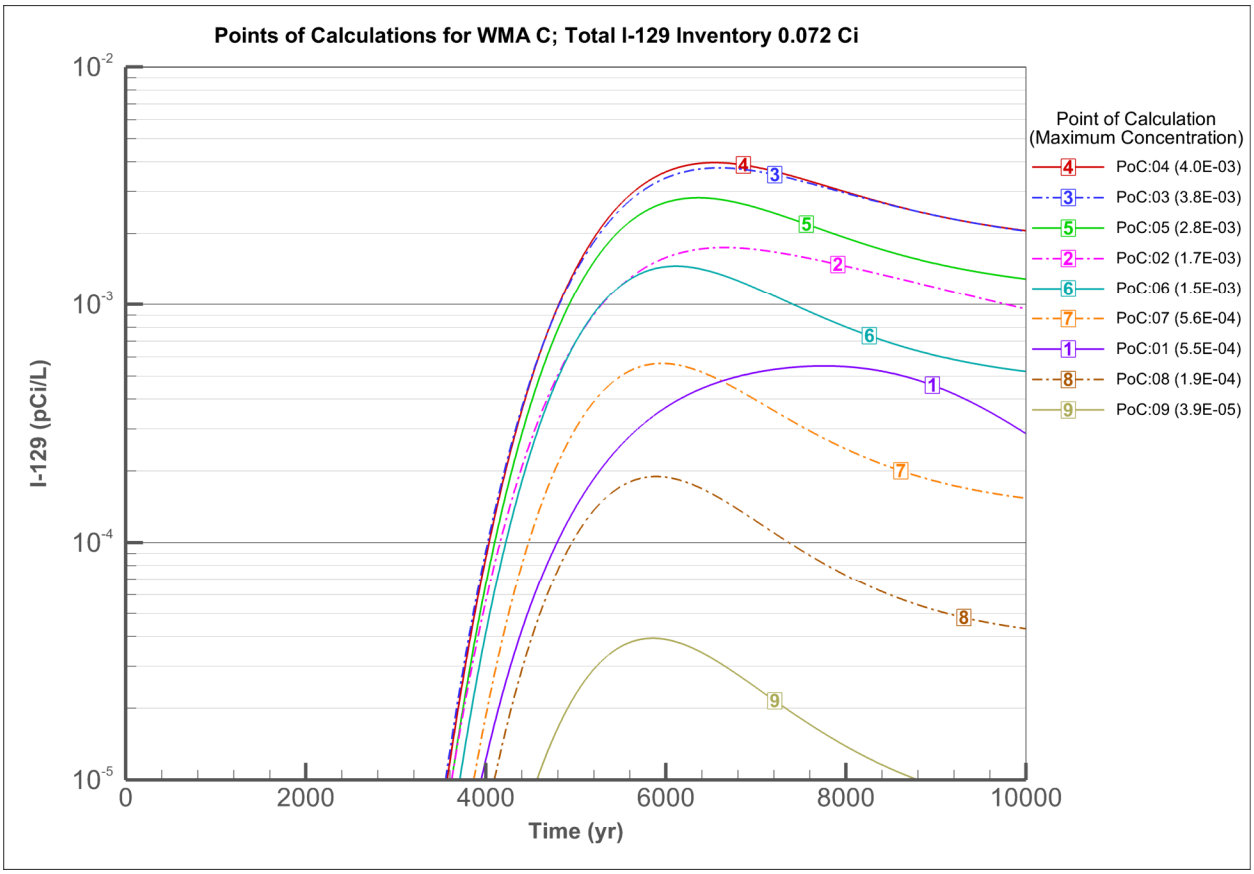

PoC = Point of Calculation WMA = Waste Management Area

Figures 7-22 through 7-24 show the development of the ^{99}Tc plume in the groundwater at 500, 1,000, and 1,570 years post-closure. These times correspond to the surface barrier design life, the end of the compliance time period, and the approximate time of the peak concentration. At 500 years after closure, the first arrival approximately occurs near the south corner of the facility, in the vicinity of the 244-CR vault as shown in Figure 7-22. Technetium-99 from residuals in both the vault and the pipelines has reached the water table in this area. Although the plume increases in size from 500 to 1,000 years into the future, peak concentration in groundwater remains very low (less than 1 pCi/L) as shown in Figure 7-23. At the time of the maximum

concentration at the point of compliance, shown in Figure 7-24, the plume shows much higher concentrations from all sources, but the peak concentration becomes dominated by inventory released from tank C-105.

Figure 7-18. Groundwater Concentration of Iodine-129 from Each Source at Point of Calculation 4.

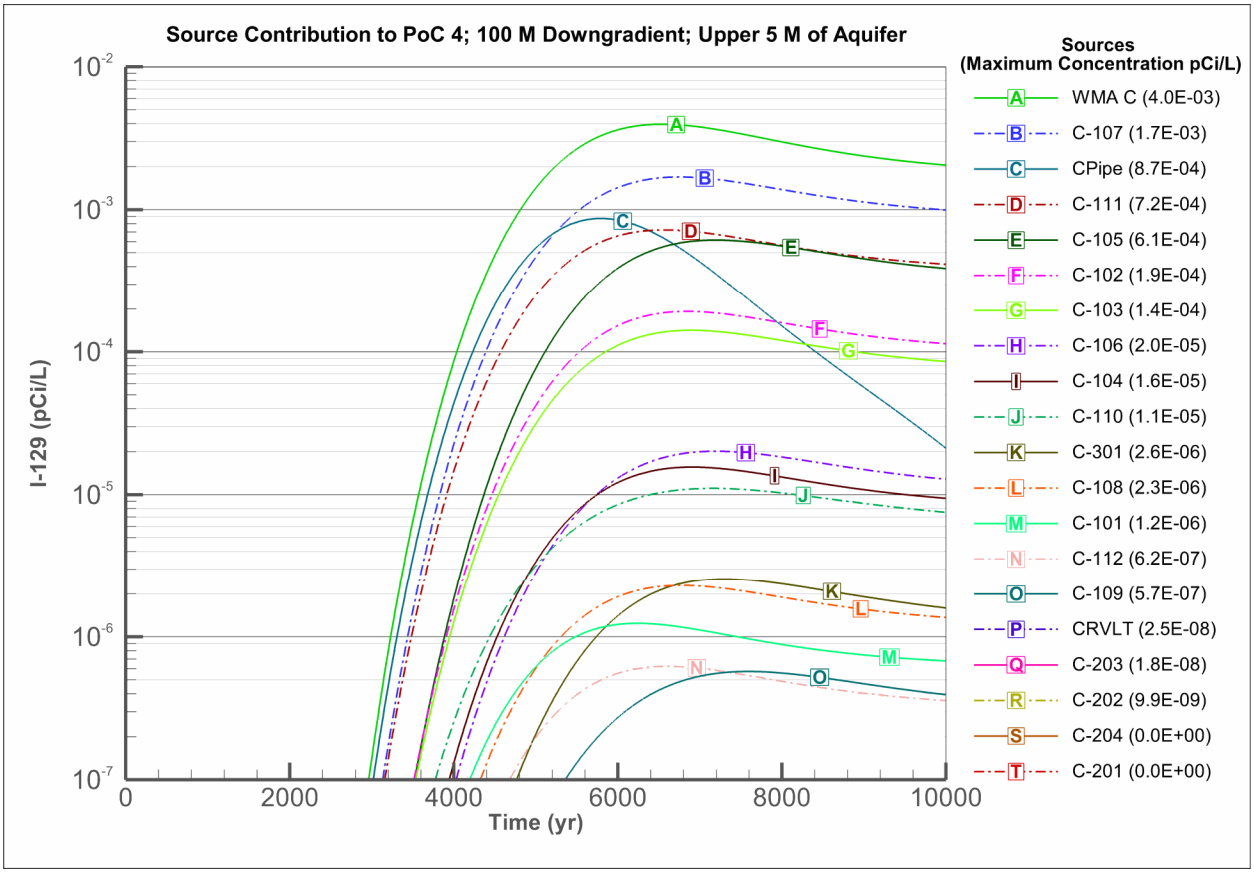

PoC = Point of Calculation WMA = Waste Management Area

Plot of breakthrough curves for ^{99}Tc at different PoCals (PoCal 3, 4, 5, and 6) at different downgradient locations (e.g., fenceline, 100 m, and 200 m) illustrate small differences in ^{99}Tc concentrations in modeling results at different PoCals and downgradient locations from WMA C (see Figure 7-25).

7.2.1.2.3 Evaluation of Correlation between Leachate Flux to Water Table and Groundwater Concentration. There is a linear relationship between the concentration in the groundwater and the radionuclide flux entering the water table. Figure 7-26 shows the breakthrough curves of ^{99}Tc relative to the flux of ^{99}Tc (pCi/yr) entering the water table. As seen in the figures, the curves overlay one another fairly closely, indicating that the downgradient concentration in groundwater is likely correlated to the flux of ^{99}Tc and concentration of the leachate entering the aquifer. This relationship provides an indication of the extent to which the correlation is linear. As a result of this linearity, groundwater concentrations in this 3-D system may be evaluated more simply, using flux rates or leachate concentration entering the water table

and a simple linear convolution. This approach is referred to as a dilution-attenuation factor (EPA/540/R-95/128).

Figure 7-19. Predicted Groundwater Concentration of Uranium-238 at All Points of Calculation 100 Meters Downgradient from Waste Management Area C.

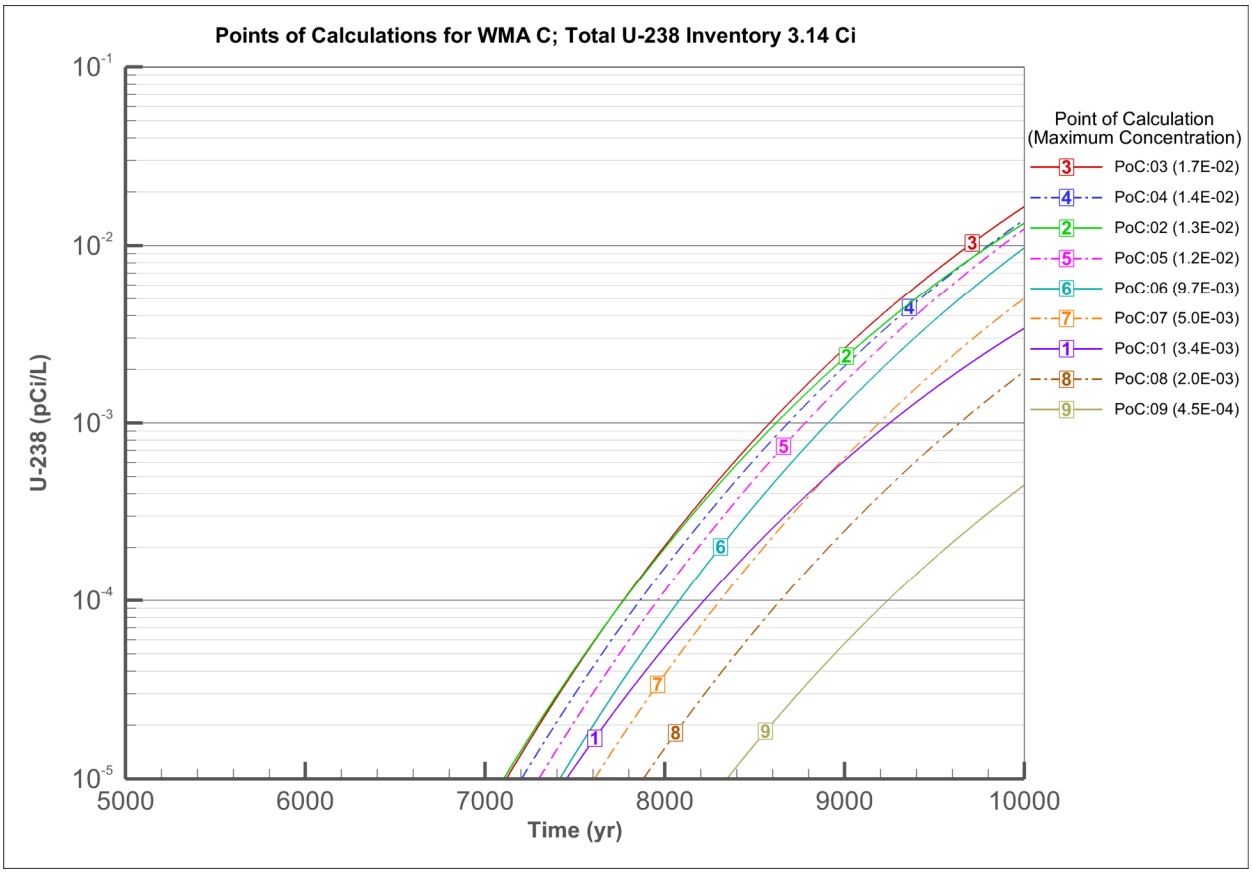

PoC = Point of Calculation WMA = Waste Management Area

The coefficient of determination for the regression lines is very close to 1, which means the lines fit the values almost perfectly. Thus, the downgradient concentration in groundwater of ^{99}Tc can be estimated by either the flux or concentration of ^{99}Tc in the leachate entering the aquifer and a linear scalar particular to each source. In the case of the ^{99}Tc flux, the scalar needs only to account for the aquifer flow rate. For the base case evaluation at PoCal 4 for ^{99}Tc from the tank C-105 residuals, the inverse of the slope of the regression line between the groundwater and leachate concentration indicates that the leachate concentration is reduced by a factor of 305 in the aquifer, i.e., 1/0.003273. For residuals from the pipelines, the scalar for PoCal 5 is 1/0.001504 = 665. Because of differences in source and PoCal locations, the relationship will be different for each combination of source and PoCal, as indicated by the comparison of the tank C-105 and pipelines scalars. However, once the scalars are established, variability in the aquifer flow parameters may be estimated simply as a function of the scalars.

Figure 7-20. Groundwater Concentration of Uranium-238 According to Each Source at Point of Calculation 3 Where the Maximum Concentration Occurs 100 Meters Downgradient from Waste Management Area C.

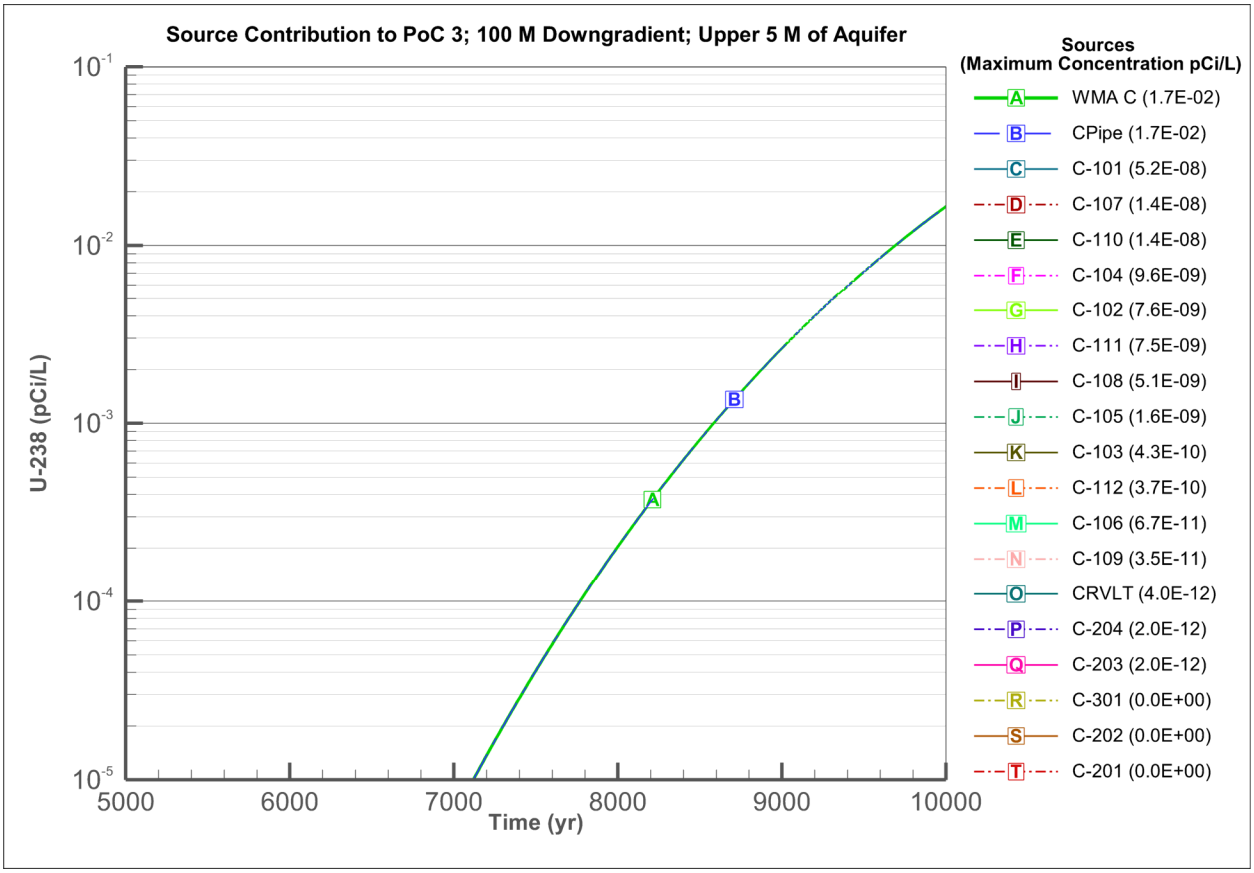

PoC = Point of Calculation WMA = Waste Management Area

7.2.2 Air Transport of Radionuclides

The atmospheric release is modeled for only those radionuclides that can partition into the gas phase from the dissolved phase (in water). These radionuclides are ^{14}C, ^{3}H (tritium), ^{129}I, and ^{222}Rn. The atmospheric release calculation methodology is described in Section 6.3.2.3 (Atmospheric Pathway) for WMA C sources, where the diffusive flux from the residual waste to the surface of the facility is calculated first. For the radionuclides that are included in the air pathway performance objective (see Section 2.1), an air transport calculation is performed to calculate the concentration at a receptor located 100 m (328 ft) downwind from the WMA C fenceline. The results of this calculation are presented in Figure 7-27 for ^{14}C, ^{3}H (tritium), and ^{129}I.[1]

[1] As discussed in Section 2, ^{222}Rn is not included in the air pathway performance objective. Instead, it has a separate criterion for flux from the facility surface.

Figure 7-21. Maximum Calculated Groundwater Concentration at 100 Meters Downgradient from Waste Management Area C.

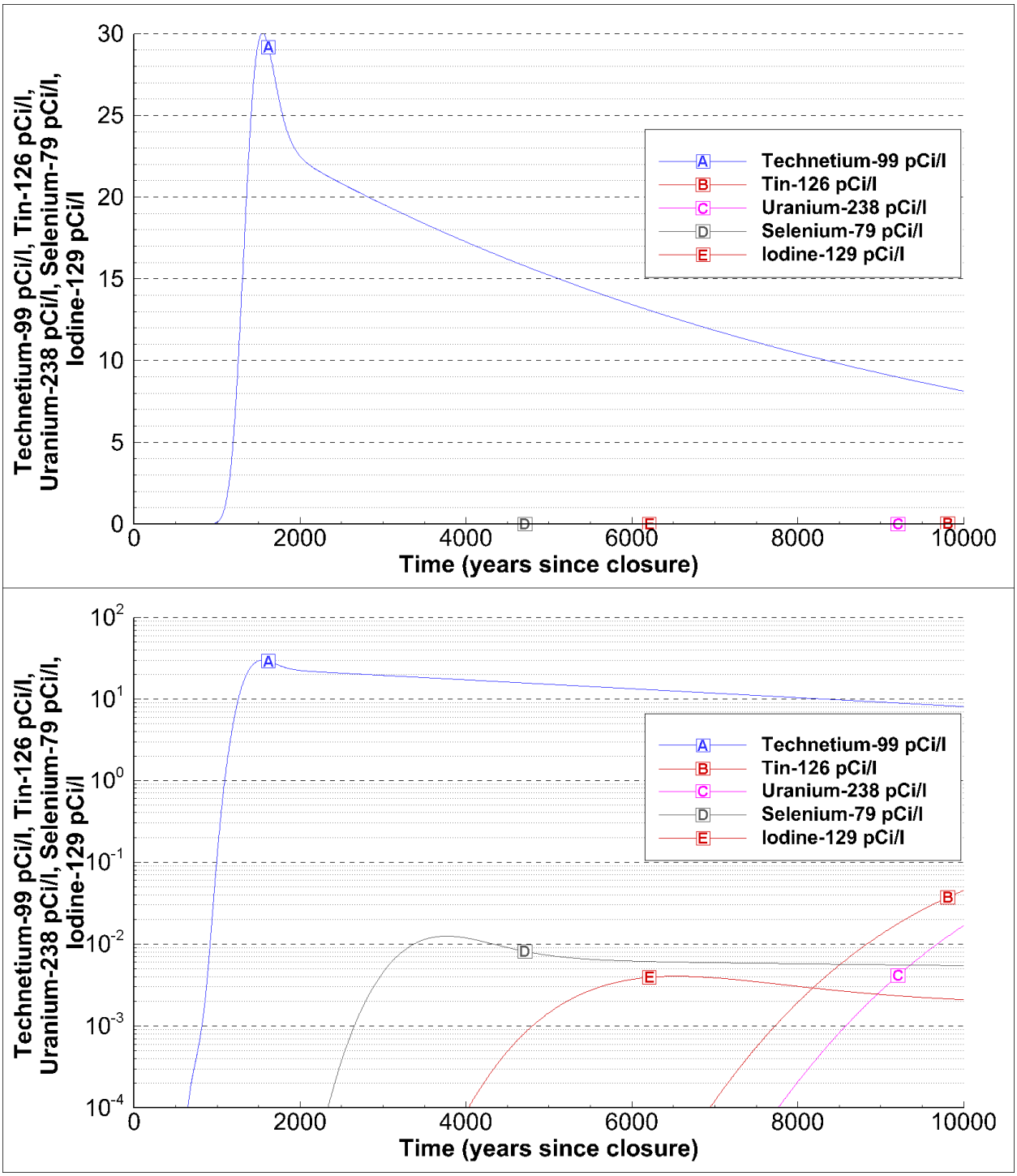

Figure 7-22. Extent of Technetium-99 Plume in Groundwater 500 Years after Closure at the End of the Surface Barrier Design Life.

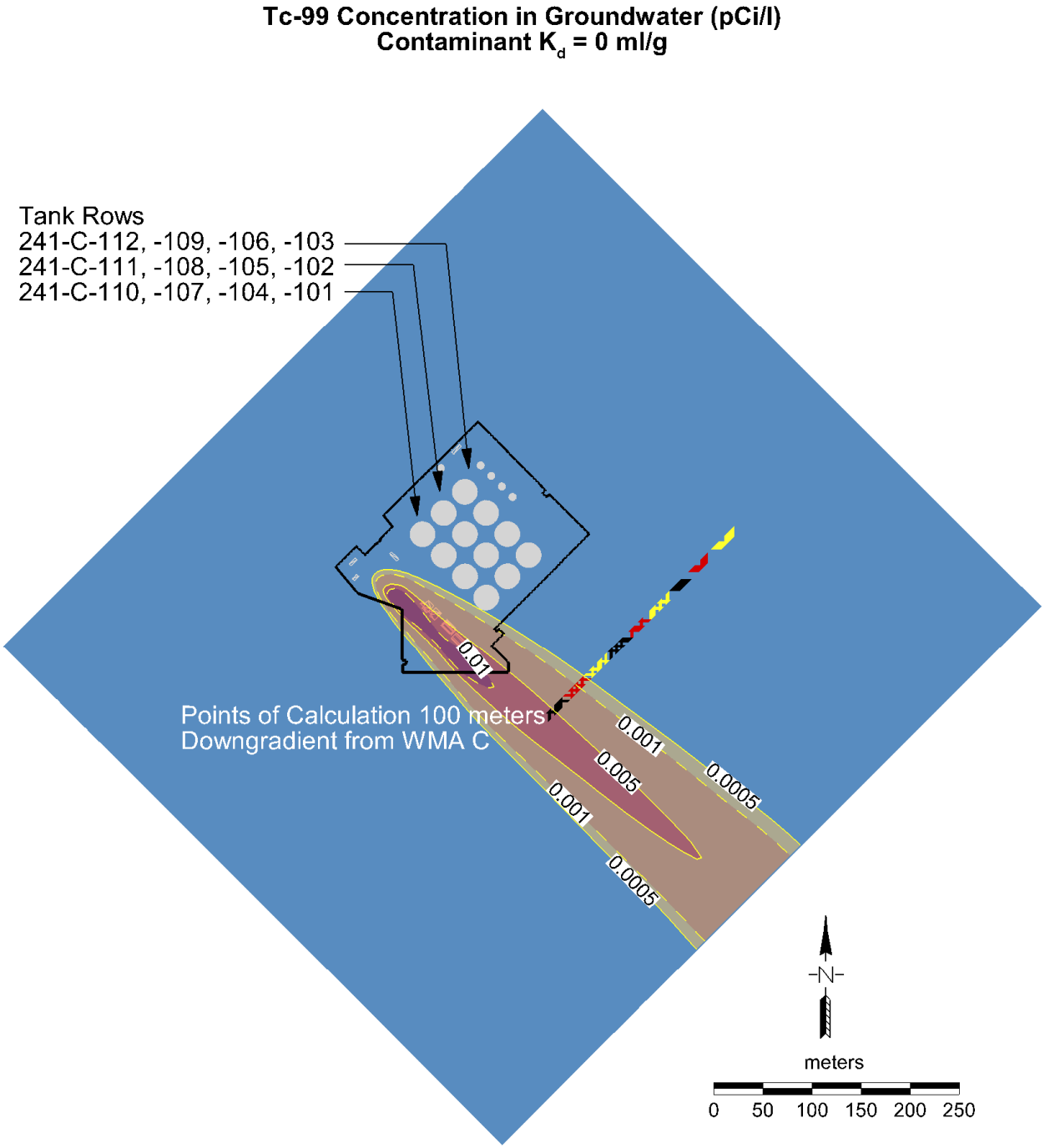

500 Years after Closure
End of barrier design life
WMA = Waste Management Area

Figure 7-23. Extent of Technetium-99 Plume in Groundwater 1,000 Years after Closure at the End of the Compliance Time Frame.

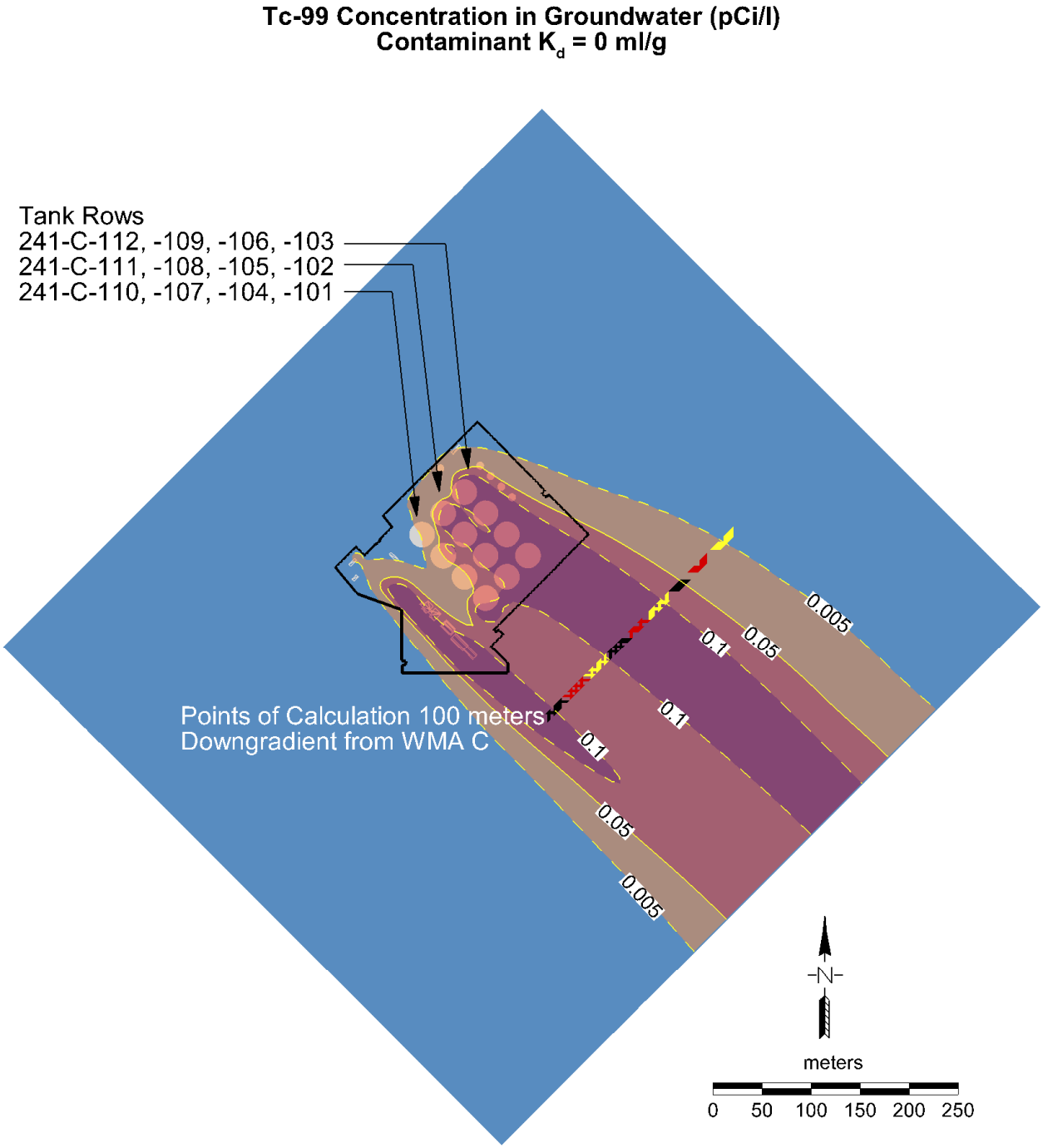

End of the 1,000 Year Compliance Period

WMA = Waste Management Area

Figure 7-24. Extent of Technetium-99 Plume in Groundwater 1,570 Years after Closure at the Time of the Maximum Concentration at the Point of Compliance.

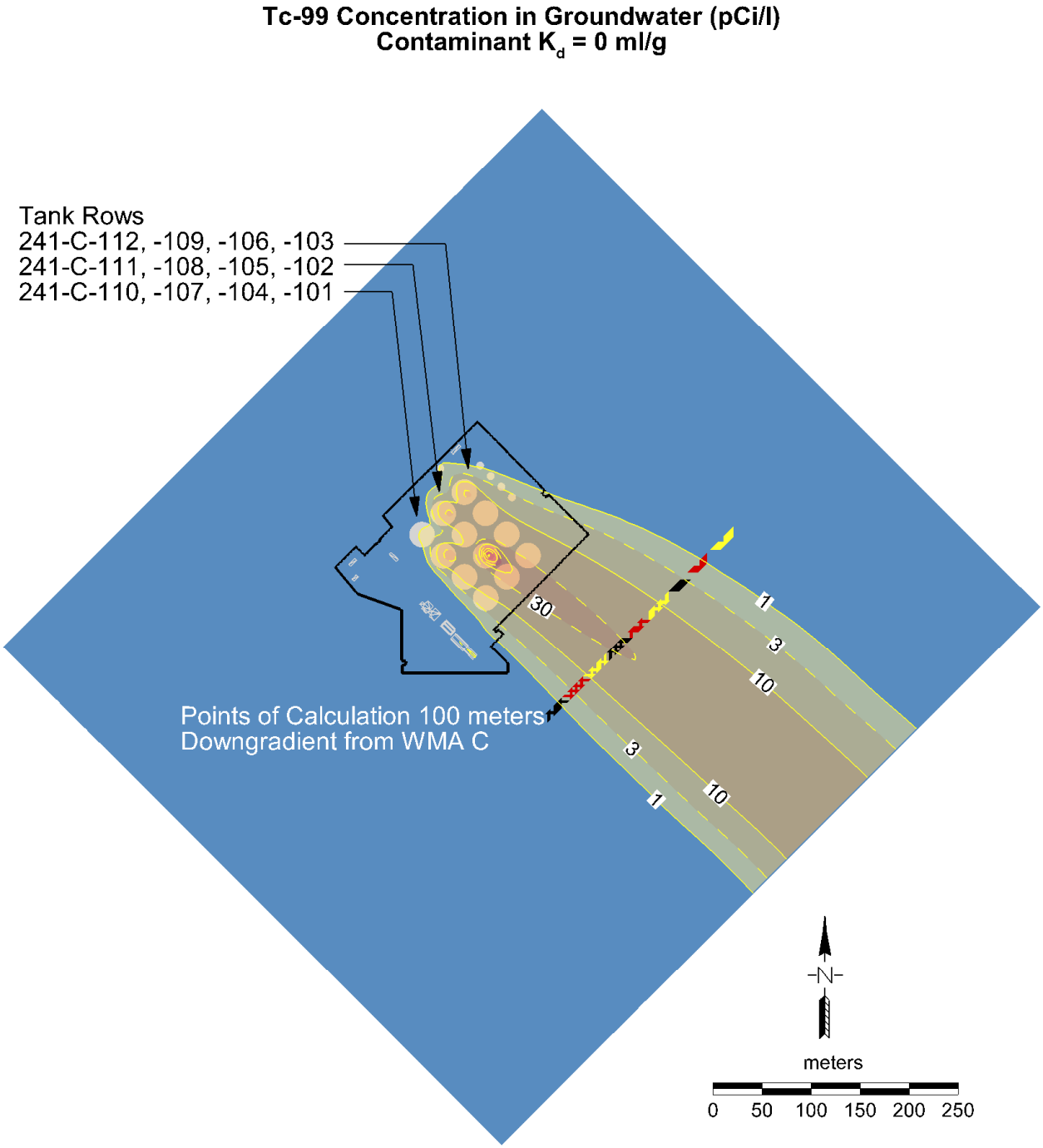

Approximate time of peak concentration at point of calculation

WMA = Waste Management Area

Figure 7-25. Technetium-99 Concentration Breakthrough Curves in Groundwater after Closure at Different Points of Calculation and Downgradient Locations.

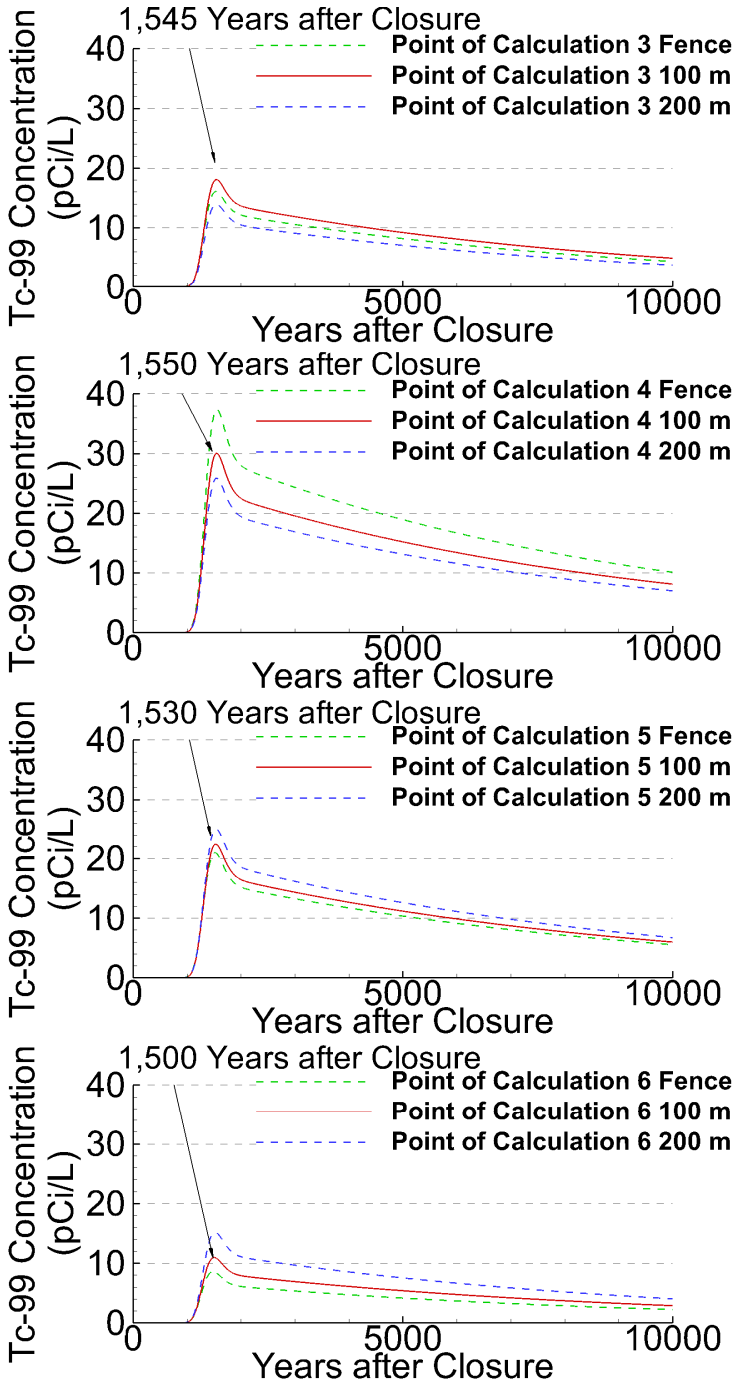

The results in Figure 7-27 indicate that the atmospheric ^{3}H (tritium) release produces much higher concentrations than the other two at early times. The differences between the curves are attributable to differences in the K_d and Henry's Law behavior for the three contaminants. As discussed in Section 6, the release rate into the gas phase is dependent on both the K_d (which controls the partitioning between solid and liquid) and the Henry's Law constant (which controls

the partitioning between liquid and vapor). The ^{3}H concentration declines sharply, both because of its short half-life and because the entire inventory is immediately available for release, having a low K_d and relatively high Henry's Law constant. By contrast, ^{129}I has a low K_d and a low Henry's Law constant (and a low inventory), so while its aqueous phase concentration is relatively high, it does not readily partition into the gas phase. The high K_d of ^{14}C keeps the aqueous concentration of ^{14}C low, limiting its availability to partition into the gas phase. The three contaminants therefore exhibit qualitatively different behavior because of the differences in their properties.

The radon flux at the surface of the WMA C facility is calculated for each source separately. These sources are presented in Figure 7-28. The relative magnitude of the fluxes are the result of the initial residual inventory of ^{226}Ra and the amount of uranium inventory that decays to form ^{226}Ra and then to ^{222}Rn. The radon flux increases with time resulting from ingrowth due to decay of ^{234}U and ^{238}U inventory. The peak flux of 7×10^{-3} pCi/m^2/sec results from tank C-203 at the end of the simulation. This value is much lower than the 20 pCi/m^2/sec performance objective. The flux from other 200-series tanks and C-301 is also relatively high compared to the 100-series tanks. This is due to combination of high initial inventories of ^{234}U (and ^{238}U), smaller residual volume, and smaller cross-sectional area for the 200-series tanks and C-301 compared to the 100-series tanks and ancillary equipment resulting in higher concentration (and flux) of radon. As discussed in Section 6, for the analysis of radon flux, releases of contaminants from the residual waste are set to zero, so the inventory of ^{226}Ra is allowed to build up in the residual layer. This is a significant conservatism at long times, since uranium migrating downward through the groundwater pathway would decrease the later peaks. Despite this conservatism, even at 10,000 years the peak radon flux is several orders of magnitude below the performance objective. Tank C-106 contains little uranium and ^{230}Th, and as expected, ^{222}Rn flux decreases as the ^{226}Ra inventory is depleted through decay (Figure 7-28). The peak radon flux for the 1,000-year compliance period is about 2×10^{-4} pCi/m^2/s.

7.3 DOSE ANALYSIS

In this section, results are presented of the dose analyses conducted for the PA to demonstrate compliance with performance objectives outlined in DOE O 435.1, as discussed in Section 1. Results are presented as a set of deterministic "base case" results that represent reasonable best estimates for the input parameters, and for a situation in which all the safety functions discussed in Section 1 behave as expected. These results are supported by a suite of sensitivity cases (see Section 8.2), which have been selected to evaluate the importance of the safety functions on compliance. They are also supported by probabilistic analyses (see Section 8.1) that evaluate the importance of parameter uncertainty on the PA, and which demonstrate that the base case represents a central tendency of the range of outputs from the probabilistic analysis.

In this section, dose results are presented for the all-pathways performance objective and for the air pathway objective. Doses for the intruder performance objectives are presented in Section 9. As discussed in Section 2, the remaining performance objectives for the PA do not require dose calculations, and are presented in appropriate sections of the report.

Figure 7-26. Results and Regression Lines Associated with the Vadose Leachate Flux to Groundwater for the Base Case Evaluation of Technetium-99.

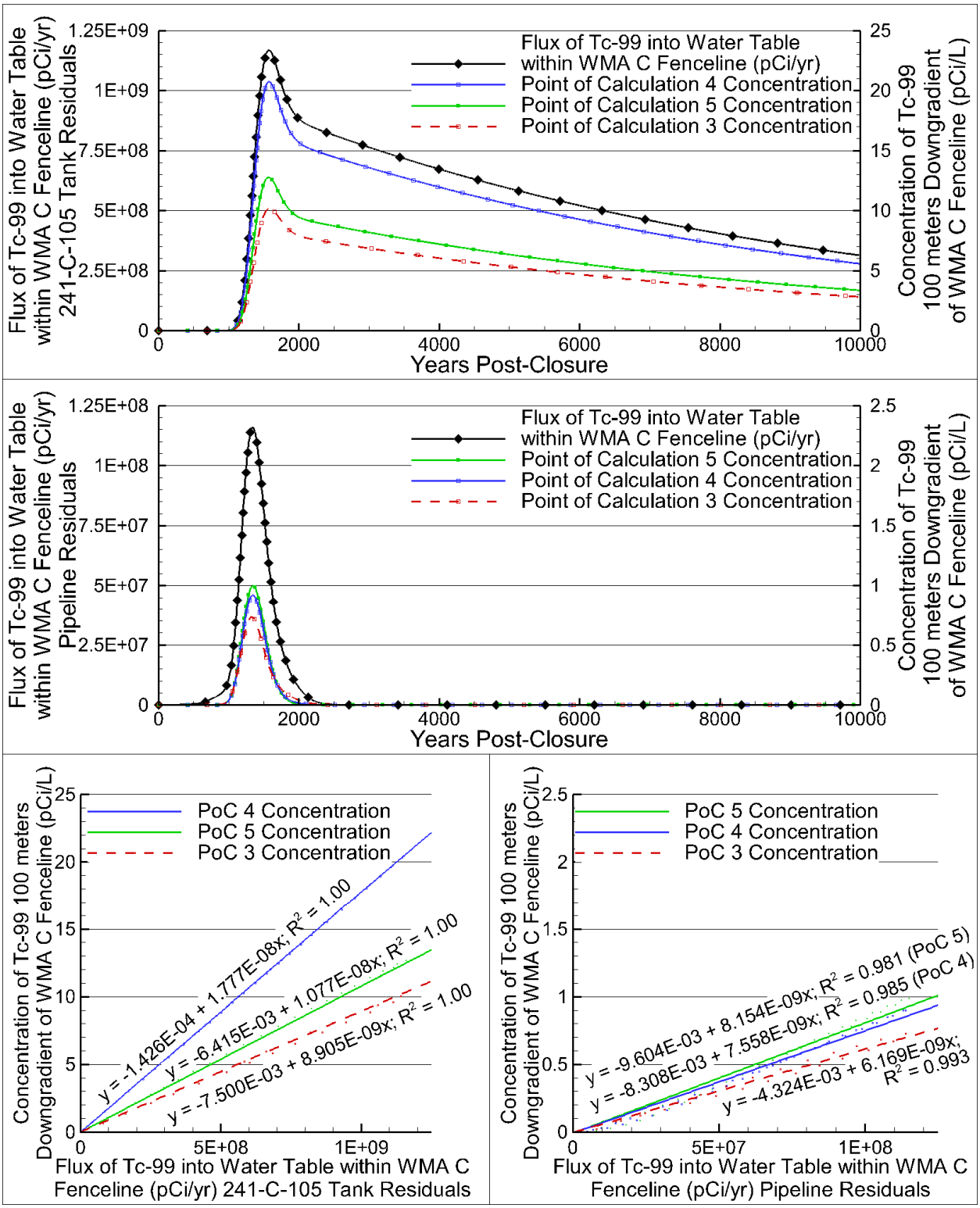

WMA = Waste Management Area

Figure 7-27. Air Concentration for Volatiles at Receptor Location in pCi/L.

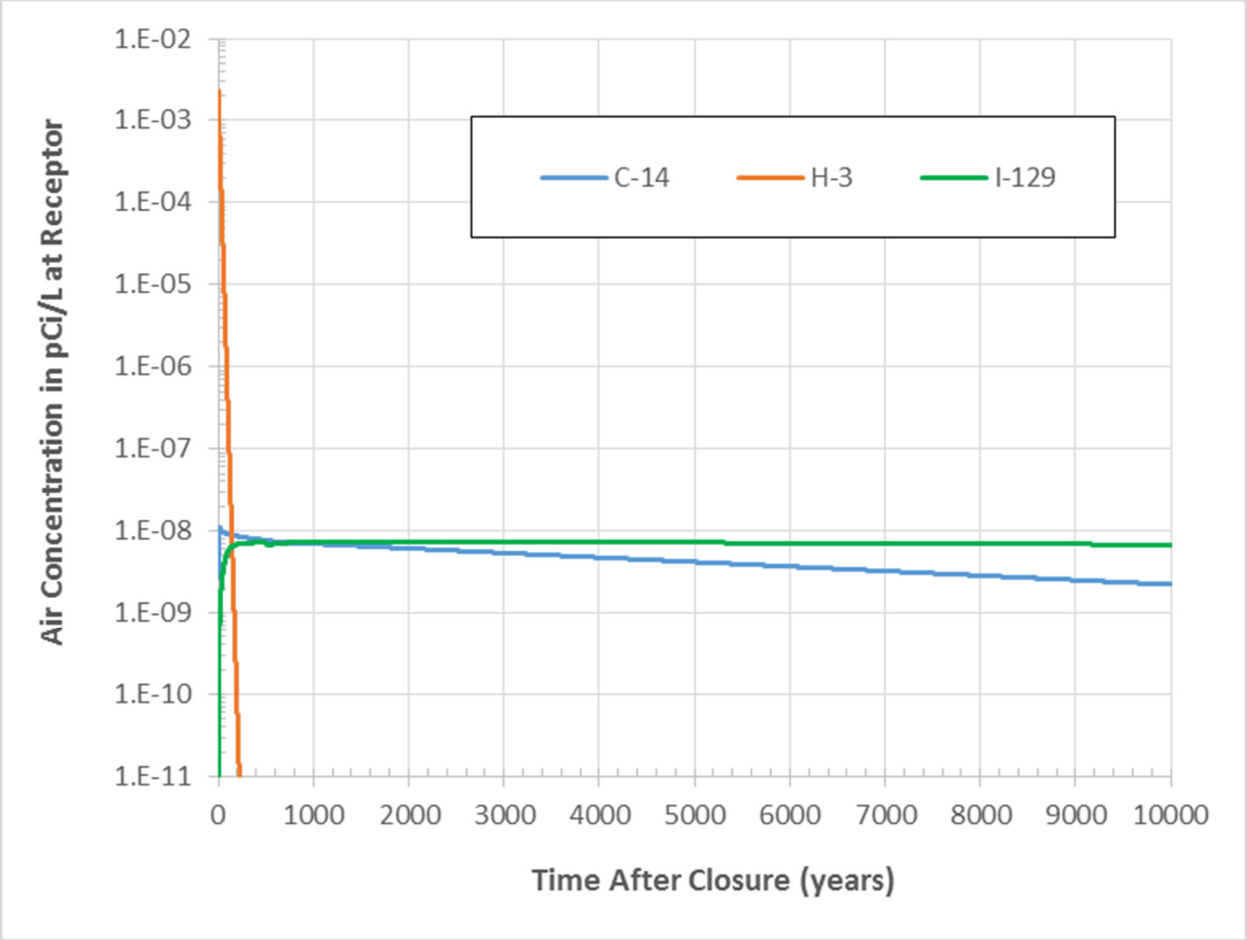

7.3.1 All-Pathways Dose

The all-pathways dose is a combination of dose from the groundwater pathway and air pathway, with the concentrations calculated according to the methodology presented in Section 6. The receptor is considered to be a reasonably maximally-exposed individual and assumed to be located along the centerline of the air pathway plume and getting water from the well located at the highest concentration point in the aquifer at the 100 m (328 ft) boundary. The groundwater concentrations are used as the concentrations at the wellhead. This approach has been taken to maintain consistency between the groundwater protection performance objectives and the all-pathways dose performance objective, but does not take account of any dilution that may occur in the well as it is pumped.

Doses associated with the groundwater pathway are presented in Figure 7-29 for the 100 m (328 ft) compliance distance for each PoCal. Consistent with the groundwater protection concentration calculations, the peak dose in space is found at PoCal 4. Consequently, PoCal 4 is used as the compliance point for the PA all-pathways analysis.

Figure 7-28. Radon Flux at Surface of Waste Management Area C.

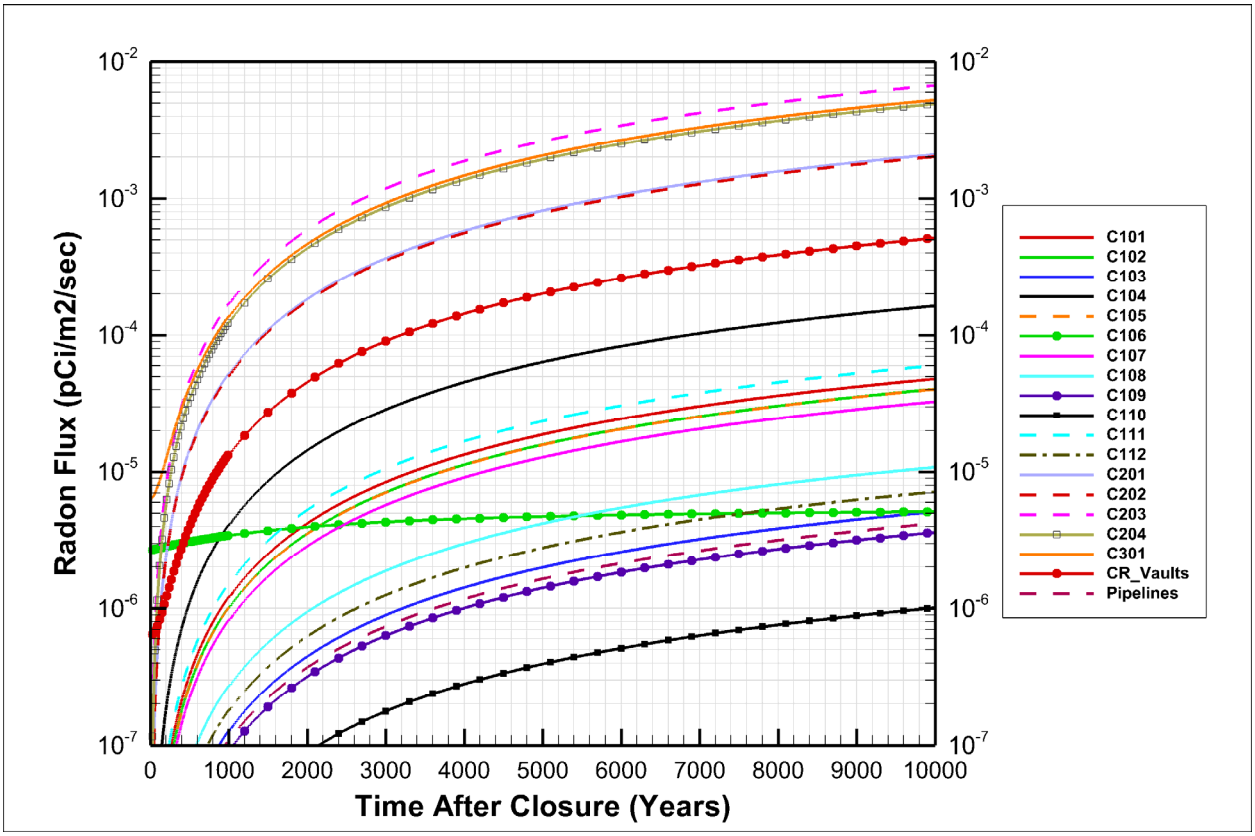

The all-pathway dose results for the groundwater (PoCal 4) and the air pathway are presented in Figure 7-30 for all radionuclides that produced a nonzero dose result within 10,000 years. Also shown on the figure are the DOE O 435.1 compliance time and compliance dose, for comparison. The peak dose summed over all radionuclides within the compliance time period is about 4×10^{-3} mrem/yr, primarily from ^{3}H release. Within the compliance time period, the early dose is due to contribution of ^{3}H and ^{129}I from the air pathway but after about 800 years the dose is dominated by ^{99}Tc contribution from the groundwater pathway. Within the sensitivity/uncertainty analysis time period (1,000 to 10,000 years), the peak dose summed over all radionuclides is 0.10 mrem/yr, which occurs about 1,500 years after closure.

The dose resulting from exposure along the groundwater pathway (PoCal 4) is by far the dominant dose in the sensitivity/uncertainty analysis time period (1,000 to 10,000 years) and is presented separately in Figure 7-31 along with the major dose-contributing radionuclides. The highest total dose from the groundwater pathway within the compliance time period is 4×10^{-4} mrem/yr and within the sensitivity/uncertainty analysis time period is 0.10 mrem/yr resulting from release of ^{99}Tc. Minor contributors to the total dose at long times are ^{79}Se, ^{129}I, ^{126}Sn, and uranium isotopes and their progeny.[2] A summary of the peak doses and time of peak occurrence is presented in Table 7-5.

[2] Radium-226+D includes doses associated with all its progeny, excluding inhalation doses from ^{222}Rn, as required in DOE O 435.1.

Figure 7-29. Groundwater Pathway Dose (mrem/yr) as a Function of Time for All Points of Calculation at the 100 Meters Compliance Distance.

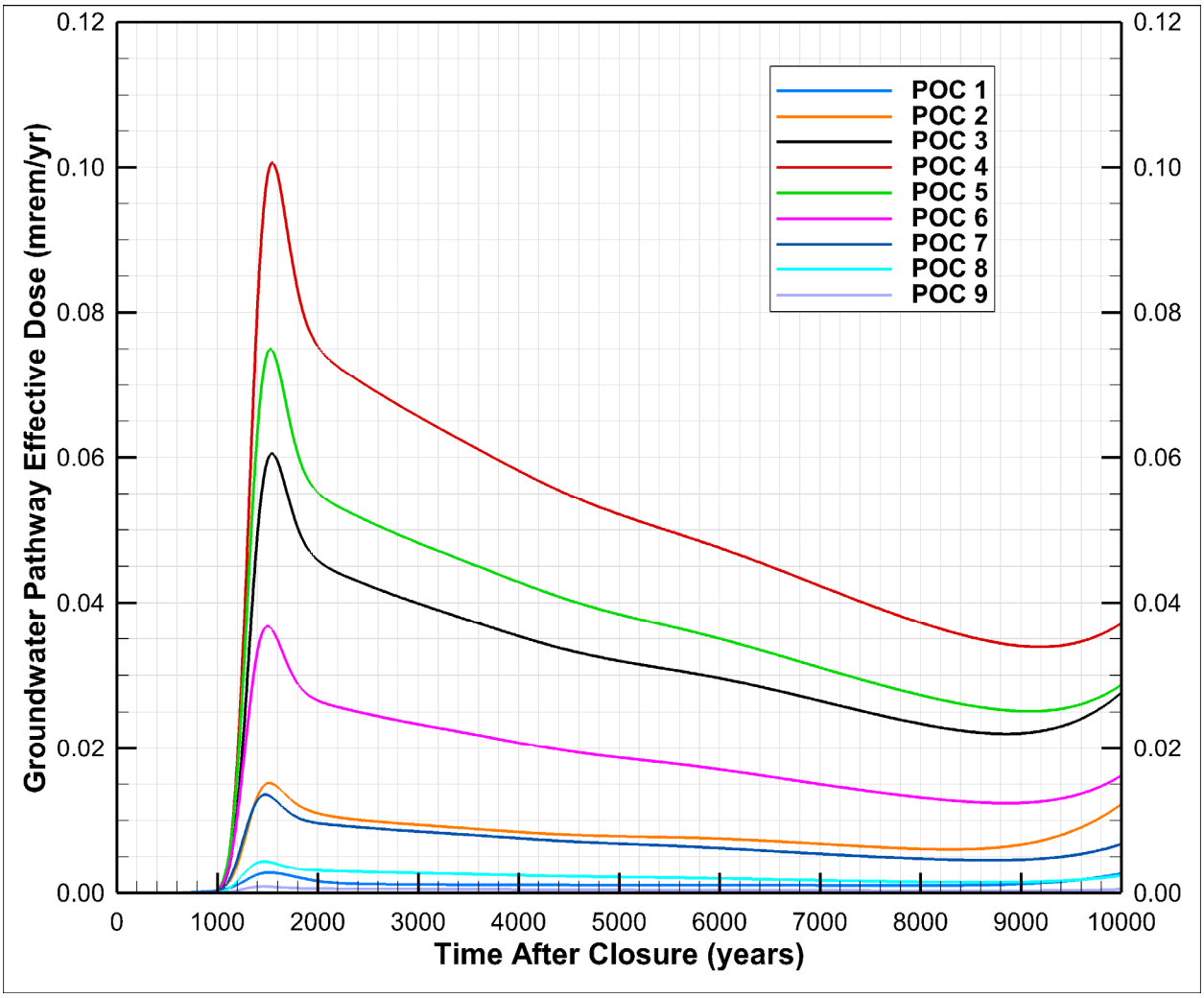

POC = Point of Calculation

7.3.2 Air Pathway Dose

Doses from radionuclides that may potentially be released in gaseous form are presented in Figure 7-32 along with the 10 mrem/yr air pathway dose performance objective from DOE O 435.1. Doses are very small, orders of magnitude below the dose performance objective, at all times. The peak dose of 4×10^{-3} mrem/yr occurs at very early time with ^{3}H being the primary dose contributor. Around 100 years, ^{129}I takes over as the primary dose contributor as ^{3}H dose declines due to its short half-life. Iodine-129 persists within the tank due to its long half-life and retention in the grout (from sorption), leading to a slow continuous diffusive flux. By about 300 years the ^{129}I dose reaches a steady value of 2×10^{-5} mrem/yr, indicating that the concentration gradient in the air phase from the tank to the surface has reached a steady state.

Figure 7-30. All-Pathways Dose Results that Includes Air and Groundwater Pathway Contributions at the Maximum Point of Concentration. The DOE Order 435.1 compliance time (1,000 years) is shown as a vertical blue dashed line, and the compliance dose (25 mrem/yr) is shown as the black horizontal dashed line. Note the logarithmic vertical axis.

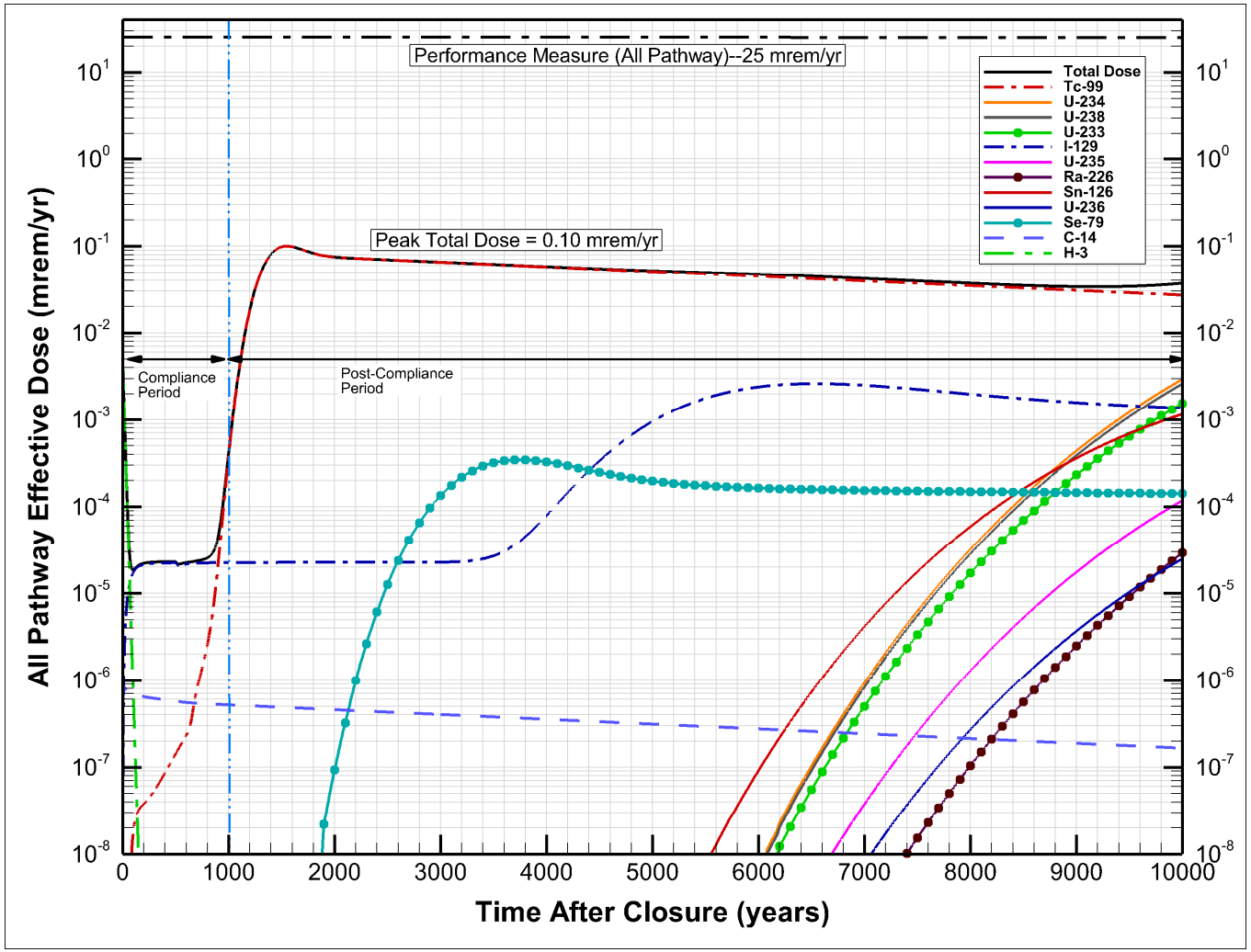

Reference: DOE O 435.1, Radioactive Waste Management.

Figure 7-31. Results of the Groundwater Pathway Dose Analysis at the Maximum Point of Concentration.

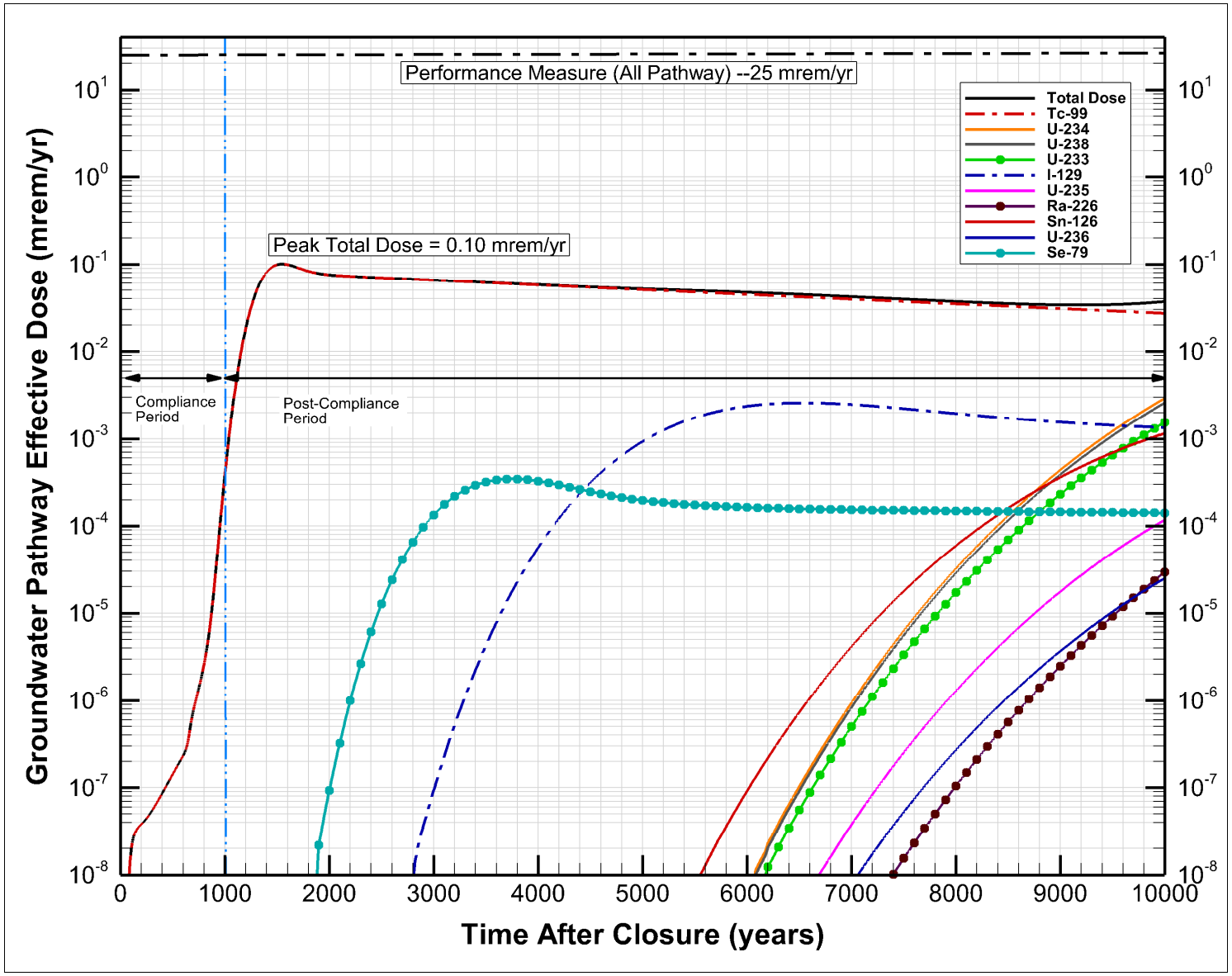

Table 7-5. Summary of Peak Doses (mrem/yr) for the Groundwater Pathway and the Time of Occurrence for All Radionuclides Giving Nonzero Doses in the Base Case Analysis.

Radionuclide	Peak Dose (mrem/yr)	Post-Closure Time of Peak Dose (year)	Peak Dose within 1,000 years Post-Closure (mrem/yr)
^{99}Tc	0.1	1,500	4E-4
^{79}Se	3.4E-4	3,800	0
^{129}I	2.6E-3	6,500	0
^{126}Sn	1.2E-3	10,000	0
^{238}U	2.6E-3	10,000	0
^{236}U	2.5E-5	10,000	0
^{235}U	1.2E-4	10,000	0
^{234}U	3.0E-3	10,000	0
^{233}U	1.6E-3	10,000	0
^{230}Th	1.3E-7	10,000	0
$^{226+D}$Ra*	2.8E-5	10,000	0

*Radium-226+D includes doses associated with all its progeny, excluding inhalation doses from ^{222}Rn, as required in DOE O 435.1, Radioactive Waste Management.

Figure 7-32. Results of the Air Pathway Dose Analysis. Note the logarithmic vertical and horizontal axis.

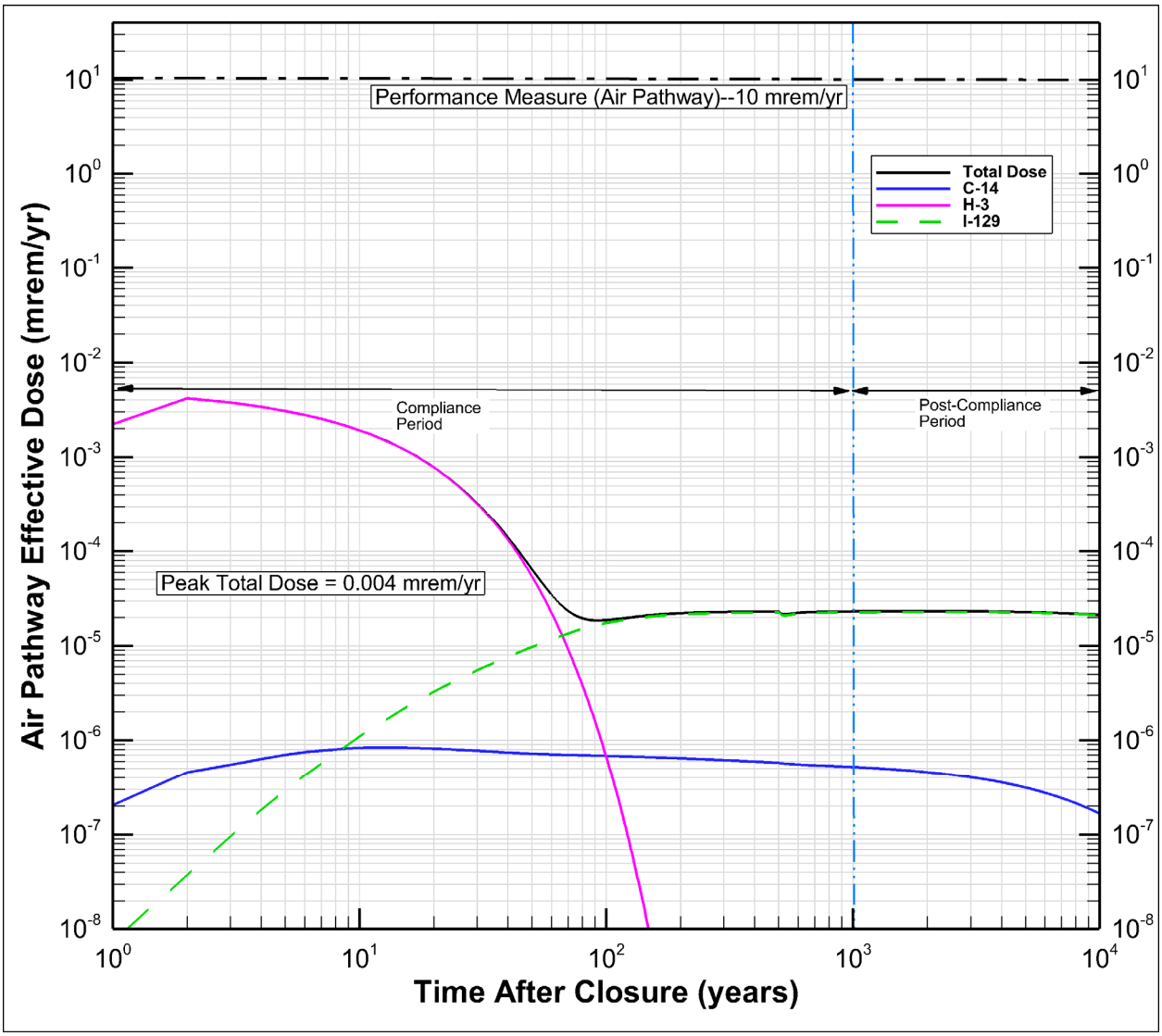

This page intentionally left blank.

8.0 UNCERTAINTY AND SENSITIVITY ANALYSIS

The guidance for completing the uncertainty and sensitivity analyses (DOE G 435.1-1) states that the dose rates have associated uncertainties, and a discussion of uncertainties should be included in expressing the outcomes of any PA. The guidance further states that an estimate of the degree of uncertainty is needed for the analysis that includes the calculation of the maximum impact of the disposal facility beyond the 1,000-year compliance period.

The intent of the uncertainty and sensitivity analysis is to identify the assumptions and parameters that have the greatest impact on the projected doses, and evaluate the consequences of the associated uncertainties relative to the performance objectives. This is because exact or precise estimates of future impacts are not truly quantifiable, and even the sources of uncertainty remain unquantifiable because they must include elements of subjectivity (NCRP Report 152).

Uncertainty analysis evaluates how uncertainty in analysis inputs collectively affect uncertainty in the analysis outcomes (for example, estimate of dose). As part of the uncertainty analysis, all uncertain inputs are evaluated together within a system model to estimate plausible range of outcomes. It helps evaluate how combination of various parameters could lead to various outcomes (for example, high dose or low dose). The sensitivity analysis quantifies the cause-and-effect relationships due to single-parameter or limited number of multiple-parameter changes in the parameter estimates. The results of the sensitivity analysis identify those parameters for which the variability in their estimates, either because of lack of knowledge or foreknowledge, limited data, or inherent randomness, introduces the greatest uncertainty into the estimates of potential radionuclide contamination levels. The uncertainty and sensitivity analysis are complementary to each other.

8.1 UNCERTAINTY ANALYSIS

Projections of environmental processes are inherently uncertain. Assessment of uncertainty in model results arising from assumptions and parameter values is necessary to support the determination that there is reasonable expectation of meeting the performance objectives. The objective of the uncertainty analysis is to estimate the plausible range of radionuclide dose that results from selecting parameter values within their uncertainty ranges. When a sufficient number of parameter combinations is evaluated over their plausible range, the calculated range of potential radionuclide dose can be used to quantify the uncertainty in the dose estimates. This analysis supports the demonstration of meeting the requirements of DOE M 435.1-1.

The objectives of this section are to develop uncertainty ranges and probability distributions of input parameter values for use in the PA, and to perform a fully probabilistic uncertainty analysis. The methodology that will be applied to propagate uncertainty through these models is first presented, followed by a discussion of the rationale that guided the probability distribution functions of input parameters. Uncertainty in model parameters is subsequently examined, followed by an evaluation of uncertainty in the groundwater and air pathway.

8.1.1 Methodology for Propagation of Uncertainty

One of the primary expectations of the PA modeling is to provide sufficient explanation of the uncertainty in the dose estimates. A probabilistic uncertainty analysis as described is intended to quantify and capture, where possible, the uncertainty in the process-level models, input parameters, and assumptions about current or future events. The intent of these analyses is to improve understanding of what uncertain factors exert the greatest influence on the model results.

The uncertainty analysis is conducted using a model that is developed by abstracting the results of the process-level models. The process-level models are defined as those that are specifically developed to rigorously solve the governing equations of flow and transport with appropriate boundary conditions at the scale of the processes that can incorporate changes to physical, chemical, and hydrologic properties. The abstraction-based approach is adopted because exercising the process-level models to adequately cover all combinations of parameter values across their full ranges of uncertainty would be very time-consuming and challenging.

To streamline this process in order to examine the uncertainty in a timely manner, an abstraction-based approach has been adopted for performing uncertainty analyses. For this purpose, the GoldSim© software (GoldSim Technology Group 2009) is used. GoldSim© is specifically designed for performing PA analyses. It not only provides the platform for coupling all of the processes in the PA in a system-level model, but also provides tools for propagation of the uncertainty. Similar approaches have been used at other DOE sites for examining uncertainty, for example, SRR-CWDA-2009-00017, "Performance Assessment for the Saltstone Disposal Facility at the Savannah River Site"; LA-UR-08-06764, "Performance Assessment and Composite Analysis for Los Alamos National Laboratory Technical Area 54, Area G"; and DOE/NV/25946--107, "Probabilistic Performance Assessment of a Low-Level Radioactive Waste Disposal Site on the Nevada Test Site."

The vadose zone flow rates as a function of time were abstracted from the STOMP©-based process-level models. STOMP© results were then used to generate the flow field (spatially and temporally varying Darcy flux and moisture content), which were abstracted along with their uncertainty estimates for use in GoldSim©-based models. Because changes in hydraulic properties and recharge rates introduce uncertainty in the computed flow field in a non-linear manner, the abstraction was performed by first propagating the uncertainty in flow parameters using the STOMP©-based model and then evaluating the resulting flow field. Since running 3-D STOMP©-based models is numerically intensive, a selected combination of pre-determined hydraulic properties and recharge rates were used by assigning parameter values from select percentiles of their distribution. This approach led to development of a possible range of flow fields (vertical Darcy flux and moisture contents) that were abstracted as inputs to the transport calculations using the GoldSim©-based system model for uncertainty analysis.

8.1.2 Rationale for Assigning Probability Distributions

The lack of knowledge about the appropriate value to use in a model is generally called epistemic uncertainty. Epistemic uncertainty is distinct from variability, which arises from

heterogeneity or an inherent randomness in the behavior of the system. The knowledge of experts cannot be expected to reduce uncertainty due to variability, although their knowledge may be useful for quantifying it ("Uncertainty and sensitivity analysis techniques for use in performance assessment for radioactive waste disposal" [Helton 1993]). Both uncertainty and variability may be quantified using probability distributions. They can be tracked and evaluated separately during an analysis, or they can be analyzed within the same computational framework. However, EPA/630/R-97/001, Guiding Principles for Monte Carlo Analysis recommends that variability and uncertainty are tracked and evaluated separately to identify parameters where additional data are needed (i.e., to identify reducible uncertainty through further study).

Among the different uncertainty and sensitivity analysis approaches available, the Monte Carlo method has been widely used for PA of radioactive waste disposals. In this method, discrete sets of input parameter values are selected at random from probability distribution functions; each set is run through the model, and a probability distribution function of model output is constructed. That distribution represents the uncertainty in model output associated with uncertain input parameters. Among its main assets, this method is conceptually simple and able to cover the full range of parameter uncertainties. More importantly, the method allows for obtaining the predictive uncertainty results without using surrogate models to map relations between uncertain inputs and analysis results (Helton 1993).

The Monte Carlo approach involves the following steps ("Uncertainty and sensitivity analysis techniques for hydrologic modeling" [Mishra 2009]):

- Selecting model input parameters
- Assigning probability distributions to input parameters to quantify uncertainty
- Generating many sample sets (realizations) through sampling of probability distribution
- Propagating the uncertainty (via realizations) through the analysis
- Determining parametric and nonparametric estimates of the reliability in the model output once an appropriate sample size is reached that ensures stable estimates of the output distribution.

A Monte Carlo approach was implemented in the WMA C PA using the GoldSim© software, using stochastic variables that represent the range of uncertain parameters in the WMA C model.

Although an infinite number of theoretical distributions can be used to fit an empirical data set, only a handful of distributions are considered in practice (Technical Report TR-02-11, "Assigning probability distributions to input parameters of performance assessment models"). The key features of these distributions are described in Table 8-1.

Several studies have tried to assess the impact of a chosen distribution function on the sensitivity analysis results. For instance, the results obtained by "The Effect of Distribution Choice for Uncertain Parameters in a Monte Carlo Analysis" (Hoffman 1996) can be used as a rule of

thumb for focusing the attention on parameter distributions that will have a relevant impact. Hoffman's conclusions are summarized in the following:

- As long as the uncertainty of a given parameter is small (coefficient of variation ≤30%), it makes very little difference which distribution is chosen

- As the coefficient of variation approaches and exceeds 30%, the use of distributions of log-transformed values is recommended

- The choice of distribution shape will be important if the analyst is interested in extreme values.

Table 8-1. Main Uses of Several Common Distribution Functions.

Distribution	Useful for Representing
Uniform (log-uniform) Triangular (log-triangular)	Low state of knowledge and/or subjective judgment
Normal	Errors due to additive processes
Log-normal	Errors due to multiplicative processes
Weibull	Component failure rates
Poisson	Frequency of rare events
Beta	Bounded, unimodal, random variables

Reference: Technical Report TR-02-11, "Assigning probability distributions to input parameters of performance assessment models."

Technical Report TR-02-11 recommends using, as a starting point, the guidelines given by EPA/630/R-97/001, the context of probabilistic health risk assessment. In selecting a distributional form, EPA/630/R-97/001 recommends that the analyst first considers the quality of the information in the database, and answers a series of questions including, but not limited to, the following:

- Is there any mechanistic basis for choosing a distribution family?

- Is the shape of the distribution likely to be dictated by physical or biological properties or other mechanisms?

- Is the variable discrete or continuous?

- What are the bounds of the variable?

- Is the distribution skewed or symmetric?

- If the distribution is thought to be skewed, in which direction?

- What other aspects of the shape of the distribution are known?

- How well do the tails of the distribution represent the observations?

For distributions representing the epistemic uncertainties common in PA analyses, Technical Report TR-02-11 recommends choosing a probability distribution function by considering the principle of maximum entropy. In this approach, a distribution is chosen that preserves the maximum uncertainty about the data, similar to the well-known concept of thermodynamic entropy related to the degree of disorder or randomness. The principle of maximum entropy seeks to choose a probability distribution function that maximizes the informational entropy, subject to known constraints. When developing the uncertainty distribution, the range was chosen carefully so as to be realistic and not to make the distribution excessively wide, which may have the potential of causing "risk dilution" (i.e., the peak dose using the peak-of-the-mean approach can be smaller for a wide parameter distribution than if a narrower distribution was used) ("History and Value of Uncertainty and Sensitivity Analyses at the Nuclear Regulatory Commission and Center for Nuclear Waste Regulatory Analyses" [CNWRA/NRC 2011]).

From a practical perspective, the use of the maximum entropy principle in assigning a distribution function implies the following considerations.

- If all the samples are equally likely because no constraint on the plausible parameter values is available, the maximum entropy is reached and corresponds to the uniform distribution.

- If some information is available, uncertainty is reduced as much as possible by using all information (i.e., by satisfying all constraints) but no further by unnecessary assumptions. This ensures that ignorance is acknowledged, and forces the analyst to retain maximum uncertainty in the distribution developed from the data. In that case, the distribution function will have a concentration of probability away from the extreme values, leading to a reduction of uncertainty and hence a reduction of entropy in comparison to the uniform distribution.

Based on these considerations, the maximum entropy principle implies that certain probability distribution functions are more appropriate for representing data with specific constraints, as summarized in Table 8-2. This approach has been used in this PA for assigning distribution functions.

8.1.3 Parameter Uncertainty Distributions

This section provides a description of the parameter uncertainty distributions evaluated in the uncertainty analysis for the WMA C PA.

8.1.3.1 Uncertainty in Recharge Rates. Recharge rates have been estimated from studies conducted at the Hanford Site over the last 30 years. Recharge rates are based on the estimate of

the downward water flux below the evapotranspiration zone representing deep drainage. Recharge rates are available for natural and disturbed soils, for soils with and without vegetation, and for various plant communities. In addition, recharge has been estimated for surface covers with varying plant communities. These estimates are based on lysimeter records, tracer tests (chloride mass balance), and computer simulations to match field data. PNNL-16688 and PNNL-14702 provide primary sources of information on recharge estimates for the Hanford Site that are relevant to tank farms. There is no site-specific information to WMA C on natural recharge. Natural recharge at WMA C is inferred from measurements made at the FLTF (Section 3.1.5.2.2).

Table 8-2. Guidance for Selection of Probability Distribution Function Considering the Data Constraints.

Constraint	Distribution
Upper bound, lower bound	Uniform
Minimum, maximum, mode	Triangular
Mean, standard deviation	Normal
Range, mean, standard deviation	Beta
Mean occurrence rate	Poisson

Reference: Reliability-Based Design in Civil Engineering (Harr 1987).

Spatial variability in recharge occurs at WMA C and surrounding areas due to variations in vegetative cover and disturbed surface conditions. Spatially, two zones have been identified with different disturbed surface conditions: one within the WMA C fenceline, designated as the WMA C Disturbed Surface, and the other outside the WMA C fenceline, designated as the Non-Tank Farm Disturbed Surface. After closure, it is expected that the disturbed areas will revegetate fully within 30 years.

The temporal uncertainty in recharge occurs due to time-varying changes resulting from construction and operations at WMA C and future changes after closure. These temporal recharge estimates have been grouped into a pre-operational phase, an operational phase, a post-closure phase with intact surface cover, and a post-closure phase with degraded surface. While both spatial and past temporal changes have influenced the recharge rates at WMA C and need to be considered, the focus of the PA is on developing uncertainty in long-term post-closure recharge rates, since that will influence the transport of contaminants from the residual waste in the future. In this regard, the temporal variability observed in the past climate records (50% to 128% of modern levels [Section 3.1.2.6]) is considered.

The area outside the WMA C fenceline, designated as the Non-Tank Farm Disturbed Surface, is not likely to influence the contaminant transport in the vadose zone, and, therefore, constant best-estimate values are used for those areas in the following manner.

- Disturbed areas observed during the operations phase using aerial photographs, where vegetation appears to have grown, are assigned a value of 22 mm/yr (0.87 in./yr) based

on estimates presented in PNNL-14702. These areas include surfaces where the existing shrub-steppe vegetation has been destroyed (e.g., by fire or Hanford operations), but shallow-rooted plants have been allowed, or were reintroduced, to re-vegetate the land.

- Disturbed areas observed during the operations phase using aerial photographs that appear to be reworked such that vegetation does not grow are assigned a value of 63 mm/yr (2.5 in./yr) based on estimates presented in PNNL-14702. These disturbed areas include construction and operations outside WMA C that removed the surface soil, broke up any near-surface layering, and exposed Hanford formation sands. These sediments tend to be coarser than the original soil, and, as indicated in photographs of the area around WMA C, plants have difficulty growing on them. The selected recharge rate is supported by drainage data collected from the 300 North Lysimeter, which contains coarse Hanford formation material screened to less than 1% gravel, where the long-term recharge rate averaged 62 mm/yr (2.4 in./yr) from 1981 to 2005 (PNNL-16688).

- Disturbed areas are allowed 30 years to revegetate fully after closure. Therefore, over time the disturbed area recharge changes to that assigned for the undisturbed natural vegetated land surface. Thirty years appears to be a reasonable estimate for the time required for the young shrub steppe to become mature and reclaim the land. Sagebrush and/or other native plant species at Hanford often reclaim the land within 5 years of planting or seeding (BHI-01745, "2004 Environmental Restoration Contractor Revegetation Monitoring Report"; WCH-223, "2007 River Corridor Closure Contractor Revegetation Monitoring Report"). The plant community at the Prototype Hanford Barrier began working almost immediately to transpire water and eliminate recharge (PNNL-17176), and 24 species of vegetation were identified on it one year after it burned (PNNL-18845). Data from other arid and semi-arid areas in the United States indicate that many stands of mountain big sagebrush achieve greater than 20% crown cover within 25 years of burning ("Trend of Mountain Big Sagebrush Crown Cover and Ground Cover on Burned Sites, Uinta Mountains and West Tavaputs Plateau, Utah" [Goodrich et al. 2008]). In a study conducted at 38 sites in southwest Montana, the average time to full recovery of basin sagebrush (ssp. *Tridentata*, the subspecies most prevalent at Hanford) required less than 32 years after burning ("Recovery of Big Sagebrush Following Fire in Southwest Montana" [Lesica et al. 2007]).

For the area within the WMA C fenceline, designated WMA C Disturbed Surface, the temporal evolution is presented below with the uncertainty estimates.

<u>Pre-Operation Period</u>: During the time prior to construction (before 1945), the area currently occupied by WMA C appears to have been covered by a mature shrub-steppe plant community growing in Rupert sand or Burbank loamy sand soil. It is difficult to distinguish between the two soil types because the divide between the Rupert sand and Burbank loamy sand soil appears to coincide with the northeastern boundary of WMA C.

For the vegetated Rupert sand, PNNL-14702 recommended using a value estimated using the Wye Barricade data (4 mm/yr [0.16 in./yr]) as the best-estimate value, although the surface is described as a stabilized dune area with low shrub cover. PNNL-16688 later

revised the estimate by considering an average of the three available tracer estimates (4, 0.26, and 0.9 mm/yr [0.16, 0.01 and 0.04 in./yr]). Moreover, they reported a good agreement between their suggested mean value (1.7 mm/yr) and their modeling results that considered a 50-year weather record (including the two wettest years: 1995 and 1996) and yielded a rate of 1.9 mm/yr (0.07 in./yr). Consequently, they recommended using an estimate of 1.7 mm/yr (0.07 in./yr) for vegetated Rupert sand soil.

For the vegetated Burbank loamy sand, PNNL-14702 recommended the average value of 3.0 mm/yr (0.12 in./yr) based on three chloride tracer-based estimates of recharge (0.66 mm/yr, 2.8 mm/yr, and 5.5 mm/yr [0.03 in./yr, 0.11 in./yr and 0.22 in./yr]). PNNL-16688 augmented these data with five additional tracer-based estimates that decreased the average to 1.9 mm/yr (0.07 in./yr), along with a simulation that suggested a rate of 5.2 mm/yr (0.2 in./yr), which is near the upper end of the range of tracer estimates.

Based on the available information, uncertainty in pre-operational (natural vegetation) recharge is developed through selection of a triangular distribution, with a minimum value of 0.5 mm/yr (0.02 in./yr), maximum value of 5.2 mm/yr (0.2 in./yr), and mode of 1.9 mm/yr (0.07 in./yr).

Operations Period: During the operations period, which started in 1945 and is assumed to last until 2020, two recharge zones have been defined within the WMA C fenceline: one that is disturbed, has no vegetation, and is covered with gravel; and the other that is largely undisturbed and characterized by a vegetative cover. For the latter, the same uncertainty distribution and range is considered that is developed for the pre-operations phase. For the former (the disturbed zone without vegetation [bare soil]), the range in recharge is based on the following discussion.

Disturbed zone recharge rates for the tank farms have been estimated to vary from 40 mm/yr to 140 mm/yr (1.57 in./yr to 5.51 in./yr). A reasonably conservative estimate of 100 mm/yr (3.94 in./yr) was recommended for disturbed Rupert sand zone without vegetation and with gravel cover (Gee et al. 1992). The upper bound value of 140 mm/year (5.51 in./yr) results from an enhanced precipitation experiment on the "sandy gravel side slope" of the Hanford Prototype Barrier installed at the 216-B-57 Crib. This treatment is referenced as being "useful for characterizing deep drainage at the high-level waste tank farms at Hanford" (PNNL-14744). Enhanced precipitation represented three times the average precipitation. Approximately 140 mm (5.51 in./yr) of the applied precipitation was observed to have infiltrated. For a lower bounding value, CP-14873, "200-BP-1 Prototype Hanford Barrier Annual Monitoring Report for Fiscal Year 2002" reported that 21.5% of precipitation (37.8 mm/yr [1.49 in./yr]) became recharge through sparsely vegetated sandy gravel representing the "sandy gravel side slope." Such a percentage (i.e., 21.5%) represents a lower value of approximately 40 mm/yr (1.57 in./yr).

Based on the available information, uncertainty in operational period recharge for the disturbed zone within WMA C is developed through selection of a triangular distribution,

with a minimum value of 40 mm/yr (1.57 in./yr), maximum value of 140 mm/yr (5.51 in./yr), and mode of 100 mm/yr (3.94 in./yr).

Post-Closure Period with Intact Surface Cover: For the area covered by the intact surface barrier, the recharge rate is expected to decline to nearly zero, as the modified RCRA-compliant surface cover is designed to prevent or significantly limit recharge. The design criteria of such a barrier are identified in BHI-00007, "Prototype Hanford Surface Barrier: Design Basis Document" and DOE/RL-93-33, and include limiting recharge to 0.5 mm/yr (0.02 in./yr). The design life of surface cover as a recharge barrier is assumed to be 500 years (DOE/RL-93-33).

Extensive laboratory and modeling work, and limited field testing of surface barriers, have been performed with results summarized in PNNL-14744. Lysimeter testing has been performed for different surface barrier concepts, including a Modified RCRA Subtitle C Barrier with silt-loam layers having depths between 1 and 2 m (3.3 to 6.6 ft). Lysimeter data from the prototype Hanford barrier (Wing and Gee 1994) have also been collected and analyzed. Finally, modeling has been performed to address potential climate change impacts and no vegetation impacts on surface barrier performance.

The lysimeter drainage data that have been collected since 1989 suggest that the recharge rate beneath surface barriers having at least 1 m (3.3 ft) of silt loam is zero under ambient precipitation conditions. Most of these lysimeters did not contain an asphalt layer. Simulation results reported in PNNL-14744 investigated the sensitivity of the lysimeter data to climate change, silt-loam hydraulic properties, vegetation changes, erosion, and dune formation above the surface barrier. Results indicated that the performance of these surface barriers was robust in that the estimated recharge rates remained below 0.1 mm/yr (0.004 in./yr). For the cases investigated, only in the case of dune formation and no vegetation on the surface barrier were the simulated recharge rates above 0.1 mm/yr (0.004 in./yr). To account for such uncertainty (dune formation and no vegetation) within the design life of the barrier, an upper-bound recharge of 0.9 mm/yr (0.04 in./yr) is considered as suggested by PNNL-14744 for the post-barrier design life.

Based on the available information, uncertainty in recharge during post-closure period with intact surface is developed through selection of a triangular distribution, with a minimum value of 0.1 mm/yr (0.004 in./yr), a maximum value of 0.9 mm/yr (0.04 in./yr), and mode of 0.5 mm/yr (0.02 in./yr).

Post-Closure Period with Degraded Surface Cover: In the post-closure period after 500 years, the recharge barrier capability of the surface cover is assumed to be degraded. This recharge rate is applicable to the entire simulated duration (except for the first 500 years after closure) and influences the contaminant transport of residual tank waste through the vadose zone. It is expected that once the surface cover is degraded, the recharge will be similar to the recharge during the pre-operational phase, since the surface will most likely be indistinguishable from the surrounding surface in terms of vegetative cover. PNNL-14744 suggests that the performance of the barrier is not expected to change after its design life. Conclusions in PNNL-14744 indicate that the

possibility of the most likely natural failure mechanisms (i.e., bioturbation of the silt loam layer, wind erosion, and accretion of windblown sand) of these natural systems is quite low with an appropriate design. The emplaced silt-loam soils should continue to perform as long as they remain in place.

To propagate uncertainty in post-closure recharge rate following degraded surface cover, a triangular distribution is chosen, with a minimum value of 0.5 mm/yr (0.02 in./yr), a mode value of 1.9 mm/yr (0.07 in./yr), and a maximum value of 5.2 mm/yr (0.2 in./yr). This uncertainty range is the same as that chosen for the pre-operational phase recharge rates and covers the natural variability observed in annual precipitation in the climate record for the last 100,000 years (Section 3.1.2.6).

The range in recharge rates selected for the various time periods are summarized in Table 8-3.

Table 8-3. Spatial and Temporal Uncertainty in Recharge Rates Considered for Waste Management Area C.

Spatially Distinct Zone	Uncertainty in Recharge Estimate (mm/yr)		
	Minimum	Maximum	Most Likely
Pre-operations Period (Prior to Year 1945)			
Undisturbed (Natural Vegetation)[a]	0.5	5.2	1.9
Operations Period (Years 1945 – 2020)			
Undisturbed (Natural Vegetation)[a]	0.5	5.2	1.9
Waste Management Area C Disturbed Surface	40	140	100
Non-Tank Farm Disturbed Surface[b]	22 / 63	22 / 63	—
Post-Closure Period with Intact Surface Cover (Years 2020 – 2520)			
Undisturbed (Natural Vegetation)[a]	0.5	5.2	1.9
Waste Management Area C Surface Barrier	0.1	0.9	0.5
Non-Tank Farm Disturbed Surface[a,c]	0.5	5.2	1.9
Late Post-Closure Period with Degraded Surface Cover (Years > 2520)			
Undisturbed (Natural Vegetation)[a]	0.5	5.2	1.9
Waste Management Area C Surface Barrier	0.5	5.2	1.9
Non-Tank Farm Disturbed Surface[a]	0.5	5.2	1.9

[a]Waste Management Area C late post-closure surface barrier assumed to acquire natural vegetation recharge rate.
[b]Disturbed areas that allow vegetation are assigned 22 mm/yr. Disturbed areas that are reworked such that vegetation does not grow are assigned 63 mm/yr.
[c]Disturbed areas are allowed 30 years to revegetate fully.

8.1.3.2 Uncertainty in Residual Inventory Estimates. A best estimate of the residual inventory for tanks and ancillary equipment was developed and evaluated in the PA (Section 3.2.2). However, considerable uncertainty exists in estimating the residual inventory due to mixing of various waste types, differentiation between inventory associated with sludge and salt-cake, and the limited availability of direct measurements of contaminant concentrations. These uncertainties have been recognized in the BBI database, which is the official database for tank waste inventory. Uncertainties in concentration, waste volume, and waste density for each tank are accounted by developing standard deviation (SD) estimates in those parameters (assuming a normal distribution), which are then propagated to calculate the inventory uncertainty in 46 radionuclides and 25 chemicals that are tracked in the BBI. For the retrieved tanks, the uncertainty is based primarily on sample-based results. However, where information is lacking for a particular analyte, a template based on process knowledge is used to fill in the gaps.

For WMA C, the BBI database currently contains residual inventory information from 10 retrieved tanks: C-103, C-104, C-106, C-108, C-109, C-110, C-201, C-202, C-203, and C-204. These are the tanks from which post-retrieval samples were collected, and uncertainty in concentration (in solid phase), residual volume, and density is quantified in terms of relative standard deviations (RSD), which is SD divided by the mean value. All the relevant information related to 46 radionuclides and 25 chemicals from the BBI was obtained for these 10 tanks. The following steps were undertaken to reduce the dataset.

- Removal of the analytes that were below detection limits. This resulted in 25 radionuclides and 12 chemicals.

- Identification of mean solid-phase concentration, residual volume, and waste density for each analyte for the sludge waste form for each tank.

- Identification of RSD of concentration for each analyte, residual volume, and waste density for the sludge waste form for each tank.

- Calculation of SDs in concentration, residual volume, and waste density from the RSDs by multiplying by the mean values.

Since the residual inventory for a given analyte is calculated by multiplying the concentration in solid phase (sludge) with the residual waste volume and waste density, the mean inventory is calculated based on the mean values of these parameters.

Next, normal probability distributions were developed for the concentration of each analyte, residual volume, and density for each tank. This was done by defining the mean and SD for the parameter and implementing them in the GoldSim©-based system model. Following this, 10,000 realizations were run using Latin Hypercube Sampling (LHS), leading to 10,000 estimates of inventory for each analyte for each tank. The sampled inventory estimates were normalized by dividing by the mean inventory, leading to 10,000 normalized inventories for each analyte for each tank. These results can be expressed as a cumulative distribution function (CDF) of the normalized inventory. An example CDF for ^{99}Tc is presented in

Figure 8-1 for each tank. In addition, an average CDF was calculated by averaging the CDF values for all the tanks.

Figure 8-1. Cumulative Distribution Function of Normalized Inventory of Technetium-99 for Retrieved Tanks, and the Average Cumulative Distribution Function.

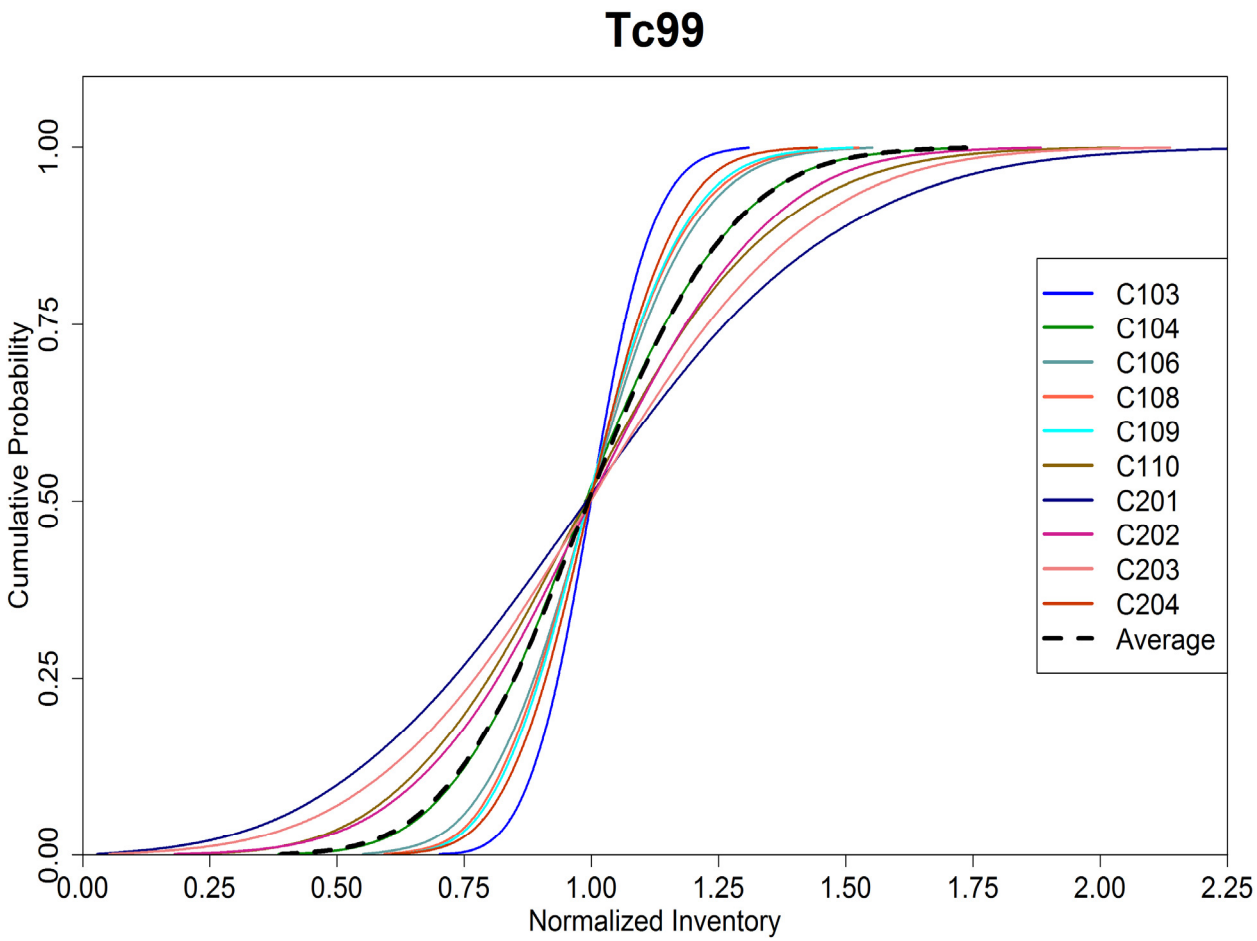

Development of normalized inventory CDF is attractive because the sampled value can be multiplied with the mean inventory to estimate inventory for a given realization. As shown in Figure 8-1, the average normalized inventory CDF for ^{99}Tc ranges from 0.4 to 1.75 and therefore indicates the factor by which the mean inventory can vary. Since the CDF of normalized inventory is calculated separately for each analyte for each tank, each CDF could be separately sampled for each tank to determine the multiplier factor for the inventory. However, this approach leads to a very large number of uncertain parameters related to inventory, due to the large number of analytes considered per source term. The analysis has therefore been simplified by sampling the analyte specific average CDF (averaged over the tanks) and then multiplying the sampled value by the mean inventory for a given analyte for each source term. This approach significantly simplifies the analysis while preserving the uncertainty in the analyte inventory.

The uncertainties in inventory for various analytes are presented in Figure 8-2. Not all the tanks have uncertainty in all the analytes quantified. This is because some analytes are below

detection limits in some of the tanks. In such cases, the average CDF is calculated based on the CDF of the tanks for which uncertainty estimates were available. For analytes for which uncertainty information is not available in the BBI, no uncertainty is propagated in the inventory. For the tanks where post-retrieval sampling-based inventory uncertainty estimates were not available in the BBI database, the uncertainty estimates based on average normalized CDF presented earlier are applied. This is a reasonable approximation, given that several tanks within WMA C have similar waste types (Table 3-12) and were operated in a similar manner.

In addition to developing uncertainty in the inventory, uncertainty is also propagated separately in the residual volume, as it is a key parameter in the source term release calculations. The methodology for deriving the uncertainty in residual volume is similar to that for the inventory derivation and is based on the same dataset. The normalized residual waste volume is derived from 10,000 LHS realizations of the same GoldSim© model file used for inventory uncertainty. The model file samples the underlying normal distribution for each tank and divides by the mean residual volume for that tank. The CDF of normalized residual waste volume uncertainty is presented in Figure 8-3 for each tank, along with the average CDF (average of all tanks). The average CDF of normalized waste volume is sampled to scale the mean residual volume for each source term. As shown in Figure 8-3, the normalized values in the average CDF vary from 0.75 to 1.25. Because some correlation is expected between residual waste volume and the residual inventory, the uncertainty distribution of residual waste volume is correlated to the uncertainty distribution of the residual uranium inventory, since it is the dominant radionuclide in terms of mass and forms mineral phases that contribute to the residual volume.

8.1.3.3 Uncertainty in Source Term Transport Parameters. The waste form degradation and release mechanisms from the source term are described in Section 6.3.1. Several interacting parameters determine the release rate from the base of the tanks and ancillary equipment into the underlying vadose zone. The uncertainty in these parameter estimates is described in Section 6.3.1 and summarized below.

- The initial release fraction of ^{99}Tc is observed to vary between 4.5% and 15%. Without additional information, a uniform distribution is applied.

- The remaining fraction of ^{99}Tc undergoes a slower release that is modeled using a first order reaction rate. The available information was used to identify a uniform distribution with a minimum of 5×10^{-4} day^{-1} and a maximum of 8×10^{-4} day^{-1}.

- The solubility of uranium is also considered to be uncertain. The uncertainties arise from both the value of the solubility at any time and the mineral phases assumed to be controlling the solubility. The mean solubility is assumed to change from 10^{-4} M to 10^{-6} M at 1,000 years after closure, based on the assumption that solubility will be controlled by amorphous mineral phases early on, and later by a $CaUO_4$ mineral phase under $Ca(OH)_2$-saturated conditions. A factor of two uncertainty multiplier to solubility is imposed by assigning a log-uniform distribution varying from 0.5 to 2. This distribution is chosen because the median value of this distribution is 1 (and mean is about 1.1); therefore, the mean/median sampled multiplier will retain the base case solubility value.

- Uncertainty in the effective diffusion coefficient through the base mat is propagated through a log-uniform distribution with a minimum and maximum value of 6×10^{-9} cm^2/s and 2×10^{-7} cm^2/s, based on the range of effective diffusion coefficients measured for ^{99}Tc as presented in Figure 6-32. This distribution leads to a median value of 3.5×10^{-8} cm^2/s, which is close to the best-estimate value of 3×10^{-8} cm^2/s.

- Uncertainty in sorption on cementitious material is represented using a triangular distribution of K_d values for each analyte (see Table 6-5). This distribution is appropriate for representing the mean values and ranges, which are the only values available in the literature. Where information is not available, a zero K_d value is used.

8.1.3.4 Uncertainties in Vadose Zone Hydraulic Properties. Uncertainties in vadose zone hydraulic properties are derived from a set of laboratory (core-scale) experiments conducted on samples representative of Hanford H1, H2, and H3 units and backfill material. The laboratory-measured soil-moisture retention and unsaturated hydraulic conductivity datasets were fit using van Genuchten-Mualem constitutive relationships to derive uncertainty in the following parameters[1]:

- The saturated hydraulic conductivity K_s

- The van Genuchten fitting parameter α, which is proportional to inverse of air-entry matric potential (cm^{-1})

- The van Genuchten fitting parameter n, which is a dimensionless fitting parameter commonly taken to be the inverse of the pore-size SD

- The saturated and residual moisture contents (θ_s and θ_r).

A single, large, internally consistent soil-moisture retention and unsaturated hydraulic conductivity dataset consisting of 44 soil samples from the nearby IDF was analyzed for the H2 sand-dominated unit. The IDF is located southwest of WMA C within 200 East Area, and the dataset includes 44 samples to evaluate uncertainty and to derive probability distribution functions for K_s, α, n, θ_s, and θ_r for H2 sand-dominated unit.

The laboratory procedures used to analyze the IDF H2 borehole samples and to derive the van Genuchten-Mualem parameters are summarized in Appendix B (Section B.2) with additional details presented in RPP-20621, "Far-Field Hydrology Data Package for the Integrated Disposal Facility Performance Assessment." The fitted van Genuchten-Mualem parameters for the IDF H2 sandy sequence (44 samples) are reproduced in Table B-3. The fitted moisture retention curves and unsaturated conductivity curves for H2 sandy sequence, as well as the WMA C H2 composite curves, are shown in Figures B-12 and B-13, respectively. A 20% gravel correction was applied to IDF H2 samples for use at WMA C based on empirical evidence of a greater gravel fraction being present at WMA C than IDF (Appendix B, Section B.2.1).

[1] The pore size distribution factor, ℓ (Mualem 1976) was kept fixed at 0.5 in this exercise.

Figure 8-2. Cumulative Distribution Function of Normalized Inventory of Various Analytes for the Retrieved Tanks along with the Average Cumulative Distribution Function. (sheet 1 of 10)

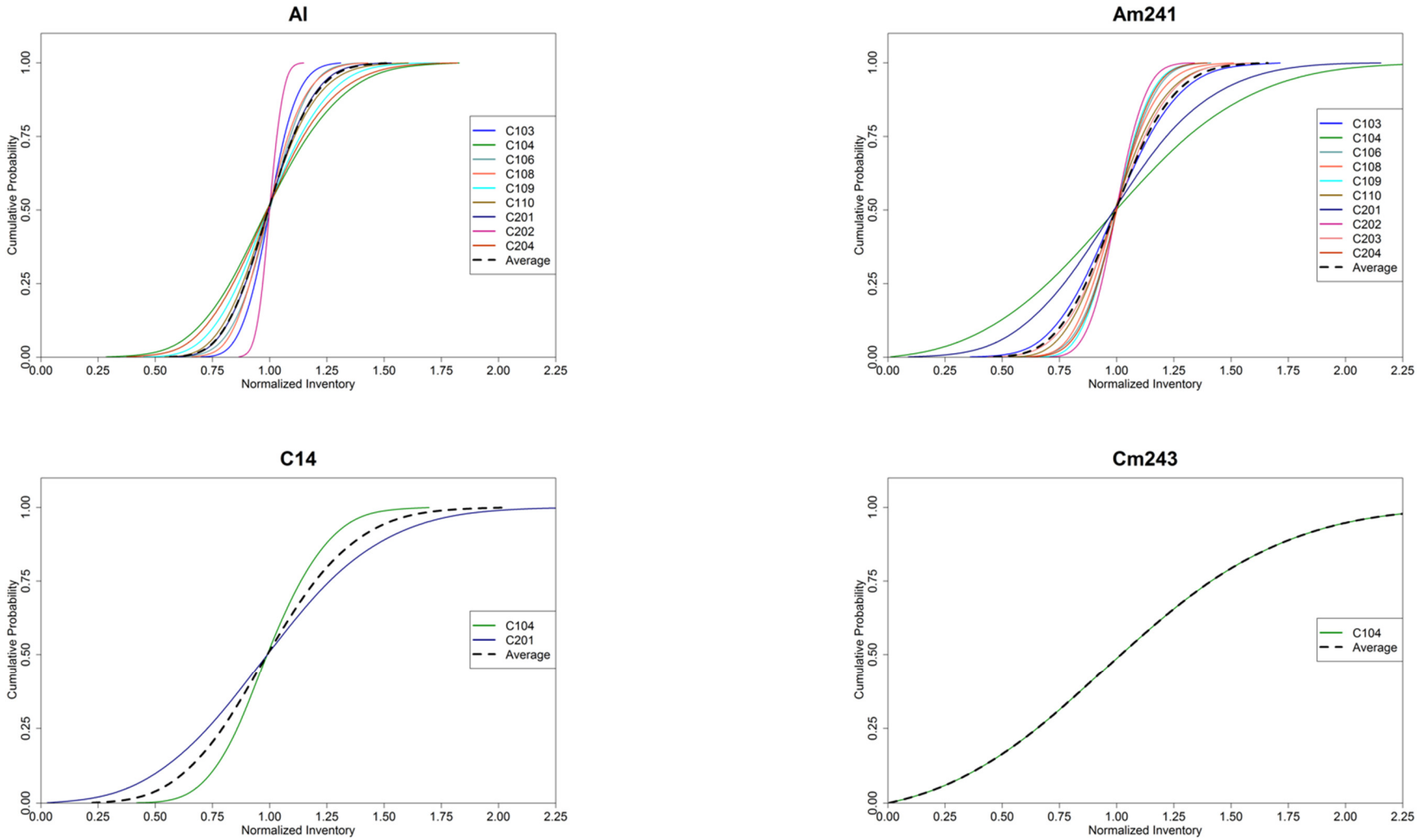

Figure 8-2. Cumulative Distribution Function of Normalized Inventory of Various Analytes for the Retrieved Tanks along with the Average Cumulative Distribution Function. (sheet 2 of 10)

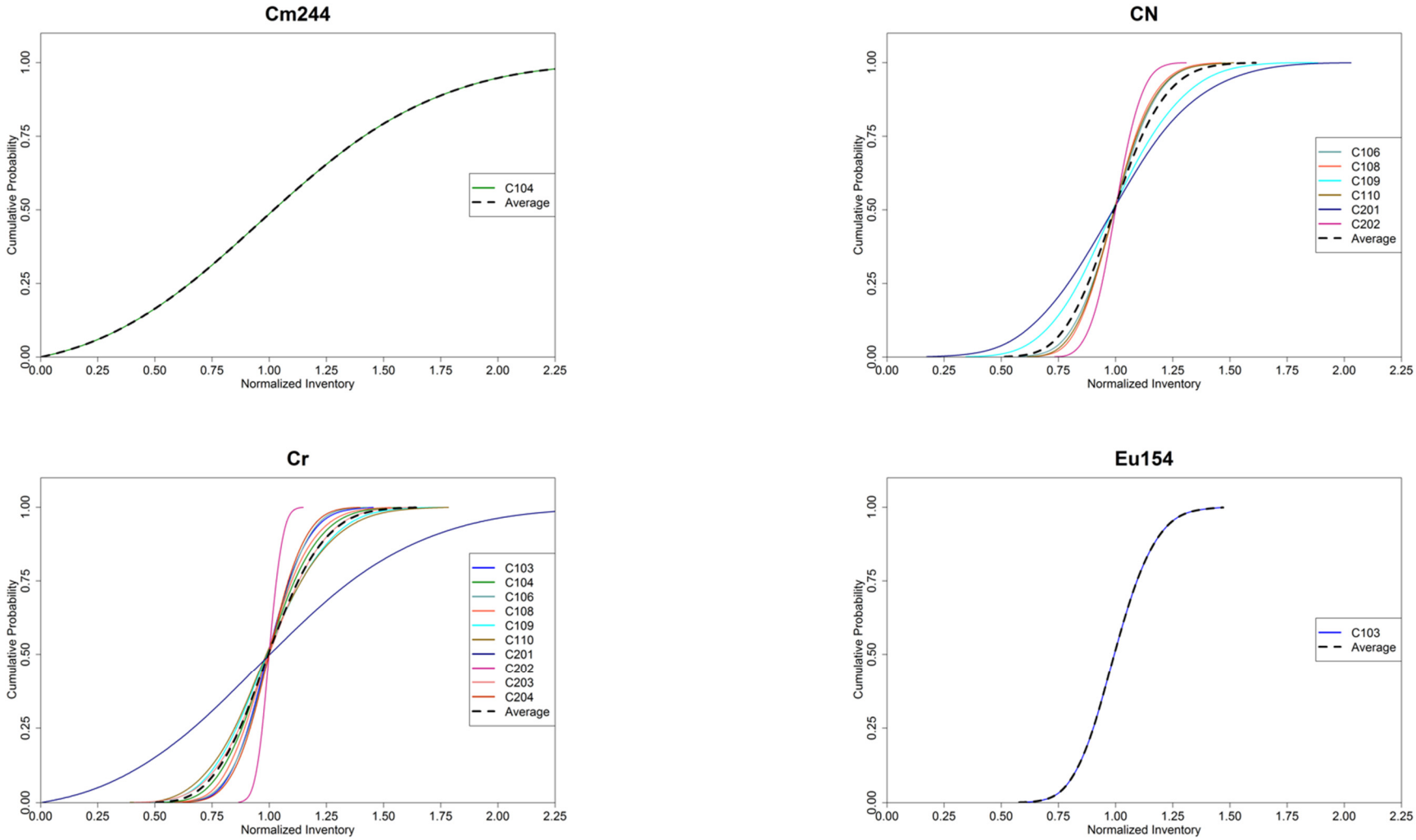

Figure 8-2. Cumulative Distribution Function of Normalized Inventory of Various Analytes for the Retrieved Tanks along with the Average Cumulative Distribution Function. (sheet 3 of 10)

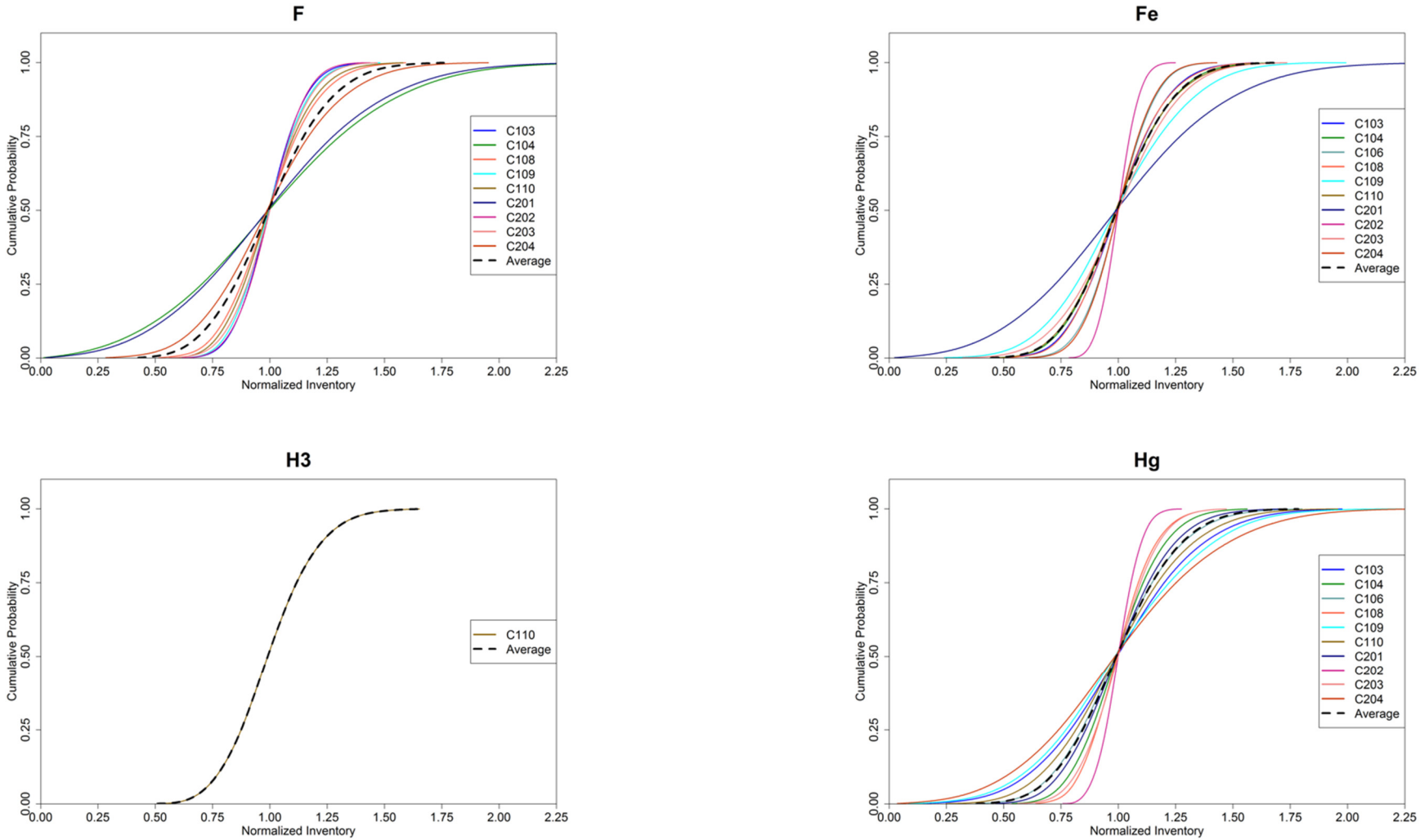

Figure 8-2. Cumulative Distribution Function of Normalized Inventory of Various Analytes for the Retrieved Tanks along with the Average Cumulative Distribution Function. (sheet 4 of 10)

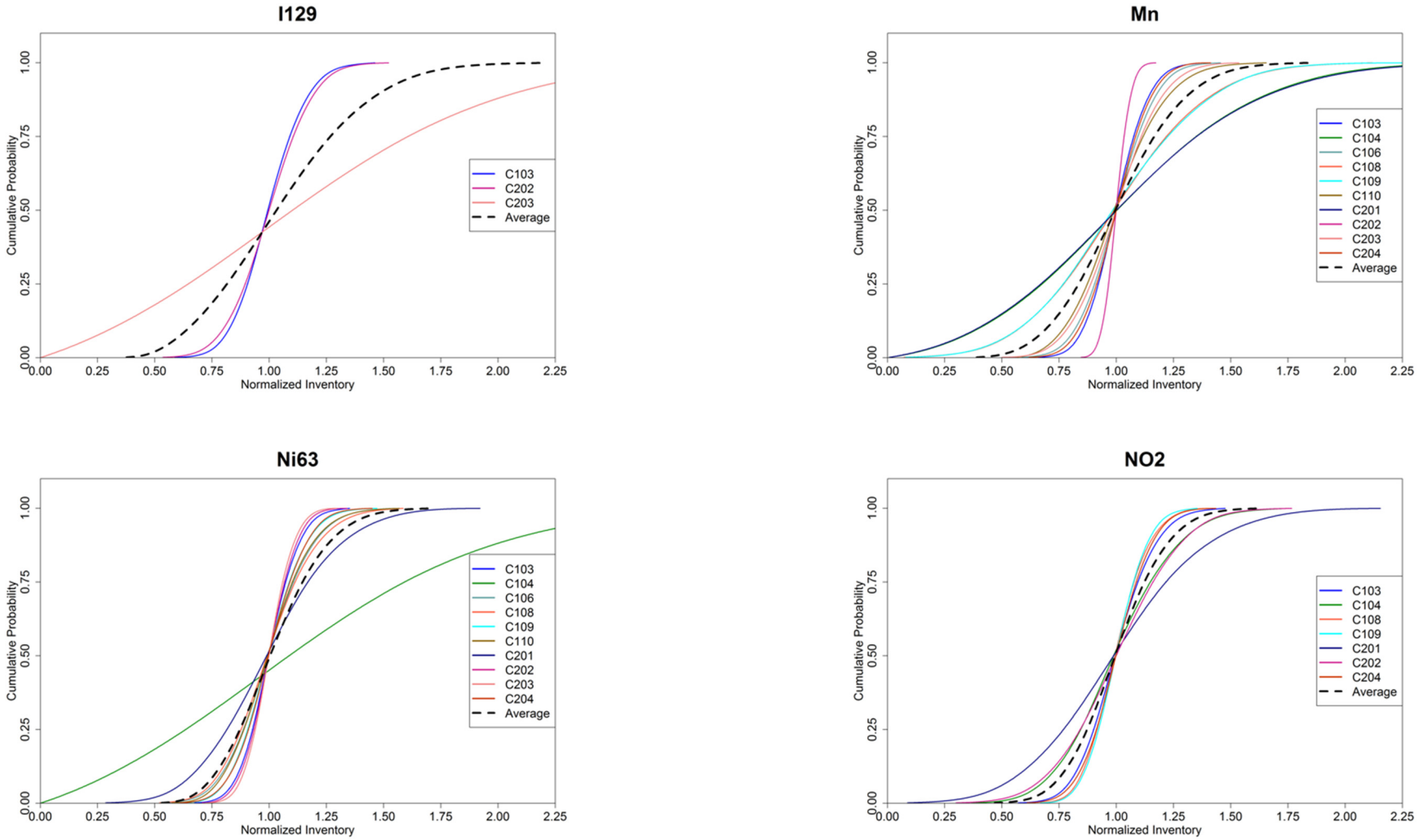

Figure 8-2. Cumulative Distribution Function of Normalized Inventory of Various Analytes for the Retrieved Tanks along with the Average Cumulative Distribution Function. (sheet 5 of 10)

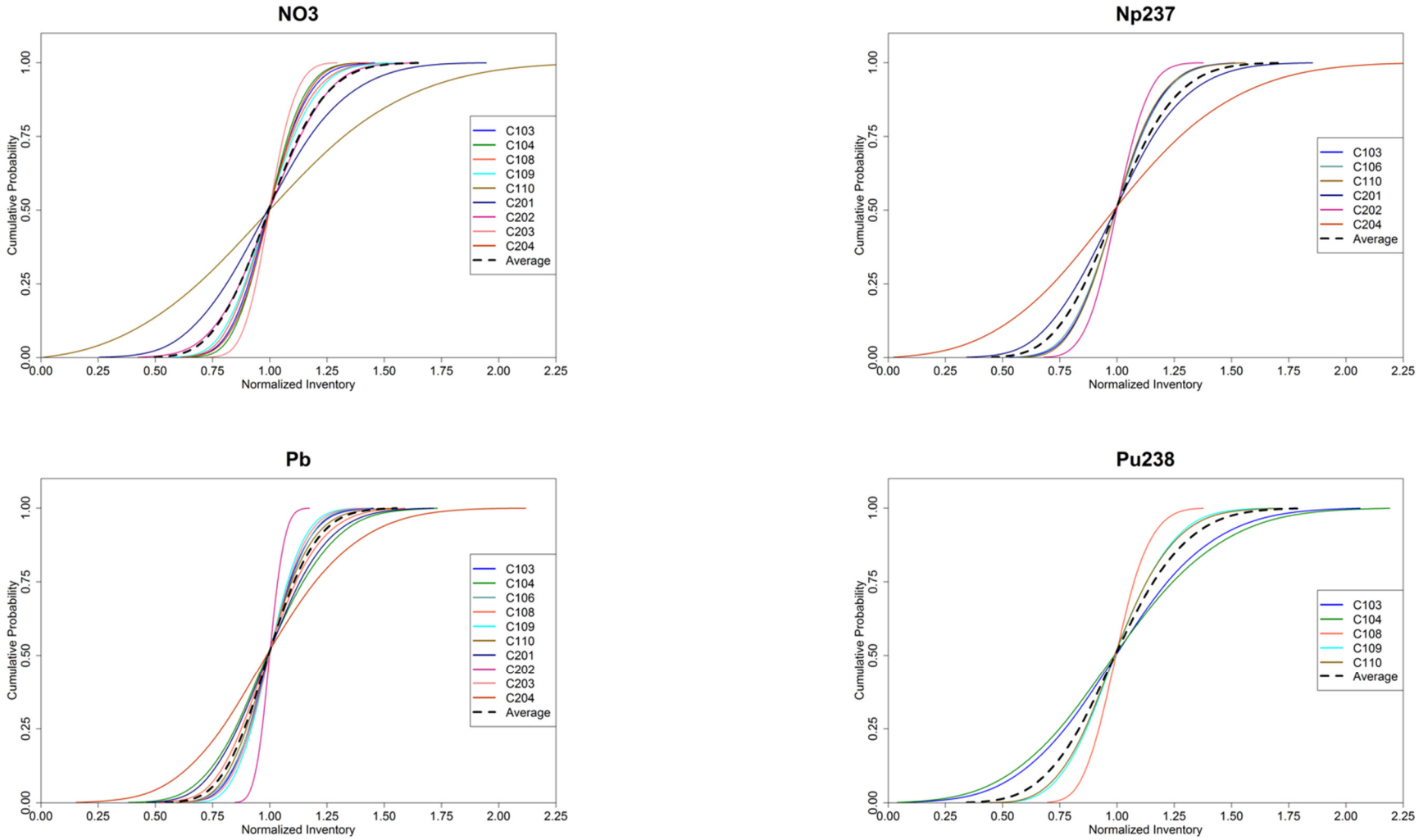

Figure 8-2. Cumulative Distribution Function of Normalized Inventory of Various Analytes for the Retrieved Tanks along with the Average Cumulative Distribution Function. (sheet 6 of 10)

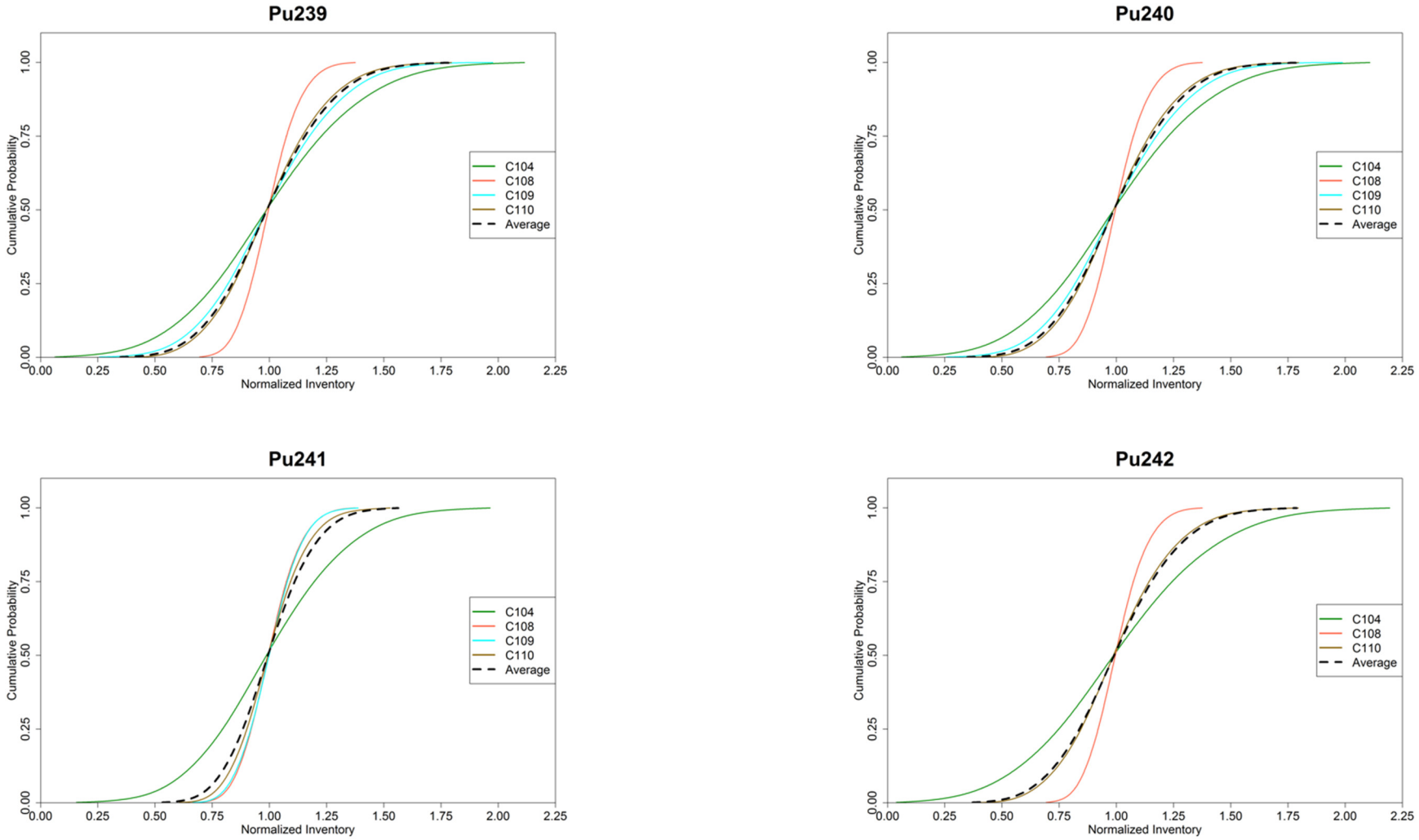

Figure 8-2. Cumulative Distribution Function of Normalized Inventory of Various Analytes for the Retrieved Tanks along with the Average Cumulative Distribution Function. (sheet 7 of 10)

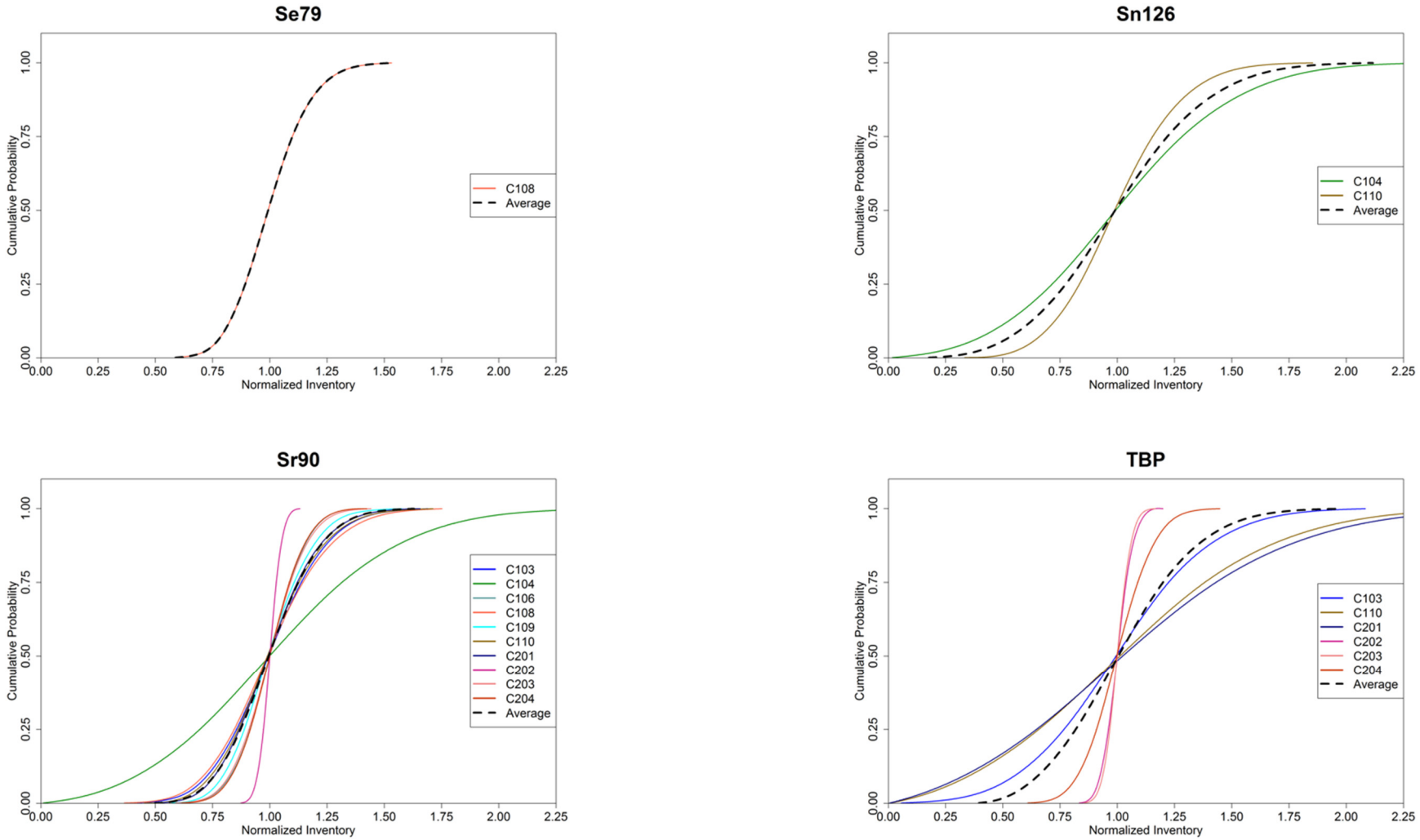

Figure 8-2. Cumulative Distribution Function of Normalized Inventory of Various Analytes for the Retrieved Tanks along with the Average Cumulative Distribution Function. (sheet 8 of 10)

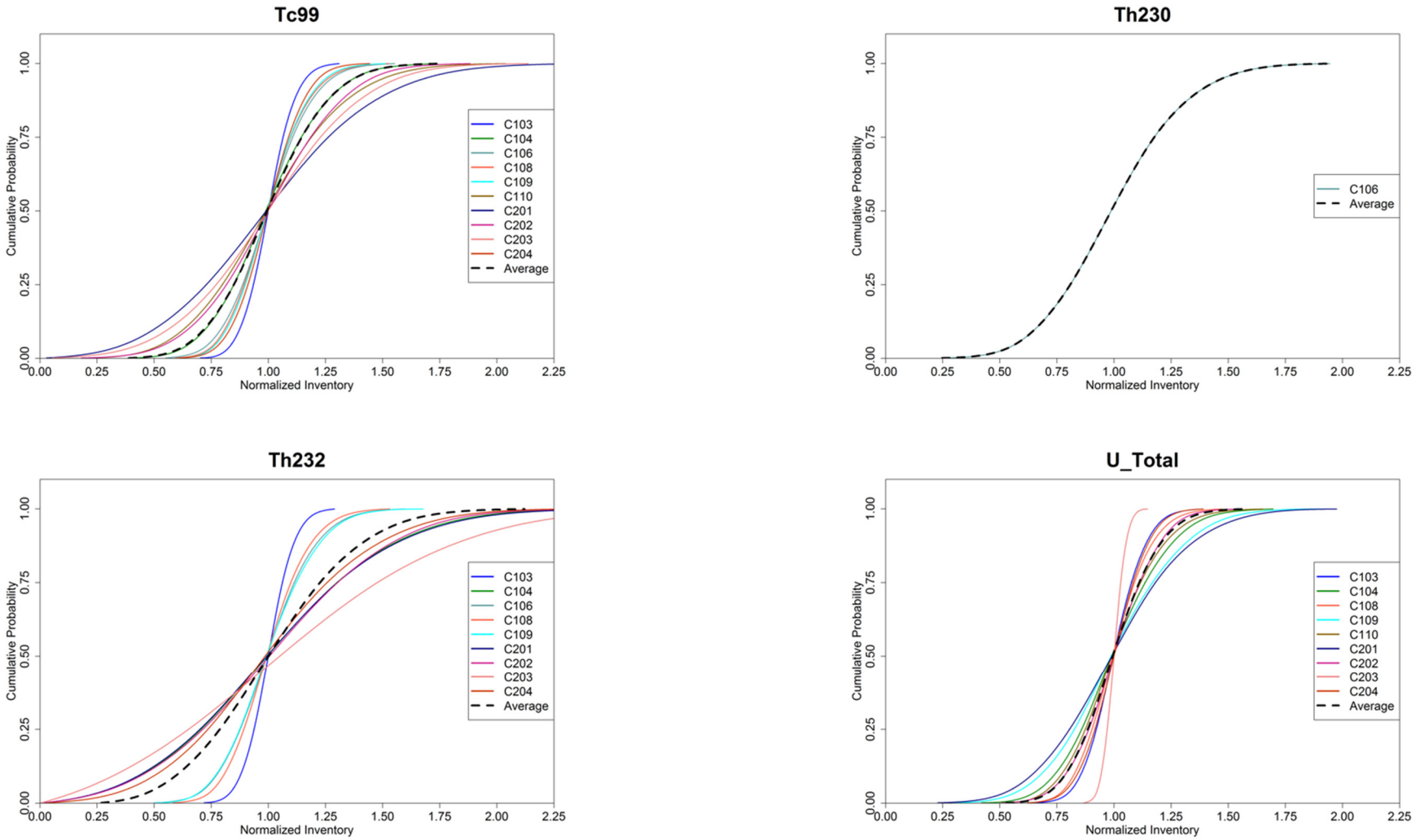

Figure 8-2. Cumulative Distribution Function of Normalized Inventory of Various Analytes for the Retrieved Tanks along with the Average Cumulative Distribution Function. (sheet 9 of 10)

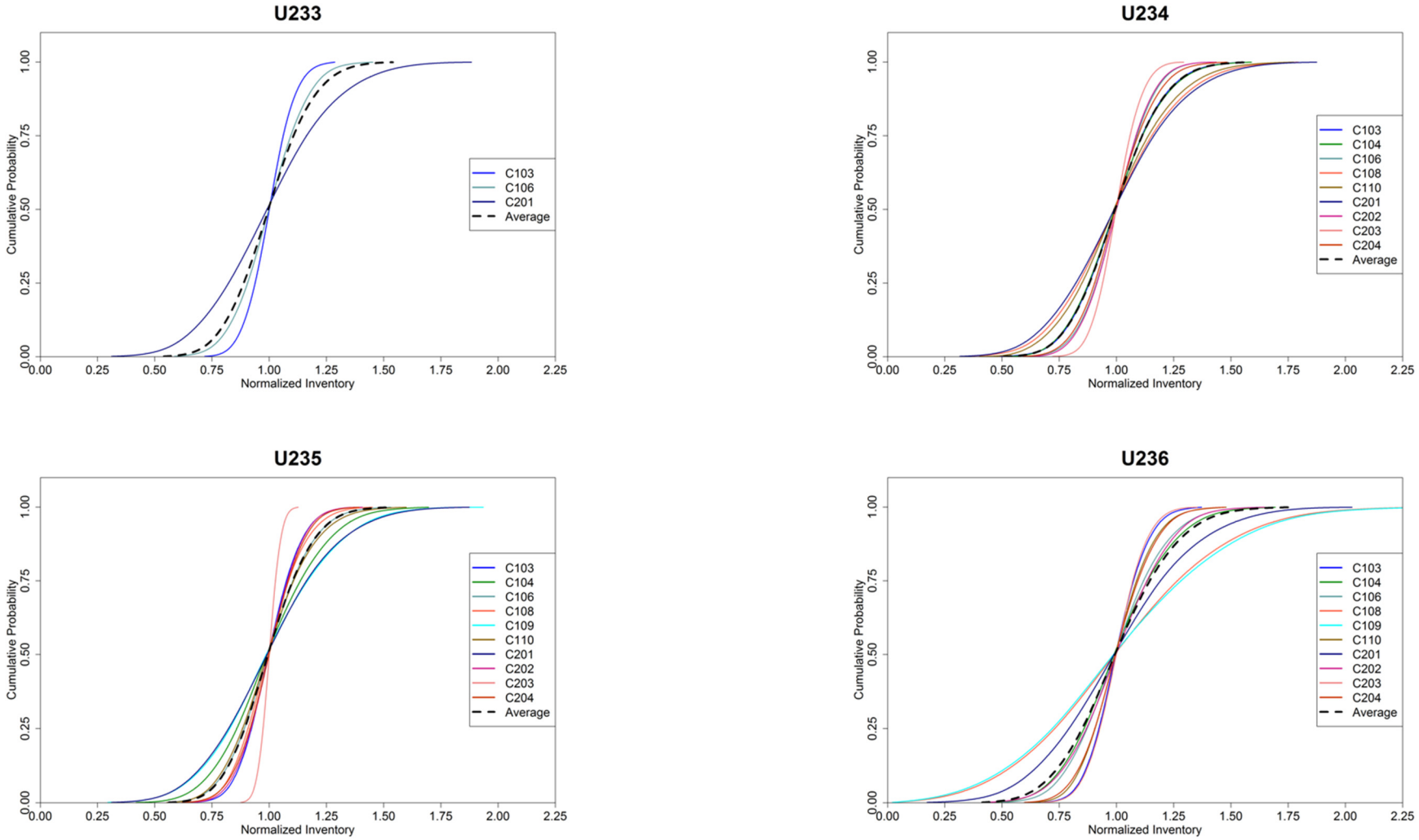

Figure 8-2. Cumulative Distribution Function of Normalized Inventory of Various Analytes for the Retrieved Tanks along with the Average Cumulative Distribution Function. (sheet 10 of 10)

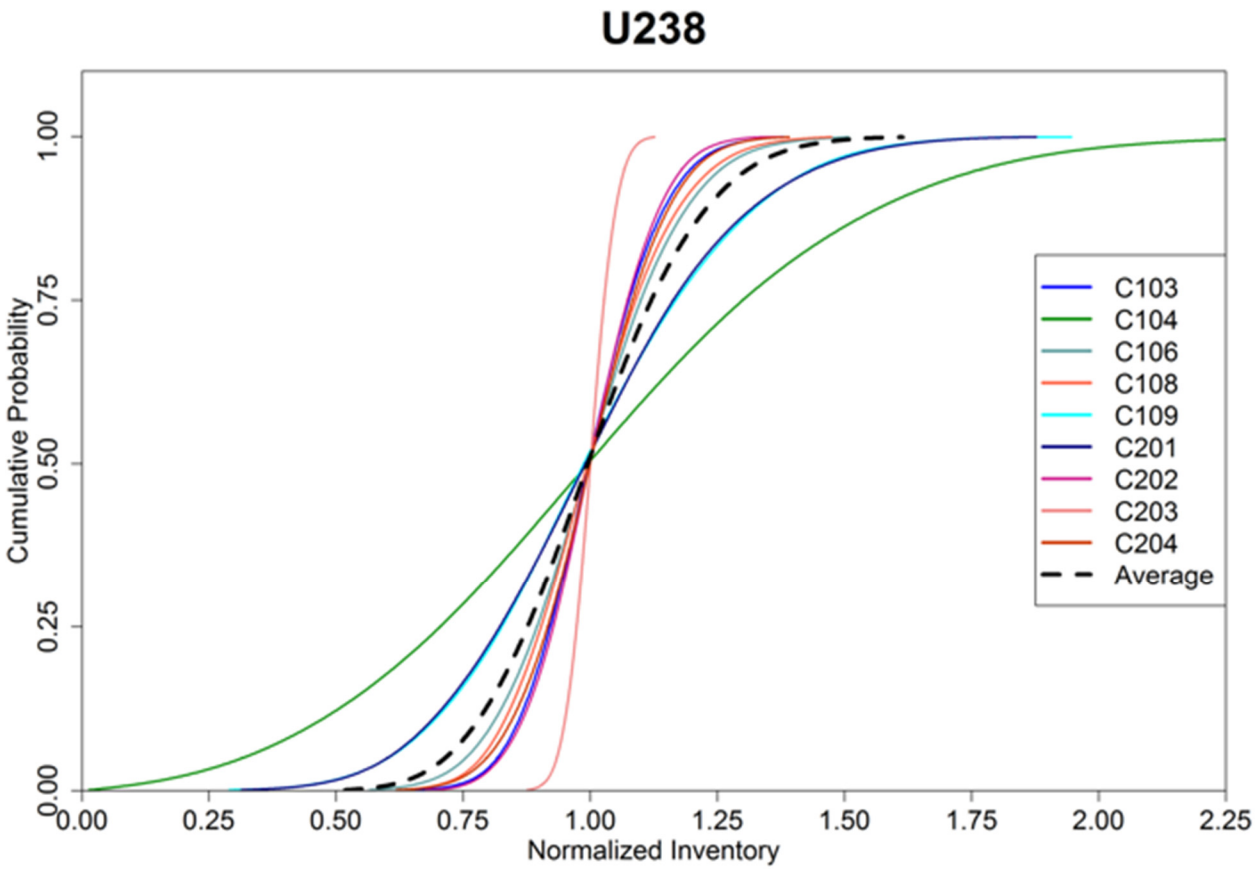

Similar uncertainty analyses were undertaken for the gravel-dominated Hanford H1 and H3 units and for the backfill sediments based on the soil-moisture dataset from other representative samples. Appendix B (Section B.2.2) discusses the methodology for measuring moisture retention data and unsaturated hydraulic conductivities for samples representative of gravel-dominated H1 and H3 units. A total of 17 sample measurements were used to represent the H1 and H3 gravelly units, and the fitted van Genuchten-Mualem parameters are reproduced in Table B-5 and displayed in Figures B-18 and B-19. For the backfill material (gravel-dominated), ten samples were used to derive van Genuchten-Mualem parameters. The results are presented in Table B-6 and shown in Figures B-20 and B-21.

8.1.3.4.1 Uncertainty in Saturated Hydraulic Conductivity (K_s) Parameter for H2 Unit. The derived K_s values from each of the 44 laboratory-measured, soil-moisture retention and unsaturated hydraulic conductivity datasets were fit to a log-normal distribution (Figure 8-4), as the number of samples allow an estimate of a mean and standard deviation. The distribution was

truncated at the minimum and maximum values of the data. The K_s distribution has the following characteristics:

- Geometric mean = 4.2×10^{-3} cm/s
- Geometric SD = 4.3
- Minimum = 2.5×10^{-4} cm/s and Maximum = 5×10^{-2} cm/s.

Figure 8-3. Cumulative Distribution Function of Normalized Residual Volume for the Retrieved Tanks along with the Average Cumulative Distribution Function.

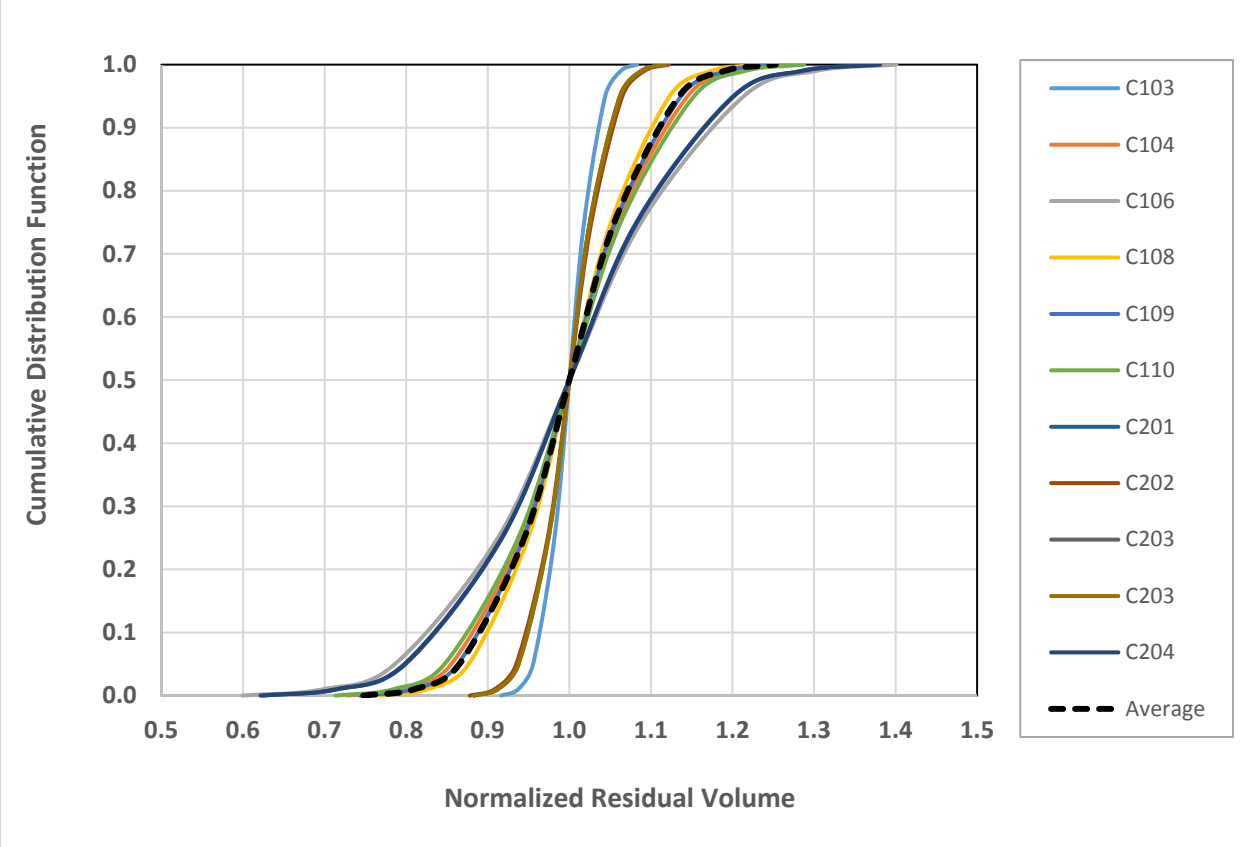

8.1.3.4.2 Uncertainty in van Genuchten Alpha (α) Parameter for H2 Unit. The derived van Genuchten alpha (α) values from each of the 44 laboratory-measured, soil-moisture retention and unsaturated hydraulic conductivity datasets were fit to a log-normal distribution (Figure 8-5). The distribution was truncated at the minimum and maximum values of the data. The α distribution has the following characteristics:

- Geometric mean = 0.060 cm^{-1}
- Geometric SD = 1.85
- Minimum = 0.0058 cm^{-1} and Maximum = 0.201 cm^{-1}.

8.1.3.4.3 Uncertainty in van Genuchten *n* Parameter for H2 Unit. The derived van Genuchten *n* parameter values from each of the 44 laboratory-measured, soil-moisture

retention and unsaturated hydraulic conductivity datasets were fit to a log-normal distribution (Figure 8-6). The distribution is truncated at the minimum and maximum values of the data. The *n* distribution has the following characteristics:

- Geometric mean = 1.81
- Geometric SD = = 1.15
- Minimum = 1.5 and Maximum = 3.18.

Figure 8-4. Fitted Log-Normal Distribution to the Saturated Hydraulic Conductivity Dataset Used for H2 Unit.

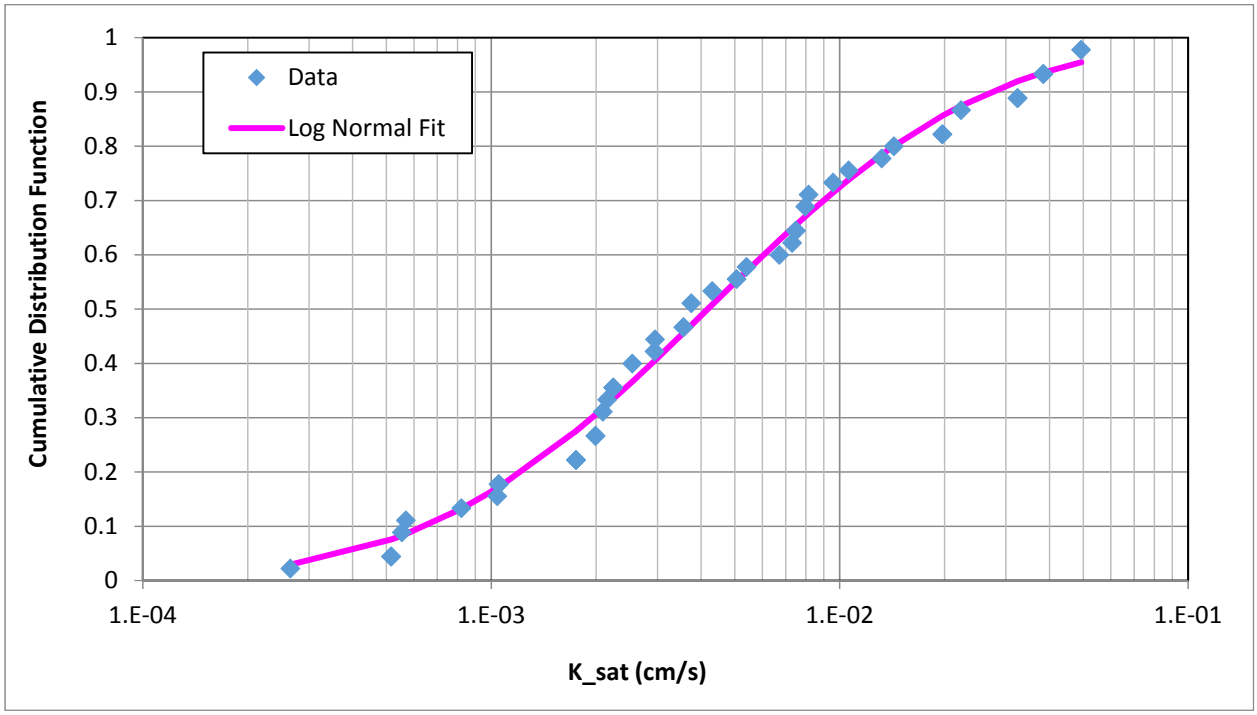

8.1.3.4.4 Uncertainty in Saturated and Residual Moisture Content (θ_s and θ_r) for H2 Unit. The derived saturated and residual moisture content values (θ_s and θ_r) from each of the 44 laboratory-measured soil-moisture retention datasets were considered with a 20% gravel correction for WMA C. The fitted values have a small range, and as a result, a uniform distribution was assumed with the following minimum and maximum values:

- Saturated moisture content (θ_s): Minimum = 0.239 and Maximum = 0.355
- Residual moisture content (θ_r): Minimum = 0 and Maximum = 0.037.

8.1.3.4.5 Correlation between Parameters. The K_s, α, and *n* parameters were evaluated to see if any correlation exists that needs to be preserved. Based on rank correlation, it was found that α and K_s have a correlation coefficient of 0.77, while α and *n* have a correlation coefficient of -0.33. This correlation was implemented while sampling the above-defined log-normal distributions to preserve the relationships in the measured dataset.

Figure 8-5. Fitted Log-Normal Distribution to the van Genuchten "Alpha" Parameter Dataset Used for H2 Unit.

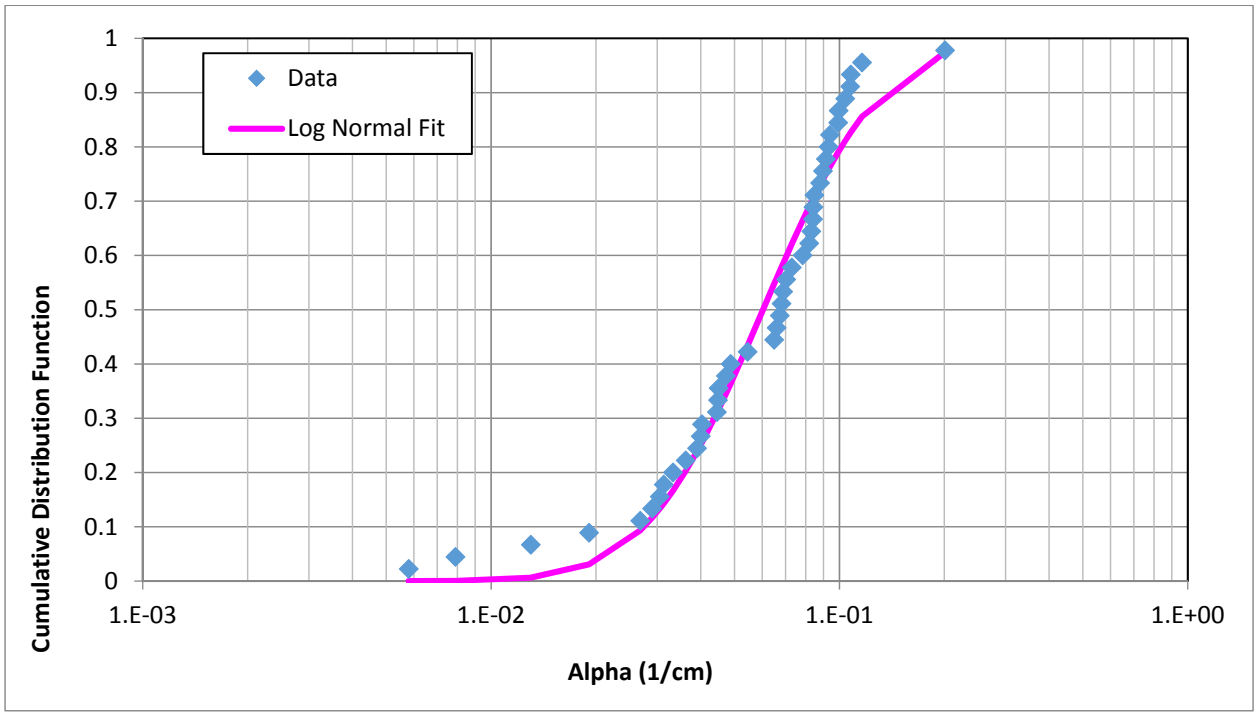

Figure 8-6. Fitted Log-Normal Distribution to the van Genuchten "*n*" Parameter Dataset Used for H2 Unit.

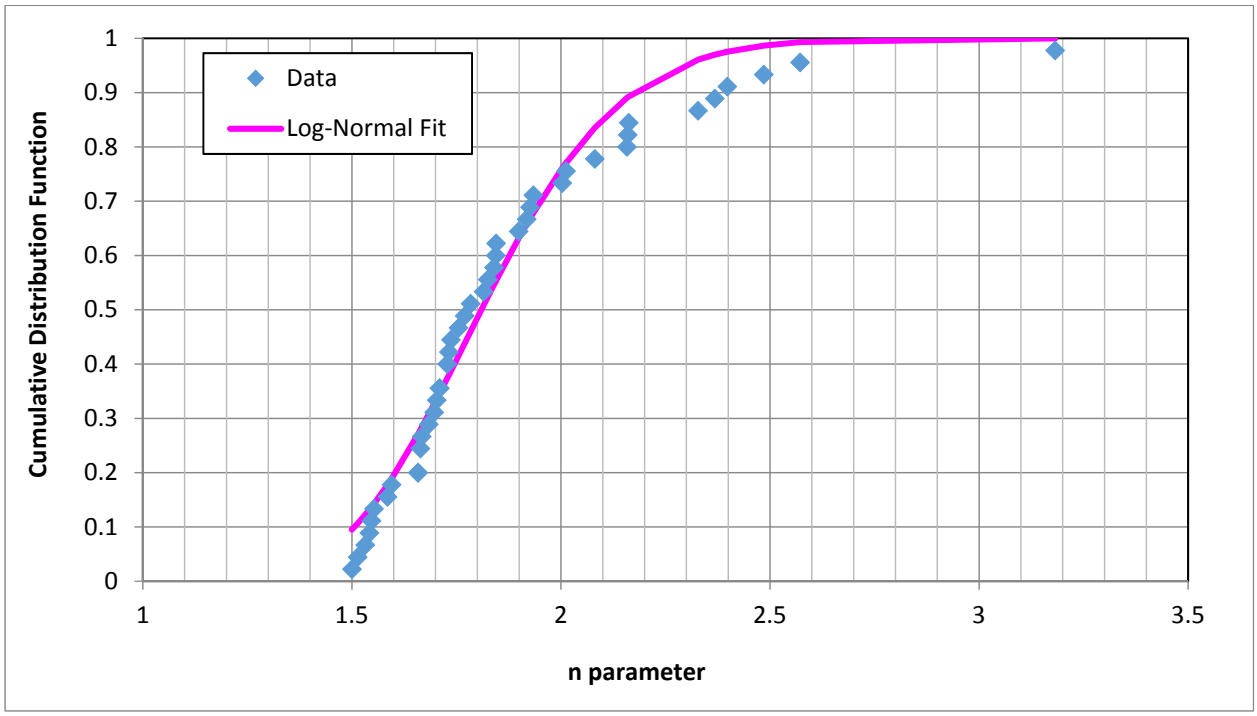

Using Monte Carlo analysis with LHS, functions of the van Genuchten parameters (including the correlation between parameters) were sampled 200 times. Using the van Genuchten-Mualem constitutive relationship functions, 200 realizations were generated of unsaturated hydraulic conductivity as a function of matric potential, and soil-moisture characteristic curves. These realizations are shown in Figure 8-7 and Figure 8-8 for the H2 unit. The 200 realizations were judged adequate based on the comparison of the distribution of moisture characteristic curves to the soil-moisture retention and unsaturated hydraulic conductivity datasets.

Figure 8-7. 200 Realizations of Unsaturated Hydraulic Conductivity as a Function of Matric Potential for H2 Unit. Red line indicates the Composite curve used in the Base Case.

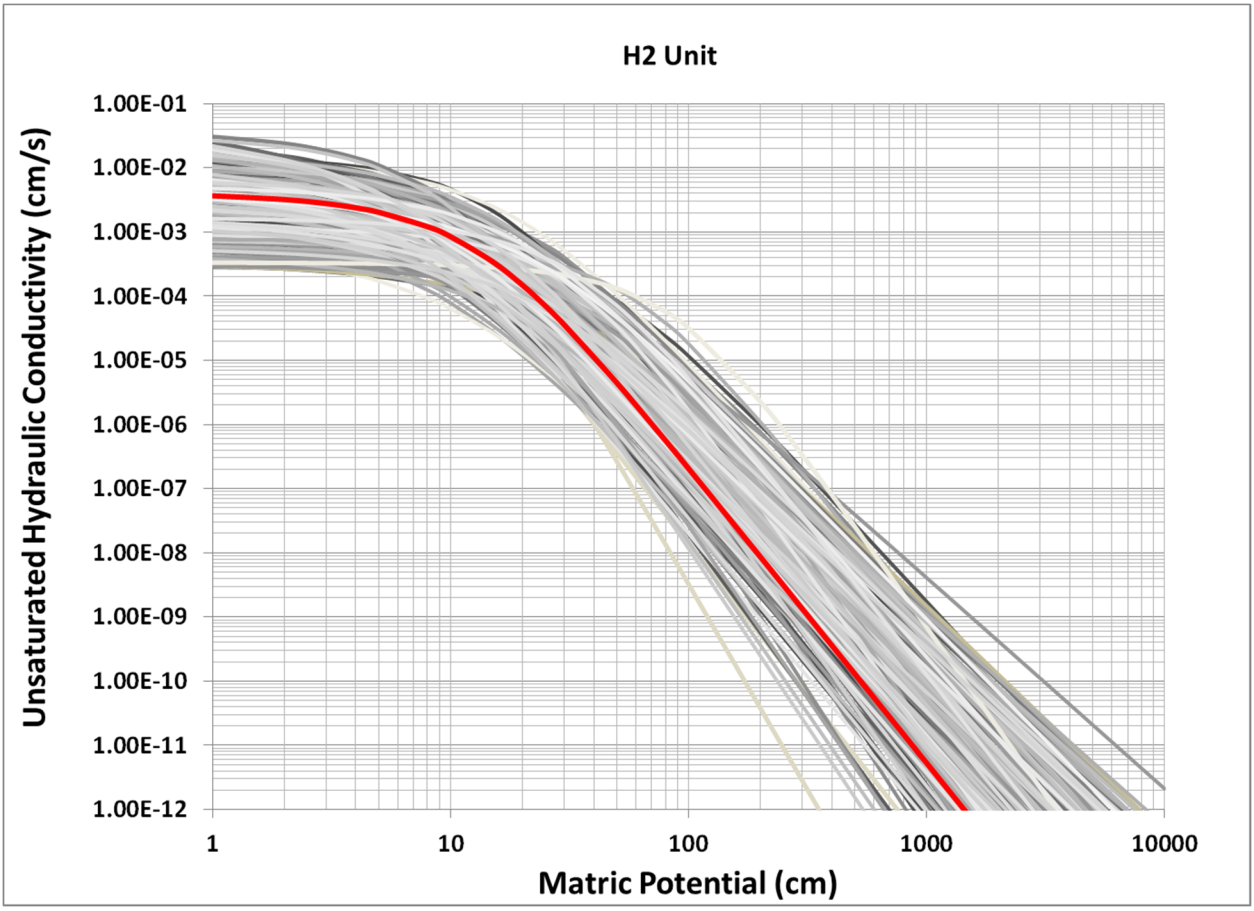

Similar to the sand-dominated H2 unit, uncertainty in the hydraulic properties for the gravel-dominated H1 and H3 units (assumed to have the same properties) and the backfill material was developed. For the H1/H3 units, the derived uncertainty distributions are summarized in Table 8-4. The fitted log-normal distributions are presented in Figures 8-9 through 8-11. Using the van Genuchten-Mualem constitutive relationship functions, 200 realizations of unsaturated hydraulic conductivity as a function of matric potential and soil-moisture characteristic curves are generated, which are shown in Figure 8-12 and Figure 8-13.

Figure 8-8. 200 Realizations of Soil-Moisture as a Function of Matric Potential for H2 Unit. Red line indicates the Composite curve used in the Base Case.

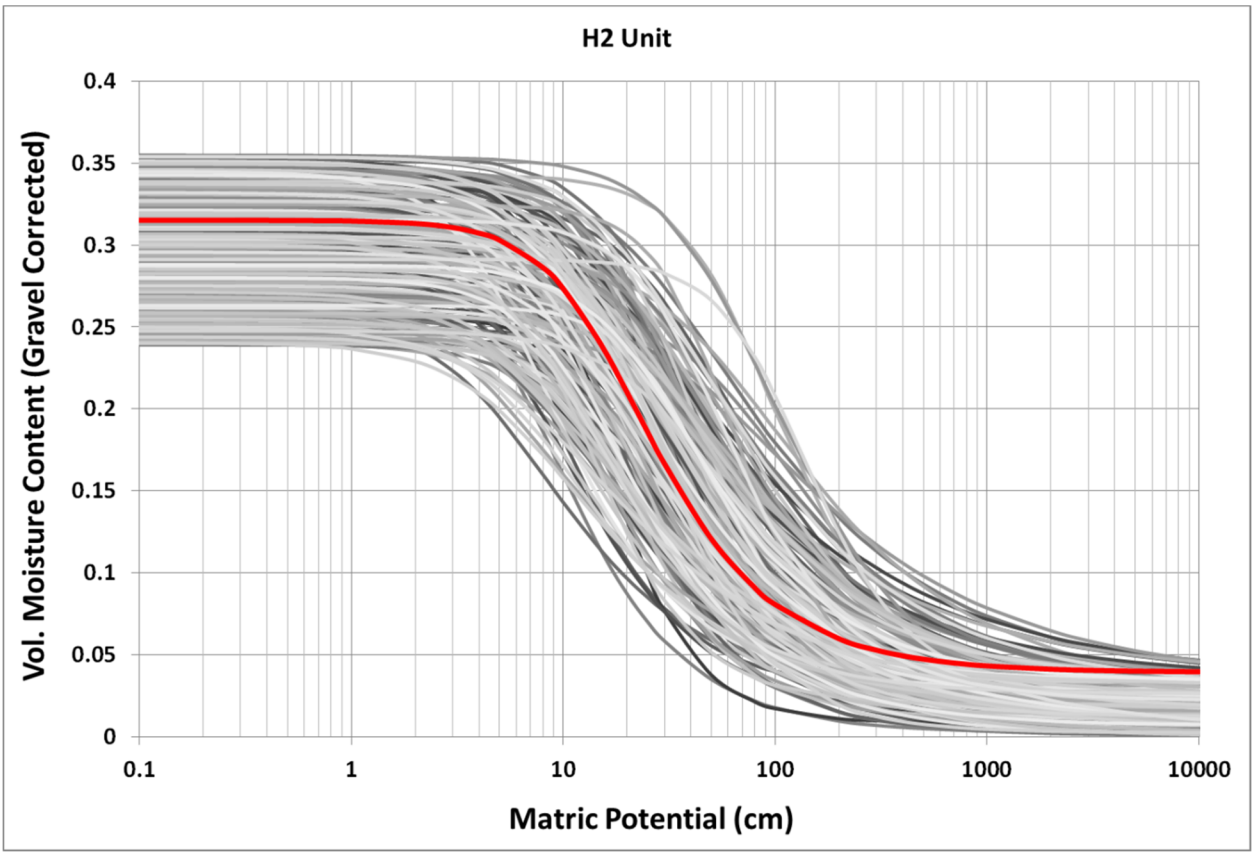

For the backfill material, the uncertainty distributions are summarized in Table 8-5.

8.1.3.5 Uncertainty in Sorption Parameter for Natural System. A linear sorption isotherm (K_d) was implemented for evaluating the interaction of contaminants with soils, as discussed in Section 6.3.1.4. These values represent intermediate impact zones, which are defined as zones (or areas) in which the acidic or basic nature of the released waste was expected to have been largely neutralized by reaction with the natural sediment.

Uncertainties in K_d values were developed using a triangular distribution as shown in Table 8-6 for sand. The sampled K_d value is then corrected for gravel fraction based on the average gravel content as discussed in Section 6.3.1.4. To be consistent with the hydraulic properties, the average gravel content for H2 unit is 20% (Section B.2.1) and for H1 and H3 units is 42% (Table B-6).

8.1.3.6 Uncertainty in Darcy Flux in Saturated Zone. Uncertainty exists in determination of the saturated hydraulic conductivity and the future hydraulic gradient within the aquifer. As discussed in Appendix C, the base case effective hydraulic conductivity was derived from the current calibrated CPGWM. The CPGWM provides calibrated hydraulic conductivity estimates for the model layers and HSUs present within the aquifer in the vicinity of WMA C. The

weighted average hydraulic conductivity of the CPGWM HSUs mapped onto the WMA C flow domain provides the base case estimate of approximately 11,000 m/day (36,000 ft/day). However, estimates based on pumping tests and other modeling studies have indicated values both lower and higher than the CPGWM calibrated values. Hence, the uncertainty in saturated zone hydraulic conductivity was chosen to range from 1,000 m/day to 21,000 m/day (3,280 ft/day to 69,000 ft/day) based on evaluation of all available information presented in Appendix C (Section C.4).

Table 8-4. Uncertainty Distributions Developed for H1/H3 Hydraulic Properties.

Hydraulic Property	Selected Uncertainty Distribution	Parameters for Defining Uncertainty Distribution
Saturated hydraulic conductivity (K_s)	Log-Normal (truncated)	Geometric Mean = 1.95E-4 cm/s Geometric Standard Deviation = 8.37 Minimum = 1E-6 cm/s; Maximum = 7.77E-3 cm/s
van-Genuchten Alpha (α) parameter	Log-Normal (truncated)	Geometric Mean = 0.015 cm^{-1} Geometric Standard Deviation = 2.42 Minimum = 0.0043 cm^{-1}; Maximum = 0.0438 cm^{-1}
van-Genuchten n parameter	Log-Normal (truncated)	Geometric Mean = 1.58 Geometric Standard Deviation = 1.13 Minimum = 1.31; Maximum = 2.25
Saturated Moisture Content (θ_s)	Uniform	Minimum = 0.1; Maximum = 0.357
Residual Moisture Content (θ_r)	Uniform	Minimum = 0; Maximum = 0.033
Rank Correlation between hydraulic properties		Alpha and K_s = 0.92 Alpha and n = 0.38

Uncertainty also exists in the hydraulic gradient within 200 East Area. Even though the hydraulic gradients are likely to remain very small (around 10^{-5} m/m) as the water table declines in the future, current monitoring has indicated that gradients can vary by a factor of two, due to Columbia River stage fluctuations and interconnections to the aquifer in the Central Plateau.

While the uncertainties in hydraulic conductivity and hydraulic gradient can be defined independently, the parameters need to be considered together as they result in determination of Darcy flux, which is the parameter that is used in the system model. Consequently, the uncertainty in hydraulic conductivity and gradient is propagated by developing uncertainty in the Darcy flux relative to the base case value. This is implemented as a multiplicative factor to the base case Darcy flux at the upgradient boundary of the WMA C system model.

The uncertainty in the Darcy flux multiplier is dominated by uncertainty in the saturated zone hydraulic conductivity, which varies by an order of magnitude or more. To derive the Darcy flux multiplier, the saturated hydraulic conductivity range (1,000 to 21,000 m/day [3,280 ft/day to

69,000 ft/day]) was divided by the best-estimate value (11,000 m/day [36,000 ft/day]) and a triangular distribution was chosen with the following parameters:

- Minimum = 0.09
- Most Likely = 1
- Maximum = 1.91.

Figure 8-9. Fitted Log-Normal Distribution to the Saturated Hydraulic Conductivity Dataset Used for H1/H3 Units.

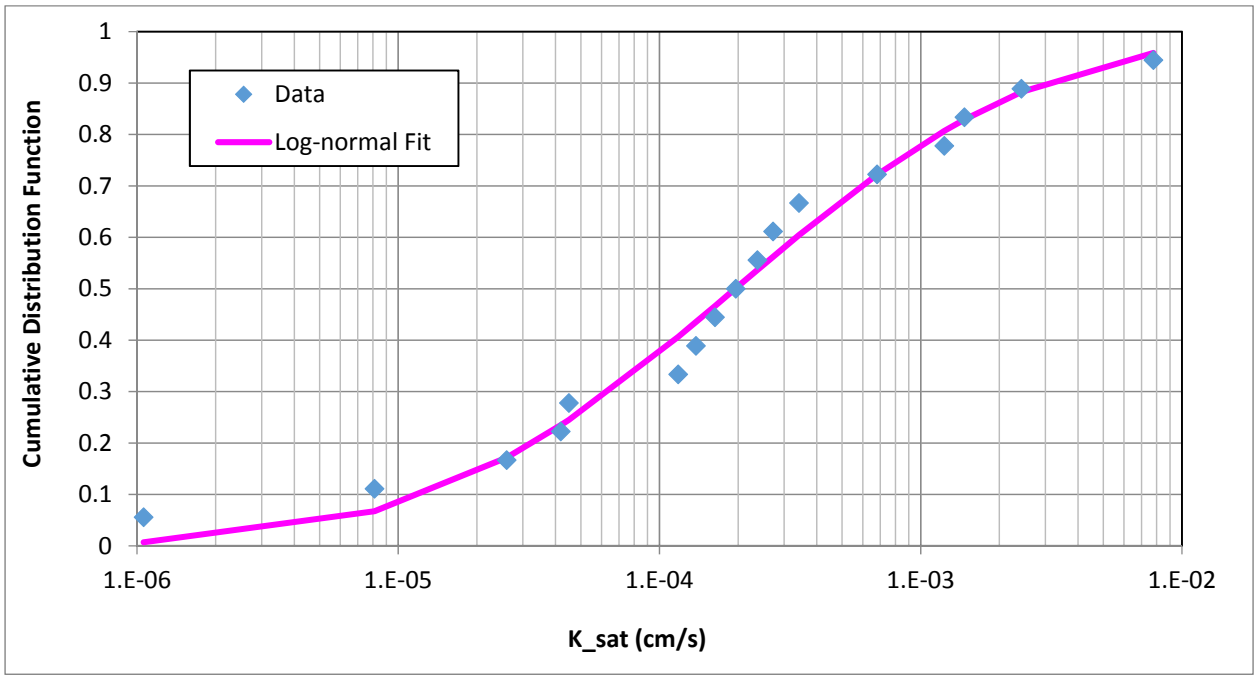

8.1.3.7 Uncertainty in Macrodispersivity in the Vadose Zone and the Saturated Zone. In unsaturated media, the longitudinal macrodispersivity is dependent on soil moisture content (or matric potential) and differs when the primary flow and transport is parallel to the bedding plane versus being primarily perpendicular to the bedding. A range of estimates are presented in Appendix B (Section B.4.3). These estimates are based on numerical simulations, stochastic theory, and experimental observations applicable to the relatively dry conditions observed in the vadose zone at WMA C. Table B-11 summarizes the various estimates for the H2 sand-dominated unit. A range from 25 cm to 100 cm (9.8 in. to 39.4 in.) is recommended for longitudinal macrodispersivity. Under the relatively dry conditions within the WMA C vadose zone, and because the primary flow and transport direction is vertical (perpendicular to the bedding plane in the H2 unit), the lower value of 25 cm (9.8 in.) is deemed as a best estimate. Consequently, a triangular distribution is used for the H2 unit with the following parameters:

- Minimum = 25 cm (9.8 in.)
- Most Likely = 25 cm (9.8 in.)
- Maximum = 100 cm (39.4 in.).

Figure 8-10. Fitted Log-Normal Distribution to the van Genuchten "Alpha" Parameter Dataset Used for H1/H3 Units.

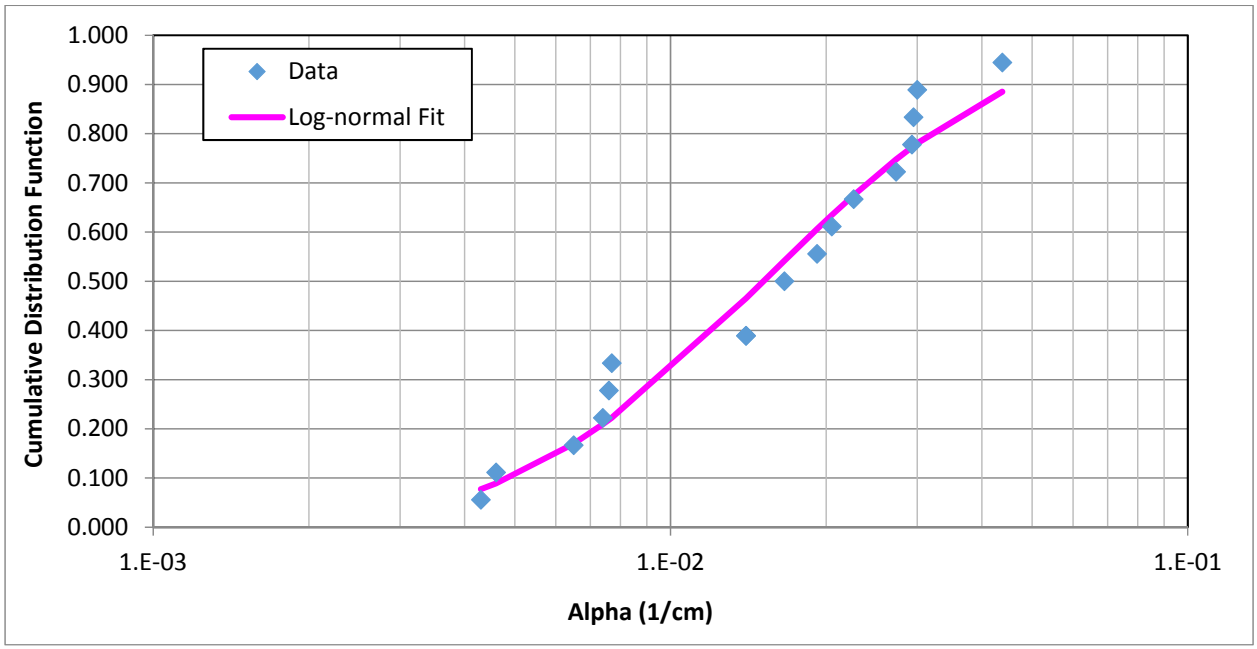

Figure 8-11. Fitted Log-Normal Distribution to the van Genuchten "*n*" Parameter Dataset Used for H1/H3 Units.

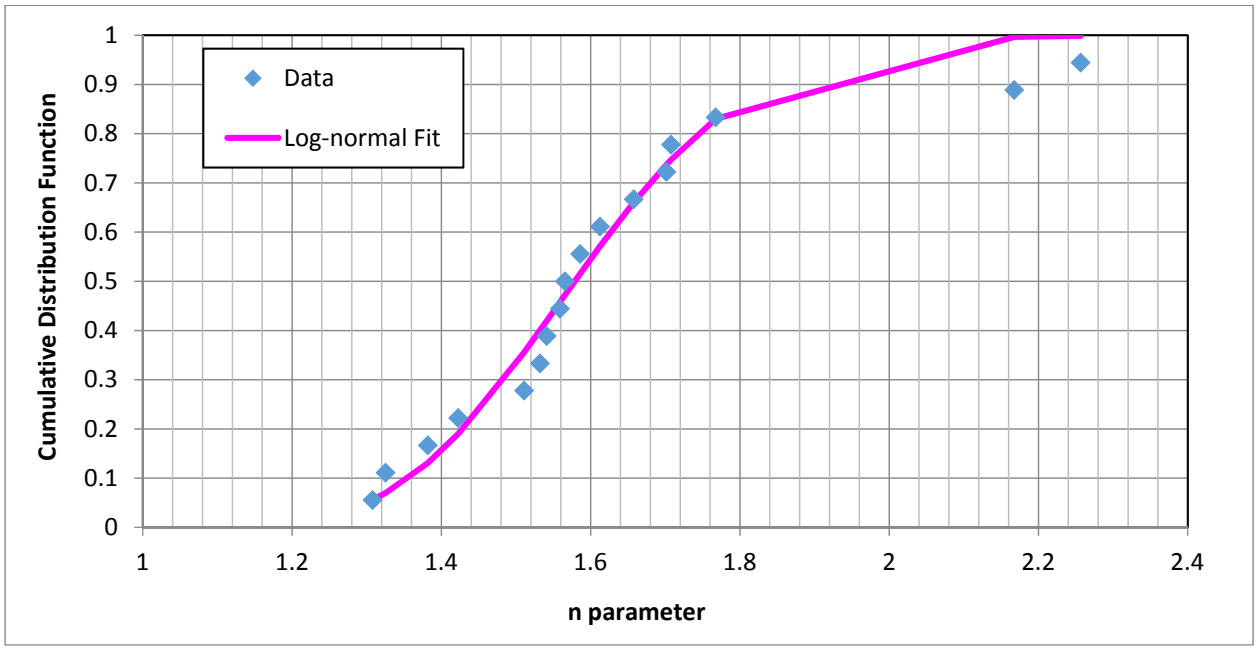

A range in the saturated zone macrodispersivity is discussed in Appendix C (Section C.4.2.2), based on a review of literature-based, scale-dependent relationships. The range in saturated zone macrodispersivity at the scale of the WMA C model is estimated to be from 1 m to 20 m (3.3 ft

to 65.6 ft). In the system model, it is necessary to use different macrodispersivity values for each source, as the transport distance in the saturated zone to the 100 m (328 ft) boundary varies by the location of the source (tank and ancillary equipment), and the appropriate macrodispersivity is dependent on the distance. It is therefore necessary to use different macrodispersivities for each source so that the results match with the STOMP© 3-D process-level model results for each source term. This is best accomplished by defining an uncertain parameter that multiplies (scales) the chosen macrodispersivity values for each source. To propagate uncertainty in macrodispersivity multiplier, a uniform distribution was chosen by taking the minimum and maximum values of the macrodispersivity range and dividing by the median value. This results in the following parameters that define the uniform distribution:

- Minimum = 0.095
- Maximum = 1.9.

Figure 8-12. 200 Realizations of Unsaturated Hydraulic Conductivity as a Function of Matric Potential for H1/H3 Units. Red line indicates the Composite curve used in the Base Case.

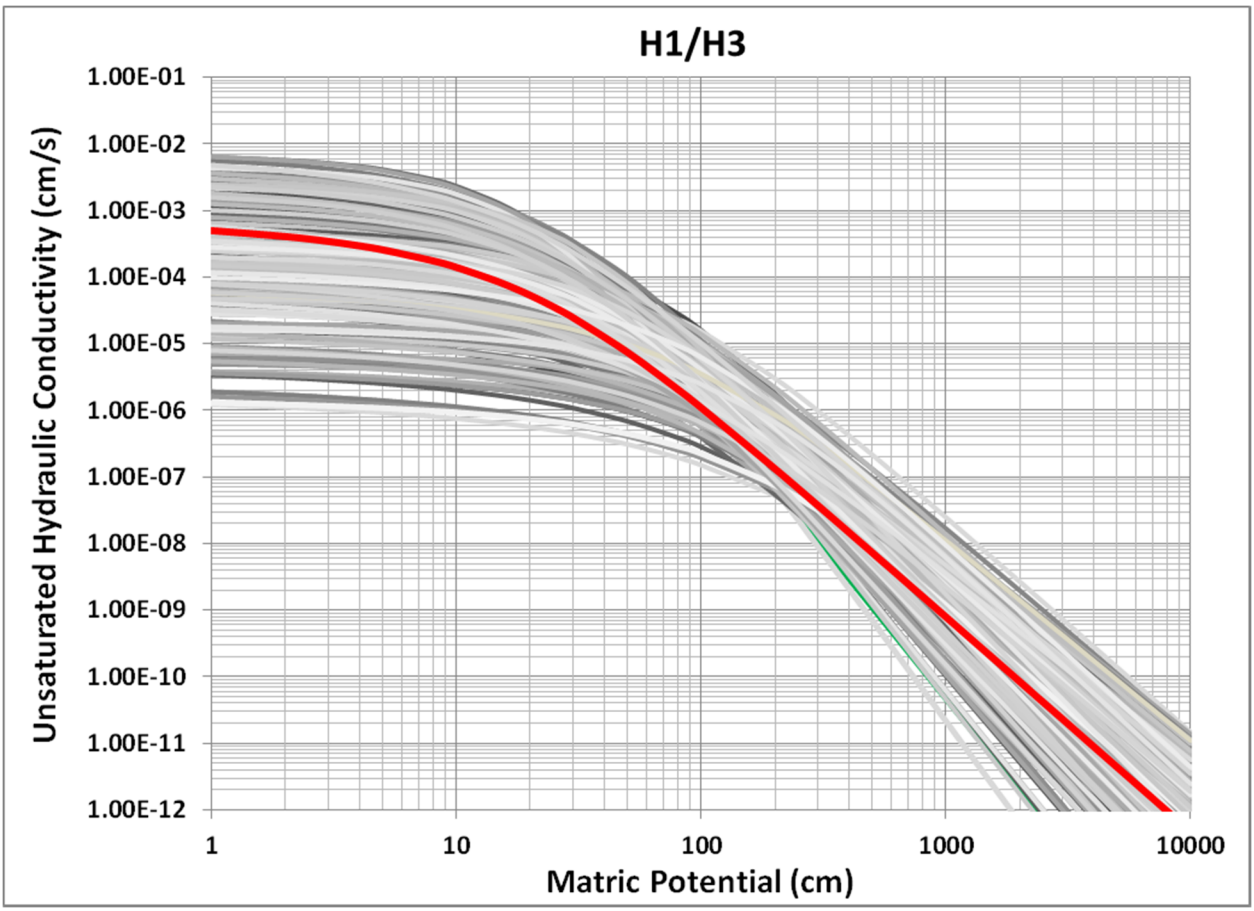

8.1.3.8 Uncertainty in Gas-Phase Tortuosity. Gas-phase tortuosity is considered to be a key parameter in the air-pathway transport calculation. Uncertainty in this parameter was implemented as a triangular distribution based on the fitted tortuosity models shown in

Figure 6-59 (and discussed in Section 6.3.2.5.2). The most likely value of the triangular distribution is based on the best fit line given by Equation 8-2. The minimum and maximum values are described below.

- The minimum envelope curve obtained with the model of Millington and Quirk (1961) with Φ, fitted total porosity = 0.8.

$$\tau = \frac{\theta_a^{10/3}}{\Phi^2} = \frac{(\phi-\theta_w)^{10/3}}{\Phi^2} \tag{8-1}$$

- The maximum envelope curve obtained with the model of Millington and Quirk (1960) with Φ, fitted total porosity = 0.4.

$$\tau = \frac{\theta_a^2}{\Phi^{2/3}} = \frac{(\phi-\theta_w)^2}{\Phi^{2/3}} \tag{8-2}$$

Where:

τ = the tortuosity
θ_a = the air content (or air-filled porosity) of the porous medium
θ_w = the water content (or water-filled porosity) of the porous medium
ϕ = the total porosity (measured)
Φ = fitted total porosity.

Two different triangular distributions were implemented related to gas-phase tortuosity, one for the gaseous transport through the tank grout and the other through the soil overburden due to different air contents.

8.1.3.9 Uncertainty in Annual Wind Speed. As discussed in Section 3.1.2.4, the wind speed at Hanford varies on a monthly basis, with speeds being higher in summer and lower during winter months. The monthly and annual average speeds from Years 1945 through 2004 are summarized in Tables 5.1 through 5.4 of PNNL-15160. The annual average wind speed for meteorological records kept from 1945 to 2004 is calculated to be ~3.4 m/s (7.6 mi/hr) at 15.2 m (50 ft) above the ground, with a maximum annual average value of 3.9 m/s (8.8 mi/hr) and a minimum annual average value of 2.8 m/s (6.2 mi/hr). Although seasonal variability in wind speed is observed, since the dose evaluations are performed on an annual basis, the annual averaged wind speeds are considered for evaluating the effect of uncertainty in this parameter. Based on the available information, a triangular distribution was implemented with the following parameters:

- Minimum = 2.8 m/s (6.2 mi/hr)
- Most Likely = 3.4 m/s (7.6 mi/hr)
- Maximum = 3.9 m/s (8.8 mi/hr).

Figure 8-13. 200 Realizations of Soil-Moisture as a Function of Matric Potential for H1/H3 Units. Red line indicates the Composite curve used in the Base Case.

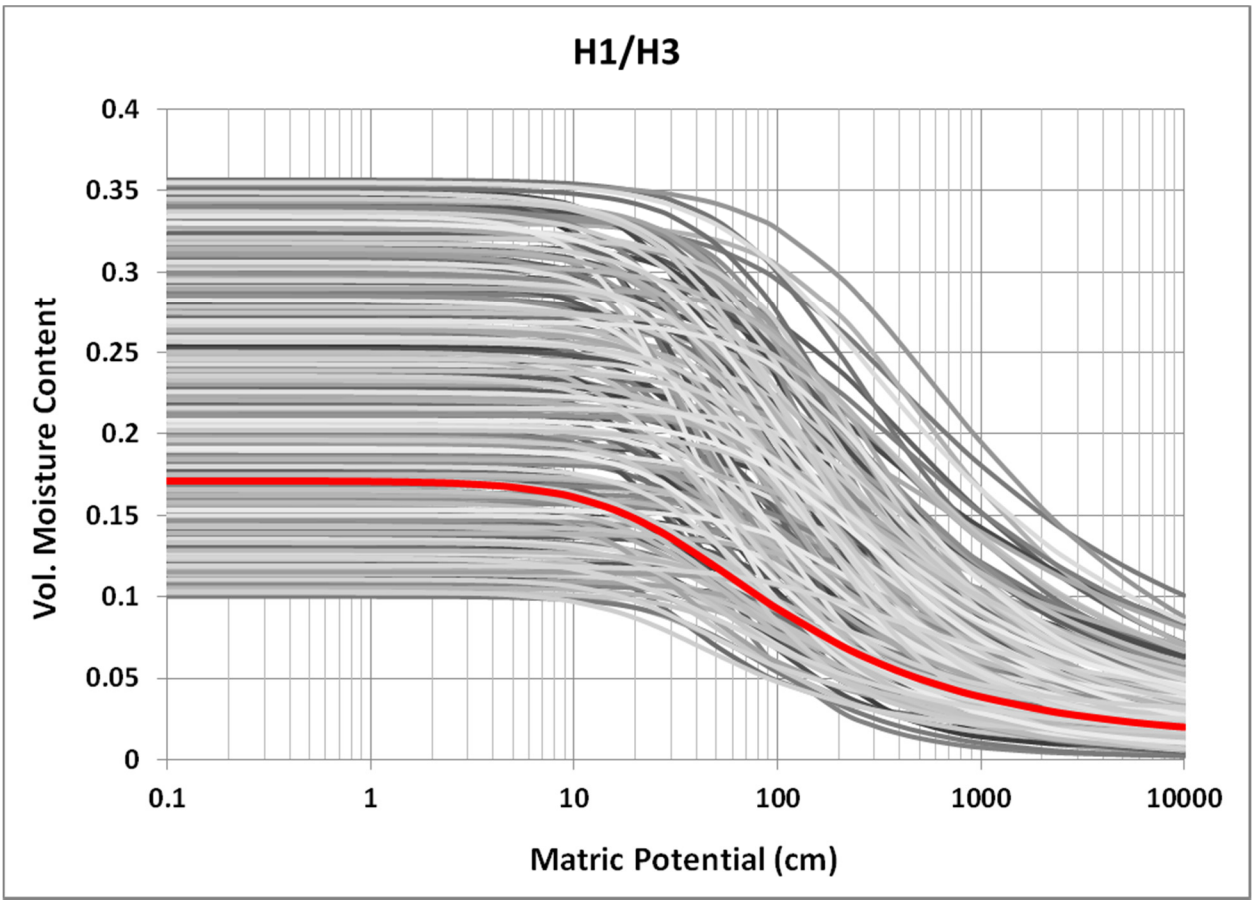

8.1.4 Development of Vadose Zone Flow Fields and Propagation of Uncertainty

The flow field for the vadose zone was abstracted from the 3-D STOMP© results as a way to efficiently evaluate the effects of uncertainty in the vadose-zone flow using the GoldSim©-based system model. The 1-D transport model implemented in GoldSim© relies on the user to provide the time-varying vertical Darcy flux and volumetric moisture content as inputs. These flow field-related parameters were extracted from the 3-D STOMP©-based model. The flow-field abstractions were performed separately for the 100-series and 200-series tanks because of different tank dimensions and thickness of HSUs within the vadose zone. The details of the flow-field abstraction approach are discussed in Section 6.3.2.2. The reasonableness of the abstraction approach was demonstrated by comparisons of the results of the transport analysis conducted using the 1-D abstracted system model to the full 3-D STOMP©-based model (Section 6.3.2.2.1).

In this section, the methodology for propagating uncertainty in the flow field is discussed. The vadose zone flow field is a function of the imposed recharge rate and vadose zone hydraulic properties. The uncertainties in these two parameters are discussed in Section 8.1.4. The uncertainty in the flow field is propagated by jointly considering the uncertainty in vadose zone

hydraulic properties and the uncertainty in recharge rates. Because a comprehensive Monte Carlo analysis using the 3-D STOMP©-based model was too computationally intensive and impractical for propagating the uncertainty in the flow field, the STOMP©-based Monte Carlo analysis was approximated by a discrete number of analyses that span the range of behavior of the flow fields for a limited number of runs. This was accomplished by selecting 5 discrete hydraulic property sets along with 3 discrete recharge rates to cover the uncertainty range. Five sets of hydraulic properties were chosen because of the larger uncertainty range in the flow parameters relative to recharge rates. The combination of 5 hydraulic property sets with 3 recharge rates results in a matrix of 15 parameter sets. These 15 combinations of flow parameters were each run using the 3-D STOMP© model. For each STOMP© calculation, the resulting flow field was abstracted using the methodology discussed in Section 6.3.2.2.

Table 8-5. Uncertainty Distributions Developed for Backfill Hydraulic Properties.

Hydraulic Property	Selected Uncertainty Distribution	Parameters for Defining Uncertainty Distribution
Saturated hydraulic conductivity (K_s)	Log-Normal (truncated)	Geometric Mean = 5.52E-5 cm/s Geometric Standard Deviation = 5.48 Minimum = 1E-6 cm/s; Maximum = 3.42E-4 cm/s
van-Genuchten Alpha (α) parameter	Log-Normal (truncated)	Geometric Mean = 0.0086 cm^{-1} Geometric Standard Deviation = 2.63 Minimum = 0.0025 cm^{-1}; Maximum = 0.030 cm^{-1}
van-Genuchten n parameter	Log-Normal (truncated)	Geometric Mean = 1.53 Geometric Standard Deviation = 1.07 Minimum = 1.31; Maximum = 1.66
Saturated Moisture Content (θ_s)	Uniform	Minimum = 0.1; Maximum = 0.236
Residual Moisture Content (θ_r)	Uniform	Minimum = 0; Maximum = 0.018
Rank Correlation between hydraulic properties		Alpha and K_s = 0.71 Alpha and n = 0.47

A simplification of the flow-field sampling approach was identified by observing that variations in recharge could be reproduced using an appropriate scaling method using the base case recharge rate. Therefore, instead of implementing 15 flow fields, only 5 flow fields had to be implemented, defined by the combination of 5 hydraulic parameters with base case recharge rate. Therefore, the remaining 10 flow fields calculated by the 3-D STOMP©-based model were used to corroborate the scaling approach, but were not directly used in the GoldSim©-based system model.

The flow-field abstraction approach is described in following five steps.

Step 1 – Selection of Vadose Zone Hydraulic Properties:

The uncertainty in the vadose zone hydraulic properties is discussed in Section 8.1.3. For each HSU in the vadose zone, 200 realizations of unsaturated hydraulic conductivity (as a function of matric potential) and soil-moisture characteristic curves were generated. Although different

curves could be randomly selected from the 200 realizations, by using insights regarding the flow fields, the uncertainties relevant to the PA were more tightly defined. First is the recognition that under the post-closure conditions, the flow will closely approach a unit gradient flow field as the vertical Darcy flux equilibrates with the imposed recharge rate. Using the long-term base recharge rate of 3.5 mm/yr (0.14 in./yr) as an estimate of vertical Darcy flux, and with the unit hydraulic gradient assumption, the associated unsaturated hydraulic conductivity is ~1×10^{-8} cm/s. This allows the analysis to focus on a specific part of the characteristic curves at unsaturated hydraulic conductivity of ~1×10^{-8} cm/s (see Figure 8-7) in which the range of matric potential is smaller than the full range over all conditions.

Table 8-6. Uncertainty in K_d Values (mL/g) for Sand As a Triangular Distribution. (2 sheets)

Element	Most Likely	Minimum	Maximum	Reference
Ac	350	100	1,500	PNNL-16663
Al	1,500	1,500	1,500	RPP-RPT-46088
Am	600	200	2,000	PNNL-17154
B	3	3	3	RPP-RPT-46088
C	1	0	100	PNNL-17154
Cd	6.7	6.7	6.7	RPP-RPT-46088
Cm	350	100	1,500	PNNL-16663
CN	0	0	0	RPP-RPT-46088
Co	0	0	10	PNNL-17154
Cr	0	0	3	PNNL-17154
Cs	100	10	1,000	PNNL-17154
Eu	10	3	100	PNNL-17154
F	0	0	1	PNNL-17154
Fe	25	25	25	RPP-RPT-46088
H	0	0	0	PNNL-17154
Hg	52	52	100	RPP-RPT-46088
I	0.2	0	2	PNNL-17154
Mn	65	65	65	RPP-RPT-46088
Nb	0	0	0.1	PNNL-16663
Ni	3	1	20	PNNL-17154
NO_2	0	0	0.1	PNNL-17154
NO_3	0	0	0.1	PNNL-17154
Np	10	2	30	PNNL-17154

Table 8-6. Uncertainty in K_d Values (mL/g) for Sand As a Triangular Distribution. (2 sheets)

Element	Most Likely	Minimum	Maximum	Reference
Pa	300	40	500	PNNL-17154
Pb	10	3	100	PNNL-17154
Pu	600	200	2,000	PNNL-17154
Ra	10	5	20	PNNL-17154
Rn	0	0	0	No relevant information available
Se	0.1	0	3	PNNL-17154
Sm	10	3	100	PNNL-17154
Sn	0.5	0	20	PNNL-17154
Sr	10	5	100	PNNL-17154
TBP	1.89	1.89	1.89	RPP-RPT-46088
Tc	0	0	0.1	PNNL-16663
Th	300	40	500	PNNL-16663
U	0.6	0.2	2	RPP-RPT-46088
U_total	0.6	0.2	2	PNNL-17154
Zr	300	40	500	PNNL-16663

References:
PNNL-16663, "Geochemical Processes Data Package for the Vadose Zone in the Single-Shell Tank Waste Management Areas at the Hanford Site."
PNNL-17154, "Geochemical Characterization Data Package for the Vadose Zone in the Single-Shell Tank Waste Management Areas at the Hanford Site."
RPP-RPT-46088, "Flow and Transport in the Natural System at Waste Management Area C."

Fixing the unsaturated hydraulic conductivity, the following procedure was undertaken to derive uncertainty in hydraulic properties.

- The 200 realizations of the unsaturated hydraulic conductivity as a function of matric potential was first interrogated (for example, see Figure 8-7 for H2 unit and Figure 8-12 for H1/H3 units). For each realization, the matric potential corresponding to 1×10^{-8} cm/s unsaturated hydraulic conductivity was determined.

- Next, the 200 realizations of the soil-moisture characteristic curves (for example, see Figure 8-8 for H2 unit and Figure 8-13 for H1/H3 units) were interrogated based on the matric potential determined in the previous step, to determine the corresponding volumetric moisture content for that realization.

- The vertical pore water velocity was calculated for each realization by dividing the 1×10^{-8} cm/s unsaturated hydraulic conductivity by the corresponding volumetric moisture content.

- The resulting 200 vertical pore water velocity estimates were then sorted, and an empirical CDF was developed. For example, see the CDF shown in Figure 8-14 for the H2 unit.

- The above steps were repeated for each HSU, and the CDFs are presented in Figures 8-14 through 8-16.

- From the CDF, five pore water velocity values associated with the 5th, 25th, 50th, 75th, and 95th percentiles were chosen to represent the uncertainty in pore water velocity for a given HSU. The realizations associated with these percentiles were selected, and the hydraulic properties associated with the realization are noted for the HSU. Table 8-7 summarizes the sampled van Genuchten-Mualem parameters (K_s, α, n, θ_s, and θ_r) associated with the various percentiles. For the purpose of comparison, the parameters chosen for the base case are also presented.

Figure 8-14. Cumulative Distribution Function of Pore Water Velocity from 200 Realizations for the H2 Unit.

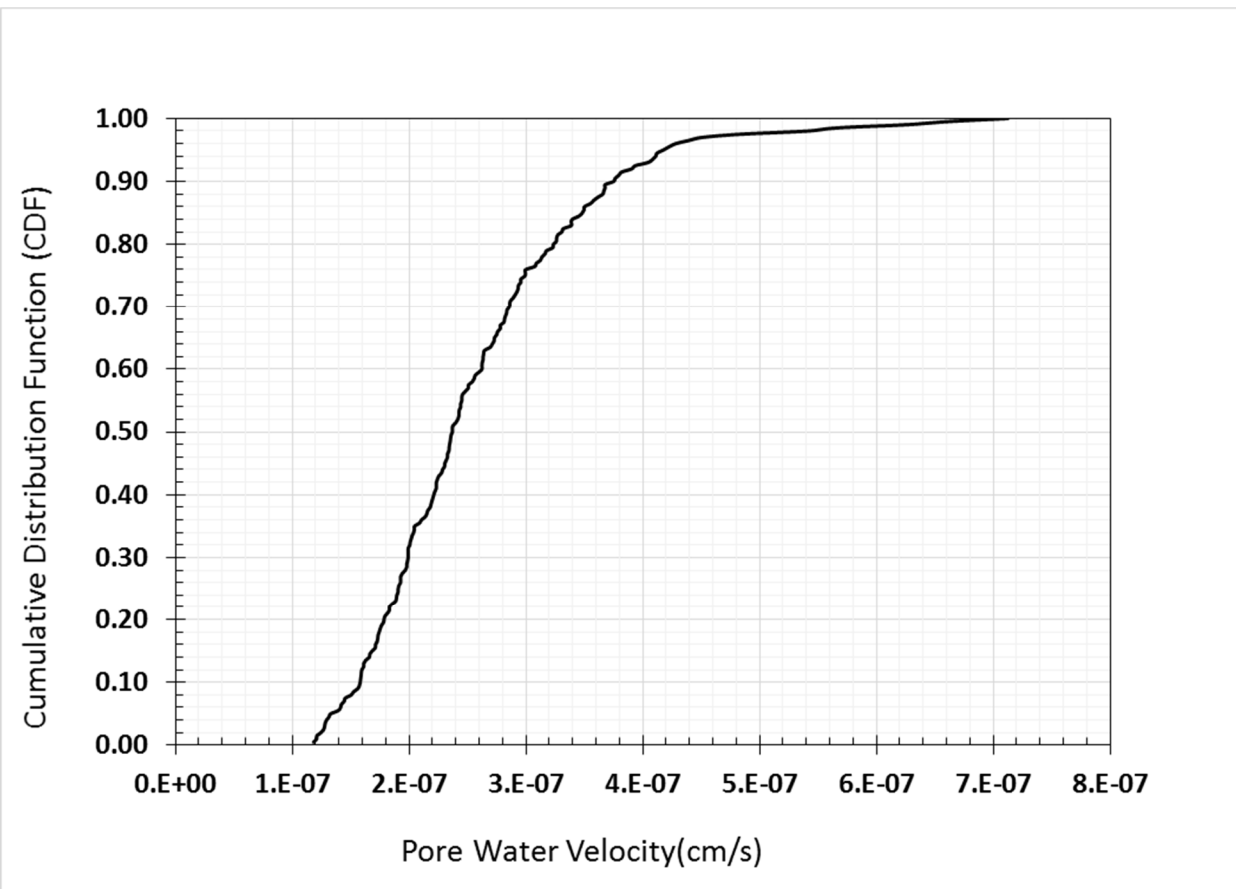

Figure 8-15. Cumulative Distribution Function of Pore Water Velocity from 200 Realizations for the H1/H3 Unit.

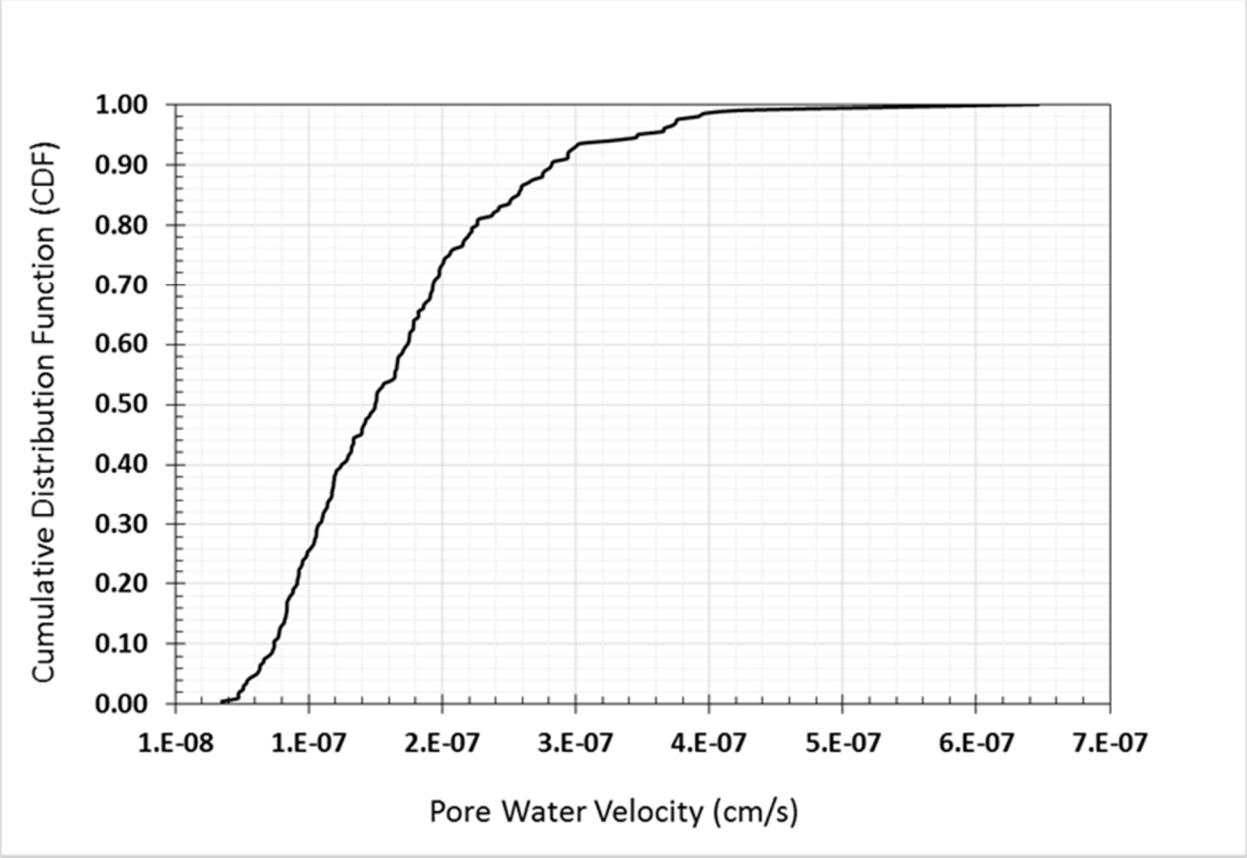

Step 2 – Selection of Recharge Rates:

Recharge rate varies both temporally and spatially as discussed in Section 8.1.3.1. Table 8-3 presents the uncertainty distribution in recharge rates for various time periods. For the purpose of abstracting the flow field, the time periods of interest are operational and post-closure periods, and the spatial area of interest is the one designated as WMA C since all of the contaminant sources are within this area. From the triangular distributions developed for each time period, the 5th percentile and the maximum (100th percentile) recharge rate values are selected along with the base case recharge rate values for the flow-field calculations. These values are representative of the uncertainty in recharge rates (the minimum value was not used due to very low probability of occurrence). The selected recharge rates are summarized in Table 8-8.

Step 3 – Flow-Field Abstraction:

The five hydraulic property sets corresponding to the vertical pore velocity percentiles (selected in Step 1 and presented in Table 8-7) and the three recharge rates (selected in Step 2 and presented in Table 8-8) were used to develop 15 combinations of flow-field inputs. The 3-D STOMP©-based model was used to calculate the flow field for each input combination. The results from the 3-D model were abstracted to generate separate flow fields for the 100-series

and 200-series tanks. Each flow field contains time-dependent vertical Darcy flux and volumetric moisture content that is applicable to the vertical grid discretization used in the GoldSim©-based system model (Table 6-16).

Figure 8-16. Cumulative Distribution Function of Pore Water Velocity from 200 Realizations for the Backfill Unit.

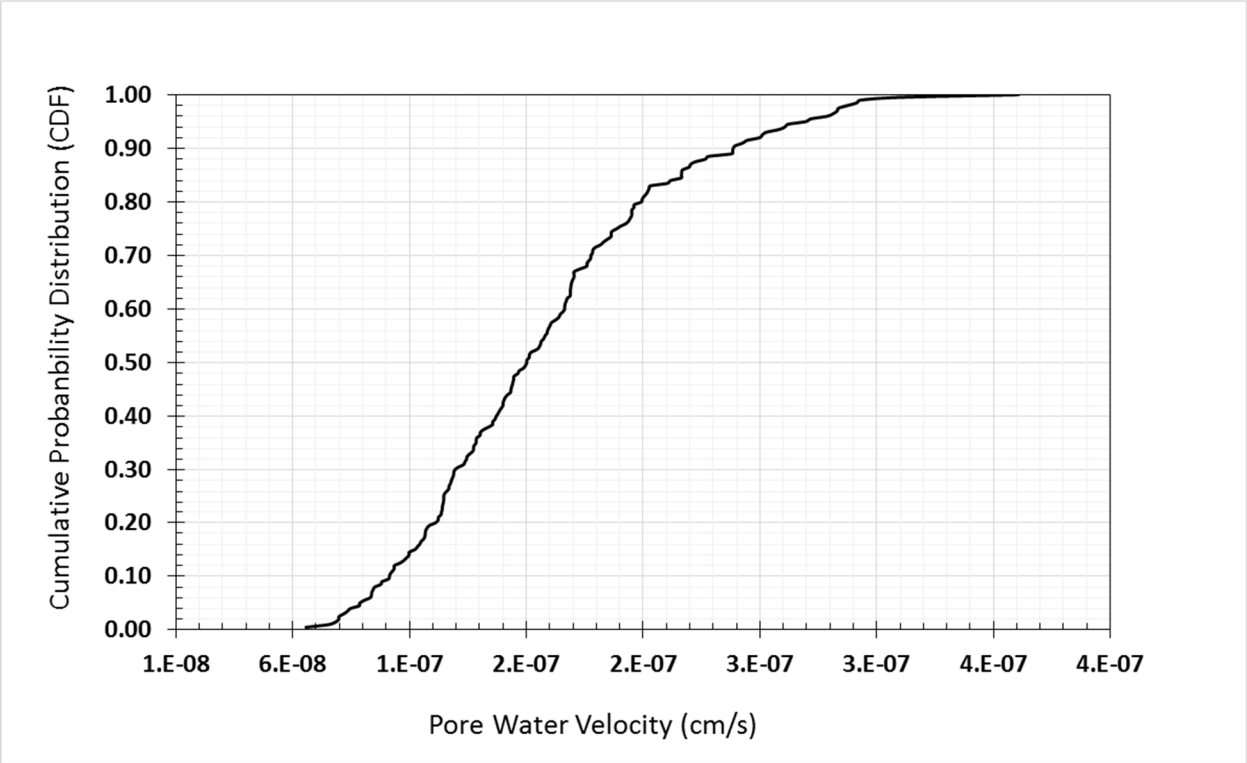

Step 4 – Scaling of Flow Field by Recharge Rate:

Upon evaluation of the 15 flow fields, it was found that a linear relationship exists between vertical Darcy flux and the recharge rate when hydraulic properties remain unchanged. Similarly, a linear relationship exists between volumetric moisture content and recharge rate. This information was used to reduce the number of flow fields being implemented in the system model to only five flow fields. The five flow fields were generated based on the combination of five hydraulic property sets with the *base case* recharge rate. These flow fields can be scaled based on sampled recharge rate using the regression equations. This approach allows to quickly and directly estimate the Darcy flux and volumetric moisture content for any sampled recharge rate without going through a demanding abstraction process.

The development of the regression equations was done as follows.

- For a selected hydraulic property percentile, the 3-D STOMP© model was used for three recharge rates presented in Table 8-8.

- Vertical Darcy flux and volumetric moisture content values were abstracted from STOMP© model nodes that correspond to the GoldSim© 1-D discretization. This was done for Calendar Year 2300 (to represent early the post-closure time period from Calendar Year 2020 to 2520 while the surface cover is intact) and at Calendar Year 5020 (to represent the late post-closure period beyond Calendar Year 2520 following surface barrier degradation).

- For the set of flow fields where the hydraulic property is held constant but recharge rate varies, the extracted vertical Darcy flux and volumetric moisture content were normalized by the base case recharge flow field. Table 8-9 provides an example of normalized Darcy flux for Calendar Year 2300 below tank C-105 (a representative column) for the 3-D STOMP© simulations with 5th percentile hydraulic properties at different recharge rates. This analysis was done for each time period.

- Normalized Darcy flux was plotted against the normalized recharge rates, and a linear regression analysis was performed to determine the relationships shown in Figures 8-17 and 8-18. These relationships are representative of the H1 unit and the deeper H2 and H3 units. Results of the regression analysis shown in Figure 8-17 are based on a STOMP© node located in H1 unit (node 66), and are used to scale the flow field for all other nodes in H1 unit in the GoldSim©-based system model. For the deeper H2 and H3 units, the regression analysis shown in Figure 8-18 was performed after averaging the results of several STOMP© nodes located in H2 and H3 units (nodes 63, 61, 55, 47, 39, 31, 24, 18, and 14). The averaging was performed because the vertical Darcy flux within the deeper nodes does not vary appreciably. Results of the regression analysis were used to scale the flow field for all nodes that define H2 and H3 in GoldSim©-based system model.

- A regression equation was also developed between normalized volumetric moisture content and normalized recharge rate in the same way. This is shown in Figures 8-19 and 8-20.

- These steps were repeated for each of the five hydraulic properties. This resulted in the development of linear relationships between normalized Darcy flux and normalized recharge rate, and between normalized volumetric moisture content and normalized recharge rate.

This algorithm resulted in a total of 40 regression equations, which were implemented in the GoldSim©-based system model for Darcy flux scaling calculations. The large number of regression equations was the result of separate regression relationships for the early post-closure time period (while the surface cover was intact) and the late post-closure time period (after surface cover is degraded), and then calculated separately for H1 unit and H2/H3 units for the 100-series tanks and 200-series tanks. The regression equations are presented in Table 8-10 for the 100-series tanks and in Table 8-11 for the 200-series tanks. Once a value is calculated from the regression equation, then the Darcy flux derived from the base case recharge rate abstraction process can be scaled to generate a new Darcy flux for the selected hydraulic property.

Table 8-7. van Genuchten-Mualem Parameters Corresponding to the Percentiles Selected from the Vertical Pore Water Velocity Cumulative Distribution Functions.

Strata (tension)	Percentile	K_s (cm/s)	θ_s	θ_r	α (1/cm)	n
Backfill	5th Percentile	7.91E-06	0.2217	1.23E-02	0.0026	1.441
	25th Percentile	1.08E-05	0.1319	1.57E-02	0.0031	1.310
	50th Percentile	7.31E-05	0.203	5.94E-03	0.0086	1.577
	75th Percentile	1.98E-04	0.1409	1.42E-02	0.0123	1.470
	95th Percentile	3.13E-04	0.1287	1.35E-02	0.0298	1.635
	Base Case	5.60E-04	0.138	1.10E-02	0.021	1.374
Hanford H1/H3	5th Percentile	7.78E-05	0.2887	3.24E-02	0.0121	1.335
	25th Percentile	5.14E-06	0.2118	2.08E-02	0.0062	1.733
	50th Percentile	1.49E-04	0.1735	3.06E-02	0.0124	1.603
	75th Percentile	1.58E-03	0.309	7.01E-03	0.0238	1.717
	95th Percentile	2.99E-04	0.102	1.45E-02	0.0152	1.760
	Base Case	7.70E-04	0.171	1.11E-02	0.036	1.491
Hanford H2	5th Percentile	1.79E-03	0.3541	2.89E-02	0.0402	1.633
	25th Percentile	1.15E-03	0.2893	2.99E-02	0.0266	1.971
	50th Percentile	2.20E-02	0.3304	2.72E-02	0.1253	1.889
	75th Percentile	3.79E-02	0.3474	2.05E-02	0.0966	1.966
	95th Percentile	1.68E-02	0.2652	2.11E-03	0.1076	1.724
	Base Case	4.15E-03	0.315	3.92E-02	0.063	2.047

Note: The connectivity parameter ℓ is assumed to be 0.5 for all strata and all percentile values.

During the regression analyses, it was observed that linear regression relationships between normalized volumetric moisture content and normalized recharge rate do not vary appreciably when different hydraulic properties were used, and between 100-series and 200-series tanks. As a result, only four regression equations are needed for scaling the volumetric moisture content. These are calculated separately for the H1 unit and the H2/H3 units for early post-closure and late post-closure time periods, and are summarized in Table 8-12. Once a value is calculated from the regression equation, then the volumetric moisture content derived from the base case recharge rate can be scaled by multiplying with this value to generate the new volumetric moisture content.

This scaling method was verified by comparing flow fields calculated using the regression equation with the flow field from 3-D STOMP© simulations for each of the hydraulic properties. An example of the comparison for the 5th percentile hydraulic property case is shown in Figure 8-21(a-d) for representative nodes from H1 and H2 units under 100-series and 200-series tanks. Very good agreement is observed between vertical Darcy flux calculated using the

regression equation and that obtained from STOMP© over the long simulated time period. Slight divergence that occurs just past Calendar Year 2500 results from switching from early post-closure period regression equation to late post-closure regression equation at Calendar Year 2520. This is because, although the step change in recharge rate occurs at Calendar Year 2520—reflecting degradation of surface cover (loss of hydraulic barrier capability)—the vertical Darcy flux in the STOMP© model slowly transitions to equilibrate to the new recharge rates. This transition period is not captured in the regression equations and leads to slight divergence in predicting the vertical Darcy flux.

Table 8-8. Recharge Rate Used in Scaling Flow Field.

	Base Case Recharge Rate	5th Percentile Recharge Rate	Maximum Recharge Rate
Operational Period (Calendar Year 1945-2020)	100 mm/yr	57.30 mm/yr	140 mm/yr
Early Post-Closure (Calendar Year 2020-2520)	0.5 mm/yr	0.23 mm/yr	0.9 mm/yr
Late Post-Closure (Calendar Year >2520)	3.5 mm/yr	1.07 mm/yr	5.2 mm/yr

Table 8-9. Example of Normalized Darcy Flux at Calendar Year 2300 from Selected Three-Dimensional STOMP©-Based Model Nodes under Tank 241-C-105 Using 5th Percentile Hydraulic Property.

Node Location	Normalized Darcy Flux: Base Recharge Rate	Normalized Darcy Flux: 5th Percentile Recharge Rate	Normalized Darcy Flux: Maximum Recharge Rate
C-105_66	1	0.5012	1.3086
C-105_63	1	0.5079	1.2964
C-105_61	1	0.4588	1.3587
C-105_55	1	0.4936	1.3802
C-105_47	1	0.5427	1.3820
C-105_39	1	0.5947	1.3560
C-105_31	1	0.6407	1.3188
C-105_24	1	0.6765	1.2864
C-105_18	1	0.6759	1.2861
C-105_14	1	0.6832	1.2791

Subsurface Transport Over Multiple Phases (STOMP)© is copyrighted by Battelle Memorial Institute, 1996.

Figure 8-17. Normalized Darcy Flux for H1 Unit (Node 66) for 100-Series Representative Column during (a) Early Post-Closure Period (b) Late Post-Closure Period.

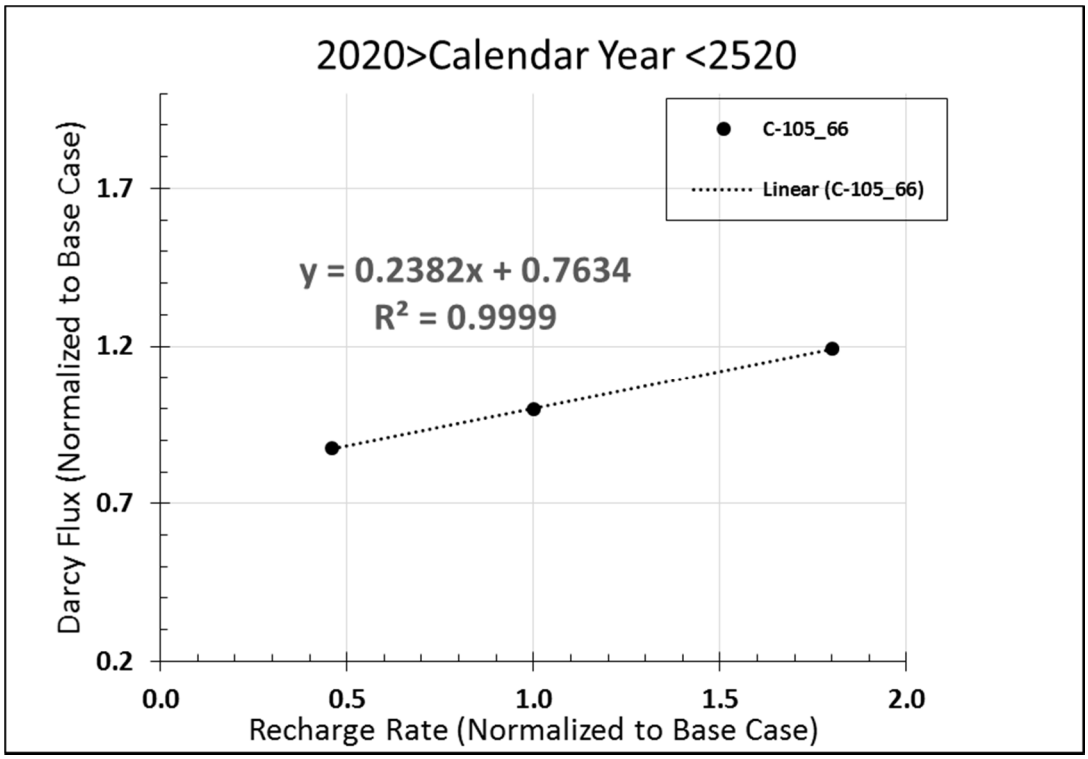

(a)

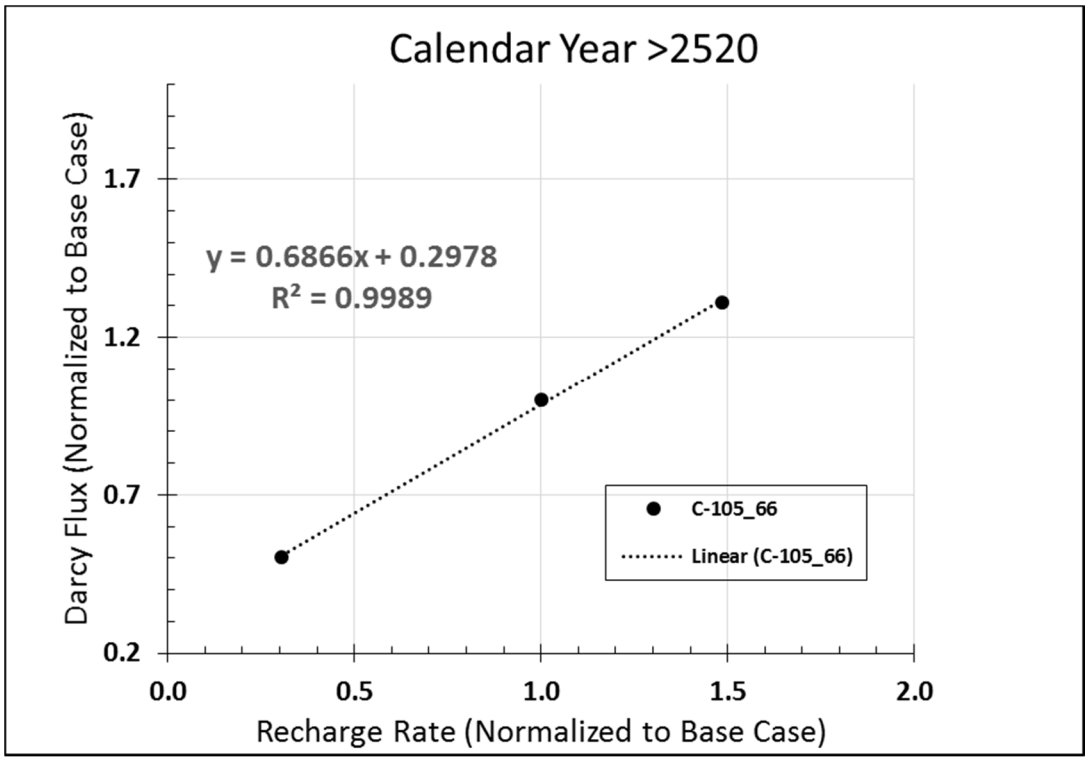

(b)

Figure 8-18. Normalized Darcy Flux for H2 and H3 Units for 100-Series Representative Column during (a) Early Post-Closure Period (b) Late Post-Closure Period.

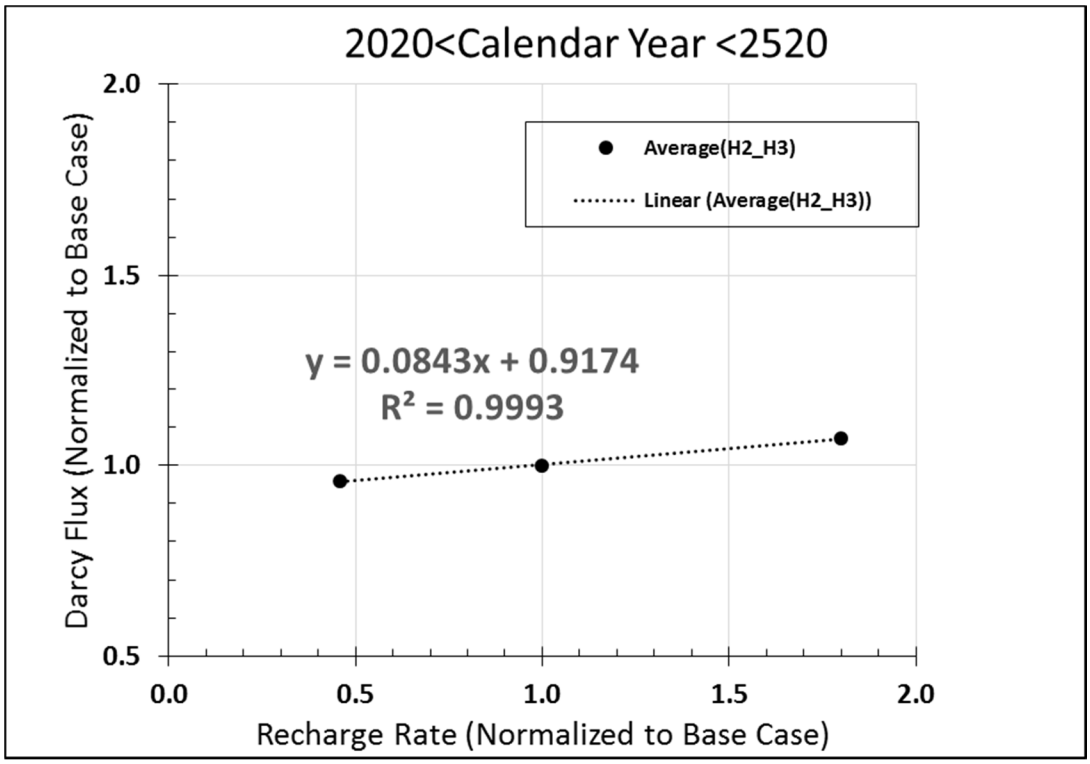

(a)

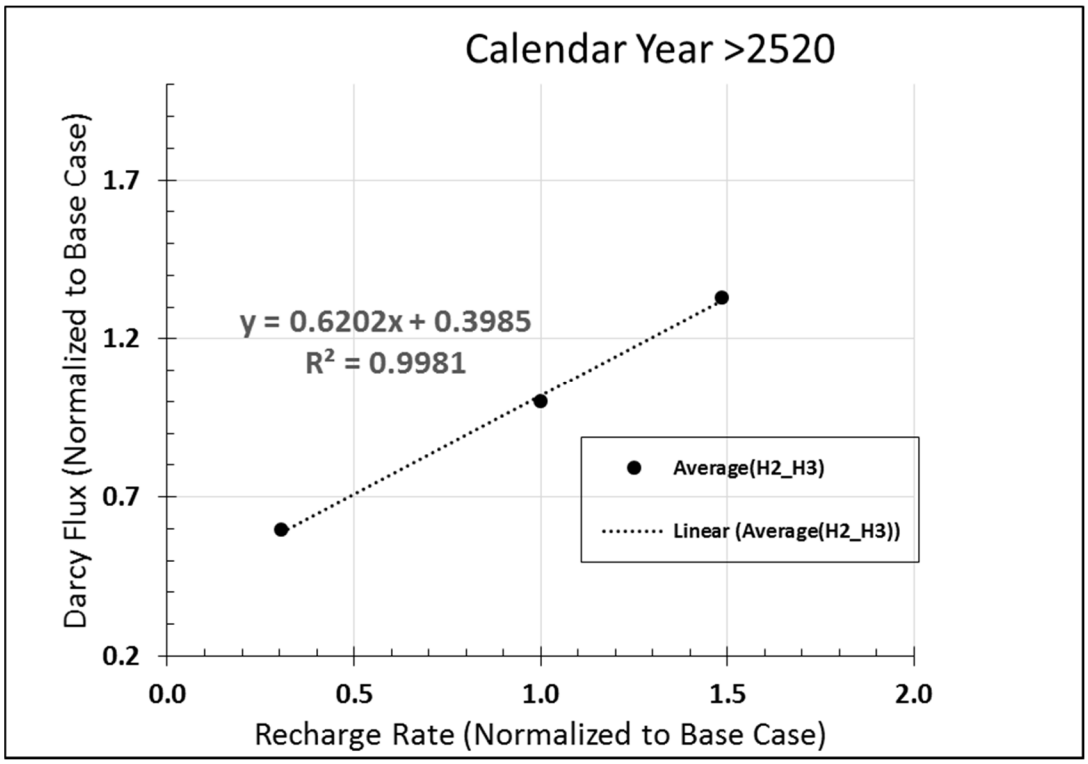

(b)

Figure 8-19. Normalized Moisture Content for H1 Unit (Node 66) for 100-Series Representative Column during (a) Early Post-Closure Period (b) Late Post-Closure Period.

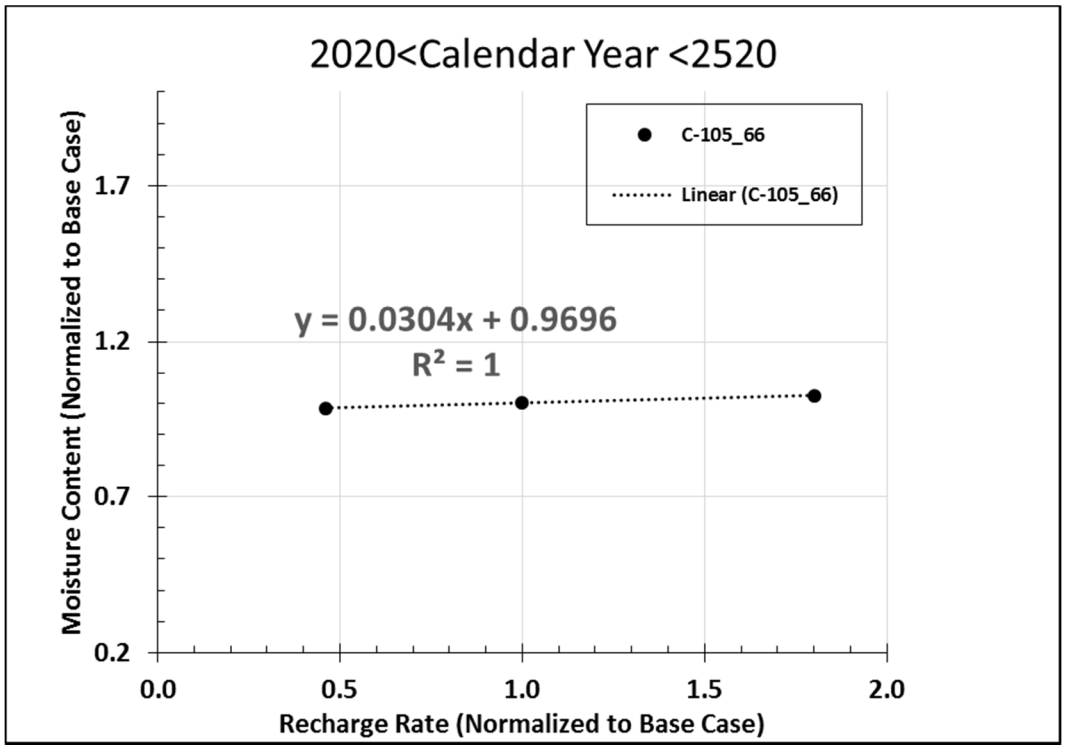

(a)

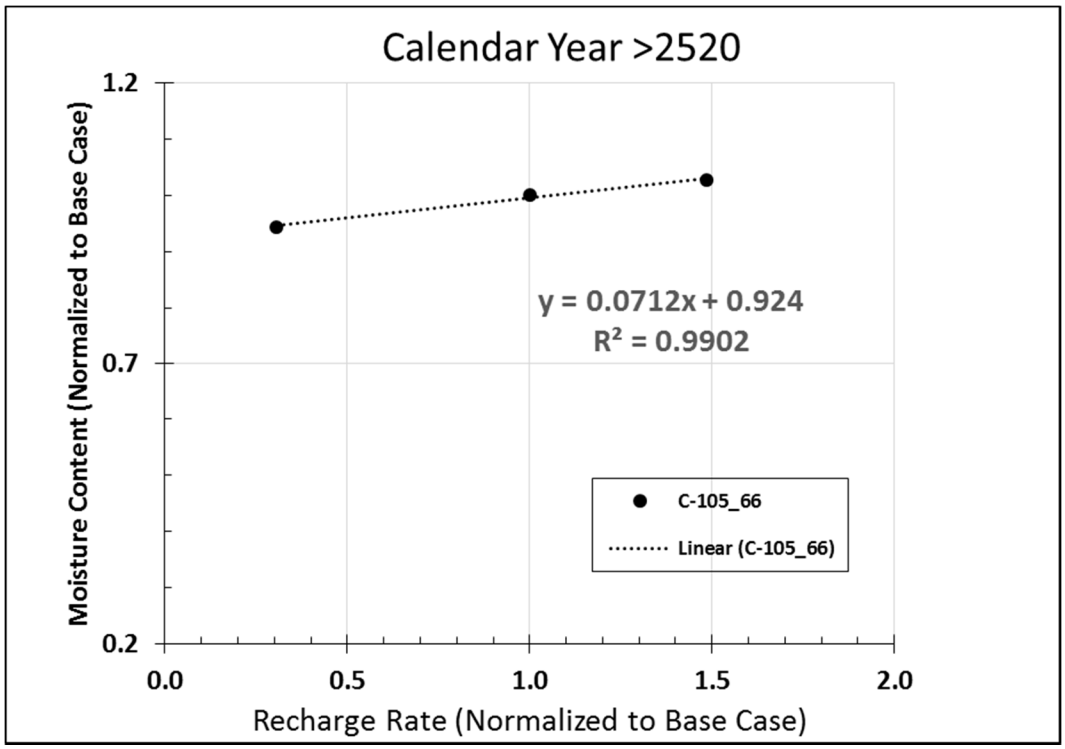

(b)

Figure 8-20. Normalized Moisture Content for H2 and H3 Units for 100-Series Representative Column during (a) Early Post-Closure Period (b) Late Post-Closure Period.

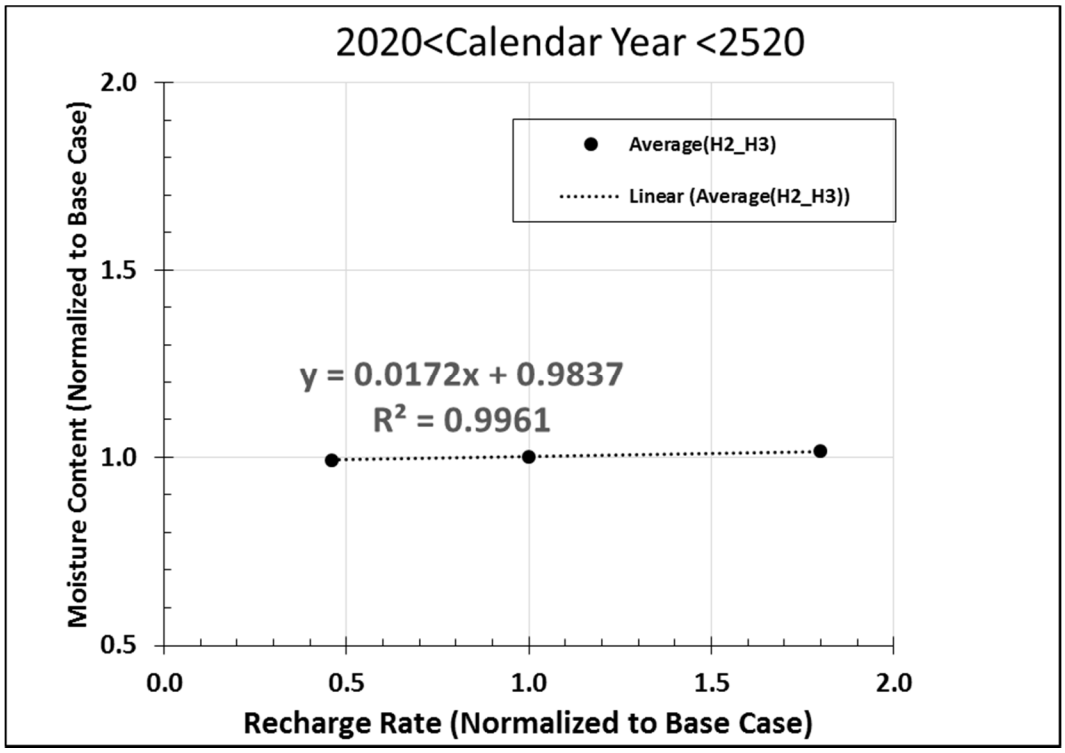

(a)

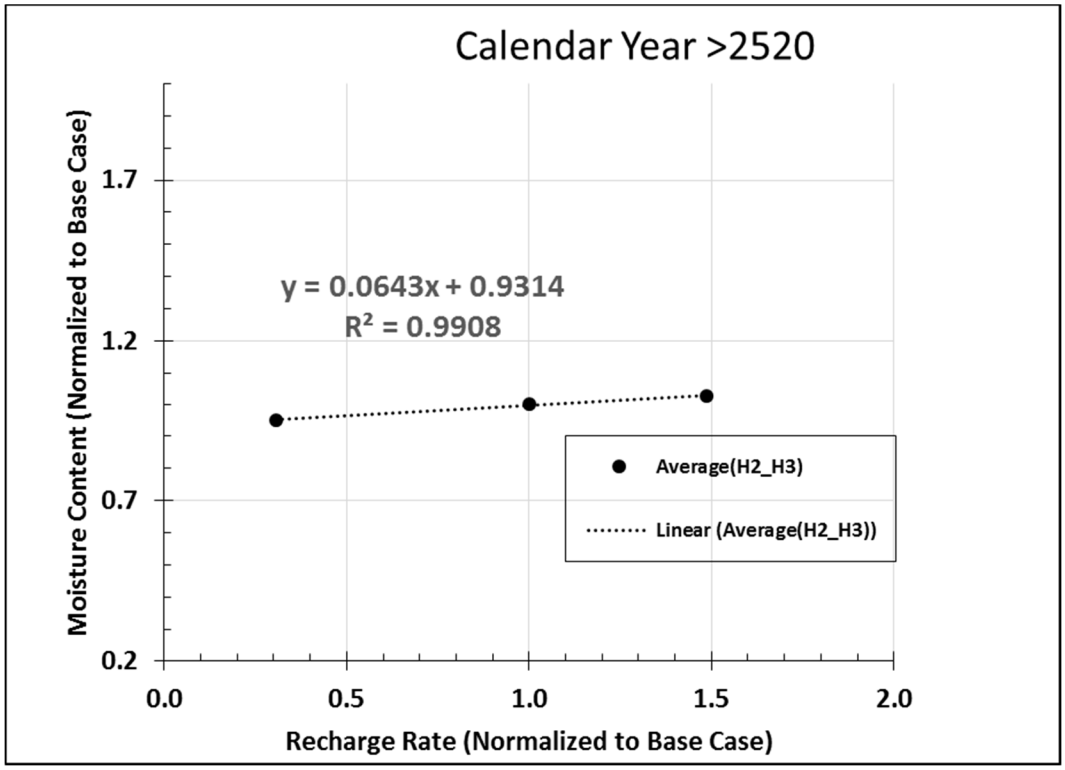

(b)

Table 8-10. Regression Equations for Scaling Darcy Flux for 100-Series Tank.

Vadose Zone Hydraulic Properties	Normalized Darcy Flux: 100 Series Tank			
	H1 Unit		H2/H3 Unit	
	2020<Calendar Year<2520	Calendar Year>2520	2020<Calendar Year<2520	Calendar Year>2520
5th Percentile Case Hydraulic Properties	0.2382*x+0.7634	0.6866*x+0.2978	0.0843*x+0.9174	0.6202*x+0.3985
25th Percentile Case Hydraulic Properties	0.2562*x+0.7406	0.5083*x+0.4701	0.1261*x+0.8763	0.7149*x+0.3032
50th Percentile Case Hydraulic Properties	0.2652*x+0.7363	0.7305*x+0.2670	0.2243*x+0.7829	0.8141*x+0.1940
75th Percentile Case Hydraulic Properties	0.3265*x+0.6721	0.7233*x+0.2580	0.2602*x+0.7474	0.8109*x+0.1946
95th Percentile Case Hydraulic Properties	0.8006*x+0.2164	0.899*x+0.0660	0.2795*x+0.7409	0.9497*x+0.0775

x = Sampled recharge rate / Base case recharge rate

Table 8-11. Regression Equations for Scaling Darcy Flux for 200-Series Tank.

Vadose Zone Hydraulic Properties	Normalized Darcy Flux: 200 Series Tank			
	H1 Unit		H2/H3 Unit	
	2020<Calendar Year<2520	Calendar Year>2520	2020<Calendar Year<2520	Calendar Year>2520
5th Percentile Case Hydraulic Properties	0.2456*x+0.7566	0.7221*x+0.2714	0.0485*x+0.9523	0.4389*x+0.5651
25th Percentile Case Hydraulic Properties	0.2832*x+0.7155	0.7253*x+0.2754	0.0781*x+0.9237	0.5536*x+0.4573
50th Percentile Case Hydraulic Properties	0.2604*x+0.7415	0.7512*x+0.2540	0.1236*x+0.8783	0.5572*x+0.4463
75th Percentile Case Hydraulic Properties	0.3260*x+0.6735	0.7614*x+0.2361	0.1472*x+0.8554	0.6110*x+0.3950
95th Percentile Case Hydraulic Properties	0.3731*x+0.6336	0.8759*x+0.1345	0.1480*x+0.8567	0.6252*x+0.3798

x = Sampled recharge rate / Base case recharge rate

Note that the scaling multipliers developed for vertical Darcy flux and volumetric moisture content are dimensionless and are applied to values calculated under base recharge conditions, as abstracted from the 3-D STOMP© model results for each of the five hydraulic properties. The results of using the regression equations over the minimum and maximum recharge rates are presented in Appendix I. The purpose of Appendix I is to illustrate the uncertainty range in

vertical average linear pore water velocities within the vadose zone for the post-closure time period. Based on the uncertainty ranges calculated for each hydraulic property under minimum and maximum recharge rates, it is found that the range in vertical linear pore water velocities is the largest for the 95th percentile hydraulic property (around a factor of 6.5) and minimum for the 25th percentile hydraulic property (factor of 2 to 2.5). For other hydraulic properties the range varies from factor of 3 to 4. These results indicate that for realizations where 95th percentile hydraulic property is selected during uncertainty analysis, greater variance in travel times can be expected compared to other hydraulic properties (under similar recharge rate range).

Table 8-12. Regression Equations for Scaling Volumetric Moisture Content.

Normalized Volumetric Moisture Content			
H1 Unit		**H2/H3 Unit**	
2020<Calendar Year<2520	**Calendar Year>2520**	**2020<Calendar Year<2520**	**Calendar Year>2520**
0.0304*x+0.9696	0.0712*x+0.9240	0.0172*x+0.9837	0.0643*x+0.9314

x = Sampled recharge rate / Base case recharge rate

Step 5 – Sampling of Flow Fields:

In the Monte Carlo analysis for the system model, a flow field is selected for each realization. Using the approach described in Steps 1 through 4, the flow fields are developed for five hydraulic property sets based on the selection of various percentiles from the vertical pore water velocity CDF (for example, see Figure 8-14 for the H2 unit). The percentiles selected were 5th, 25th, 50th, 75th, and 95th to discretely represent the uncertainty in the CDF (Table 8-7). A discrete probability distribution was developed for sampling the five hydraulic properties (flow fields). The 5th and 95th percentile hydraulic properties were given a probability of 0.1 each, the 25th and 75th percentile hydraulic properties were given a probability of 0.25 each, and the 50th percentile hydraulic property was given a probability of 0.3, leading to a discrete probability distribution with a median value being represented by the 50th percentile hydraulic property. The rationale for this probability weighting was based on the understanding that the 5th and 95th percentile hydraulic properties represent the extremes of the pore water velocity distribution, and should have a lower probability of being selected compared to the other percentile hydraulic properties, with the 50th percentile hydraulic property being the most probable. As a result, the 25th and 75th percentile hydraulic properties are given slightly lower weighting than the 50th percentile hydraulic property. The selected discrete probability distribution results in the median being the 50th percentile hydraulic property, which is also the most probable flow field.

8.1.5 Results of Uncertainty Analyses

A full uncertainty analysis is undertaken by performing multi-realization simulations in the probabilistic mode using the GoldSim©-based system model. The uncertainties are propagated using the Monte Carlo sampling methodology and the LHS scheme. In the Monte Carlo simulation, the entire system is simulated a large number of times. Each simulation is equally likely and is referred to as a *realization* of the system. For each realization, all of the uncertain

parameters are sampled, and the system is simulated through time (with the given set of input parameters) such that the performance of the system can be computed. At the start of each realization, each stochastic element generates a new random seed that forms the basis for sampling the element during the realization. The LHS scheme allows for efficient sampling of the probability space so that full uncertainty can be represented without a large number of realizations (GoldSim Technology Group 2014c). In this scheme, each stochastic element's probability distribution (0 to 1) is divided into equally likely strata or slices equal to the number of realizations. The strata are then "shuffled" into a random sequence, and a random value is picked from each stratum in turn. This approach ensures that uniform spanning sampling is achieved. Note that each element has an independent sequence of shuffled strata that are a function of the element's random number seed and the number of realizations in the simulation. The LHS appears to have a significant benefit for problems involving a few independent stochastic parameters, and with moderate number of realizations (GoldSim Technology Group 2014c).

The total mean annual dose, $\overline{D}(\tau)$, for a multi-realization case is estimated at time τ by numerically evaluating

$$\overline{D}(\tau) = \int_E D(\tau|\mathbf{e})\, d_E(\mathbf{e}) dE \tag{8-3}$$

where E is a probability space comprising the epistemic uncertain parameters, and $D(\tau|\mathbf{e})$ computes the annual dose at time τ for a given element $\mathbf{e}$ (a vector of all uncertain parameters evaluated per realization) in E. The evaluation of the function $D(\tau|\mathbf{e})$ is performed by numerically solving a complex, coupled system of differential equations such as describing radionuclide decay, mass transport, flow, and other physical processes. The numerical integration is performed by the Monte Carlo technique and employing LHS of epistemic uncertain parameters.

The GoldSim©-based system model is exercised by running 300 realizations. The results are presented in Figure 8-22 in terms of mean of total dose (from all radionuclides from the groundwater and atmospheric transport pathways) along with the mean dose contribution of individual radionuclides. The early dose (from 100 to 600 years after closure) primarily results from the release of ^{3}H (tritium) and ^{129}I to the air pathway, and the late dose (past 1,000 years after closure) results primarily from the ^{99}Tc release to the groundwater pathway. The mean dose reaches a peak value of about 0.17 mrem/yr around 3,400 years after closure and then declines gradually. Although the contribution of ^{99}Tc steadily declines, the mean total dose remains virtually unchanged beyond 7,000 years after closure until the end of the analysis time. This is because of increasing dose contributions from uranium isotopes (primarily ^{234}U, ^{238}U, and ^{233}U) that have relatively long half-lives and are relatively mobile (low K_d value).

Besides ^{99}Tc and uranium isotopes, other radionuclides of interest are ^{129}I, ^{226}Ra, ^{126}Sn, and ^{79}Se. The dose contribution of ^{129}I in the first 1,000 years after closure is primarily from the atmospheric pathway, and beyond that primarily from the groundwater pathway. Radium-226 dose results from it being in equilibrium with the uranium decay series, and therefore—although it has a high K_d by itself—it appears at the PoCal. Tin-126 and ^{79}Se are relatively mobile (low

K_d) and have relatively long half-lives (>200,000 years after closure), and therefore show breakthrough at PoCal within the simulated time period.

8.1.5.1 Evaluation of Uncertainty in Groundwater Pathway. Figure 8-23 shows the results of propagating parameter uncertainties in the groundwater pathway dose for 300 realizations, along with the mean, median, 5th, and 95th percentile values. The highest mean and median doses occur around 3,400 years after closure. For comparison purposes, the dose from base case is also presented. Comparing the base case dose with the mean dose from 300 realizations indicates that the peak occurs earlier in the base case, reflecting faster transport through the vadose zone and saturated zone. For all realizations, ^{99}Tc is the primary dose contributor, and thus the uncertainty in groundwater pathway dose is almost entirely due to uncertainty in ^{99}Tc dose. The mean of the total dose is higher than the median of the total dose and closer to the 75th percentile curve. This occurs because the values range over several orders of magnitude, so that an arithmetic mean will tend to be skewed to the higher values. The variance in dose, defined by the difference in 5th and 95th percentiles at a given time slice, is observed to decrease after 4,000 years following closure. This is due to occurrence of larger number of realizations having relatively similar breakthrough curves. Prior to this time, some realizations that have earlier ^{99}Tc breakthrough show a decline due to variable influence of flow fields, leading to increased variance. At late time also (>7,000 years after closure), the variance in dose increases marginally. This results from the increasing importance of uranium isotopes at late times.

To understand the relative influence of uncertain parameters on the peak dose resulting from the groundwater pathway, two realizations (Rlz# 142 and Rlz# 295) are shown in Figure 8-24, and demonstrate the highest dose values (Figure 8-24).

In Rlz# 142, the peak dose value is ~2.5 mrem/yr, and it occurs around 2,400 years after closure. This high dose value results from a combination of sampling the Darcy flux multiplier (0.33) near the low end of the uncertainty distribution and sampling the residual waste instantaneous ^{99}Tc release fraction (0.149) from the upper end of the distribution. In addition, the saturated zone dispersivity (2.3 m [7.5 ft]) is sampled at the lower end of the distribution. The high instantaneous release fraction leads to larger diffusive flux from the base of the tanks, and the lower Darcy flux multiplier leads to less dilution in the saturated zone leading to increased concentration in the aquifer. In addition, sampling lower dispersivity in the saturated zone leads to less dispersion and higher peak concentration that results in a high dose.

In Rlz# 295, the peak dose value is ~1.8 mrem/yr and it occurs around 5,000 years after closure. Unlike Rlz# 142, where the peak occurs quickly followed by steep decline, the dose curve in Rlz# 295 shows a gradual rise and a more gradual decline. This behavior results from a combination of sampling the Darcy flux multiplier (0.19) near the minimum value of the uncertainty distribution and sampling the ^{99}Tc inventory multiplier (1.36) from the upper end of the uncertainty distribution. This combination leads to increased residual inventory being available, along with lowest possible dilution in the saturated zone resulting in greater peak concentration. In this realization, the 25th percentile flow field is sampled that leads to lower pore water velocity in the vadose zone, and therefore the mass continues to arrive from the source term over a longer time period. This leads to a gradual rise and gradual decline in the dose curve.

Figure 8-21. Comparison between Darcy Flux Calculated Using Regression Equation and that Obtained from Three-Dimensional Subsurface Transport Over Multiple Phases-Based Model Simulation for the 5th Percentile Hydraulic Property Case for (a) H1 Unit under 100-Series Tank (Node 66); (b) H2 Unit under 100-Series Tank (Node 47); (c) H1 Unit under 200-Series Tank (Node 66); and (d) H2 Unit under 200-Series Tank (Node 43). (sheet 1 of 4)

(a)

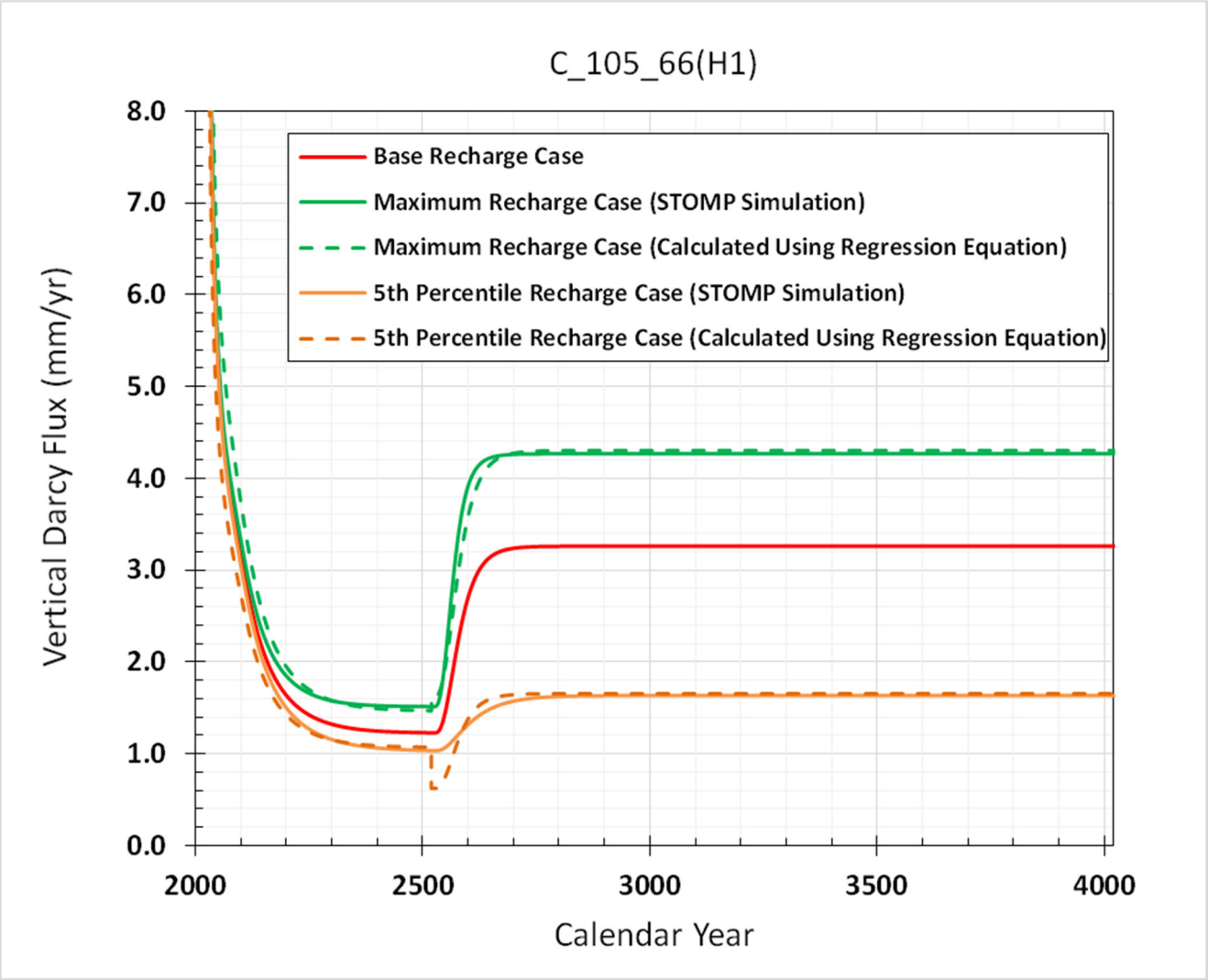

Figure 8-21. Comparison between Darcy Flux Calculated Using Regression Equation and that Obtained from Three-Dimensional Subsurface Transport Over Multiple Phases Based Model Simulation for the 5th Percentile Hydraulic Property Case for (a) H1 Unit under 100-Series Tank (Node 66); (b) H2 Unit under 100-Series Tank (Node 47); (c) H1 Unit under 200-Series Tank (Node 66); and (d) H2 Unit under 200-Series Tank (Node 43). (sheet 2 of 4)

(b)

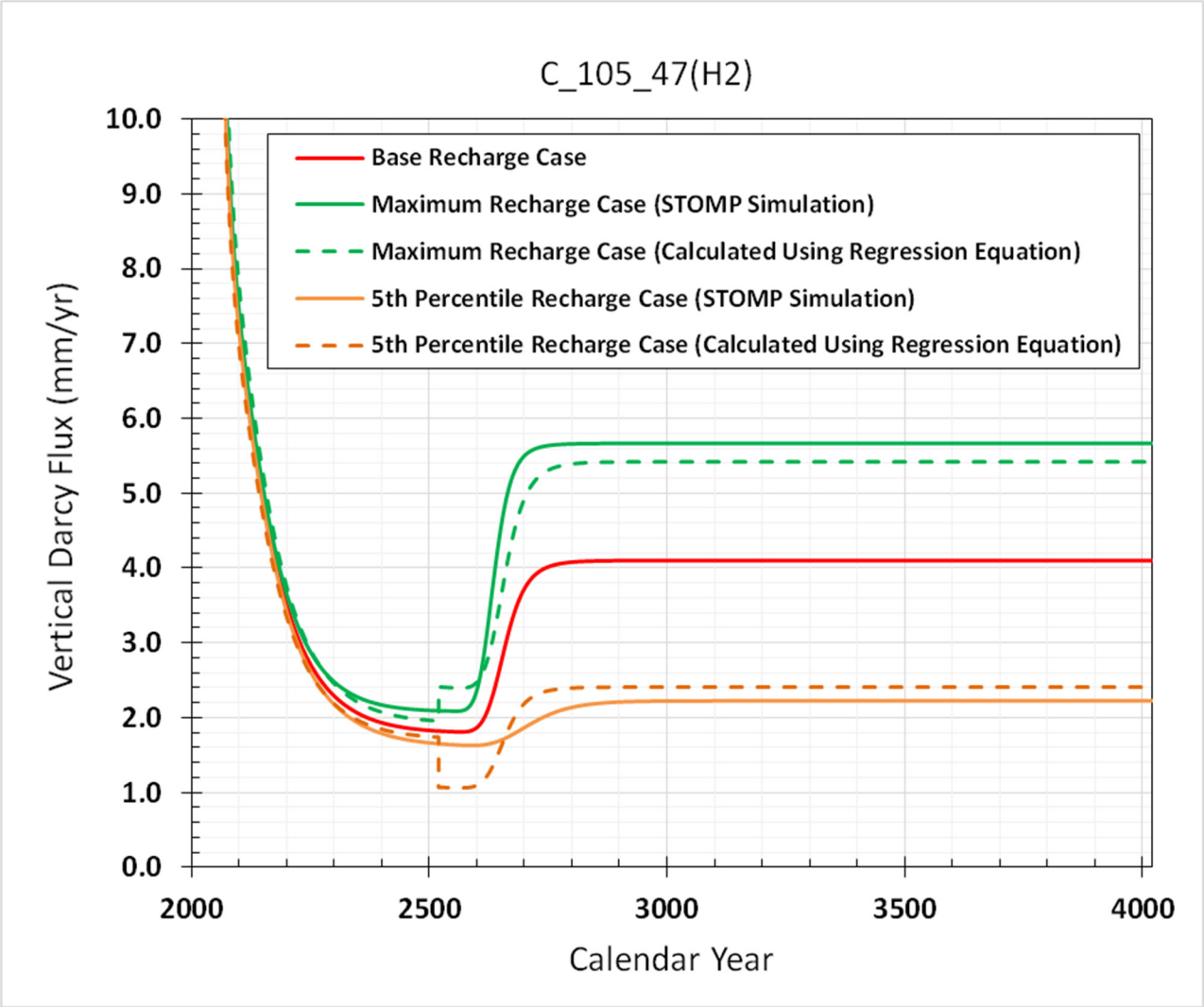

Figure 8-21. Comparison between Darcy Flux Calculated Using Regression Equation and that Obtained from Three-Dimensional Subsurface Transport Over Multiple Phases Based Model Simulation for the 5th Percentile Hydraulic Property Case for (a) H1 Unit under 100-Series Tank (Node 66); (b) H2 Unit under 100-Series Tank (Node 47); (c) H1 Unit under 200-Series Tank (Node 66); and (d) H2 Unit under 200-Series Tank (Node 43). (sheet 3 of 4)

(c)

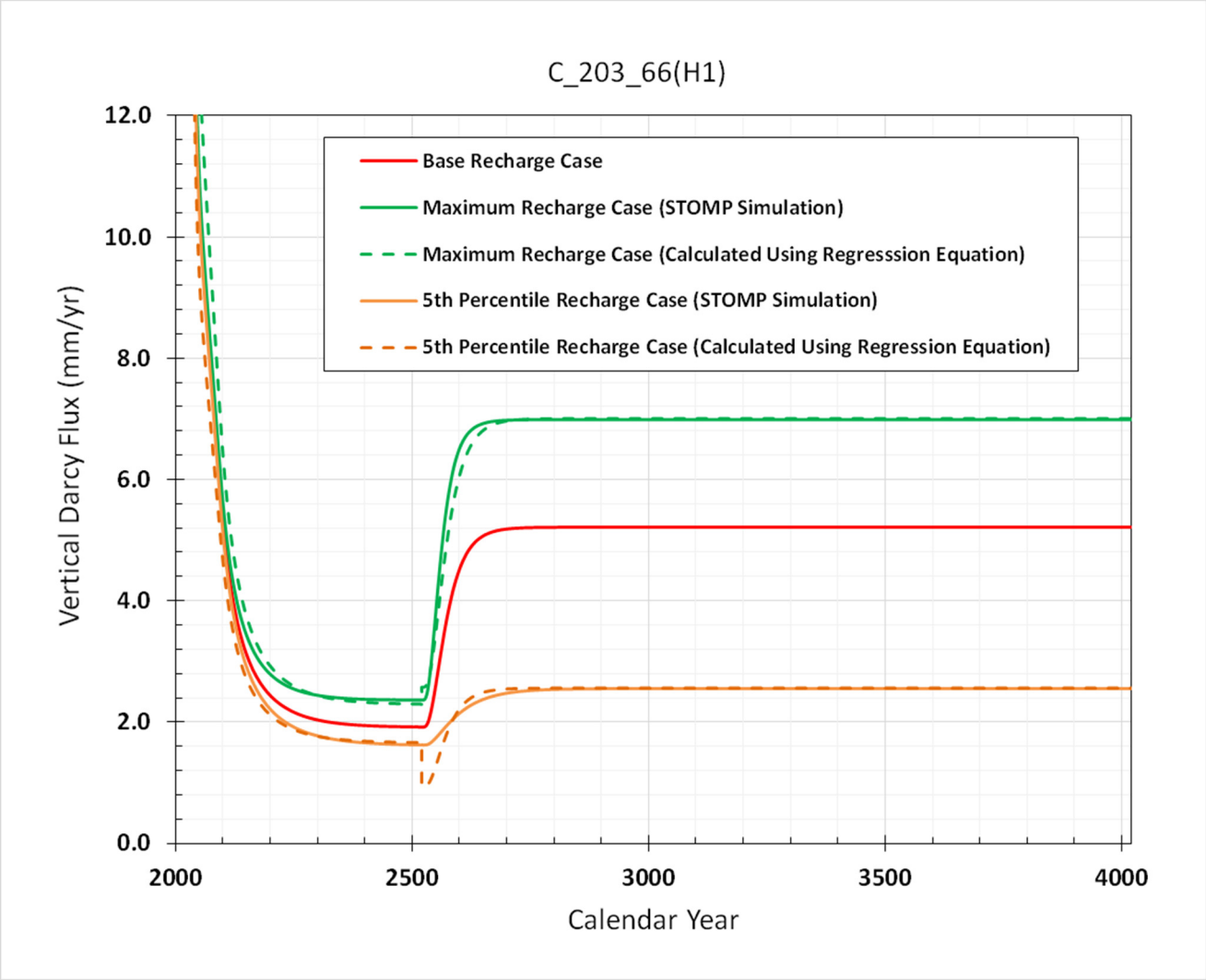

Figure 8-21. Comparison between Darcy Flux Calculated Using Regression Equation and that Obtained from Three-Dimensional Subsurface Transport Over Multiple Phases Based Model Simulation for the 5th Percentile Hydraulic Property Case for (a) H1 Unit under 100-Series Tank (Node 66); (b) H2 Unit under 100-Series Tank (Node 47); (c) H1 Unit under 200-Series Tank (Node 66); and (d) H2 Unit under 200-Series Tank (Node 43). (sheet 4 of 4)

(d)

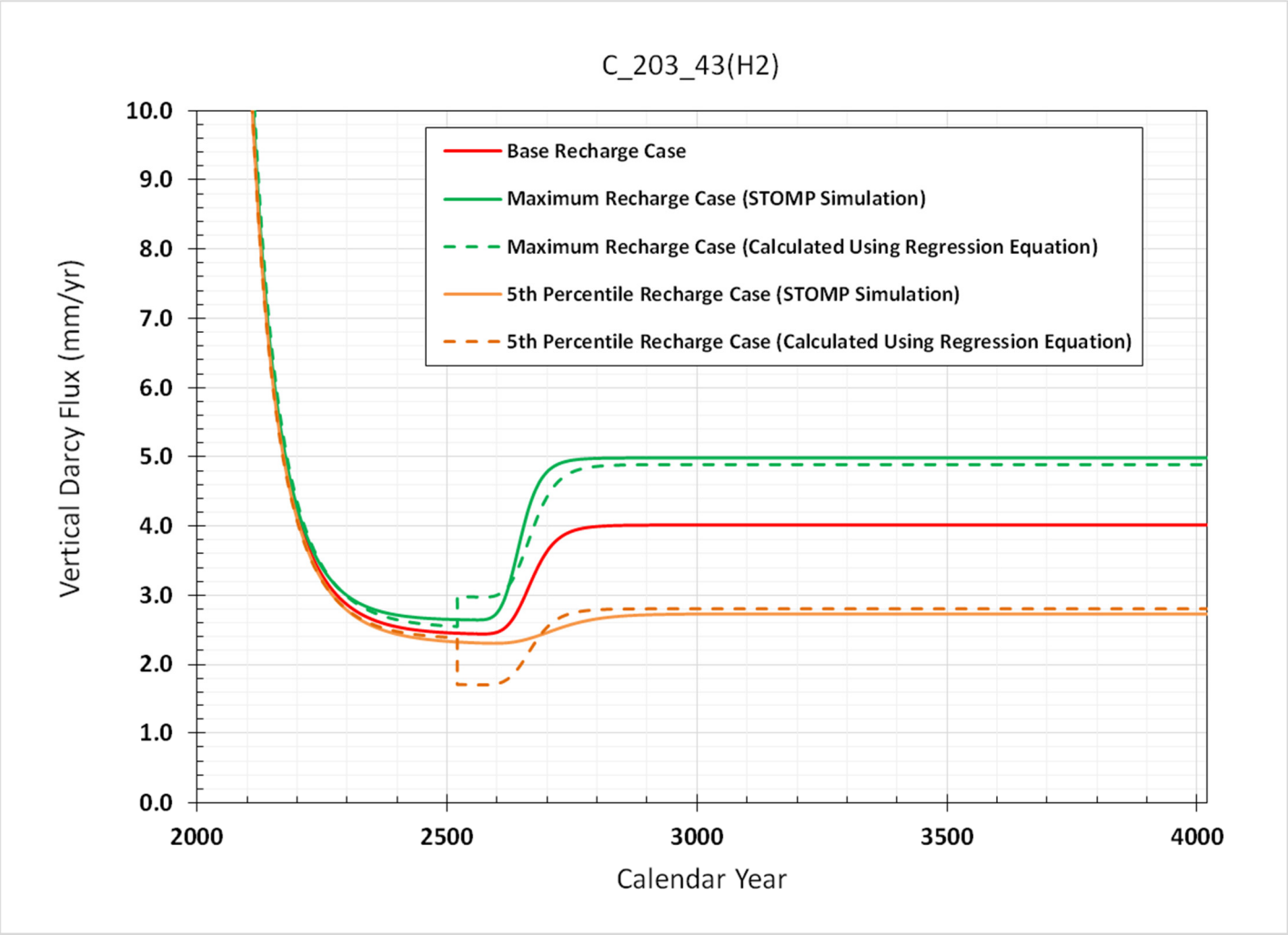

Subsurface Transport Over Multiple Phases (STOMP)© is copyrighted by Battelle Memorial Institute, 1996.

Figure 8-22. All-Pathway Mean Dose Calculation Results Based on 300 Realizations.

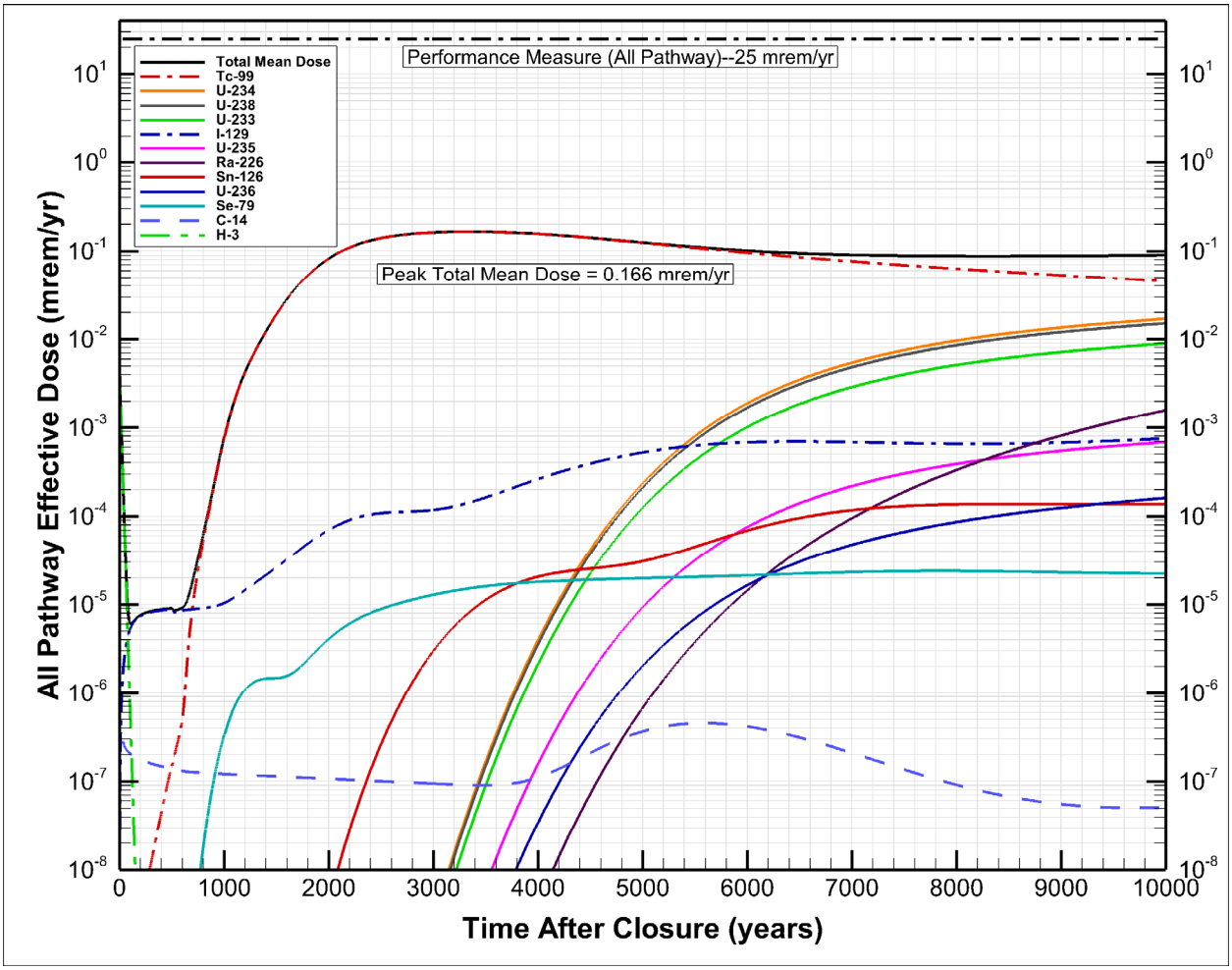

Some of the realizations presented in Figure 8-24 show a gradual rise late in time. This gradual increase is attributed to the increasing dose influence from uranium isotopes. Some of the realizations that show early peak dose result from sampling the 95th percentile flow field that leads to high pore-water velocity and earlier breakthrough.

Multivariate analyses were conducted to evaluate the importance of uncertain parameters on the groundwater pathway dose calculations. The analysis was conducted at the time of peak mean dose, which occurs about 3,400 years after closure. The analysis was based on the ranks (rather than values) of the uncertain parameters. Two types of analyses were conducted: (a) the rank (Spearman) correlation coefficient and (b) the Importance Measure. Standardized rank regression coefficients and partial rank correlation coefficients were also computed, but they do not provide additional insight and are not discussed further. The total number of uncertain parameters that are implemented in the system model is 130.

Figure 8-23. Uncertainty in Groundwater Pathway Dose Based on 300 Realizations.

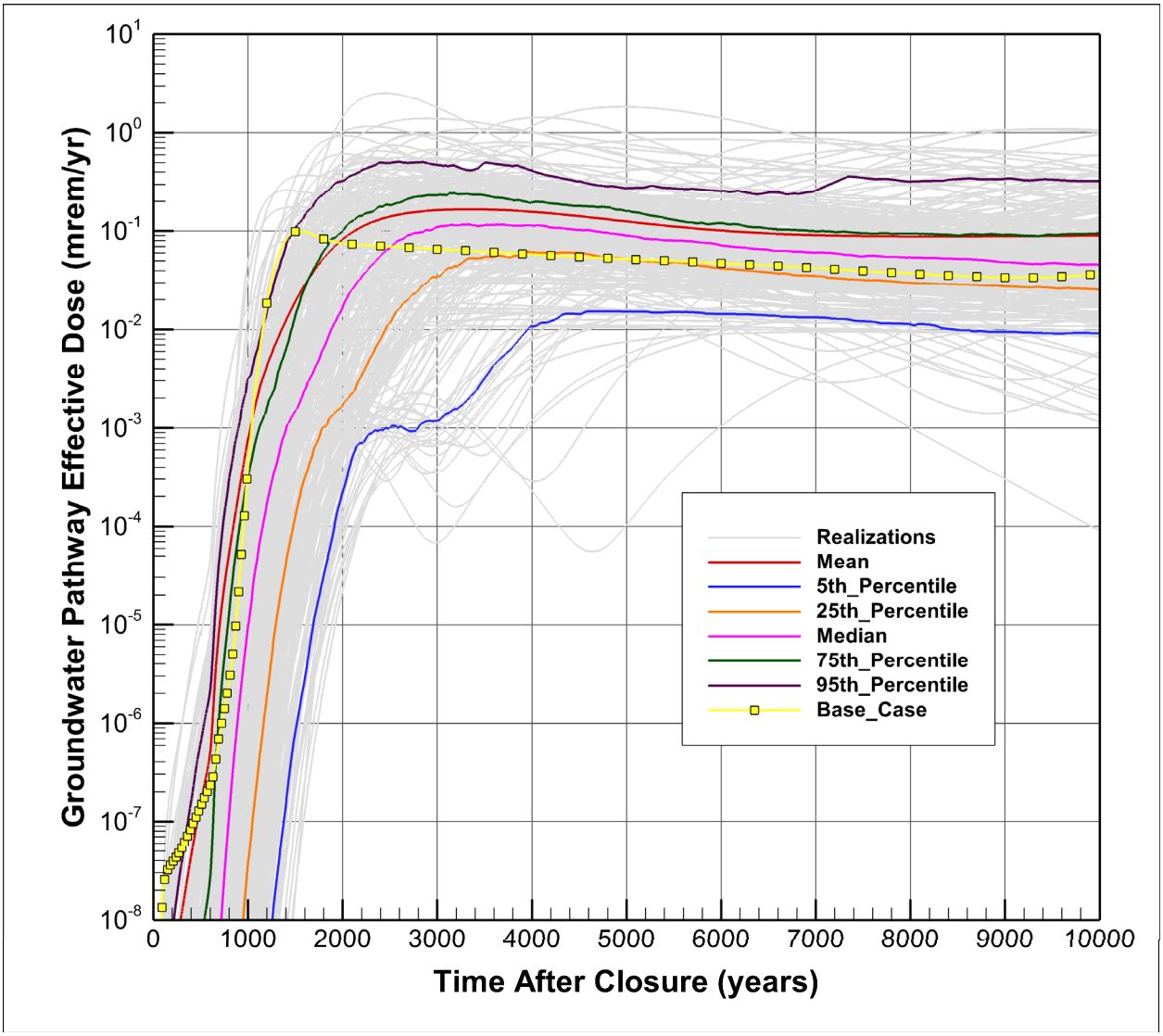

The rank correlation coefficient expresses the extent to which there is a linear relationship between the selected result and an input variable. The coefficients range between -1 and 1 with extreme values indicating strong negative or positive correlations. The calculation is performed using the following equation (GoldSim Technology Group 2014c):

$$C_{rp,rank} = \frac{\sum_{i=1}^{n}(Rp_i - m_{Rp})(Rr_i - m_{Rr})}{\sqrt{\sum_{i=1}^{n}(Rp_i - m_{Rp})^2 \sum_{i=1}^{n}(Rr_i - m_{Rr})^2}} \quad (8\text{-}4)$$

Where:

$C_{rp,rank}$ = the rank correlation coefficient
n = the number of selected data points (realizations)

Rp_i = the rank (from 1 to n) of output p for realization I
m_{Rp} = mean value of the rank of output p
m_{Rr} = mean value of the rank of output r.

Figure 8-24. Selected Realizations for Groundwater Pathway Dose Analysis.

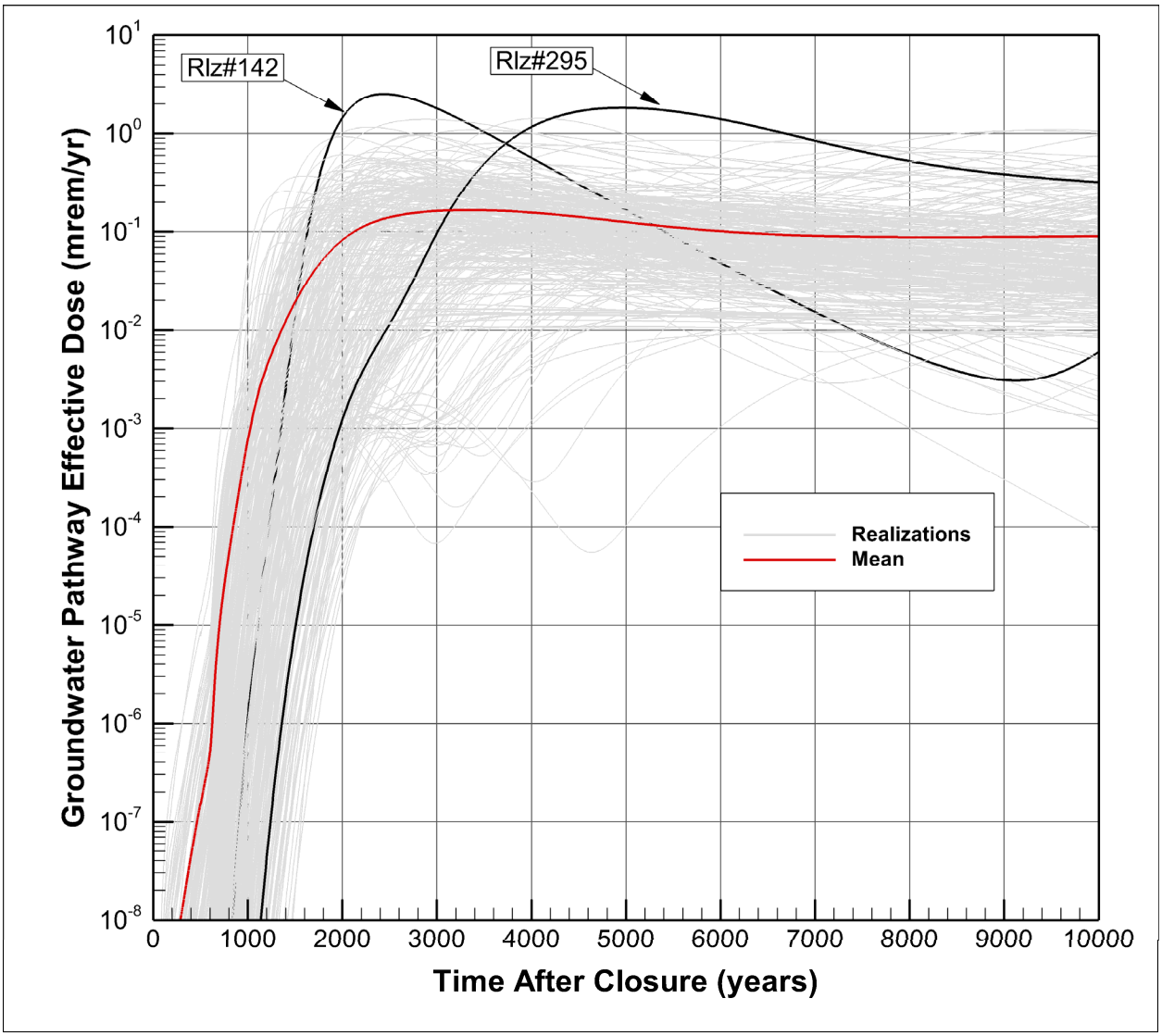

The standardized rank regression coefficients and partial rank correlation coefficients also vary between -1 and 1. These calculations are based on the variable ranks rather than on the actual values of the variables. The standardized rank regression coefficients provide a normalized measure of the linear relationship between variables and the result (dose). They are regression coefficients found when all of the variables and the results are transformed and expressed in terms of the number of standard deviations away from the mean. The partial correlation coefficients reflect the extent of the linear relationship between the selected result and an input variable, after removing the effects of any linear relationships between the other input variables and both the results and the input variable in question. Both formulations are based on

NUREG/CR-4122, A FORTRAN 77 Program and User's Guide for the Calculation of Partial Correlation and Standardized Regression Coefficients.

The importance measure (as calculated using GoldSim©) expresses the nonlinear, non-monotonic relationship between an input variable and the result, which the conventional correlation coefficient may not reveal. This measure varies between 0 and 1, and represents the fraction of the result's variance that is explained by the variable. The importance measure presented here is a normalized version of a measure discussed in "On the Relative Importance of Input Factors in Mathematical Models: Safety Assessment of Nuclear Waste Disposal" (Saltelli and Tarantola 2002), and is calculated as:

$$M_{y,i} = 1 - \frac{E[V_y(Y|X_i)]}{V_y} \tag{8-5}$$

Where:

$M_{y,i}$ = the importance measure for the sensitivity of the result (Y) to input variable X_i

V_y = the current variance in the result Y

$E[V_y(Y|X_i)]$ = the expected value of V_y if the input variable X_i was perfectly known.

Thus, the Importance Measure $M_{y,i}$ represents the fraction of the result variance that is explained by X_i. For additional computational details, refer to Appendix B of the GoldSim User's Guide (GoldSim Technology Group 2014b).

The uncertainty analysis results of the 300 realization case for the groundwater pathway are presented at the end of 1,000 years after closure (Table 8-13a) which is the end of compliance time period, and at 3,400 years after closure (Table 8-13b), the approximate time when the peak occurs in the mean dose. Only those parameters are presented that contribute significantly to the uncertainty in total dose for the groundwater pathway. The results are sorted by the uncertain parameters from highest to lowest in terms of their Importance Measures, for those parameters that have correlation coefficients equal to or greater than ~0.2. Other uncertainty analysis measures (e.g., partial correlation coefficients) generally follow the same trend. The uncertainty analysis for the groundwater pathway is conducted by evaluating the dose from all realizations at 1,000 years and 3,400 years after closure. The results of the multivariate analysis are only applicable to these times.

Based on the uncertainty analysis for the groundwater pathway conducted at 1,000 years after closure (end of compliance time period), the most important uncertain parameter is found to be the K_d of ^{99}Tc in the vadose zone sediments (Table 8-13a). It shows a high negative correlation with the dose at 1,000 years, which is primarily due to ^{99}Tc. Since the 1,000-year time is near the arrival time of ^{99}Tc at the water table (breakthrough time) and since the dose curves are rising steeply, the magnitude of the dose is being directly affected by the uncertainty in the K_d of ^{99}Tc in the vadose zone sediments. Due to steep rise in the dose curves, a small delay in arrival at the water table leads to a much lower magnitude of dose at the 1,000-year time plane compared to a realization where the arrival at the water table occurs marginally earlier. Therefore, even though

the uncertainty range in the K_d of ^{99}Tc in the vadose zone sediments is very small (0 to 0.1 mL/g), it leads to significant changes in the breakthrough time at the water table at 1,000 years. The coefficient of determination based on linear rank regression is ~0.96 and thus explains 96% of the variance in the dose at 1,000 years. All other uncertain parameters show much lower correlation to the dose at 1,000 years. The second and third most important parameters are related to uncertainty in dispersivity within the vadose zone and saturated zone. These parameters also affect the arrival times at the water table and receptor location.

Based on the uncertainty analysis for the groundwater pathway conducted at the time of peak dose (around 3,400 years after closure), the two most important uncertain parameters are found to be the vadose zone flow-field selector (hydraulic properties corresponding to the percentiles chosen from the vertical pore-water velocity CDF) and the saturated zone Darcy flux multiplier (scales the base case Darcy flux in the aquifer). Both uncertain parameters are negatively correlated to the groundwater pathway dose. The linear relationships in these parameters can be inferred from the scatter plots shown in Figure 8-25. Choosing higher flow field (higher percentile vadose zone hydraulic property set) leads to increased vertical pore water velocities, resulting in ^{99}Tc peak dose occurring earlier than 3,400 years after closure. In such realizations, dose from ^{99}Tc (which is approximately the total dose) shows a declining trend at 3,400 years after closure. On the other hand, realizations where lower flow field (lower percentile vadose zone hydraulic property set) is selected tend to have delayed peak dose from ^{99}Tc due to decreased vertical pore water velocities, resulting in an upwardly increasing dose trend at 3,400 years after closure. This combination results in a negative correlation between flow field and dose at 3,400 years after closure. The negative correlation observed for the saturated zone Darcy flux multiplier is more intuitive (Figure 8-25b), as the Darcy flux multiplier directly affects the volumetric flow rate in the aquifer, leading to dilution of the mass flux arriving from the vadose zone. Therefore, increasing the Darcy flux reduces the concentrations in the saturated zone for the simulated duration. The coefficient of determination based on linear rank regression for uncertain parameters shown in Table 8-13b is ~0.75. This indicates that these six parameters represent about 75% of the total variance in the peak dose result (around 3,400 years after closure). The first two parameters alone account for more than half (59%) of the total variance in the dose.

The above uncertainty analyses are performed at fixed time planes and therefore provide information on important uncertain parameters that influence dose at that time. But since peak dose for each realization occurs at different times, a separate analysis is performed where correlation is performed between the input parameters and the peak dose regardless of the time. In this evaluation, the peak dose values from all 300 realizations are taken and a correlation is performed to identify uncertain parameters that influence the peak dose. The magnitude of peak dose for the groundwater pathway is shown in Figure 8-26 for all realizations. It shows that the peak dose values vary within about two orders of magnitude range (0.01 to 1 mrem/yr). The correlation coefficient analysis shows that the three most important uncertain parameters are saturated zone Darcy flux multiplier (correlation coefficient of -0.48), vadose zone flow-field selector (correlation coefficient of -0.45), and ^{99}Tc normalized inventory multiplier (correlation coefficient of 0.24). The scatter plots indicating the relationship between input parameters and peak dose are presented in Figure 8-27 (a,b,c). The parameters determined to be important are a subset of the parameters that were previously identified during uncertainty analysis performed at

3,400 years (Table 8-13b), which indicates that these parameters continue to affect the peak dose irrespective of time within the 10,000-year evaluation time period.

Figure 8-27(b) shows the relationship between the peak groundwater dose as a function of vadose zone hydraulic property (flow-field selector). The peak dose results from varying flow-field selectors mostly overlap except for flow-field #5 (corresponding to the 95th percentile hydraulic property), which shows somewhat lower peak dose and therefore causes an overall negative correlation. This result is likely due to greater variance in vertical pore water velocity estimated for the 95th percentile hydraulic property compared to other hydraulic properties (see Appendix I for illustration of the range). Since pore water velocity also affects the dispersion coefficient, larger variation in velocity also results in larger dispersion of solute mass within the vadose zone that affects the magnitude of the peak groundwater dose. Ignoring the results from 95th percentile hydraulic property results in lowering the negative correlation, which indicates that this parameter has lower influence on affecting peak dose than probably inferred based on simple correlation.

8.1.5.2 Evaluation of Uncertainty in the Atmospheric Pathway. Figure 8-28 presents the uncertainty in the atmospheric pathway dose for all 300 realizations, along with the mean, median, and other percentiles. In the first 100 years after closure, ^{3}H (tritium) dose is the primary atmospheric pathway dose contributor, and after that it is ^{129}I (Figure 8-22). Hydrogen-3 dose declines sharply within the first 100 years after closure due to its short half-life and limited inventory. The ^{129}I dose, however, increases gradually and reaches a steady value after 500 years following closure. This is attributed to a relatively lower degree of partitioning into the air phase compared to ^{3}H (and ^{14}Co), and a relatively larger degree of sorption to the tank infill grout material compared to ^{3}H. Due to these reasons, and in combination with long half-life, ^{129}I persists within the tank for a long time period. As shown in Figure 8-28, the dose resulting from atmospheric pathway remains negligibly small for all time periods.

The uncertainty analysis results of the 300 realization case for the atmospheric pathway are presented in Table 8-14 based on dose results at three different times: (a) early time period (at 2 years after closure) to represent the early peak followed by steep decline; (b) intermediate time period (at 100 years after closure) to represent the slowly increasing dose; and (c) long time period (at 1,000 years after closure) to represent the steady dose. Only the parameters are presented that contribute significantly to the uncertainty in total dose for the atmospheric pathway. The results are sorted by the uncertain parameters from highest to lowest numbers in terms of Importance Measure (that have correlation coefficient of greater than 0.2).

At early time period represented by sharp rise and fall, since ^{3}H (tritium) dominates the dose, the most important uncertain parameter is found to be associated with the inventory. A strong positive correlation observed between dose and inventory uncertainty is not unexpected, indicating that increased inventory leads to larger concentration in the air pathway (see scatter plot presented in Figure 8-29). Uncertainty in wind speed shows a weak negative correlation, as it acts to dilute the concentration in air resulting from upward diffusive mass flux from the tanks.

Table 8-13. Uncertain Parameters Important to Groundwater Pathway at (a) End of Compliance Time Period (1,000 Years after Closure) and (b) Time of Peak Dose (about 3,400 Years after Closure).

Stochastic Parameter ID	Description	Correlation Coefficient Based on Ranks	Standardized Regression Coefficient Based on Ranks	Partial Correlation Coefficient Based on Ranks	Importance Measures Based on Ranks
Kd_Sand_Uncert[Tc]	Uncertainty in K_d of Tc-99 for sand	-0.98	-0.97	-0.99	0.92
SZ_Dispersivity	Dispersivity in the saturated zone; used to scale the 1-D transport model values	-0.16	-0.02	-0.14	0.06
VZ_H2_Dispersivity_Uncert	Dispersivity in the vadose zone for the H2 Unit	0.18	0.11	0.64	0.06

(a)

Stochastic Parameter ID	Description	Correlation Coefficient Based on Ranks	Standardized Regression Coefficient Based on Ranks	Partial Correlation Coefficient Based on Ranks	Importance Measures Based on Ranks
Hyd_Prop_Uncert	Vadose Zone Flow-Field selector based on pore-water velocity CDF	-0.63	-0.59	-0.78	0.40
Darcy_Flux_Mult_SZ	Darcy flux multiplier in the saturated zone	-0.44	-0.42	-0.67	0.22
Recharge_Late_PC_Uncert	Long-term recharge rate after degradation of surface cover; used in scaling the flow field	0.29	0.23	0.41	0.14
SZ_Dispersivity	Dispersivity in the saturated zone; used to scale the 1-D transport model values	-0.26	-0.23	-0.42	0.09
Kd_Sand_Uncert[Tc]	Uncertainty in K_d of Tc-99 for sand	-0.22	-0.18	-0.36	0.08
Tc99_Inv_Mult	Uncertainty in Tc-99 inventory; multiplies the base case value	0.22	0.19	0.36	0.06

(b)

1-D = one-dimensional CDF = cumulative distribution function

Figure 8-25. Scatter Plots of Selected Uncertain Parameters Against Groundwater Pathway Dose at 3,400 Years after Closure.

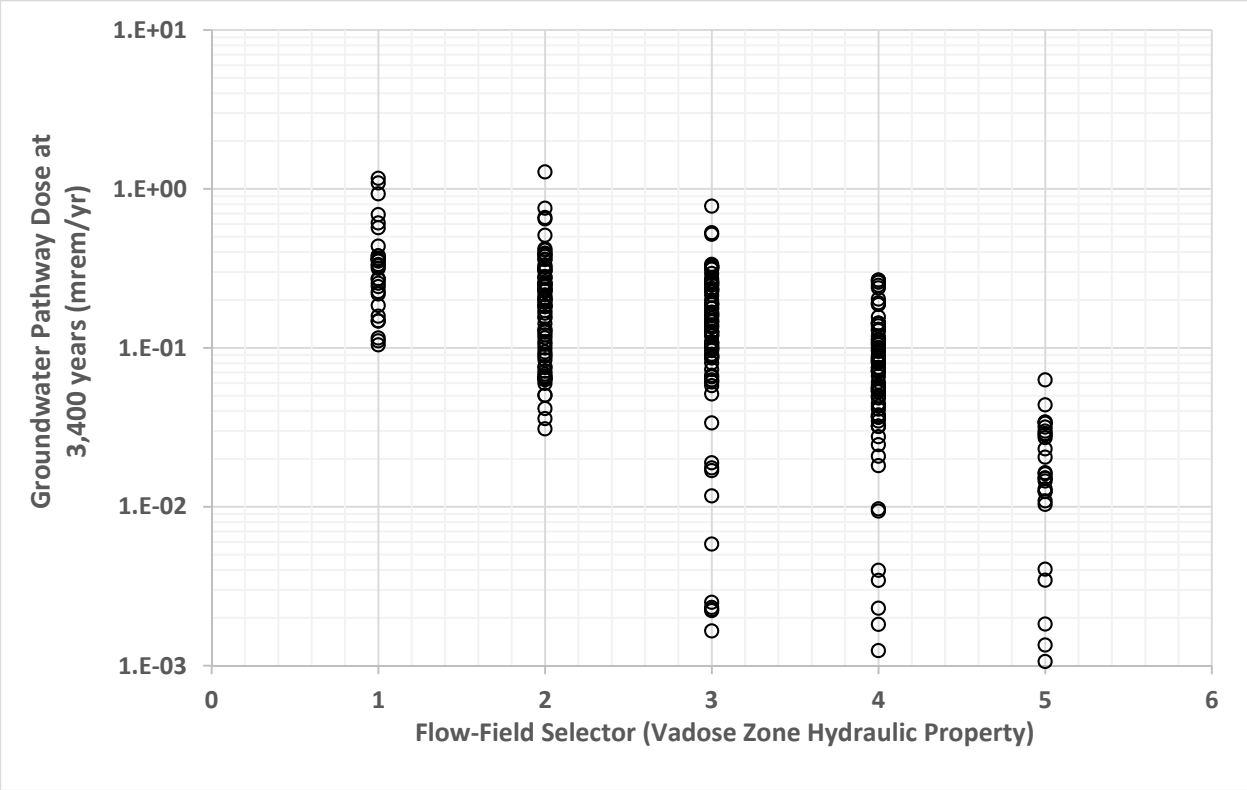

(a)

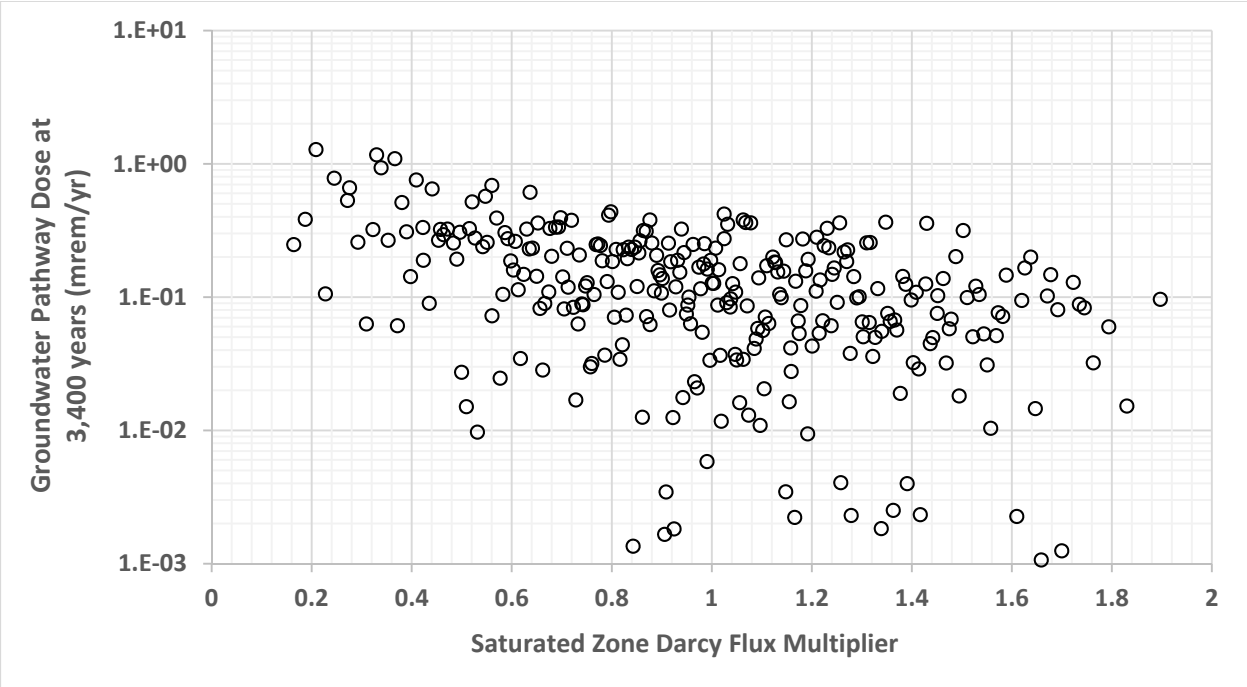

(b)

Figure 8-26. Peak Dose Values from Groundwater Pathway for 300 Realizations.

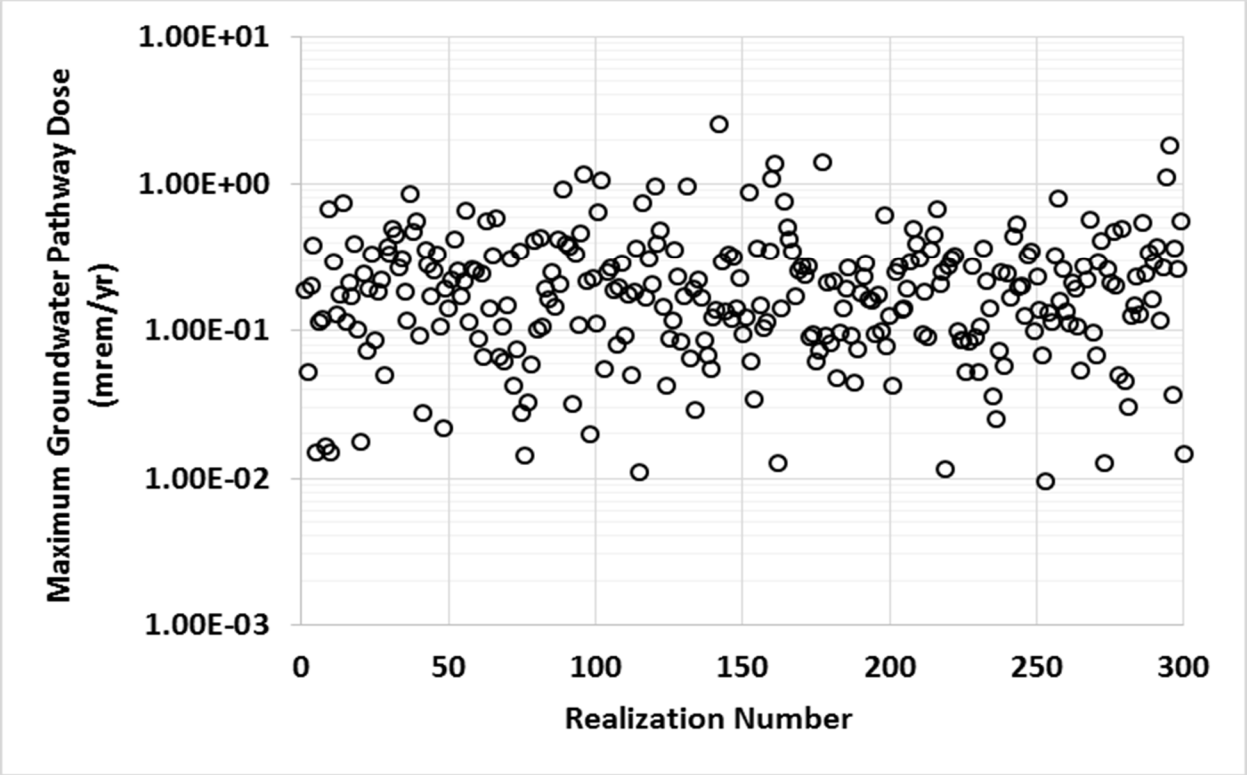

In the intermediate time period (around 100 years after closure), ^{129}I gradually becomes the dominant dose driver as ^{3}H dose continues to decline and ^{14}Co dose remains negligibly small. During this time, the total dose is seen to gradually increase with time. The most important uncertain parameter is associated with the K_d of ^{129}I for the grout tank infill material. A strong negative correlation is seen. This is expected as increased sorption of ^{129}I on the in-tank grout material will reduce the diffusive mass flux along the air pathway. Other important uncertain parameters in this time are related to tortuosity in the air pathway (used to calculate the effective diffusion coefficient) and residual inventory. See the scatter plots presented in Figure 8-30.

In the long time period (around 1,000 years after closure), the ^{129}I dose reaches a steady value, indicating that the concentration gradient in the air phase from the tank to the surface has reached a steady state. The most important uncertain parameter is associated with the K_d of ^{129}I for the grout tank infill material; a strong negative correlation is seen. The second most important uncertain parameter is associated with the residual inventory (see Figure 8-31).

8.1.6 Statistical Stability

A stability analysis was conducted to determine whether a sufficient number of realizations were used to ensure that the results of the calculations are statistically stable. The 1-D abstraction model is statistically stable if the mean annual dose computed by the model is stable. Demonstrating stability of the mean annual dose requires evaluation of the sufficiency of sample size of uncertain parameters so that possible parameter combinations are adequately represented

in the system analyzed. Performing uncertainty analysis with an inadequate number of realizations can result in erroneous interpretation of important uncertain parameters. Statistical stability is generally determined by demonstrating that the estimate of the mean annual dose does not depend on the sample size.

For stability analysis, the mean annual dose and uncertainty in underlying distribution is evaluated by performing calculations with different number of realizations (i.e., by varying the sample size). Since atmospheric pathway dose remains negligibly small over all time compared to the groundwater dose, the stability analysis was performed with respect to the dose from groundwater pathway. Three cases are performed with an increasing number of realizations: (a) 100 realizations, (b) 300 realizations, and (c) 500 realizations. The dose statistics (mean, median, and 95th percentile) derived from these cases are compared in Figure 8-32. The results indicate that mean and median values among various cases are very similar. About 10% variance in the peak mean values between the three cases is seen, while the variance in the median values is even smaller. The variance in the 95th percentile values among different cases is slightly greater near the peak time, but still the peak mean dose is within a factor of two for all cases. The larger variation noticed in the 95th percentile for the 100 realization case indicates that only a few realizations have breakthrough at the 100 m (328 ft) downgradient location around 3,000 years after closure, and as such the dose results are not stable due to small sample size. However, the 95th percentile curves for the 300 realization and 500 realization case are very similar, indicating adequate sample size has been reached. Based on these results, it can be concluded that 300 realizations are adequate for the purpose of performing uncertainty analysis.

Figure 8-33 provides the upper and lower confidence limits on the grand mean (mean of the means) based on the three different cases at a 95% confidence level (significance level, $\alpha = 0.05$). The grand mean is shown in a thick black line and virtually overlaps the mean value from the 300 realization case. The range between the confidence bounds encompasses the mean from all three cases, indicating sufficiency of using 300 realizations for uncertainty analysis.

8.2 SENSITIVITY ANALYSIS FOR THE GROUNDWATER PATHWAY

Sensitivity analyses evaluate changes in calculated groundwater impacts that result from changes in input parameter estimates. Parameter value ranges used in these analyses were selected by one of several methods. As discussed in Section 1, as part of the scoping process leading up to the implementation of the PA, stakeholders expressed specific interest in seeing the results of specific sets of input parameters. In addition to these agreed sets of sensitivity analyses, additional sensitivity cases were identified during the implementation of the PA to evaluate the importance of specific safety functions on the behavior of the disposal system. The result is a set of sensitivity analyses intended to represent the effects of changing a broad set of input assumptions. It is also emphasized that these sensitivity analyses have been augmented by probabilistic uncertainty analyses (Section 8.1), which specifically evaluate parameter uncertainties. By contrast, the sensitivity analyses are generally intended to evaluate changes in parameters and modeling assumptions, to demonstrate the effect that alternatives have on the groundwater concentrations at the PoCal.

Figure 8-27. Scatter Plots of Selected Uncertain Parameters Against Peak Dose for Groundwater Pathway for 300 Realizations. (sheet 1 of 2)

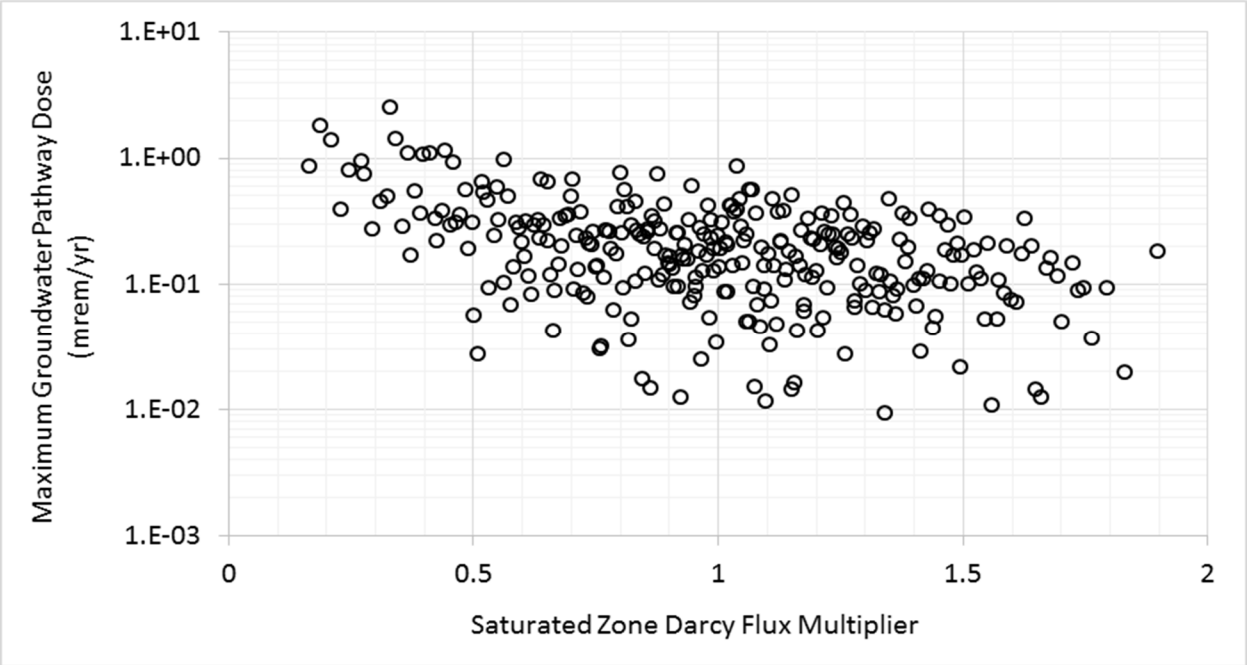

(a)

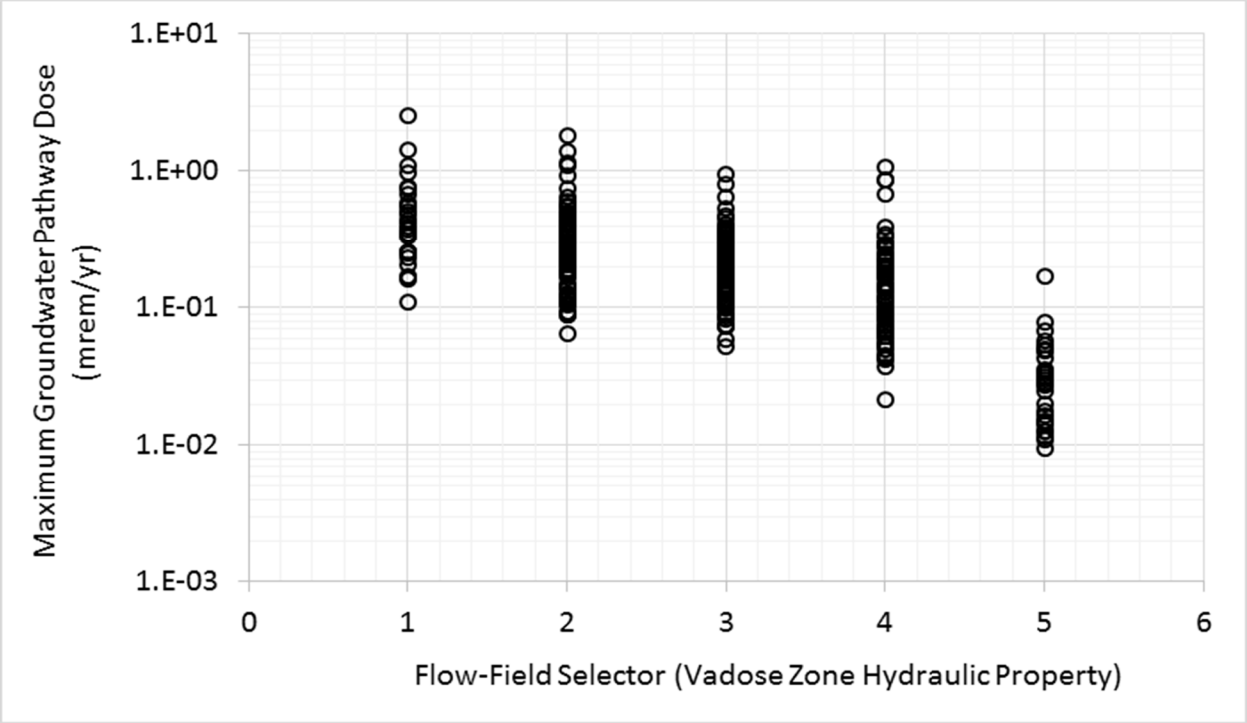

(b)

Figure 8-27. Scatter Plots of Selected Uncertain Parameters Against Peak Dose for Groundwater Pathway for 300 Realizations. (sheet 2 of 2)

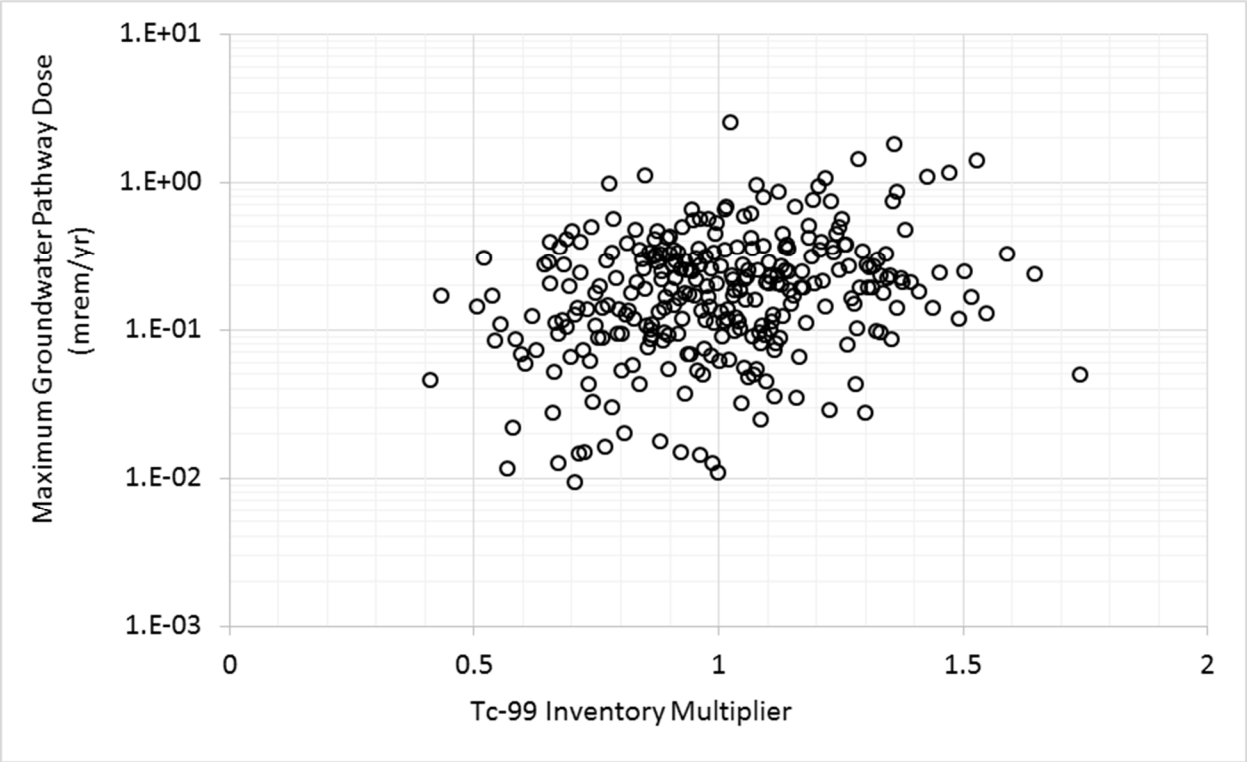

(c)

Primary sources of alternative modeling assumptions are natural system heterogeneities, long-term engineered surface barrier performance, and human actions. Such assumptions can be categorized as scenario or model uncertainties, and as such are not readily amenable to the use of probabilistic methods (NCRP Report 152; "Decision Analysis for Low-Level Radioactive Waste Disposal Facilities" [Kozak 1994]). Consequently, these analyses are run as deterministic sensitivity analyses, without assigning a likelihood of occurrence to a particular result other than (in some cases) a qualitative evaluation of its likelihood.

The sensitivity analyses quantify the ranges of calculated groundwater concentration outcomes due to single-parameter or multiple-parameter changes that represent an underlying shift in the conceptual model. With respect to the defense-in-depth concept, the analyses quantify the impacts that alternative views of the engineered barriers and natural attenuation may have on groundwater concentrations in the evaluation of total system performance. These analyses are an effective tool for supporting closure action decisions for WMA C, because they demonstrate the complementary and redundant nature of the safety functions evaluated in the PA.

The set of sensitivity analyses are presented in Table 8-15. Each sensitivity analysis is assigned a shorthand designator so it can be easily referenced. A brief explanation of each sensitivity analysis is also provided in the table, to provide insight into the alternative assumptions it is intended to evaluate. Depending on the nature of the sensitivity analysis, it was either run in STOMP© or using the GoldSim© abstraction of the STOMP© model; the selection of how to run

the analysis was made solely for pragmatic considerations. It is much faster to run the GoldSim© model, so when possible, that is the preferred approach. However, when the sensitivity case involved changes in the underlying flow field, by necessity, the analysis could only be done using STOMP©. Table 8-15 also identifies which numerical model was used in the sensitivity analyses.

Figure 8-28. Uncertainty in Atmospheric Pathway Dose Based on 300 Realizations.

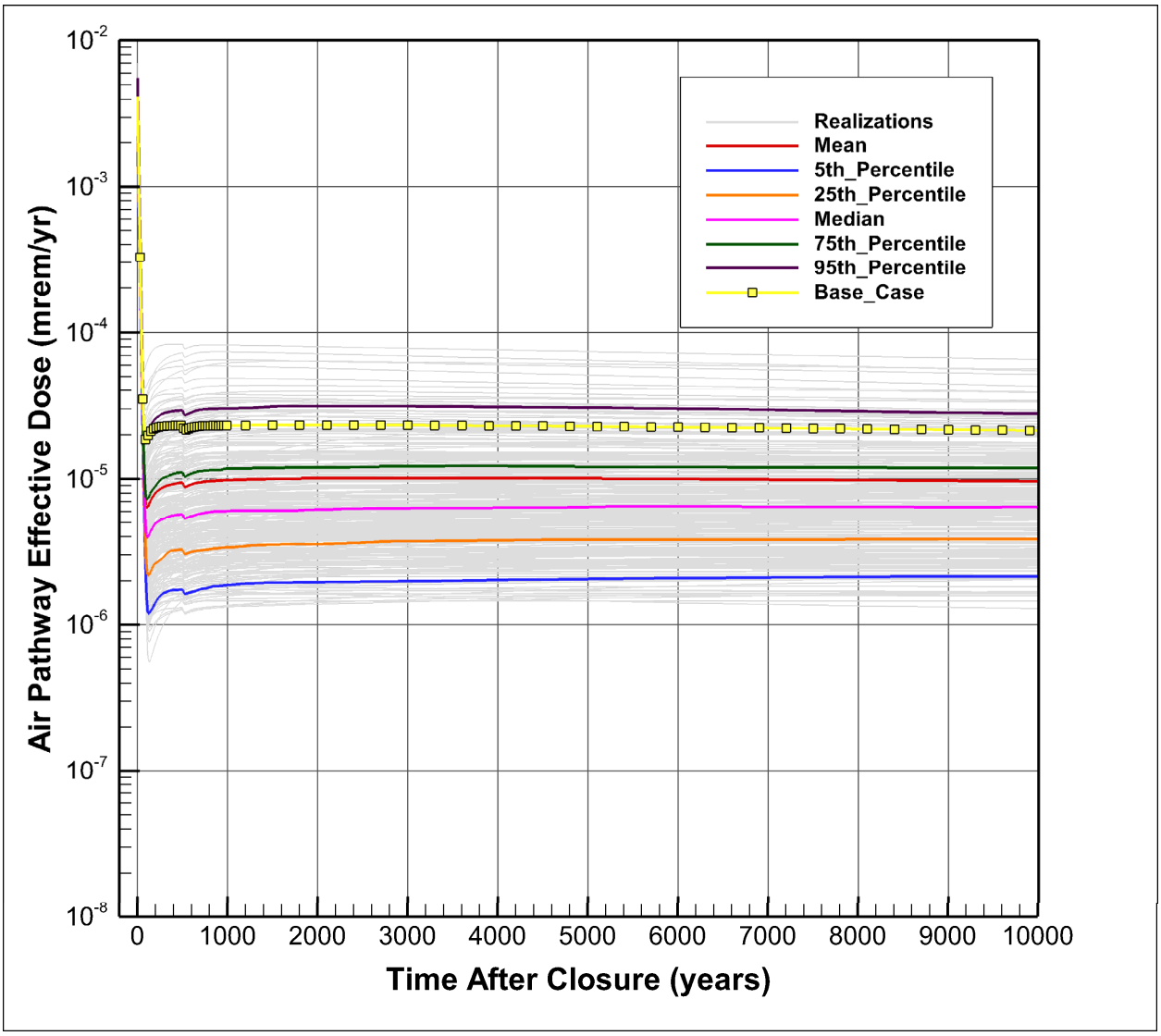

In Table 8-15, the sensitivity analyses are subdivided into several categories corresponding to the categories of safety functions they are intended to evaluate. The sensitivity cases conducted using the 3-D STOMP© model can be grouped in three categories: (1) changes in aquifer properties, (2) changes in recharge, and (3) changes in vadose zone geology and hydrologic parameters. The sensitivity analysis for the aquifer parameters examines the impacts associated with radionuclide transport and mixing in the aquifer between WMA C and the PoCal 100 m (328 ft) downgradient of the facility. The recharge category of sensitivity simulations addresses

elements associated with the surface barrier function and the impacts of changes in recharge rate estimates during both pre- and post-design life performance periods of the surface barrier. The hydrologic cases examine the impacts of changes in the hydrologic parameters and address those elements of the natural attenuation within the vadose zone. This category includes the evaluation of Alternative Geologic Model II and the hypothesized presence of a clastic dike within the WMA C fenceline. Because the screening analysis and base case results indicate that only the most mobile radionuclides break through to a peak concentration in groundwater within the 10,000-year sensitivity-uncertainty evaluation time frame, comparative results are presented for radionuclides with K_d values equal to zero, in particular, ^{99}Tc. Technetium-99 was chosen for the sensitivity analyses because it accounts for the majority of the dose (Section 8.1.6 and Figure 8-22).

8.2.1 Surface Barrier Flow Sensitivity Analyses

In this evaluation, recharge-related parameters were varied to examine the impact of temporal and spatial variations in recharge at the 100 m (328 ft) PoCal. The recharge sensitivity evaluations address the safety function related to surface barrier flow. Because of the spatial component of this analysis, it was conducted using STOMP©. For this analysis, the vadose zone and aquifer hydraulic properties remain unchanged from their base case values.

Five recharge sensitivity cases were evaluated. Cases inf01 and inf02 address the minimum and maximum estimated values of net infiltration (recharge) after the design life of the surface barrier. Case inf03 represents significantly different conditions on the cover, with very high infiltration rate characteristic of infiltration rates for bare soil that existed during the operational period, and was specifically requested by Ecology during the scoping sessions. This case involves the assumption of present-day estimates of tank farm recharge resuming at WMA C after a 100-year period of institutional controls. Cases unc01 and unc02 address variability in recharge estimates outside WMA C. Case unc02 also applies to the evaluation of the impact of including additional water at the edge of the cover to represent runoff from the top surface and additional recharge occurring through the side-slopes and at the base of the barrier.

The peak groundwater concentration of ^{99}Tc ranges between 22 and 36 pCi/L for these cases (Table 8-16). This includes recharge rates applied to areas outside of WMA C ranging from 0.5 mm/yr to 100 mm/yr (0.02 in./yr to 3.94 in./yr) to evaluate the impact the outside recharge rates have on the results. The latter of these two cases also addresses the concern that increased recharge may occur through the side-slopes and around the base of the surface barrier.

Figures 8-34 and 8-35 show the overall results for ^{99}Tc at the nine PoCals for the minimum and maximum estimated values of post-design life barrier net infiltration, respectively, with a breakdown by source at the maximum PoCal. Figure 8-36 shows a comparison of the specific ^{99}Tc results for tank C-105 and the pipelines at the maximum PoCal. For the case with the post-design life recharge rate set to the minimum value, the maximum concentration of ^{99}Tc decreases from the base case value of 30 pCi/L to 22 pCi/L, a decrease of 27%. For the case with the maximum post-design life recharge rate, the peak groundwater concentration of ^{99}Tc increases from the base case value of 30 pCi/L to 36 pCi/L, an increase of 20% (Table 8-16).

Table 8-14. Uncertain Parameters Important to Atmospheric Pathway Dose at Various Times.

Stochastic Parameter ID	Description	Correlation Coefficient Based on Ranks	Standardized Regression Coefficient Based on Ranks	Partial Correlation Coefficient Based on Ranks	Importance Measures Based on Ranks
At Early Time (2 years after Closure)					
H3_Inv_Mult	Uncertainty in H-3 inventory; multiplies the base case value	0.92	0.94	0.98	0.82
Wind_Speed_Stoch	Uncertainty in wind speed	-0.25	-0.3	-0.82	0.07
At Intermediate Time (100 years after Closure)					
Grout_Kd_Uncert[I]	Uncertainty in K_d of Iodine for Grout	-0.78	-0.70	-0.85	0.59
Soil_Air_Tort_Stoch	Uncertainty in tortuosity term for diffusive transport along the air pathway in the backfill soil	0.38	0.22	0.46	0.16
Grout_Air_Tort_Stoch	Uncertainty in tortuosity term for diffusive transport along the air pathway in the Grout material within the tank	0.28	0.31	0.58	0.13
I129_Inv_Mult	Uncertainty in I-129 inventory; multiplies the base case value	0.34	0.28	0.54	0.11
At Late Time (1,000 years after Closure)					
Grout_Kd_Uncert[I]	Uncertainty in K_d of Iodine for Grout	-0.88	-0.83	-0.94	0.74
I129_Inv_Mult	Uncertainty in I-129 inventory; multiplies the base case value	0.42	0.33	0.73	0.16
Soil_Air_Tort_Stoch	Uncertainty in tortuosity term for diffusive transport along the air pathway in the backfill soil	0.26	0.08	0.25	0.08

Recharge in the areas outside WMA C has an inverse relationship with the results: peak ^{99}Tc concentration in groundwater decreases as recharge in the areas outside WMA C increases. The magnitude of the increase or decrease is within the range of values determined from the WMA C

surface barrier evaluation (Table 8-16). Therefore, for this range of recharge rates, the recharge outside of WMA C is encompassed in the uncertainty analysis. For very high infiltration, characteristic of alternative assumptions about future surface conditions leading to extreme infiltration, the peak groundwater concentration of ^{99}Tc increases by approximately 50% from the base case results and arrives at the PoCal approximately 50 years after the barrier ceases to exist (Table 8-16).

Figure 8-29. Scatter Plot of Selected Uncertain Parameters Against the Atmospheric Pathway Dose at Early Time Period (2 Years after Closure).

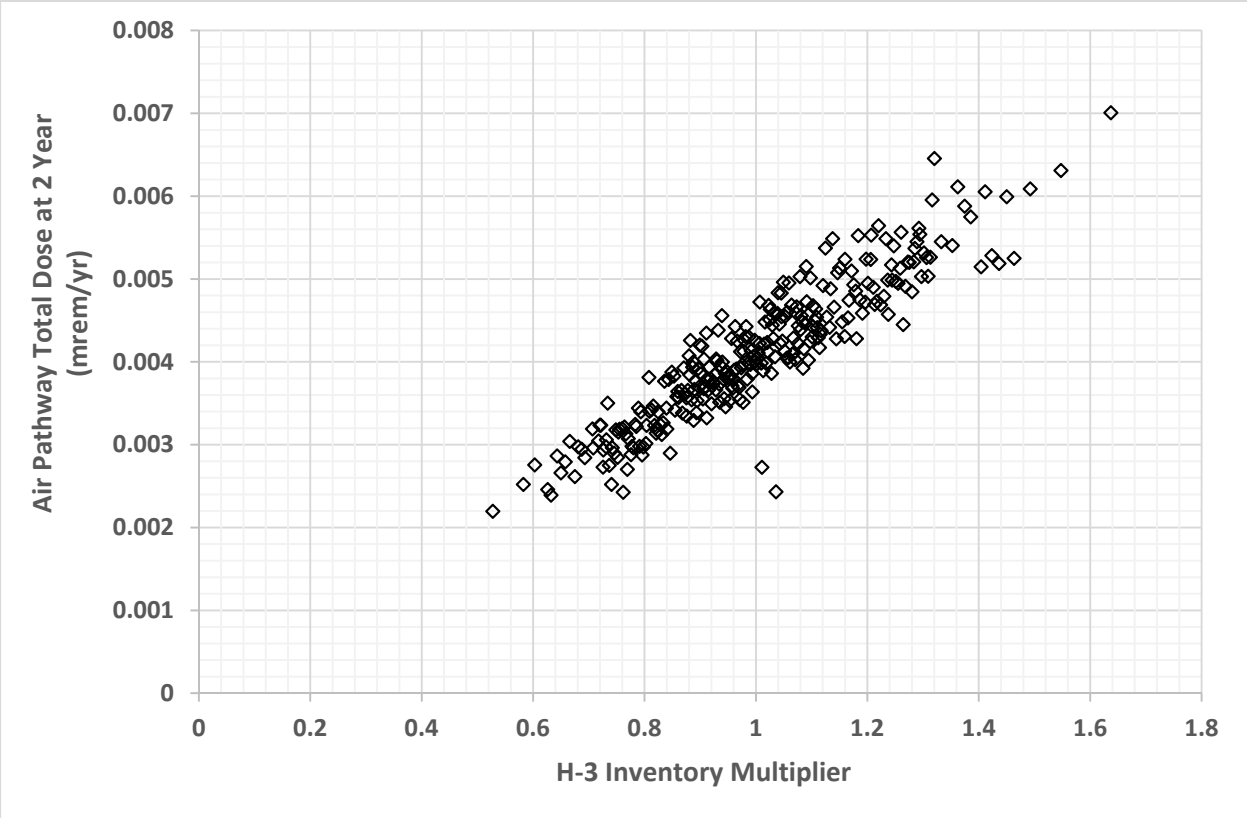

8.2.2 Aquifer Dilution Sensitivity Analyses

The aquifer property sensitivity evaluations address the safety function component related to dilution caused by the groundwater flux in the aquifer. The parameters that determine the groundwater flux and the amount of dilution that occurs in the aquifer are the hydraulic conductivity and hydraulic gradient. In a natural system, the two parameters offset one another. If the groundwater flux through an aquifer volume remains constant, then in areas with high hydraulic conductivity, the hydraulic gradient will be less, and vice versa. They are considered to be coupled parameters because changes to the flux term caused by changes made to one term are inseparable from changes made to the other term. These parameters act inversely proportional to one another, and the same change in the flux can be made by making the same proportional change to either parameter. Therefore, only one of the parameters, e.g., hydraulic

conductivity, needs to be varied to produce the variability in the flux necessary to conduct the sensitivity analysis. For this sensitivity evaluation, the hydraulic conductivity is varied.

The sensitivity analysis includes two values of hydraulic conductivity, the 5th percentile value (4,200 m/day [13,800 ft/day] [gwp01]) and the 95th percentile value (17,800 m/day [58,400 ft/day] [gwp03]). The results provide some insight into the dilution mechanism of the aquifer (Table 8-17). Figures 8-37 and 8-38 show the overall results for WMA C at the nine PoCals for the 5th and 95th percentile values, respectively, with a breakdown by source at the maximum PoCal. Figure 8-39 shows a comparison of the specific results for tank C-105 and the pipelines at the maximum PoCal. Tank C-105 has the largest estimated residual inventory of ^{99}Tc, and the release from the pipelines is approximated as being advection-controlled instead of diffusion-controlled release used in the tanks. The results of the evaluation using the 5th percentile value are a factor of 2.6 greater than the base case; the hydraulic conductivity is a factor of 2.6 less than the base case value. Similarly, the results of the evaluation using the 95th percentile value are a factor of 1.6 less than the base case; the hydraulic conductivity is a factor of 1.6 greater than the base case value. The amount of dilution appears inversely proportional to the flux through an aquifer as determined from the hydraulic conductivity. The proportionality is observed in the tank C-105 and pipeline residuals evaluations. The results of the 5th percentile hydraulic conductivity evaluation indicate an approximate factor of 2.6 increase in the peak concentration compared to the base case, and the results of the 95th percentile hydraulic conductivity evaluation indicate an approximate factor of 1.6 decrease in the peak concentration compared to the base case. These results indicate that the aquifer flow parameters that affect the flux rate of water have an inversely proportional impact on the groundwater concentration. The timing of the peak arrival at the PoCals is essentially the same for all cases because the groundwater velocity for all three cases exceeds 100 m (328 ft) (the distance to the line of PoCals) per year.

8.2.3 Vadose Zone Flow and Dispersion Sensitivity Analyses

The vadose zone hydraulic properties were varied to determine the impact that the inherent variability in these parameters has on the groundwater results. This set of vadose zone hydraulic properties sensitivity evaluations addresses the safety functions associated with flow and dispersion in the vadose zone. Four vadose zone parameters were varied: van Genuchten α and n (coupled), saturated moisture content (θ_s), residual moisture content (θ_r), and fitted saturated hydraulic conductivity (K_s). The parameters were varied in accordance with the percentile relationships determined in the uncertainty analysis. Therefore, for the evaluations using the 5th percentile values, all of the geologic soil units were assigned their 5th percentile values. It is important to note that the percentiles refer to sets of parameter values and not to the properties individually (as discussed in Appendix B). Thus, the maximum van Genuchten residual saturation parameter does not necessarily represent the largest value of θ_r, but instead represents the value associated with the fitted unsaturated hydraulic conductivity curve that produces the highest flow velocity at the pre-Hanford operations recharge rate. The values of four vadose zone parameters, van Genuchten α and n (coupled), θ_s, θ_r, and fitted saturated hydraulic conductivity (K_s) varied for the three percentile cases (5th [vzp01], median [vzp02], and 95th [vzp03]) are presented in Section 8.1.4 (see Table 8-7). These evaluations used the base case recharge values and time sequence.

Figure 8-30. Scatter Plots of Selected Uncertain Parameters Against the Atmospheric Pathway Dose at Intermediate Time Period (100 Years after Closure).

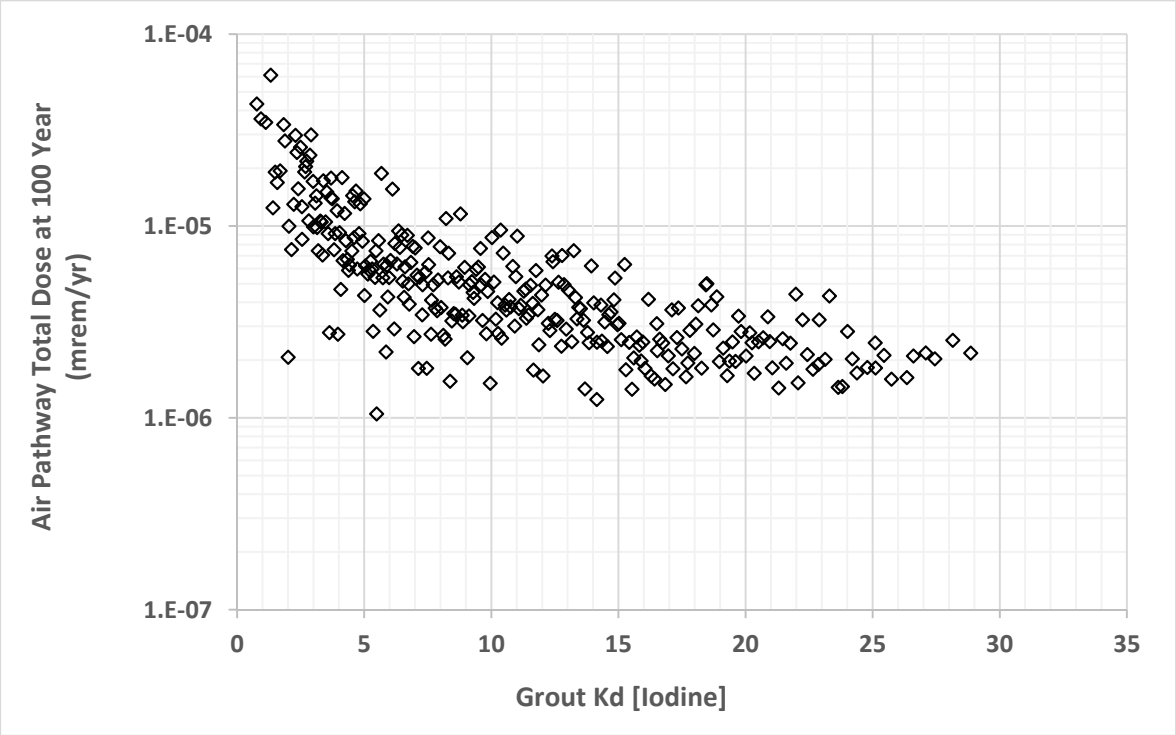

(a)

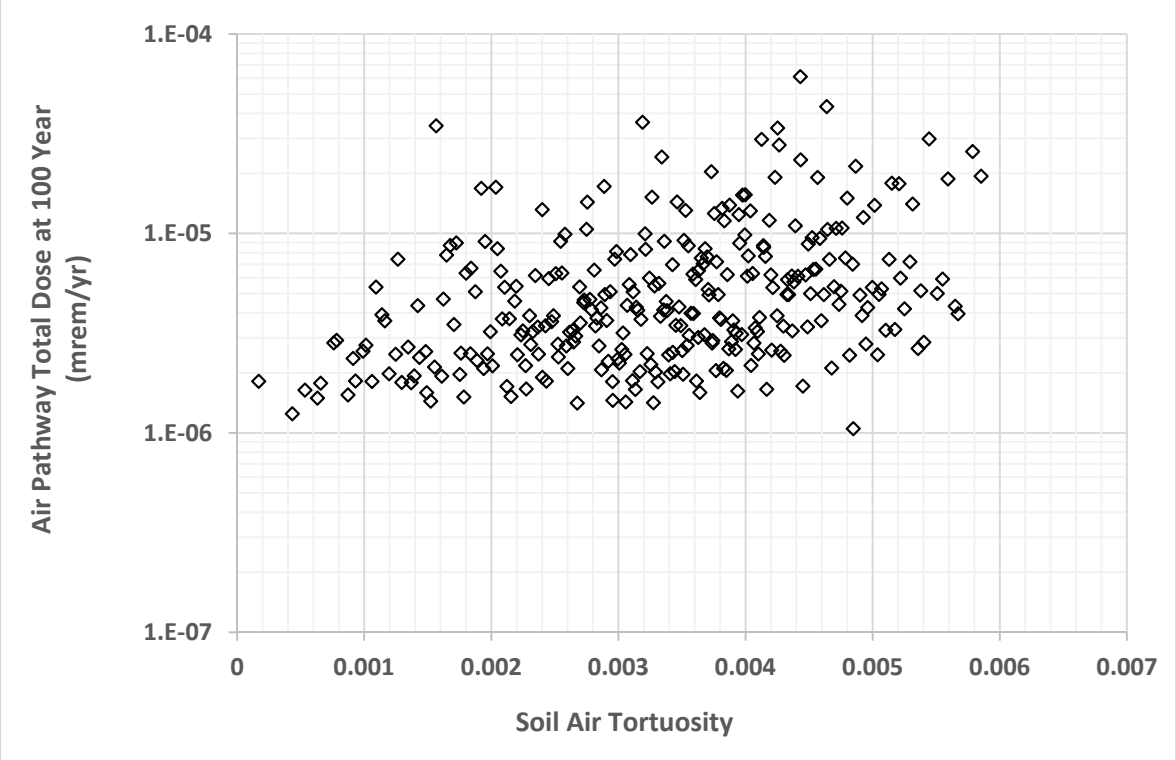

(b)

Figure 8-31. Scatter Plots of Selected Uncertain Parameters Against the Atmospheric Pathway Dose at Late Time Period (1,000 Years after Closure).

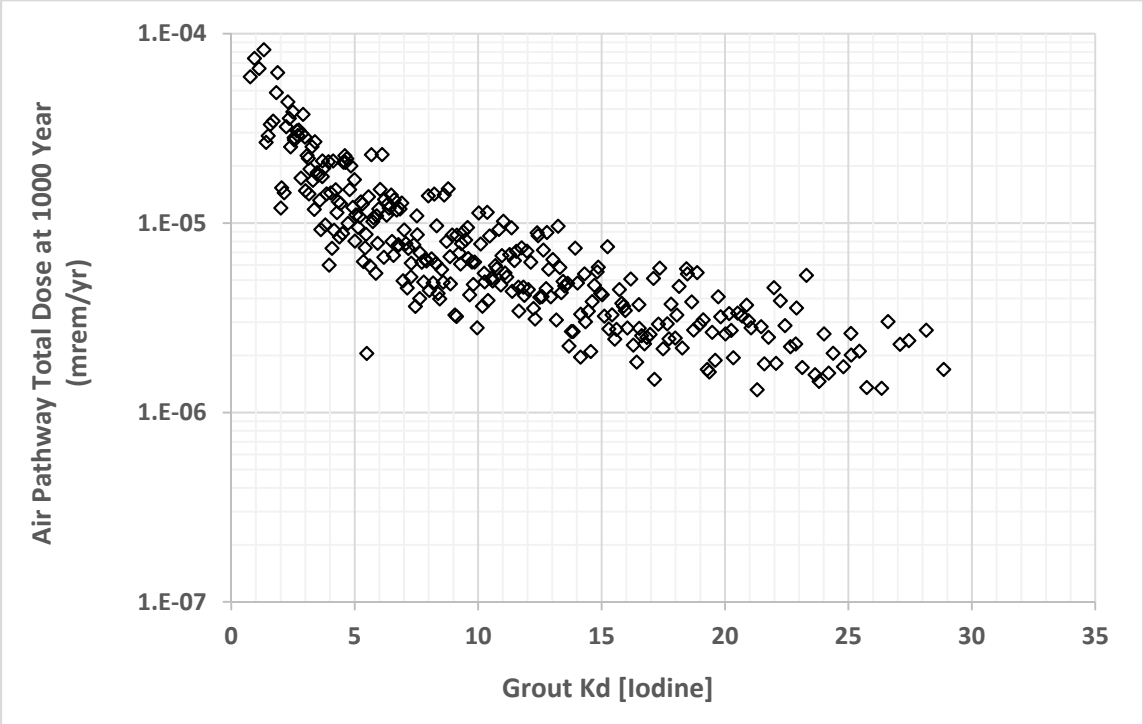

(a)

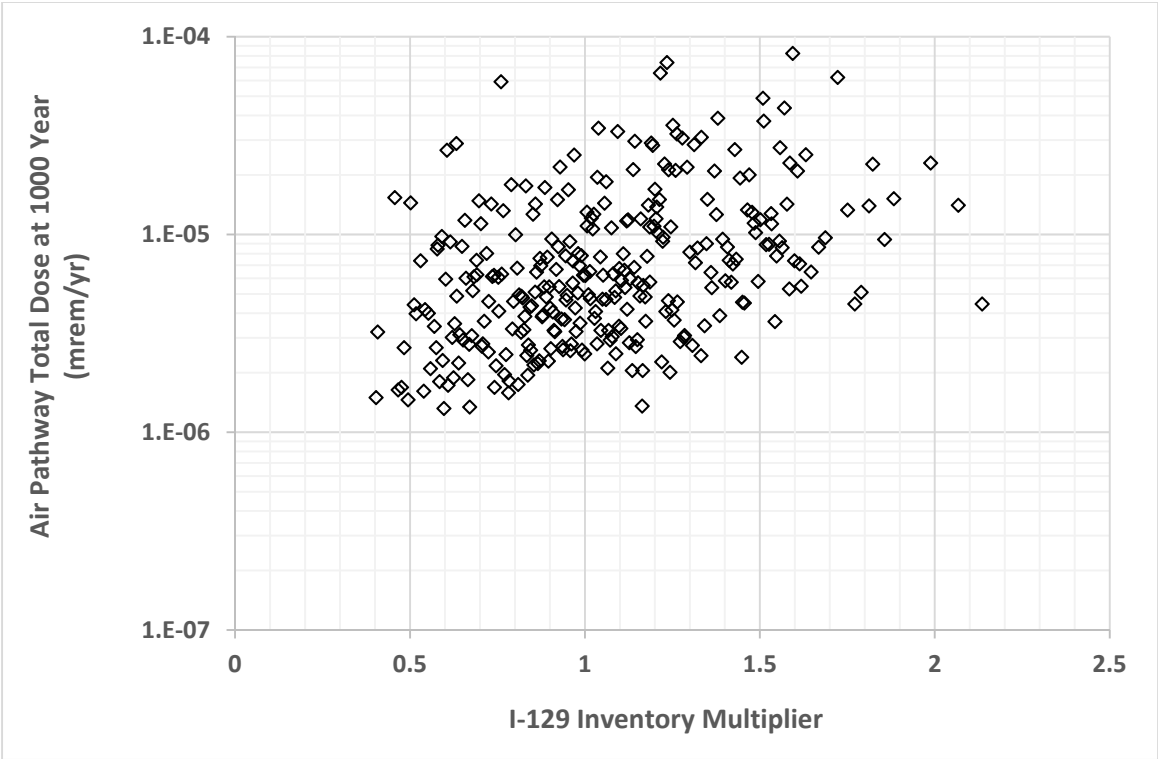

(b)

Figure 8-32. Statistical Stability Analysis with Different Number of Realizations, Comparing (a) Mean, (b) Median, and (c) 95th Percentile Values of the Groundwater Pathway Dose. (sheet 1 of 3)

(a)

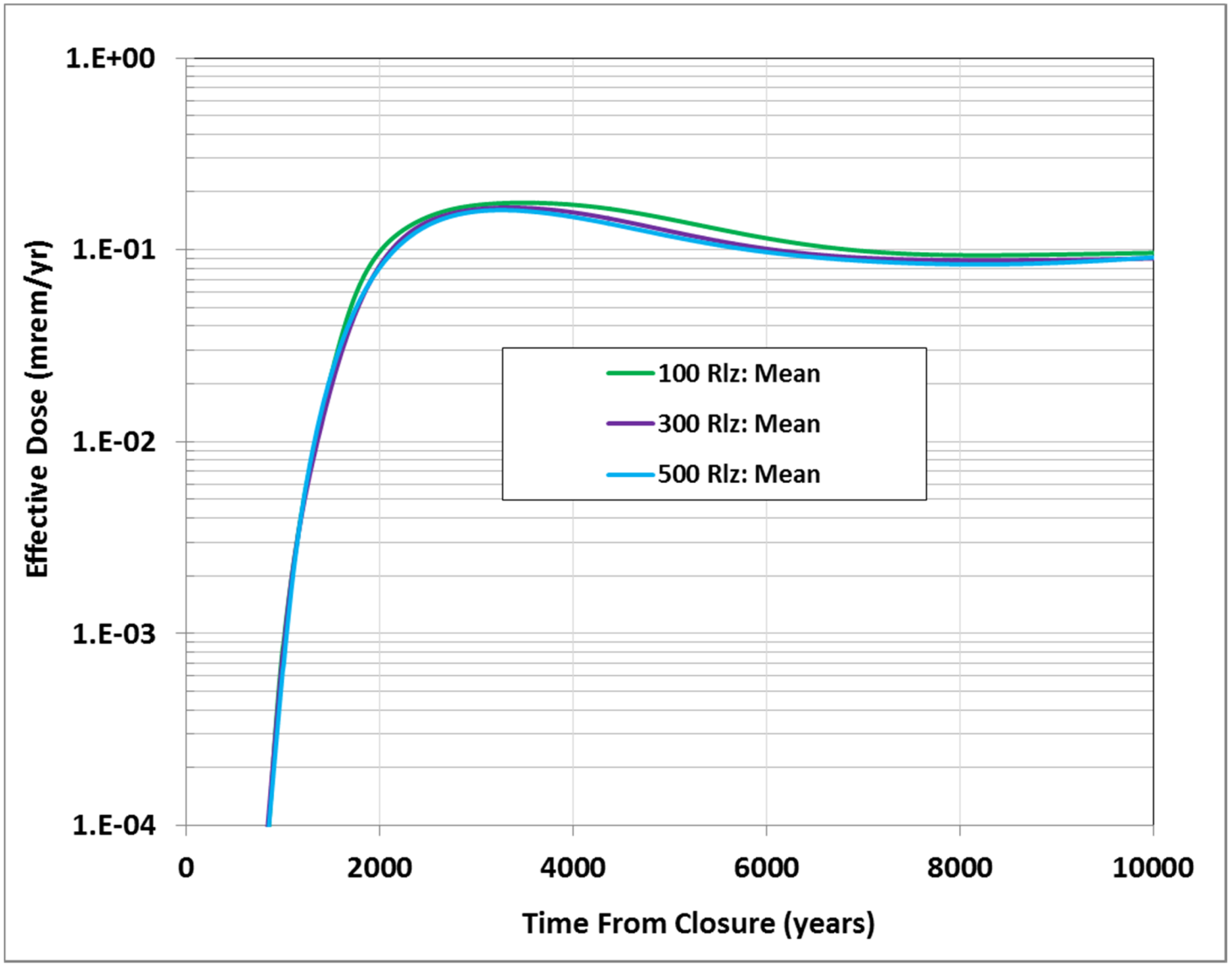

Figure 8-32. Statistical Stability Analysis with Different Number of Realizations, Comparing (a) Mean, (b) Median, and (c) 95th Percentile Values of the Groundwater Pathway Dose. (sheet 2 of 3)

(b)

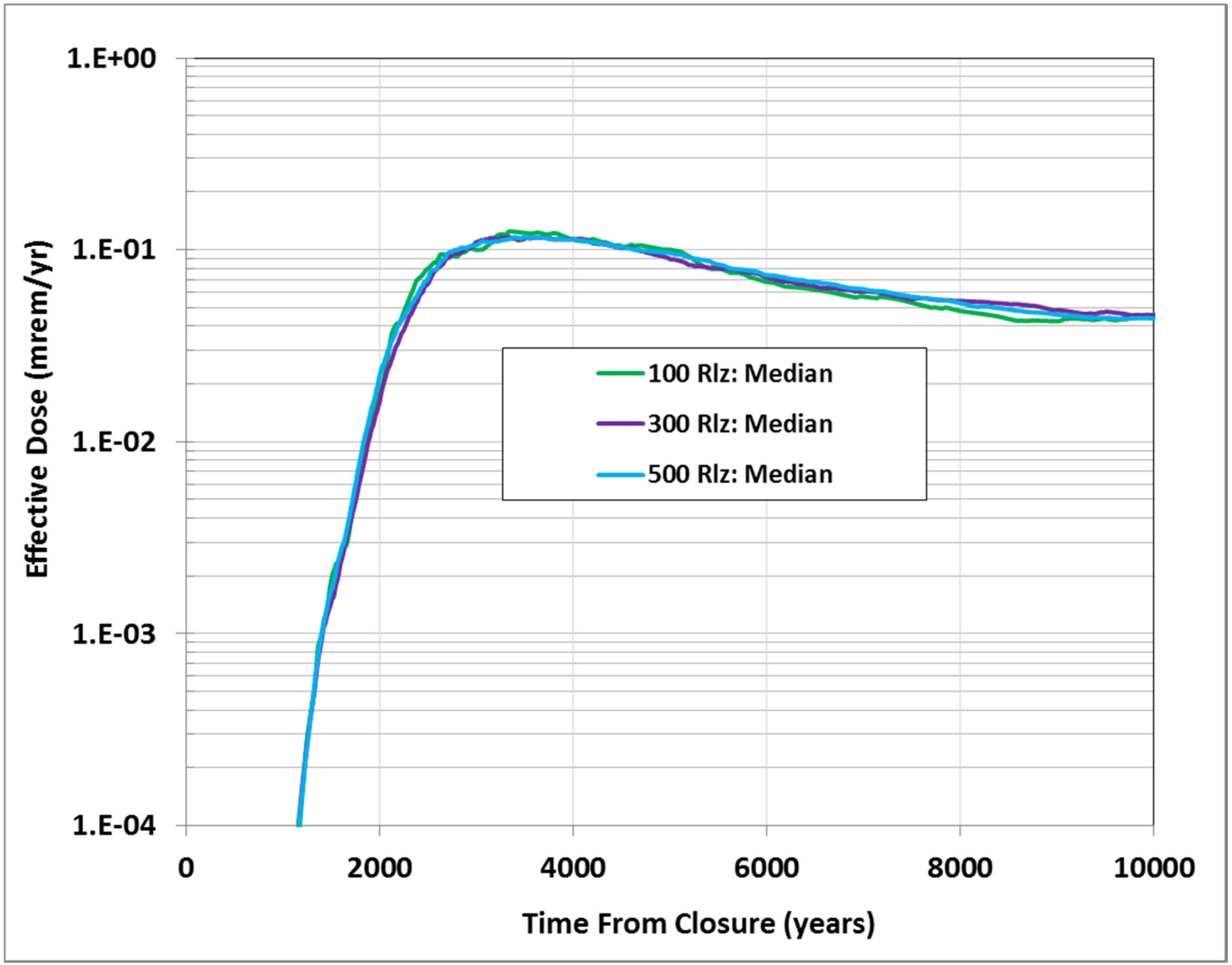

Figure 8-32. Statistical Stability Analysis with Different Number of Realizations, Comparing (a) Mean, (b) Median, and (c) 95th Percentile Values of the Groundwater Pathway Dose. (sheet 3 of 3)

(c)

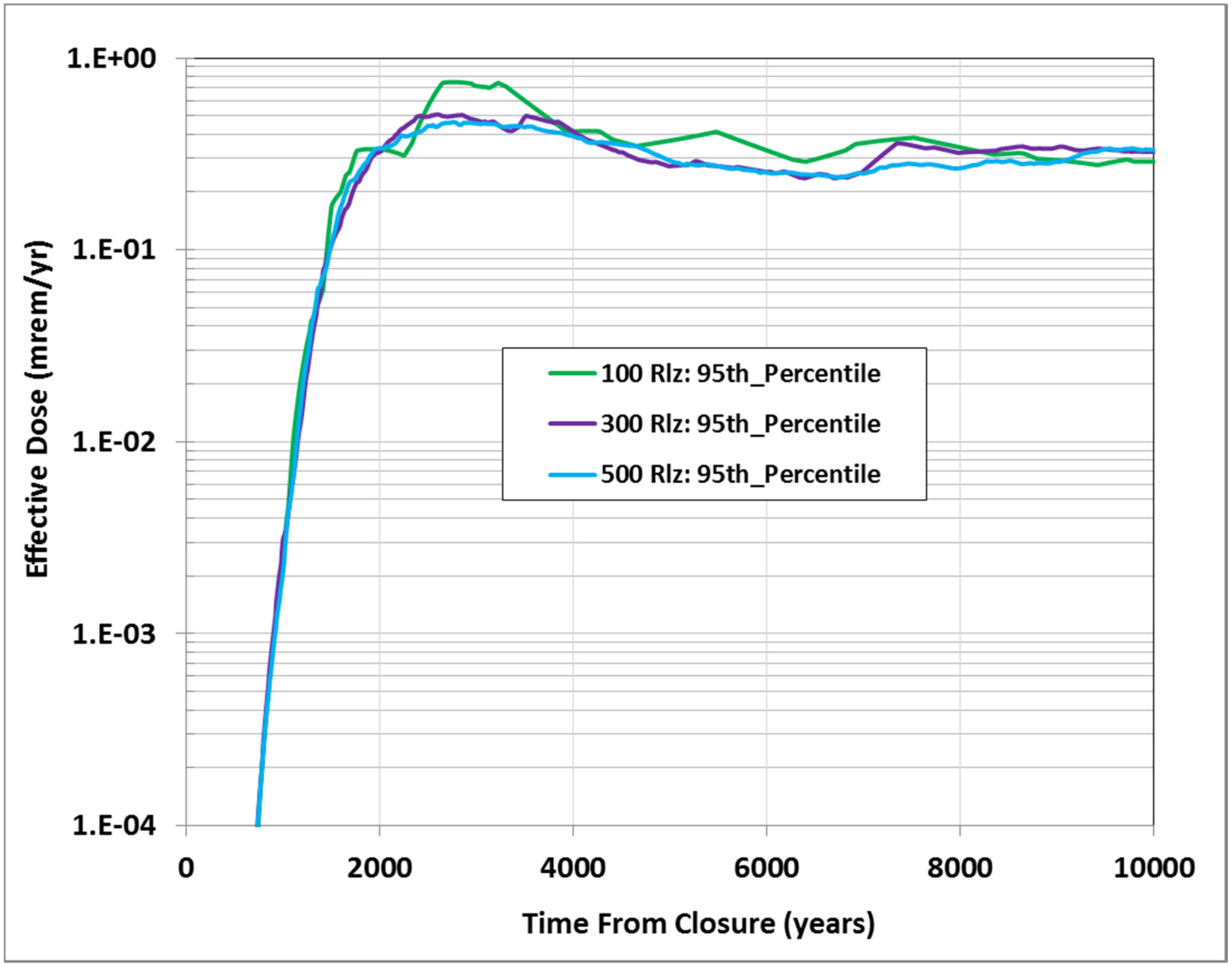

Figure 8-33. Confidence Limits on the Mean Effective Groundwater Pathway Dose.

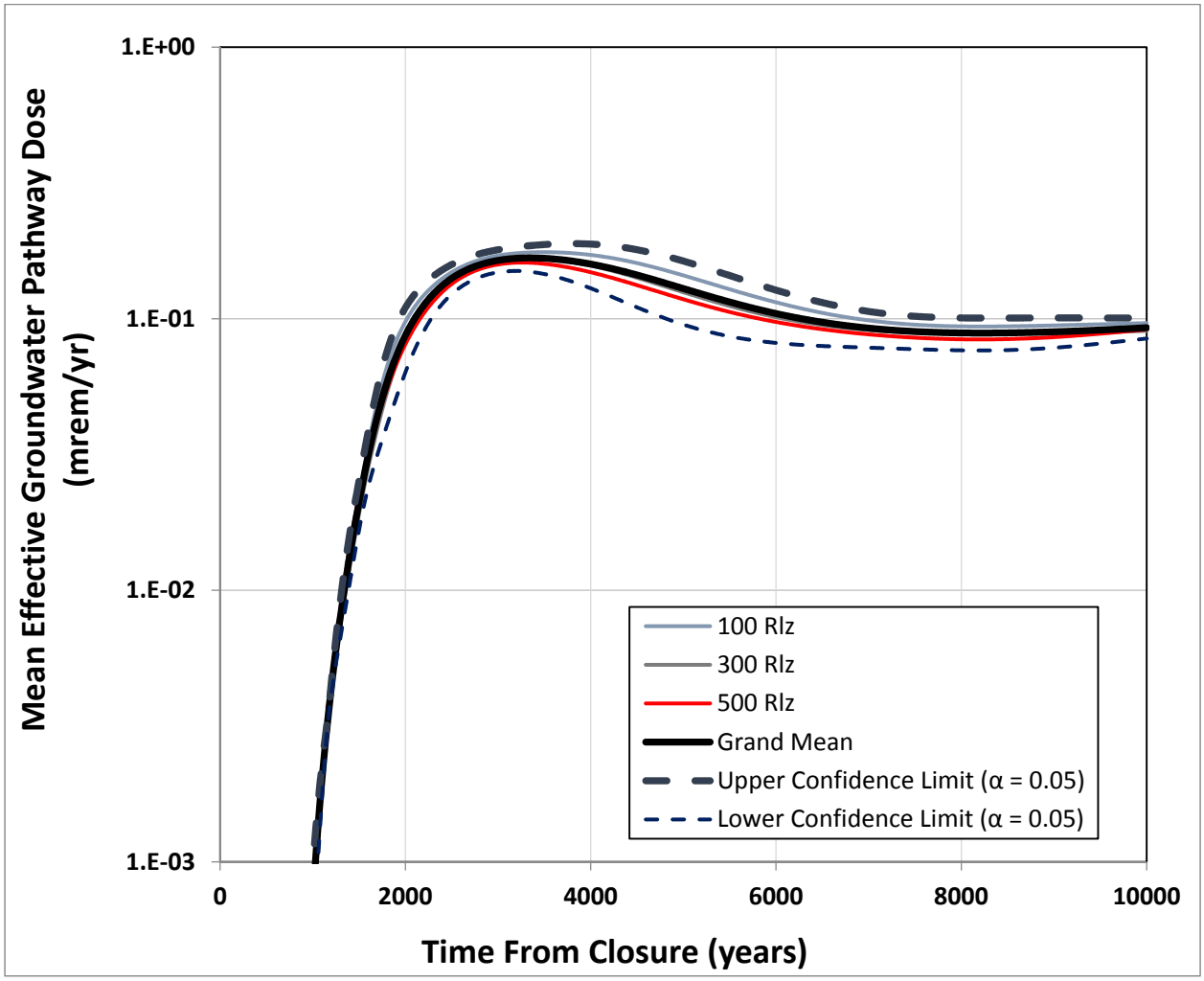

The vadose zone evaluation also included two alternate conceptual models of the geology. One alternative, referred to as Alternative II (vzp04), considers the Hanford H2 Sand unit to consist of three subunits that each possess different hydraulic characteristics (Figure D-7b). Most of the formation remains identified as H2 Sand and the hydraulic properties for it remain unchanged from the base case analysis. Near the base of the Hanford H2 Sand unit in Alternative II are fine and coarse sand subunits. For this sensitivity evaluation, these subunits are assigned the Hanford H2 Sand 5th and 95th percentile hydraulic property sets, respectively. The second alternative conceptual model of the geology includes the representation of a preferential pathway, such as a clastic dike or unsealed borehole, located underneath tank C-105 (vzp05). Clastic dikes are discrete polygonal (plan view) features, and typically range in width from 3 cm to 1 m (1.2 in. to 3.3 ft), from 1.5 m to 100 m (4.9 ft to 328 ft) in segment length, and from 2 m (6.6 ft) to greater than 20 m (65.6 ft) in depth (BHI-01103). An especially long clastic dike segment does not appear to exist within WMA C because, if one did, then the many neutron and drywell moisture measurements would likely have detected evidence of a continuous band of high moisture. For the sensitivity case, the length of the dike is assumed to extend for 7.6 m (25 ft), and 3-D model discretization imposes a minimum width of 3.8 m (12 ft) for the dike.

Although a width of 3.8 m (12 ft) is more representative of a planar feature than a dike, finer resolution of the model grid is not practicable with the available computational resources. The planar area of the dike is 29 m^2 (312 ft^2), which is comparable to a 1-m (3.3-ft)-wide dike that extends the entire diameter of the tank (23 m^2 [246 ft^2]). Clastic dikes of this size typically occur in sand, silt, and only occasionally in gravel (BHI-01103); therefore, the model representation of the dike extends throughout the depth of the Hanford H2 Sand (Figure D-7a shows the location of tank C-105; the clastic dike is centered beneath the tank in the Hanford H2 Sand shown in the figure). The hydraulic parameters assigned to the clastic dike material were selected to determine whether the flux conditions exist at WMA C such that the clastic dikes provide a preferential flow path for the residual waste. Thus, the set of clastic dike hydraulic parameters from among the samples listed in PNNL-23711, "Physical, Hydraulic, and Transport Properties of Sediments and Engineered Materials Associated with Hanford Immobilized Low-Activity Waste" that produced the highest pore water velocity at the undisturbed recharge rate of 3.5 mm/yr (0.14 in./yr) were assigned to the clastic dike material.

Table 8-15. Summary of Sensitivity Cases. (3 sheets)

Sensitivity Case Shorthand	Explanation	Model
Surface Barrier Flow Safety Function		
inf01	All parameters same as base case, except that post-design surface barrier net infiltration = 1.0 mm/yr. This is a case in which the surface barrier continues to provide limitation to flow beyond its design life.	STOMP©
inf02	All parameters same as base case, except that post-design surface barrier net infiltration = 5.2 mm/yr. This is a case in which the surface barrier behaves worse than expected after its design life, and allows more infiltration than the base case Hanford infiltration.	STOMP©
inf03	All parameters same as base case, except that operational period net infiltration = 140 mm/yr, and post-institutional control net infiltration = 100 mm/yr. This corresponds to future scenarios in which land use or vegetative cover are significantly different and disadvantageous compared to the base case. This may include vegetative progression, migration of sand dunes onto Waste Management Area (WMA) C, or agricultural irrigation on the site.	STOMP©
unc01	All parameters same as base case, except that net infiltration for all surfaces outside WMA C = 0.5 mm/yr for all times. This corresponds to future scenarios in which land use or vegetative cover are significantly different and advantageous compared to the base case, but the cover continues to have a nominal functionality.	STOMP©
unc02	All parameters same as base case, except that net infiltration for all surfaces outside WMA C = 100 mm/yr for all times. This corresponds to future scenarios in which land use or vegetative cover are significantly different and disadvantageous compared to the base case, but the cover continues to have a nominal functionality.	STOMP©
Aquifer Dilution Safety Function		
gwp01	All parameters same as base case, except that aquifer flow parameters are 5th percentile values. This corresponds to altered aquifer flow producing minimal aquifer dilution compared to the base case.	STOMP©

Table 8-15. Summary of Sensitivity Cases. (3 sheets)

Sensitivity Case Shorthand	Explanation	Model
gwp03	All parameters same as base case, except that aquifer flow parameters are 95th percentile values. This corresponds to altered aquifer flow producing a higher level of aquifer dilution compared to the base case.	STOMP©
Vadose Zone Flow and Dispersion Safety Functions		
vzp01	All parameters same as base case, except that vadose zone hydraulic properties are 5th percentile values. This is an exploration of the effect of vadose zone parameters.	STOMP©
vzp02	All parameters same as base case, except that vadose zone hydraulic properties are 50th percentile values (median). This is an exploration of the effect of vadose zone parameters.	STOMP©
vzp03	All parameters same as base case, except that vadose zone hydraulic properties are 95th percentile values. This is an exploration of the effect of vadose zone parameters.	STOMP©
vzp04	All parameters same as base case, except that the geologic model is Alternative II with 5th and 95th percentile values of H2 Sand applied to H2 Fine and H2 Coarse Sand, respectively. This is an exploration of the effect of vadose zone parameters.	STOMP©
vzp05	All parameters same as base case, except that the geologic conceptualization includes clastic dikes. This is an alternative conceptual model representing an unknown feature below the site.	STOMP©
Inventory Estimate		
inv1	All parameters same as base case, except that the estimated inventory is based on the TC&WM EIS (2012) values. This is an exploration of the effect of alternative inventory assumptions.	GoldSim©
inv2	All parameters same as base case, except that the estimated inventory is based on the upper bound values. This is an exploration of the effect of alternative inventory assumptions.	GoldSim©
Grout Flow Safety Function		
grt1	All parameters same as base case, except that after 5,000 years following closure, the grout degrades and the flow properties change to Hanford H2 sand values, with a step function change in the flow rate occurring at this time. This may represent an alternative in which the grout degradation is more rapid than the base case, either through weathering processes that are not included in the base case, or if failure occurs from unanticipated seismic activity.	GoldSim©
grt2	All parameters same as base case, except that after 1,000 years following closure, the grout degrades and the flow properties change to Hanford H2 sand values, with a step function change in the flow rate occurring at this time. This may represent an alternative in which the grout degradation is more rapid than the base case, either through weathering processes that are not included in the base case, or if failure occurs from unanticipated seismic activity.	GoldSim©

Table 8-15. Summary of Sensitivity Cases. (3 sheets)

Sensitivity Case Shorthand	Explanation	Model
grt3	All parameters same as base case, except that after 500 years following closure, the grout degrades and the flow properties change to Hanford H2 sand values, with a step function change in the flow rate occurring at this time. This may represent an alternative in which the grout degradation is more rapid than the base case, either through weathering processes that are not included in the base case, or if failure occurs from unanticipated seismic activity.	GoldSim©
grt4	All parameters same as base case, except that after 0 years following closure, the grout degrades and the flow properties change to Hanford H2 sand values, with a step function change in the flow rate occurring at this time.	GoldSim©
Residual Chemistry Safety Function		
rls1	All parameters same as base case, except that the release function is calculated assuming all waste is instantly available. This case evaluates a more conservative release function compared to the base case.	GoldSim©
Tank Flow Safety Function		
dif1	All parameters same as base case, except that the release function is based on diffusion coefficient 1E-7 cm^2/s. This case represents the tank and base mat in worse condition than the base case, but still limited by diffusion.	GoldSim©
dif2	All parameters same as base case, except that the release function is based on linearly changing diffusion coefficient over 500 years after closure from 1E-14 to 3E-8 cm^2/s. This case represents the tank and base mat degrading over 500 years after closure, but still limited by diffusion.	GoldSim©
dif4	All parameters same as base case, except that the tanks remain intact (no release) for 5,000 years after closure, followed by advective release beginning immediately. This case represents the steel shell remaining intact for longer than the base case, potentially allowing ingrowth of uranium progeny, followed by advective release with associated potential for higher releases of the progeny.	GoldSim©

GoldSim© simulation software is copyrighted by GoldSim Technology Group LLC of Issaquah, Washington (see http://www.goldsim.com).
Subsurface Transport Over Multiple Phases (STOMP)© is copyrighted by Battelle Memorial Institute, 1996.

TC&WM EIS = Tank Closure and Waste Management Environmental Impact Statement (DOE/EIS-0391, 2012, "Final Tank Closure and Waste Management Environmental Impact Statement for the Hanford Site, Richland, Washington," U.S. Department of Energy, Washington, D.C.)

Figures 8-40 through 8-42 show the overall results for ^{99}Tc at the nine PoCals for the 5th, median, and 95th percentile values, respectively, with a breakdown by source at the maximum PoCal. Figure 8-43 shows a comparison of the specific ^{99}Tc results for tank C-105 and the pipelines at the maximum PoCal. The peak groundwater concentration ranges between 23 and 48 pCi/L for these cases (Figure 8-39). The median hydraulic property values produce peak concentration results very similar to the base case results (27 pCi/L arriving 1,465 years after closure compared to 30 pCi/L arriving 1,550 years after closure for the base case; see Table 8-18). The range of

results for the vadose zone sensitivity analysis produced a similar range of results to that of the recharge estimates.

Table 8-16. Recharge Sensitivity Evaluation.

Sensitivity Case Shorthand	Pre-WMA C and Undisturbed Ground Recharge Rate Percentile (Value)	Recharge Rate of WMA C Ground During Operations Percentile (Value)	Design Life Surface Barrier and Degraded Liner Recharge Rate Percentile (Value)	Post-Design Life Surface Barrier Recharge Rate Percentile (Value)	Time of Arrival of Maximum Concentration at Downgradient Point of Calculation (Years after Closure)	Maximum Concentration at Downgradient Point of Calculation (pCi/L)
Base Case	3.5 mm/yr	100 mm/yr	0.5 mm/yr	3.5 mm/yr	1,555	30
inf01	3.5 mm/yr	100 mm/yr	0.5 mm/yr	1.0 mm/yr	3,150	22
inf02	5.2 mm/yr[a]	100 mm/yr	0.5 mm/yr	5.2 mm/yr	1,260	36
inf03	3.5 mm/yr	140 mm/yr	0.5 mm/yr	100 mm/yr[b]	174	47
unc01	3.5 mm/yr[c]	100 mm/yr[c]	0.5 mm/yr[c]	3.5 mm/yr[c]	1,630	32
unc02	3.5 mm/yr[d]	100 mm/yr[d]	0.5 mm/yr[d]	3.5 mm/yr[d]	1,230	26

[a]Only recharge in the area that will be occupied by Waste Management Area (WMA) C is 5.2 mm/yr. Recharge everywhere else remains the base case value of 3.5 mm/yr.

[b]Post-design recharge begins 100 years after closure.

[c]Recharge in the areas not occupied by WMA C is 0.5 mm/yr.

[d]Recharge in the areas not occupied by WMA C is 100 mm/yr.

This evaluation of the alternative conceptual model of the geology indicates that these heterogeneous features do not strongly affect the results of the PA. Figures 8-44 and 8-45 show the overall results for WMA C at the nine PoCals for Alternative Model II and for the clastic dike analysis, respectively, with a breakdown by source at the maximum PoCal. Figure 8-46 shows a comparison of the specific results for tank C-105 and the pipelines at the maximum PoCal. The peak concentration values show little change from the base case value, although the clastic dike analysis shows a slightly reduced travel time (Table 8-18).

8.2.4 Inventory Sensitivity Analyses

An upper bound estimate of inventory is provided in Section 3.2.2.3 for both the retrieved tanks and for tanks undergoing retrieval (Tables 3-16 and 3-17). Since ^{99}Tc is the primary dose contributor for the groundwater pathway, a sensitivity case was performed by replacing the base case ^{99}Tc inventory with the upper bound value to evaluate the impact in terms of groundwater concentration at the PoCal. Additionally, the residual volume based on the upper bound estimate

was also updated to be consistent with the change in inventory. All other parameters were kept the same as in the system model base case.

Upper bound residual inventory of 89.7 Ci was estimated for ^{99}Tc for all the sources in WMA C, of which 81.40 Ci was estimated for tank C-105. In comparison, the estimated total ^{99}Tc inventory for the base case was 14.70 Ci of which 7.83 Ci was for tank C-105. Results for these analyses are summarized and compared with the base case in Table 8-19. Figure 8-47(a) presents the results of the sensitivity case compared to the system-model base case. The peak groundwater concentration increased by a factor of five (compared to the base case), which is approximately the ratio of the inventories between the two cases (factor of six). Figure 8-47(b) presents the source term release rate (pCi/yr) of ^{99}Tc from tank C-105 to the vadose zone immediately below the tank. This release rate is proportional to the residual inventory change and indicates that source term release provides the predominant control on the observed differences in groundwater concentrations at the PoCal. In the base case, the source term release rates show a decline after 500 years following closure as most of the ^{99}Tc inventory is depleted by that time, while the upper bound case shows continued increase in the release rate until 1,000 years after closure because of the higher inventory and longer time to deplete. For this reason, the peak groundwater concentration for the upper bound case occurs after 600 years following closure compared to the base case.

8.2.5 Grout Flow Sensitivity Analyses

In the base case, the grouted tanks were assumed to remain intact throughout the 10,000-year analysis time, based on the evaluation of grout durability presented in Section 6.2.12. To assess the impact of early failure of the tank due to unforeseen events, sensitivity cases are performed where the infill grout in the tank is assumed to provide no barrier to flow through the tank. For this purpose, the grout properties are replaced by H2 sand properties and flow through the tank is initiated at the following four degradation times:

1. Tank Degrades at 5,000 years after closure (GRT1)
2. Tank Degrades at 1,000 years after closure (GRT2)
3. Tank Degrades at 500 years after closure (GRT3)
4. Tank Degrades at 0 years after closure (GRT4)

Results for these analyses are summarized and compared with the base case in Table. Figure 8-48(a) presents the ^{99}Tc concentration in the saturated zone at the PoCal (cumulative for all the sources) and Figure 8-48(b) presents the ^{99}Tc release rate (pCi/yr) from tank C-105 to the vadose zone immediately below the tank for the four cases in comparison to the base case. Where the tank grout is degraded at closure (0 years) the ^{99}Tc release rate from the tank at early times is much higher, primarily due to advection, and drops sharply as the mass is depleted. This is in contrast to the release rate for the tanks that are assumed to degrade later, where the release occurs by diffusion (same as base case) until the tank degrades, and by both advection and diffusion after the tank degradation. Until the degradation time, the tank release curves track the base case results.

Figure 8-34. Recharge (Net Infiltration) Sensitivity Analysis Results of the Technetium-99 Concentration in Groundwater for the Minimum (inf01) Post-Design Life Value.

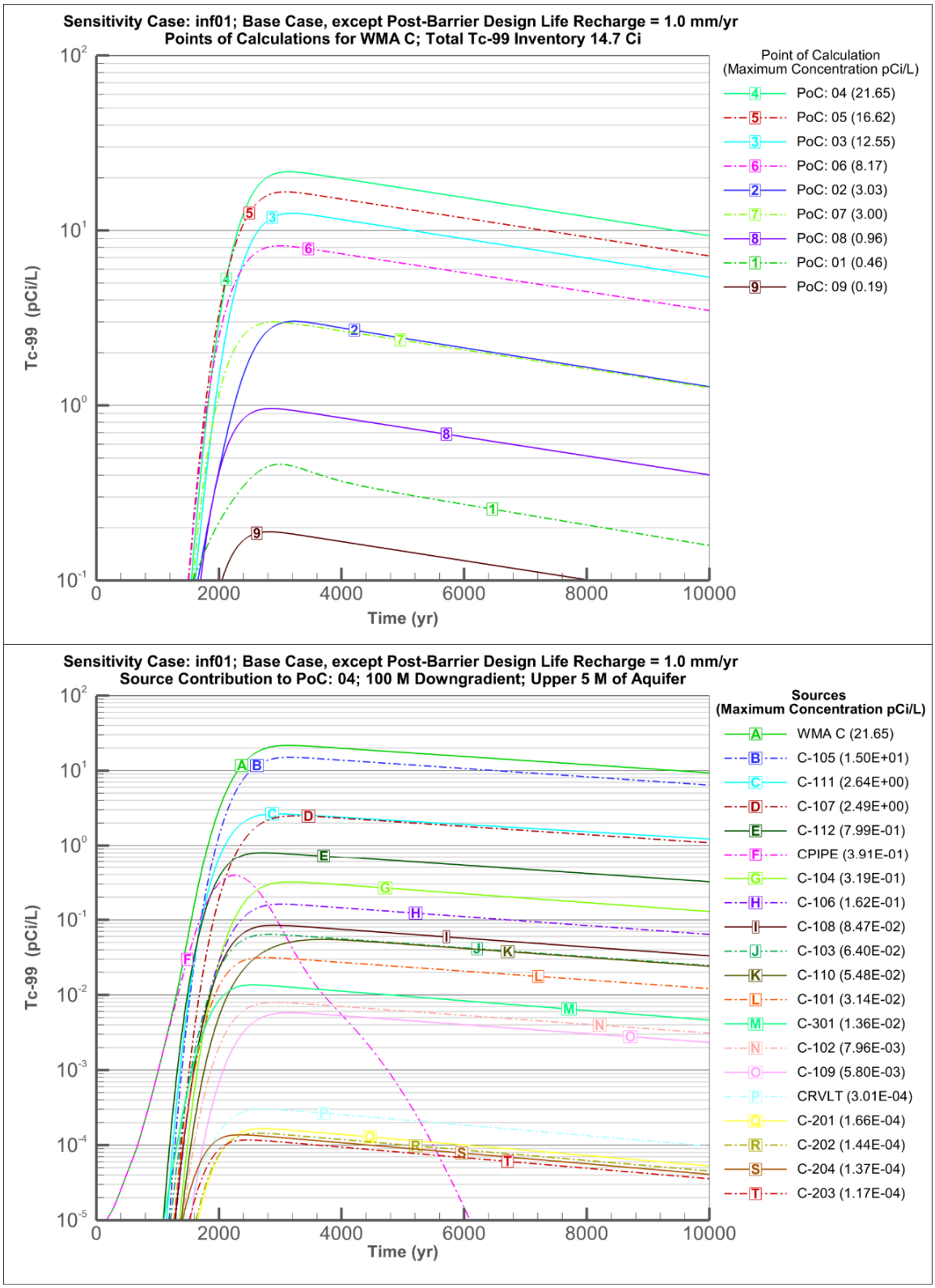

PoCal = Point of Calculation WMA = Waste Management Area

Figure 8-35. Recharge (Net Infiltration) Sensitivity Analysis Results of the Technetium-99 Concentration in Groundwater for the Maximum (inf02) Post-Design Life Value.

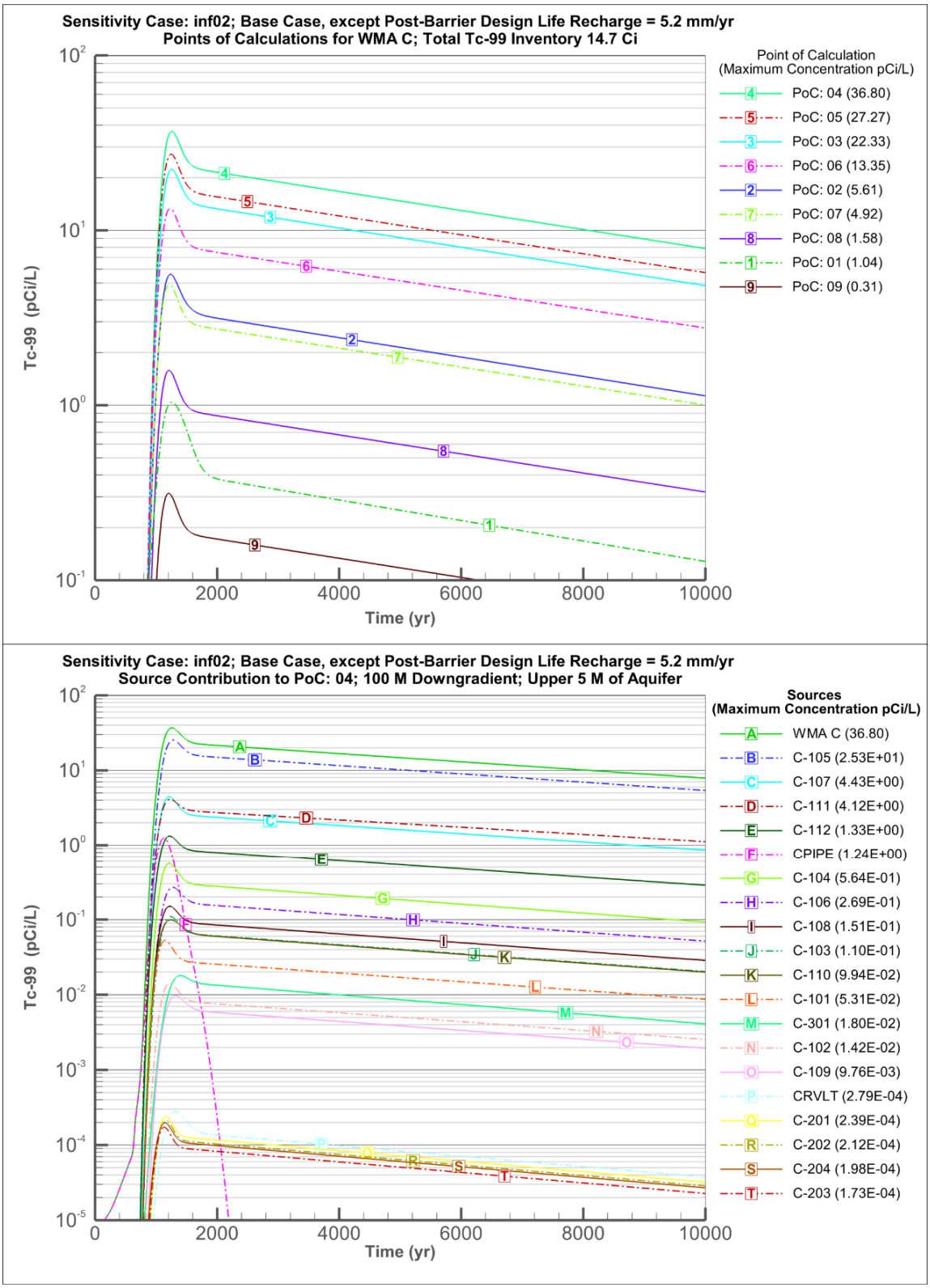

PoCal = Point of Calculation WMA = Waste Management Area

Figure 8-36. Comparison of Recharge (Net Infiltration) Sensitivity Analysis Results of the Technetium-99 Concentration in Groundwater for the Base Case, Minimum (inf01), and Maximum (inf02) Post-Design Life Values.

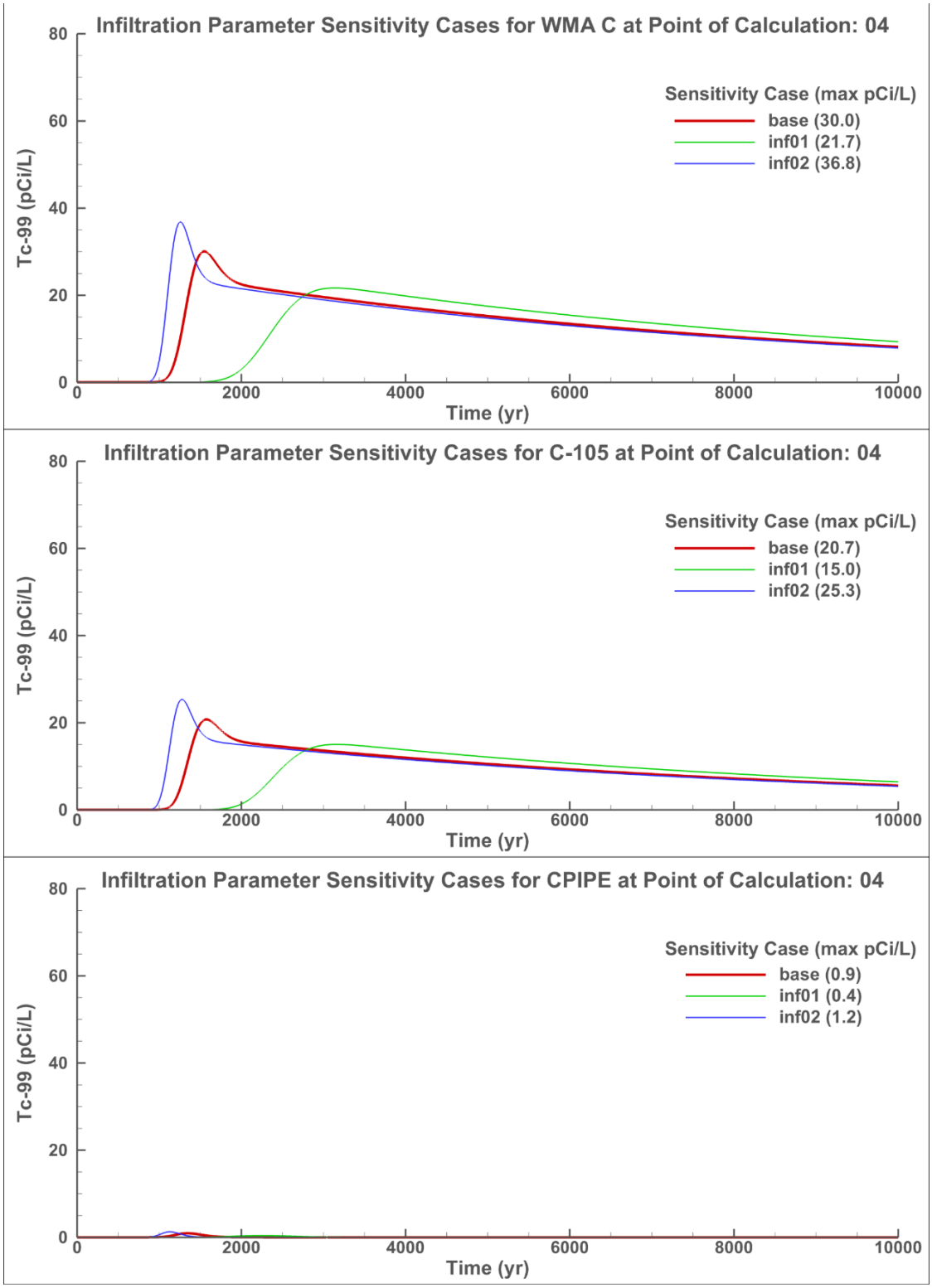

CPIPE = WMA C Pipeline WMA = Waste Management Area

Table 8-17. Aquifer Property Sensitivity Evaluation.

Aquifer Property	Sensitivity Case Shorthand	Aquifer Hydraulic Conductivity (m/day)	Time of Arrival of Maximum Concentration at Downgradient Point of Calculation (Years after Closure)	Maximum Concentration at Downgradient Point of Calculation (pCi/L)
5th Percentile Hydraulic Conductivity Value	gwp01	4,200	1,560	78
Median Hydraulic Conductivity Value	Base Case	11,000	1,555	30
95th Percentile Hydraulic Conductivity Value	gwp03	17,800	1,555	19

The magnitude in peak concentration (and peak release rate) in the saturated zone reduces with the delayed tank degradation time due to inventory depletion from diffusive release prior to the start of advection. For the case where the tank grout is degraded at closure (0 years) the peak concentration in the saturated zone is marginally higher than the case where the tank grout is degraded at 500 years after closure, and the peak concentration occurs after 1,500 years indicating delayed transport through the vadose zone.

8.2.6 Waste Form Sensitivity Analysis

In the base case, waste form degradation and dissolved concentration limits are applied in determining the source term release for some analytes, as discussed in Section 6.3.1. In this sensitivity analysis, such limits are removed to evaluate the impact on saturated zone concentration at the PoCal.

As described in Section 6.3.1, the following source term release models are applied for ^{99}Tc and uranium in the base case:

- For ^{99}Tc, 6% of the inventory is considered to be instantaneously available for release while the remaining 94% undergoes relatively slower release at the fractional rate of 6×10^{-4} day^{-1}

- For uranium, a solubility limit of 1×10^{-4} mol/L is applied for 1,000 years after closure and 1×10^{-6} mol/L after 1,000 years after closure under intact tank conditions.

For the purpose of conducting the sensitivity analysis, all of the ^{99}Tc inventory was assumed to be instantaneously available for release and the solubility limit or dissolved concentration limits are not imposed for uranium.

Figure 8-37. Aquifer Property Sensitivity Analysis Results of the Technetium-99 Concentration in Groundwater for the 5th Percentile (gwp01) Hydraulic Conductivity Values.

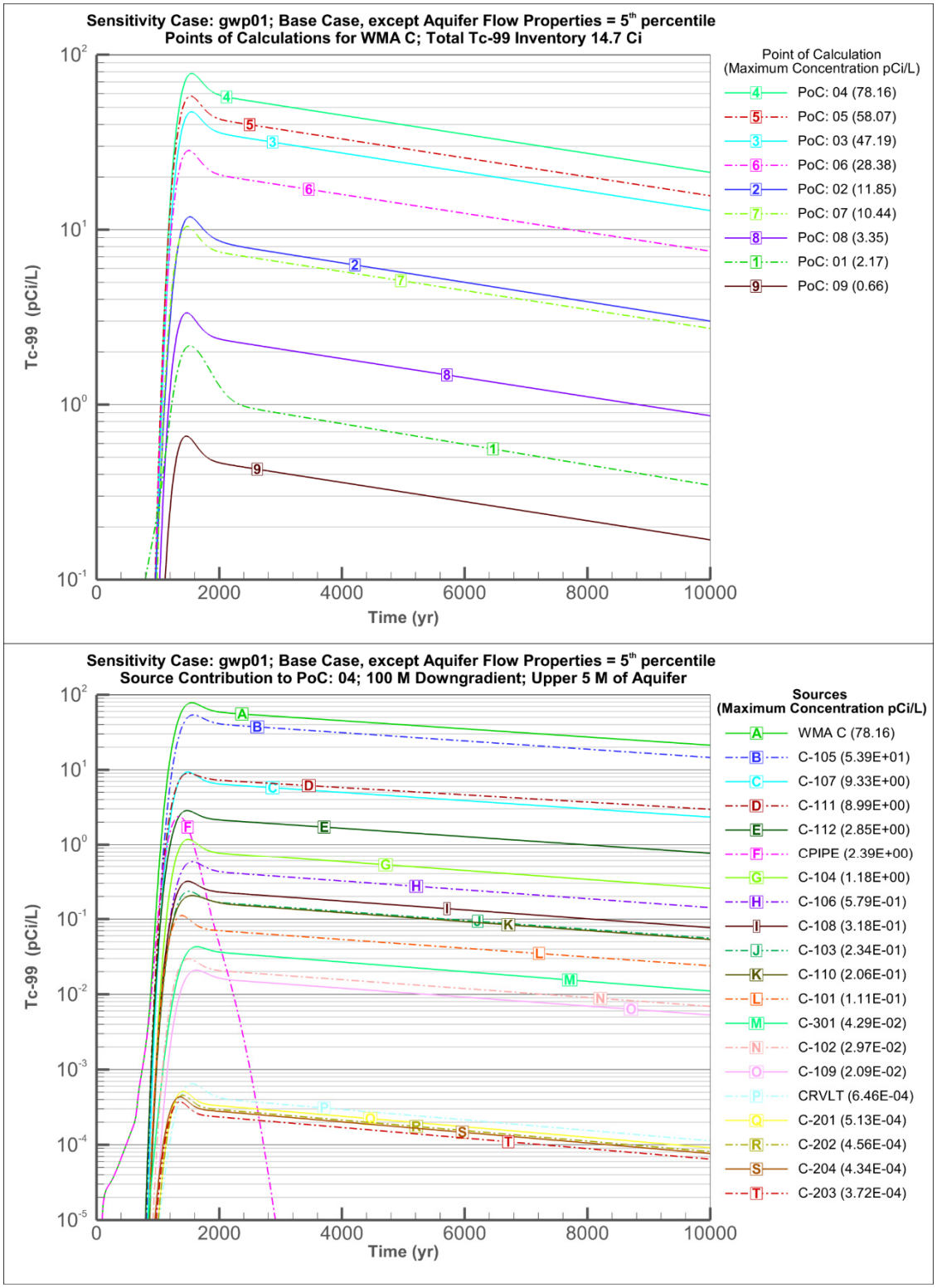

CPIPE = WMA C Pipeline WMA = Waste Management Area

Figure 8-38. Aquifer Property Sensitivity Analysis Results of the Technetium-99 Concentration in Groundwater for the 95th Percentile (gwp03) Hydraulic Conductivity Values.

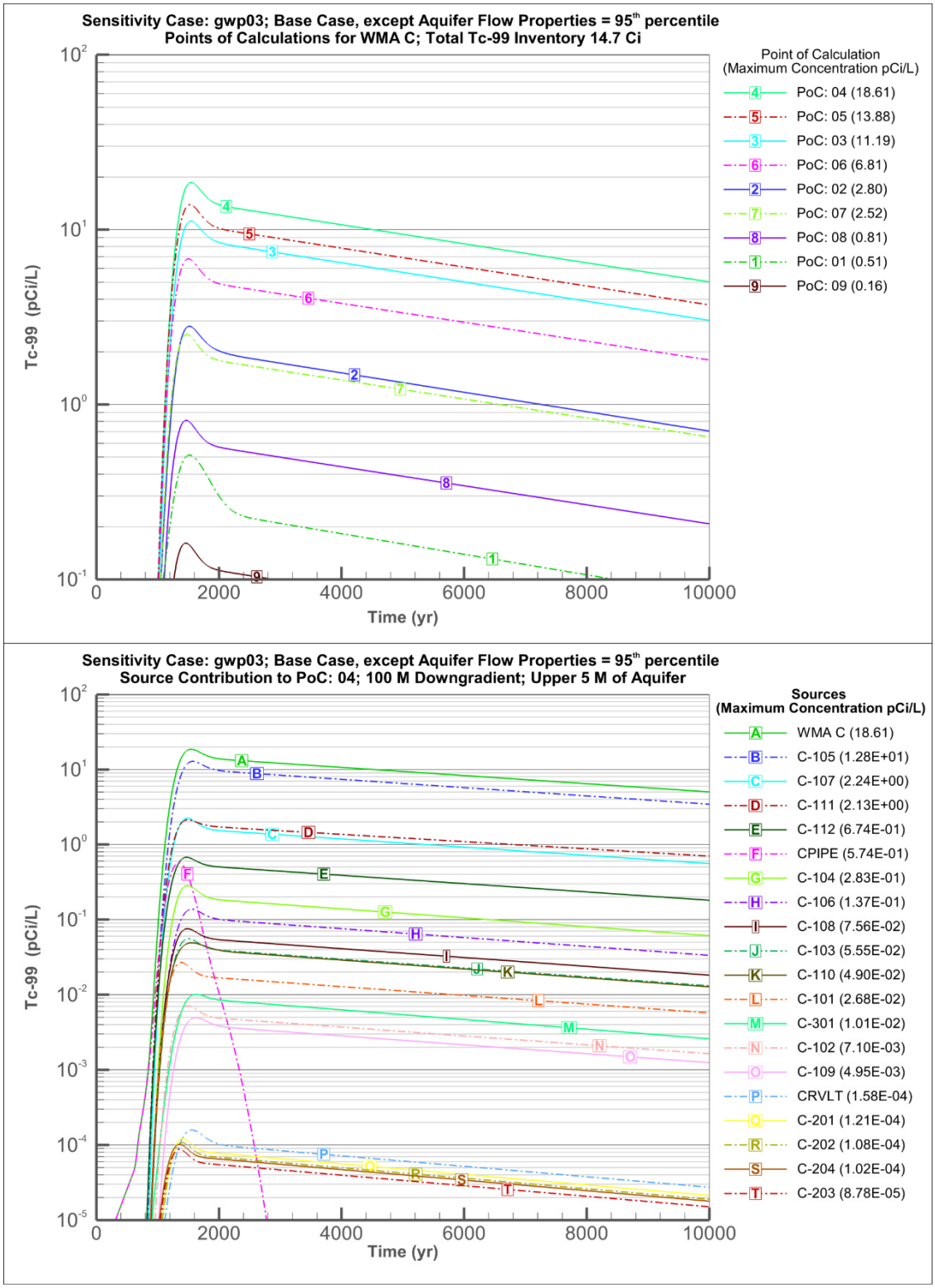

CPIPE = WMA C Pipeline WMA = Waste Management Area

Figure 8-39. Comparison of the Aquifer Property Sensitivity Analysis Results of the Technetium-99 Concentration in Groundwater for the Base Case, 5th Percentile (gwp01), and 95th Percentile (gwp03) Hydraulic Conductivity Values at Point of Calculation 4.

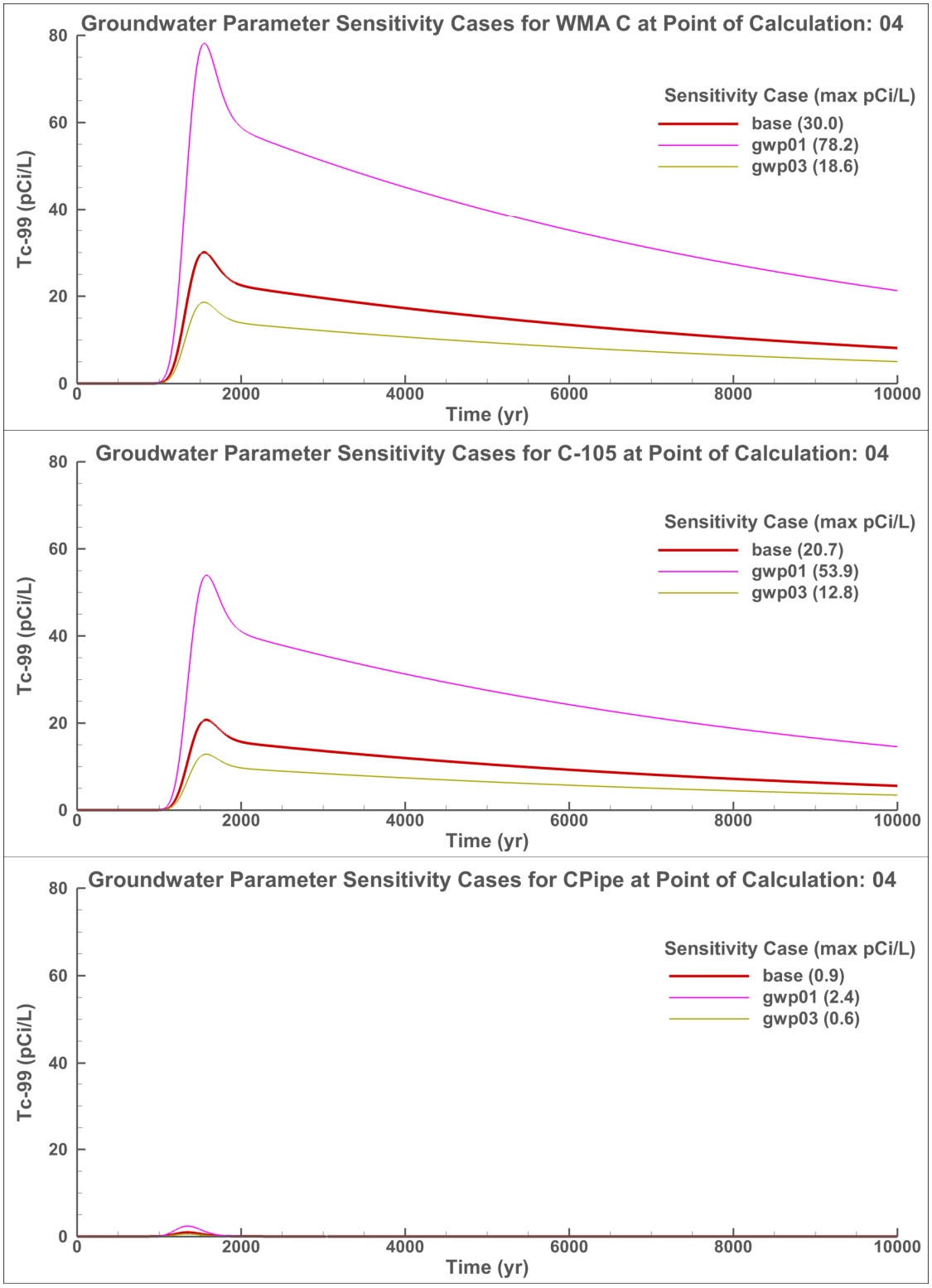

CPipe = WMA C Pipeline WMA = Waste Management Area

Figure 8-40. Vadose Zone Property Sensitivity Analysis Results of the Technetium-99 Concentration in Groundwater for the 5th (vzp01) Percentile Hydraulic Parameter Values.

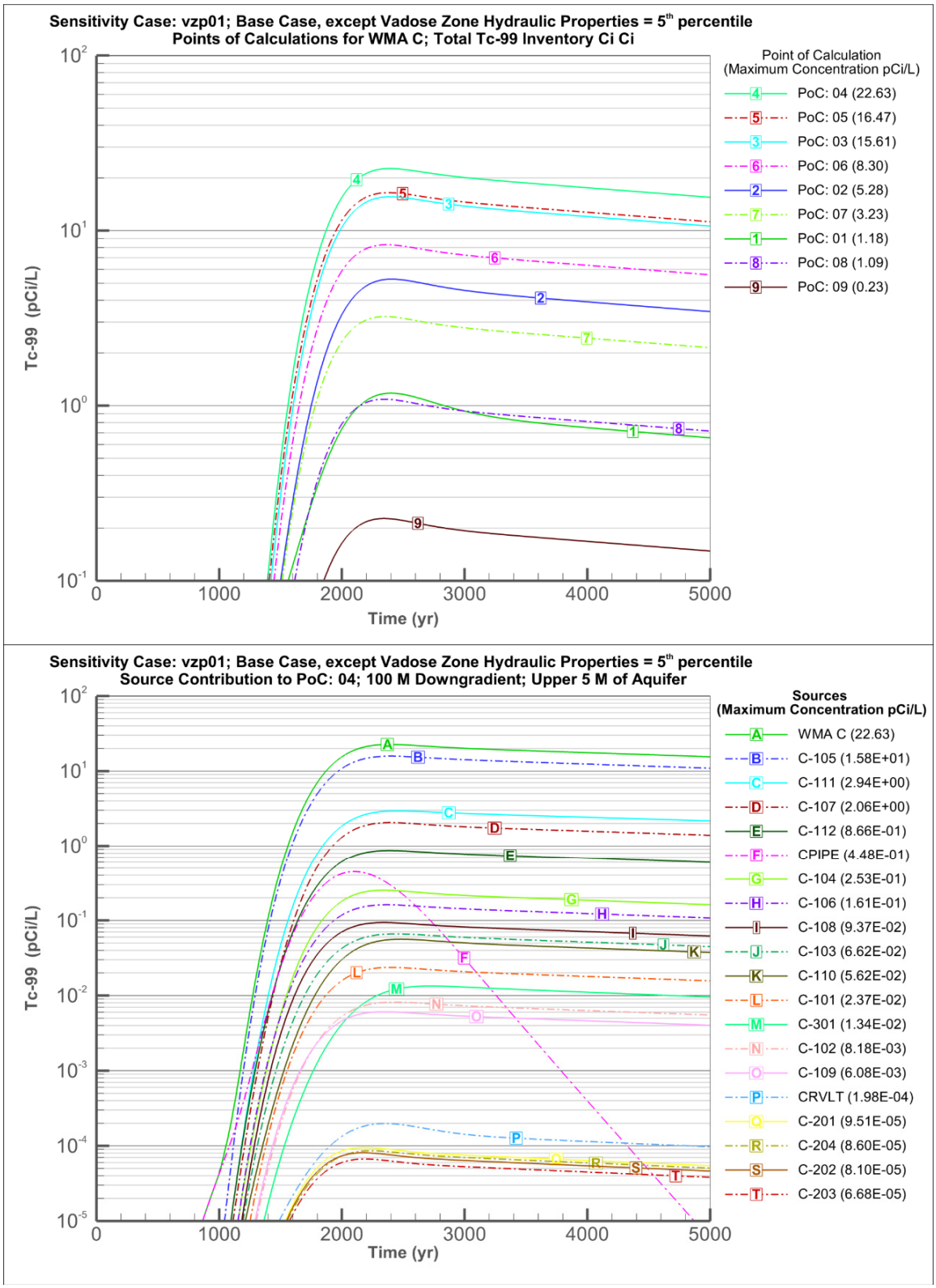

CPIPE = WMA C Pipeline WMA = Waste Management Area

Figure 8-41. Vadose Zone Property Sensitivity Analysis Results of the Technetium-99 Concentration in Groundwater for the Median (vzp02) Percentile Hydraulic Parameter Values.

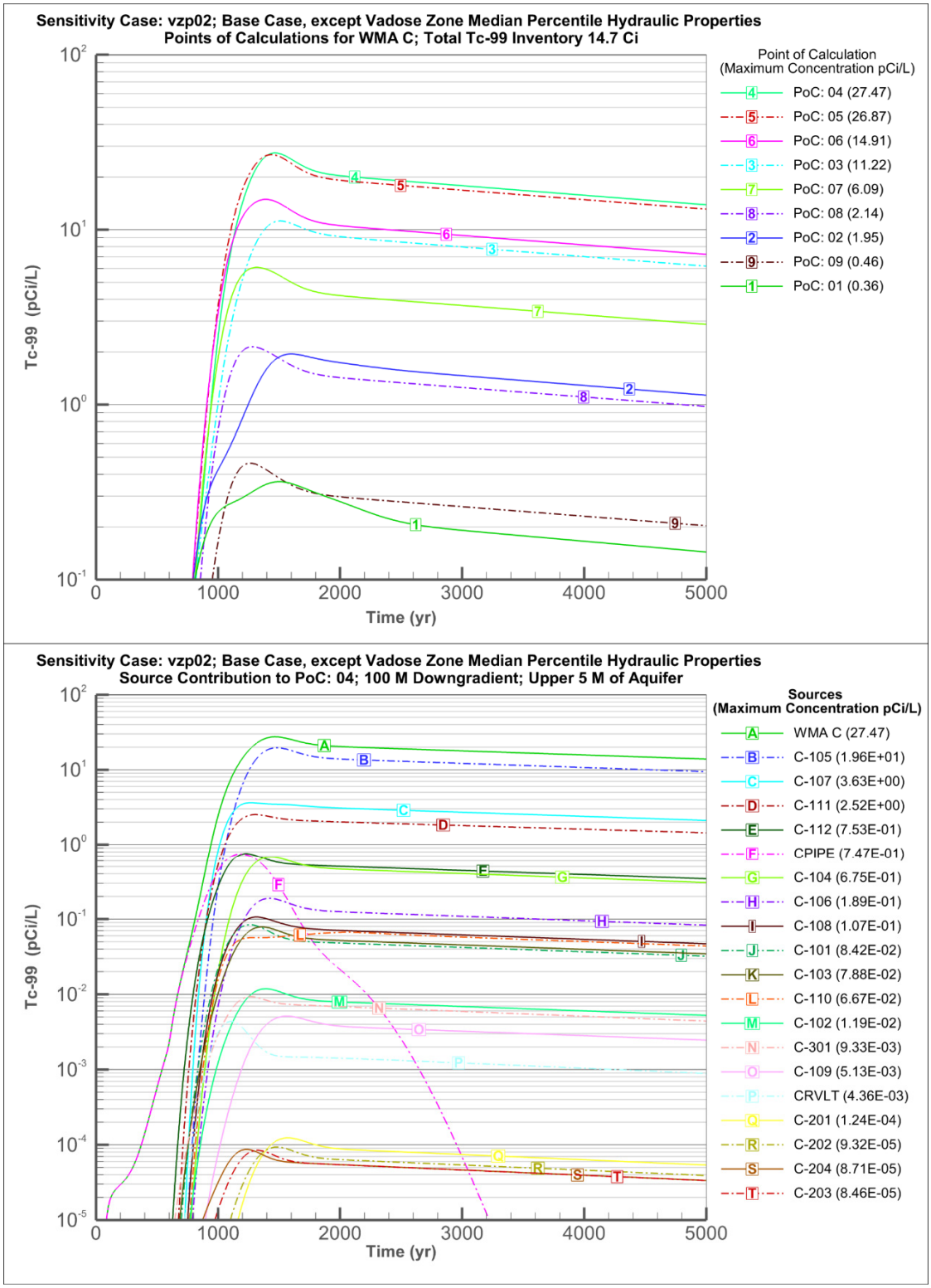

CPIPE = WMA C Pipeline WMA = Waste Management Area

Figure 8-42. Vadose Zone Property Sensitivity Analysis Results of the Technetium-99 Concentration in Groundwater for the 95th (vzp03) Percentile Hydraulic Parameter Values.

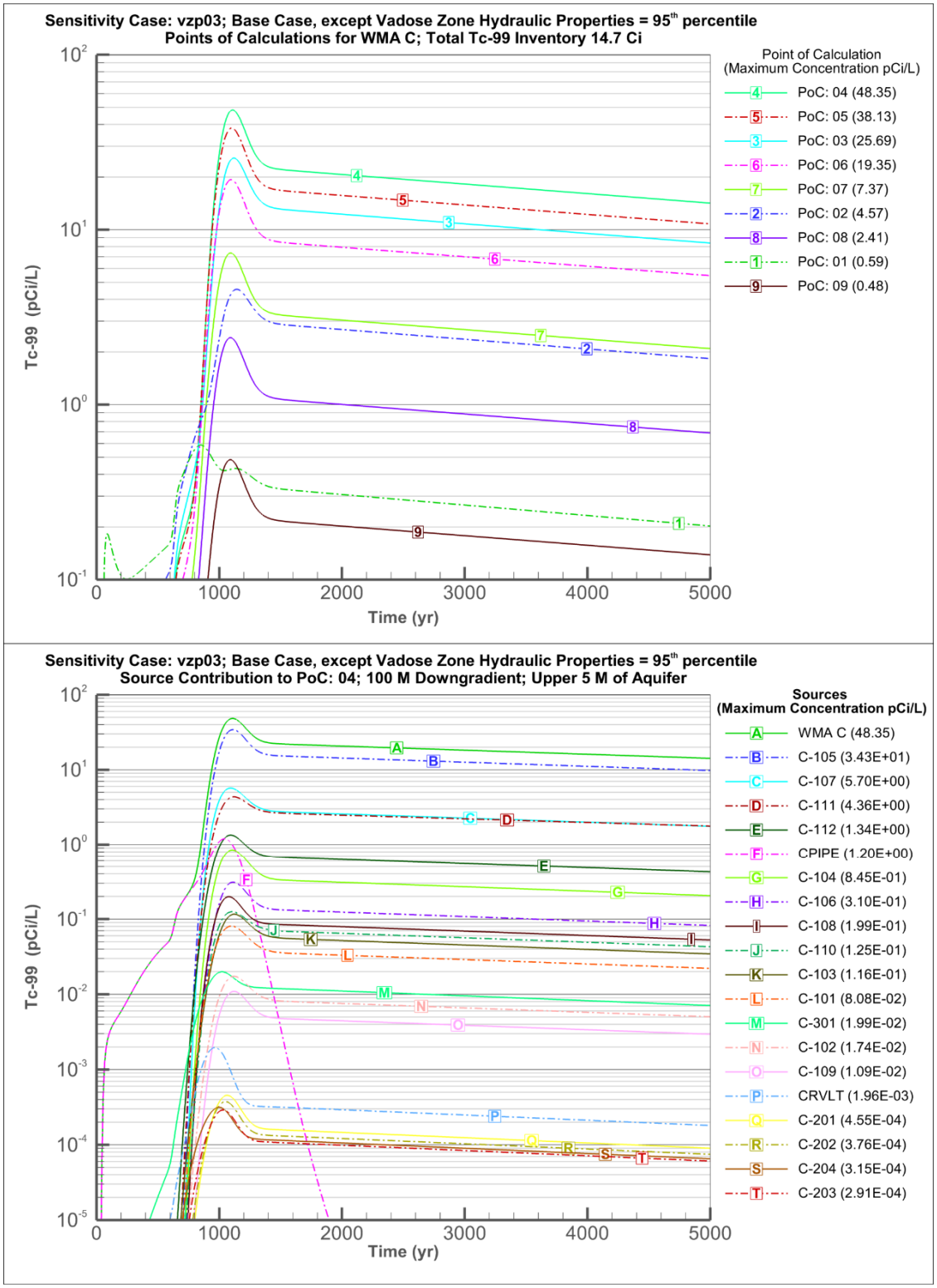

CPIPE = WMA C Pipeline WMA = Waste Management Area

Figure 8-43. Comparison of Vadose Zone Property Sensitivity Analysis Results of the Technetium-99 Concentration in Groundwater for the Base Case, 5th (vzp01), Median (vzp02), and 95th Percentile (vzp03) Hydraulic Parameter Values.

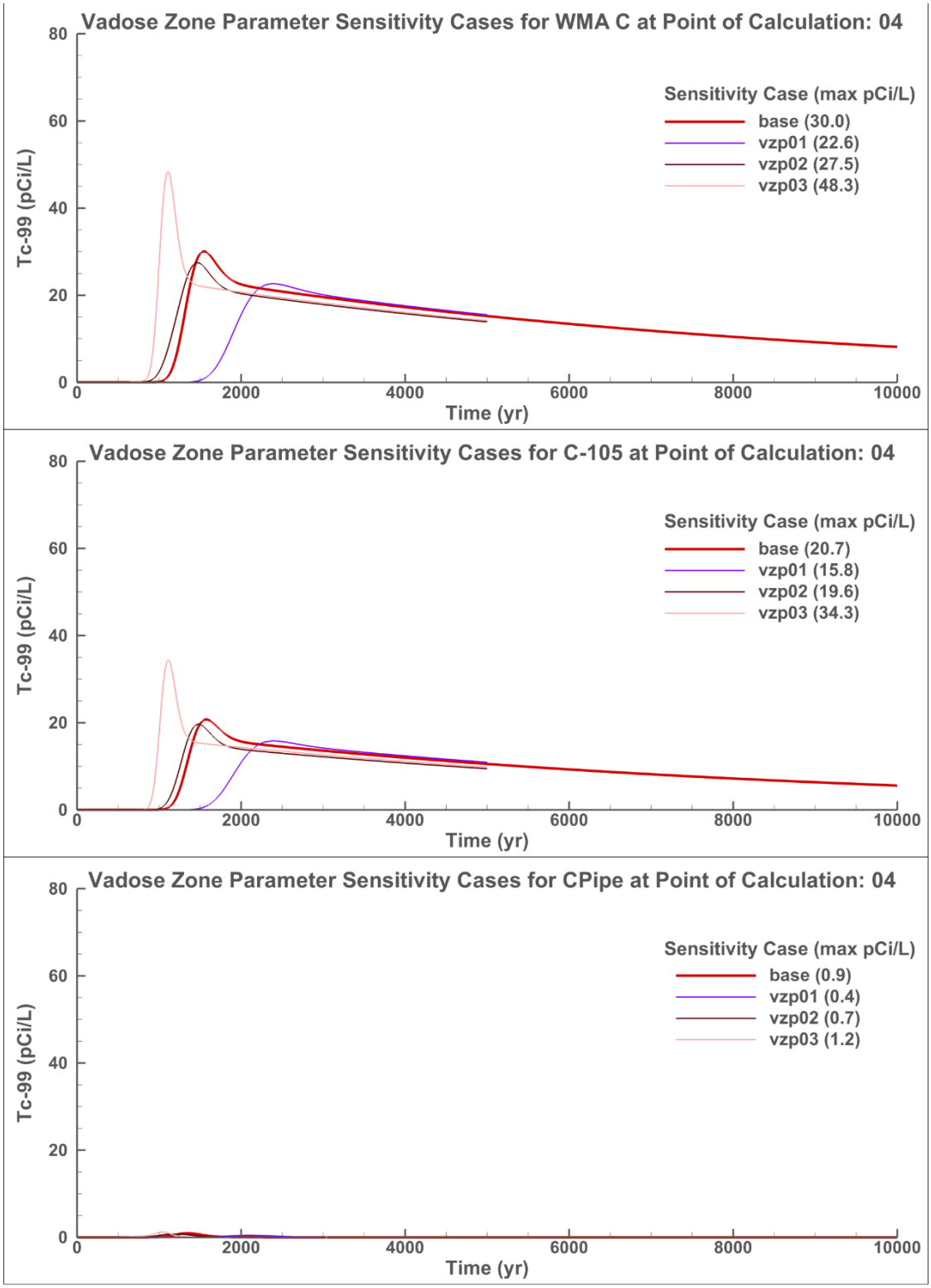

CPipe = WMA C Pipeline WMA = Waste Management Area

Table 8-18. Vadose Zone Sensitivity Evaluation.

Vadose Zone Sensitivity	Sensitivity Case Shorthand	Time of Arrival of Maximum Concentration at Downgradient Point of Calculation (Years after Closure)	Maximum Concentration at Downgradient Point of Calculation (pCi/L)
Base Case	Base Case	1,555	30
5th Percentile Parameter Values	vzp01	2,390	23
Median Percentile Parameter Values	vzp02	1,465	27
95th Percentile Parameter Values	vzp03	1,110	48
Alternative Geologic Model II	vzp04	1,395	29
Presence of Clastic Dike	vzp05	1,460	26

Figure 8-49(a) presents the ^{99}Tc concentration in the saturated zone at the PoCal (cumulative for all the sources) and Figure 8-49(b) presents the ^{99}Tc release rate from tank C-105 to the vadose zone immediately below the tank. Results for these analyses for ^{99}Tc are summarized and compared with the base case in Table 8-21. Figure 8-50 presents the ^{238}U concentration in the saturated zone.

For ^{99}Tc, very little difference is observed between the base case and sensitivity case (Table 8-21). This is because the degradation rate used in the base case itself results in almost all of the ^{99}Tc inventory being available for release within a few years after closure. The small difference in time in the waste form degradation results in negligible difference in the saturated zone concentrations due to larger dispersion caused by vadose zone and saturated zone processes.

For ^{238}U the increase in concentrations are appreciable, indicating the influence of the solubility/dissolved concentration limits. The effect on ^{238}U concentration is relatively small because the breakthrough curve for uranium is primarily from advective release from pipeline sources. Uranium is retarded within the tank due to sorption on the base mat (grout + concrete layer).

Figure 8-44. Alternative Geologic Model Evaluation Results of the Technetium-99 Concentration in Groundwater for the Alternative Geologic Model (vzp04) Geologic Conceptualization.

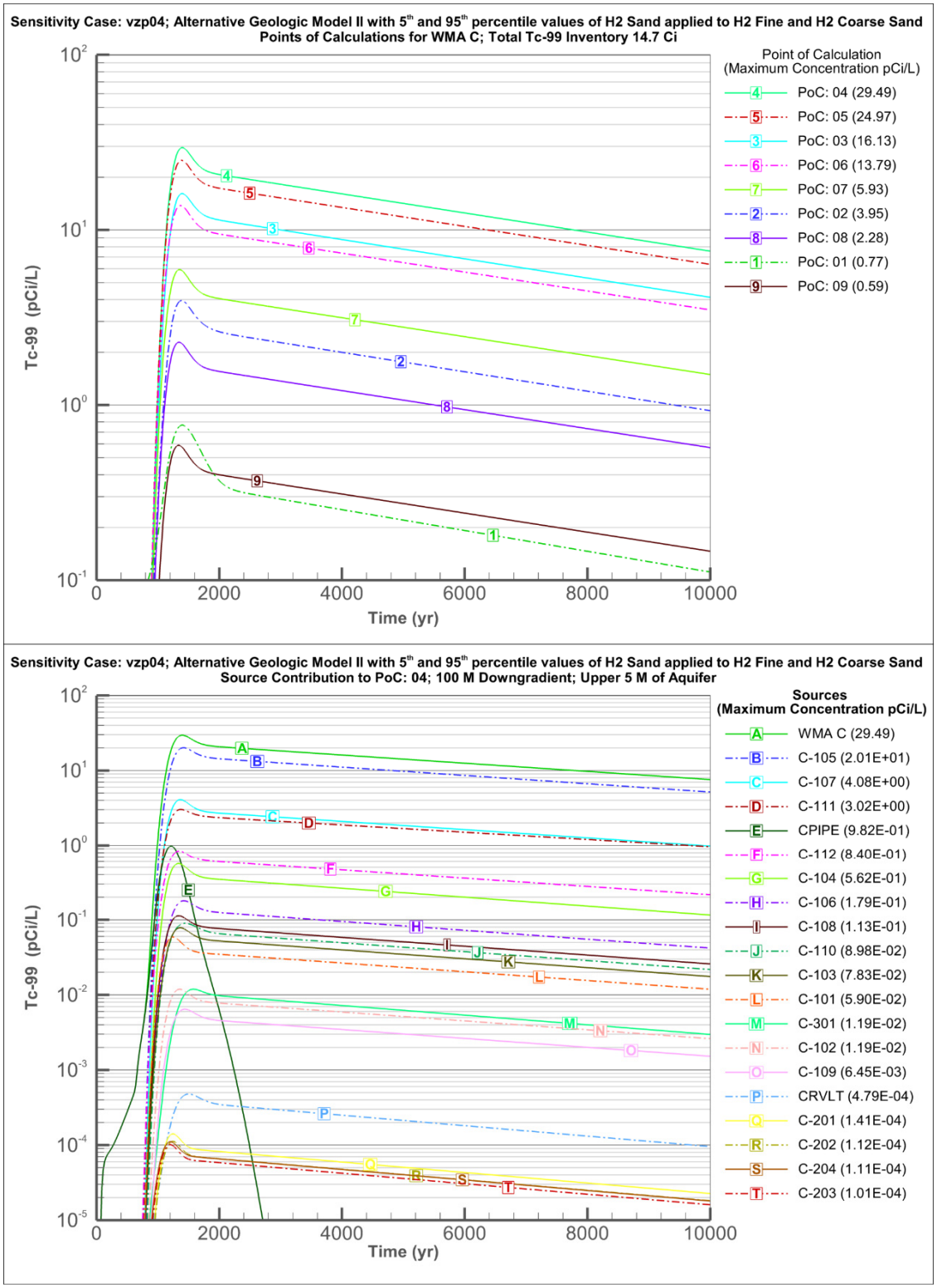

CPIPE = WMA C Pipeline WMA = Waste Management Area

Figure 8-45. Alternative Geologic Model Evaluation Results of the Technetium-99 Concentration in Groundwater for the Hypothesized Clastic Dike (vzp05) Geologic Conceptualization.

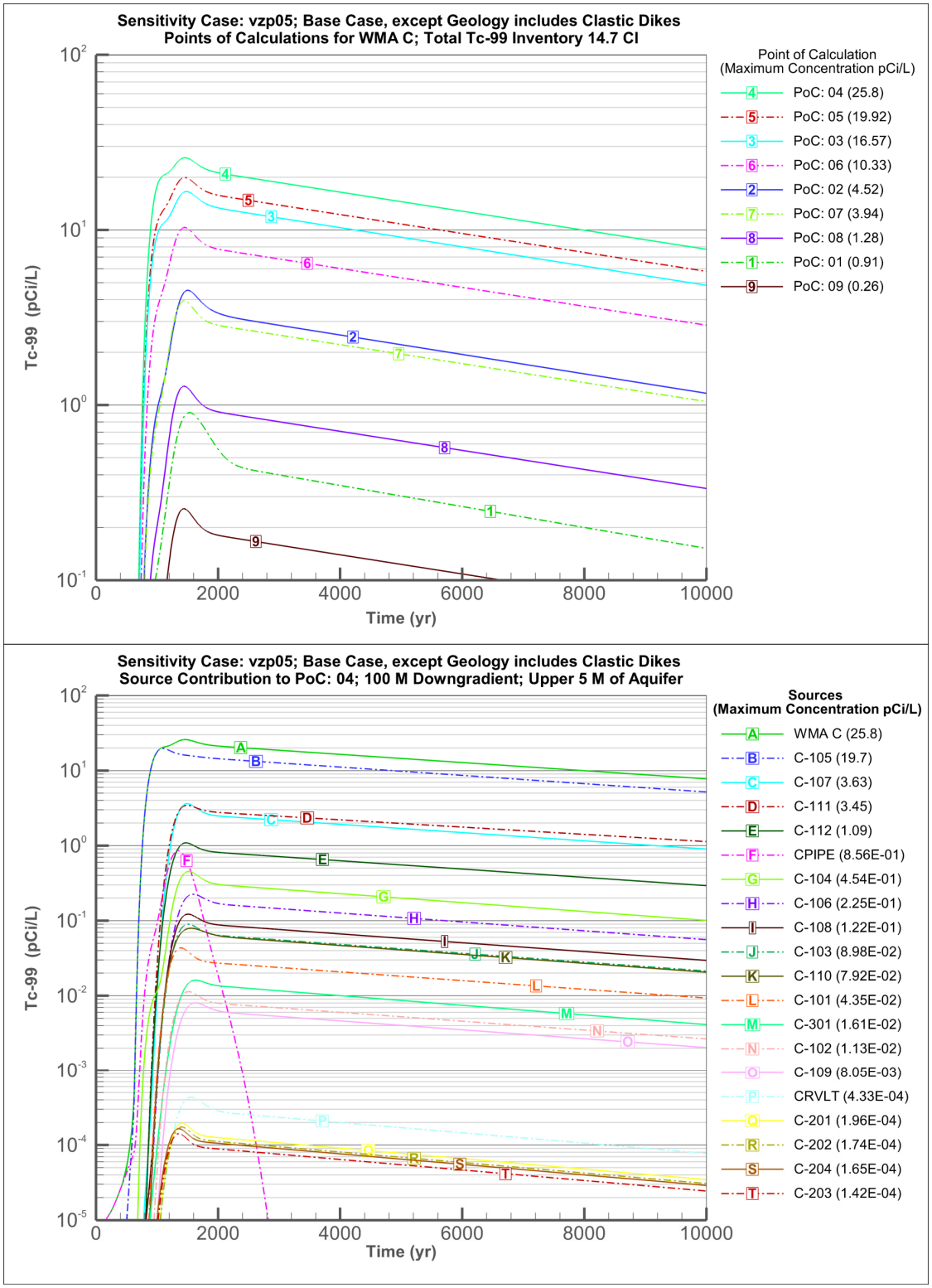

CPIPE = WMA C Pipeline WMA = Waste Management Area

Figure 8-46. Comparison of the Results of the Technetium-99 Concentration in Groundwater for the Alternative Geologic Model (vzp04) and the Hypothesized Clastic Dike (vzp05) Geologic Conceptualizations.

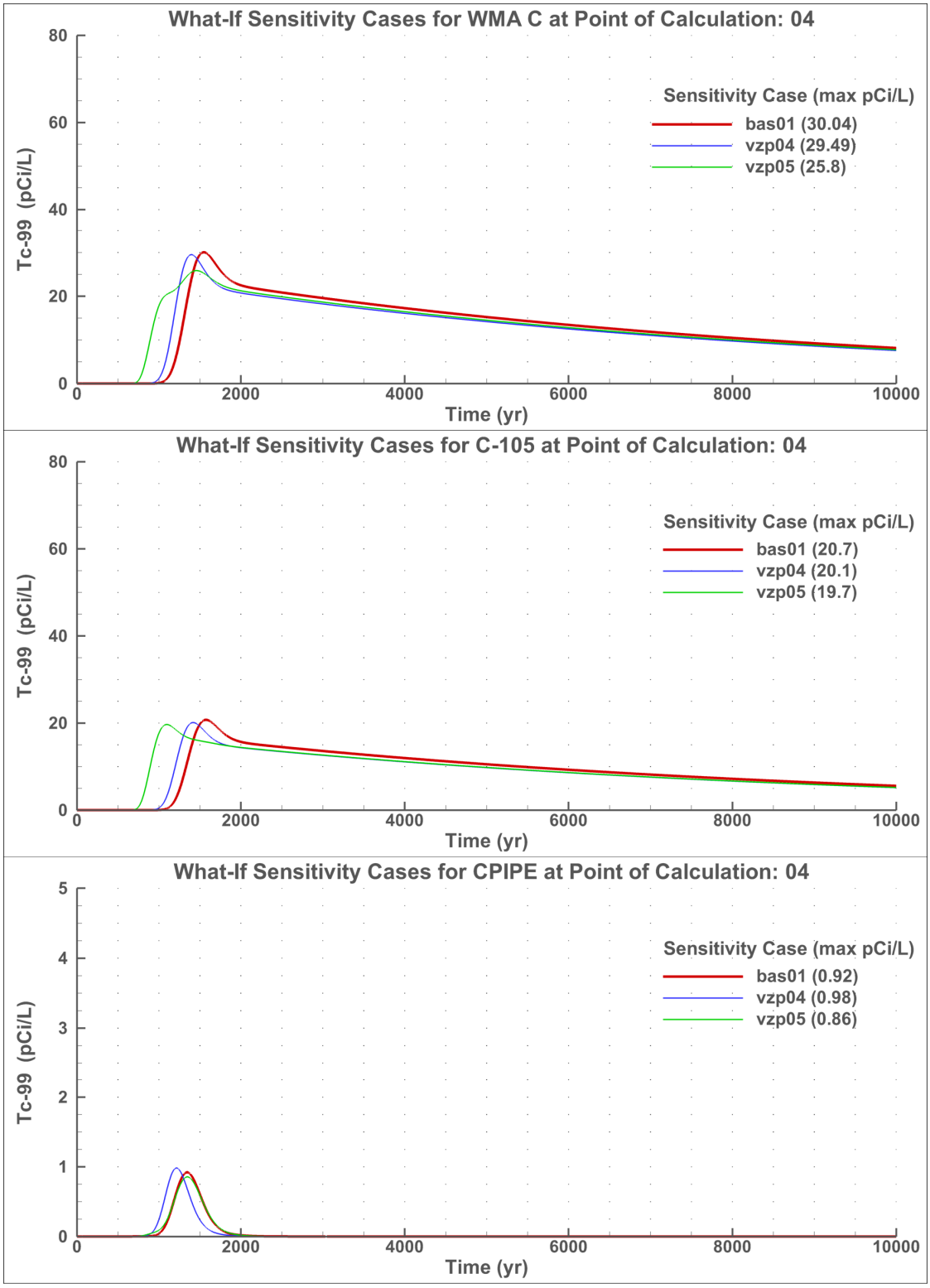

CPIPE = WMA C Pipeline WMA = Waste Management Area

Table 8-19. Inventory Estimate Sensitivity Evaluation.

Inventory	Sensitivity Case Shorthand	Time of Arrival of Maximum Concentration at Downgradient Point of Calculation (Years after Closure)	Maximum Concentration at Downgradient Point of Calculation (pCi/L)
Base case*	Base case	2,030	32
Upper bound Inventory for Technetium-99	inv2	2,480	144

*The base case analysis was run using the system model for this comparison. The results differ slightly from the base case analysis results from Subsurface Transport Over Multiple Phases (STOMP)© (copyrighted by Battelle Memorial Institute, 1996).

8.2.7 Tank Flow Sensitivity Analyses

Diffusive release through the base of the tank (made up of grout and concrete layer) is the primary release mechanism from the tanks in the base case. The effective diffusion coefficient through the concrete and grout layer is a key parameter in determining the diffusive flux. For the base case, an effective diffusion coefficient of 3×10^{-8} cm^2/s was considered (Section 6.3.1); the following three sensitivity cases were performed to evaluate the impact of changing the effective diffusion coefficient based on stakeholder inputs from the scoping process.

1. Effective diffusion coefficient for the grout is changed to 1×10^{-7} cm^2/s (DIF1).

2. Effective diffusion coefficient for the grout varies linearly from 1×10^{-14} to 3×10^{-8} cm^2/s in the first 500 years after closure and remains constant afterwards at 3×10^{-8} cm^2/s (DIF2).

3. Tanks (including 244-CR vault) remain fully intact with no advective release until 5,000 years after closure. The tank becomes fully degraded at 5,000 years after closure, resulting in both advective and diffusive releases. The effective diffusion coefficient remains the same as the base case (DIF3).

Results for these analyses are summarized and compared with the base case in Table 8-22. Figure 8-51(a) presents the ^{99}Tc concentration in the saturated zone at the PoCal and Figure 8-51(b) presents the ^{99}Tc release from tank C-105 to the vadose zone immediately below the tank for the three cases in comparison to the base case. For the DIF1 case, higher diffusion coefficient results in higher diffusive release and higher peak concentration. Once the source inventory depletes (following the peak value) the curves follow the same trend as the base case. For the DIF2 case, due to lower diffusion coefficient in the first 500 years after closure, the diffusive flux and therefore the concentration is lower than the base case early on. For the DIF3 case, since no release is allowed from the grouted tank sources in the first 5,000 years after closure, the only release prior to this time is from the pipeline source that results in a small increase in groundwater concentration around 1,000 years after closure [Figure 8-51(a)]. After 5,000 years after closure, both advective and diffusive release start resulting in higher peak concentration than the base case.

Figure 8-47. Comparison of Base Case and INV1 Case (a) Technetium-99 Concentration at 100 meter Boundary (b) Technetium-99 Release Rate to Vadose Zone from Tank 241-C-105.

(a)

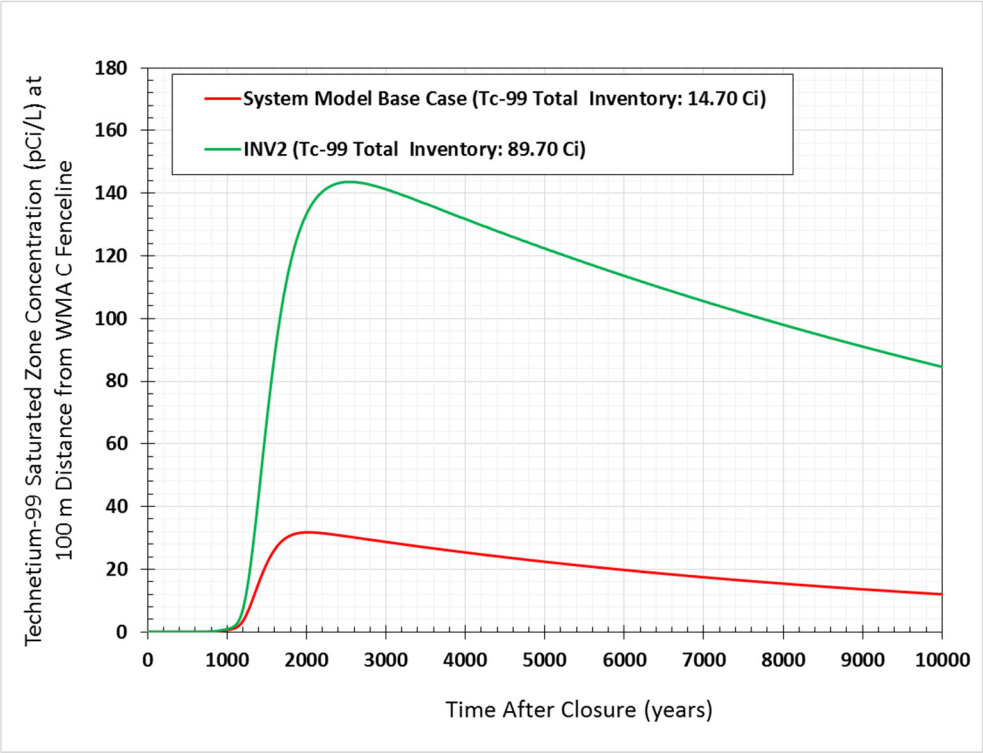

(b)

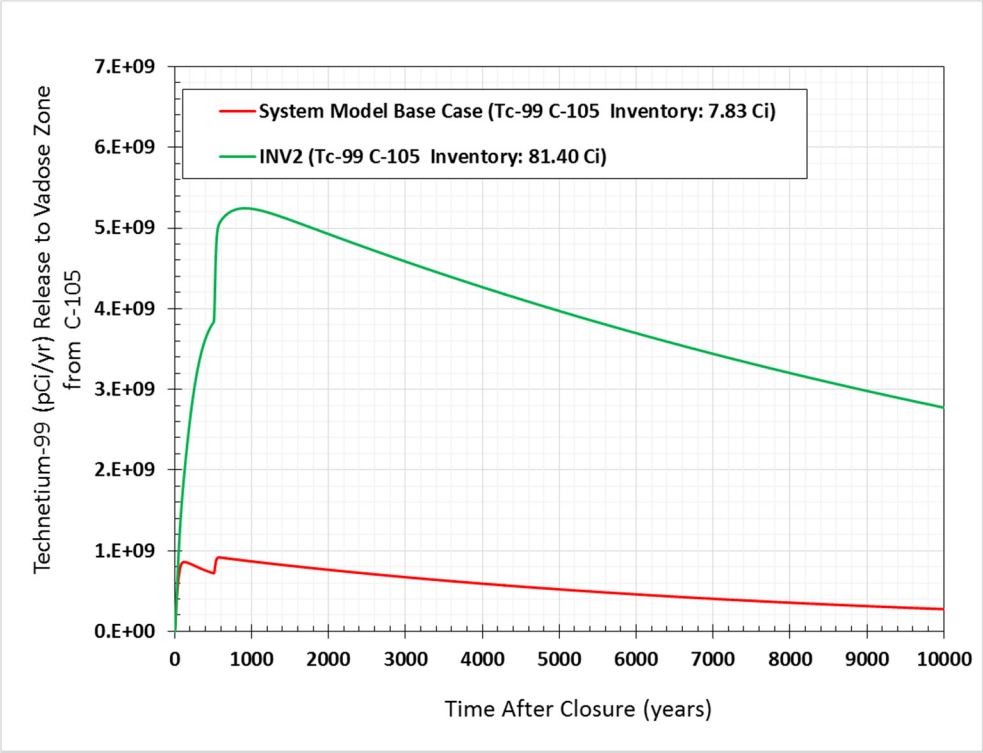

WMA = Waste Management Area

Table 8-20. Grout Flow Safety Function Sensitivity Evaluation.

Tank Degradation Time	Sensitivity Case Shorthand	Time of Arrival of Maximum Concentration at Downgradient Point of Calculation (Years after Closure)	Maximum Concentration at Downgradient Point of Calculation (pCi/L)
Base case*	Base case	2,030	32
Tank Degrades at 5,000 yr	grt1	2,030	32
Tank Degrades at 1,000 yr	grt2	2,630	43
Tank Degrades at 500 yr	grt3	2,190	45
Tank Degrades at 0 yr	grt4	1,520	46

*The base case analysis was run using the system model for this comparison. The results differ slightly from the base case analysis results from Subsurface Transport Over Multiple Phases (STOMP)© (copyrighted by Battelle Memorial Institute, 1996).

8.2.8 Evaluation of Long-Term Peak Dose

An additional evaluation case was run to evaluate the peak dose beyond the 10,000-year post-closure time frame. For this purpose, the base case flow-field that was developed for the 10,000-year post-closure time period was extended such that assumptions of constant recharge rate were maintained and all the processes that were applicable over the 10,000-year post-closure time frame were assumed to be applicable for the extended duration. The only change made to the base case is the one where the grouted tanks (including the 244-CR vault) are considered to be degraded at 30,000 years after closure. At this time, flow through the tank is applied based on the degraded tank flow field. The calculations were run for a period of 400,000 years after closure and the results are presented in Figure 8-52 in terms of effective dose from the groundwater pathway. The peak dose of 0.27 mrem/yr occurs around 15,000 years after closure. It is controlled by ^{99}Tc, uranium isotopes, and ^{226}Ra. The peak dose from uranium isotopes results primarily from advective release from pipeline inventory that occurs at closure, indicating significant delay in the vadose and saturated zone. Following the peak, the dose from uranium isotopes declines sharply and then gradually increases over the simulated time period, indicating delayed arrival from tank sources that are diffusion controlled. The slower diffusive release from the tanks along with retardation in the natural system lead to very small dose from the long-lived uranium isotopes. The dose after 20,000 years following closure is dominated by ^{226}Ra (including progeny) that results from ingrowth due to decay of parent uranium isotopes. After 30,000 years following closure, a small rise in the ^{99}Tc dose is noticeable, which results from an increased release when advection through the tank is assumed. At the end of 400,000 years of simulation, the dose contributions from ^{226}Ra and ^{210}Pb are increasing. Both result from the decay of parent uranium isotopes, indicating establishment of secular equilibrium.

Figure 8-48. Comparison of Base Case and GRT1, GRT2, GRT3, GRT4 Case (a) Technetium-99 Concentration at 100 meter Boundary (b) Technetium-99 Release Rate to Vadose Zone from Tank 241-C-105.

(a)

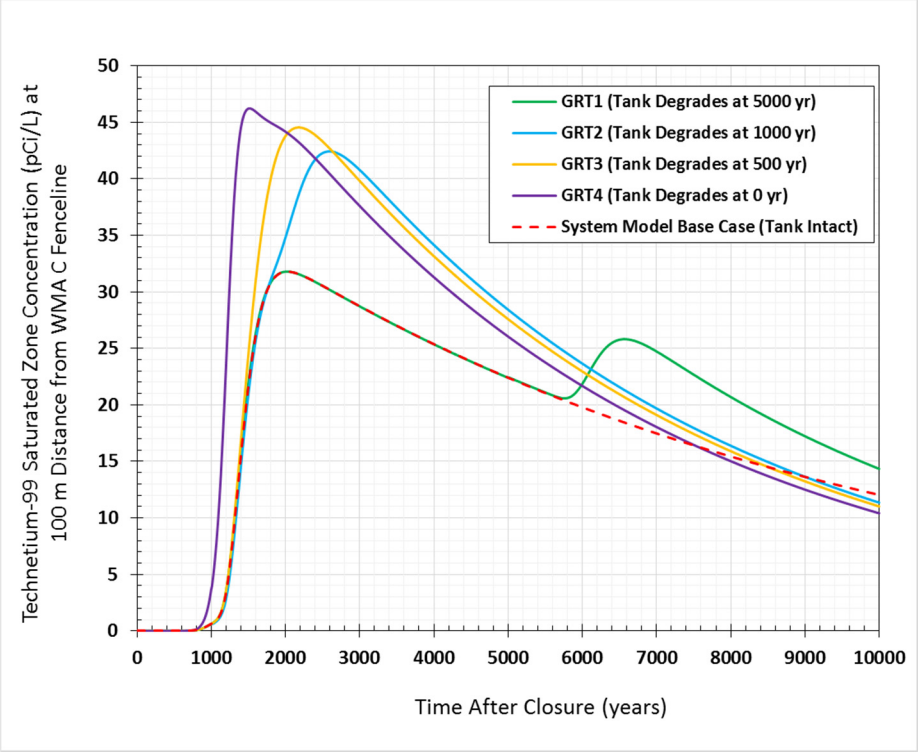

(b)

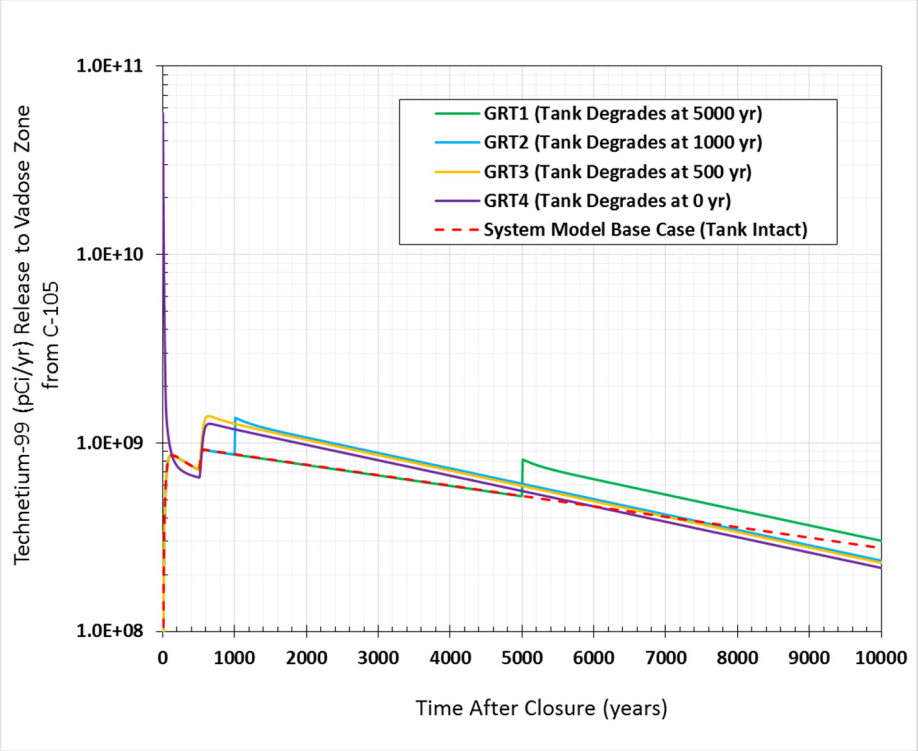

WMA = Waste Management Area

Figure 8-49. Comparison of Base Case and RLS1 Case (a) Technetium-99 Concentration at 100 meter Boundary (b) Technetium-99 Release to Vadose Zone from Tank 241-C-105.

(a)

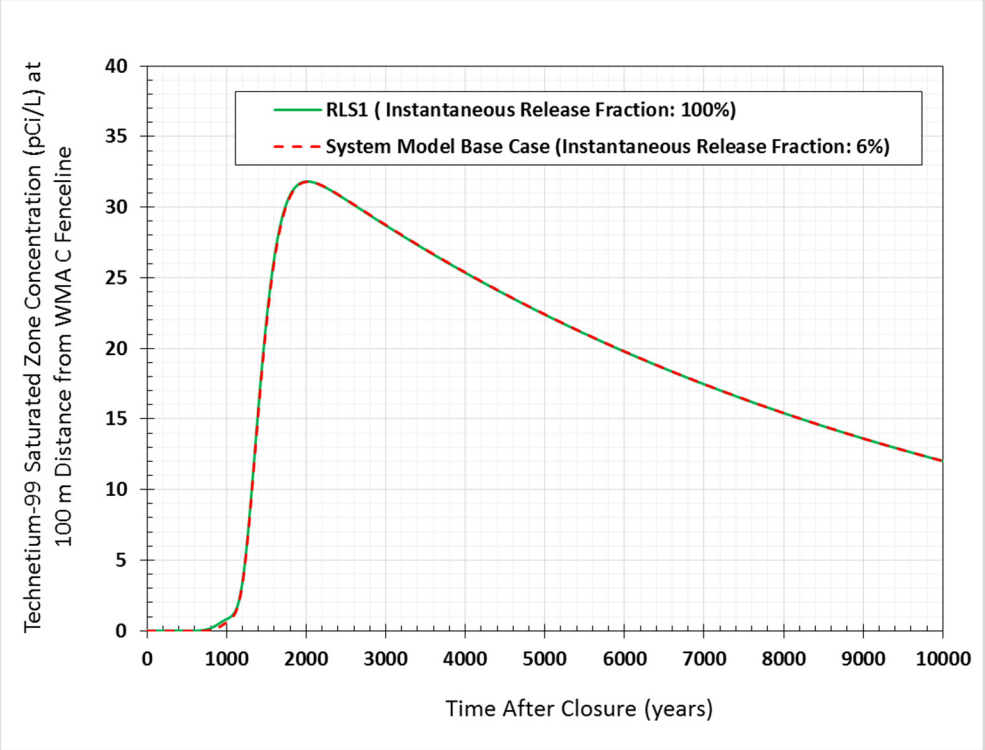

(b)

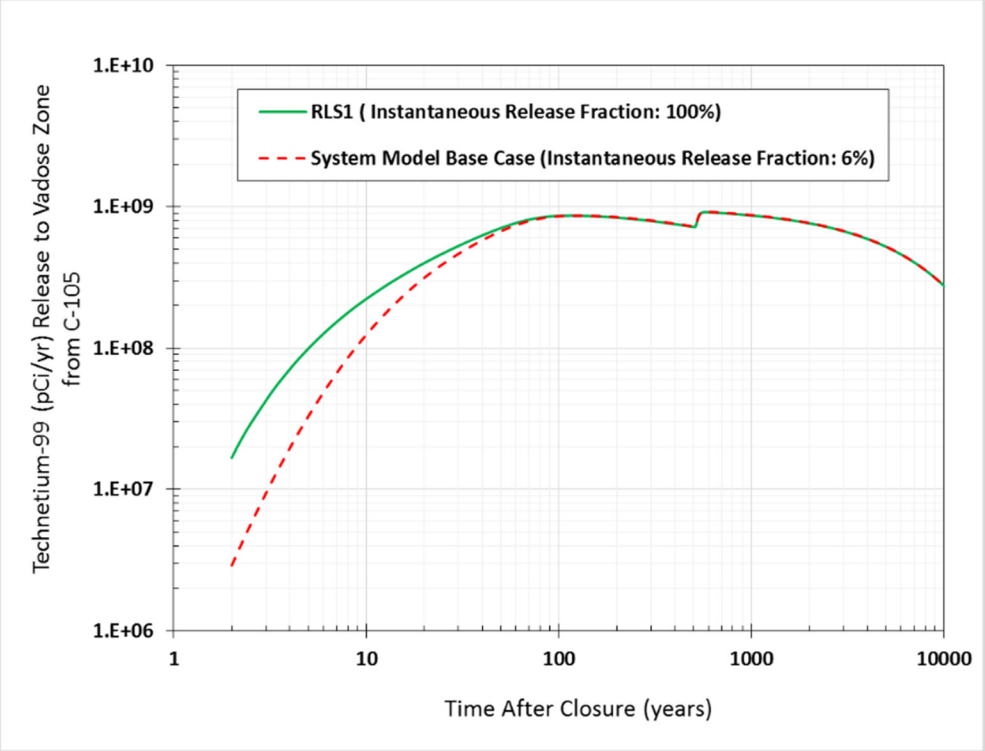

WMA = Waste Management Area

Table 8-21. Residual Chemistry Safety Function.

Residual Chemistry	Sensitivity Case Shorthand	Time of Arrival of Maximum Concentration at Downgradient Point of Calculation (Years after Closure)	Maximum Concentration at Downgradient Point of Calculation (pCi/L)
Base case for technetium-99*	Base case	2,030	32
100% Instantaneous release fraction for technetium-99	rls1(technetium-99)	2,030	32
Solubility Limited release for Uranium	rls1(Uranium-238)	Maximum concentration did not arrive within 10,000 years	Maximum concentration did not arrive within 10,000 years

*The base case analysis was run using the system model for this comparison. The results differ slightly from the base case analysis results from Subsurface Transport Over Multiple Phases (STOMP)© (copyrighted by Battelle Memorial Institute, 1996).

Figure 8-50. Comparison of Base Case and RLS1 Case for Uranium-238 Concentration at 100 meter Boundary.

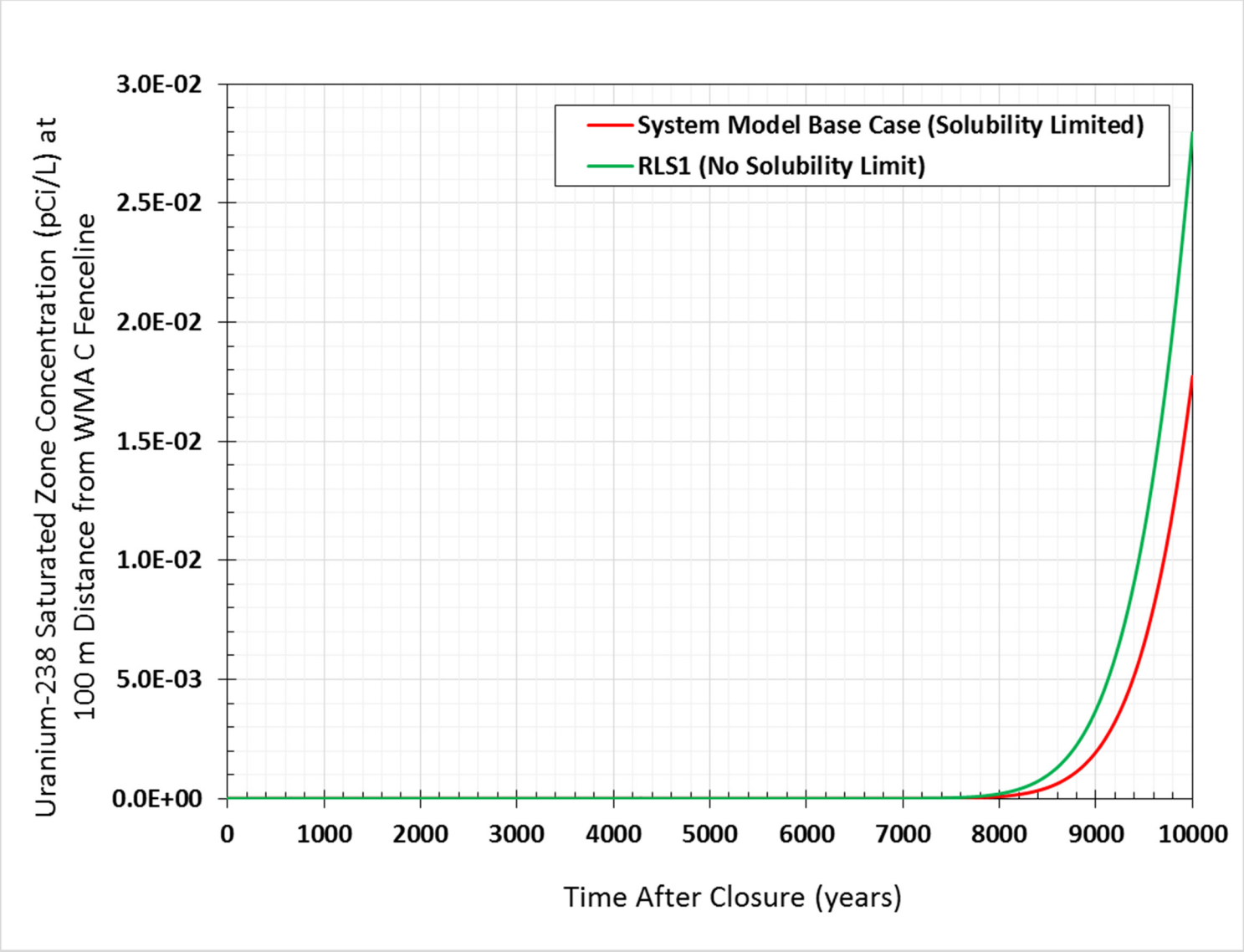

WMA = Waste Management Area

Table 8-22. Tank Flow Safety Function Sensitivity Evaluation.

Tank Flow	Sensitivity Case Shorthand	Time of Arrival of Maximum Concentration at Downgradient Point of Calculation (Years after Closure)	Maximum Concentration at Downgradient Point of Calculation (pCi/L)
Base case*	Base case	2,030	32
Diffusion coefficient 1E-7 cm^2/s	dif1	1,920	34
Linearly changing diffusion coefficient over 500 years from 1E-14 to 3E-8 cm^2/s	dif2	2,230	31
Tanks remain intact (no release) for 5,000 years, followed by advective release beginning immediately.	dif3	6,930	44

*The base case analysis was run using the system model for this comparison. The results differ slightly from the base case analysis results from Subsurface Transport Over Multiple Phases (STOMP)© (copyrighted by Battelle Memorial Institute, 1996).

Figure 8-51. Comparison of Base Case and DIF1, DIF2, DIF3 Case (a) Technetium-99 Concentration at 100 meter Boundary (b) Technetium-99 Release to Vadose Zone from Tank 241-C-105.

(a)

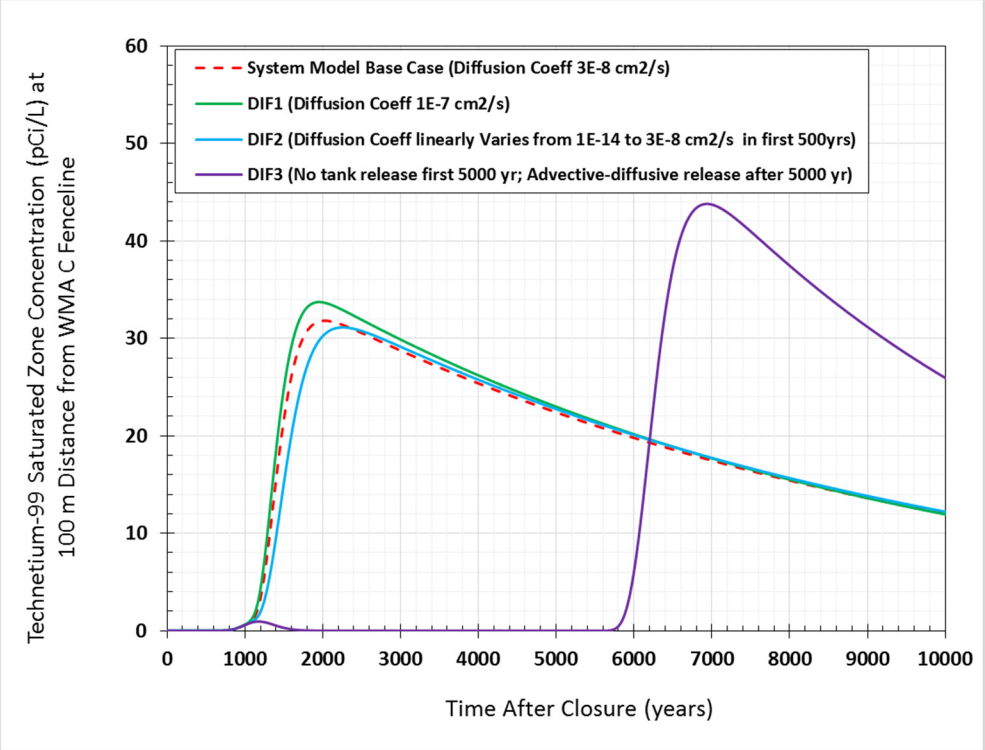

(b)

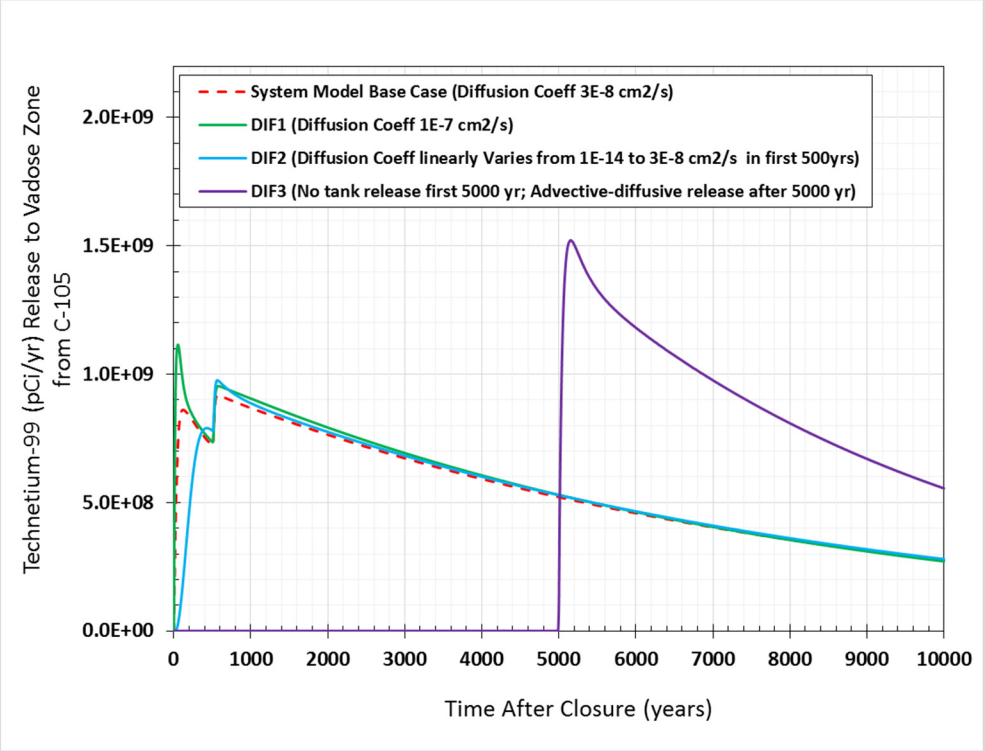

WMA = Waste Management Area

Figure 8-52. Sensitivity Case Showing the Results of Peak Groundwater Pathway Dose Calculations.

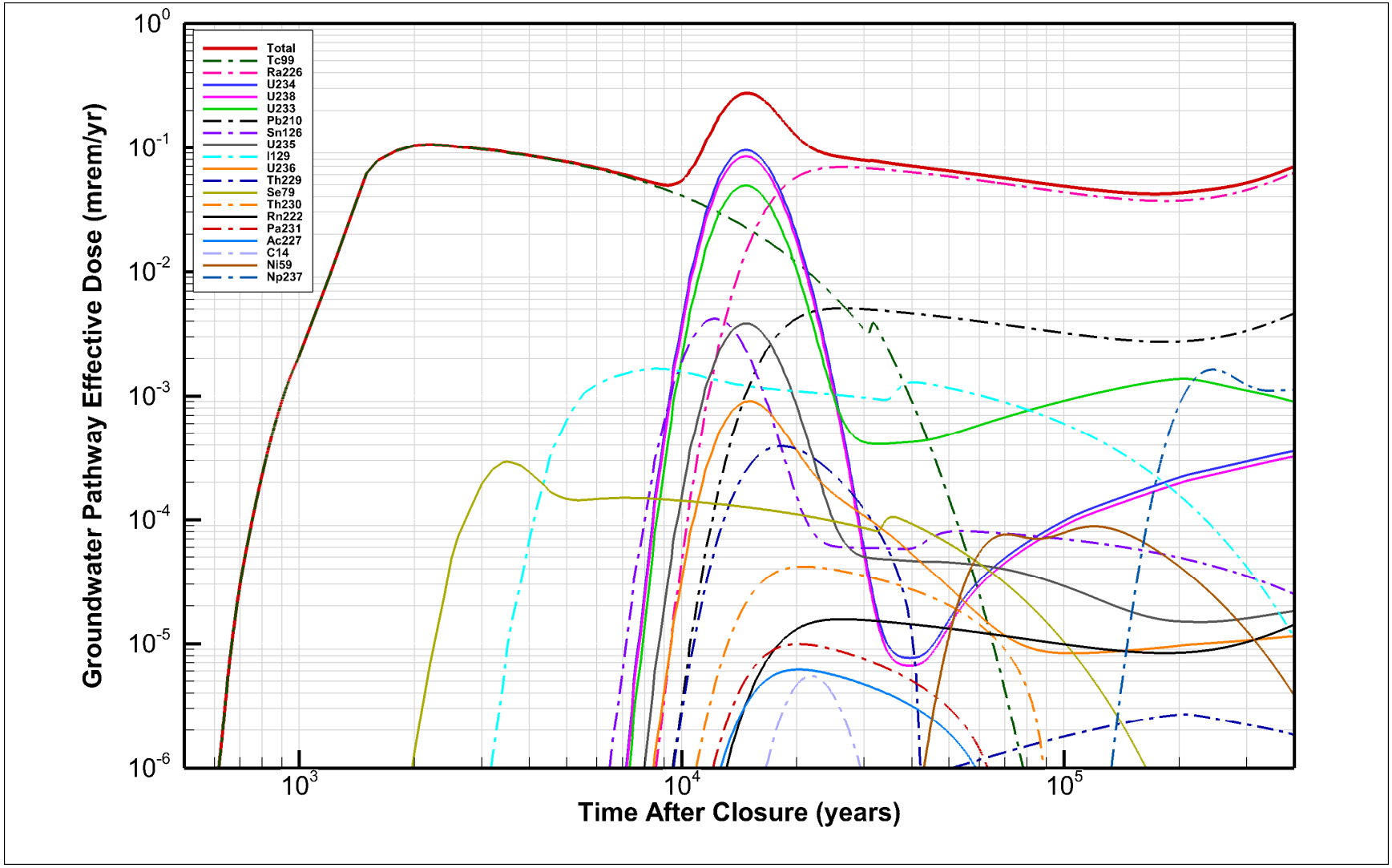

This page intentionally left blank.

9.0 INADVERTENT INTRUDER ANALYSIS

This section presents the analysis of the doses to a hypothetical individual who inadvertently intrudes into tanks or ancillary equipment at WMA C. The analyses were performed in accordance with DOE O 435.1 and DOE M 435.1-1 requirements. Guidance for the inadvertent intruder analysis comes from DOE G 435.1-1, which states the following:

> "Although DOE is committed to retaining control of land containing residual radioactive material, such as disposed low-level waste, it is nonetheless appropriate to consider the impacts of potential inadvertent intrusion. Intrusion should be considered as an accident scenario which could occur during lapses of institutional controls. It is a hypothetical situation assumed simply to provide a basis for determining the acceptability of waste for near-surface disposal and may be used for establishing concentrations of radioactive material in a near-surface disposal facility."

DOE G 435.1-1 states that the development of inadvertent intruder scenarios needs to be consistent with best management practices and other current industry standards, such as those issued by the NCRP and ICRP. In developing these scenarios, a supplemental document to DOE G 435.1-1 provides the following guidance on the groundwater pathway for use in the inadvertent intruder analysis (DOE G 435.1-2):

> "The purpose of this *[the inadvertent intruder]* analysis is to provide a surrogate for the determination of LLW that is acceptable for near-surface disposal. The purpose of this analysis is not to protect future members of the public. As a result, the ingestion of contaminated water need not be considered as part of the inadvertent intruder analysis because protection of water resources is considered explicitly as one of the performance criteria for the performance assessment."

Two types of exposure scenarios are considered to estimate dose to the hypothetical intruder: (1) acute scenarios and (2) chronic scenarios. Acute scenarios evaluate the dose received from well drilling and subsequent exposure to residual waste in the drill cuttings; exposure is evaluated over a short time period. Chronic scenarios evaluate the dose received from spreading the drill cuttings over a specific area while living and/or working on that area. One acute exposure scenario and three chronic exposure scenarios are evaluated in this PA, and brief descriptions of each scenario are provided in Table 9-1. The equations and input parameters are presented in the following sections, but additional details are provided in RPP-ENV-58813. Parameters common to all intruder scenarios are presented in Table 9-2.

Inadvertent intruder dose is calculated at times consistent with regulatory guidance contained in NUREG-1854. NUREG-1854 notes that it is inappropriate to strictly apply the waste classification system in 10 CFR 61.55 to tank farm residual wastes, because the underlying assumptions used in developing the generic waste classification system in 10 CFR 61.55 differ from the site-specific considerations at DOE tank farms. Nevertheless, NUREG-1854 further describes appropriate approaches for evaluating the conditions at DOE tank farms using the logic applied to the development of 10 CFR 61.55. They note that the depth to the waste and the use

of robust intruder barriers are the determining conditions for the type and timing of intruder scenarios. A robust intruder barrier is defined as one that will prevent intrusion into the waste for 500 years.

Table 9-1. Descriptions of the Inadvertent Intruder Scenarios Evaluated in the Waste Management Area C Performance Assessment.

Scenario	Description
Acute Exposure: Well Driller	Dose is the result of drilling through WMA C. Exposure pathways include external exposure, inhalation of soil particulates, and incidental soil ingestion. Exposure occurs during the drilling operation while in contact with the drill cuttings. Exposure does not depend on the borehole diameter.
Chronic Exposure: Rural Pasture	Dose is the result of drilling a well that serves a rural pasture. Contaminated drill cuttings are mixed with the soil over the pasture area. Exposure pathways include external exposure, inhalation of soil particulates, incidental soil ingestion, and milk consumption.
Chronic Exposure: Suburban Garden	Dose is the result of drilling a well that serves a suburban garden. Contaminated drill cuttings are mixed with the soil over the area where a residence and a garden are constructed. Exposure pathways include external exposure, inhalation of soil particulates, incidental soil ingestion, and fruit and vegetable consumption.
Chronic Exposure: Commercial Farm	Dose is the result of drilling a well that serves a commercial farm. Contaminated drill cuttings are mixed with the soil over the commercial farm area. Exposure pathways are external exposure, inhalation of soil particulates, and incidental soil ingestion.

Reference: RPP-ENV-58813, "Exposure Scenarios for Risk and Performance Assessments in Tank Farms at the Hanford Site, Washington."

NUREG-1854 concludes that for wastes at relatively shallow depths without robust intrusion barriers, it is appropriate to carry out the intrusion calculation at the end of institutional control: 100 years. For deeper wastes when robust intruder barriers exist, it is appropriate to assume that intrusion is prevented for at least 500 years, and therefore the intrusion calculation should be carried out at 500 years. For WMA C, these principles are applied by assuming that pipelines do not represent a significant intrusion barrier, and consequently the intrusion calculation is conducted beginning at 100 years after closure (end of institutional control period). By contrast, the tanks and infill grout represent very significant and robust barriers to intrusion, and therefore the intrusion calculation is conducted beginning at 500 years.

These principles are consistent with prior DOE and NRC approaches to evaluating inadvertent intrusion. DOE O 435.1 allows institutional controls to be effective in deterring intrusion for at least 100 years following closure.

Intruder scenarios are evaluated for each of the 19 waste sources (twelve 100-series tanks, four 200 series-tank, CR-vaults, C-301 catch tank and pipe line). The dose calculations are based on the emplaced radionuclide inventory in WMA C (considering radioactive decay and ingrowth), but ignoring any depletion due to transport of radionuclides from the waste site. The best-estimate inventory as mentioned in Tables 3-13a, 3-14a, and 3-15a is used for the intruder dose calculation. For all inadvertent intruder scenarios, the emplaced wastes are assumed to be distributed uniformly throughout the bottom area of the waste source.

Table 9-2. Parameters Common to the Inadvertent Intruder Scenarios.

Parameter	Notation	Value	Unit	Reference
Radionuclide concentration in residual waste	C_{ws}	Isotope-specific	pCi/g	Source term-specific
Soil dry bulk density for soil layers below WMA C	ρ_{sl}	2.05	g/cm^3	Site-specific
Bulk density of residual waste	ρ_{ws}	2.05	g/cm^3	Site-specific
Time of intrusion	t	100 years and 500 years after closure	year	DOE O 435.1
Radionuclide half-life	$t_{1/2}$	Isotope-specific	Year	ICRP 2008
Decay constant	λ	Isotope-specific	(year)$^{-1}$	ICRP 2008
Depth to groundwater	Z_{gw}	7,900	cm	Site-specific
Thickness of wastes intercepted by the borehole	Z_{ws}	Calculated	cm	Source term-specific

DOE = U.S. Department of Energy
ICRP = International Commission on Radiological Protection
WMA = Waste Management Area

References:
DOE O 435.1, Radioactive Waste Management.
"ICRP Publication 107: Nuclear Decay Data for Dosimetric Calculations" (ICRP 2008).

According to RPP-PLAN-47559, there are ~11.2 km (7 mi) of pipelines at WMA C, with the majority of pipelines being pumped waste transfer pipelines (98% by length) and the remaining being gravity-fed cascade lines between the 100-series SSTs (including one known plugged pipeline, V122). The waste transfer pipelines are assumed to be 5% full, while the cascade lines (including pipeline V122) are assumed to be fully plugged and the residual inventory is estimated using average BBI concentration for retrieved tanks (Section 3.2.2.4.4). The waste transfer pipelines are more likely to be intruded as they cover 98% of the total pipeline length and correspondingly the area over which pipelines are distributed within WMA C. Based on assumptions and justifications in RPP-PLAN-47559, intrusion is considered through the 7.6-cm (3-in.)-diameter waste transfer pipeline (the most common pipe diameter) that is assumed to be 5% full of waste. Impact of improbable intrusion through a fully plugged cascade pipeline is evaluated as part of the sensitivity analysis to estimate the bounding dose.

9.1 CONSIDERATION OF THE PROBABILITY OF INTRUSION

As discussed in DOE G 435.1-1, NCRP Report No. 152, and NUREG-1854, the primary purpose of intrusion analyses is to establish waste classification identifying wastes appropriate for near-surface disposal. An intrusion calculation is not intended to represent a realistic calculation of doses to a future member of the public, but rather a stylized representation of hypothetical doses to people living in the future under extreme scenarios of uncertain but generally very low likelihood. The analyses are therefore usually carried out as deterministic calculations assuming

the occurrence of the intrusion event without regard to the likelihood of their occurrence, and the deterministic results have the potential to be misinterpreted as representing a higher risk than they actually do.

Therefore, in this section a qualitative discussion is presented on the likelihood of inadvertent human intrusion at WMA C. This discussion is intended solely to help put intrusion results in a risk-informed context; likelihoods of occurrence are not considered explicitly or included in any further regulatory use of the intrusion analysis results.

The only credible potential intrusion event at WMA C is a drilling intrusion, owing to the depth of the wastes (greater than 5 m after the modified RCRA Subtitle C barrier is put in place) in the final closed facility. For a drilling event to intersect the waste, exhume contamination, and lead to exposures to that contamination, a series of necessary events must occur, as shown in Figure 9-1. These events can generally be regarded as independent, and each can only occur if all of the previous necessary events have occurred. If at any stage of the sequence the necessary event does not occur, the overall intrusion event will not occur. Also shown on the figure are a set of precursor conditions that help to understand the likelihood of occurrence of each necessary event. The precursor conditions relate to issues such as societal change, and motivations and actions of the intruder. As such they are not readily amenable to rigorous probabilistic calculation, but the evolution of each over the post-closure performance period can be qualitatively assessed, supported by logical arguments.

The initial necessary event leading to intrusion is the loss of institutional control. It is reasonable to assume that as long as DOE and the U.S. Government exist, some form of governmental control over the Central Plateau will be maintained as required under DOE P 454.1[1]. Therefore, a precursor condition to the loss of control would be an unforeseen major change in the governance of the United States, to the extent that previously-established administrative controls would be forgotten or deliberately disregarded. Such possibilities are regarded as extremely low over the next 100 years, but moderate over 1,000 years. Such judgments are, of course, a function of the optimism or pessimism with which one regards the future, but the general trend should be for increasing likelihood of such changes over increasing longer time periods.

The second necessary event in the chain is the loss of societal memory of the existence of the Hanford Site, and of waste disposal activities in the Central Plateau. This would involve both loss of individuals' knowledge of the existence of Hanford as well as the loss of relevant records and deed restrictions that would warn future inhabitants of the residual hazards existing under the Central Plateau. The precursor condition for this event is similar to the loss of institutional control: a profound societal change with disruption of the continuity of government. The loss of memory is regarded as less likely than the loss of institutional control, since governmental records of land ownership and deed restrictions are often maintained even when profound changes in governments occur. Nevertheless, as time increases, there is an increasing likelihood that such an event will occur.

[1] This policy specifically states the following: "DOE will maintain the institutional controls as long as necessary to perform their intended protective purposes and seek sufficient funds."

Figure 9-1. Sequence of Events Necessary for Inadvertent Human Intrusion at Waste Management Area C.

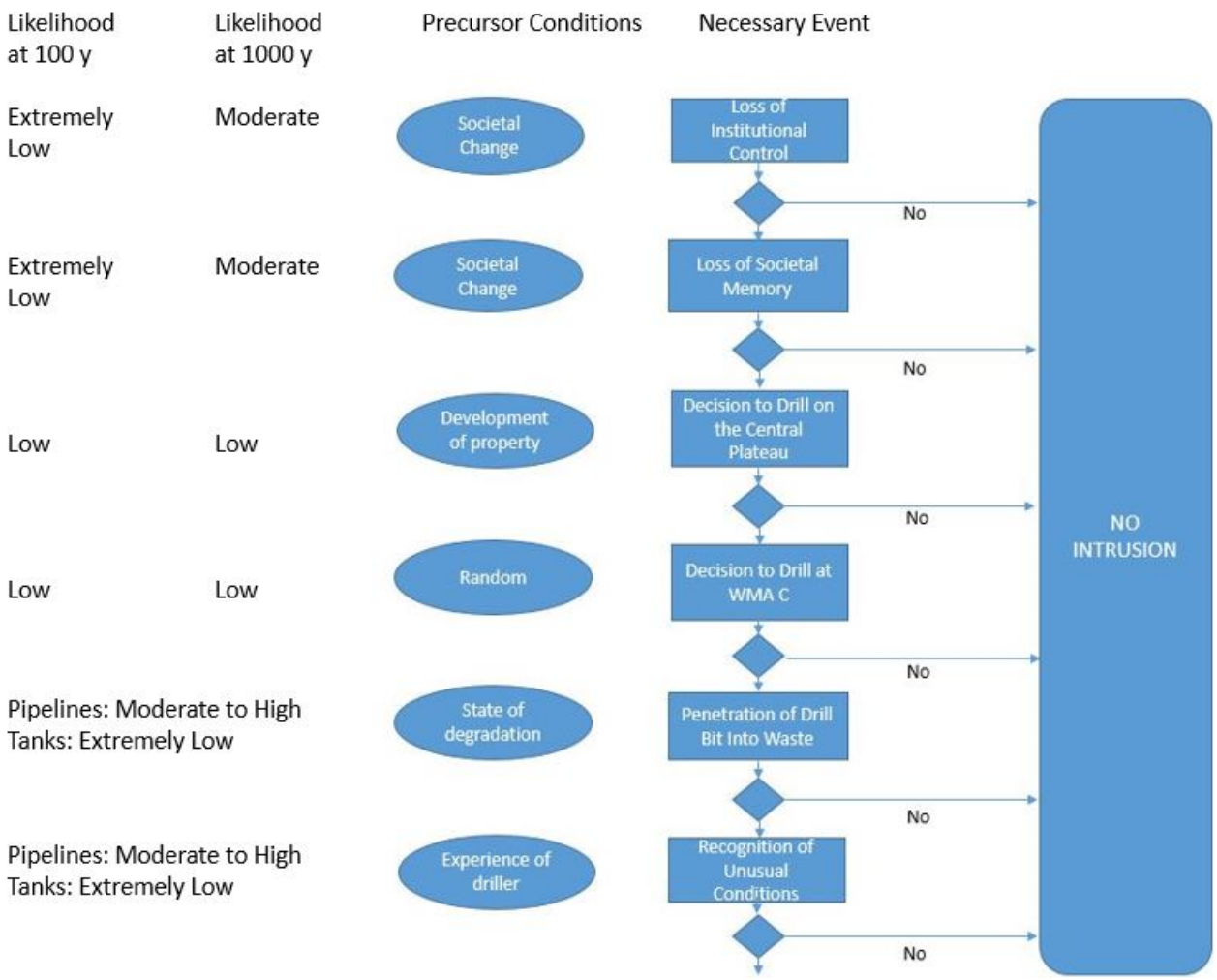

The third necessary event would be a decision to drill on the Central Plateau. The likelihood that this would occur is dependent on the motivation for drilling for water, so the precursor condition is a desire for some sort of property development on the Central Plateau that needs a source of water, such as a housing project or farm. It is also dependent on a desire to drill a local well rather than pump water from the Columbia River. This event is also conditional on the loss of institutional control and memory of Hanford; it is therefore reasonable to assume that in the absence of the Hanford worker base the population of the area would be substantially smaller than today, and would be concentrated closer to the river and focused on agriculture. Given these considerations, the likelihood that this event will occur is considered low; these motivational issues would not necessarily change in time, so it is regarded as low throughout the performance period.

The fourth necessary event would be a decision to drill at WMA C given the previous decision to drill on the Central Plateau, and furthermore to drill in a spot that would intersect residual contamination. In the absence of notable distinguishing features to modify the likelihood across

the Central Plateau, this can be regarded as a purely random decision. Therefore, in this case one could in principle evaluate the probability using the ratios of the area of WMA C to the area of the Central Plateau multiplied by the area of tanks or ancillary equipment over the area of WMA C. This event is the first in the chain of events that allows one to distinguish between the likelihood of intrusion into tanks as opposed to ancillary equipment. This likelihood depends on the definitions of these areas, but is low to extremely low for both tanks and ancillary equipment, and does not change in time.

The fifth necessary event is the penetration of the drill bit into waste. Here there is a clear distinction between drilling into tanks and drilling into ancillary equipment. The conditional likelihood, assuming all the previous events have occurred, of drilling into waste is reasonably high for pipelines, and would increase as the pipelines degrade in time. By contrast, it is extremely low for tanks, owing to the integrity and strength of the structure of the tank and infill grout. There are not expected to be significant changes in the structural integrity of the tanks and grout over the performance period (see Section 6.2.1.2 for estimates of the longevity of tank structures), and the likelihood of intrusion into a tank remains very small until much longer times in the future when the tank and infill grout may be considered degraded.

The sixth and final necessary event would be that the driller would not recognize that the drill had encountered unusual conditions as they drill to the depth of the waste. The conditional likelihood, assuming all the previous events have occurred, of not recognizing that one has hit a pipeline is reasonably high, and would increase as the pipelines degrade in time. By contrast, to reach residual material in a tank one must traverse an extended thickness of unusual material that would be obvious to the driller. The precursor condition for this necessary event to occur would be that the driller would have to be inexperienced or inattentive to not recognize the unusual nature of the tank and grout materials in the well bore. It is regarded as extremely unlikely that someone would not notice this, and would penetrate to the depth of the residual waste. Furthermore, the conditional likelihood of this event would not increase even at very long times when the tank materials may be structurally degraded, because the texture and color of the grout will continue to be easily distinguishable from the surrounding sands for the indefinite future.

Since these events are independent and sequential, one could in principle assign numerical conditional probabilities to each and calculate a joint probability of occurrence of the sequence as the product of the probabilities. Given the speculative and judgmental nature of any assessment of the precursor conditions, using such numerical probabilities is not recommended for this analysis. However, from a qualitative viewpoint, one can say that multiplying six low to extremely low numbers together would give a vanishingly small joint probability of the entire sequence occurring, regardless of the specific assignment of numerical values. It can therefore be concluded that the likelihood of occurrence into tanks at WMA C is vanishingly small, while the likelihood of intrusion into a pipeline is also very small, but somewhat larger than for tanks.

9.2 ACUTE EXPOSURE SCENARIOS

A single acute hypothetical inadvertent intruder exposure scenario is evaluated for the WMA C tank farm PA. This scenario evaluates the short-term exposure of a well driller to drill cuttings

that are exhumed from a well that is installed to the depth of the water table for the supply of water. As the well is drilled through the WMA C tank farm waste residuals, the driller will be exposed to the radiation dose from the drill cuttings. The well driller is assumed to be exposed to drill cuttings for a total of five days (8 hours per day for a total of 40 hours). The dose is calculated by assuming that the cuttings are uniformly spread across the drill pad and are not diluted by mixing with clean soil. As discussed above, the timing of the intrusion event is assumed to be 100 years for pipelines and 500 years for more highly stabilized wastes with robust intrusion barriers.

The borehole diameter is not a factor in determining dose for this scenario because the radionuclide concentrations in the drill cuttings are independent of the size of the borehole, and because the cuttings are assumed to be distributed over the drill pad with no mixing with clean soil. For the purpose of calculating dose from external exposure, the thickness and lateral extent of the contaminated layer is assumed to be infinite. Exposure pathways evaluated for the well driller scenario are incidental soil ingestion, inhalation of soil particulates, and direct external exposure as illustrated in Figure 9-2. Exposure parameters for the acute well driller scenario are provided in Table 9-3. Radionuclide-specific shielding factors and dose conversion factors are presented in Section 6.3.3, Tables 6-24 and 6-25, respectively.

Figure 9-2. Exposure Pathways Considered in the Inadvertent Intruder Acute Well Driller Scenario.

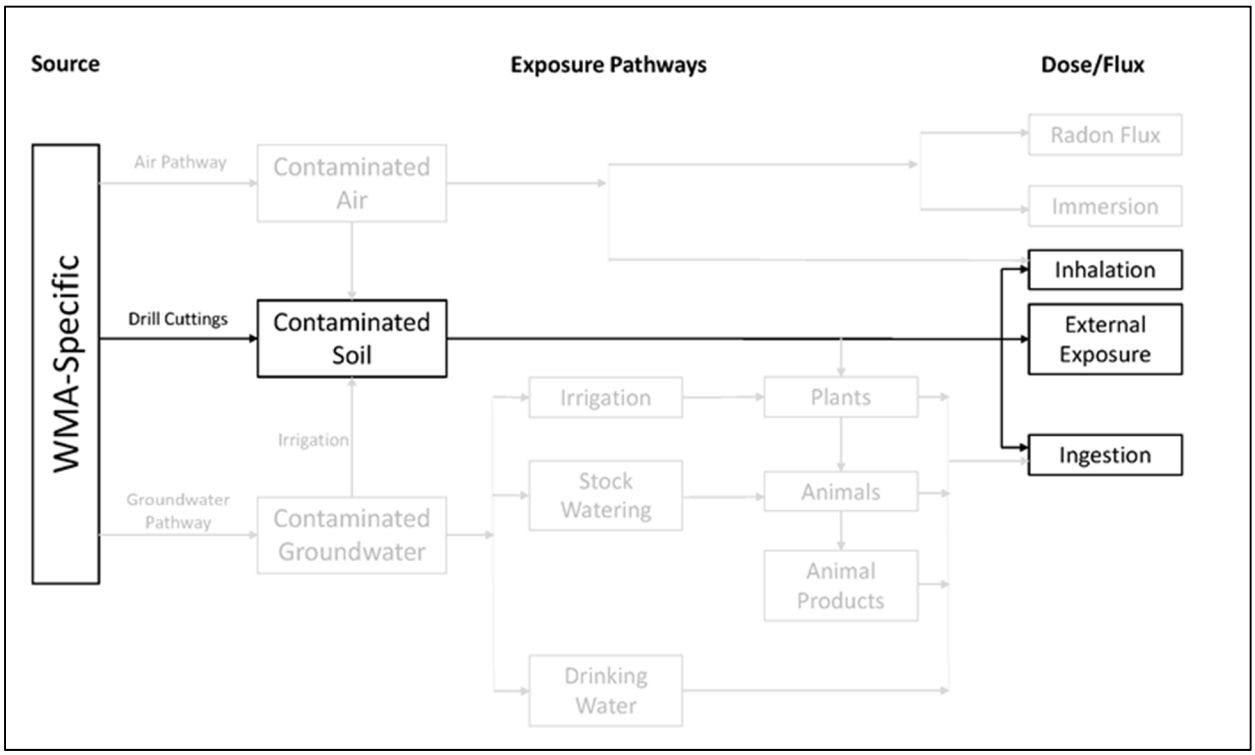

WMA = Waste Management Area

The intruder dose scenario is applied to an adult receptor but the dose conversion factors are derived for a Representative Person (Section 6.3.3.1). This is a conservative simplification

because these dose conversion factors represent effective dose coefficients calculated for a Reference Person and are generally marginally greater than that for the adult.

Table 9-3. Exposure Parameters for the Acute Well Driller Exposure Scenario.

Parameter	Notation	Value	Units	Reference
Radionuclide concentration in drill cuttings	C_{ds}	Calculated	pCi/g	—
Area of the well	A_{well}	1,379.51	cm^2	HNF-SD-WM-TI-707, Rev. 5
Diameter of the well	D_{well}	41.91	cm	HNF-SD-WM-TI-707, Rev. 5
Soil ingestion rate – well driller	$IR_{s,wd}$	100	mg/day	OSWER Directive 9285.6-03
Exposure frequency – well driller	EF_{wd}	5	days/yr	HNF-SD-WM-TI-707, Rev. 5
Enrichment factor	Ef	4	unitless	NCRP Report No. 129
Outdoor inhalation rate – well driller	$INH_{out,wd}$	12,775	m^3/yr	NCRP Report No. 129
Mass loading factor	M	6.66E-05	g/m^3	ICRP 1994
Fraction of time spent outdoors	$t_{out,wd}$	0.0046	unitless	HNF-SD-WM-TI-707, Rev. 5 (40 hours in a year)
Unit conversion factor	UCF_1	0.001	g/mg	0.001 g = 1 mg

ICRP = International Commission on Radiological Protection NCRP = National Council on Radiation Protection

References:
HNF-SD-WM-TI-707, "Exposure Scenarios and Unit Factors for the Hanford Tank Waste Performance Assessment."
"ICRP Publication 66: Human Respiratory Tract Model for Radiological Protection" (ICRP 1994).
NCRP Report No. 129, "Recommended Screening Limits for Contaminated Surface Soil and Review of Factors Relevant to Site-Specific Studies."
OSWER Directive 9285.6-03, Risk Assessment Guidance for Superfund, Volume I: Human Health Evaluation Manual, Supplemental Guidance "Standard Default Exposure Factors" Interim Final.

9.2.1 Radionuclide Concentration in Drill Cuttings

Radionuclide concentrations in the drill cuttings are calculated as shown in Equations 9-1 through 9-3 (RPP-ENV-58813).

$$A_{well} = \pi \times \left(\frac{d_{well}}{2}\right)^2 \tag{9-1}$$

$$C_{ds} = \frac{C_{ws} \times A_{well} \times Z_{ws} \times \rho_{ws}}{A_{well} \times Z_{ws} \times \rho_{ws} + A_{well} \times (Z_{gw} - Z_{ws}) \times \rho_{sl}} = \frac{C_{ws} \times Z_{ws} \times \rho_{ws}}{Z_{ws} \times \rho_{ws} + (Z_{gw} - Z_{ws}) \times \rho_{sl}} \tag{9-2}$$

Because bulk density of residual waste and the soil is very similar, to simplify the equations it is assumed that $\rho_{ws} = \rho_{sl}$. As a result, the above equation simplifies to:

$$C_{ds} = \frac{C_{ws} \times Z_{ws}}{Z_{gw}} \tag{9-3}$$

Where:

A_{well} = area of well (cm^2)
d_{well} = diameter of well (cm)
C_{ds} = radionuclide concentration in drill cuttings (pCi/g)
C_{ws} = radionuclide concentration in the residual waste (pCi/g), varies as a function of time due to radioactive decay and ingrowth
Z_{ws} = thickness of waste intercepted by borehole (cm)
ρ_{ws} = residual waste bulk density (g/cm^3)
Z_{gw} = depth to groundwater (cm)
ρ_{sl} = soil dry bulk density for soil layers below WMA C (g/cm^3).

The following sections provide the equations used to calculate dose for this scenario.

9.2.2 Acute Well Driller Scenario – Incidental Soil Ingestion

The following equation is used to calculate dose to the well driller resulting from incidental ingestion of soil (RPP-ENV-58813):

$$D_s = C_{ds} \times IR_{s,wd} \times EF_{wd} \times UCF_1 \times DCF_{ing} \quad (9\text{-}4)$$

Where:

D_s = dose resulting from incidental soil ingestion (mrem/yr)
C_{ds} = radionuclide concentration in drill cuttings (pCi/g)
$IR_{s,wd}$ = soil ingestion rate – well driller (mg/day)
EF_{wd} = exposure frequency – well driller (days/yr)
UCF_1 = unit conversion factor (g/mg)
DCF_{ing} = ingestion dose conversion factor (mrem/pCi).

9.2.3 Acute Well Driller Scenario – Inhalation of Soil Particulates

The following equation is used to calculate dose to the well driller resulting from inhalation of soil particulates (RPP-ENV-58813):

$$D_{inh} = C_{ds} \times E_f \times INH_{out,wd} \times M \times t_{out,wd} \times DCF_{inh} \quad (9\text{-}5)$$

Where:

D_{inh} = dose resulting from inhalation of soil (mrem/yr)
C_{ds} = radionuclide concentration in drill cuttings (pCi/g)
E_f = enrichment factor (unitless)
$INH_{out,wd}$ = outdoor inhalation rate – well driller (m^3/yr)
M = mass loading factor (g/m^3)

$t_{out,wd}$ = fraction of time spent outdoors – well driller (unitless)
DCF_{inh} = inhalation dose conversion factor (mrem/pCi).

9.2.4 Acute Well Driller Scenario – External Exposure

The following equation is used to calculate dose to the well driller resulting from external exposure (RPP-ENV-58813):

$$D_{ext} = C_{ds} \times t_{out,wd} \times DCF_{ext} \tag{9-6}$$

Where:

D_{ext} = dose resulting from external exposure to drill cuttings (mrem/yr)
C_{ds} = radionuclide concentration in drill cuttings (pCi/g)
$t_{out,wd}$ = fraction of time spent outdoors by well driller (unitless)
DCF_{ext} = external exposure dose conversion factor (mrem/yr)/(pCi/g).

9.3 CHRONIC SCENARIOS

Three chronic hypothetical inadvertent intruder exposure scenarios are evaluated for the WMA C tank farm PA which are representative of lifestyles in and around the Hanford Site. These scenarios evaluate the long-term exposure of three different receptors from previously exhumed drill cuttings that have been uniformly spread and tilled onto three different land areas or target fields. The three different target fields include the following: a rural pasture, a suburban garden, and a commercial farm. Radionuclide concentrations in the target field are dependent on the diameter of the well that is drilled to support the scenario, the area of the target field over which the drill cuttings are spread, and the depth to which the drill cuttings are tilled into the soil. In the chronic scenarios, the exposed individual does not drill or add the cuttings to the soil but simply lives or works on the land where the cuttings have been spread and tilled into the soil.

Based on well log data from the State of Washington from 1960 to 2003, the diameter of boreholes can range from 2.5 cm (1 in.) up to 76 cm (30 in.), with about 70% of the domestic water wells having about a 16.5-cm (6.5-in.) diameter (HNF-SD-WM-TI-707, "Exposure Scenarios and Unit Factors for the Hanford Tank Waste Performance Assessment"). Although a 16.5-cm (6.5-in.) well diameter may be common, it is not considered representative for the target fields in each scenario. Although irrigation of a rural pasture is a small-scale operation, it typically requires a larger diameter well because a larger pump is needed as compared to a normal well that is used for domestic purposes. Therefore, a well diameter of 26.67 cm (10.5 in.) was selected for the rural pasture scenario, and a 16.5-cm (6.5-in.) well diameter was selected for the suburban garden scenario. Similarly, a commercial farm using irrigation would require a larger diameter well than the rural pasture to extract water at a higher flow rate. As a result, a well diameter of 41.91 cm (16.5 in.) was selected for the commercial farm scenario. The size of target fields also varies over a broad range. The sizes of the target fields selected are 5,000 m^2 (1.24 acre) for the rural pasture scenario, 2,500 m^2 (0.62 acre) for the suburban garden scenario, and 64,750,000 m^2 (160 acre) for the commercial farm scenario (HNF-SD-WM-TI-707). In

selecting the well diameters and target field areas, characteristics specific to the Hanford Site and values selected from previous PAs were considered. Sensitivity analyses provide confidence that the calculated performance parameters are robust enough to support sound decisions.

The intruder dose scenario is applied to an adult receptor but the dose conversion factors are derived for a Representative Person (Section 6.3.3.1). This is a conservative simplification because these dose conversion factors represent effective dose coefficients calculated for a Reference Person and are generally marginally greater than that for the adult. The various exposure parameters used in the dose calculations were selected from DOE and EPA guidance documents, and from national and international standards such as the NCRP and ICRP, as appropriate for an adult. The exposure pathways are determined by the use of the target field.

9.3.1 Chronic Rural Pasture Scenario

The rural pasture scenario evaluates the long-term exposure to an individual who uses the target field as a residence, with a pasture used for milk production from dairy cows. In this scenario, a well diameter of 26.67 cm (10.5 in.) is assumed, the drill cuttings are spread over a pasture area of 5,000 m^2 (1.24 acre), and the cuttings are tilled to a depth of 15 cm (5.9 in.). This scenario represents an individual who resides and has a pasture on the target field area. The pasture is used to raise dairy cattle that eat fodder grown from the pasture, and the resident subsequently drinks the pasture cows' milk. In addition to exposure from milk consumption, the resident is exposed by incidental soil ingestion, inhalation of the soil particulates, and external exposure; these exposure pathways are illustrated in Figure 9-3. Exposure parameters for the chronic rural pasture scenario are provided in Table 9-4. Element-specific bioconcentration factors, radionuclide-specific shielding factors, and dose conversion factors are presented in Section 6.3.3, Tables 6-23, 6-24 and 6-25, respectively.

9.3.1.1 Radionuclide Activity in Drill Cuttings. The concentration of radionuclides in pasture soil resulting from the drill cuttings is determined by first calculating the activity of each radionuclide in the drill cuttings, and then calculating the radionuclide concentration in the pasture soil. Equation 9-7 and Equation 9-8 are used to calculate the radionuclide activities and radionuclide concentrations for all three of the chronic scenarios. The differences in radionuclide activities for each scenario are the well diameters and the depth that the drill cuttings are tilled into the soil of the target field (rural pasture, suburban garden, or commercial farm).

The following equation is used to calculate the total radionuclide activity in the drill cuttings (RPP-ENV-58813):

$$S_A = T_A \times \left(\frac{A_{well}}{A_{source_term}}\right) \tag{9-7}$$

Where:

S_A = radionuclide activity in drill cuttings (pCi) at any given time

T_A = residual radionuclide activity in the source term (pCi), varies with time due to radioactive decay and ingrowth

A_{well} = area of the well (cm^2)
A_{source_term} = area over which the residual waste is spread in the source term (cm^2).

Figure 9-3. Exposure Pathways Considered for the Inadvertent Intruder Chronic Rural Pasture Exposure Scenario.

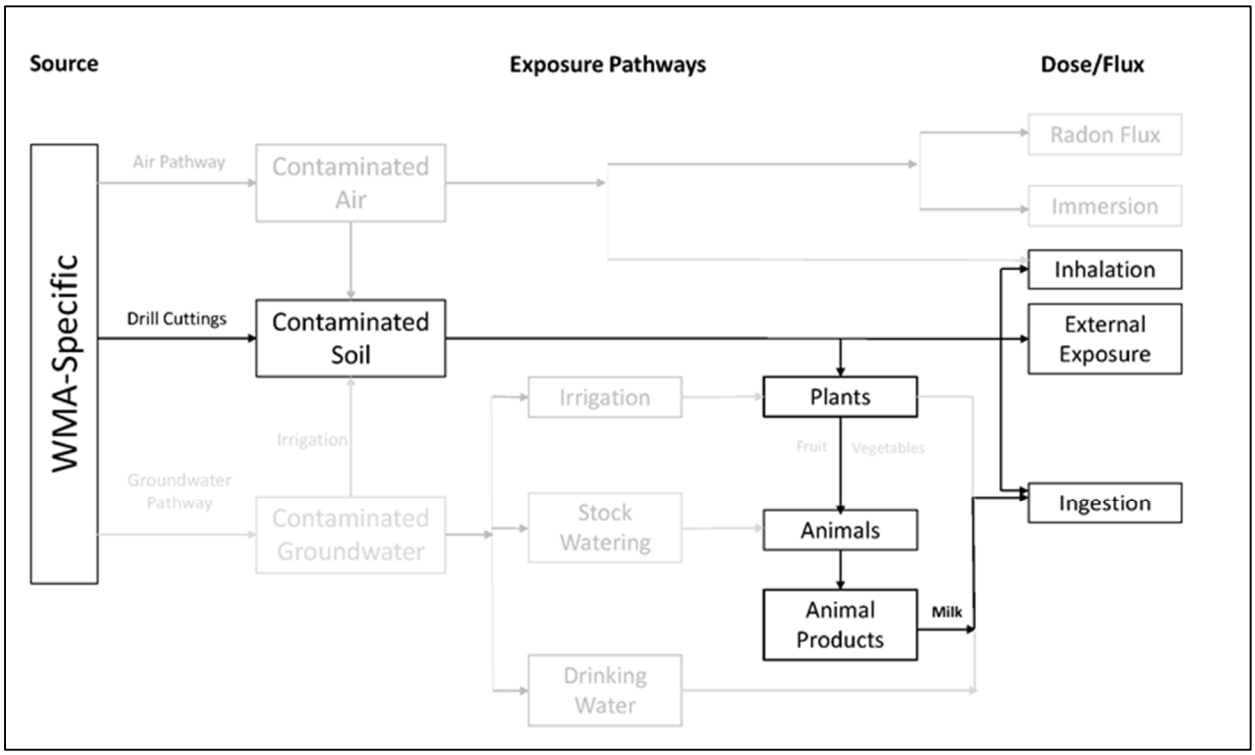

WMA = Waste Management Area

For the pipeline source term, the activity in the drill cuttings is based on the contaminated pipeline area that is interrogated by the borehole. If the borehole diameter is greater than the pipeline diameter, then the width of the contaminated zone is restricted to the pipeline diameter.

9.3.1.2 Radionuclide Concentrations in Pasture Soil. The following equation is used to calculate the radionuclide concentration in the pasture soil (RPP-ENV-58813):

$$C_{ps} = \frac{S_A}{A_p \times Z_p \times \rho_p + A_{well} \times Z_{gw} \times \rho_s} \tag{9-8}$$

Where:

C_{ps} = radionuclide concentration in pasture soil (pCi/g) at any given time
S_A = radionuclide activity in soil from drill cuttings (pCi/g) at any given time
A_p = area of the pasture (cm^2)
Z_p = depth the drill cuttings are tilled into the pasture (cm)
ρ_p = soil dry bulk density in the pasture (g/cm^3)
A_{well} = area of the well (cm^2)

Z_{gw} = depth to groundwater (cm)
ρ_s = dry bulk density of the drill cuttings (g/cm^3).

Table 9-4. Exposure Parameters for the Chronic Rural Pasture Exposure Scenario. (2 sheets)

Parameter	Notation	Value	Units	Reference
Area over which residual waste is spread	A_{source_term}	Calculated	cm^2	Source term-specific
Area of the well	A_{well}	558.6	cm^2	HNF-SD-WM-TI-707, Rev. 5
Diameter of the well	D_{well}	26.67	cm	HNF-SD-WM-TI-707, Rev. 5
Area of rural pasture	A_p	5.00E+07	cm^2	HNF-SD-WM-TI-707, Rev. 5
Tilled depth of rural pasture	Z_p	15	cm	HNF-SD-WM-TI-707, Rev. 5
Soil ingestion rate – resident	$IR_{s,rp}$	100	mg/day	OSWER Directive 9285.6-03
Exposure frequency – resident	EF_{rp}	350	days/yr	OSWER Directive 9285.6-03
Milk ingestion rate	IR_m	155.96	L/yr	EPA/600/R-090/052F
Fraction of locally-produced dairy products that are consumed	F_a	1	unitless	PRGfR 2015
Water ingestion rate for dairy cattle	$IR_{w,d}$	92	L/day	PRGfR 2015
Radionuclide concentration in water consumed by dairy cattle	C_w	0	pCi/L	No groundwater contamination assumed
Soil ingestion rate for dairy cattle	$IR_{s,d}$	0.41	kg/day	PRGfR 2015
Radionuclide concentration in pasture soil consumed by dairy cattle	C_{ps}	Isotope-specific	pCi/g	Source term-specific
Fodder ingestion rate for dairy cattle	$IR_{fodder,d}$	16.9	kg/day	PRGfR 2015
Pasture-soil bioconcentration factor through uptake	B_p	Isotope-specific	(pCi/kg dry weight of crop)/(pCi/kg dry weight of soil)	See Table 6-23
Pasture-soil bioconcentration factor from resuspension processes	B'_p	0.1	(pCi/kg dry weight of crop)/(pCi/kg dry weight of soil)	NCRP Report No. 129

Table 9-4. Exposure Parameters for the Chronic Rural Pasture Exposure Scenario. (2 sheets)

Parameter	Notation	Value	Units	Reference
Enrichment factor	E_f	0.7	unitless	NCRP Report No. 129
Indoor inhalation rate – resident	$INH_{in,r}$	7,300	m^3/yr	NCRP Report No. 129
Mass loading factor	M	6.66E-05	g/m^3	NCRP Report No. 129
Fraction of time spent indoors – rural pasture	$t_{in,rp}$	0.656	unitless	PRGfR 2015 (16.42 hours per day, 350 days per year)
Outdoor inhalation rate – rural pasture	INH_{out_rp}	9,125	m^3/yr	NCRP Report No. 129
Fraction of time spent outdoors – rural pasture	t_{out}	0.16	unitless	HNF-SD-WM-TI-707, Rev. 5 (4 hours per day, 350 days per year)
Ratio of radionuclide concentrations in indoor versus outdoor air	I/O	0.3	unitless	NCRP Report No. 129
Unit conversion factor	UCF_1	0.001	g/mg	0.001 g = 1 mg
Unit conversion factor	UCF_2	1,000	g/kg	1,000 g = 1 kg

NCRP = National Council on Radiation Protection

References:
EPA/600/R-090/052F, Exposure Factors Handbook: 2011 Edition.
HNF-SD-WM-TI-707, "Exposure Scenarios and Unit Factors for the Hanford Tank Waste Performance Assessment."
NCRP Report No. 129, "Recommended Screening Limits for Contaminated Surface Soil and Review of Factors Relevant to Site-Specific Studies."
OSWER Directive 9285.6-03, Risk Assessment Guidance for Superfund, Volume I: Human Health Evaluation Manual, Supplemental Guidance "Standard Default Exposure Factors" Interim Final.
Preliminary Remediation Goals for Radionuclides (PRGfR), Queried 07/2015, [PRG User's Guide], http://epa-prgs.ornl.gov/radionuclides/prg_guide.html.

9.3.1.3 Chronic Rural Pasture Scenario – Incidental Soil Ingestion. The following equation is used to calculate dose to the rural pasture resident resulting from incidental ingestion of pasture soil (RPP-ENV-58813):

$$D_s = C_{ps} \times IR_{s,rp} \times EF_{rp} \times UCF_1 \times DCF_{ing} \quad (9\text{-}10)$$

Where:

D_s = dose resulting from incidental soil ingestion (mrem/yr)
C_{ps} = radionuclide concentration in pasture soil (pCi/g) at any given time
$IR_{s,rp}$ = soil ingestion rate – rural pasture (mg/day)
EF_{rp} = exposure frequency – rural pasture (days/yr)

UCF_1 = unit conversion factor (g/mg)
DCF_{ing} = ingestion dose conversion factor (mrem/pCi).

9.3.1.4 Chronic Rural Pasture Scenario – Consumption of Milk. The following equations are used to calculate the concentration of contaminant in livestock fodder, the concentration of contaminant in milk, and the dose from consumption of milk (RPP-ENV-58813).

The equation used to calculate the concentration of contaminant in livestock fodder is given by:

$$C_{fodder} = C_{ps} \times (B_p + B'_p) \tag{9-11}$$

Where:

C_{fodder} = radionuclide concentration in livestock fodder (pCi/g) at any given time
C_{ps} = radionuclide concentration in the pasture soil (pCi/g) at any given time
B_p = pasture-soil bioconcentration factor through uptake $\left(\frac{\left(\frac{pCi}{kg\ dry\ weight\ of\ fodder}\right)}{\left(\frac{pCi}{kg\ dry\ weight\ of\ soil}\right)}\right)$
B'_p = pasture-soil bioconcentration factor for resuspension effects $\left(\frac{\left(\frac{pCi}{kg\ dry\ weight\ of\ fodder}\right)}{\left(\frac{pCi}{kg\ dry\ weight\ of\ soil}\right)}\right)$.

The following equation is used to calculate the concentration of contaminant in milk resulting from consumption of contaminated water (if any), contaminated fodder, and contaminated soil by the dairy animal:

$$C_m = \left(C_w \times IR_{w,d} + C_{fodder} \times IR_{fodder,d} \times UCF_2 + C_{ps} \times IR_{s,d} \times UCF_2\right) \times BCF_{milk} \tag{9-12}$$

Where:

C_m = radionuclide concentration in milk (pCi/L) at any given time
C_w = radionuclide concentration in water (pCi/L) at any given time (assumed zero for the intruder scenario)
$IR_{w,d}$ = ingestion rate of water by dairy cattle (L/day)
$IR_{fodder,d}$ = ingestion rate of fodder by dairy cattle (kg/day)
UCF_2 = unit conversion factor (g/kg)
C_{ps} = radionuclide concentration in the pasture soil (pCi/g) at any given time
$IR_{s,d}$ = ingestion rate of soil by dairy cattle (kg/day)
BCF_{milk} = bioconcentration factor of radionuclides in milk (day/L).

The equation used to calculate the dose from ingestion of milk is given by:

$$D_m = C_m \times IR_m \times F_a \times DCF_{ing} \tag{9-13}$$

Where:

D_m = dose resulting from ingestion of milk (mrem/yr)
C_m = radionuclide concentration in milk (pCi/L) at any given time
IR_m = milk ingestion rate (L/yr)
F_a = fraction of locally-produced milk that is consumed (unitless)
DCF_{ing} = ingestion dose conversion factor (mrem/pCi).

9.3.1.5 Chronic Rural Pasture Scenario – Inhalation of Soil Particulates. The following equation is used to calculate dose to the rural pasture resident resulting from inhalation of dust particulates (RPP-ENV-58813):

$$D_{inh} = C_{ps} \times E_f \times M \times \left(INH_{in,rp} \times t_{in,rp} \times \left(\frac{I}{O}\right) + INH_{out,rp} \times t_{out,rp}\right) \times DCF_{inh} \quad (9\text{-}14)$$

Where:

D_{inh} = dose resulting from inhalation of soil
C_{ps} = the radionuclide concentration in the pasture soil surface layer (pCi/g)
E_f = enrichment factor (unitless)
M = mass loading factor (g/m^3)
$INH_{in,rp}$ = indoor inhalation rate – rural pasture (m^3/yr)
$t_{in,rp}$ = fraction of time spent indoors – rural pasture (unitless)
$\frac{I}{O}$ = ratio of radionuclide concentrations in indoor and outdoor air (unitless)
$INH_{out,rp}$ = outdoor inhalation rate – rural pasture (m^3/yr)
$t_{out,rp}$ = fraction of time spent outdoors – rural pasture (unitless)
DCF_{inh} = inhalation dose conversion factor (mrem/pCi).

9.3.1.6 Chronic Rural Pasture Scenario – External Exposure. The following equation is used to calculate dose to the rural pasture resident resulting from external exposure (RPP-ENV-58813):

$$D_{ext} = C_{ps} \times \left(t_{in,rp} \times \varepsilon + t_{out,rp}\right) \times DCF_{ext} \quad (9\text{-}15)$$

Where:

D_{ext} = dose resulting from external exposure to pasture soil (mrem/yr)
C_{ps} = radionuclide concentration in the pasture soil (pCi/g) at any given time
$t_{in,rp}$ = fraction of time spent indoors – rural pasture (unitless)
ε = transmission or shielding factor (unitless)
$t_{out,rp}$ = fraction of time spent outdoors – rural pasture (unitless)
DCF_{ext} = external exposure dose conversion factor (mrem/yr)/(pCi/g).

9.3.2 Chronic Suburban Garden Scenario

The suburban garden scenario evaluates the long-term exposure to an individual who uses the target field as a home construction lot with a garden. In this scenario, a well diameter of 16.51 cm (6.5 in.) is assumed that was drilled prior to the construction of the house and garden, and the drill cuttings are spread over the 2,500-m^2 (0.62-acre) lot and tilled to a depth of 15 cm (5.9 in.). The size of the home garden was chosen to be 100 m^2 (1,076 ft^2) based on the discussions presented in Revision 5 of HNF-SD-WM-TI-707, where this garden size was deemed reasonable to provide 25% of the daily vegetable diet for a family of four living in the home. In addition to exposure from fruit and vegetable consumption, the resident is exposed by incidental soil ingestion, inhalation of the soil particulates, and external exposure; these exposure pathways are illustrated in Figure 9-4. Exposure parameters for the chronic suburban garden scenario are provided in Table 9-5.

Figure 9-4. Exposure Pathways Considered in the Inadvertent Intruder Chronic Suburban Garden Exposure Scenario.

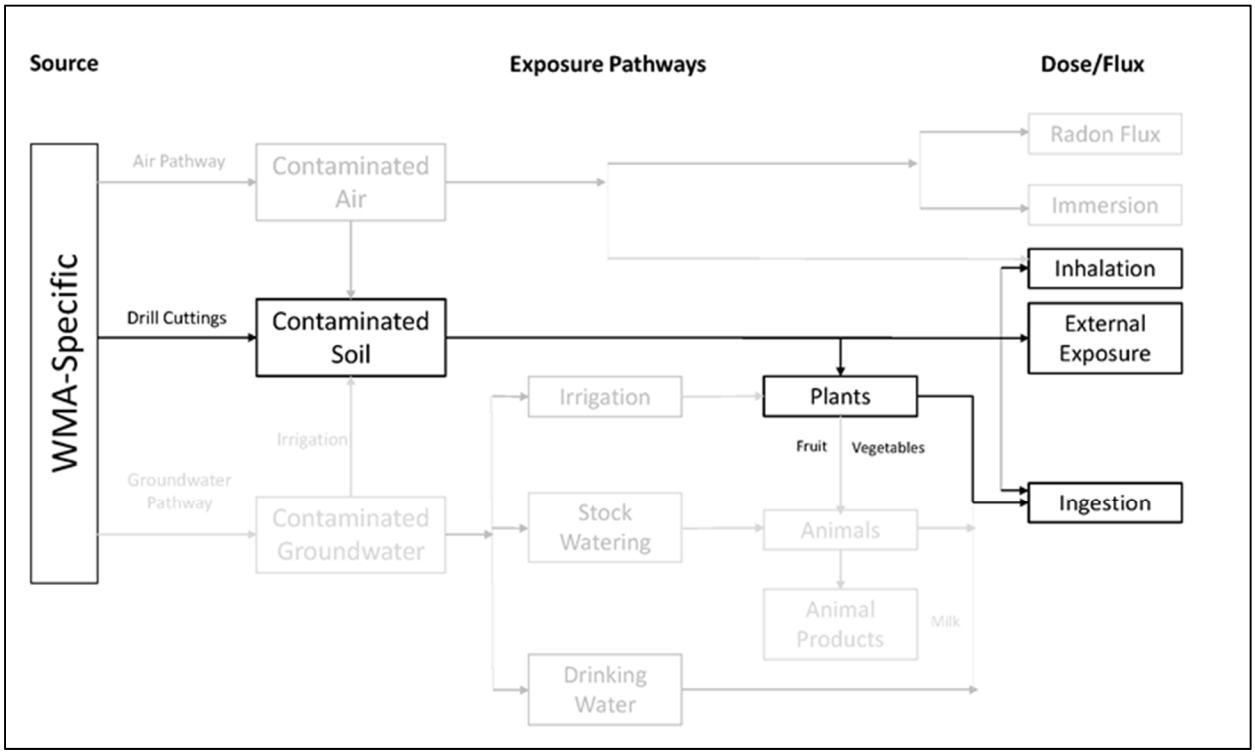

WMA = Waste Management Area

As discussed in Section 9.3.1.1, Equation 9-7 is used to calculate the radionuclide activities, and Equation 9-8 is used to calculate the radionuclide concentrations for the suburban garden scenario (C_{gs}), with corresponding well area and target field area (home construction lot). Element-specific bioconcentration factors, radionuclide-specific shielding factors, and dose conversion factors are presented in Section 6.3.3, Tables 6-23, 6-24 and 6-25 respectively.

Table 9-5. Exposure Parameters for the Chronic Suburban Garden Exposure Scenario. (2 sheets)

Parameter	Notation	Value	Units	Reference
Radionuclide concentration in garden soil	C_{gs}	Calculated	pCi/g	Equation 9-8
Area over which residual waste is spread	A_{source_term}	Calculated	cm^2	Source term-specific
Diameter of the well	D_{well}	16.51	cm	HNF-SD-WM-TI-707, Rev. 5
Area of the well	A_{well}	214.08	cm^2	Calculated
Area of home construction lot (target field)	A_{tf}	25,000,000	cm^2	HNF-SD-WM-TI-707, Rev. 5
Tilled depth of garden	Z_g	15	cm	HNF-SD-WM-TI-707, Rev. 5
Soil ingestion rate – suburban garden	$IR_{s,sg}$	100	mg/day	OSWER Directive 9285.6-03
Exposure frequency – resident	EF_{sg}	350	day/yr	OSWER Directive 9285.6-03
Crop (fruit and vegetables) ingestion rate	IR_c	106.51	kg/yr	PRGfR 2015
Crop-soil bioconcentration factor from uptake	B_v	Element-specific	(pCi/kg fresh wt crop)/ (pCi/kg dry wt soil)	NCRP Report No. 129
Crop-soil bioconcentration factor from resuspension/ soil adhesion	B_v'	0.004	(pCi/kg fresh wt crop)/ (pCi/kg dry wt soil)	NCRP Report No. 129
Fraction of locally-produced crop (fruit and vegetables) that are consumed	F_v	0.25	unitless	EPA/600/P-95/002Fa
Enrichment factor	E_f	0.7	unitless	NCRP Report No. 129
Indoor inhalation rate – suburban garden	$INH_{in,sg}$	7,300	m^3/yr	NCRP Report No. 129
Mass loading factor	M	6.66E-05	g/m^3	ICRP 1994
Fraction of time spent indoors – suburban garden	$t_{in,sg}$	0.656	unitless	PRGfR 2015 (16.42 hours per day, 350 days per year)
Outdoor inhalation rate – suburban garden	$INH_{out,sg}$	9,125	m^3/yr	NCRP Report No. 129
Fraction of time spent outdoors	$t_{out,sg}$	0.080	unitless	HNF-SD-WM-TI-707, Rev. 5 (2 hours per day, 350 days per year)

Table 9-5. Exposure Parameters for the Chronic Suburban Garden Exposure Scenario. (2 sheets)

Parameter	Notation	Value	Units	Reference
Ratio of radionuclide concentrations in indoor versus outdoor air	I/O	0.3	unitless	NCRP Report No. 129
Unit conversion factor	UCF_1	0.001	g/mg	0.001 g = 1 mg
Unit conversion factor	UCF_2	1,000	g/kg	1,000 g = 1 kg

ICRP = International Commission on Radiological Protection NCRP = National Council on Radiation Protection

References:
EPA/600/P-95/002Fa, Exposure Factors Handbook Volume 1: General Factors.
EPA/600/R-090/052F, Exposure Factors Handbook: 2011 Edition.
HNF-SD-WM-TI-707, "Exposure Scenarios and Unit Factors for the Hanford Tank Waste Performance Assessment."
"ICRP Publication 66: Human Respiratory Tract Model for Radiological Protection" (ICRP 1994).
NCRP Report No. 129, "Recommended Screening Limits for Contaminated Surface Soil and Review of Factors Relevant to Site-Specific Studies."
OSWER Directive 9285.6-03, Risk Assessment Guidance for Superfund, Volume I: Human Health Evaluation Manual, Supplemental Guidance "Standard Default Exposure Factors" Interim Final.
Preliminary Remediation Goals for Radionuclides (PRGfR), Queried 07/2015, [PRG User's Guide], http://epa-prgs.ornl.gov/radionuclides/prg_guide.html.

9.3.2.1 Chronic Suburban Garden Scenario – Incidental Soil Ingestion. The following equation is used to calculate dose to the suburban garden resident resulting from incidental ingestion of garden soil (RPP-ENV-58813):

$$D_s = C_{gs} \times IR_{s,sg} \times EF_{sg} \times UCF_1 \times DCF_{ing} \tag{9-16}$$

Where:

D_s = dose resulting from incidental soil ingestion (mrem/yr)
C_{gs} = radionuclide concentration in garden soil (pCi/g)
$IR_{s,sg}$ = soil ingestion rate – suburban garden (mg/day)
EF_{sg} = exposure frequency – resident (days/yr)
UCF_1 = unit conversion factor (g/mg)
DCF_{ing} = ingestion dose conversion factor (mrem/pCi).

9.3.2.2 Chronic Suburban Garden Scenario – Consumption of Homegrown Crops (Fruits and Vegetables). The following equations are used to calculate the concentration of contaminant in the crop (homegrown fruits and vegetables) and the dose from consumption of the crop. The following equation is used to calculate the concentration of contaminant in the crop (RPP-ENV-58813):

$$C_c = C_{gs} \times (B_v + B_v') \tag{9-17}$$

Where:

C_c = radionuclide concentration in crop (pCi/g)
C_{gs} = radionuclide concentration in garden soil (pCi/g)
B_v = crop-soil bioconcentration factor through uptake $\left(\frac{\left(\frac{pCi}{kg\ fresh\ weight\ of\ crop}\right)}{\left(\frac{pCi}{kg\ dry\ weight\ of\ soil}\right)}\right)$
B'_v = crop-soil bioconcentration factor representing all resuspension-soil adhesion processes $\left(\frac{\left(\frac{pCi}{kg\ fresh\ weight\ of\ crop}\right)}{\left(\frac{pCi}{kg\ dry\ weight\ of\ soil}\right)}\right)$.

The following equation is used to calculate dose resulting from consumption of homegrown fruits and vegetables (RPP-ENV-58813):

$$D_c = C_c \times IR_c \times F_v \times UCF_1 \times DCF_{ing} \quad (9\text{-}18)$$

Where:

D_c = dose resulting from consumption of crops (homegrown fruits and vegetables) (mrem/yr)
C_c = radionuclide concentration in crop (pCi/g)
IR_c = crop ingestion rate (kg/yr)
F_v = fraction of homegrown fruits and vegetables consumed (unitless)
UCF_1 = unit conversion factor (1,000 g/kg)
DCF_{ing} = ingestion dose conversion factor (mrem/pCi).

9.3.2.3 Chronic Suburban Garden Scenario – Inhalation of Soil Particulates. The following equation is used to calculate dose to the suburban garden resident resulting from inhalation of dust particulates (RPP-ENV-58813):

$$D_{inh} = C_{gs} \times E_f \times M \times \left(INH_{in,sg} \times t_{in,sg} \times \frac{I}{O} + INH_{out,sg} \times t_{out,sg}\right) \times DCF_{inh} \quad (9\text{-}19)$$

Where:

D_{inh} = dose resulting from inhalation of soil (mrem/yr)
C_{gs} = radionuclide concentration in garden soil (pCi/g)
E_f = enrichment factor (unitless)
M = mass loading factor (g/m^3)
$INH_{in,sg}$ = indoor inhalation rate – suburban garden (m^3/yr)
$t_{in,sg}$ = fraction of time spent indoors – suburban garden (unitless)
I/O = ratio of radionuclide concentrations in indoor and outdoor air (unitless)
$INH_{out,sg}$ = outdoor inhalation rate –suburban garden (m^3/yr)
$t_{out,sg}$ = fraction of time spent outdoors – suburban garden (unitless)
DCF_{inh} = inhalation dose conversion factor (mrem/pCi).

9.3.2.4 Chronic Suburban Garden Scenario – External Exposure. The following equation is used to calculate dose to the suburban garden resident resulting from external exposure (RPP-ENV-58813):

$$D_{ext} = C_{gs} \times \left(t_{in,sg} \times \varepsilon + t_{out,sg}\right) \times DCF_{ext} \quad (9\text{-}20)$$

Where:

D_{ext} = dose resulting from external exposure (mrem/yr)
C_{gs} = radionuclide concentration in garden soil (pCi/g)
$t_{in,sg}$ = fraction of time spent indoors – suburban garden (unitless)
ε = transmission or shielding factor
$t_{out,sg}$ = fraction of time spent outdoors – suburban garden (unitless)
DCF_{ext} = external exposure dose conversion factor (mrem/yr)/(pCi/g).

9.3.3 Chronic Commercial Farm Scenario

The commercial farm scenario evaluates the long-term exposure to an individual who uses the target field as a commercial farm. In this outdoor scenario, a well diameter of 41.91 cm (16.5 in.) is assumed and the drill cuttings are spread over a farm area of 647,000 m^2 (160 acres) for growing food crops. This scenario represents an individual who works on the commercial farm, and grows and tends to the crops but does not consume what is produced. The commercial farm worker is exposed by incidental soil ingestion, inhalation of soil particulates, and external exposure; these exposure pathways are illustrated in Figure 9-5. Exposure parameters for the chronic commercial farm scenario are provided in Table 9-6.

As discussed in Section 9.3.1.1, Equation 9-7 is used to calculate the radionuclide activities, and Equation 9-8 is used to calculate the radionuclide concentrations for the commercial farm scenario (C_{cf}) with corresponding well area and target field area. Radionuclide-specific shielding factors and dose conversion factors are presented in Section 6.3.3, Tables 6-24 and 6-25, respectively. Because the fraction of time spent indoors is assumed to be zero, the indoor shielding factor is not applicable in this scenario.

9.3.3.1 Chronic Commercial Farm Scenario – Incidental Soil Ingestion. The following equation is used to calculate dose to the commercial farmer resulting from incidental ingestion of soil (RPP-ENV-58813):

$$D_s = C_{cf} \times IR_{s,cf} \times EF_{cf} \times UCF_1 \times DCF_{ing} \quad (9\text{-}18)$$

Where:

D_s = dose resulting from incidental soil ingestion (mrem/yr)
C_{cf} = radionuclide concentration in the commercial farm soil (pCi/g)
$IR_{s,cf}$ = soil ingestion rate – commercial farmer (mg/day)
EF_{cf} = exposure frequency – commercial farmer (days/yr)

UCF_1 = unit conversion factor (g/mg)
DCF_{ing} = ingestion dose conversion factor (mrem/pCi).

Figure 9-5. Exposure Pathways Considered for the Inadvertent Intruder Chronic Commercial Farm Exposure Scenario.

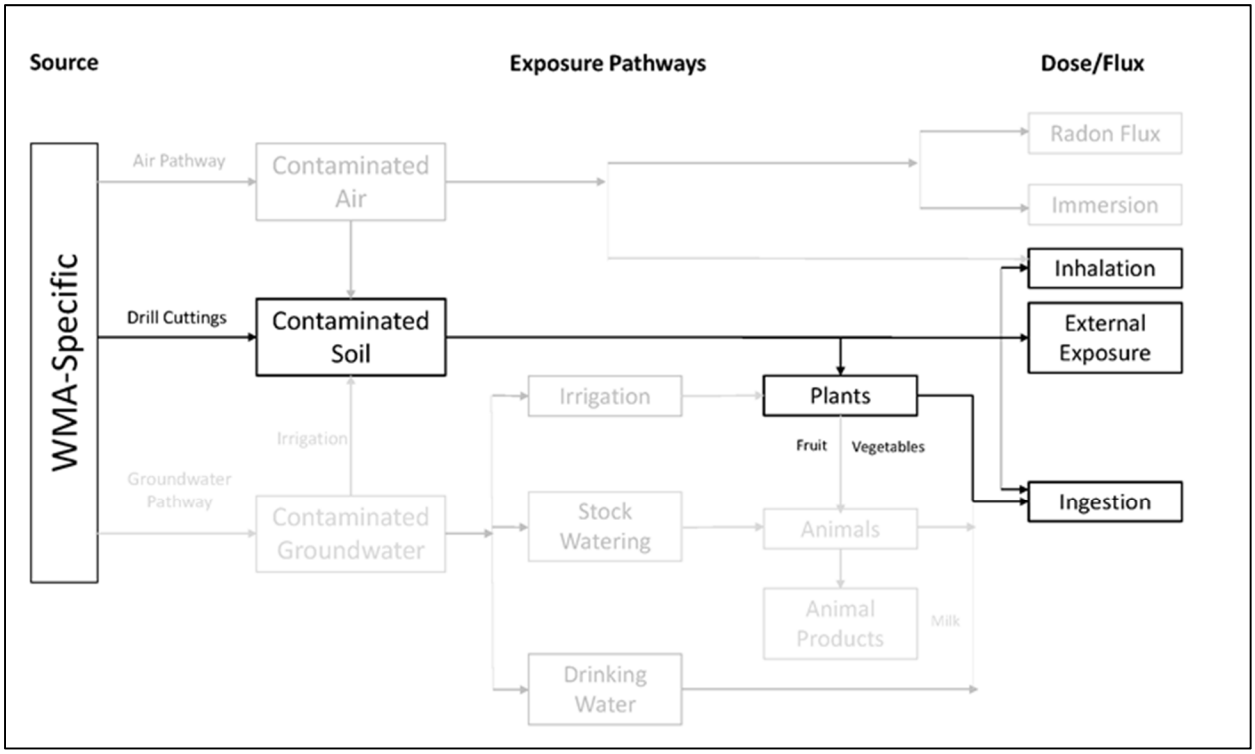

WMA = Waste Management Area

9.3.3.2 Chronic Commercial Farm Scenario – Inhalation of Soil Particulates. The following equation is used to calculate dose to the commercial farmer resulting from inhalation of dust particulates (RPP-ENV-58813):

$$D_{inh} = C_{cf} \times E_f \times M \times \left(INH_{in,cf} \times t_{in,cf} \times \frac{I}{O} + INH_{out,cf} \times t_{out,cf}\right) \times DCF_{inh} \quad (9\text{-}21)$$

Where:

D_{inh} = dose resulting from inhalation of soil (mrem/yr)
C_{cf} = radionuclide concentration in commercial farm soil (pCi/g)
E_f = enrichment factor (unitless)
M = mass loading factor (g/m^3)
$INH_{in,cf}$ = indoor inhalation rate – commercial farmer (m^3/yr)
$t_{in,cf}$ = fraction of time spent indoors – assumed to be zero for commercial farmer
I/O = ratio of radionuclide concentrations in indoor and outdoor air (unitless)
$INH_{out,cf}$ = outdoor inhalation rate – commercial farmer (m^3/yr)

$t_{out,cf}$ = fraction of time spent outdoors – commercial farmer (unitless)
DCF_{inh} = inhalation dose conversion factor (mrem/pCi).

Table 9-6. Exposure Parameters for the Chronic Commercial Farm Exposure Scenario.

Parameter	Notation	Value	Units	Reference
Area over which residual waste is spread	A_{source_term}	Calculated	cm^2	Source term-specific
Area of the well	A_{well}	1,379.51	cm^2	Calculated
Diameter of the well	D_{well}	41.91	cm	HNF-SD-WM-TI-707, Rev. 5
Area of commercial farm	A_{cf}	6.475E+09	cm^2	HNF-SD-WM-TI-707, Rev. 5
Tilled depth of commercial farm	Z_{cf}	15	cm	HNF-SD-WM-TI-707, Rev. 5
Soil ingestion rate – commercial farmer	$IR_{s,cf}$	100	mg/day	OSWER Directive 9285.6-03
Exposure frequency – commercial farmer	EF_{cf}	350	days/yr	OSWER Directive 9285.6-03
Enrichment factor	E_f	0.7	unitless	NCRP Report No. 129
Indoor inhalation rate – commercial farmer	$INH_{in,cf}$	7,300	m^3/yr	NCRP Report No. 129
Mass loading factor	M	6.66E-05	g/m^3	NCRP Report No. 129
Fraction of time spent indoors – commercial farmer	$t_{in,cf}$	0	unitless	NCRP Report No. 129; Outdoor scenario
Outdoor inhalation rate – commercial farmer	$INH_{out,cf}$	10,950	m^3/yr	HNF-SD-WM-TI-707, Rev. 5
Fraction of time spent outdoors – commercial farmer	$t_{out,cf}$	0.164	unitless	HNF-SD-WM-TI-707, Rev. 5
Ratio of radionuclide concentrations in indoor versus outdoor air	I/O	0.3	unitless	NCRP Report No. 129
Unit conversion factor	UCF_1	0.001	g/mg	0.001 g = 1 mg

NCRP = National Council on Radiation Protection

References:
HNF-SD-WM-TI-707, "Exposure Scenarios and Unit Factors for the Hanford Tank Waste Performance Assessment."
NCRP Report No. 129, "Recommended Screening Limits for Contaminated Surface Soil and Review of Factors Relevant to Site-Specific Studies."
OSWER Directive 9285.6-03, Risk Assessment Guidance for Superfund, Volume I: Human Health Evaluation Manual, Supplemental Guidance "Standard Default Exposure Factors" Interim Final.

9.3.3.3 Chronic Commercial Farm Scenario – External Exposure. The following equation is used to calculate dose to the resident resulting from external exposure (RPP-ENV-58813):

$$D_{ext} = C_{cf} \times \left(t_{in,cf} \times \varepsilon + t_{out,cf}\right) \times DCF_{ext} \quad (9\text{-}22)$$

Where:

D_{ext} = dose resulting from external exposure
C_{cf} = radionuclide concentration in commercial farm soil (pCi/g)
$t_{in,cf}$ = fraction of time spent indoors – assumed to be zero for commercial farmer
ε = transmission or shielding factor
$t_{out,cf}$ = fraction of time spent outdoors – commercial farmer (unitless)
DCF_{ext} = external exposure dose conversion factor (mrem/yr)/(pCi/g).

9.4 INTRUDER ANALYSIS RESULTS

Sections 9.3.1 and 9.3.2 summarize the calculated effective dose for each of the four inadvertent intruder scenarios. Graphic displays show the effective dose starting 100 years after closure for intrusion into a pipeline source and 500 years after closure for the other sources that produce significant intruder dose. Over the compliance time period (1,000 years after closure), the relative contribution of radionuclides vary, but the total dose decreases, with highest dose being at 100 years after closure. Table 9-7 summarizes the calculated effective doses for each intruder scenario, assuming intrusion at 100 years for intrusion into a pipeline source and 500 years after closure for the other 18 waste sources. Although inadvertent intrusions into many of the tanks lead to potential doses, the likelihood of intrusion is considered to be very small due to the significant mechanical barrier to drilling from the large thickness of grout that will fill tanks at closure compared to drilling outside of grouted tank area. On the other hand, the inadvertent intrusion through pipelines is more likely as pipelines would not provide any appreciable mechanical barrier to drilling compared to drilling through the Hanford unit sediments.

For the purpose of analysis, the total intruder dose and doses from major radionuclide contributors from intrusion into tank C-301 (maximum intruder dose causing source term at 500-year intrusion time) and intrusion into a pipeline (most likely intruder source term) are presented separately for each intruder scenario. The relative importance of various pathways is presented for each intruder scenario in Table 9-8 for intruding through the pipeline.

9.4.1 Acute Exposure Dose

Figure 9-6 shows the calculated acute dose to the well driller assuming the intrusion takes place 100 years or beyond for pipelines and 500 years or beyond for sources with substantial intrusion barriers. Among the 19 residual waste sources, the sources with the top six intruder doses are displayed in the figure. For all sources, the dose remains below the 500 mrem performance measure. Figure 9-7(a) shows the total well driller dose produced by tank C-301 residual waste source along with major dose-contributing radionuclides, while Figure 9-7(b) shows the results for the intruded pipeline source. The major contributor to dose to the well driller is ^{239}Pu for both sources, although ^{137}Cs is an important contributor to intrusion into pipelines at early times. The major pathway for well driller dose is external exposure.

Table 9-7. Peak Effective Dose for the Inadvertent Intruder Scenarios for All Residual Waste Sources.

Source	Well Driller Acute Dose (mrem)	Commercial Farm Chronic Dose (mrem/yr)	Rural Pasture Chronic Dose (mrem/yr)	Suburban Garden Chronic Dose (mrem/yr)
241-C-101	1.24E+00	2.17E-03	1.44E-01	3.22E-01
241-C-102	4.59E+00	8.09E-03	5.37E-01	1.20E+00
241-C-103	4.09E-01	7.25E-04	6.14E-02	1.10E-01
241-C-104	5.77E-01	1.10E-03	1.21E-01	1.70E-01
241-C-105	3.80E+00	6.69E-03	7.18E-01	1.23E+00
241-C-106	3.47E+00	8.75E-03	8.93E-01	9.57E-01
241-C-107	1.49E+01	2.66E-02	1.82E+00	3.90E+00
241-C-108	5.80E-02	1.05E-04	1.09E-02	1.71E-02
241-C-109	3.10E-02	5.57E-05	7.63E-03	9.33E-03
241-C-110	8.24E-02	1.78E-04	1.99E-02	2.44E-02
241-C-111	7.47E+00	1.32E-02	1.40E+00	2.13E+00
241-C-112	3.48E-01	6.10E-04	9.17E-02	1.41E-01
241-C-201	1.45E+01	2.52E-02	1.58E+00	3.75E+00
241-C-202	1.28E+01	2.22E-02	1.39E+00	3.32E+00
241-C-203	4.61E-01	8.51E-04	7.25E-02	1.26E-01
241-C-204	5.60E-02	1.77E-04	2.97E-02	2.49E-02
241-C-301	2.12E+01	**3.86E-02**	2.69E+00	**5.57E+00**
CR-VAULT	3.91E+00	7.10E-03	4.96E-01	1.03E+00
Pipeline*	**3.60E+01**	1.13E-03	**8.21E+00**	3.92E+00

Note: Peak dose calculated at 500 years for all sources except for pipeline, which is reported at 100 years after closure.

*Maximum dose at 100 years after closure.

The peak dose for each scenario is shown in **bold**.

9.4.2 Chronic Exposure Dose

Figure 9-8 shows the calculated dose for the rural pasture scenario for the top six residual waste sources. All remain below the 100 mrem/yr performance measure throughout the simulated time period. Figure 9-9(a) shows the total rural pasture dose produced by intrusion into tank C-301 along with major dose-contributing radionuclides, while Figure 9-9(b) shows the results for intrusion into a pipeline. Strontium-90 is the major contributor to pipelines up until almost 500 years after closure, with major pathways being milk ingestion. Cesium-137 through the milk

ingestion pathway is also a major contributor to dose at early time period. Plutonium-239 becomes the major contributor for both pipelines and tank residuals after 500 years following closure.

Table 9-8. Relative Fraction of Pathway Contributions to the Inadvertent Intruder Dose for Pipeline at 100 Years After Closure.

Scenario	Pathways				
	External Exposure	**Soil Inhalation**	**Soil Ingestion**	**Milk Ingestion**	**Vegetable Ingestion**
Well Driller	**0.59**	0.30	0.11	x	x
Rural Pasture	0.01	<0.01	<0.01	**0.98**	x
Suburban Garden	0.03	<0.01	<0.01	x	**0.96**
Commercial Farm	**0.69**	0.05	0.26	x	x

x = pathway not considered

Pathway contributing the most is highlighted for each scenario.

Figure 9-10 shows the calculated dose for the suburban garden scenario for the top six residual waste sources. All doses remain below the 100 mrem/yr performance measure throughout the compliance time period. Figure 9-11(a) shows the total suburban garden dose produced by intrusion into tank C-301 along with major dose-contributing radionuclides, while Figure 9-11(b) shows the results for intruded pipeline source. Strontium-90 is the major contributor up until about 300 years after closure (for intrusion into a pipeline source), with major pathways being vegetable ingestion. Cesium-137 through the vegetable ingestion pathway is also a major contributor to dose at early times. Plutonium-239 becomes the major contributor after 500 years for both pipelines and tank residuals.

Figure 9-12 shows the calculated dose for the commercial farm scenario for the top six residual waste sources. The dose from all residual waste sources remains below the 100 mrem/yr performance measure throughout the simulated time period.

Figure 9-13(a) shows the total commercial farm dose produced by intrusion into tank C-301 along with major dose-contributing radionuclides, while Figure 9-13(b) shows the results for intrusion into a pipeline source. For intrusion into a pipeline source, ^{137}Cs and ^{90}Sr are the major contributor up until almost 300 years after, with major pathways being external exposure. Plutonium-239 and ^{241}Am become the major contributor to both pipelines and tank residuals after 500 years.

Figure 9-14(a-b) shows the total dose produced by intrusion into tank C-301 and a pipeline residual waste source for all three chronic scenarios. For about the first 300 years after closure (for intrusion into a pipeline source), the rural pasture scenario produces higher dose than the other chronic scenarios; after that time the suburban garden dose is highest among all of the chronic scenarios. Within the first 300 years for intrusion into a pipeline after closure, the milk

ingestion dose (dominant pathway in rural pasture scenario) from ^{90}Sr is higher than the vegetable ingestion dose (dominant pathway in suburban garden scenario). After that, the total vegetable ingestion dose from ^{90}Sr, ^{241}Am and ^{239}Pu exceeds the total milk ingestion dose from ^{90}Sr, ^{241}Am and ^{239}Pu. So, if intrusion occurs at 100 years after closure, the rural pasture scenario will produce the highest chronic dose.

Figure 9-6. Effective Dose for the Well Driller Acute Exposure Scenario.

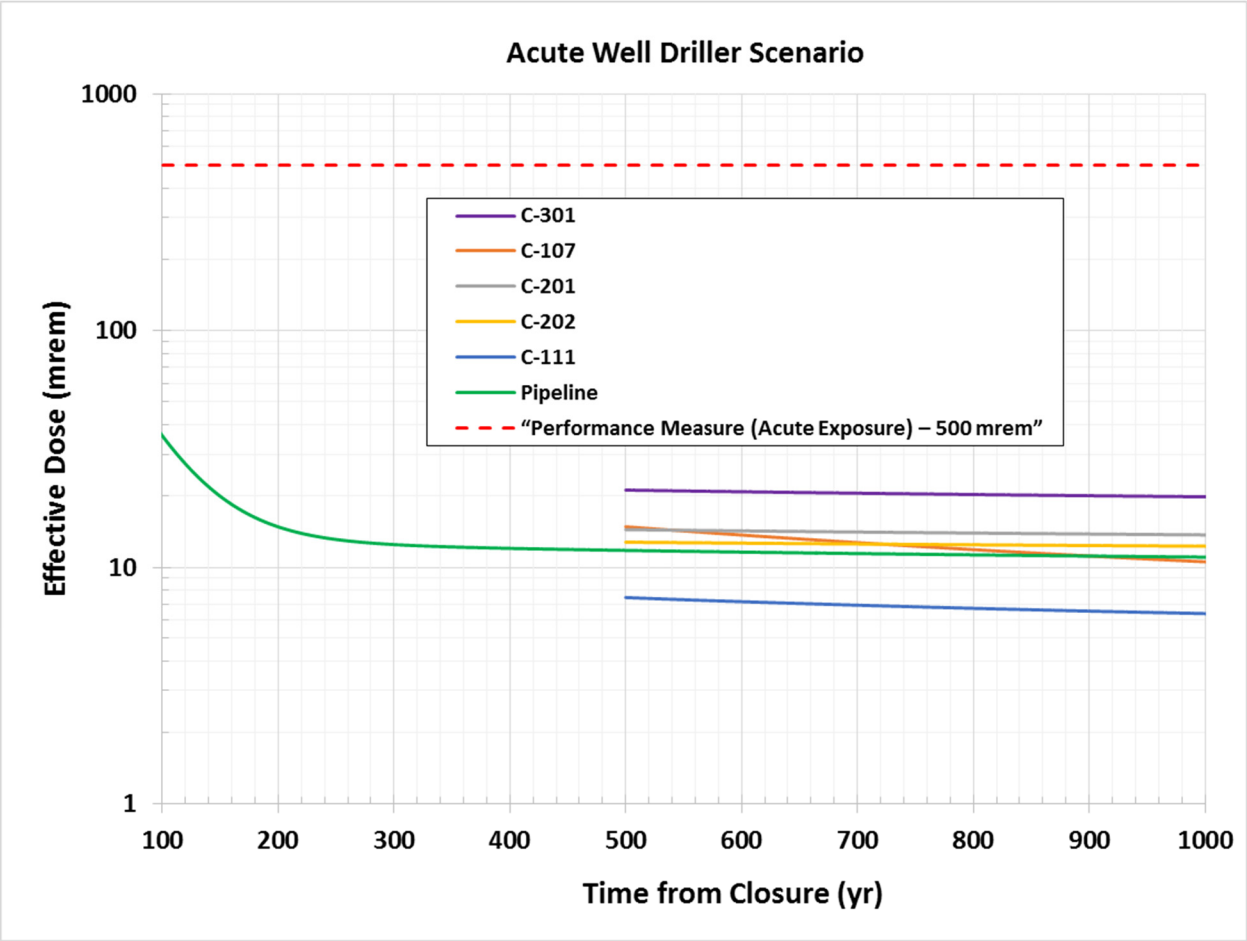

For intrusion into tank wastes, the suburban garden scenario produces the maximum chronic dose, with tank C-301 producing the highest dose. The commercial farm scenario is always lower than the other chronic scenarios.

9.5 INTRUDER SENSITIVITY/UNCERTAINTY ANALYSIS

Sensitivity and uncertainty analyses for intruder analyses are somewhat limited, owing to the stylized and speculative nature of the scenarios. Consequently, for this PA only qualitative discussions are provided in this section.

Figure 9-7. Effective Dose for the Well Driller Acute Exposure Scenario for (a) Tank 241-C-301 and (b) Pipeline Residual Waste.

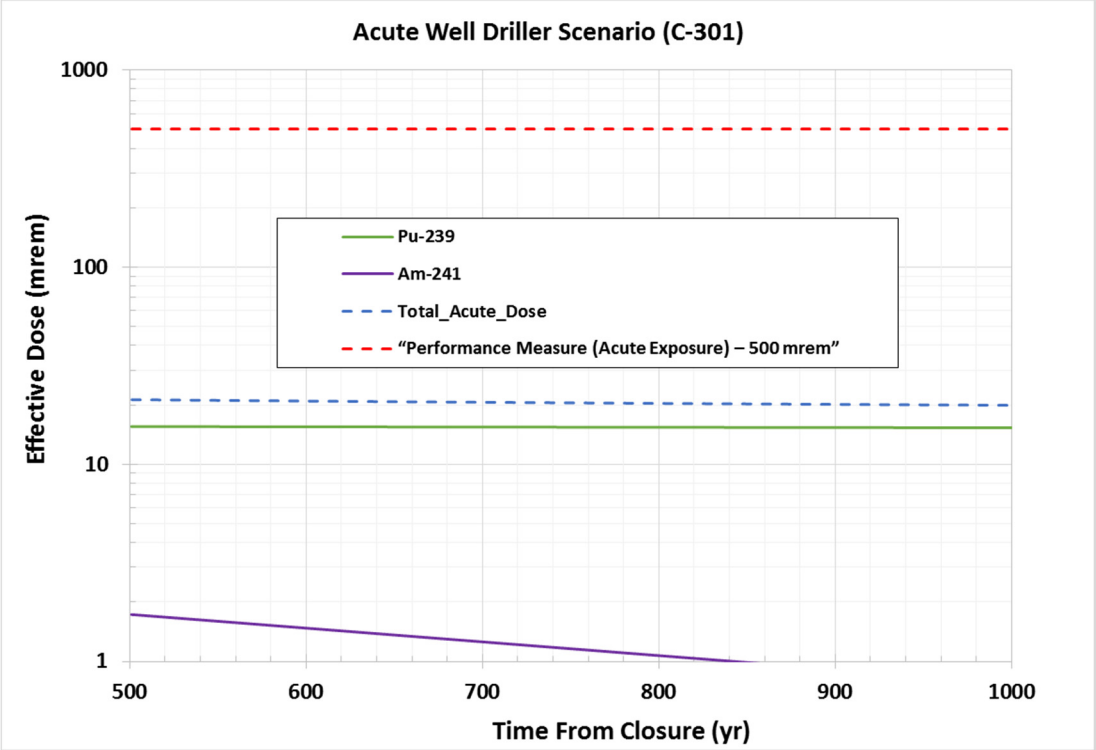

(a)

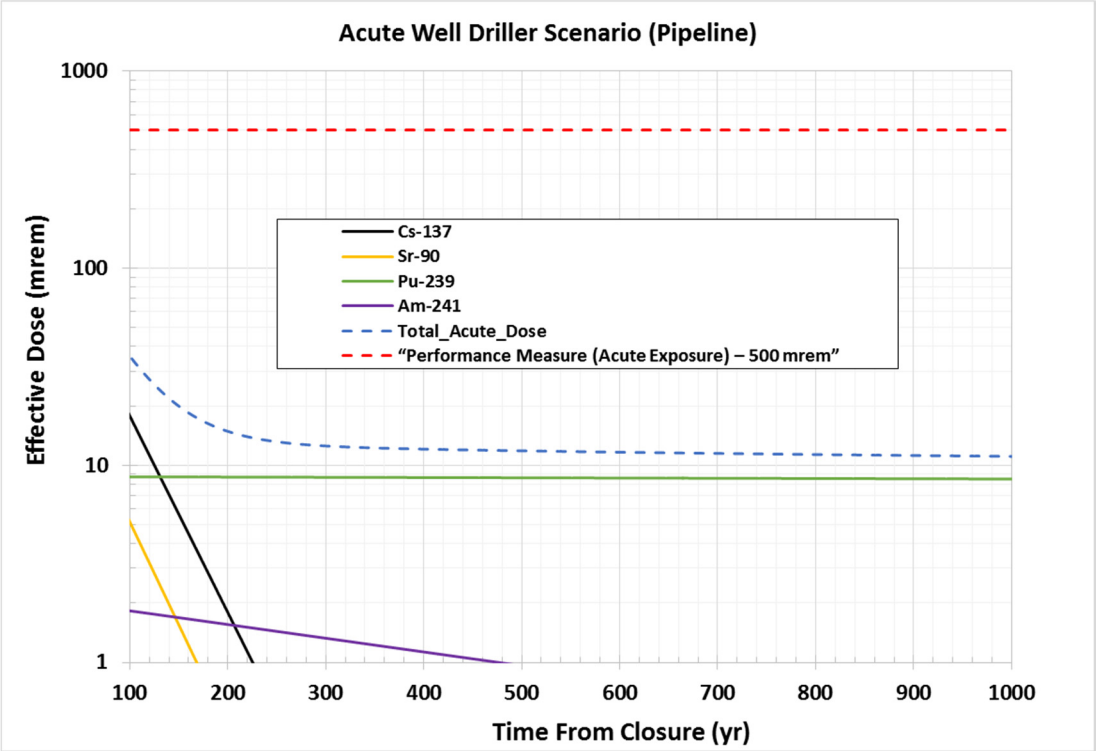

(b)

Figure 9-8. Effective Dose for the Rural Pasture Chronic Exposure Scenario.

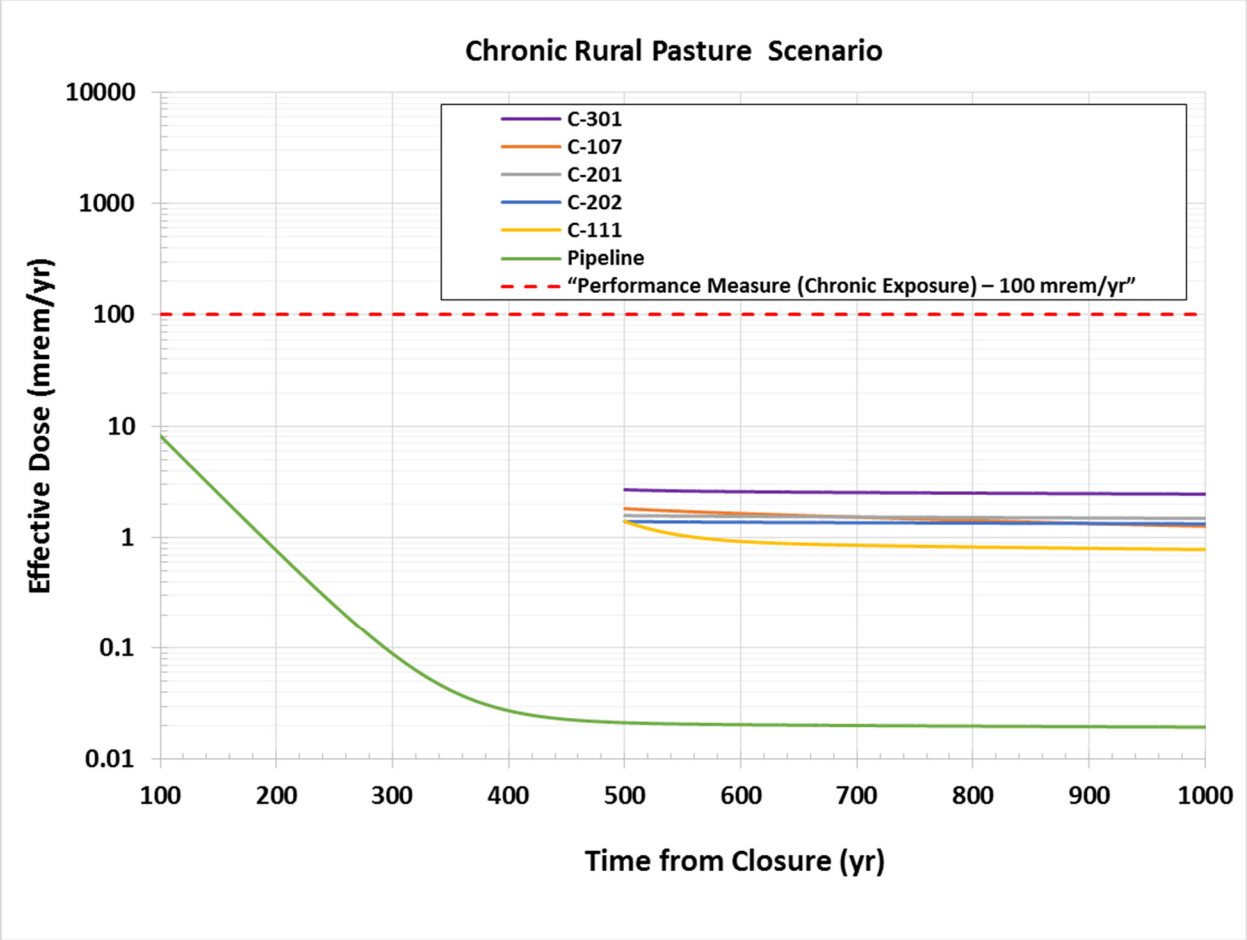

The key parameter in the intruder analysis is concentration in the residual wastes. Calculated doses are linear with the activity of waste exhumed in the intrusion event. For example, the limiting inadvertent intruder scenario is the rural pasture scenario, as it leads to the highest dose at 100 years after closure. The major dose contributors in this scenario are ^{90}Sr and ^{137}Cs. Decreasing the closure inventory (or concentration) of those two nuclides would result in a proportional decrease in the rural pasture dose.

Sensitivities of other key parameters depend on which exposure pathways are the most important dose contributors. The relative importance of various pathways is presented for each scenario in Table 9-8 for pipeline (most likely source for intrusion) at 100 years after closure. It provides insight into the group of parameters that will have the greatest impact on the dose, and therefore the uncertainty in dose would be most impacted by the uncertainty in those parameter values. The relative contribution to the overall dose by a given pathway is provided. Based on the results presented in Table 9-8, the parameters associated with external exposure pathway are deemed to be most important for well driller and commercial farm scenarios, parameters associated with milk ingestion pathway are most important for rural pasture scenario, and for suburban garden scenario the parameters associated with vegetable ingestion pathway are most important.

Figure 9-9. Effective Dose for the Rural Pasture Chronic Exposure Scenario for (a) Tank 241-C-301 and (b) Pipeline Residual Waste.

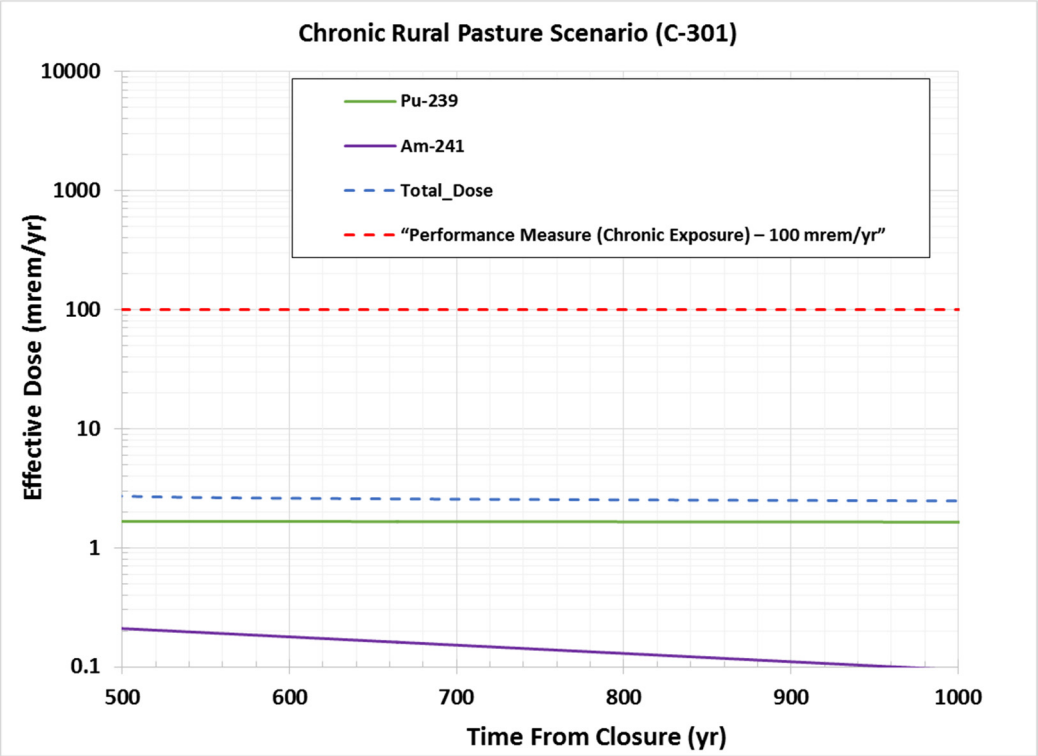

(a)

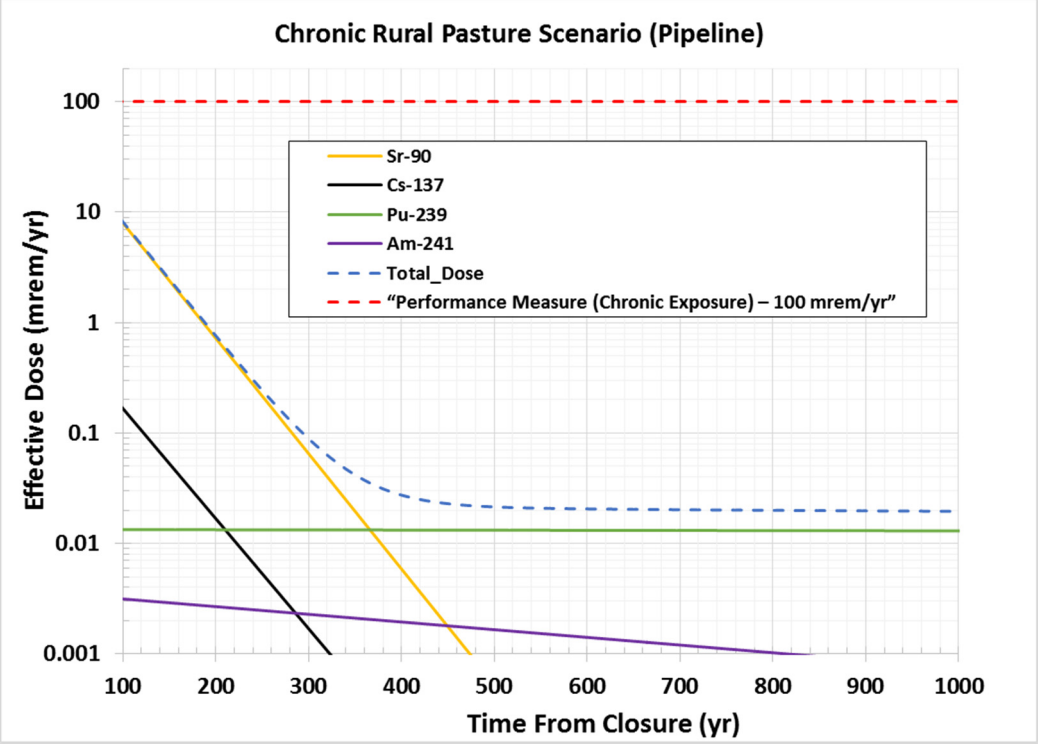

(b)

Figure 9-10. Effective Dose for the Suburban Garden Chronic Exposure Scenario.

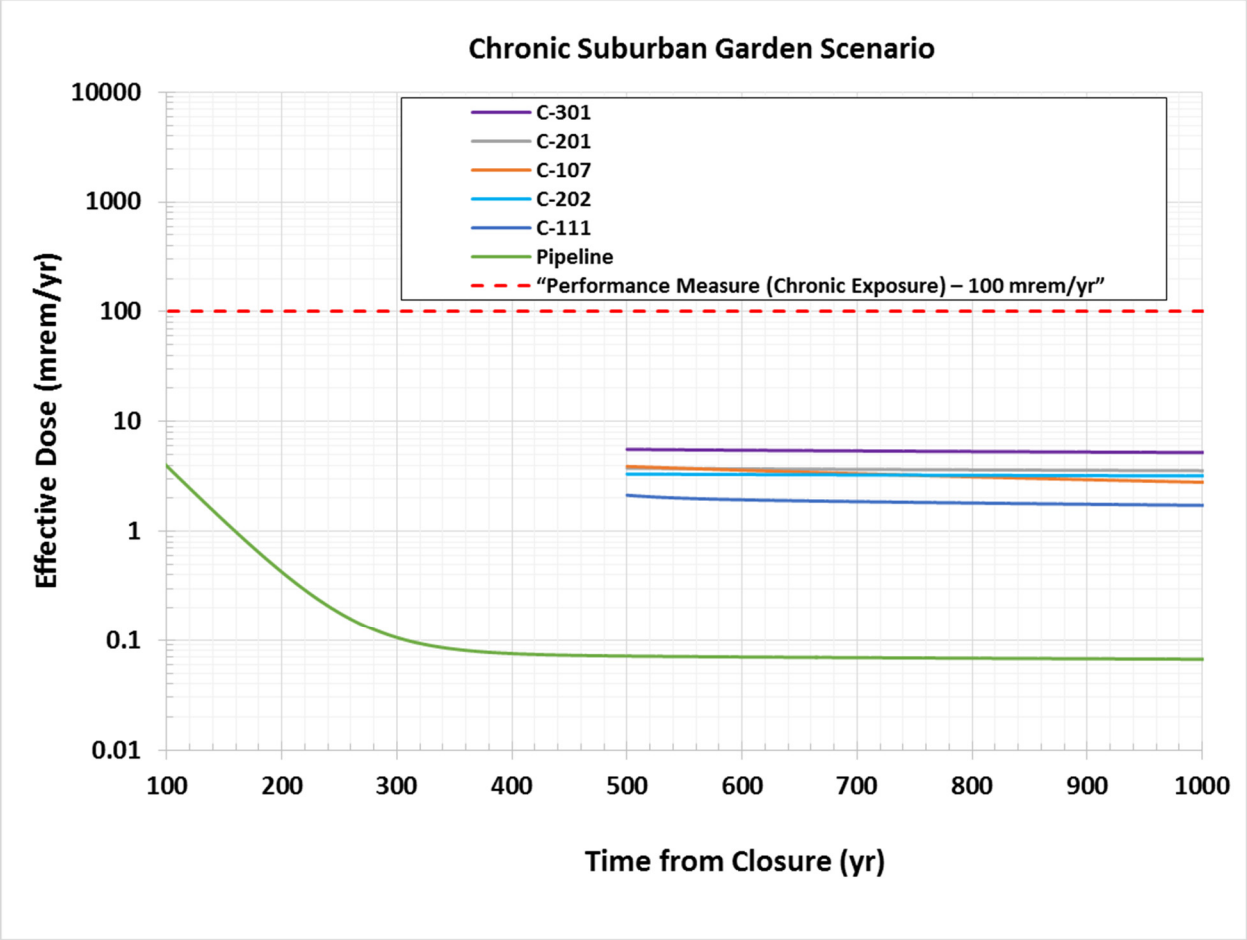

A sensitivity analysis was performed to evaluate the impact of intrusion through a fully plugged cascade pipeline. As discussed earlier, the plugged pipelines only occupy about 2% of the total pipeline length within WMA C. Performing intrusion calculation through the fully plugged cascade line will provide the bounding dose estimate for intrusion into a pipeline source. The calculations are performed in the same manner as discussed earlier for a pipeline source except that the cascade pipeline is assumed to be completely full (instead of 5% full for a waste transfer pipeline). The results of the three chronic scenarios are presented in Figure 9-15. Only the dose from the rural pasture scenario exceeds the performance measure at 100 years (about 160 mrem/yr) but quickly drops below within 20 years due to decay of ^{90}Sr. When compared to the dose estimates presented in Figure 9-14(b) for the transfer pipeline, the cascade pipeline dose values are a factor of 20 higher, indicating that the dose scales linearly with the waste volume assumption. The acute scenario dose for the cascade pipeline remains the same as that for the transfer pipeline [Figure 9-7(b)] as the calculation depends on the concentration of the residual waste, which is assumed to be the same.

Figure 9-11. Effective Dose for the Suburban Garden Chronic Exposure Scenario for (a) Tank 241-C-301 and (b) Pipeline Residual Waste.

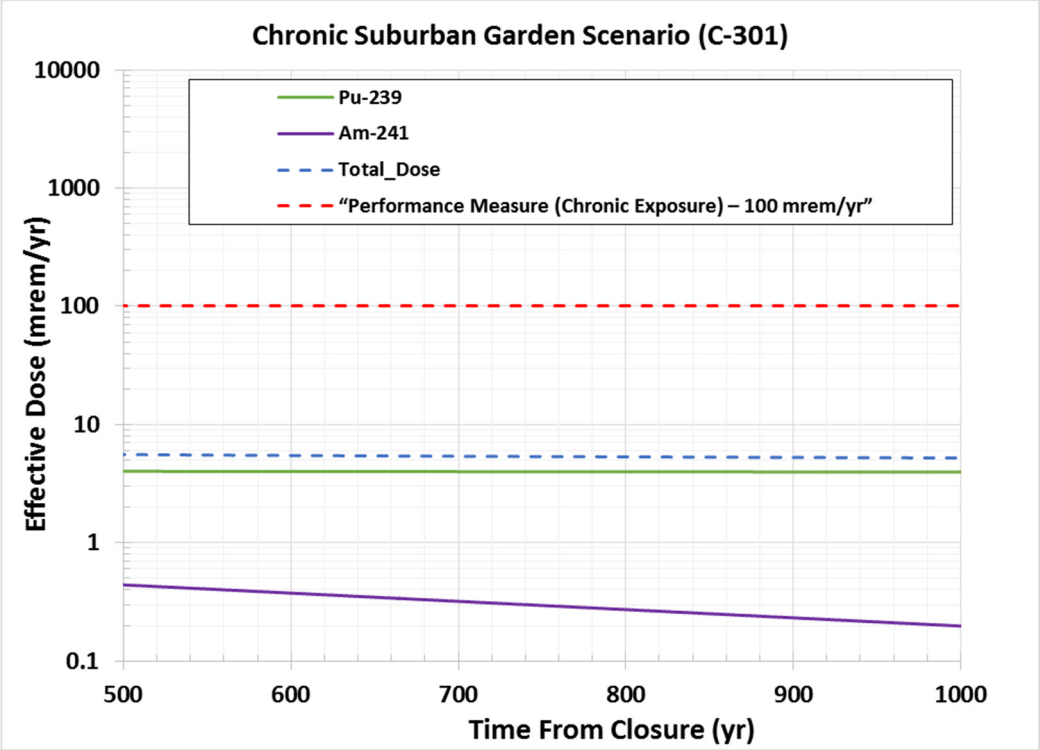

(a)

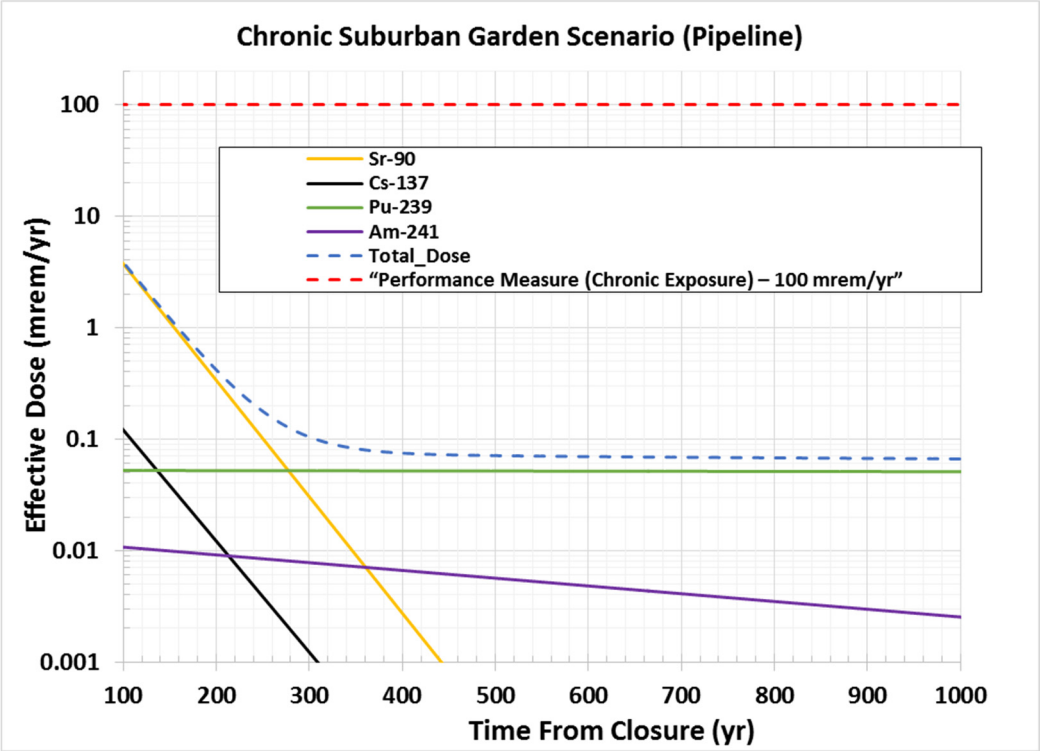

(b)

Figure 9-12. Effective Dose for the Commercial Farm Chronic Exposure Scenario.

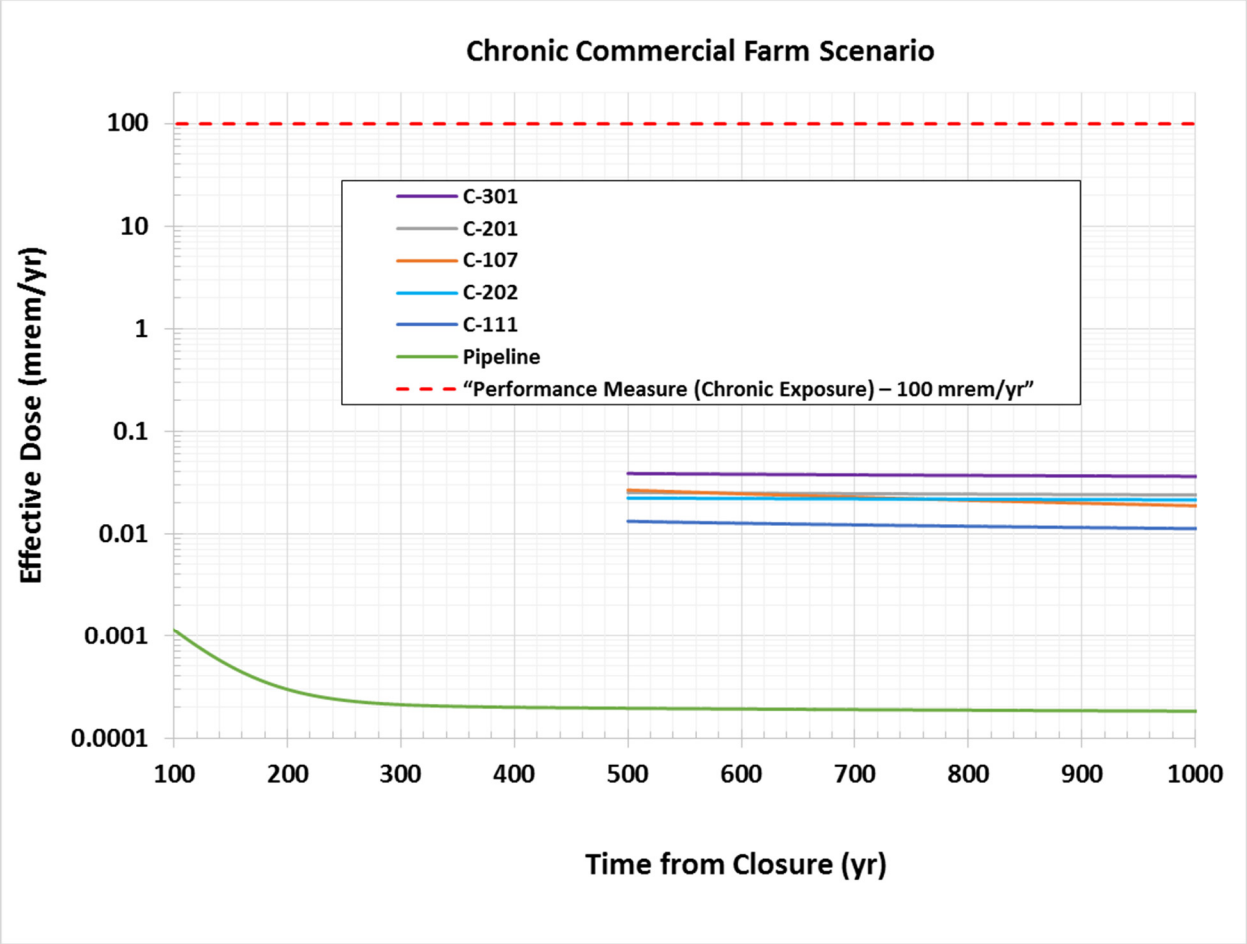

Figure 9-13. Effective Dose for the Commercial Farm Chronic Exposure Scenario for (a) Tank 241-C-301 and (b) Pipeline Residual Waste.

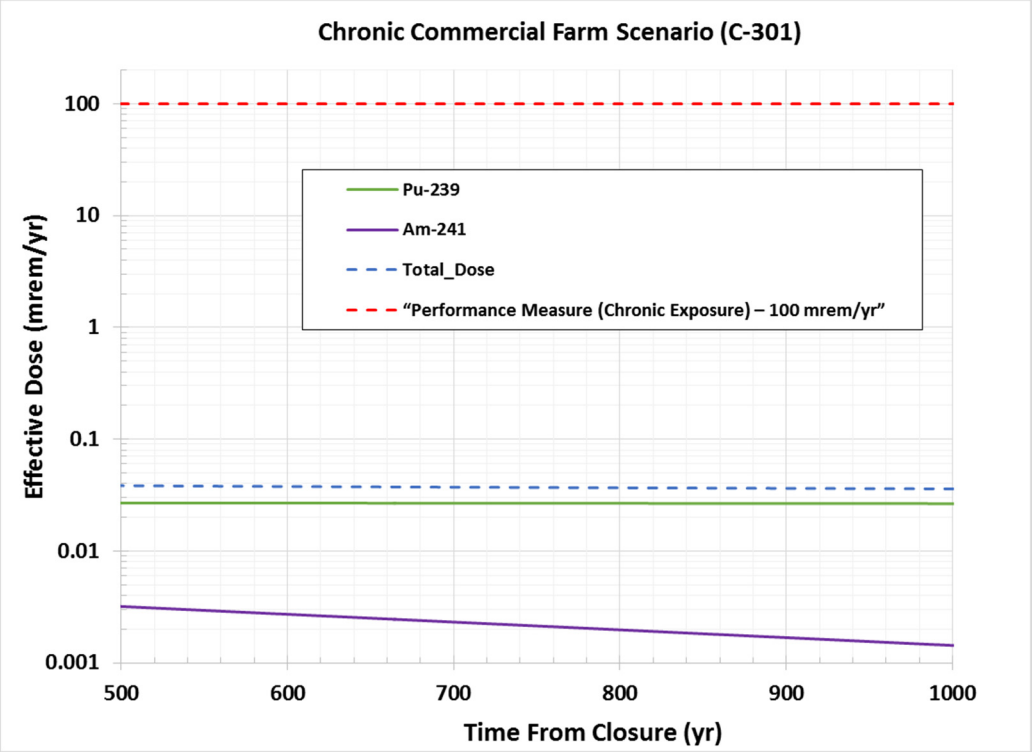

(a)

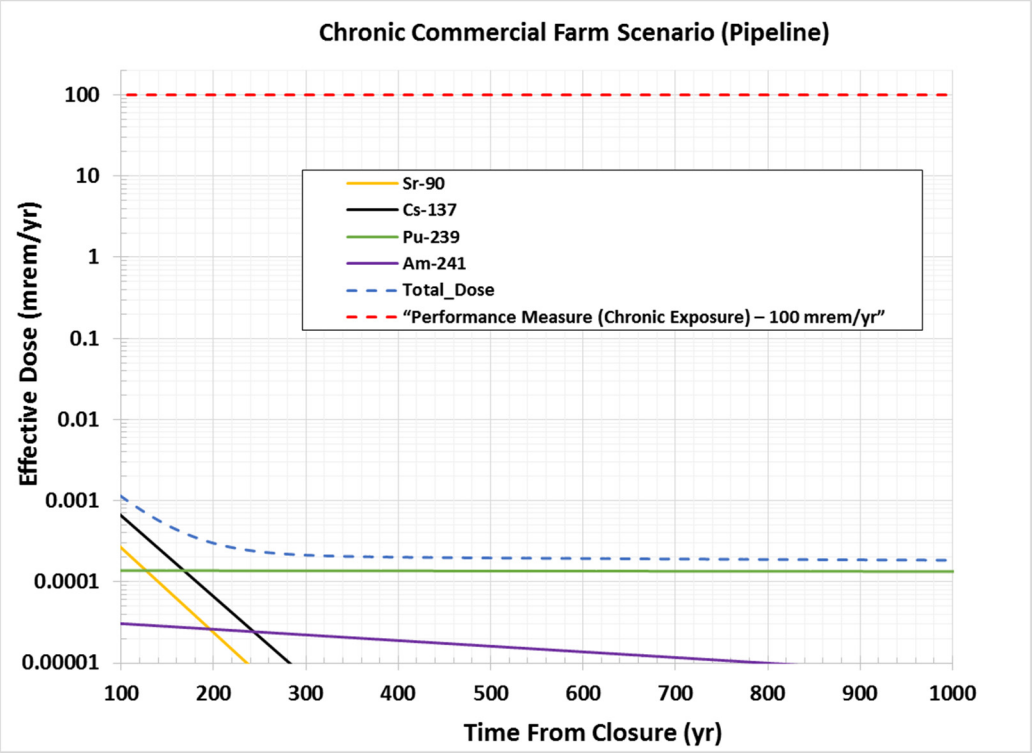

(b)

Figure 9-14. Effective Dose for All Three Chronic Exposure Scenarios for (a) Tank 241-C-301 and (b) Pipeline Residual Waste.

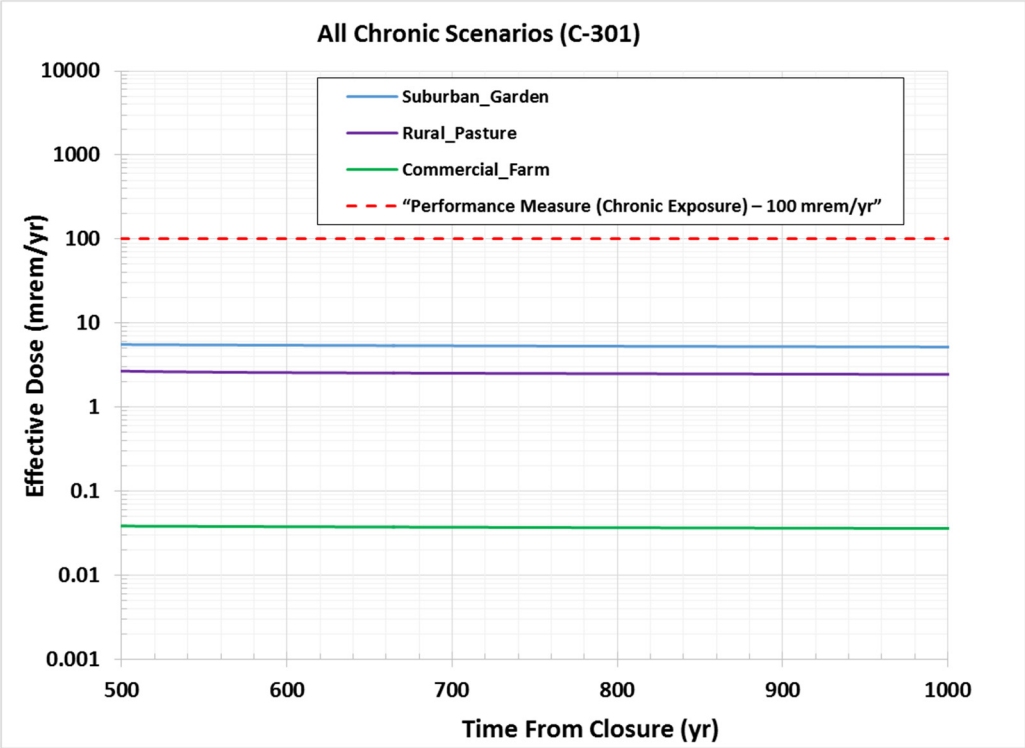

(a)

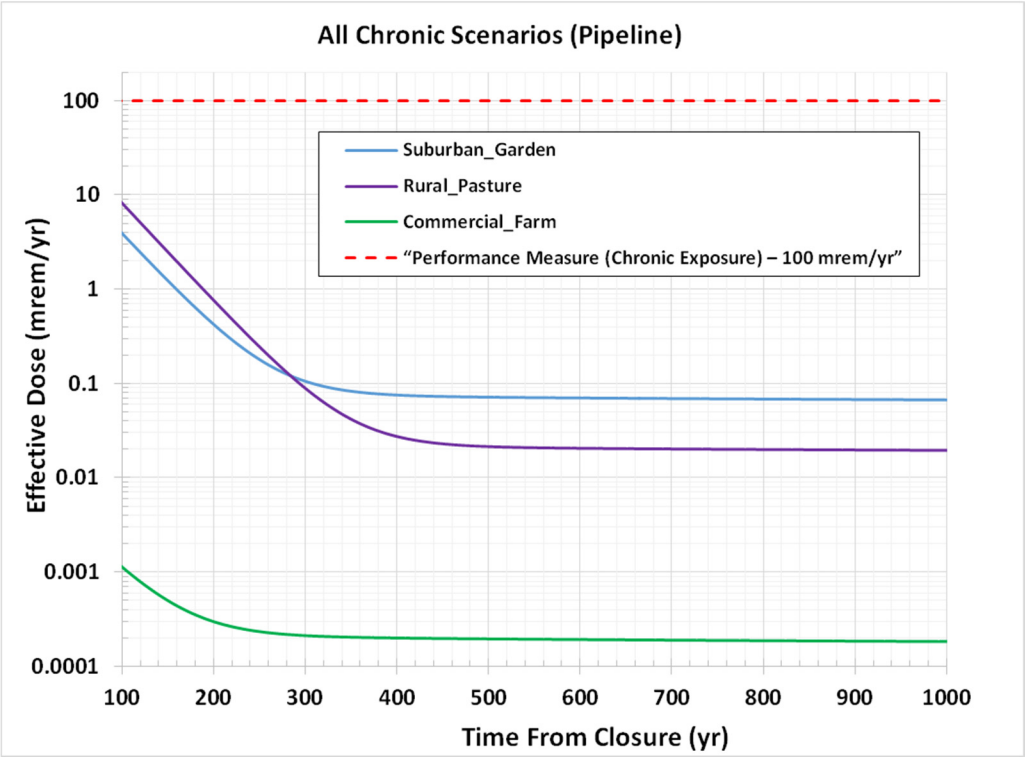

(b)

Figure 9-15. Effective Dose for All Three Chronic Exposure Scenarios for a Fully Plugged Cascade Pipeline.

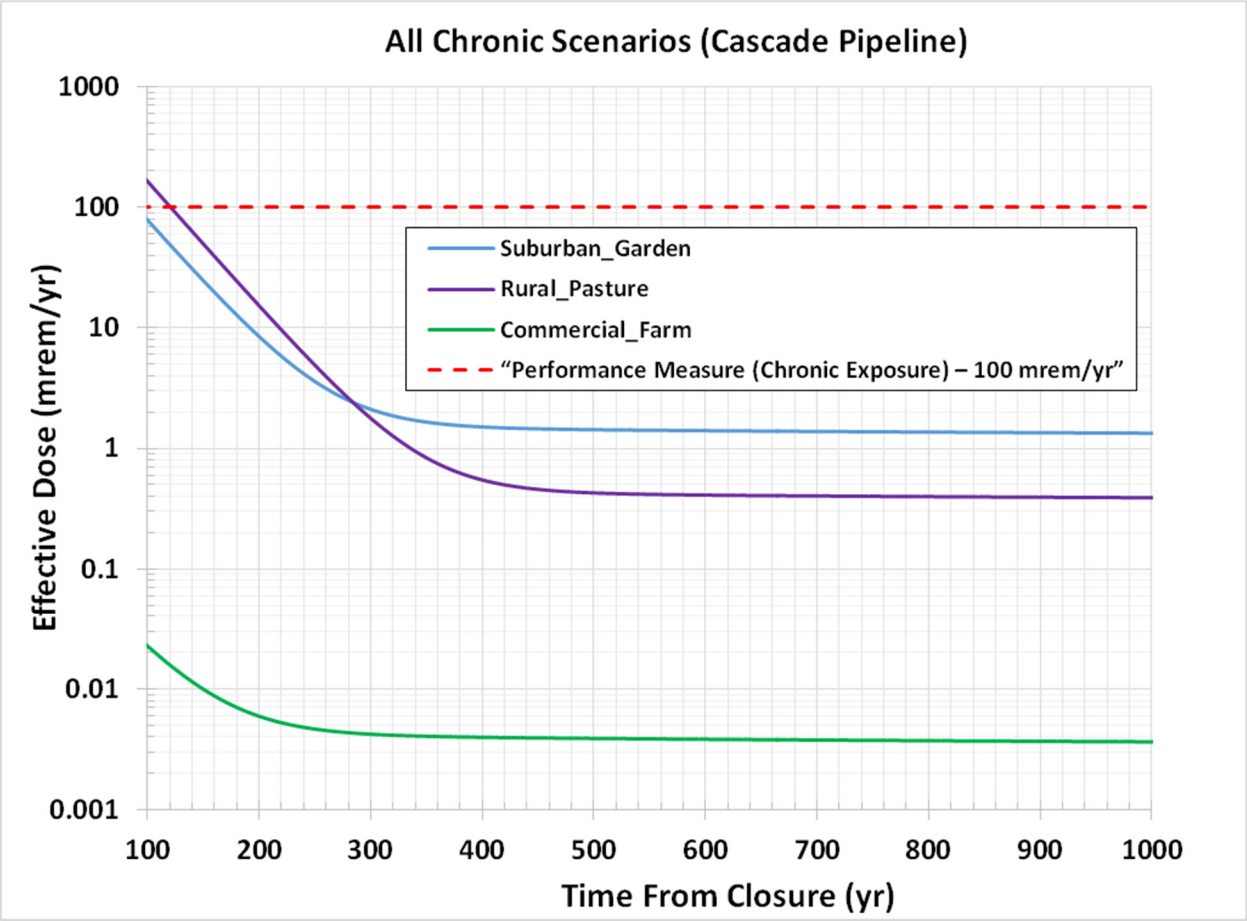

10.0 PERFORMANCE EVALUATION AND INTERPRETATION OF RESULTS

In this section, the results of the PA are consolidated and compared against the performance objectives, to interpret their meaning and significance. The goals of this section are as follows:

- To compare the results of the PA against the applicable DOE O 435.1 performance objectives
- To provide a basis to conclude that the performance of waste residuals in tanks and ancillary equipment left at WMA C at closure has been adequately addressed, and that the results provide a sufficient basis for concluding that the closed facility meets the performance objectives in DOE O 435.1
- To provide context for the results of the sensitivity and uncertainty analyses, and the support they provide to the conclusion that release of radionuclides remaining in the tank and ancillary residuals at a closed WMA C meets the performance objectives
- To provide results and interpretation of human health and environmental impacts for the post-compliance sensitivity and uncertainty time period.

The results are presented and interpreted for the following performance objectives and measures:

- All-pathways analysis
- Radon flux analysis
- Biotic pathways
- Groundwater resource protection analysis
- Inadvertent intruder analysis
- Sensitivity analyses for the groundwater pathway.

10.1 ALL-PATHWAYS ANALYSIS

Doses from releases to the groundwater and the air pathways were combined and evaluated against performance objectives for the all-pathways analysis required by DOE O 435.1. The main analysis used to compare against these performance objectives has been called the "base case." The base case is a deterministic analysis using a set of parameters that evaluates the condition when the safety functions provide their expected contribution to the performance of the facility[1]. The all-pathways analysis combines the groundwater pathway analysis and the air pathway analysis for the base case, as discussed in Section 6. The all-pathways dose results are given in Section 7.3.1.

[1] The exceptions to this statement are the safety functions for institutional control and societal memory. As discussed in Section 1, under DOE O 435.1, performance assessment is predicated on the assumption that these safety functions are lost 100 years in the future, allowing exposures of members of the public to occur. If these safety functions were to remain intact, exposure of the kind evaluated in the performance assessment could not occur.

The peak dose from the all-pathways analysis during the 0- to 1,000-year compliance period is associated with the air pathway, with the peak dose of 4×10^{-3} mrem/yr dominated by tritium resulting from upward gaseous diffusive flux from the residual waste. This peak dose occurs in the institutional control period, between 10 and 20 years after closure. This peak dose does not consider the active monitoring measures that are anticipated during institutional control. The all-pathways dose remains substantially lower (approximately 4×10^{-5} mrem/yr) for about 800 years after closure, but shows a rapid increase near the end of the compliance time period due to breakthrough of ^{99}Tc at the PoCal along the groundwater pathway. The peak all-pathways dose during the post-compliance time period (1,000 to 10,000 years after closure) evaluated for the purpose of sensitivity and uncertainty analysis occurs at about 1,500 years after closure, and results primarily from peak in ^{99}Tc concentration at the PoCal in the groundwater pathway. The peak all-pathways' dose within the post-compliance time period is 0.1 mrem/yr.

The all-pathways' peak dose results are summarized in Table 10-1. This peak dose is over two orders of magnitude below the DOE O 435.1 performance objective of 25 mrem/yr during the 1,000-year compliance period, as well as in the sensitivity/uncertainty analysis period (1,000 to 10,000 years).

Table 10-1. Summary of All-Pathways Analysis Results for the Base Case.

Compliance Period (<1,000 yr)		**Sensitivity/Uncertainty Period (1,000 – 10,000 yr)**	
Peak Dose (mrem/yr)	Time of Peak (years after closure)	Peak Dose (mrem/yr)	Time of Peak (years after closure)
4E-3	10	0.1	1,500
Key radionuclide tritium dominates the peak dose		Key radionuclide ^{99}Tc is nearly 100% of this dose	

The results of the base case are supported by a number of sensitivity and uncertainty analyses, which are described below in Section 10.6.

10.2 AIR PATHWAY ANALYSIS

Potential releases into the gaseous pathway were evaluated and compared to the DOE O 435.1 performance objective of 10 mrem/yr for doses from airborne contamination. The number of contaminants that could potentially be released into the air is very limited, and the inventory of these radionuclides is not large. The results of the analyses (see Section 7.3.2) were orders of magnitude below the performance objective, as shown in Table 10-2. Additional sensitivity analyses were not considered necessary, owing to the negligible releases to the air.

10.3 RADON FLUX

Releases of radon from the facility were evaluated and compared to the 20 pCi/m^2/s radon flux performance objective in DOE O 435.1. The inventory of ^{226}Ra (the parent of ^{222}Rn) in WMA C residual waste is small, and initial radon fluxes are very low compared to the performance objectives. Ingrowth of ^{226}Ra from decay of the ^{238}U decay chain leads to increasing radon

fluxes at longer times (Section 7.2.2). However, the fluxes remain many orders of magnitude below the performance objective at all times, as presented in Table 10-3.

Table 10-2. Summary of Results for the Air Pathway.

Compliance Period (<1,000 yr)		Sensitivity/Uncertainty Period (1,000 – 10,000 yr)	
Peak Dose (mrem/yr)	Time of Peak (years after closure)	Peak Dose (mrem/yr)	Time of Peak (years after closure)
4E-3	0	2E-5	1,000 – 10,000
Key radionuclide ^{3}H at early times, ^{129}I in the sensitivity/uncertainty period. The dose is approximately constant in the period 1,000 to 10,000 years.			

Table 10-3. Summary of Radon Flux Analyses.

Compliance Period (<1,000 yr)		Sensitivity/Uncertainty Period (1,000 – 10,000 yr)	
Peak Flux ($pCi/m^2/yr$)	Time of Peak (years after closure)	Peak Dose ($pCi/m^2/s$)	Time of Peak (years after closure)
2E-4	1,000	7E-3	10,000
Flux from Tank 301		Flux from Tank 201	

10.4 INADVERTENT HUMAN INTRUSION

Doses associated with hypothetical inadvertent human intrusion were calculated for all sources in WMA C (see Section 9.0), and compared to the acute and chronic performance measures in DOE O 435.1. However, the calculated doses do not take account of the likelihood of intrusion into the various sources, and there are significant differences between them.

As discussed in Section 3, the tank domes were constructed of reinforced concrete; they are still in good condition and will likely provide a very substantial barrier to a drilling intrusion. Furthermore, upon closure the tanks will be filled with grout, which will add a second, very significant barrier to drilling intrusion. As a result of these barriers, intrusion into grouted tanks is not regarded as a credible event, as the tank domes and infill grout form very substantial and long-lasting barriers to the intrusion. Consequently, while the potential doses that might arise from intrusion into a tank are the highest calculated, the likelihood of occurrence of intrusion into a tank is regarded as very small. As a result, the intrusion analyses for tanks should be regarded as informational, and should not be compared to the performance measures.

By contrast, barriers are much less robust or nonexistent for pipelines and other ancillary equipment, and as a result the primary potential for intrusion is considered to be into ancillary equipment. The likely event for ancillary equipment would be intrusion into a waste transfer pipeline, as discussed in Section 9. This event was used to represent intrusion into any ancillary equipment, and these results are used for comparison with performance measures.

The calculated doses associated with the acute and chronic exposure scenarios for intrusion into a waste transfer pipeline are summarized in Table 10-4 for the compliance time period and for the sensitivity/uncertainty analysis period. The calculated doses for acute and chronic exposure scenario from potential intrusion into a waste transfer pipeline remain below the DOE O 435.1 performance measure for the time period evaluated beyond 100 years after closure. The acute scenario dose is dominated by ^{137}Cs and ^{239}Pu, while chronic scenario doses are dominated by ^{90}Sr, ^{137}Cs and ^{239}Pu. The total dose generally shows a steep decline, compared to the timescales evaluated in the PA, due to short half-lives of ^{90}Sr and ^{137}Cs but becomes stable once long-lived ^{239}Pu becomes the dominant dose contributor. The dominant exposure condition for the assessment was the acute scenario, which had higher doses than the chronic exposure scenarios at 100 years after closure. At longer times (greater than about 500 years after closure), the acute scenario also produced higher calculated doses for the intrusion into waste transfer pipelines, mainly because long-lived ^{239}Pu plays a more important role in the dose calculation.

Table 10-4. Summary of Inadvertent Human Intrusion Analyses for Intrusion into Ancillary Equipment.

Exposure Scenario	Compliance Period (<1,000 yr)		Sensitivity/Uncertainty Period (1,000 – 10,000 yr)	
	Peak Dose (mrem/yr)	Time of Peak (years after closure)	Peak Dose (mrem/yr)	Time of Peak (years after closure)
Acute inadvertent intruder Performance measure – 500 mrem	36.0	100	11.1	1,000
Chronic inadvertent intruder Performance measure – 100 mrem/yr	8.2	100	0.07	1,000

10.5 GROUNDWATER RESOURCE PROTECTION

Groundwater protection was evaluated by comparing calculated concentrations in groundwater 100 m (328 ft) downgradient from the WMA C boundary during the compliance and sensitivity/uncertainty analysis time periods with the National Primary Drinking Water Regulations for MCLs for radionuclides listed in 40 CFR 141.66. The State of Washington has adopted the Federal drinking water regulations (revised as of July 1, 2009) for MCLs for radionuclides in WAC 246-290, “Group A Public Water Supplies” [WAC 246-290-025, “Adoption by Reference” and WAC 246-290-310, “Maximum Contaminant Levels (MCLs) and Maximum Residual Disinfectant Levels (MRDLs)”].

Peak calculated radionuclide groundwater concentrations are summarized and compared to applicable groundwater protection criteria in Table 10-4. For beta/gamma-emitting radionuclides (^{99}Tc, ^{129}I, ^{79}Se, and ^{126}Sn), an assessment of compliance with the radionuclides’ respective MCLs was conducted by computing the dose equivalent and comparing the sum of the dose over time to the 4-mrem/yr dose equivalent limit. For the man-made radionuclides other than tritium (^{3}H) and ^{90}Sr, 40 CFR 141.66 requires the maximum concentration limits to be calculated based on 4-mrem total body or organ dose equivalents from 2 L/day (0.5 gal/day) drinking water intake using the 168-hour data list in NBS 69 “Maximum Permissible Body

Burdens and Maximum Permissible Concentrations of Radionuclides in Air and in Water for Occupational Exposure" (National Bureau of Standards Handbook 69). Using this handbook, the MCLs for ^{99}Tc and ^{129}I are 900 pCi/L and 1 pCi/L, respectively. The maximum permissible concentrations in water for ^{79}Se and ^{126}Sn are not mentioned specifically in the handbook, and the MCL for these two radionuclides could not be established.

Table 10-5. Comparison of Peak Groundwater Pathway Results to Groundwater Protection Criteria.

Groundwater Performance Measure (Based on 40 CFR 141)	Compliance Period (100 m Downgradient) (Years 2035–3035)	Post-Compliance Period (100 m Downgradient) (Years 3035–12035)	Comments
Beta/gamma dose equivalent ≤ 4 mrem/yr	5E-4 mrem/yr [a]	0.13 mrem/yr [a]	Peak concentrations of ^{99}Tc within the compliance and post-compliance time periods are ~0.12 pCi/L and 30 pCi/L, respectively. ^{99}Tc accounts for almost all of the peak dose. Other minor contributors to dose are ^{129}I, ^{79}Se, and ^{126}Sn.
Gross alpha activity concentration (excluding radon and uranium) ≤ 15 pCi/L	0 pCi/L	1E-10 pCi/L [b]	No arrival at the water table due to high K_d of radionuclides such as ^{237}Np, ^{230}Th, and ^{226}Ra.
Combined ^{226}Ra and ^{228}Ra concentration ≤ 5 pCi/L	0 pCi/L	7E-7 pCi/L	Ingrowth from ^{238}U, ^{238}Pu, ^{234}U, and ^{232}Th.
Uranium concentration ≤ 30 µg/L MCL	0 µg/L	0.05 µg /L	—
^{90}Sr concentration ≤ 8 pCi/L MCL	NA [c]	NA [c]	—
^{3}H concentration ≤ 20,000 pCi/L	0 pCi/L	1E-10 pCi/L [b]	—

[a] Calculated using the formula (C_{Peak}/MCL) × 4 mrem/yr. For example, using C_{Peak} (peak concentration for ^{99}Tc) = 30 pCi/L and MCL = 900 pCi/L for ^{99}Tc, which is the most significant dose contributor, the equivalent dose is calculated to be 0.13 mrem/yr.

[b] Concentrations less than 1E-10 pCi/L are essentially zero.

[c] Not applicable; ^{90}Sr was not released to the groundwater pathway during the 10,000-year period due to its relatively short half-life and its low mobility in the subsurface.

MCL = maximum contaminant level NA = not applicable

Reference: 40 CFR 141, "National Primary Drinking Water Regulations," Code of Federal Regulations, as amended.

For beta/gamma-emitting radionuclides, the peak dose equivalent was 5×10^{-4} mrem/yr during the compliance time period and about 0.13 mrem/yr for the post-compliance time period, which was dominated by contribution of ^{99}Tc. This dose is below the 4-mrem/yr dose equivalent limit.

The peak gross alpha activity—combined ^{226}Ra and ^{228}Ra concentration, ^{90}Sr concentration, and tritium concentration in the groundwater—is zero during the compliance period, and is projected to be essentially zero during the post-compliance period. The peak uranium concentrations within the compliance and post-compliance time periods are 0 µg/L and 0.05 µg/L, respectively.

All of the groundwater protection performance metrics are well below the performance measures, which provide confidence that there is a reasonable expectation that the facility will meet the requirements under the Safe Drinking Water Act of 1974 or 40 CFR 141.66.d.

10.6 SENSITIVITY AND UNCERTAINTY ANALYSES FOR THE GROUNDWATER PATHWAY

The interpretations and discussion in Sections 10.1 through 10.5 were based on the base case analysis. In Section 8, a series of sensitivity and uncertainty analyses were reported that evaluate changes in calculated groundwater impacts that result from changes in selected input parameter estimates.

A set of deterministic sensitivity analyses were conducted that show the effects when the safety functions are degraded compared to their expected behavior. The FEPs that may lead to this degraded behavior are identified in Appendix H. For the purposes of the PA, it is not necessary to quantify the likelihood that the FEPs will influence the system; if there is the potential for a safety function to be degraded, it is evaluated as a sensitivity analysis. The specific safety functions examined in this way relate to the various physical components of the disposal system that included model evaluations of groundwater impacts with the following:

- Higher than expected infiltrations rates; these may be the result of a number of potential effects, ranging from unexpectedly poor performance of the cover, through changes in land use with irrigation on top of the facility
- Changes in the effectiveness of the tanks and infill grout to act as barriers, by assuming that the hydraulic conductivity of the tanks increases at times earlier than expected
- Changes in the leachability of the residual wastes, by assuming that the material would dissolve instantly and completely upon contact with water
- Bounding inventories for unretrieved tanks
- Alternative conceptualizations of the stratigraphy of the vadose zone
- Alternative assumptions about dilution in the aquifer.

The maximum deviation from the base case was a factor of 4.8 higher than the base case, which occurred for sensitivity case INV01, which assumed the maximum ^{99}Tc inventory in the unretrieved tanks, as shown in Table 10-5. For this case, there is no change in the time dependence of the results compared to the base case; the peak occurs in the

sensitivity/uncertainty time period, and the concentration in the compliance time period is small. This case represents an assumption that no further retrieval of ^{99}Tc from tanks will be possible.

Of the sensitivity cases that evaluated safety functions, the maximum deviation from the base case was produced by cases that evaluated the aquifer safety function, as shown in Table 10-6. By setting the aquifer flow properties to their 5th percentile, the peak concentration increased by a factor of 2.6 compared to the base case. There is no change in the time dependence of the results compared to the base case; the peak occurs in the sensitivity/uncertainty time period, and the concentration in the compliance time period is small. This case represents an assumption of minimal dilution in the aquifer.

Table 10-6. Summary of Maximum Results from Sensitivity Cases.

Highest Calculated Peak Concentration of ^{99}Tc divided by the base case	**Change in Time of Peak (years after closure) compared to base case**
4.8	No change
Sensitivity case INV01, with maximum ^{99}Tc inventory in unretrieved tanks.	
Highest Calculated Peak Concentration of ^{99}Tc divided by the base case	**Time of Peak (years after closure)**
2.6	No change
Sensitivity case GWP01, with 5% aquifer properties leading to minimal dilution.	

For all of these sensitivity analyses, the disposal system met the performance objectives. This result demonstrates the robustness of the PA to alternative assumptions with respect to the behavior of the safety functions.

In addition to these deterministic analyses of the effect of the safety functions evaluated in Section 8, probabilistic analyses were conducted to show the effects of parameter uncertainty on the performance of the system. A number of parameters were assigned probability density functions, the PA was run probabilistically, and the results were evaluated as a probability density function of dose. The highest calculated groundwater dose in the compliance period was about 0.07 mrem/yr, and the highest calculated peak dose in the sensitivity/uncertainty analysis period was 2.5 mrem/yr, as shown in Table 10-7. The most important uncertain parameters that affect the peak dose in the groundwater pathway are the vadose zone hydraulic properties and Darcy flux in the saturated zone (see Section 8.1.4.4 for details).

For the entire range of input parameters, even including the extreme of the sampled inputs, the disposal system met the performance objectives. These results show the robustness of the PA to uncertainties in the input parameters used in the model.

Table 10-7. Summary of Relevant Results from the Probabilistic Uncertainty Analysis of Groundwater Pathway.

Compliance Period (<1,000 yr)		Sensitivity/Uncertainty Period (1,000 – 10,000 yr)	
Mean Peak Dose (mrem/yr)	Time of Peak (years after closure)	Mean Peak Dose (mrem/yr)	Time of Peak (years after closure)
7E-4	1,000	0.17	3,400
Key radionuclide ^{99}Tc comprises nearly 100% of these doses			
Highest Calculated Peak Dose (mrem/yr)	Time of Peak (years after closure)	Highest Calculated Peak Dose (mrem/yr)	Time of Peak (years after closure)
0.07	1,000	2.5	2,400
Key radionuclide ^{99}Tc comprises nearly 100% of these doses			

10.7 USE OF PERFORMANCE ASSESSMENT RESULTS

The PA has substantiated that landfill closure of residual wastes in WMA C can meet applicable performance objectives and measures. The result can be used to support decisions regarding further retrieval from tanks, in supporting determinations that sufficient retrieval has been accomplished. This will be done as part of a determination that the projected releases of radionuclides to the environment are maintained ALARA. DOE O 413.3B, Program and Project Management for the Acquisition of Capital Assets requires an analysis of ALARA analysis during the design and construction of DOE facilities. The purpose of an ALARA options analysis is to consider those actions that could be taken to reduce both costs and dose. For WMA C, the ALARA options analysis is in part addressed through the process associated with retrieval as documented in Retrieval Data Reports. Although ALARA is not specifically called out in the Retrieval Data Reports, these reports evaluate available waste retrieval technologies to identify (1) retrieval function requirements, (2) retrieval technologies, and (3) appropriate retrieval alternatives. The Retrieval Data Report is considered complete when “no retrieval” is identified as the preferred option, indicating that the amount of retrieval achieved is optimized.

The key result that supports these decisions is the sensitivity analysis case in which no further retrieval was assumed (see Section 10.6 sensitivity case INV01). This analysis case showed that the closed WMA C disposal system met the performance objectives without further retrieval.

In addition to these ALARA considerations that are embedded in the retrieval process, it is anticipated that the PA will be used to support optimization during final detailed design of the facility. This can be done using the PA to establish functional requirements for the design features, such as a functional requirement for infiltration through the surface cover barrier.

In addition, the PA will be used to support decisions related to WIR that will be left at closure within tanks and ancillary equipment. DOE M 435.1-1 Chapter IIB.(2)(a)2. is the second criteria for the WIR evaluation process. This criterion states that such wastes “(w)ill be managed to meet the safety requirements comparable to the performance objectives set out in 10 CFR 61

Subpart C, *Performance Objectives*." This PA will be the primary tool used to demonstrate that 10 CFR 61.41 and 10 CFR 61.42 are met. Further, the PA will be used to develop the site-specific factors related to 10 CFR 61.55 Class C comparison.

10.8 FUTURE WORK

The current PA is based on partial retrieval of residual wastes from WMA C, and continued retrieval is ongoing. The PA will be updated to reflect updated inventory information when the tanks are considered to be fully retrieved and sample-based inventories are available. Additionally, detailed design of the closure system needs to be performed, including the specific grout formulation to be used in filling the tanks, and the detailed design of the final closure engineered surface cover system. These detailed designs may require updates of the PA.

Grout infill material and the tank concrete shell diverts any infiltrating water from flowing through the tank. Understanding the long-term degradation rates of these cementitious materials under Hanford shallow vadose zone conditions should be considered as an area of future research.

DOE M 435.1-1 Chg 1 [IV.P.(4)] includes a requirement for PA maintenance to evaluate the impact of design and operational changes and to incorporate any new information regarding waste forms, site characteristics, etc. In addition to a PA maintenance plan, required documentation in support of the Tier 1 Closure Authorization Statement (CAS) for WMA C includes a closure plan, monitoring plan, and annual reports documenting any recent changes to the plans for the facility or changes in the understanding of the environmental impacts from the facility. The path forward in the near term includes the following:

- Preparation of an updated PA that addresses key findings, secondary issues, and observations provided by the Low-Level Waste Disposal Facility Federal Review Group (LFRG) during its review of this document

- Development of an additional revision of the PA that resolves review comments by outside agencies (NRC, State Regulators, Public)

- Development and implementation of a change control process to address potential effects of changes in closure actions and decisions that could affect the validity of the analysis and conclusion of this PA.

This page intentionally left blank.

11.0 QUALITY ASSURANCE

Model development and application for the WMA C PA was performed under a general project plan for modeling for RCRA closure analyses and DOE O 435.1 PAs. This general project plan implements the requirements of Title 10, CFR, Part 830, "Nuclear Safety Management" (10 CFR 830) Subpart A, "Quality Assurance Requirements"; DOE O 414.1D, Quality Assurance; and State and Federal environmental regulations. Additionally, this general project plan follows EPA guidance provided in EPA/240/R-02/007, Guidance for Quality Assurance Project Plans for Modeling, EPA QA/G-5M. It addresses as relevant and important all nine "Group A" elements presented in EPA/240/B-01/003, EPA Requirements for Quality Assurance Project Plans, EPA QA/R-5. The nine elements include problem definition and background, quality objectives and criteria for measurements and data acquisition leading to model inputs and outputs, data validation and usability, references, documentation and records management, special training requirements and certifications for modelers, and assessments and reports to management. The model documentation requirements identified during project planning align with DOE management expectations for compliance listed in Revision 1 of EM-QA-001, EM Quality Assurance Program, Attachment H, "Model Development, Use, and Validation."

11.1 ENVIRONMENTAL MODEL LIFECYCLE QUALITY ASSURANCE PROCESS

The development, application, and preservation of environmental models used to support regulatory decision-making and analysis is conducted under a general project plan that implements the requirements of DOE O 414.1D and the direction related to modeling in EM-QA-001, as well as EPA guidance provided in EPA/240/R-02/007. This plan provides for modeling to be performed in a framework for quality assurance of the full lifecycle, with integrated control of models, implementing software, applications, and supporting information as depicted in Figure 11-1.

Highlights of the general plan requirements under which this PA was developed include the following.

- Training is stipulated in the general plan for modelers to complete that ensured the requirements and quality assurance process for model development and application are communicated.

- Software used to implement environmental models is controlled per the requirements of DOE O 414.1D (refer to Section 11.2, below, for further details on this with respect to this PA). Modeling software management is provided at the Hanford Site by CHPRC as part of that contractor's integration role for Hanford Site modeling activities. CHPRC's controlled software management procedure implements the DOE O 414.1D software requirements. This control includes configuration management of code; use of a central registry for software registration, grading and classification, approval tracking, and use logging; and software quality assurance documentation requirements. Software users are required to complete software-specific training assignments, obtain code from the

software owner (configuration management system), complete installation testing for specific computers per the test plan, and submit software installation and checkout documentation to record tested installations.

- A process for model documentation, control, and preservation is specified (refer to Section 11.3, below, for further details on this with respect to this PA). Features of this process include documentation of model development in model package reports (a qualify configuration item); documentation of model applications in an Environmental Model Calculation File (EMCF, also a quality configuration item); and preservation of models, model applications, and model basis information (non-direct measurements) in an integrated archive. Full checking and senior review of model package reports and EMCFs is required as part of this process.

The general plan follows the EPA guidance in structure, and provides for flexibility to support with a specific plan for modeling projects that require additional quality assurance/quality control requirements. The WMA C PA modeling work was developed under the general plan and a complementary project-specific plan.

11.2 CONTROLLED SOFTWARE USE

Software used for model implementation was managed following a controlled software management procedure (PRC-PRO-IRM-309, "Controlled Software Management") that implements the requirements of 10 CFR 830 Subpart A, "Quality Assurance Requirements"; DOE O 414.1D; and State and Federal environmental regulations. This controlled software management procedure directs management of all software including configuration control, evaluation, implementation, acceptance and installation testing (verification and validation), and operation and maintenance. Software used to implement the models and perform calculations was approved for use under this controlled software management procedure that also implements the requirements of, and is compliant with, DOE management expectations for compliance listed in Revision 1 of EM-QA-001, Attachment G, "Software Quality Requirements."

The WMA C PA relies on two primary controlled-use software packages to simulate the flow and transport in the subsurface, simulate source term releases, conduct inadvertent intruder calculations, and simulate air-pathway transport in order to calculate doses resulting from the disposal of waste at the facility. These primary software packages are STOMP© and GoldSim© Pro, which are qualified for controlled use at the Hanford Site in accordance with their respective software management and testing plans. These software packages are registered in the Hanford Information Systems Inventory (HISI). HISI provides the platform for tracking all software in use at the Hanford Site. For safety software (which includes STOMP© and GoldSim© Pro), the HISI entry is used to record approval for use of software versions, to maintain a registry of authorized users, and to log all instances of the software's usage. Software is maintained using the established Hanford Site configuration management system, MKS Integrity™[1], which is the Hanford Site standard for preserving and managing source code and executable versions of

[1] MKS Integrity, Integrity, and all other PTC product names and logos are trademarks or registered trademarks of Parametric Technology Corporation or its subsidiaries in the United States and in other countries.

software. MKS Integrity™ provides a "checkpoint" feature that locks files at particular points, such as when an executable has passed quality assurance testing, been documented in an acceptance test report, and been approved for use.

Software-specific descriptions, and associated quality assurance documentation for each software package used in the PA, are summarized below for the primary model implementation software packages used for the WMA C PA (STOMP© and GoldSim©).

11.2.1 Subsurface Transport Over Multiple Phases

The vadose zone fate and transport calculations are performed using "CHPRC Build 4" of the STOMP© simulator software (PNNL-12030; PNNL-15782, "STOMP Subsurface Transport Over Multiple Phases Version 4.0 User's Guide"). STOMP© is registered in the HISI under identification number 2471. The STOMP© simulator was developed at PNNL, which maintains a program to test STOMP© code to meet ASME NQA-1-2008, "Quality Assurance Requirements for Nuclear Facility Applications" software requirements, as well as the requirements specified under DOE O 414.1D for Safety Software. The "Water" and "Water-Transport" operational modes of STOMP© were used for the WMA C PA, and all code elements of those modes that were used have been ASME NQA-1-2008 tested by PNNL. STOMP© use for the WMA C PA is managed and controlled such that the computational needs filled by use of STOMP© (and any associated utility codes) and the specific roles and responsibilities for management and the modeling staff and subcontractors have been identified and traced. These responsibilities include modeler training, source code installation and testing, preserving the software and verification test results, operation and maintenance of the original Fortran source code and executable files provided by PNNL, validation and verification that the PNNL quality assurance documentation demonstrate that STOMP© meets the CHPRC modeling needs and purposes, reporting and documenting any software errors (none were encountered during the development of the WMA C PA), management of the STOMP© input files, and contingency and disaster recovery (which was not encountered during development of the WMA C PA). Acceptance and installation tests of the STOMP© simulation software demonstrate that it is appropriate for its intended uses for the WMA C PA and that it has been successfully installed on computing systems used for STOMP© simulations to develop the WMA C PA.

STOMP© was executed on two independent computer systems. The first of these is the GREEN Linux®[2] system that is owned and managed by INTERA, Incorporated, which is a subcontractor to WRPS. The GREEN system is physically located at INTERA's Richland, Washington office, and is comprised of a Dell™[3] PowerEdge™ R510 with two 6-core Intel® Xeon®[4] X5660 processors @ 2.80GHz and 48 GB of RAM. The second system used was the Tellus Subsurface Simulation Platform, a Linux® cluster system that is owned and managed by CHPRC to support Hanford Site integrated environmental modeling needs. The Tellus cluster system is comprised of a Dell™ PowerEdge™ M1000e blade enclosure with 16 Dell™ PowerEdge™ M610 and

[2] Linux® is a registered trademark of Linus Torvalds in the U.S. and other countries.

[3] Dell and PowerEdge are trademarks of Dell Inc.

[4] Intel and Xeon are trademarks of Intel Corporation in the U.S. and other countries.

1 Dell™ PowerEdge™ M710 blade servers. The M610 blade servers each have 6-core Intel®
Xeon X5670 processors @ 2.93 GHz (12MB cache) and 96 GB of RAM.

DOE/RL-2011-50 contains a summary of the main model attributes and code selection criteria that serve as the basis for the demonstration of the adequacy of the STOMP© code for use in vadose zone modeling at the Hanford Site. The results of the evaluation in DOE/RL-2011-50 show that the STOMP© code is capable of meeting or exceeding the identified attributes and criteria.

11.2.2 GoldSim©

Software development of GoldSim© Pro meets ASME NQA-1-2008 software requirements, as well as the requirements specified under DOE O 414.1D for Safety Software. GoldSim© Pro use at the Hanford Site is managed and controlled such that the computational needs filled by use of GoldSim© Pro (and any associated utility codes) and the specific roles and responsibilities for management and the modeling staff and subcontractors have been identified and traced. These responsibilities include modeler training, source code installation and testing, preserving the software and verification test results, validation and verification that the GoldSim© Pro quality assurance documentation demonstrate that GoldSim© Pro meets identified modeling needs and purposes, reporting and documenting any software errors (none were encountered during the development of the WMA C PA), management of the GoldSim© Pro input files, and contingency and disaster recovery (which was not encountered during the development of the WMA C PA). Acceptance and installation tests of the GoldSim© Pro simulation software demonstrate that it is appropriate for its intended uses for the WMA C PA and that it has been successfully installed on the computing systems used to conduct WMA C PA modeling.

11.2.3 Other Hanford Site Tank Waste Management Software Tools

The PA effort makes use of other tank waste management software tools available at the Hanford Site in the preparation of model inputs.

11.2.3.1 Tank Waste Information Network System/Best Basis Inventory. TWINS is a web-based database system providing access to Hanford tank waste data, documents, graphics, photos and reports via the Hanford Local Area Network (HLAN) and to approved offsite users via the Internet. This legacy software was developed over time and contains a number of primary databases, reporting tools, and support tools. The database system consists of the Tank Characterization Database, Tank Vapor Database, BBI Estimates and BBI Model tool, the Automated Tank Characterization Report system, Data Source Access, Automated Statistics tool, and Automated Vector creation tool. These systems were developed by various projects over a number of years and have been consolidated within the TWINS architecture. A system description can be found in RPP-RPT-39487, “TWINS Software Description.” TWINS changes are tracked in accordance with internal WRPS procedures used for TWINS software change control.

Figure 11-1. Lifecycle Quality for Environmental Models.

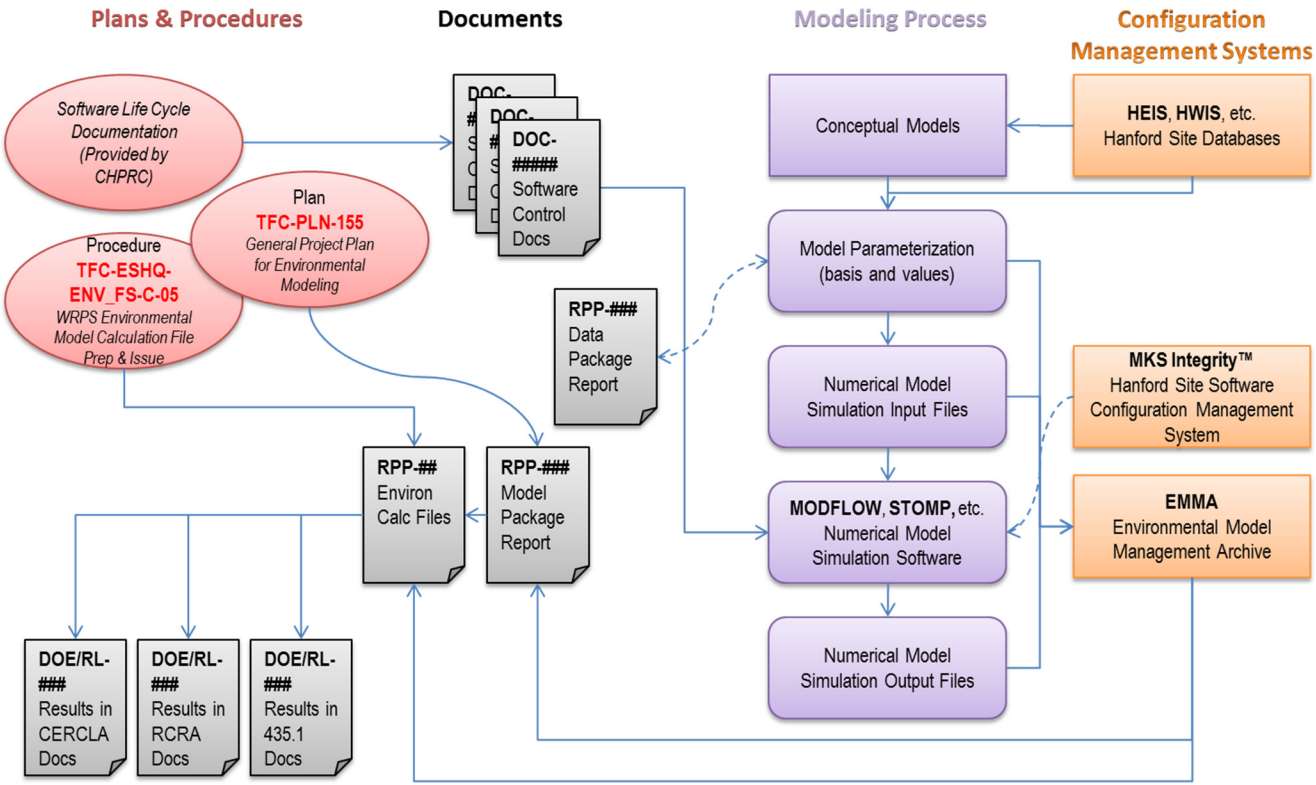

435.1 = DOE O 435.1, 2001, Radioactive Waste Management, U.S. Department of Energy, Washington, D.C.
CERCLA = Comprehensive Environmental Response, Compensation, and Liability Act of 1980, 42 USC 9622, et seq.
CHPRC = CH2M HILL Plateau Remediation Company
HEIS = Hanford Environmental Information System
HWIS = Hanford Well Information System
RCRA = Resource Conservation and Recovery Act of 1976, 42 USC 6901, et seq.

References:

TFC-ESHQ-ENV_FS-C-05, "WRPS Environmental Model Calculation Preparation and Issuance," Washington River Protection Solutions LLC (WRPS) Tank Farms, Richland, Washington.
TFC-PLN-155, "General Project Plan for Environment Modeling," Washington River Protection Solutions LLC (WRPS) Tank Farms, Richland, Washington.

MKS Integrity, Integrity, and all other PTC product names and logos are trademarks or registered trademarks of Parametric Technology Corporation or its subsidiaries in the United States and in other countries.
MODFLOW software has been developed and distributed by the U.S. Geological Survey, Washington, D.C.
Battelle Memorial Institute (Battelle) retains copyright on all versions, revisions, and operational modes of the Subsurface Transport Over Multiple Phases (STOMP©) software simulator, as permitted by the U.S. Department of Energy. STOMP© is used here under a limited government use license.

Except as noted, BBI estimates with radionuclides decayed to January 1, 2020 were used as source terms for the PA. The BBI is developed using applicable output from the Tank Characterization Database, Automated Statistics tool, Automated Vector creation tool and BBI Model tool. The BBI values are based on sample- and/or model-based composition estimates multiplied by waste volume estimates. Best-Basis process outputs are described in Section 3.2.2. The BBI was developed in accordance with RPP-7625, "Guidelines for Updating Best-Basis Inventory" and TFC-ENG-CHEM-P-53, "Best-Basis Inventory Evaluations." BBI Model tool output was downloaded to a spreadsheet which was reviewed and checked in accordance with internal WRPS procedures used in the preparation and review of engineering calculations and incorporated into RPP-RPT-42323. Output from RPP-RPT-42323 is included in Tables 3-13 through 3-16 in this report.

11.2.3.2 Hanford Tank Waste Operations Simulator. The HTWOS model is a dynamic flowsheet mass balance model that tracks and predicts the movement of waste over the full River Protection Project mission (that is, from current tank contents through treatment to disposal). It establishes the timing of key process steps and the life-cycle system mass balance using a well-defined set of assumptions (the current set being described in Revision 6 of ORP-11242, "River Protection Project System Plan"). The various processes are modeled in sufficient detail to estimate the overall timing of each process and the quantities and composition of the primary and secondary waste streams, taking into account the interactions, including recycle, between the various processes and unit operations. The HTWOS model and validation of the model is described in RPP-RPT-39908, "Hanford Tank Waste Operations Simulator Model (HTWOS) Version 3.0 Verification and Validation Report." The HTWOS spreadsheet output for residual inventories is SVF-2109, Rev. 0, "Tank_Residuals_4MinTimestep(6Melters)-mmr-11-031-6.5-8.3r1-2011-03-18-at-01-31-58_M1.xlsm.

HTWOS residual inventories provided lower bound inventory estimates in the PA for tanks not yet retrieved as of September 1, 2014 (see Section 3.2.2.3.3). The HTWOS model is controlled in accordance with RPP-50816, "Software Management Plan for Grade D Custom Developed Hanford Tank Waste Operations Simulator (HTWOS)." The HTWOS output was downloaded to a spreadsheet to back decay values to January 1, 2020 and scale the values for a waste volume of 360 ft^3. The spreadsheet was reviewed and checked in accordance with internal WRPS procedures used in the preparation and review of engineering calculations and incorporated into RPP-RPT-42323. HTWOS residual inventory estimates are included in Table 3-17 in this report.

11.2.3.3 Video Camera Computer-Aided Design Modeling System. The CCMS was used to estimate the volume of residual waste in retrieved tanks. The CCMS approach consists of obtaining in-tank videos showing the location of residual solids and liquid waste remaining in a tank after retrieval. The videos are reviewed and a 3-D CAD drawing of the residual waste is developed using a template of an empty tank. The volume of the residual waste is then calculated using CAD software. The CCMS approach and quality assurance/quality control requirements are described in RPP-52784, "Video camera/CAD Modeling System for Retrieval: HISI #3254 Software Management Plan." CCMS modelers are trained and qualified in accordance with internal WRPS procedures used for post-retrieval volume determinations. Uncertainty in CCMS estimates is described in RPP-23403. Actual and upper bound volumes

based on CCMS estimates are documented in applicable waste volume reports and incorporated into the BBI.

11.2.3.4 Other Legacy Software. This section provides information about legacy software tools, namely the HDW software and the ORIGEN2 software, that are cited in the PA but are not currently managed as controlled use software.

11.2.3.4.1 Hanford Defined Waste Model. The HDW model (RPP-19822) uses a spreadsheet format to combine tank waste transfer and process information with Hanford Site irradiated fuel and separation plant process records from the ORIGEN2 model (RPP-13489) to produce total chemical and radionuclide compositions by waste type. These estimates comprise 46 radionuclides (the standard radioisotopes in the BBI) and 33 nonradioactive species (24 of the 25 standard chemicals from the BBI plus citrate, N-[hydroxyethyl]-ethylenediaminetriacetic acid, ethylenediaminetetraacetic acid, glycolate, acetate, dibutyl phosphate, butanol, ammonia, and ferrocyanide) and four properties (density, water wt%, total organic carbon wt% and sludge void fraction [total organic carbon is a standard constituent in BBI]).

The HDW model concentration estimates are considered to have higher uncertainty compared to sample-based concentrations and are used in BBI to fill gaps where sample data do not exist for a waste type and/or constituent. RPP-19822 (HDW model, Revision 5) was checked in accordance with company procedures (see RPP-19822, Appendix G). Revision 5 uses the same software and formulas as Revision 4, but includes updated ORIGEN2 results and tank waste process inputs to estimate tank waste type compositions and does not include the supernatant mixing model, tank waste layering model, or tank-specific inventory estimates in Revision 4. Additional description of the waste type compositions model is provided in LA-UR-96-3860, "Hanford Tank Chemical and Radionuclide Inventories: HDW Model Rev. 4."

11.2.3.4.2 Oak Ridge Isotope Generation and Depletion Code 2. The primary radionuclide input to the HDW model consists of a file of "pre-decayed" isotopic inventories (Fuel Activity Records) generated using the ORIGEN2 and Radioactive Decay (DK) and Processing (PRO) (DKPRO) codes. The ORIGEN2 code is used to calculate initial radionuclide inventories as a function of fuel type, fuel burn-up, and reactor type, with subsequent decay and processing computed by the DKPRO code. Input to the DKPRO code includes an archive file of separations processing records by fuel batch, a file of processing directives, a file of summary directives, and a set of ORIGEN2 inventory files representing unprocessed radionuclide inventories. The ORIGEN2 and DKPRO software and outputs are described in RPP-13489. Review and checking ORIGEN2 results and verification and validation of DKPRO code are presented in Appendices A and F of RPP-13489.

11.3 MODEL DOCUMENTATION, CONTROL, AND PRESERVATION

The four basic model components necessary to provide traceable, reproducible models are (1) the basis for the model inputs, including data packages, (2) the models themselves, (3) the applications of the models, and (4) the implementing software.

As noted above regarding controlled software use, software used for the development of the WMA C PA is maintained using the established Hanford Site configuration management system, MKS Integrity™. However, models are comprised of more than just software. Control and preservation of the other three identified model components (basis, models, and applications) are necessary as well. Under the general project plan for modeling for RCRA closure analyses and DOE O 435.1 PAs followed for development of the WMA C PA, these components are maintained in the WRPS Environmental Model Management Archive (EMMA). The EMMA is the approved means to maintain traceability and reproducibility for these model components by providing for version documentation and preservation of the model basis, inputs, and output, along with identification of the software packages and specific versions used. The EMMA is fundamentally a highly disciplined file system, with defined structure, controls on staging and uploading content, requirements for content preservation, and an active backup plan that ensures the EMMA is frequently synchronized to a controlled, managed disk space inside HLAN. EMMA's organization aligns to the three components mentioned: basis, models, and applications.

- The EMMA "basis" bin includes Electronic Model Data Transmittal coversheets to document preserved data and information that form the basis of model parameterization.

- The EMMA "model" bin includes model package reports that provide the description and explanation of the modeling objectives, conceptualization, implementation, uncertainty and sensitivity evaluations, version configuration control, and the limitations of the models. Model input files that form the specific version of a configuration-controlled model are preserved with the model package report that documents that specific model and version.

- The EMMA "application" bin includes documentation of model applications. While the model package reports include information regarding the complete configuration managed version of the WMA C PA models, the EMCF documents information on specific cases analyzed with the models. This includes the application of the STOMP© and GoldSim© Pro models used to perform the calculations for the WMA C PA.

12.0 PREPARERS

Marcel P. Bergeron, Washington River Protection Solutions, LCC

M.A., Geology, Indiana University, Bloomington, Indiana
B.A., Geology, University of Vermont, Burlington, Vermont

Mr. Bergeron has more than 35 years of experience in a wide variety of subsurface investigations and studies at radioactive and hazardous waste facilities and contaminated sites. He is experienced in planning and implementation of environmental characterization and risk assessment investigations in a variety of roles including as a technical contributor, a project and task manager, and a line manager. He has performed quantitative analysis of subsurface systems using analytical and numerical models and visualization tools. He has significant technical project experience in managing technical teams, schedules, and budgets for multi-disciplinary projects and communication of project results with clients, regulators, and stakeholders.

For this document, Mr. Bergeron is the technical project lead for Washington River Protection Solutions, LLC and the document manager in the preparation for this performance assessment.

Michael P. Connelly, TecGeo, Inc.

M.S., Geology, University of Utah
B.S., Geology, University of Utah

Mr. Connelly provided technical support to the performance assessment team for the Tank Farm Vadose Zone Project and is a contributing author to this document. He has over 16 years of experience in environmental geohydrology including project management, groundwater modeling, and using computer techniques to analyze and interpret field data for remedial action and site characterization activities.

For this document, Mr. Connelly was the lead author for Section 3 (Site and Facility Characteristics) and provided technical support in the preparation of graphics and visualizations used in Sections 7 (Results of Analysis) and 8.2 (Sensitivity Analysis for the Groundwater Pathway).

James Field, Washington River Protection Solutions, LLC

Ph.D., Engineering Science, Washington State University, May 1989
M.S., Engineering Science, Washington State University, December 1986
B.S., Agricultural Engineering, University of Wyoming, August 1984

Dr. Field has 26 years of experience as engineer and manager in retrieval operations, RCRA/CERCLA waste site closure, technology testing and implementation, characterization, and data management. Dr. Field provides engineering support to the closure program. He was

lead for the inventory data package for the Hanford Closure and Waste Management EIS and prepared inventory data packages for tank residuals and releases to the soil in WMA C and WMA A-AX.

For this document, Dr. Field was the lead author for Section 3.2.2 (Tank Residual Waste Inventory) and provided inventory support for the performance assessment.

Nazmul Hasan, INTERA, Inc.

M.S., Environmental Engineering, Washington State University
B.S., Civil Engineering, University of Engineering & Technology, Bangladesh

Mr. Hasan has over eight years of experience performing numerical modeling in the saturated and unsaturated zones, including model calibration and sensitivity analysis, geostatistical analysis, and programming.

For this document, Mr. Hasan provided technical assistance in checking flow and transport models, developing the flow-fields for the abstraction model, and performing uncertainty analyses. He also prepared Section 9 (Inadvertent Intruder Analysis) and technically supported the overall document preparation and generation of figures and tables.

Raziuddin Khaleel, INTERA, Inc.

Ph.D., Soil and Water Engineering, Texas A&M University
M.S., Water Science and Engineering, Asian University of Technology
B.S., Civil Engineering, Bangladesh University of Engineering and Technology

Dr. Khaleel has over 25 years of experience in groundwater hydrology and numerical simulations of subsurface flow and transport. He was a key contributor to the Hanford Site Performance Assessment for the Disposal of Low-Level Waste in the 200 West Area Burial Grounds, the Performance Assessment for the Disposal of Low-Level Waste in the 200 East Area Burial Grounds, and the Hanford Immobilized Low-Activity Tank Waste Performance Assessment, particularly in the area of conceptual model development, direction of modeling, and in writing the document.

For this document, Dr. Khaleel developed the hydraulic parameter sets for the vadose zone, technical basis for conceptual vadose zone flow and transport model discussed in Appendix A, and document preparation.

Matthew W. Kozak, INTERA, Inc.

Ph.D., 1988, Chemical Engineering, University of Washington
B.S., 1981, Chemical Engineering, Cleveland State University

Dr. Kozak has more than 27 years of experience in the areas of performance assessment of near-surface and geological radioactive waste repositories, regulatory development, dose assessment for residual contamination of soils and buildings, toxic materials risk assessment, and mixed waste issues. He is the author of over 100 publications on these topics. He has supported national programs in the U.S. and countries in Europe, Asia, and Africa to site, develop, construct, and analyze facilities for disposal of radioactive waste.

He has participated in a number of international research programs, including the International Atomic Energy Agency's (IAEA) Coordinated Research Program on Improvement of Safety Assessment Methodologies (ISAM), and its successor programs: Application of Safety Assessment Methodologies (ASAM), Practical Illustration and Use of the Safety Case Concept in the Management of Near-Surface Disposal (PRISM), and most recently Modelling and Data for Radiological Impact Assessments (MODARIA).

For this document, Dr. Kozak has been one of the principal investigators, and was the lead author for Sections 1 (Introduction), 2 (Assessment Context), and 10 (Performance Evaluation and Interpretation of Results), and Appendix H (List of Features, Events, and Processes Applied to Waste Management Area C), with additional input on project coordination, reviews, and overall document preparation.

Sunil Mehta, INTERA, Inc.

Ph.D., Earth Sciences (Hydrogeology specialization), University of Kentucky
M.S., Geosciences, University of Louisiana at Monroe
M.Sc., Geology, University of Poona, India
B.Sc., Chemistry, Zoology, and Geology, University of Jodhpur, India

Dr. Mehta has more than 18 years of experience related to groundwater flow and transport modeling, reactive transport modeling, total system performance assessment, uncertainty analysis, geophysical logging, and well testing. He has worked on projects involving geologic isolation of radioactive wastes, environmental restoration activities, and water resources exploration and evaluation. Dr. Mehta has over 10 years of experience in designing, developing, and applying probabilistic tools to assess the long-term performance of radioactive waste storage and disposal facilities. He has performed reactive transport modeling and groundwater flow modeling to study behavior of contaminants such as uranium and hexavalent chromium in periodically rewetted zones influenced by aquifer-river interactions.

For this document, Dr. Mehta has been one of the principal investigators, performing the flow and transport abstraction modeling for uncertainty analysis and dose calculations, inadvertent

intruder analysis, and air-pathway analysis, focusing on project coordination, reviews, and overall document preparation.

William J. McMahon, CH2M HILL – Plateau Remediation Contractor

M.S., Agricultural Engineering, Texas A&M University
B.S., Agricultural Engineering, University of California, Davis

Mr. McMahon specializes in hydrologic data collection, analysis, and interpretation, and groundwater and vadose zone numerical modeling to support groundwater and vadose remedial projects. He has experience with a number of vadose zone and groundwater modeling packages. His other duties include directing hydrologic data collection efforts, analyzing and interpreting hydrologic data, assessing the effectiveness of groundwater remedial actions, developing work plans for data collection and interpretation, and performing numerical modeling to predict facility impacts to the aquifer to support remediation and construction decisions.

For this study, Mr. McMahon has been the one of the principal investigators, focusing on the flow and transport modeling using STOMP© code, groundwater pathway compliance calculations, sensitivity analysis, and document preparation.

Donna Morgans, INTERA, Inc.

M.S., Environmental Toxicology, Oregon State University
B.S., Microbiology, Oregon State University

Ms. Morgans has 27 years of experience in assessing the potential for adverse human health effects associated with exposure to radiological and chemical contaminants in air, soil, water, and plant and animal tissues. She has managed and performed complex risk assessment and data compilation efforts to address Federal and State regulations that include CERCLA and RCRA lifecycle decisions and DOE O 435.1 requirements. Her experience includes the development and review of elements within work plans, remedial investigations and RCRA facility investigations, and feasibility studies and corrective measure studies.

For this document, Ms. Morgans provided technical support in the development of exposure parameters and equations presented in Section 6.3.3 (Exposure and Dose Analysis). Exposure scenarios included in the performance assessment include the All-Pathways Representative Person Scenario, the Atmospheric Pathway, and the hypothetical Inadvertent Intruder scenarios. The exposure scenario included in the RCRA closure analysis includes the EPA tap water (resident) scenario used in the RCRA analysis.

Benjing Sun, Ramboll Environ, Inc.

Ph.D., Environmental Analytical/Atmospheric Chemistry, Brigham Young University
M.S., Environmental Sciences, Beijing Normal University
B.S., Physics, Beijing Normal University

Dr. Sun has expertise in managing and conducting projects in the areas of risk assessment, performance assessment, environmental chemistry, and air quality modeling. He also has experience in permitting, regulatory compliance and environmental forensic investigation. He has in-depth knowledge in fate and transport modeling among multiple environmental media, sensitivity and uncertainty analyses, and risk-based remediation goal setup following the technical guidance under CERCLA and RCRA, and other Federal and State regulations. He has managed and performed many risk assessment projects in support of remedial investigation/feasibility study, permit application, regulatory compliance, and risk management.

For this document, Dr. Sun developed exposure scenarios and associated parameters, dose calculation methodologies for various exposure pathways, and validation activities for the air pathway.

Kristin M. Singleton, Washington River Protection Solutions, LLC

B.S., Cellular and Molecular Biology, University of Nevada, Reno

Mz. Singleton has six years of experience performing extensive risk assessments across the Hanford Site Tank Farms and River Corridor. She has experience developing risk-based remediation goals in compliance with Federal and State regulations and interpreting modeling results for hazardous waste facilities and contaminated sites.

In this document, Mz. Singleton provided technical support in the development of waste inventories and screening analysis and supported the preparation of Sections 3.2.2 (Tank Residual Waste Inventory) and 4 (Screening Approaches).

This page intentionally left blank.

13.0 REFERENCES

04-TPD-083, 2004, "Agreement on Content of Tank Waste Retrieval Work Plans" (external letter from R. J. Schepens to M. A. Wilson, Nuclear Waste Program, State of Washington Department of Ecology, August 20), U.S. Department of Energy, Office of River Protection, Richland, Washington.

10 CFR 61, "Licensing Requirements for Land Disposal of Radioactive Waste," Subpart C—Performance Objectives, Code of Federal Regulations, as amended.

10 CFR 61, "Licensing Requirements for Land Disposal of Radioactive Waste," Subpart C—Performance Objectives, § 61.41, Protection of the General Population from Releases of Radioactivity, Code of Federal Regulations, as amended.

10 CFR 61, "Licensing Requirements for Land Disposal of Radioactive Waste," Subpart C—Performance Objectives, § 61.42, Protection of individuals from inadvertent intrusion, Code of Federal Regulations, as amended.

10 CFR 61, "Licensing Requirements for Land Disposal of Radioactive Waste," Subpart D—Technical Requirements for Land Disposal Facilities, § 61.52, Land disposal facility operation and disposal site closure, Code of Federal Regulations, as amended.

10 CFR 61, "Licensing Requirements for Land Disposal of Radioactive Waste," Subpart D—Technical Requirements for Land Disposal Facilities, § 61.55, Waste classification, Code of Federal Regulations, as amended.

10 CFR 830, "Nuclear Safety Management," Code of Federal Regulations, as amended.

10 CFR 830, "Nuclear Safety Management, Subpart A—Quality Assurance Requirements," Code of Federal Regulations, as amended.

1301789, 2012, "Modeling to Support Regulatory Decisionmaking at Hanford" (internal memorandum from A. C. Williams to M. S. Mccormick [Richland Operations Office] and S. L. Samuelson [Office Of River Protection], October 9), Associate Principal Deputy Assistant Secretary for Environmental Management, U.S. Department of Energy, Washington, D.C.

14-ECD-0030, 2014, "Transmittal of Clean Closure Practicability Demonstration for the Single-Shell Tanks DOE/ORP-2014-02" (letter from K. W. Smith to J. A. Hedges, Nuclear Waste Program, Washington State Department of Ecology, July 23), U.S. Department of Energy, Office of River Protection, Richland, Washington.

40 CFR 141, "National Primary Drinking Water Regulations," Subpart G—National Primary Drinking Water Regulations: Maximum Contaminant Levels and Maximum Residual Disinfectant Levels, §141.66 Maximum contaminant levels for radionuclides, Code of Federal Regulations, as amended.

62 FR 8693, 1997, "Record of Decision for the Tank Waste Remediation System, Hanford Site, Richland, WA," Federal Register, Vol. 62, pp. 8693–8704 (February 26).

64 FR 61615, 1999, "Record of Decision: Hanford Comprehensive Land-Use Plan Environmental Impact Statement (HCP EIS)," Federal Register, Vol. 64, pp. 61615–61625 (November 12).

65 FR 37253, 2000, "Establishment of the Hanford Reach National Monument," Federal Register, Vol. 65, pp. 37253–37257 (June 13).

73 FR 55824, 2008, "Amended Record of Decision for the Hanford Comprehensive Land-Use Plan Environmental Impact Statement," Federal Register, Vol. 73, pp. 55824–55826 (September 26).

78 FR 75913, 2013, "Record of Decision: Final Tank Closure and Waste Management Environmental Impact Statement for the Hanford Site, Richland, Washington," Federal Register, Vol. 78, pp. 75913–75919 (December 13).

80 FR 16082, 2015, "Low-Level Radioactive Waste Disposal," Federal Register, Vol. 80, pp. 16082-16125 (March 26).

ANL/EAD-4, 2001, "User's Manual for RESRAD Version 6," Environmental Assessment Division, Argonne National Laboratory, Argonne, Illinois.

ARH-CD-775, 1976, "Geohydrologic Study of the West Lake Basin," Atlantic Richfield Hanford Company, Richland, Washington.

ARH-LD-132, 1976, "Geology of the 241-C Tank Farm," Atlantic Richfield Hanford Company, Richland, Washington.

ASME NQA-1, 2000, "Quality Assurance Requirements for Nuclear Facility Applications," American National Standards Institute/American Society of Mechanical Engineers, New York, New York.

ASTM A283/A283M-03, 2005, "Standard Specification for Low and Intermediate Tensile Strength Carbon Steel Plates," ASTM International, West Conshohocken, Pennsylvania.

Atomic Energy Act of 1954, 42 USC 2011, et seq., as amended.

Baker, V. R., B. N. Bjornstad, A. J. Busacca, K. R. Fecht, E. P. Kiver, U. L. Moddy, J. G. Rigby, D. F. Stradling, and A. M. Tallman, 1991, "Quaternary Geology of the Columbia Plateau," The Geology of North America, Quaternary Nonglacial Geology: Conterminous U.S., Vol. K-2, Chapter 8, pp. 215–250.

Bear, J. 1972, Dynamics of Fluids in Porous Media, American Elsevier Publishing Company, Inc., New York, New York.

BHI-00007, 1994, "Prototype Hanford Surface Barrier: Design Basis Document," Rev. 00, Bechtel Hanford, Inc., Richland, Washington.

BHI-00144, 1995, "Long-term Climate Change Effects Task for the Hanford Site Permanent Isolation Barrier Development Program: Final Report," Bechtel Hanford Company, Richland, Washington.

BHI-00169, 1995, "Environmental Restoration Disposal Facility Performance Assessment," Revision 00, Bechtel Hanford, Inc., Richland, Washington.

BHI-00184, 1995, "Miocene- to Pliocene-Aged Suprabasalt Sediments of the Hanford Site, South-Central Washington," Rev. 00, Bechtel Hanford, Inc., Richland, Washington.

BHI-00230, 1996, "Geologic Field Inspection of the Sedimentary Sequence at the Environmental Restoration Disposal Facility," Bechtel Hanford, Inc., Richland, Washington.

BHI-01103, 1999, "Clastic Injection Dikes of the Pasco Basin and Vicinity – Geologic Atlas Series," Rev. 0, Bechtel Hanford, Inc., Richland, Washington.

BHI-01745, 2004, "2004 Environmental Restoration Contractor Revegetation Monitoring Report," Bechtel Hanford Inc., Rev. 0, Richland, Washington.

Bjornstad, B. N., K. R. Fecht, and C. J. Pluhar, 2001, "Long History of Pre-Wisconsin, Ice Age Cataclysmic Floods: Evidence from Southeastern Washington State," The Journal of Geology, Vol. 109, pp. 695–713.

BNWL-243, 1966, "Soil Survey Hanford Project in Benton County Washington," Pacific Northwest Laboratory, Richland, Washington.

BNWL-1709, 1973, "Collection and Analysis of Pump Test Data for Transmissivity Values," Pacific Northwest Laboratories, Richland, Washington.

BNWL-B-360, 1974, "Selected Water Table Contour Maps and Well Hydrographs for the Hanford Reservation, 1944-1973," Pacific Northwest Laboratory, Richland, Washington.

BPF-73550, 1944, "Specifications For Construction of Composite Storage Tanks Bldg. No. 241 Hanford Engineer Works Project 9536," Rev. 2, Richland, Washington.

Bredehoeft, J. D., C. E. Neuzil, and P. C. D. Milly, 1983, "Regional Flow in the Dakota Aquifer: A Study of the Role of Confining Layers," Water-Supply Paper 2237, U.S. Geological Survey, Alexandria, Virginia.

Bredehoeft, J. D. and L. F. Konikow, 1993, "Ground-Water Models: Validate or Invalidate," Groundwater, Vol. 31, No. 2, pp. 178–179.

Brown, K. G., J. Arnold, S. Sarkar, G. Flach, H. van der Sloot, J.C.L. Meeussen and D. S. Kosson, 2013, "Modeling Carbonation of High-Level Waste Tank Integrity and Closure," EPJ Web of Conferences, Vol. 56, pp. 1–10.

Bruckler, L., B. C. Ball, and P. Renault, 1989, "Laboratory Estimation of Gas Diffusion Coefficient and Effective Porosity in Soils," Soil Science, Vol. 147, pp. 1–10.

Cantrell, K. J., K. C. Carroll, E. C. Buck, D. Neiner, K. N. Geiszler, 2013, "Single-pass flow-through test elucidation of weathering behavior and evaluation of contaminant release models for Hanford tank residual radioactive waste," Applied Geochemistry, Vol. 28, pp. 119–127.

Cantrell, K. J., W. J. Deutsch, and M. J. Lindberg, 2011, "Thermodynamic Model for Uranium Release from Hanford Site Tank Residual Waste," Environmental Science & Technology, Vol. 45, No. 4, pp. 1473–1480.

CHPRC-00269, 2013, "STOMP Requirements Traceability Matrix CHPRC Build 4," Rev. 3, CH2M HILL Plateau Remediation Company, Richland, Washington.

CNWRA/NRC, 2011, "History and Value of Uncertainty and Sensitivity Analyses at the Nuclear Regulatory Commission and Center for Nuclear Waste Regulatory Analyses," Center for Nuclear Waste Regulatory Analyses, San Antonio, Texas/U.S. Nuclear Regulatory Commission, Washington, D.C.

Comprehensive Environmental Response, Compensation, and Liability Act of 1980, 42 USC 9622, et seq.

Consent Decree, State of Washington v. Department of Energy, Case No. CV-08-5085-RMP, United States District Court, Eastern District of Washington (October 25, 2010).

CP-14873, 2003, "200-BP-1 Prototype Hanford Barrier Annual Monitoring Report for Fiscal Year 2002," Rev. 0, Fluor Hanford, Inc., Richland, Washington.

CP-47631, 2011, "Model Package Report: Central Plateau Groundwater Model Version 3.3," Rev. 0, CH2M HILL Plateau Remediation Company, Richland, Washington.

CP-47631, 2015, "Model Package Report: Central Plateau Groundwater Model Version 6.3.3," Rev. 2, INTERA, Inc., Richland, Washington.

D&D-25575, 2005, "Silt Borrow Source Field Investigation Report," Rev. 0, Fluor Hanford, Inc., Richland Washington.

Deutsch, W. J., K. J. Cantrell, K. M. Krupka, M. L. Lindberg, and R. J. Serne, 2011, "Hanford tank residual waste – Contaminant source terms and release models," Applied Geochemistry, Vol. 26, pp. 1681–1693.

DOE/EIS-0222-F, 1999, "Final Hanford Comprehensive Land-Use Plan Environmental Impact Statement," U.S. Department of Energy, Richland Operations Office, Richland, Washington.

DOE/EIS-0222-SA-01, 2008, "Hanford Comprehensive Land-Use Plan Environmental Impact Statement Supplement Analysis," Rev. 0, U.S. Department of Energy, Richland Operations Office, Richland, Washington.

DOE/EIS-0222-SA-02, 2015, "Supplement Analysis of the Hanford Comprehensive Land-Use Plan Environmental Impact Statement," Rev. 0, U.S. Department of Energy, Richland Operations Office, Richland, Washington.

DOE/EIS-0310, 2000, "Final Programmatic Environmental Impact Statement for Accomplishing Expanded Civilian Nuclear Energy Research and Development and Isotope Production Missions in the United States, Including the Role of the Fast Flux Test Facility," U.S. Department of Energy, Office of Nuclear Energy, Science and Technology, Washington, D.C.

DOE/EIS-0391, 2012, "Final Tank Closure and Waste Management Environmental Impact Statement for the Hanford Site, Richland, Washington," U.S. Department of Energy, Washington, D.C.

DOE G 435.1-1, 1999, Implementation Guide for Use with DOE M 435.1-1, Radioactive Waste Management Manual, U.S. Department of Energy, Washington, D.C.

DOE G 435.1-2, DRAFT, Implementation Guide for use with DOE M 435.1-1, Format and Content Guide for U.S. Department of Energy Low-Level Waste Disposal Facility Performance Assessments and Composite Analyses, U.S. Department of Energy, Washington, D.C.

DOE M 435.1-1, 2007, Radioactive Waste Management Manual, U.S. Department of Energy, Washington, D.C.

DOE/NV/25946--107, 2008, "Probabilistic Performance Assessment of a Low-Level Radioactive Waste Disposal Site on the Nevada Test Site," National Security Technologies, LLC for the U.S. Department of Energy, National Nuclear Security Administration Nevada Site Office.

DOE O 413.3B, 2010, Program and Project Management for the Acquisition of Capital Assets, U.S. Department of Energy, Washington, D.C.

DOE O 414.1D, 2011, Quality Assurance, U.S. Department of Energy, Washington, D.C.

DOE O 430.1B, 2008, Real Property Asset Management, U.S. Department of Energy, Washington, D.C.

DOE O 435.1, 2001, Radioactive Waste Management, U.S. Department of Energy, Washington, D.C.

DOE O 458.1, 2013, Radiation Protection of the Public and the Environment, U.S. Department of Energy, Office of Health, Safety and Security, Washington, D.C.

DOE/ORP-2000-24, 2001, Hanford Immobilized Low-Activity Waste Performance Assessment: 2001 Version, Rev. 0, U.S. Department of Energy, Office of River Protection, Richland, Washington.

DOE/ORP-2003-11, 2003, Preliminary Performance Assessment for Waste Management Area C at the Hanford Site, Washington, Rev. 0, U.S. Department of Energy, Office of River Protection, Richland, Washington.

DOE/ORP-2005-01, 2006, Initial Single-Shell Tank System Performance Assessment for the Hanford Site, Rev. 0, U.S. Department of Energy, Office of River Protection, Richland, Washington.

DOE/ORP-2008-01, 2010, RCRA Facility Investigation Report for Hanford Single-Shell Tank Waste Management Areas, Rev. 1, U.S. Department of Energy, Office of River Protection, Richland, Washington.

DOE/ORP-2014-02, 2014, Clean Closure Practicability Demonstration for Single-Shell Tanks, Rev. 1, U.S. Department of Energy, Office of River Protection, Richland, Washington.

DOE P 454.1, 2011, Use of Institutional Controls, U.S. Department of Energy, Washington, D.C.

DOE/RL-88-30, 2015, Hanford Site Waste Management Units Report, Rev. 24, U.S. Department of Energy, Richland Operations Office, Richland, Washington.

DOE/RL-91-45, 1995, Hanford Site Risk Assessment Methodology, Rev. 3, U.S. Department of Energy, Richland Operations Office, Richland, Washington.

DOE/RL-92-04, 1993, PUREX Source Aggregate Area Management Study Report, Rev. 0, U.S. Department of Energy, Richland Operations Office, Richland, Washington.

DOE/RL-92-94, 2001, Hanford Site Background: Part 1, Soil Background for Nonradioactive Analytes, Rev. 4, 2 vols., U.S. Department of Energy, Richland Operations Office, Richland, Washington.

DOE/RL-93-33, 1996, Focused Feasibility Study of Engineered Barriers for Waste Management Units in the 200 Areas, Rev. 1, U.S. Department of Energy, Richland Operations Office, Richland, Washington.

DOE/RL-95-55, 1995, Hanford Site Background: Evaluation of Existing Soil Radionuclide Data, Rev. 0, U.S. Department of Energy, Richland Operations Office, Richland, Washington.

DOE/RL-96-12, 1996, Hanford Site Background: Part 2, Soil Background for Radionuclides, Rev. 0, U.S. Department of Energy, Richland Operations Office, Richland, Washington.

DOE/RL-96-16, 1998, Screening Assessment and Requirements for a Comprehensive Assessment: Columbia River Comprehensive Impact Assessment, Rev. 1, U.S. Department of Energy, Richland Operations Office, Richland, Washington.

DOE/RL-96-81, 1997, Waste Site Grouping for 200 Areas Soil Investigations, Rev. 0, U.S. Department of Energy, Richland Operations Office, Richland, Washington.

DOE/RL-97-02, 1997, National Register of Historic Places Multiple Property Documentation Form - Historic, Archaeological and Traditional Cultural Properties of the Hanford Site, Washington, Rev. 0, U.S. Department of Energy, Richland Operations Office, Richland, Washington.

DOE/RL-99-11, 1999, 200-BP-1 Prototype Barrier Treatability Test Report, Rev. 0, U.S. Department of Energy, Richland Operations Office, Richland, Washington.

DOE/RL-99-36, 2000, Phase 1 RCRA Facility Investigation/Corrective Measures Study Work Plan for Single-Shell Tank Waste Management Areas, Rev. 1, U.S. Department of Energy, Richland Operations Office, Richland, Washington.

DOE/RL-2001-41, 2009, Sitewide Institutional Controls Plan for Hanford CERCLA Response Actions, Rev. 4, U.S. Department of Energy, Richland Operations Office, Richland, Washington.

DOE/RL-2001-54, 2002, Ecological Evaluation of the Hanford 200 Areas-Phase 1: Compilation of Existing 200 Areas Ecological Data, Draft A, U.S. Department of Energy, Richland Operations Office, Richland, Washington.

DOE/RL-2001-54, 2005, Central Plateau Ecological Evaluation, Rev. 0, U.S. Department of Energy, Richland Operations Office, Richland, Washington.

DOE/RL-2002-39, 2002, Standardized Stratigraphic Nomenclature for Post-Ringold-Formation Sediments Within the Central Pasco Basin, Rev. 0, U.S. Department of Energy, Richland Operations Office, Richland, Washington.

DOE/RL-2002-59, 2004, Hanford Site Groundwater Strategy Protection, Monitoring, and Remediation, U.S. Department of Energy, Richland Operations Office, Richland, Washington.

DOE/RL-2007-50, 2011, Central Plateau Ecological Risk Assessment Data Package Report, Rev. 1, U.S. Department of Energy, Richland Operations Office, Richland, Washington.

DOE/RL-2009-10, 2013, Hanford Site Cleanup Completion Framework, Rev. 1, U.S. Department of Energy, Richland Operations Office, Richland, Washington.

DOE/RL-2009-77, 2010, Groundwater Quality Assessment Plan for the Single-Shell Tank Waste Management Area C, Rev. 0, U.S. Department of Energy, Richland Operations Office, Richland, Washington.

DOE/RL-2009-85, 2012, Remedial Investigation Report for the 200-PO-1 Groundwater Operable Unit, Rev. 1, U.S. Department of Energy, Richland Operations Office, Richland, Washington.

DOE/RL-2010-97, 2011, Remedial Investigation/Feasibility Study for the 100-KR-1, 100-KR-2, and 100-KR-4 Operable Units, Draft A, U.S. Department of Energy, Richland Operations Office, Richland, Washington.

DOE/RL-2011-50, 2012, Regulatory Basis and Implementation of a Graded Approach to Evaluation of Groundwater Protection, Rev. 1, U.S. Department of Energy, Richland Operations Office, Richland, Washington.

DOE/RL-2013-22, 2013, Hanford Site Groundwater Monitoring Report for 2012, Rev. 0, CH2M HILL Plateau Remediation Company, Richland, Washington.

DOE/RL-2014-32, 2014, Hanford Site Groundwater Monitoring Report for 2013, Rev. 0, U.S. Department of Energy, Richland Operations Office, Richland, Washington.

DOE/RW-0070, 1986, Nuclear Waste Policy Act (Section 112), Environmental Assessment, Reference Repository Location, Hanford Site, Washington, U.S. Department of Energy, Office of Civilian Radioactive Waste Management, Washington, D.C.

DOE/RW-0164, 1988, Consultation Draft Site Characterization Plan Reference Repository Location, Hanford Site, Washington, U.S. Department of Energy, Office of Civilian Radioactive Waste Management, Washington, D.C.

DOE-STD-1196-2011, 2011, Derived Concentration Technical Standard, U.S. Department of Energy, Washington, D.C.

DOE-STD-XXX, 2014 (Draft), Radioactive Waste Management Disposal Authorization Statement Technical Basis Documentation Technical Standard, U.S. Department of Energy, Washington, D.C.

Ecology, EPA, and DOE, 1989, Hanford Federal Facility Agreement and Consent Order – Tri-Party Agreement, 2 vols., as amended, State of Washington Department of Ecology, U.S. Environmental Protection Agency, and U.S. Department of Energy, Olympia, Washington.

EM-QA-001, 2012, EM Quality Assurance Program (QAP), Rev. 1, Office of Environmental Management, U.S. Department of Energy, Washington, D.C.

EPA, 2014, CAP88-PC Version 4.0 User Guide, U.S. Environmental Protection Agency, Washington, D.C.

EPA/240/B-01/003, 2001, EPA Requirements for Quality Assurance Project Plans, EPA QA/R-5, U.S. Environmental Protection Agency, Office of Environmental Information, Washington, D.C.

EPA/240/R-02/007, 2002, Guidance for Quality Assurance Project Plans for Modeling, EPA QA/G-5M, U.S. Environmental Protection Agency, Office of Environmental Information, Washington, D.C.

EPA-402-R-93-081, 1993, Federal Guidance Report No. 12, External Exposure to Radionuclides in Air, Water, and Soil, Office of Radiation and Indoor Air, U.S. Environmental Protection Agency, Washington, D.C.

EPA/540/F-95/041, 1996, Soil Screening Guidance: Fact Sheet, Publication 9355.4-14FSA, U.S. Environmental Protection Agency, Office of Solid Waste and Emergency Response, Washington, D.C.

EPA/540/R-92/003, 1991, Guidance for Data Useability in Risk Assessment (Part A) Final, Office of Research and Development, U.S. Environmental Protection Agency, Washington, D.C.

EPA/540/R-92/003, 1991, Risk Assessment Guidance for Superfund: Volume I – Human Health Evaluation Manual (Part B, Development of Risk-based Preliminary Remediation Goals) Interim, Publication 9285.7-01B, Office of Research and Development, U.S. Environmental Protection Agency, Washington, D.C.

EPA/540/R-95/128, 1996, Soil Screening Guidance: Technical Background Document, Second Edition, U.S. Environmental Protection Agency, Washington, D.C.

EPA/540/R-96/018, 1996, Soil Screening Guidance: User's Guide, Second Edition, Publication 9355.4-23, Office of Solid Waste and Emergency Response, U.S. Environmental Protection Agency, Washington, D.C.

EPA/600/2-91/065, 1991, The RETC Code for Quantifying the Hydraulic Functions of Unsaturated Soils, Office of Research and Development, U.S. Environmental Protection Agency, Washington, D.C.

EPA/600/P-95/002Fa, 1997, Exposure Factors Handbook Volume 1: General Factors, U.S. Environmental Protection Agency, National Center for Environmental Assessment, Washington, D.C.

EPA/600/R-090/052F, 2011, Exposure Factors Handbook: 2011 Edition, National Center for Environmental Assessment, Office of Research and Development, U.S. Environmental Protection Agency, Washington, D.C.

EPA/630/R-97/001, 1997, Guiding Principles for Monte Carlo Analysis, Risk Assessment Forum, U.S. Environmental Protection Agency, Washington, D.C.

EPA-SAB-RAC-ADV-99-006, 1999, An SAB Advisory: Modeling of Radionuclide Releases from Disposal of Low Activity Mixed Waste, U.S. Environmental Protection Agency, Science Advisory Board, Washington, D.C.

ERDA-1538, 1975, "Final Environmental Impact Statement, Waste Management Operations, Hanford Reservation, Richland, Washington," U.S. Energy Research and Development Administration, Richland, Washington.

Fayer, M. J., and G. W. Gee, 2006, "Multiple-Year Water Balance of Soil Covers in a Semiarid Setting," Journal of Environmental Quality, Vol. 35, No. 2, pp. 366–377.

Fayer, M. J., G. W. Gee, M. L. Rockhold, M. D. Freshley, and T. B. Walters, 1996, "Estimating Recharge Rates for a Groundwater Model Using a GIS," Journal of Environmental Quality, Vol. 25, pp. 510–518.

Fecht, K. R., S. P. Reidel, and A. M. Tallman, 1987, "Paleodrainage of the Columbia River System on the Columbia Plateau of Washington State – A Summary," Selected Papers on the Geology of Washington, Washington Division of Geology and Earth Resources, Washington State Department of Natural Resources, Bulletin 77, pp. 219–248.

Gee, G. W., M. J. Fayer, M. L. Rockhold, and M. D. Campbell, 1992, "Variations in Recharge at the Hanford Site," Northwest Science, Vol. 66, No. 4, pp. 237–250.

Gelhar, L. W., 1993, Stochastic Subsurface Hydrology, Prentice Hall, New York, New York.

Gelhar, L. W. and C. L. Axness, 1983, "Three-dimensional stochastic analysis of macrodispersion in aquifers," Water Resources Research, Vol. 19, pp. 161–180.

Gelhar, L. W., C. Welty, and K. R. Rehfeldt, 1992, "A Critical Review of Data on Field-Scale Dispersion in Aquifers," Water Resources Research, Vol. 28, pp. 1955–1974.

GJO-98-39-TAR/GJO-HAN-18, 1998, "Hanford Tank Farms Vadose Zone: C Tank Farm Report," U.S. Department of Energy, Grand Junction Office, Grand Junction, Colorado.

GJO-98-39-TARA/GJO-HAN-18, 2000, "Hanford Tank Farms Vadose Zone: Addendum to the C Tank Farm Report," U.S. Department of Energy, Grand Junction Office, Grand Junction, Colorado.

GoldSim Technology Group, 2014a, "GoldSim Contaminant Transport Module User's Guide," Version 6.4, GoldSim Technology Group, Issaquah, Washington.

GoldSim Technology Group, 2014b, "GoldSim Distributed Processing Module User's Guide," Version 11.1, GoldSim Technology Group LLC, Issaquah, Washington.

GoldSim Technology Group, 2014c, "GoldSim Probabilistic Simulation Environment User's Guide," Version 11.1, GoldSim Technology Group LLC, Issaquah, Washington.

Goodrich, S., A. Huber, and B. Monroe, 2008, "Trend of Mountain Big Sagebrush Crown Cover and Ground Cover on Burned Sites, Uinta Mountains and West Tavaputs Plateau, Utah," in Proceedings—Shrublands Under Fire: Disturbance and Recovery in a Changing World, Cedar City, Utah.

Hall, E. R., 1981, The Mammals of North America, John Wiley and Sons, Inc., New York, New York.

Hanford Site (Hanford.gov), Queried 07/2015, [Hanford Meteorological Station], http://www.hanford.gov/page.cfm/HMS.

Harr, M. E., 1987, Reliability-Based Design in Civil Engineering, McGraw-Hill, New York, New York.

Haynes, W. M. and D. R. Lide, 2011, CRC Handbook of Chemistry and Physics, 92nd Edition, CRC Press, Talyor & Francis Group, Boca Raton, Florida.

Helton, J. C., 1993, "Uncertainty and sensitivity analysis techniques for use in performance assessment for radioactive waste disposal," Reliability Engineering & System Safety, Vol. 42, Issues 2–3, pp. 327–367.

HFSUWG 1992a, "The Future for Hanford: Uses and Cleanup, Summary of the Final Report of the Hanford Future Site Uses Working Group," Hanford Future Site Uses Working Group, Westinghouse Hanford Company, Richland, Washington.

HFSUWG, 1992b, "The Future for Hanford: Uses and Cleanup, The Final Report of the Hanford Future Site Uses Working Group," Hanford Future Site Uses Working Group, Westinghouse Hanford Company, Richland, Washington.

HGLP-MBL-018, 2016, "241-C-102 Tank Waste Retrieval Project Final Report of Drywell Monitoring Data," Rev. 0, Stoller Newport News Nuclear, Richland, Washington.

HNF-4769, 1999, "Far-Field Hydrology Data Package for Immobilized Low-Activity Tank Waste Performance Assessment," Rev. 1, Fluor Daniel Northwest, Inc., Richland, Washington.

HNF-EP-0182, 2005, "Waste Tank Summary Report for Month Ending August 31, 2005," Rev. 209, CH2M HILL Hanford Group, Inc., Richland, Washington.

HNF-EP-0182, 2014, "Waste Tank Summary Report for Month Ending September 30, 2013," Rev. 306, Washington River Protection Solutions, LLC, Richland, Washington.

HNF-EP-0182, 2014, "Waste Tank Summary Report for Month Ending May 31, 2014," Rev. 317, Washington River Protection Solutions, LLC, Richland, Washington.

HNF-EP-0182, 2014, "Waste Tank Summary Report for Month Ending July 31, 2014," Rev. 319, Washington River Protection Solutions, LLC, Richland, Washington.

HNF-EP-0182, 2015, "Waste Tank Summary Report for Month Ending February 28, 2015," Rev. 326, Washington River Protection Solutions, LLC, Richland, Washington.

HNF-EP-0182, 2016, "Waste Tank Summary Report for Month Ending February 29, 2016," Rev. 338, Washington River Protection Solutions, LLC, Richland, Washington.

HNF-SD-RE-TI-178, 2007, "Single-Shell Tank Interim Stabilization Record," Rev. 9a, CH2M HILL Hanford Group, Inc., Richland, Washington.

HNF-SD-WM-SP-012, 2007, "Tank Farm Contractor Operation and Utilization Plan," Rev. 6, CH2M HILL Hanford Group, Inc., Richland, Washington.

HNF-SD-WM-TI-707, 2007, "Exposure Scenarios and Unit Factors for the Hanford Tank Waste Performance Assessment," Rev. 5, CH2M HILL Hanford Group, Inc., Richland, Washington.

HNF-SD-WM-TI-740, 1999, "Standard Inventories of Chemicals and Radionuclides in Hanford Site Tank Wastes," Rev. 0C, Lockheed Martin Hanford Corporation, Richland, Washington.

Hoffman F. O., 1996, "The Effect of Distribution Choice for Uncertain Parameters in a Monte Carlo Analysis," presented at Society of Risk Analysis Annual Meeting, Workshop on Quantitative Techniques for Analysis of Variability and Uncertainty in Exposure and Risk Assessment (December 8), New Orleans, Louisiana.

HW-7-1388-DEL, 1945, "Hanford Engineer Works Monthly Report February 1945," E. I. du Pont de Nemours and Company, Richland, Washington.

IAEA, 1994, "Technical Reports Series No. 364, Handbook of Parameter Values for the Prediction of Radionuclide Transfer in Temperate Environments," International Atomic Energy Agency, Vienna, Austria.

IAEA, 2010, "Technical Reports Series No. 472, Handbook of Parameter Values for the Prediction of Radionuclide Transfer in Terrestrial and Freshwater Environments," International Atomic Energy Agency, Vienna, Austria.

ICRP, 1994, "ICRP Publication 66: Human Respiratory Tract Model for Radiological Protection," Annals of the ICRP, International Commission on Radiation Protection, Vol. 24, No. 1–3, pp. 1–482.

ICRP, 1996, "ICRP Publication 72: Age-dependent Doses to the Members of the Public from Intake of Radionuclides - Part 5 Compilation of Ingestion and Inhalation Coefficients," Annals of the ICRP, International Commission on Radiation Protection, Vol. 26, No. 1.

ICRP, 2006, "ICRP Publication 101a: Assessing Dose of the Representative Person for the Purpose of the Radiation Protection of the Public," Annals of the ICRP, International Commission on Radiation Protection, Vol. 36, No. 3.

ICRP, 2007, "ICRP Publication 103: The 2007 Recommendations of the International Commission on Radiological Protection," Annals of the ICRP, International Commission on Radiation Protection, Vol. 37, No. 2–4, pp. 1–332.

ICRP, 2008, "ICRP Publication 107: Nuclear Decay Data for Dosimetric Calculations," Annals of the ICRP, International Commission on Radiation Protection, Vol. 38, No. 3, pp. 7–96.

INDC-356-VOL3, 1945, "Construction Hanford Engineer Works U.S. Contract Number W-7412-ENG-1 Du Pont Project 9536 History of the Project Volume III," E. I. du Pont de Nemours and Company, Wilmington, Delaware.

INEEL/EXT-01-00273, 2006, "Biological Data to Support Operable Unit 7-13/14 Modeling of Plant and Animal Intrusion at Buried Waste Sites," Rev. 1, Idaho Cleanup Project, Idaho Falls, Idaho.

Jannik, T., 2014, "Environmental Dosimetry," Savannah River Chapter of Health Physics Society Seminar, Savannah River National Laboratory, Aiken, South Carolina.

Jin, Y. and W. A. Jury, 1996, "Characterizing the Dependence of Gas Diffusion Coefficient on Soil Properties," Soil Science Society of America Journal, Vol. 60, No. 1, pp. 66–71.

Jones, V. C., 1985, United States Army in World War II, Special Studies -- Manhattan: The Army and the Atomic Bomb, Center of Military History, United States Army, Washington, D.C.

Jury, W. A., W. R. Gardner, and W. H. Gardner, 1991, Soil Physics, 5th edition, Wiley and Sons, Inc., New York, New York.

Jury, W. A. and R. Horton, 2004, Soil Physics, 6th edition, Wiley and Sons, Inc., New York, New York.

Karimi, A. A., W. J. Farmer, and M. M. Cliath, 1987, "Vapor-phase Diffusion of Benzene in Soil," Journal of Environmental Quality, Vol. 16, No. 1, pp. 38–43.

Karl, T. R., J. M. Melillo, and T. C. Peterson, (eds.), 2009, Global Climate Change Impacts in the United States: A State of Knowledge Report from the U.S. Global Change Research Program, Cambridge University Press, New York, New York.

Khaleel, R., 1989, "Scale Dependence of Continuum Models for Fractured Basalts," Water Resources Research, Vol. 25, No. 8, pp. 1847–1855.

Khaleel, R. and J. F. Relyea, 1997, "Correcting Laboratory-Measured Moisture Retention Data for Gravels," Water Resources Research, Vol. 33, Issue 8, pp. 1875–1878.

Khaleel, R., J. F. Relyea, and J. L. Conca, 1995, "Evaluation of van Genuchten-Mualem Relationships to Estimate Unsaturated Hydraulic Conductivity at Low Water Contents," Water Resources Research, Vol. 31, Issue 11, pp. 2659–2668.

Khaleel, R. and P. R. Heller, 2003, "On the Hydraulic Properties of Coarse-Textured Sediments at Intermediate Water Contents," Water Resources Research, Vol. 39, Issue 9, pp. 1233–1237.

Klute, A., 1986, Methods of Soil Analysis, Part 1—Physical and Mineralogical Methods, Second Edition, American Society of Agronomy-Soil Science Society of America, Madison, Wisconsin.

Kozak, M. W., 1994, "Decision analysis for low-level radioactive waste disposal facilities," Radioactive Waste Management and Environmental Restoration, Vol. 18, pp. 209–223.

Kozak, M. W., 2010, "Safety assessment for near-surface disposal of low- and intermediate-level radioactive waste," in Geological repository systems for safe disposal of spent nuclear fuels and radioactive waste, J. Ahn and M. J. Apted eds., Woodhead Publishing Limited, Cambridge, UK and CRC Press LLC, Boca Raton, Florida.

LA-UR-08-06764, 2008, "Performance Assessment and Composite Analysis for Los Alamos National Laboratory Technical Area 54, Area G," Rev. 4, Los Alamos National Laboratory, Los Alamos, New Mexico.

LA-UR-96-3860, 1997, "Hanford Tank Chemical and Radionuclide Inventories: HDW Model Rev. 4," Los Alamos National Laboratory, Los Alamos, New Mexico.

Leary, K. D., 1990, Analysis of Techniques for Estimating Potential Recharge and Shallow Unsaturated Zone Water Balance near Yucca Mountain, Nevada, M.S. Thesis, University of Nevada, Reno, Nevada.

Lesica, P., S. V. Cooper and G. Kudray, 2007, "Recovery of Big Sagebrush Following Fire in Southwest Montana," Rangeland Ecology & Management, Vol. 60, Issue 3, pp. 261–269.

Liu, G., B. Li, K. Hu, and M. T. van Genuchten, 2006, "Simulating the Gas Diffusion Coefficient in Macropore Network Images: Influence of Soil Pore Morphology," Soil Science Society of America Journal, Vol. 70, pp. 1252–1261.

MASSFLUX-1, 2010, "Use and Measurement of Mass Flux and Mass Discharge," The Interstate Technology & Regulatory Council, Integrated DNAPL Site Strategy Team, Washington, D.C.

Millington, R. J., and J. P. Quirk, 1960, "Transport in porous media," in Transactions of the 7th International Congress of Soil Science, Madison, Wisconsin, Vol. 1, pp. 97–106.

Millington, R. J. and J. P. Quirk, 1961, "Permeability of Porous Solids," Transactions of the Faraday Society, Vol. 57, pp. 1200–1207.

Mishra, S., 2009, "Uncertainty and sensitivity analysis techniques for hydrologic modeling," Journal of Hydroinformatics, Vol. 11, No. 3–4, pp. 282–296.

Moldrup, P., S. Yoshikawa, T. Olesen, T. Komatsu, and D. E. Rolston, 2003, "Gas Diffusivity in Undisturbed Volcanic Ash Soils: Test of Soil-Water-Characteristic-Based Prediction Models," Soil Science Society of America Journal, Vol. 67, No. 1, pp. 41–51.

Moldrup, P., T. Oleson, S. Yoshikawa, T. Komatsu, and D. E. Rolston, 2004, "Three-Porosity Model for Predicting the Gas Diffusion Coefficient in Undisturbed Soil," Soil Science Society of America Journal, Vol. 68, No. 3, pp. 750–759.

Mote, P. E., E. P. Salathé, V. Dulière, and E. Jump, 2008, Scenarios of future climate for the Pacific Northwest, Climate Impacts Group, University of Washington, Seattle, Washington.

Mualem, Y., 1976, "A New Model for Predicting the Hydraulic Conductivity of Unsaturated Porous Media," Water Resources Research, Vol. 12, No. 3, pp. 513–522.

Murray, C. J., A. L. Ward, and J. L. Wilson, 2007, "Influence of Clastic Dikes on Vertical Migration of Contaminants at the Hanford Site," Vadose Zone Journal, Vol. 6, No. 4, pp. 959–970.

NAGRA NTB 02-20, 2002, "Cementitious Near-Field Sorption Data Base for Performance Assessment of an ILW Repository in Opalinus Clay," Technical Report 02-20, National Cooperative for the Disposal of Radioactive Waste, Hardstrasse, Zurich, Switzerland.

National Bureau of Standards Handbook 69, 1963, "Maximum Permissible Body Burdens and Maximum Permissible Concentrations of Radionuclides in Air and in Water for Occupational Exposure," as amended, U.S. Department of Commerce, Washington, D.C.

National Environmental Policy Act of 1969, 42 USC 4321-4347, et seq.

Nazaroff, W. W. and A. V. Nero, 1988, Radon and Its Decay Products in Indoor Air, John Wiley & Sons, New York, New York.

NCRP Report No. 93, 1987, "Ionizing Radiation Exposure of the Population of the United States," National Council on Radiation Protection, Bethesda, Maryland.

NCRP Report No. 103, 1989, "Control of Radon in Houses," National Council on Radiation Protection, Bethesda, Maryland.

NCRP Report No. 129, 1999, "Recommended Screening Limits for Contaminated Surface Soil and Review of Factors Relevant to Site-Specific Studies," National Council on Radiation Protection, Bethesda, Maryland.

NCRP Report No. 152, 2005, "Performance Assessment of Near-Surface Facilities for Disposal of Low-Level Radioactive Waste," National Council on Radiation Protection and Measurements, Bethesda, Maryland.

NEA, 1987, "Shallow Land Disposal of Radioactive Waste: Reference Levels for Acceptance of Long-Lived Radionuclides," Nuclear Energy Agency, Organisation for Economic Co-operation and Development, Paris, France.

Neuman, S. P., 1992, "Validation of safety assessment models as a process of scientific and public confidence building," in International High Level Radioactive Waste Management (IHLRWM) Conference Proceedings, Las Vegas, Nevada.

Newcomb, R. C., 1958, "Ringold Formation of Pleistocene Age in Type Locality, the White Bluffs, Washington," American Journal of Science, Vol. 256, pp. 328–340.

Newcomb, R. C., J. R. Strand, and F. J. Frank, 1972, "Geology and Ground-Water Characteristics of the Hanford Reservation of the U.S. Atomic Energy Commission, Washington," Professional Paper 717, U.S. Geological Survey, Washington, D.C.

NIROND-TR 2008-23 E, 2009, "Review of sorption values for the cementitious near field of a near surface radioactive waste disposal facility, Project near surface disposal of category A waste at Dessel," Belgian Agency for Radioactive Waste and Enriched Fissile Materials, Brussels, Belgium.

NOAA Manual NOS NGS 5, 1990, "State Plane Coordinate System of 1983," National Geodetic Survey, U.S. Department of Commerce, National Oceanic and Atmospheric Administration, Rockville, Maryland.

Northern California Earthquake Data Center, Queried 09/2005, [Advanced National Seismic System (ANSS) Catalog Search], http://www.quake.geo.berkeley.edu/anss/catalog-search.html.

NUREG-1573, 2000, A Performance Assessment Methodology for Low-Level Radioactive Waste Disposal Facilities: Recommendations of NRC's Performance Assessment Working Group, U.S. Nuclear Regulatory Commission, Office of Nuclear Material Safety and Safeguards, Washington, D.C.

NUREG-1636, 1999, Regulatory Perspectives on Model Validation in High-Level Radioactive Waste Management Programs: A Joint NRC/SKI White Paper, U.S. Nuclear Regulatory Commission, Office of Nuclear Material Safety and Safeguards, Washington, D.C.

NUREG-1854, 2007, NRC Staff Guidance for Activities Related to U.S. Department of Energy Waste Determinations – Draft Final Report for Interim Use, U.S. Nuclear Regulatory Commission, Office of Federal and State Materials and Environmental Management Programs, Washington, D.C.

NUREG-2175, 2015, Guidance for Conducting Technical Analyses for 10 CFR Part 61 – Draft Report for Comment, U.S. Nuclear Regulatory Commission, Office of Nuclear Material Safety and Safeguards, Washington, D.C.

NUREG/CR-4122, 1985, A FORTRAN 77 Program and User's Guide for the Calculation of Partial Correlation and Standardized Regression Coefficients, SAND85-0044, U.S. Nuclear Regulatory Commission, Washington, D.C.

NUREG/CR-4370, 1986, Update of Part 61 Impacts Analysis Methodology, U.S. Nuclear Regulatory Commission, Washington, D.C.

NUREG/CR-5512, 1992, Residual Radioactive Contamination From Decommissioning, Vol. 1, Technical Basis for Translating Contamination Levels to Annual Total Effective Dose Equivalent, Final Report, PNL-7994, U.S. Nuclear Regulatory Commission, Washington, D.C.

Nyame, B. K. and J. M. Illston, 1981, "Relationships between permeability and pore structure of hardened cement paste," Magazine of Concrete Research, Vol. 33, No. 116, p. 139–146.

O'Connor, J. E. and V. R. Baker, 1992, "Magnitudes and implications of peak discharges from glacial Lake Missoula," Geological Society of America Bulletin, Vol. 104, No. 3, pp. 267–279.

Olander, A. R. 2016-05-03, "RE: WMA C PA - Editing" (e-mail to J. G. Field), Washington River Protection Solutions LLC (WRPS) Tank Farms, Richland, Washington.

Olander, A. R. 2016-08-18, "RE: WMA C PA - Editing" (e-mail to M. P. Bergeron), Washington River Protection Solutions LLC (WRPS) Tank Farms, Richland, Washington.

Open File Report 87-222, 1987, "Subsurface Transport of Radionuclides in Shallow Deposits of the Hanford Nuclear Reservation, Washington – Review of Selected Previous Work and Suggestions for Further Study," U.S. Geological Survey, Tacoma, Washington.

Open File Report 94-8, 1994, "Geologic Map of the Richland 1:100,000 Quadrangle, Washington," Washington Division of Geology and Earth Resources, Washington State Department of Natural Resources, Olympia, Washington.

Open File Report 96-8, 1996, "The Miocene to Pliocene Ringold Formation and Associated Deposits of the Ancestral Columbia River System, South-Central Washington and North-Central Oregon," Washington Division of Geology and Earth Resources, Washington State Department of Natural Resources, Olympia, Washington.

ORP-11242, 2011, "River Protection Project System Plan," Rev. 6, U.S. Department of Energy, Office of River Protection, Richland, Washington.

OSWER Directive 9200.1-120, 2014, "Human Health Evaluation Manual, Supplemental Guidance: Update of Standard Default Exposure Factors" (Memorandum from D. Stalcup to Superfund National Policy Managers, Regions 1 – 10, February 6), Office of Solid Waste and Emergency Response, U.S. Environmental Protection Agency, Washington, D.C.

OSWER Directive 9285.6-03, 1991, Risk Assessment Guidance for Superfund, Volume I: Human Health Evaluation Manual, Supplemental Guidance "Standard Default Exposure Factors" Interim Final, Office of Emergency and Remedial Response, Toxics Integration Branch, U.S. Environmental Protection Agency, Washington, D.C.

OSWER Directive 9841.00-6C, 1987, Alternate Concentration Limit Guidance, Part I, ACL Policy and Information Requirements, Interim Final, EPA/530-SW-87-017, Office of Solid Waste, Waste Management Division, U.S. Environmental Protection Agency, Washington, D.C.

Pacific Northwest National Laboratory, Queried 12/18/2015, [STOMP User Guide], http://stomp.pnnl.gov/user_guide/STOMP_guide.stm.

Pasquill, F., 1961, "The Estimation of the Dispersion of Windborne Material," The Meteorological Magazine, Vol. 90, No. 1063, pp. 33–49.

Plummer, M. A., L. C. Hull, and D. T. Fox, 2004, "Transport of Carbon-14 in a Large Unsaturated Soil Column," Vadose Zone Journal, Vol. 3, No. 1, pp. 109–121.

PNL-2774, 1979, "Characterization of the Hanford 300 Area Burial Grounds Task IV - Biological Transport," Pacific Northwest Laboratory, Richland, Washington.

PNL-5247, 1985, "Rooting Depth and Distributions of Deep-Rooted Plants in the 200 Area Control Zone of the Hanford Site," Pacific Northwest Laboratory, Richland, Washington.

PNL-5289, 1984, "Investigation of Ground-Water Seepage from the Hanford Shoreline of the Columbia River," Pacific Northwest Laboratory, Richland, Washington.

PNL-6328, 1988, "Estimation of Ground-Water Travel Time at the Hanford Site: Description, Past Work, and Future Needs," Pacific Northwest Laboratory, Richland, Washington.

PNL-6464, 1988, "Environmental Monitoring at Hanford for 1987," Pacific Northwest Laboratory, Richland, Washington.

PNL-7297, 1990, "Hanford Waste-Form Release and Sediment Interaction – A Status Report with Rationale and Recommendations for Additional Studies," Pacific Northwest Laboratory, Richland, Washington.

PNL-7662, 1991, "An Evaluation of the Chemical, Radiological, and Ecological Conditions of West Lake on the Hanford Site," Pacific Northwest Laboratory, Richland, Washington.

PNL-8337, 1992, "Summary and Evaluation of Available Hydraulic Property Data for the Hanford Site Unconfined Aquifer System," Pacific Northwest Laboratory, Richland, Washington.

PNL-8478, 1993, "Soil Erosion Rates Caused by Wind and Saltating Sand Stresses in a Wind Tunnel," Pacific Northwest Laboratory, Richland, Washington.

PNL-8889, 1993, "Solid-Waste Leach Characteristics and Contaminant-Sediment Interactions, Volume 1: Batch Leach and Adsorption Tests and Sediment Characterization," Pacific Northwest Laboratory, Richland, Washington.

PNL-10195, 1994, "Three-Dimensional Conceptual Model for the Hanford Site Unconfined Aquifer System: FY 1994 Status Report," Pacific Northwest Laboratory, Richland, Washington.

PNL-10817, 1995, "Hydrochemistry and Hydrogeologic Conditions within the Hanford Site Upper Basalt Confined Aquifer System," Pacific Northwest Laboratory, Richland, Washington.

PNL-10835, 1995, Comparison of Constant-Rate Pumping Test and Slug Interference Test Results at the Hanford Site B Pond Multilevel Test Facility, Pacific Northwest Laboratory, Richland, Washington.

PNL-10886, 1995, "Development of a Three-Dimensional Ground-Water Model of the Hanford Site Unconfined Aquifer System: FY 1995 Status Report," Pacific Northwest National Laboratory, Richland, Washington.

PNL-SA-23121 S, 1993, "Hanford Technical Exchange Program: Process Chemistry at Hanford (Genesis of Hanford Wastes)," Pacific Northwest Laboratory, Richland, Washington.

PNNL-6415, 2005, "Hanford Site National Environmental Policy Act (NEPA) Characterization," Rev. 17, Pacific Northwest National Laboratory, Richland, Washington.

PNNL-6415, 2007, "Hanford Site National Environmental Policy Act (NEPA) Characterization," Rev. 18, Pacific Northwest National Laboratory, Richland, Washington.

PNNL-11216, 1997, "STOMP Subsurface Transport Over Multiple Phases Application Guide," Pacific Northwest National Laboratory, Richland, Washington.

PNNL-11485, 1996, "Radionuclide Adsorption Distribution Coefficients Measured in Hanford Sediments for the Low Level Waste Performance Assessment Project," Pacific Northwest National Laboratory, Richland, Washington.

PNNL-11800, 1998, "Composite Analysis for Low-Level Waste Disposal in the 200 Area Plateau of the Hanford Site," Pacific Northwest National Laboratory, Richland, Washington.

PNNL-11810, 1998, "Results of Phase I Groundwater Quality Assessment for Single-Shell Tank Waste Management Areas S-SX at the Hanford Site," Pacific Northwest National Laboratory, Richland, Washington.

PNNL-11965, 1998, "Effects of Aging Quartz Sand and Hanford Site Sediment with Sodium Hydroxide on Radionuclide Sorption Coefficients and Sediment Physical and Hydrologic Properties: Final Report for Subtask 2a," Pacific Northwest National Laboratory, Richland, Washington.

PNNL-12030, 2000, "STOMP Subsurface Transport Over Multiple Phases Version 2.0 Theory Guide," Pacific Northwest National Laboratory, Richland, Washington.

PNNL-12261, 2000, "Revised Hydrogeology for the Suprabasalt Aquifer System, 200-East Area and Vicinity, Hanford Site, Washington," Pacific Northwest National Laboratory, Richland, Washington.

PNNL-13024, 2001, "RCRA Groundwater Monitoring Plan for Single-Shell Tank Waste Management Area C at the Hanford Site," as amended, Pacific Northwest National Laboratory, Richland, Washington.

PNNL-13033, 1999, "Recharge Data Package for the Immobilized Low-Activity Waste 2001 Performance Assessment," Pacific Northwest National Laboratory, Richland, Washington.

PNNL-13037, 2000, "Geochemical Data Package for the Hanford Immobilized Low-Activity Tank Waste Performance Assessment (ILAW PA)," Rev. 1, Pacific Northwest National Laboratory, Richland, Washington.

PNNL-13037, 2004, "Geochemical Data Package for the 2005 Hanford Integrated Disposal Facility Performance Assessment," Rev. 2, Pacific Northwest National Laboratory, Richland, Washington.

PNNL-13080, 2000, "Hanford Site Groundwater Monitoring: Setting, Sources, and Methods," Pacific Northwest National Laboratory, Richland, Washington.

PNNL-13342, 2000, "Analysis of the Hydrologic Response Associated with Shutdown and Restart of the 200-ZP-1 Pump-and-Treat System," Pacific Northwest National Laboratory, Richland, Washington.

PNNL-13378, 2001, "Results of Detailed Hydrologic Characterization Tests – Fiscal Year 1999," Pacific Northwest National Laboratory, Richland, Washington.

PNNL-13514, 2001, "Results of Detailed Hydrologic Characterization Tests – Fiscal Year 2000," Pacific Northwest National Laboratory, Richland, Washington.

PNNL-13641, 2001, "Uncertainty Analysis Framework – Hanford Site-Wide Groundwater Flow and Transport Model," Pacific Northwest National Laboratory, Richland, Washington.

PNNL-13653, 2005, "A Catalog of Geologic Data for the Hanford Site," Rev. 2, Pacific Northwest National Laboratory, Richland, Washington.

PNNL-13672, 2002, "A Catalog of Vadose Zone Hydraulic Properties for the Hanford Site," Rev. 1, Pacific Northwest National Laboratory, Richland, Washington.

PNNL-13674, 2001, "Zone of Interaction Between Hanford Site Groundwater and Adjacent Columbia River: Progress Report for the Groundwater/River Interface Task Science and Technology Groundwater/Vadose Zone Integration Project," Pacific Northwest National Laboratory, Richland, Washington.

PNNL-13895, 2003, "Hanford Contaminant Distribution Coefficient Database and Users Guide," Rev. 1, Pacific Northwest National Laboratory, Richland, Washington.

PNNL-14058, 2002, "Prototype Database and User's Guide of Saturated Zone Hydraulic Properties for the Hanford Site," Pacific Northwest National Laboratory, Richland, Washington.

PNNL-14113, 2002, "Results of Detailed Hydrologic Characterization Tests – Fiscal Year 2001," Pacific Northwest National Laboratory, Richland, Washington.

PNNL-14133, 2003, "Blanket Biological Review for General Maintenance Activities Within Active Burial Grounds, 200 E and 200 W Areas, ECR #2002-200-034," Pacific Northwest National Laboratory, Richland, Washington.

PNNL-14143, 2002, "The Hanford Site 1000-Year Cap Design Test," Pacific Northwest National Laboratory, Richland, Washington.

PNNL-14202, 2003, "Mineralogical and Bulk-Rock Geochemical Signatures of Ringold and Hanford Formation Sediments," Pacific Northwest National Laboratory, Richland, Washington.

PNNL-14233, 2003, "Biological Review of the Hanford Solid Waste EIS – Borrow Area C (600 Area), Stockpile and Conveyance Road Area (600 Area), Environmental Restoration Disposal Facility (ERDF) (600 Area), Central Waste Complex (CWC) Expansion (200 West), 218-W-5 Expansion Area (200 West), New Waste Processing Facility (200 West), Undeveloped Portion of 218-W-4C (200 West), Western Half & Northeastern Corner of 218-W-6 (200 West), Disposal Facility Near Plutonium-Uranium Extraction (PUREX) Facility (200 East), ECR #2002-600-012b," Pacific Northwest National Laboratory, Richland, Washington.

PNNL-14398, 2003, "Transient Inverse Calibration of the Site-Wide Groundwater Flow Model (ACM-2): FY 2003 Progress Report," Pacific Northwest National Laboratory, Richland, Washington.

PNNL-14548, 2004, "Hanford Site Groundwater Monitoring for Fiscal Year 2003," Pacific Northwest National Laboratory, Richland, Washington.

PNNL-14586, 2004, "Geologic Data Package for 2005 Integrated Disposal Facility Waste Performance Assessment," Rev. 1, Pacific Northwest National Laboratory, Richland, Washington.

PNNL-14656, 2004, "Borehole Data Package for Four CY 2003 RCRA Wells 299-E27-4, 299-E27-21, 299-E27-22, and 299-E27-23 at Single-Shell Tank, Waste Management Area C, Hanford Site, Washington," Pacific Northwest National Laboratory, Richland, Washington.

PNNL-14702, 2006, "Vadose Zone Hydrogeology Data Package for Hanford Assessments," Rev. 1, Pacific Northwest Laboratory, Richland, Washington.

PNNL-14744, 2004, "Recharge Data Package for the 2005 Integrated Disposal Facility Performance Assessment," Pacific Northwest National Laboratory, Richland, Washington.

PNNL-14753, 2006, "Groundwater Data Package for Hanford Assessments," Rev. 1, Pacific Northwest National Laboratory, Richland, Washington.

PNNL-14804, 2004, "Results of Detailed Hydrologic Characterization Tests – Fiscal Year 2003," Pacific Northwest National Laboratory, Richland, Washington.

PNNL-14903, 2007, "Hanford Tanks 241-C-203 and 241-C-204: Residual Waste Contaminant Release Model and Supporting Data," Rev. 1, Pacific Northwest National Laboratory, Richland, Washington.

PNNL-14960, 2005, "200-BP-1 Prototype Hanford Barrier Annual Monitoring Report for Fiscal Year 2004," Pacific Northwest National Laboratory, Richland, Washington.

PNNL-15160, 2005, "Hanford Site Climatological Summary 2004 with Historical Data," Pacific Northwest National Laboratory, Richland, Washington.

PNNL-15187, 2007, "Hanford Tank 241-C-106: Residual Waste Contaminant Release Model and Supporting Data," Rev. 1, Pacific Northwest National Laboratory, Richland, Washington.

PNNL-15503, 2008, "Characterization of Vadose Zone Sediments Below the C Tank Farm: Borehole C4297 and RCRA Borehole 299-E27-22," Rev. 1, Pacific Northwest National Laboratory, Richland, Washington.

PNNL-15782, 2006, "STOMP Subsurface Transport Over Multiple Phases Version 4.0 User's Guide," Pacific Northwest National Laboratory, Richland, Washington.

PNNL-15955, 2007, "Geology Data Package for the Single-Shell Tank Waste Management Areas at the Hanford Site," Rev. 1, Pacific Northwest National Laboratory, Richland, Washington.

PNNL-16229, 2007, "Hanford Tanks 241-C-202 and 241-C-203: Residual Waste Contaminant Release Models and Supporting Data," Pacific Northwest National Laboratory, Richland, Washington.

PNNL-16346, 2007, "Hanford Site Groundwater Monitoring for Fiscal Year 2006," Pacific Northwest National Laboratory, Richland, Washington.

PNNL-16407, 2007, "Geology of the Waste Treatment Plant Seismic Boreholes," Rev. 1, Pacific Northwest National Laboratory, Richland, Washington.

PNNL-16620, 2007, "Ecological Data in Support of the Tank Closure and Waste Management Environmental Impact Statement Part 2: Results of Spring 2007 Field Surveys," Pacific Northwest National Laboratory, Richland, Washington.

PNNL-16663, 2007, "Geochemical Processes Data Package for the Vadose Zone in the Single-Shell Tank Waste Management Areas at the Hanford Site," Pacific Northwest National Laboratory, Richland, Washington.

PNNL-16688, 2007, "Recharge Data Package for Hanford Single-Shell Tank Waste Management Areas," Pacific Northwest National Laboratory, Richland, Washington.

PNNL-16738, 2008, "Hanford Tank 241-C-103 Residual Waste Contaminant Release Models and Supporting Data," Pacific Northwest National Laboratory, Richland, Washington.

PNNL-17154, 2008, "Geochemical Characterization Data Package for the Vadose Zone in the Single-Shell Tank Waste Management Areas at the Hanford Site," Pacific Northwest National Laboratory, Richland, Washington.

PNNL-17176, 2007, "200-BP-1 Prototype Hanford Barrier Annual Monitoring Report for Fiscal Years 2005 Through 2007," Pacific Northwest National Laboratory, Richland, Washington.

PNNL-18845, 2011, "200-BP-1 Prototype Hanford Barrier – 15 Years of Performance Monitoring," Rev. 1, Pacific Northwest National Laboratory, Richland, Washington.

PNNL-18934, 2009, "The Effects of Fire on the Function of the 200-BP-1 Engineered Surface Barrier," Pacific Northwest National Laboratory, Richland, Washington.

PNNL-19425, 2010, "Hanford Site Tank 241-C-108 Residual Waste Contaminant Release Models and Supporting Data," Pacific Northwest National Laboratory, Richland, Washington.

PNNL-19702, 2010, "Hydrogeologic Model for the Gable Gap Area, Hanford Site," Pacific Northwest National Laboratory, Richland, Washington.

PNNL-20302, 2011, "First Quarter Hanford Seismic Report for Fiscal Year 2011," Pacific Northwest National Laboratory, Richland, Washington.

PNNL-20548, 2011, "Hanford Site Environmental Report for Calendar Year 2010 (Including Some Early 2011 Information)," Pacific Northwest National Laboratory, Richland, Washington.

PNNL-20616, 2011, "Contaminant Release from Hanford Tank Residual Waste – Results of Single-Pass Flow-Through Tests," Pacific Northwest National Laboratory, Richland, Washington.

PNNL-20631, 2011, "Hanford Site Regional Population – 2010 Census," Pacific Northwest National Laboratory, Richland, Washington.

PNNL-23711, 2015, "Physical, Hydraulic, and Transport Properties of Sediments and Engineered Materials Associated with Hanford Immobilized Low-Activity Waste," RPT-IGTP-004, Rev. 0, Pacific Northwest National Laboratory, Richland, Washington.

PNNL-23841, 2014, "Radionuclide Migration through Sediment and Concrete: 16 Years of Investigations," Pacific Northwest National Laboratory, Richland, Washington.

PNNL-SA-32152, 1999, "A Short History of Plutonium Production and Nuclear Waste Generation, Storage, and Release at the Hanford Site," Pacific Northwest National Laboratory, Richland, Washington.

Polmann, D. J., 1990, "Application of Stochastic Methods to Transient Flow and Transport in Heterogeneous Unsaturated Soils," Ph.D. Thesis, Massachusetts Institute of Technology, Cambridge, Massachusetts.

Portland State University College of Urban & Public Affairs: Population Research Center, Queried 05/17/2015, [Population Estimates and Reports], http://www.pdx.edu/prc/population-reports-estimates.

PRC-PRO-IRM-309, 2014, "Controlled Software Management," Rev. 5, CH2M HILL Plateau Remediation Company, Richland, Washington.

Preliminary Remediation Goals for Radionuclides (PRGfR), Queried 07/2015, [PRG User's Guide], http://epa-prgs.ornl.gov/radionuclides/prg_guide.html.

PSI Bericht Nr. 95-06, 1995, "Sorption Databases for the Cementitious Near-Field of a L/ILW Repository for Performance Assessment," Paul Scherrer Institute, Switzerland.

Radiation Risk Assessment Software: CAP-88 and CAP-88 PC (EPA 2014), Queried 07/2015, [CAP88-PC Version 4.0 User Guide], http://www.epa.gov/radiation/assessment/CAP88/index.html.

RCW 70.105, "Hazardous Waste Management," Revised Code of Washington, as amended.

RCW 70.105D, "Hazardous Waste Cleanup — Model Toxics Control Act," Revised Code of Washington, as amended.

Reidel, S. P., N. P. Campbell, K. R. Fecht, and K. A. Lindsey, 1994, "Late Cenozoic Structure and Stratigraphy of South-Central Washington," Regional Geology of Washington State, Washington Division of Geology and Earth Resources, Washington State Department of Natural Resources, Bulletin 80, pp. 159–180.

Reidel, S. P. and P. R. Hooper (editors), 1989, "Volcanism and Tectonism in the Columbia River Flood-Basalt Province," Special Paper 239, The Geological Society of America, Inc., Boulder, Colorado.

Relander, C., 1956, Drummers and Dreamers, Caxton Printers, Caldwell, Idaho.

Resource Conservation and Recovery Act of 1976, 42 USC 6901, et seq.

RHO-BWI-C-64, 1979, "Clastic Dikes Of The Pasco Basin, Southeastern Washington, Final Report," Rockwell Hanford Operations, Richland, Washington.

RHO-BWI-C-120/PNL-4219, 1981, "Flood Risk Analysis of Cold Creek near the Hanford Site," prepared by Pacific Northwest Laboratory for Rockwell Hanford Operations, Richland, Washington.

RHO-BWI-ST-4, 1979, "Geologic Studies of the Columbia Plateau: A Status Report," Rockwell Hanford Operations, Richland, Washington.

RHO-BWI-ST-14, 1981, "Subsurface Geology of the Cold Creek Syncline," "Chapter 2 – Suprabasalt Sediments of the Cold Creek Syncline Area," Rockwell Hanford Operations, Richland, Washington.

RHO-BWI-ST-14, 1981, "Subsurface Geology of the Cold Creek Syncline," "Chapter 3 – Wanapum and Saddle Mountains Basalts of the Cold Creek Syncline Area," Rockwell Hanford Operations, Richland, Washington.

RHO-RE-CR-2, 1982, "Strength and Elastic Properties Tests of Hanford Concrete Cores – 241-SX-115 Tank and 202-A Purex Canyon Building," Construction Technology Laboratories, Skokie, Illinois.

RHO-SA-211, "Invasion of radioactive waste burial sites by the Great Basin Pocket Mouse (*Perognathus parvus*)," Hanford Engineering Development Laboratory, Richland, Washington.

RHO-ST-23, 1979, "Geology of the Separation Areas, Hanford Site, South-Central Washington," Rockwell Hanford Operations, Richland, Washington.

RHO-ST-46 P, 1984, "Field Calibration of Computer Models for Application to Buried Liquid Discharges: A Status Report," Rockwell International, Richland, Washington.

Rohay, A. C., 1989, "Earthquake Recurrence Rate Estimates for Eastern Washington and the Hanford Site," CONF-8910192--18, in Proceedings, Second DOE Natural Phenomena Hazards Mitigation Conference, Knoxville, Tennessee.

Ronald W. Reagan National Defense Authorization Act for Fiscal Year 2005, Public Law 108-375.

RPP-7494, 2001, "Historical Vadose Zone Contamination from A, AX, and C Tank Farm Operations," Rev. 0, Fluor Federal Services, Richland, Washington.

RPP-7625, 2015, "Guidelines for Updating Best-Basis Inventory," Rev. 12, Washington River Protection Solutions, LLC, Richland, Washington.

RPP-8847, 2007, "Best-Basis Inventory Template Compositions of Common Tank Waste Layers," Rev. 1B, CH2M HILL Hanford Group, Inc., Richland, Washington.

RPP-13033, 2014, "Tank Farms Documented Safety Analysis," Rev. 5-C, Washington River Protection Solutions, LLC, Richland, Washington.

RPP-13489, 2002, "Activity of Fuel Batches Processed Through Hanford Separations Plants, 1944 Through 1989," Rev. 0, CH2M HILL Hanford Group, Inc., Richland, Washington.

RPP-13774, 2004, "Single-Shell Tank System Closure Plan," Rev. 2, CH2M HILL Hanford Group, Inc., Richland, Washington.

RPP-13889, 2004, "Tank 241-C-106 Component Closure Action Data Quality Objectives," Rev. 1, CH2M HILL Hanford Group, Inc., Richland, Washington.

RPP-14430, 2003, "Subsurface Conditions Description of the C and A-AX Waste Management Area," Rev. 0, CH2M HILL Hanford Group, Inc., Richland, Washington.

RPP-15043, 2003, "Single-Shell Tank System Description," Rev. 0, CH2M HILL Hanford Group, Inc., Richland, Washington.

RPP-19822, 2005, "Hanford Defined Waste Model – Revision 5.0," Rev. 0-A, CH2M HILL Hanford Group, Inc./Technical Resources International, Inc., Richland, Washington.

RPP-19866, 2004, "Calculation for the Post-Retrieval Waste Volume Determination for Tank 241-C-106," Rev. 1, CH2M HILL Hanford Group, Inc., Richland, Washington.

RPP-20577, 2007, "Stage II Retrieval Data Report for Single-Shell Tank 241-C-106," Rev. 0, CH2M HILL Hanford Group, Inc., Richland, Washington.

RPP-20621, 2004, "Far-Field Hydrology Data Package for the Integrated Disposal Facility Performance Assessment," Rev. 0, CH2M HILL Hanford Group, Inc., Richland, Washington.

RPP-20658, 2008, "Basis for Exception to the Hanford Federal Facility Agreement and Consent Order Waste Retrieval Criteria for Single-Shell Tank 241-C-106," Rev. 3, CH2M HILL Hanford Group, Inc., Richland, Washington.

RPP-23403, 2006, "Single-Shell Tank Component Closure Data Quality Objectives," Rev. 3, CH2M HILL Hanford Group, Inc., Richland, Washington.

RPP-23403, 2013, "Single-Shell Tank Component Closure Data Quality Objectives," Rev. 5, Washington River Protection Solutions, LLC, Richland, Washington.

RPP-26744, 2005, "Hanford Soil Inventory Model, Rev. 1," Rev. 0, CH2M HILL Hanford Group, Inc., Richland, Washington.

RPP-29441, 2006, "Post-Retrieval Waste Volume Determination for Single Shell Tank 241-C-201," Rev. 0, Freestone Environmental Services, Inc./CH2M HILL Hanford Group, Inc., Richland, Washington.

RPP-32681, 2013, "Process to Assess Tank Farm Leaks in Support of Retrieval and Closure Planning," Rev. 2, Washington River Protection Solutions, LLC, Richland, Washington.

RPP-35484, 2008, "Field Investigation Report for Waste Management Areas C and A-AX," Rev.1, CH2M HILL Hanford Group, Inc., Richland, Washington.

RPP-50233, 2011, "Waste Management Area C Closure Conceptual Design Support Report," Rev. 0, Washington River Protection Solutions, LLC, Richland, Washington.

RPP-50816, 2013, "Software Management Plan for Grade D Custom Developed Hanford Tank Waste Operations Simulator (HTWOS)," Rev. 1, Washington River Protection Solutions, LLC, Richland, Washington.

RPP-52784, 2012, "Video Camera/CAD Modeling System for Retrieval: HISI #3254 Software Management Plan," Rev. 0, Washington River Protection Solutions, LLC, Richland, Washington.

RPP-ASMT-46452, 2010, "Tank 241-C-105 Leak Assessment Completion Report," Rev. 0, Washington River Protection Solutions, LLC, Richland, Washington.

RPP-CALC-54266, 2013, "Post-Hard Heel Retrieval Camera/CAD Modeling System Waste Volume Estimate for Tank 241-C-108," Rev. 0, Washington River Protection Solutions, LLC, Richland, Washington.

RPP-CALC-54284, 2013, "Post-Hard Heel Retrieval Camera/CAD Modeling System Waste Volume Estimate for Tank 241-C-104," Rev. 0, Washington River Protection Solutions, LLC, Richland, Washington.

RPP-CALC-54759, 2013, "Post-Hard Heel Retrieval Camera/CAD Modeling System Waste Volume Estimate for Tank 241-C-109," Rev. 0, Washington River Protection Solutions, LLC/Weirich Consulting Services Inc., Richland, Washington.

RPP-CALC-56399, 2013, "Post-Hard Heel Retrieval Camera/CAD Modeling System Waste Volume Estimate for Tank 241-C-110," Rev. 0, Washington River Protection Solutions, LLC, Richland, Washington.

RPP-CALC-56434, 2013, "Post-Retrieval Camera/CAD Modeling System Waste Volume Estimate for Tank 241-C-101," Rev. 0, Washington River Protection Solutions, LLC/ Weirich Consulting Services Inc., Richland, Washington.

RPP-CALC-56856, 2014, "Estimated Waste Volume Remaining in Single Shell Tank 241-C-112 after Hard Heel Retrieval," Rev. 0, Washington River Protection Solutions, LLC, Richland, Washington.

RPP-CALC-59985, 2014, "Post-Retrieval Camera/CAD Modeling System Waste Volume Estimate for Tank 241-C-107," Rev. 0, Washington River Protection Solutions, LLC/ Weirich Consulting Services Inc., Richland, Washington.

RPP-CALC-60345, 2016, "Heterogeneous Media Model for Waste Management Area C Performance Assessment," Rev. 0, Washington River Protection Solutions, LLC, Richland, Washington.

RPP-ENV-33418, 2016, "Hanford C-Farm Leak Inventory Assessments Report," Rev. 4, Washington River Protection Solutions, LLC, Richland, Washington.

RPP-ENV-58806, 2016, "RCRA Closure Analysis of Tank Waste Residuals Impacts at Waste Management Area C, Hanford Site, Washington," Rev. 0, Washington River Protection Solutions, LLC, Richland, Washington.

RPP-ENV-58813, 2016, "Exposure Scenarios for Risk and Performance Assessments in Tank Farms at the Hanford Site, Washington," Rev. 0, Washington River Protection Solutions, LLC, Richland, Washington.

RPP-PLAN-39114, 2012, "Phase 2 RCRA Facility Investigation/Corrective Measures Study Work Plan for Waste Management Area C," Rev. 2, Washington River Protection Solutions, LLC, Richland, Washington.

RPP-PLAN-47559, 2012, "Single-Shell Tank Waste Management Area C Pipeline Feasibility Evaluation," Rev. 1, Washington River Protection Solutions, LLC/Cenibark International, Inc., Richland, Washington.

RPP-RPT-24257, 2005, "244-CR Vault Liquid Level Assessment and Video Inspection Completion Report," Rev. 0, CH2M HILL Hanford Group, Inc., Richland, Washington.

RPP-RPT-26475, 2008, "Retrieval Data Report for Single-Shell Tank 241-C-203," Rev. 1-A, CH2M HILL Hanford Group, Inc., Richland, Washington.

RPP-RPT-29095, 2006, "Retrieval Data Report for Single-Shell Tank 241-C-202," Rev. 0, CH2M HILL Hanford Group, Inc., Richland, Washington.

RPP-RPT-30181, 2006, "Retrieval Data Report for Single-Shell Tank 241-C-201," Rev. 0-B, CH2M HILL Hanford Group, Inc., Richland, Washington.

RPP-RPT-33060, 2007, "Retrieval Data Report for Single-Shell Tank 241-C-103," Rev. 0, CH2M HILL Hanford Group, Inc., Richland, Washington.

RPP-RPT-34062, 2007, "Retrieval Data Report for Single-Shell Tank 241-C-204," Rev. 0, CH2M HILL Hanford Group, Inc., Richland, Washington.

RPP-RPT-39487, 2008, "TWINS Software Description," Rev. 0, Washington River Protection Solutions, LLC, Richland, Washington.

RPP-RPT-39908, 2009, "Hanford Tank Waste Operations Simulator Model (HTWOS) Version 3.0 Verification and Validation Report," Rev. 0, Washington River Protection Solutions, LLC, Richland, Washington.

RPP-RPT-41918, 2010, "Assessment Context for Performance Assessment for Waste in C Tank Farm Facilities after Closure," Rev. 0, Washington River Protection Solutions, LLC, Richland, Washington.

RPP-RPT-42294, 2016, "Hanford Waste Management Area C Soil Contamination Inventory Estimates," Rev. 2, Washington River Protection Solutions, LLC, Richland, Washington.

RPP-RPT-42323, 2015, "Hanford C-Farm Tank and Ancillary Equipment Residual Waste Inventory Estimates," Rev. 3, Washington River Protection Solutions, LLC, Richland, Washington.

RPP-RPT-44042, 2010, "Recharge and Waste Release within Engineered System in Waste Management Area C," Rev. 0, Washington River Protection Solutions, LLC, Richland, Washington.

RPP-RPT-45845, 2010, "Completion of Pumpable Liquid Removal from 244-CR Vault," Rev. 0, Washington River Protection Solutions, LLC, Richland, Washington.

RPP-RPT-46088, 2016, "Flow and Transport in the Natural System at Waste Management Area C," Rev. 2, Washington River Protection Solutions, LLC/GSI Water Solutions, Inc., Richland, Washington.

RPP-RPT-46879, 2016, "Corrosion and Structural Degradation within Engineered System in Waste Management Area C," Rev. 3, Washington River Protection Solutions, LLC, Richland, Washington.

RPP-RPT-47479, 2016, "Exposure Scenarios for the Waste Management Area C Performance Assessment," Rev. 2, Washington River Protection Solutions, LLC, Richland, Washington.

RPP-RPT-48490, 2011, "Technical Approach and Scope for Flow and Contaminant Transport Analysis in the Initial Performance Assessment of Waste Management Area C," Washington River Protection Solutions, LLC, Richland, Washington.

RPP-RPT-49089, 2011, "Hanford B-Farm Leak Inventory Assessments Report," Rev. 0, Washington River Protection Solutions, LLC, Richland, Washington.

RPP-RPT-49425, 2011, "Ecological Risk Assessment Approach for Hanford Waste Management Area C," Rev. 1, Washington River Protection Solutions, LLC, Richland, Washington.

RPP-RPT-49701, 2011, "Waste Management Area C Closure – Conceptual Design Report," Rev. 0, Washington River Protection Solutions, LLC, Richland, Washington.

RPP-RPT-50097, 2011, "Hanford 241-U Farm Leak Inventory Assessment Report," Rev. 0, Washington River Protection Solutions, LLC, Richland, Washington.

RPP-RPT-50870, 2013, "Hanford 241-TX Farm Leak Inventory Assessment Report," Rev. 0, Washington River Protection Solutions, LLC, Richland, Washington.

RPP-RPT-50934, 2012, "Inspection and Test Report for the Removed 241-C-107 Dome Concrete," Rev. 0, Washington River Protection Solutions, LLC, Richland, Washington.

RPP-RPT-54072, 2014, "Retrieval Data Report for Single-Shell Tank 241-C-104," Rev. 0, Washington River Protection Solutions, LLC/YAHSGS, LLC, Richland, Washington.

RPP-RPT-55084, 2013, "Hanford 241-T Farm Leak Inventory Assessment Report," Rev. 0, Washington River Protection Solutions LLC, Richland, Washington.

RPP-RPT-55284, 2014, "Retrieval Data Report for Single-Shell Tank 241-C-109," Rev. 0, Washington River Protection Solutions, LLC/YAHSGS, LLC, Richland, Washington.

RPP-RPT-55896, 2013, "Retrieval Data Report for Single-Shell Tank 241-C-108," Rev. 1, Washington River Protection Solutions, LLC/YAHSGS, LLC, Richland, Washington.

RPP-RPT-56356, 2014, "Development of Alternative Digital Geologic Models of Waste Management Area C," Rev. 0, Freestone Environmental Services Inc./Washington River Protection Solutions, LLC, Richland, Washington.

RPP-RPT-56796, 2014, "Retrieval Data Report for Single-Shell Tank 241-C-110," Rev. 0, Washington River Protection Solutions, LLC, LLC, Richland, Washington.

RPP-RPT-58254, 2014, "Concrete Core Testing Report for the Single-Shell Tank 241-A-106 Sidewall Coring Project," Rev. 0, Washington River Protection Solutions LLC, Richland, Washington.

RPP-RPT-58295, 2015, "Retrieval Data Report for Single-Shell Tank 241-C-107," Rev. 1, Washington River Protection Solutions, LLC, LLC, Richland, Washington.

RPP-RPT-58329, 2016, "Baseline Risk Assessment for Waste Management Area C," Rev. 1, INTERA, Inc./Washington River Protection Solutions, LLC, Richland, Washington.

RPP-RPT-58339, 2014, "Phase 2 RCRA Facility Investigation Report for Waste Management Area C," Draft A, Washington River Protection Solutions, LLC, Richland, Washington.

RPP-RPT-58386, 2015, "Retrieval Data Report for Single-Shell Tank 241-C-101," Rev. 2, Washington River Protection Solutions, LLC, Richland, Washington.

RPP-RPT-58490, 2015, "Retrieval Data Report for Single-Shell Tank 241-C-112," Rev. 2B, Washington River Protection Solutions, LLC, Richland, Washington.

RPP-RPT-58676, 2015, "Practicability Evaluation Request to Forego a Third Retrieval Technology for Tank 241-C-102," Rev. 0, Washington River Protection Solutions, LLC, Richland, Washington.

RPP-RPT-59197, 2016, "Analysis of Past Tank Waste Leaks and Losses in the Vicinity of Waste Management Area C at the Hanford Site, Southeast Washington," Rev. 0, Washington River Protection Solutions LLC, Richland, Washington.

Safe Drinking Water Act of 1974, 42 USC 300, et seq.

Sakoda, A., Ishimori, Y., and Yamaoka, K., 2011, "A comprehensive review of radon emanation measurements for mineral, rock, soil, mill tailing and fly ash," Applied Radiation and Isotopes, Vol. 69, Issue 10, pp. 1422–1435.

Saltelli, A. and S. Tarantola, 2002, "On the Relative Importance of Input Factors in Mathematical Models: Safety Assessment of Nuclear Waste Disposal," Journal of the American Statistical Association, Vol. 97, No. 459, pp. 702–709.

Sander, R., 1999, "Compilation of Henry's Law Constants for Inorganic and Organic Species of Potential Importance in Environmental Chemistry," Version 3, Max-Planck Institute of Chemistry, Mainz, Germany.

Scanlon, B. R., K. E. Keese, A. L. Flint, L. E. Flint, C. B. Gaye, W. M. Edmunds, and I. Simmers, 2006, "Global synthesis of groundwater recharge in semiarid and arid regions," Hydrological Processes, Vol. 20, Issue 15, pp. 3335–3370.

Scheibe, T. D., E. M. Murphy, X. Chen, A. K. Rice, K. C. Carroll, B. J. Palmer, A. M. Tartakovsky, I. Battiato, and B. D. Wood, 2015, "An Analysis Platform for Multiscale Hydrogeologic Modeling with Emphasis on Hybrid Multiscale Methods," Groundwater, Vol. 53, No. 1, pp. 38–56.

SD-BWI-TI-335, 1988, "Fresh-Water Potentiometric Map and Inferred Flow Direction of Ground Water Within the Mabton Interbed, Hanford Site, Washington State – January 1987," Rockwell Hanford Operations, Richland, Washington.

Seyfried, M. S., S. Schwinning, M. A. Walvoord, W. T. Pockman, B. D. Newman, R. B. Jackson, and F. M. Phillips, 2005, "Ecohydrological Control of Deep Drainage in Arid and Semiarid Regions," Ecology, Vol. 86, No. 2, pp. 277–287.

SGW-54165, 2014, "Evaluation of the Unconfined Aquifer Hydraulic Gradient Beneath the 200 East Area, Hanford Site," Rev. 0, CH2M HILL Plateau Remediation Company, Richland, Washington.

SGW-58561, 2015, "WMA C Quarterly October through December 2014 Quarterly Groundwater Monitoring Report," Rev. 0, CH2M HILL Plateau Remediation Company, Richland, Washington.

Slate, J. L., 1996, "Buried carbonate paleosols developed in Pliocene-Pleistocene deposits of the Pasco Basin, south-central Washington, U.S.A.," Quaternary International, Vol. 34–36, pp. 191–196.

SKB Rapport R-05-75, 2005, "Assessment of uncertainty intervals for sorption coefficients, SFR-1 uppföljning av SAFE," Swedish Nuclear Fuel and Waste Management Company, Stockholm, Sweden.

SRNL-STI-2008-00421, 2008, "Hydraulic and Physical Properties of Saltstone Grouts and Vault Concretes," Rev. 0, Savannah River National Laboratory, Savannah River Nuclear Solutions, Aiken, South Carolina.

SRR-CWDA-2009-00017, 2009, "Performance Assessment for the Saltstone Disposal Facility at the Savannah River Site," Rev. 0, SRR Closure & Waste Disposal Authority, Savannah River Remediation, Aiken, South Carolina.

State of Washington Office of Financial Management, Queried 05/17/2015, [April 1 official population estimates], http://www.ofm.wa.gov/pop/april1/default.asp.

SVF-2109, Rev. 0, "Tank_Residuals_4MinTimestep(6Melters)-mmr-11-031-6.5-8.3r1-2011-03-18-at-01-31-58_M1.xlsm," Present residual waste inventory data for System Plan, Rev. 6, Case 1 - Baseline Case, R. A. Kirkbride, Base Ops. Proc. Engrng./Modeling, B1-55, 372-2115, 4/5/2011

Tank Waste Information Network System [TWINS], Queried 02/10/2014, [WMA C Tanks, wt% water in sludge/solid waste type], http://twins.pnl.gov/twins.htm.

Technical Report TR-02-11, 2002, "Assigning probability distributions to input parameters of performance assessment models," INTERA Inc. for Swedish Nuclear Fuel and Waste Management Company, Stockholm, Sweden.

TFC-ENG-CHEM-P-53, "Best-Basis Inventory Evaluations," Washington River Protection Solutions LLC (WRPS) Tank Farms, Richland, Washington.

TFC-ESHQ-ENV_FS-C-05, "WRPS Environmental Model Calculation Preparation and Issuance," Washington River Protection Solutions LLC (WRPS) Tank Farms, Richland, Washington.

TFC-PLN-155, "General Project Plan for Environment Modeling," Washington River Protection Solutions LLC (WRPS) Tank Farms, Richland, Washington.

Tsang, C.-F., 1991, "The Modeling Process and Model Validation," Ground Water, Vol. 29, No. 6, pp. 825–831.

The Nature Conservancy, 1998, "Biodiversity Inventory and Analysis of the Hanford Site, 1997 Annual Report," The Nature Conservancy of Washington, Seattle, Washington.

UCRL-21069, 1988, "Probabilistic Flood Hazard Assessment for the N Reactor, Hanford, Washington," Jack R. Benjamin and Associates, Inc., Mountain View, California.

United States Environmental Protection Agency, Queried 01/2012, [EPA On-line Tools for Site Assessment Calculation], https://www3.epa.gov/ceampubl/learn2model/part-two/onsite/estdiffusion.html.

United States Environmental Protection Agency, Queried 06/18/2015, [Preliminary Remediation Goals for Radionuclides], http://epa-prgs.ornl.gov/radionuclides/.

USACE, 1951, "Artificial Flood Possibilities on the Columbia River," U.S. Army Corps of Engineers, 45 Washington District, Washington, D.C.

USACE, 1989, "Water Control Manual for McNary Lock and Dam, Columbia River, Oregon and Washington," U.S. Army Corps of Engineers, Walla Walla District, Walla Walla, Washington.

U.S. Department of Agriculture, Natural Resources Conservation Service, Queried 12/18/2015, [Fact Sheets & Plant Guides/Artemisia tridentata ssp. tridentata], http://plants.usda.gov/plantguide/pdf/pg_artrt.pdf.

U.S. Geological Survey, Queried 09/2015, [USGS Water Data for the Nation], http://waterdata.usgs.gov/nwis/nwis.

USGS Bulletin 1457-G, 1979, "Revisions in stratigraphic nomenclature of the Columbia River Basalt Group," U.S. Geological Survey, Washington, D.C.

van Genuchten, M. Th., 1980, "A Closed-form Equation for Predicting the Hydraulic Conductivity of Unsaturated Soils," Soil Science Society of America Journal, Vol. 44, No. 5, pp. 892–898.

WA7 89000 8967, 2007, "Hanford Facility Resource Conservation and Recovery Act Permit, Dangerous Waste Portion Revision 8C for the Treatment, Storage, and Disposal of Dangerous Waste," State of Washington Department of Ecology, Richland, Washington.

WAC 173-160, "Minimum Standards for Construction and Maintenance of Wells," Washington Administrative Code, as amended.

WAC 173-201A, "Water Quality Standards for Surface Waters of the State of Washington," Washington Administrative Code, as amended.

WAC 173-216, "State Waste Discharge Permit Program," Washington Administrative Code, as amended.

WAC 173-303, "Dangerous Waste Regulations," Washington Administrative Code, as amended.

WAC 173-303-610, "Closure and Post-Closure," Washington Administrative Code, as amended.

WAC 173-303-640, "Tank Systems," Washington Administrative Code, as amended.

WAC 173-303-665, "Landfills," Washington Administrative Code, as amended.

WAC 173-340-745, "Soil Cleanup Standards for Industrial Properties," Washington Administrative Code, as amended.

WAC 173-340-747, "Deriving Soil Concentrations for Groundwater Protection," Washington Administrative Code, as amended.

WAC 246-290, "Group A Public Water Supplies," Washington Administrative Code, as amended.

WAC 246-290-025, "Adoption by Reference," Washington Administrative Code, as amended.

WAC 246-290-310, "Maximum Contaminant Levels (MCLs) and Maximum Residual Disinfectant Levels (MRDLs)," Washington Administrative Code, as amended.

Wang, J. S. Y. and T. N. Narasimhan, 1985, "Hydrologic Mechanisms Governing Fluid Flow in a Partially Saturated, Fractured, Porous Medium," Water Resources Research, Vol. 21, No. 12, pp. 1861–1874.

Waters, A. C., 1961, "Stratigraphic and Lithologic Variations in the Columbia River Basalt," American Journal of Science, Vol. 259, pp. 583–611.

WCH-223, 2007, "2007 River Corridor Closure Contractor Revegetation Monitoring Report," Rev. 0, Washington Closure Hanford, Richland, Washington.

WCH-520, 2013, "Performance Assessment for the Environmental Restoration Disposal Facility, Hanford Site, Washington," Rev. 1, Washington Closure Hanford, Richland, Washington.

Webster, G. D. and J. W. Crosby, 1982, "Appendix 2R - Stratigraphic Investigation of the Skagit/Hanford Nuclear Project," in Skagit/Hanford Nuclear Project, Preliminary Safety Analysis Report, Volume 5, Pudget Power, Pudget Sound Power and Light Company, Bellevue, Washington.

WHC-EP-0216, 1989, "Primary Operable Units Designation Project," Westinghouse Hanford Company, Richland, Washington.

WHC-EP-0332, 1989, "Simulations of Infiltration of Meteoric Water and Contaminant Plume Movement in the Vadose Zone at Single-Shell Tank 241-T-106 at the Hanford Site," Westinghouse Hanford Company, Richland, Washington.

WHC-EP-0595, 1993, "Westinghouse Hanford Company Operational Groundwater Status Report, 1990-1992," Westinghouse Hanford Company, Richland, Washington.

WHC-EP-0645, 1995, "Performance Assessment for the Disposal of Low-Level Waste in the 200 West Area Burial Grounds," Westinghouse Hanford Company, Richland, Washington.

WHC-EP-0673, 1994, "Permanent Isolation Surface Barrier Development Plan," Westinghouse Hanford Company, Richland, Washington.

WHC-EP-0698, 1994, "Groundwater Impact Assessment Report for the 216-U-14 Ditch," Westinghouse Hanford Company, Richland, Washington.

WHC-EP-0707, 1994, "216-U-10 Pond and 216-Z-19 Ditch Characterization Studies," Rev. 0 (formerly RHO-ST-45), Westinghouse Hanford Company, Richland, Washington.

WHC-EP-0772, 1994, "Characterization of the Corrosion Behavior of the Carbon Steel Liner in Hanford Site Single-Shell Tanks," Rev. 0, Westinghouse Hanford Company, Richland, Washington.

WHC-EP-0815, 1995, "Groundwater Impact Assessment Report for the 216-T-4-2 Ditch," Westinghouse Hanford Company, Richland, Washington.

WHC-EP-0883, 1995, "Variability and Scaling of Hydraulic Properties for 200 Area Soils, Hanford Site," Westinghouse Hanford Company, Richland, Washington.

WHC-MR-0293, 1992, "Legend and Legacy: Fifty Years of Defense Production at the Hanford Site," Rev. 2, Westinghouse Hanford Company, Richland, Washington.

WHC-MR-0521, 1996, "The Plutonium Production Story at the Hanford Site: Processes and Facilities History," Rev. 0, Westinghouse Hanford Company, Richland, Washington.

WHC-SA-1252-S, 1991, "Mammal Occurrence and Exclusion at the Hanford Site," Westinghouse Hanford Company, Richland, Washington.

WHC-SD-EN-AP-012, 1991, "Interim-Status Groundwater Monitoring Plan for the Single-Shell Tanks," Rev. 1, Westinghouse Hanford Company, Richland, Washington.

WHC-SD-EN-EE-004, 1991, "Revised Stratigraphy for the Ringold Formation, Hanford Site, South-Central Washington," Rev. 0, Westinghouse Hanford Company, Richland, Washington.

WHC-SD-EN-TI-012, 1992, "Geologic Setting of the 200 East Area: An Update," Rev. 0, Westinghouse Hanford Company, Richland, Washington.

WHC-SD-EN-TI-014, 1992, "Hydrogeologic Model for the 200 West Groundwater Aggregate Area," Rev. 0, Westinghouse Hanford Company, Richland, Washington.

WHC-SD-EN-TI-019, 1992, "Hydrogeologic Model for the 200 East Groundwater Aggregate Area," Rev. 0, Westinghouse Hanford Company, Richland, Washington.

WHC-SD-EN-TI-290, 1994, "Geologic Setting of the Low-Level Burial Grounds," Rev. 0, Westinghouse Hanford Company, Richland, Washington.

WHC-SD-ER-TI-003, 1991, "Geology and Hydrology of the Hanford Site: A Standardized Text for Use in Westinghouse Hanford Company Documents and Reports," Rev. 0, Westinghouse Hanford Company, Richland, Washington.

WHC-SD-GN-ER-30009, 1992, "Bibliography and Summary of Geotechnical Studies at the Hanford Site," Rev. 2, Westinghouse Hanford Company, Richland, Washington.

WHC-SD-GN-ER-30038, 2012, "Volcano Ashfall Loads for the Hanford Site," Rev. 2, Washington River Protection Solutions LLC, Richland, Washington.

WHC-SD-W236A-TI-0002, 1993, "Probabilistic Seismic Hazard Analysis, DOE Hanford Site, Washington," Rev. 0, prepared for Westinghouse Hanford Company by Geomatrix Consultants, Richland, Washington.

WHC-SD-WM-EE-004, 1995, "Performance Assessment of Grouted Double-Shell Tank Waste Disposal at Hanford," Rev. 1, Westinghouse Hanford Company, Richland, Washington.

WHC-SD-WM-TI-632, 1995, "Hanford Defined Wastes: Chemical and Radionuclide Compositions," Rev. 0, Westinghouse Hanford Company, Richland, Washington.

WHC-SD-WM-TI-730, 1996, "Performance Assessment for the Disposal of Low-Level Waste in the 200 East Area Burial Grounds," Rev. 0, Westinghouse Hanford Company, Richland, Washington.

Whitlock, C. and P. J., Bartlein, 1997, "Vegetation and climate change in northwest America during the past 125 kyr," Nature, Vol. 388, pp. 57–61.

Wing, N. R. and G. W. Gee, 1994, "Quest for the Perfect Cap," Civil Engineering, Vol. 64, No. 10, pp. 38–41.

WMP-17524, 2003, "Vadose Zone Hydraulic Property Letter Reports," Rev. 0, Fluor Hanford, Richland, Washington.

WMP-20570, 2006, "Central Plateau Terrestrial Ecological Risk Assessment Data Quality Objectives Summary Report – Phase I," Rev. 0, Fluor Hanford, Richland, Washington.

WSRC-MS-2003-00582, 2004, "Performance Assessment/Composite Analysis Modeling to Support a Holistic Strategy for the Closure of F Area, a Large Nuclear Complex at the Savannah River Site," Rev. 1, Savannah River Technology Center, Aiken, South Carolina.

WSRC-STI-2007-00369, 2007, "Hydraulic and Physical Properties of Tank Grouts and Base Mat Surrogate Concrete for FTF Closure," Rev. 0, Savannah River National Laboratory, Aiken, South Carolina.

WSRC-STI-2007-00607, 2007, "Chemical Degradation Assessment of Cementitious Materials for the HLW Tank Closure Project (U)," Rev. 0, Washington Savannah River Company/Savannah River National Laboratory, Aiken, South Carolina.

WSRC-TR-2005-00195, 2005, "Summary of Grout Development and Testing for Single Shell Tank Closure at Hanford," Rev. 0, Savannah River National Laboratory, Aiken, South Carolina.

Xu, X., J. L. Nieber, and S. C. Gupta, 1992, "Compaction Effect on the Gas Diffusion Coefficient in Soils," Soil Science Society of America Journal, Vol. 56, No. 6, pp. 1743–1750.

Ye, M. and R. Khaleel, 2008, "A Markov chain model for characterizing medium heterogeneity and sediment layering structure," Water Resources Research, Vol. 44, Issue 9, W09427.

Ye, M., R. Khaleel, M. G. Schaap, and J. Zhu, 2007, "Simulation of field injection experiments in heterogeneous unsaturated media using cokriging and artificial neural network," Water Resources Research, Vol. 43, Issue 7, W07413.

Ye, M., R. Khaleel, T. J. Yeh, 2005, "Stochastic analysis of moisture plume dynamics of a field injection experiment," Water Resources Research, Vol. 41, W03013.

Yeh, T.-C. J., M. Ye, R. Khaleel, 2005, "Estimation of effective unsaturated hydraulic conductivity tensor using spatial moments of observed moisture plume," Water Resources Research, Vol. 41, W03014.

Zhang, Z. F. and R. Khaleel, 2010, "Simulating field-scale moisture flow using a combined power-averaging and tensorial connectivity-tortuosity approach," Water Resources Research, Vol. 46, Issue 9, W09505.

APPENDIX A

KEY ASSUMPTIONS IN THE PERFORMANCE ASSESSMENT

This page intentionally left blank.

LIST OF TERMS

Abbreviations and Acronyms

DOE	U.S. Department of Energy
RCRA	Resource Conservation and Recovery Act of 1976
WMA	Waste Management Area

This page intentionally left blank.

APPENDIX A

KEY ASSUMPTIONS IN THE PERFORMANCE ASSESSMENT

In this Appendix, a set of key assumptions used in the base case analysis of the Performance Assessment are listed. However, it is emphasized that the structure of the Performance Assessment is founded on the extensive use of sensitivity and uncertainty analyses that explore the consequences if alternative assumptions are used. The alternative analyses include sensitivity cases evaluating conditions well outside the range of the base case analysis. In all cases the calculations produced results that are below the performance measures. Therefore, it is not possible to identify key assumptions or design variables that must be met in order to meet the regulatory goals of DOE O 435.1, Radioactive Waste Management.

- It has been assumed that the landfill closure of Waste Management Area (WMA) C occurs in 2020, consistent with planning assumptions in the Tank Closure and Waste Management Environmental Impact Statement (DOE/EIS-0391). The results of the performance assessment are not significantly affected by alternative assumptions about closure timing.

- The Central Plateau has been designated Industrial-Exclusive for the indefinite future, based on several Records of Decision [64 FR 61615, "Record of Decision: Hanford Comprehensive Land-Use Plan Environmental Impact Statement (HCP EIS)"; 73 FR 55824, "Amended Record of Decision for the Hanford Comprehensive Land-Use Plan Environmental Impact Statement"]. This area, which includes the 200 East and 200 West Areas, includes WMA C. There is no stated intention to release the Central Plateau from this designation or from U.S. Department of Energy (DOE) control at any time in the future. Despite this designation, it is assumed in this analysis that institutional control and societal memory of the disposal activities are lost 100 years after site closure, for consistency with DOE O 435.1 requirements. This assumption is necessary to allow future hypothetical individuals to come onto the Central Plateau and engage in activities that might result in exposure.

- In the base case, the land use and land cover, including the barrier, remain shrub steppe indefinitely after closure. Alternative infiltration rates in the future are included in alternative analysis cases, which are intended to address a variety of potential future conditions, including progression to different land uses and land covers.

- The engineered cover for WMA C is not yet designed but is assumed to be similar to the Modified Resource Conservation and Recovery Act of 1976 (RCRA) Subtitle C Barrier that limits infiltration through the waste primarily by evapotranspiration processes (i.e., surface barrier) based on the work done for the Hanford Prototype barrier (DOE/ORP-2008-01, RCRA Facility Investigation Report for Hanford Single-Shell Tank Waste Management Areas, Appendix C). These processes are not modeled directly for this report, but those processes have been studied through field measurements, tracer studies, and numerical models to estimate net infiltration (PNNL-14744, "Recharge Data Package for the 2005 Integrated Disposal Facility Performance Assessment";

PNNL-14960, "200-BP-1 Prototype Hanford Barrier Annual Monitoring Report for Fiscal Year 2004"; "Multiple-Year Water Balance of Soil Covers in a Semiarid Setting" [Fayer and Gee 2006]). Instead, the recommended net infiltration rates from those reports are applied to the area under the engineered cover and are varied spatially and temporally as appropriate according to the estimated or assumed time-dependent performance of a surface barrier.

- The design life of the cover is assumed to be 500 years in the base case, following which the infiltration through the cover is assumed to return to the site-wide average infiltration rate for undisturbed soil. Alternative infiltration rates in the future are included in alternative analysis cases, which are intended to address a variety of potential future conditions, including progression to different land uses and land covers.

- It is assumed the tanks will be filled with grout according to the basic assumptions outlined for landfill closure in DOE/EIS-0391 (2012). The specific formulation of the grout has not yet been established, but consistent with DOE/EIS-0391 (2012), it is assumed the fill material for the tanks will be similar to the cold-cap grout formulation developed by the U.S. Army Corps of Engineers for the Hanford Grout Vault Program. This type of grout is assumed to behave chemically like ordinary cementitious material. It has been assumed that the grout formulation does not provide any specific or unusual chemical conditions, such as reducing conditions.

- Radionuclide and chemical release mechanisms from the sources are assumed to occur by one of two mechanisms: (a) the entire inventory of the residual waste is assumed to be instantly available for release and transport out of the tanks, or (b) a semi-empirical release function is applied based on leach tests performed on residual waste from WMA C.

- Transport of contamination from the tanks is assumed to be primarily controlled by diffusion from the grouted tanks through the base mat below the tank. Alternative assumptions are included as sensitivity cases that evaluate the consequences of hydraulic failure (i.e., fracturing) of the grouted tanks and base mat.

- The specific formulation of the grout has not yet been established, and site-specific measurements of the chemical influence of the grout have not been performed. The chemical effect of the grout is represented by contaminant-specific distributions of distribution coefficients (K_d), which have been developed from international literature on sorption of radionuclides on cementitious materials. These values are generally consistent with or more conservative than comparable values used for the facility-specific grout at the Savannah River F and H tank farm performance assessments [WSRC-STI-2007-00369, "Hydraulic and Physical Properties of Tank Grouts and Base Mat Surrogate Concrete for FTF Closure" and WSRC-STI-2007-00607, "Chemical Degradation Assessment of Cementitious Materials for the HLW Tank Closure Project (U)"].

- Release from one WMA C solute source and migration are independent of other solute transport and source terms in the model.

- The post-retrieval inventory of contaminants in WMA C is assumed to be uniformly distributed throughout the waste residual volume. The residual volume in the tanks is assumed to be a uniform layer distributed at the bottom of the tanks. In pipelines and ancillary equipment, the residual waste is assumed to be distributed in a homogeneous layer across WMA C at the depth and area of the pipelines.

- Progeny radionuclides with a half-life of less than two years are assumed to be in secular equilibrium with their parent, which allows a reduction in the number of species tracked but still accounts for the radiological effects of the progeny.

- Inventories of contaminants in retrieved tanks are based on post-retrieval sampling and measurements. It is assumed that the sampling results are representative of the entire waste residual. Inventories for tanks that have not yet completed retrieval use the best estimates of post-retrieval conditions available at this time. These data have been estimated as of September 30, 2014. Additional sensitivity cases were executed based on alternative inventories in the 2009 to 2011 working sessions.

- The vadose zone is modeled as an aqueous-gas porous media system where flow and transport through the gas phase are assumed to be negligible.

- Hydraulic property heterogeneity is assumed to be insignificant within geologic units. Hence, each geologic unit within the vadose zone is assigned upscaled, effective hydraulic properties. These properties have been updated from the input parameters presented in the 2009 and 2011 data packages based on consideration of field data for moisture content, as discussed in Appendix B.

- Post-closure groundwater flow beneath WMA C is assumed to be northwest to southeast and parallel to the four tank arrays of 100-series tanks in WMA C. The justification for this assumption is found in RPP-RPT-46088, "Flow and Transport in the Natural System at Waste Management Area C." Groundwater flow parameters have been derived from the Central Plateau groundwater model (CP-47631, "Model Package Report: Central Plateau Groundwater Model Version 6.3.3").

- Distribution coefficients (K_d) are used to represent sediment-contaminant chemical interaction that best represent plausible levels of reactivity. The K_d values are chosen assuming low-salt, near-neutral waste chemistry in the vadose and saturated zone. Justification for the selected parameter values is found in RPP-RPT-46088; PNNL-16663, "Geochemical Processes Data Package for the Vadose Zone in the Single-Shell Tank Waste Management Areas at the Hanford Site"; and PNNL-17154, "Geochemical Characterization Data Package for the Vadose Zone in the Single-Shell Tank Waste Management Areas at the Hanford Site." In addition, uncertainties in K_d values have been assessed as part of the uncertainty analysis.

- The point of calculation used in the calculation of the groundwater concentrations corresponds to the location 100 m (328 ft) downgradient from the facility per DOE O 435.1. For the purpose of calculating groundwater concentrations for comparison with groundwater protection requirements, it is necessary to identify the peak location in space at which the concentration occurs. The approach for identifying the location of peak groundwater concentrations is described in Section 6.3.9.

- For volatiles released from the residual wastes, it is assumed that transport through the tank infill grout material and the soil overburden is controlled by diffusion.

- Once volatile radionuclides reach the ground surface, a simplified Gaussian plume model with uniform velocity and atmospheric conditions is assumed for the air transport analysis.

- Assumptions used in the exposure scenarios to define input parameter values are based on appropriate regulatory guidance as detailed in RPP-ENV-58813, "Exposure Scenarios for Risk and Performance Assessments in Tank Farms at the Hanford Site, Washington." These values represent conservative inputs to the exposure scenario calculations characteristic of a highly exposed individual.

- Age- and gender-weighted intake rates are generally developed for a Representative Person in accordance with the recommendations described in DOE-STD-1196-2011, Derived Concentration Technical Standard. The 95th percentile intake rates were obtained from EPA/600/R-090/052F, Exposure Factors Handbook: 2011 Edition, National Center for Environmental Assessment, based on available information. Even though mean intake rates were available, the 95th percentile values from the underlying distribution were chosen conservatively to maximize the likely exposure. Typically, the 95th percentile intake rates weighted by age and gender are calculated (Appendix P of RPP-ENV-58813). The exceptions to this approach were the indoor inhalation rate (taken directly from a reference source) and the soil ingestion rates (where simple age weighting is performed for children and adults).

- The following assumptions are specific to inadvertent human intrusion.

    - The only credible intrusion event is a drilling event. Both depth of disposal and the existence of concrete and grout intrusion barriers limit credible intrusion scenarios.

    - Although results are provided for intrusion into individual single-shell tanks, the most credible intrusion event is assumed to be into the ancillary equipment rather than a tank. This type of event is more credible than a tank intrusion, since the tank dome and grout form a substantial intruder protection barrier.

    - For the analysis of intrusion into the pipelines, the driller is assumed to penetrate a transfer line at 100 years after closure. Sensitivity analyses have investigated intrusion into a cascade line, which would release a larger inventory relative to other pipeline locations in WMA C.

- For the intrusion analysis for the 100- and 200-series tanks, the C-301 catch tank, and the 244-CR Process Tank Vault, the intruder is assumed to penetrate the tank dome, tank shell, grout, and residual waste at 500 years after closure.

- The acute exposure to the driller is calculated using representative local assumptions about the duration of the drilling.

- Acute exposures are limited to a well driller that is exposed to waste exhumed by the drill bit during the drilling.

- Chronic post-intrusion exposures are calculated for several alternative exposure scenarios. In these scenarios, waste exhumed by the intrusion event is assumed to be mixed with a surface soil layer. In each scenario, the volume of soil in this layer represents the minimum area consistent with the assumed activities of the scenario. For instance, the residential garden scenario mixes the contamination in an area of a garden sufficient to grow vegetables, whereas the rural pasture scenario mixes the contamination in an area sufficient for cattle grazing. The effect of this assumption is that different post-intrusion chronic scenarios have different soil concentrations, and the relative importance of the scenarios is strongly dependent on the assumed area of contamination.

REFERENCES

64 FR 61615, 1999, "Record of Decision: Hanford Comprehensive Land-Use Plan Environmental Impact Statement (HCP EIS)," Federal Register, Vol. 64, pp. 61615–61625 (November 12).

73 FR 55824, 2008, "Amended Record of Decision for the Hanford Comprehensive Land-Use Plan Environmental Impact Statement," Federal Register, Vol. 73, pp. 55824–55826 (September 26).

CP-47631, 2015, "Model Package Report: Central Plateau Groundwater Model Version 6.3.3," Rev. 2, INTERA, Inc., Richland, Washington.

DOE/EIS-0391, 2012, "Final Tank Closure and Waste Management Environmental Impact Statement for the Hanford Site, Richland, Washington," U.S. Department of Energy, Washington, D.C.

DOE O 435.1, 2001, Radioactive Waste Management, U.S. Department of Energy, Washington, D.C.

DOE/ORP-2008-01, 2010, RCRA Facility Investigation Report for Hanford Single-Shell Tank Waste Management Areas, Rev. 1, U.S. Department of Energy, Office of River Protection, Richland, Washington.

DOE-STD-1196-2011, 2011, Derived Concentration Technical Standard, U.S. Department of Energy, Washington, D.C.

EPA/600/R-090/052F, 2011, Exposure Factors Handbook: 2011 Edition, National Center for Environmental Assessment, Office of Research and Development, U.S. Environmental Protection Agency, Washington, D.C.

Fayer, M. J., and G. W. Gee, 2006, "Multiple-Year Water Balance of Soil Covers in a Semiarid Setting," Journal of Environmental Quality, Vol. 35, No. 2, pp. 366–377.

PNNL-14744, 2004, "Recharge Data Package for the 2005 Integrated Disposal Facility Performance Assessment," Pacific Northwest National Laboratory, Richland, Washington.

PNNL-14960, 2005, "200-BP-1 Prototype Hanford Barrier Annual Monitoring Report for Fiscal Year 2004," Pacific Northwest National Laboratory, Richland, Washington.

PNNL-16663, 2007, "Geochemical Processes Data Package for the Vadose Zone in the Single-Shell Tank Waste Management Areas at the Hanford Site," Pacific Northwest National Laboratory, Richland, Washington.

PNNL-17154, 2008, "Geochemical Characterization Data Package for the Vadose Zone in the Single-Shell Tank Waste Management Areas at the Hanford Site," Pacific Northwest National Laboratory, Richland, Washington.

Resource Conservation and Recovery Act of 1976, 42 USC 6901, et seq.

RPP-ENV-58813, 2016, "Exposure Scenarios for Risk and Performance Assessments in Tank Farms at the Hanford Site, Washington," Rev. 0, Washington River Protection Solutions, LLC, Richland, Washington.

RPP-RPT-46088, 2016, "Flow and Transport in the Natural System at Waste Management Area C," Rev. 2, Washington River Protection Solutions, LLC/GSI Water Solutions, Inc., Richland, Washington.

WSRC-STI-2007-00369, 2007, "Hydraulic and Physical Properties of Tank Grouts and Base Mat Surrogate Concrete for FTF Closure," Rev. 0, Savannah River National Laboratory, Aiken, South Carolina.

WSRC-STI-2007-00607, 2007, "Chemical Degradation Assessment of Cementitious Materials for the HLW Tank Closure Project (U)," Rev. 0, Washington Savannah River Company/Savannah River National Laboratory, Aiken, South Carolina.

APPENDIX B

BASIS FOR DEVELOPMENT OF VADOSE ZONE HYDRAULIC PROPERTIES AT WASTE MANAGEMENT AREA C

This page intentionally left blank.

TABLE OF CONTENTS

APPENDIX B – BASIS FOR DEVELOPMENT OF VADOSE ZONE HYDRAULIC PROPERTIES AT WASTE MANAGEMENT AREA C B-1

B.1 MOISTURE CONTENT MEASUREMENTS AT WASTE MANAGEMENT AREA C B-1

B.1.1 Moisture Content Measurements for Hanford H2 Sand-Dominated Unit B-2

B.1.2 Moisture Content Measurements for Hanford H1, Hanford H3 and Backfill Gravelly Units B-15

B.2 LABORATORY-SCALE MEASUREMENTS FOR HYDRAULIC PROPERTIES B-16

B.2.1 Properties of the Hanford H2 Sand Unit B-17

B.2.2 Properties of the Hanford H1 and H3 Gravelly Units B-27

B.2.3 Properties for the Backfill Gravelly Unit B-30

B.3 EFFECTIVE (UPSCALED) FLOW PARAMETERS FOR VADOSE ZONE B-31

B.3.1 Composite Macroscopic Relationships and Effective Parameters B-33

B.3.2 Stochastic Model for Macroscopic Anisotropy B-34

B.3.3 Macroscopic Anisotropy Relations B-36

B.4 EFFECTIVE TRANSPORT PARAMETERS B-36

B.4.1 Bulk Density and K_d B-38

B.4.2 Diffusivity B-39

B.4.3 Vadose Zone Macrodispersivities B-40

B.5 REFERENCES B-55

LIST OF FIGURES

Figure B-1. Distribution of Moisture Content Measurements Collected in and around Waste Management Area C (a) Plan View with All Moisture Content Data, (b) Plan View with All Moisture Content Data Inside the Single-Shell Tank Footprint, (c) Plan View with All Moisture Content Data Outside the Single-Shell Tank Footprint and (d) a Side View Looking Northwest. B-3

Figure B-2a. Waste Management Area C Moisture Content Histogram for All H2 Data (Includes the Data from Both Inside and Outside of the Single-Shell Tank Footprint). B-4

Figure B-2b. Waste Management Area C Moisture Content Histogram for H2 Data Within the Single-Shell Tank Footprint. B-5

Figure B-2c. Waste Management Area C Moisture Content Histogram for H2 Data Outside of the Single-Shell Tank Footprint. B-6

Figure B-3. Location of Sisson and Lu Site, Integrated Disposal Facility and Selected Boreholes in 200 Area. B-7

Figure B-4. (a) Pre- and (b) Post-Injection Moisture Plumes for the Field Injection Experiment in the 200 East Area. B-8

Figure B-5. Borehole Location Map for Waste Management Area C. B-9

Figure B-6a. Borehole C4297 Lithology and Gravimetric Moisture Content Measurements (the shaded areas in light blue and gray are regions of increased moisture). B-10

Figure B-6b. Borehole 299-E27-22 Lithology and Gravimetric Moisture Content Measurements (the shaded areas in light blue and gray are regions of increased moisture). B-11

Figure B-7a. Matric Potentials Measured by Filter Paper Technique on Core Samples from Borehole C4297. ..... B-13

Figure B-7b. Matric Potentials Measured by Filter Paper Technique on Core Samples from Borehole 299-E27-22. ..... B-14

Figure B-8a. Comparison of Gravimetric Moisture Content Measurements for Boreholes C4297 and 299-E27-22. ..... B-18

Figure B-8b. Comparison of Soil Moisture Tension Measurements for Boreholes C4297 and 299-E27-22. ..... B-19

Figure B-9a. Waste Management Area C Moisture Content Histogram for All H1 Data (Includes the Data from Both Inside and Outside of the Single-Shell Tank Footprint). B-20

Figure B-9b. Waste Management Area C Moisture Content Histogram for H1 Data Within the Single-Shell Tank Footprint. B-20

Figure B-9c. Waste Management Area C Moisture Content Histogram for H1 Data Outside of the Single-Shell Tank Footprint. B-21

Figure B-10a. Waste Management Area C Moisture Content Histogram for All Backfill Data (Includes the Data from Both Inside and Outside of the Single-Shell Tank Footprint). B-21

Figure B-10b. Waste Management Area C Moisture Content Histogram for Backfill Data Inside of the Single-Shell Tank Footprint. B-22

Figure B-10c. Waste Management Area C Moisture Content Histogram for Backfill Data Outside the Single-Shell Tank Footprint. B-23

Figure B-11. Waste Management Area C Hanford H2 Sand-Dominated Core. B-24

Figure B-12. Moisture Retention Data for H2 Unit (44 Samples). B-28

Figure B-13. Unsaturated Hydraulic Conductivity Data for H2 Unit (44 Samples). B-29

Figure B-14. Comparison of Simulated (Blue) and Observed (Circle) Moisture Content for Hanford H2 Sand-Dominated Unit. B-30

Figure B-15. Moisture Retention Curves for Various Hydrostratigraphic Units and Selected Properties for Alternative Geologic Model II. B-32

Figure B-16. Unsaturated Hydraulic Conductivity Curves for Various Hydrostratigraphic Units and Selected Properties for Alternative Geologic Model II. B-33

Figure B-17. Unsaturated Hydraulic Conductivity Measurements for Sand-Dominated and Gravel-Dominated Samples. B-34

Figure B-18. Moisture Retention Data for H1 and H3 Units (17 Samples). B-38

Figure B-19. Unsaturated Hydraulic Conductivity Data for H1 and H3 Units (17 Samples). B-39

Figure B-20. Moisture Retention Data for Backfill Unit (10 Samples). B-42

Figure B-21. Unsaturated Hydraulic Conductivity Data for Backfill Units (10 Samples). B-43

Figure B-22. Experimental (Triangles) and Fitted Theoretical (Squares) Variogram for Saturated Hydraulic Conductivity (LnK_s). B-44

Figure B-23. Calculated Macroscopic Anisotropy as a Function of Mean Matric Potential for the H2 Sand-Dominated Unit..... B-45

Figure B-24. Calculated Macroscopic Anisotropy as a Function of Mean Matric Potential for the H1 and H3 Gravelly Units. B-45

Figure B-25. Calculated Macroscopic Anisotropy as a Function of Mean Matric Potential for Backfill Gravelly Unit..... B-46

Figure B-26. (a) Ks, (b) α, and (c) n Random Distribution for a Single Realization. B-47

Figure B-27. Simulated Concentration Distribution for a Single Realization at (a) 400 days, (b) 700 days, and (c) 1,000 days and (d) the Averaged Concentration Profile at Those Times for Flow Perpendicular to Bedding for a Mean Pressure Head (H) of -1 m. B-48

Figure B-28. Simulated Concentration Distribution for a Single Realization at (a) 400 days, (b) 700 days, and (c) 1,000 days and (d) the Averaged Concentration Profile at Those Times for Flow Parallel to Bedding for a Mean Pressure Head (H) of -1 m. B-50

Figure B-29. Longitudinal Laboratory- and Field-Scale Dispersivities in Unsaturated Media as a Function of Overall Problem Scale. B-54

LIST OF TABLES

Table B-1. Summary Statistics for Waste Management Area C Moisture Content (% Volume) Database. B-4

Table B-2. Mean Moisture and Matric Potentials for Borehole Samples Inside and Outside of Waste Management Area C. B-15

Table B-3. van Genuchten Parameters (Based on the Multistep Method) and Saturated Hydraulic Conductivity Data for 44 Integrated Disposal Facility Borehole Samples from the H2 Sandy Sequence. B-25

Table B-4. Wet Sieve Particle Size Distribution for Borehole 299-E27-22 Sediments. B-27

Table B-5. van Genuchten Parameters, Fitted Saturated Hydraulic Conductivity, and Measured Bulk Density Data for H1/H3 Units (17 Samples). B-37

Table B-6. van Genuchten Parameters, Fitted Saturated Hydraulic Conductivity, and Measured Bulk Density Data for Backfill Unit (10 Samples). B-41

Table B-7. Composite van Genuchten-Mualem Parameters for Waste Management Area C Hydrostratigraphic Units. B-43

Table B-8. Simulated Average Tension Ranges for Polmann Anisotropy Model. B-44

Table B-9. Variable, Macroscopic Anisotropy Parameter Estimates for Various Waste Management Area C Units. B-44

Table B-10. Effective Bulk Density (g/cm^3) Estimates for Waste Management Area C Hydrostratigraphic Units. B-46

Table B-11. Longitudinal Macrodispersivity Estimates (cm). B-55

LIST OF TERMS

Abbreviations and Acronyms

ACM-I/ACM1	Alternative Geologic Model I
ACM-II/ACM2	Alternative Geologic Model II
EHM	equivalent homogeneous medium
ERDF	Environmental Restoration Disposal Facility
HSU	hydrostratigraphic unit
IDF	Integrated Disposal Facility
MC	Monte Carlo
MPa	megapascal
PA	performance assessment
RCRA	Resource Conservation and Recovery Act of 1976
RETC	RETention Curve
S&L	Sisson and Lu
SST	single-shell tank
WMA	Waste Management Area

APPENDIX B

BASIS FOR DEVELOPMENT OF VADOSE ZONE HYDRAULIC PROPERTIES AT WASTE MANAGEMENT AREA C

This appendix provides a description of the basis for the selection of hydraulic properties for hydrostratigraphic units (HSUs) identified at Waste Management Area (WMA) C. No WMA C site-specific data are available that can be used to directly develop estimates of hydraulic properties needed for the performance assessment (PA). As a result, a process has been developed for identifying surrogate hydraulic properties based on samples collected at other sites within the 200 Areas that are considered to be representative of sediments characteristic of the major HSUs identified at WMA C. The selected properties were then used to simulate a WMA C vadose zone flow field and the simulation results were cross-checked against field moisture contents for different WMA C units. This step allowed an updating of the properties by incorporating data sets developed from data collected at other nearby sites within the 200 Areas that are consistent with WMA C field data.

The following information is included in this Appendix:

- WMA C moisture content database, its consistency with nearby field data, and a summary of available data on 241-C Tank Farm (C Farm) soil-water matric potential and their impact on the selection of moisture characteristic data for PA modeling (see Section B.1)

- Evaluation of laboratory measurements for vadose zone soil moisture retention, saturated and unsaturated hydraulic conductivity for samples in the vicinity of C Farm and 200 Areas (see Section B.2 below) as the basis for the selection of hydraulic properties for the major HSUs identified at WMA C (see Section B.2)

- Comparison of observed and simulated moisture content using selected hydraulic properties (see Section B.2.1.1)

- Moisture characteristic curves for major HSUs identified for Alternative Geologic Models I and II (see Section B.2.1.2)

- Effective (upscaled) moisture retention, saturated and unsaturated hydraulic conductivity, bulk density, diffusivity, and macrodispersivity estimates for various strata (see Sections B.3 and B.4).

B.1 MOISTURE CONTENT MEASUREMENTS AT WASTE MANAGEMENT AREA C

As part of WMA C site characterization, an extensive database of moisture content information is available for various HSUs. The moisture content database was developed as part of a direct push campaign conducted at WMA C in 2008, and understood as being long after the occurrence

of past leaks and discharges at the farm. A summary of these measurements for the WMA C area and associated statistics presented in this Appendix is provided in RPP-CALC-60450, "Process for Determining the Volumetric Moisture Content for the Vadose Zone Geologic Units Underlying Waste Management Area."

The spatial distribution of all moisture measurements collected in and around WMA C is shown in Figure B-1(a); the database includes moisture content data collected both within the footprint of the single-shell tanks (SSTs) (i.e., where the backfill is thickest) [Figure B-1(b)] and outside this area (where the backfill is thin or non-existent) [Figure B-1(c)]. The green line on Figure B-1(b) and (c) reflects the approximate demarcation of areas inside and outside of the SST footprint. In each of the four plots on Figure B-1, the size of the circles depicted at each borehole is indicative of the magnitude of moisture content. The larger-diameter circles (higher moisture content) are more prevalent in the shallower units and outside the farm. Figure B-1(d) is a perspective view looking north-northwest, showing both the vertical direct pushes, dry wells, groundwater well, characterization borehole, and slant direct pushes.

A summary of the statistics of the moisture content measurements by major HSUs is provided in Table B-1. Overall, the moisture content data show considerable variability: the range varies from a low of 0.11 (% volume) for backfill to as high as 30.64 (% volume) for H1 unit (Table B-1).

B.1.1 Moisture Content Measurements for Hanford H2 Sand-Dominated Unit

The Hanford H2 (sand-dominated) unit is the dominant unit at WMA C in terms of vadose zone thickness. The largest number of the moisture content measurements is associated with the Hanford H2 unit (Table B-1).

Figure B-1(a) and (b) show the location of where moisture content measurements were made in the Hanford H2 unit relative to the green line that marks the boundary of where the backfill is thickest (i.e., within the footprint of the SSTs). Figure B-2a shows the histogram for H2 moisture data for all measurements inside and outside of the SST footprint. Figure B-2b shows the histogram for measurements inside the SST footprint, whereas Figure B-2c shows the histogram for measurements outside the SST footprint. While the average for all H2 measurements (inside as well as outside of SST footprint) is ~5.15 (% volume) (Figure B-2a), inside the tank farm, the average is 5.09 (% volume), with the range varying from ~1.86% to 19.9% and a variance of 3.03% (Figure B-2b). Outside the SST footprint, the average is 5.17 (% volume), with the range varying from ~1.06% to 26.32% and a variance of 3.39% (Figure B-2c). The statistics suggest that the averages for moisture content measurements inside and outside the SST footprint are not significantly different. The variance for measurements inside the SST footprint is lower, compared to variance for measurements outside the SST footprint. This may simply be a reflection of a smaller sample size (a count of 5,143 inside of the SST footprint versus a count of 15,733 outside of the SST footprint), or may reflect differences in media heterogeneities within the H2 unit.

Figure B-1. Distribution of Moisture Content Measurements Collected in and around Waste Management Area C (a) Plan View with All Moisture Content Data, (b) Plan View with All Moisture Content Data Inside the Single-Shell Tank Footprint, (c) Plan View with All Moisture Content Data Outside the Single-Shell Tank Footprint and (d) a Side View Looking Northwest.

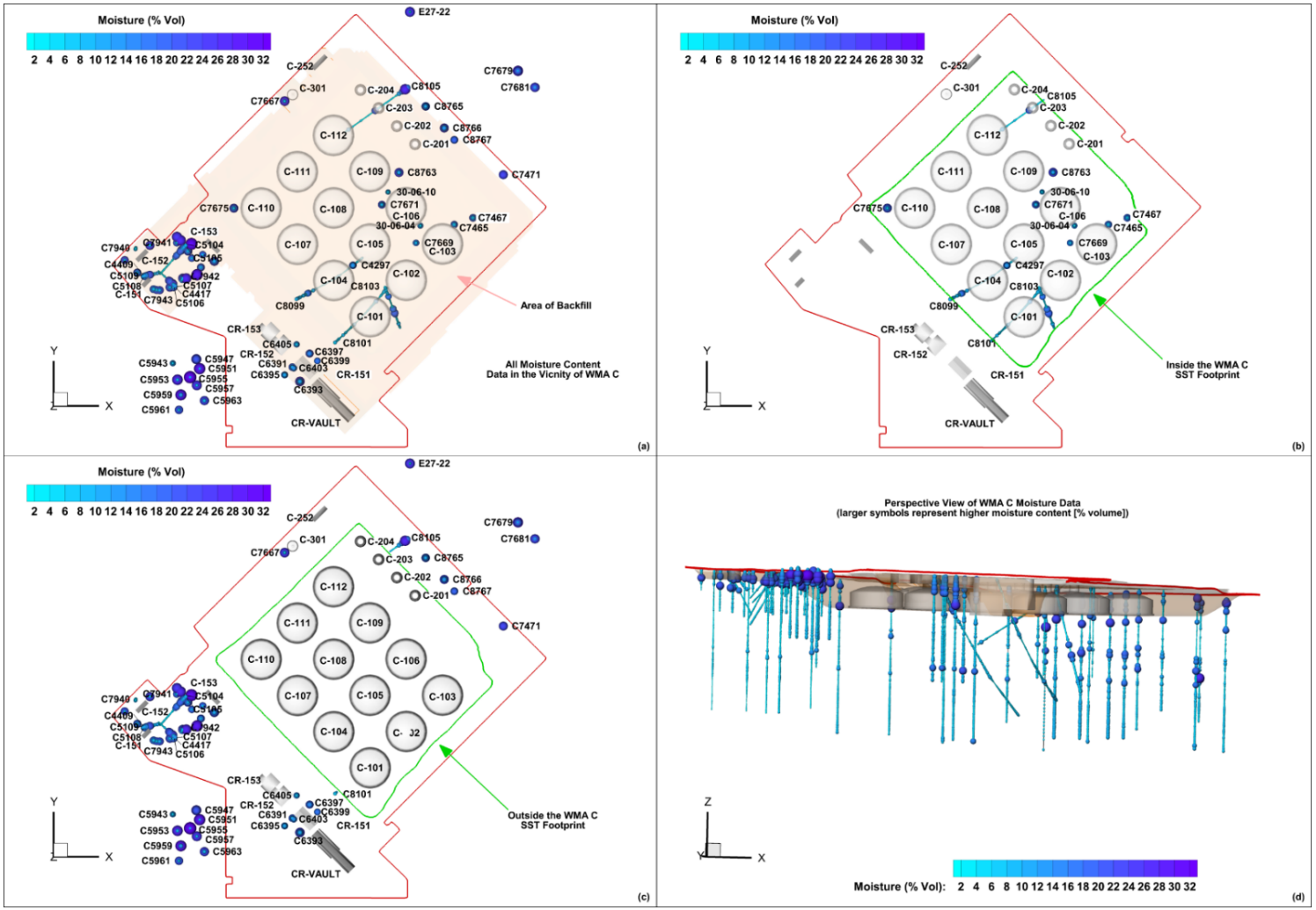

SST = single-shell tank WMA = waste management area

Table B-1. Summary Statistics for Waste Management Area C Moisture Content (% Volume) Database.

Unit	Count	Minimum	Maximum	Average
Backfill	4,052	0.11	30.61	8.09
H1	7,977	0.13	30.64	5.88
H2	20,876	1.06	26.32	5.15
H3	7	5.54	7.09	6.18
All Units	32,912	0.11	30.64	5.69

Figure B-2a. Waste Management Area C Moisture Content Histogram for All H2 Data (Includes the Data from Both Inside and Outside of the Single-Shell Tank Footprint).

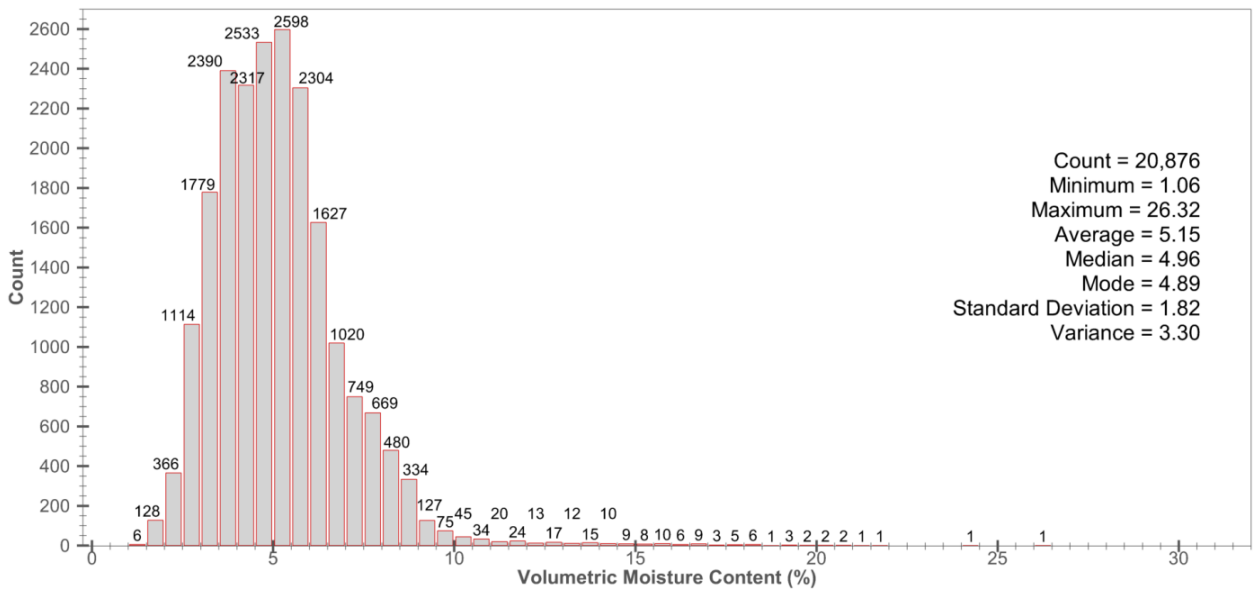

B.1.1.1 Comparison with Sisson and Lu Site Moisture Content Measurements. In this section of the Appendix, the moisture content measurements for the Hanford H2 unit at WMA C are compared to, and checked for consistency against, another extensive set of moisture content measurements collected at the nearby Sisson and Lu (S&L) field injection site in 200 East Area (Figure B-3). Unlike WMA C, soil hydraulic properties data are available for the S&L site (PNNL-14284, "Laboratory Measurements of the Unsaturated Hydraulic Properties at the Vadose Zone Transport Field Study Site"; "Evaluation of van Genuchten-Mualem relationships to estimate unsaturated hydraulic conductivity at low water contents" [Khaleel et al. 1995]). Furthermore, unlike WMA C, moisture content measurements are available before and after application of anthropogenic recharge at the S&L site. Thus, the S&L site serves as a backdrop for WMA C moisture measurements for Hanford H2 unit. Details of the S&L site, field injections and the spatio-temporal distribution of observed moisture plume are described elsewhere ("Stochastic analysis of moisture plume dynamics of a field injection experiment"

[Ye et al. 2005]; PNNL-13795, "Vadose Zone Transport Field Study: Soil Water Content Distributions by Neutron Moderation").

Figure B-2b. Waste Management Area C Moisture Content Histogram for H2 Data Within the Single-Shell Tank Footprint.

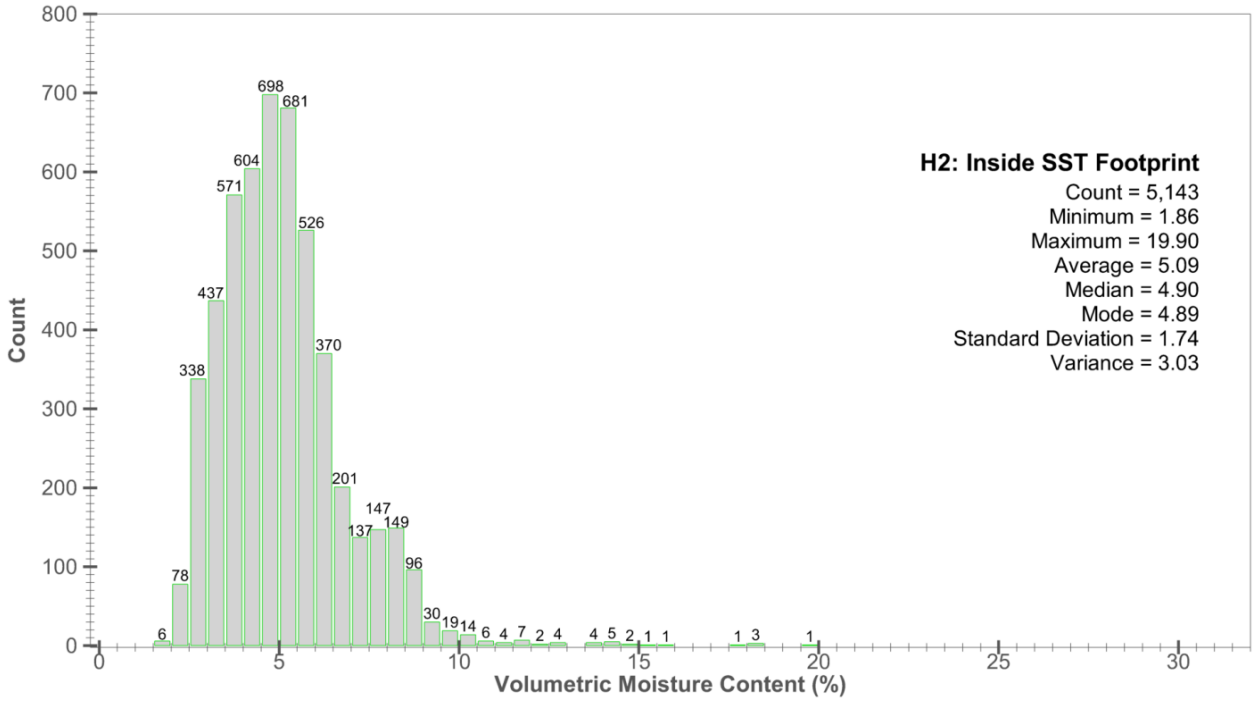

SST = single-shell tank

Figure B-4 shows the composite set of all moisture content measurements collected before and after injection at the S&L site. The S&L site initial moisture content data were collected on May 5, 2000 [Figure B-4 (a)] and post-injection and post-redistribution data were collected about two months later [Figure B-4(b)]. These measurements are all within an HSU that would correlate with the Hanford H2 sand unit identified at WMA C. The S&L moisture content profiles are in general agreement with the known stratigraphic cross-section (Ye et al. 2005), with larger moisture content values being associated with the fine-textured sediments and smaller values being associated with the coarse-textured sediments. In addition to the 2000 S&L field experiment, data also exist on the 1980 field experiment conducted at the same site (RHO-ST-46P, "Field Calibration of Computer Models for Application to Buried Liquid Discharges: A Status Report"). Although not shown here, the 1980 moisture content measurements are nearly identical to the 2000 moisture content measurements. The consistency in the moisture content profiles over the 20-year time interval suggests that, in the absence of anthropogenic recharge, the moisture content distribution is under a state of natural equilibrium with meteoric recharge. The S&L moisture content profiles (Figure B-4) clearly illustrate the impact of media heterogeneities and natural capillary breaks ("Simulating field-scale moisture flow using a combined power-averaging and tensorial connectivity-tortuosity approach" [Zhang and Khaleel 2010]; Ye et al. 2005). During and following field injections, the capillary breaks created due to textural discontinuities allow flow to occur laterally until the pressure head in the fine layer is sufficient to overcome the entry pressure head of the underlying coarse layer.

Nonetheless, as indicated in Figure B-4, the pre- and post-injection moisture plumes are essentially confined within three layers (i.e., two fine-textured layers and a coarse-textured layer that is sandwiched in between the two fine-textured layers).

Figure B-2c. Waste Management Area C Moisture Content Histogram for H2 Data Outside of the Single-Shell Tank Footprint.

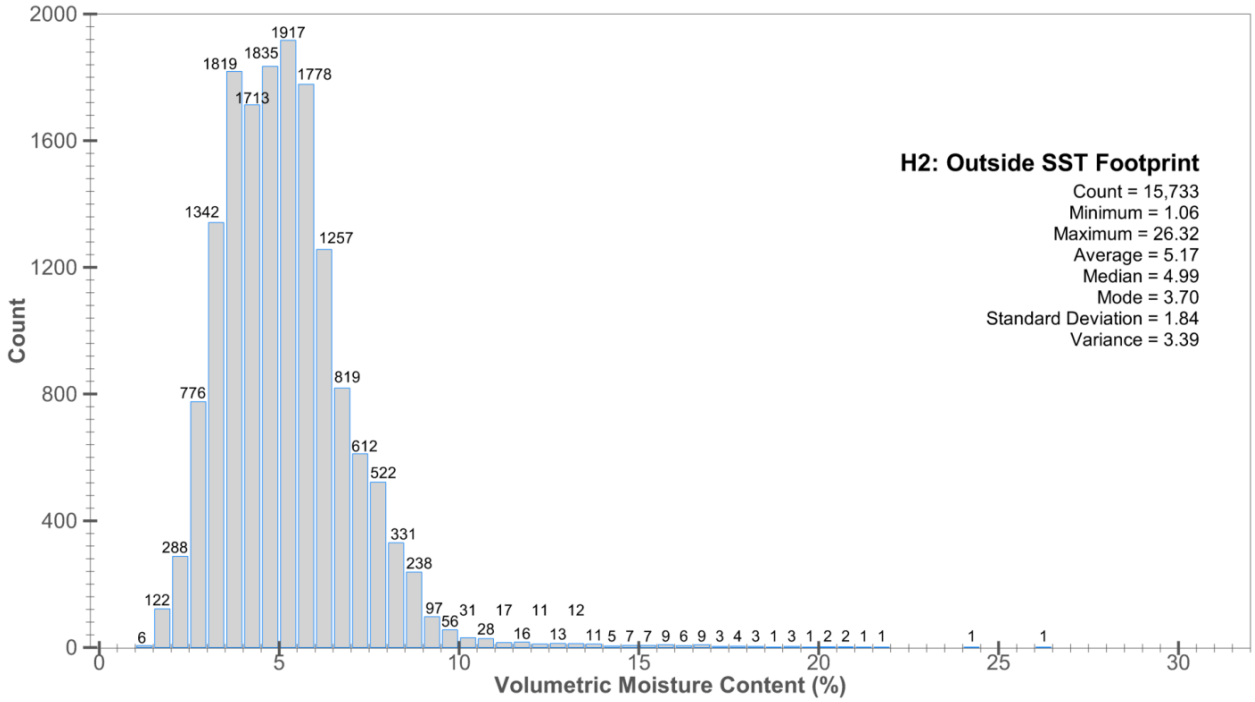

SST = single-shell tank

At WMA C, the volumetric moisture content for the Hanford H2 unit inside the tank farm (see Figure B-2c) ranges from 1.86 to 19.90 with a mean of 5.09 (% volume), whereas at the S&L site the volumetric moisture content ranges from 4.60 to 24.50 with a mean of 8.92 (% volume) (Ye at al. 2005). Even though the natural recharge at the two sites are not identical and the sediment textural data are different, the WMA C H2 unit moisture contents compare well and show similar trends relative to variability with field-measured H2 moisture contents at the nearby S&L site (i.e., higher moisture contents for fine-textured units and lower moisture contents for coarse-textured units as illustrated in Figure B-4). However, the S&L mean moisture content is much higher than the WMA C (inside the tank farm) mean value. This is consistent with the ubiquitous occurrence of fine-textured units at the S&L site (Ye at al. 2005), and the apparent non-occurrence of such units at WMA C. These data show that the field measurements at both WMA C and S&L sites are significantly impacted by small-scale heterogeneities. However, if the moisture content data is used as a surrogate for characterizing media heterogeneities, the higher mean (~8.92 [% volume]) moisture values at the S&L site suggest that the Hanford H2 unit is much coarser at WMA C than at the nearby S&L site. Therefore, while the comparison with the S&L site generally corroborates the understanding of the WMA C H2 unit, the S&L site is not a useful surrogate for development of hydraulic properties for the Hanford H2 sand unit at WMA C. Furthermore, the comparison demonstrates that substantial variability can occur in the H2 unit over fairly short spatial distances.

Figure B-3. Location of Sisson and Lu Site, Integrated Disposal Facility and Selected Boreholes in 200 Area.

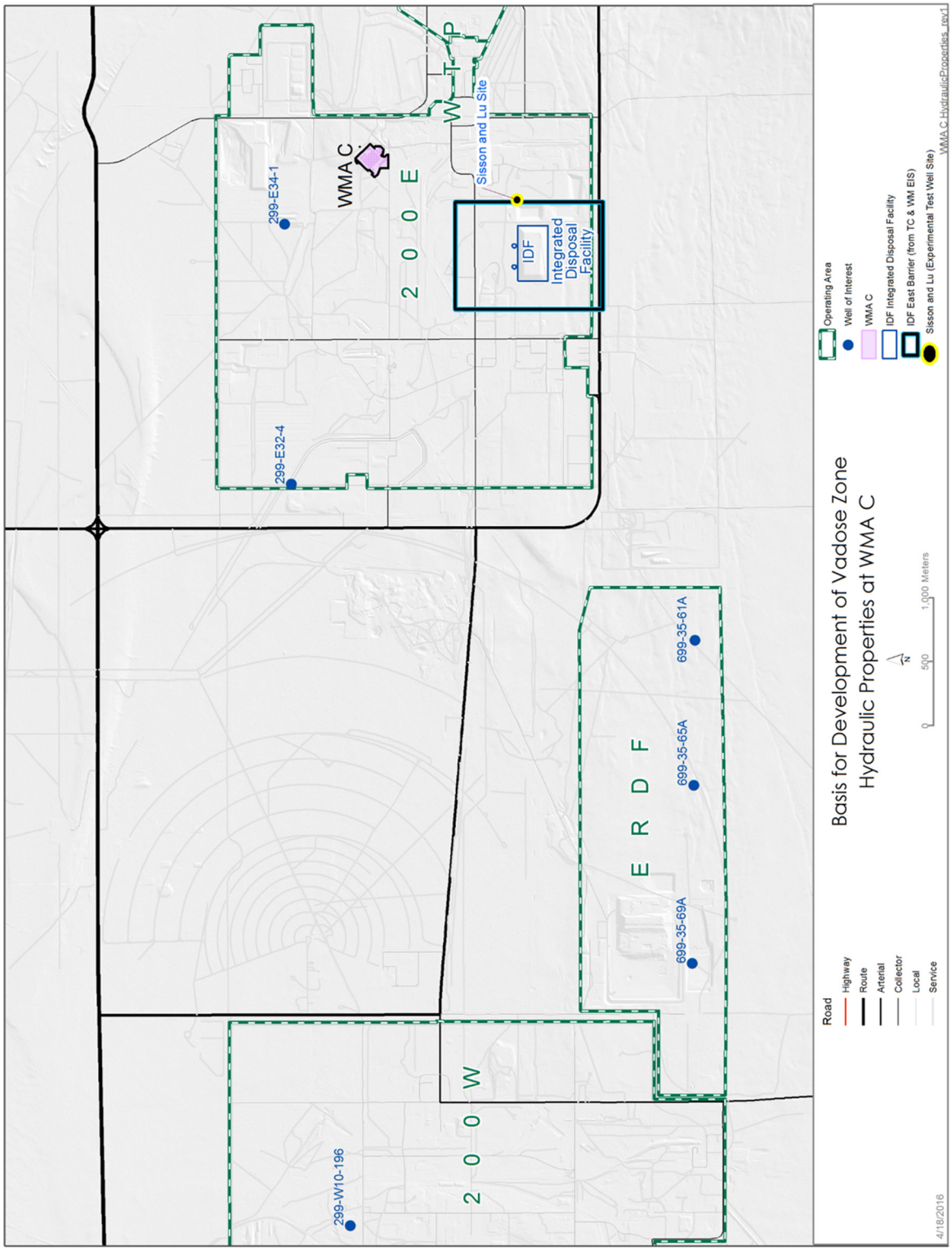

ERDF = Environmental Restoration Disposal Facility WMA = Waste Management Area
TC & WM EIS = Tank Closure and Waste Management Environmental Impact Statement
WTP = Waste Treatment Plant

Figure B-4. (a) Pre- and (b) Post-Injection Moisture Plumes for the Field Injection Experiment in the 200 East Area.

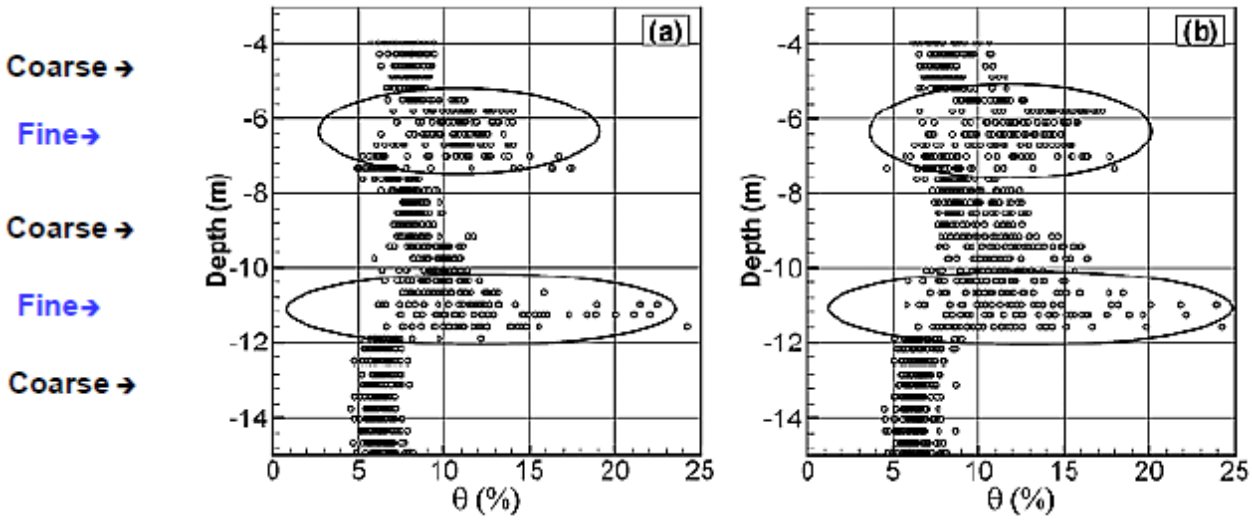

Profiles of volumetric moisture content (%) measured on (a) May 5, 2000, and (b) July 31, 2000. The figures illustrate the fact that, in the absence of anthropogenic recharge, moisture contents at the field site are in equilibrium with natural recharge at the site.

Reference: "Stochastic analysis of moisture plume dynamics of a field injection experiment" (Ye et al. 2005).

B.1.1.2 Soil-Moisture and Matric Potential Data for Borehole Samples Inside and Outside the Tank Farm. In addition to the moisture content measurements developed from neutron logging of direct push boreholes presented in Section B.1, additional moisture content data as well as matric potential information are available for two individual boreholes. Boreholes C4297 (inside the tank farm near tank C-105) and 299-E27-22 (Resource Conservation and Recovery Act of 1976 [RCRA] borehole just outside the tank farm) (Figure B-5) provide moisture content (gravimetric) measurements as well as matric potential (using filter paper) data (PNNL-15503, "Characterization of Vadose Zone Sediments Below the C Tank Farm: Borehole C4297 and RCRA Borehole 299-E27-22"). The two sets of data on moisture content and matric potential were collected to evaluate differences between one being outside the farm (a lower expected average moisture content and a more negative matric potential) and the other inside the farm (a higher expected average moisture content and a less negative matric potential indicative of a draining soil profile). However, as stated earlier (Section B.1.1), the averages for moisture content measurements inside and outside the SST footprint were not significantly different.

The moisture content profiles for the two boreholes are shown in Figures B-6a and B-6b, respectively. Zones with relatively high moisture are illustrated via a light blue bar immediately to the right of the lithologic log in these diagrams. The moisture content and lithological data are generally consistent; the elevated levels of moisture in the vadose zone at C Farm are associated with fine-grained lenses of fine sand and/or silt. Most of these occur within the Hanford formation H2 unit, although there is also one at the base of the backfill in borehole C4297, and within the H1 unit in RCRA borehole 299-E27-22, which is consistent with the concentration of moisture at an abrupt, large contrast in grain size. This is illustrated at the 82-ft depth in RCRA borehole 299-E27-22 (Figure B-6b), where there is a sharp contact between gravelly sand overlying fine to coarse sand (PNNL-15503).

Figure B-5. Borehole Location Map for Waste Management Area C.

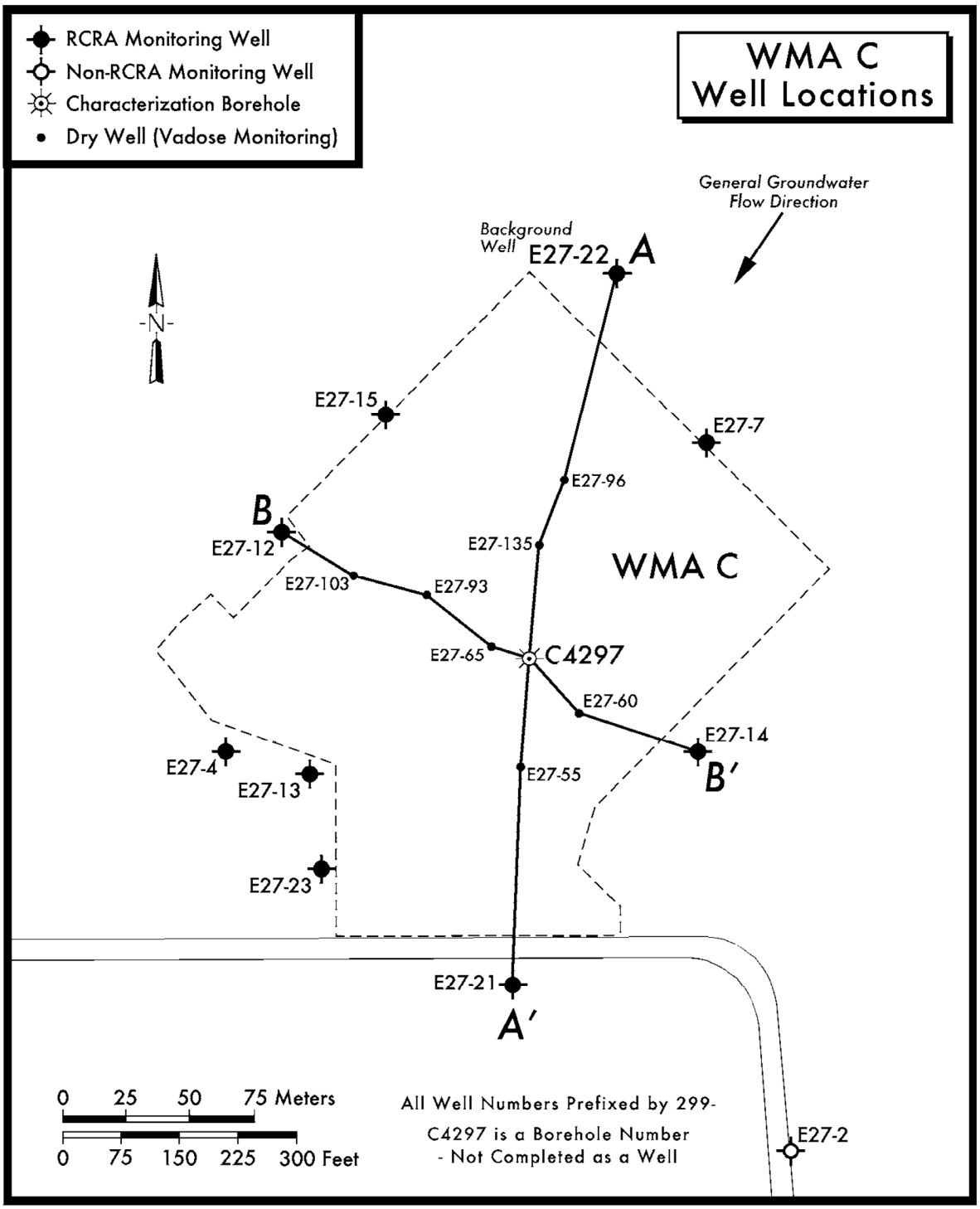

RCRA = Resource Conservation and Recovery Act of 1976 WMA = Waste Management Area

Source: PNNL-15503, "Characterization of Vadose Zone Sediments Below the C Tank Farm: Borehole C4297 and RCRA Borehole 299-E27-22."

Note: Cross-sections AA' and BB' are Figures 2.4 and 2.5, respectively, in PNNL-15503.

Figure B-6a. Borehole C4297 Lithology and Gravimetric Moisture Content Measurements (the shaded areas in light blue and gray are regions of increased moisture).

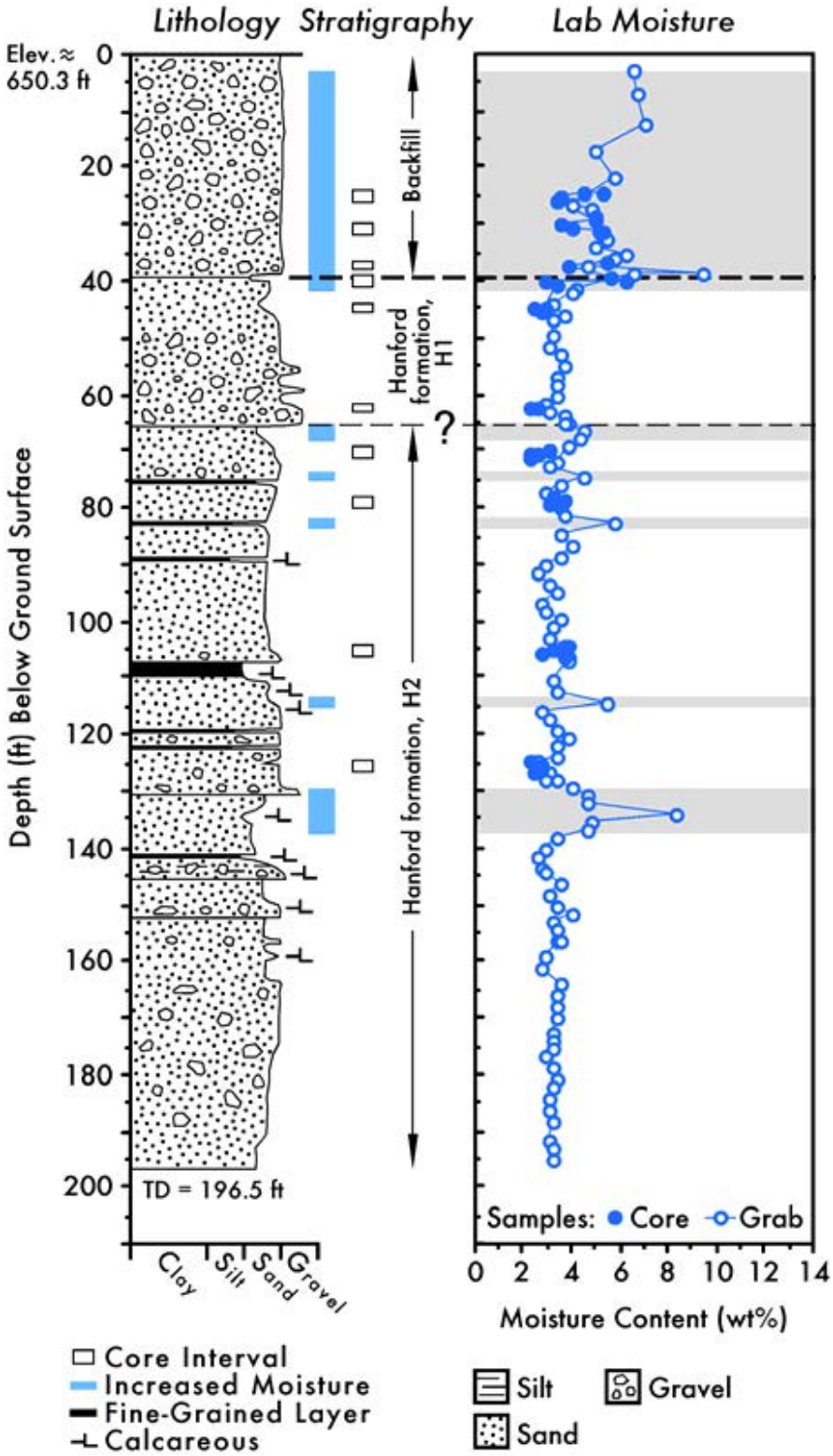

Reference: PNNL-15503, "Characterization of Vadose Zone Sediments Below the C Tank Farm: Borehole C4297 and RCRA Borehole 299-E27-22."

Figure B-6b. Borehole 299-E27-22 Lithology and Gravimetric Moisture Content Measurements (the shaded areas in light blue and gray are regions of increased moisture).

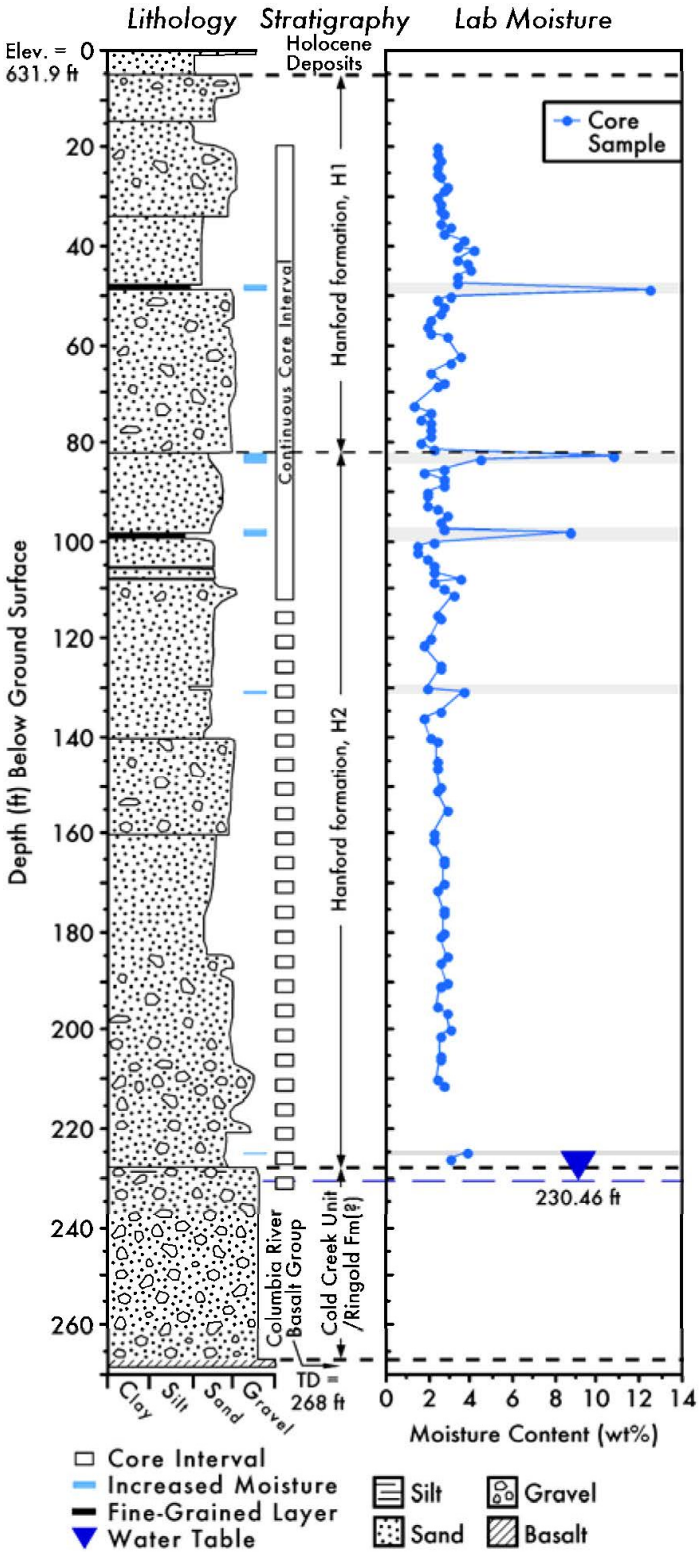

Reference: PNNL-15503, "Characterization of Vadose Zone Sediments Below the C Tank Farm: Borehole C4297 and RCRA Borehole 299-E27-22."

The distribution of moisture in the vadose zone at these two borehole locations was developed by gravimetric moisture measured directly from core samples in the laboratory (Figures B-6a and B-6b). Moisture data based on grab sampling is only available for one of the two boreholes (C4297), and these data generally corroborate the laboratory-measured moisture content measurements (Figure B-6a). However, several pronounced spikes that appear on the laboratory-moisture plot do not appear in the moisture log. This is likely the result of a number of thin (a few inches or less) fine-grained layers that were preferentially sampled during core processing. These thin layers are not visible on the geophysical log because the neutron flux is averaged over a larger area beyond the limits of the fine-grained layer, including adjacent relatively dry layers. Thus, the resulting field logging signal is dampened. In general, the neutron-moisture log appears to accurately reflect the relative bulk moisture content, and can confidently be used as a substitute to estimate bulk moisture conditions when core samples are unavailable. However, most thin (<6 in.) moist zones go undetected on neutron-moisture logs (PNNL-15503).

While the moisture content profiles provide useful information, the moisture profiles, by themselves, cannot be used to describe the soil-water energy status and the vadose zone flow dynamics. Data on soil-moisture matric potentials are needed to establish the energy level and the subsequent flow status. A simple measure of direction of flow can be approximated by plotting field-measured matric potentials versus the height above the water table. The hydraulic potential at any given elevation is given by the sum of matric potential and gravitational potential and the flux is calculated from the Darcy-Buckingham law (Soil Physics [Jury and Horton 2004]).

Figures B-7a and B-7b illustrate the respective filter paper-based matric potential measurements, as a function of depth for sediment samples from the two boreholes: C4297 (inside the farm) and 299-E27-22 (outside the farm), with the potentials (MPa) shown as absolute values (PNNL-15503). With the filter paper technique, the moisture in a filter material reaches equilibrium with the surrounding environment. In both figures, the red line, labeled “theoretical value” is the theoretical line that represents the steady-state equilibrium condition. Matric potential values to the left of the theoretical line suggest a draining profile. The general trend for the data is that the measured potentials for both boreholes are consistent with those of a draining profile.

For borehole 299-E27-22 (Figure B-7b), matric potentials for three of the samples (27.0, 72.0, and 74.5 ft below ground surface) suggest very dry conditions; these appear to be erroneous because of inadvertent drying of the samples or weighing errors (PNNL-15503). The matric suction values are generally below 0.5 MPa (~5,000 cm) for the sediment profile in borehole 299-E27-22 as well as borehole C4297.

Filter paper-based soil matric potentials are point measurements, and are not consistent with the use of averaged upscaled (effective) properties (Section 6) for the large blocks used in the PA simulations. In addition, the error bar for filter paper measurements is rather large (0.1 to 0.2 MPa). Soil moisture measurements are typically more accurate than matric potential measurements, and the matric potential variability is typically larger than the soil moisture variability (PNNL-15503). Overall, however, the WMA C moisture and tension data appear to be internally consistent and represent a relatively dry moisture regime.

Figure B-7a. Matric Potentials Measured by Filter Paper Technique on Core Samples from Borehole C4297. Matric potentials are presented as absolute values.

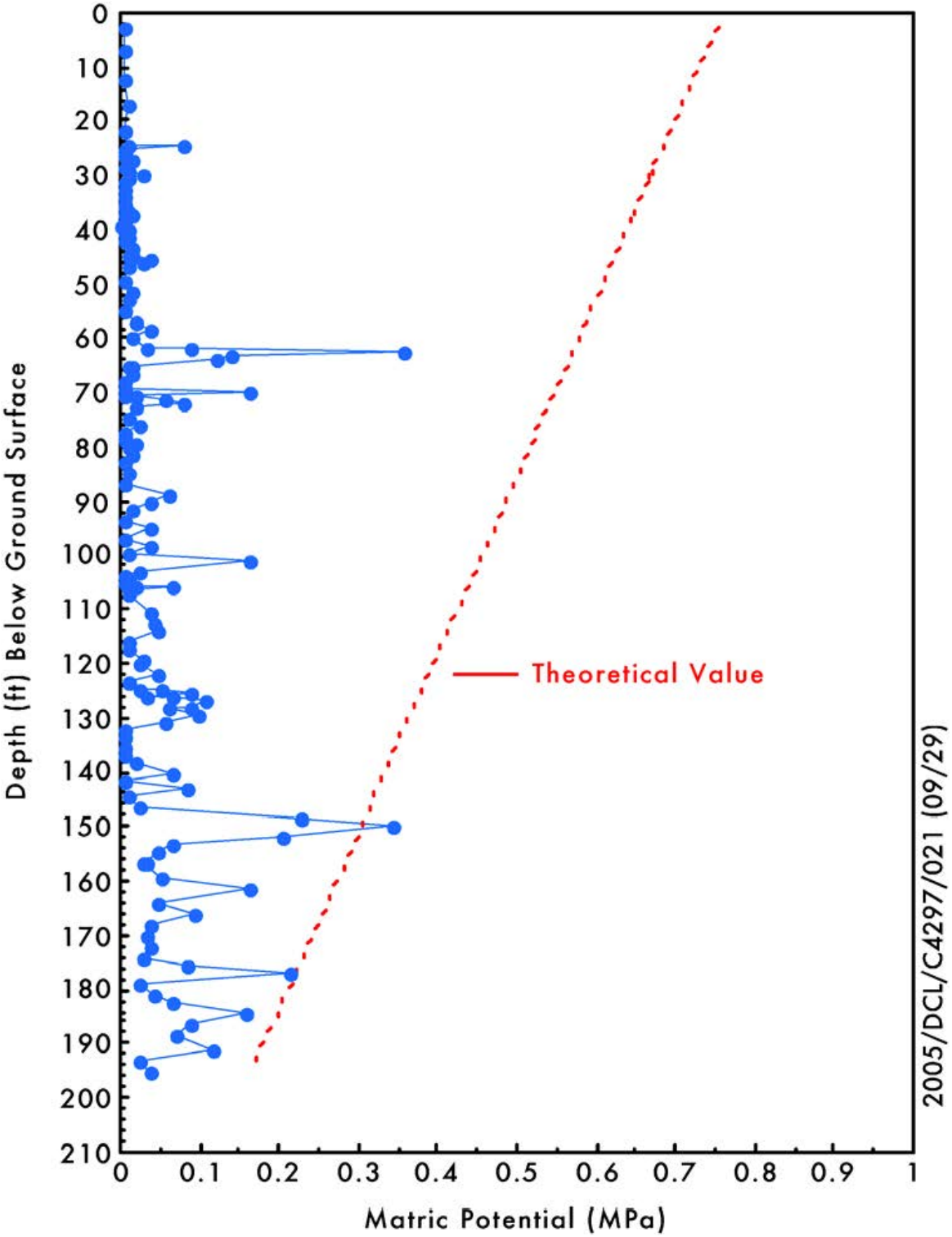

Reference: PNNL-15503, "Characterization of Vadose Zone Sediments Below the C Tank Farm: Borehole C4297 and RCRA Borehole 299-E27-22."

Figure B-7b. Matric Potentials Measured by Filter Paper Technique on Core Samples from Borehole 299-E27-22. Matric potentials are presented as absolute values.

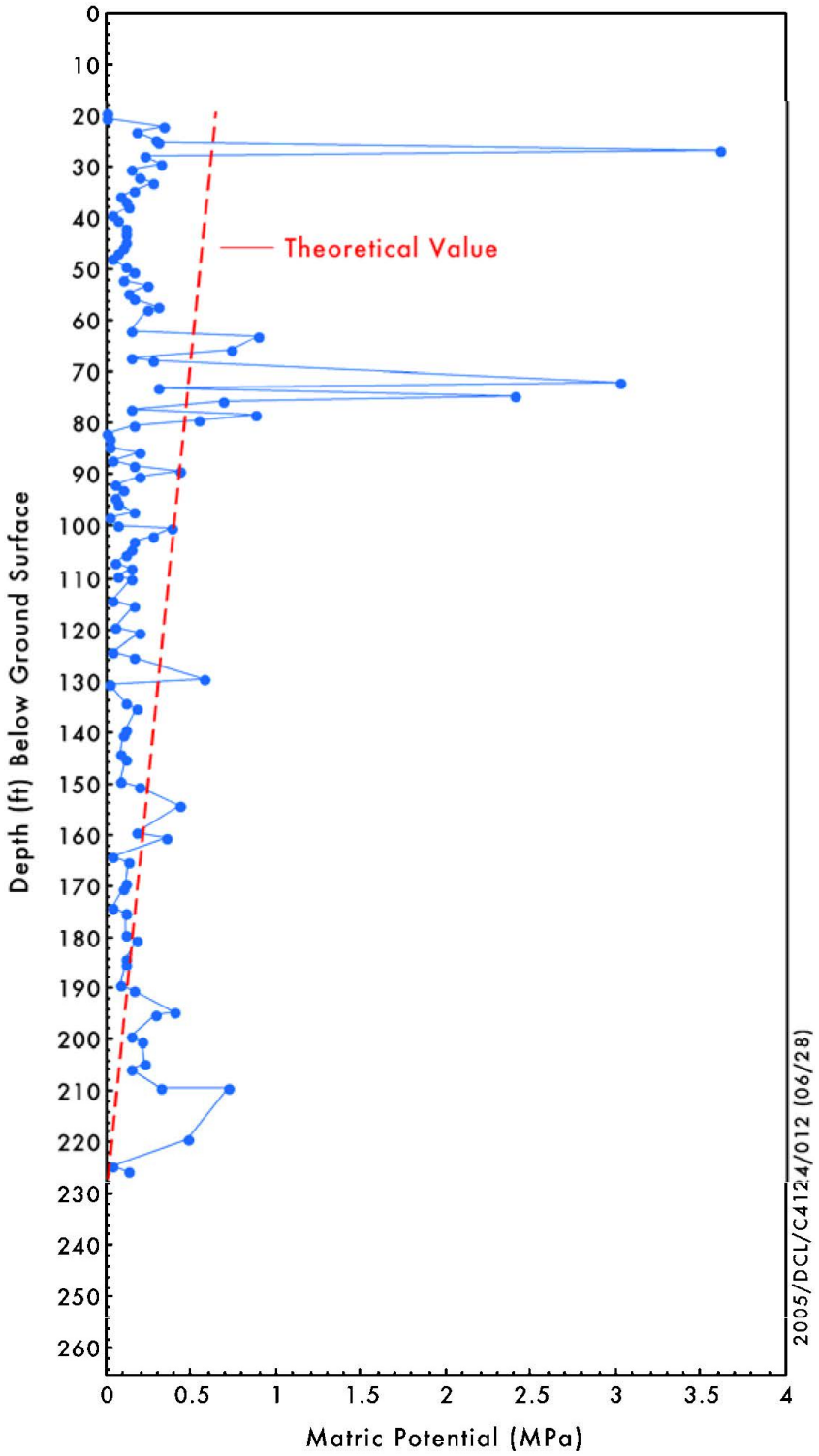

Reference: PNNL-15503, "Characterization of Vadose Zone Sediments Below the C Tank Farm: Borehole C4297 and RCRA Borehole 299-E27-22."

Table B-2 summarizes the mean moisture content and mean filter paper-based matric potential measurements for the two borehole samples. The data show a drier moisture content for measurements outside the farm compared to those inside the farm. A comparison of the moisture and matric potential profiles for the two boreholes is shown in Figures B-8a and B-8b, respectively.

Table B-2. Mean Moisture and Matric Potentials for Borehole Samples Inside and Outside of Waste Management Area C.

Borehole	C4297 (inside tank farm)	299-E27-22 (outside tank farm)
Mean moisture content (% volume)*	6.00	4.60
Mean matric potential (-cm)	498.45	1,616.43

*Gravimetric data were converted to volumetric moisture content using an assumed sediment bulk density of 1.7 g cm^{-3}.

Reference: PNNL-15503, "Characterization of Vadose Zone Sediments Below the C Tank Farm: Borehole C4297 and RCRA Borehole 299-E27-22."

As stated earlier, matric potential measurements for both boreholes suggest a draining soil profile (PNNL-15503). Intuitively, it might be postulated that the higher mean observed moisture and a less negative mean matric potential inside the farm is due to the combined effects of both natural recharge and the operational use of water during the period of past tank farm operations. However, whereas the mean moisture contents for the two borehole samples suggest a slightly higher moisture content from measurements inside the tank farm, the much more negative mean matric potential for outside borehole samples (Table B-2) could simply be a reflection of differences in moisture retention characteristics for the two datasets, albeit being of similar lithology. A comparison of the field-measured and simulated moisture contents for the sand-dominated H2 unit is provided in Section B.2.1.1.

B.1.2 Moisture Content Measurements for Hanford H1, Hanford H3 and Backfill Gravelly Units

The statistics of moisture content measurement for Hanford H1 and H3 gravelly units and backfill gravelly unit are summarized in Table B-1. As indicated in Table B-1, unlike moisture content measurements made in the H1 gravelly unit, the sample size of moisture content measurements made in the H3 gravelly unit is too small to generate any meaningful statistics.

B.1.2.1 Hanford H1 Gravelly Unit. Figure B-9a shows the histogram for all moisture content measurements made in the H1 gravelly unit inside and outside the tank farm (Figure B-2c). Figure B-9b shows the histogram for measurements inside the SST footprint, whereas Figure B-9c shows the histogram for measurements outside the SST footprint. While the average for all H1 measurements is about 5.88% on a volume basis (Figure B-9a), inside the tank farm the average is 4.24 (% volume), with the range varying from ~1.47% to 23.11% and a variance of 3.76% (Figure B-9b). Outside of the SST footprint the average is 6.41 (% volume), with the range varying from ~0.13% to 30.64% and a large variance of 15.42% (Figure B-9c). Once again, similar to H2 data and contrary to expectation, the statistics suggest a considerably higher H1 average moisture content for measurements outside the SST footprint, compared with

the average for measurements inside the SST footprint. The variance for H1 measurements outside the SST footprint is higher, compared to variance for measurements inside the SST footprint. This might simply be a reflection of a smaller sample size (a count of 1,921 inside versus a count of 6,056 outside), and/or media heterogeneities that are prevalent within the H1 unit.

It is questionable as to whether the observed high moisture contents (e.g., 30.64 [% volume] for the gravel-dominated H1 unit) are reflective of the natural moisture regime. As discussed earlier, other moisture data in the nearby S&L test site suggest that, in the absence of anthropogenic recharge, the moisture profiles are typically in equilibrium with meteoric recharge. Furthermore, in the absence of anthropogenic recharge, moisture contents correlate with sediment texture (i.e., coarse-textured sediments have a lower moisture content and fine-textured sediments have a higher moisture content) (Figure B-4). Nonetheless, none of the S&L moisture content measurements for the fine-textured horizons approach as high as 30.64% (% volume); such an unusually high value for the gravel-dominated H1 unit is considered an outlier.

B.1.2.2 Backfill Gravelly Unit. In general, tank farm backfill materials consist of unstructured, poorly-sorted mixtures of gravel, sand, and silt removed during tank excavation, and then later used as fill around the tanks. Backfill materials extend to depths of ~50 ft (~15.24 m) within the tank farms. Most or all of the recent deposits of eolian sand and silt material found elsewhere across the Hanford Site have been removed and replaced with backfill in the immediate vicinity of the tank farms.

For the backfill unit, the average moisture content is 8.08 (% volume) (Table B-1), and is the highest among averages for all the units. The backfill unit also has the lowest measured moisture content of 0.11 (% volume) among all units. The maximum measured moisture content for backfill is 30.61 (% volume).

Figure B-10a shows the histogram for all moisture content measurements made in the backfill gravelly unit inside and outside the tank farm (Figure B-2c). Figure B-10b shows the histogram for measurements inside the SST footprint, whereas Figure B-10c shows the histogram for measurements outside the SST footprint. While the average for all backfill measurements is ~8.09% (% volume) (Figure B-10a), inside the tank farm, the average is 6.61 (% volume), with the range varying from ~0.31% to 23.05% and a variance of 7.69% (Figure B-10b). Outside of the SST footprint, the average is considerably higher (9.30 [% volume]), with the range varying from ~0.11% to 30.61% and a large variance of 15.47% (Figure B-10c).

B.2 LABORATORY-SCALE MEASUREMENTS FOR HYDRAULIC PROPERTIES

The purpose of this section is to summarize data sources and laboratory measurements of core-scale sample properties for different HSUs; these are later upscaled for use in WMA C PA modeling (Section B.3 below). Core-scale measurements and their parameterization are described below for the following HSUs:

- Hanford H2 Sand Unit

- Hanford H1 and H3 Gravelly Units
- Backfill Gravelly Unit.

B.2.1 Properties of the Hanford H2 Sand Unit

Figure B-11 shows a representative sample of sediments associated with the Hanford H2 sand-dominated unit identified at WMA C. Because site-specific hydraulic properties data are unavailable, the available hydraulic properties database for coarse sands as well as the WMA C moisture content distribution were used to identify and characterize hydraulic properties for the Hanford H2 sand unit identified at WMA C. Soils used to characterize the WMA C Hanford H2 unit properties were similar to those shown in Figure B-11. Using moisture as a proxy, the nearby 200 East Area Integrated Disposal Facility (IDF) site (Figure B-3) coarse sand unit correlates well with the Hanford H2 sand unit identified at WMA C; the IDF coarse sands were thus used as surrogate for the WMA C H2 sands. The primary mission of RCRA-permitted IDF (Figure B-3) is disposal of low-level wastes, mixed low-level wastes, and Immobilized Low-Activity Waste (i.e., the Hanford tank waste that has undergone separations treatment to remove the bulk of the radionuclides and then solidified at the Hanford Waste Treatment and Immobilization Plant).

As part of site characterization for IDF, sediment samples were obtained in fiscal years 1998, 2001 and 2002 via a borehole drilling and sampling program. The Hanford formation sandy H2 sequence identified at the IDF site is ~200 ft (~61 m) thick and, like WMA C, is the dominant facies at the site.

The laboratory procedures used to analyze the IDF H2 borehole samples and analysis of samples from the three boreholes are described in appendices found in RPP-20621, "Far-Field Hydrology Data Package for the Integrated Disposal Facility Performance Assessment." Briefly, the multistep and steady-state methods were used to obtain moisture retention and unsaturated conductivity data. The specific details for the two methods are described in RPP-20621 appendices. Both methods were performed on the same core using the same sensor locations. In addition to cumulative outflow, the multistep method provides water content-matric potential (θ-ψ) pairs. These data were used in conjunction with a numerical inversion procedure ("Optimization of Hydraulic Functions from Transient Outflow and Soil Water Pressure Data" [Eching and Hopmans 1993]) to determine the optimal set of van Genuchten model ("A Closed-form Equation for Predicting the Hydraulic Conductivity of Unsaturated Soils" [van Genuchten 1980]) parameters (RPP-20621). The steady-state method, described in "Hydraulic Conductivity and Diffusivity: Laboratory Methods" (Klute and Dirksen 1986), provides water content-matric potential-unsaturated conductivity (θ-ψ-K) triplets; the method was primarily used as a check on the multistep method.

RPP-20621 (Tables 1 through 3) provides the van Genuchten model parameters determined using the numerical inversion procedure and data from the multistep test. The pore-size distribution parameter ℓ ("A New Model for Predicting the Hydraulic Conductivity of Unsaturated Porous Media" [Mualem 1976]) was kept fixed at 0.5. The fitted van Genuchten-Mualem parameters for the IDF H2 sandy sequence (44 samples) are reproduced in Table B-1.

Figure B-8a. Comparison of Gravimetric Moisture Content Measurements for Boreholes C4297 and 299-E27-22.

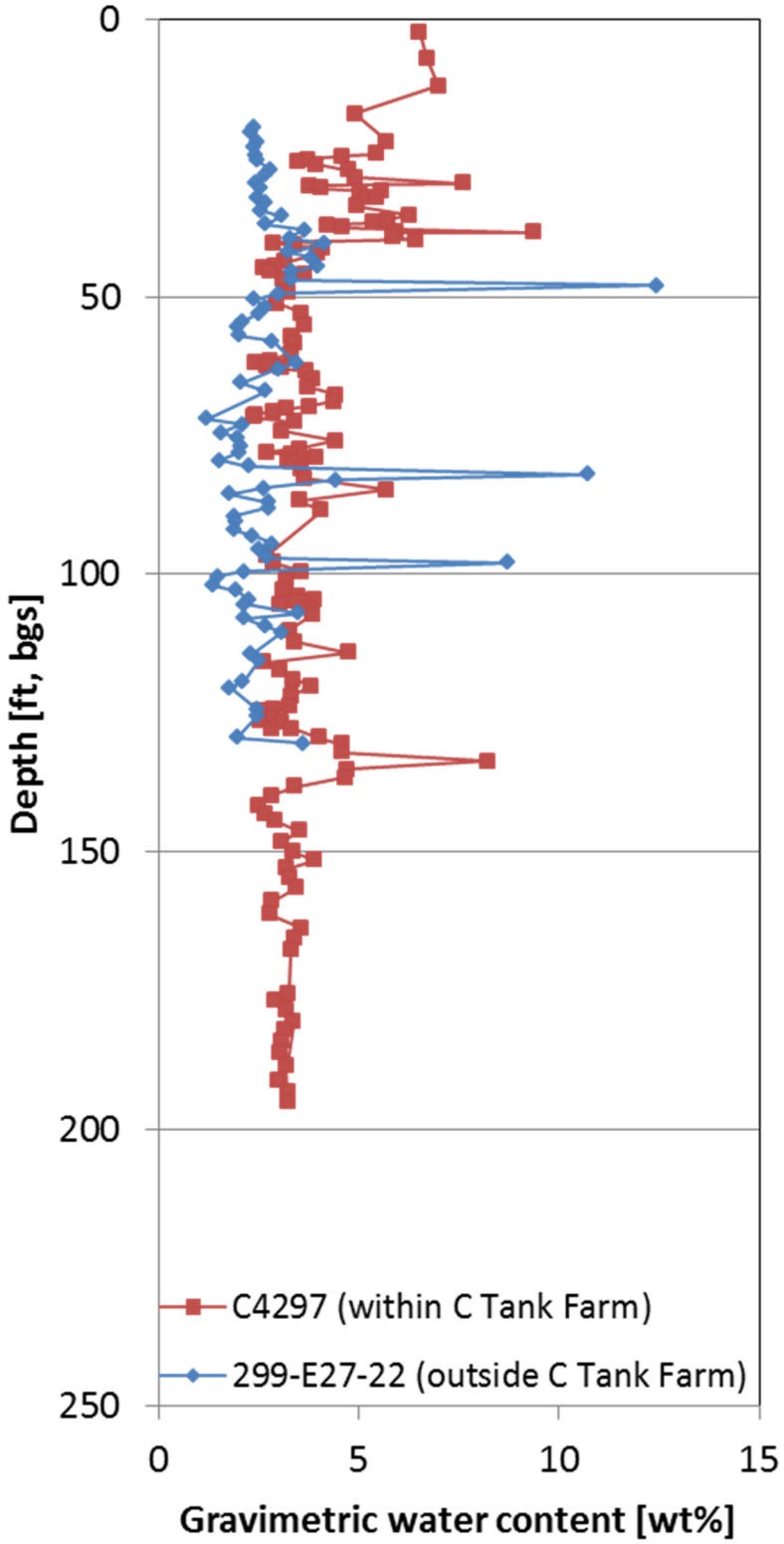

Reference: PNNL-15503, "Characterization of Vadose Zone Sediments Below the C Tank Farm: Borehole C4297 and RCRA Borehole 299-E27-22."

Figure B-8b. Comparison of Soil Moisture Tension Measurements for Boreholes C4297 and 299-E27-22.

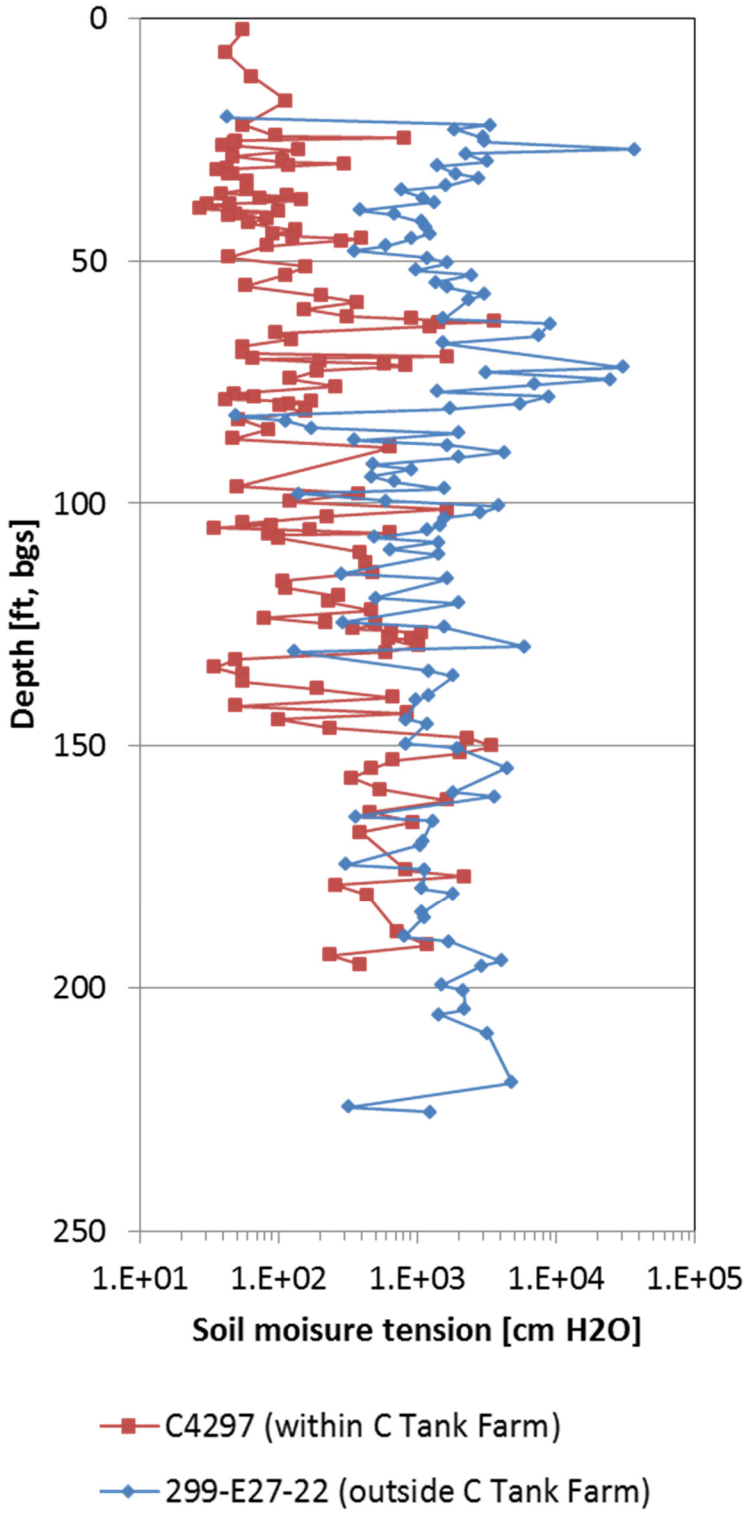

Reference: PNNL-15503, "Characterization of Vadose Zone Sediments Below the C Tank Farm: Borehole C4297 and RCRA Borehole 299-E27-22."

Figure B-9a. Waste Management Area C Moisture Content Histogram for All H1 Data (Includes the Data from Both Inside and Outside of the Single-Shell Tank Footprint).

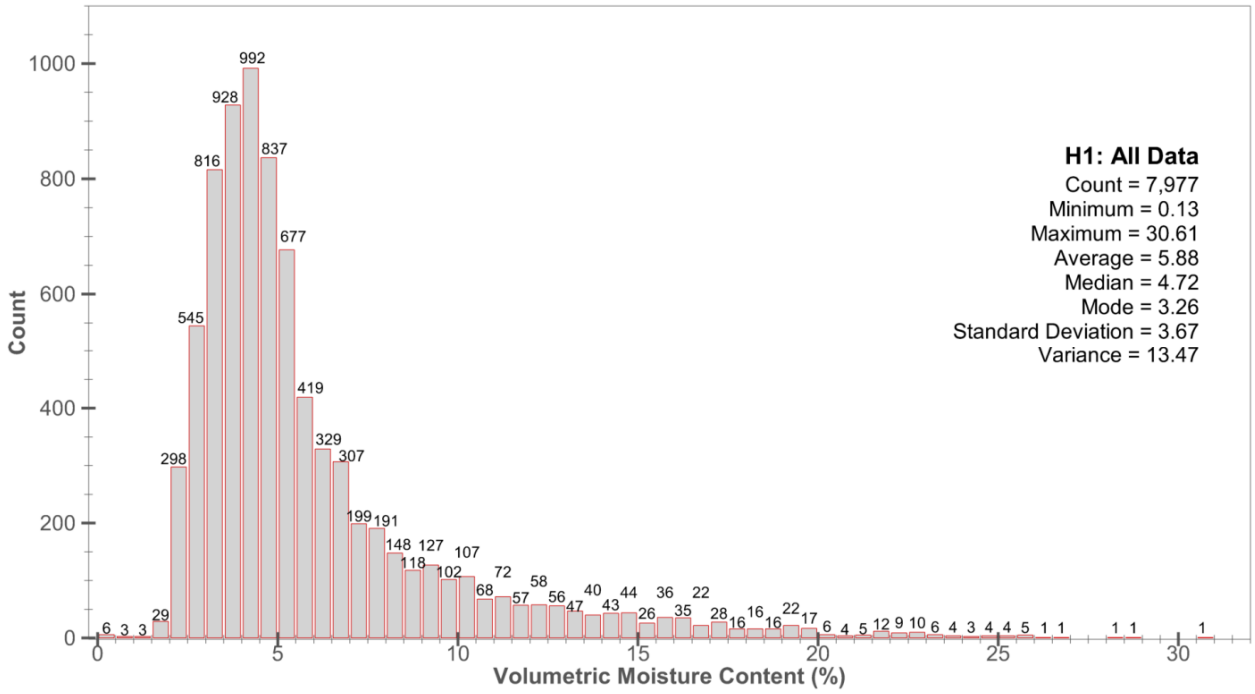

Figure B-9b. Waste Management Area C Moisture Content Histogram for H1 Data Within the Single-Shell Tank Footprint.

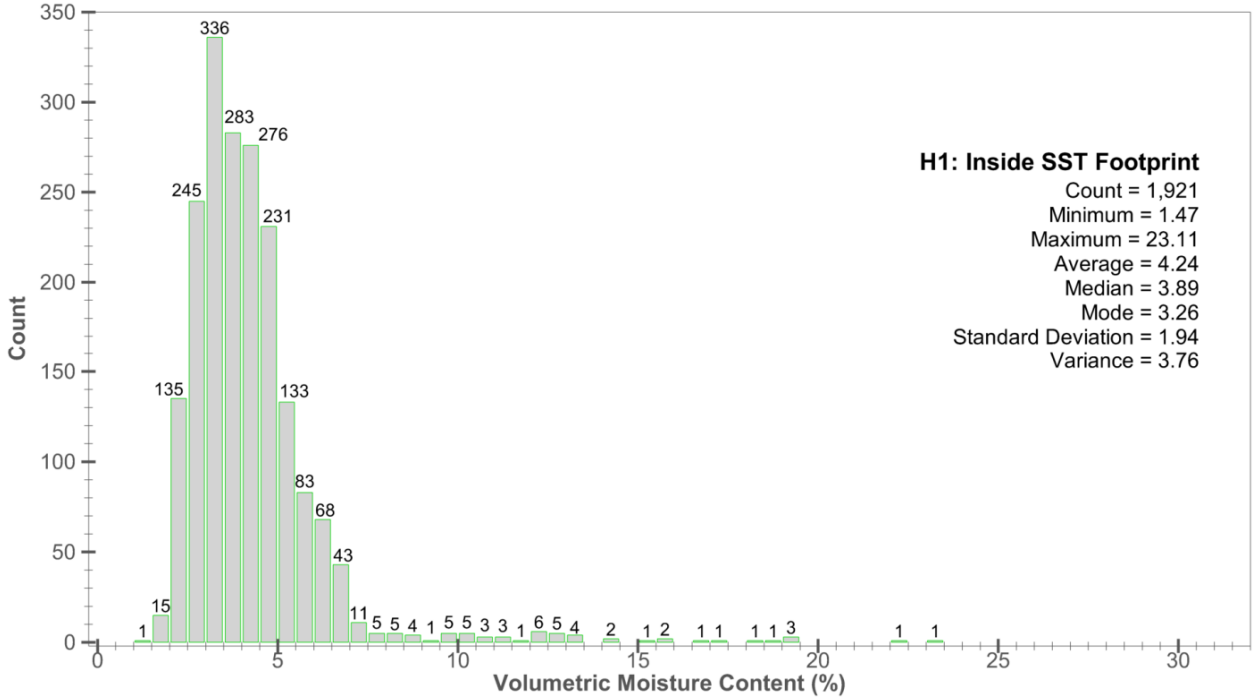

SST = single-shell tank

Figure B-9c. Waste Management Area C Moisture Content Histogram for H1 Data Outside of the Single-Shell Tank Footprint.

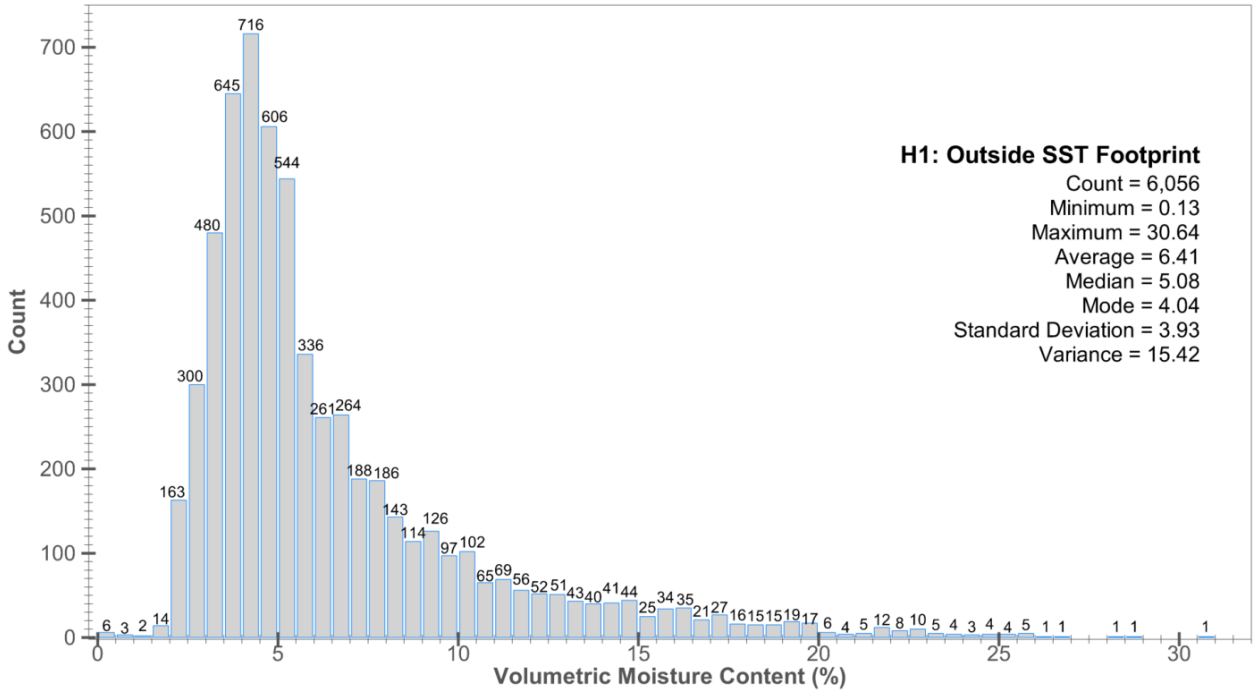

SST = single-shell tank

Figure B-10a. Waste Management Area C Moisture Content Histogram for All Backfill Data (Includes the Data from Both Inside and Outside of the Single-Shell Tank Footprint).

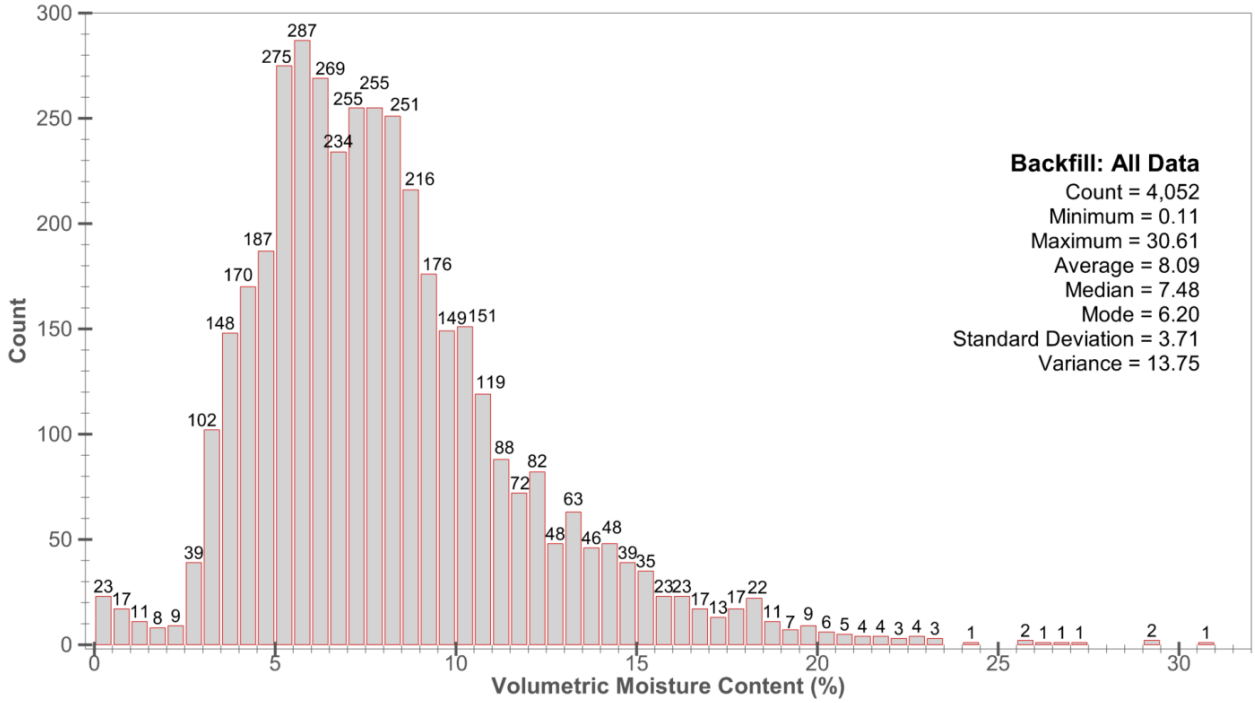

Figure B-10b. Waste Management Area C Moisture Content Histogram for Backfill Data Inside of the Single-Shell Tank Footprint.

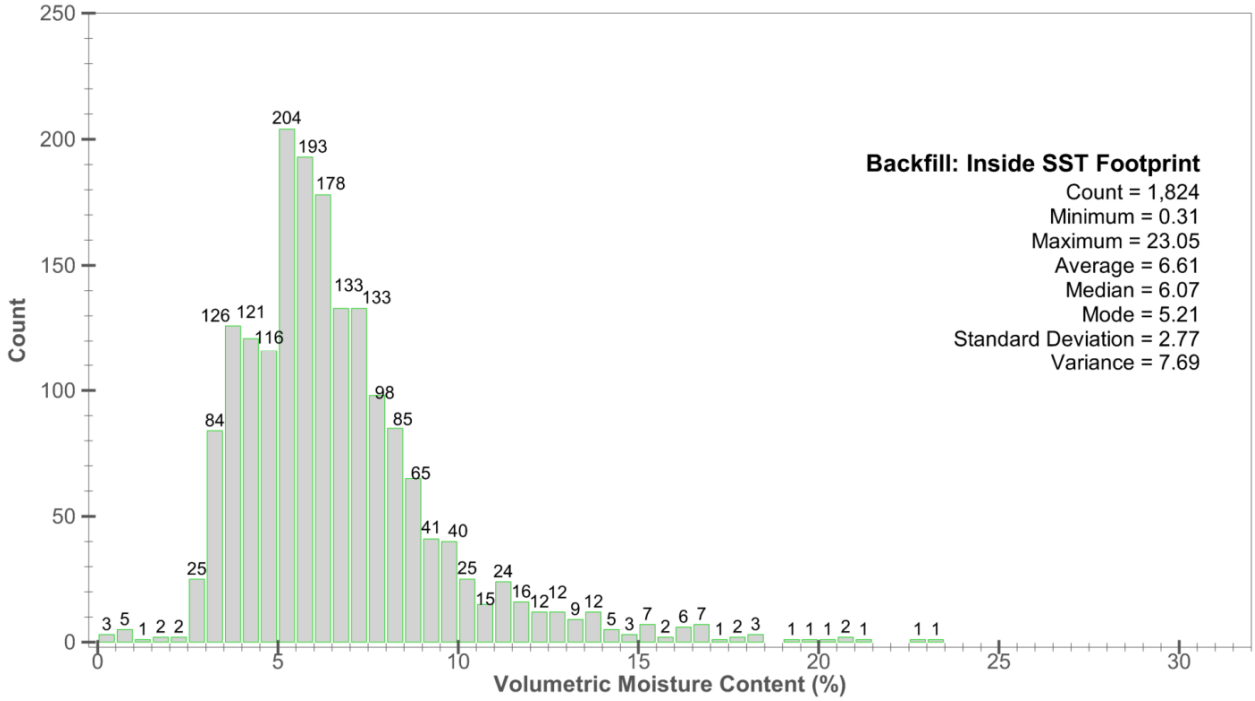

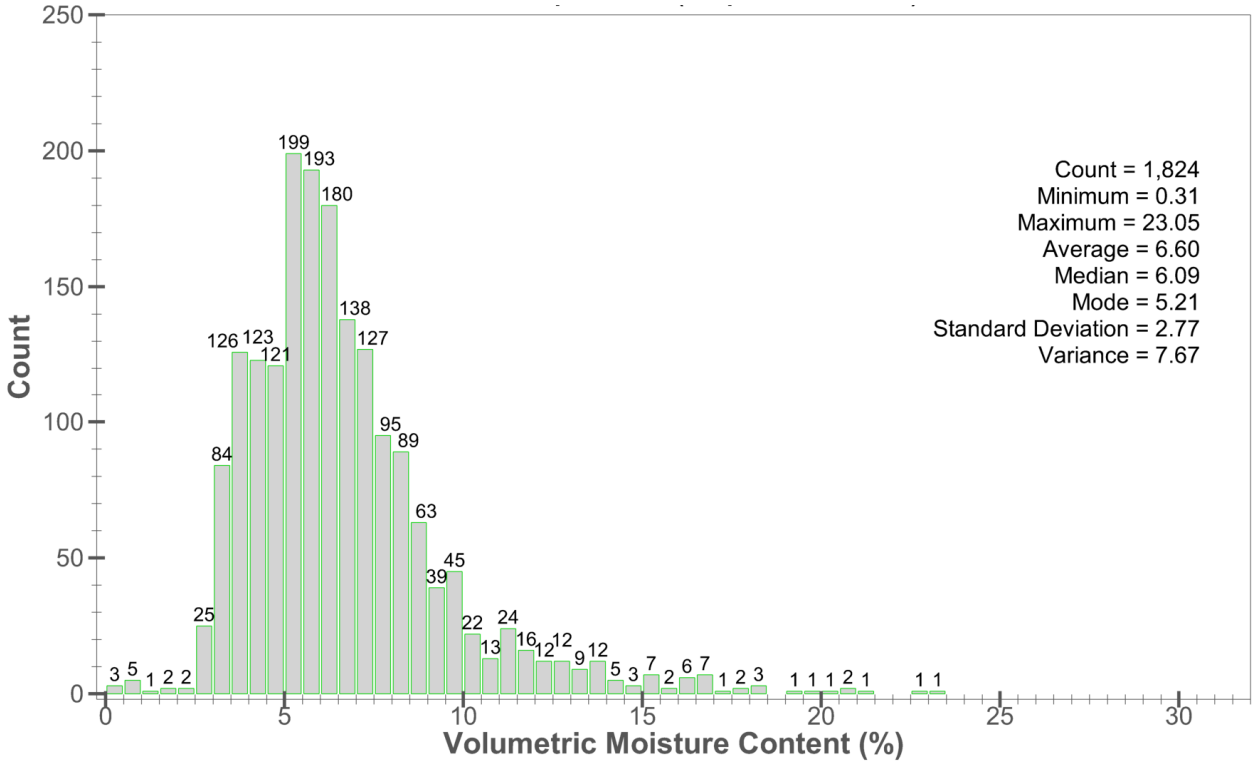

SST = single-shell tank

Figure B-10c. Waste Management Area C Moisture Content Histogram for Backfill Data Outside the Single-Shell Tank Footprint.

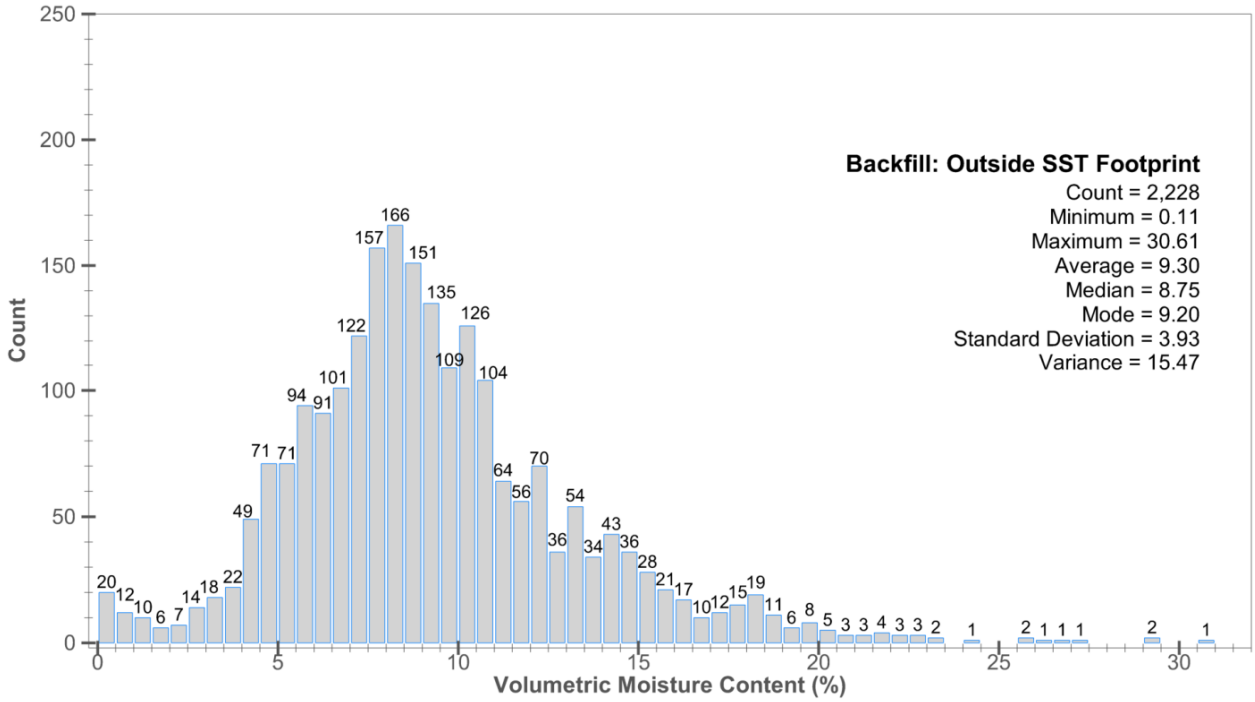

SST = single-shell tank

The IDF H2 samples contain very little gravel (>2-mm size) (RPP-20621). To account for the presence of gravel fraction for WMA C samples, the IDF H2 moisture retention data (Table B-3) were corrected ("Correcting laboratory-measured moisture retention data for gravels" [Khaleel and Relyea 1997]). Table B-4 data suggest that the gravel fraction for the H2 unit can range from less than 1% to about 25%. Also, borehole logs (PNNL-15503) suggest the presence of a high gravel fraction, and many WMA C H2 samples are characterized as "sandy pebble gravel" and "pebbly sand." A gravel fraction of 20% was assumed and applied to correct the IDF retention data. The fitted moisture retention curves and unsaturated conductivity curves for H2 sandy sequence as well as the WMA C H2 composite curves are shown in Figures B-12 and B-13, respectively. To obtain the composite curves, all measurements for an equivalent homogeneous medium (EHM) were pooled and the composite van Genuchten parameters were obtained via RETC (RETention Curve) code (EPA/600/2-91/065, The RETC Code for Quantifying the Hydraulic Functions of Unsaturated Soils) and a simultaneous fit of both moisture retention and unsaturated conductivity data. The composite curves account for gravel correction (Khaleel and Relyea 1997).

B.2.1.1 Comparison of Simulated and Observed Moisture Content. As stated earlier, the selected properties were used to simulate a vadose zone flow field and the simulation results were cross-checked against WMA C field-measured moisture contents. Figure B-14 shows a comparison of measured moisture profile for borehole C4297 (Figure B-5) and the simulated steady-state moisture profile for WMA C. As indicated, for an expected long-term recharge estimate of 3.5 mm/yr, the simulated H2 moisture profile compares well with the measurements. Overall, the simulated H2 moisture content of ~6 (% volume) is in agreement with the average

WMA C H2 moisture of ~5.15 (% volume) (Table B-1). As stated in Section B.1.1, the averages for moisture content measurements for H2 inside and outside the SST footprint were not significantly different even though the recharge conditions outside the farm are different (lower infiltration) from those inside the farm (higher infiltration). As expected, the field-measured moisture contents are significantly impacted by small-scale heterogeneities and exhibit considerable variability (Figure B-14). To the contrary, the PA simulations are based on upscaled or effective hydraulic properties; each heterogeneous formation is replaced by its homogeneous equivalent, and the upscaled or effective flow parameters are used to represent the EHM. This effectively results in a smoothing of the model estimates (Figure 6-3). Therefore, the variability of field-measured moisture contents, induced by media heterogeneities, is inherently larger in comparison to that based on PA simulations using homogenized upscaled properties, and the ensemble average, embedded in EHM approximation, cannot capture the field-scale variability.

Figure B-11. Waste Management Area C Hanford H2 Sand-Dominated Core.

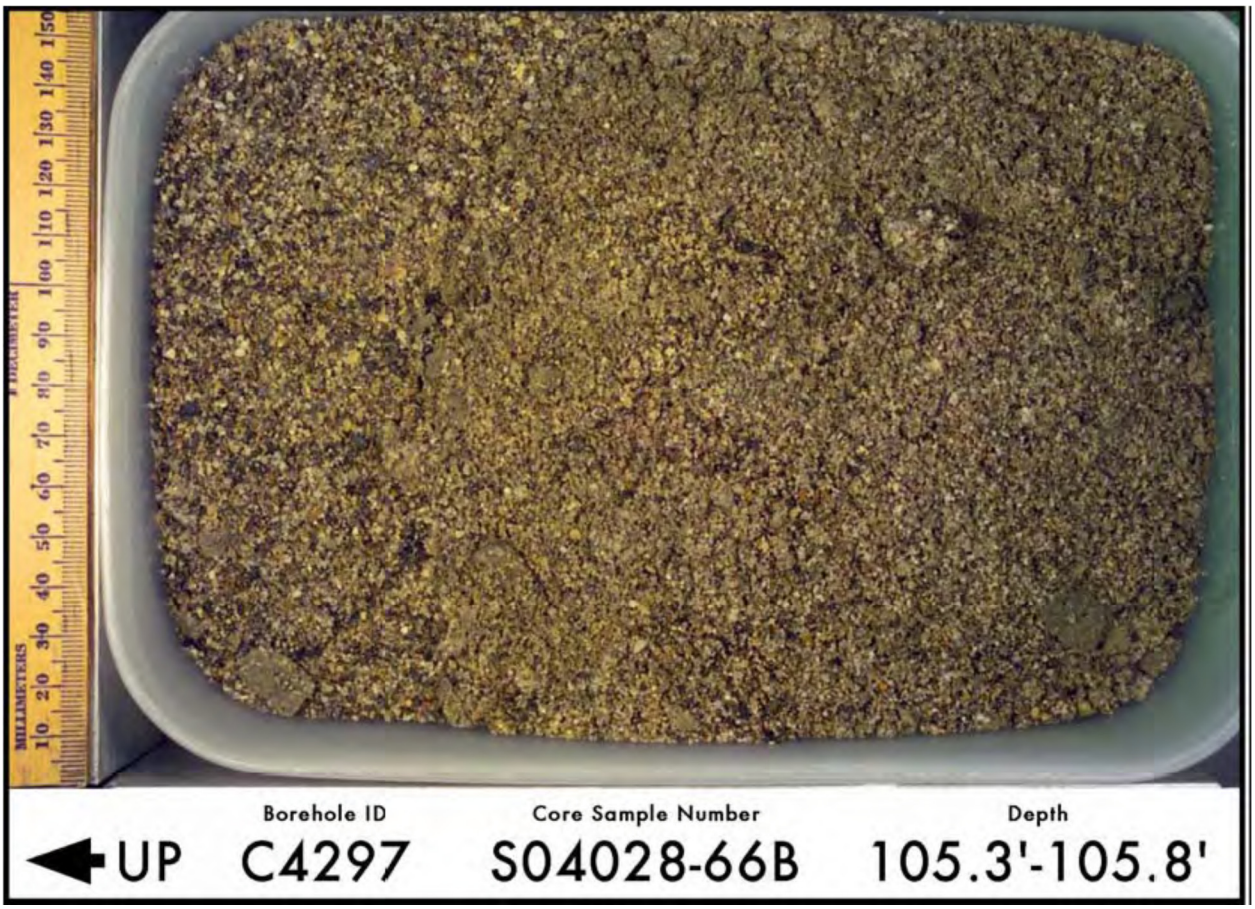

Reference: PNNL-15503, "Characterization of Vadose Zone Sediments Below the C Tank Farm: Borehole C4297 and RCRA Borehole 299-E27-22."

Similar comparison was also made for other units using their selected properties (presented below); for a recharge estimate of 3.5 mm/yr, the steady-state simulated moisture contents and the field-measured average moisture contents (Table B-1) compared well.

Table B-3. van Genuchten Parameters (Based on the Multistep Method) and Saturated Hydraulic Conductivity Data for 44 Integrated Disposal Facility Borehole Samples from the H2 Sandy Sequence. (2 sheets)

Sample	θ_s (cm^3/cm^3)	θ_r (cm^3/cm^3)	α (1/cm)	n (-)	Saturated Hydraulic Conductivity (cm/s)
7A[1]	0.377	0.0404	0.0290	1.825	1.04E-03
10A[1]	0.413	0.0279	0.1161	1.784	2.95E-03
12A[1]	0.363	0.0309	0.0650	1.755	2.15E-03
14A[1]	0.416	0.0324	0.0445	1.728	1.99E-03
15A[1]	0.380	0.0254	0.0487	1.844	2.09E-03
16A[1]	0.420	0.0228	0.0682	1.710	9.57E-03
17A[1]	0.423	0.0382	0.0689	1.899	1.99E-03
19A[1]	0.444	0.0279	0.2010	1.542	4.31E-03
20A[1]	0.419	0.0321	0.0305	2.081	2.54E-03
21A[1]	0.403	0.0276	0.0545	1.926	2.94E-03
22A[1]	0.352	0.0252	0.1078	1.585	5.06E-03
23A[1]	0.371	0.0411	0.0079	1.553	2.65E-04
24A[1]	0.321	0.0413	0.0130	1.684	5.69E-04
25A[1]	0.345	0.0267	0.0842	2.158	5.40E-03
27A[1]	0.377	0.0354	0.0830	1.532	8.14E-03
29A[1]	0.359	0.0317	0.0784	1.732	3.75E-03
31A[1]	0.418	0.0444	0.0058	2.012	8.21E-04
32A[1]	0.359	0.0401	0.0931	1.703	6.71E-03
34A[1]	0.316	0.0324	0.0819	2.398	1.32E-02
35A[1]	0.299	0.0428	0.0897	2.160	1.06E-02
45L[2]	0.385	0.008	0.1039	1.737	3.24E-2
45U[2]	0.385	0.005	0.088	1.664	3.24E-2
50L[2]	0.420	0.025	0.073	1.710	1.75E-3
50U[2]	0.420	0.013	0.045	1.667	1.75E-3
80L[2]	0.359	0.031	0.0403	2.368	1.05E-3
80U[2]	0.359	0.033	0.0313	2.572	1.05E-3

Table B-3. van Genuchten Parameters (Based on the Multistep Method) and Saturated Hydraulic Conductivity Data for 44 Integrated Disposal Facility Borehole Samples from the H2 Sandy Sequence. (2 sheets)

Sample	θ_s (cm^3/cm^3)	θ_r (cm^3/cm^3)	α (1/cm)	n (-)	Saturated Hydraulic Conductivity (cm/s)
85L[2]	0.406	0.023	0.1074	1.697	3.84E-2
85U[2]	0.406	0.027	0.0847	1.595	3.84E-2
110L[2]	0.412	0.039	0.0362	2.328	5.16E-4
110U[2]	0.412	0.046	0.0268	3.182	5.16E-4
130L[2]	0.358	0.032	0.0940	2.003	1.97E-2
130U[2]	0.358	0.036	0.0674	1.934	1.97E-2
150L[2]	0.431	0.015	0.0992	1.547	7.48E-3
150U[2]	0.431	0.024	0.0703	1.514	7.48E-3
200L[2]	0.410	0.002	0.0995	2.162	4.93E-2
215L[2]	0.370	0.028	0.0448	1.918	2.24E-3
215U[2]	0.370	0.023	0.0333	1.815	2.24E-3
230L[2]	0.309	0.040	0.0472	1.658	3.56E-3
230U[2]	0.309	0.038	0.0400	1.658	3.56E-3
251L[2]	0.427	0.032	0.084	1.845	1.43E-2
261L[2]	0.390	0.045	0.0191	2.485	5.54E-4
C3826-171[3]	0.382	0.0226	0.0390	1.840	7.96E-3
C3827-63.5[3]	0.444	0.0	0.0914	1.500	2.23E-2
C3827-221[3]	0.361	0.0220	0.0660	1.770	7.30E-3

[1]Fiscal year 1998 borehole.
[2]Fiscal year 2001 borehole.
[3]Fiscal year 2002 borehole.

Reference: RPP-20621, "Far-Field Hydrology Data Package for the Integrated Disposal Facility Performance Assessment."

B.2.1.2 Alternative Geologic Model Properties. The preceding sections have identified parameters for the soils in Alternative Geologic Model I (ACM-I). Alternative Geologic Model II (ACM-II) is a slight variation (see Section 6) of ACM-I. The primary difference between the two alternative models concerns whether or not a sandy gravel facies followed by a silty sandy layer exist at the bottom of the H2 unit in the vicinity of WMA C. Figure B-15 illustrates the moisture retention curves for ACM-II, whereas Figure B-16 illustrates the unsaturated conductivity curves for ACM-II.

Table B-4. Wet Sieve Particle Size Distribution for Borehole 299-E27-22 Sediments.

Depth (ft bgs)	Stratigraphic Unit (Hanford formation)	Weight Percent		
		Gravel	Sand	Silt/Clay
28.0	H1	28.2	62.9	8.78
40.5	H1	0.104	85.1	14.3
45.5	H1	0.136	88.9	10.5
48.0	H1	0	61.6	36.3
50.5	H1	22.1	72.3	5.58
78.0	H1	11.0	77.6	11.2
82.0	H2	0.165	87.5	11.9
85.5	H2	1.74	89.6	8.61
95.5	H2	1.10	88.4	10.4
100.5	H2	0.424	90.8	8.62
139.5	H2	0.112	88.4	11.0
145.5	H2	24.7	66.1	9.09
160.5	H2	15.9	68.8	15.2
164.5	H2	3.21	89.1	7.53
185.5	H2	18.9	60.9	20.0
200.5	H2	17.3	73.5	9.12
210.5	H2	17.1	68.5	14.2
225.5	H2	11.7	76.2	11.9

Reference: PNNL-15503, "Characterization of Vadose Zone Sediments Below the C Tank Farm: Borehole C4297 and RCRA Borehole 299-E27-22."

B.2.2 Properties of the Hanford H1 and H3 Gravelly Units

Similar to the Hanford H2 sand-dominated unit, no site-specific data are available for the WMA C Hanford H1 and H3 gravelly units. However, as part of other Hanford Site projects, particle-size distribution, bulk density, saturated hydraulic conductivity, moisture retention, and unsaturated conductivity data have been collected for several borehole samples (Figure B-3) at other sites in the vicinity of C Farm and within 200 Areas. These sites include the 218-E-12B and 218-E-10 low-level solid waste burial grounds in 200 East Area, the Environmental Restoration Disposal Facility site located in between the 200 West and 200 East Areas, and the 241-T-106 tank site located in 200 West Area. Borehole sediment samples from these sites were used as surrogates to represent the hydraulic properties for WMA C H1 and H3 gravel-dominated units.

Figure B-12. Moisture Retention Data for H2 Unit (44 Samples). The Waste Management Area C H2 composite curve is shown in red.

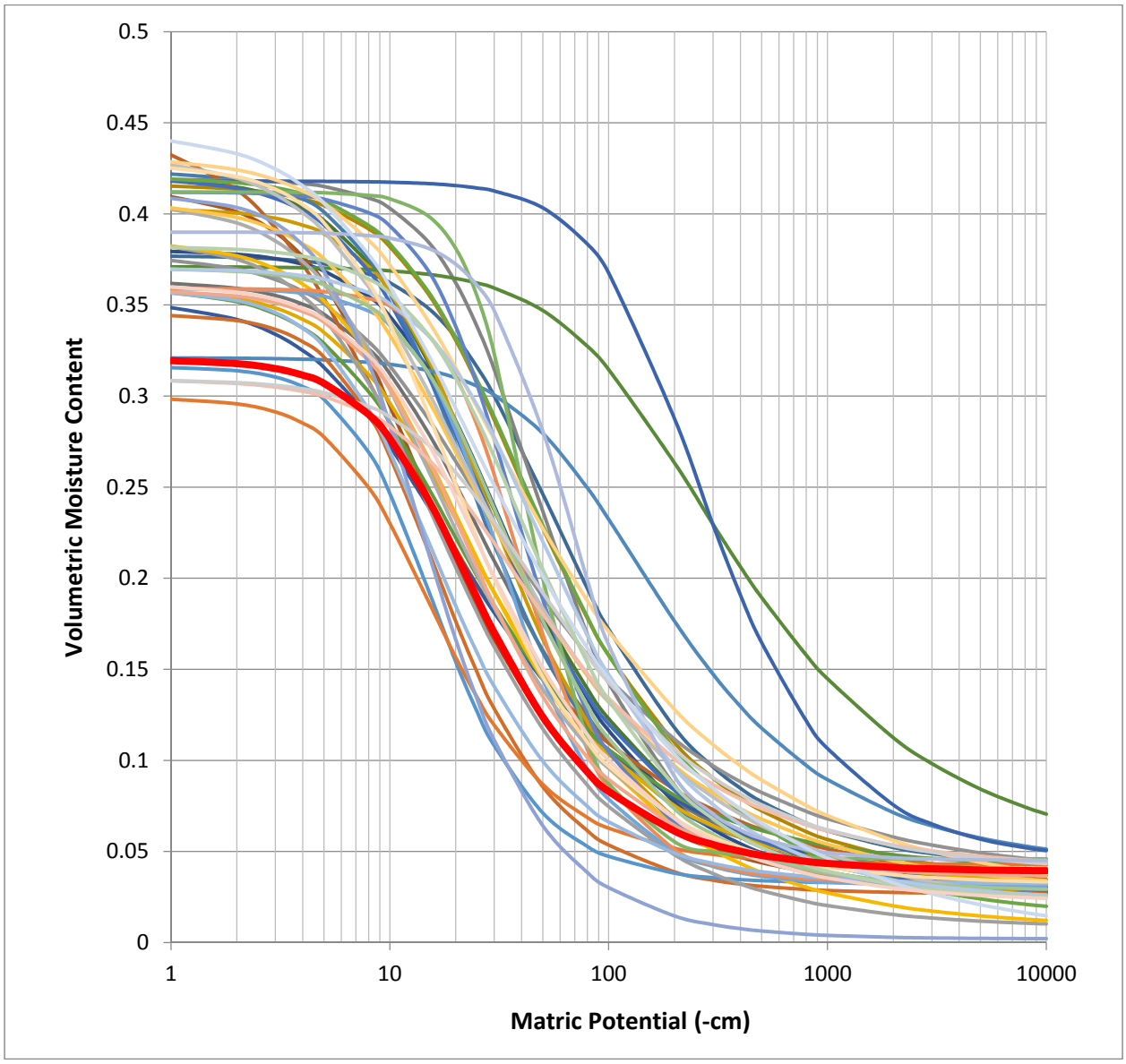

Reference: RPP-20621, "Far-Field Hydrology Data Package for the Integrated Disposal Facility Performance Assessment."

Unlike H2 sediments, both H1 and H3 sediments are comprised of a significant gravel (>2-mm size) fraction. To explore the impact of gravelly sediments for the drier moisture regime, a separate study was conducted ("Variability of Gardner's α for coarse-textured sediments" [Khaleel and Relyea 2001]); a total of 79 gravelly and sandy samples were analyzed in the laboratory. The gravel fraction for 41 samples ranged from 20 to 71% (by weight); the remaining 38 samples were sandy with very little gravel fraction (Figure B-17). A noteworthy feature of Figure B-17 is the fact that the variability in saturated conductivity is much greater than the variability in unsaturated conductivity near saturation. Furthermore, the measured unsaturated conductivities for the gravelly samples showed less variability for the drier moisture

regime, fell within a narrower range, and were well within the range of measured unsaturated conductivities for the sandy samples (see Figure B-17). Such a generic behavior for the gravelly sediments for the drier moisture regime prompted assigning similar properties for both H1 and H3 units.

Figure B-13. Unsaturated Hydraulic Conductivity Data for H2 Unit (44 Samples). The Waste Management Area C H2 composite curve is shown in red.

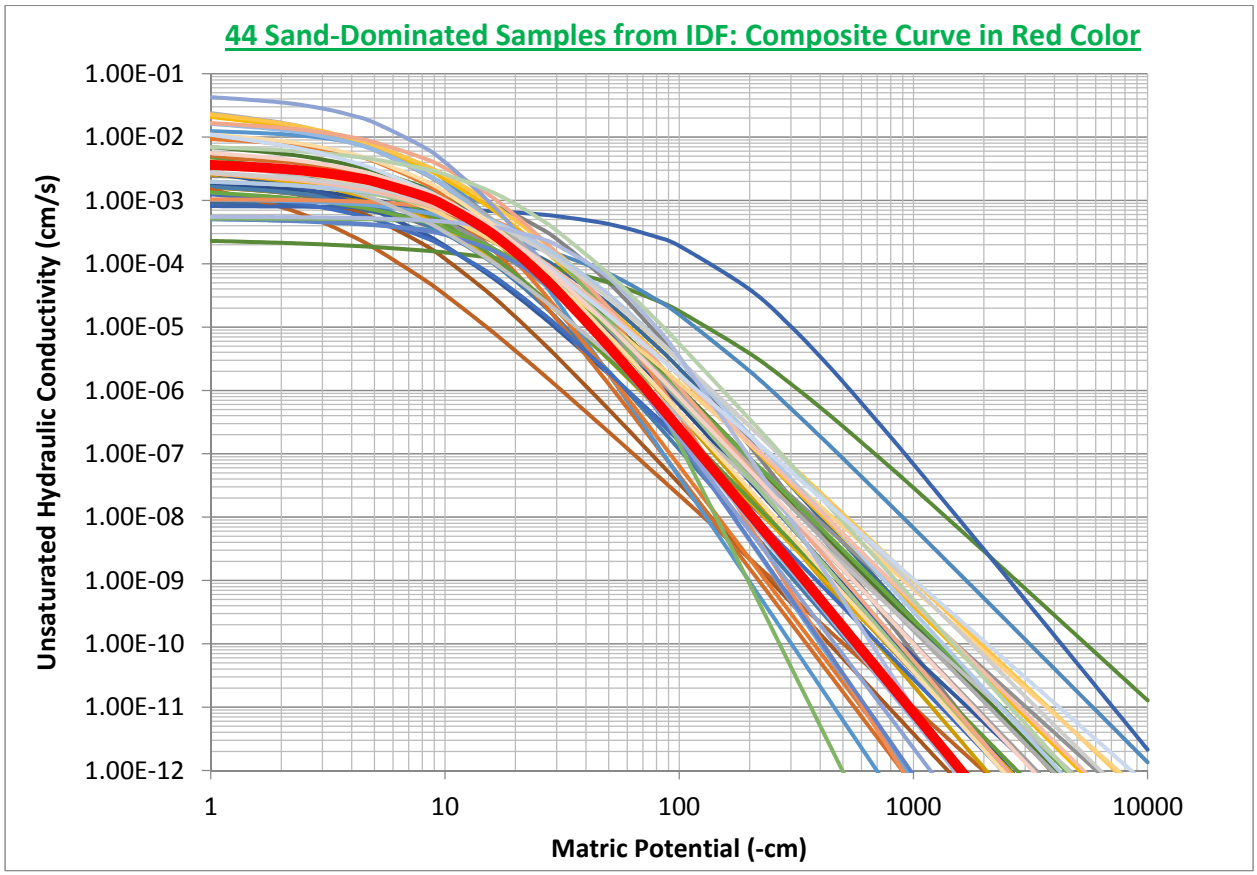

Reference: RPP-20621, "Far-Field Hydrology Data Package for the Integrated Disposal Facility Performance Assessment."

Standard laboratory and Westinghouse Hanford Company quality assurance procedures (WHC-IP-0635, "Geotechnical Engineering Procedure Manual") were used to analyze the H1 and H3 sediment samples. The moisture retention data for the fine fraction (<2 mm) and the drainage cycle of up to -1,000 cm of pressure head were measured using "Tempe" pressure cells; the rest of the drainage data up to -15,000 cm was measured using the pressure plate extraction method ("Water Retention: Laboratory Methods" [Klute 1986]). A variation of the unit gradient method (Klute and Dirksen 1986, Khaleel et al. 1995) was used to measure unsaturated hydraulic conductivities for the bulk samples. The laboratory measured data on <2 mm size fraction were corrected for the gravel fraction ("Water Content" in Methods of Soils Analysis, Part 1—Physical and Mineralogical Methods [Gardner 1986]; Khaleel and Relyea 1997). No correction was needed for the saturated and unsaturated conductivities, since these were measured on the bulk sample.

Figure B-14. Comparison of Simulated (Blue) and Observed (Circle) Moisture Content for Hanford H2 Sand-Dominated Unit.

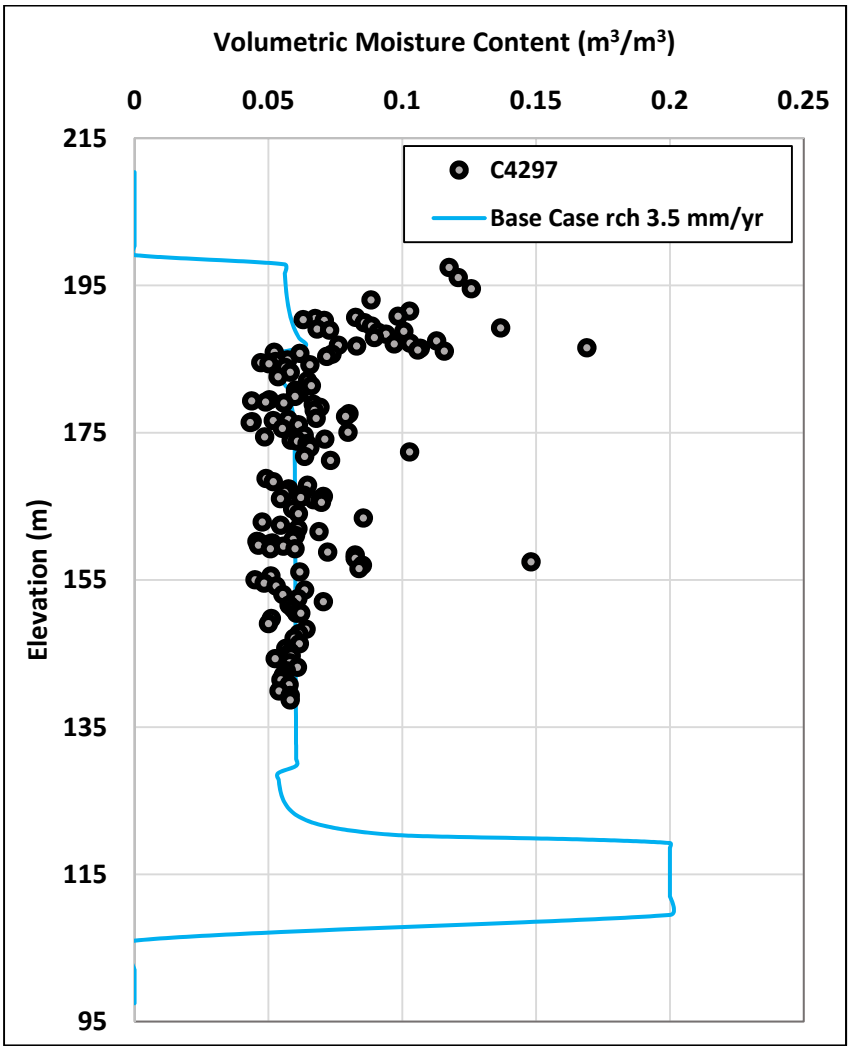

As was done for the Hanford H2 sandy unit, a simultaneous fit of both laboratory-measured moisture retention and unsaturated conductivity data was used; and all five unknown parameters (i.e., θ_r, θ_s, α, n, and K_s), with m=1-1/n (van Genuchten 1980), were fitted to the data via RETC (EPA/600/2-91/065). The pore size distribution factor, ℓ (Mualem 1976), was kept fixed at 0.5 during the simultaneous fitting. The fitted parameters, based on moisture retention and unsaturated conductivity measurements for H1 and H3 units, are shown in Table B-5. The fitted retention and conductivity curves for H1 and H3 units are shown in Figure B-18 and Figure B-19, respectively.

B.2.3 Properties for the Backfill Gravelly Unit

Because of high gravel content, the backfill hydraulic properties are expected to be similar to H1 and H3 gravelly media properties. Table B-6 catalogs the van Genuchten-Mualem parameters for samples that were selected from the 200 Areas database to represent the WMA C tank farm

backfill sediments. Because the backfill includes a significant gravel fraction, most of the samples (Table B-6) are the same as the 17 samples used to represent the H1 and H3 gravelly units. The fitted retention and conductivity curves for the backfill unit are shown in Figure B-20 and Figure B-21, respectively.

B.3 EFFECTIVE (UPSCALED) FLOW PARAMETERS FOR VADOSE ZONE

Data on hydraulic properties, described in the preceding sections, were obtained via laboratory tests on core samples (scales of the order of a few centimeters). However, numerical models of fluid flow and contaminant transport in the unsaturated zone require specifying hydraulic properties for each discretized grid block (scales of the order of meters), which are much larger than the core scale at which the unsaturated properties are measured. The process of defining large-scale properties for the numerical grid blocks based on small, core-scale measurements is called upscaling ("Upscaled Flow and Transport Properties for Heterogeneous Unsaturated Media" [Khaleel et al. 2002]).

For stratified sediments such as those existing in the 200 Areas, the effective hydraulic conductivity tensor is anisotropic with a moisture-dependent (or tension-dependent) degree of anisotropy. The anisotropy ratio of horizontal hydraulic conductivity to vertical hydraulic conductivity increases with decreasing moisture content. Theoretical work on variable anisotropy includes, for example, "Stochastic Analysis of Unsaturated Flow in Heterogeneous Soils, 2. Statistically Anisotropic Media with Variable α" (Yeh et al. 1985), "Stochastic Modeling of Large-Scale Transient Unsaturated Flow Systems" (Mantoglou and Gelhar 1987), and "Estimation of effective unsaturated hydraulic conductivity tensor using spatial moments of observed moisture plume" (Yeh et al. 2005). Experimental studies supporting variable anisotropy include, for example, "Dependence of Anisotropy on Saturation in a Stratified Sand" (Stephens and Heermann 1988), "Effective Unsaturated Hydraulic Conductivity of Layered Sands" (Yeh and Harvey 1990), and "Hysteresis and State-Dependent Anisotropy in Modeling Unsaturated Hillslope Hydrologic Processes" (McCord et al. 1991). Variable, moisture-dependent anisotropy in unsaturated soils, in effect, is an effective, large-scale (macroscopic) flow property which results from media heterogeneities at a smaller scale, and provides a framework for upscaling laboratory-scale measurements to delineate the effective or upscaled properties for the large-scale vadose zone. A stochastic model (i.e., "Application of Stochastic Methods to Transient Flow and Transport in Heterogeneous Unsaturated Soils" [Polmann 1990]) is used to describe moisture- or tension-dependent anisotropy for WMA C sediments. Such an upscaling process recognizes the spatial variability inherent in heterogeneous media such as those existing at WMA C.

Effective or upscaled values of flow parameters for the WMA C vadose zone are presented in Section B.3.1. Specific upscaled flow parameters include moisture retention, saturated, and unsaturated hydraulic conductivity. Transport parameters (e.g., bulk density, diffusivity, sorption coefficients, and macrodispersivity) are discussed later in Section B.4.

Figure B-15. Moisture Retention Curves for Various Hydrostratigraphic Units and Selected Properties for Alternative Geologic Model II.

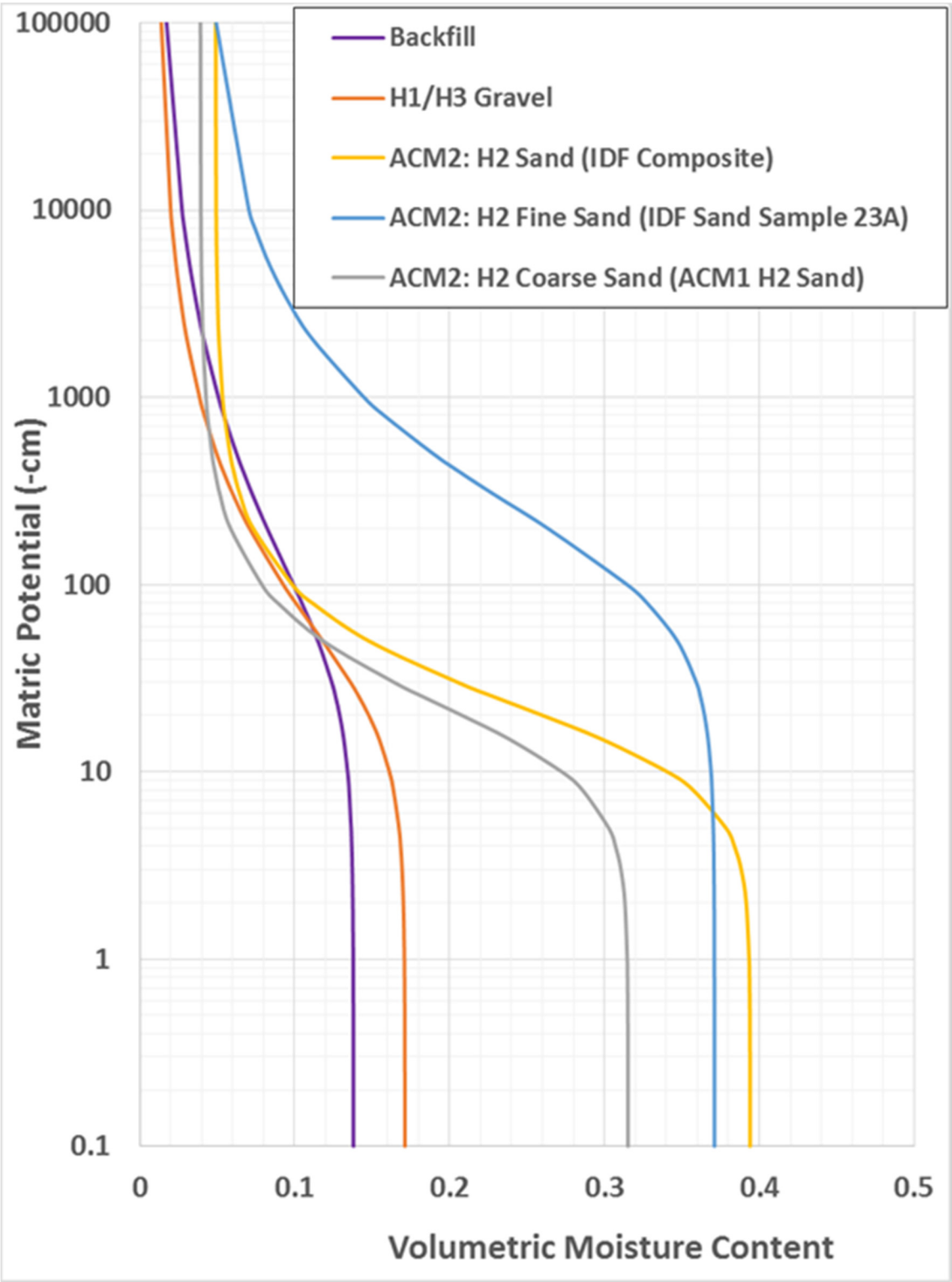

ACM1 = Alternative Geologic Model I
ACM2 = Alternative Geologic Model II
IDF = Integrated Disposal Facility

Figure B-16. Unsaturated Hydraulic Conductivity Curves for Various Hydrostratigraphic Units and Selected Properties for Alternative Geologic Model II.

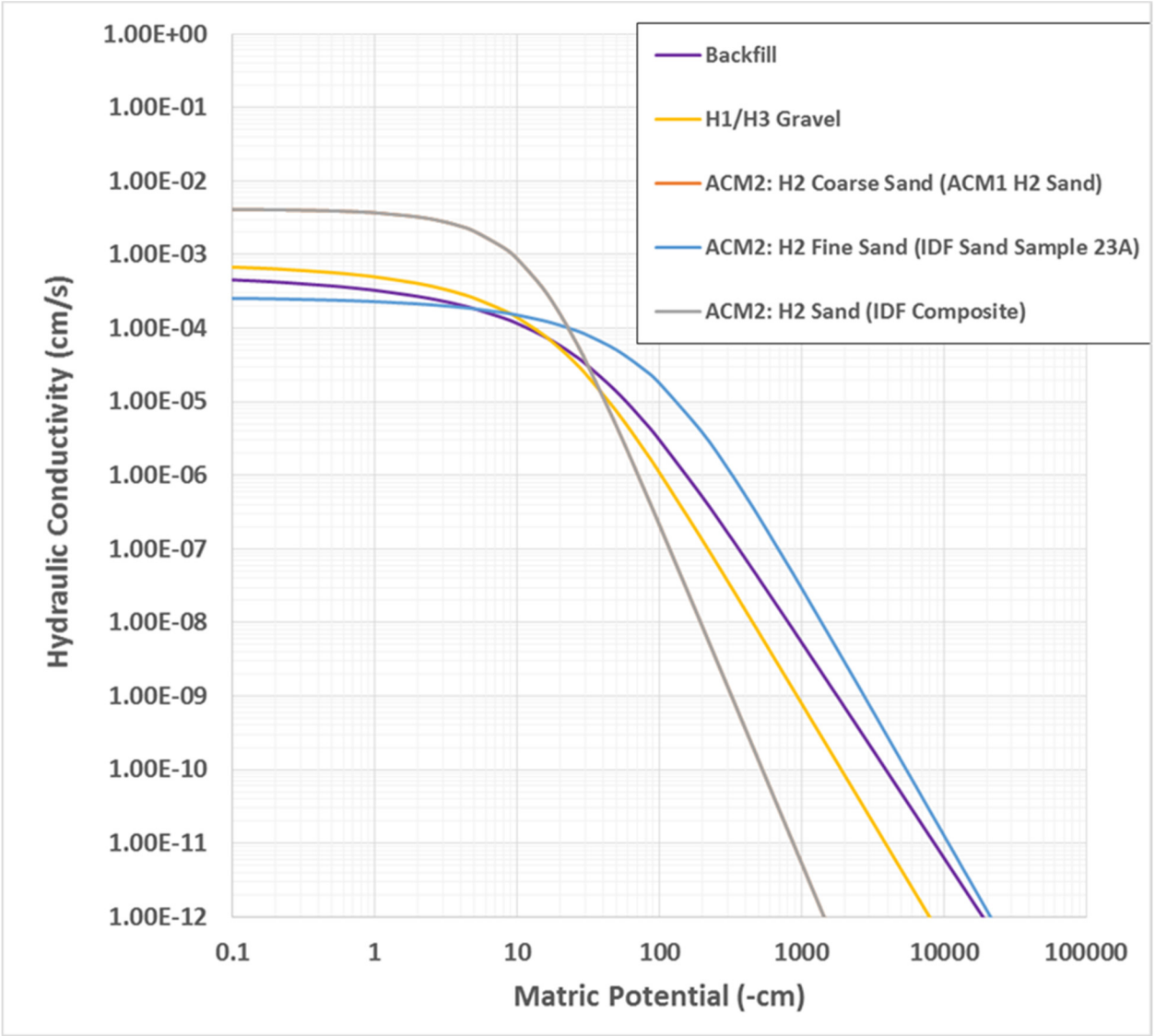

ACM1 = Alternative Geologic Model I
ACM2 = Alternative Geologic Model II
IDF = Integrated Disposal Facility

B.3.1 Composite Macroscopic Relationships and Effective Parameters

The WMA C composite parameters for moisture characteristics are derived based on laboratory measurements presented in preceding sections. The fitted moisture retention curves (e.g., Figure B-12 for H2 unit) show spatial variability, albeit the degree of variation at a given tension is more modest than that of hydraulic conductivity (e.g., Figure B-13 for H2 unit). For both sandy (e.g., H2 unit) and gravelly (e.g., H1, H3, and backfill units) sediments, the composite van Genuchten parameters were obtained via RETC (EPA/600/2-91/065) and a simultaneous fit of both moisture retention and unsaturated conductivity data. The pore size

distribution factor ℓ (van Genuchten 1980) was kept constant at 0.5 during the simultaneous fitting.

Figure B-17. Unsaturated Hydraulic Conductivity Measurements for Sand-Dominated and Gravel-Dominated Samples.

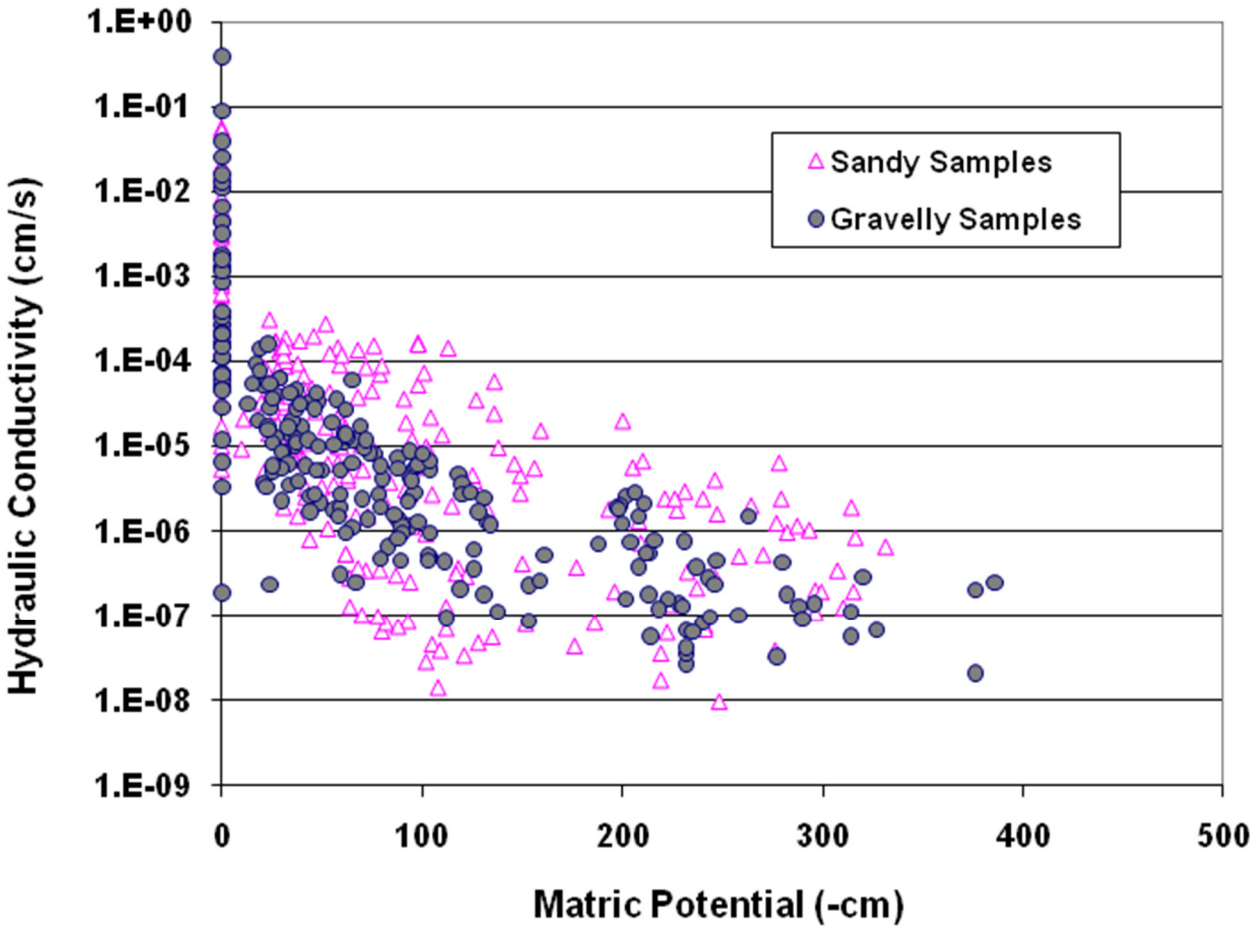

Reference: "Variability of Gardner's α for coarse-textured sediments" (Khaleel and Relyea 2001).

The fitted composite van Genuchten-Mualem parameters for different HSUs are shown in Table B-7. Estimates for the equivalent horizontal and vertical hydraulic conductivities are discussed in Section B.3.2.

B.3.2 Stochastic Model for Macroscopic Anisotropy

As discussed earlier, variable, tension-dependent anisotropy provides a framework for upscaling small-scale measurements to the effective or upscaled properties for the large-scale vadose zone. A stochastic model is used to describe tension-dependent anisotropy for sediments at the C Farm.

Yeh et al. (1985) analyzed steady unsaturated flow through heterogeneous porous media using a stochastic model. Parameters such as hydraulic conductivity are treated as random variables rather than as deterministic quantities. The Gardner relationship ("Some Steady-State Solutions

of the Unsaturated Moisture Flow Equation with Application to Evaporation from a Water Table" [Gardner 1958]) was used by Yeh et al. (1985) to describe unsaturated hydraulic conductivity (K) as a function of saturated hydraulic conductivity (K_s) and tension (h), as shown in Equations B-1 and B-2.

$$K(h)=K_s\ exp(-\beta h) \tag{B-1}$$

Where β is a fitting parameter.

Equation B-1 can be written as

$$ln(K(h)) = ln(K_s) - \beta h \tag{B-2}$$

Equation B-2 is referred to as the log-linear model, since ln(K(h)) is linearly related to h through the constant slope β. However, such a constant slope is often inadequate in describing ln(K(h)) over ranges of tension of practical interest for field applications. As an alternative, the slope β can be approximated locally by straight lines over a fixed range of tension. The pseudo "ln(K_s)" term in Equation B-2 can then be derived by extrapolating the local slopes back to zero tension.

Using a linear correlation model between the log-conductivity zero-tension intercept and β, Polmann (1990) presents a generalized model that accounts for the cross-correlation of the local soil property [i.e., ln(K_s) and β] residual fluctuations. When compared with the uncorrelated ln(K_s) - β model, a partial correlation of the properties is shown to have a significant impact on the magnitude of the effective parameters derived from the stochastic theory. The Polmann (1990) equations for deriving the effective parameters are shown in Equation B-3.

$$\begin{aligned}
&< LnK > = < LnK_s > - A < h > - \sigma^2_{LnKs}\lambda[p - p^2 < h > - \zeta^2 < h >]/(1 + A\lambda) \\
&\sigma^2_{LnK} = \sigma^2_{LnKs}[(1 - p < h >)^2 + \zeta^2 < h >^2]/(1 + A\lambda) \\
&K_h^{eq} = \exp[< LnK > + (\sigma^2_{LnK}/2)] \\
&K_v^{eq} = \exp[< LnK > - (\sigma^2_{LnK}/2)]
\end{aligned} \tag{B-3}$$

Where:

σ^2_{LnK}	=	variance of log unsaturated conductivity (which depends on mean tension)
$<h>$	=	mean tension (positive) = |ψ|
ψ	=	matric potential (negative)
σ^2_{LnKs}	=	variance of pseudo "log saturated conductivity"
$<LnK_s>$	=	mean of ln(K_s)
p	=	slope of the β versus ln(K_s) regression line, where β is the slope of the unsaturated conductivity curve and approximated locally based on Gardner's (1958) exponential model
ζ	=	$\sigma_\delta/\sigma_{ln(Ks)}$

σ_δ = standard deviation of the residuals in the β versus ln(K_s) regression
A = mean slope, β, for ln(K) vs. h
λ = vertical correlation lengths for ln(K_s) (assumed to be same as that of β)
K_h^{eq} = equivalent unsaturated horizontal conductivity
K_v^{eq} = equivalent unsaturated vertical conductivity.

B.3.3 Macroscopic Anisotropy Relations

Results of application of Equation B-3 for variable anisotropy are presented below. The data for individual HSUs (Tables B-3, B-5 and B-6) are used to obtain the Polmann parameters < ln(K_s)>, σ^2_{LnKs}, p, ζ, and A (Equation B-3). The slope and pseudo ln(K_s) estimates, discussed in the preceding section, are evaluated for the expected moisture regime of interest (i.e., relatively high tension range) (Table B-8). However, it should be noted that often no experimental data are available for unsaturated conductivities in the tension range of interest; β and ln(K_s) estimates are then based on the fitted van Genuchten-Mualem curves.

An estimate of correlation length λ is needed for anisotropy calculations. Most of the measurements in the 200 Areas have been obtained at sampling intervals that are too coarse to yield a reasonable estimate for the correlation length. However, one data set is available that provides saturated conductivity estimates at about 30-cm intervals for a depth of 18 m within the Hanford formation; the site is located about 0.5 mi east of the IDF site (Figure B-3) in the 200 East Area. Figure B-22 shows the experimental variogram and the fitted theoretical variogram for saturated conductivities. The fitted variogram suggests a correlation length λ of about 50 cm (i.e., the distance at which the variogram drops to [1-(1/e)] times the sill) (Figure B-22). Correlation length λ for both ln(K_s) and β were assumed to be equal.

Table B-9 lists the variable, macroscopic anisotropy parameter estimates for various WMA C units. The calculated macroscopic variable anisotropy relations for various HSUs are shown in Figures B-23, B-24, and B-25. A supporting document presents the anisotropy calculations (RPP-CALC-60452, "Moisture Dependent Anisotropy Calculations Supporting WMA C PA").

Note that values listed in Table B-7 are the composite van Genuchten-Mualem parameters for different units. Equation B-3 is used to assign the variable Polmann anisotropy (i.e., the ratio of equivalent unsaturated horizontal conductivity to equivalent unsaturated vertical conductivity) as a function of saturation. The van Genuchten-Mualem parameters in Table B-7 are then used to assign the actual unsaturated hydraulic conductivity estimates. The fitted K_s values in Table B-7 represent the vertical components.

B.4 EFFECTIVE TRANSPORT PARAMETERS

Base case effective transport parameter (bulk density, diffusivity, and dispersivity) estimates are presented in this section. Because of natural variability, the transport parameters are all spatially variable. The purpose is again, similar to the flow parameters, to evaluate the effect of such variability on the large-scale transport process.

Table B-5. van Genuchten Parameters, Fitted Saturated Hydraulic Conductivity, and Measured Bulk Density Data for H1/H3 Units (17 Samples).

Sample	Site/Operable Unit	Borehole Number	Depth m	Percent Gravel	Θs cm^3/cm^3	Θr cm^3/cm^3	α 1/cm	n	Fitted Ks cm/s	Bulk Density g/cm^3
5-0150	218-E-12B	299-E34-1	24.84	17	0.240	0.023	0.030	1.7077	1.47E-03	1.95
5-0157	218-E-10	299-E32-4	3.50	13	0.293	0.033	0.027	2.1675	7.77E-03	1.88
5-0152	218-E-12B	299-E34-1	65.50	26	0.280	0.025	0.044	1.3253	2.43E-03	1.85
5-0158	218-E-10	299-E32-4	71.50	44	0.214	0.013	0.008	1.4226	1.38E-04	2.15
5-0148	218-E-12B	299-E34-1	15.25	54	0.148	0.013	0.021	1.5589	2.72E-04	2.16
4-1080	ERDF	699-35-61A	93.50	43	0.178	0.000	0.007	1.3819	8.11E-06	2.00
4-0791	ERDF	699-35-65A	63.20	0	0.338	0.026	0.023	2.2565	6.81E-04	1.60
4-0792	ERDF	699-35-65A	75.40	71	0.100	0.008	0.030	1.5858	3.42E-04	2.32
4-1076	ERDF	699-35-61A	76.40	0	0.357	0.000	0.029	1.7015	1.23E-03	1.74
4-1079	ERDF	699-35-61A	90.90	61	0.163	0.000	0.014	1.3079	1.18E-04	2.06
4-1013	ERDF	699-35-69A	77.90	65	0.139	0.013	0.007	1.5656	1.06E-06	2.20
4-1012	ERDF	699-35-69A	73.90	55	0.147	0.000	0.008	1.5109	4.50E-05	2.19
3-0668	241-T-106	299-W10-196	38.90	62	0.175	0.000	0.019	1.6124	1.63E-04	2.13
3-0682	241-T-106	299-W10-196	46.10	51	0.224	0.000	0.017	1.6577	2.37E-04	2.14
3-0210	241-T-106	299-W10-196	3.10	48	0.186	0.029	0.014	1.7674	1.96E-04	2.11
3-0688	241-T-106	299-W10-196	48.50	49	0.199	0.000	0.004	1.5321	2.60E-05	2.17
3-0690	241-T-106	299-W10-196	53.7	53	0.182	0.018	0.005	1.5410	4.19E-05	2.19

ERDF = Environmental Restoration Disposal Facility

Figure B-18. Moisture Retention Data for H1 and H3 Units (17 Samples). The composite curve is shown in red.

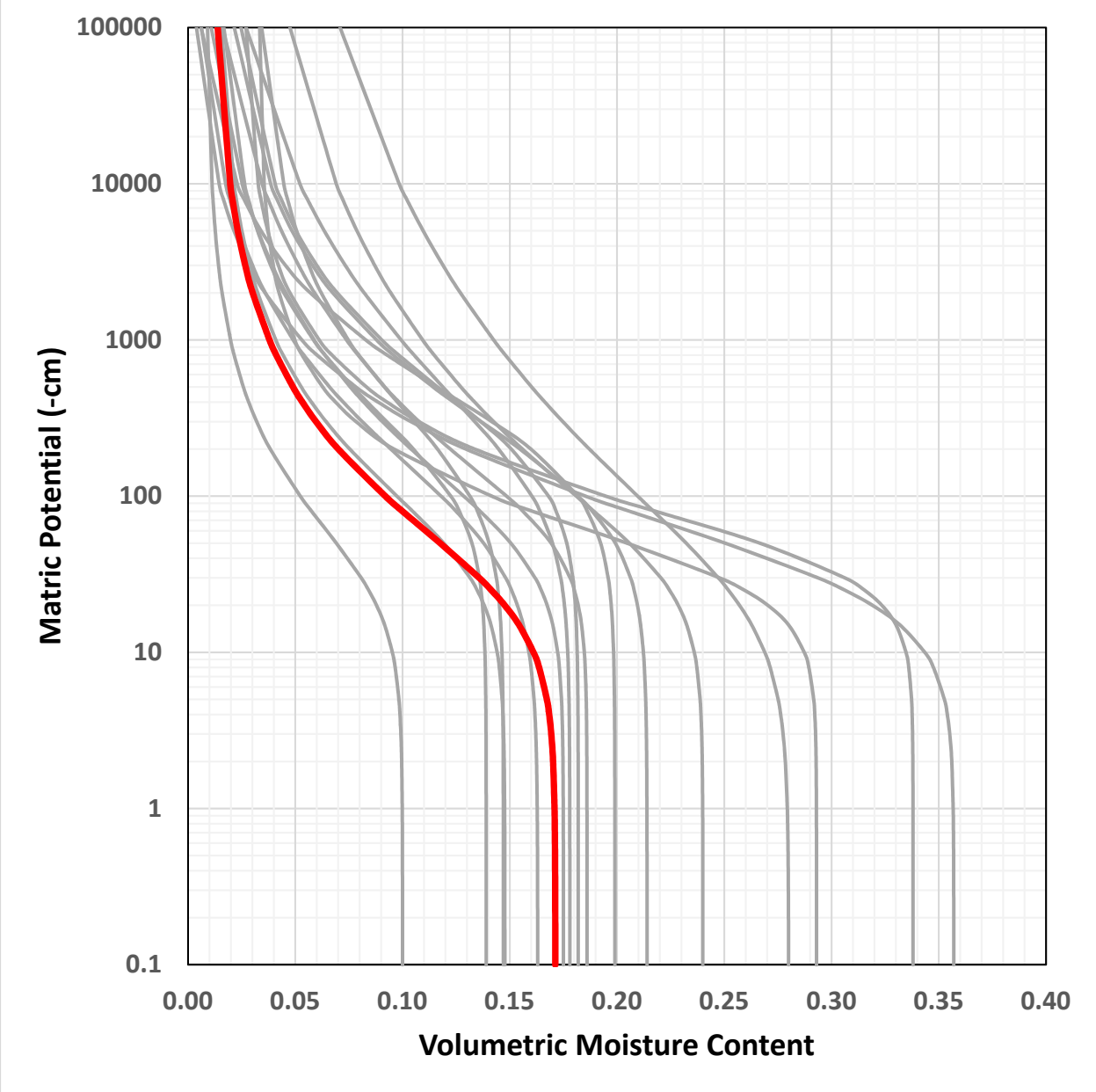

B.4.1 Bulk Density and K_d

Both bulk density (ρ_b) and K_d estimates are needed to calculate retardation factors for different species. The effective, large-scale estimate for bulk density is the average of the small-scale laboratory measurements for bulk density (Stochastic Subsurface Hydrology [Gelhar 1993]). Table B-10 provides the effective, large-scale bulk density estimates for WMA C HSUs. The K_d values, presented in Section 6, were corrected for the gravel (>2-mm size) fraction, and are not repeated here. The correction procedure followed is described in PNNL-17154, "Geochemical Characterization Data Package for the Vadose Zone in the Single-Shell Tank Waste Management

Areas at the Hanford Site." For materials that contain significant amounts of gravel (notably H1 and H3), K_d values are typically lower than those determined with <2-mm size material because the surface area and the corresponding quantity of adsorption sites is lower (PNNL-17154).

Figure B-19. Unsaturated Hydraulic Conductivity Data for H1 and H3 Units (17 Samples). The composite curve is shown in red.

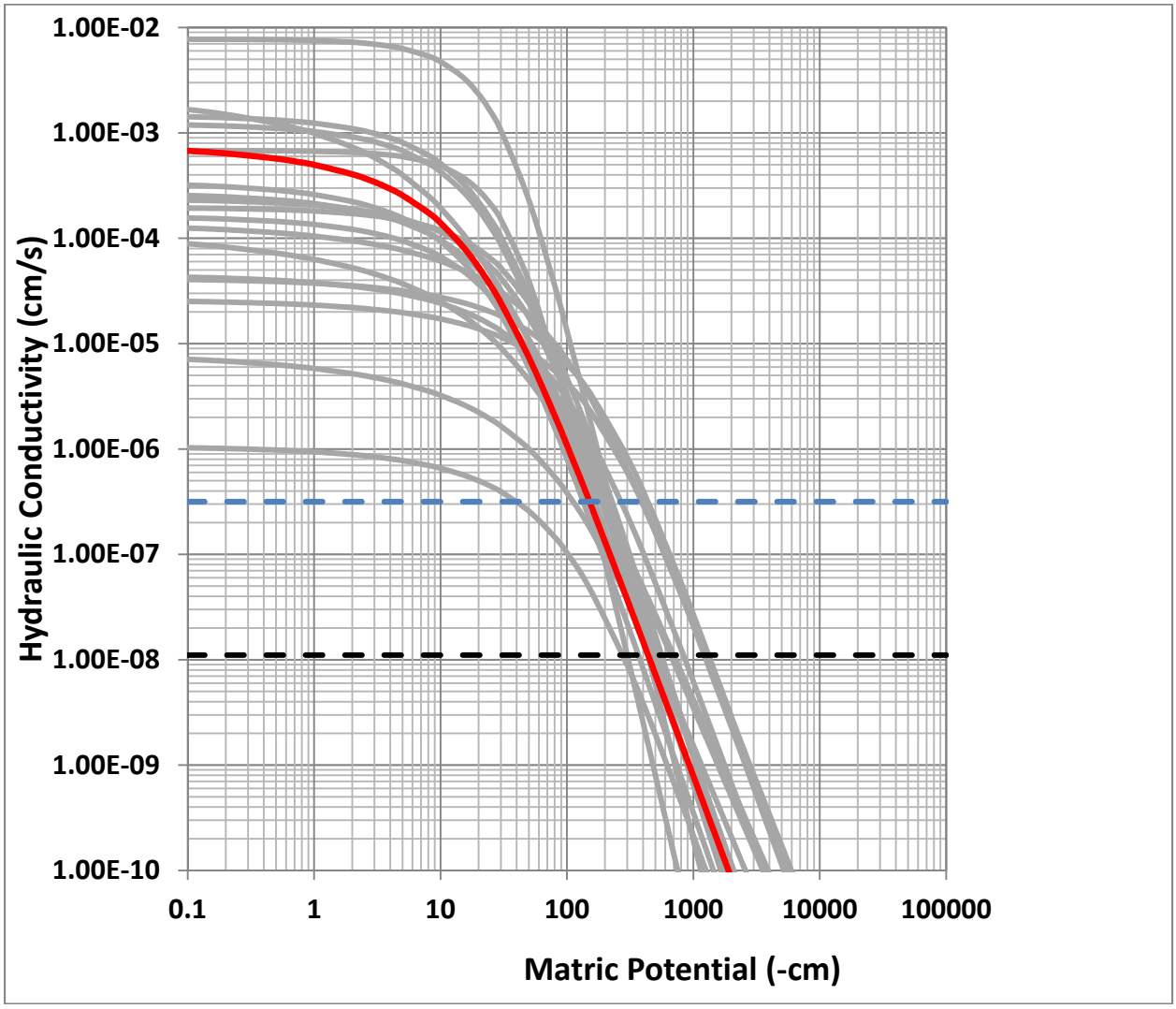

B.4.2 Diffusivity

It is assumed that the effective, large-scale diffusion coefficients for all HSUs are a function of volumetric moisture content, θ, and can be estimated based on an empirical relation ("Permeability of Porous Solids" [Millington and Quirk 1961]):

$$D_e(\theta) = D_0 \frac{\theta^{10/3}}{\theta_s^2} \tag{B-4}$$

where $D_e(\theta)$ is the effective diffusion coefficient of an ionic species, and D_0 is the effective diffusion coefficient for the same species in free water. The molecular diffusion coefficient for all species in pore water is assumed to be 2.5×10^{-5} cm^2/sec (WHC-SD-WM-EE-004, "Performance Assessment of Grouted Double-Shell Tank Waste Disposal at Hanford").

B.4.3 Vadose Zone Macrodispersivities

Field-scale dispersivities are referred to as macrodispersivities. The terms macrodispersivity and dispersivity are used interchangeably in this section. Readers can go directly to Section B.4.3.4 for the macrodispersivity values recommended for WMA C PA calculations. Details on how the selections are made using different methods are provided in Section B.4.3.1 (Numerical Simulations), Section B.4.3.2 (Stochastic Theory) and Section B.4.3.3 (Experimental Observations).

Field observations indicate that the dispersion coefficients required to describe the large-scale transport processes, at field scales of tens or hundreds of meters, are much different from those observed in small-scale laboratory experiments (Gelhar 1993). In fact, field-scale dispersivities may often be orders of magnitude larger than those observed in the laboratory. Consequently, laboratory-scale dispersivities, which are typically ~1 cm or less, are of little use in estimating field-scale dispersivities.

There is general agreement in hydrology literature that hydraulic conductivity variations induced by field-scale heterogeneities play an important role in field-scale transport processes. However, there does not appear to be a clear consensus about how best to describe such processes quantitatively (Gelhar 1993). While well-designed, large-scale tracer experiments would provide useful information, limited field data are available at this time to quantify macrodispersivities in unsaturated media.

Dispersivities are a function of matric potential (or soil moisture content) in unsaturated media (Mantoglou and Gelhar 1987). As with saturated media, heterogeneities that exist at various length scales result also in a scale dependence of macrodispersivities in unsaturated media ("A Critical Review of Data on Field-Scale Dispersion in Aquifers" [Gelhar et al. 1992]). Dispersivities increase with time, or equivalently with distance, until they tend to converge on their unique asymptotic (large-time) values. However, it can take a long time (e.g., years or decades) for the asymptotic Fickian approximation to take hold. Nonetheless, the second-moment evolution or the time-dependent, preasymptotic dispersivities are of marginal interest in simulations involving long-times or large-mean travel distances such as those in the WMA C PA modeling. This well-known behavior is usually attributed to heterogeneity-induced spreading and mixing until the point at which all of the heterogeneity has effectively been "sampled" by the contaminant plume such that dispersion becomes constant. The use of a constant (asymptotic) macrodispersivity is thus considered appropriate in PA simulations (NUREG/CR-6114, Auxiliary Analyses in Support of Performance Assessment of a Hypothetical Low-Level Waste Facility: Groundwater Flow and Transport Simulation, Vol. 3; NUREG/CR-5965, Modeling Field Scale Unsaturated Flow and Transport Processes).

Table B-6. van Genuchten Parameters, Fitted Saturated Hydraulic Conductivity, and Measured Bulk Density Data for Backfill Unit (10 Samples).

Sample	Site	Borehole Number	Depth (m)	Percent Gravel	θ_s (cm^3/cm^3)	θ_r (cm^3/cm^3)	α (1/cm)	n (-)	Fitted K_s (cm/s)	Bulk Density (g/cm^3)
4-0792	ERDF	699-35-65A	75.4	71	0.100	0.0084	0.03	1.5858	3.42E-04	2.32
4-1012	ERDF	699-35-69A	73.9	55	0.147	0	0.0076	1.5109	4.50E-05	2.19
4-1013	ERDF	699-35-69A	77.9	65	0.139	0.0127	0.0065	1.5656	1.06E-06	2.20
4-1079	ERDF	699-35-61A	90.9	61	0.163	0	0.014	1.3079	1.18E-04	2.06
4-1080	ERDF	699-35-61A	93.5	43	0.178	0	0.0074	1.3819	8.11E-06	2.00
3-0668	241-T-106	299-W10-196	38.9	62	0.175	0	0.0192	1.6124	1.63E-04	2.13
3-0682	241-T-106	299-W10-196	46.1	51	0.224	0	0.0166	1.6577	2.37E-04	2.14
3-0688	241-T-106	299-W10-196	48.5	49	0.199	0	0.0043	1.5321	2.60E-05	2.17
3-0689	241-T-106	299-W10-196	52.2	28	0.236	0	0.0025	1.4747	4.58E-05	1.93
3-0690	241-T-106	299-W10-196	53.7	53	0.1819	0.0177	0.0046	1.541	4.19E-05	2.19

ERDF = Environmental Restoration Disposal Facility

Figure B-20. Moisture Retention Data for Backfill Unit (10 Samples). The composite curve is shown in red.

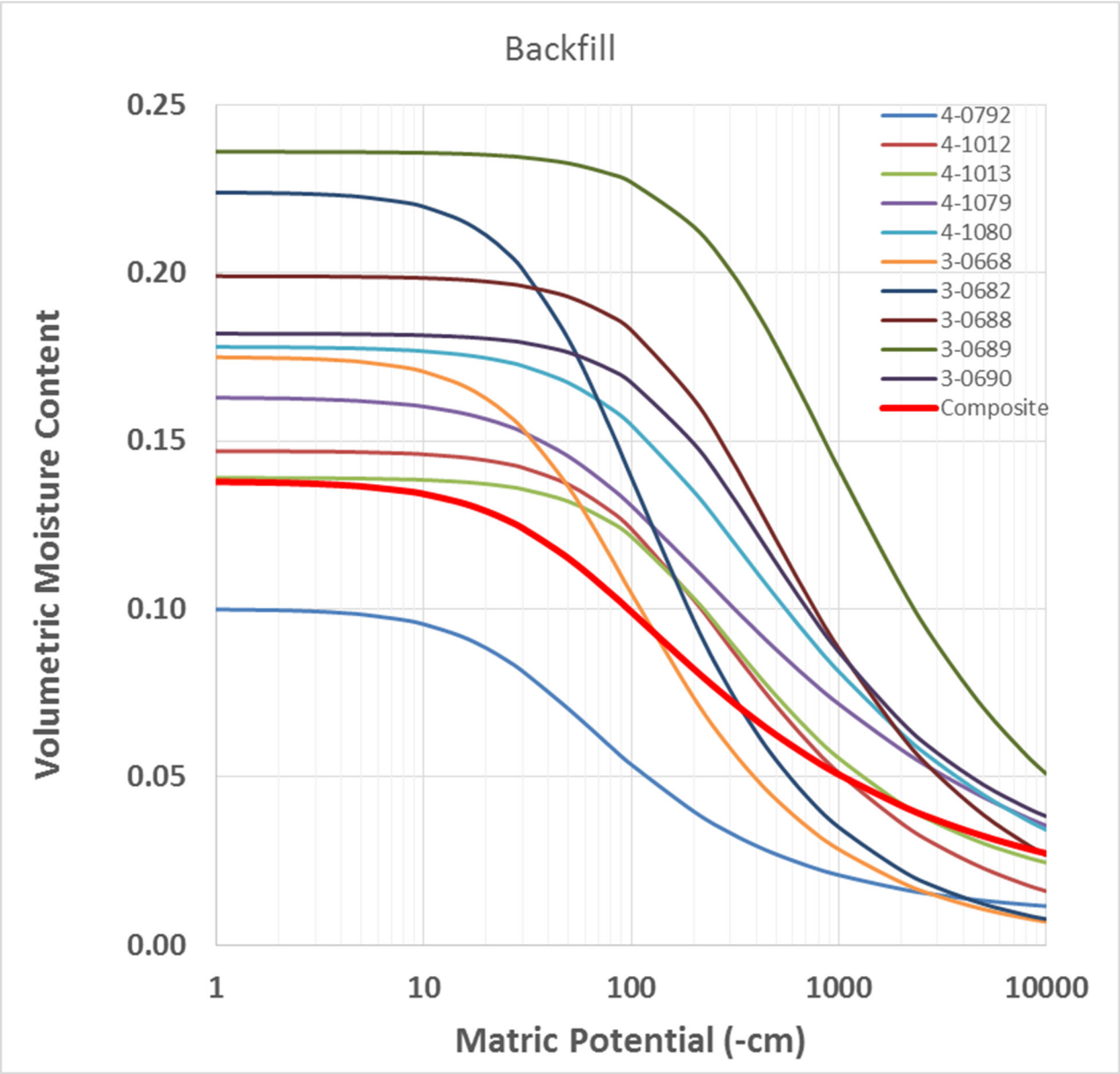

Note that, because of the relatively dry moisture regime, unsaturated media macrodispersivity estimates are expected to be smaller, compared to saturated media estimates. Below, a range of estimates on the basis of numerical simulations (Section B.4.3.1), stochastic theory (Section B.4.3.2) and experimental observations (Section B.4.3.3) is provided. To obtain macrodispersivity, the local pore-scale dispersivities, which are typically small (<1 cm), are not included either in numerical simulations or stochastic solutions. This is consistent with the approach used by other investigators ("Stochastic analysis of adsorbing solute transport in three-dimensional, heterogeneous, unsaturated soils" [Yang et al. 1997]; Gelhar 1993; "Three-Dimensional Stochastic Analysis of Macrodispersion in Aquifers" [Gelhar and Axness 1983]).

Figure B-21. Unsaturated Hydraulic Conductivity Data for Backfill Units (10 Samples). The composite curve is shown in red.

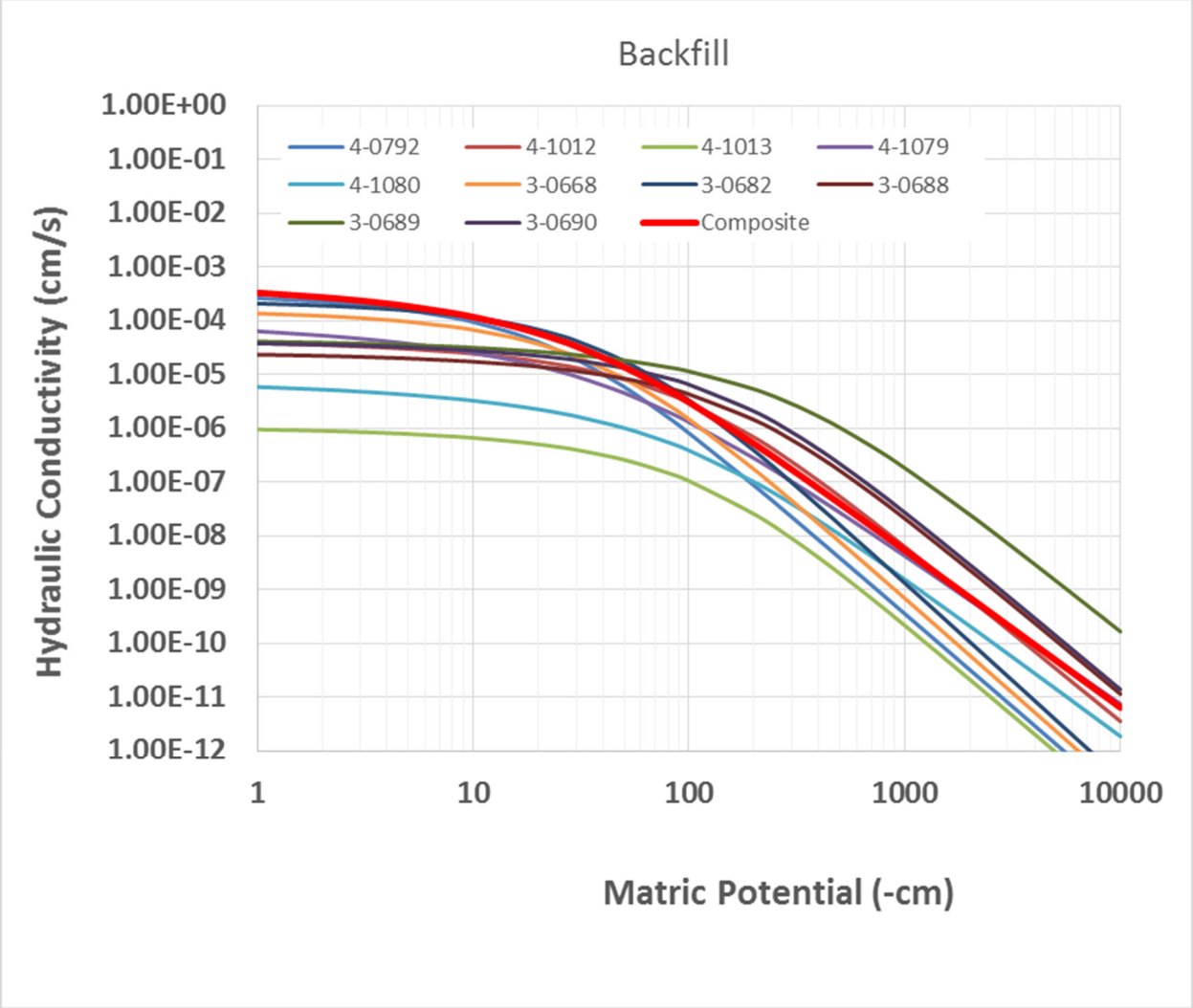

Table B-7. Composite van Genuchten-Mualem Parameters for Waste Management Area C Hydrostratigraphic Units.

Hydrostratigraphic Unit	Number of samples	θ_s	θ_r	α (1/cm)	n	ℓ	Fitted K_s (cm/s)
Backfill Gravelly Unit	10	0.138	0.010	0.021	1.374	0.5	5.60E-04
H1 and H3 Gravelly Units	15	0.171	0.011	0.036	1.491	0.5	7.70E-04
H2 Sand-Dominated Unit	44	0.315	0.0392	0.0631	2.047	0.5	4.15E-03

Table B-8. Simulated Average Tension Ranges for Polmann Anisotropy Model.

Hydrostratigraphic Unit	Simulated Average Tension (cm)
Backfill Gravelly Unit	400 – 750
H1 and H3 Gravelly Units	150 – 400
H2 Sand-Dominated Unit	80 – 300

Figure B-22. Experimental (Triangles) and Fitted Theoretical (Squares) Variogram for Saturated Hydraulic Conductivity (LnK_s).

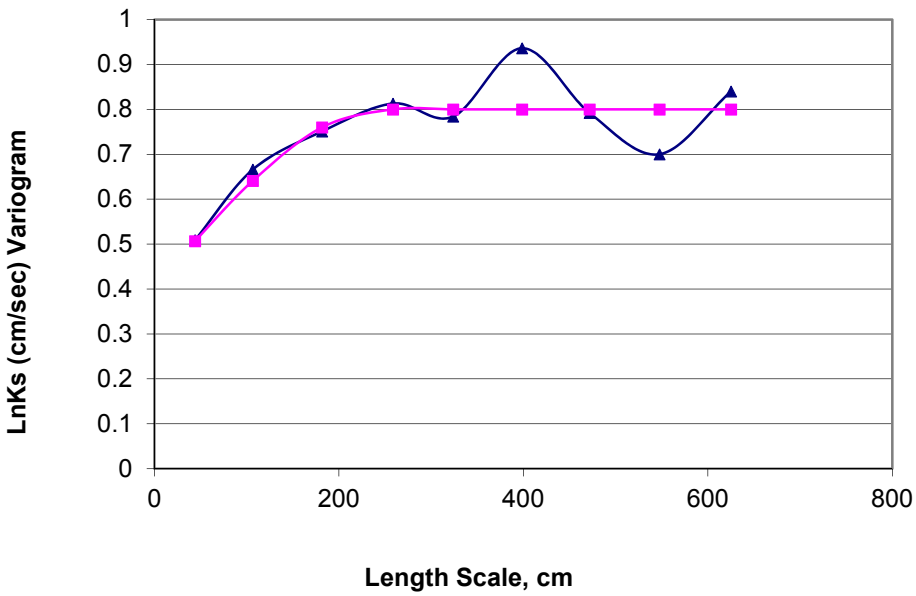

Reference: RPP-20621, "Far-Field Hydrology Data Package for the Integrated Disposal Facility Performance Assessment."

Table B-9. Variable, Macroscopic Anisotropy Parameter Estimates for Various Waste Management Area C Units.

Hydrostratigraphic Unit	Number of samples	$\langle LnK_s \rangle$	$\sigma^2_{LnK_s}$	p	ζ	λ (cm)	A
Backfill Gravelly Unit	10	-14.60	2.98	-2.28E-04	3.53E-04	30	0.00534
H1 and H3 Gravelly Units	17	-12.34	1.41	1.04E-03	2.68E-03	30	0.01249
H2 Sand-Dominated Unit	44	-11.79	2.50	-7.45E-04	3.33E-03	50	0.02415

Figure B-23. Calculated Macroscopic Anisotropy as a Function of Mean Matric Potential for the H2 Sand-Dominated Unit.

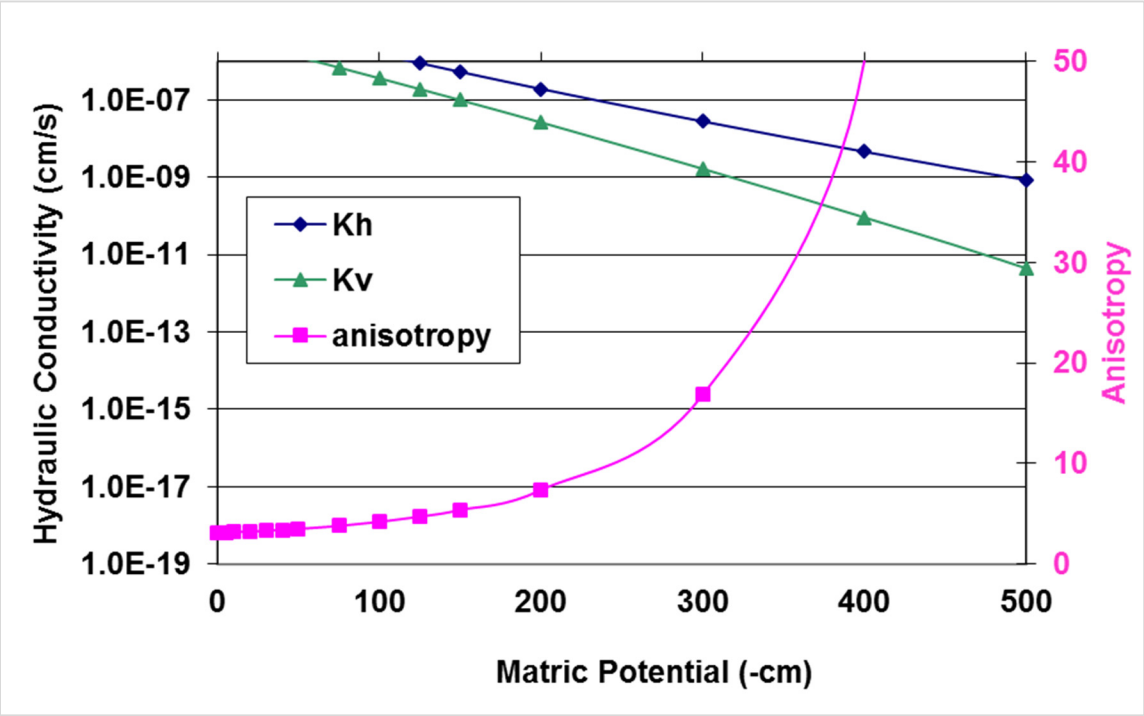

Figure B-24. Calculated Macroscopic Anisotropy as a Function of Mean Matric Potential for the H1 and H3 Gravelly Units.

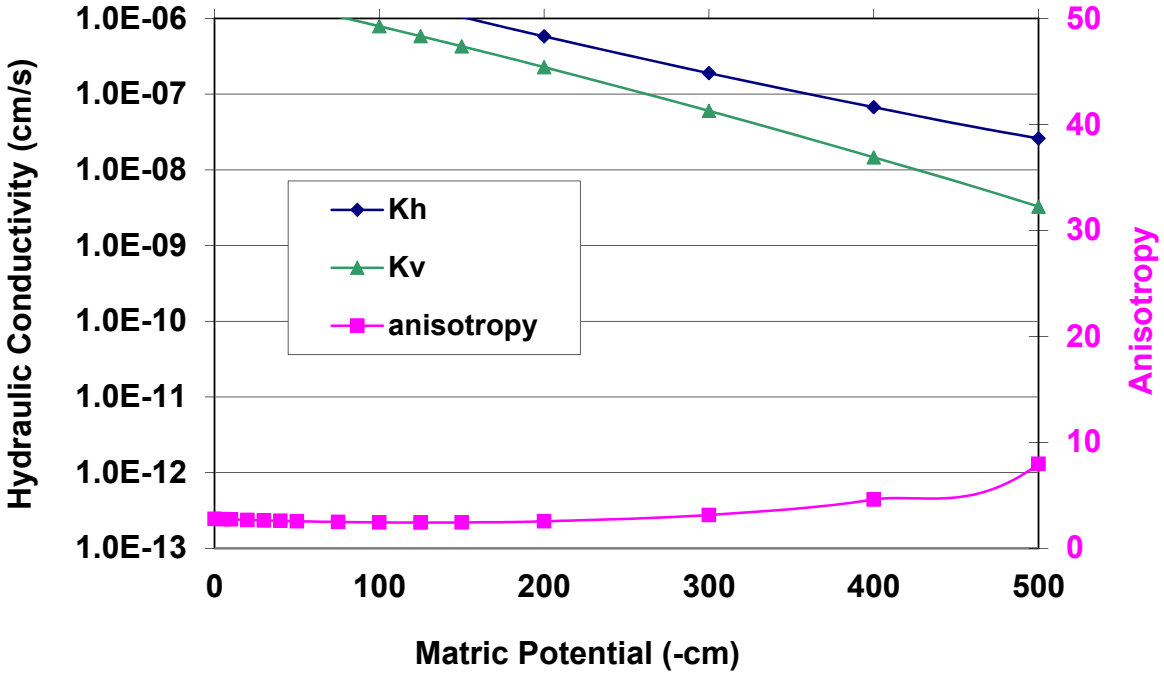

Figure B-25. Calculated Macroscopic Anisotropy as a Function of Mean Matric Potential for Backfill Gravelly Unit.

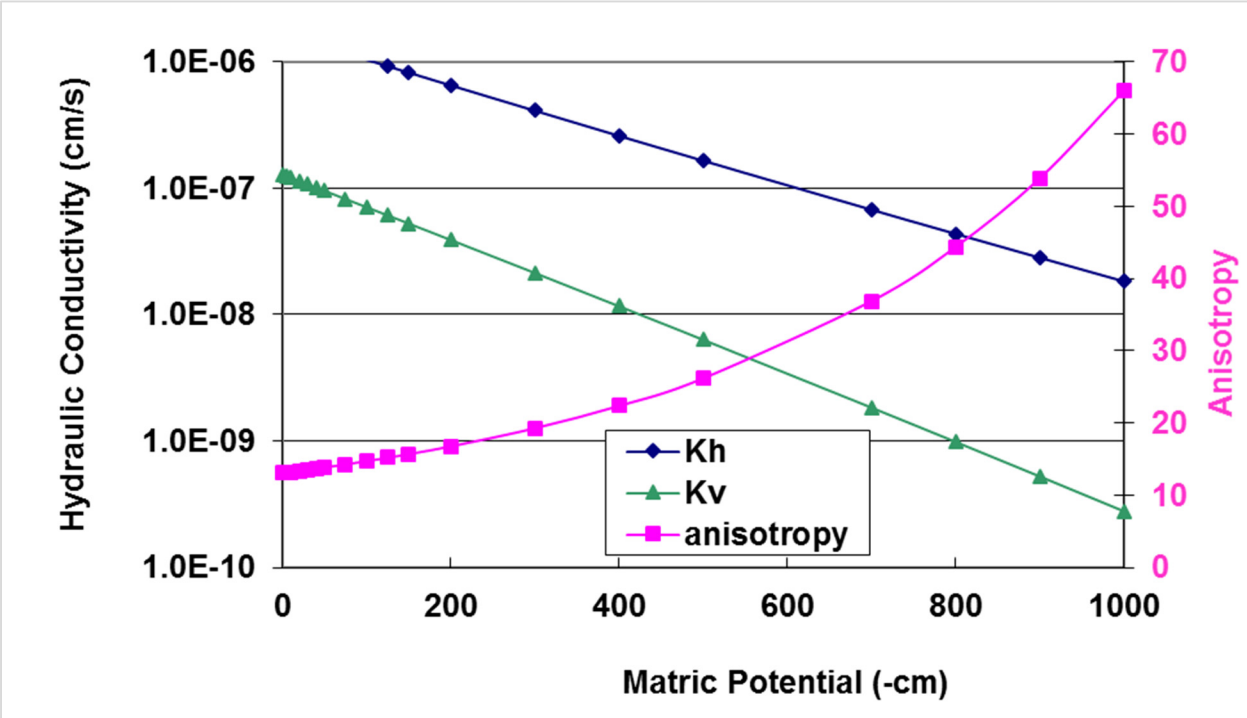

Table B-10. Effective Bulk Density (g/cm^3) Estimates for Waste Management Area C Hydrostratigraphic Units.

Hydrostratigraphic Unit	E[ρ_b]*
Backfill Gravelly Unit	2.13
Hanford H2 Sand-dominated Unit	1.71
Hanford H1 and H3 Gravelly Units	2.05

*E = Expectation.

B.4.3.1 Numerical Simulations. Details of the numerical simulation approach are described in Khaleel et al. (2002). Briefly, Monte Carlo (MC) simulations are used to obtain upscaled (effective) properties. The simulations mimic steady state, gravity infiltration for 50 realizations in two-dimensional (20 m × 20 m) heterogeneous flow regions. Constitutive relations for unsaturated media at the mesh-size scale are based on the van Genuchten-Mualem relationships. A realization of the flow field is shown in Figure B-26. The sediment properties are based on laboratory measurements of moisture retention and unsaturated *K* for coarse-textured sandy samples from the upper Hanford formation (HNF-4769, "Far-Field Hydrology Data Package for Immobilized Low-Activity Tank Waste Performance Assessment"); these data show somewhat less variability when compared to the 44 Hanford formation H2 samples discussed earlier. A unit-mean-gradient approach is used to derive upscaled properties for flow perpendicular to

bedding. For a specified infiltration rate, the simulated pressure head distributions for 50 realizations are averaged to yield a mean pressure head, H. Because the simulated flow field is under a unit mean gradient condition, the infiltration rate is equal to the effective conductivity at the calculated H.

Figure B-26. (a) Ks, (b) α, and (c) n Random Distribution for a Single Realization.

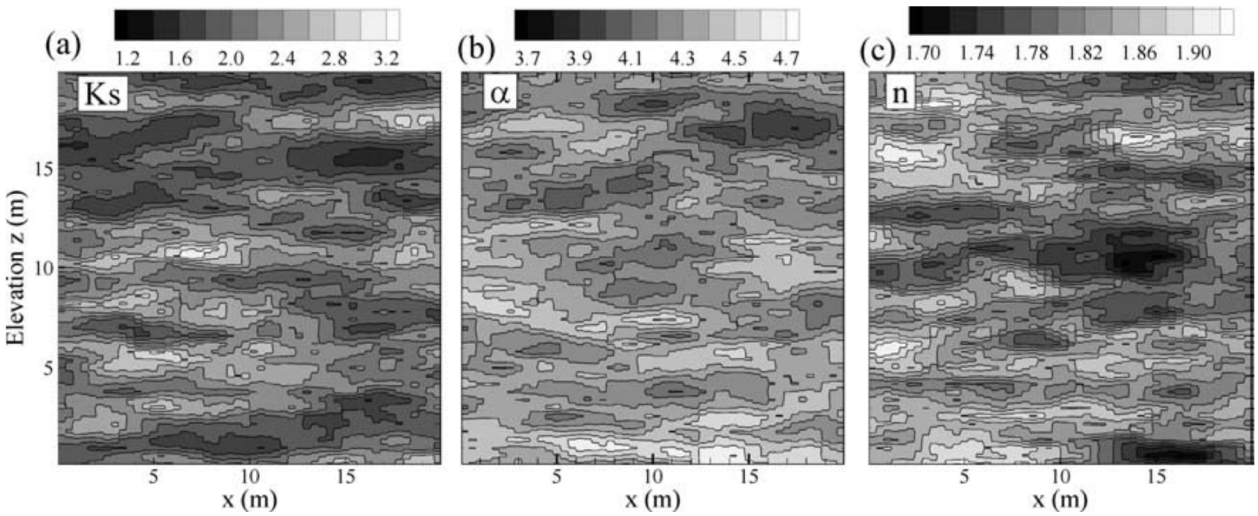

Reference: "Upscaled Flow and Transport Properties for Heterogeneous Unsaturated Media" (Khaleel et al. 2002).

Following flow simulations, macrodispersivities are calculated on the basis of spatial moments of the ensemble-mean plume (Khaleel et al. 2002). For a given steady flow and a prescribed flux, the migration and spread of a slug of simulated tracer is simulated. Snapshots are taken of the two-dimensional plume distribution at different times. The snapshot at each sampling time is then averaged over the length across the flow domain to obtain the solute concentration profiles as a function of depth. The concentration profiles for all realizations are averaged to obtain the ensemble mean profile; these profiles are then used to evaluate their spatial moments. The calculated second spatial moment of the plume about the center of mass (i.e., spatial variance) over time allows estimation of the longitudinal macrodispersivity.

Figures B-27a, B-27b and B-27c are snapshots, for a mean pressure head of -1.0 m, of the simulated plume for a single realization and for flow perpendicular to bedding at 400, 700, and 1,000 days after simulating the release of a conservative tracer across the top boundary of a mildly heterogeneous media (Figure B-26). The averaged concentration profiles for the flow regime and for the corresponding sampling times are illustrated in Figure B-27d. Bedding perpendicular to flow direction enhances lateral mixing and prevents growth of irregular flow paths. Consequently, the averaged concentration profiles for flow perpendicular to bedding (Figure B-27d) exhibit the typical bell-shaped distribution as described by the classical Fickian advection-dispersion equation. The computed longitudinal macrodispersivity for a mean pressure head (H) of -2 m was ~25 cm, ranging from ~15 cm to ~40 cm for the 50 realizations. On the other hand, for a mean H of -20 m, the macrodispersivity was ~100 cm, ranging from ~70 cm to ~130 cm for the 50 realizations. As the MC simulations indicate, considerable variability in longitudinal macrodispersivity estimates is expected depending on the mean matric potential. Nonetheless, results show a clear dependence of longitudinal macrodispersivity on the

moisture regime; longitudinal macrodispersivity estimates are higher for the drier moisture regime.

Figure B-27. Simulated Concentration Distribution for a Single Realization at (a) 400 days, (b) 700 days, and (c) 1,000 days and (d) the Averaged Concentration Profile at Those Times for Flow Perpendicular to Bedding for a Mean Pressure Head (H) of -1 m.

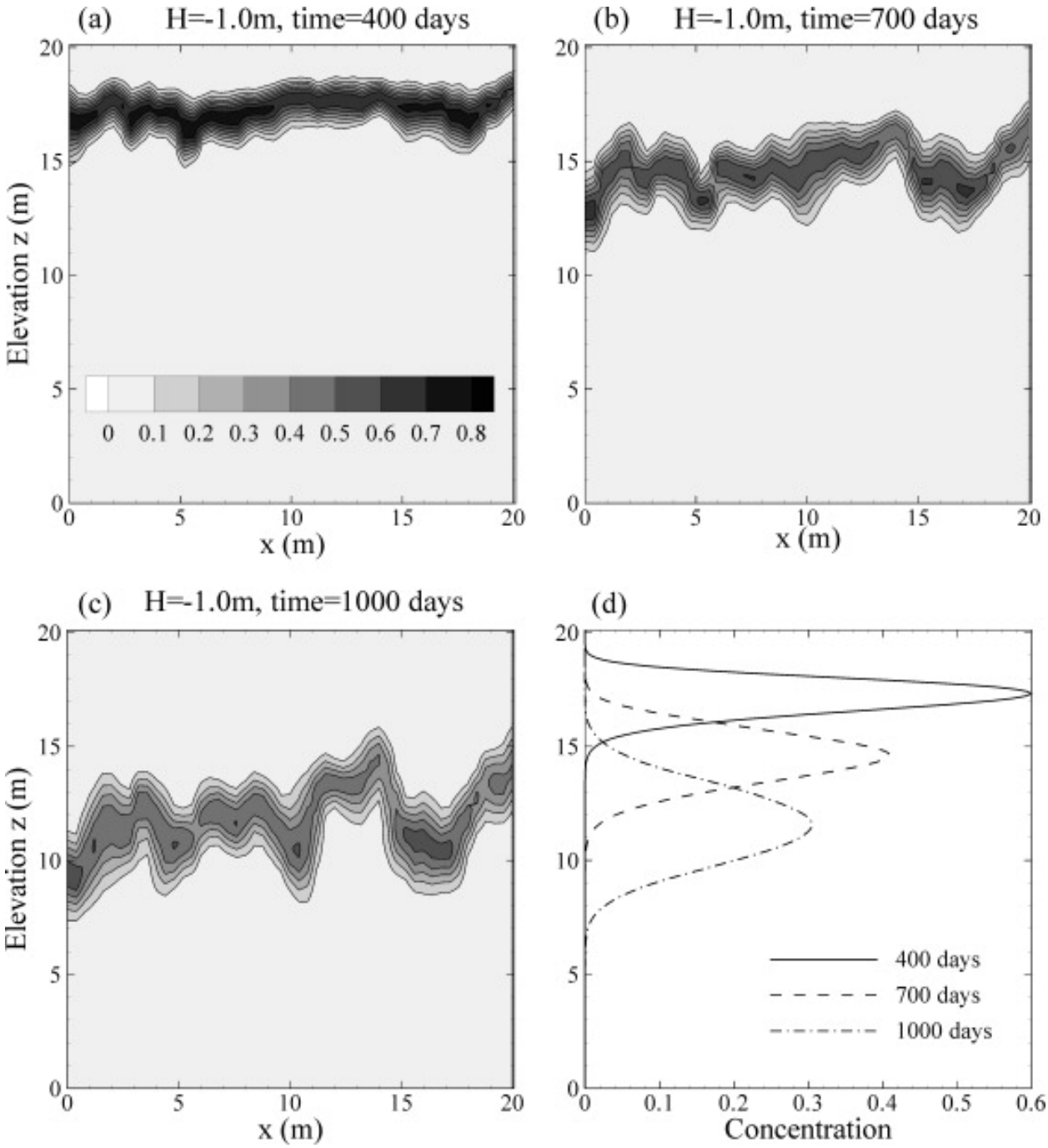

Reference: "Upscaled Flow and Transport Properties for Heterogeneous Unsaturated Media" (Khaleel et al. 2002).

To evaluate directional dependence, simulations were also run for flow parallel to geologic bedding for the same flow domain. Figures B-28a, B-28b, and B-28c are snapshots of the plume at identical times for flow parallel to bedding for the same realization and for H=-1 m; Figure B-28d shows the averaged profile. A comparison of Figures B-27 and B-28 shows that the two-dimensional concentration distribution is more irregular in case of flow parallel to bedding than for flow perpendicular to bedding (Figures B-28a, B-28b, and B-28c versus Figures B-27a, B-27b, and B-27c). Compared with flow perpendicular to bedding, the concentration profiles for flow parallel to bedding are highly skewed and characterized by multiple peaks, and spread out over greater distances, characteristics of a non-Fickian behavior. Thus, while the averaged concentration profiles for flow perpendicular to bedding show "textbook like" Fickian behavior, the averaged profiles for flow parallel to bedding are highly skewed and non-Fickian. At H=-2 m, the computed longitudinal macrodispersivity for flow parallel to bedding is considerably higher (~120 cm) than for flow perpendicular to bedding (~25 cm). For a mean H of -20 m, the macrodispersivity is ~180 cm for flow parallel to bedding versus ~100 cm for flow perpendicular to bedding.

In summary, the numerical results for Hanford H2 sands having mild heterogeneity (HNF-4769) show that the longitudinal dispersivities for flow parallel to bedding are higher than those for flow perpendicular to bedding (Khaleel et al. 2002). For both perpendicular and parallel to bedding, macrodispersivities increase as the mean matric potential becomes more negative. However, the Fickian regime is reached much earlier for cases with flow perpendicular to bedding than parallel to bedding (Khaleel et al. 2002). For WMA C PA modeling, the flow is mostly perpendicular to geologic bedding; nonetheless, the preceding analysis provides estimates in situations where the flow is not necessarily perpendicular to bedding.

B.4.3.2 Stochastic Models. For unsaturated media, in addition to the size of flow domain and media heterogeneities, macrodispersivities are expected to be a function of soil moisture content (or matric potential). Furthermore, as demonstrated via preceding MC simulations, macrodispersivities are larger for flow parallel to bedding than for flow perpendicular to bedding. The following describes two stochastic models to estimate WMA C longitudinal macrodispersivities for flow perpendicular to the geologic bedding.

B.4.3.2.1 Mantoglou Model. Using spectral perturbation techniques (Gelhar and Axness 1983; Gelhar 1993), an approximate equation was derived for macrodispersivities in unsaturated media for flow perpendicular to bedding ("Large-Scale Models of Transient Unsaturated Flow and Contaminant Transport Using Stochastic Methods" [Mantoglou 1984]). Mantoglou showed that the asymptotic value of tension-dependent longitudinal macrodispersivity, $A_{\perp}$ under unit mean gradient condition, for flow perpendicular to bedding, is

$$A_{\perp}(H) = \frac{\sigma^2_{LnK_u}\lambda_u}{\gamma^2} \tag{B-5}$$

where $A_{\perp}$ depends on the mean pressure head H, σ^2_{LnKu} is the variance in log unsaturated K, λ_u is the correlation length scale for unsaturated hydraulic conductivity, and γ is a flow factor that

depends on the direction of mean flow and the orientation of heterogeneity (Gelhar and Axness 1983).

Figure B-28. Simulated Concentration Distribution for a Single Realization at (a) 400 days, (b) 700 days, and (c) 1,000 days and (d) the Averaged Concentration Profile at Those Times for Flow Parallel to Bedding for a Mean Pressure Head (H) of -1 m.

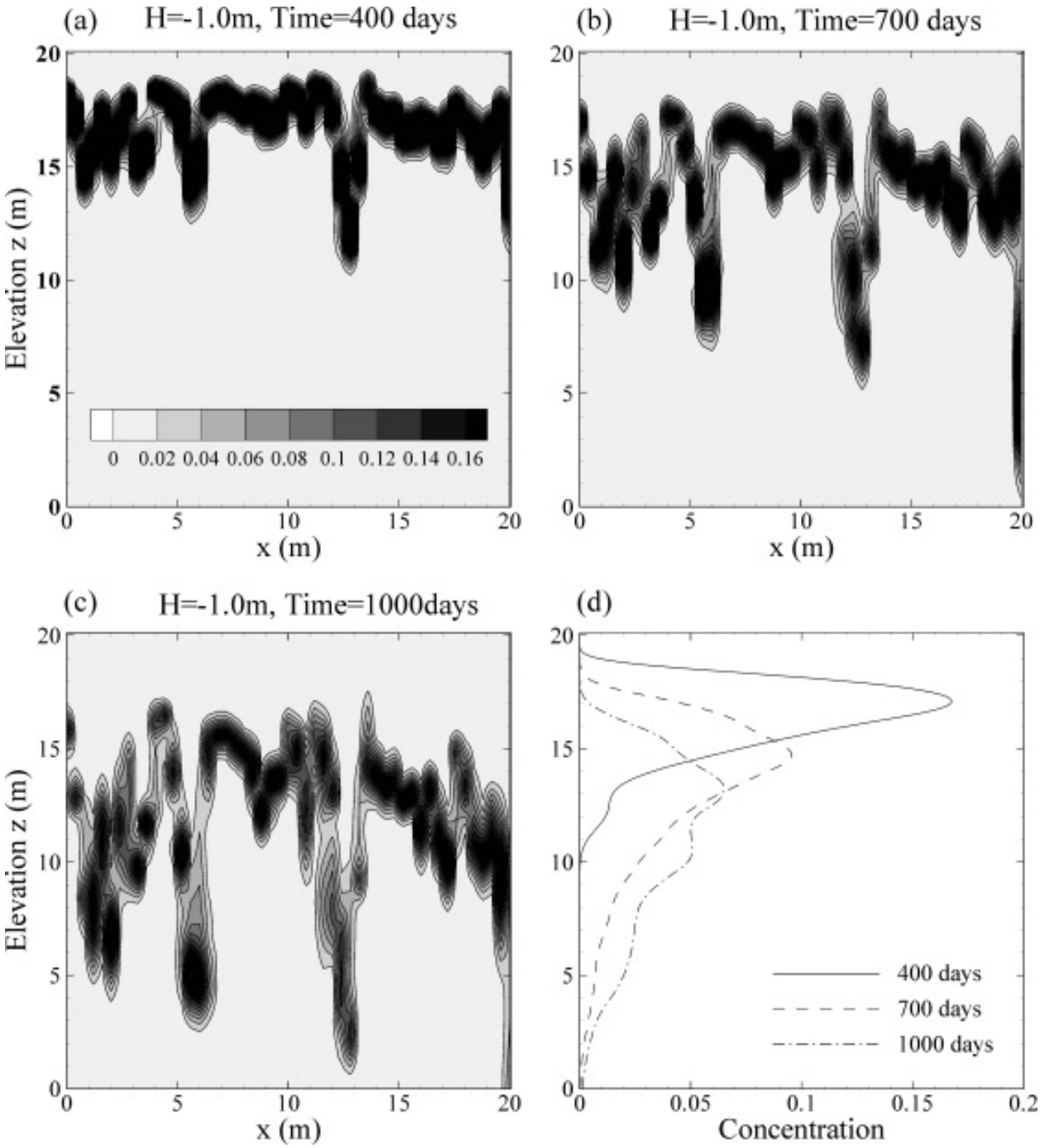

Reference: "Upscaled Flow and Transport Properties for Heterogeneous Unsaturated Media" (after Khaleel et al. 2002).

Equation B-5 represents the asymptotic macrodispersivity estimate for steady-state uniform flow with uniform mean tension. Because macrodispersivity modeled by Equation B-5 is an asymptotic parameter, it applies only when the concentration plume has traveled a large distance in a geologic unit and has encountered numerous heterogeneities in the formation. Furthermore, it is important to note that similar to other stochastic perturbation approaches (Gelhar 1993), the validity of Equation B-5 relies on the variance of hydraulic properties being relatively small (i.e., $\sigma^2_{LnK_u} < 1$).

Mantoglou (1985; Figure 5.9) presents longitudinal macrodispersivity estimates, based on Equation B-5, for Maddock sandy loam ("Spatial Variability of in Situ Unsaturated Hydraulic Conductivity of Maddock Sandy Loam" [Carvallo et al. 1976]) and Panoche silty clay loam ("Spatial Variability of Field-Measured Soil-Water Properties" [Nielsen et al. 1973]) soil types. Mantoglou results show considerable variability even for mild tensions. Based on the Mantoglou model (Equation B-5), for Maddock soil type, the asymptotic longitudinal macrodispersivity was 2.4 m at a mean tension of 50 cm. For Panoche soil type, the estimate was 0.8 m at a mean tension of 300 cm.

B.4.3.2.2 Russo Model. Using the Lagrangian framework in conjunction with the Yeh et al (1985) velocity covariance, theoretical expressions were developed for evolution of contaminant plume spatial moments in unsaturated heterogenous media under steady-state conditions ("Stochastic Analysis of Simulated Vadose Zone Solute Transport in a Vertical Cross Section of Heterogeneous Soil During Nonsteady Water Flow" [Russo 1991]). The spatial moments were then used to assess the preasymptotic evolution of macrodispersivity.

$$A_{zz}(t) = \sigma^2_{LnK_u} \lambda_u \left\{ 1 - 3(2\tau)^{-1} - 3(\tau)^{-2} \exp(-\tau) + 3(\tau)^{-3}[1 - \exp(-\tau)] \right\} \qquad \text{(B-6)}$$

where A_{zz} is the longitudinal macrodispersivity (i.e., similar to $A_\perp$), z denotes vertical direction, t is time, λ_u is vertical correlation length, and $\tau = z_c(t)/\lambda_u$. The unsaturated conductivity variance $\sigma^2_{LnK_u}$ was derived by Russo (1991) using the Gardner (1958) exponential model for unsaturated conductivity. At large times, $\tau \rightarrow \infty$; the longitudinal asymptotic macrodispersivity is therefore

$$A_{zz}(\infty) = \sigma^2_{LnK_u} \lambda_u \,. \qquad \text{(B-7)}$$

Note that this is the same as Mantoglou Equation B-5 without the flow factor γ in the denominator. For hypothetical vadose zone flow domains having $\sigma^2_{LnK_u}$ = 0.29 and extending 15 m and 10 m in the horizontal and vertical directions, respectively, and a correlation length of 0.12 m in the vertical direction, Russo (1991) computed an asymptotic longitudinal macrodispersivity (Equation B-7) of 3.48 cm. As discussed later, the conductivity variance of 0.29 is, however, much smaller compared to variance for Hanford H2 unsaturated conductivity data.

B.4.3.2.3 Stochastic Theory-Based Macrodispersivity Estimates for Waste Management Area C. To apply stochastic Equations B-5 and B-7, an estimate of λ_u for unsaturated K is needed. As discussed earlier, a correlation length of the order of 50 cm was used for saturated conductivity. However, as saturation decreases, an increase in the variance of log unsaturated conductivity is accompanied by a decrease in the correlation scale of log unsaturated K ("Stochastic Modeling of Macrodispersion for Solute Transport in a Heterogeneous Unsaturated Porous Formation" [Russo 1993]). Also, the Equation B-5 flow factor γ (Mantoglou 1984) in a predominantly vertical unsaturated flow through a layered system would be less than 1; it is approximately the ratio of the harmonic and geometric means of unsaturated K (Gelhar 1993; Gelhar and Axness 1983). Assuming a correlation length of 10 cm (approximate measurement scale for small-scale unsaturated K measurements), and γ estimates based on the ratio of the harmonic and geometric means (Khaleel et al. 2002), for H2 sands, Mantoglou's model yields asymptotic macrodispersivity estimates, for flow perpendicular to bedding, that are ~360 cm at relatively low tensions of ~2 m. For the Russo (1991) model (Equation B-7), at ~2 m tension, the asymptotic longitudinal macrodispersivity for H2 sands is ~32 cm. Note that the MC simulations (Khaleel et al. 2002) yielded a longitudinal macrodispersivity of ~25 cm for flow perpendicular to bedding and for H=-2m. However, the favorable comparison with Russo's model is coincidental since σ^2_{LnK} and mean tension values are different.

Reported values have a relatively low tension of 2 m because of the limitation of low perturbation for stochastic models. The variance $\sigma^2_{LnK_u}$ in Equation B-5 becomes rather large for H2 sands; at a mean tension of 1 m, $\sigma^2_{LnK_u}$ is about 1.96, whereas at a tension of 2 m, $\sigma^2_{LnK_u}$ is about 4.73. Compared to H2 sands, $\sigma^2_{LnK_u}$ for the H1/H3/Backfill gravelly units is significantly lower; at a mean tension of 150 cm, $\sigma^2_{LnK_u}$ is about 1.22, whereas at a mean tension of 400 cm, σ^2_{LnK} is about 2.02. Such variance results are consistent with the unsaturated *K* data reported earlier for sandy and gravelly samples (Figure B-17). Unsaturated *K* for gravelly samples fall within a narrow range, and well within the range of measured *K* for sandy samples. At a matric potential of -1 m, the unsaturated *K* for sandy samples ranges over four orders of magnitude, whereas the unsaturated *K* for gravelly samples ranges over two orders of magnitude (Figure B-17).

B.4.3.3 Experimental Data from 200 Areas and Other Sites. Field experiments were conducted at a location in 200 East Area, using potassium chloride as a tracer (RPP-20621 Appendix E, "Hanford Low-Activity Tank Waste Performance Assessment Activity: Determination of in Situ Hydraulic Parameters of the Upper Hanford Formation"). Analysis of the data, using moment analysis, provided dispersivities that ranged from 1.3 cm to 7.8 cm for travel distances ranging from 25 cm to 125 cm. Although these estimates are for the Hanford formation, the transport distance within the vadose zone is indeed of limited extent. Nonetheless, results based on the limited data are consistent with the concept of a scale-dependent dispersivity; it is expected that the asymptotic value will be larger than those based on the small-scale tracer experiment. In fact, extrapolation of the trend line for the data (RPP-20621 Appendix E) suggests that an asymptotic dispersivity estimate of ~1 m is not

unlikely if the heterogeneity at the field site is similar to that of the sandy sediments underlying C Farm, and if the entire sandy sequence of the Hanford formation is treated as EHM.

In addition to the preceding data, results of artificial tracer experiments are available from several arid/semi-arid regions. Two massively instrumented solute transport experiments were performed in desert soils near Las Cruces, New Mexico ("The Las Cruces Trench Site: Characterization, Experimental Results, and One-Dimensional Flow Predictions" [Wierenga et al. 1991]; "The Second Las Cruces Trench Experiment: Experimental Results and Two-Dimensional Flow Predictions" [Hills et al. 1991]). Drip emitters were used to irrigate a plot adjoining a deep trench in heterogeneous media, with well in excess of one order of magnitude standard deviation in saturated hydraulic conductivity. Monitoring of the trench face showed a spatially uniform progression of the wetting front and did not reveal indications of preferential flow (Wierenga et al. 1991). Hills et al. (1991) found that a dispersivity of 5 cm provided reasonably realistic simulations of tritium and bromine tracer distributions.

One additional study ("Chlorine 36 and Tritium From Nuclear Weapons Fallout as Tracers for Long-Term Liquid and Vapor Movement in Desert Soils" [Phillips et al. 1988]) assessed the degree of mixing in desert soils using the conventional advection-dispersion modeling, yielding a dispersion coefficient of 50 cm^2/yr. This compares with the calculated effective diffusion coefficient of 25 cm^2/yr. A similar study ("Evaluation of Liquid and Vapor Water Flow in Desert Soils Based on Chlorine 36 and Tritium Tracers and Nonisothermal Flow Simulations" [Scanlon 1992]) at another southwestern arid site obtained a dispersion coefficient of about 14 cm^2/yr. These, then, lead to effective dispersivities of about 7 cm and 4 cm at the two arid sites, and Peclet numbers (displacement divided by dispersivity) of 23 and 17. In summary, long-term environmental tracer studies at several arid southwestern sites indicate vadose zone dispersivities being less than 10 cm.

Based on a different survey of literature, Gelhar (1993) presented the longitudinal vadose zone dispersivities as a function of the scale of the experiment (Figure B-29). The figure shows sparse data for scales larger than 2 m. Nonetheless, similar to saturated flow (Gelhar et al. 1992), Figure B-29 shows an increase of dispersivity with an increase in scale. Also, shown in Figure B-29 are results of the 200 East Area field experiment (RPP-20621 Appendix E); the trend line dispersivity estimate at a field scale of ~10 m is in close agreement with "Field Scale Transport of Bromide in an Unsaturated Soil, 2. Dispersion Modeling" (Butters and Jury 1989) field data.

B.4.3.4 Recommended Macrodispersivities for Waste Management Area C Performance Assessment. Table B-11 summarizes the macrodispersivity estimates based on results of numerical simulation, stochastic theory, and 200 Areas experimental data. Table B-11 shows that, for H2 sands, estimates are available by all three methods. For the H2 sand unit, for the PA modeling, the recommendation is to use longitudinal macrodispersivity values ranging from 25 cm (based on numerical simulations) to 100 cm (based on field experiments). For H1/H3/Backfill sediments, the recommendation is to use, based on stochastic theory, longitudinal macrodispersivity values ranging from 20 cm to 100 cm. The transverse macrodispersivity is typically much lower; in saturated media, it may range from 1 to 10% of the longitudinal macrodispersivity (Gelhar and Axness 1983). In the absence of unsaturated media

experimental data, the recommendation is to use a transverse macrodispersivity 1/10th of the longitudinal macrodispersivity.

Figure B-29. Longitudinal Laboratory- and Field-Scale Dispersivities in Unsaturated Media as a Function of Overall Problem Scale.

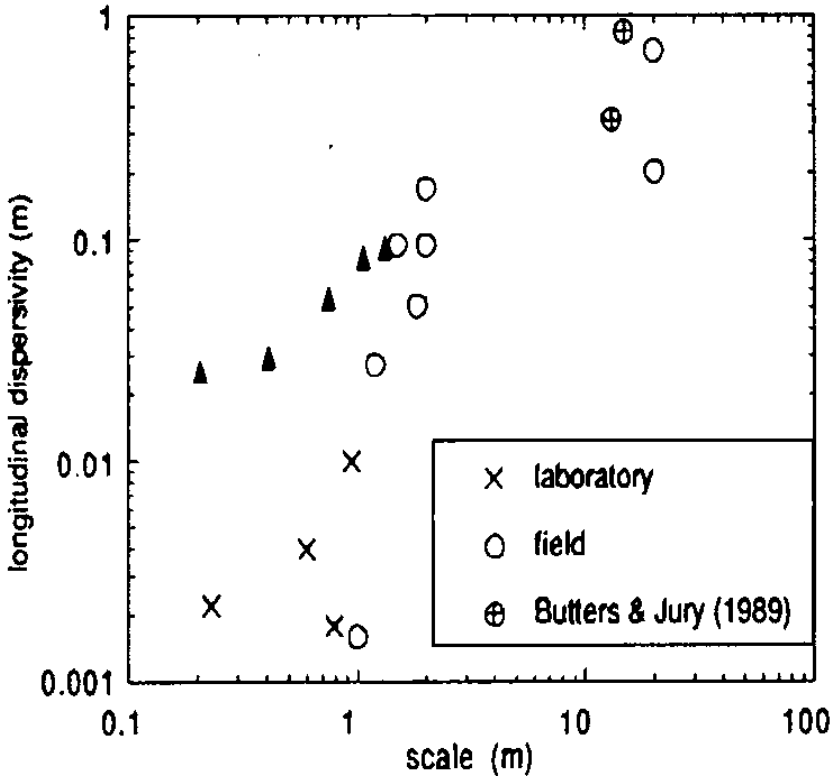

Note: The triangles are data from RPP-20621, "Far-Field Hydrology Data Package for the Integrated Disposal Facility Performance Assessment," Appendix E, "Hanford Low-Activity Tank Waste Performance Assessment Activity: Determination of In Situ Hydraulic Parameters of the Upper Hanford Formation."

References:
"Field Scale Transport of Bromide in an Unsaturated Soil, 2. Dispersion Modeling" (Butters and Jury 1989).
Stochastic Subsurface Hydrology (Gelhar 1993).

Table B-11. Longitudinal Macrodispersivity Estimates (cm).

Hydrostratigraphic Unit	Numerical Simulation	Stochastic Theory (Russo and Mantoglou Equations 5 and 7)	200 Area Field Experiments
H2 Sand-Dominated Unit	25	~32[a] – 360[a]	~100[c]
H1, H3, and Backfill Gravelly Units	NA	~20[b] – 100[b]	NA

[a]Evaluated at a mean tension of 2 m.

[b]Evaluated at a mean tension of 4 m.

[c]Extrapolated experimental data (RPP-20621, "Far-Field Hydrology Data Package for the Integrated Disposal Facility Performance Assessment," Appendix E, "Hanford Low-Activity Tank Waste Performance Assessment Activity: Determination of In Situ Hydraulic Parameters of the Upper Hanford Formation").

NA = Not Available

References:
"Large-Scale Models of Transient Unsaturated Flow and Contaminant Transport Using Stochastic Methods" (Mantoglou 1984).
"Stochastic Analysis of Simulated Vadose Zone Solute Transport in a Vertical Cross Section of Heterogeneous Soil During Nonsteady Water Flow" (Russo 1991).

B.5 REFERENCES

Butters, G. L., and W. A. Jury, 1989, "Field Scale Transport of Bromide in an Unsaturated Soil, 2. Dispersion Modeling," Water Resources Research, Vol. 25, No. 7, pp. 1583–1589.

Carvallo, H. O., D. K. Cassel, J. Hammond, and A. Bauer, 1976, "Spatial Variability of in Situ Unsaturated Hydraulic Conductivity of Maddock Sandy Loam," Soil Science, Vol. 121, pp. 1–8.

Eching, S. O. and J. W. Hopmans, 1993, "Optimization of Hydraulic Functions from Transient Outflow and Soil Water Pressure Data," Soil Science Society of America Journal, Vol. 57, No. 5, pp. 1167–1175.

EPA/600/2-91/065, 1991, The RETC Code for Quantifying the Hydraulic Functions of Unsaturated Soils, Office of Research and Development, U.S. Environmental Protection Agency, Washington, D.C.

Gardner, W. H., 1986, "Water Content," in Methods of Soils Analysis, Part 1—Physical and Mineralogical Methods, pp. 493–544, American Society of Agronomy-Soil Science Society of America, Madison, Wisconsin.

Gardner, W. R., 1958, "Some Steady-State Solutions of the Unsaturated Moisture Flow Equation with Application to Evaporation from a Water Table," Soil Science, Vol. 85, No. 4, pp. 228–232.

Gelhar, L. W., 1993, Stochastic Subsurface Hydrology, Prentice Hall, New York, New York.

Gelhar, L. W. and C. L. Axness, 1983, "Three-Dimensional Stochastic Analysis of Macrodispersion in Aquifers," Water Resources Research, Vol. 19, No. 1, pp. 161–180.

Gelhar, L. W., C. Welty, and K. R. Rehfeldt, 1992, "A Critical Review of Data on Field-Scale Dispersion in Aquifers," Water Resources Research, Vol. 28, No. 7, pp. 1955–1974.

HNF-4769, 1999, "Far-Field Hydrology Data Package for Immobilized Low-Activity Tank Waste Performance Assessment," Rev. 1, Fluor Daniel Northwest, Richland, Washington.

Hills, R. G., P. J. Wierenga, D. B. Hudson, and M. R. Kirkland, 1991, "The Second Las Cruces Trench Experiment: Experimental Results and Two-Dimensional Flow Predictions," Water Resources Research, Vol. 27, No. 10, pp. 2707–2718.

Jury, W. A. and R. Horton, 2004, Soil Physics, 6th edition, Wiley and Sons, Inc., New York, New York.

Khaleel, R. and J. F. Relyea, 1997, "Correcting laboratory-measured moisture retention data for gravels," Water Resources Research, Vol. 33, No. 8, pp. 1875–1878.

Khaleel, R. and J. F. Relyea, 2001, "Variability of Gardner's α for coarse-textured sediments," Water Resources Research, Vol. 37, No. 6, pp. 1567–1575.

Khaleel, R., J. F. Relyea and J. L. Conca, 1995, "Evaluation of van Genuchten-Mualem relationships to estimate unsaturated hydraulic conductivity at low water contents," Water Resources Research, Vol. 31, No. 11, pp. 2659–2668.

Khaleel, R., T.-C. J. Yeh, and Z. Lu, 2002, "Upscaled Flow and Transport Properties for Heterogeneous Unsaturated Media," Water Resources Research, Vol. 38, No. 5, pp. 11.1–11.12.

Klute, A., 1986, "Water Retention: Laboratory Methods," in Methods of Soil Analysis, Part 1—Physical and Mineralogical Methods, pp. 635–660, American Society of Agronomy-Soil Science Society of America, Madison, Wisconsin.

Klute, A. and C. Dirksen, 1986, "Hydraulic Conductivity and Diffusivity: Laboratory Methods," in Methods of Soil Analysis, Part 1—Physical and Mineralogical Methods, pp. 687–734, American Society of Agronomy-Soil Science Society of America, Madison, Wisconsin.

Mantoglou, A., 1984, "Large-Scale Models of Transient Unsaturated Flow and Contaminant Transport Using Stochastic Methods," Ph.D. Thesis, Massachusetts Institute of Technology, Department of Civil Engineering, Cambridge, Massachusetts.

Mantoglou, A. and L. W. Gelhar, 1987, "Stochastic Modeling of Large-Scale Transient Unsaturated Flow Systems," Water Resources Research, Vol. 23, No. 1, pp. 37–46.

McCord, J. T., D. B. Stephens, and J. L. Wilson, 1991, "Hysteresis and State-Dependent Anisotropy in Modeling Unsaturated Hillslope Hydrologic Processes," Water Resources Research, Vol. 27, No. 7, pp. 1501–1518.

Millington, R. J. and J. P. Quirk, 1961, "Permeability of Porous Solids," Transactions of the Faraday Society, Vol. 57, pp. 1200–1207.

Mualem, Y., 1976, "A New Model for Predicting the Hydraulic Conductivity of Unsaturated Porous Media," Water Resources Research, Vol. 12, No. 3, pp. 513–522.

Nielsen, D. R., J. M. Biggar, and K. T. Erh, 1973, "Spatial Variability of Field-Measured Soil-Water Properties," Hilgardia, Vol. 42, No. 7, pp. 215–260.

NUREG/CR-5965, 1994, Modeling Field Scale Unsaturated Flow and Transport Processes, Nuclear Regulatory Commission, Washington, D.C.

NUREG/CR-6114, 1994, Auxiliary Analyses in Support of Performance Assessment of a Hypothetical Low-Level Waste Facility: Groundwater Flow and Transport Simulation, Vol. 3, U.S. Nuclear Regulatory Commission, Washington, D.C.

Phillips, F. M., J. L. Mattick, T. A. Duval, D. Elmore, and P. W. Kubik, 1988, "Chlorine 36 and Tritium From Nuclear Weapons Fallout as Tracers for Long-Term Liquid and Vapor Movement in Desert Soils," Water Resources Research, Vol. 24, No. 11, pp. 1877–1891.

PNNL-13795, 2000, "Vadose Zone Transport Field Study: Soil Water Content Distributions by Neutron Moderation," Pacific Northwest National Laboratory, Richland, Washington.

PNNL-14284, 2003, "Laboratory Measurements of the Unsaturated Hydraulic Properties at the Vadose Zone Transport Field Site," Pacific Northwest National Laboratory, Richland, Washington.

PNNL-15503, 2008, "Characterization of Vadose Zone Sediments Below the C Tank Farm: Borehole C4297 and RCRA Borehole 299-E27-22," Rev. 1, Pacific Northwest National Laboratory, Richland, Washington.

PNNL-17154, 2008, "Geochemical Characterization Data Package for the Vadose Zone in the Single-Shell Tank Waste Management Areas at the Hanford Site," Pacific Northwest National Laboratory, Richland, Washington.

Polmann, D. J., 1990, "Application of Stochastic Methods to Transient Flow and Transport in Heterogeneous Unsaturated Soils," Ph.D. Thesis, Massachusetts Institute of Technology, Department of Civil Engineering, Cambridge, Massachusetts.

Resource Conservation and Recovery Act of 1976, 42 USC 6901, et seq.

RHO-ST-46P, 1984, "Field Calibration of Computer Models for Application to Buried Liquid Discharges: A Status Report," Rockwell Hanford Operations, Richland, Washington.

RPP-20621, 2004, "Far-Field Hydrology Data Package for the Integrated Disposal Facility Performance Assessment," Rev. 0, CH2M HILL Hanford Group, Inc., Richland, Washington.

RPP-20621, 2004, "Far-Field Hydrology Data Package for the Integrated Disposal Facility Performance Assessment," Appendix E, "Hanford Low-Activity Tank Waste Performance Assessment Activity: Determination of In Situ Hydraulic Parameters of the Upper Hanford Formation," Rev. 0, CH2M HILL Hanford Group, Inc., Richland, Washington.

RPP-CALC-60450, 2016, "Process for Determining the Volumetric Moisture Content for the Vadose Zone Geologic Units Underlying Waste Management Area," Rev. 0, Washington River Protection Solutions, LLC, Richland, Washington.

RPP-CALC-60452, 2016, "Moisture Dependent Anisotropy Calculations Supporting WMA C PA," Rev. 0, Washington River Protection Solutions, LLC, Richland, Washington.

Russo, D., 1991, "Stochastic Analysis of Simulated Vadose Zone Solute Transport in a Vertical Cross Section of Heterogeneous Soil During Nonsteady Water Flow," Water Resources Research, Vol. 27, No. 3, pp. 267–283.

Russo, D., 1993, "Stochastic Modeling of Macrodispersion for Solute Transport in a Heterogeneous Unsaturated Porous Formation," Water Resources Research, Vol. 29, No. 2, pp. 383–397.

Scanlon, B. R., 1992, "Evaluation of Liquid and Vapor Water Flow in Desert Soils Based on Chlorine 36 and Tritium Tracers and Nonisothermal Flow Simulations," Water Resources Research, Vol. 28, No. 1, pp. 285–297.

Stephens, D. B., and S. Heermann, 1988, "Dependence of Anisotropy on Saturation in a Stratified Sand," Water Resources Research, Vol. 24, No. 5, pp. 770–778.

van Genuchten, M. Th., 1980, "A Closed-form Equation for Predicting the Hydraulic Conductivity of Unsaturated Soils," Soil Science Society of America Journal, Vol. 44, No. 5, pp. 892–898.

WHC-IP-0635, 1991, "Geotechnical Engineering Procedure Manual," Vols. 1 and 2, Westinghouse Hanford Company, Richland, Washington.

WHC-SD-WM-EE-004, 1995, "Performance Assessment of Grouted Double-Shell Tank Waste Disposal at Hanford," Rev. 1, Westinghouse Hanford Company, Richland, Washington.

Wierenga, P. J., R. G. Hills, and D. B. Hudson, 1991, "The Las Cruces Trench Site: Characterization, Experimental Results, and One-Dimensional Flow Predictions," Water Resources Research, Vol. 27, No. 10, pp. 2695–2705.

Yang, J., R. Zhang, J. Wu, and M. B. Allen, 1997, "Stochastic analysis of adsorbing solute transport in three-dimensional, heterogeneous, unsaturated soils," Water Resources Research, Vol. 33, No. 3, pp. 1947–1956.

Ye, M., R. Khaleel, and T.-C. J. Yeh, 2005, "Stochastic analysis of moisture plume dynamics of a field injection experiment," Water Resources Research, Vol. 41, W03013, pp. 1–13.

Yeh, T.-C. J., and D. J. Harvey, 1990, "Effective Unsaturated Hydraulic Conductivity of Layered Sands," Water Resources Research, Vol. 26, No. 6, pp. 1271–1279.

Yeh, T.-C. J., L. W. Gelhar and A. L. Gutjahr, 1985, "Stochastic Analysis of Unsaturated Flow in Heterogeneous Soils, 2. Statistically Anisotropic Media with Variable α," Water Resources Research, Vol. 21, No. 4, pp. 457–464.

Yeh, T.-C. J., M. Ye, and R. Khaleel, 2005, "Estimation of effective unsaturated hydraulic conductivity tensor using spatial moments of observed moisture plume," Water Resources Research, Vol. 41, W03014, pp. 1–12.

Zhang, Z. F. and R. Khaleel, 2010, "Simulating field-scale moisture flow using a combined power-averaging and tensorial connectivity-tortuosity approach," Water Resources Research, Vol. 46, W09505, pp. 1–14.

This page intentionally left blank.

APPENDIX C

TECHNICAL BASIS FOR WASTE MANAGEMENT AREA C UNCONFINED AQUIFER CONCEPTUAL MODEL: FIELD DATA AND RELATED INVESTIGATIONS

This page intentionally left blank.

TABLE OF CONTENTS

APPENDIX C – TECHNICAL BASIS FOR WASTE MANAGEMENT AREA C UNCONFINED AQUIFER CONCEPTUAL MODEL: FIELD DATA AND RELATED INVESTIGATIONS C-1

C.1 HIERARCHY OF LENGTH SCALES AND SCALE DEPENDENCE OF MEDIA PROPERTIES C-2

C.2 HYDROGEOLOGIC CONDITIONS AND STRUCTURE C-3

C.2.1 Paleochannel Configuration and Flow Paths C-4

C.2.2 Theoretical Basis for Hydraulic Conductivity Estimates of Paleochannel Sediments C-6

C.3 ESTIMATES OF UNCONFINED AQUIFER FLOW AND TRANSPORT PROPERTIES C-7

C.3.1 Groundwater Flow Velocities and Fluxes C-7

C.3.2 Hydraulic Conductivity of Unconfined Aquifer Sediments C-8

C.3.3 Groundwater Flow Directions and Hydraulic Gradients C-12

C.3.4 Anisotropy C-16

C.3.5 Properties for Contaminant Transport C-16

C.4 UNCONFINED AQUIFER FLOW AND TRANSPORT PROPERTIES USED IN THE WASTE MANAGEMENT AREA C PERFORMANCE ASSESSMENT C-21

C.4.1 Flow Properties C-21

C.4.2 Contaminant Transport Properties C-23

C.5 DEVELOPMENT OF UNCERTAINTY IN GROUNDWATER FLUX AND MACRODISPERSIVITY FOR SATURATED ZONE C-23

C.6 REFERENCES C-25

LIST OF FIGURES

Figure C-1. Schematic Illustrating Scale in a Heterogeneous Media and Scale Dependence of Saturated Hydraulic Conductivity. C-2

Figure C-2. Interpreted Extent of a Paleochannel Associated with the Ancestral Columbia River in 200 East Area in the Vicinity of Waste Management Area C. C-5

Figure C-3. Digital Photo Log for Borehole 299-E27-4 with an Expansion Showing the Open Framework Gravel below the Water Table. C-9

Figure C-4. (a) An Idealized Hexagonal Model Approximation of Open-Framework Gravelly Media, and (b) Representative Flow Regions used to Determine Equivalent Hydraulic Conductivity. C-10

Figure C-5. Plan View of the Central Plateau Groundwater Model Representing the Aquifer and the Volumetric Flux Calculation Window in the Vicinity of Waste Management Area C. C-13

Figure C-6. Hanford Formation Saturated Hydraulic Conductivity Estimates Based on Slug Tests, Pump Tests, and Model Calibration. C-14

Figure C-7. Borehole Log of Well 299-E27-22. ..... C-15

Figure C-8. Pacific Northwest National Laboratory Site-Wide Model Calibration of Hydraulic Conductivity of the Unconfined Aquifer with the Location of Waste Management Area C and Magnitude of Hydraulic Conductivity Indicated. C-16

Figure C-9. Central Plateau Groundwater Model Layer Discretization In the Saturated Zone and Extent of Various Hydrostratigraphic Units within the Model Layer in the Vicinity of Waste Management Area C (shown by the Rectangle). C-17

Figure C-10. Longitudinal Macrodispersivity in Saturated Media as a Function of Overall Problem Scale with Data Classified by Reliability. C-19

Figure C-11. Central Plateau Groundwater Model Calibration Results in the Vicinity of Waste Management Area C. C-22

Figure C-12. Low-Gradient Low-Level Waste Management Area 1 Monitoring Network Results. C-24

LIST OF TABLES

Table C-1. Calculation of Weighted Average Hydraulic Conductivity Value and Volumetric Water Flux from the Central Plateau Groundwater Model. C-18

Table C-2. Relationship Between Saturated Longitudinal Macrodispersivity (α_L) and Scale of Measurement (L_s). C-20

Table C-3. Triangular Distribution of Aquifer Flux and Proportional Hydraulic Conductivity Values Applicable to the Uncertainty Analysis. C-25

LIST OF TERMS

CCu	Cold Creek unit
CPGWM	Central Plateau Groundwater Model
EHM	equivalent homogeneous medium
FY	fiscal year
HSU	hydrostratigraphic unit
LLWMA	Low-Level Waste Management Area
PA	Performance Assessment
RCRA	Resource Conservation and Recovery Act of 1976
STOMP	Subsurface Transport Over Multiple Phases
TC&WM EIS	Tank Closure and Waste Management Environmental Impact Statement
WMA	Waste Management Area

APPENDIX C

TECHNICAL BASIS FOR WASTE MANAGEMENT AREA C UNCONFINED AQUIFER CONCEPTUAL MODEL: FIELD DATA AND RELATED INVESTIGATIONS

The groundwater pathway analysis is an important aspect of the Waste Management Area C (WMA C) Performance Assessment (PA). As the contaminant mass flux arriving from the vadose zone enters the aquifer, it mixes with the groundwater and undergoes dilution, dispersion, and retardation while traveling along the flow path. The amount of dilution is strongly dependent on the ratio of volumetric groundwater flux to contaminant mass flux within the mixing zone. However, groundwater flux is not ordinarily a measurable quantity. Instead, it is inferred from hydraulic head measurements and from hydraulic properties of the aquifer (i.e., estimates of the hydraulic gradients and hydraulic conductivities), which are deduced from a variety of measurement methods, such as pump and slug tests, or derived from inverse modeling of the aquifer to estimate conductivity from measured head values.

Past and present measured field data (hydraulic heads) in observation boreholes in the vicinity of WMA C must be used carefully as the region is recovering from the effects of both surface (ponds, cribs, trenches, and ditches) and subsurface (leaking pipelines, leaking tanks, and injection wells) liquid discharges from Hanford operations for many years. Groundwater mounding continues to dissipate to an equilibrium condition that is likely to be similar to the pre-Hanford operations condition (see Section 3.1.5.4.2 and Figure 3-35). As a result, the post-closure position of the water table, and its hydraulic gradient, can only be estimated through evaluating the current water table and forecasting the anticipated changes. Modeling is a critical tool in this evaluation, as it can be used to estimate both the hydraulic gradient and the recovery of hydraulic heads from the operational liquid discharges. Consequently, this analysis uses modeling tools to calculate the future groundwater flux, based on aquifer hydraulic properties and the projected hydraulic gradient.

This appendix provides a detailed assessment and evaluation of saturated media field data used to estimate the aquifer hydraulic properties, including saturated hydraulic conductivity, groundwater fluxes, and hydraulic gradients, and specifies the technical basis for parameter selection and use in the WMA C PA modeling. Included in this assessment/evaluation is the following:

- A brief review of scale dependence of saturated media parameters (Section C.1)
- A brief overview of the hydrogeologic conditions pertinent to WMA C (Section C.2)
- A summary of measured and theoretically-estimated aquifer hydraulic parameter estimates available for the areas near WMA C (Section C.3)
- A summary of how this information is used for the PA (Section C.4), including a discussion of the sensitivity and uncertainties of groundwater flux and flow parameters used in the PA (Section C.5).

C.1 HIERARCHY OF LENGTH SCALES AND SCALE DEPENDENCE OF MEDIA PROPERTIES

A variety of methods exist which can be used to estimate hydraulic conductivity, including permeameter cells, slug tests, pump tests, and model calibration. In general, estimates of saturated hydraulic conductivity, either inferred by aquifer testing or determined from calibrated models, tend to increase as the scale of the flow domain increases (e.g., U.S. Geological Survey Water-Supply Paper 2237, "Regional Flow in the Dakota Aquifer: A Study of the Role of Confining Layers"). The evolving heterogeneities at various length scales result in a scale dependence of effective parameters such as saturated hydraulic conductivity ("An Analysis Platform for Multiscale Hydrogeologic Modeling with Emphasis on Hybrid Multiscale Methods" [Scheibe et al. 2015]). For WMA C PA saturated media modeling, the flow domain size of interest is shown on the right side of Figure C-1, with the characteristic length scale for flow and transport on the order of hundred meters. As the length scale of observation increases, the effective properties increase in discretely hierarchical stages or evolve continuously (Scheibe et al. 2015). The effects of large-scale heterogeneity on flow and determination of media properties can therefore be inferred most effectively by using regional scale groundwater models.

Figure C-1. Schematic Illustrating Scale in a Heterogeneous Media and Scale Dependence of Saturated Hydraulic Conductivity.

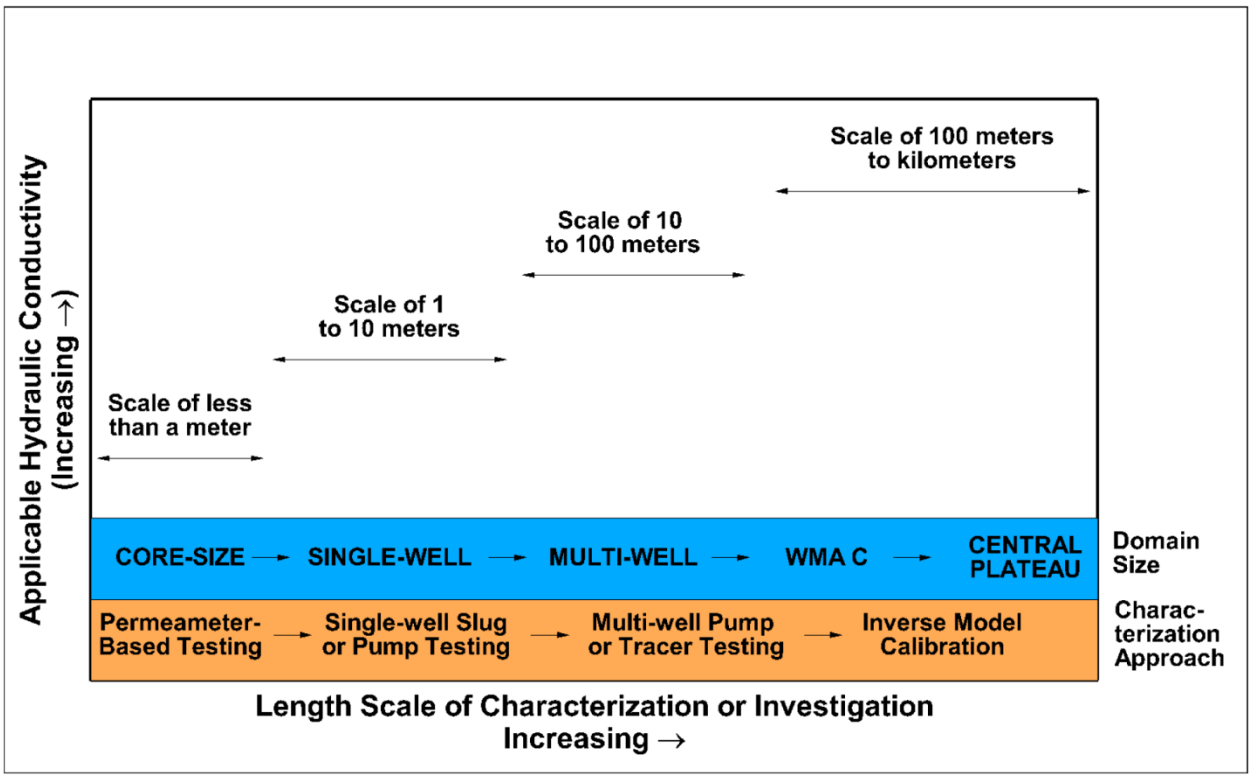

WMA = Waste Management Area

Determining effective hydraulic conductivities applicable to the field scale appears to be best evaluated using inverse modeling conditioned by available data, using appropriate boundary

conditions. Measurements of hydraulic conductivity appear to be dependent on the test scale, and increase as the scale increases, particularly in heterogeneous media ("Scale Dependency of Hydraulic Conductivity Measurements" [Rovey and Cherkauer 1995]; "Scale Dependency of Hydraulic Conductivity in Heterogeneous Media" [Schulze-Makuch et al. 1999]). In-situ measures of aquifer flow and hydraulic properties inferred from hydraulic testing represent relatively small areas (Figure C-1) compared to the overall scale and dimensions of the model domain, and therefore do not provide representative results appropriate for the field scale ("Use and Measurement of Mass Flux and Mass Discharge" [ITRC 2010]). Similarly, individual well-based slug and pump tests provide information at a relatively small scale, albeit larger than core-scale permeameter tests. Permeameter, slug, and pump tests are also limited in their ability to quantify spatial averages or trends, and are less likely to produce central measures of flow magnitudes than a regional model (ITRC 2010). Field estimates for saturated hydraulic conductivity based on slug tests, for example, provide estimates of hydraulic representation at a scale of meters and are not considered generally appropriate to be used directly in the modeling, even though slug and pumping test data are important input for model calibration (ITRC 2010).

Consequently, in evaluating available information for the aquifer at WMA C, hydraulic conductivities derived from a calibrated model are regarded as more reliable than direct measurements by permeameter, slug, or pump tests. This distinction is important because, as Section C.2 will show, substantially different values for hydraulic conductivity have been estimated by various investigators using different methods.

C.2 HYDROGEOLOGIC CONDITIONS AND STRUCTURE

To understand the groundwater flow conditions in the vicinity of WMA C, and in particular the large-scale saturated hydraulic conductivity and hydraulic gradient, it is important to note the regional geology and the hydrogeologic conditions and geologic structure in the 200 Areas. Groundwater in the unconfined aquifer at Hanford generally flows from recharge areas in the elevated region near the western boundary of the Hanford Site, toward the Columbia River on the eastern and northern boundaries. The Columbia River is the primary discharge area for the unconfined aquifer.

The unconsolidated sediments of the present-day Central Plateau reflect deposits of the ancient Columbia River, and the Pleistocene cataclysmic flooding (Section 3.1.4 and 3.1.9 provide a detailed discussion of the regional and local geology that is not repeated here). Briefly, WMA C lies on the northern flank of the Cold Creek bar, a large compound flood bar formed during Pleistocene cataclysmic flooding, which last occurred about 15,000 years ago (On the Trail of the Ice Age Floods: A Geological Field Guide to the Mid-Columbia Basin [Bjornstad 2006]). The cataclysmic floods caused repeated large erosional and depositional events, which have significantly shaped the Central Plateau and the present WMA C geology. Erosion by Ice-Age flooding and the ancestral Columbia River are believed to have removed much of the Ringold Formation from the area and created a highly transmissive paleochannel. The cataclysmic floods deposited into the channel the gravel-dominated facies of the Hanford formation that consist of coarse-grained basaltic sand and granule- to boulder-size gravel displaying an open framework. These large-scale features significantly influence groundwater flow and plume migration because

the deposits in the channel are much more transmissive than those outside of the channel. The groundwater flow direction in the unconfined aquifer in the vicinity of WMA C trends toward the southeast. This conclusion is based on the following: 1) slightly higher hydraulic heads to the northwest, 2) the orientation of the southeast trending paleochannel in the area, and 3) the configuration of the major contamination plumes.

C.2.1 Paleochannel Configuration and Flow Paths

As discussed above, the paleochannel has a significant influence on flow and contaminant transport under WMA C. The open-framework gravels of the paleochannel are highly conductive, and as such constitute a potential fast pathway for migration of contaminants. It is therefore important to characterize the spatial extent of the paleochannel in the vicinity of WMA C, and to appropriately estimate its permeability.

Based on current understanding of the ancestral Columbia River deposits, a large paleochannel is interpreted extending southeast through Gable Gap (Figure C-2) that bifurcates just south of the gap. One sub-channel trends easterly following along the direction of strike of the Gable Mountain anticline while the other sub-channel trends in a more southerly direction through the eastern portion of the 200 Area Inner Boundary (the paleochannel identified in Figure C-2). The southerly trending paleochannel configuration, flow path, and dimensions have been the subject of numerous studies, owing to their importance to site-wide contaminant transport.

Recent reports providing information supporting the current interpretation of the extent of the paleochannel include the following.

- PNNL-12261, "Revised Hydrogeology for the Suprabasalt Aquifer System, 200-East Area and Vicinity, Hanford Site, Washington." The report includes detailed interpretations on the paleo and flood channels, and has several cross sections and figures displaying their configuration and flow paths.

- Aero-Metric LiDAR, "RCCC-Hanford Battelle/PNNL/DOE, Digital Orthophotography & LiDAR Surveys Photogrammetric Report," prepared by Aero-Metric, Seattle, Washington. The report includes LiDAR data; surficial expression of paleochannel outlines are apparent from ground-proofed Aero-Metric LiDAR data collected in 2008.

- Fiscal year (FY) 2013 and 2014 Annual Groundwater Monitoring Reports, CHPRC. Interpretation of tritium and ^{129}I plume extents follow the highly conductive flow paleochannel flow path.

- ECF-Hanford-13-0029, "Development of the Hanford South Geologic Framework Model, Hanford Site, Washington." The report shows areas where interpolated sediment volumes are not present, suggesting scouring along the paleochannel flow paths. All but two of the wells used in ECF-Hanford-13-0029 in the immediate vicinity of WMA C lie within the paleochannel. Geologic and geophysical logging data from the wells were also used in estimating paleochannel location.

Figure C-2. Interpreted Extent of a Paleochannel Associated with the Ancestral Columbia River in 200 East Area in the Vicinity of Waste Management Area C.

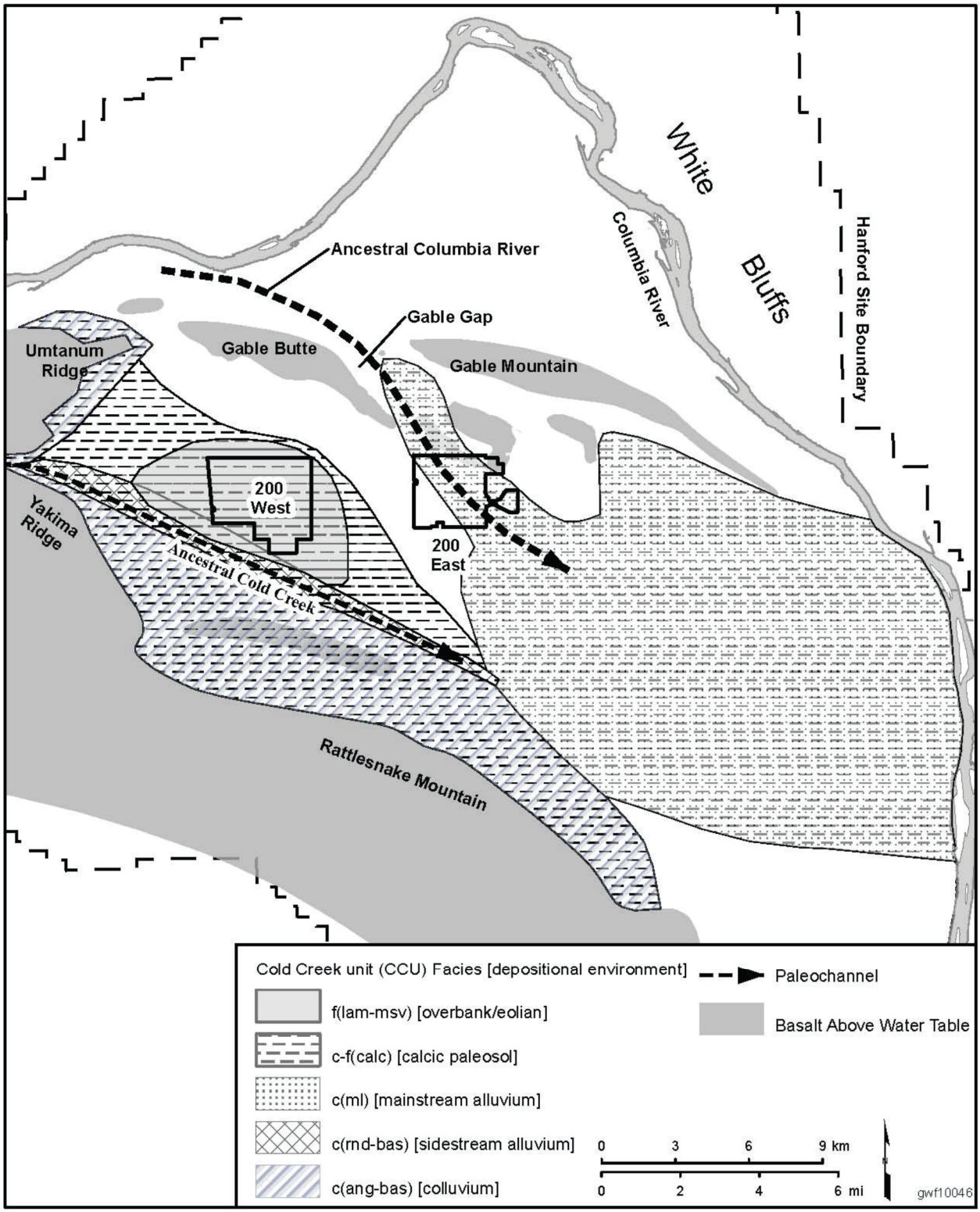

Source: DOE/RL-2011-118, Hanford Site Groundwater Monitoring for 2011, Appendix E.

Scouring of suprabasalt sediments in the paleochannels is evident in that, along much of its path, only the Hanford formation overlies the top of the basalt. Hanford formation material makes up almost entirely the material within the paleochannels in general, as well as all of the material within the paleochannel at the WMA C water table. Removal of pre-Hanford formation suprabasalt sediments, with the possible exception of a thin layer of Cold Creek unit (CCu) beneath the eastern half of WMA C, is apparent suggesting a paleochannel width of over 500 m beneath WMA C. Wells 299-E27-14 and 299-E27-15 penetrate the Hanford formation within the paleochannel beneath WMA C. The Hanford formation is ~86 m thick and the saturated thickness from the water table to the top of the basalt is ~13 m.

C.2.2 Theoretical Basis for Hydraulic Conductivity Estimates of Paleochannel Sediments

As discussed above, the paleochannel comprises an open-framework gravelly medium below WMA C. Figure C-3 is a digital photo log for borehole 299-E27-4 showing its proximity to WMA C and the open-framework gravelly media below the water table (the broken blue line is the water table location). The importance of the paleochannel to groundwater transport in the central plateau has led to a number of efforts to characterize its permeability, which can be applied to the WMA C PA.

Permeability measurements in open-framework gravelly media present special challenges, as the permeabilities are so high that they are above the measurement range of most laboratory constant-head permeameters—the head difference is too small to be measured. "Measuring the permeability of open-framework gravel" (Ferreira et al. 2010) addresses the challenge of measuring the high permeability by using a 3-m long permeameter. The head difference over this length was of the order of 10^{-2} to 10^{-3} m, which could be measured to the nearest 10^{-5} m. Measured permeability values varied between 3,456 m/day (for uniform pebbles) to 86,400 m/day (for open-framework gravels).

Figure C-4 illustrates an idealized unit cell model of an open-framework gravelly medium. "Scale Dependence of Continuum Models for Fractured Basalts" (Khaleel 1989) derived an expression (Equation C-1) for the isotropic saturated hydraulic conductivity (K) for such idealized media.

$$K_1 = K_2 = \frac{b^3 g}{12\sqrt{3}\ell\nu} \qquad \text{(C-1)}$$

where g is the acceleration (LT^{-2}) due to gravity, b is the open space aperture (L), ℓ is the coordinate length (L) along the opening of the unit cell, and ν is the kinematic viscosity (L^2T^{-1}) of the fluid. By inspection of equation (C-1) for equivalent isotropic *K*, the aperture size or width *b* is the most sensitive parameter in influencing conductivity estimates. For different aperture widths, and for a hexagon side length of 0.005 m (i.e., representative of 0.01-m [10-mm]-diameter pebbles), the calculated equivalent K estimates range from a low of 8 m/day to 65,000 m/day for aperture widths (*b*) ranging from a rather modest spacing of 0.1 mm to as high as 2 mm. In regard to WMA C, according to sieve results of sandy gravel samples collected from near the water table and below at well 299-E27-4, the grain size of approximately 35% to 40% of the material exceeds 10 mm (PNNL-14656, "Borehole Data Package for Four CY 2003

RCRA Wells 299-E27-4, 299-E27-21, 299-E27-22, and 299-E27-23 at Single-Shell Tank, Waste Management Area C, Hanford Site, Washington").

A theoretical estimate of the permeability of a uniform pebble network can also be obtained using the Kozeny-Carman equation (Dynamics of Fluids in Porous Media [Bear 1972]):

$$k = \frac{d}{180}\frac{\phi^3}{(1-\phi)^2} \tag{C-2}$$

The 10-mm diameter (d) uniform pebble model having a measured porosity ϕ=40% yields a permeability of about 86,000 m/day. Therefore, the two theoretical approaches are the same order of magnitude, and both provide very high estimates of saturated conductivity that are comparable to those based on the large-scale permeameter experiments (Ferreira et al. 2010).

C.3 ESTIMATES OF UNCONFINED AQUIFER FLOW AND TRANSPORT PROPERTIES

Estimation of aquifer flow and transport parameters at WMA C are necessary for evaluating the rate and extent of migration of contaminants arriving from the vadose zone and to assess the groundwater quality as required under the Resource Conservation and Recovery Act of 1976 (RCRA). The RCRA groundwater quality assessment program requires determination of whether past releases from WMA C are affecting groundwater quality and estimation of the rate and extent of migration of dangerous waste or dangerous waste constituents in the groundwater (DOE/RL-2009-77, Groundwater Quality Assessment Plan for the Single-Shell Tank Waste Management Area C; SGW-54508, "WMA C September 2012 Quarterly Groundwater Monitoring Report").

C.3.1 Groundwater Flow Velocities and Fluxes

Estimates of groundwater flow velocity or Darcy flux can provide valuable information about the hydraulic properties of the aquifer. These estimates can be made by measuring the flow within a borehole (using downhole flowmeters) or by interrogating the local or regional scale flow models.

Few direct measurements of groundwater flow exist in the 200 East Area, and none are particularly relevant to the groundwater flow conditions forecast for the unconfined aquifer in the immediate vicinity of WMA C. Measurements of groundwater flow velocity (groundwater flux divided by porosity) in the vicinity of WMA B-BX-BY, collected using a colloidal borescope circa 2001, reflected the impact of the large mound caused by the discharges at 216-B-3 Pond diverting flow from the east or southeast. The results did indicate that the flow velocities appeared to be greater in magnitude in the southern half of WMA B-BX-BY than in the northern half ("Application of the Colloidal Borescope to Determine a Complex Groundwater Flow Pattern" [Narbutovskih et al. 2002]). WHC-SD-EN-WP-012, "Groundwater Screening Evaluation/Monitoring Plan -- 200 Area Treated Effluent Disposal Facility (Project W-049H)" documents the results of an evaluation conducted using a heat pulse

flowmeter used to measure the magnitude and direction of groundwater flow velocity in three wells located east of the 216-B-3 Pond complex. However, during January and February 1994 when the evaluation occurred, the 216-B-3 Pond complex still received effluent and sustained the prominent groundwater mound, and the results of the testing were influenced by the mound created by the 216-B-3 pond discharges.

Groundwater flux information for particular subareas of regional models is often difficult to obtain from previous studies, and often must be inferred from whatever information is available. DOE/EIS-0391, "Final Tank Closure and Waste Management Environmental Impact Statement for the Hanford Site, Richland, Washington" estimated the future steady-state flow velocity in the highly conductive Hanford formation sediments at the 216-BY Cribs to be approximately 2 to 3 m/day toward the southeast, according to figures in Appendix L (i.e., Figures L-55, L-56, and L-57). According to the range of specific yield values presented in Table L-12 of Appendix L of DOE/EIS-0391, the flux in the aquifer is between 0.3 and 0.9 m/day.

Groundwater flux in the aquifer is estimated using the Central Plateau Groundwater Model (CPGWM) (CP-47631, "Model Package Report: Central Plateau Groundwater Model Version 6.3.3") by evaluating the water budget through a planar rectangular window (300 m × 200 m that encompasses most of WMA C flow domain) over the unconfined aquifer thickness (Figure C-5). The results of the CPGWM include two times of interest, present day and post-closure steady state:

- For Year 2014 (approximating present day conditions), the CPGWM-calculated flow through the window volume is 1,100 m^3/day, which divided by the cross-sectional area of 3,300 m^2 translates to a Darcy flux of 0.33 m/day

- For Year 2100 (approximating post-closure steady state conditions), the CPGWM-calculated flow through the window volume is 580 m^3/day, which divided by the cross-sectional area of 3,300 m^2 translates to a Darcy flux of 0.18 m/day.

C.3.2 Hydraulic Conductivity of Unconfined Aquifer Sediments

The basis for the hydraulic conductivity of the unconfined aquifer used in the PA takes account of the accumulated knowledge and experience of many years of study of the aquifer beneath the Central Plateau, undertaken for a variety of purposes by different investigators, using a variety of measurement and modeling approaches. The hydraulic conductivity estimates from various investigations, with focus on the aquifer within the 200 East Area, are presented in Figure C-6 in such a manner that the length scale of observation increases from left to right. The results presented on the left-hand side are from slug tests (small spatial scale measurements), while the pumping test-based measurements are in the middle and the regional scale model-based estimates are on the right-hand side. Where multiple results are provided within a single report that cover slug and pump test data, the range of hydraulic conductivity is shown with a vertical line (Figure C-6). The generally increasing estimates of effective hydraulic conductivity moving from the left to the right are consistent with Figure C-1 and the description in Section C.1. The results of most hydrologic tests indicate the presence of highly permeable conditions in the unconfined aquifer within the Central Plateau, and measured hydraulic conductivity estimates range as high as 51,500 m/day.

Figure C-3. Digital Photo Log for Borehole 299-E27-4 with an Expansion Showing the Open Framework Gravel below the Water Table.

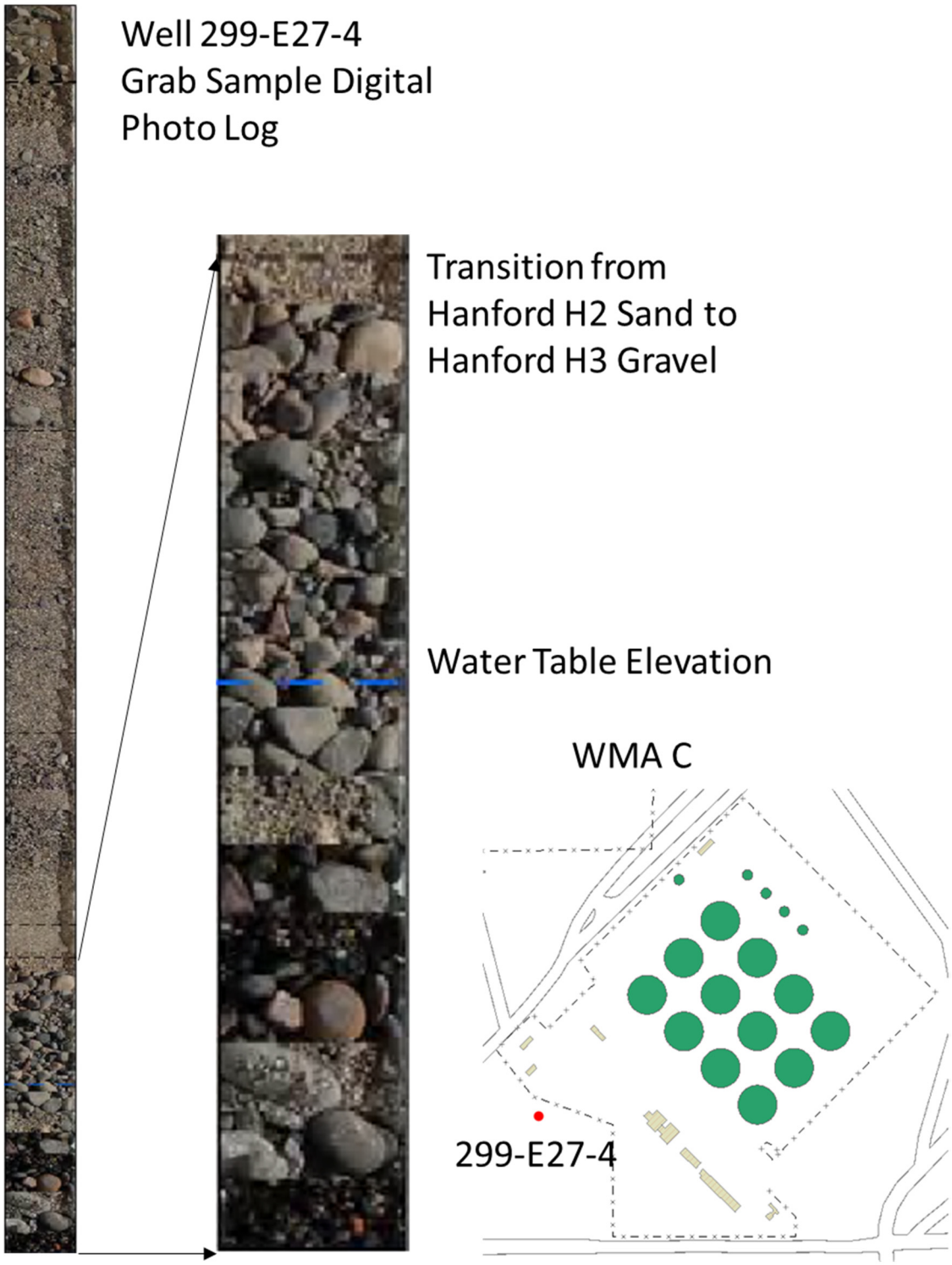

Adapted from PNNL-14656, "Borehole Data Package for Four CY 2003 RCRA Wells 299-E27-4, 299-E27-21, 299-E27-22, and 299-E27-23 at Single-Shell Tank, Waste Management Area C, Hanford Site, Washington."

WMA = Waste Management Area

Figure C-4. (a) An Idealized Hexagonal Model Approximation of Open-Framework Gravelly Media, and (b) Representative Flow Regions used to Determine Equivalent Hydraulic Conductivity.

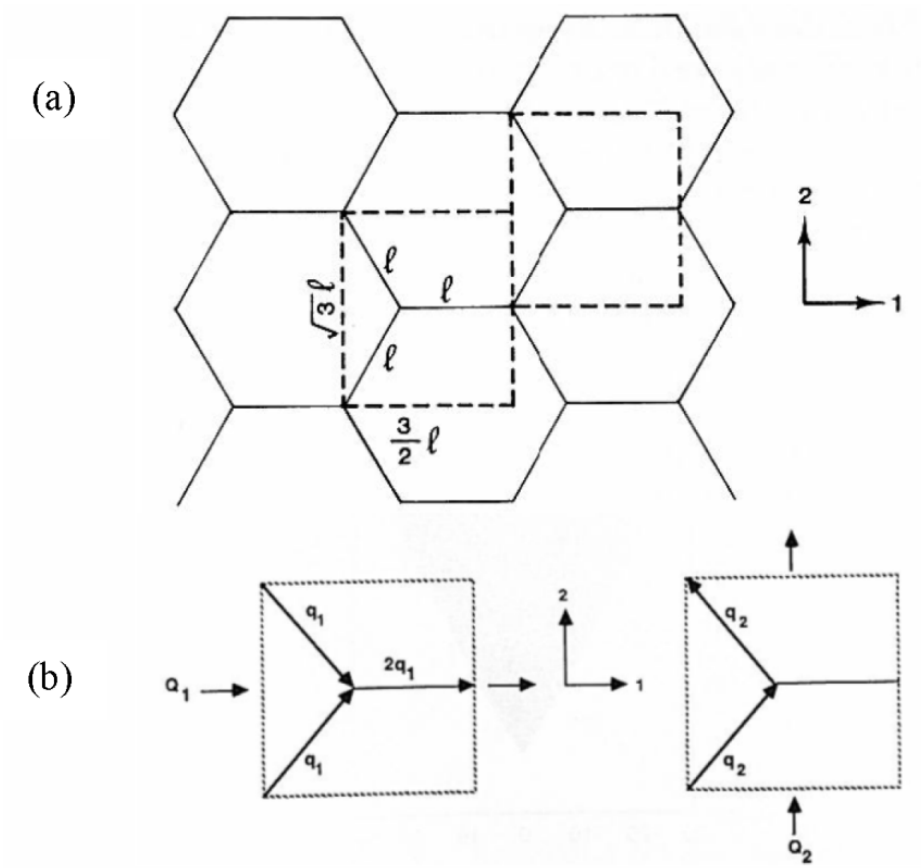

SGW-54508 considers hydraulic conductivity of the Hanford gravel at WMA C to range from 100 to 2,100 m/day on the basis of the results of slug and pumping tests conducted in the immediate vicinity of WMA C. Excluded from this range are unpublished slug test results from well 299-E27-24 that produced hydraulic conductivity estimates ranging from 3,650 to 51,500 m/day, and slug test results from well 299-E27-22 that range from 1,888 to 6,888 m/day (shown in Figure C-6). SGW-54508 discounts the results from well 299-E27-24 because the open interval and well radius were not controlled and sloughing conditions existed before testing. SGW-54508 also discounts the results from well 299-E27-22 because the sediment borehole log description at well 299-E27-22 indicates a more dominant silt matrix with less gravel content than at well 299-E27-23, where slug test results indicated that the hydraulic conductivity measures 100 to 108 m/day. However, the borehole log of well 299-E27-22 (Figure C-7) does indicate the presence of the open-framework gravel in the aquifer, and SGW-54508 does not explain why sloughing would cause hydraulic conductivity estimates derived from a slug test to be overestimated. In addition, the slug test data presented in SGW-48722, "Borehole Summary Report for the ARRA Installation of Five RCRA Groundwater Monitoring Wells in the 200 Areas, FY 2010" collected from wells 299-E27-24 and 299-E27-25 exhibit the oscillatory response indicative of highly permeable conditions. While the summary of data presented in SGW-54508 is appropriate for the purposes of the RCRA groundwater quality assessment

program, which include collecting and analyzing the available data, the data represent measurements made at a much smaller observation scale than is appropriate for developing an effective hydraulic conductivity estimate for WMA C (Figure C-1).

PNNL-14656 indicates that the high values measured at the wells are indicative of, and consistent with, the geologic interpretation of the open, highly permeable lower Hanford H3 gravels. The slug test and well screen development drawdown data also indicate comparable highly permeable conditions in the aquifer at wells 299-E27-21 and 299-E27-22 (PNNL-14656). Lastly, the results of an aquifer test with multiple observation wells conducted at well 699-55-50 indicate an aquifer hydraulic conductivity of 2,700 m/day (HW-60601, "Aquifer Characteristics and Ground-Water Movement at Hanford"). HW-60601 describes the aquifer as consisting of "Glaciofluviatile sands and gravels," which are described as unconsolidated sands and gravels occurring chiefly as glacial outwash. This description matches that given to the highly permeable gravel contained in the paleochannel.

Past calibration efforts (e.g., PNL-10886, "Development of a Three-Dimensional Ground-Water Model of the Hanford Site Unconfined Aquifer System: FY 1995 Status Report"; PNNL-11801, "Three-Dimensional Analysis of Future Groundwater Flow Conditions and Contaminant Plume Transport in the Hanford Site Unconfined Aquifer System: FY 1996 and 1997 Status Report") estimated that an upper limit of hydraulic conductivity for coarse-gravel flood deposits found in the central part of the Hanford Site is on the order of several tens of thousands of meters per day (Figure C-8). Figure C-8 shows the influence of the high hydraulic conductivity paleochannel in the aquifer beneath WMA C, as denoted by the swath of red. This swath indicates hydraulic conductivity exceeding 7,000 m/day, extending from the Gable Gap through the southeast corner of the 200 East Area. In one calibration effort, the hydraulic conductivity ranged from 271 m/day to 8,840 m/day within the WMA C PA model domain, and a value of 7,020 m/day in the immediate vicinity of WMA C (PNNL-14753, "Groundwater Data Package for Hanford Assessments"). In another effort, the hydraulic conductivity of the Hanford formation sediments ranged up to about 1,000,000 m/day for the Hanford flood deposits (PNNL-13641, "Uncertainty Analysis Framework – Hanford Site-Wide Groundwater Flow and Transport Model"). The Tank Closure and Waste Management Environmental Impact Statement (TC&WM EIS) model estimates the hydraulic conductivity of the highly conductive Hanford gravel present at WMA C to be ~4,000 m/day (DOE/EIS-0391). In a more recent modeling effort, CP-57037, "Model Package Report: Plateau to River Groundwater Transport Model Version 7.1" developed a calibrated estimate of 17,000 m/day for the Hanford formation associated with the paleochannel.

The CPGWM provides calibrated hydraulic conductivity estimates for the hydrostratigraphic units (HSUs) present within the aquifer. The CPGWM represents the most recent culmination of understanding of the unconfined aquifer under the Central Plateau and, given the rigorous nature of the development effort, is deemed to be the most suitable for predicting flow. The thicknesses and extent of the different HSUs within the selected model layers in the vicinity of WMA C for the saturated zone are shown in Figure C-9. The equivalent hydraulic conductivity for a given layer within the rectangular area (approximate extent of WMA C) ranges between 5,802 m/day and 17,000 m/day (Table C-1). Using a layer thickness weighted averaging scheme, the effective hydraulic conductivity for an equivalent homogeneous medium (EHM) is estimated to be 11,000 m/day for the entire aquifer (Table C-1). The EHM approach is used for representing

the saturated zone in the three-dimensional WMA C PA model using Subsurface Transport Over Multiple Phases (STOMP)©[1], as discussed in Appendix D, and therefore the value of 11,000 m/day is used for the aquifer.

C.3.3 Groundwater Flow Directions and Hydraulic Gradients

In the vicinity of WMA C, directions of groundwater flow and hydraulic gradients are inferred from water-level measurements in another part of the 200 East Area, around Low-Level Waste Management Area (LLWMA)-1 (DOE/RL-2013-22, Hanford Site Groundwater Monitoring Report for 2012), which is located northwest of WMA C. According to DOE/RL-2014-32, Hanford Site Groundwater Monitoring Report for 2013, the hydraulic gradient ranges between 2.2×10^{-5} m/m and 2.9×10^{-5} m/m, with flow moving in a southeastern direction. The average hydraulic gradient estimated from July 2011 through September 2012 was 2.5×10^{-5} ($\pm 0.4 \times 10^{-5}$) m/m toward the south (SGW-54165, "Evaluation of the Unconfined Aquifer Hydraulic Gradient Beneath the 200 East Area, Hanford Site"). SGW-54165 indicates that while the hydraulic gradient determination represents a spatial average across the entire Low-gradient Monitoring Network in the vicinity of LLWMA-1, mapping of water levels from August 2011 indicates that the flow direction directly beneath LLWMA-1 is more toward the southeast rather than toward the south.

Hydraulic gradient estimates in groundwater based on the CPGWM estimates of future conditions within the Central Plateau are summarized in Table C-1. Although water levels in the 200 East Area continue to decline, an evaluation of current groundwater flow directions and rates at WMA C is difficult due to the very low hydraulic gradient (on the order of 10^{-5} m/m). The hydraulic gradient according to the CPGWM is calculated from the volumetric flux through the window described in Section C.3.1.2 and the hydraulic conductivity value described in Section C.3.1.2. As indicated previously, the results of the CPGWM include two times of interest, present day and post-closure steady state (Table C-1), as follows.

- For Year 2014 (approximating present day conditions), the CPGWM-calculated flow through the window volume is 1,000 m^3/day, which divided by the cross-sectional area of 3,300 m^2 and equivalent hydraulic conductivity of 11,000 m/day translates to a hydraulic gradient of 3×10^{-5}. The direction of flow inferred from the modeling and consistent with plume movements is in a south-to-southeasterly direction.

- For Year 2100 (approximating post-closure steady state conditions), the CPGWM-calculated flow through the window volume is 730 m^3/day, which divided by the cross-sectional area of 3,300 m^2 and equivalent hydraulic conductivity of 11,000 m/day translates to a hydraulic gradient of 2×10^{-5}. The direction of flow inferred from the model is in a southeasterly direction.

[1] Subsurface Transport Over Multiple Phases (STOMP)© is copyrighted by Battelle Memorial Institute, 1996.

Figure C-5. Plan View of the Central Plateau Groundwater Model Representing the Aquifer and the Volumetric Flux Calculation Window in the Vicinity of Waste Management Area C.

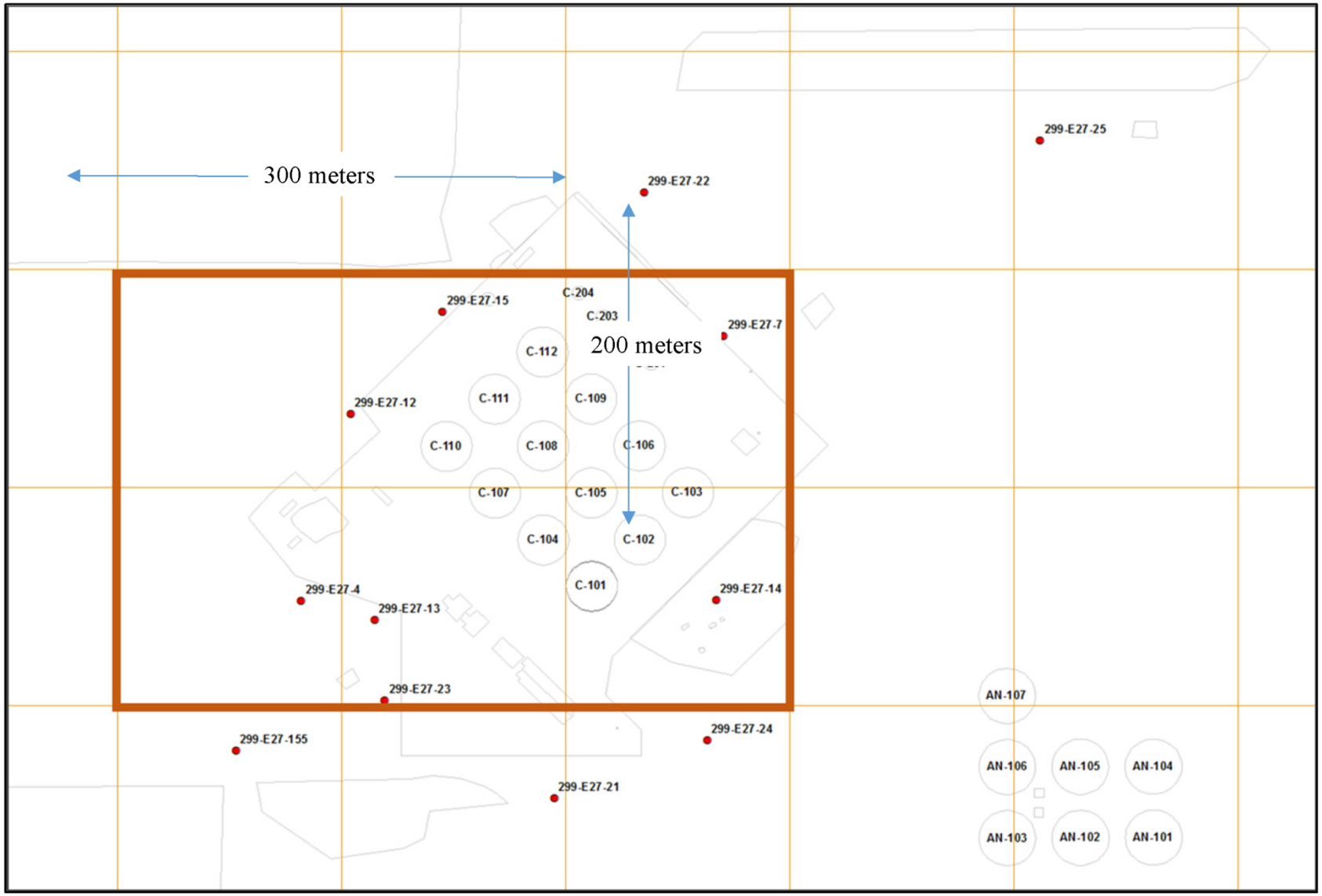

Figure C-6. Hanford Formation Saturated Hydraulic Conductivity Estimates Based on Slug Tests, Pump Tests, and Model Calibration.

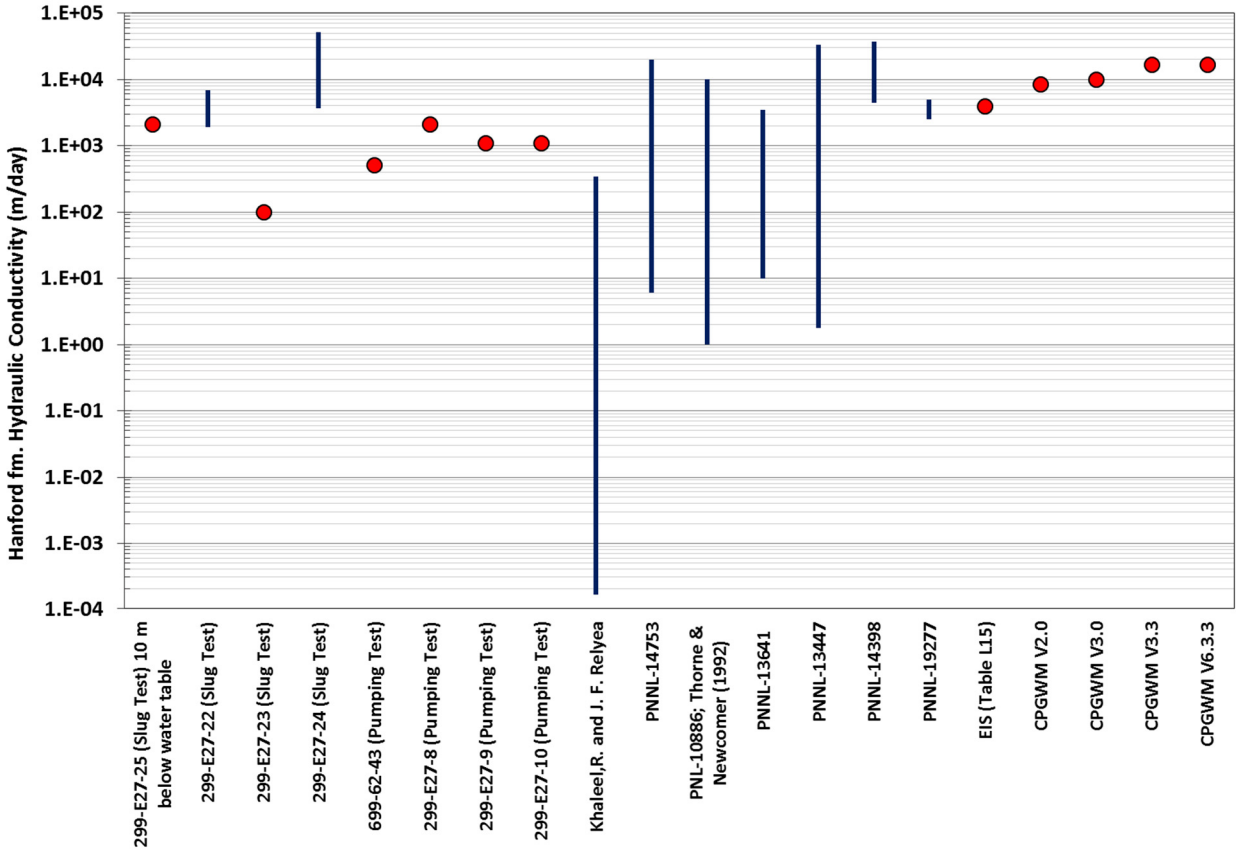

References:

"Correcting Laboratory-Measured Moisture Retention Data for Gravels" (Khaleel and Relyea 1997).

CP-47631, "Model Package Report: Central Plateau Groundwater Model Version [as amended]."

DOE/EIS-0391, "Final Tank Closure and Waste Management Environmental Impact Statement for the Hanford Site, Richland, Washington."

PNL-10886, "Development of a Three-Dimensional Ground-Water Model of the Hanford Site Unconfined Aquifer System: FY 1995 Status Report."

PNNL-13447, "Transient Inverse Calibration of Hanford Site-Wide Groundwater Model to Hanford Operational Impact – 1943 to 1996."

PNNL-13641, "Uncertainty Analysis Framework – Hanford Site-Wide Groundwater Flow and Transport Model."

PNNL-14753, "Groundwater Data Package for Hanford Assessments."

PNNL-14398, "Transient Inverse Calibration of the Site-Wide Groundwater Flow Model (ACM-2): FY 2003 Progress Report."

PNNL-19277, "Conceptual Models for Migration of Key Groundwater Contaminants Through the Vadose Zone and Into the Unconfined Aquifer Below the B-Complex."

Thorne & Newcomer (1992) = PNL-8337, "Summary and Evaluation of Available Hydraulic Property Data for the Hanford Site Unconfined Aquifer System."

The CPGWM model estimate of 3×10^{-5} m/m for year 2014 is consistent with the average gradient measured during 2013 (2.6×10^{-5} m/m) (DOE/RL-2014-32), and within the range of what is reported in SGW-54508 and SGW-58561, "WMA C Quarterly October through December 2014 Quarterly Groundwater Monitoring Report" (5.9×10^{-6} to 4.5×10^{-5} m/m).

Figure C-7. Borehole Log of Well 299-E27-22.

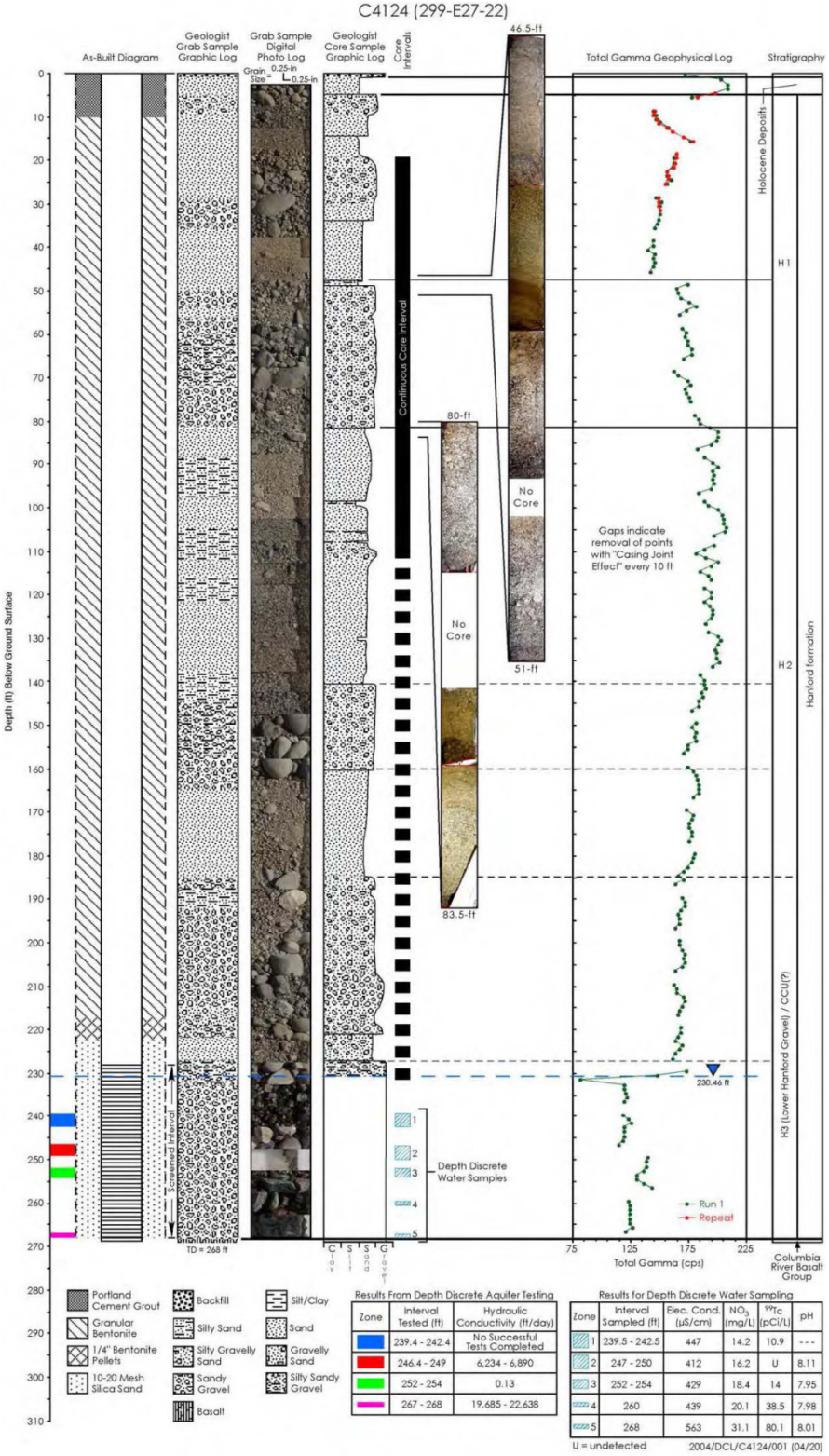

Zone	Interval Tested (ft)	Hydraulic Conductivity (ft/day)
	239.4 - 242.4	No Successful Tests Completed
	246.4 - 249	6,234 - 6,890
	252 - 254	0.13
	267 - 268	19,685 - 22,638

Zone	Interval Sampled (ft)	Elec. Cond. (µS/cm)	NO_3 (mg/L)	^{99}Tc (pCi/L)	pH
1	239.5 - 242.5	447	14.2	10.9	---
2	247 - 250	412	16.2	U	8.11
3	252 - 254	429	18.4	14	7.95
4	260	439	20.1	38.5	7.98
5	268	563	31.1	80.1	8.01

Source: PNNL-14656, "Borehole Data Package for Four CY 2003 RCRA Wells 299-E27-4, 299-E27-21, 299-E27-22, and 299-E27-23 at Single-Shell Tank, Waste Management Area C, Hanford Site, Washington."

Figure C-8. Pacific Northwest National Laboratory Site-Wide Model Calibration of Hydraulic Conductivity of the Unconfined Aquifer with the Location of Waste Management Area C and Magnitude of Hydraulic Conductivity Indicated.

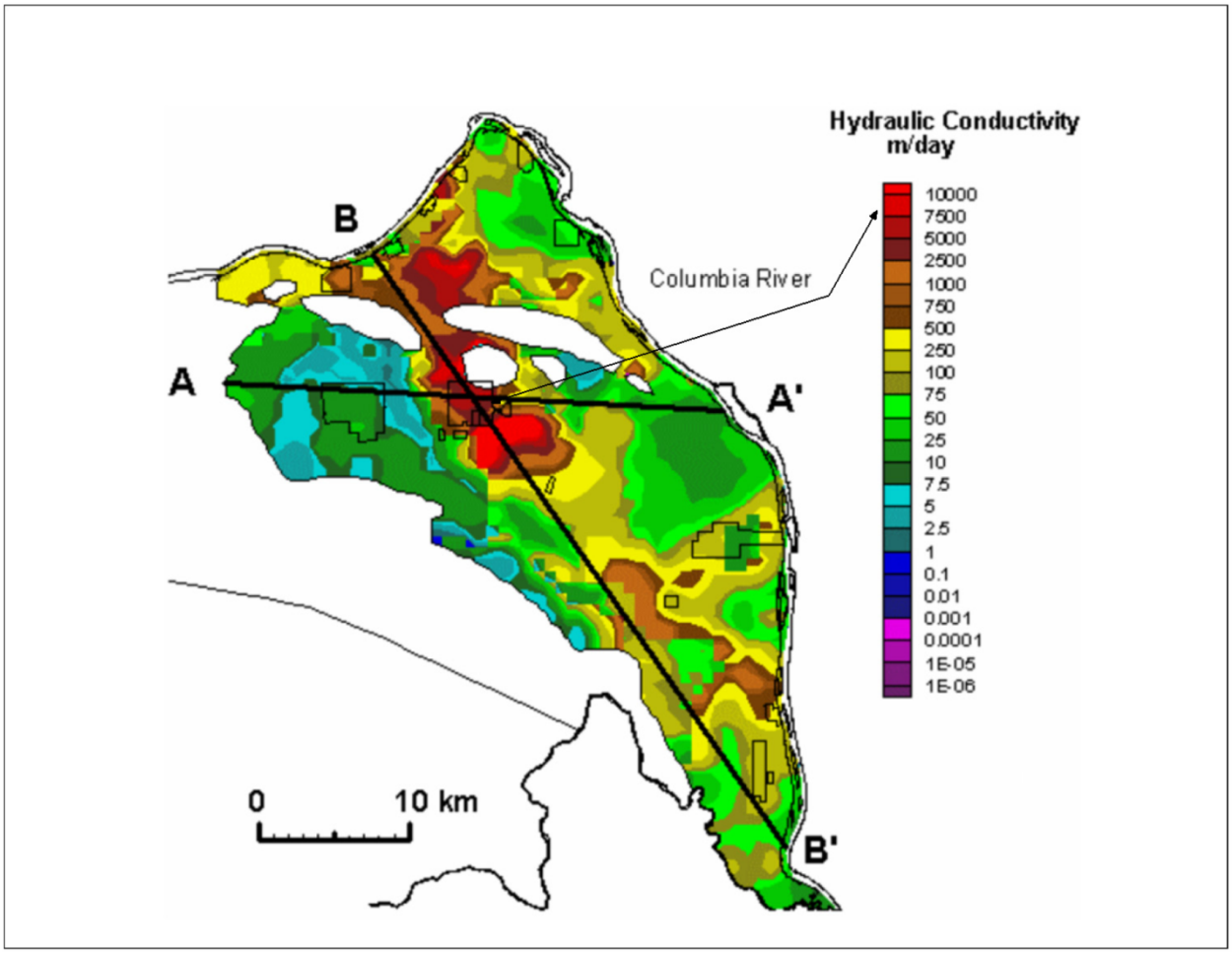

Excerpted and adapted from PNNL-13447, "Transient Inverse Calibration of Hanford Site-Wide Groundwater Model to Hanford Operational Impact – 1943 to 1996."

C.3.4 Anisotropy

Anisotropy in saturated hydraulic conductivity for Hanford H3 gravels has been estimated from pumping tests, which indicate values ranging from 0.01 to 0.1 (PNL-10886) and 0.015 to 0.5 (DOE/RL-2007-28, Feasibility Study Report for the 200-ZP-1 Groundwater Operable Unit) for post-year 2000 testing. Previous modeling analyses (e.g., PNNL-14398, "Transient Inverse Calibration of the Site-Wide Groundwater Flow Model [ACM-2]: FY 2003 Progress Report"; PNNL-14753; DOE/EIS-0391; and CPGWM [CP-47631]) estimate anisotropy to be 0.1.

C.3.5 Properties for Contaminant Transport

The transport of contaminants also requires estimates of the porosity, the volume of pore space in the aquifer, and the macrodispersivity, which accounts for the mixing that occurs because of variations in the flow and velocity caused by heterogeneities.

Figure C-9. Central Plateau Groundwater Model Layer Discretization In the Saturated Zone and Extent of Various Hydrostratigraphic Units within the Model Layer in the Vicinity of Waste Management Area C (shown by the Rectangle).

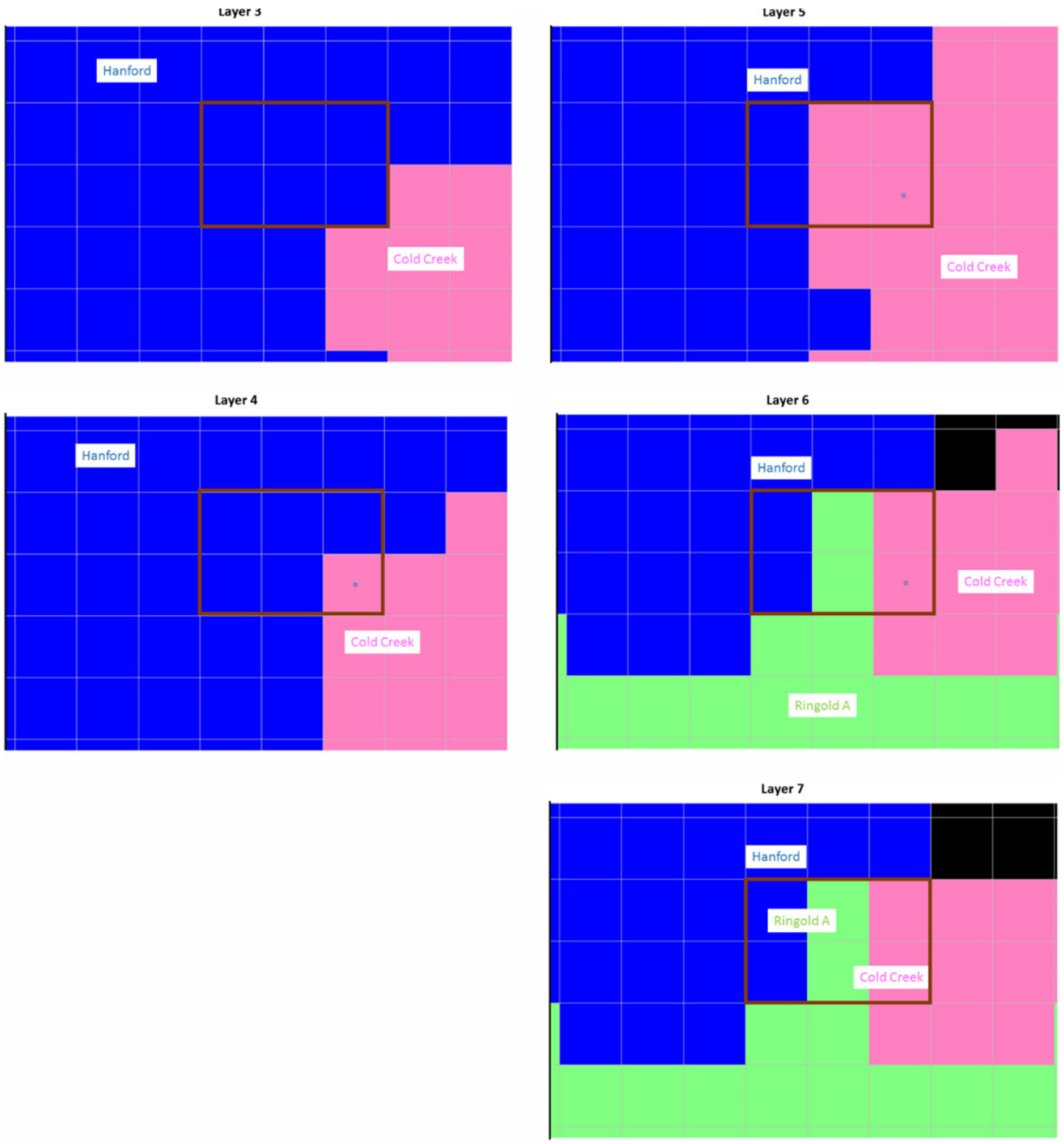

C.3.5.1 Porosity. According to RPP-14430, "Subsurface Conditions Description of the C and A-AX Waste Management Area," porosity is generally estimated to be about 30% for unconsolidated coarse-grained sediments, but a value closer to 20% may be more appropriate where boulders and cobbles are present and mixed with sand and gravels, such as at WMA C. Other estimated values include 0.06 determined from an aquifer pumping test at a well

(699-62-43) screened within the Hanford gravel sequence similar to that at WMA C (HW-60601); 0.1 derived from laboratory tests of Hanford gravels discussed in PNNL-19277, "Conceptual Models for Migration of Key Groundwater Contaminants Through the Vadose Zone and Into the Unconfined Aquifer Below the B-Complex"; and 0.25 in RPP-RPT-46088, "Flow and Transport in the Natural System at Waste Management Area C." DOE/EIS-0391 identified 0.15 to 0.30 as a reasonable range for the storage property value (expressed as specific yield values) of the highly conductive Hanford formation present in the paleochannel. CP-57037 estimated porosity of the Hanford formation associated with the paleochannel to be 0.2.

Table C-1. Calculation of Weighted Average Hydraulic Conductivity Value and Volumetric Water Flux from the Central Plateau Groundwater Model.

Year	Model Layer	Predicted Volumetric Water Flux (m^3/day)	Length of Window (m)	Layer Thickness (m)	Hanford Unit Calibrated Horizontal Hydraulic Conductivity (m/day)	Calculated Gradient (m/m)
2014	3	277.1	300	3	17,000	1.81E-05
2014	4	319.1	300	3	14,233	2.49E-05
2014	5	253.4	300	3	5,933	4.75E-05
2014	6	143.1	300	1	5,802	8.22E-05
2014	7	52.5	300	1	5,802	3.02E-05
2100	3	161.3	300	3	17,000	1.05E-05
2100	4	238.4	300	3	14,233	1.86E-05
2100	5	188.7	300	3	5,933	3.53E-05
2100	6	104.6	300	1	5,802	6.01E-05
2100	7	38.5	300	1	5,802	2.21E-05
Layer Thickness Weighted Hydraulic Conductivity (m/day, rounded):						11,000
Hydraulic Gradient 2014 (m/m, rounded):						3E-05
Hydraulic Gradient 2200 (m/m, rounded):						2E-05

C.3.5.2 Macrodispersivity Estimates. Field-scale dispersivities are referred to as macrodispersivities. Field observations indicate that the dispersion coefficients required to describe the large-scale transport processes, at field scales of tens or hundreds of meters, are much different from those observed in small-scale laboratory experiments (Stochastic Subsurface Hydrology [Gelhar 1993]). In fact, macrodispersivities may often be orders of magnitude larger than those observed in the laboratory. Consequently, laboratory-scale dispersivities, which are typically ~1 cm or less, are of little use in estimating field-scale dispersivities.

There is general agreement in hydrology literature that hydraulic conductivity variations induced by field-scale heterogeneities play an important role in field-scale transport processes. However, there does not appear to be a clear consensus about how best to describe such processes quantitatively (Gelhar 1993). While well-designed, large-scale tracer experiments would provide

useful information, limited field data are available at this time to quantify macrodispersivities in unsaturated media.

Heterogeneities that exist at various length scales result in a scale dependence of macrodispersivities (Figure C-10; "A Critical Review of Data on Field-Scale Dispersion in Aquifers" [Gelhar et al. 1992]). Dispersivities increase with time, or equivalently with distance, until they tend to converge on their unique asymptotic (large-time) values. However, it can take a long time (e.g., years or decades) for the asymptotic Fickian approximation to take hold. Nonetheless, the second-moment evolution or the time-dependent, preasymptotic dispersivities are of marginal interest in simulations involving long-times or large-mean travel distances such as those in PA modeling. The use of a constant (asymptotic) macrodispersivity is thus considered appropriate in PA simulations (NUREG/CR-6114, Auxiliary Analyses in Support of Performance Assessment of a Hypothetical Low-Level Waste Facility: Groundwater Flow and Transport Simulation).

Figure C-10. Longitudinal Macrodispersivity in Saturated Media as a Function of Overall Problem Scale with Data Classified by Reliability.

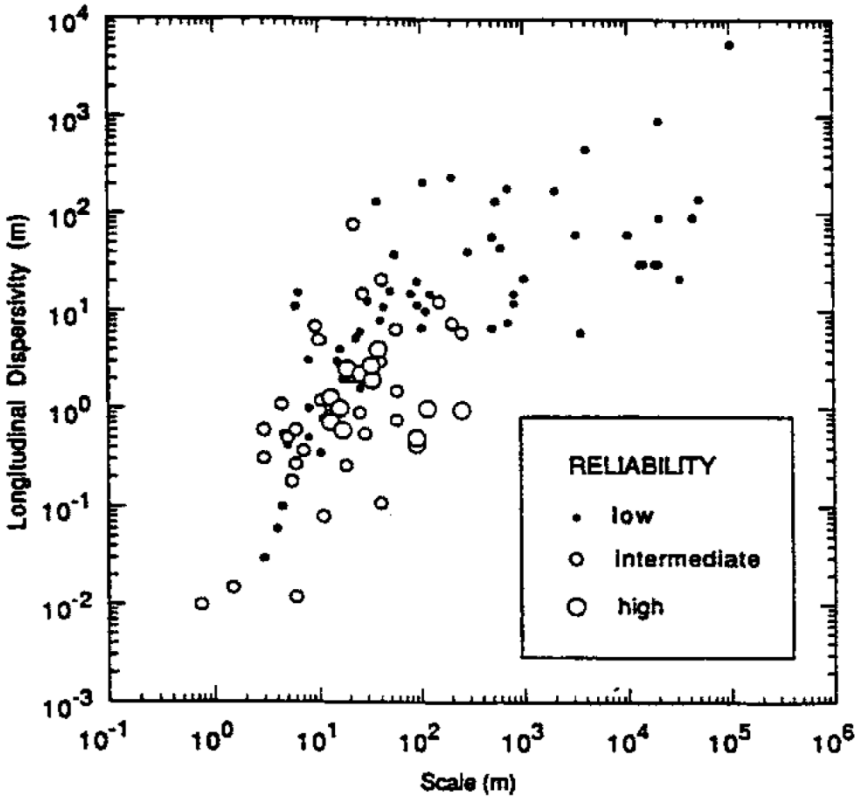

Reference: "A Critical Review of Data on Field-Scale Dispersion in Aquifers" (Gelhar et al. 1992).

The longitudinal and transverse macrodispersivity estimates in the saturated zone are based on a review of three general relationships ("Universal Scaling of Hydraulic Conductivities and Dispersivities in Geologic Media" [Neuman 1990]; "Longitudinal Dispersivity Data and Implications for Scaling Behavior" [Schulze-Makuch 2005]; and "Use of Weighted Least-Squares Method in Evaluation of the Relationship Between Dispersivity and Field Scale"

[Xu and Eckstein 1995]) that quantify the dependence of this parameter on measurement scale (L_s). For the 100 m scale of transport calculations considered in the PA effort, which is the approximate distance of transport from source areas to a compliance well located in the saturated zone, the calculated values fall within the range of 3.5 to 17 m (Table C-2).

Table C-2. Relationship Between Saturated Longitudinal Macrodispersivity (α_L) and Scale of Measurement (L_s).

Reference	Relationship	Origin	Saturated Longitudinal Macrodispersivity Estimate (m) for a Scale ≈ 100 m
Neuman (1990)	$\alpha_L \approx 0.017 L_s^{1.5}$	"Universal relationship" established considering both field and laboratory data (excluding modeling results)	17
Schulze-Makuch (2005)	$\alpha_L \approx 0.085 L_s^{0.81}$	Established considering field and modeling results (all reliabilities) and excluding laboratory data	3.5
Xu and Eckstein (1995)	$\alpha_L \approx 0.94(\log_{10} L_s)^{2.693}$	Established considering the same data set as Neuman (1990) including numerical model results	6

References:
"Universal Scaling of Hydraulic Conductivities and Dispersivities in Geologic Media" (Neuman 1990).
"Longitudinal Dispersivity Data and Implications for Scaling Behavior" (Schulze-Makuch 2005).
"Use of Weighted Least-Squares Method in Evaluation of the Relationship Between Dispersivity and Field Scale" (Xu and Eckstein 1995).

RPP-17209, "Modeling Data Package for an Initial Assessment of Closure of the S and SX Tank Farms," and "Field Study of a Long and Very Narrow Contaminant Plume" (van der Kamp et al. 1994) indicate that a value of 10 represents a reasonable estimate of the ratio of longitudinal to transverse macrodispersivity, and the aquifer lateral and vertical dispersivity values used in the model appear to be consistent with the distribution of the ^{99}Tc in the aquifer observed around WMA C. The elevated ^{99}Tc concentrations around WMA C appear to extend throughout the depth of the aquifer, indicating that the plume is well mixed. The peak ^{99}Tc activity (20,800 pCi/L) was determined at a depth of ~9 m below the water table in well 299-E27-23 during depth discrete sampling, although the activity was relatively constant at each depth measured in the well (i.e., 19,900 pCi/L and 20,500 pCi/L at depths of 3 m and 6 m, respectively) (DOE/RL-2011-01, Hanford Site Groundwater Monitoring Report for 2010). Depth discrete samples collected at wells 299-E27-4, 299-E27-7, and 299-E27-21 further indicate that ^{99}Tc activity increases with depth and that the ^{99}Tc is not contained in the upper part of the aquifer. For example, well 299-E27-4 had activity measurements of 727 and 761 pCi/L in the first two intervals but 7,260 pCi/L in the lowest sample interval (DOE/RL-2011-01). Thus, the aquifer dispersivity values appear to be consistent with the distribution indicated by the measured data.

C.4 UNCONFINED AQUIFER FLOW AND TRANSPORT PROPERTIES USED IN THE WASTE MANAGEMENT AREA C PERFORMANCE ASSESSMENT

The WMA C PA mostly adopted flow and transport properties derived from results developed from the calibrated CPGWM. The CPGWM takes into account the accumulated knowledge and experience of many years of study of the aquifer beneath the Central Plateau. One of the objectives for the CPGWM is to create a common modeling platform that can be used for investigations that support remedial activities and decisions in the four groundwater operable units that exist in the Central Plateau region (CP-47631). As discussed in Section C.1, the scale of the WMA C PA requires aquifer flow property estimates consistent with large area model calibration studies that are on the appropriate spatial scale.

The CPGWM incorporates the large-scale geologic and hydrogeologic features, and provides estimates of water levels, hydraulic gradients, and groundwater flows throughout the 200 West and 200 East Areas for current and expected future groundwater conditions. The model domain includes six suprabasalt HSUs with hydraulic properties established primarily through a transient calibration of the model to historical water level measurements. The CPGWM calibration places emphasis on matching water level data from the 1940s, early 1950s, and first decade of the 21st century to estimate hydraulic properties using flow conditions relatively unperturbed by site operations. Simulated water levels are compared to observed values for wells located upgradient and downgradient of WMA C (Figure C-11). The observed heads and CPGWM-simulated heads, representing a time span of over 20 years, compare well as indicated in Figure C-11, providing confidence in the predictive capabilities of the CPGWM.

The CPGWM is not a single-time-use tool, but represents the product of ongoing development and continued improvement that began in FY 2009 (CP-47631). The CPGWM represents the most recent culmination of understanding of the unconfined aquifer under the Central Plateau. CP-47631 provides information pertaining to the CPGWM objectives; conceptualization; model implementation; sensitivity, calibration, and uncertainty analyses; configuration control; and limitations of the groundwater flow component of the CPGWM.

The CPGWM has undergone several revisions (currently at Revision 6.3.3) to improve its performance with respect to calibration. CPGWM 6.3.3 takes account of the historical development of understanding the unconfined aquifer, along with current interpretations of the geology (including the extent of the paleochannel), and up-to-date measurements of the recovery of the water table from operational discharges. Hence, it represents the best current understanding of flow under the Central Plateau.

C.4.1 Flow Properties

C.4.1.1 Hydraulic Conductivity. As discussed in Section C.3.2, the effective hydraulic conductivity for the entire aquifer at WMA C using an EHM approach is estimated to be 11,000 m/day (Table C-1). This is based on the layer thickness weighted averaging scheme of calibrated hydraulic conductivity of the HSUs in the CPGWM in the vicinity of WMA C flow domain.

Figure C-11. Central Plateau Groundwater Model Calibration Results in the Vicinity of Waste Management Area C.

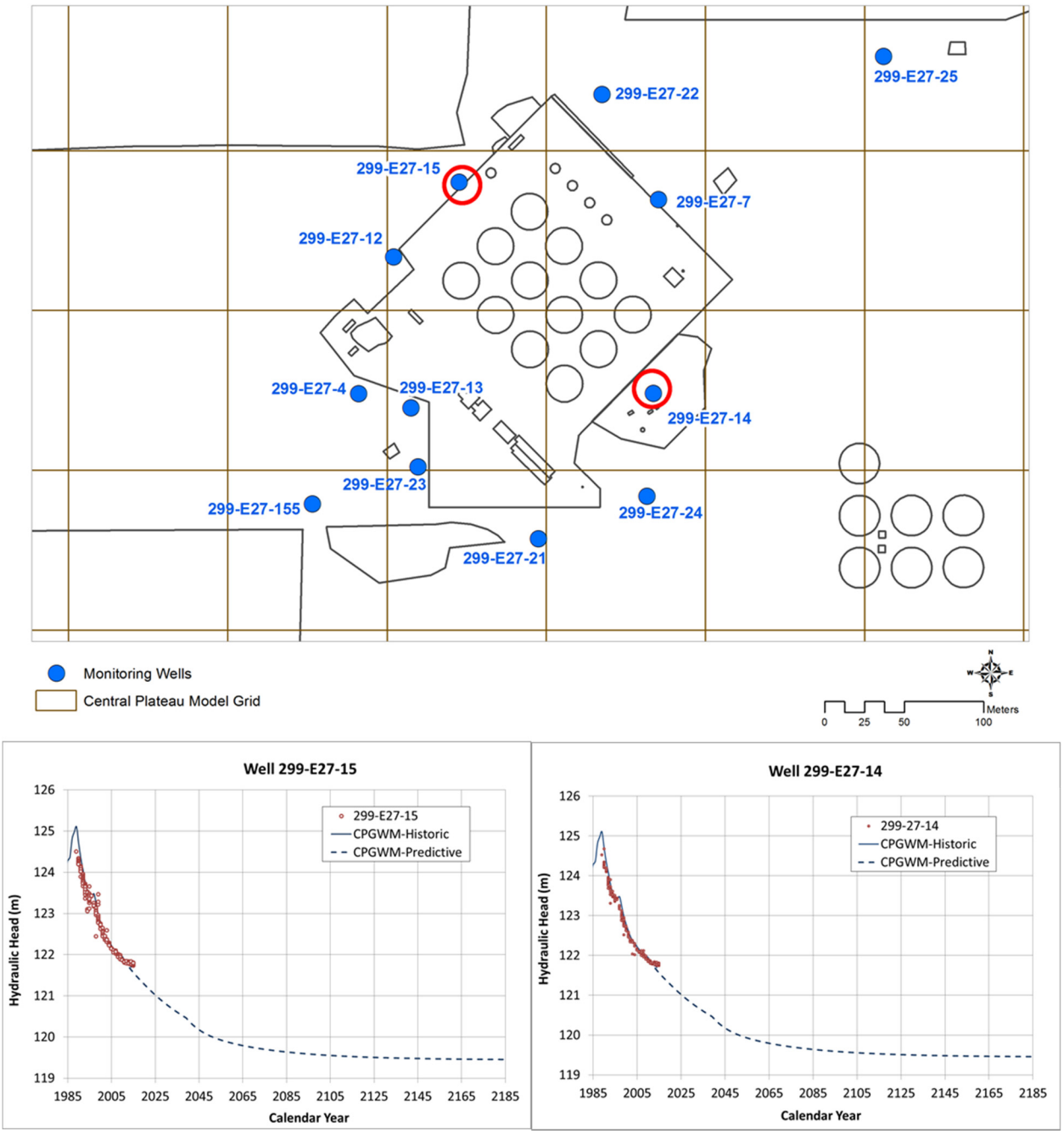

CPGWM = Central Plateau Groundwater Model

C.4.1.2 Hydraulic Gradient. The hydraulic gradient estimate (2×10^{-5} m/m, Table C-1) is based on the CPGWM estimates of future conditions within the Central Plateau. Water levels in the 200 East Area continue to decline, and evaluation of current flow direction and rate of groundwater flow at WMA C is difficult due to the very low hydraulic gradient. However, no appreciable change in hydraulic gradient is expected to occur after about 100 years after closure of WMA C, once the remedial actions in the nearby operable units are completed and the water

table is at or near steady state. It is expected that by the time the contaminants are released from WMA C and reach the water table, several hundred years would have passed and the water table would be at a steady-state condition. These conditions justify the use of a single value of hydraulic gradient for the water table, even though it is known to have changed substantially in the past owing to operational releases.

C.4.1.3 Anisotropy. The CPGWM estimate of 0.1 (CP-47631) for the anisotropy, which is defined here as the ratio of vertical to horizontal hydraulic conductivity, is consistent with previous modeling analyses (e.g., PNNL-14398, PNNL-14753, and DOE/EIS-0391).

C.4.2 Contaminant Transport Properties

C.4.2.1 Porosity. The CPGWM value of 0.20 is consistent with the conclusion in RPP-14430, the vadose zone value of 0.17 for the Hanford H1 and H3 sediments discussed in Section 6.3.2.2, and with the aquifer test results presented in HW-60601. The porosity value is within the range of other estimated values (e.g., PNNL-19277 and RPP-RPT-46088).

C.4.2.2 Macrodispersivity Estimates. A value of 10.5 m is considered representative and the midpoint of the range of values presented in Section C.3.5.2. The ratio of longitudinal to transverse macrodispersivity is chosen to be 10. The reasonableness of these selected macrodispersivity values for the PA effort is discussed in Section C.3.5.2.

C.5 DEVELOPMENT OF UNCERTAINTY IN GROUNDWATER FLUX AND MACRODISPERSIVITY FOR SATURATED ZONE

In the WMA C PA, the contaminant concentrations in the aquifer largely depend on the groundwater flux through the aquifer. While the groundwater flux can vary spatially due to local changes in hydraulic properties, the peak concentration at a particular location appears to correlate strongly to the mean groundwater flux, even in a heterogeneous aquifer (ITRC 2010; NUREG/CR-6767, Evaluation of Hydrologic Uncertainty Assessments for Decommissioning Sites Using Complex and Simplified Models).

Groundwater flux is linearly proportional to the hydraulic conductivity and hydraulic gradient. In the vicinity of WMA C, estimates of hydraulic gradient appear to include much less variability than estimates of hydraulic conductivity, as indicated by the results of detailed studies of the hydraulic gradient in the 200 East Area (Figure C-12). Because changes in one of the parameters can be negated by reciprocal changes to the other, for the purpose of evaluating uncertainty range in the groundwater flux, only the uncertainty in effective hydraulic conductivity is considered.

The general understanding of the groundwater flux in the aquifer around WMA C was used to evaluate the uncertainty in that parameter. The groundwater flux estimate from the calibrated CPGWM is considered to be the best estimate. The uncertainty in groundwater flux is represented by propagation of uncertainty in hydraulic conductivity (K_s) and by holding the long-term hydraulic gradient constant (2×10^{-5} m/m). A lower bound estimate of K_s is chosen to be 1,000 m/day and the upper bound estimate is chosen to be 21,000 m/day with the best estimate of 11,000 m/day. The lower bound estimate of 1,000 m/day is in the middle of the

range of test results presented in DOE/RL-2013-22, but appears to substantially underestimate the regional-scale value estimated using the CPGWM. The upper bound estimate of 21,000 m/day is chosen as a reasonable upper bound given that the hydraulic gradient is kept fixed. Based on this information, the uncertainty distribution for K_s is represented by a triangular distribution with minimum of 1,000 m/day, maximum of 21,000 m/day, and mode of 11,000 m/day.

Figure C-12. Low-Gradient Low-Level Waste Management Area 1 Monitoring Network Results.

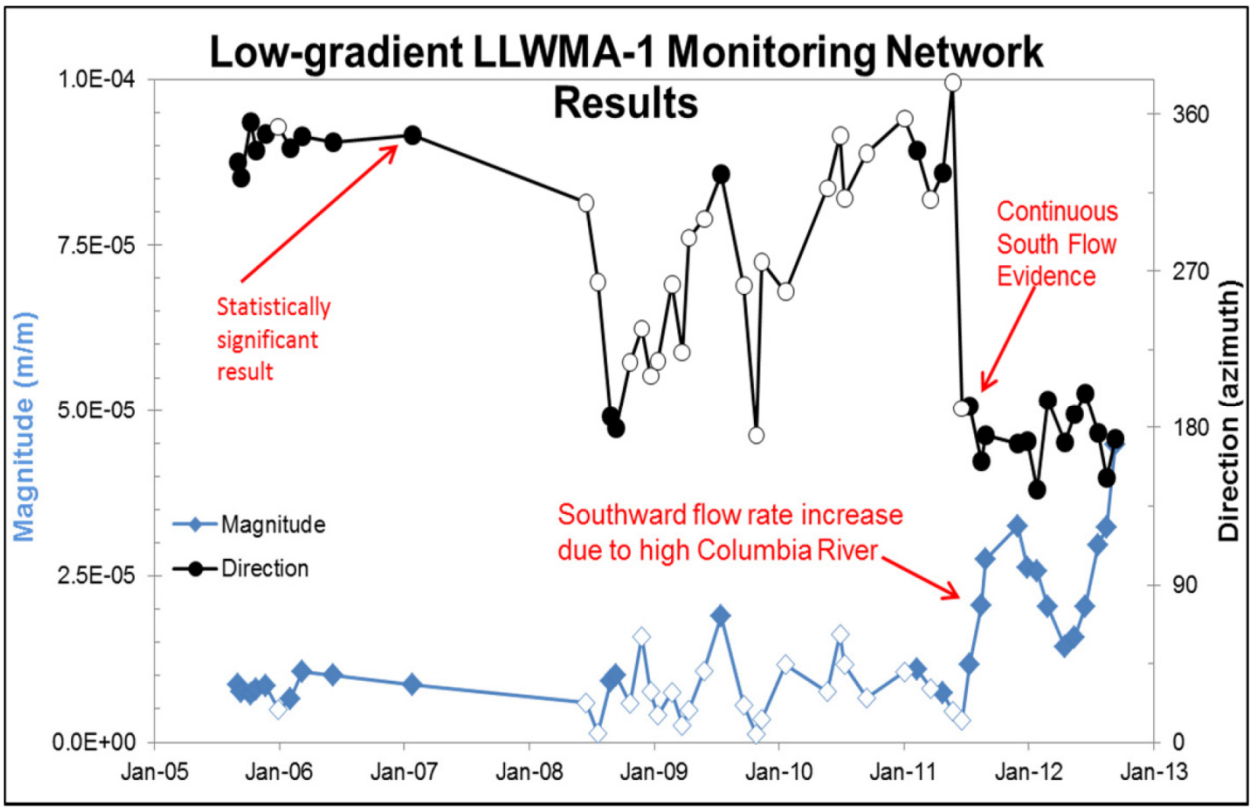

Excerpted from SGW-54165, "Evaluation of the Unconfined Aquifer Hydraulic Gradient Beneath the 200 East Area, Hanford Site."

LLWMA-1 = Low-Level Waste Management Area 1

The base case groundwater flux (Darcy flux) value of 0.22 m/day is calculated from best-estimate hydraulic gradient and hydraulic conductivity. This represents the mode of the triangular distribution with the minimum and maximum values estimated to be 0.02 m/day and 0.42 m/day, respectively. The minimum and maximum values are chosen in the same proportion (relative to the best estimate) as for the K_s, as discussed above. The uncertainty distributions are summarized in Table C-3.

The uncertainty in macrodispersivity within the unconfined aquifer was based on a review of literature-based, scale-dependent relationships for this parameter as discussed in Section C.3.5.2.

The range in saturated zone macrodispersivity at the scale of the WMA C model is estimated to be from 1 m to 20 m.

Table C-3. Triangular Distribution of Aquifer Flux and Proportional Hydraulic Conductivity Values Applicable to the Uncertainty Analysis.

Triangular Distribution	Minimum	Mode/Median	Maximum
Aquifer Flux (m/day)	0.02	0.22	0.42
Resultant Hydraulic Conductivity (m/day)	1,000	11,000	21,000

Uncertainty in the anisotropy and porosity in the aquifer are not considered as they have small range and are not likely to appreciably impact the contaminant concentrations (WCH-520, "Performance Assessment for the Environmental Restoration Disposal Facility, Hanford Site, Washington"). Furthermore, the uncertainty associated with these effects is considered to be minor and included within the uncertainty in the concentration results associated with the uncertainty in the groundwater flux.

C.6 REFERENCES

Aero-Metric LiDAR, 2008, "RCCC-Hanford Battelle/PNNL/DOE, Digital Orthophotography & LiDAR Surveys Photogrammetric Report," Aero-Metric, Inc., Seattle, Washington.

Bear, J. 1972, Dynamics of Fluids in Porous Media, American Elsevier Publishing Company, Inc., New York, New York.

Bjornstad, B., 2006, On the Trail of the Ice Age Floods: A Geological Field Guide to the Mid-Columbia Basin, Keokee Co. Publishing, Inc., Sandpoint, Idaho.

CP-47631, 2015, "Model Package Report: Central Plateau Groundwater Model Version 6.3.3," Rev. 2, INTERA, Inc., Richland, Washington.

CP-57037, 2015, "Model Package Report: Plateau to River Groundwater Transport Model Version 7.1," Rev. 0, CH2M HILL Plateau Remediation Company, Richland, Washington.

DOE/EIS-0391, 2012, "Final Tank Closure and Waste Management Environmental Impact Statement for the Hanford Site, Richland, Washington," U.S. Department of Energy, Washington, D.C.

DOE/RL-2007-28, 2008, Feasibility Study Report for the 200-ZP-1 Groundwater Operable Unit, Rev. 0, U.S. Department of Energy, Richland Operations Office, Richland, Washington.

DOE/RL-2009-77, 2010, Groundwater Quality Assessment Plan for the Single-Shell Tank Waste Management Area C, Rev. 0, U.S. Department of Energy, Richland Operations Office, Richland, Washington.

DOE/RL-2011-01, 2011, Hanford Site Groundwater Monitoring Report for 2010, Rev. 0, U.S. Department of Energy, Richland Operations Office, Richland, Washington.

DOE/RL-2011-118, 2012, Hanford Site Groundwater Monitoring for 2011, Rev. 0, U.S. Department of Energy, Richland Operations Office, Richland, Washington.

DOE/RL-2013-22, 2013, Hanford Site Groundwater Monitoring Report for 2012, Rev. 0, CH2M HILL Plateau Remediation Company, Richland, Washington.

DOE/RL-2014-32, 2014, Hanford Site Groundwater Monitoring Report for 2013, Rev. 0, U.S. Department of Energy, Richland Operations Office, Richland, Washington.

ECF-Hanford-13-0029, 2015, "Development of the Hanford South Geologic Framework Model, Hanford Site, Washington," Rev. 1, CH2M HILL Plateau Remediation Company, Richland, Washington.

Ferreira, J. T., R. W. Ritzi, and D. F. Dominic, 2010, "Measuring the permeability of open-framework gravel," Ground Water, Vol. 48, pp. 593–597.

Gelhar, L. W., 1993, Stochastic Subsurface Hydrology, Prentice Hall, New York, New York.

Gelhar, L. W., C. Welty, and K. R. Rehfeldt, 1992, "A Critical Review of Data on Field-Scale Dispersion in Aquifers," Water Resources Research, Vol. 28, pp. 1955–1974.

HW-60601, 1959, "Aquifer Characteristics and Ground-Water Movement at Hanford," General Electric Company, Hanford Atomic Products Operation, Richland, Washington.

ITRC, 2010, "Use and Measurement of Mass Flux and Mass Discharge," The Interstate Technology & Regulatory Council, Integrated DNAPL Site Strategy Team, Washington, D.C.

Khaleel, R., 1989, "Scale Dependence of Continuum Models for Fractured Basalts," Water Resources Research, Vol. 25, No. 8, pp. 1847–1855.

Khaleel, R. and J. F. Relyea, 1997, "Correcting Laboratory-Measured Moisture Retention Data for Gravels," Water Resources Research, Vol. 33, Issue 8, pp. 1875–1878.

Narbutovskih, S. M., J. P. McDonald, R. Schalla, M. D. Sweeney, 2002, "Application of the Colloidal Borescope to Determine a Complex Groundwater Flow Pattern," in Evaluation and Remediation of Low Permeability and Dual Porosity Environments, pp. 176–190, Symposium on Evaluation and Remediation of Low Permeability and Dual Porosity Environments, Reno, Nevada.

Neuman, S. P., 1990, "Universal Scaling of Hydraulic Conductivities and Dispersivities in Geologic Media," Water Resources Research, Vol. 26, No. 8, pp. 1749–1758.

NUREG/CR-6114, 1994, Auxiliary Analyses in Support of Performance Assessment of a Hypothetical Low-Level Waste Facility: Groundwater Flow and Transport Simulation, Vol. 3, U.S. Nuclear Regulatory Commission, Washington, D.C.

NUREG/CR-6767, 2002, Evaluation of Hydrologic Uncertainty Assessments for Decommissioning Sites Using Complex and Simplified Models, PNNL-13832, Pacific Northwest National Laboratory prepared for Division of Systems Analysis and Regulatory Effectiveness, Office of Nuclear Regulatory Research, U.S. Nuclear Regulatory Commission, Washington, D.C.

PNL-8337, 1992, "Summary and Evaluation of Available Hydraulic Property Data for the Hanford Site Unconfined Aquifer System," Pacific Northwest Laboratory, Richland, Washington.

PNL-10886, 1995, "Development of a Three-Dimensional Ground-Water Model of the Hanford Site Unconfined Aquifer System: FY 1995 Status Report," Pacific Northwest Laboratory, Richland, Washington.

PNNL-11801, 1997, "Three-Dimensional Analysis of Future Groundwater Flow Conditions and Contaminant Plume Transport in the Hanford Site Unconfined Aquifer System: FY 1996 and 1997 Status Report," Pacific Northwest National Laboratory, Richland, Washington.

PNNL-12261, 2000, "Revised Hydrogeology for the Suprabasalt Aquifer System, 200-East Area and Vicinity," Hanford Site, Washington, Pacific Northwest National Laboratory, Richland, Washington.

PNNL-13447, 2001, "Transient Inverse Calibration of Hanford Site-Wide Groundwater Model to Hanford Operational Impact – 1943 to 1996," Pacific Northwest National Laboratory, Richland, Washington.

PNNL-13641, 2001, "Uncertainty Analysis Framework – Hanford Site-Wide Groundwater Flow and Transport Model," Pacific Northwest National Laboratory, Richland, Washington.

PNNL-14398, 2003, "Transient Inverse Calibration of the Site-Wide Groundwater Flow Model (ACM-2): FY 2003 Progress Report," Rev. 0, Pacific Northwest National Laboratory, Richland, Washington.

PNNL-14656, 2004, "Borehole Data Package for Four CY 2003 RCRA Wells 299-E27-4, 299-E27-21, 299-E27-22, and 299-E27-23 at Single-Shell Tank, Waste Management Area C, Hanford Site, Washington," Pacific Northwest National Laboratory, Richland, Washington.

PNNL-14753, 2006, "Groundwater Data Package for Hanford Assessments," Rev. 1, Pacific Northwest National Laboratory, Richland, Washington.

PNNL-19277, 2010, "Conceptual Models for Migration of Key Groundwater Contaminants Through the Vadose Zone and Into the Unconfined Aquifer Below the B-Complex," Rev. 0, Pacific Northwest National Laboratory, Richland, Washington.

Resource Conservation and Recovery Act of 1976, 42 USC 6901, et seq.

Rovey, C. W. II and D. S. Cherkauer, 1995, "Scale Dependency of Hydraulic Conductivity Measurements," Ground Water Vol. 33, No. 5, pp. 769–780.

RPP-14430, 2003, "Subsurface Conditions Description of the C and A-AX Waste Management Area," Rev. 0, CH2M HILL Hanford Group, Inc., Richland, Washington.

RPP-17209, 2006, "Modeling Data Package for an Initial Assessment of Closure of the S and SX Tank Farms," Rev. 1, CH2M HILL Hanford Group, Inc., Richland, Washington.

RPP-RPT-46088, 2016, "Flow and Transport in the Natural System at Waste Management Area C," Rev. 2, Washington River Protection Solutions, LLC/GSI Water Solutions, Inc., Richland, Washington.

Scheibe, T. D., E. M. Murphy, X. Chen, A. K. Rice, K. C. Carroll, B. J. Palmer, A. M. Tartakovsky, I. Battiato, and B. D. Wood, 2015, "An Analysis Platform for Multiscale Hydrogeologic Modeling with Emphasis on Hybrid Multiscale Methods," Ground Water, Vol. 53, No. 1, pp. 38–56.

Schulze-Makuch, D., 2005, "Longitudinal Dispersivity Data and Implications for Scaling Behavior," Ground Water, Vol. 43, No. 3, pp. 443–456.

Schulze-Makuch, D., D. A. Carlson, D. S. Cherkauer, P. Malik, 1999, "Scale Dependency of Hydraulic Conductivity in Heterogeneous Media," Ground Water, Vol. 37, No. 6, pp. 904–919.

SGW-48722, 2011, "Borehole Summary Report for the ARRA Installation of Five RCRA Groundwater Monitoring Wells in the 200 Areas, FY 2010," Rev. 0, Freestone Environmental Services, Inc., Richland, Washington.

SGW-54165, 2014, "Evaluation of the Unconfined Aquifer Hydraulic Gradient Beneath the 200 East Area, Hanford Site," Rev. 0, CH2M HILL Plateau Remediation Company, Richland, Washington.

SGW-54508, 2013, "WMA C September 2012 Quarterly Groundwater Monitoring Report," Rev. 0, CH2M HILL Plateau Remediation Company, Richland, Washington.

SGW-58561, 2015, "WMA C Quarterly October through December 2014 Quarterly Groundwater Monitoring Report," Rev. 0, CH2M HILL Plateau Remediation Company, Richland, Washington.

U.S. Geological Survey Water-Supply Paper 2237, 1983, "Regional Flow in the Dakota Aquifer: A Study of the Role of Confining Layers," U.S. Government Printing Office, Alexandria, Virginia.

van der Kamp, G., L. D. Luba, J. A. Cherry, and H. Maathuis, 1994, "Field Study of a Long and Very Narrow Contaminant Plume," Ground Water, Vol. 32, No. 6, pp. 1008–1016.

WCH-520, 2013, "Performance Assessment for the Environmental Restoration Disposal Facility, Hanford Site, Washington," Rev. 1, Washington Closure Hanford, Richland, Washington.

WHC-SD-EN-WP-012, 1996, "Groundwater Screening Evaluation/Monitoring Plan -- 200 Area Treated Effluent Disposal Facility, Project W-049H," Rev. 1, Westinghouse Hanford Company, Richland, Washington.

Xu, M. and Y. Eckstein, 1995, "Use of Weighted Least-Squares Method in Evaluation of the Relationship Between Dispersivity and Field Scale," Ground Water, Vol. 33, No. 6, pp. 905–908.

This page intentionally left blank.

APPENDIX D

FLOW AND CONTAMINANT TRANSPORT NUMERICAL MODEL FOR THE WASTE MANAGEMENT AREA C PERFORMANCE ASSESSMENT

This page intentionally left blank.

TABLE OF CONTENTS

D1.0 INTRODUCTION D-1

D2.0 PURPOSE D-2

D3.0 MODELING OBJECTIVES D-3

D4.0 MODEL CONCEPTUALIZATION D-4

D4.1 FEATURES, EVENTS, AND PROCESSES D-4

D4.1.1 Model Domain and Boundary Conditions D-6

D4.1.2 Geologic Setting D-7

D4.1.3 Source Term D-8

D4.1.4 Vadose Zone Hydrogeology and Contaminant Transport D-14

D4.1.5 Infiltration and Recharge D-19

D4.1.6 Geochemistry and Sorption D-22

D4.1.7 Groundwater Domain D-24

D4.1.8 Point of Calculation, Protectiveness Metric, and Time Frame Considerations D-26

D4.2 NATURE AND EXTENT OF CONTAMINATION D-30

D5.0 STOMP© SOFTWARE D-32

D5.1 STOMP© CONTROLLED CALCULATION SOFTWARE D-33

D5.2 SOFTWARE INSTALLATION AND CHECKOUT D-33

D5.3 STATEMENT OF VALID SOFTWARE APPLICATION D-34

D6.0 MODEL IMPLEMENTATION D-34

D6.1 DISCRETIZATION D-34

D6.2 PARAMETERIZATION D-40

D6.3 MODELING STAGES D-41

D6.4 CALIBRATION D-42

D6.5 SCREENING D-42

D7.0 MODEL LIMITATIONS D-46

D8.0 MODEL CONFIGURATION MANAGEMENT D-48

D9.0 MODEL APPLICATION D-50

D10.0 REFERENCES D-50

LIST OF FIGURES

Figure D-1. Waste Management Area C Tanks and Associated Infrastructure and Unplanned Releases. D-3

Figure D-2. Plan View of Waste Management Area C Performance Assessment Model Domain Showing the Horizontal Distribution and Surface Type of the Irregularly-Spaced Calculation Nodes. The resolution increases in the area of Waste Management Area C. D-9

Figure D-3. Fence Diagram of Alternative Geologic Models Used in the Performance Assessment for Waste Management Area C. D-11

Figure D-4. Central Plateau Groundwater Model Calibration Results in the Vicinity of Waste Management Area C. D-28

Figure D-5. Points of Calculation 100 Meters Downgradient of Waste Management Area C. D-31

Figure D-6. Horizontal Alignment of Three-Dimensional Model Computational Nodes with Waste Management Area C Single-Shell Tanks, 241-C-301 Catch Tank, 244-CR-Vault, and Other Waste Management Area C Ancillary Equipment. D-35

Figure D-7. Horizontal and Vertical Alignment and Distribution of Waste Management Area C Performance Assessment Three-Dimensional Model Computational Nodes. D-37

Figure D-8. Relative Change in Moisture Content from the Pre-Hanford Steady State Condition at the Four Vertical Boundaries of the Model at Three Times of Interest: Year 2020, Year 2520, and Year 3020. ..... D-38

Figure D-9. Comparison of the Technetium-99 Concentration at the Nine Points of Calculation Located 100 Meters Downgradient between the Base Case Dispersivity Values and the Numerical Dispersion Test Case Dispersivity Values. D-39

LIST OF TABLES

Table D-1. Post-Retrieval Residual Waste Inventory for Waste Management Area C Tanks, Ancillary Equipment, and Pipelines. D-15

Table D-2. Summary Explanation and List of Parameters Used to Develop the Source-Term Release Calculations and Functions. D-17

Table D-3. Partition Coefficient Values for Grout/Concrete Used for Waste Management Area C Performance Assessment Source Release Functions. D-20

Table D-4. Composite van Genuchten-Mualem Parameters for Various Strata at the Waste Management Area C Site Used in the Base Case Evaluations of Alternative Geologic Models I and II. D-21

Table D-5. Effective Bulk Density (E[ρb], g/cm^3) Estimates for Various Strata at Waste Management Area C Used in the Base Case Evaluations of Alternative Geologic Models I and II. D-21

Table D-6. Macrodispersity Estimates for Various Strata at Waste Management Area C Used in the Base Case Evaluations of Alternative Geologic Models I and II. D-22

Table D-7. Base Case Recharge Rate (Net Infiltration) Estimates for Surface Conditions during the Pre-Construction, Operational, and Post-Closure Periods. D-23

Table D-8. Summary of the Waste Management Area C Performance Assessment Base Case K_d (mL/g) Values. D-24

Table D-9. Relationship Between Saturated Longitudinal Macrodispersivity (αL) and Scale of Measurement (L_s). D-29

Table D-10. Waste Management Area C Performance Assessment Unconfined Aquifer Flow and Transport Properties. D-30

Table D-11. Width of Point of Calculation Segments 100 Meters Downgradient of Waste Management Area C. D-32

Table D-12. Horizontal and Vertical Spacing of the Finite Difference Cells in the Three-Dimensional Waste Management Area C Flow and Transport Model Domain. D-36

Table D-13. Waste Management Area C Performance Assessment Vadose Zone Dispersivity Values and Numerical Dispersion Evaluation. D-40

Table D-14. Waste Management Area C Performance Assessment Vadose Zone Courant Criteria and Numerical Dispersion Evaluation. D-41

Table D-15. Summary of Key Elements and Base Case Parameters Associated with Site-Specific Model Components for Waste Management Area C (The basis for the elements and parameter selection provided in the individual model components sections)..... D-43

Table D-16. van Genuchten-Mualem Parameters Associated with the Maximum Pore Water Velocity at Specific Tension Ranges Based on Cumulative Distribution Functions. D-45

Table D-17. Maximum Net Infiltration (Recharge) Estimates Used in the Screening Analysis for Pre-Construction Period, Operational Period, and Post-Closure of Waste Management Area C (Section 8.1.4). D-45

Table D-18. First-Arrival Time (in Calendar Year) of Radionuclides for Various K_d Values Based on Screening Analysis Using Subsurface Transport Over Multiple Phases. D-46

Table D-19. Radionuclides that Arrive at the Water Table within the 1,000-Year Compliance and 10,000-Year Sensitivity and Uncertainty Time Frame Based on the Screening Analysis Conducted Using Subsurface Transport Over Multiple Phases..... D-49

LIST OF TERMS

3-D	three-dimensional
CERCLA	Comprehensive Environmental Response, Compensation, and Liability Act of 1982
CHPRC	CH2M HILL Plateau Remediation Company
Ci	curie(s)
cm	centimeter(s)
cm/s	centimeters per second
CPGWM	Central Plateau Groundwater Model
Cr	chromium
DOE	U.S. Department of Energy
EHM	equivalent homogeneous medium
EMMA	Environmental Model Management Archive
EPA	U.S. Environmental Protection Agency
FEPs	Features, Events, and Processes
ft	feet
g	gram(s)
h	hour(s)
HSU	hydrostratigraphic unit
in.	inch
kg	kilogram(s)
K-U-T	potassium, uranium, and thorium
m	meter(s)
µg/L	micrograms per liter
mg/kg	milligrams per kilogram

mi	mile(s)
mL/g	microliters per gram
mm/yr	millimeters per year
NAVD88	North American Vertical Datum of 1988, National Geodetic Survey, U.S. Department of Commerce.
PA	Performance Assessment
PNNL	Pacific Northwest National Laboratory
RCRA	Resource Conservation and Recovery Act of 1976
RETC	RETention Curve (software)
STOMP	Subsurface Transport Over Multiple Phases
UPR	unplanned release
WMA	Waste Management Area
WRPS	Washington River Protection Solutions
yr	year

D1.0 INTRODUCTION

This appendix documents the development of the vadose zone flow and transport model for the Waste Management Area (WMA) C performance assessment (PA). The results of the flow and transport model are intended to assist in evaluating the potential long-term impact on groundwater of post-retrieval single-shell tank waste residuals, and waste left in ancillary equipment, including pipelines. Impacts related to historical unplanned releases (UPRs) are outside the scope of this modeling effort. The objectives are to address the requirements outlined in Appendix I of the Hanford Federal Facility Agreement and Consent Order (Ecology et al. 1989) for assessment of radiological impacts of waste residuals in a closed WMA C under U.S. Department of Energy (DOE) Order 435.1, Radioactive Waste Management, and evaluation of hazardous chemical impacts for the same wastes under the Resource Conservation and Recovery Act of 1976 (RCRA). The modeling results are used to estimate the possible future concentration in groundwater of various radionuclides and non-radiological contaminants to support WMA C closure decisions associated with the PA. The overall objective of the modeling effort is to provide a basis for making informed closure decisions pertinent to WMA C.

This appendix discusses the development and translation of the conceptual model for flow and contaminant transport into the WMA C three-dimensional (3-D) numerical flow and transport model evaluated using the Subsurface Transport Over Multiple Phases (STOMP)©[1] simulator. The development of the geologic conceptual model is described, along with the implementation of waste release models used to represent contaminant releases from waste residuals remaining in tanks and ancillary equipment. The technical basis for specific model parameters and boundary conditions, along with description of modeling assumptions, is provided. The methodology used in estimating the peak concentrations in the groundwater from residual contamination in the tank residuals and ancillary equipment is described in detail. The modeling includes a screening process used to identify and narrow the list of contaminants of potential concern that require specific evaluation in the 3-D numerical flow and transport model of the post-retrieval closed WMA C. Control of all software used to implement the model is directed by the requirements of PRC-PRO-IRM-309, “Controlled Software Management.”

This appendix documents the 3-D numerical flow and transport model itself and its applicability, along with certain calculations that are necessary to demonstrate the soundness of the model. This appendix does not discuss base case results, or the uncertainty and sensitivity analyses. Those results are presented in Sections 7 and 8. Parameters, values, and ranges identified for evaluation in the uncertainty and sensitivity analyses are presented in Sections 5, 7, and 8.

[1] Subsurface Transport Over Multiple Phases (STOMP)© is copyrighted by Battelle Memorial Institute, 1996.

D2.0 PURPOSE

The 3-D WMA C PA flow and transport model evaluates quantitatively foreseeable or plausible future radiological and non-radiological contaminant concentrations in groundwater to determine the extent of protection to human health and the environment that the planned WMA C retrieval and closure activities provide. The purpose of the WMA C PA flow and transport modeling is to evaluate the impacts to groundwater associated with waste remaining in tank residuals after closure of WMA C. While there are no Federal requirements for protection of water resources for a radioactive waste disposal facility, the impacts from the WMA C tank residuals must comply with any applicable State or local law, regulation, or other legally-applicable requirement for water resource protection (DOE M 435.1-1, Radioactive Waste Management Manual). Therefore, water resources protection impacts are assessed on the basis of comparison to Washington State (Washington Administrative Code [WAC] 173-340, "Model Toxics Control Act – Cleanup") or Federal Drinking Water Standards (Title 40, Code of Federal Regulations, Part 141, "National Primary Drinking Water Regulations"), whichever are more restrictive.

The modeling is conducted in accordance with the DOE G 435.1-1, Implementation Guide for Use with DOE M 435.1-1, Radioactive Waste Management Manual PA guidelines. The modeling includes both a screening phase and detailed evaluation of the groundwater concentrations and radionuclide arrival times during the 1,000-year compliance and 10,000-year sensitivity-uncertainty periods per DOE O 435.1, Radioactive Waste Management. This analysis does not consider contaminant release during WMA C operations, only the post-closure impacts of the radionuclides and non-radiological contaminants to the environment. The intent of the screening phase is to limit the model analysis to those radionuclides sufficiently mobile to impact groundwater within the compliance and sensitivity-uncertainty periods. The screening phase follows Federal soil screening guidance and DOE PA guidelines (EPA/540/F-95/041, Soil Screening Guidance: Fact Sheet; DOE G 435.1-1, Chapter 4) that approve of the use of simple site-specific models for risk assessment screening purposes. For the WMA C PA reference case evaluation, the flow and transport model is 3-D to account for the lateral movement of water and radionuclides and to maintain comparability with other vadose zone transport analyses conducted at the Hanford Site.

Details of the site and facilities (Figure D-1) are provided in Sections 2 and 3 that describe to date the conditions, geologic and hydrologic interpretations, subsurface contamination approximations, and source term estimates. During its operational history, a number of confirmed or suspected waste release events have occurred at WMA C. These included suspected tank leaks and known UPRs from waste transfer lines and systems. Although these suspected tank leaks and UPRs are believed to have impacted groundwater, the evaluation of their impacts to groundwater is outside the scope of this WMA C PA model.

Figure D-1. Waste Management Area C Tanks and Associated Infrastructure and Unplanned Releases.

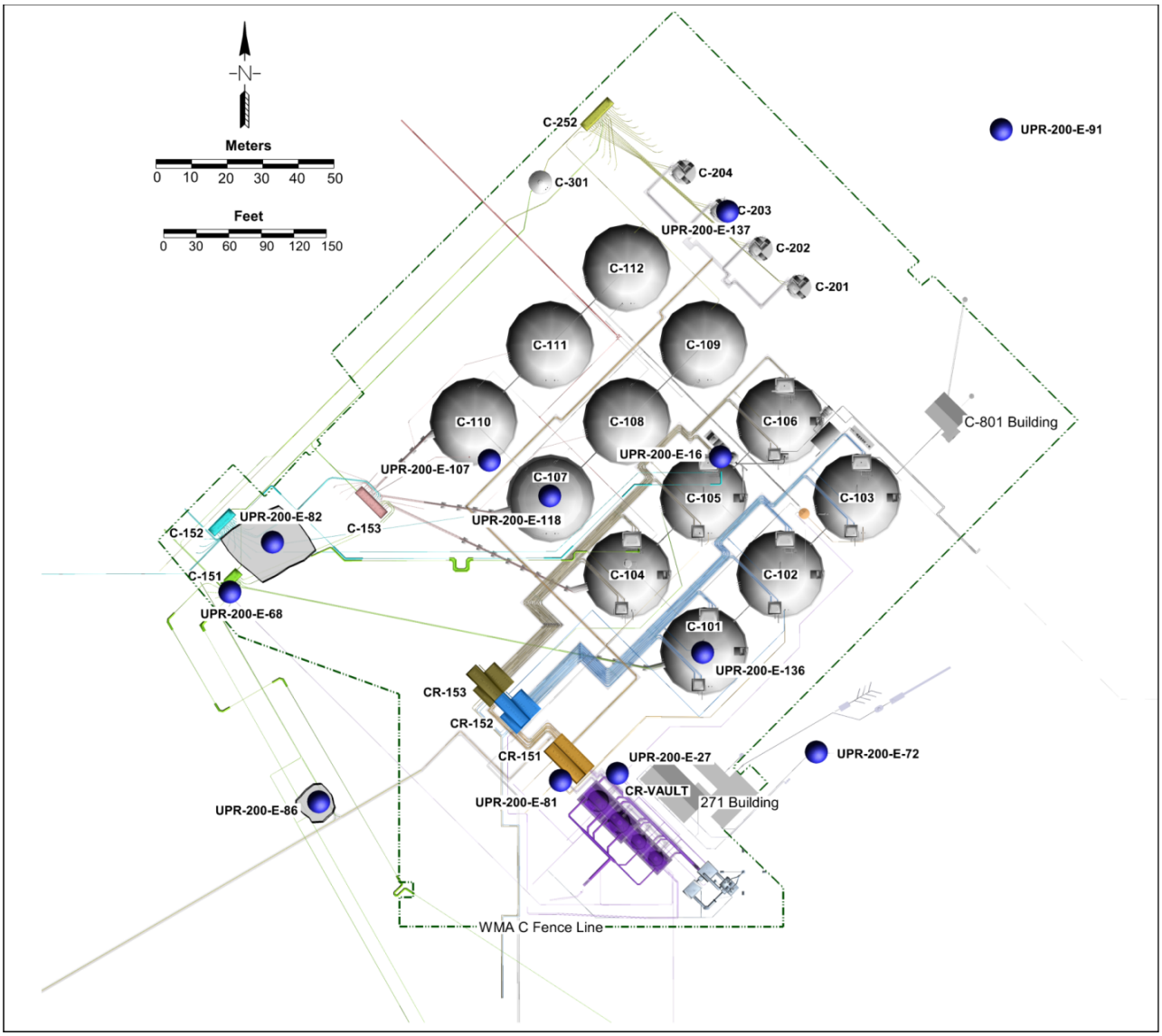

WMA = Waste Management Area

D3.0 MODELING OBJECTIVES

The objectives of the vadose zone fate and transport modeling include the capability to provide results that support the water resource impact evaluation and the estimation of dose at the point of assessment for the "all-pathways" exposure scenario described in DOE M 435.1-1. The analysis needs to include time history results of the transport of radionuclides and non-radiological contaminants individually and collectively, and be suitable for estimating the maximum concentration in the environment. DOE M 435.1-1 requires that the WMA C PA

includes calculations of potential doses to representative future members of the public and environmental impacts from potential releases from the tank residuals for a 1,000-year period after closure. The point of compliance for this performance objective is at the point of highest calculated concentration or dose, with an allowance for some volume averaging based on projected groundwater use, beyond a 100-m buffer zone around WMA C.

The modeling objectives also include conducting sensitivity and uncertainty analyses with the goal of defining bounding estimates for modeling predictions. The sensitivity-uncertainty analyses extend to 10,000 years to calculate the maximum dose and the time of that dose. These analyses take account of parameter values, initial conditions, boundary conditions, and changes in properties with time that are appropriate for the longer time frame. These sensitivity-uncertainty analyses are used to evaluate the significance of the assumptions used in the development of the transport modeling and their relevance to the controlling pathways or scenarios analyzed in DOE M 435.1-1. Assumptions necessary to develop inputs to the transport models, or to address uncertainties, data gaps, or linkages to other models used in the analysis are identified, justified, and shown to be consistent with the conceptual model.

D4.0 MODEL CONCEPTUALIZATION

This section describes the modeling methodology and approach for the determination of the WMA C residual waste impacts to groundwater. A synopsis of vadose zone conceptual model, conceptual model components, and the technical basis and rationale for the selection of parameters is provided here, along with supporting information and rationale. This section includes a description of the WMA C vadose zone geology and the pertinent vadose zone physical and chemical features, events, and processes (FEPs). A summary of the rationale and basis for selection of the Point of Calculation, a protectiveness metric, and the time frame for compliance is also presented.

D4.1 FEATURES, EVENTS, AND PROCESSES

The development of conceptual models and exposure scenarios for the WMA C PA builds upon work that began in 1999 with the intent to promote consistency and completeness in the development of conceptual models to support ongoing long-term assessments at Hanford through implementation of the FEPs methodology developed by the Nuclear Energy Agency for the Organization for Economic Co-operation and Development (RPP-RPT-41918, “Assessment Context for Performance Assessment for Waste in C Tank Farm Facilities after Closure”). The FEPs methodology, as adopted by the Hanford Site, identifies a list of FEPs that are relevant to the assessment of long-term safety or risks associated with solid radioactive waste repositories and other waste disposal sites (RPP-RPT-41918). DOE/RL-2011-50, Regulatory Basis and Implementation of a Graded Approach to Evaluation of Groundwater Protection identifies and describes the FEPs applicable to most vadose zone modeling applications in the 200 Areas, and concludes with the development of a “basic” Hanford Site-specific vadose zone conceptual

model. This conceptual model provides a basis for identifying the model attributes and criteria that lead to the selection of the appropriate model type and computer code applicable for most Hanford Site vadose zone modeling needs (DOE/RL-2011-50).

The following list of key conceptual model components derives from the basic Hanford Site vadose zone conceptual model identified in DOE/RL-2011-50 and includes:

- Model domain and boundary conditions
- Geologic setting
- Source term
- Vadose zone hydrogeology and contaminant transport
- Infiltration and recharge
- Geochemistry and sorption
- Groundwater domain.

These conceptual model components are consistent with those identified in EPA guidelines for the evaluation of the protection of groundwater pathway [EPA 402-R-94-012, A Technical Guide to Ground-Water Model Selection at Sites Contaminated with Radioactive Substances; OSWER No. 9200.4-18, "Establishment of Cleanup Levels for CERCLA Sites with Radioactive Contamination"; and HNF-5294, "Computer Code Selection Criteria for Flow and Transport Code(s) To Be Used in Vadose Zone Calculations for Environmental Analyses in the Hanford Site's Central Plateau"]. The principal FEPs associated with these conceptual model components include the following:

- Relatively thick vadose zone composed of predominantly similar sediments (geologic setting conceptual model component)

- Semi-arid region (infiltration recharge conceptual model component)

- Underlying unconfined aquifer (groundwater domain conceptual model component)

- Relatively few contaminants of concern in the vadose zone soils (source term) that have potential impacts to groundwater.

To apply the general or basic FEPs to the WMA C PA, conceptual model components must account for the source release of radionuclides and non-radiological contaminants from the grouted tanks, contaminant transport through engineered barriers, and contaminant transport through the natural environment, while accounting for decay and ingrowth of daughter isotopes (RPP-RPT-48490, "Technical Approach and Scope for Flow and Contaminant Transport Analysis in the Initial Performance Assessment of Waste Management Area C"). Transport through engineered barriers must take into account the degradation of the tank structures, as well as flow of water through the waste in the tanks and contaminant releases into the vadose zone (RPP-RPT-41918). These processes include details of physical and chemical mechanisms on a refined local scale.

The key conceptual model components listed above and their associated FEPs are discussed in the following subsections. The discussion includes the rationale and basis for each of the conceptual model components, and describes the function each conceptual model component and corresponding FEPs serve in the model, the assumptions associated with them, a description of the FEPs included in each component, and a qualitative assessment of the impact the component has on the model results.

D4.1.1 Model Domain and Boundary Conditions

The model domain and boundary conditions establish both a framework and limiting conditions for the numerical model. The model domain for flow and transport in the vadose zone is represented in 3-D space, with one of the horizontal axes aligned in the general direction of groundwater flow. Aligning an axis with the general direction of groundwater flow allows concentrations to be calculated more easily downgradient of the waste sites. The numerical model adapts the physical elements of the conceptual model to a Cartesian grid, and also assigns numerical values to the parameters used in algorithms to represent the physical and geochemical systems and processes.

The WMA C model domain is 737.9 m (2,421 ft) northwest to southeast by 795.3 m (2,609 ft) southwest to northeast by 116 m (381 ft) vertically, extending about 12 m (49 ft) below the water table. The southwestern and northwestern boundaries of the model are 574656.09 m, 136454.41 m, and 575218.45 m, 137016.78 m, respectively (Lambert Coordinate system easting, NOAA Manual NOS NGS 5, "State Plane Coordinate System of 1983"). The southeastern and northeastern boundaries are 575177.86 m, 135932.64 m, and 575740.22 m, 136495.00 m, respectively. The vertical base elevation of the model is nominally 95 m (North American Vertical Datum of 1988 [NAVD88]), although the bottom and top of the model domain vary spatially according to the top of basalt elevation and surface relief, respectively (RPP-RPT-56356, "Development of Alternative Digital Geologic Models of Waste Management Area C").

A specified-flux boundary condition is applied at the surface, and net infiltration rates representing recharge vary spatially and temporally along the upper boundary depending on site and surface conditions simulated, the location and physical dimensions of WMA C (recharge parameterization is discussed in Section 3.1.5), and the time of WMA C operations (RPP-RPT-44042, "Recharge and Waste Release within Engineered System in Waste Management Area C") (Figure D-2). The bottom boundary of the unsaturated (vadose) zone is the water table, and the bottom of the model (aquifer) is defined as a vertical no flow boundary condition. Boundary conditions at the sides of the model domain are assumed to be no flow in the vadose zone and prescribed flux and prescribed head in the aquifer on the upgradient and downgradient boundaries, respectively.

The boundary condition in the aquifer on the upgradient boundary applies a prescribed flux calculated on the basis of the aquifer hydraulic conductivity and gradient, independent of recharge. The prescribed flux boundary condition value includes a factor to account for the fact that the thickness of the unconfined aquifer varies because of the uneven surface of the underlying basalt. To account for the non-uniform aquifer thickness from the underlying basalt

boundary, the nominal flux rate calculated as the product of the hydraulic conductivity and gradient (base case values of 11,000 m/day and 2.0×10^{-5} m/m, respectively; see Section D4.1.7) is proportioned according to the ratio of the average aquifer area throughout the model domain (9,440 m^2) and the aquifer area along the southwest-northwest boundary (6,151 m^2) where the prescribed flux is applied. The aquifer area refers to the area perpendicular to the direction of groundwater flow.

D4.1.2 Geologic Setting

The geological setting information presented here is a summary of the information presented in RPP-RPT-46088, "Flow and Transport in the Natural System at Waste Management Area C" and RPP-RPT-56356. Waste Management Area C is located near the eastern edge of the 200 East Area on the Hanford Site on what is known as the Central Plateau. The vadose zone is ~80 to 100 m (262.4 to 328.1 ft) thick, and there are ~68 m between the base of WMA C and the present-day water table. Waste Management Area C lies within the gravel-dominated H1 unit in the vadose zone. The stratigraphic units recognized in the WMA C area include:

- Recent (Holocene) backfill material (Hdb) (~10 m thick)
- Hanford formation unit H1 – Gravel-dominated sequence (~10 m to 30 m thick)
- Hanford formation unit H2 –
    - Hanford H2 Sand-dominated sequence (~45 m to 70 m thick)
    - Hanford H2 Coarse subunit (gravel/coarse-grained facies that underlies the H2 sands)
    - Hanford H2 Silty sand subunit (silty sand lower permeability laminations/lenses)
- Hanford formation unit H3 – gravel-dominated sequence (~0 m to 20 m thick)
- Columbia River Basalt Group.

As part of the RCRA facility investigations (DOE/ORP-2008-01, RCRA Facility Investigation Report for Hanford Single-Shell Tank Waste Management Areas and RPP-PLAN-39114, "Phase 2 RCRA Facility Investigation/Corrective Measures Study Work Plan for Waste Management Area C"), the geologic strata underlying WMA C have been characterized in conjunction with soil sampling and borehole logging for radionuclides and hazardous waste constituents. The geophysical and geologic logging from the boreholes has been used to identify the elevations of tops of the geologic units in the vicinity of WMA C. Specifically, potassium, uranium, and thorium (K-U-T) data from geophysical logs were used to map the tops of the different geologic units at WMA C (RPP-RPT-56356).

In discussions associated with the 2009 to 2011 working sessions and additional discussions with regulators in 2013 and 2014, two alternative geological models were proposed and developed on

the basis of the data discussed in the preceding paragraph. Both of these models have been incorporated into the PA as a means to explore the performance implications of the alternative conceptualizations. This section provides a brief summary of important differences between these alternative models. Details on the basis for their development are provided in RPP-RPT-56356 and only briefly summarized here.

The primary difference between the two alternative models concerns whether or not a sandy gravel facies followed by a silty sand layer exist at the bottom of the H2 subunit in the vicinity of WMA C. The K-U-T data (i.e., a lower gross gamma and potassium count) indicates that there is a coarsening of the sand at the bottom of the H2 that turns more into a sandy gravel. Underlying this sandy gravel facies is a silty sand unit that presents a strong potassium peak and an occasional but strong natural uranium peak. The difficulty in making the determination between the two alternative models is that there are few direct pushes or drywells that go deep enough in which there are both good geophysical logs and geologic logs (with drill cuttings). For the most part, only the nearby groundwater wells extend to a sufficient depth. The drill cuttings from nearby ground wells indicate that there is a definite fining of the sands, along with some silty sands found at the vertical location as indicated by the K-U-T data in the geophysical logs, but a competent silt layer was not observed. Alternative Model I does not distinguish the sandy gravel and underlying silty sand unit distinctly from Hanford H2, while Alternative Model II does distinguish them. The significance of distinguishing these layers is that their differing characteristics, as expressed by different soil hydraulic property values, could cause increased lateral movement in the vadose zone. A series of fence diagrams showing the differences between the two models within WMA C is given in RPP-RPT-56356. The fence diagram for both these models running southwest to northeast through the center of WMA C is given in Figure D-3.

The WMA C PA includes the evaluation of Alternative Model II in its sensitivity analysis. This appendix includes the discussion of Alternative Model II because Alternative Model II represents an alternative conceptualization of the entire geologic model, and not a parametric variation.

D4.1.3 Source Term

The radionuclide inventory information presented here is a summary of the information presented in RPP-RPT-42323, “Hanford C-Farm Tank and Ancillary Equipment Residual Waste Inventory Estimates” and the WMA C PA. The source term conceptual model component defines the characteristics of the inventory and the release of residual waste from the tanks, ancillary equipment, and pipelines. RPP-RPT-42323 presents the basis for chemical and radiological inventory estimates for residual waste remaining in 241-C Tank Farm single-shell tanks and associated transfer equipment after tank waste is retrieved. As discussed in RPP-RPT-42323, a conservative or bounding bias is built into the inventory estimating process, generally resulting in larger than likely inventory estimates. Inventory estimates applicable to the vadose zone fate and transport evaluation presented in Table D-1 are derived from the values presented in RPP-RPT-42323 (Appendix B-1, C-3 and C-5), with the radionuclides decayed to January 1, 2020.

Figure D-2. Plan View of Waste Management Area C Performance Assessment Model Domain Showing the Horizontal Distribution and Surface Type of the Irregularly-Spaced Calculation Nodes. The resolution increases in the area of Waste Management Area C.

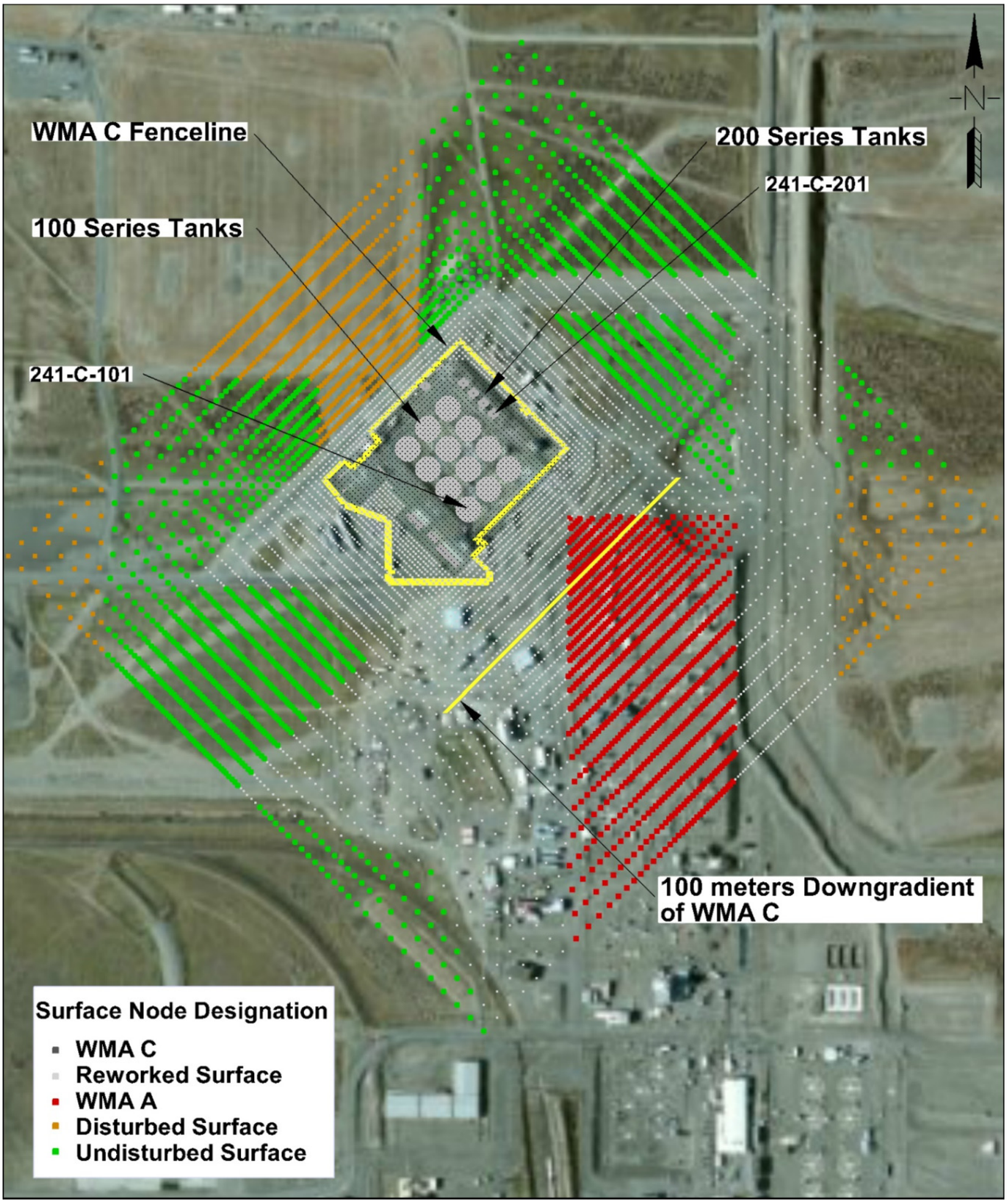

WMA = Waste Management Area

Figure D-3. Fence Diagram of Alternative Geologic Models Used in the Performance Assessment for Waste Management Area C.

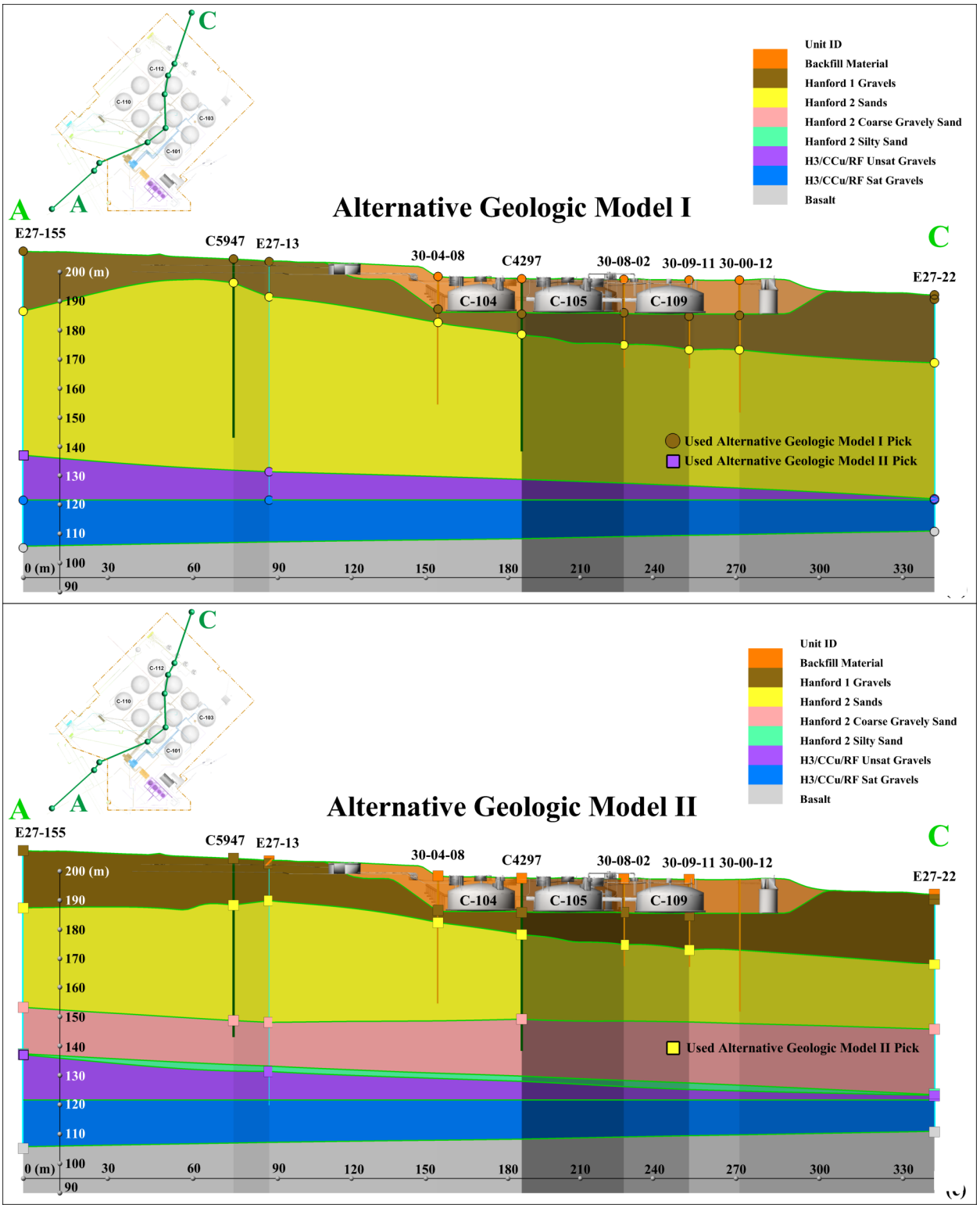

H3/CCu/RF = undifferentiated H3, Cold Creek unit and Ringold Formation

Both mineral phase solubility-limited and matrix degradation rate-limited processes are considered for the key radionuclides and non-radiological contaminants ^{99}Tc, chromium, and uranium. Release processes associated with these three contaminants have been studied in detail in the laboratory, and the laboratory results have been incorporated in the source term analysis. In particular, the following release models are used, which are based on empirical evidence (Section 6.3.1):

- Matrix-degradation-rate-based release of ^{99}Tc that considers an initial 6% fraction of the ^{99}Tc inventory to be instantaneously available for release while the remaining 94% fraction undergoes relatively slower release at the fractional rate of 6×10^{-4} day^{-1}

- Solubility-controlled releases of uranium that impose a solubility limit of 1×10^{-4} M for 1,000 years followed by solubility limit of 1×10^{-6} M

- Dissolved concentration limited release for chromium that imposes a dissolved concentration upper limit of 2,000 µg/L.

For the other analytes evaluated in the WMA C PA, conservative source-term calculations are performed whereby all the analytes are assumed to be instantly and completely available in solution within the residual waste volume, and available for an immediate diffusive release.

While the tank (and ancillary equipment) infill material remains intact, it is assumed that releases occur by a diffusion process through the base of the tank base mat, consisting of grout and concrete layers. The diffusive thickness being considered is the 8-in. combined thickness of concrete and grout layer located at the base of the tank (ignoring the steel plate) because the shortest diffusive pathway for release to the near-field environment is through the base of the tank. The aqueous phase diffusive transport occurs along the thin water films within the pore spaces of the grout and concrete layer. The effective diffusion coefficient of contaminant (which includes effects of tortuosity), and sorption behavior within the grout and concrete layer, control the diffusive mass flux, in addition to the concentration gradient.

Section 6.3.1 of the WMA C PA presents detailed discussion about the theoretical and empirical development and applicability of the equations and the parameters incorporated into the release functions for the individual radionuclides and non-radiological contaminants. That discussion and all of those equations are not repeated here. The discussion and equations presented here only intend to provide context for the relationship between the equations and parameters used to develop the release functions, and an indication of the magnitude of the parameter values associated with the different radionuclides and non-radiological contaminants.

Conceptually, the diffusive release occurs in response to the solute concentration gradient that develops through the interstitial fluid contained in the tank grout and the surrounding soil. Diffusive mass transport is proportional to the concentration gradient. Solute mass diffuses from fluid volumes containing the higher concentration to volumes containing the lower concentration in proportion to the diffusive conductance. Diffusive conductance is a function of the properties

of the contaminant, the fluid media, and the geometry of the diffusive process. For the diffusion release model, the diffusive conductance for a contaminant solute (D_s) is computed as:

$$D_s = \frac{(A\, d\, \tau)}{L} \tag{D-1}$$

Where:

D_s = diffusive conductance of the solute in the fluid (L^3/T)
A = mean cross-sectional area of the connection (L^2)
d = free-water diffusivity of the contaminant solute (L^2/T)
τ = tortuosity of the porous medium that implicitly includes the effect of porosity and saturation (dimensionless)
L = diffusive length, i.e., the length through which diffusion occurs (L).

The diffusive flux f_s (M/T) through the fluid is computed as follows:

$$f_s = D_s(C_{high} - C_{low}) \tag{D-2}$$

where C_{high} and C_{low} (M/L^3) are the high concentration to low concentration values of the dissolved solute. The parameters used to populate the diffusion equations in Section 6.3.1 of the WMA C PA are presented in Table D-2.

As the solute mass diffuses through the fluid in the grout, it instantaneously partitions between the solid (grout and/or soil) and fluid (water and/or air) media. The partitioning is controlled by the partition coefficients defined for each solute in each media, and the quantities of fluid and solid media present. Thus, there becomes a concentration in each medium. In the absence of solubility limits, the concentration of the solute in a particular medium (referred to as medium "m" in Equation 3) is calculated as follows:

$$C_{ims} = \left(\frac{K_{dm}}{\sum_{g=1}^{NM} K_{grs}.VM_g}\right) m_s \tag{D-3}$$

Where:

C_{ims} = concentration of solute in a particular medium (medium "m"), either fluid or solid ([M/L^3] for fluid media or [M/M] for solid media)
m_s = total mass of solute present (M)
K_{dm} = partition coefficient of the solute between medium "m" and a reference fluid ([L^3/L^3] for fluid media or [L^3/M] for solids)
g = media identifying index
K_{grs} = partition coefficient between the other media present, as identified by the index, and a reference fluid for the solute ([L^3/L^3] for fluid media or [L^3/M] for solids)
VM_g = quantity (volume or mass) of a particular medium present (L^3 for fluids or M for solids)
NM = the number of media present.

The partition coefficients for the radionuclides and non-radiological contaminants evaluated in the vadose zone flow and transport model are listed in Table D-3.

D4.1.4 Vadose Zone Hydrogeology and Contaminant Transport

The vadose zone hydrogeology and transport information presented here is a summary of the information presented in Section 6.3.2.2. Detailed discussion and description of the data available and the methods used to develop the parameters, distributions, and percentile values are not repeated here.

The flow and transport pathway process used for the WMA C vadose zone modeling is porous media continuum flow. The porous media continuum assumption and the soil relative permeability/saturation/capillary pressure relations provide the basis for vadose zone flow and transport modeling (PNNL-11216, "STOMP Subsurface Transport Over Multiple Phases Application Guide"; PNNL-12030, "STOMP Subsurface Transport Over Multiple Phases Version 2.0 Theory Guide"). The vadose zone at the Hanford Site is composed of sediments ranging in particle size associated with gravels to silts or clays. In the model domain, the hydraulic properties describing fluid transport characteristics associated with each geologic layer are approximated by average upscaled values, with each unit having different flow and transport parameter values (hydraulic conductivity, bulk density, and dispersivity). The model describes bulk (or mean) flow and radionuclide transport behavior in the vadose zone, limiting the applicability of the evaluation to estimating overall and eventual radionuclide impacts to groundwater. Porous media continuum transport in unsaturated media of this type is regarded as the fundamental process and feature for modeling contaminant fate and transport behavior in the vadose zone at the Hanford Site (DOE/RL-2011-50).

Table D-4 lists the upscaled composite-fitted van Genuchten-Mualem parameters for the various strata at the WMA C site ("A Closed-form Equation for Predicting the Hydraulic Conductivity of Unsaturated Soils" [van Genuchten 1980]; "A New Model for Predicting the Hydraulic Conductivity of Unsaturated Porous Media" [Mualem 1976]; EPA/600/2-91/065, The RETC Code for Quantifying the Hydraulic Functions of Unsaturated Soils). A simultaneous fit of both laboratory-measured moisture retention and unsaturated conductivity data was used in this work, and all five unknown parameters θ_r, θ_s, α, n, and K_s, with m=1-1/n (van Genuchten 1980) were fitted to the data via a code named RETention Curve (RETC) (EPA/600/2-91/065). K_s is treated as a fitted parameter during the curve fitting process in order to obtain a better agreement with experimental data for the region of interest (i.e., relatively dry moisture regime). Estimated unsaturated conductivities, based on saturated conductivity (K_s) and the van Genuchten retention model parameters, have been shown to differ by up to several orders of magnitude with measured conductivities at the dry end (e.g., "Evaluation of van Genuchten-Mualem Relationships to Estimate Unsaturated Hydraulic Conductivity at Low Water Contents" [Khaleel et al. 1995]). The pore size distribution factor ℓ (Mualem 1976) was kept fixed at 0.5 during the simultaneous fitting.

Table D-1. Post-Retrieval Residual Waste Inventory for Waste Management Area C Tanks, Ancillary Equipment, and Pipelines.

Source	241-C-101	241-C-102	241-C-103	241-C-104	241-C-105	241-C-106	241-C-107	241-C-108	241-C-109	241-C-110	241-C-111	241-C-112	241-C-201	241-C-202	241-C-203	241-C-204	241-C-301	244-CR-Vault	Pipelines
Carbon-14 (Ci)	0.003	0.001	0.007	0.003	0.05	0.008	0.02	0.008	0.0008	0.002	0.1	0.02	0.0008	0.0002	0.0002	0.0002	0.002	0.002	0.003
Cobalt-60 (Ci)	0.0002	0.21	0.02	0.47	0.68	2.2	0.0009	0.0007	0.0005	0.0001	0.1	0.0007	0.002	0.002	0.002	0.002	0.12	0.12	0.19
Tritium (Ci)	0.02	2E-5	0.004	0.009	4.1	0.004	0.01	0.02	0.004	0.002	2.6	0.01	0.0002	0.0002	0.0001	0.0001	0.002	0.002	0.003
Iodine-129 (Ci)	6E-5	0.003	0.003	0.0005	0.009	0.0006	0.04	4E-5	3E-5	0.0003	0.01	4E-5	5E-7	7E-6	1E-5	4E-7	0.0002	0.0002	0.0003
Niobium-93m (Ci)	2E-5	0.01	0.0004	0.03	0.001	5.9	0.08	0.05	0.05	0.01	0.1	0.06	0.0007	0.0008	0.0006	0.0006	0.23	0.24	0.38
Radium-226 + Daughters (Ci)	6E-7	3E-7	2E-8	3E-7	2E-7	0.0005	6E-7	5E-7	3E-7	9E-8	5E-6	4E-7	1E-9	1E-9	8E-10	8E-10	2E-5	2E-5	3E-5
Selenium-79 (Ci)	0.0003	2E-6	3E-5	0.009	0.0002	0.01	0.0003	0.002	0.0001	4E-5	0.004	0.0002	5E-5	6E-5	5E-5	4E-5	0.001	0.001	0.002
Tin-126 + Daughters (Ci)	0.0005	0.0002	5E-5	0.009	0.0003	1.8	0.0005	0.0004	0.0003	0.02	0.007	0.0004	0.0001	0.0001	9E-5	9E-5	0.07	0.07	0.11
Technetium-99 (Ci)	0.04	0.004	0.04	0.3	7.8	0.16	2.1	0.05	0.009	0.04	2.2	1.7	0.003	0.002	0.002	0.003	0.04	0.04	0.06
Uranium-232* (Ci)	2E-6	0.03	4E-6	0.04	9E-6	0.0005	2E-6	5E-7	1E-7	2E-8	2E-5	5E-7	2E-6	2E-6	7E-6	5E-6	0.002	0.002	0.003
Uranium-233* (Ci)	2E-7	2.2	0.006	2.2	5E-7	0.002	2E-7	4E-8	1E-8	2E-9	5E-5	4E-8	1E-5	1E-5	3E-5	3E-5	0.12	0.12	0.19
Uranium-234* (Ci)	0.17	0.11	0.01	0.42	0.24	0.0009	0.21	0.03	0.009	0.003	0.77	0.04	0.04	0.04	0.11	0.08	0.23	0.24	0.37
Uranium-235* (Ci)	0.008	0.004	0.0007	0.02	0.01	4E-5	0.009	0.002	0.0004	0.0001	0.03	0.002	0.001	0.001	0.005	0.003	0.01	0.01	0.02
Uranium-236* (Ci)	0.002	0.001	0.0004	0.005	0.005	2E-5	0.002	0.0003	1E-4	3E-5	0.01	0.0005	0.0005	0.0004	0.0008	0.0005	0.002	0.002	0.003
Uranium-238 +Daughters (Ci)	0.17	0.1	0.02	0.44	0.24	0.0009	0.21	0.04	0.01	0.003	0.79	0.04	0.04	0.03	0.11	0.08	0.23	0.23	0.36
Chromium (VI) (dissolved) (Kg)	7.2	11.3	2.4	3.1	37	3.8	55.4	0.63	0.18	1.1	73.3	57.8	12.2	9.1	2.6	1.4	17.9	18.3	28.6
Fluoride (Kg)	34.6	0.006	0.16	15.4	79.2	0.54	605	121	96.8	138	807	709	2.7	2.3	1.6	0.008	21.2	21.8	34.1
Nitrite (Kg)	564	0.03	0.48	5.1	647	41.4	2,148	5.8	3.8	2.7	5,500	675	0.53	0.45	0.99	0.03	3.9	4	6.2
Nitrate (Kg)	8,200	0.1	0.87	9.4	783	34.8	3,588	9.2	4.5	6.7	14,700	8,760	1.4	1.3	3.8	0.02	7.5	7.7	12
Total Uranium (soluble salts) (Kg)	516	293	49.1	1320	734	2.7	632	121	28.6	5.5	2,360	129	111	98.8	326	243	676	693	1,084
Cobalt (Kg)	0	0	0.09	0.04	0	0.38	0	0.05	0.01	0.02	0	0	0.08	0.08	0.02	0.04	0	0	0
Cyanide (Kg)	0	0	0.01	0.02	0	0.08	0	0.16	0.39	0.008	0	0	0.002	0.004	0.004	0.0007	0	0	0
Selenium and compounds (Kg)	0	0	0.69	0.14	0	2.9	0	0.31	0.08	0.04	0	0	0.11	0.09	0.18	0.4	0	0	0
Tin (Kg)	0	0	1.1	0.37	0	2.4	0	0.15	0.04	0.85	0	0	0.13	0.38	0.15	0.2	0	0	0
Tributyl Phosphate (Kg)	0	0	1	0.02	0	0	0	0.05	0.009	0.1	0	0	19.9	5.3	8.7	65.5	0	0	0

*The base case analysis also includes Uranium-232, Uranium-233, Uranium-234, Uranium-235, and Uranium-236, but these isotopes were not evaluated directly using the STOMP© model.

Subsurface Transport Over Multiple Phases (STOMP)© is copyrighted by Battelle Memorial Institute, 1996.

Table D-2. Summary Explanation and List of Parameters Used to Develop the Source-Term Release Calculations and Functions. (2 sheets)

Parameter	Value	Reference
Release Type	Diffusive release from the tanks and CR-Vaults under intact conditions; Both advective and diffusive release for the Pipelines; Both advective and diffusive release for tanks and CR-Vaults under degraded conditions.	
Technetium-99 release	6% of the waste inventory available for release instantaneously; remaining 94% waste form inventory made available based on first order fractional release rate of 6E-4 day^{-1}.	Waste Management Area (WMA) C Performance Assessment (PA) Section 6.3.1
Chromium dissolved concentration limit	2,000 µg/L dissolved concentration limit imposed	WMA C PA Section 6.3.1
Uranium solubility for intact tank conditions	1E-4 M for 1,000 years; 1E-6 M for time >1,000 years	WMA C PA Section 6.3.1
Uranium solubility for degraded tank conditions	1E-4 M for 1,000 years; 2E-5 M for time >1,000 years	WMA C PA Section 6.3.1
Contaminant K_d values for transport through the grout and concrete layer	Variable; See Table D-3	WMA C PA Table 6-5
Porosity of Residual Waste Layer	0.4	Assumed
Saturation of Residual Waste Layer	1	Assumed fully saturated to maximize diffusive release
Residual Waste Volume	Variable by source	WMA C PA Section 3.1
Porosity of Concrete and Grout layer below the waste layer	0.11	SRNL-STI-2008-00421, Table 39
Saturation of Concrete and Grout layer below the waste layer	1	Assumed to maximize diffusive release
Bulk Density of Concrete and Grout layer below the waste layer	2.41 g/cm^3	RPP-RPT-50934, pp. C-3 (C-107 dome core density of 151 lb/ft^3)
Diffusive Length of Waste form layer	0 m	Assumed to maximize diffusive release
Diffusive Length of Concrete and Grout layer below the waste layer	0.203 m (8 in.)	Minimum diffusive thickness based on tank bottom geometry

Table D-2. Summary Explanation and List of Parameters Used to Develop the Source-Term Release Calculations and Functions. (2 sheets)

Parameter	Value	Reference
Diffusive Area for source term release	410.4 m^2 for 100-Series Tanks; 29. 2 m^2 for 200-Series Tanks and C-301 catch tank; 162.4 m^2 for CR_Vaults; 22,500 m^2 for Pipelines	Base area for tanks based on circular geometry; area of CR-Vault is based on rectangular area with length of 92 ft and average width of 19 ft; area of Pipeline assumed to be 150 m × 150 m.
Effective Diffusion Coefficient through grout and concrete layer (incorporates effects of tortuosity)	3E-8 cm^2/s	WMA C PA Section 6.3.1

References:
RPP-RPT-50934, "Inspection and Test Report for the Removed 241-C-107 Dome Concrete."
SRNL-STI-2008-00421, "Hydraulic and Physical Properties of Saltstone Grouts and Vault Concretes."

A stochastic model of variable moisture or tension-dependent anisotropy provides the framework for upscaling small-scale measurements to the effective (upscaled) properties for the large-scale vadose zone ("Application of Stochastic Methods to Transient Flow and Transport in Heterogeneous Unsaturated Soils" [Polmann 1990]). The upscaling processes factor the inherent spatial variability that occurs on different scales in heterogeneous media into the field scale parameter estimates ("Stochastic analysis of moisture plume dynamics of a field injection experiment" [Ye et al. 2005]; "Estimation of effective unsaturated hydraulic conductivity tensor using spatial moments of observed moisture plume" [Yeh et al. 2005]). Specific upscaled flow parameters include moisture retention, and saturated and unsaturated hydraulic conductivity. Upscaled transport parameters include bulk density, diffusivity, sorption coefficients, and macrodispersivity. Detailed discussion of the Polmann (1990) model and the derivation of the upscaled parameters are presented in Section 6.3.2.2.

For the Alternative Geologic Model II evaluation, the Hanford H2 gravel/coarse sand subunit was assumed to be more transmissive, and the Hanford H2 silty sand less transmissive, than the Hanford H2 sand. Therefore, as an initial estimate of these properties, the hydraulic properties associated with the 5th and 95th percentile realizations of unsaturated hydraulic conductivity curves developed for the Hanford H2 sand unit were considered representative of the Hanford H2 gravel/coarse sand and the Hanford H2 silty sand subunits, respectively.

The effective transport parameter (i.e., macrodispersivity, bulk density, and diffusivity) estimates used in the base case and sensitivity cases are presented. Because of natural variability, the transport parameters are all spatially variable. The purpose is similar to the upscaled flow parameters, to evaluate the effect of such variability on the large-scale transport process. Effective bulk density (ρ_b) estimates are needed to calculate retardation factors for different species. The average ρ_b ($E[\rho_b]$) estimates for various strata at WMA C are presented in Table D-5. These estimates are derived from bulk density values listed in Section 3.2.2. According to "Solute transport in heterogeneous porous formations" (Dagan 1984),

macrodispersivity reaches a constant, asymptotic value after the solute travels a few tens of correlation scales (~50 cm) of the hydraulic conductivity field; therefore, the use of a constant (asymptotic) macrodispersivity value is considered appropriate in PA simulations (Section 3.2.2). On the basis of results of numerical simulation, stochastic theory, and 200 Areas experimental data, the recommendation is to use a longitudinal macrodispersivity value of 25 cm for the H2 sand unit in the WMA C PA base case. For H1/H3/Backfill sediments, the recommendation is to use a longitudinal macrodispersivity value of 20 cm. The transverse macrodispersivity is typically much lower; in saturated media, it may range from 1 to 10% of the longitudinal macrodispersivity ("Three-dimensional stochastic analysis of macrodispersion in aquifers" [Gelhar and Axness 1983]). In the absence of unsaturated media experimental data, the recommendation is to use a transverse macrodispersivity 1/10th of the longitudinal macrodispersivity. The estimated values of macrodispersivity applicable to the scale of the WMA C PA model for the base case are shown in Table D-6. It is assumed that the effective, large-scale diffusion coefficients for all strata in the vadose zone at the WMA C site are a function of volumetric moisture content, θ, and can be expressed using the Millington-Quirk ("Permeability of Porous Solids" [Millington and Quirk 1961]) empirical relation:

$$D_e(\theta) = D_0 \frac{\theta^{10/3}}{\theta_s^2} \tag{4-1}$$

Where:

$D_e(\theta)$ = the effective diffusion coefficient of an ionic species
D_0 = the effective diffusion coefficient for the same species in free water
θ = the localized volumetric moisture content.

The tortuosity formulation in the Millington-Quirk model is based on theoretical considerations absent from other empirical models, and accounts for the ranges of moisture contents present in the vadose zone around WMA C. The molecular diffusion coefficient for all species in pore water is assumed to be 2.5×10^{-5} cm^2/sec (WHC-SD-WM-EE-004, "Performance Assessment of Grouted Double-Shell Tank Waste Disposal at Hanford") which is consistent with, and representative of, values used in other Hanford PAs.

D4.1.5 Infiltration and Recharge

The magnitude of recharge for soils at the Hanford Site varies as a function of the soil type, condition of the vegetation cover, and soil integrity (e.g., disturbed versus undisturbed). The range of recharge values reported in RPP-RPT-44042 represents distinct populations of data based on lysimetry and isotopic measurements, and based on interpretation and, in some instances, extrapolation by Hanford Site subject matter experts. The natural background recharge rates represent a population for natural vegetated conditions. The range of values for operational conditions represents a population of recharge rates for vegetation-free disturbed soil. Table D-7 presents a summary of the base case recharge rates applied to the different surface types.

Table D-3. Partition Coefficient Values for Grout/Concrete Used for Waste Management Area C Performance Assessment Source Release Functions.

Radionuclide or Non-radiological Contaminant	Best Estimate K_d Value (mL/g)	Reference
C	2.53E+03	PSI Bericht Nr. 95-06
CN	0.00E+00	No relevant information
Co	4.00E+01	SKB R-05-75
Cr	0.00E+00	No relevant information
F	0.00E+00	No relevant information
H	1.00E-01	NAGRA NTB 02-20
I	3.00E+00	SKB R-05-75
Nb	5.00E+02	SKB R-05-75
NO_2	0.00E+00	No relevant information
NO_3	0.00E+00	No relevant information
Ra	5.00E+01	SKB R-05-75
Rn	0.00E+00	No relevant information
Se	6.00E+00	SKB R-05-75
Sn	5.00E+02	SKB R-05-75
Tri-butyl Phosphate	0.00E+00	No relevant information
Tc	1.00E+00	NAGRA NTB 02-20
U isotopes	2.00E+03	NAGRA NTB 02-20
U_total	2.00E+03	NAGRA NTB 02-20

References:
NAGRA NTB 02-20, "Cementitious Near-Field Sorption Data Base for Performance Assessment of an ILW Repository in Opalinus Clay."
PSI Bericht Nr. 95-06, "Sorption Databases for the Cementitious Near-Field of a L/ILW Repository for Performance Assessment."
SKB Rapport R-05-75, "Assessment of uncertainty intervals for sorption coefficients, SFR-1 uppföljning av SAFE."

The design for the WMA C surface barrier at closure has not been finalized, but it is expected to function comparably to a Modified RCRA Subtitle C Barrier. Summary of data collected over 13 years at the Prototype Hanford Barrier (PNNL-17176, "200-BP-1 Prototype Hanford Barrier Annual Monitoring Report for Fiscal Years 2005 Through 2007"; DOE/RL-93-33, Focused Feasibility Study of Engineered Barriers for Waste Management Units in the 200 Areas) indicates that infiltration through the prototype is much less than 0.1 mm/yr, and evaluations of the design using lysimeter data indicate that the barrier is capable of limiting recharge to this amount even with a complete lack of vegetation ("Multiple-Year Water Balance of Soil Covers in a Semiarid Setting" [Fayer and Gee 2006]). However, for PA simulations involving WMA C

with a functioning surface barrier, a base case recharge rate of 0.5 mm/yr is assumed, which is consistent with the drainage design specification in DOE/RL-93-33.

Table D-4. Composite van Genuchten-Mualem Parameters for Various Strata at the Waste Management Area C Site Used in the Base Case Evaluations of Alternative Geologic Models I and II.

Strata	Number of Samples	θ_s	θ_r	α (1/cm)	n	ℓ^c	Fitted K_s (cm/s)
Backfill (Gravelly)	10	0.138	1.11E-02	0.021	1.374	0.5	5.60E-04
Hanford H1/H3 (Gravel-dominated)	15	0.171	1.11E-02	0.036	1.491	0.5	7.70E-04
Hanford H2 (Sand-dominated)	44	0.315	3.92E-02	0.063	2.047	0.5	4.15E-03
Hydrostratigraphic Units only applicable to Alternative Geologic Model II							
Hanford H2 – Gravel/coarse sand subunit*	not applicable (75th Percentile)	0.265	2.11E-03	0.108	1.724	0.5	1.68E-02
Hanford H2 – Silty sand subunit*	not applicable (5th Percentile)	0.354	2.89E-02	0.040	1.633	0.5	1.79E-03

* Hydraulic properties of these units are only used in numerical model simulation of Alternative Geologic Model II. As an initial estimate of these properties, the hydraulic properties associated with the 5th and 95th percentile realizations of unsaturated hydraulic conductivity curves developed in the Uncertainty and Sensitivity Analysis for the Hanford H2 sand unit were considered to be representative of the Hanford H2 gravel/coarse sand and the Hanford H2 silty sand subunits.

Table D-5. Effective Bulk Density (E[ρb], g/cm^3) Estimates for Various Strata at Waste Management Area C Used in the Base Case Evaluations of Alternative Geologic Models I and II.

Strata	$E[\rho_b]$
Backfill (Gravelly)	2.13
Hanford H1/H3 (Gravel-dominated)	2.05
Hanford H2 (Sand-dominated)	1.71
Hydrostratigraphic Units only applicable to Alternative Geologic Model II	
Hanford H2 – Gravel/coarse sand subunit*	1.83
Hanford H2 – Silty sand subunit*	1.61

* Effective bulk densities of these units are only used in numerical model simulation of Alternative Geologic Model II.

At the end of 500 years, the surface barrier performance is assumed to degrade to permit an infiltration rate of 3.5 mm/yr and maintain that infiltration rate for the remainder of the sensitivity and uncertainty analysis time frame. No quantifying data are available for specifying the performance of the barrier top after its design life. According to PNNL-13033, “Recharge

Data Package for the Immobilized Low-Activity Waste 2001 Performance Assessment," the erosion of the silt loam layer and deposition of dune sand on the barrier is not likely to alter the barrier performance significantly. The value of 3.5 mm/yr (0.14 in./yr) corresponds to the recharge in an undisturbed area, which indicates that native vegetation is assumed to reclaim the land.

Table D-6. Macrodispersivity Estimates for Various Strata at Waste Management Area C Used in the Base Case Evaluations of Alternative Geologic Models I and II.

Strata	A_L (cm)	A_T (cm)
Backfill (Gravelly)	~20	2
Hanford H1/H3 (Gravel-dominated)	~20	2
Hanford H2 (Sand-dominated)	~25	2.5
Hydrostratigraphic Units only applicable to Alternative Geologic Model II		
Hanford H2 –Gravel/coarse sand subunit*	~25	2.5
Hanford H2 – Silty sand subunit*	~25	2.5

* Macrodispersivities of these units are only used in numerical model simulation of Alternative Geologic Model II.

Although the side slopes and berm are likely to function and perform differently than the surface of the barrier, they are included as part of the barrier surface. The impact of the side slopes on the overall recharge rate is expected to be relatively minor. The sandy gravel/gravelly sand barrier side slope and berm are assumed eventually to resemble a Burbank loamy sand, and PNNL-16688, "Recharge Data Package for Hanford Single-Shell Tank Waste Management Areas" indicates that the long-term recharge rate for that soil type is 1.9 mm/yr, which is less than the value of 3.5 mm/yr used in the analysis for the degraded barrier surface.

D4.1.6 Geochemistry and Sorption

The geochemistry conceptual model component involves the partitioning behavior or sorption characteristics regarding release, retardation, and attenuation mechanisms, and any simplifying assumptions for specific radionuclides and non-radiological contaminants. The key aspects of this geochemistry conceptual model and its applicability to the Hanford Site 200 Areas include the following, and are discussed in detail in DOE/RL-2011-50:

- The use of a linear K_d isotherm is a reasonable description for the release and attenuation of radionuclides in the context of providing an upper-bounding condition
- The source(s) of the data used in the selection of radionuclide K_d values
- The use of a single K_d in the individual vadose zone hydrostratigraphic units (HSUs).

Table D-7. Base Case Recharge Rate (Net Infiltration) Estimates for Surface Conditions during the Pre-Construction, Operational, and Post-Closure Periods.

Period	Waste Management Area (WMA) C Region and Surface Condition	Base Case Value of Recharge Rate (mm/yr)
Pre-construction (before 1944)	Undisturbed region (Rupert sand with vegetation)	3.5
Operational period (1945 to 2020)	Undisturbed region (Rupert sand with vegetation)	3.5
	WMA C Surface region (Gravel without vegetation)	100
	WMA A Surface region (Gravel without vegetation)	100
	Disturbed revegetated region (Rupert sand with vegetation)	22
	Disturbed unrevegetated region (Rupert sand with no vegetation)	63
Early post-closure (2020 to 2520)	Undisturbed region (Rupert sand with vegetation)	3.5
	WMA C Surface region (Surface barrier with vegetation)	0.5
	WMA A Surface region (Surface barrier with vegetation beginning in 2050)	0.5
	Disturbed revegetated region (Rupert sand with vegetation beginning in 2050 with vegetation recovery completed in 2080)	3.5
	Disturbed unrevegetated region (Rupert sand with no vegetation until vegetation recovery begins in 2050 and completes in 2080)	3.5
Late post-closure (2520 to 3020 and beyond)	Undisturbed region (Rupert sand with vegetation)	3.5
	WMA C Surface region (Surface barrier with vegetation)	3.5
	WMA A Surface region (Degraded surface barrier with vegetation begins in 2550)	3.5
	Disturbed revegetated region (Rupert sand with vegetation recovery completed in 2080)	3.5
	Disturbed unrevegetated region (Rupert sand with vegetation recovery completed in 2080)	3.5

The geochemistry conceptual models for the Hanford Site are based on extensive laboratory studies, testing, and measurements of adsorption and desorption coefficients under saturated and unsaturated conditions involving Hanford Site-specific sediments, contaminants, and conditions (DOE/RL-2011-50; RPP-RPT-46088; PNNL-13895, "Hanford Contaminant Distribution Coefficient Database and Users Guide"). The basis and rationale for the K_d values used to approximate the transport of the radionuclides is presented in RPP-RPT-46088, and the base case values are presented in Table D-8. The differing values for the different geologic units represent the adjustment of values resulting from the approximate gravel content of each unit.

The radionuclides and non-radiological contaminants listed in Table D-8 are limited to those with K_d values less than 2 mL/g (prior to any adjustments because of gravel content) because the

results of the screening analysis indicated that radionuclides with K_d values greater than 2 mL/g did not impact groundwater within the 10,000-year sensitivity-uncertainty time frame (see Section 7.2.1.1 Result of Screening Analysis for Groundwater Pathway regarding this determination).

Table D-8. Summary of the Waste Management Area C Performance Assessment Base Case K_d (mL/g) Values.

Radionuclide or Non-radiological Contaminant	K_d (mL/g)			
	Backfill	H1	H2	H3
Carbon-14 (C-14)	0.46	0.58	0.8	0.58
Cobalt/Cobalt-60 (Co/Co-60)	0	0	0	0
Chromium (Cr)	0	0	0	0
Fluoride (F)	0	0	0	0
Tritium (H-3)	0	0	0	0
Iodine-129 (I-129)	0.09	0.12	0.16	0.12
Niobium-93m (Nb-93m)	0	0	0	0
Nitrite (NO_2)	0	0	0	0
Nitrate (NO_3)	0	0	0	0
Radon-222 (Rn-222)	0	0	0	0
Selenium/Selenium-79 (Se/Se-79)	0.05	0.06	0.08	0.06
Tin/Tin-126 (Sn/Sn-126)	0.23	0.29	0.4	0.29
Technetium-99 (Tc-99)	0	0	0	0
Total Uranium/Uranium-238 (U Total/U-238*)	0.28	0.35	0.48	0.35
Tri-butyl Phosphate (TBP)	1.89	0.87	1.1	1.5

* The base case analysis also includes Uranium-232, Uranium-233, Uranium-234, Uranium-235, Uranium-236, and the Uranium-238 daughter products, but these isotopes were not evaluated directly using the STOMP© model.

Subsurface Transport Over Multiple Phases (STOMP)© is copyrighted by Battelle Memorial Institute, 1996.

D4.1.7 Groundwater Domain

The integrated, saturated-unsaturated, 3-D WMA C model calculates groundwater concentrations of contaminants approximately 100 m downgradient of the WMA C fenceline that are estimated to occur several hundred to several thousand years into the future. The unconfined aquifer flow and transport parameters play a critical role in WMA C PA modeling because of the dilution that occurs as recharge containing contaminants enters the aquifer. Additional dilution and concentration attenuating dispersion occurs as the contaminants travel through the aquifer. The dilution and dispersion are strongly dependent on the groundwater flux, which is a rate measure defined as the flow through a defined area. Groundwater flow beneath WMA C has been

difficult to measure historically because the hydraulic gradient is very small and the hydraulic conductivity is very large in this region of the Hanford Site.

The groundwater in the aquifer system in the vicinity of WMA C has been studied extensively as part of the site characterization as discussed in RPP-RPT-46088 and Appendix C. The groundwater conceptual model for WMA C includes the uppermost unconfined aquifer system that exists within a channel eroded by the cataclysmic floods of the Pleistocene. The base of the aquifer is the underlying basalt surface. The undifferentiated lower sands and gravels associated with the Hanford formation, Cold Creek unit, and the Ringold Formation (Unit A) that comprise the aquifer sediments are simply categorized as saturated Hanford H3 sediments in the model. The thickness of the uppermost aquifer beneath WMA C is approximately 12 m (39 ft). The model results provided represent concentrations in the upper 5 m (16.4 ft) of the aquifer. The 5-m vertical interval corresponds to the well screen length of a conceptual groundwater monitoring well, and the basis for that delimiter to the groundwater concentrations calculation is presented in Section D4.1.8 Point of Calculation, Protectiveness Metric, and Time Frame Considerations. The aquifer, identified as Hanford H3 – aquifer, is separated from that portion of the Hanford H3 above the water table, reflecting the distinctly different saturation conditions.

For the WMA C PA modeling, the unconfined aquifer is treated as an equivalent homogeneous medium (EHM) that requires parameterization for the appropriate scale. Effective parameterization for WMA C saturated media hydraulic conductivity appears to be best achieved via a field-scale calibrated regional groundwater model that accounts for appropriate local-scale boundary conditions, flow configuration, and history matching of well head data (WMA C PA Appendix C). The Central Plateau Groundwater Model (CPGWM) provides calibrated hydraulic conductivity estimates for the model layers and HSUs present within the aquifer in the vicinity of WMA C. The thicknesses of the different aquifer HSUs are mapped from the CPGWM onto the WMA C PA STOMP© model flow domain, and an averaging scheme weighted according to HSU thickness provides estimates of the EHM effective saturated hydraulic conductivity and the hydraulic gradient.

The weighted average of hydraulic conductivity of the CPGWM HSUs mapped onto the WMA C flow domain indicates that the effective STOMP© EHM saturated hydraulic conductivity is approximately 11,000 m/day. As discussed previously, field-scale calibrated groundwater models provide an effective parameterization for WMA C saturated media hydraulic conductivity for the overall dimensions of the WMA C PA model domain. The hydraulic gradient is calculated from a planar rectangular window (300 m × 200 m) in the CPGWM having an unconfined aquifer depth that encompasses most of the WMA C flow domain (Figure D-4, adapted from CP-47631, “Model Package Report: Central Plateau Groundwater Model Version 3.4”) by taking into account the net volumetric flux through the domain. Volumetric flux through the window is divided by the vertical cross-sectional area of the aquifer and the STOMP© EHM hydraulic conductivity to calculate the hydraulic gradient.

In the future, the gradient is generally expected to be from northwest to southeast. The water table in the unconfined aquifer is expected to continue declining because the large discharges of operational liquid to the ground at 216-B-3 Pond system and other large discharge sites in 200 East Area have ceased. The hydraulic heads around WMA C are expected to continue

declining slowly until they stabilize around year 2030 at 119.5 m (392 ft) (Figure D-4). For Year 2100 (approximating post-closure steady state conditions), the CPGWM-calculated flow through the window volume is 580 m^3/day, which divided by the cross-sectional area of 3,300 m^2 translates to a Darcy flux of 0.18 m/day with a hydraulic gradient of 2×10^{-5}, which is close to the one observed prior to start of Hanford operations, as estimated from Figure 6-42 (adapted from Figure 2-8 in WHC-EP-0645, "Performance Assessment for the Disposal of Low-Level Waste in the 200 West Area Burial Grounds"). Changes in hydraulic gradient are only expected to occur within the first 10 to 50 years of the post-closure simulation period, which, according to the screening analysis (see Sections 6.3.2.3 Groundwater Pathway Screening Analysis Methodology and 7.2.1.1 Result of Screening Analysis for Groundwater Pathway), is before the mobile radionuclides reach the water table. Thus, the hydraulic gradient is assumed to be stable for this analysis.

According to RPP-14430, "Subsurface Conditions Description for C and A-AX Waste Management Area," porosity is generally estimated to be about 30% for unconsolidated coarse-grained sediments, but a value closer to 20% may be more appropriate where boulders and cobbles are present and mixed with sand and gravels, such as at WMA C. The STOMP© EHM porosity value of 0.20 is consistent with the vadose zone value of 0.17 for the Hanford H1 and H3 sediments, and with the aquifer test results from well 699-55-50 presented in HW-60601, "Aquifer Characteristics and Ground-Water Movement at Hanford." The STOMP© EHM includes the CPGWM estimate of 0.1 (CP-47631) for the anisotropy, which is defined here as the ratio of vertical to horizontal hydraulic conductivity. The longitudinal and transverse macrodispersivity estimates in the saturated zone are based on a review of three general relationships ("Universal Scaling of Hydraulic Conductivities and Dispersivities in Geologic Media" [Neuman 1990]; "Longitudinal Dispersivity Data and Implications for Scaling Behavior" [Schulze-Makuch 2005]; and "Use of Weighted Least-Squares Method in Evaluation of the Relationship Between Dispersivity and Field Scale" [Xu and Eckstein 1995]) that quantify the dependence of this parameter on measurement scale (L_s). For 100 m, which is the approximate distance of travel to the compliance well located in the saturated zone, the calculated values fall within the range of 1 to 20 m (Table D-9). Thus, a value of 10.5 m is chosen for the base calculation. The ratio of longitudinal to transverse macrodispersivity is chosen to be 10 based on RPP-17209, "Modeling Data Package for an Initial Assessment of Closure of the S and SX Tank Farms" and "Field Study of a Long and Very Narrow Contaminant Plume" (van der Kamp et al. 1994). Table D-10 presents a summary of the aquifer hydraulic parameters for the Hanford H3 – aquifer used for the base case.

D4.1.8 Point of Calculation, Protectiveness Metric, and Time Frame Considerations

In accordance with risk and performance assessment guidelines, the determination of soil contamination impacts to groundwater also requires the definition and rationale for (1) the point of calculation, i.e., the place and points in the groundwater domain where modeled groundwater concentrations are to be assessed for potential impacts and protectiveness; (2) the protectiveness metric, i.e., the groundwater metric(s) to be used in the assessment of protectiveness at the point of calculation; and (3) the time frame considered applicable for the calculation of impacts to groundwater. The point of calculation is intended to effectively serve as the point where exposure point groundwater concentrations are evaluated in the model for the purpose of

evaluating the achievement of the groundwater protection performance objectives. The point of calculation for the protection of groundwater is related to "Point of Compliance" in Federal PA requirements (DOE M 435.1-1; DOE G 435.1-1, Chapter 4) and described as follows:

> "The point of compliance shall correspond to the point of highest projected dose or concentration beyond a 100 meter buffer zone surrounding the disposed waste. A larger or smaller buffer zone may be used if adequate justification is provided."

Thus, the point of calculation for the groundwater impact analysis is 100 m downgradient from the WMA C fenceline. While the DOE manual and guide state that point of compliance is the point of highest calculated dose (groundwater concentration), neither indicates how that groundwater concentration should be calculated—i.e., within what volume the concentration is to be calculated, apart from indicating that the aquifer mixing must be consistent with State or local laws, regulations, or agreements.

The approach identified in EPA/540/R-95/128, Soil Screening Guidance: Technical Background Document and WAC 173-340-747, "Deriving Soil Concentrations for Groundwater Protection" indicates that the cross section of the aquifer volume is usually prescribed to be a unit width of 1 m (3.3 ft), because the equations are developed on the basis of a unit width. This implies that the cross section width is equal to the width of contamination entering the aquifer. Consistent with this reasoning, other performance assessments conducted at Hanford and other DOE facilities have used an aquifer mixing width equal to the width of the facility (e.g., WCH-520, "Performance Assessment for the Environmental Restoration Disposal Facility, Hanford Site, Washington"; WSRC-MS-2003-00582, "Performance Assessment/Composite Analysis Modeling to Support a Holistic Strategy for the Closure of F Area, a Large Nuclear Complex at The Savannah River Site").

To calculate the highest groundwater concentration, the base case evaluated the average concentration in the aquifer within nine segments along the line perpendicular to, and 100 m beyond, the southeast edge of WMA C (Figure D-5). Concentrations calculated in the nine segments of the aquifer are assumed to be comparable to concentrations that would be measured by sampling a monitoring well at that location. The nine segments are approximately 30 m long (Table D-11), and aligned such that the centerlines of the plumes in the groundwater resulting from the residuals released from a single line of 100-series tanks parallel to the direction of groundwater flow (e.g., the centerline of the plumes resulting from the tank residuals in 241-C-102, 241-C-105, 241-C-108, and 241-C-111) intersect the perpendicular line within the same segment.

The WAC specifies a 5-m mixing zone in groundwater that is consistent with a 5-m vertical interval corresponding to a conceptual groundwater monitoring well with the 15-ft well screen length (and mixing zone dimension) associated with State monitoring well descriptions (e.g., see Equation 747-4 in WAC 173-340-747). The aquifer mixing zone extends into the upper 5 m of the aquifer for the purpose of the evaluations. DOE M 435.1-1 does not specify the level of protection required for water resources, and there are no applicable parameterization requirements or guidelines indicated in DOE G 435.1-1, Chapter 4.

Figure D-4. Central Plateau Groundwater Model Calibration Results in the Vicinity of Waste Management Area C.

a)

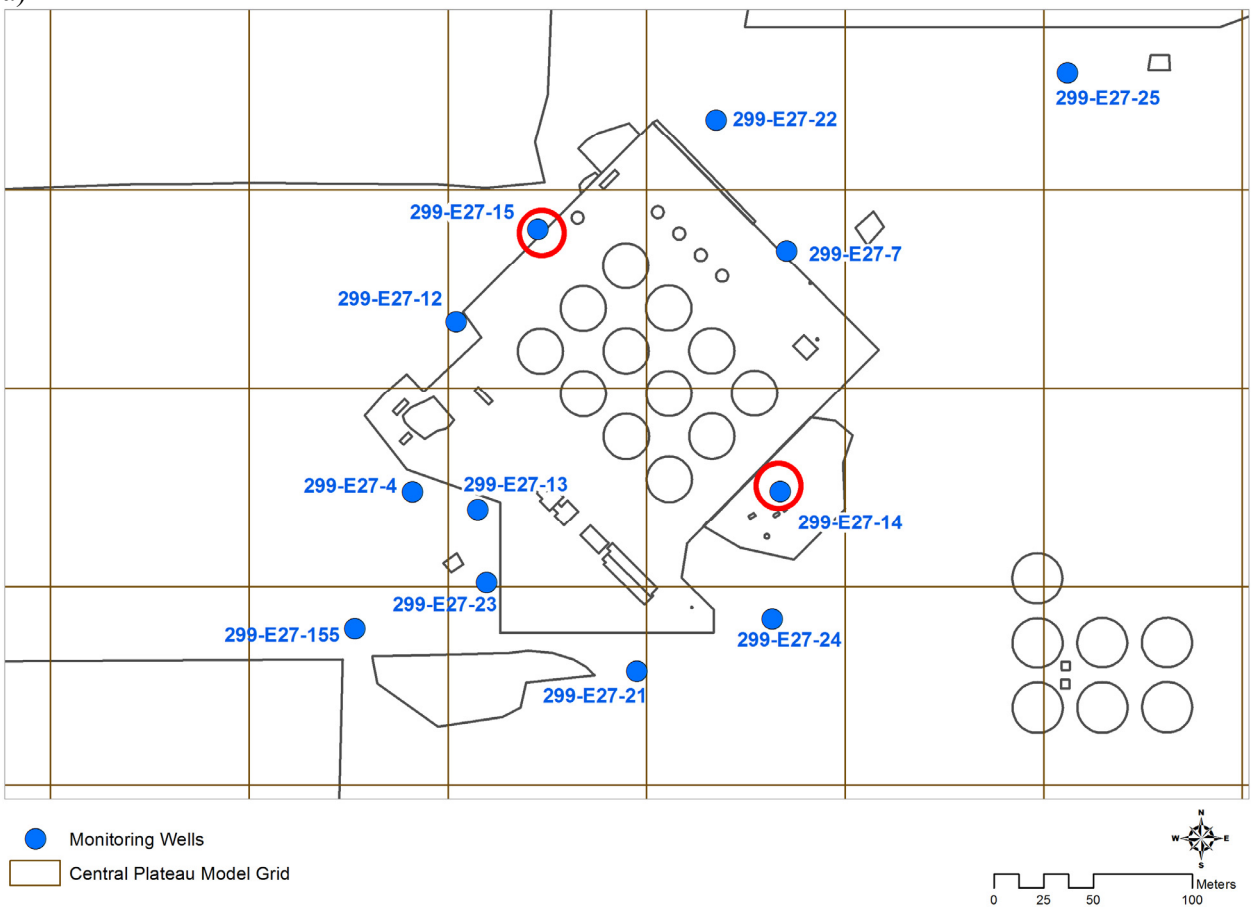

b)

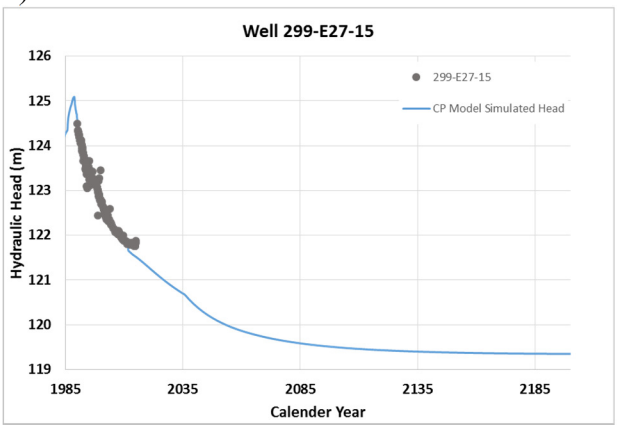

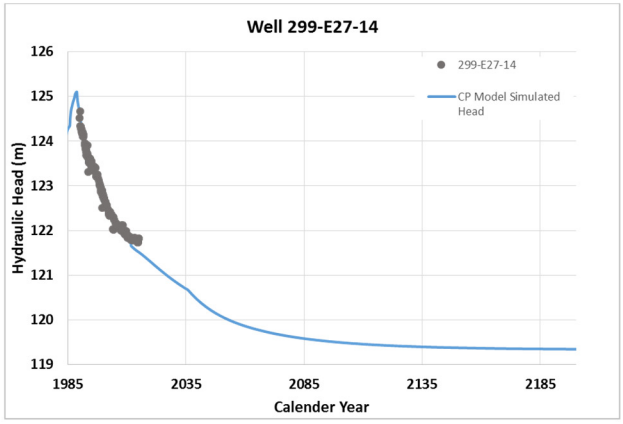

The compliance time frame is defined as 1,000 years following closure of the facility (DOE M 435.1-1; DOE G 435.1-1, Chapter 4). The sensitivity-uncertainty analysis along with the Nuclear Regulatory Commission's guidance (NUREG-1854, NRC Staff Guidance for Activities Related to U.S. Department of Energy Waste Determinations – Draft Final Report for

Interim Use) extends the evaluation to 10,000 years, which is sufficient to evaluate the peak dose from all of the radionuclides that the screening analysis indicates may not impact groundwater within the compliance period. DOE M 435.1-1 and DOE G 435.1-1, Chapter 4 state that the sensitivity-uncertainty analysis time frame should include calculation of the maximum dose regardless of the time at which the maximum occurs, as a means of increasing confidence in the outcome of the modeling and increasing the understanding of the models used. However, EPA-SAB-RAC-ADV-99-006, An SAB Advisory: Modeling of Radionuclide Releases from Disposal of Low Activity Mixed Waste warns that extending the modeling time frame beyond 10,000 years could make the results irrelevant, and hinder public acceptance of the results because of the inherent scientific and social uncertainties associated with such an extended time frame. The 10,000-year time frame is sufficient to address uncertainty associated with radionuclides that impact groundwater during the compliance period (NUREG-1573, A Performance Assessment Methodology for Low-Level Radioactive Waste Disposal Facilities: Recommendations of NRC's Performance Assessment Working Group).

Table D-9. Relationship Between Saturated Longitudinal Macrodispersivity (αL) and Scale of Measurement (L_s).

Reference	Relationship	Origin	Saturated Longitudinal Macrodispersivity Estimate (m) for a Scale ≈ 100 m
Neuman (1990)	$\alpha_L \approx 0.017\ L_s^{1.5}$	"Universal relationship" established considering both field and laboratory data (excluding modeling results)	17
Schulze-Makuch (2005)	$\alpha_L \approx 0.085\ L_s^{0.81}$	Established considering field and modeling results (all reliabilities) and excluding laboratory data	3.5
Xu and Eckstein (1995)	$\alpha_L \approx 0.94(\log_{10} L_s)^{2.693}$	Established considering the same data set as Neuman (1990) including numerical model results	6

References:
"Longitudinal Dispersivity Data and Implications for Scaling Behavior" (Schulze-Makuch 2005).
"Universal Scaling of Hydraulic Conductivities and Dispersivities in Geologic Media" (Neuman 1990).
"Use of Weighted Least-Squares Method in Evaluation of the Relationship Between Dispersivity and Field Scale" (Xu and Eckstein 1995).

DOE G 435.1-1, Chapter 4 states that DOE low-level waste disposal facilities must comply with legally applicable requirements for water resource protection. The protectiveness metrics determined to be most appropriate for the evaluation of impacts to groundwater during the compliance period from the radionuclide and contaminant inventory in WMA C are the maximum concentration limits. Maximum concentration limits represent the "allowable concentrations" and/or "acceptable limits" of a radionuclide for minimizing further degradation of groundwater in accordance with the conditions identified in State and Federal anti-degradation goals (e.g., EPA/540/R-92/003, Guidance for Data Useability in Risk Assessment (Part A) Final; EPA/530-SW-87-017, Alternate Concentration Limit Guidance; DOE/RL-2002-59, Hanford Site Groundwater Strategy Protection, Monitoring, and Remediation).

Table D-10. Waste Management Area C Performance Assessment Unconfined Aquifer Flow and Transport Properties.

Property	Waste Management Area C
Horizontal saturated hydraulic conductivity (m/day)[a]	11,000
Ratio of vertical to horizontal saturated hydraulic conductivity	0.1
Specific storage (1/m)[b]	1.1E-3
Effective porosity (dimensionless)	0.20 (Hanford Gravel)
Hydraulic gradient (m/m)[c]	2.0E-5
Depth to water table (m)	80
Longitudinal macrodispersivity (m)	10.5
Longitudinal to transverse macrodispersivity ratio	10

[a] Thickness weighted average conductivity estimate derived from Central Plateau Groundwater Model based on Equivalent Homogeneous Media approach adopted for representing the aquifer in the model.

[b] Using the assumed values of an aquifer compressibility of 1.0E-7 1/Pa (STOMP default), a water compressibility of 0.0046 1/atm (CRC Handbook of Chemistry and Physics [Haynes and Lide 2011]), and a water density of 1,000 kg/m^3 (Haynes and Lide 2011).

[c] Thickness weighted gradient estimate derived from Central Plateau Groundwater Model based on Equivalent Homogeneous Media approach adopted for representing the aquifer in the model.

Defining the protection of groundwater in the context of vadose zone fate and transport requires consideration of the soil and groundwater media as a hybrid or coupled pathway. This pathway involves the determination of future concentrations in the groundwater medium that result from the transport of the radionuclide and contaminant inventory existing in the WMA C tank residuals. The working definition of protectiveness for the protection of groundwater pathway is considered achieved if the radionuclide and contaminant levels in the WMA C tank residuals do not cause groundwater concentrations to exceed maximum concentration limits at the point of calculation within 1,000 years after closure, which is assumed to begin in 2020.

D4.2 NATURE AND EXTENT OF CONTAMINATION

The WMA C PA addresses the radionuclide and non-radiological contaminant inventory contained in waste residuals in tanks and ancillary equipment in WMA C at the assumed time of closure. Tank waste can be grouped into three types based on physical properties: supernate, salt, and sludge (RPP-RPT-42323). The 241-C Tank Farm contains little salt types, and with the supernate having been pumped out as part of interim stabilization, the tanks now mainly contain sludge (RPP-RPT-42323). As of the summer of 2015, all retrieval has been completed in all but three tanks.

Figure D-5. Points of Calculation 100 Meters Downgradient of Waste Management Area C.

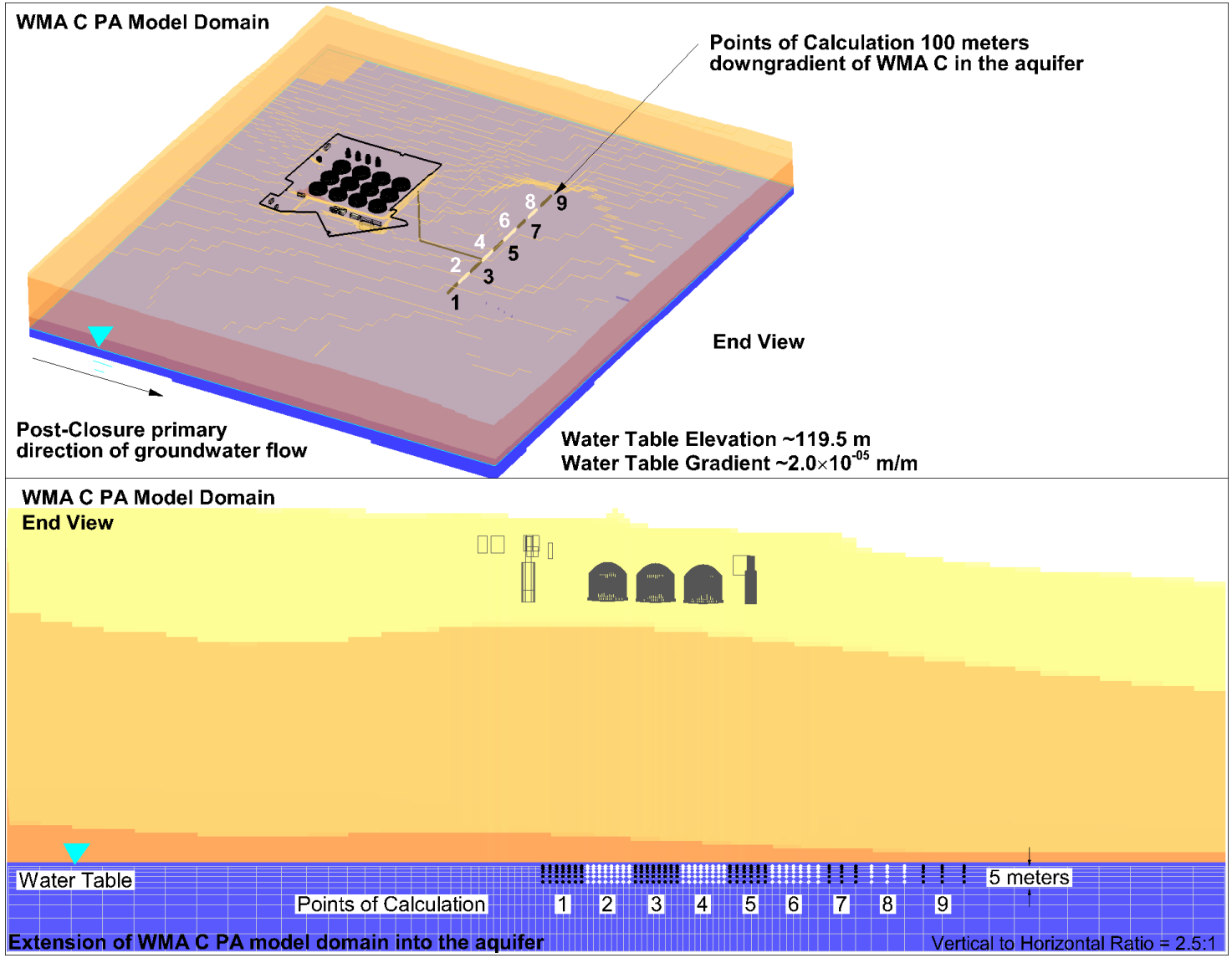

PA = Performance Assessment WMA = Waste Management Area

Table D-11. Width of Point of Calculation Segments 100 Meters Downgradient of Waste Management Area C.

Point of Calculation Segment	1	2	3	4	5	6	7	8	9
Width (m)	28.8	30.5	30.4	29.6	27	34.5	36	34	28

The residual waste volume for tanks not yet retrieved is unknown; therefore, assumptions about the inventory have been made based on current threshold requirements. Most constituents' inventory uncertainties vary by a factor of 5 or less, but may vary by as much as a factor of 10 for certain constituents in tanks not yet retrieved. For tanks already retrieved, uncertainty in residual waste estimates is on the order of 20 to 30% for most constituents, assuming no additional retrieval is required.

Specific information about the residual inventory and the release of the radionuclide and non-radiological contaminant inventory from the tanks, ancillary equipment, and pipelines is presented in Section D4.1.3.

D5.0 STOMP© SOFTWARE

STOMP© is used to solve the Richards equation (the water mass conservation equation in PNNL-12030) and the Advection-Dispersion equation (the solute mass conservation equation in PNNL-12030) that govern water flow and solute transport, respectively, under variably-saturated conditions in the vadose zone and groundwater in and around WMA C. STOMP© (PNNL-11216; PNNL-12030; PNNL-15782, "STOMP Subsurface Transport Over Multiple Phases Version 4.0 User's Guide") was selected to simulate the transport of contaminants in the vadose zone of the 100 Area because it fulfills the following specifications.

- The STOMP© simulator operational modes needed for implementation of this model are available free for government use under a limited government-use agreement.
- The STOMP© simulator solves the necessary governing equations, e.g., the Richards equation, the van Genuchten soil water retention equation, the Mualem unsaturated hydraulic conductivity equation, and the Advection-Dispersion equation.
- It is capable of directly simulating the principal FEPs that are relevant (see Section D4.1).
- The STOMP© simulator is well documented (PNNL-11216; PNNL-12030; PNNL-15782).
- The STOMP© simulator development is compliant with DOE O 414.1C, Quality Assurance requirements [PNNL-SA-54024, "Project Management Plan for Subsurface Transport Over Multiple Phases (STOMP) Software Maintenance and Development";

PNNL-SA-54022, "STOMP Software Test Plan Rev. 1.0"; PNNL-SA-54023, "STOMP Software Configuration Management Plan Rev. 1.3"; PNNL-SA-54079, "Requirements for STOMP Subsurface Transport Over Multiple Phases"].

- The STOMP© simulator is distributed with source code, enhancing transparency.
- The modeling team implementing this model has expertise in use of this simulator.
- There is an extensive history of application of STOMP© at Hanford and elsewhere including verification, validation, and benchmarking (DOE/RL-2011-50).
- Use of STOMP© is in keeping with DOE direction for simulation of vadose zone flow and transport at the Hanford Site (Letter 06-AMCP-0133, "Hanford Groundwater Modeling Integration").

The software used to implement this model and perform calculations was approved under the requirements of, and use was compliant with, PRC-PRO-IRM-309. This software is managed under the following software quality assurance documents consistent with PRC-PRO-IRM-309 that address all aspects of STOMP© usage and management: functional requirements, software management, software installation and acceptance testing and reporting, and the preparation of a requirements traceability matrix.

D5.1 STOMP© CONTROLLED CALCULATION SOFTWARE

The following describes the STOMP© controlled calculation software.

- Software Title: STOMP-W (a scientific tool for analyzing single- and multiple-phase subsurface flow and transport using the integrated finite volume discretization technique with Newton-Raphson iteration).
- Software Version: STOMP-W was provided by Pacific Northwest National Laboratory on January 30, 2013, and was tested and approved for use by CH2M HILL Plateau Remediation Company (CHPRC) as "CHPRC Build 4."
- Hanford Information System Inventory Identification Number: 2471 (Safety Software S3, graded Level C).

D5.2 SOFTWARE INSTALLATION AND CHECKOUT

Safety Software (CHPRC Build 4 of STOMP©) is checked out in accordance with procedures specified in the software management plan. Source or executable files are obtained from the CHPRC software owner, who maintains the configuration-managed copies in MKS Integrity™[2].

[2] MKS Integrity is a trademark of MKS, Incorporated.

Installation tests identified in the test plan are performed. Upon confirmation of successful installation, software installation and checkout forms are required and must be approved for installations used to perform model runs. Approved users are registered in the Hanford Information System Inventory for safety software.

D5.3 STATEMENT OF VALID SOFTWARE APPLICATION

Use of the STOMP© software for implementing the model described in this report is consistent with its intended use for CHPRC (DOE/RL-2011-50), as identified in the functional requirements document.

D6.0 MODEL IMPLEMENTATION

The 3-D model incorporates spatial heterogeneity and temporal changes of geologic and recharge conditions, with the ability to include lateral spreading, commingling of plumes, and preferential flow. The gridding scheme and extent of the domain intend to minimize the numerical error and impact that the boundary conditions have on the model calculations in the areas of interest, i.e., the points of calculation. The discretization scheme allows the distinct representation of the different sources within WMA C such that no sources, with the exception of the pipelines, overlap one another.

D6.1 DISCRETIZATION

The horizontal node spacing varies between 3.0 and 20 m to optimize the discretization in the areas attempting to approximate the slopes associated with construction of WMA C and the 100-series tanks without overwhelming the available computational resources. Within the confines of WMA C, the horizontal grid cell dimensions ranged between 3 and 4 m to align the nodes with the tanks, vault, and other ancillary equipment (Figure D-6). Outside of WMA C, the grid cells expanded in size such that no adjoining grids differed in length by more than a factor of 1.5. Table D-12 presents the pattern of the spacing of the finite difference cells. Vertical spacing in the vadose zone ranged between 1 and 1.25 m, except around the water table where the spacing decreased to 0.5 m to capture the impact of the capillary fringe above the water table (Figure D-7).

The total number of nodes in the modeled rectangular prism equaled 736,653. During the pre-operational phase, the engineered structures were non-existent. Hence, the number of active nodes equaled 640,565 with 96,088 inactive. During the operational and post-closure phases, WMA C backfill replaced Hanford H1 Gravel, and the number of active nodes equaled 637,543 with 99,110 inactive. The increase in inactive nodes is attributed to the inactivation of the tank and ancillary equipment nodes within the WMA C excavation. Figure D-8 shows the relative change in moisture content from the pre-Hanford steady-state condition at the four vertical boundaries of the model at three times of interest: at Year 2020, at the end of the WMA C

operational period; at Year 2520, at the end of the design life of the WMA C surface barrier; and at Year 3020, which is the end of the compliance time frame and when the system has reacquired or nearly reacquired steady-state conditions. In general, the effects are contained within a relatively small segment along the boundaries near the water table and appear to be minor (less than 1.0×10^{-5}). The changes in moisture content are negligibly small in magnitude, which indicates that the boundaries are far enough removed from the area of interest to avoid unintentional impacts to the model solution. Consequently, they are not considered to affect adversely the evaluation of radionuclide transport and groundwater impacts associated with the radionuclide and non-radiological contaminant inventory in WMA C.

Figure D-6. Horizontal Alignment of Three-Dimensional Model Computational Nodes with Waste Management Area C Single-Shell Tanks, 241-C-301 Catch Tank, 244-CR-Vault, and Other Waste Management Area C Ancillary Equipment.

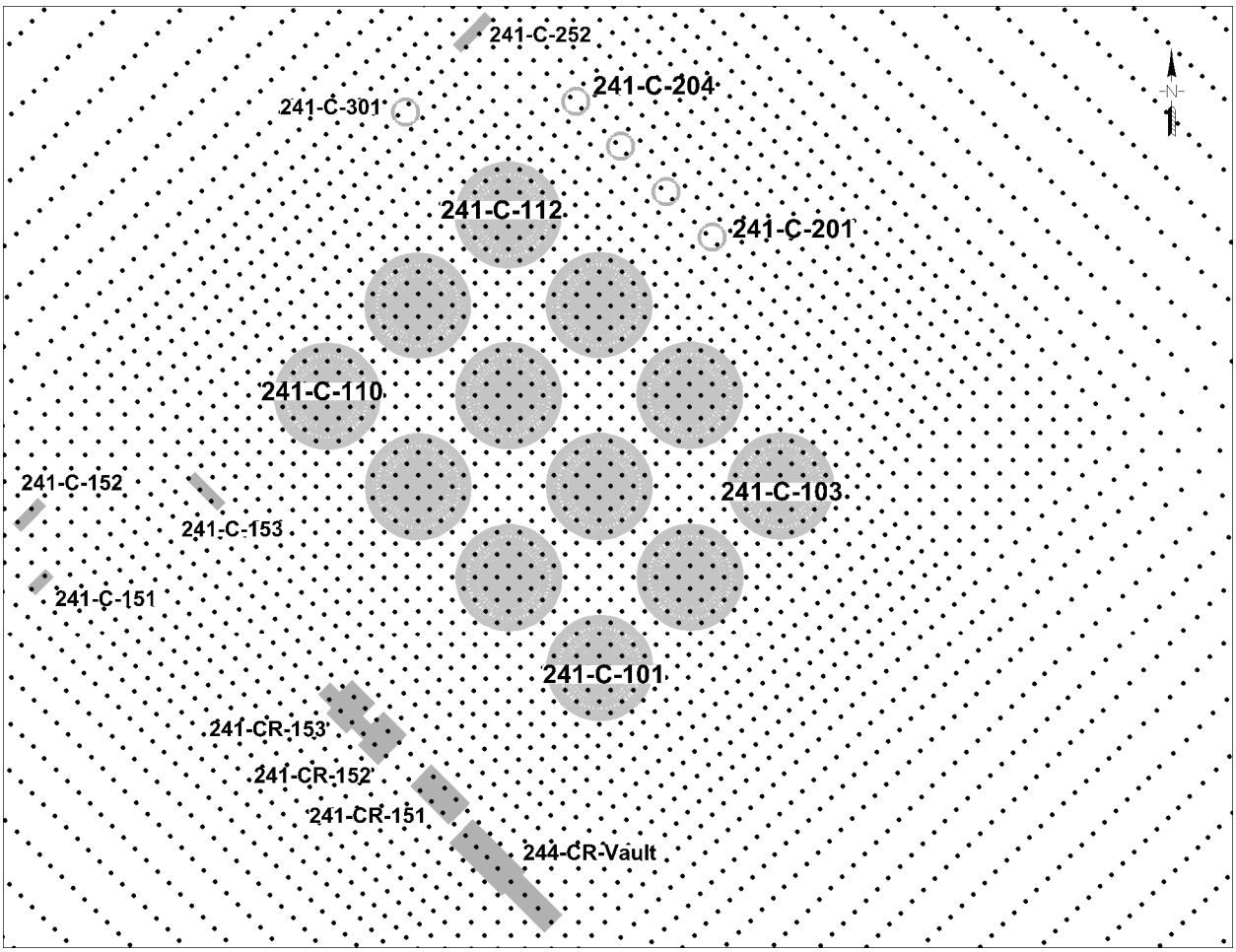

For the base case, the vadose Peclet number equaled approximately 6 (1.25 m / 0.20 m), with an imposed Courant (number) restriction of 10. While the value of 1 for these numbers is often considered ideal, it has been demonstrated that acceptably small numerical oscillations may be obtained with local Peclet numbers as high as 10 (Computational Methods in Subsurface Flow [Huyakorn and Pinder 1983]). It is difficult to assess numerical impacts on the solution caused

by the grid spacing, apart from consideration of the Peclet criteria. The total number of nodes in the model is close to the maximum that the computer hardware and solver can accommodate, so evaluating solution stability through grid refinement is not feasible. Other comparably-scaled models indicate that the WMA C PA grid size and spacing is sufficient. DOE/EIS-0391, "Final Tank Closure and Waste Management Environmental Impact Statement for the Hanford Site, Richland, Washington," Appendix N indicates that the horizontal grid size and spacing of 5 m within WMA C, and vertical spacing of 2 m, are small enough in that 3-D model to provide accurate simulation of flow and transport.

Table D-12. Horizontal and Vertical Spacing of the Finite Difference Cells in the Three-Dimensional Waste Management Area C Flow and Transport Model Domain.

West to East Spacing; Southeastern Boundary Coordinate = 574656 m (Lambert Coordinate System[1] Easting)						
4@ 20.00 m	2@ 16.00 m	2@ 12.00 m	2@ 10.00 m	2@ 8.00 m	2@ 6.00 m	7@ 4.50 m
1@ 3.70 m	6@ 3.80 m	2@ 3.85 m	14@ 3.80 m	2@ 3.85 m	6@ 3.80 m	1@ 3.00 m
7@ 4.50 m	3@ 6.00 m	4@ 8.00 m	10@ 10.00 m	2@ 12.00 m	1@ 16.00 m	9@ 20.00 m
South to North Spacing; Southwestern Boundary Coordinate = 136454 m (Lambert Coordinate System[1] Northing)						
8@ 20.00 m	3@ 16.00 m	2@ 12.00 m	4@ 10.00 m	3@ 8.00 m	2@ 6.00 m	11@ 4.50 m
4@ 4.00 m	8@ 3.80 m	1@ 3.90 m	15@ 3.80 m	1@ 3.00 m	11@ 4.50 m	2@ 6.00 m
2@ 8.00 m	3@ 10.00 m	3@ 12.00 m	4@ 16.00 m	6@ 20.00 m		
Vertical Spacing; Bottom Elevation = 95 m (NAVD88[2])						
1@ 5.00 m	2@ 4.00 m	1@ 3.00 m	1@ 2.00 m	2@ 1.50 m	1@ 1.25 m	1@ 1.00 m
1@ 0.75 m	3@ 0.50 m	1@ 0.75 m	12@ 1.00 m	40@ 1.25 m	4@ 1.00 m	19@ 1.25 m

[1] NOAA Manual NOS NGS 5, State Plane Coordinate System of 1983.

[2] North American Vertical Datum of 1988, National Geodetic Survey, U.S. Department of Commerce.

Note: The sequences read left to right. The number preceding the "@" symbol indicates the number of columns (west to east), rows (south to north), or vertical layers (bottom to top) that have the length indicated by the distance following it.

Figure D-9 shows a comparison of the ^{99}Tc concentration at the nine points of calculation located 100 m downgradient between the base case dispersivity values and dispersivity values intended to test numerical dispersion (Table D-13). These values represent the approximate maximum values associated with the different HSUs. The perceptible increase in maximum concentration observed in the base case results, compared to the numerical dispersion test case results, indicates that the grid is sized adequately such that numerical dispersion is not unduly affecting or obscuring the model computations.

Figure D-7. Horizontal and Vertical Alignment and Distribution of Waste Management Area C Performance Assessment Three-Dimensional Model Computational Nodes.

a) Alternative Geologic Model I

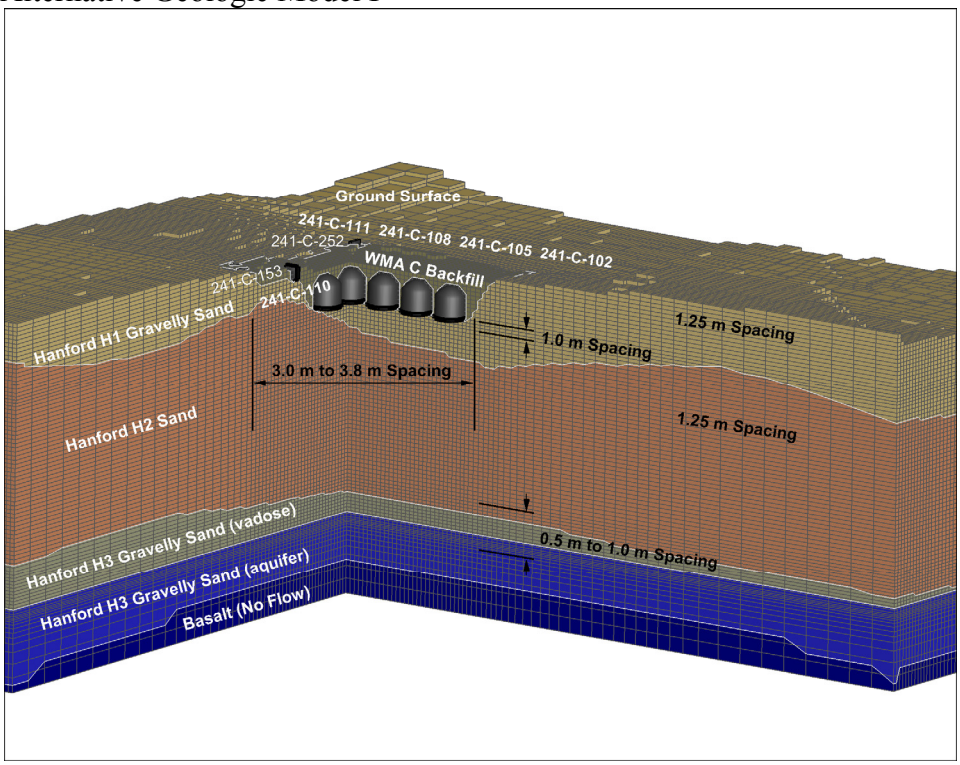

b) Alternative Geologic Model II

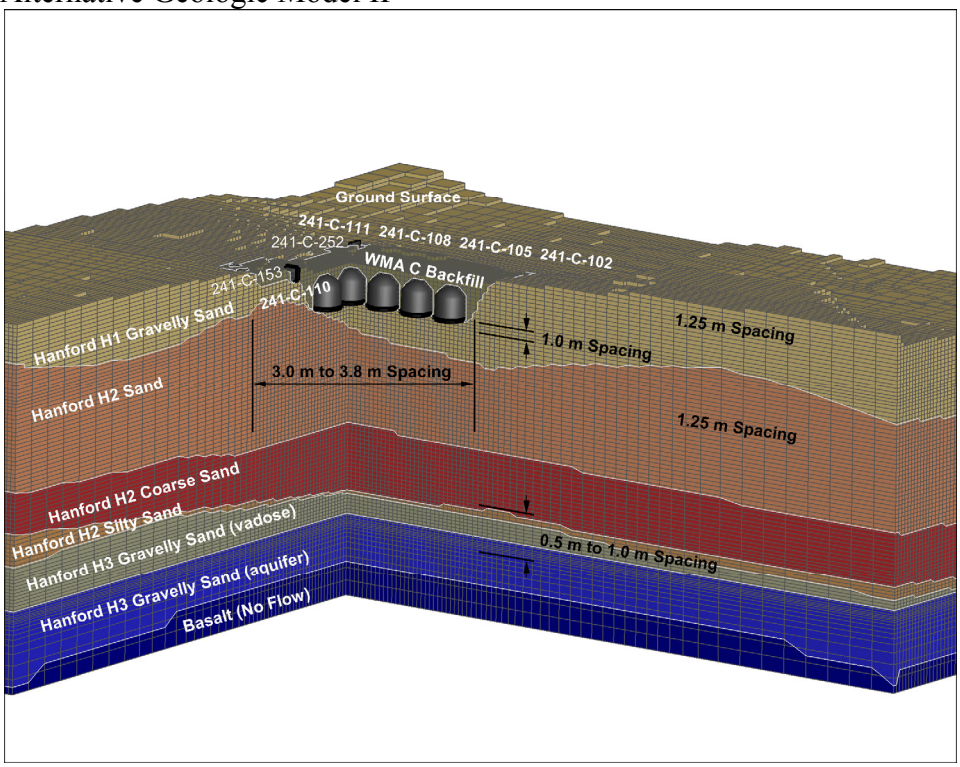

WMA = Waste Management Area

Figure D-8. Relative Change in Moisture Content from the Pre-Hanford Steady State Condition at the Four Vertical Boundaries of the Model at Three Times of Interest: Year 2020, Year 2520, and Year 3020.

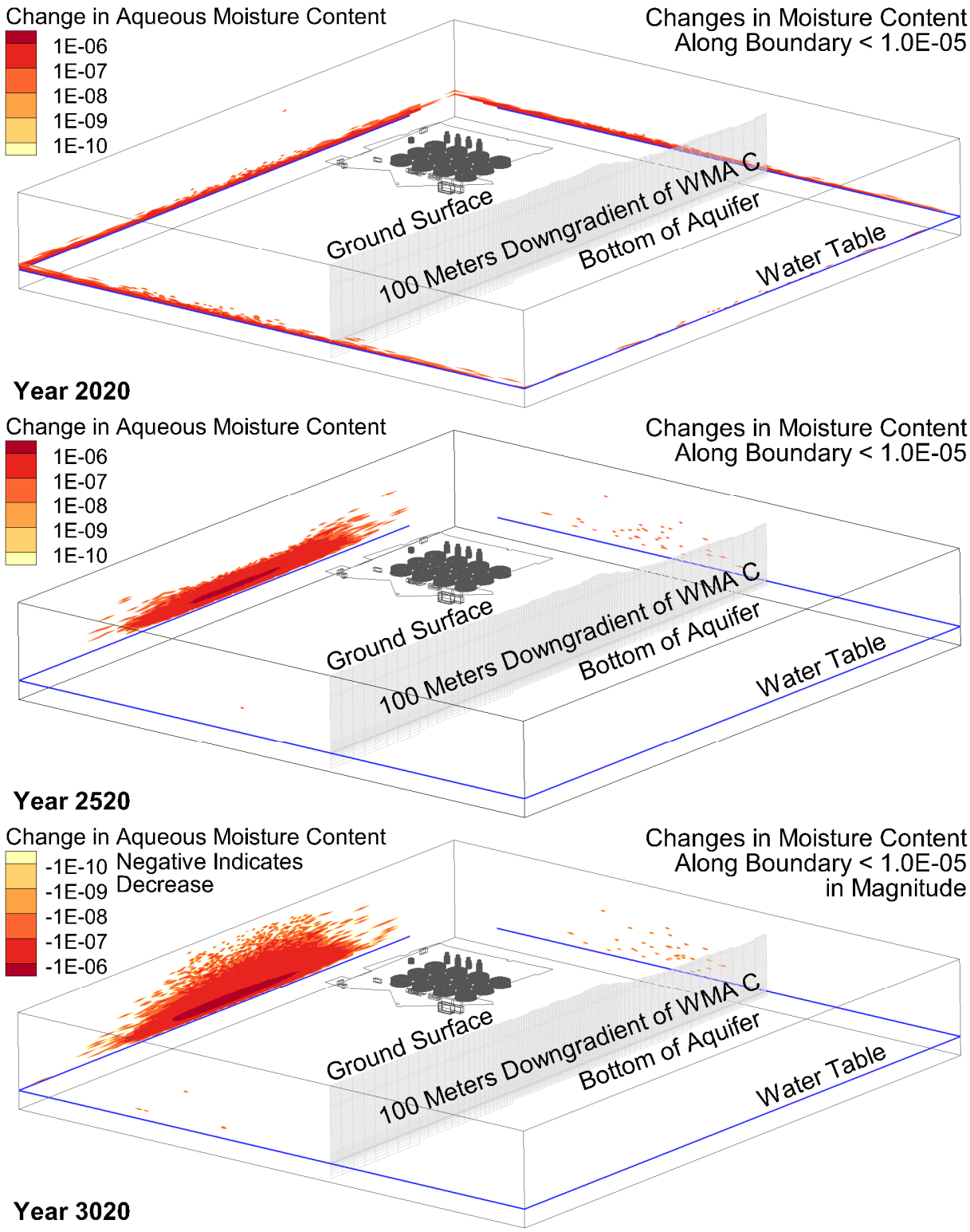

WMA = Waste Management Area

Figure D-9. Comparison of the Technetium-99 Concentration at the Nine Points of Calculation Located 100 Meters Downgradient between the Base Case Dispersivity Values and the Numerical Dispersion Test Case Dispersivity Values.

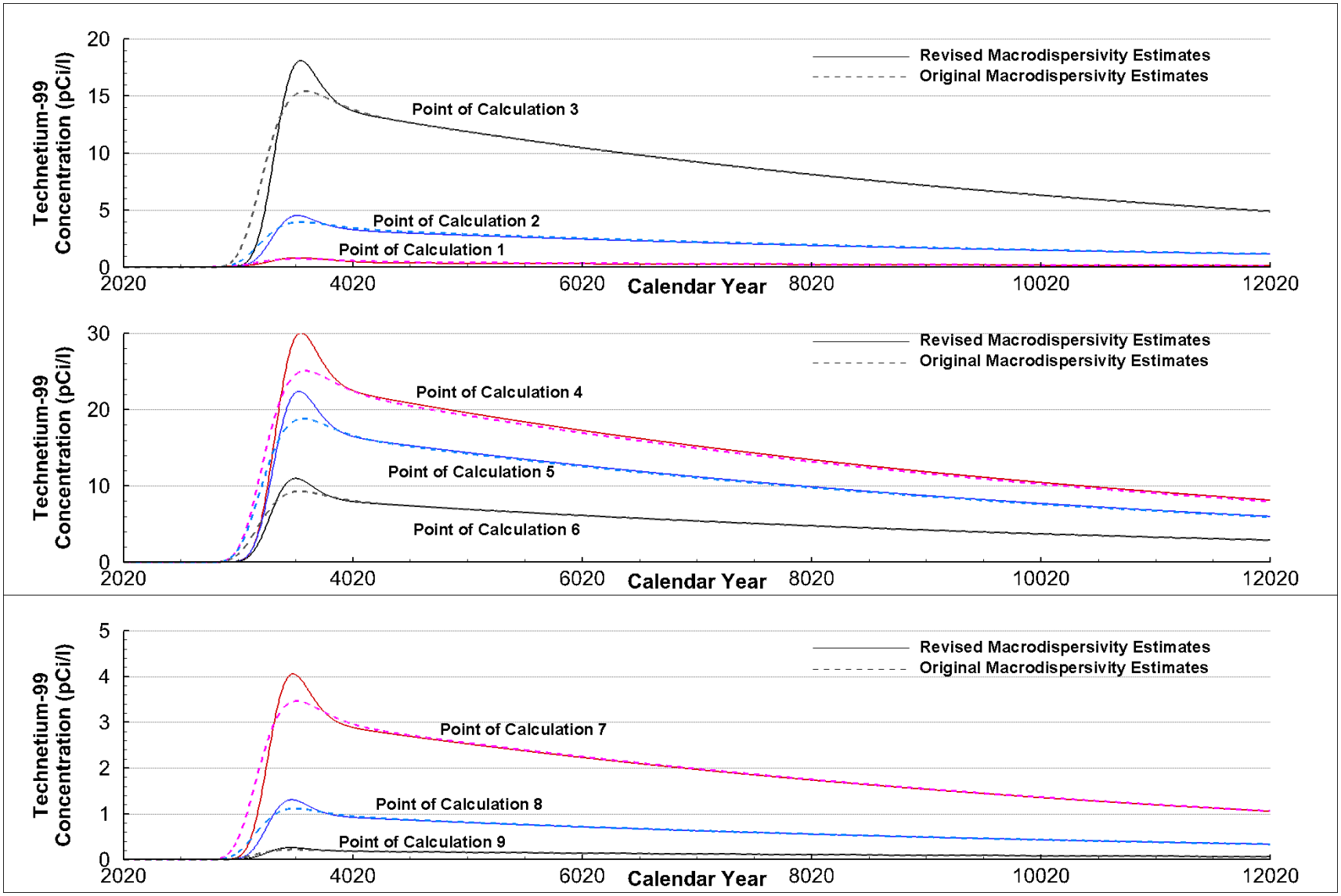

Table D-13. Waste Management Area C Performance Assessment Vadose Zone Dispersivity Values and Numerical Dispersion Evaluation.

Hydrostratigraphic Unit	Numerical Dispersion Test Case Longitudinal Macrodispersivity (cm)	Base Case Longitudinal Macrodispersivity (cm)
Backfill	150	20
Hanford H1	100	20
Hanford H2	200	25
Hanford H3	100	20
Point of Calculation 100 meters downgradient of Waste Management Area C	Maximum Concentration (pCi/L)	Maximum Concentration (pCi/L)
1	0.80	0.83
2	4.0	4.5
3	15	18
4	25	30
5	19	22
6	9.2	11
7	3.4	4.1
8	1.1	1.3
9	0.22	0.26

The vertical Courant numbers in the vadose zone tend to be small (e.g., 10 yr × 0.0035 m/yr recharge / 0.05 moisture content / 1 m grid spacing = 0.7), but the horizontal Courant numbers become large near the water table and capillary fringe where the velocity approaches 400 m/yr. These few places impose an impractical limit on the time step while the Courant number remains small elsewhere. Table D-14 presents the results of a Courant criteria evaluation, which evaluated the maximum concentration of ^{99}Tc at the points of calculation associated with a subset of the WMA C sources: tank 241-C-105, tank 241-C-203, and the pipelines contained in a single STOMP© input file. The negligible differences in the results indicate that an overly strict Courant restriction does not affect the solution and appears to be unwarranted, especially considering the improved efficiency in solution time when the Courant restriction is relaxed to 10. These evaluations indicate that the grid is adequately discretized.

D6.2 PARAMETERIZATION

Table D-15 presents a summary of the model parameters and values assigned, including boundary and initial conditions, and identifies the section where the data sources and data quality are discussed. Parameters and values that are already tabularized in the subsections of Section D4.1 are simply referenced by the applicable table number.

Table D-14. Waste Management Area C Performance Assessment Vadose Zone Courant Criteria and Numerical Dispersion Evaluation.

	Numerical Dispersion Test Case Courant Number = 1 (pCi/L)			Base Case Courant Number = 10 (pCi/L)		
Simulation Duration and Time to Complete	4,000 years completed in 112.51 hours			10,000 years completed in 32.08 hours		
Point of Calculation 100 meters downgradient of Waste Management Area C	Maximum Concentration (pCi/L)			Maximum Concentration (pCi/L)		
	Source			Source		
	241-C-105	241-C-203	Pipelines	241-C-105	241-C-203	Pipelines
1	0.02	0	0.36	0.02	0	0.36
2	0.86	0	0.53	0.86	0	0.53
3	10	0.000003	0.74	10	0.000003	0.73
4	21	0.0001	0.94	21	0.0001	0.92
5	13	0.002	1.0	13	0.002	1.0
6	4.1	0.006	0.74	4.1	0.006	0.73
7	0.92	0.007	0.34	0.91	0.007	0.34
8	0.22	0.004	0.12	0.22	0.004	0.12
9	0.03	0.001	0.03	0.03	0.001	0.03

D6.3 MODELING STAGES

The WMA C tank residual simulations using STOMP© require running three separate stages of the model in sequence. The first stage is a long-term transient simulation of only water flow resulting from historic recharge conditions. This stage is needed to obtain near steady-state soil moisture conditions throughout the model domain at the start time for the second stage. The second stage begins with the initial moisture distribution provided from the first stage, and simulates only water flow during the operational period of WMA C, which is the time between the construction of WMA C in 1945 and its assumed closure in 2020. The use of a previously simulated condition as a starting point for another simulation is referred to as a "restart" condition in STOMP©. The contaminant transport stage (stage 3) begins with the moisture distribution provided from the second stage, and simulates flow and transport for 10,000 years, from 2020 to 12020. Each tank, ancillary equipment, and pipeline residual source is simulated individually. The groundwater concentrations resulting from each source are summed according to the principle of superposition to produce time series concentration breakthrough curves at the points of calculation identified in Section D4.1.8. The principle of superposition also applies to the spatial distribution of the pore water concentrations in the vadose zone resulting from each

source. The superposition and summing of the concentration results occurs outside of STOMP©, and is not addressed in this appendix.

D6.4 CALIBRATION

DOE G 435.1-1 and Federal risk assessment guidelines [e.g., EPA/540/1-89/002, Risk Assessment Guidance for Superfund Volume I Human Health Evaluation Manual (Part A) Interim Final] acknowledge that the assessment of uncertainties associated with how well models approximate actual relationships and conditions in the field (i.e., field validation) is desirable, but that field data for model calibration is generally not available and/or attainable for vadose zone models. No specific effort to calibrate the WMA C PA flow and transport model has been made; however, a comparison of measured and simulated water contents was carried out for this analysis, and parameters were adjusted accordingly (Appendix B).

D6.5 SCREENING

The screening analysis uses the 3-D model to determine the maximum K_d value of contaminants in the WMA C tank residuals that reach the water table in 1,000 and 10,000 years. The purpose of this screening phase was to streamline the PA modeling by identifying those contaminants sufficiently mobile to impact groundwater during the compliance, sensitivity and uncertainty analysis time frames. This analysis was performed to considerably reduce the computation time required to conduct the PA modeling by limiting the number of radionuclides evaluated in the model. According to the facility performance requirements in DOE O 435.1, performance objectives must be met for 1,000 years, and post-closure evaluations must extend out to 10,000 years to clarify long-term impacts. Given the combination of low infiltration rates and a deep vadose zone below the facility, it is evident that contaminants that are highly sorptive on the soils may not reach the water table within 10,000 years,[3] even for combinations of input parameters that are highly conservative. If the travel time exceeds 10,000 years, even for conservative combinations of input parameters, the contaminant will not affect any of the calculated results in the PA, and can reasonably be screened from the analysis.

The specific methodology, basis for the parameters selected, and key assumptions used in the screening phase analysis are described in detail in Section 6.3.2.3 Groundwater Pathway Screening Analysis Methodology. The screening analysis includes vadose zone hydraulic property values and recharge rates developed for the uncertainty analysis, which are discussed in Section 8.1.4. In particular, the screening analysis applies the maximum recharge rates associated with each period for each surface type (Table D-16), assigns the vadose zone hydraulic properties that produce the fastest pore water velocity for each HSU as determined for the uncertainty analysis (Table D-17), and implements an advection release function for the radionuclides. Other parameters (e.g., dispersivity, distribution coefficient gravel correction, and aquifer hydraulic properties) remain the same as the base case parameters. The use of these

[3] In this analysis, the travel time to the aquifer is defined as the time to first arrival of the contaminant at the aquifer, taking into account advection, diffusion, and dispersion. This metric will tend to screen fewer contaminants than using the arrival of the peak concentration.

parameter values prevents the occurrence of a false negative, i.e., that a radionuclide or non-radioactive contaminant that could impact groundwater within the 1,000- or 10,000-year simulation time frames is screened from the fate and transport evaluations. Model results indicating the time of first arrival at the water table for contaminants with distribution coefficients ranging between 0.1 and 2.0 mL/g are summarized in Table D-18 and presented in graphical form in Figure 7-6.

Table D-15. Summary of Key Elements and Base Case Parameters Associated with Site-Specific Model Components for Waste Management Area C (The basis for the elements and parameter selection provided in the individual model components sections). (2 sheets)

Model Domain and Boundary Conditions	Rectangular Prism: 737. 9 m (2,421 ft) × 795. 3 m (2,609 ft) × 116 m (381 ft) Prescribed flux across the top (Recharge); no-flow along vertical side boundaries in the vadose zone; prescribed flux and head along the upgradient and downgradient vertical side boundaries in the aquifer, respectively; no-flow along the bottom of the model (aquifer). The prescribed volumetric water flux boundary condition is calculated to maintain mass conservation in the aquifer independent of recharge.

Geologic Setting	The Waste Management Area (WMA) C cross section includes the following anthropogenic or natural units that occur from surface to groundwater (RPP-RPT-56356, "Development of Alternative Digital Geologic Models of Waste Management Area C," Rev. 0):
	• WMA C Backfill
	• Hanford H1 (gravel-dominated, generally identified as gravel or very coarse sand)
	• Hanford H2 Sand (sand-dominated facies generally identified as fining upward sequences of gravel, sandy/gravel to sand to very fine sand)
	• Hanford H3 (coarse-grained open framework gravel to sandy gravel; in the vicinity of WMA C is often referred to as undifferentiated H3 gravels, Cold Creek, and Ringold)
	• In Alternative Geologic Model II, the Hanford H2 Sand includes following two additional subunits
	  o Hanford H2 Coarse (gravel/coarse-grained facies that underlies the H2 fines)
	  o Hanford H2 Silty Sand – (a silty sand unit that is only observed in deep groundwater wells and a mappable unit may not be readily identified)

Groundwater Domain and Characteristics	WMA C post-closure water table elevation ~119.5 m NAVD88 and average hydraulic gradient ~0.00001 m/m Aquifer area along northwest cross section boundary = 6,151.04 m^2 Aquifer area along southeast cross section boundary = 13,997.55 m^2 Average aquifer area along all aquifer cross sections = 9,439.56 m^2 Prescribed flux along northwest cross section boundary (saturated K = 11,000 m/d); 11,000 m/d × 0.2000E-04 × 365.25 d/yr = 0.80355E+02 m/yr; 0.0.80355E+02 m/yr × 9,439.56 m^2 / 6,151.04 m^2 = 0.12331E+03 m/yr Prescribed head along southeast cross section boundary = 119.49 m Groundwater thickness is ~12 m (39 ft) in the aquifer; Groundwater concentrations evaluated for upper 5 m (16 ft) of the aquifer (rationale for aquifer depth presented in section D4.1.8 Point of Calculation, Protectiveness Metric, and Time Frame Considerations)
Source Term/ Inventory	WMA C Base Case inventory presented in Table D-3. Diffusion controlled release from the grouted tanks and advection controlled release from the pipelines along with equilibrium sorption-desorption processes (i.e., K_d control).

Table D-15. Summary of Key Elements and Base Case Parameters Associated with Site-Specific Model Components for Waste Management Area C (The basis for the elements and parameter selection provided in the individual model components sections). (2 sheets)

Vadose Zone Hydrogeology and Fluid Transport	WMA C Base Case hydrogeologic properties presented in Table D-4. Aquifer Hydraulic Conductivity Horizontal to Vertical Anisotropy **10:1**; Vadose Zone Hydraulic Conductivity Anisotropy allowed to vary as a function of the moisture content in accordance with the Polmann model ("Application of Stochastic Methods to Transient Flow and Transport in Heterogeneous Unsaturated Soils" [Polmann 1990]). Aquifer and Vadose Zone Dispersion Horizontal to Vertical Anisotropy **10:1**. K_d-control for radionuclide transport in the vadose zone and groundwater.				
Recharge	Phase	Recharge on Surface (mm/yr [in./yr])			
		Natural Vegetation	Tank Farm Disturbed Surface	Non-Tank Farm Disturbed Surface*	Surface Barrier
	Pre-operations	3.5 [0.14]	NP	NP	NP
	Operations	3.5 [0.14]	100 [3.9]	22 [0.87]/63 [2.5]	NP
	First 100 years Post-Closure	3.5 [0.14]	NP	3.5 [0.14]	0.5 [0.02]
	Early Post-Closure (100 to 500 years)	3.5 [0.14]	NP	3.5 [0.14]	0.5 [0.02]
	Late Post-Closure (after 500 years)	3.5 [0.14]	NP	3.5 [0.14]	3.5 [0.14]
	* Disturbed areas that allow vegetation are assigned 22 mm/yr [0.87 in./yr]. Disturbed areas that are reworked such that vegetation does not grow are assigned 63 mm/yr [2.5 in./yr].				
Sorption Characteristics	WMA C Base Case K_d values (partition coefficients) presented in Table 6-11.				

*Applies to all subfacies of this unit.

NAVD88 = North American Vertical Datum of 1988, National Geodetic Survey, U.S. Department of Commerce.

NP = Not present

The results of the screening analysis indicate that, even when using parameter estimates biased to produce the greatest pore water velocity in the vadose zone, contaminants with a K_d in the fine fraction > 0.15 mL/g do not reach groundwater within the 1,000-year compliance time frame, and radionuclides with a K_d > 1.5 mL/g do not reach groundwater within the 10,000-year

post-compliance period (Table D-18). The screening evaluation helps in reducing the number of radionuclides to be evaluated using 3-D modeling analysis.

Table D-16. van Genuchten-Mualem Parameters Associated with the Maximum Pore Water Velocity at Specific Tension Ranges Based on Cumulative Distribution Functions.

Strata	θ_s	θ_r	α (1/cm)	n	Fitted K_s (cm/s)
Hanford H1 (gravelly sand)	0.100	0.0006	0.0190	1.789	5.07E-04
Hanford H2 (sand-dominated)	0.239	0.0006	0.0743	2.042	8.84E-04
Hanford H3 (gravelly sand)	0.100	0.0006	0.0190	1.789	5.07E-04
Backfill	0.100	0.0003	0.0116	1.601	9.42E-05
Aquifer	0.20	0.016	0.0190	1.789	3.49E-03*

* The vertical aquifer hydraulic conductivity value is determined from the horizontal hydraulic conductivity value and the aquifer anisotropy.

Table D-17. Maximum Net Infiltration (Recharge) Estimates Used in the Screening Analysis for Pre-Construction Period, Operational Period, and Post-Closure of Waste Management Area C (Section 8.1.4).

Surface Status	Pre-Construction (mm/yr)	Operational Period (mm/yr)	Post Closure	
			Until End of Barrier Design Life (500 yr after closure) (mm/yr)	After End of Barrier Design Life (mm/yr)
Waste Management Area C	5.2	140	1.0	5.2
Undisturbed	5.2	5.2	5.2	5.2
Disturbed	5.2	22	5.2	5.2
Reworked	5.2	63	5.2	5.2
Waste Management Area A	5.2	140	1.0	5.2

Of the list of radionuclides in the WMA C residuals inventory and on the basis of the results of the screening phase, only 12 (Table D-19) appear to be sufficiently mobile to arrive at groundwater during the compliance period, with 6 others sufficiently mobile to arrive at groundwater during the sensitivity and uncertainty analysis time frame. During the sensitivity and uncertainty analysis time frame, even some contaminants that undergo appreciable retardation in the vadose zone, e.g., ^{129}I, ^{14}C, and ^{238}U, are sufficiently mobile to arrive at groundwater within the sensitivity and uncertainty analysis time frame. The other contaminants in the WMA C residual inventory are not included in further groundwater impact analysis because they do not reach the water table within the evaluation time frames.

Table D-18. First-Arrival Time (in Calendar Year) of Radionuclides for Various K_d Values Based on Screening Analysis Using Subsurface Transport Over Multiple Phases.

Contaminant K_d (mL/g)				Calendar Year of First Arrival at the Water Table	Time of Arrival, Post-Closure (Closure occurring in 2020) Years
Fine Fraction	Backfill	Hanford H1 and H3	Hanford H2		
0.10	0.05	0.06	0.08	2517.5	497.5
0.15	0.07	0.09	0.12	3022.5	1,002.5
0.20	0.09	0.12	0.16	3505	1,485
0.25	0.12	0.15	0.20	3900	1,880
0.30	0.14	0.17	0.24	4210	2,190
0.40	0.18	0.23	0.32	4840	2,820
0.60	0.28	0.35	0.48	6110	4,090
0.80	0.37	0.46	0.64	7390	5,370
1.0	0.46	0.58	0.80	8680	6,660
1.5	0.69	0.87	1.2	11900	9,880
2.0	0.92	1.2	1.6	>12020	>10,000

D7.0 MODEL LIMITATIONS

The evaluation of WMA C PA tank residuals model limitations must consider two types of limitations: (1) the limitations associated with the model that affect the results, and (2) the limitations associated with the applicability of the model results outside the model's intended purpose. Model limitations primarily depend on the inherent capabilities of the model; the scale and boundary conditions of the model domain; assumptions used in the model design; the extent to which the model input parameters represent actual, bounding, or limiting conditions; and the ability of the model and code to represent individual and combinations of dynamic FEPs. Limitations associated with the applicability of the model results concern the extent to which the model results are relevant and applicable to model conditions, parameters, or assumptions that differ from those of the specific modeling purpose and objectives (e.g., attempting to apply the tank residuals model to the evaluation of past UPRs).

DOE/RL-2011-50 identifies generalized model and code limitations associated with the relevant FEPs for the 200 Areas vadose zone. Other limitations specific to WMA C were considered during FEPs process working sessions conducted from 2009 to 2011, and additional discussions with regulators in 2013 and 2014. The description of the limitations involves a summary of those FEPs considered and not considered in the model, along with possible consequences of their omission on the model results. The limitations also address or involve uncertainties in the

model results. Some specific examples of limitations in the applicability of the WMA C PA tank residuals vadose zone model results include the following.

- Domain and scale limitations:
  - Results represent incremental groundwater contamination from WMA C residuals and do not include interaction with earlier WMA C waste releases or contamination from other sources
  - Applicability of model results limited to releases containing no accompanying water discharges within the model domain.
- Geologic setting limitations:
  - Applicability of model results limited to evaluations with a comparable stratigraphy to WMA C.
- Source-term limitations:
  - Applicability of model results limited to source-term components of finite or estimable volume within the model domain
  - Applicability of model results limited to contaminant release and retardation mechanisms based on the assumption of diffusion control or reversible equilibrium conditions.
- Groundwater domain limitations:
  - Applicability of model results limited to sites with dilution effects comparable to WMA C aquifer hydrologic properties.
- Hydrogeologic parameter limitations:
  - Applicability of WMA C model results limited to evaluations where flow and transport are dominated by unsaturated porous media continuum flow, with comparable or acceptably bounding moisture content profiles
  - Applicability of WMA C model results limited to evaluations where hydrogeologic parameter values remain constant (unchanging) over time
  - Applicability of model results limited to sites where preferential pathways (e.g., discordant voids such as well seals/casing, clastic dikes, and sills) are not considered important.

- Recharge limitations:
  - Applicability of model results limited to conditions similar to or bounded by the values of recharge rates evaluated in the WMA C PA.
- Geochemical limitations:
  - Applicability of model results limited to radionuclides and non-radiological contaminants exhibiting linear isotherm behavior for contaminant release and attenuation, which neglect surface complexation and precipitation
  - Applicability of model results limited to the radionuclides and non-radiological contaminants for which the assumption applies that the adsorption K_d and desorption K_d values are equivalent
  - Applicability of model results limited to radionuclides and non-radiological contaminants with transport characteristics similar to, or within the range of, evaluated K_d values.

For the purposes of establishing that the requirements of DOE O 435.1 to protect the public and environment from exposure to radiation from radioactive materials are being met, these limitations appear to be acceptable because the results represent reasonable (upper) bounding or limiting conditions, or the risk implications of the results are not sensitive to the limitations apart from those identified through the sensitivity analysis (DOE/RL-2011-50; Section 8).

D8.0 MODEL CONFIGURATION MANAGEMENT

Consistent with the requirements of CHPRC-00189, "CH2M Hill Plateau Remediation Company Environmental Quality Assurance Program Plan," Revision 9, all inputs and outputs for the development of WMA C PA models are committed to the Environmental Model Management Archive (EMMA) to maintain and preserve configuration managed models. Basis information (that information collected to form the basis for model input parameterization) is also stored in the EMMA for traceability purposes.

The STOMP© software is used to implement the models collectively described in this report. These models are managed as discussed in Section 11.2.1. Safety Software (CHPRC Build 4 of STOMP©) is checked out in accordance with procedures specified in CHPRC-00176, "STOMP Software Management Plan." Source or executable files are obtained from the CHPRC software owner, who maintains the configuration-managed copies in MKS Integrity™. Installation tests identified in CHPRC-00211, "STOMP Software Test Plan" are performed and successful installation confirmed, and software installation and checkout forms (see Appendix A) are required and must be approved for installations used to perform model runs. Approved users are registered in the Hanford Information System Inventory for Safety Software.

Table D-19. Radionuclides that Arrive at the Water Table within the 1,000-Year Compliance and 10,000-Year Sensitivity and Uncertainty Time Frame Based on the Screening Analysis Conducted Using Subsurface Transport Over Multiple Phases.

Contaminant	K_d [Fine Fraction] (mL/g)	K_d [Backfill] (mL/g)	K_d [Hanford H1 and H3] (mL/g)	K_d [Hanford H2] (mL/g)
Radionuclides and non-radiological contaminants that may arrive at the water table within 1,000 years				
CN	0	0	0	0
Co/Co-60	0	0	0	0
Cr	0	0	0	0
F	0	0	0	0
H-3	0	0	0	0
Hg	0	0	0	0
Nb-93m	0	0	0	0
NO_2	0	0	0	0
NO_3	0	0	0	0
Rn-222	0	0	0	0
Tc-99	0	0	0	0
Se/Se-79	0.1	0.05	0.06	0.08
Radionuclides and non-radiological contaminants that may arrive at the water table within 10,000 years				
I-129	0.2	0.09	0.12	0.16
Sn/Sn-126	0.5	0.23	0.29	0.40
U-238	0.6	0.28	0.35	0.48
U Total	0.6	0.28	0.35	0.48
C-14	1.0	0.46	0.58	0.80
Tri-butyl Phosphate	1.89	0.87	1.1	1.5

Use of the STOMP© software for implementing the model described in this report is consistent with its intended use for CHPRC, as identified in CHPRC-00222, "STOMP Functional Requirement Document."

D9.0 MODEL APPLICATION

The STOMP© simulation results developed from this modeling effort are recommended for use in the WMA C PA residual waste evaluation. These results provide adequate confidence that the radioactive waste management requirements of DOE O 435.1 are being met. The activities associated with the disposition of the tank, ancillary equipment, and pipeline residual waste of WMA C are being systematically planned, documented, executed, and evaluated. These activities appear sufficient to protect the environment and the public from exposure to radiation from radioactive materials per the requirements contained in DOE O 5400.1, General Environmental Protection Program and DOE O 5400.5, Radiation Protection of the Public and the Environment. The results also indicate that any eventual groundwater impacts will comply with applicable Federal, State, and local laws and regulations.

The WMA C PA tank residuals model represents a closure condition, and would therefore need to be evaluated for applying this model to other conditions, such as in the evaluation of past releases. In addition, the effects of preferential pathways or other phenomena that direct or deflect transport may become important considerations because of the enhanced net infiltration of precipitation through the gravel surface and the planned and unplanned anthropogenic releases of water.

D10.0 REFERENCES

06-AMCP-0133, 2006, "Hanford Groundwater Modeling Integration" (external letter from K. A. Klein to P. L. Pettiette, Washington Closure Hanford, March 9) U.S. Department of Energy, Richland Operations Office, Richland, Washington.

40 CFR 141, "National Primary Drinking Water Regulations," Code of Federal Regulations, as amended.

CHPRC-00176, 2011, "STOMP Software Management Plan," Rev. 2, CH2M HILL Plateau Remediation Company, Richland, Washington.

CHPRC-00189, 2012, "CH2M Hill Plateau Remediation Company Environmental Quality Assurance Program Plan," Rev. 9, CH2M HILL Plateau Remediation Company, Richland, Washington.

CHPRC-00211, 2014, "STOMP Software Test Plan," Rev. 2, CH2M HILL Plateau Remediation Company, Richland, Washington.

CHPRC-00222, 2011, "STOMP Functional Requirement Document," Rev. 1, CH2M HILL Plateau Remediation Company, Richland, Washington.

CP-47631, 2013, "Model Package Report: Central Plateau Groundwater Model Version 3.4," Rev. 1, CH2M HILL Plateau Remediation Company, Richland, Washington.

Dagan, G., 1984, "Solute transport in heterogeneous porous formations," Journal of Fluid Mechanics, Vol. 145, pp. 151–177.

DOE/EIS-0391, 2012, "Final Tank Closure and Waste Management Environmental Impact Statement for the Hanford Site, Richland, Washington," U.S. Department of Energy, Washington, D.C.

DOE G 435.1-1, 1999, Implementation Guide for Use with DOE M 435.1-1, Radioactive Waste Management Manual, U.S. Department of Energy, Washington, D.C.

DOE M 435.1-1, 2007, Radioactive Waste Management Manual, U.S. Department of Energy, Washington, D.C.

DOE O 414.1C, 2005, Quality Assurance, U.S. Department of Energy, Washington, D.C.

DOE O 435.1, 2001, Radioactive Waste Management, U.S. Department of Energy, Washington, D.C.

DOE O 5400.1, 1990, General Environmental Protection Program, Change 1, U.S. Department of Energy, Washington, D.C.

DOE O 5400.5, 1993, Radiation Protection of the Public and the Environment, U.S. Department of Energy, Washington, D.C.

DOE/ORP-2008-01, 2010, RCRA Facility Investigation Report for Hanford Single-Shell Tank Waste Management Areas, Rev. 1, U.S. Department of Energy, Office of River Protection, Richland, Washington.

DOE/RL-93-33, 1996, Focused Feasibility Study of Engineered Barriers for Waste Management Units in the 200 Areas, Rev. 1, U.S. Department of Energy, Richland Operations Office, Richland, Washington.

DOE/RL-2002-59, 2004, Hanford Site Groundwater Strategy Protection, Monitoring, and Remediation, U.S. Department of Energy, Richland Operations Office, Richland, Washington.

DOE/RL-2011-50, 2012, Regulatory Basis and Implementation of a Graded Approach to Evaluation of Groundwater Protection, Rev. 1, U.S. Department of Energy, Richland Operations Office, Richland, Washington.

Ecology, EPA, and DOE, 1989, Hanford Federal Facility Agreement and Consent Order – Tri-Party Agreement, 2 vols., as amended, State of Washington Department of Ecology, U.S. Environmental Protection Agency, and U.S. Department of Energy, Olympia, Washington.

EPA 402-R-94-012, 1994, A Technical Guide to Ground-Water Model Selection at Sites Contaminated with Radioactive Substances, U.S. Environmental Protection Agency, Washington, D.C.

EPA/530-SW-87-017, 1987, Alternate Concentration Limit Guidance, Interim Final, OSWER Directive 9841.00-6C, U.S. Environmental Protection Agency, Office of Emergency Response, Washington, D.C.

EPA/540/1-89/002, 1989, Risk Assessment Guidance for Superfund Volume I Human Health Evaluation Manual (Part A) Interim Final, U.S. Environmental Protection Agency, Washington, D.C.

EPA/540/F-95/041, 1996, Soil Screening Guidance: Fact Sheet, Publication 9355.4-14FSA, U.S. Environmental Protection Agency, Office of Solid Waste and Emergency Response, Washington, D.C.

EPA/540/R-92/003, 1991, Guidance for Data Useability in Risk Assessment (Part A) Final, U.S. Environmental Protection Agency, Office of Research and Development, Washington, D.C.

EPA/540/R-95/128, 1996, Soil Screening Guidance: Technical Background Document, Second Edition, U.S. Environmental Protection Agency, Office of Solid Waste and Emergency Response, Washington, D.C.

EPA/600/2-91/065, 1991, The RETC Code for Quantifying the Hydraulic Functions of Unsaturated Soils, Office of Research and Development, U.S. Environmental Protection Agency, Washington, D.C.

EPA-SAB-RAC-ADV-99-006, 1999, An SAB Advisory: Modeling of Radionuclide Releases from Disposal of Low Activity Mixed Waste, U.S. Environmental Protection Agency, Science Advisory Board, Washington, D.C.

Fayer, M. J., and G. W. Gee, 2006, "Multiple-Year Water Balance of Soil Covers in a Semiarid Setting," Journal of Environmental Quality, Vol. 35, No. 2, pp. 366–377.

Gelhar, L. W. and C. L. Axness, 1983, "Three-dimensional stochastic analysis of macrodispersion in aquifers," Water Resources Research, Vol. 19, pp. 161–180.

Haynes, W. M. and D. R. Lide, 2011, CRC Handbook of Chemistry and Physics, 92nd Edition, CRC Press, Talyor & Francis Group, Boca Raton, Florida.

HNF-5294, 1999, "Computer Code Selection Criteria for Flow and Transport Code(s) To Be Used in Vadose Zone Calculations for Environmental Analyses in the Hanford Site's Central Plateau," Rev. 0, CH2M HILL Hanford Group, Inc. Richland, Washington.

Huyakorn, P. S. and G. F. Pinder, 1983, Computational Methods in Subsurface Flow, Academic Press, Salt Lake City, Utah.

HW-60601, 1959, "Aquifer Characteristics and Ground-Water Movement at Hanford," General Electric Company, Richland, Washington.

Khaleel, R., J. F. Relyea, and J. L. Conca, 1995, "Evaluation of van Genuchten-Mualem Relationships to Estimate Unsaturated Hydraulic Conductivity at Low Water Contents," Water Resources Research, Vol. 31, Issue 11, pp. 2659–2668.

Millington, R. J. and J. P. Quirk, 1961, "Permeability of Porous Solids," Transactions of the Faraday Society, Vol. 57, pp. 1200–1207.

Mualem, Y., 1976, "A New Model for Predicting the Hydraulic Conductivity of Unsaturated Porous Media," Water Resources Research, Vol. 12, No. 3, pp. 513–522.

NAGRA NTB 02-20, 2002, "Cementitious Near-Field Sorption Data Base for Performance Assessment of an ILW Repository in Opalinus Clay," Technical Report 02-20, National Cooperative for the Disposal of Radioactive Waste, Hardstrasse, Zurich, Switzerland.

Neuman, S. P., 1990, "Universal Scaling of Hydraulic Conductivities and Dispersivities in Geologic Media," Water Resources Research, Vol. 26, No. 8, pp. 1749–1758.

NOAA Manual NOS NGS 5, 1989, "State Plane Coordinate System of 1983," National Geodetic Survey, Rockville, Maryland.

NUREG-1573, 2000, A Performance Assessment Methodology for Low-Level Radioactive Waste Disposal Facilities: Recommendations of NRC's Performance Assessment Working Group, U.S. Nuclear Regulatory Commission, Office of Nuclear Material Safety and Safeguards, Washington, D.C.

NUREG-1854, 2007, NRC Staff Guidance for Activities Related to U.S. Department of Energy Waste Determinations – Draft Final Report for Interim Use, U.S. Nuclear Regulatory Commission, Office of Federal and State Materials and Environmental Management Programs, Washington, D.C.

OSWER No. 9200.4-18, 1997, "Establishment of Cleanup Levels for CERCLA Sites with Radioactive Contamination" (memorandum from S. D. Luftig and L. Weinstock to Addressees, August 22), U.S. Environmental Protection Agency, Washington, D.C.

PNNL-11216, 1997, "STOMP Subsurface Transport Over Multiple Phases Application Guide," Pacific Northwest National Laboratory, Richland, Washington.

PNNL-12030, 2000, "STOMP Subsurface Transport Over Multiple Phases Version 2.0 Theory Guide," Pacific Northwest National Laboratory, Richland, Washington.

PNNL-13033, 1999, "Recharge Data Package for the Immobilized Low-Activity Waste 2001 Performance Assessment," Pacific Northwest National Laboratory, Richland, Washington.

PNNL-13895, 2003, "Hanford Contaminant Distribution Coefficient Database and Users Guide," Rev. 1, Pacific Northwest National Laboratory, Richland, Washington.

PNNL-15782, 2006, "STOMP Subsurface Transport Over Multiple Phases Version 4.0 User's Guide," Pacific Northwest National Laboratory, Richland, Washington.

PNNL-16688, 2007, "Recharge Data Package for Hanford Single-Shell Tank Waste Management Areas," Pacific Northwest National Laboratory, Richland, Washington.

PNNL-17176, 2007, "200-BP-1 Prototype Hanford Barrier Annual Monitoring Report for Fiscal Years 2005 Through 2007," Pacific Northwest National Laboratory, Richland, Washington.

PNNL-SA-54022, 2007, "STOMP Software Test Plan Rev. 1.0," Pacific Northwest National Laboratory, Richland, Washington.

PNNL-SA-54023, 2007, "STOMP Software Configuration Management Plan Rev. 1.3," Pacific Northwest National Laboratory, Richland, Washington.

PNNL-SA-54024, 2007, "Project Management Plan for Subsurface Transport Over Multiple Phases (STOMP) Software Maintenance and Development," Rev. 1, Pacific Northwest National Laboratory, Richland, Washington.

PNNL-SA-54079, 2007, "Requirements for STOMP Subsurface Transport Over Multiple Phases," Pacific Northwest National Laboratory, Richland, Washington.

Polmann, D. J., 1990, "Application of Stochastic Methods to Transient Flow and Transport in Heterogeneous Unsaturated Soils," Ph.D. Thesis, Massachusetts Institute of Technology, Cambridge, Massachusetts.

PRC-PRO-IRM-309, 2014, "Controlled Software Management," Rev. 5, CH2M HILL Plateau Remediation Company, Richland, Washington.

PSI Bericht Nr. 95-06, 1995, "Sorption Databases for the Cementitious Near-Field of a L/ILW Repository for Performance Assessment," Paul Scherrer Institute, Switzerland.

Resource Conservation and Recovery Act of 1976, 42 USC 6901, et seq.

RPP-14430, 2003, "Subsurface Conditions Description of the C and A-AX Waste Management Area," Rev. 0, CH2M HILL Hanford Group, Inc., Richland, Washington.

RPP-17209, 2006, "Modeling Data Package for an Initial Assessment of Closure of the S and SX Tank Farms," Rev. 1, CH2M HILL Hanford Group, Inc., Richland, Washington.

RPP-PLAN-39114, 2012, "Phase 2 RCRA Facility Investigation/Corrective Measures Study Work Plan for Waste Management Area C," Rev. 2, Washington River Protection Solutions, LLC, Richland, Washington.

RPP-RPT-41918, 2010, "Assessment Context for Performance Assessment for Waste in C Tank Farm Facilities after Closure," Rev. 0, Washington River Protection Solutions, LLC, Richland, Washington.

RPP-RPT-42323, 2015, "Hanford C-Farm Tank and Ancillary Equipment Residual Waste Inventory Estimates," Rev. 3, Washington River Protection Solutions, LLC, Richland, Washington.

RPP-RPT-44042, 2016, "Recharge and Waste Release within Engineered System in Waste Management Area C," Rev. 1, Washington River Protection Solutions, LLC, Richland, Washington.

RPP-RPT-46088, 2016, "Flow and Transport in the Natural System at Waste Management Area C," Rev. 2, Washington River Protection Solutions, LLC/GSI Water Solutions, Inc., Richland, Washington.

RPP-RPT-48490, 2011, "Technical Approach and Scope for Flow and Contaminant Transport Analysis in the Initial Performance Assessment of Waste Management Area C," Washington River Protection Solutions, LLC, Richland, Washington.

RPP-RPT-50934, 2012, "Inspection and Test Report for the Removed 241-C-107 Dome Concrete," Rev. 0, Washington River Protection Solutions, LLC, Richland, Washington.

RPP-RPT-56356, 2014, "Development of Alternative Digital Geologic Models of Waste Management Area C," Rev. 0, Freestone Environmental Services Inc./Washington River Protection Solutions, LLC, Richland, Washington.

Schulze-Makuch, D., 2005, "Longitudinal Dispersivity Data and Implications for Scaling Behavior," Groundwater, Vol. 43, No. 3, pp. 443–456.

SKB Rapport R-05-75, 2005, "Assessment of uncertainty intervals for sorption coefficients, SFR-1 uppföljning av SAFE," Swedish Nuclear Fuel and Waste Management Company, Stockholm, Sweden.

SRNL-STI-2008-00421, 2008, "Hydraulic and Physical Properties of Saltstone Grouts and Vault Concretes," Rev. 0, Savannah River National Laboratory, Savannah River Nuclear Solutions, Aiken, South Carolina.

van der Kamp, G., L. D. Luba, J. A. Cherry, and H. Maathuis, 1994, "Field Study of a Long and Very Narrow Contaminant Plume," Groundwater, Vol. 32, No. 6, pp. 1008–1016.

van Genuchten, M. Th., 1980, "A Closed-form Equation for Predicting the Hydraulic Conductivity of Unsaturated Soils," Soil Science Society of America Journal, Vol. 44, No. 5, pp. 892–898.

WAC 173-340, "Model Toxics Control Act – Cleanup," Washington Administrative Code, as amended.

WAC 173-340-747, "Deriving Soil Concentrations for Groundwater Protection," Washington Administrative Code, as amended.

WCH-520, 2013, "Performance Assessment for the Environmental Restoration Disposal Facility, Hanford Site, Washington," Rev. 1, Washington Closure Hanford, Richland, Washington.

WHC-EP-0645, 1995, "Performance Assessment for the Disposal of Low-Level Waste in the 200 West Area Burial Grounds," Westinghouse Hanford Company, Richland, Washington.

WHC-SD-WM-EE-004, 1995, "Performance Assessment of Grouted Double-Shell Tank Waste Disposal at Hanford," Rev. 1, Westinghouse Hanford Company, Richland, Washington.

WSRC-MS-2003-00582, 2003, "Performance Assessment/Composite Analysis Modeling to Support a Holistic Strategy for the Closure of F Area, a Large Nuclear Complex at The Savannah River Site," Rev. 1, Savannah River Technology Center, Aiken, South Carolina.

Xu, M. and Y. Eckstein, 1995, "Use of Weighted Least-Squares Method in Evaluation of the Relationship Between Dispersivity and Field Scale," Groundwater, Vol. 33, No. 6, pp. 905–908.

Ye, M., R. Khaleel, T. J. Yeh, 2005, "Stochastic analysis of moisture plume dynamics of a field injection experiment," Water Resources Research, Vol. 41, W03013.

Yeh, T.-C. J., M. Ye, R. Khaleel, 2005, "Estimation of effective unsaturated hydraulic conductivity tensor using spatial moments of observed moisture plume," Water Resources Research, Vol. 41, W03014.

APPENDIX E

VALIDATION OF THE AIR-PATHWAY MODELING APPROACH

This page intentionally left blank.

TABLE OF CONTENTS

APPENDIX E – VALIDATION OF THE AIR-PATHWAY MODELING APPROACH.....E-1

E.1 AIR CONCENTRATIONS USING WASTE MANAGEMENT AREA C PERFORMANCE ASSESSMENT MODEL E-1

E.2 MODELED AIR CONCENTRATIONS USING EPA CAP88-PC SOFTWARE E-2

E.2.1 Receptor Location and Population.....E-2

E.2.2 Meteorological Data.....E-2

E.2.3 Source and Radionuclide Data.....E-4

E.2.4 CAP88 Modeling Results E-4

E.3 COMPARISON OF MODELED AIR CONCENTRATIONS E-4

E.4 COMPARISON AGAINST HANFORD SITE NATIONAL ENVIRONMENTAL POLICY ACT CHARACTERIZATION REPORT.....E-5

E.5 REFERENCES E-6

LIST OF FIGURES

Figure E-1. 2011 Wind Rose for Hanford Meteorological Station Showing the Incoming Wind Direction. E-3

LIST OF TABLES

Table E-1. Predicted Maximum Air Concentration Using Waste Management Area C Performance Assessment Model.....E-1

Table E-2. Source Terms for CAP88 Run. E-4

Table E-3. Maximum Air Concentrations Based on CAP88 Model. E-4

Table E-4. Estimated Air Concentrations at the Receptor Location.....E-5

LIST OF TERMS

EPA	U.S. Environmental Protection Agency
HMS	Hanford Meteorological Station
NEPA	National Environmental Policy Act
PA	performance assessment
WMA C	Waste Management Area C

APPENDIX E
VALIDATION OF THE AIR-PATHWAY MODELING APPROACH

As a part of the performance assessment (PA) requirements, potential gas emissions and the resulting air concentrations of radionuclides originating from Waste Management Area C (WMA C) need to be modeled for calculating potential doses by the atmospheric pathway. Among the radionuclides contained in the wastes in WMA C at closure, three of them can potentially emanate in gaseous form. These radionuclides are ^{14}C (as CO_2), ^{3}H (as H_2), and ^{129}I (as I_2). Using the WMA C PA model, the release rates and concentrations for the three radionuclides over WMA C are calculated. The PA model conceptualization for air-pathway modeling is discussed in Section 6.3.2.5 (Atmospheric Transport Pathway).

This section provides evidence that the air-pathway modeling approach has been adequately modeled to meet the performance requirements of the PA. This is done by comparing the PA model for air-pathway calculations to modeling results generated using the U.S. Environmental Protection Agency's (EPA) CAP88-PC code, and to those reported in the recent Hanford Site National Environmental Policy Act (NEPA) Characterization Report [PNNL-6415, "Hanford Site National Environmental Policy Act (NEPA) Characterization"]. The comparison of results indicates that the GoldSim®[1]-based WMA C PA model built for the air-pathway calculation is appropriate for its intended purpose.

E.1 AIR CONCENTRATIONS USING WASTE MANAGEMENT AREA C PERFORMANCE ASSESSMENT MODEL

The WMA C PA air pathway model was used to calculate the release rates and concentrations for three radionuclides—^{14}C (as CO_2), ^{3}H (as H_2), and ^{129}I (as I_2)—at the receptor location (see Sections 6.3.2.5 and 7.2.2). The PA model calculates the diffusive flux of volatiles to the surface of WMA C and then transports them through the air to the receptor location. The air concentrations for the volatiles (^{14}C [as CO_2], ^{3}H [as H_2], ^{129}I) from all residual waste sources in WMA C are calculated out to 10,000 years. The maximum calculated air concentration is presented in Table E-1. These values were used for comparison.

Table E-1. Predicted Maximum Air Concentration Using Waste Management Area C Performance Assessment Model.

Nuclides	Unit	Maximum Air Concentration
^{14}C	pCi/m^3	2.4E-6
^{3}H		1.1
^{129}I		3.5E-6

[1] GoldSim® Pro is a registered trademark of GoldSim Technologies, Issaquah, Washington, in the United States and other countries.

E.2 MODELED AIR CONCENTRATIONS USING EPA CAP88-PC SOFTWARE

To verify the modeled radionuclide concentrations by the WMA C PA model, a comparative modeling study was performed using the CAP88-PC Version 4 computer program (EPA 2014). The CAP88 (which stands for Clean Air Act Assessment Package – 1988) computer model is a set of computer programs, databases, and associated utility programs for estimation of concentrations, dose, and risk from radionuclide emissions to the air.

CAP88-PC uses a modified Gaussian plume equation to estimate the average dispersion of radionuclides released from up to six emitting sources. The sources may be either elevated stacks (such as a smoke stack) or uniform area sources (such as a landfill or a pile of uranium mill tailings). Plume rise can be calculated assuming either a momentum or buoyant-driven plume. Assessments are done for a circular grid of distances and directions for a radius of up to 80 km (50 mi) around the facility. The Gaussian plume model produces results that agree with experimental data, and with other similar regulatory models.

The CAP88-PC model requires the following inputs:

- Facility data
- Receptor location and population
- Meteorological data
- Source data
- Radionuclide data
- Agriculture data (for dose estimation and risk calculation).

For this comparative study, the CAP88-PC modeling was conducted using the options and input parameters described in the following sections.

E.2.1 Receptor Location and Population

The CAP88 modeling was set up for “individual assessment” (rather than for “population assessment”) to be consistent with modeled results in the PA effort. The modeled receptor distance was calculated as the distance from the center of the tank farm within WMA C to 100 m downwind from the fenceline. As a result, a total receptor distance for the CAP88 modeling was set to be 175 m.

E.2.2 Meteorological Data

The following site-specific meteorological input parameters for the comparative modeling were determined based on the averages of 30-year meteorological data collected at the Hanford Meteorological Station (HMS). The HMS is located near the center of the Hanford Site, just outside the northeast corner of the 200 West Area:

- Annual ambient temperature: 10°C
- Annual precipitation: 17 cm/year

- Height of the mixing layer: 1,000 m (default)
- Absolute humidity: 8.00 g/m^3 (default, similar to the HMS value).

The wind rose for HMS for 2011 is presented in Figure E-1. The figure showed that the prevailing wind direction is from west-northwest towards the east-southeast.

Figure E-1. 2011 Wind Rose for Hanford Meteorological Station Showing the Incoming Wind Direction.

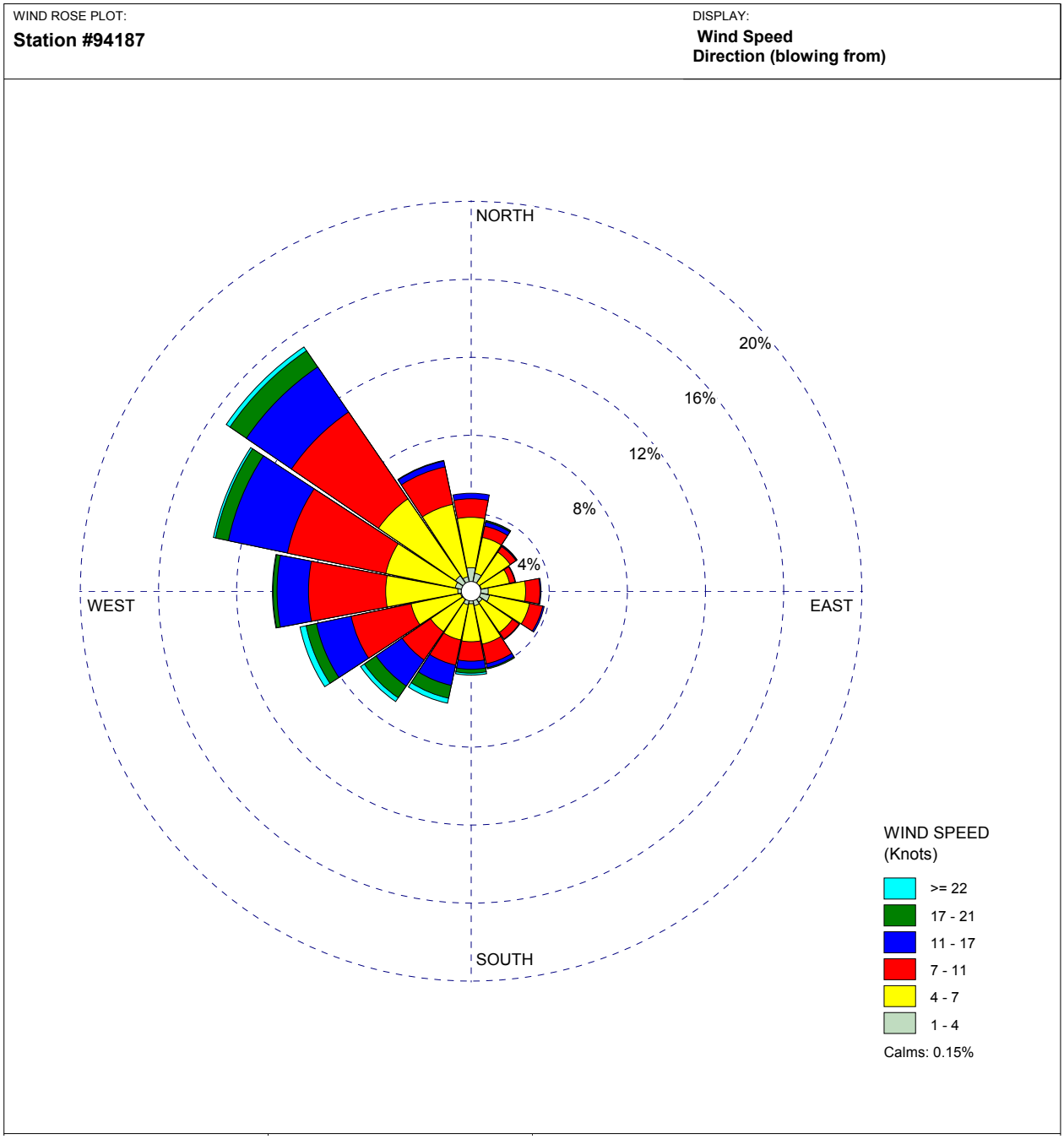

E.2.3 Source and Radionuclide Data

The emissions from the tank farm within WMA C were modeled as a point source (stack emission) at a height of 2 m above the ground level. The point source is conceptualized to be conservative and located at the center of the tank farm. The effective diameter for the stack was set to be the 100-series tank diameter (75 ft).

The combined diffusive flux for the volatiles (^{14}C [as CO_2], ^{3}H [as H_2], ^{129}I) from all sources was used as the source term for stack emission for CAP88 calculation. For the purpose of verification, the maximum emission rate for each radionuclide at the surface of WMA C calculated by the WMA C PA model was selected. The maximum emission rates are presented in Table E-2.

Table E-2. Source Terms for CAP88 Run.

Nuclides	Unit	Emission Rate
^{14}C	Ci/yr	4.35E-7
^{3}H		2.06E-1
^{129}I		6.54E-7

E.2.4 CAP88 Modeling Results

Using the wind file from HMS (200 Area), the CAP88 modeling determined the maximum concentration for each radionuclide at the receptor location; those concentrations are presented in Table E-3. The maximum concentration occurred along the 175 m distance in the southeast direction from the center of the tank farm, consistent with the predominant wind direction.

Table E-3. Maximum Air Concentrations Based on CAP88 Model.

Nuclides	Unit	Maximum Air Concentration
^{14}C	pCi/m^3	1.57E-6
^{3}H		0.744E-1
^{129}I		2.37E-6

E.3 COMPARISON OF MODELED AIR CONCENTRATIONS

Tables E-1 and E-3 present maximum air concentration results for three radionuclides—^{14}C (as CO_2), ^{3}H (as H_2), and ^{129}I (as I_2)—at the receptor location using the WMA C PA model and CAP88 model. The results showed that the maximum concentrations for both models are in reasonable agreement, with the PA model producing results about 50% higher than CAP88. The difference between the two models lies in an approximation used in the PA model where

concentration along the center of the plume is calculated at the same height as the stack without accounting for horizontal and vertical dispersion.

E.4 COMPARISON AGAINST HANFORD SITE NATIONAL ENVIRONMENTAL POLICY ACT CHARACTERIZATION REPORT

As part of the annual Hanford Site NEPA Characterization Report, an atmospheric dispersion analysis is performed to characterize the distribution of the identified radionuclides in the ambient air and to estimate the potential exposure. These are presented in Revision 18 of PNNL-6415. The annual sector-averaged dispersion coefficients for the major Hanford Site areas are presented, taking into account the wind-related data from 1983 through 2006 from various meteorological stations on the Hanford Site. These dispersion factors are presented as a function of direction and distance from the release point.

The atmospheric dispersion analysis in the PNNL-6415 report was conducted using simple dispersion models and the joint frequency distribution of atmospheric stability, wind speed, and wind direction to compute diffusion factors for both chronic and acute releases. Joint frequency distributions for atmospheric stability, wind speed, and transport direction have been estimated and presented for the meteorological data collected from the 100-N, 200, 300, and 400 Areas at two release heights (9.1 m [30 ft] and 60 m [197 ft]).

To verify the WMA C PA air-pathway modeling results, an evaluation was performed by comparing the WMA C PA modeled concentrations at a selected distance with the derived air concentrations for the same distance. This evaluation used the reported annual sector average dispersion coefficients (X/Q', where X is the air concentration [Ci/m^3] and Q' is the emission rate) in PNNL-6415 for a given WMA C gas emission rate.

For this comparison analysis, joint frequency distributions presented for the 200 Area were used (PNNL-6415). The atmospheric dispersion coefficient (X/Q') of 1.1×10^{-4} s·m^{-3} for the ground level release was selected based on a distance of 175 m (approximate effective distance of receptor from the center of WMA C) in the southeast direction (the predominant direction of flow) from Table A11 of PNNL-6415. The emission rates for three radionuclides are presented in Table E-2. The atmospheric dispersion coefficient (X/Q') was multiplied with the emission rates for three radionuclides to calculate their estimated ground level air concentrations at 175 m downgradient from the source. The results are presented in Table E-4.

Table E-4. Estimated Air Concentrations at the Receptor Location.

Nuclides	X/Q (s/m^3)	Emission Rate		Estimated Air Concentrations at 175 m Downgradient (pCi/m^3) = X/Q (s/m^3) × Emission Rate (pCi/s)
		(Ci/yr)	(pCi/s) = (Ci/yr) × (10^{12} pCi/Ci) × (1 yr/3.15E7 s)	
^{14}C	1.1E-4	4.35E-7	1.38E-02	1.52E-06
^{3}H		2.06E-1	6.54E+03	7.20E-01
^{129}I		6.54E-7	2.07E-02	2.28E-06

Comparison with the WMA C concentrations (Table E-1) shows that, like the CAP88 comparison, the WMA C results are about 50% higher. As in that comparison, the difference is attributable to the centerline approximation used in the WMA C PA model, which tends to overestimate concentrations relative to other models.

E.5 REFERENCES

EPA, 2014, CAP88-PC Version 4.0 User Guide, U.S. Environmental Protection Agency, Washington, D.C.

National Environmental Policy Act of 1969, 42 USC 4321-4347, et seq.

PNNL-6415, 2007, "Hanford Site National Environmental Policy Act (NEPA) Characterization," Rev. 18, Pacific Northwest National Laboratory, Richland, Washington.

APPENDIX F

DEVELOPMENT OF HETEROGENEOUS MEDIA MODEL AND COMPARISON TO BASE CASE MODEL RESULTS FOR WASTE MANAGEMENT AREA C PERFORMANCE ASSESSMENT

This page intentionally left blank.

TABLE OF CONTENTS

APPENDIX F – DEVELOPMENT OF HETEROGENEOUS MEDIA MODEL AND COMPARISON TO BASE CASE MODEL RESULTS FOR WASTE MANAGEMENT AREA C PERFORMANCE ASSESSMENT F-1

F.1 INTRODUCTION F-1

F.2 METHODOLOGY FOR DEVELOPING TWO-DIMENSIONAL CROSS-SECTION MODELS FROM THE THREE-DIMENSIONAL MODEL F-2

F.2.1 Waste Management Area C Performance Assessment Three-Dimensional STOMP© Model F-2

F.2.2 Development of Three-Dimensional Distributions of Moisture Content F-2

F.2.3 Development of Two-Dimensional STOMP©-Based Models from Three-Dimensional Models F-2

F.3 RESULTS F-14

F.3.1 Moisture Content Prediction F-14

F.3.2 Matric Potential Measurements F-14

F.3.3 Calculation of Technetium-99 Concentration F-15

F.4 CONCLUSIONS F-15

F.5 REFERENCES F-25

LIST OF FIGURES

Figure F-1. Geologic Layers in the Three-Dimensional Waste Management Area C Performance Assessment Model. F-5

Figure F-2. Plan View of Waste Management Area C Performance Assessment Model and Moisture Content-Based Model. F-6

Figure F-3. Waste Management Area C Basemap with Moisture Content (vol %) Data Locations. F-7

Figure F-4. Cross Section B-B' with Continuous Contours for Moisture Content (vol %) Interpolation. F-8

Figure F-5. Cross Section C-C' with Continuous Contours for Moisture Content (vol %) Interpolation. F-9

Figure F-6. Location of Selected Cross Sections for the Two-Dimensional Models. F-10

Figure F-7. View along Cross Section 1 (North to South) Shown in Figure F-6. F-11

Figure F-8. View along Cross Section 2 (North to South) Shown in Figure F-6. F-12

Figure F-9. View along Cross Section 3 (West to East) Shown in Figure F-6. F-13

Figure F-10. Moisture Retention Curves and Unsaturated Hydraulic Conductivity Curves for the 44 Integrated Disposal Facility Samples. F-16

Figure F-11. Moisture Retention Curves and Unsaturated Hydraulic Conductivity Curves for the Four New Units. F-17

Figure F-12. Location of Contaminant Source and Point of Calculation. F-18

Figure F-13. Location of Well C4297 and 299-E27-22 Relative to Cross Section 1. F-19

Figure F-14. Comparison of Measured (C4297) and Simulated Moisture Contents for (a) Base Case (Equivalent Homogeneous Medium) Model, and (b) Heterogeneous Model for Cross Section 1. F-20

Figure F-15. Comparison of Measured (299-E27-22) and Simulated Moisture Contents for (a) Base Case (Equivalent Homogeneous Medium) Model, and (b) Heterogeneous Model for Cross Section 1. F-21

Figure F-16. Technetium-99 Breakthrough Curves for Cross Section 1. F-22

Figure F-17. Technetium-99 Breakthrough Curves for Cross Section 2. F-23

Figure F-18. Technetium-99 Breakthrough Curves for Cross Section 3. F-24

LIST OF TABLES

Table F-1. Vadose Zone Hydraulic Properties for Waste Management Area C Hydrostratigraphic Units (Appendix B). F-14

Table F-2. Summary of Vadose Zone Hydraulic Properties for the New Units (Appendix B). F-18

Table F-3. Average Moisture and Matric Potentials for Borehole Samples Inside and Outside of Waste Management Area C. F-21

Table F-4. Summary of Technetium-99 Transport Model Results. F-24

LIST OF TERMS

Abbreviations and Acronyms

2D	two-dimensional
3D	three-dimensional
cm	centimeter
EHM	equivalent homogeneous medium
HSU	hydrostratigraphic unit
L	Liter
m	meter
MPa	megapascal
NAVD88	North American Vertical Datum of 1988
pCi	picocurie
PA	performance assessment
RCRA	Resource Conservation and Recovery Act of 1976
s	second
S&L	Sisson and Lu
STOMP	Subsurface Transport Over Multiple Phases
WMA	Waste Management Area

APPENDIX F

DEVELOPMENT OF HETEROGENEOUS MEDIA MODEL AND COMPARISON TO BASE CASE MODEL RESULTS FOR WASTE MANAGEMENT AREA C PERFORMANCE ASSESSMENT

F.1 INTRODUCTION

Small-scale laboratory measurements were used to estimate field-scale parameters for the Waste Management Area (WMA) C model (Section 6). Each heterogeneous geologic unit was replaced by an equivalent homogeneous medium (EHM) with macroscopic flow properties. Each heterogeneous unit was assigned its upscaled or effective hydraulic properties; the simulated flow fields calculated the bulk or mean flow behavior at the field scale. Upscaling, in effect, accounts for differences in scale between small, core-scale measurements and large, field-scale modeling.

While the EHM model is the base case for performance assessment (PA) modeling, an alternative case is considered here based on the natural moisture content distribution. For heterogeneous media, the natural moisture content distribution, in the absence of anthropogenic recharge, can be used as an indicator of sediment texture (Appendix B). Field-measured moisture contents can then be used as indirect evidence from which estimates of soil hydraulic properties can be inferred.

In the absence of anthropogenic recharge, moisture content data correlate well with sediment texture ("Stochastic analysis of moisture plume dynamics of a field injection experiment" [Ye et al. 2005]). Higher moisture contents are associated with fine-textured sediments and lower moisture contents are associated with coarse-textured sediments. In the absence of anthropogenic recharge, field-measured moisture contents are assumed to be in equilibrium with natural recharge. These inferences, as well as the results of geostatistical analysis of the moisture content database, are used to identify and select hydraulic properties for input into a vadose zone model for WMA C.

An extensive set of moisture content data exists at WMA C for neutron moisture logging of direct push borehole and drywell locations. Using a geostatistical interpretation of the moisture data, an alternative vadose zone conceptual model has been developed, which is denoted as the "Heterogeneous Case" (RPP-CALC-60345, "Heterogeneous Media Model for Waste Management Area C Performance Assessment"). From the three-dimensional (3D) WMA C base case model, three cross sections have been selected to develop two-dimensional (2D) Subsurface Transport Over Multiple Phases (STOMP)©[1] models for both the EHM base case model and heterogeneous case model. The results are compared to identify the impact of heterogeneity for predicting concentrations in the water table.

[1] Subsurface Transport Over Multiple Phases (STOMP)© is copyrighted by Battelle Memorial Institute, 1996.

F.2 METHODOLOGY FOR DEVELOPING TWO-DIMENSIONAL CROSS-SECTION MODELS FROM THE THREE-DIMENSIONAL MODEL

Two-dimensional cross sections are developed from a 3D moisture content distribution model by interpolating on the grid discretization developed for the 3D STOMP© WMA C PA model. These selected cross sections form the basis for developing alternative heterogeneous case models based on moisture content data. The details of the approach for developing the 2D cross-sectional model are described in Sections F.2.1 through F.2.3.

F.2.1 Waste Management Area C Performance Assessment Three-Dimensional STOMP© Model

Figure F-1 (Section 6.3.2.2) presents a cutaway section of geologic units in the 3D STOMP© WMA C PA model domain. The WMA C PA 3D STOMP©-based model domain is 737.9 m (2,421 ft) northwest to southeast by 795.3 m (2,609 ft) southwest to northeast by 116 m (381 ft), vertically, extending about 12 m (49 ft) below the water table.

For the purpose of developing the heterogeneous geologic models, the moisture content distribution was interpolated on the 3D STOMP© WMA C PA model domain and then cross sections were developed.

F.2.2 Development of Three-Dimensional Distributions of Moisture Content

A 3D model of the distribution of moisture content has been developed based on a geostatistical evaluation of soil moisture data collected at WMA C. An extensive set of moisture content data and information exists at WMA C from neutron moisture logging of direct push borehole and drywell locations. These moisture content data have been collected long after the occurrence of past leaks and discharges at the farm (RPP-CALC-60345), and therefore are regarded as representing the vadose zone at equilibrium with natural recharge. A geostatistical analysis of the moisture content data yielded vertical as well as horizontal correlation length scales for moisture content. The experimental variograms for moisture content used in the geostatistical analysis were fit with an exponential model having a vertical correlation length of ~15 m and a horizontal correlation length of ~85 m. Subsequent krigging yielded a heterogeneous moisture distribution, which, unlike the EHM approximation, captures a higher level of spatial variability of moisture content and associated variability in hydraulic properties (RPP-CALC-60345). Figure F-2 represents the plan view of 3D WMA C PA model domain and krigged moisture content based on the level of discretization of the model domain. Figure F-3 (RPP-CALC-60345) presents the location of the different cross sections of the model; Figure F-4 and Figure F-5 show the 2D cross sections of the model.

F.2.3 Development of Two-Dimensional STOMP©-Based Models from Three-Dimensional Models

F.2.3.1 Base Case Two-Dimensional Model. From the 3D base case model, 2D models were extracted for three different cross sections for comparison to the heterogeneous case model-based cross sections. Figure F-6 shows the location of the selected cross sections. These cross sections

were selected to be in the same locations as the cross section B-B' and cross section C-C' shown in Figure F-3. Two orthogonal directions were chosen to represent behavior in different directions. Only cross section 1 slices through the tanks. Heterogeneity was only considered for the H1 and H2 units because of lack of moisture data for the deeper units.

F.2.3.1.1 Interpretation of the Three-Dimensional Moisture Model. The following steps were followed to develop the geology of the heterogeneous model from the moisture content model.

1. Four different moisture content bands were used to define the heterogeneous layers in the H1 and H2 units based on the histogram of the observed moisture content data reported in RPP-CALC-60345. These moisture content bands qualitatively correlate with the sand/silt content of the sediments as inferred from the characterization of vadose zone sediments within WMA C (PNNL-15503, "Characterization of Vadose Zone Sediments Below the C Tank Farm: Borehole C4297 and RCRA Borehole 299-E27-22"). Typically, increasing volumetric moisture content from 6% to >10% reflects increasing silt content in the sediments. Based on the characterization of vadose zone sediments in WMA C (PNNL-15503), it is observed that <6% moisture content is associated with sediments with no, or negligible, silt content (primarily sand or gravelly sand), while sediment with >10% volumetric moisture content is silt-dominated. For volumetric moisture contents within 6% and 10%, the increasing moisture content is understood to reflect increasing silt content. To define the moisture content bands for the purpose of model parameterization, two additional classes are introduced, one with 6% to 8% and the other with 8% to 10% volumetric moisture content. The four moisture content bands are summarized below:

    - 2%-6% – correlates to sand with some gravel fraction
    - 6%-8% – correlates to sandy units with minor silt fraction
    - 8%-10% – correlates to sandy-silty sand units
    - >10% – correlates to predominantly silty units.

2. The moisture content values from the moisture model were interpolated on the 3D STOMP© model grid.

3. The STOMP© model zonation number for each of the model grid blocks was printed out along with the moisture content values.

4. The base case 3D STOMP© model has five different hydrostratigraphic units (HSUs) defined as implemented in STOMP© as rock/soil zones:

    - Backfill: gravel-dominated
    - H1: gravel-dominated unit
    - H2: sand-dominated unit
    - H3: gravel-dominated unit
    - Aquifer.

5. Four additional rock/soil zones are introduced corresponding to the four moisture content bands by altering the original zones. These four zones are added within the WMA C model domain defined by the krigged area in Figure F-6 (red rectangular box). For areas outside this box, the original five rock/soil zones are retained, thus leading to total of nine different rock/zones.

6. Generate 2D models for the heterogeneous case and the base case along three selected cross sections. Figure F-7, Figure F-8, and Figure F-9 contrast the geologic representation of the PA base case model and the heterogeneous model for the selected cross sections.

F.2.3.2 Vadose Zone Hydraulic Properties for Different Units. Table F-1 shows the vadose zone hydraulic properties for the HSUs defined in the base case model. For the heterogeneous case, hydraulic properties for four additional zones/layers have been selected that compare favorably with the moisture content data under current recharge conditions.

The hydraulic properties for the new zones/layers have been selected by analyzing 44 Integrated Disposal Facility sandy samples as presented in Appendix B, Basis for Development of Vadose Zone Hydraulic Properties at Waste Management Area C. Figure F-10 shows the moisture retention curves and unsaturated hydraulic conductivity curves for the 44 Integrated Disposal Facility samples. Four samples out of the 44 samples were selected to represent the new moisture content-based units. The four samples were chosen such that the resulting moisture content distribution at unit gradient condition corresponds to the moisture content bands represented by the samples. Figure F-11 shows the moisture retention curves and unsaturated hydraulic conductivity curves for the four new units that correlate with the four zones based on moisture content. Table F-2 summarizes the properties for all the new units.

Moisture-dependent anisotropy was applied to the 2D cross-section model derived from the 3D base case model to be consistent with the upscaling methodology used for EHM-based models. However, the impact of anisotropy was assumed to be represented by the heterogeneous distribution of sediments and was therefore not applied for the 2D heterogeneous models.

F.2.3.2.1 Contaminant Source and Model Output. For each cross-sectional model, an arbitrary source concentration of 1,000 pCi/m^3 of ^{99}Tc (in bulk volume) was injected into the subsurface at the base of the backfill material beginning in the calendar year 2020. Here the objective was to compare the transport behavior of the contaminant between the EHM and heterogeneous model. Figure F-12 shows the location of the source and the point of calculation for all the cases. The vertical location of the contaminant mass is positioned 68 m above the water table. The output concentrations were observed at a point of calculation 100 m downgradient from the source location.

F.2.3.2.2 Recharge Rate. A 3.5 mm/yr recharge rate corresponding to long-term recharge rate for the WMA C base model domain was applied throughout the simulation duration.

Figure F-1. Geologic Layers in the Three-Dimensional Waste Management Area C Performance Assessment Model.

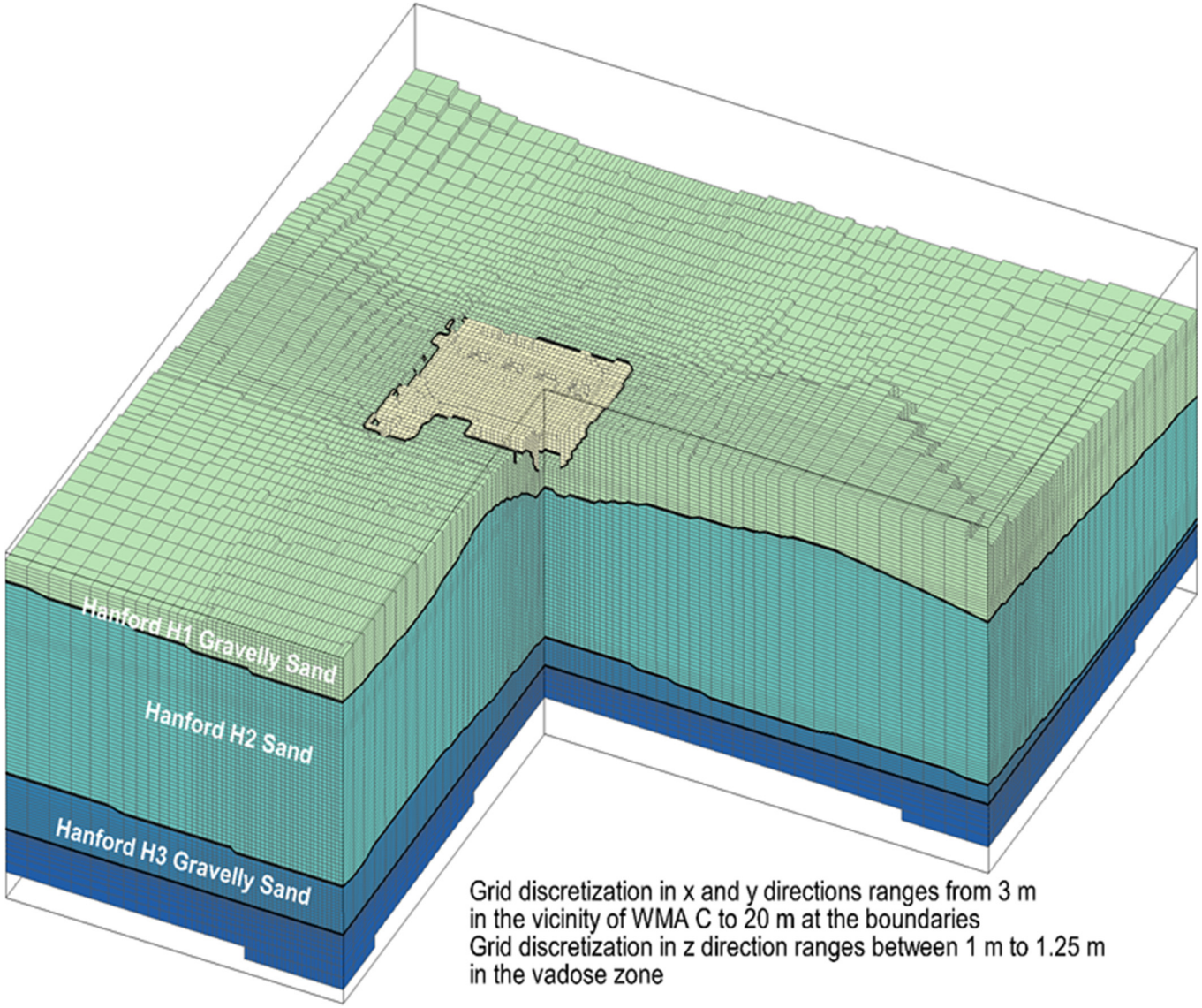

WMA = Waste Management Area

Figure F-2. Plan View of Waste Management Area C Performance Assessment Model and Moisture Content-Based Model.

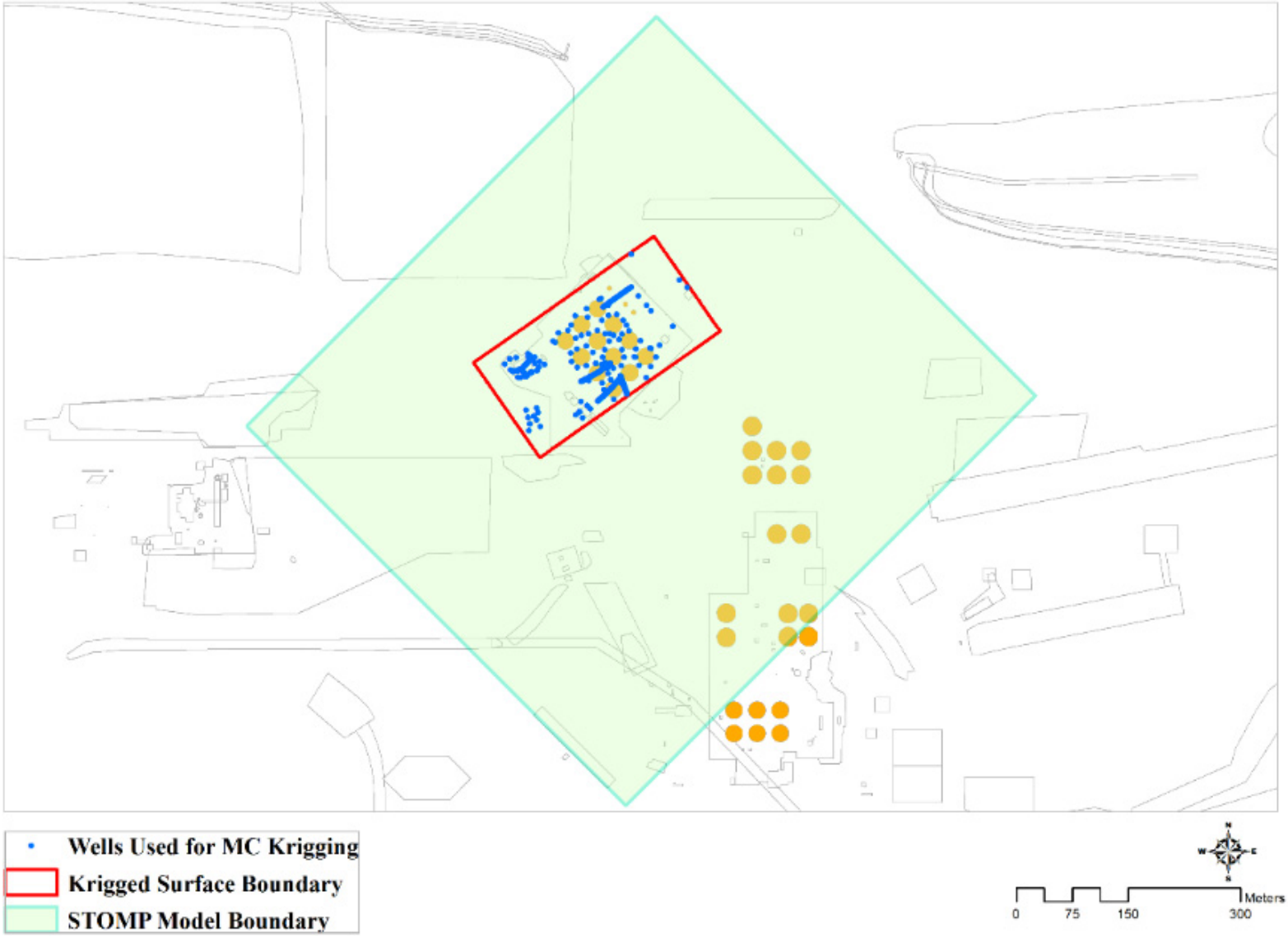

Subsurface Transport Over Multiple Phases (STOMP)© is copyrighted by Battelle Memorial Institute, 1996.

Figure F-3. Waste Management Area C Basemap with Moisture Content (vol %) Data Locations.

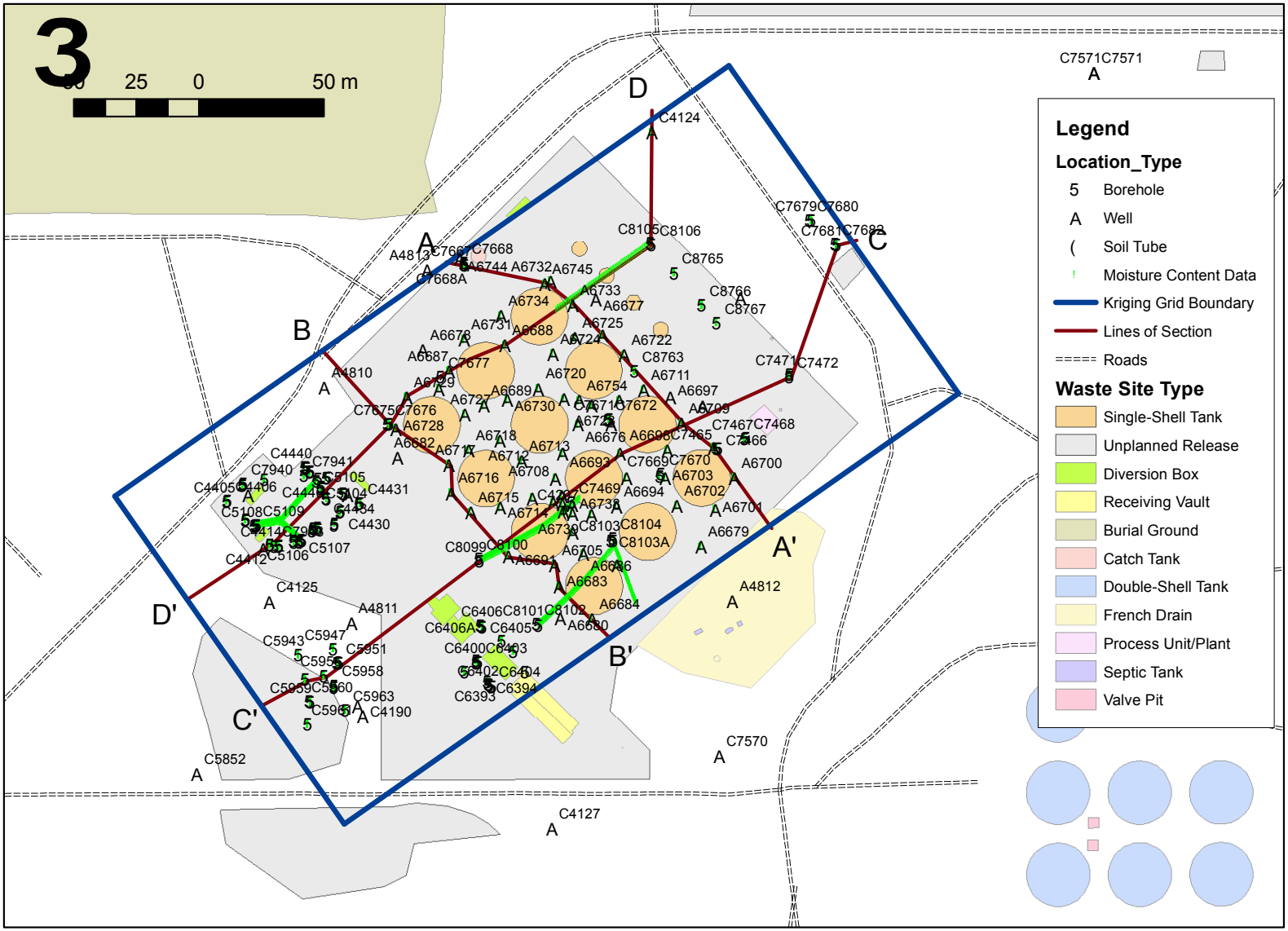

Reference: RPP-CALC-60345, "Heterogeneous Media Model for Waste Management Area C Performance Assessment."

Figure F-4. Cross Section B-B' with Continuous Contours for Moisture Content (vol %) Interpolation.

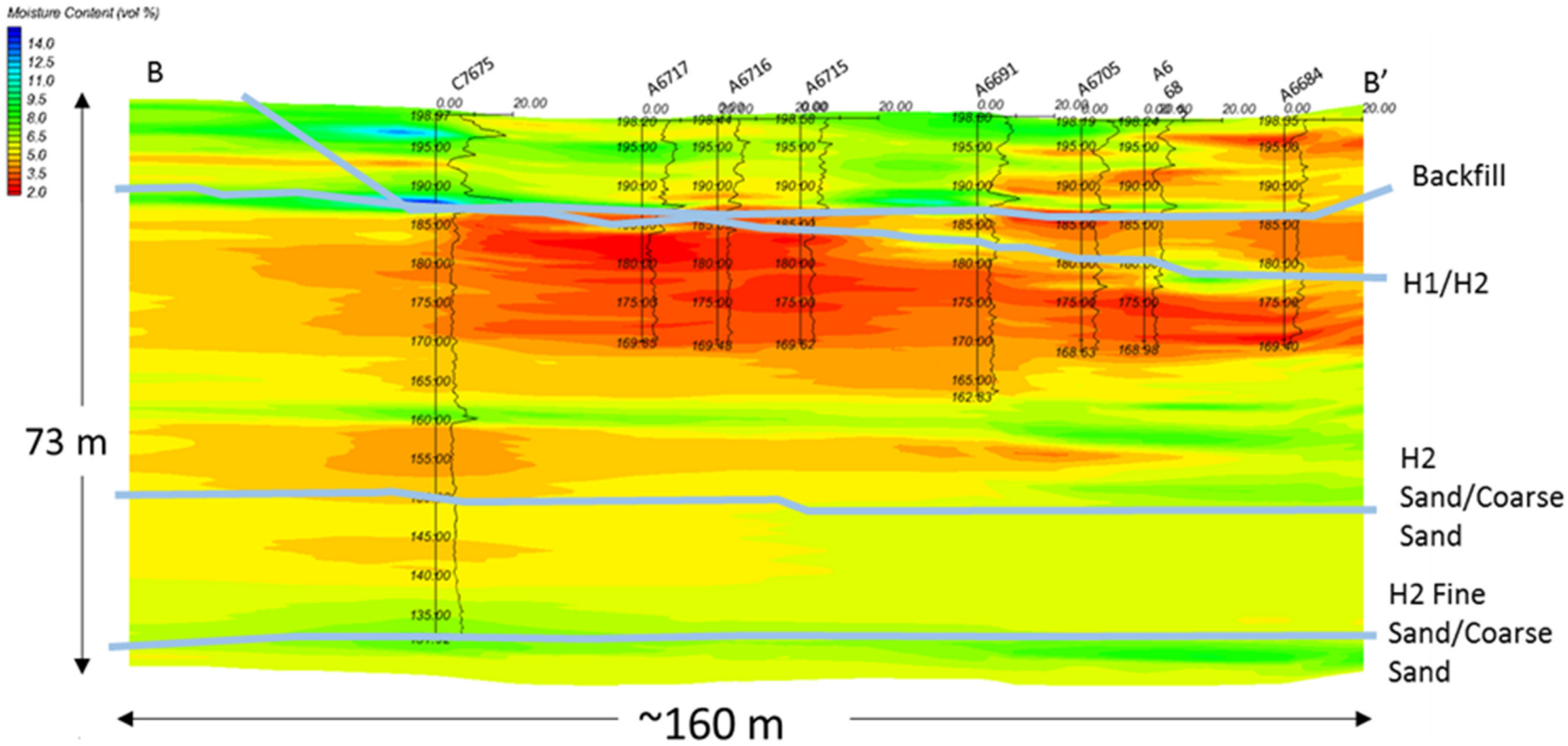

Reference: RPP-CALC-60345, "Heterogeneous Media Model for Waste Management Area C Performance Assessment."

Figure F-5. Cross Section C-C' with Continuous Contours for Moisture Content (vol %) Interpolation.

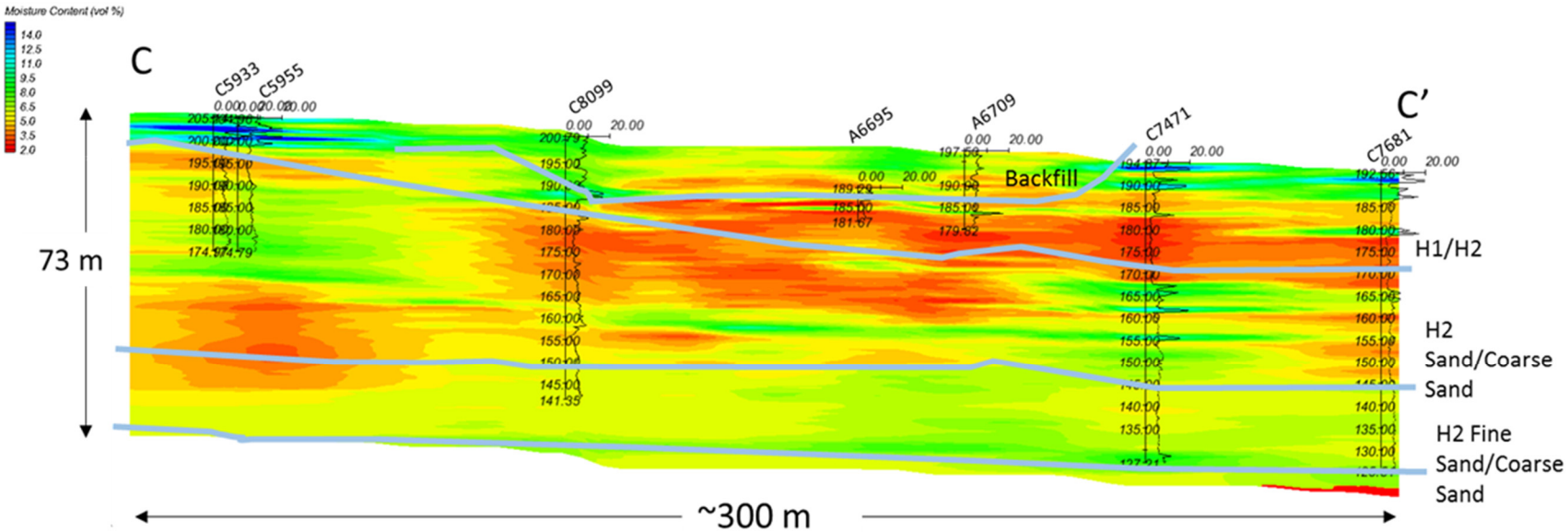

Reference: RPP-CALC-60345, "Heterogeneous Media Model for Waste Management Area C Performance Assessment."

Figure F-6. Location of Selected Cross Sections for the Two-Dimensional Models.

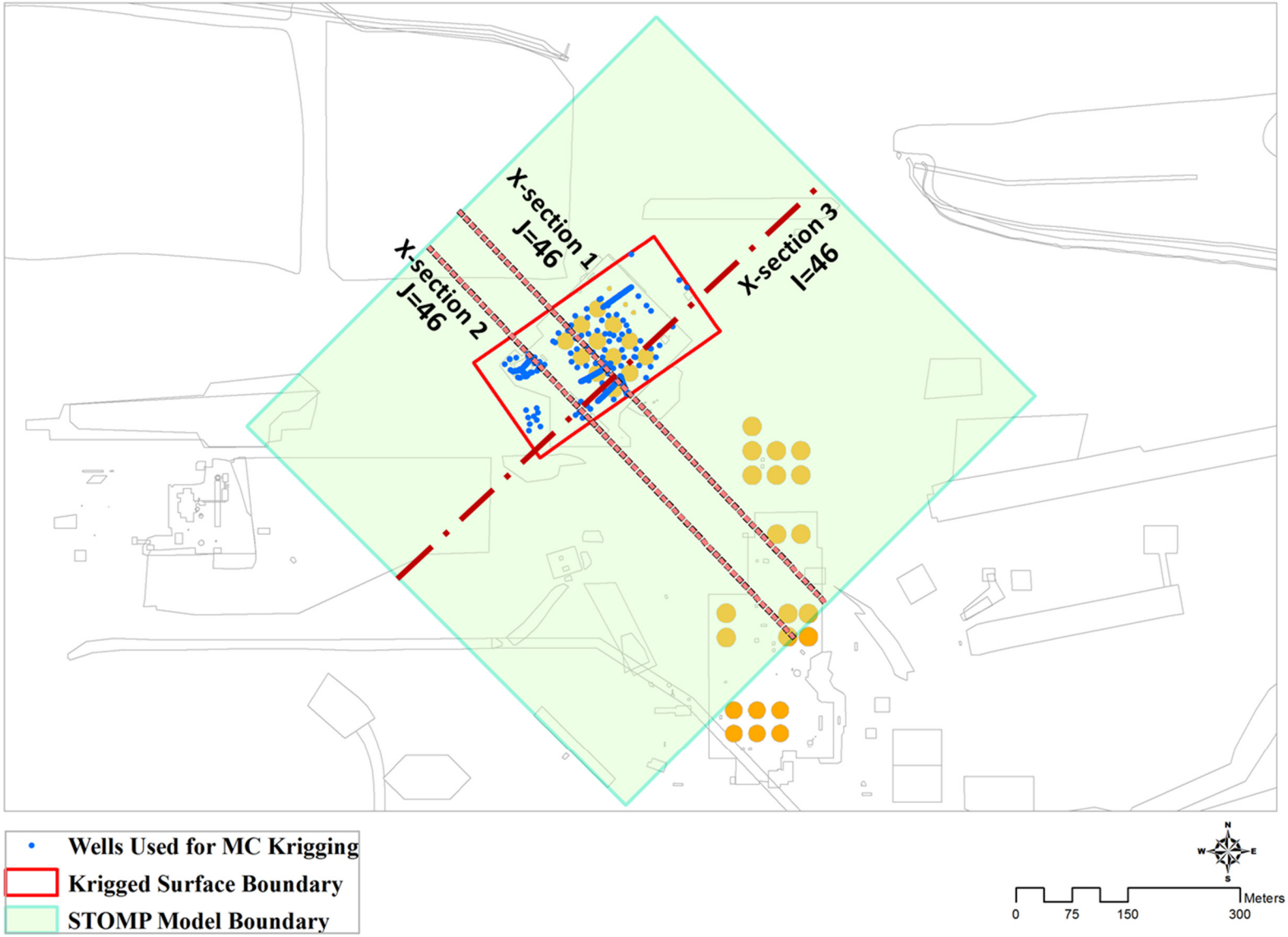

Subsurface Transport Over Multiple Phases (STOMP)© is copyrighted by Battelle Memorial Institute, 1996.

Figure F-7. View along Cross Section 1 (North to South) Shown in Figure F-6.

The left hand figure has the original 5 rock/soil zones (hydrostratigraphic units) while the right hand figure has 4 additional rock/soil zones to incorporate the moisture content bands-based heterogeneity within the krigged area shown in Figure F-6.

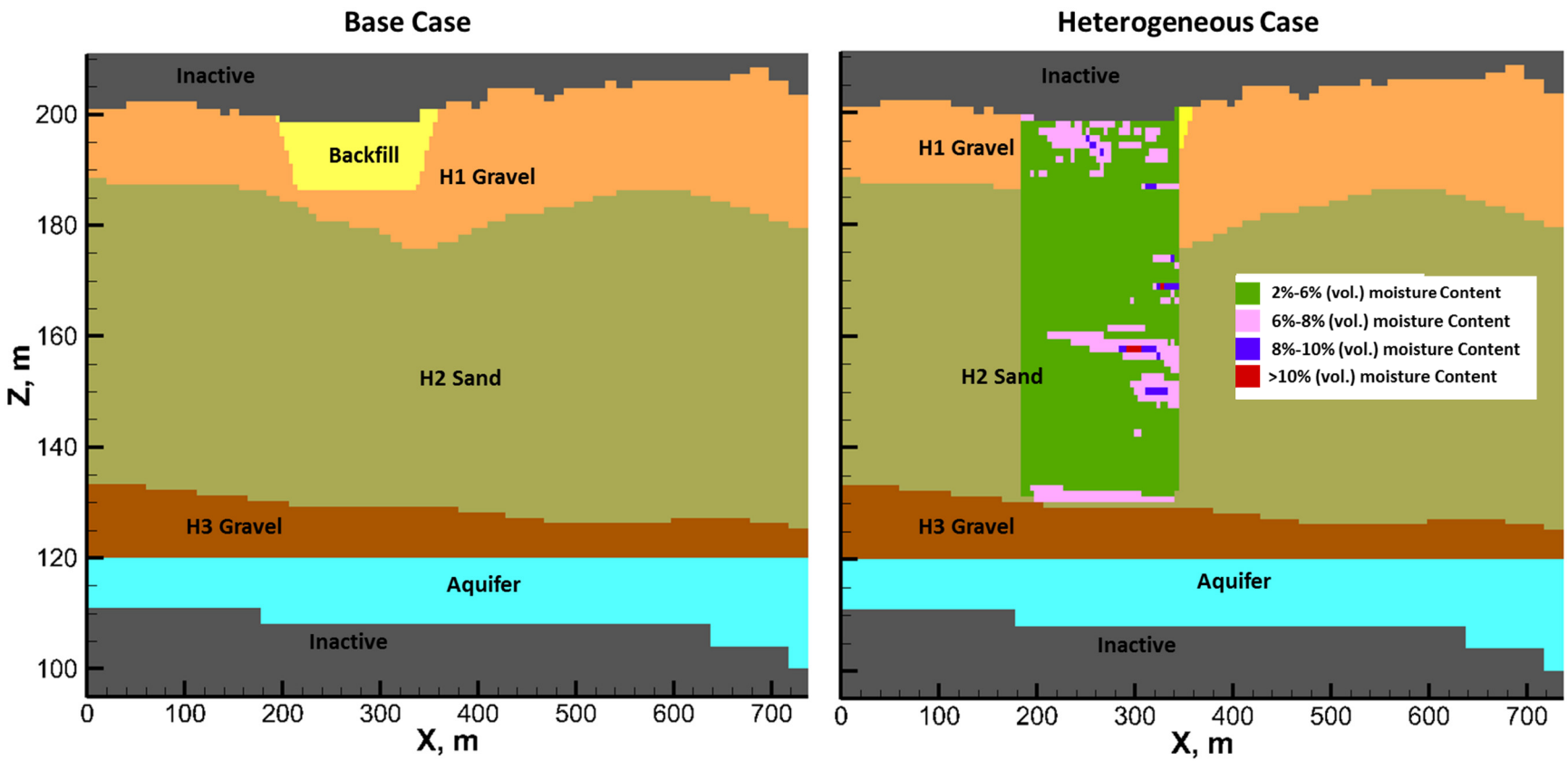

Figure F-8. View along Cross Section 2 (North to South) Shown in Figure F-6.

The left hand figure has the original 5 rock/soil zones (hydrostratigraphic units) while the right hand figure has 4 additional rock/soil zones to incorporate the moisture content bands-based heterogeneity within the krigged area shown in Figure F-6.

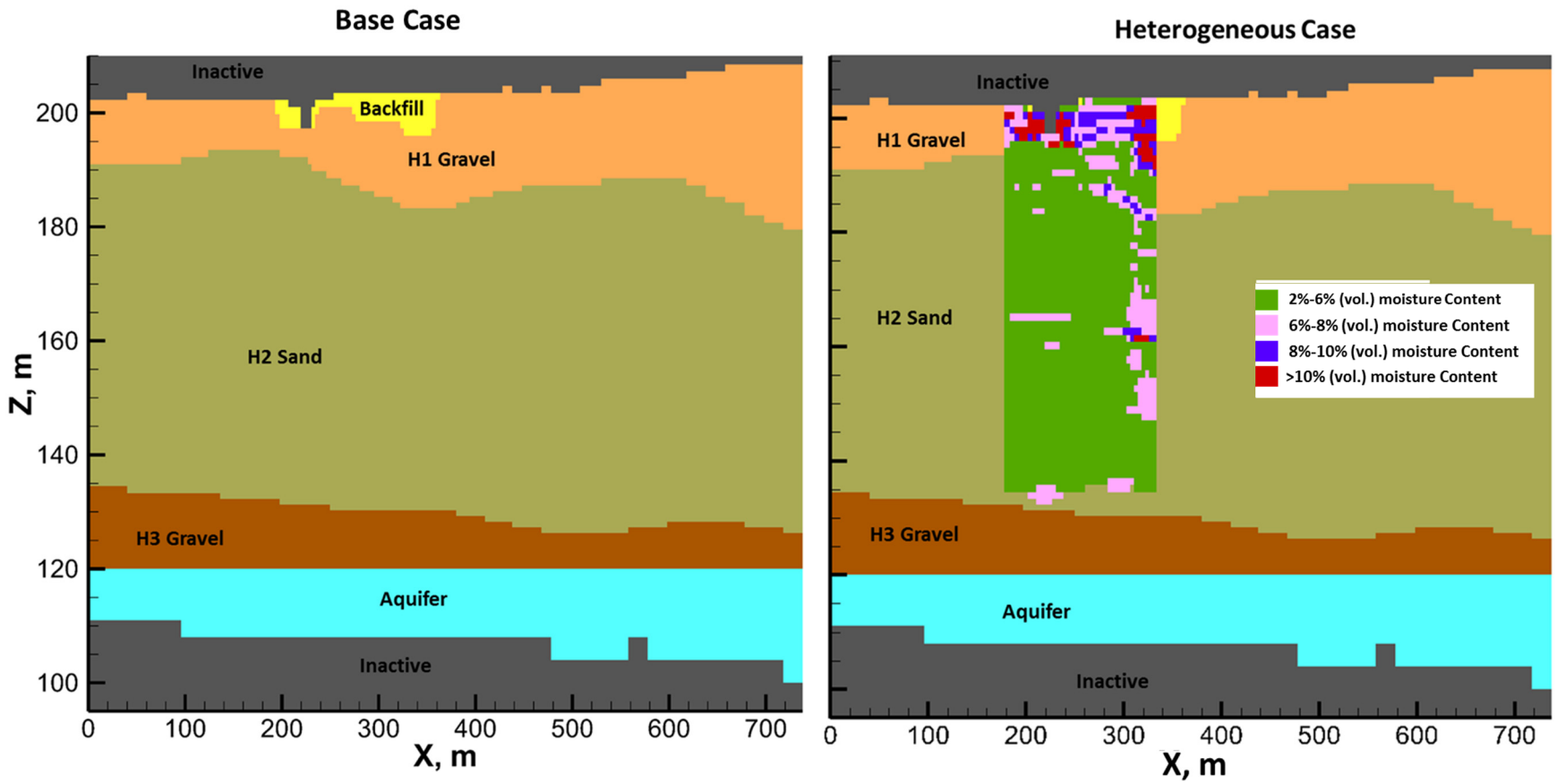

Figure F-9. View along Cross Section 3 (West to East) Shown in Figure F-6.

The left hand figure has the original 5 rock/soil zones (hydrostratigraphic units) while the right hand figure has 4 additional rock/soil zones to incorporate the moisture content bands-based heterogeneity within the krigged area shown in Figure F-6.

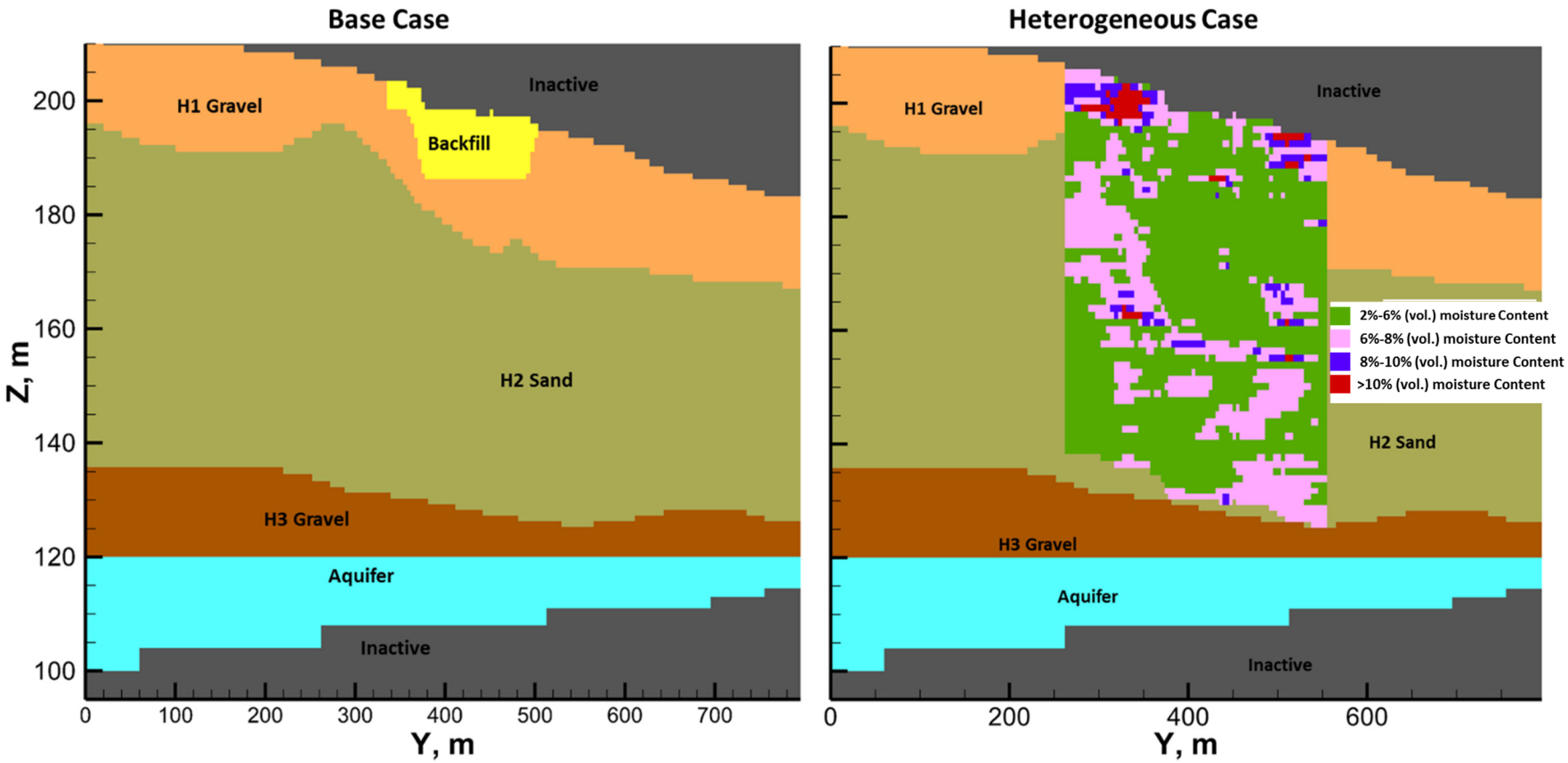

Table F-1. Vadose Zone Hydraulic Properties for Waste Management Area C Hydrostratigraphic Units (Appendix B).

Hydrostratigraphic Unit	θ_s	θ_r	α (1/cm)	n	ℓ	Fitted K_s (cm/s)
Backfill Gravelly Unit	0.138	0.010	0.021	1.374	0.5	5.60E-04
H1 and H3 Gravelly Units	0.171	0.011	0.036	1.491	0.5	7.70E-04
H2 Sand-Dominated Unit	0.315	0.039	0.063	2.047	0.5	4.15E-03

θs = Saturated water content
θr = Residual water content
α = van Genuchten alpha
n = van Genuchten n
ℓ = Pore size connectivity factor
K_s = Saturated Conductivity

F.3 RESULTS

The STOMP© modeling results are presented in this section for the base case and the heterogeneous case. Comparisons are made for simulated moisture contents and contaminant breakthrough curves.

F.3.1 Moisture Content Prediction

The simulated moisture content values from the STOMP© models were compared to the observed moisture profiles from two wells (C4297 and 299-E27-22). Moisture content data at boreholes C4297 (located near tank 241-C-105) and 299-E27-22 (outside the tank) were obtained from PNNL-15503. The borehole C4297 is in close proximity to cross section 1 (Figure F-13). Figure F-14 shows a comparison of simulated steady-state moisture contents from the cross section 1 model and measured moisture profile for borehole C4297, and Figure F-15 does the same for well 299-E27-22. As indicated, for a recharge of 3.5 mm/yr, the simulated moisture content profile (blue line) for cross section 1 compares well with the measurements (black circles) for both the base case (EHM approximation) and the heterogeneous case. In the heterogeneous case, the model simulation also shows higher moisture contents observed at depth.

F.3.2 Matric Potential Measurements

Table F-3 summarizes the average moisture content and the average filter paper-based matric potential measurements for the two borehole samples C4297 (near tank 241-C-105) and 299-E27-22 (Figure F-13), and the model-predicted average moisture content and matric potential values for both cases. As indicated, the simulated steady-state moisture contents (0.06) for the Hanford H2 unit compare well with field-measured moisture contents for both the cases (Table F-3). However, when compared to the model results, the simulated matric potentials for the Hanford H2 unit were much smaller in magnitude (~ -150 cm) for both cases. The base case results in a smoothing of the model estimates. By contrast, the filter paper-based soil matric potentials are point measurements, and are not consistent with the smoothing resulting from the use of averaged upscaled or effective properties for the large grid blocks used in PA simulations. Therefore, the variability of filter paper-based point measurements is inherently larger compared to that based on PA simulations using homogenized upscaled properties. In addition, the error

bar for filter paper measurements is rather large (0.1 to 0.2 MPa or ~1,000 to ~2,000 cm). Similar arguments are applicable to the heterogeneous case. Soil moisture measurements are typically more accurate than matric potential measurements, and the matric potential variability is typically larger than the soil moisture variability. Nonetheless, the overall characterization data are consistent with the relatively dry moisture regime predicted by the PA simulations. The deviation in soil matric potential values is due to a mismatch between the modeling scale and the measurement scale.

F.3.3 Calculation of Technetium-99 Concentration

The breakthrough curves of ^{99}Tc for both cases for three different cross-section models are presented in Figure F-16, Figure F-17, and Figure F-18.

Table F-4 summarizes all the ^{99}Tc transport model results for all the cases. In all three cross-sectional models, the base case shows a higher peak concentration than the heterogeneous model. In cross section 3, the heterogeneous case shows a much lower concentration than the base case because the contrast is greater: there is more heterogeneity than in the other cross sections.

Peak concentrations for the heterogeneous model and the base case are very similar, with the heterogeneities leading to a smearing of the contaminant plume, resulting in a slightly lower peak concentration than the base case. The good agreement between the two models supports the use of the base case model for the post-closure evaluation of releases of residuals.

F.4 CONCLUSIONS

The following summarizes the conclusions of the alternative heterogeneous conceptual model:

- Calculated moisture contents are in very good agreement with field measurements for both the base case and the heterogeneous case.

- The peak concentrations are in good agreement between the two models, with the peak for the heterogeneous cases slightly lower than the base cases. These results support the use of the EHM modeling approach for the post-closure period when the flow is in equilibrium with natural recharge.

Figure F-10. Moisture Retention Curves and Unsaturated Hydraulic Conductivity Curves for the 44 Integrated Disposal Facility Samples.

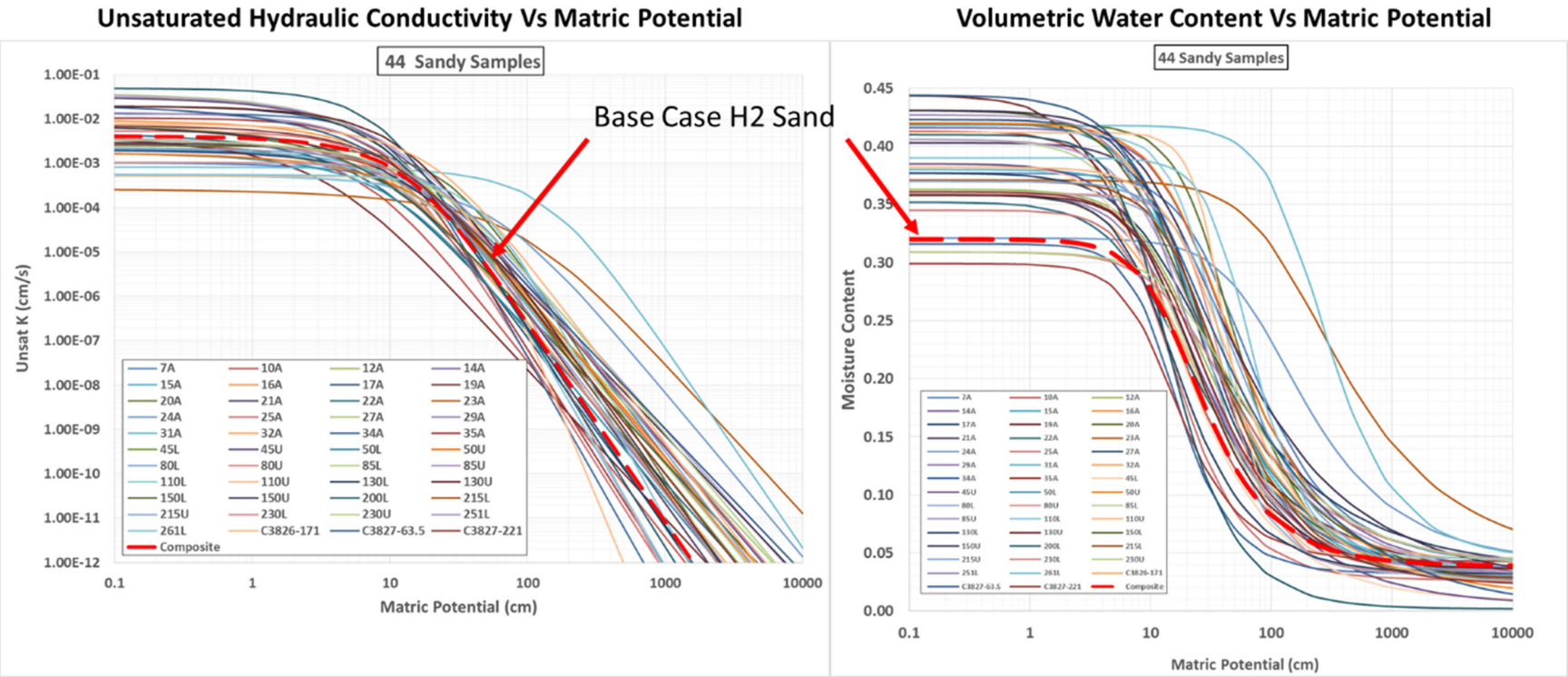

Figure F-11. Moisture Retention Curves and Unsaturated Hydraulic Conductivity Curves for the Four New Units.

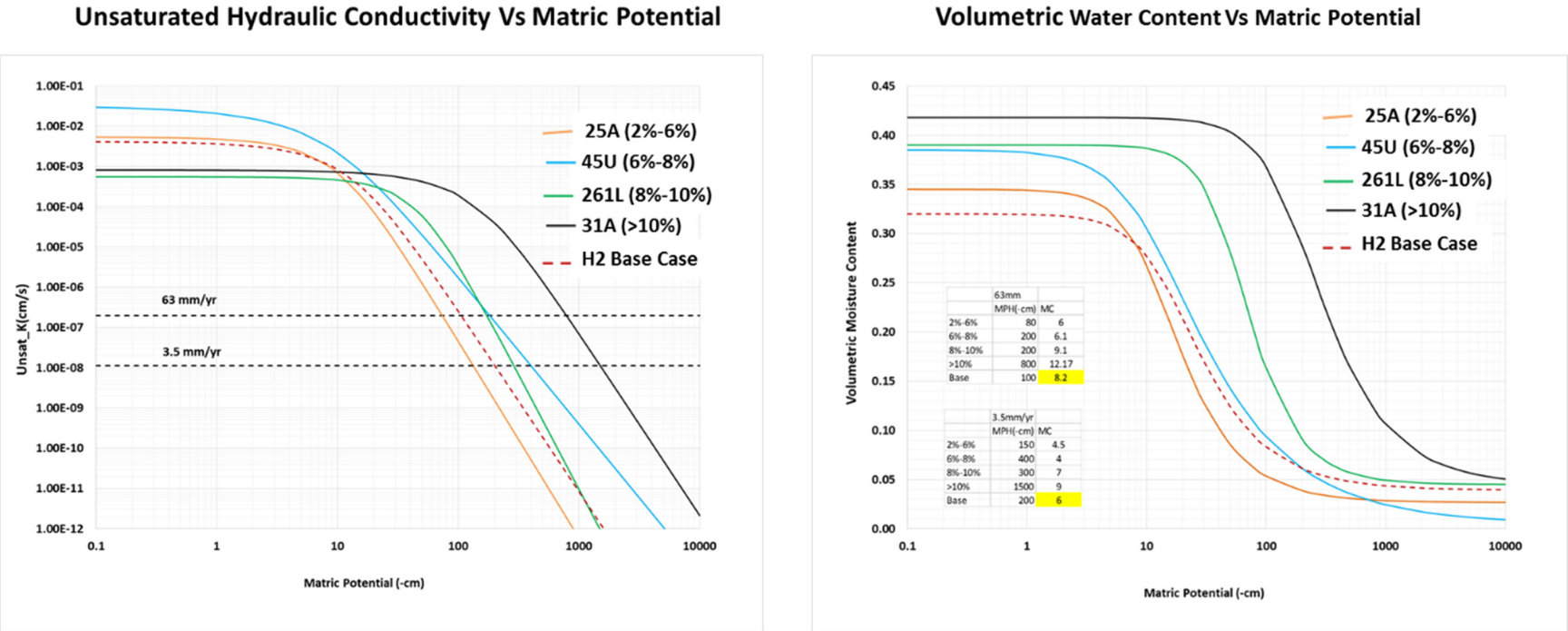

Table F-2. Summary of Vadose Zone Hydraulic Properties for the New Units (Appendix B).

Samples (Moisture Content zones)	θ_s	θ_r	α (1/cm)	n	ℓ	Fitted K_s (cm/s)
25A (2%-6%)	0.345	0.0267	0.0842	2.158	0.5	5.40E-03
45U (6%-8%)	0.385	0.0050	0.0880	1.664	0.5	3.24E-02
261L (8%-10%)	0.390	0.0450	0.0191	2.485	0.5	5.54E-04
31A (>10%)	0.418	0.0444	0.0058	2.012	0.5	8.21E-04

Figure F-12. Location of Contaminant Source and Point of Calculation.

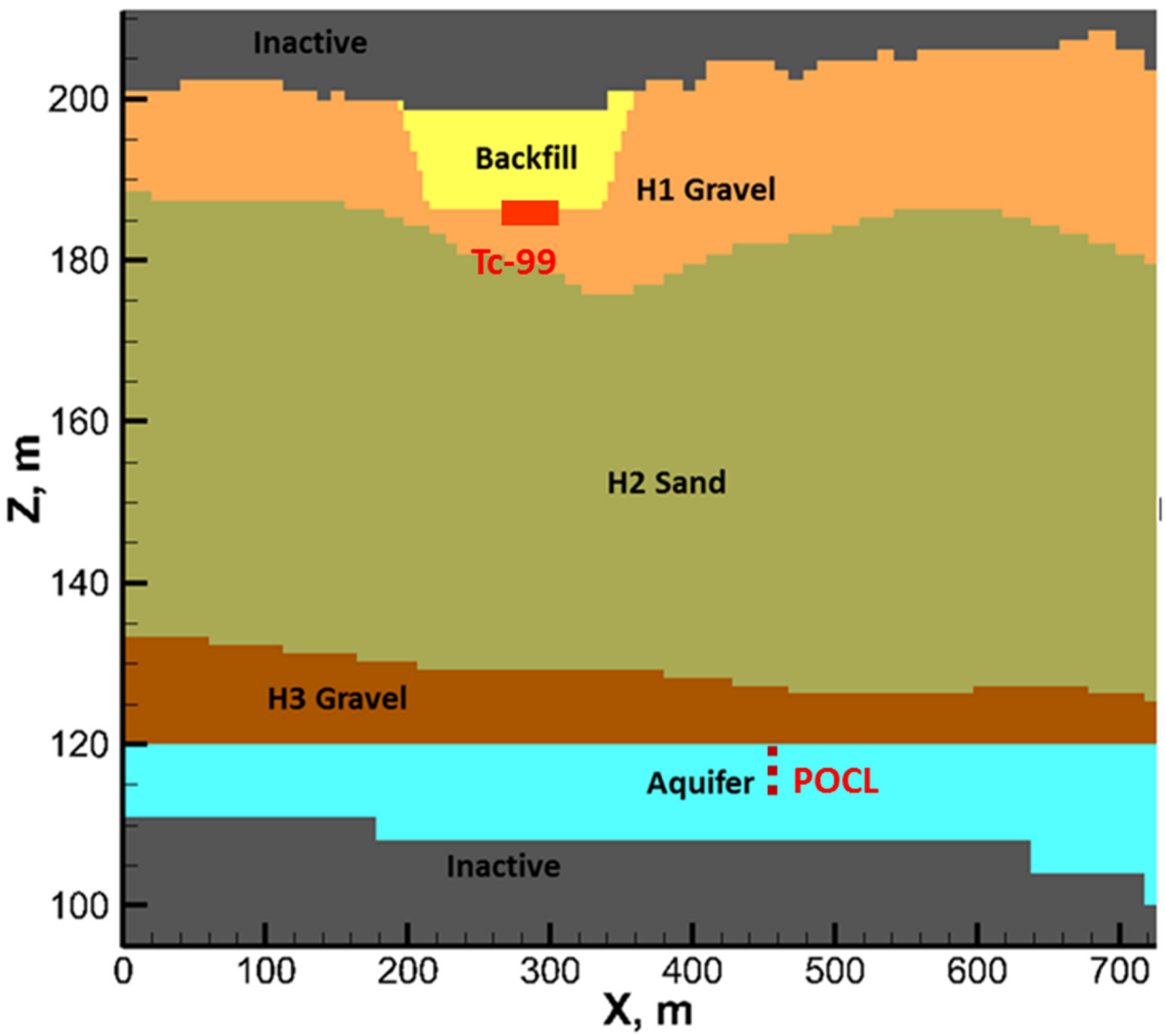

Figure F-13. Location of Well C4297 and 299-E27-22 Relative to Cross Section 1.

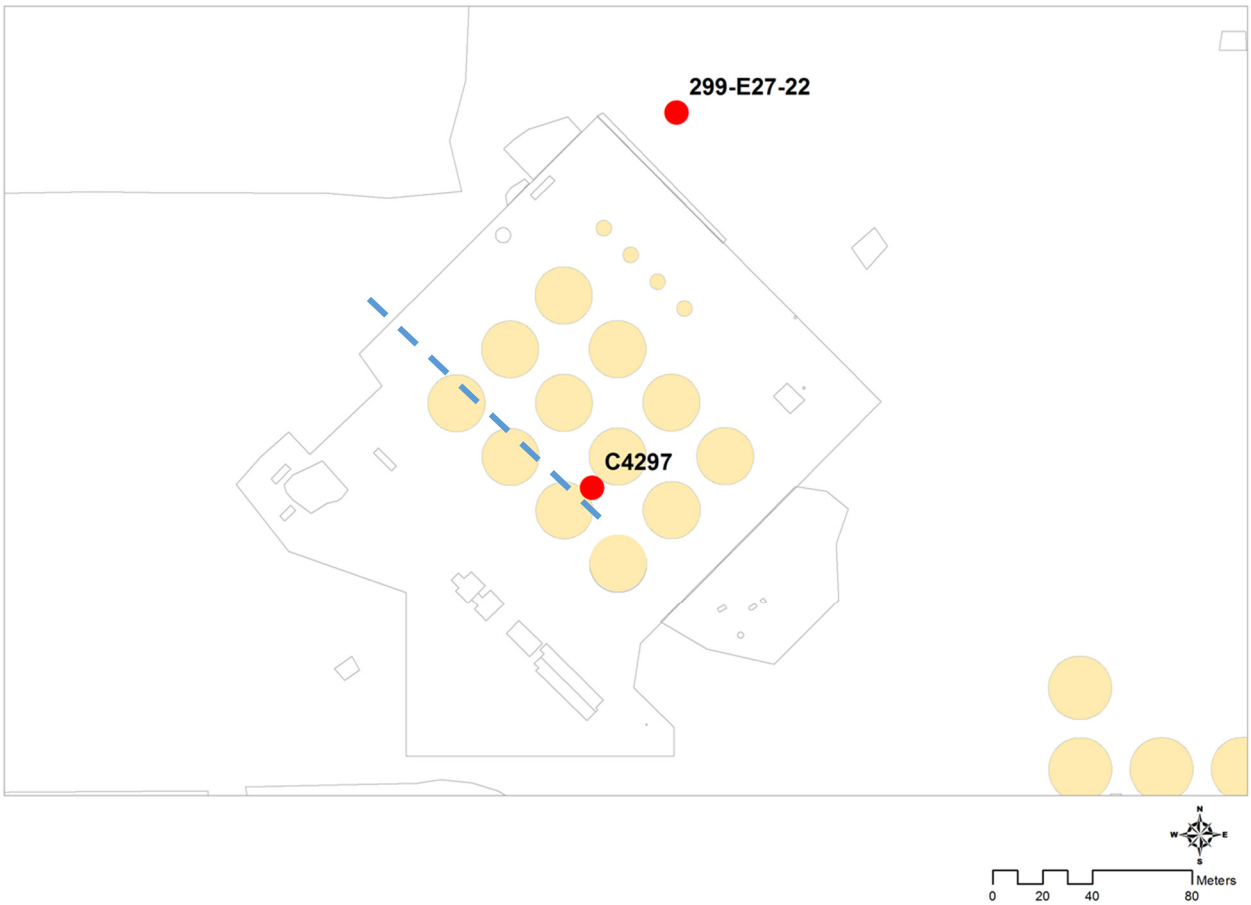

Figure F-14. Comparison of Measured (C4297) and Simulated Moisture Contents for (a) Base Case (Equivalent Homogeneous Medium) Model, and (b) Heterogeneous Model for Cross Section 1.

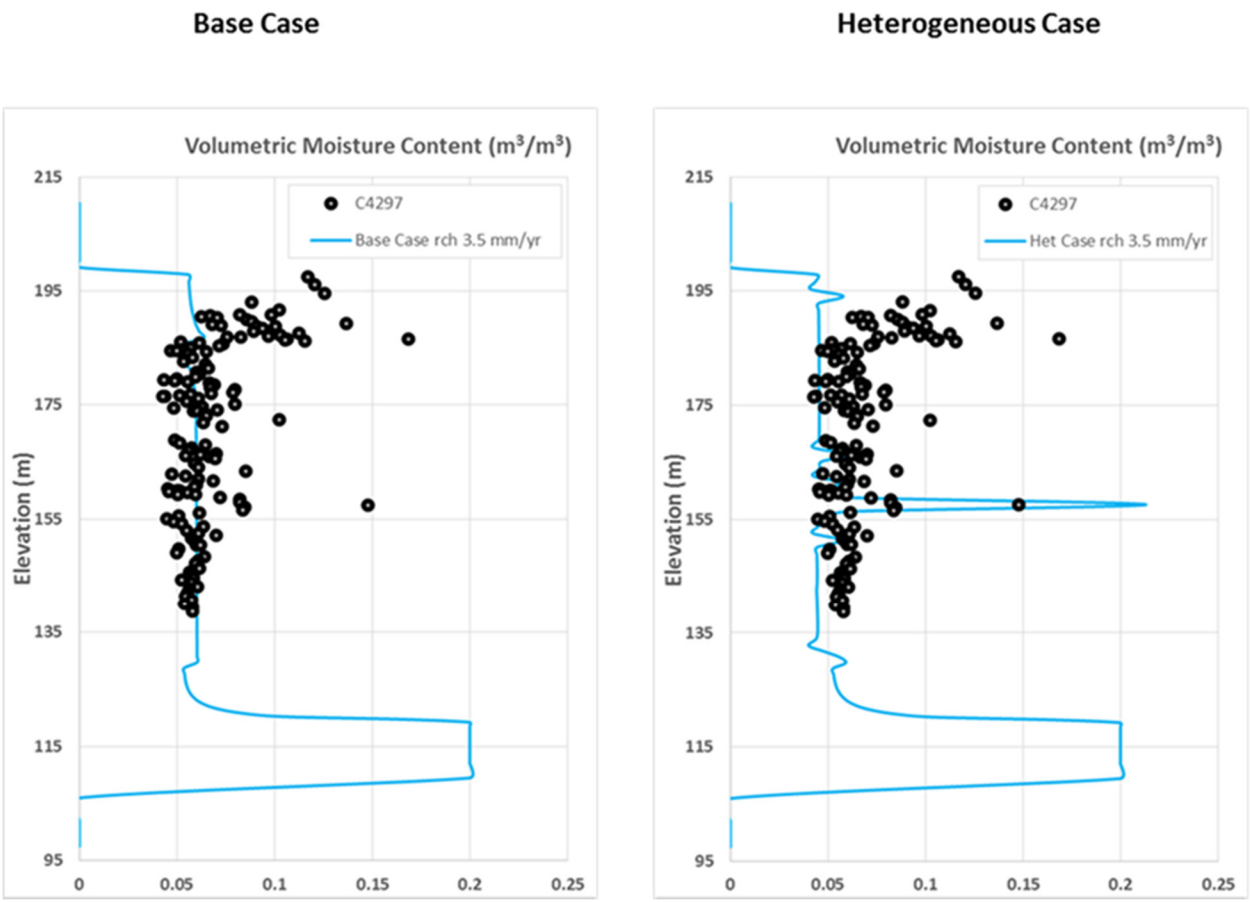

(a) (b)

Figure F-15. Comparison of Measured (299-E27-22) and Simulated Moisture Contents for (a) Base Case (Equivalent Homogeneous Medium) Model, and (b) Heterogeneous Model for Cross Section 1.

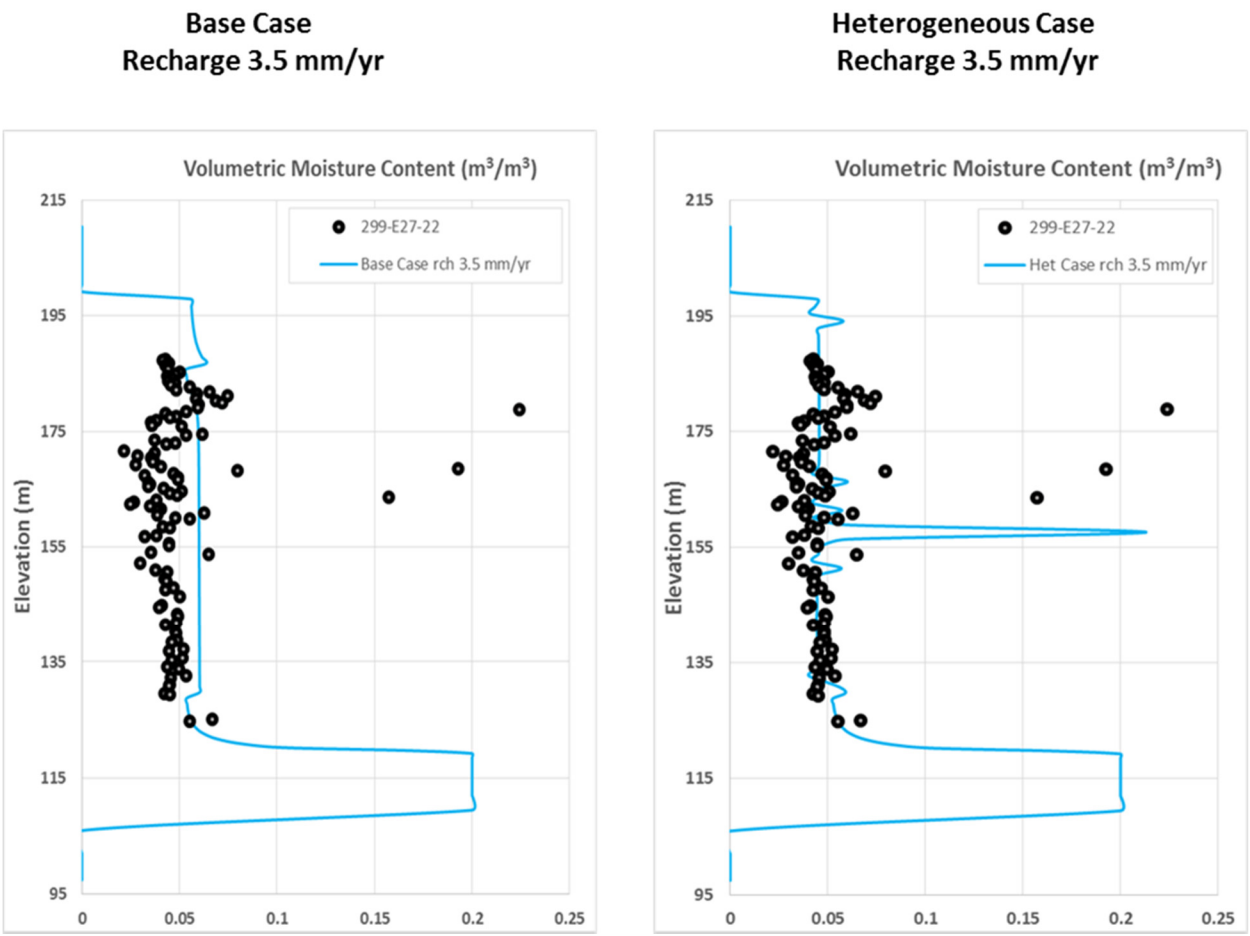

(a) (b)

Table F-3. Average Moisture and Matric Potentials for Borehole Samples Inside and Outside of Waste Management Area C.

Borehole	C4297 (inside tank farm)	299-E27-22 (outside tank farm)
Mean moisture content *	0.060	0.046
Mean matric potential (-cm)	498.45	1,616.43

*Gravimetric data were converted to volumetric moisture content using an assumed sediment bulk density of 1.7 g cm^{-3}.

Source: PNNL-15503, "Characterization of Vadose Zone Sediments Below the C Tank Farm: Borehole C4297 and RCRA Borehole 299-E27-22."

Figure F-16. Technetium-99 Breakthrough Curves for Cross Section 1.

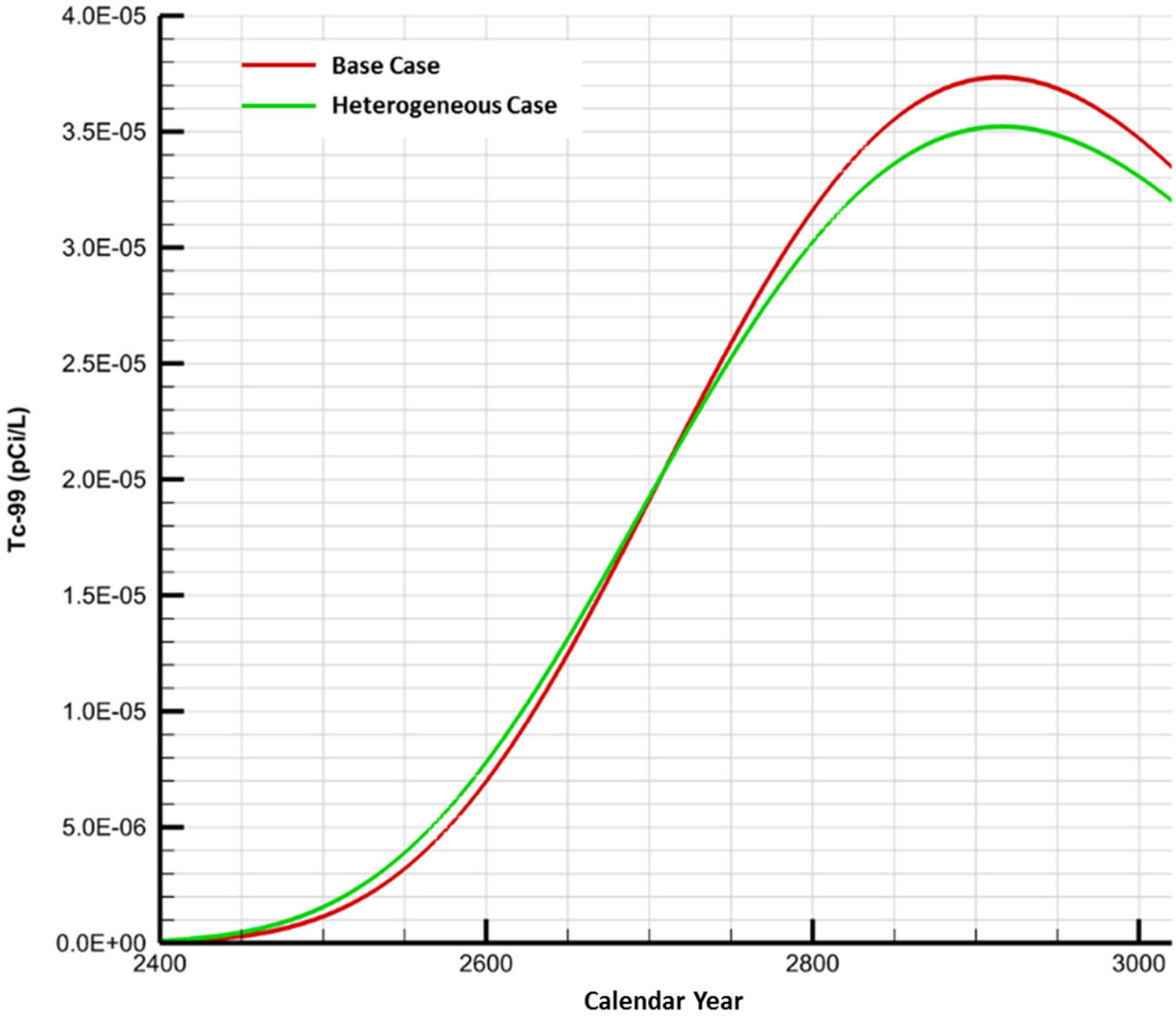

Figure F-17. Technetium-99 Breakthrough Curves for Cross Section 2.

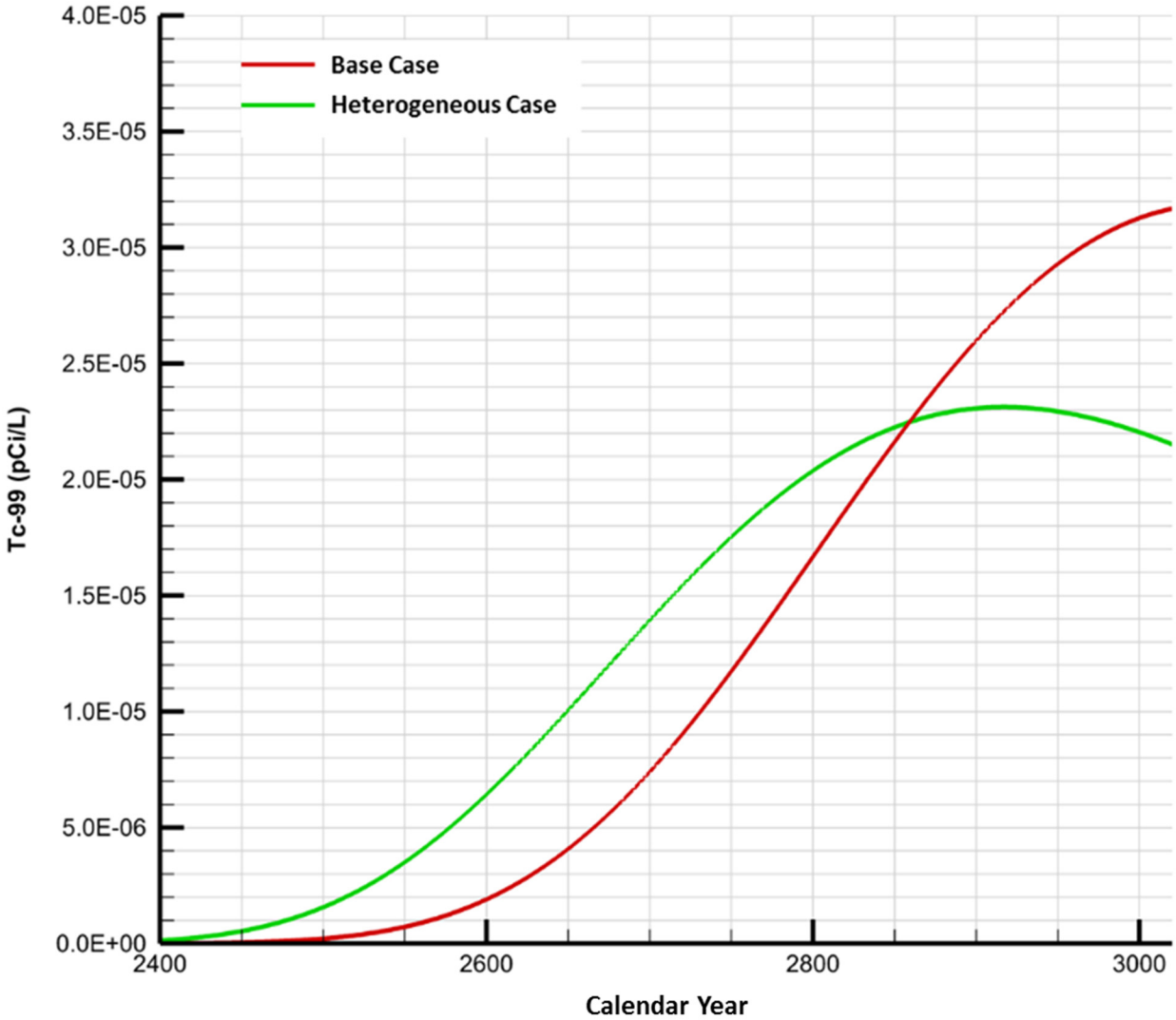

Figure F-18. Technetium-99 Breakthrough Curves for Cross Section 3.

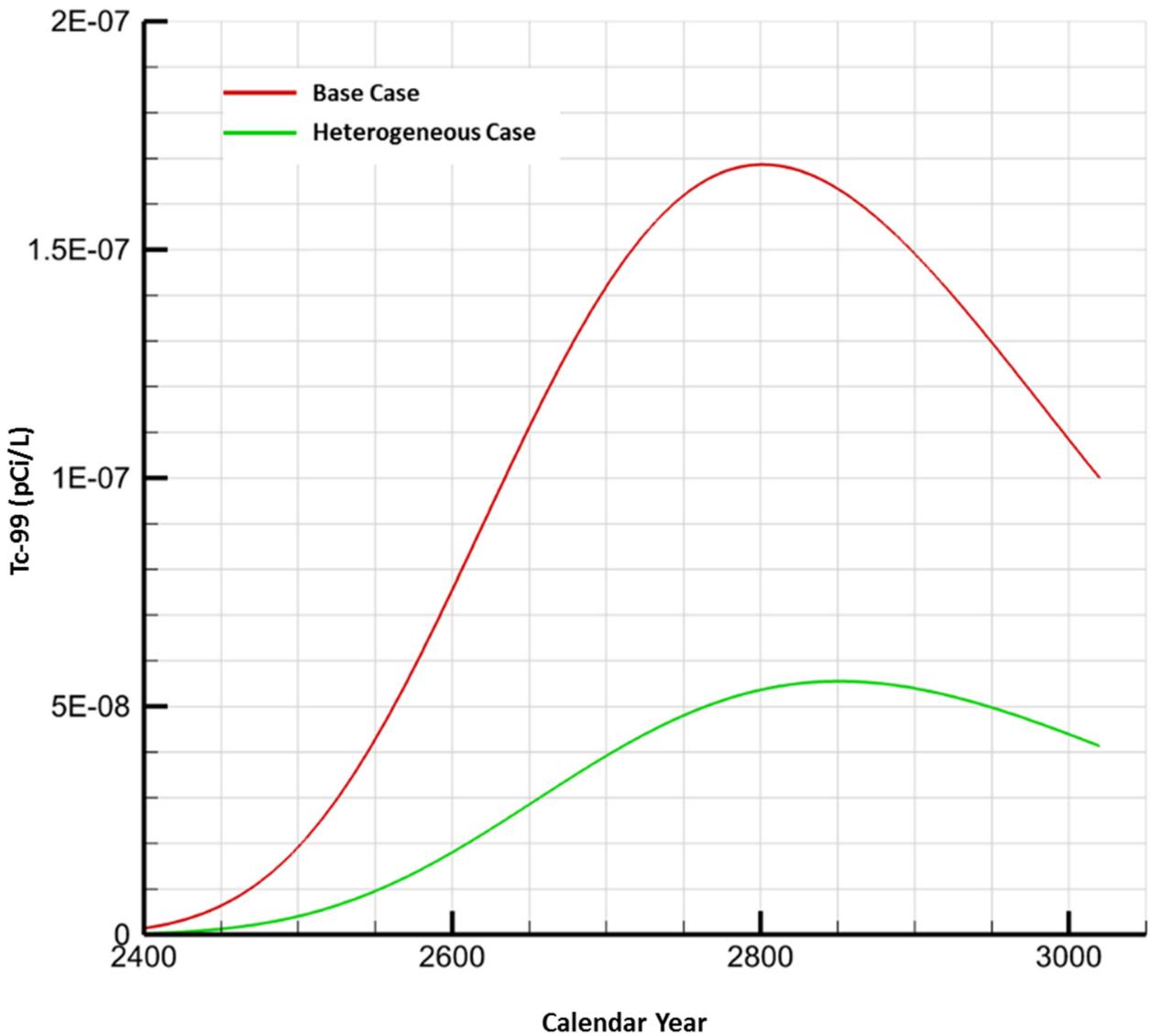

Table F-4. Summary of Technetium-99 Transport Model Results.

Cross Section	Time of Breakthrough (Calendar Year)		Time of Peak (Calendar Year)		Peak Concentration (pCi/L)	
	Base Case	Heterogeneous Case	Base Case	Heterogeneous Case	Base Case	Heterogeneous Case
1	2226	2210	2916	2916	3.73E-05	3.52E-5
2	2253	2205	>3000	2918	>3.16E-5	2.31E-5
3	2212	2232	2798	2843	1.69E-7	5.44E-8

F.5 REFERENCES

NOAA Manual NOS NGS 5, 1990, "State Plane Coordinate System of 1983," National Geodetic Survey, U.S. Department of Commerce, National Oceanic and Atmospheric Administration, Rockville, Maryland.

PNNL-15503, 2008, "Characterization of Vadose Zone Sediments Below the C Tank Farm: Borehole C4297 and RCRA Borehole 299-E27-22," Rev. 1, Pacific Northwest National Laboratory, Richland, Washington.

Resource Conservation and Recovery Act of 1976, 42 USC 6901, et seq.

RPP-CALC-60345, 2016, "Heterogeneous Media Model for Waste Management Area C Performance Assessment," Rev. 0, Washington River Protection Solutions, LLC, Richland, Washington.

RPP-CALC-60448, 2016, "WMA C Performance Assessment Contaminant Fate and Transport Model to Evaluate Impacts to Groundwater," Rev. 0, Washington River Protection Solutions, LLC, Richland, Washington.

Ye, M., R. Khaleel, T. J. Yeh, 2005, "Stochastic analysis of moisture plume dynamics of a field injection experiment," Water Resources Research, Vol. 41, W03013.

This page intentionally left blank.

APPENDIX G

COMPARISON OF SELECTED MODEL RESULTS FOR ALTERNATIVE 2B FROM THE TANK CLOSURE AND WASTE MANAGEMENT ENVIRONMENTAL IMPACT STATEMENT FOR WASTE MANAGEMENT AREA C WITH EQUIVALENT RESULTS USING THE WASTE MANAGEMENT AREA C PERFORMANCE ASSESSMENT BASE CASE MODEL

This page intentionally left blank.

TABLE OF CONTENTS

APPENDIX G – COMPARISON OF SELECTED MODEL RESULTS FOR ALTERNATIVE 2B FROM THE TANK CLOSURE AND WASTE MANAGEMENT ENVIRONMENTAL IMPACT STATEMENT FOR WASTE MANAGEMENT AREA C WITH EQUIVALENT RESULTS USING THE WASTE MANAGEMENT AREA C PERFORMANCE ASSESSMENT BASE CASE MODEL G-1

G.1 GENERAL DESCRIPTION OF ALTERNATIVE 2B RESULTS USING THE 2012 TANK CLOSURE AND WASTE MANAGEMENT ENVIRONMENTAL IMPACT STATEMENT MODEL FOR WASTE MANAGEMENT AREA C G-1

G.2 GENERAL APPROACH FOR COMPARISON OF THE ALTERNATIVE 2B RESULTS USING PERFORMANCE ASSESSMENT AND THE 2012 TANK CLOSURE AND WASTE MANAGEMENT ENVIRONMENTAL IMPACT STATEMENT MODELS OF WASTE MANAGEMENT AREA C G-2

G.3 COMPARISONS OF MODEL INPUTS FOR 2012 TANK CLOSURE AND WASTE MANAGEMENT ENVIRONMENTAL IMPACT STATEMENT AND PERFORMANCE ASSESSMENT MODELS OF WASTE MANAGEMENT AREA C G-5

G3.1 Inventory Estimates G-5

G3.2 Inventory Release Rates G-5

G3.3 Recharge G-6

G3.4 Hydrogeologic Framework and Hydrologic Properties G-7

G3.5 Partitioning Coefficients and Dispersivity G-9

G.4 COMPARISON OF SELECTED RESULTS FOR ALTERNATIVE 2B USING THE PERFORMANCE ASSESSMENT AND TANK CLOSURE AND WASTE MANAGEMENT ENVIRONMENTAL IMPACT STATEMENT MODELS OF WASTE MANAGEMENT AREA C 9

G.5 REFERENCES 12

LIST OF FIGURES

Figure G-1. Lines of Analysis in the Tank Closure and Waste Management Environmental Impact Statement. G-3

Figure-G-2. STOMP© Model Horizontal Grid Distribution Showing the Source Area for the Waste Management Area C Tank Residual Component of the Tank Closure and Waste Management Environmental Impact Statement. G-6

Figure G-3. Time Series of Net Infiltration Tank Closure and Waste Management Environmental Impact Statement. G-8

Figure G-4. Waste Management Area C Vadose Zone Stratigraphy as Depicted in the Tank Closure and Waste Management Environmental Impact Statement. G-8

Figure G-5. Tank Closure and Waste Management Environmental Impact Statement Analysis of Iodine-129 Flux from the Vadose Zone into the Aquifer for Alternative 2b (Baseline) and Three Flux Reduction Sensitivity Cases. G-10

Figure G-6. Waste Management Area C Performance Assessment Analysis of Tank Closure and Waste Management Environmental Impact Statement Alternative 2b Model of Iodine-129 Flux from the Vadose Zone into the Aquifer. G-11

LIST OF TABLES

Table G-1. Peak Constituent of Potential Concern Concentrations (pCi/L) and Time of Occurrence (Calendar Year) at the A Barrier Calculated in the Environmental Impact Statement Associated with All Tank Residuals and Ancillary Equipment. G-4

Table G-2. Summary of Rates of Release for Iodine-129. ..... G-7

LIST OF TERMS

PA	performance assessment
STOMP	Subsurface Transport Over Multiple Phases (computer code)
TC&WM EIS	Tank Closure and Waste Management Environmental Impact Statement
WMA	Waste Management Area

APPENDIX G

COMPARISON OF SELECTED MODEL RESULTS FOR ALTERNATIVE 2B FROM THE TANK CLOSURE AND WASTE MANAGEMENT ENVIRONMENTAL IMPACT STATEMENT FOR WASTE MANAGEMENT AREA C WITH EQUIVALENT RESULTS USING THE WASTE MANAGEMENT AREA C PERFORMANCE ASSESSMENT BASE CASE MODEL

The purpose of this appendix is to compare, to the extent possible, the model developed for the Waste Management Area (WMA) C performance assessment (PA) to results from DOE/EIS-0391, "Final Tank Closure and Waste Management Environmental Impact Statement for the Hanford Site, Richland, Washington" (TC&WM EIS). The intent is to show the similarities and differences between the models, and to demonstrate that both models are appropriate for their intended purposes. The extent to which the two models can be directly compared is limited, given the different modeling objectives, spatial scales and levels of detail in the treatment of the engineered barrier system. However, a comparison provides perspectives on interpreting modeling results within the context of the modeling objectives.

G.1 GENERAL DESCRIPTION OF ALTERNATIVE 2B RESULTS USING THE 2012 TANK CLOSURE AND WASTE MANAGEMENT ENVIRONMENTAL IMPACT STATEMENT MODEL FOR WASTE MANAGEMENT AREA C

The analysis in the TC&WM EIS supports U.S. Department of Energy decisions regarding proposed actions to retrieve, treat, and dispose of tank waste; decommission the Fast Flux Test Facility; and expand waste disposal capacity at Hanford. The TC&WM EIS evaluates the potential sitewide cumulative environmental impacts and cost consequences associated with 11 proposed alternatives for tank closure, including the preferred alternative to retrieve at least 99% of the tank waste and institute landfill closure of the single-shell tank farms. The TC&WM EIS describes groundwater impacts in terms of the concentrations of ^{129}I, ^{99}Tc, chromium, nitrate, ^{3}H (tritium), ^{238}U, and total uranium at prescribed polygonal "lines of interest" or "barriers," including one that surrounds WMA C and WMA A-AX. The results at a line of interest or barrier represent the outcome of vadose zone model results evaluated using Subsurface Transport Over Multiple Phases (STOMP)©[1] (Appendix N of DOE/EIS-0391) input to a groundwater flow field developed in MODFLOW[2] (Appendix L of DOE/EIS-0391), with concentration calculated using a proprietary particle-tracking code (Appendix O of DOE/EIS-0391).

The TC&WM EIS evaluated a local-scale vadose zone-only model representing WMA C, and used the vadose zone releases from this model as a source to a regional groundwater model to estimate the impacts of residual wastes and past releases originating in WMA C at specific points for analysis. However, the groundwater impact results reported in Appendix O of DOE/EIS-0391 do not distinguish between the impacts caused by the residual wastes, past leaks, and releases in WMA C from those originating in other tank farms in the A Complex of the

[1] Subsurface Transport Over Multiple Phases (STOMP)© is copyrighted by Battelle Memorial Institute, 1996.
[2] MODFLOW software has been developed and distributed by the U.S. Geological Survey, Washington, D.C.

200 East Area. In addition, the point of analyses in the TC&WM EIS groundwater impact analysis are not coincident with the 100 meter point of calculation prescribed by DOE M 435.1-1, Radioactive Waste Management Manual. Instead, the TC&WM EIS reported cumulative results from facilities at a number of polygonal "lines of analysis" that are shown in Figure G-1. The line of analysis most relevant to WMA C is the "A Barrier," at which the cumulative contributions and impacts from tank farm residual waste and past leaks from WMAs C, A, and AX, and other nearby double-shell tank farm facilities are evaluated in groundwater. The WMA C PA provides concentration-based results along a hypothetical line of analysis located 100 m downgradient of the WMA C fenceline. The line of analysis is divided into nine segments to account for the spatial distribution of the impacts along the line of analysis resulting from the spatial distribution of sources within WMA C. The results for each segment distinguish between the impacts caused by residuals from the different tanks and ancillary equipment, including pipelines within WMA C, and integrate the individual results into a composite concentration.

Therefore, while the "A Barrier" results are not directly comparable to the PA model results, they still provide the best available comparison point between the analyses, and are summarized here (Table G-1). According to the groundwater transport analysis results of Preferred Alternative 2B at A Barrier (found in Table O-26 in Appendix O of DOE/EIS-0391), the peak concentrations of radionuclides ^{99}Tc and ^{129}I at A Barrier related to tank residuals are 160 pCi/L and 0.1 pCi/L, respectively, with the years of peak arrival being 3685 and 3896, respectively. The peak concentrations of chromium and nitrate are 5 µg/L and 536 µg/L, respectively, with the years of peak arrival being 3451 and 3614, respectively. The peak concentrations of radionuclides ^{99}Tc and ^{129}I related to ancillary equipment at A Barrier are 31 pCi/L and 0.1 pCi/L, respectively, with the years of peak arrival being 3610 and 3694, respectively. The peak concentrations of chromium and nitrate are 1 µg/L and 183 µg/L, respectively, with the years of peak arrival being 3647 and 3606, respectively (Table O-22 in Appendix O of DOE/EIS-0391).

G.2 GENERAL APPROACH FOR COMPARISON OF THE ALTERNATIVE 2B RESULTS USING PERFORMANCE ASSESSMENT AND THE 2012 TANK CLOSURE AND WASTE MANAGEMENT ENVIRONMENTAL IMPACT STATEMENT MODELS OF WASTE MANAGEMENT AREA C

To compare the WMA C PA and TC&WM EIS models for consistency, it was necessary to modify the base case results to provide a common technical basis between the two models. The tank residual waste inventory, residual waste release functions, and spatial and temporal recharge from the small-scale TC&WM EIS WMA C vadose zone-only model were introduced into the WMA C PA vadose zone-groundwater model.

As a metric for comparisons, Appendix U of DOE/EIS-0391 includes a figure that shows the modeling results for Alternative 2B for the ^{129}I radionuclide fluxes exiting the vadose zone. The results from this plot are compared against similar results using similar source term and assumption for Alternative 2B using the PA model of WMA C. To facilitate this comparison, the tank residual waste inventory, residual waste release functions, and spatial and temporal

recharge from the small-scale TC&WM EIS WMA C vadose zone-only model were introduced into the WMA C PA vadose zone-groundwater model.

Figure G-1. Lines of Analysis in the Tank Closure and Waste Management Environmental Impact Statement.

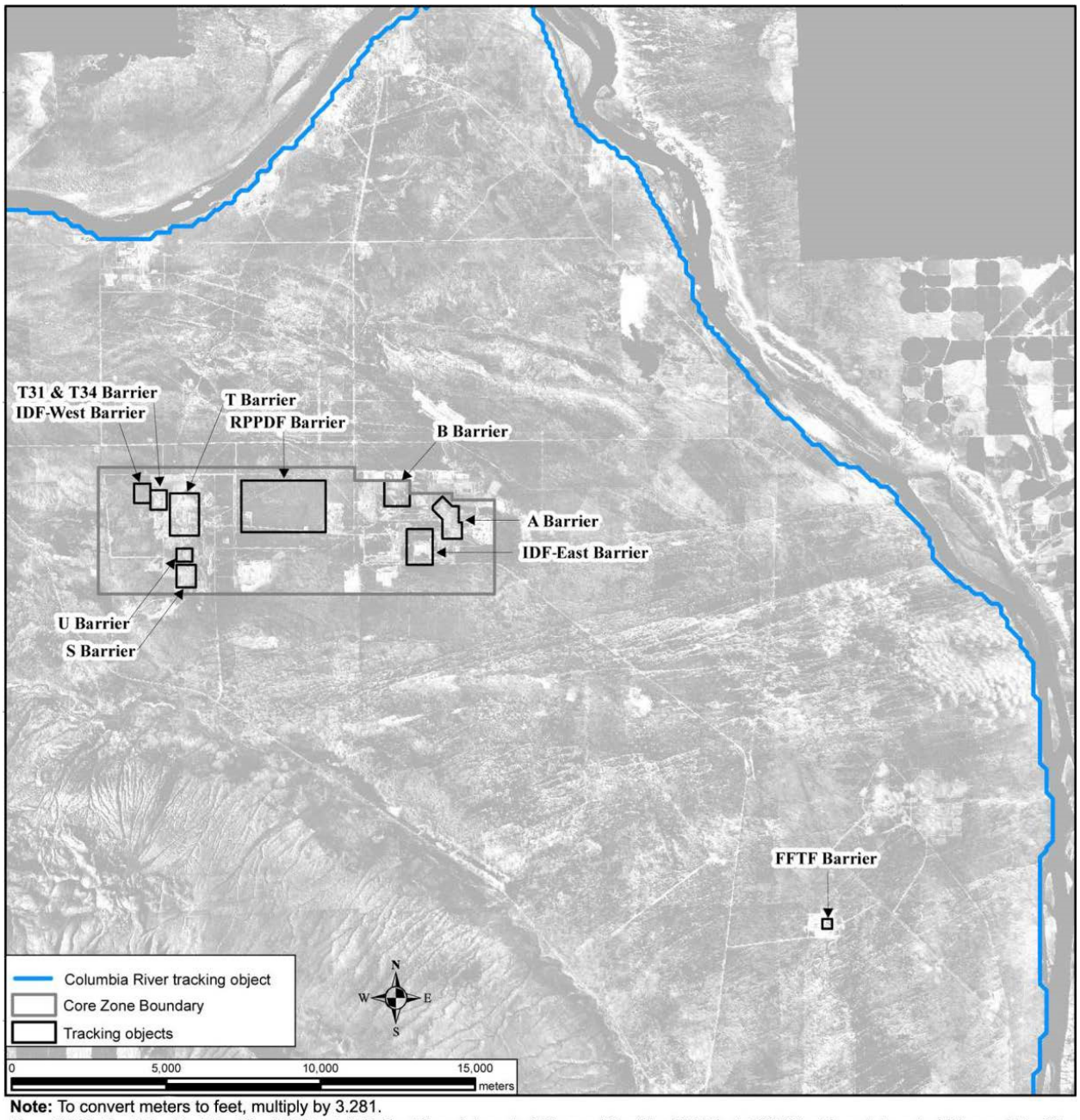

Note: To convert meters to feet, multiply by 3.281.
Key: FFTF=Fast Flux Test Facility; IDF-East=200-East Area Integrated Disposal Facility; IDF-West=200-West Area Integrated Disposal Facility; RPPDF=River Protection Project Disposal Facility; T31 & T34=trenches 31 and 34.

Excerpted from DOE/EIS-0391, "Final Tank Closure and Waste Management Environmental Impact Statement for the Hanford Site, Richland, Washington," Appendix O, pp. O-16.

Table G-1. Peak Constituent of Potential Concern Concentrations and Time of Occurrence (Calendar Year) at the A Barrier Calculated in the Environmental Impact Statement Associated with All Tank Residuals and Ancillary Equipment.

Radionuclide	Tank Residuals (Calendar Year Time of Peak)	Ancillary Equipment (Calendar Year Time of Peak)
Tc-99	160 pCi/L (3685)	31 pCi/L (3610)
I-129	0.1 pCi/L (3896)	0.1 pCi/L (3694)
Contaminant		
Cr	5 µg/L (3451)	1 µg/L (3647)
Nitrate	536 µg/L (3614)	183 µg/L (3606)

Values excerpted from DOE/EIS-0391, "Final Tank Closure and Waste Management Environmental Impact Statement for the Hanford Site, Richland, Washington" Tables O-22 and O-26.

Other elements of the models are similar. As in the WMA C PA, the assumed end state of the tanks evaluated in DOE/EIS-0391 was that the single-shell tank waste system would be filled with grout to immobilize residual waste, prevent long-term degradation of the tanks, and discourage intruder access. The closed tank system would be covered with an engineered modified Resource Conservation and Recovery Act of 1976 Subtitle C barrier with a design life of 500 years. The TC&WM EIS STOMP©-based vadose zone model incorporates a number of elements that are similar in approach to the WMA C PA model:

- Residual waste inventory in tanks and ancillary equipment
- Three-dimensional representation of geology, hydraulic properties, and grid geometry
- Temporal and spatial variability of net infiltration at the ground surface
- Temporal variability of radionuclide and non-radiological contaminant introduction (i.e., source term) at specific horizontal locations and vertical depths
- Water and radionuclide and non-radiological contaminant output fluxes at specified locations (referred to in STOMP© as surfaces)
- Radionuclide and non-radiological contaminant movement through, and exit from the vadose zone.

Unlike the WMA C PA, the TC&WM EIS modeling methodology calculates the following outside of STOMP©:

- Contaminant movement in the groundwater to various calculation points
- Concentrations calculated at a contiguous polygon surrounding WMA C and WMA A-AX in the saturated-zone model (referred to in DOE/EIS-0391 as "A Barrier").

G.3 COMPARISONS OF MODEL INPUTS FOR 2012 TANK CLOSURE AND WASTE MANAGEMENT ENVIRONMENTAL IMPACT STATEMENT AND PERFORMANCE ASSESSMENT MODELS OF WASTE MANAGEMENT AREA C

The primary areas where the models differ internally involve inventory estimates, waste release rates, geological description and hydrological properties, the partitioning coefficients and dispersivity applied to certain radionuclides, and the spatial distribution of recharge rates. The following discussion describes these differences and any adjustments made to the WMA C PA model so that the two model predictions could be compared.

G3.1 Inventory Estimates

DOE/ORP-2003-02, Environmental Impact Statement for Retrieval, Treatment, and Disposal of Tank Waste and Closure of Single-Shell Tanks at the Hanford Site, Richland, WA: Inventory and Source Term Data Package provides the estimated radionuclide inventory present at each tank farm as of December 1, 2002. According to Table M-24 in Appendix M of DOE/EIS-0391, the estimated quantities of ^{129}I under tank closure Alternative 2B are 0.00993 of ^{129}I. The alternatives analysis evaluated impacts from the tank farms as entities, not individual tanks; thus, the tank residual wastes are composited into a single source for the entire tank farm. The TC&WM EIS model represents the residual wastes in the tanks as a uniform concentration distributed across an area that approximately encompasses the 100- and 200-series tanks of the tank farm (Figure G-2). The residual waste inventory estimates have been revised since the issuance of DOE/EIS-0391 because more waste has been retrieved from the tanks, and the new inventory is based on direct measurement of the end state of the retrieval. The WMA C PA includes the updated information.

For the purpose of comparing the two model results for Alternative 2B, the WMA C PA model was modified to run with the TC&WM EIS inventory estimates and an approximation of the TC&WM EIS release area in its evaluation.

G3.2 Inventory Release Rates

DOE/EIS-0391 calculated the release of contaminants from stabilized tank grout using a partitioning-limited, advective-flow release model (Table M-2 of Appendix M of DOE/EIS-0391). In this model, only the rate of water movement through the waste volume, and the partitioning of the contaminant between the solid and liquid phases of the waste volume, control the release of contaminants from the waste form to the vadose zone (Appendix M of DOE/EIS-0391). Contaminant concentrations are assumed to maintain equilibrium between the liquid and solid phases within the pore space of the waste form according to the contaminant's partitioning coefficient in the waste form material. The amount of contaminant mass exiting the waste form is therefore equal to the quantity of liquid exiting from the waste form and the concentration of the contaminant in that liquid.

For the purpose of comparing the two model results of Alternative 2B, the WMA C PA model was run using the TC&WM EIS (2012) release function for ^{129}I in its evaluation. Equations M-1

through M-8 in Appendix M of DOE/EIS-0391 provide the basis for the release models used to develop the release functions for the solid sources. Summarized rates of release for ^{129}I developed according to this model are presented in Table G-2.

Figure-G-2. STOMP© Model Horizontal Grid Distribution Showing the Source Area for the Waste Management Area C Tank Residual Component of the Tank Closure and Waste Management Environmental Impact Statement.

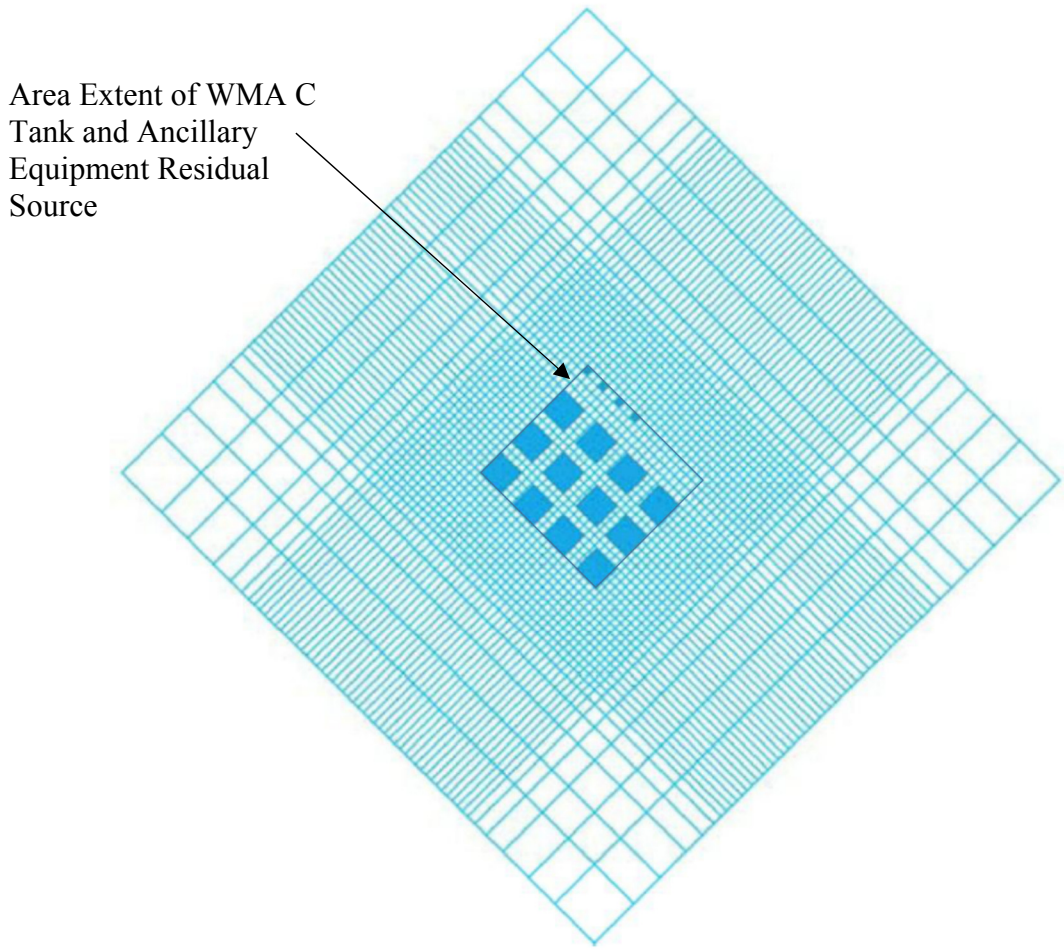

Excerpted and adapted from Figure N-4, Appendix N of DOE/EIS-0391, "Final Tank Closure and Waste Management Environmental Impact Statement for the Hanford Site, Richland, Washington."

Subsurface Transport Over Multiple Phases (STOMP)© is copyrighted by Battelle Memorial Institute, 1996.

WMA = Waste Management Area

G3.3 Recharge

In the TC&WM EIS release model calculations, the quantity of liquid exiting from the waste form is assumed to equal the water infiltrating into it. The water infiltrating into the waste form is assumed to be equal to the net infiltration at the surface, which is subject to change according to the conditions at the surface such as natural vegetation or the presence of an engineered barrier. Figure M-2 in Appendix M of DOE/EIS-0391 displays the time series of net infiltration

rates applicable to tank farms (Figure G-3). For WMA C, the background conditions represent a steady state net infiltration rate of 3.5 mm/yr. The disturbed conditions (100 mm/yr) coincide with the beginning of tank farm operations and the assumed closure of the farm in 2050. The cap conditions follow closure, and last 500 years until the cap becomes degraded and the net infiltration reverts to the background value. The net infiltration applied to surfaces outside the WMA C source area does not change from the background conditions throughout the simulation period.

Table G-2. Summary of Rates of Release for Iodine-129.

Year	I-129 Release Rate (Ci/yr)
2050	4.57E-06
2267	4.09E-06
2510	3.81E-06
2550	2.64E-05
2551	2.46E-05
2592	2.12E-05
2639	1.78E-05
2695	1.44E-05
2764	1.10E-05
2854	7.62E-06
2984	4.15E-06
3223	6.07E-07
4515	0

Values based on Equations M-1 through M-8 in Appendix M of DOE/EIS-0391, "Final Tank Closure and Waste Management Environmental Impact Statement for the Hanford Site, Richland, Washington."

For the purpose of comparing the two models of Alternative 2, the WMA C PA model was run using the TC&WM EIS recharge sequence in its evaluation.

G3.4 Hydrogeologic Framework and Hydrologic Properties

In the TC&WM EIS geologic model, most of the vadose zone consists of units identified as Hanford sand with a layer of Hanford gravel at the bottom and another layer of Hanford gravel existing about two-thirds the depth from the surface to groundwater. Both gravel units vary in thickness, and the shallower sand is not continuous and is not present in the southeastern corner of the model (Figure G-4). The TC&WM EIS geologic model does not account for the presence of the WMA C tanks and ancillary equipment. The volumes associated with those features remain active in the model and unchanged from the natural system. The TC&WM EIS developed hydraulic properties for the Hanford sand and gravel units according to the procedure described in Section N.3.6.1 in Appendix N of DOE/EIS-0391.

Figure G-3. Time Series of Net Infiltration Tank Closure and Waste Management Environmental Impact Statement.

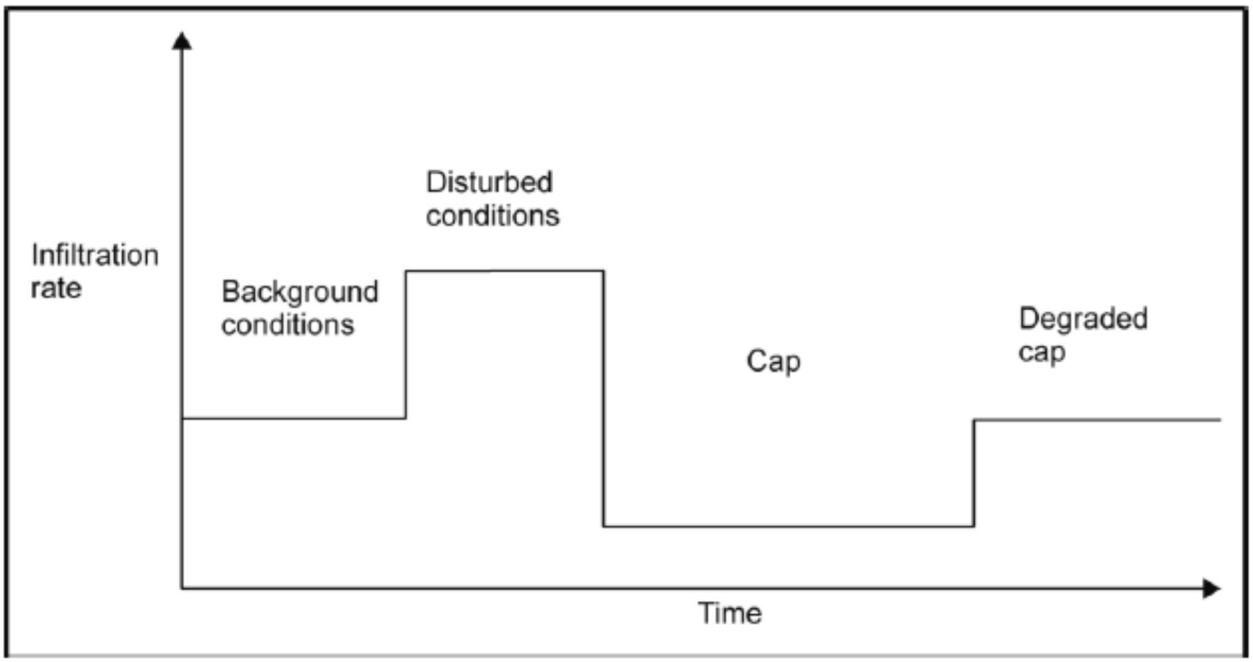

Excerpted from Figure M-1, Appendix M of DOE/EIS-0391, "Final Tank Closure and Waste Management Environmental Impact Statement for the Hanford Site, Richland, Washington."

Figure G-4. Waste Management Area C Vadose Zone Stratigraphy as Depicted in the Tank Closure and Waste Management Environmental Impact Statement.

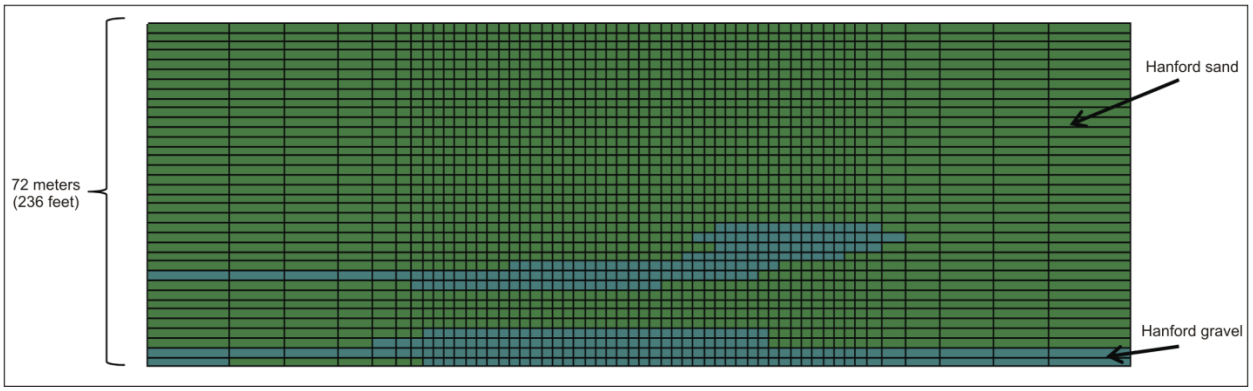

Figure U–58. West-to-East Cross Section of Vadose Zone Lithology for C Tank Farm

Excerpted from Figure U-58, Appendix U of DOE/EIS-0391, "Final Tank Closure and Waste Management Environmental Impact Statement for the Hanford Site, Richland, Washington"; green is Hanford Sand and blue is Hanford Gravel).

For the purpose of comparing the two model results for Alternative 2B, the WMA C PA model was not modified, and includes the geology and hydraulic properties developed for the PA using local scale information on the hydrogeologic conditions at WMA C. In the PA model of WMA C, the inactive nodal areas representing the tanks and selective ancillary equipment

volumes were treated as active using hydraulic properties being used to represent properties of Hanford H2 Sand hydrostratigraphic unit.

G3.5 Partitioning Coefficients and Dispersivity

The TC&WM EIS model applied a constant partitioning coefficient value of 0 mL/g to ^{129}I. The WMA C PA base case analysis partitioning coefficient value for ^{129}I is 0.2 mL/g in fine-grained material. This value is then adjusted downward for the different hydrogeologic units in the WMA C PA model according to the estimated gravel content associated with those hydrogeologic units.

The TC&WM EIS model applied the same longitudinal and transverse dispersivity values of 1 m and 0.1 m, respectively, to all hydrogeologic units. The WMA C PA base case analysis vadose zone longitudinal and transverse dispersivity values vary according to the hydrogeologic unit. For Hanford H2 Sand, the longitudinal and transverse dispersivity values are 25 cm and 2.5 cm, respectively. For backfill and both Hanford H1 and H3 Sandy Gravel/Gravelly Sand, the longitudinal and transverse dispersivity values are 20 cm and 2.0 cm, respectively.

For the purpose of comparing the two model results for Alternative 2B, the PA model of WMA C was run with constant partitioning coefficient values of 0 mL/g to ^{129}I, respectively for all hydrogeologic units. The longitudinal and transverse dispersivity values for the hydrogeologic units remained the same as in the WMA C PA base case.

G.4 COMPARISON OF SELECTED RESULTS FOR ALTERNATIVE 2B USING THE PERFORMANCE ASSESSMENT AND TANK CLOSURE AND WASTE MANAGEMENT ENVIRONMENTAL IMPACT STATEMENT MODELS OF WASTE MANAGEMENT AREA C

The WMA C base case was run with the adaptations described in Sections G.2 and G.3. The flux of ^{129}I into the water table generated by this analysis was compared to the results presented in Figure U-122 in Appendix U of DOE/EIS-0391, which is replicated as Figure G-5. Comparable results of the WMA C PA model are shown in Figure G-6.

The time series releases of ^{129}I to the groundwater calculated in both models include two relative maxima, and there is negligible difference between the two peak values calculated by the different models. The primary difference between the model results is that the WMA C model shows the release of ^{129}I to the groundwater continuing throughout the simulation period. This tail of the release rate curve is a consequence of the inclusion of the aquifer in the WMA C PA model, which introduces some persistence of transport between the capillary fringe and water table.

The results of the comparison show that the two models are capable of producing consistent results. To make the comparison meaningful, several differences in inputs had to be reconciled, e.g., the radionuclide inventory and release functions associated with the release of the radionuclides from the grout. When these differences are reconciled, the two models agree well.

Figure G-5. Tank Closure and Waste Management Environmental Impact Statement Analysis of Iodine-129 Flux from the Vadose Zone into the Aquifer for Alternative 2b (Baseline) and Three Flux Reduction Sensitivity Cases.

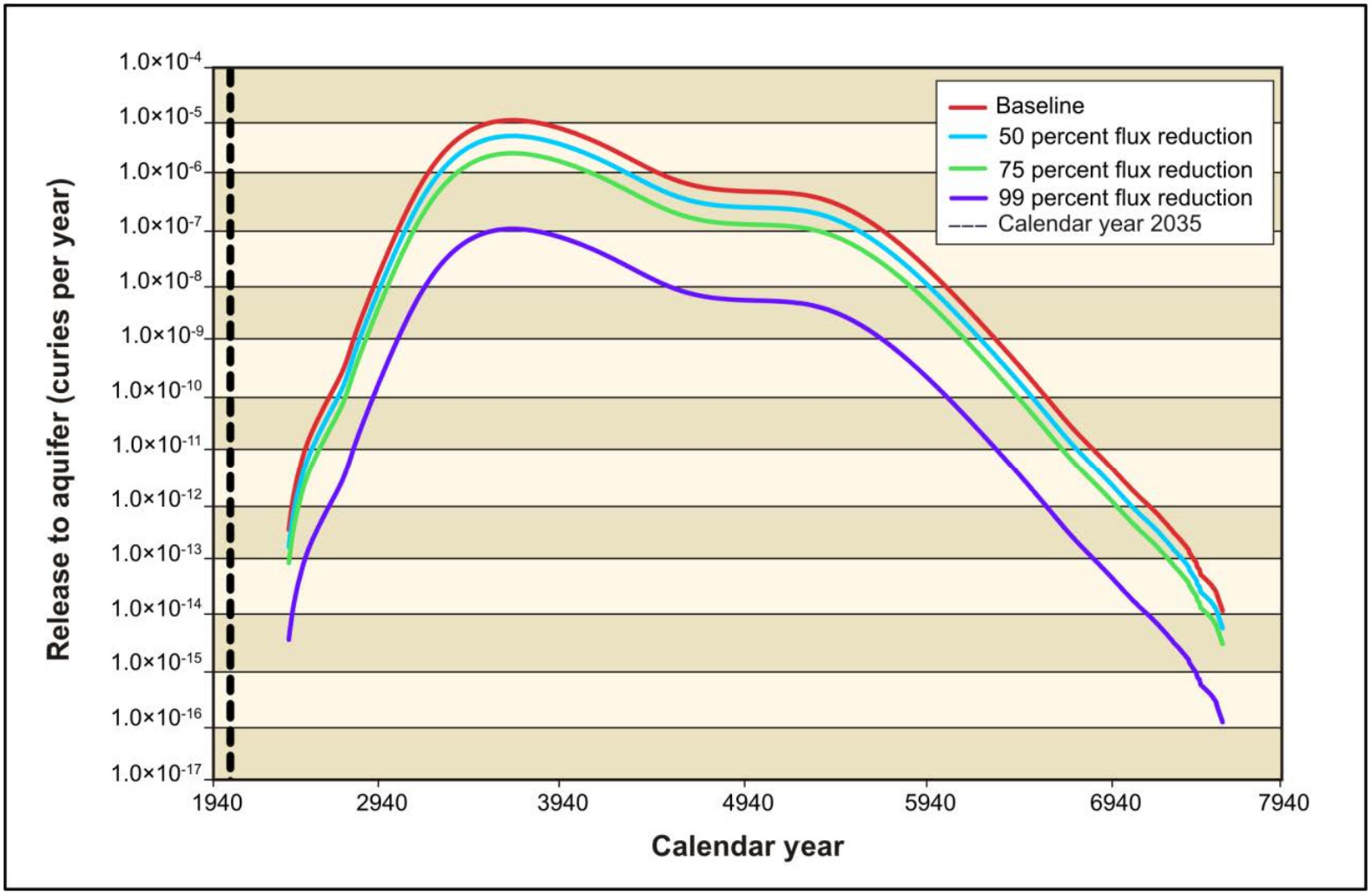

Figure U–122. Iodine-129 Flux to Aquifer Versus Time, C Tank Farm, Tank Residuals

Excerpted from Figure U-122, Appendix U of DOE/EIS-0391, "Final Tank Closure and Waste Management Environmental Impact Statement for the Hanford Site, Richland, Washington."

Figure G-6. Waste Management Area C Performance Assessment Analysis of Tank Closure and Waste Management Environmental Impact Statement Alternative 2b Model of Iodine-129 Flux from the Vadose Zone into the Aquifer.

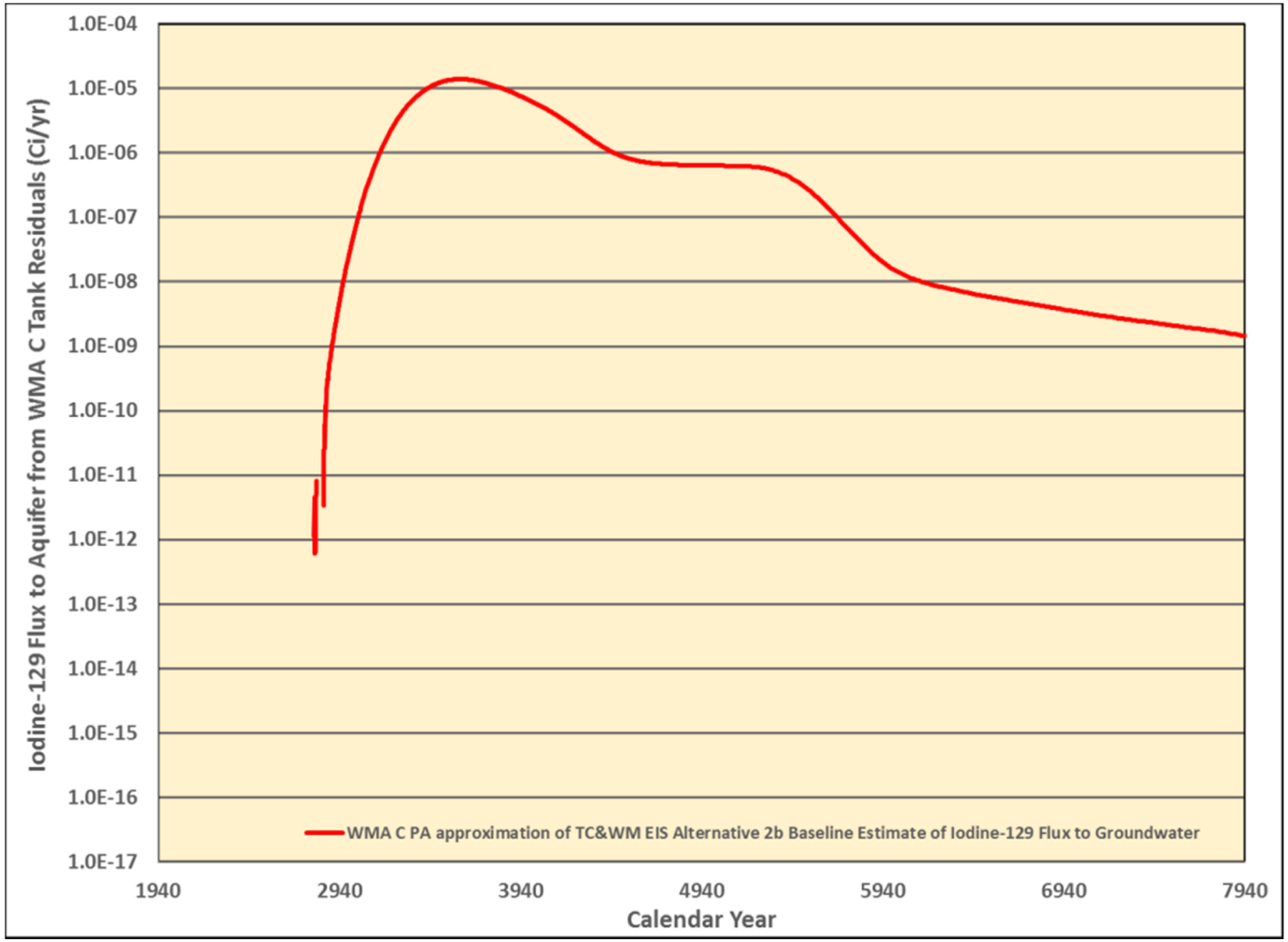

PA = performance assessment WMA = Waste Management Area
TC&WM EIS = Tank Closure and Waste Management Environmental Impact Statement

Reference: DOE/EIS-0391, "Final Tank Closure and Waste Management Environmental Impact Statement for the Hanford Site, Richland, Washington."

G.5 REFERENCES

DOE/EIS-0391, 2012, "Final Tank Closure and Waste Management Environmental Impact Statement for the Hanford Site, Richland, Washington," U.S. Department of Energy, Office of River Protection, Richland, Washington.
Appendix M, Release to Vadose Zone
Appendix N, Vadose Zone Flow and Transport
Appendix O, Groundwater Transport Analysis
Appendix U, Supporting Information for the Long-Term Cumulative Impact Analyses

DOE M 435.1-1, 1999, Radioactive Waste Management Manual, U.S. Department of Energy, Washington, D.C.

DOE/ORP-2003-02, 2003, Environmental Impact Statement for Retrieval, Treatment, and Disposal of Tank Waste and Closure of Single-Shell Tanks at the Hanford Site, Richland, WA: Inventory and Source Term Data Package, Rev. 0, U.S. Department of Energy, Office of River Protection, Richland, Washington.

Resource Conservation and Recovery Act of 1976, 42 USC 6901, et seq.

APPENDIX H

LIST OF FEATURES, EVENTS AND PROCESSES APPLIED TO WASTE MANAGEMENT AREA C

This page intentionally left blank.

TABLE OF CONTENTS

H.1 BACKGROUND ON FEATURES, EVENTS AND PROCESSES EVALUATION H-1

H.2 INTRODUCTION TO SAFETY FUNCTIONS H-2

H.3 SAFETY CONCEPT AND SAFETY FUNCTIONS FOR WASTE MANAGEMENT AREA C H-3

H.4 INTERNATIONAL FEATURES, EVENTS, AND PROCESSES LIST WITH EVALUATIONS OF APPLICABILITY TO WASTE MANAGEMENT AREA C ... H-11

H.5 MAPPING SAFETY FUNCTIONS TO FEATURES, EVENTS AND PROCESSES H-12

H.6 REFERENCES H-88

LIST OF FIGURES

Figure H-1. Feature, Event, and Process Numbering Classification System H-12

LIST OF TABLES

Table H-1. Safety Functions, Associated Features, Events, and Processes, and Potentially Deleterious Features, Events, and Processes Identified for the Waste Management Area C Residual Waste Performance Assessment. Details for individual Features, Events, and Processes and associated numbers identified in this table can be found in Section H.4. ..... H-4

Table H-2. Applicability of Features, Events, and Processes to Waste Management Area C Safety Functions. H-15

LIST OF TERMS

Abbreviations and Acronyms

DOE	U.S. Department of Energy
FEP	Features, Events, and Processes
IAEA	International Atomic Energy Agency
ISAM	Improvement of Safety Assessment Methodologies
WMA	Waste Management Area

APPENDIX H

LIST OF FEATURES, EVENTS AND PROCESSES APPLIED TO WASTE MANAGEMENT AREA C

H.1 BACKGROUND ON FEATURES, EVENTS AND PROCESSES EVALUATION

The use of Features, Events, and Processes (FEPs) is a well-established approach for improving the traceability and transparency of a performance assessment (PA). The intent of the use of FEPs is to identify conditions that may occur in the future that may affect the ability of the disposal system to perform successfully.

In general, the process of using FEPs consists of four steps: (1) identifying a comprehensive list of FEPs, (2) screening the comprehensive list to a manageable number, (3) describing the relationships between the FEPs, and (4) arranging them into calculational cases, or scenarios, for the safety assessment. Differences between published FEP evaluation approaches are comprised of differences between methods for one of these steps, or different ordering of the steps. For instance, the original scenario development procedure described in NUREG/CR-1667 (SAND80-1429), "Risk Methodology for Geologic Disposal of Radioactive Waste: Scenario Selection Procedure" only calls for screening the full scenarios, whereas more recent scenario development approaches emphasize screening at the FEP level (SKB Technical Report 95-22, "The Use of Interaction Matrices for Identification, Structuring, and Ranking of FEPs in a Repository System") or screening both FEPs and full scenarios (SAND94-0482, "Scenario Development for the Waste Isolation Pilot Plant: Building Confidence in the Assessment"). Despite the differences in approaches and ordering, the concepts of these four steps are the same for all scenario development procedures.

Considerable international effort has been expended to develop comprehensive FEP lists for geological (deep) disposal systems. There is only one approach that has been used for this step: collection and elicitation of expert opinion. Excellent summaries of the comprehensive FEP lists for geological disposal have been provided by Chapman et al. (SKI Report 95:26, "Systems Analysis, Scenario Construction and Consequence Analysis Definition for SITE-94") and by Guzowski and Newman (SAND93-7100, "Preliminary Identification of Potentially Disruptive Scenarios at the Greater Confinement Disposal Facility, Area 5 of the Nevada Test Site"). Chapman et al. (SKI Report 95:26) suggest that a comprehensive list of FEPs for a geological disposal system in Sweden was comprised of over 1,200 entries (SKI Technical Report 93:27, "SITE-94 Scenario Development FEP Audit List Preparation: Methodology and Presentation").

Work on formal scenario development for near-surface disposal is more recent and based heavily on the prior geological disposal literature. The International Atomic Energy Agency (IAEA) (IAEA-ISAM-1, "Safety Assessment Methodologies for Near Surface Disposal Facilities, Results of a co-ordinated research project, Volume 1: Review and enhancement of safety assessment approaches and tools") published the first comprehensive set of FEPs for near-surface disposal based on the results of the Improvement of Safety Assessment Methodologies (ISAM) coordinated research program. This FEP list was an adaptation of a

geological disposal comprehensive FEP list for near-surface conditions (IAEA-ISAM-1), and was audited against previously developed site-specific FEP lists for near-surface disposal [e.g., AECL-MISC-295, "Preliminary Safety Analysis Report (PSAR) for the Intrusion Resistant Underground Structure (IRUS)"], providing a good degree of confidence that the list was substantially complete and reliable. This international FEP list is attached to this report as Appendix A.

FEP approaches have also been used increasingly within the U.S. Department of Energy (DOE) Environmental Management and Tank Waste programs (e.g., "2002 LLW Repository PCSC – FEP Consideration [Phifer 2011]; FCRD-USED-2011-000297, "Features, Events and Processes for the Disposal of Low Level Radioactive Waste – FY 2011 Status Report"). Lists of Hanford-relevant FEPs have been developed [BHI-01573, "Groundwater/Vadose Zone Integration Project – The Application of Feature, Event, and Process Methodology at the Hanford Site"; WMP-22922, "Prototype Hanford Features, Events, and Processes (HFEP) Graphical User Interface"] and applied to recent PAs (WCH-520, "Performance Assessment for the Environmental Restoration Disposal Facility, Hanford Site, Washington"). The Hanford FEP lists differ in some regards from the international FEP list, mainly in being focused at a very fine level of detail, which has limited their utility in PAs.

While FEP analyses have been widely used, they have also been identified to have a number of drawbacks. In particular, as a bottom-up approach, they seek to identify all conditions of concern, without necessarily focusing on the key issues. As a result, they have in some cases led to large amounts of effort, but without a commensurate improvement in the traceability of the PA.

As a result of these issues with FEP-based analyses, in recent years there has been increasing attention given to safety function approaches in structuring PAs. Recent guidance on the conduct of PAs has de-emphasized the importance of purely FEP-based approaches, and has instead recommended a blended approach (NEA Report 6923,"Methods of Safety Assessment of Geological Disposal Facilities for Radioactive Waste, Outcomes of the NEA MeSA Initiative"). These approaches are reviewed in the next section.

H.2 INTRODUCTION TO SAFETY FUNCTIONS

The drawbacks to the FEPs process have led to a more recent emphasis in the literature on the use of an alternative approach to identifying conditions that need to be included in the PA. Increasingly, the literature on PA emphasizes the use of safety functions as either a replacement for FEP analyses or as an augmentation of FEP analyses (e.g., SKB Technical Report TR-10-45, "FEP report for the safety assessment SR-Site"; NEA Report 6923). A safety function is a feature of the system that provides a specific function that is relevant to the performance (or safety) of the facility. The set of these safety functions presents a high-level summary of the strategy by which the performance of the disposal system is assured. In addition to providing a technical approach to development of scenarios, the use of safety functions is beneficial in emphasizing the overall safety strategy with stakeholders.

Increasingly, PAs include both FEP evaluations as a bottom-up approach and safety functions as a top-down approach to identifying conditions that need to be evaluated in the PA ("A methodology for scenario development based on understanding of long-term evolution of geological disposal systems" [Wakasugi et al. 2012]; "Natural and Engineering Barriers – the Safety Concept Basis for LILW Repository in Vrbina, Krško" [Virsek et al. 2014]). In this hybrid approach, FEPs are used in a more targeted manner than the traditional FEPs concept. In the hybrid approach, FEPs are identified that may affect the ability of the safety function to provide assurance of performance in the future. That is, FEPs are identified that may degrade or modify the performance of the safety function in some way. For instance, performance of an engineered cover system may be influenced by a wide variety of FEPs that would change the rate of water movement through it. These FEPs might include (for example) mechanical changes to the cover soil, changes in the vegetation on top of the cover, climate changes that lead to different precipitation patterns on top of the cover, loss of institutional control leading to onsite irrigation, and so on. Since all of these FEPs influence the system in a similar manner (i.e., changes in water flow through the cover), sensitivity analyses that vary this safety function represent an aggregated view of the potential negative effects of a suite of FEPs. In this way the PA can be organized to evaluate a large number of FEPs with fewer sensitivity cases and scenarios.

H.3 SAFETY CONCEPT AND SAFETY FUNCTIONS FOR WASTE MANAGEMENT AREA C

The safety concept is the overall approach by which a disposal system is intended to provide the performance required in regulation. The safety concept can be thought of as the set of safety functions, acting together in concert, to provide that performance. Ideally, the safety functions represent multiple and redundant barriers, so that the loss of one or some of the safety functions continues to result in adequate performance of the overall system. A set of safety functions for Waste Management Area (WMA) C are shown in Table H-1. The goal of the PA is to evaluate these safety functions, to provide reasonable assurance of performance even when some of the safety functions are lost or degraded through time or disruptive events.

A significant part of the safety concept lies in the land ownership of the Central Plateau by DOE. It is noteworthy that all of the technical calculations that are presented in a PA of WMA C are predicated on the loss of the first two safety functions: loss of institutional control of the Central Plateau by DOE, followed by loss of societal memory that the Hanford Site existed. If either or both of these safety functions remain in place, the radiological impacts of releases or residual wastes from WMA C are very low and greatly delayed in time, as shown in the TC&WM EIS analyses for tank residual wastes (DOE/EIS-0391, "Final Tank Closure and Waste Management Environmental Impact Statement for the Hanford Site, Richland, Washington"). In the assessment context of PAs conducted under DOE O 435.1, Radioactive Waste Management (see Section 2), both of these safety functions are assumed to disappear after 100 years.

Table H-1. Safety Functions, Associated Features, Events, and Processes, and Potentially Deleterious Features, Events, and Processes Identified for the Waste Management Area C Residual Waste Performance Assessment. Details for individual Features, Events, and Processes and associated numbers identified in this table can be found in Section H.4. (6 sheets)

Designation		Description	Associated FEPs	Deleterious FEPs	Associated Analyses
I1	Institutional Control	By DOE O 435.1, Radioactive Waste Management, it is assumed that control of the site will be retained for 100 years. A strong potential exists that the U.S. government will retain control of the site for a much more extended period of time. DOE O 458.1, Radiation Protection of the Public and the Environment requires that plans for management and disposal of wastes provide for institutional controls and long-term stewardship. DOE P 454.1, Use of Institutional Controls identifies how that stewardship is to be carried out.	1.1.06 1.1.09 1.1.10 1.4 (all)		Treated conservatively in all
I2	Societal memory	Societal memory is represented by records, deed restrictions, and other passive controls that would warn someone that additional care should be taken in the area. For a member of the public to come onsite to experience exposures to contamination from Waste Management Area (WMA) C, records that the Hanford Site existed would need to be forgotten or ignored. DOE O 458.1 requires record keeping that would lessen the likelihood of this occurrence. DOE P 454.1 identifies how that stewardship is to be carried out.	1.1.06 1.1.09 1.1.10 1.4 (all)		Treated conservatively in all
I3	Exposure	By DOE O 435.1, it is assumed that a post-closure well is established 100 m downgradient at the point of highest exposure. It is highly unlikely that this situation will occur, and potential wells in other locations would produce much lower impacts to a member of the public. Furthermore, even if control of the site is lost, the 100 m boundary for WMA C lies under the A Complex, and does not represent a realistic exposure point. Exposures would be more likely to occur further downgradient.	1.1 (all) 1.4 (all) 3.3 (all) 2.2.13(intruder) 2.3.03 2.3.08 2.3.09 2.3.13 2.4 (all)		Treated conservatively in all

Table H-1. Safety Functions, Associated Features, Events, and Processes, and Potentially Deleterious Features, Events, and Processes Identified for the Waste Management Area C Residual Waste Performance Assessment. Details for individual Features, Events, and Processes and associated numbers identified in this table can be found in Section H.4. (6 sheets)

Designation		Description	Associated FEPs	Deleterious FEPs	Associated Analyses
S1	Site characteristics	WMA C is a semi-arid site with low precipitation. The Central Plateau is remote from members of the public, with a substantial buffer area under U.S. Department of Energy (DOE) control. The vadose zone is thick, with long travel times in the vadose zone.	2.3.01 2.3.02 2.3.03 2.3.07 2.3.07 2.3.08 2.3.09 2.3.10 2.3.11 2.3.12 2.3.13		All
EB1	RCRA Cover (infiltration reduction)	The final design cover has not yet been established, but is believed to be able to produce very low initial flow rates. Over some period of time this function may deteriorate, with the rate of deterioration associated with a variety of processes.	1.1.02 1.1.08 1.1.12 1.2.04 1.2.07 1.3.01 1.3.02 1.3.04 1.3.06 1.3.07 1.3.08 1.4 (all) 2.1.05 2.3.01 2.3.02 2.3.07 2.3.08 2.3.10 2.3.11 2.3.12 2.3.13	1.1.08 1.1.12 1.2.04 1.2.07 2.3.08 2.3.12 2.3.13	INF0 – INF4 Treated in GoldSim© uncertainty analysis

Table H-1. Safety Functions, Associated Features, Events, and Processes, and Potentially Deleterious Features, Events, and Processes Identified for the Waste Management Area C Residual Waste Performance Assessment. Details for individual Features, Events, and Processes and associated numbers identified in this table can be found in Section H.4. (6 sheets)

Designation		Description	Associated FEPs	Deleterious FEPs	Associated Analyses
EB2	RCRA Cover (depth of disposal)	Limitation of types of potential inadvertent human intrusion by depth of disposal.	1.1.02 1.1.05 1.4 (all)		Intrusion
EB3	Steel Shell (permeability)	The function of the carbon steel shell to limit flow through the tank is not currently explicitly accounted for in the performance assessment. The shell is part of the overall assessment of low flow through the tank for long periods of time. Its potential eventual failure is considered as part of the generic barrier failure cases. DIF4 explores what happens if the tank behaves *better* than expected, and retains integrity for thousands of years, allowing ingrowth of progeny before releases commence.	1.1.02 2.1.05 2.1.08		DIF4
EB4	Steel Shell (chemical)	The carbon steel shell will corrode over a period of time, leaving behind corrosion products of (primarily) iron oxides. These corrosion products are highly sorptive and tend to produce reducing conditions that are highly advantageous for limiting solubilities of key radionuclides, particularly technetium.	1.1.02 2.1.05 2.1.09		None
EB5	Tank structure (structural)	The dome and walls provide structural support preventing subsidence of the closed facility.	1.1.02 1.2.03 2.1.05		No credible deleterious FEPs
EB6	Tank structure (intrusion)	The tank structure provides a barrier to intrusion.	1.1.02 1.4.03 2.1.05		Intrusion analysis
EB7	Tank structure (chemical)	The concrete of the tank acts to condition the chemistry of the waste residuals, with sorption characteristic of high pH environments.	1.1.02 2.1.05 2.1.09		Treated in GoldSim© uncertainty analysis GRT4 (Barrier analysis)
EB8	Tank structure (permeability)	The concrete of the tank structure is substantially intact and provides a barrier to flow into the tank.	1.1.02 1.2.03 2.1.05	1.2.03	GRT1, GRT2, GRT3

Table H-1. Safety Functions, Associated Features, Events, and Processes, and Potentially Deleterious Features, Events, and Processes Identified for the Waste Management Area C Residual Waste Performance Assessment. Details for individual Features, Events, and Processes and associated numbers identified in this table can be found in Section H.4. (6 sheets)

Designation		Description	Associated FEPs	Deleterious FEPs	Associated Analyses
EB9	Grout in tank (permeability)	The grout acts to limit water flow through the facility, making releases dominated by diffusion from the waste.	1.1.02 1.1.03 1.1.04 1.1.05 1.1.08 1.2.03 2.1.04	1.1.08 1.2.03	GRT1, GRT2, GRT3
EB10	Grout in Tank (chemical)	The grout acts to condition the chemistry of the waste residuals, with sorption characteristic of high pH environments.	1.1.02 2.1.04 2.1.09		Treated in GoldSim© uncertainty analysis GRT4 (Barrier analysis)
EB11	Grout in tank (structural)	The grout provides structural support preventing subsidence of the closed facility.	1.1.02 2.1.04		No credible deleterious FEPs
EB12	Grout (intrusion)	The structural strength of the grout provides a barrier to intrusion.	1.1.02 1.4.03 2.1.04 2.2.13		Intrusion analysis
EB13	Tank Base Mat (permeability)	The tank base mat, if intact, will provide a barrier that will limit flow and contaminant transport from the tank residual wastes situated at the tank bottom into the underlying vadose zone sediments.	1.1.02 2.1.05	2.1.05	GRT0 GRT1 GRT2 GRT3 (Barrier analysis)
EB14	Tank Base Mat (chemical)	The concrete pad is anticipated to continue to provide a high pH environment, with associated sorption, for an extended time in the future.	1.1.02 2.1.05 2.1.09 2.1.10		GoldSim© uncertainty analysis
EB15	Pipelines (permeability)	The pipelines, if intact, provide a delay to releases of waste in ancillary equipment.	2.1.06		All
AP1	Grout (air pathway)	Limitation of releases to air owing to low air permeability and long pathway to the surface.	2.1.12 2.3.07 3.1.04 3.2.09 3.2.10		Air pathway analysis

Table H-1. Safety Functions, Associated Features, Events, and Processes, and Potentially Deleterious Features, Events, and Processes Identified for the Waste Management Area C Residual Waste Performance Assessment. Details for individual Features, Events, and Processes and associated numbers identified in this table can be found in Section H.4. (6 sheets)

Designation		Description	Associated FEPs	Deleterious FEPs	Associated Analyses
WF1	Residual Waste (chemical)	The residual waste is recalcitrant by nature, providing limitations to the amount and rate of release of contamination from it upon contact with water.	2.1.01 2.1.02 2.1.12 3.1 (all) (except 3.1.06) 3.2 (all) (except 3.2.08)	2.1.1	RLS1 INV0, INV1, INV2 GoldSim© uncertainty
VZ1	Vadose zone thickness	The vadose zone is thick with slow rates of water flow, leading to long delay times in the vadose zone.	2.2.01 2.2.02 2.2.03 2.2.05 2.2.07 2.2.08 2.2.09 2.2.12 2.3.02 3.1.01 3.2.07	1.1.01 2.2.12	VZP0 VZP1 VZP2 VZP3 VZP4 VZP5 VZP6 VZP7 Treated in GoldSim© uncertainty analysis VZP9 (Barrier analysis)
VZ2	Sorption on vadose zone soils	Vadose zone soils sorb some of the contaminants of potential concern, delaying their arrival at the water table. A number of key contaminants are not believed to sorb significantly.	1.4.07 2.2.08 2.2.09 2.3.02 3.2.03 3.2.04 3.2.05 3.2.06 3.2.07	1.4.07 2.2.08 3.2.03	Treated in GoldSim© uncertainty analysis VZP6
VZ3	Dispersion in vadose zone	Spreading of contaminants in the vadose zone, dispersing them and decreasing concentrations.	2.2.01 2.2.02 2.2.03 2.2.05 2.2.07 2.3.02	2.2.12	Treated in GoldSim© uncertainty analysis VZP7

Table H-1. Safety Functions, Associated Features, Events, and Processes, and Potentially Deleterious Features, Events, and Processes Identified for the Waste Management Area C Residual Waste Performance Assessment. Details for individual Features, Events, and Processes and associated numbers identified in this table can be found in Section H.4. (6 sheets)

Designation		Description	Associated FEPs	Deleterious FEPs	Associated Analyses
SZ1	Water flow in saturated zone	Advective flow in the saturated zone leading to dilution of the contaminants.	1.2.10 1.3.01 1.3.02 1.3.03 1.3.07 1.4.10 2.2.03 2.2.05 2.2.07 2.3.03 2.3.04 3.1.01 3.2.07	1.3.01 1.3.02 1.3.03 1.3.07 2.3.03	Treated in GoldSim© uncertainty analysis GWP0 GWP1 GWP2 GWP3 (Barrier analysis)
SZ2	Sorption on saturated zone soils	Saturated zone soils sorb some of the contaminants of potential concern, delaying their arrival at the point of compliance. A number of key contaminants are not believed to sorb significantly.	2.2.08 2.2.09 3.2.03 3.2.04 3.2.07		Treated in GoldSim© uncertainty analysis
SZ3	Dispersion in saturated zone	Spreading of the plume in the saturated zone, adding dilution to the contaminant plume and lowering concentrations.	2.2.03 2.2.05 2.2.07		Treated in GoldSim© uncertainty analysis
SZ4	Dilution in well	Dilution caused by pumping a groundwater well to the surface where it is useable and accessible by a member of the public.	1.4.10 2.2.13 3.2.07 3.2.12 3.3.01 3.3.02 3.3.04		By groundwater protection rule, not taken into account. Groundwater concentrations at each point in space used for all analyses.

FEPs = Features, Events, and Processes RCRA = Resource Conservation and Recovery Act of 1976

GoldSim© simulation software is copyrighted by GoldSim Technology Group LLC of Issaquah, Washington (see http://www.goldsim.com).

DOE O 435.1 also introduces another administrative safety function into the analysis: the point of compliance. If the first two safety functions (institutional control and societal memory) are lost, DOE O 435.1 requires an assumption that a groundwater well is installed 100 m from the disposal facility in the location of peak concentration. This assumption means that relatively little credit is given for delay and dilution in the groundwater aquifer. Even in the event that memory of the Hanford Site is lost, people would not necessarily move to the Central Plateau and use untreated groundwater as their water source. People further downgradient or people not using groundwater would necessarily be more protected than the PA calculates. The regulation, therefore, provides an additional layer of safety to the results of the analyses via this safety function.

The remaining parts of the safety concept involve the use of the engineering and geological setting to provide multiple and redundant barriers to the release and migration of residual wastes from tanks and ancillary equipment. The barriers can be divided into one of three types: hydrological safety functions, chemical safety functions, and structural safety functions. The safety concept calls for backfilling the tanks with grout, leading to a highly stable underground structure. The resulting monolith of grout contained in the tank can be assumed to maintain its ability to support the soil overburden for very long periods of time. The hydrological safety functions limit the contact of water with the residual wastes, limit that rate at which contamination can be released and transported through the environment to the compliance point, and provide dilution of contamination through dispersion and mixing with clean surrounding water. The chemical safety functions are intended to decrease the solubility and increase the sorption of key contaminants, and to provide a stable and passive chemical environment for the engineered barriers.

As discussed above, the purpose of the PA is to evaluate the safety concept to provide reasonable assurance of performance of the safety concept, even in the event that one or more of the safety functions are lost or are degraded in time. It is therefore reasonable to ask which FEPs might affect a particular safety function in a way that might degrade its function, or to cause the safety function to act differently than expected.

This approach can be used to identify a set of sensitivity analyses that can be used to explore the implications of the loss of safety functions, while at the same time exploring the implications of aggregated FEPs that might affect the safety function in similar ways. The structure of the PA for WMA C will therefore be to identify sensitivity cases and alternative models for the safety functions shown in Table H-1, and to examine what happens in the PA model when the safety function behaves differently than expected, is degraded compared to a base case, or is lost entirely. Particular attention will be given to any FEPs identified that might affect multiple safety functions simultaneously.

The safety functions identified for the WMA C post-closure period are presented in Table H-1 along with the associated FEPs and potentially deleterious FEPs. This table was generated from a workshop of senior PA experts, and represents the collective view of that group. The workshop was held in Denver April 20 – 21, 2015, with the goal of evaluating FEPs as they relate to WMA C and mapping the FEPs to safety functions. The attendee list is below.

WRPS/INTERA/Hanford

- Marcel Bergeron
- Matt Kozak
- Mike Connelly
- Alaa Aly
- Mick Apted
- Randy Arthur
- Bob Andrews

SRR/SRNL/ Savannah River

- Roger Seitz
- Kent Rosenberger
- Steve Hommel

PNNL/Hanford

- Vicky Freedman

The workshop was undertaken to evaluate which FEPs had the potential to affect safety functions within the 10,000-year sensitivity and uncertainty analysis period. It therefore allowed the FEP team to screen out some FEPs that may be expected to occur over extremely long time periods (e.g., orogeny). The presumption in the FEP screening was that continental glaciation will not occur within 10,000 years, so FEPs associated with such extreme changes were screened out. All other FEPs that have a reasonable likelihood of occurrence in 10,000 years were evaluated for their potential effects on the safety functions.

H.4 INTERNATIONAL FEATURES, EVENTS, AND PROCESSES LIST WITH EVALUATIONS OF APPLICABILITY TO WASTE MANAGEMENT AREA C

This section contains an adaptation of Appendix C of IAEA-ISAM-1. The ISAM FEPs list is a list of FEPs relevant to the assessment of long-term safety of near-surface disposal facilities, which attempts to be comprehensive within reasonable bounds. Because these FEPS are an adaptation of the FEPs used for near-surface disposal facilities, the term repository is used to refer to the disposal system. It consists of 141 FEPs, each of which has an identifying number. The numbers reflect a classification system, as shown in Figure H-1. At its center, the classification scheme includes processes related to contaminant release, migration and exposures (radionuclide and contaminant factors). The next tier are the features of the disposal system (wastes, engineered and natural barriers and human behaviour) and events and processes which may cause the system to evolve (environment factors). Further out, there are processes and events originating outside the disposal system, but which act upon it (external factors). These external factors (or external FEPs) are often considered to be scenario-generating FEPs.

Examination of the FEPs list shows a distinction between those that are descriptive of the system and how it functions and those that have been included in the FEPs list because they have potentially disruptive effects on the disposal system. This distinction has been used to

characterize how the FEPs act on WMA C safety functions, with the results documented in Section H.3.

Figure H-1. Feature, Event, and Process Numbering Classification System.

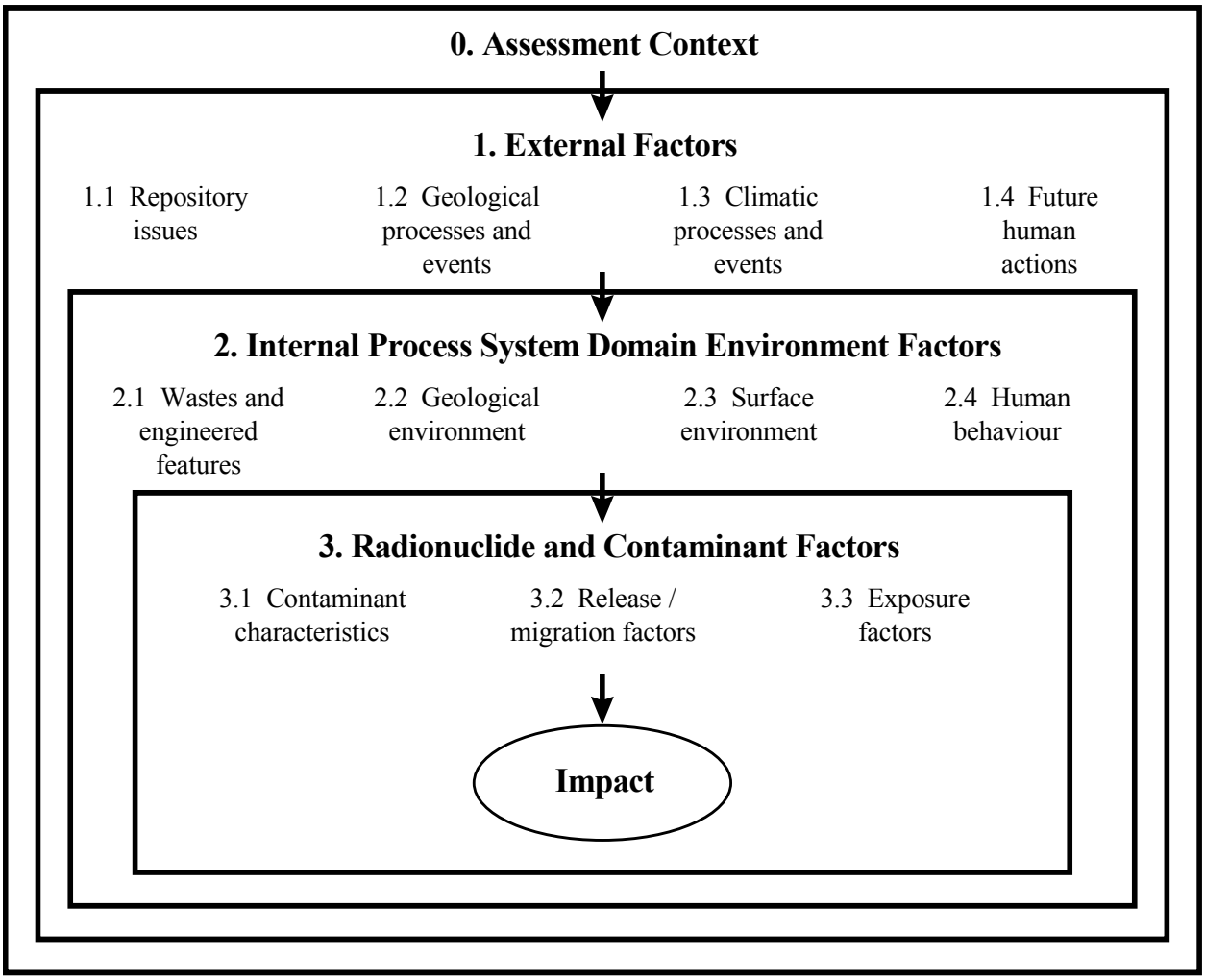

Figure excerpted from IAEA-ISAM-1, "Safety Assessment Methodologies for Near Surface Disposal Facilities, Results of a co-ordinated research project, Volume 1: Review and enhancement of safety assessment approaches and tools."

For the sake of clarity, the full list of FEPs from IAEA-ISAM-1 is included here in the same format as the original publication (refer to the list below). A new addition to the description of each FEP is a short commentary on the applicability of the FEP to the WMA C PA, and a short statement of what negative impact (if any) the FEP may have on the performance of WMA C, and how it affects safety functions.

H.5 MAPPING SAFETY FUNCTIONS TO FEATURES, EVENTS AND PROCESSES

Application of the IAEA FEPs list to the WMA C safety functions, discussed in Section H.4, leads to a mapping of applicable FEPs to each safety function. This mapping is shown in

Table H-2. A number of the FEPs have been evaluated as not applicable to WMA C, either because of the geological or geographical location, because of the assessment context, or because of the time frame of the analysis, which rules out FEPs requiring very long geological times for their occurrence. These FEPs are denoted with N in the table (for not applicable). FEPs applicable to a particular safety function are denoted with an X, whereas if the FEP is not applicable to the safety function it is left blank.

This page intentionally left blank.

Table H-2. Applicability of Features, Events, and Processes to Waste Management Area C Safety Functions. (1 of 3 sheets)

X denotes applicable to Waste Management Area C, N denotes not applicable. See Feature, Event, and Process (FEP) list for discussion and justification.

FEP	Safety Function																										
	I1	I2	I3	S1	EB1	EB2	EB3	EB4	EB5	EB6	EB7	EB8	EB9	EB10	EB11	EB12	EB13	EB14	EB15	AP1	WF1	VZ1	VZ2	VZ3	SZ1	SZ2	SZ3	SZ4
1.1.01			X																									
1.1.02			X		X	X	X	X	X	X	X	X	X	X	X	X	X	X										
1.1.03			X																									
1.1.04			X																									
1.1.05			X			X																						
1.1.06	X	X	X																									
1.1.07			X																									
1.1.08			X		X																							
1.1.09	X	X	X																									
1.1.10	X	X	X																									
1.1.11			X																									
1.1.12			X		X																							
1.2.01	N	N	N	N	N	N	N	N	N	N	N	N	N	N	N	N	N	N	N	N	N	N	N	N	N	N	N	N
1.2.02	N	N	N	N	N	N	N	N	N	N	N	N	N	N	N	N	N	N	N	N	N	N	N	N	N	N	N	N
1.2.03									X			X	X															
1.2.04					X																							
1.2.05	N	N	N	N	N	N	N	N	N	N	N	N	N	N	N	N	N	N	N	N	N	N	N	N	N	N	N	N
1.2.06	N	N	N	N	N	N	N	N	N	N	N	N	N	N	N	N	N	N	N	N	N	N	N	N	N	N	N	N
1.2.07					X																							
1.2.08	N	N	N	N	N	N	N	N	N	N	N	N	N	N	N	N	N	N	N	N	N	N	N	N	N	N	N	N
1.2.09	N	N	N	N	N	N	N	N	N	N	N	N	N	N	N	N	N	N	N	N	N	N	N	N	N	N	N	N
1.2.10																									X			
1.3.01					X																				X			
1.3.02					X																				X			
1.3.03																									X			
1.3.04	N	N	N	N	N	N	N	N	N	N	N	N	N	N	N	N	N	N	N	N	N	N	N	N	N	N	N	N
1.3.05	N	N	N	N	N	N	N	N	N	N	N	N	N	N	N	N	N	N	N	N	N	N	N	N	N	N	N	N
1.3.06					X																							
1.3.07					X																				X			
1.3.08					X																							
1.3.09	N	N	N	N	N	N	N	N	N	N	N	N	N	N	N	N	N	N	N	N	N	N	N	N	N	N	N	N
1.3.10						X																						
1.4.01	X	X	X		X																							
1.4.02	X	X	X		X																							
1.4.03	X	X	X		X					X						X												
1.4.04	X	X	X		X																							
1.4.05	X	X	X		X																							
1.4.06	X	X	X		X																							
1.4.07	X	X	X		X																		X					
1.4.08	X	X	X		X																							
1.4.09	X	X	X		X																							
1.4.10	X	X	X		X																				X			

Table H-2. Applicability of Features, Events, and Processes to Waste Management Area C Safety Functions. (2 of 3 sheets)

X denotes applicable to Waste Management Area C, N denotes not applicable. See Feature, Event, and Process (FEP) list for discussion and justification.

FEP	Safety Function																											
	I1	I2	I3	S1	EB1	EB2	EB3	EB4	EB5	EB6	EB7	EB8	EB9	EB10	EB11	EB12	EB13	EB14	EB15	AP1	WF1	VZ1	VZ2	VZ3	SZ1	SZ2	SZ3	SZ4
1.4.11	X	X	X		X																							
1.4.12	X	X	X		X																							
1.4.13	X	X	X		X																							
1.4.14	X	X	X		X																							
1.4.15	X	X	X		X																							
2.1.01																					X							
2.1.02																					X							
2.1.03	N	N	N	N	N	N	N	N	N	N	N	N	N	N	N	N	N	N	N	N	N	N	N	N	N	N	N	N
2.1.04													X	X	X	X												
2.1.05							X	X	X	X	X	X					X	X										
2.1.06																			X									
2.1.07																												
2.1.08							X																					
2.1.09								X			X			X			X	X										
2.1.10																		X										
2.1.11	N	N	N	N	N	N	N	N	N	N	N	N	N	N	N	N	N	N	N	N	N	N	N	N	N	N	N	N
2.1.12																				X	X							
2.1.13	N	N	N	N	N	N	N	N	N	N	N	N	N	N	N	N	N	N	N	N	N	N	N	N	N	N	N	N
2.1.14	N	N	N	N	N	N	N	N	N	N	N	N	N	N	N	N	N	N	N	N	N	N	N	N	N	N	N	N
2.1.15	N	N	N	N	N	N	N	N	N	N	N	N	N	N	N	N	N	N	N	N	N	N	N	N	N	N	N	N
2.2.01																						X		X				
2.2.02																						X		X				
2.2.03																						X		X	X		X	
2.2.04	N	N	N	N	N	N	N	N	N	N	N	N	N	N	N	N	N	N	N	N	N	N	N	N	N	N	N	N
2.2.05																						X		X	X		X	
2.2.06	N	N	N	N	N	N	N	N	N	N	N	N	N	N	N	N	N	N	N	N	N	N	N	N	N	N	N	N
2.2.07																						X		X	X			
2.2.08																						X	X			X		
2.2.09																						X	X			X		
2.2.10	N	N	N	N	N	N	N	N	N	N	N	N	N	N	N	N	N	N	N	N	N	N	N	N	N	N	N	N
2.2.11	N	N	N	N	N	N	N	N	N	N	N	N	N	N	N	N	N	N	N	N	N	N	N	N	N	N	N	N
2.2.12																						X						
2.2.13			X																									X
2.3.01				X	X																							
2.3.02				X	X																	X	X	X				
2.3.03			X	X																					X			
2.3.04				X																					X			
2.3.05	N	N	N	N	N	N	N	N	N	N	N	N	N	N	N	N	N	N	N	N	N	N	N	N	N	N	N	N
2.3.06	N	N	N	N	N	N	N	N	N	N	N	N	N	N	N	N	N	N	N	N	N	N	N	N	N	N	N	N
2.3.07				X	X																	X						
2.3.08			X	X	X																							
2.3.09			X	X																								
2.3.10				X	X																							

Table H-2. Applicability of Features, Events, and Processes to Waste Management Area C Safety Functions. (3 of 3 sheets)

X denotes applicable to Waste Management Area C, N denotes not applicable. See Feature, Event, and Process (FEP) list for discussion and justification.

FEP	Safety Function																											
	I1	I2	I3	S1	EB1	EB2	EB3	EB4	EB5	EB6	EB7	EB8	EB9	EB10	EB11	EB12	EB13	EB14	EB15	AP1	WF1	VZ1	VZ2	VZ3	SZ1	SZ2	SZ3	SZ4
2.3.11				X	X																							
2.3.12				X	X																							
2.3.13			X	X	X																							
2.3.14	N	N	N	N	N	N	N	N	N	N	N	N	N	N	N	N	N	N	N	N	N	N	N	N	N	N	N	N
2.4.01			X																									
2.4.02			X																									
2.4.03			X																									
2.4.04			X																									
2.4.05			X																									
2.4.06			X																									
2.4.07			X																									
2.4.08			X																									
2.4.09			X																									
2.4.10	N	N	N	N	N	N	N	N	N	N	N	N	N	N	N	N	N	N	N	N	N	N	N	N	N	N	N	N
2.4.11	N	N	N	N	N	N	N	N	N	N	N	N	N	N	N	N	N	N	N	N	N	N	N	N	N	N	N	N
3.1.01																						X			X			
3.1.02	N	N	N	N	N	N	N	N	N	N	N	N	N	N	N	N	N	N	N	N	N	N	N	N	N	N	N	N
3.1.03																												
3.1.04																				X								
3.1.05	N	N	N	N	N	N	N	N	N	N	N	N	N	N	N	N	N	N	N	N	N	N	N	N	N	N	N	N
3.1.06	N	N	N	N	N	N	N	N	N	N	N	N	N	N	N	N	N	N	N	N	N	N	N	N	N	N	N	N
3.2.01																					X							
3.2.02																					X							
3.2.03																					X		X					
3.2.04																					X		X					
3.2.05																					X		X					
3.2.06																					X		X					
3.2.07																					X	X	X		X	X		
3.2.08	N	N	N	N	N	N	N	N	N	N	N	N	N	N	N	N	N	N	N	N	N	N	N	N	N	N	N	N
3.2.09																				X	X							
3.2.10																				X	X							
3.2.11																					X							
3.2.12																					X							
3.2.13																					X							
3.3.01			X																						X			
3.3.02			X																						X			
3.3.03			X																									
3.3.04			X																						X			
3.3.05			X																									
3.3.06			X																									
3.3.07			X																									
3.3.08			X																	X								

ASSESSMENT CONTEXT	0
Definition: Factors that the analyst will consider in determining the scope of the analysis. These may include factors related to regulatory requirements, definition of desired calculation end-points, requirements in a particular phase of assessment, description of the domain of concern and a description of the target groups in the assessment. Decisions at this point will affect the phenomenological scope of a particular phase of assessment, i.e. what "physical FEPs" will be included.	
Comment: *"Assessment Context" is a category in the International FEP List and is subdivided into individual FEPs.*	

Assessment endpoints	0.01
Definition: The long-term human *health and environmental effects or risks that may arise from the disposed wastes and repository. These FEPs include health or environmental effects of concern in an* assessment (what effect and to whom/what), and health or environmental effects ruled to be of no concern.	
Comment: *From the disposed radioactive waste to the health impact to humans, various indicators and associated criteria can be defined to serve as assessment endpoints. Which one to choose, will depend on the purpose of the assessment. The indicator most frequently considered is the radiation dose or risk to man, often represented by the annual dose rate or risk to a member of a "critical group" of potentially most exposed individuals (see FEP 0.06).*	
Key concepts, examples, and related FEPs	
Annual individual dose / *Lifetime individual risk* / *Increase in radiation levels in the environment*	
Annual individual risk / *Radionuclide concentration in the environment* / *Release or concentration of non-radiological toxic contaminants*	
Collective doses / *Flux through engineered barriers* / *Dose to biota other than man*	
Lifetime individual dose / *Flux from geosphere to biosphere* / *Collective risk*	
Collective effective dose	
Application to WMA C: *Addressed in DOE Order 435.1.*	
Potentially deleterious FEP*: Not applicable*	

Timescales of concern	0.02
Definition: The time periods over which the disposed wastes and repository may present some significant human health or environmental hazard.	
Comment: *These may correspond to the timescale over which the safety of the disposed wastes and repository is estimated or discussed. In some countries national regulations set a limit up to which quantitative assessment is required, with more qualitative arguments to demonstrate safety being sufficient at later times.*	

Key concepts, examples, and related FEPs		
Until peak doses occur	*500 – 10 000 years*	*0 – 500 years*
> 60 000 years	*10 000 – 60 000 years*	
Application to WMA C: *Addressed in DOE Order 435.1.*		
Potentially deleterious FEP*: Not applicable*		

Spatial domain of concern	0.03
Definition: The domain over which the disposed wastes and repository may present some significant human health or environmental hazard.	
Comment: *This may correspond to the spatial domain over which the safety of the disposed wastes and repository is estimated, or the domain which is necessary to model in order to develop an understanding of the movement of contaminants and exposures. This may be limited by the purpose of the assessment, for example if the performance of a component of the total system have to be assessed.*	
Key concepts, examples, and related FEPs	
Description of the spatial domain of concern	
Application to WMA C: *Addressed in DOE Order 435.1.*	
Potentially deleterious FEP*: Not applicable*	

Repository assumptions		0.04
Definition: The assumptions that are made in the assessment about the construction, operation, closure and administration of the repository.		
Comment: *For example, most post-closure assessments make the assumption that a repository has been successfully closed, although, in practice such decisions may be delayed or be the subject of uncertainty*		
Key concepts, examples, and related FEPs		
Description of the construction, operation, closure and operation of the repository	*Repository has been successfully closed*	*Change in volume of disposed waste*
	Waste emplacement configuration has change	*Change in repository design*
Application to WMA C: *Addressed in the performance assessment. See Sections 1-3 for a summary.*		
Potentially deleterious FEP*: Uncertainties in repository assumptions are addressed in sensitivity analyses for various safety functions. PA Maintenance is required to address changes in actual disposal relative to assumptions in the PA.*		

Future human action assumptions	0.05
Definition: The assumptions made in the assessment concerning general boundary conditions for assessing future human actions.	
Comment: *For example, it can be expected that human technology and society will develop over the timescales of relevance for repository safety assessment. However, this development is unpredictable. Therefore, it is usual to make some assumptions in order to constrain the range of future human activities that are considered.*	
Key concepts, examples, and related FEPs	
Only present day technologies will be considered *Only technologies practised in the past will be considered* *Description of human society development* *Description of general human society* *The past is an accurate reflection of the future*	
Application to WMA C: *Addressed in DOE Order 435.1.* ***Potentially deleterious FEP****: Not applicable*	

Future human behaviour (target group) assumptions	0.06
Definition: The assumptions made concerning potentially exposed individuals or population groups that are considered in the assessment.	
Comment: *Doses or risks are usually estimated for critical groups (individuals or groups) thought to be representative of the individuals or population groups that may be at highest risk or receive the highest doses as a result of the disposed wastes and repository. This is the accepted approach for assessing radiological risk or dose to members of the public resulting from a source of radioactive release to the environment. To assess the doses or risks at times in the far future, when the characteristics of potentially exposed populations are unknown, a hypothetical critical group, or groups, is/are usually defined*	
Key concepts, examples, and related FEPs	
Description of an actual critical group *Description of a hypothetical critical group*	
Application to WMA C: *Addressed in DOE Order 435.1.* ***Potentially deleterious FEP****: Not applicable DOE Order 435.1 requires evaluation at the location and time of peak concentration during the compliance period, so deleterious assumptions are part of the application of the FEP.*	

Dose response assumptions	0.07
Definition: Those assumptions made in an assessment in order to convert received dose to a measure of risk to an individual or population.	

Comment: *Usually this will refer to individual human dose response, e.g. by a dose-risk conversion factor where the factor is the probability of a specified health effect per unit of radiation exposure. If other organisms are considered then a risk to individual organisms or a species might be considered. The variation of a given response or human health effect (e.g. cancer incidence, cancer mortality) with the amount of radiation dose an individual or a group of individuals received is referred to as the dose-response relation. It is not possible to determine the shape of the dose response curve at low doses with any precision, because the incidence of health effects is very low. A linear dose-response relation with no dose threshold is generally assumed cautious (See ICRP 60).*

Key concepts, examples, and related FEPs

None

Application to WMA C: *Addressed in DOE Order 435.1.*

Potentially deleterious FEP*: Not applicable*

Assessment purpose	0.08

Definition: The purpose for which the assessment is being undertaken.

Comment: *The aim of the assessment is likely to depend on the stage in the repository development project at which the assessment is carried out and may also affect the scope of assessment*

Key concepts, examples, and related FEPs

Site selection	*Demonstrate the feasibility of a disposal concept*	*Public confidence*
Demonstrate regulatory compliance	*Rehabilitation of contaminated site*	*System optimization*
Concept design		

Application to WMA C: *Addressed in the performance assessment. See Section 2.*

Potentially deleterious FEP*: Not applicable*

Regulatory requirements and exclusions	0.09

Definition: The specific terms or conditions in the national regulations or guidance related to all stages of the repository that will influence the post closure safety assessment.

Comment: *Regulatory requirements and exclusions may be expressed in terms of release, dose or risk limits or targets to individuals or populations effective over a specified timescale; they may also make demands about procedures following closure of the repository. In some regulations, the long-term scenarios to be assessed are specified, or some scenarios or events are specifically ruled out of consideration.*

Key concepts, examples, and related FEPs		
Independence of safety from control	*Environmental protection standards*	*Multi-factor safety case*
Optimization	*Quality assurance*	*Radiological protection standards*
Effects in the future	*Quality control*	
Application to WMA C: *Addressed in DOE Order 435.1.*		
Potentially deleterious FEP*: Not applicable*		

Model and data issues	0.10
Definition: Model and data issues in the context of a safety assessment, refers to general (i.e. methodological) issues affecting the assessment modelling process and use of data during the process.	
Comment: *A post-closure safety assessment is an attempt to quantify the exposure or risk posed by a radioactive waste disposal site to future generations of humanity and their environment. Intrinsically, to do this one can say that the observations needed for the safety assessment of a site should be carried out for the life span of the proposed disposal facility. However, this is neither physically possible nor desirable. The only viable approach to perform a complete radiological safety assessment is to try to obtain as much observational data as possible, on a limited time scale, and then simulate the future behaviour of the disposal system through what is known as a model.*	
Key concepts, examples, and related FEPs	
Treatment of uncertainty	*Modelling studies*	*Data availability*
Method of handling site data	*Model and data reduction/simplification*	*Application of conservatism*
Assessment philosophy		
Application to WMA C: *Addressed in the performance assessment. See Sections 1 – 3 for a summary.*	
Potentially deleterious FEP*: Not applicable*	

EXTERNAL FACTORS	1
Definition: FEPs with causes or origin outside the disposal system domain, i.e. natural or human factors of a more global nature and their immediate effects. Included in this category are decisions related to repository design, operation and closure since these are outside the temporal boundary of the disposal system domain for post-closure assessment.	
Comment: *"External Factors" is a category in the International FEP List and is divided into sub-categories.*	

REPOSITORY ISSUES	1.1
Definition: Decisions on designs and waste allocation (repository type), and also events related to site investigation, operations and closure (site context).	
Comment: *"Repository Issues" is a sub-category of External Factors in the International FEP List and is divided into individual FEPs.*	

Site investigation		1.1.01
Definition: FEPs related to the investigations that are carried out at a potential repository site in order to characterize the site both prior to repository excavation and during construction and operation.		
Comment: *Site investigation activities provide detailed site-specific performance assessment data and information necessary for the safety case to demonstrate the suitability of the site and to establish baseline conditions*		
Key concepts, examples, and related FEPs		
Geography and demography	*Aquifer tests*	*Ecological features*
Meteorology and climatology (regional and local)	*Investigative boreholes*	*Pre-operational monitoring programme*
Geology and seismology	*Biosphere characteristics*	*Hydrogeology characteristics*
Hydrology characteristics	*Natural resources*	*Geohydrological characteristics*
Geotechnical characteristics	*Geochemical characteristics*	*Geomorphology characteristics*
Application to WMA C: *Relevant to the performance assessment. See Section 4 for a discussion of site investigations.*		
Potentially deleterious FEP*: Drywells and boreholes may have the potential to provide relative fast paths through the vadose zone under some wetting conditions. Alternative conceptual models with preferential flow paths through the vadose zone are included in the PA.*		

Design, repository	1.1.02
Definition: FEPs related to the design of the repository including both the safety concept, i.e. the general features of design and how they are expected to lead to a satisfactory performance, and the more detailed engineering specification for excavation, construction and operation.	
Comment: *The repository design and construction is established in a general way in the disposal concept for the repository which is based on expected host lithology characteristics, waste and backfill characteristics, construction technology, and economics. Repository design includes the principle design features that are designed to provide long-term isolation of disposed waste, minimize the need for continued active maintenance after site closure, and improve the site's natural characteristics in order to protect public health and the environment. There may, nevertheless, be a range of engineering design and construction options still open. As the repository project proceeds, and more detailed site-specific information becomes available, the range of options may be constrained and decisions will be made. At any stage, repository safety assessments may only analyse a subset of the total range of option. (See FEP 1.103).*	

Key concepts, examples, and related FEPs
The general repository design features (e.g. host lithology, waste form, backfill, waste packages, construction technology, etc.) *The principle design criteria or considerations for normal and abnormal condition* *Operational monitoring programme*
Application to WMA C: *Relevant to the performance assessment. See Section 4.*
Potentially deleterious FEP*: Not applicable*

Construction, repository	1.1.03
Definition: FEPs related to the construction (e.g., excavation) of shafts, tunnels, disposal galleries, silos, trenches, vaults, etc. of a repository, as well as the stabilisation of these openings and installation/assembly of structural elements according to the design criteria.	
Comment:*. Repository construction refers to the implementation of the design considerations and specifically to the construction of features of the repository necessary to provide long-term isolation of disposed waste, minimize the need for continued active maintenance after site closure, and improve the site's natural characteristics in order to protect public health and the environment. In addition, it includes the construction methods. (See FEP 1.102).*	
Key concepts, examples, and related FEPs	
Drilling of borehole *Construction of walls, floors, mounds, layers of mounds* *Control and diversion of water* *Excavation of trenches, holes, vaults* *Site plans, engineering drawing, and construction specifications* *Site preparations* *Construction equipment*	
Application to WMA C: *Relevant to the performance assessment. For WMA C this relates both to past facility construction (Section 4), and to emplacement of grout and cover.*	
Potentially deleterious FEP*: Potential degradation of safety functions associated with the engineered components of the system may result from failure of quality control. A range of cover performance is assumed in various sensitivity cases.*	

Emplacement of wastes and backfilling	1.1.04
Definition: FEPs related to the placing of wastes (usually in containers) at their final position within the repository and placing of buffer and/of backfill materials in the disposal zone.	
Comment: *Some waste types and inventories may require special waste emplacement arrangements to simplify the disposal practice, to ensure safety or to ensure structure stability in the repository area. The backfill material is used to refill excavated portions of the repository or any void spaces left unfilled after waste has been emplaced (see also FEP 1.1.07).*	

Key concepts, examples, and related FEPs
Emplacement method *Filling of void spaces between the containers and in the rest of the repository* *Covering of waste in-between containers*
Waste emplacement configuration
Application to WMA C: *Relevant to the performance assessment with respect to the infill grout emplacement and cover emplacement.*
Potentially deleterious FEP*: Safety functions associated with the grout and cover may be degraded by incorrect emplacement of the materials. Emplacement of grout must take due account of heat of hydration and shrinkage A range of cover performance is assumed in various sensitivity cases.*

Closure, repository	1.1.05
Definition: FEPs related to the cessation of waste disposal operations at a site, the backfilling and sealing of boreholes type facilities, and the capping and covering of trenches, vaults, etc.	
Comment: *The term closure refers to the status of, or an action directed at a disposal facility at the end of its operational life. A disposal facility is placed under permanent closure usually after completion of waste emplacement, by covering a near surface disposal facility, by backfilling and/or sealing of a borehole type facility, and termination and completion of activities in any associated structure. The intention of repository capping and sealing is to prevent infiltrating water as well as human access to the wastes. Individual sections of a repository may be closed in sequence, but closure usually refers to final closure of the whole repository, and will probably include removal of surface installations. The schedule and procedure for capping, sealing and closure may need to be considered in the assessment.*	
Key concepts, examples, and related FEPs	
Trench/vault capping *Backfilling of boreholes* *Decontamination and decommissioning plan*	
Site stabilisation *Removal of surface structures* *Post-operational monitoring programme*	
Cover construction *Closure procedures* *Closure compartments*	
Application to WMA C: *Relevant to the performance assessment with respect to the infill grout emplacement and cover emplacement.*	
Potentially deleterious FEP*: Safety functions associated with the grout and cover may be degraded by incorrect closure. Emplacement of grout must take due account of heat of hydration and shrinkage. A range of cover performance is assumed in various sensitivity cases.*	

Records and markers, repository	1.1.06
Definition: FEPs related to the retention of records of the content and nature of a repository after closure and also the placing of permanent markers at or near the site.	
Comment: *It is expected that records will be kept to allow future generations to recall the existence and nature of the repository following closure. In some countries, the use of site markers has been proposed where the intention is that the location and nature of the repository might be recalled even in the event of a lapse of present-day administrative controls.*	

Key concepts, examples, and related FEPs		
Records of the content and nature of the repository	*Disposal unit and boundary markers*	*Site markers*
	Archive of the records	
Application to WMA C: *Addressed as part of institutional control assumptions in DOE Order 435.1.*		
Potentially deleterious FEP*: Safety functions associated with institutional control are treated conservatively by requirements in DOE Order 435.1. Reduction of these safety functions is not credible.*		

Waste allocation	1.1.07
Definition: FEPs related to the choices on allocation of wastes to the repository, including waste type(s) and amount(s).	
Comment: *The waste type and waste allocation is established in a general way in the repository disposal concept. There may, however, be a number of options concerning these factors. Final decisions may not be made until the repository is operating and will be subject to regulation. In safety assessments, assumptions may need to be made about future waste arisings and future waste allocation strategies (see also FEP 1.1.04).*	

Key concepts, examples, and related FEPs		
Waste allocation description	*Future waste allocation strategies*	*Waste acceptance criteria for the repository*
Future waste arisings	*Projected inventories*	
Application to WMA C: *Not applicable for tank closure. The FEP relates to future waste arisings.*		
Potentially deleterious FEP*: Not applicable*		

Quality control	1.1.08
Definition: FEPs related to quality assurance and control procedures and tests during the design, construction and operation of the repository, as well as the manufacture of the waste forms, containers and engineered features.	
Comment: *It can be expected that a range of quality control measures will be applied during construction and operation of the repository, as well as to the manufacture of the waste forms, containers etc. In an assessment these may be invoked to avoid analysis of situations which, it is expected, can be prevented by quality control. There may be specific regulations governing quality control procedures, objectives and criteria.*	

Key concepts, examples, and related FEPs		
Defects in construction of disposal system	*Improper or faulty waste emplacement and backfilling*	*Defects during the conditioning of the waste*
Defects in the construction of container		*Defects in cap constructions*

Application to WMA C: *Relevant grout emplacement, and cover emplacement.*

Potentially deleterious FEP*: Safety functions associated with grout and cover may be degraded if there is a failure of quality control. A range of cover performance is assumed in various sensitivity cases.*

Schedule and planning	1.1.09
Definition: FEPs related to the sequence of events and activities occurring during repository excavation, construction, waste emplacement and sealing.	
Comment: *Relevant events may include phased construction of units and emplacement of wastes, backfilling, sealing, capping and closure of sections of the repository after wastes are emplaced, and monitoring activities to provide data on the transient behaviour of the system or to provide input to the final assessment. The sequence of events and time between events may have implications for long term performance, e.g. decline of activity and heat production from the wastes, material degradation, chemical and hydraulic changes during a prolonged "open" phase.*	
Key concepts, examples, and related FEPs *Phased construction of units* *Planning of monitoring activities to provide data on the transient behaviour of the system* *Phased emplacement of wastes, backfilling, sealing, capping and closure of sections of the repository*	
Application to WMA C: *Project timing assumed in the performance assessment is consistent with assumptions in the TC&WM EIS.* ***Potentially deleterious FEP****: Alterations in project timing have the potential to affect safety functions associated with the grout and cover. Not foreseen as a significant issue while tanks are relatively intact.*	

Administrative control, repository site	1.1.10
Definition: FEPs related to measures to control events at or around the repository site, both during the operational period and after closure.	
Comment: *The responsibility for administrative control of the site before closure of the repository during the construction and operational phases, and subsequently following closure of the repository may not be the same. Furthermore, the type of administrative control may vary depending on the stage in the repository lifetime.*	
Key concepts, examples, and related FEPs *None*	
Application to WMA C: *Addressed in multiple DOE Orders and policies. See Section 2.* ***Potentially deleterious FEP****: Safety functions associated with institutional control are treated conservatively by requirements in DOE Order 435.1. Reduction of these safety functions is not credible.*	

Monitoring of repository	1.1.11
Definition: FEPs related to any monitoring that is carried out during operations or following closure of sections of, or the total, repository. This includes monitoring for operational safety and also monitoring of parameters related to the long-term safety and performance.	
Comment: *The extent and requirement for such monitoring activities may be determined by repository design and host lithology, regulations and public pressure.*	
Key concepts, examples, and related FEPs	
Pre-operational monitoring programme *Post-operational monitoring programme* *Operational monitoring programme*	
Application to WMA C: *Will be addressed in the performance maintenance plan.*	
Potentially deleterious FEP*: Not applicable, although potential preferential pathways through the vadose zone are addressed.*	

Accidents and unplanned events	1.1.12
Definition: FEPs related to accidents and unplanned events during construction, waste emplacement and closure, which might have an impact on long-term performance or safety.	
Comment:*. Accidents are events that are outside the range of normal operations although the possibility that certain types of accident may occur should be anticipated in repository operational planning. Unplanned events include accidents but could also include deliberate deviations from operational plans.*	
Key concepts, examples, and related FEPs	
Deviations from operations in response to an accident *Unexpected waste arising during operations* *Increase in waste delivery*	
Reduction in waste delivery *Unexpected geological event* *Earlier than anticipated container failure*	
Earlier than anticipated cap failure *Deliberate deviations from operational plans*	
Application to WMA C: *Relevant to the performance assessment.*	
Potentially deleterious FEP*: Early degradation of cap safety function from unanticipated events; unexpected geological event may lead to early degradation of hydraulic safety functions in the engineered system. Early failure of barriers is addressed in sensitivity cases.*	

Retrievability	1.1.13
Definition: FEPs related to any special design, emplacement, operational or administrative measures that might be applied or considered in order to enable or ease retrieval of wastes.	
Comment: *Designs may specifically allow for retrieval or rule it out. In some cases, an interim period might be planned, between waste emplacement and final repository closure, during which time retrieval is possible.*	

Key concepts, examples, and related FEPs

None

Application to WMA C: *Not relevant to the tank closure performance assessment. Waste has been retrieved to the extent practicable as documented in Retrieval Completion Certifications.*

Potentially deleterious FEP*: Not applicable*

GEOLOGICAL PROCESSES AND EFFECTS	1.2
Definition: Processes arising from the wider geological setting and long-term processes	
Comment*. "Geological Processes and Effects" is a sub-category of External Factors in the International FEP List and is divided into individual FEPs.*	

Orogeny and related tectonic processes at plate boundaries	1.2.01
Definition: Rock deformation and translation (commonly referred to as tectonics) of this nature arises when rock masses belonging to different plates either collide against each other or slide past each other. Literally speaking, orogeny is the process of formation of mountains, often occurring over periods of a few million years, but up to several tens of millions of years.	
Comment: *By present geological usage, orogeny is the process by which structures within mountain areas were formed through processes that include thrusting, folding and faulting in the lithosphere. The latter h is the name given to the rigid, outermost layer of the earth, made up predominantly of solid rock which are affected by processes such as metamorphism, plutonism, and, at great depth (>10 km), by plastic folding. .* *The term folding is generally used to imply the shortening of strata that results from the formation of fold structures on a broad scale, and sometimes has the connotation of general deformation of which the actual folding is only a part. A fault is a fracture in the Earth's crust accompanied by displacement of one side of the fracture relative to the other, from a few cm to several kilometres. Orogenic belts are typically characterized by compressive reverse faults as this lead to crustal shortening and duplication of geological formations. Transform faults typically occur where crustal plates slide past each other without colliding (e.g. the St. Andrea fault in California) and the relative displacement can be in the order of thousands of kilometers. Fractures and joints may be caused by compressional or tenisonal forces in the earth crust but do not present displacement between the rocks on each side. These forces may result in the reactivation of of existing faults or, less likely, in the generation of new ones* *It is important to acknowledge that orogenic processes experience periods of quiescence alternating with periods of paroxismand that such periods are not necessarily synchronous along the whole length of an orogenic belt.* ***Implications to near-surface disposal systems:*** *This type of movements should be considered with great care since orogenic processes can lead, in areas of active collision (e.g. Chile, Turkey, Iran, Morocco) to the propagation of fault and thrust planes up to the surface. In such events (see seismicity) extreme ground fracturing, faulting could lead to breakage of containment barriers*	

Key Concepts, examples, and related FEPs

Collision of the Earth's crustal plates

Transcurrent, strike-slip faults

Thrusts: low-angle reverse faults;

Subduction zones

Faulting and folding of lithosphere: Thin skinned tectonics vs. Thick skinned tectonics

Metamorphism, anatexis (partial melting/ migmatization), and plastic folding in the inner and deeper layer

Granitic to granodioritic batholiths; calc-alkaline igneous activity

Orogeny,

Neotectonics

Application to WMA C: *Not relevant on the time scale of the performance assessment.*

Potentially deleterious FEP*: Not applicable*

Anorogenic and within-plate tectonic processes (Deformation, elastic, plastic or brittle)	1.2.02

Definition: FEPs related to the physical deformation of geological structures in the interior of continental or oceanic plates in response to stress fields generated either at plate margins or in regions of anomalous stress. This includes mainly faulting and fracturing of rocks and, less frequently, also their compression and folding rocks.

Comment. *The term folding is generally used for the compression of strata in the formation of fold structures on a broad scale, and sometimes has the connotation of general deformation of which the actual folding is only a part. A fault is a fracture in the Earth's crust accompanied by displacement of one side of the fracture relative to the other, from a few centimetres to a few kilometres on scale. Fractures may be caused by compressional or tensional forces in the Earth's crust. Such forces may result in the activation of existing faults and, less likely, the generation of new faults.*

Implications to near-surface disposal systems: *Within the timescales of concern, deformation is unlikely to have an effect on near-surface disposal systems*

Key Concepts, examples, and related FEPs

Faulting: normal, extensional faults

Extrusion

Neotectonics

Alkaline volcanism, volcanoes

Dyke swarms

Fractures

Fracturing

Compression of rocks

Rifting, rift valleys

Horst and grabens

Jointing, master joints

Hot springs

Basin and range

Continental; break- up

Uplift axes

Stress field

Cross-fabrics

Application to WMA C: *Not relevant on the time scale of the performance assessment.*

Potentially deleterious FEP*: Not applicable*

Seismicity		1.2.03
Definition: FEPs related to seismic events and the potential for seismic events. Rapid relative movements within the Earth's crust, usually along existing faults or geological interfaces cause a seismic event. The accompanying release of energy may result in ground movement and/or rupture, e.g. earthquakes.		
Comment: *Seismic events may result in changes in the physical properties of rocks due to stress changes and induced hydrological changes. Seismic events are most common in tectonically active or volcanically active regions at crustal plate margins, less commonly they also occur in the interior of continental/oceanic plates. The seismic waves that are generated by a tectonic or volcanic disturbance of the ocean floor may result in a seismic (giant) sea wave, known as a tsunami. These may be amplified by submarine soft sediment slumps along steep continental margins. In extreme cases, soil liquefaction has been reported in areas where soils and sedimentary strata of appropriate moisture content and composition are subjected to strong seismic shaking.*		
Key Concepts, examples, and related FEPs		
Change in the physical properties of rocks due to stress changes	*Faulting*	*Seismic swarms*
Hydrological changes	*Tsunami*	*Soil liquefaction*
	Earthquakes	*Aftershocks*
Application to WMA C: *Relevant to the performance assessment in considering the longevity of safety functions for the engineered barriers.*		
Potentially deleterious FEP*: The primary potential effects on the disposal system is degradation of hydraulic safety functions of the tank, grout, and base mat. Other safety functions would be unaffected. Potential for preferential pathways is considered in the sensitivity cases.*		

Volcanic and magmatic activity		1.2.04
Definition: FEPs related to volcanic and magmatic activities. Magma is molten, mobile rock material, generated below the Earth's crust, which gives rise to igneous rocks when solidified. Magmatic activity occurs when there is intrusion of magma into the crust. A volcano is a vent or fissure in the Earth's surface through which molten or part-molten materials (lava) may flow, and ash and hot gases be expelled.		
Comment: *The high temperatures and pressures associated with volcanic and magmatic activity may result in permanent changes in the surrounding rocks; this process is referred to as metamorphism but is not confined to volcanic and magmatic activity (see FEP 1.2.05). Intrusive magmatic activity refers to the process of emplacement of magma in pre-existing rock. Extrusive magmatic activity refers to the process whereby magma are ejected onto the surface of the Earth.*		
Key Concepts, examples, and related FEPs		
Temperature and pressure rise	*Intrusive magmatic activity*	*Pyroclastic explosion / flow / cloud*
Change in surrounding rocks	*Extrusive magmatic activity*	*Fumaroles*
Slope tilting	*Lava flows*	*Hydrothermal alteration*
	CO_2 emissions	

Application to WMA C: *Relevant to WMA C as potential ash fall from future volcanic events in the region.*

Potentially deleterious FEP*: The effect of prior eruptions is included in the paleo record of infiltration. The effects of past ash fall events is therefore included in the uncertainty range in infiltration.*

Metamorphism	1.2.05
Definition: FEPs induced by the mineralogical and structural adjustment of solid rock to physical and chemical conditions, which have been imposed by the action of heat (T>200 C) and pressure at great depths (usually several kilometres) beneath the Earth's surface or near magmatic activity.	
Comment: *Metamorphic processes are unlikely to be important at typical repository depths, but past metamorphic history of a host lithology may be very important to understanding its present-day characteristics.* ***Implications to near-surface disposal systems:*** *Within the timescales of concern, metamorphism is unlikely to have an effect on near-surface disposal systems.*	
Key Concepts, examples, and related FEPs *Metamorphic history of a host lithology*	
Application to WMA C: *Not relevant on the time scale of the performance assessment.* ***Potentially deleterious FEP****: Not applicable*	

Hydrothermal activity	1.2.06
Definition: FEPs associated with high temperature groundwater, including processes such as density-driven groundwater flow and hydrothermal alteration of minerals in the rocks through which the high temperature groundwater flows.	
Comment: *Groundwater temperature is determined by the large-scale geological and petrophysical properties of the rock formations (e.g. radiogenic heat formation, thermal conductivity), as well as the hydrogeological characteristics (e.g. hydraulic conductivity) of the rock and by the tectonic environment. (neotectonic deformation, extension).* ***Implications to near-surface disposal systems:*** *Within the timescales of concern, hydrothermal activity is unlikely to have an effect on typical near-surface disposal systems.*	
Key Concepts, examples, and related FEPs *Hydrothermal synthesis* — *Hydrothermal alterations of minerals in the rocks* — *Scalding springs* *Density driven groundwater flow* — *Hydrothermal metamorphism*	
Application to WMA C: *Not relevant to the WMA C geological setting.* ***Potentially deleterious FEP****: Not applicable*	

Erosion and sedimentation			1.2.07
Definition: FEPs related the large-scale (geological) removal and accumulation of rocks and sediments, with associated changes in topography and geological/hydrogeological conditions of the repository host lithology.			
Comment: *Erosion is the process or group of processes whereby the earthy and rocky materials of the Earth's crust are loosened, dissolved, or worn away, and simultaneously removed from one place to another, by natural agencies that include weathering, solution, corrosion, and transportation. Compare FEP 2.3.12, which is concerned with more local processes over shorter periods of time. Sedimentation is the act or process of forming or accumulating sediment in layers, including such processes as the separation of rock particles from the material from which the sediment is derived, the transportation of these particles to the site of deposition or settling of the particles, the chemical and other (diagenetic) changes occurring in the sediment, and the ultimate consolidation of the sediment into solid rock.* ***Implications to near-surface disposal systems:*** *Within the timescales of concern, large scale erosion and sedimentation are unlikely to have an effect on near-surface disposal systems.*			
Key Concepts, examples, and related FEPs			
Change in topography, uplift	*Deposition of sediment*	*Stream erosion*	
Coastal erosion	*Changes in geological conditions*	*Changes in hydrogeological conditions*	
Application to WMA C: *Relevant to the performance assessment in considering the longevity of safety functions for the engineered cover.* ***Potentially deleterious FEP****: The primary potential effects on the disposal system is degradation of the infiltration safety functions of the cover. Other safety functions would be unaffected. Potential increases in infiltration through the cover are addressed in sensitivity cases.*			

Diagenesis and pedogenesis	1.2.08
Definition: The processes by which deposited sediment, at or near the Earth's surface are formed into rocks by compaction, cementation and crystallisation, i.e. under conditions of temperature and pressure normal to the upper few kilometres of the earth's crust.	
Comment: *Diagenesis include all the chemical, physical, and biological changes, modifications, or transformations undergone by a sediment after its initial deposition, and during and after its lithification, exclusive or surficial alteration (weathering) and metamorphism. It embraces those non-destructive or reconstructive processes (e.g., consolidation, compaction, cementation, reworking, authigenesis, replacement, solution, precipitation, crystallisation, oxidation, reduction, leaching, hydration, polymerisation, adsorption, bacterial action, and formation of concretions) that occur under conditions of pressure and temperature that are normal to the surficial or outer part of the Earth's crust.* *Pedogenesis represents the mode of origin of soils, with reference to the factors responsible for the formation of "solum", or true soil, from unconsolidated parent material. Pedogenesis may have an effect on the behaviour of near surface disposal systems as it involves geohydrologic, atmospheric and biological processes (burrowing animals, plant roots activity/invasion) operation at or near surface on time scales of few hundred to thousands of years* ***Implications to near-surface disposal systems:*** *Within the timescales of concern, diagenesis is unlikely to have an effect on near-surface disposal systems*	

Key Concepts, examples, and related FEPs   *None*
Application to WMA C: *Not relevant to the WMA C geological setting.*   ***Potentially deleterious FEP****: Not applicable*

Salt diapirism and dissolution	1.2.09
Definition: The long-term evolution of salt formations. Diapirism is the lateral or vertical intrusion or upwelling of either buoyant or non-buoyant rock into overlying strata (the overburden) from a source layer. Dissolution of the salt may occur where the evolving salt formation is in contact with groundwater with salt content below saturation.	
Comment: *Diapirism is most commonly associated with salt formations where a salt diapir comprises a mass of salt that has flowed in a ductile manner from a source layer and pierces or intrudes into the over-lying rocks. The term can also be applied to magmatic or migmatic intrusion.* ***Implications to near-surface disposal systems:*** *Within the timescales of concern, salt diapirism and dissolution are unlikely to have an effect on near-surface disposal system.*	
Key Concepts, examples, and related FEPs *Diapirism* *Brine pockets*	
Application to WMA C: *Not relevant to the WMA C geological setting.* ***Potentially deleterious FEP****: Not applicable*	

Hydrological/hydrogeological response to geological changes	1.2.10
Definition: FEPs related to changes in the hydrological or hydrogeological regime arising from the large-scale geological changes listed in FEPs 1.2.01 to 1.2.09.	
Comment: *These could include changes of hydrological boundary conditions due to effects of erosion on topography, changes of hydraulic properties of saturated and unsaturated zones due to changes in rock stress or fault movements, or a change in the geochemical behaviour of the saturated and unsaturated zones. In and below low-permeability geological formations, hydrogeological conditions may evolve very slowly and often reflect past geological conditions, i.e. be in a state of disequilibrium*	
Key Concepts, examples, and related FEPs *Geochemical change* *Changes in hydraulic properties* *Changes of hydrological boundary conditions*	
Application to WMA C: *Regional scale geological changes may influence the Columbia River, which has a controlling influence on aquifer flow under the Central Plateau.* ***Potentially deleterious FEP****: Potential effects on the saturated zone flow safety functions. Variations in saturated zone flow are considered in sensitivity analyses.*	

CLIMATIC PROCESSES AND EFFECTS	1.3
Definition: Processes related to global climate change and consequent regional effects.	
Comment: "Climatic Processes and Effects" is a sub-category of External Factors in the International FEP List and is divided into individual FEPs.	

Climate change, global	1.3.01
Definition: FEPs related to the possible future, and evidence for past, long-term change of global climate. This is distinct from resulting changes that may occur at specific locations according to their regional setting and also climate fluctuations, c.f. FEP 1.3.02.	
Comment: *The last two million years of the Quaternary have been characterized by glacial/interglacial cycling. According to the Milankovitch Theory, the Quaternary glacial/interglacial cycles are caused by long term changes in seasonal and latitudinal distribution of incoming solar radiation which are due to the periodic variations of the Earth's orbit about the Sun (Milankovitch cycles). The direct effects are magnified by factors such as changes in ice, vegetation and cloud cover, and atmospheric composition.*	
Key Concepts, examples, and related FEPs	
Description of global climate changes	*Changes in ice, vegetation and cloud cover*	*Isostatic movement (c.f. FEP 1.3.03)*
Changes in atmospheric composition	*Greenhouse effect*	*Glaciation (large scale)*
Eustatic change (c.f. FEP 1.3.03)		
Application to WMA C: *Climate change may affect infiltration and saturated zone flow safety functions. However, global climate changes are expressed locally in these processes. See FEP 1.3.02. See Section 3 for a discussion of the basis for long term precipitation estimation.*	
Potentially deleterious FEP*: Not relevant.*	

Climate change, regional and local	1.3.02
Definition: FEPs related to the possible future changes, and evidence for past changes, of climate at the repository site. This is likely to occur in response to global climate change, but the changes will be specific to situation, and may include shorter-term fluctuations, c.f. FEP 1.3.01.	
Comment: *Climate is characterized by a range of factors including temperature, humidity, precipitation and pressure as well as other components of the climate system such as oceans, ice and snow, biota and the land surface. The Earth's climate varies by location and for convenience broad climate types have been distinguished in assessments, e.g. tropical, savannah, mediterranean, temperate, boreal and tundra. Climatic changes lasting only a few decades are referred to as climatic fluctuations. These are unpredictable at the current state of knowledge although historical evidence indicates the degree of past fluctuations.*	

Key Concepts, examples, and related FEPs

Climate fluctuations	*Description of regional and local climate change*	*Increase/decrease in temperature*
Increase/decrease in precipitation)		

Application to WMA C: *Climate change may affect infiltration and saturated zone flow. However, global climate changes are expressed locally in these processes. See FEP 1.3.01. See Section 3 for a discussion of the basis for long term precipitation estimation.*

Potentially deleterious FEP*: Changes in infiltration associated with climate change are uncertain. Regional scale modelling shows either increases or decreases in future infiltration, with the magnitude of the changes within the pattern of the paleo record. The response of the aquifer system to climate change is uncertain. Climate change may potentially affect safety functions for the cover and for the saturated zone. Ranges of infiltration and aquifer flow are considered in sensitivity cases.*

Sea level change 1.3.03

Definition: FEPs related to changes in sea level, which may occur as a result of global (eustatic) change and regional geological change, e.g. isostatic movements.

Comment: *The component of sea-level change involving the interchange of water between land ice and the sea is referred to as eustatic change. As ice sheets melt so the ocean volume increases and sea levels rise. Sea level at a given location will also be affected by vertical movement of the land mass, e.g. depression and rebound due to glacial loading and unloading, referred to as isostatic change (c.f. FEP 1.3.01).*

Key Concepts, examples, and related FEPs

Flooding	*Saline intrusion into repository or geosphere*	*Change in the hydrogeological regime*

Application to WMA C: *Sea level change may affect Columbia River stage, with subsequent influence on aquifer flow.*

Potentially deleterious FEP*: Potential effect on saturated zone safety functions by alteration of the gradient.*

Periglacial effects 1.3.04

Definition: FEPs related to the physical processes and associated landforms in cold but ice-sheet-free environments. This may be at the immediate margins of former and existing glaciers and ice sheets or an environment in which frost actions is dominant.

Comment: *An important characteristic of periglacial environments is the seasonal change from winter freezing to summer thaw with large water movements and potential for erosion. The frozen subsoils are referred to as permafrost. Meltwater of the seasonal thaw is unable to percolate downwards due to permafrost and saturates the surface materials, this can result in a mass movement called solifluction (literally soil-flow). Permafrost layers may isolate the deep hydrological regime from surface hydrology, or flow may be focused at "taliks" (localized unfrozen zones, e.g. under lakes, large rivers or at regions of groundwater discharge).*

Key Concepts, examples, and related FEPs

Large water movement	*Strong seasonal influences*	*Permafrost*
Erosion	*Soil flow (movement) – solifluction*	*Saturation of surface materials*

Application to WMA C: *Not relevant on the time scale of the performance assessment. However, pollen data records provide information that extends through past glacial cycles. See Section 3.*

Potentially deleterious FEP*: Not applicable*

Glacial and ice sheet effects, local	1.3.05

Definition: FEPs related to the effects of glaciers and ice sheets within the region of a repository, e.g. changes in the geomorphology, erosion, meltwater and hydraulic effects. This is distinct from the effect of large ice masses on global and regional climate, c.f. FEPs 1.3.01, 1.3.02.

Comment: *Erosional processes (abrasion, over-deepening) associated with glacial action, especially advancing glaciers and ice sheets, and with glacial meltwaters beneath the ice mass and at the margins, can lead to morphological changes in the environment e.g. U-shaped valleys, hanging valleys, fjords and drumlins. Depositional features associated with glaciers and ice sheets include moraines and eskers. The pressure of the ice mass on the landscape may result in significant and even depression of the regional crustal plate.*

Key Concepts, examples, and related FEPs

Erosional processes (abrasion, over-deepening)

Hydrogeological change

Transportation and depositional processes and features (Moraines Eskers)

Morphological changes (Hanging valleys, Fjords, Drumlins)

Depression of the regional crustal plate

Application to WMA C: *Not relevant on the time scale of the performance assessment.*

Potentially deleterious FEP*: Not applicable*

Warm climate effects (tropical and desert)	1.3.06

Definition: FEPs related to warm tropical and desert climates, including seasonal effects, and meteorological and geomorphological effects special to these climates.

Comment: *Regions with a tropical climate may experience extreme weather patterns (monsoons, hurricanes), that could result in flooding, storm surges, high winds etc. with implications for erosion and hydrology. The high temperatures and humidity associated with tropical climates result and soils are generally thin. In arid climates, total rainfall, erosion and recharge may be dominated by infrequent storm events.*

Key Concepts, examples, and related FEPs

Extreme weather patterns	*Alkali flats*	*Effective recharge*
Monsoons	*Infrequent storm events*	*Change in hydrological regime*
Hurricanes	*High rainfall*	*Rapid biological degradation*
Flooding	*High winds*	*Erosion*
Storm surges		

Application to WMA C: *Relevant in evaluation of the infiltration rate. See Section 3.*

Potentially deleterious FEP*: Effects are included in estimates and uncertainties in the infiltration rate.*

Hydrological/hydrogeological response to climate changes 1.3.07

Definition: FEPs related to changes in the hydrological and hydrogeological regime, e.g. recharge, sediment load and seasonality, in response to climate change in a region.

Comment: *The hydrology and hydrogeology of a region is closely coupled to climate. Climate controls the amount of precipitation and evaporation, seasonal ice cover and thus the soil water balance, extent of soil saturation, surface runoff and groundwater recharge. Vegetation and human actions may modify these responses.*

Key Concepts, examples, and related FEPs

Change in groundwater recharge	*Change in regional precipitation/infiltration/evaporation*	*Change in surface runoff*
Change in sediment load	*Change in seasonal ice cover*	*Increase in groundwater velocity*
Change in soil water balance		*Creation of local ponds*

Application to WMA C: *Relevant in evaluating the infiltration rate.*

Potentially deleterious FEP*: This FEP has the potential to affect the cover infiltration safety function. Effects of climate change on infiltration are included in the range of rates derived from the paleo record on precipitation. Potential anthropogenic effects are within the range of past climates. See Section 3.*

Ecological response to climate changes 1.3.08

Definition: FEPs related to changes in ecology, e.g. vegetation, plant and animal populations, in response to climate change in a region.

Comment: *The ecology of an environment is linked to climate. Ecological adaptation has allowed flora and fauna to survive and exploit even the most hostile of environments. For example, cacti have evolved to survive extreme heat and desiccation of the desert environment, and certain plant species complete their entire lifecycle over very short time periods following rare rain events in the desert. Some tree and plant species have evolved to survive natural events such as forest fires, and may require them to complete their lifecycle*

Key Concepts, examples, and related FEPs		
Desert formation	*Change in animal life*	*Ecological adaptation*
Change in vegetation		
Application to WMA C: *Relevant in evaluating the infiltration rate.*		
Potentially deleterious FEP*: This FEP has the potential to affect the cover infiltration safety function by altering the plant community over the waste. Variation in infiltration rates are considered, barrier testing has included conditions following loss of vegetation.*		

Human response to climate changes		1.3.09
Definition: FEPs related to changes in human behaviour, e.g. habits, diet, size of communities, in response to climate change in a region.		
Comment: *Human response is closely linked to climate. Climate affects the abundance and availability of natural resources such as water, as well as the types of crops that can be grown. The more extreme a climate, the greater the extent of human control over these resources is necessary to maintain agricultural productivity, e.g. through the use of dams, irrigation systems, controlled agricultural environments (greenhouses).*		
Key Concepts, examples, and related FEPs		
Change in human habits	*Increase/decrease in usage of irrigation systems*	*Effect of climate change on water availability*
Effect of climate change on food chain	*Change in population density*	*Construction of dams*
Change in agricultural activities/products	*Change in diet*	
Application to WMA C: *Addressed in the exposure assessment requirements in DOE Order 435.1.*		
Potentially deleterious FEP*: Not applicable.*		

Other geomorphologic changes	1.3.10
Definition: FEPs related to geomorphologic (also known as physiography) changes on a regional and local scale, i.e. the general configuration of the Earth's surface.	
Comment: *Geomorphology refers to the classification, description, nature, origin and development of present landforms and their relationships to underlying structures, and of the history of geologic changes as recorded by these surface features. The term is especially applied to the generic interpretation of landforms, but has also been restricted to features produced only by erosion and deposition.*	
Key Concepts, examples, and related FEPs	
Denudation	

Application to WMA C: *Relevant in to WMA C in the morphological changes associated with adding the cover, with increased depth to the waste.*

Potentially deleterious FEP*: Not applicable*

FUTURE HUMAN ACTIONS (ACTIVE)	1.4
Definition: Human actions and regional practices, in the post-closure period, that can potentially affect the performance of the engineered and/or geological barriers, e.g. intrusive actions, but not the passive behaviour and habits of the local population, c.f. 2.4.	
Comment: *Human Actions (Active)" is a sub-category of the External Factors in the International FEP List and is divided into individual FEPs.*	

Human influences on climate	1.4.01
Definition: FEPs related to human activities that could affect the change of climate either globally or in a region.	
Comment: *These activities could be intentional or unintentional, with an indirect influence more than a direct influence on the climate.*	
Key Concepts, examples, and related FEPs	
De-forestation *Emissions of 'greenhouse' gases such as CO_2 and CH_4*	
Application to WMA C: *Relevant in evaluating the infiltration rate. Projected anthropogenic effects on future climates may be either increases or decreases in infiltration rate.*	
Potentially deleterious FEP*: This FEP has the potential to affect the cover infiltration safety function. Effects of climate change on infiltration are included in the range of rates derived from the paleo record on precipitation. Potential anthropogenic effects are within the range of past climates.*	

Motivation and knowledge issues (inadvertent/deliberate human actions)	1.4.02
Definition: FEPs related to the degree of knowledge of the existence, location and/or nature of the repository. Also, reasons for deliberate interference with, or intrusion into, a repository after closure with complete or incomplete knowledge.	
Comment: *Some future human actions e.g. see FEPs 1.4.03 and 1.4.04, could directly impact upon the repository performance. Many assessments distinguish between:* - *inadvertent actions, which are actions taken without knowledge or awareness of the repository, and* - *deliberate actions, which are actions that are taken with knowledge of the repository's existence and location, e.g. deliberate attempts to retrieve the waste, malicious intrusion and sabotage.* *Intermediate cases, of intrusion with incomplete knowledge, could also occur.*	

Key Concepts, examples, and related FEPs

Human intrusion (instigate mechanical processes

Incomplete knowledge intrusion)

Deliberate actions e.g. war, sabotage, waste recovery, malicious intrusion

Inadvertent actions e.g. exploratory drilling, resource mining, archaeological intrusion

Application to WMA C: *Not relevant for the WMA C performance assessment, since this FEP relates to probability of occurrence of inadvertent intrusion, which is not taken credit for in the assessment. Advertent intrusion is generally excluded from consideration in the international community of performance assessment.*

Potentially deleterious FEP*: Not applicable.*

Drilling activities (human intrusion)	1.4.03
Definition: FEPs related to any type of drilling activity near the repository.	
Comment: *These activities may be taken with or without knowledge of the repository and in fact is a subgroup of FEP 1.4.02.*	

Key Concepts, examples, and related FEPs

Exploratory and/or exploitation drilling for natural resources and raw materials

Drilling for research or site characterization studies

Water well drilling

Drilling for waste injection

Drilling for hydrothermal resources

Extraction of valuable components of the disposed waste

Application to WMA C: *Relevant to the intrusion scenario.*

Potentially deleterious FEP*: Addressed in the evaluation of inadvertent intrusion.*

Mining and other underground activities (human intrusion)	1.4.04
Definition: FEPs related to any type of mining or excavation activity carried out near the repository.	
Comment: *These activities may be taken with or without knowledge of the repository and in fact is a subgroup of FEP 1.4.02.*	

Key Concepts, examples, and related FEPs

Resource mining;

Excavation for industry;

Geothermal energy production

Mine drillings

Shaft construction, underground construction and tunnelling

Recovery of repository materials (re-use of waste)

The presence of mine galleries - after closure

Malicious intrusion, sabotage or war

Injection of liquid wastes and other fluids

Scientific underground investigation

Underground nuclear testing

Application to WMA C: *Drilling activities accounted for in the drilling intrusion scenario. Other mining activities excluded based on lack of resources as WMA C. Potential for intrusive activities is also limited by depth of waste disposal and presence of intrusion barriers.*

Potentially deleterious FEP*: Not applicable.*

Un-intrusive site investigation	1.4.05

Definition: FEPs related to airborne, geophysical or other surface-based investigation of a repository site after repository closure

Comment: *Such investigation, e.g. prospecting for geological resources, might occur after information of the location of a repository had been lost. The evidence of the repository itself, e.g. discovery of an old shaft, might itself prompt investigation, including research of historical archives.*

Key Concepts, examples, and related FEPs

Prospecting for geological resources

Investigation of an old shaft

Research of historical archives

Application to WMA C: *Not relevant as this FEP relates to probabilities of intrusion, which are not taken credit for in the performance assessment.*

Potentially deleterious FEP*: Not applicable.*

Surface excavations	1.4.06

Definition: FEPs related to any type of human activities during surface excavations that can potentially affect the performance of the engineered and/or natural (geological) barriers, or the exposure pathways.

Comment: *This FEP relates to the surface environment. Strictly speaking, excavation refers to an act or process of removing soil and or rock materials from one location and transporting them to another. This may include, for example, digging, blasting, breaking, loading and hauling, which may result in direct human intrusion in the case of a near-surface repository.*

Key Concepts, examples, and related FEPs

Quarrying, trenching, ploughing	*Dredging of sediments in estuaries*	*Shallow excavations for site investigations*
Digging, blasting, breaking, loading, hauling	*Excavation for construction (earthworks)*	*Excavation for military purposes*
Recycling of materials	*Excavation for storage or disposal*	

Application to WMA C: *Home construction basement scenario excluded based on depth of waste disposal and presence of intrusion barriers.*

Potentially deleterious FEP*: Not applicable.*

Pollution	1.4.07

Definition: FEPs related to any type of human activities associated with pollution that can potentially affect the performance of the engineered and/or natural (geological) barriers, or the exposure pathways.

Comment: *As used here, it refers to the alteration of the chemical composition of the surface environment in the vicinity of the repository, in such a way that the performance of the disposal system is influenced.*

Key Concepts, examples, and related FEPs

Acid rain	*Soil pollution*	*Groundwater pollution*
Chemical liquid waste disposal	*Soil fertilization*	

Application to WMA C: *Relevant to WMA C in potential changes to the degradation rates of the engineered barriers. Effects of past leaks on vadose zone properties.*

Potentially deleterious FEP*: Potential effects in engineered barrier safety functions related to flow reduction. Effects of past leaks on vadose zone properties.*

Site development	1.4.08

Definition: FEPs related to any type of human activities during site development that can potentially affect the performance of the engineered and/or natural (geological) barriers, or the exposure pathways

Comment: *As used here, site development refers to alterations to the surface environment after memory of the repository has been lost. These alterations may result in direct human intrusion in the near-surface facility, or to an alteration of the host lithology or topography.*		
Key Concepts, examples, and related FEPs		
Site occupation	*Construction of roads, houses, buildings, dams, etc.*	*Residential, industrial, transport and road construction*
Levelling of hills (e.g., airport lay out)	*Human modification of the site drainage*	*Land reclamation/extension*
Application to WMA C: *Relevant to WMA C in potential changes to the degradation rates of the cover.*		
Potentially deleterious FEP*: Potential effects in the cover function for infiltration considered in sensitivity cases.*		

Archaeology	1.4.09
Definition: FEPs related to any type of human activities associated with archaeology that can potentially affect the performance of the engineered and/or natural (geological) barriers, or the exposure pathways.	
Comment: *As used here, the FEP refers to archaeological investigations in the surface environment.*	
Key Concepts, examples, and related FEPs	
Archaeological, inadvertent human intrusion	*Archaeological artefacts find during construction*
Application to WMA C: *Not relevant as this FEP relates to probabilities of intrusion, which are not taken credit for in the performance assessment.*	
Potentially deleterious FEP*: Not applicable.*	

Water management (wells, reservoirs, dams)	1.4.10
Definition: FEPs related to groundwater and surface water management including water extraction, reservoirs, dams, and river management.	
Comment: *Water is a valuable resource and water extraction and management schemes provide increased control over its distribution and availability through construction of dams, barrages, canals, pumping stations and pipelines. Groundwater and surface water may be extracted for human domestic use (e.g. drinking water, washing), agricultural uses (e.g. irrigation, animal consumption) and industrial uses. Extraction and management of water may affect the movement of radionuclides to and in the surface environment.*	

Key Concepts, examples, and related FEPs		
Waterworks	*Intentional artificial groundwater recharge/discharge by humans*	*Extraction of contaminated water from aquifer via a well*
Artificial mixing of lakes	*Dam, barrage, canals, pumping stations and pipeline building*	*Impoundment of water for fishing/fish farming, bathing*
Reservoirs	*Desalination of water in estuaries and marines*	*Groundwater/surface water extraction for irrigation, animal consumption, drinking water, washing*
Industrial usage	*Drainage systems*	*Salt production*
Human effects on water potential		
Chemical liquid waste disposal		
Application to WMA C: *Water management activities on the Columbia River have the potential to affect river stage.*		
Potentially deleterious FEP*: Potential effects on the saturated zone safety functions are consider in sensitivity cases for aquifer flow.*		

Social and institutional developments	1.4.11
Definition: FEPs related to changes in social patterns and degree of local government, planning and regulation.	
Comment: *The decisions made in future concerning social and institutional development may have a significant influence on the disposal system, e.g., if a change in land use is promulgated or a change in the regulatory requirements.*	
Key Concepts, examples, and related FEPs	
Loss of archives/records, loss/degradation of societal memory	*Changes in land use*
Changes in planning controls and environmental legislation	*Change in regulatory requirements*
Demographic change and urban development	*Change in institutional control*
Application to WMA C: *Excluded from consideration in DOE Order 435.1.*	
Potentially deleterious FEP*: Not applicable.*	

Technological developments	**1.4.12**
Definition: FEPs related to future developments in human technology and changes in the capacity and motivation to implement technologies. This may include retrograde developments, e.g. loss of capacity to implement a technology.	

Comment: *Of interest are those technologies that might change the capacity of man to intrude deliberately or otherwise into a repository, to cause changes that would affect the movement of contaminants, to affect the exposure or its health implications. Technological developments are likely but may not be predictable especially at longer times into the future. In most assessments, assumptions are made to limit the scope of consideration.*
Key Concepts, examples, and related FEPs *Retrograde developments* *Loss of capacity to implement technology*
Application to WMA C: *Excluded from consideration in DOE Order 435.1.* ***Potentially deleterious FEP****: Not applicable.*

Remedial actions	1.4.13
Definition: FEPs related to actions that might be taken following repository closure to remediate problems with a waste repository that, either, was not performing to the standards required, had been disrupted by some natural event or process, or had been inadvertently or deliberately damaged by human actions.	
Comment:	
Key Concepts, examples, and related FEPs *None*	
Application to WMA C: *Excluded from consideration in DOE Order 435.1.* ***Potentially deleterious FEP****: Not applicable.*	

Explosions and crashes	1.4.14
Definition: FEPs related to deliberate or accidental explosions and crashes such as might have some impact on a closed repository, e.g. underground nuclear testing, aircraft crash on the site, acts of war.	
Comment:	
Key Concepts, examples, and related FEPs *Intrusions by war, sabotage, terrorism* *Likelihood of crashes onto surface facilities, e.g. plane crashes* *Underground nuclear testing*	
Application to WMA C: *Potentially relevant to the performance of the cover, but very low probability of occurrence.* ***Potentially deleterious FEP****: Potential relevance to the surface barrier safety function for infiltration. However, it is excluded from consideration based on very low probability of occurrence.*	

DISPOSAL SYSTEM DOMAIN: ENVIRONMENTAL FACTORS	2
Definition: Features and processes occurring within that spatial and temporal (post-closure) domain whose principal effect is to determine the evolution of the physical, chemical, biological and human conditions of the domain that are relevant to estimating the release and migration of radionuclides and consequent exposure to man.	
Comment: *"Disposal System Domain: Environmental Factors" is a category in the International FEP List and is divided into sub-categories.*	

WASTES AND ENGINEERED FEATURES	2.1
Definition: Features and processes within the waste and engineered components of the disposal system. (output – source term characteristics)	
Comment: *"Wastes and Engineered Features" is a sub-category of Disposal Domain:Environmental Factors in the International FEP List and is divided into individual FEPs.* *Note that FEPs 2.1.01 to 2.1.06 describe the features in the disposal system, in other words, a description of the system as it is constructed, whereas FEPs 2.1.07 to 2.1.11 describe the processes or the changes in the disposal system.*	

Inventory, radionuclide and other material	2.1.01
Definition: FEPs related to the total content of the repository of a given type of material, substance, element, individual radionuclides, total radioactivity or inventory of toxic substances.	
Comment: *The FEP often refers to content of radionuclides but the content of other materials, e.g. steels, other metals, concrete or organic materials, could be of interest.*	
Key Concepts, examples, and related FEPs	
Radionuclide content *Concrete or organic material content* *Steel and other metal content*	

Waste form materials, characteristics and degradation processes	2.1.02
Definition: FEPs related to the physical, chemical, biological characteristics of the waste form at the time of disposal and as they may evolve in the repository, including FEPs which are relevant specifically as waste degradation processes.	
Comment: *The waste form will usually be conditioned prior to disposal, e.g. by solidification and inclusion of grout materials. The waste form is a component of the waste package. The waste characteristics will evolve due to various processes that will be affected by the physical and chemical conditions of the repository environment. Processes that are relevant specifically as waste degradation processes, as compared to general evolution of the near field, are included in this FEP.*	

Key Concepts, examples, and related FEPs		
Physical degradation	*Ash*	*Activated metal*
Chemical degradation	*Cloves, clothing, plastics, paper wood*	*Sludges, evaporation residue, compacted solids, filters*
Solid matrix of resin, bitumen, cement	*Spent sources*	
Application to WMA C: *Relevant to the performance assessment.*		
Potentially deleterious FEP*: Uncertainties in the inventory of residual waste and its chemical and physical form. Uncertainty in the final amounts of waste in as-yet unretrieved tanks.*		

Container materials, characteristics and degradation/failure processes		2.1.03
Definition: FEPs related to the physical, chemical, biological characteristics of the container at the time of disposal and as they may evolve in the repository, including FEPs that are relevant specifically as container degradation/failure processes.		
Comment: *The container refers to the vessel into which the waste form is placed for handling, transportation, storage and or disposal. It is also the outer barrier protecting the waste from external intrusions. The container is a component of the waste package.*		
Key Concepts, examples, and related FEPs		
Container degradation/failure processes	*Concrete containers*	*Lead containers*
Metal drums	*Stainless steel containers*	
Application to WMA C: *Not relevant to the performance assessment. Waste is not containerized*		
Potentially deleterious FEP*: Not applicable.*		

Buffer/backfill materials, characteristics and degradation processes	2.1.04
Definition: FEPs related to the physical, chemical, biological characteristics of the buffer and/or backfill at the time of disposal and as they may evolve in the repository, including FEPs that are relevant specifically as buffer/backfill degradation processes. (Effect on hydrology / flow)	
Comment: *Buffer and backfill are sometimes used synonymously. In some HLW/spent fuel concepts, the term buffer is used to mean material immediately surrounding a waste container and having some chemical and/or mechanical buffering role whereas backfill is used to mean material used to fill other underground openings. However, in ILW/LLW concepts the term backfill is used to describe the material placed between waste containers, which may have a chemical role. Buffer/backfill materials may include clays, cement and mixtures of cement with aggregates, e.g. of crushed rock.* *The buffer/backfill characteristics will evolve due to various processes that will be affected by the physical and chemical conditions of the repository environment. Processes, which are relevant specifically as buffer/backfill degradation processes, as compared to general evolution of the near field, are included in this FEP.*	

Key Concepts, examples, and related FEPs
Buffer/backfill degradation processes *Clay, cement, sand, soil* *Mixture of clay and crushed rock*
Bentonite clay
Application to WMA C: *Relevant to the performance assessment as the grout infill.*
Potentially deleterious FEP*: Uncertainty in the performance of the grout is considered in sensitivity and uncertainty analysis.*

Engineered barrier system characteristics and degradation processes	2.1.05
Definition: FEPs related to the design, physical, chemical, hydraulic etc. characteristics of the cavern/tunnel/shaft seals at the time of sealing and closure and also as they may evolve in the repository, including FEPs which are relevant specifically as cavern/tunnel/shaft seal and cap degradation processes. (Effect on hydrology / flow – change over time).	
Comment: *Cavern/tunnel/shaft seal and cap failure may result from gradual degradation processes, or may be the result of a sudden event. The importance is that alternative routes for groundwater flow and radionuclide transport may be created along the various layers and tunnels and/or shafts and associated EDZ (see FEP 2.2.01).*	
Key Concepts, examples, and related FEPs	
Engineered caps (cover) *Intrusion resistance caps* *Cap materials: clay, concrete*	
Cover degradation	
Application to WMA C: *Relevant to the performance assessment as the tank structure, base mat, and cover system.*	
Potentially deleterious FEP*: Uncertainties in the current state and long term performance of the engineered barriers is addressed in sensitivity and uncertainty analysis.*	

Other engineered features materials, characteristics and degradation processes	2.1.06
Definition: FEPs related to the physical, chemical, biological characteristics of the engineered features (other than containers, buffer/backfill, caps and seals) at the time of disposal and also as they may evolve in the repository, including FEPs which are relevant specifically as degradation processes acting on the engineered features.	
Comment: *Examples of other engineered features are rock bolts, shotcrete, tunnel liners, silo walls, any services and equipment not removed before closure. The engineered features, materials and characteristics will evolve due to various processes that will be affected by the physical and chemical conditions of the repository environment. Processes which are relevant specifically as degradation processes acting on the features, as compared to general evolution of the near field, are be included in this FEP.*	

Key Concepts, examples, and related FEPs		
Trenches, holes, vaults *Walls, floors, mounds, layers of mounds* *Rock bolts, tunnel liners, silo walls*	*Reduction in flow through structures due to impermeable membrane and subsequent degradation of impermeable membrane*	*Cut-off walls* *Degradation processes*
Application to WMA C: *Relevant to pipes and structures associated with ancillary equipment.* ***Potentially deleterious FEP****: Not applicable, as the ancillary equipment is treated conservatively in the base case,*		

Mechanical processes and conditions (in wastes and EBS)		2.1.07
Definition: FEPs related to the mechanical processes that affect the wastes, containers, seals and other engineered features, and the overall mechanical evolution of near field with time. This includes the effects of hydraulic and mechanical loads imposed on wastes, containers and repository components by the surrounding geology.		
Comment:		
Key Concepts, examples, and related FEPs		
Waste and container compression *Container collapse* *Buffer swelling pressure* *Material volume changes*	*Subsidence as a result of compression of waste and cover layers* *Fracture formation in vault, backfill, joints, cover materials, host geology (local fractures)*	*Container movement* *Differential behaviour of joints* *Tunnel roof or lining collapse*
Application to WMA C: *Relevant to the performance assessment in the influence of the FEP to conditions of the base mat.* ***Potentially deleterious FEP****: Potential degradation in the current state and future evolution of the base mat hydraulic safety function which is considered in the sensitivity and uncertainty analysis.*		

Hydraulic/hydrogeological processes and conditions (in wastes and EBS)	2.1.08
Definition: FEPs related to the hydraulic/hydrogeological processes that affect the wastes, containers, seals and other engineered features, and the overall hydraulic/hydrogeological evolution of near field with time. This includes the effects of hydraulic/hydrogeological influences on wastes, containers and repository components by the surrounding geology.	
Comment:	

Key Concepts, examples, and related FEPs		
Failure of drainage system *Failure of cut-off walls* *Failure of cap/cover*	*Modification of pore water by cover caused by chemical* *Interaction of vault material with pore water* *pH change*	*Osmotic effects* *Infiltration and movement of fluids in the repository environment* *Resaturation/desaturation of the repository or its components*
Failure of the joints *Bathtubbing* *Fracturing of concrete components* *Effect of cap+cover+backfill* *Influence of climate change* *Influence of saline intrusion* *Gas mediated water flow* *Interaction of backfill with pore water* *pH change* *Redox change* *Sulphate attack* *Effect of chelating agents*	*Redox potential change* *Mineralization* *Modification of pore water by cover* *Interaction of container material with pore water* *Matrix corrosion* *Gas generation* *Polymer degradation (high integrity containers)* *Mineralization change* *Osmotic effect* *Interaction of vault materials with host groundwater* *Carbonation*	*Water flow and contaminant transport paths within the repository* *Induced fluid effects caused by temperature change* *-Pressure change* *-Natural convection* *-Viscosity* *Reduction in flow through structures due to grouting* *Chloride attack* *Sulphate attack* *Colloid formation*
Application to WMA C: *Relevant to the performance assessment in the influence of the FEP to release and transport of waste from tanks and ancillary equipment.* ***Potentially deleterious FEP****: Uncertainty in the current state and future evolution of the safety functions of the waste, grout, tank, and base mat is considered in the sensitivity and uncertainty analysis*		

Chemical/geochemical processes and conditions (in wastes and EBS)	2.1.09
Definition: FEPs related to the chemical/geochemical processes that affect the wastes, containers, seals and other engineered features, and the overall chemical/geochemical evolution of near field with time. This includes the effects of chemical/geochemical influences on wastes, containers and repository components by the surrounding geology.	
Comment:	

Key Concepts, examples, and related FEPs		
Chemical interaction of backfill with pore water	*Chemical interaction of waste with pore water*	*Induced galvanic metallic corrosion*
pH changes	*Metallic corrosion processes (general and pitting)*	*Polymer degradation (high integrity containers)*
Redox changes	*Polymer degradation (resins)*	*Chemical interaction of backfill with containers (including overpacks)*
Sulphate attack	*Osmotic effects*	*Induced galvanic metallic corrosion*
Osmotic effects	*Chemical interaction of containers (including overpacks) with pore water*	*Polymer degradation (high integrity containers)*
Chemical interaction of vault materials with pore water	*Metallic corrosion*	*Chemical interaction of non-radioactive waste components with radioactive waste components*
pH changes	*Polymer degradation (high integrity containers)*	*pH changes*
Redox potential changes	*Osmotic effects*	*Redox potential changes*
Chemical interaction of vault materials with host groundwater	*Chemical interaction of waste with containers*	*Change in chemical reaction rate caused by temperature change*
Carbonation	*Precipitation/dissolution reactions*	*Electrochemical processes*
Chloride attack	*Evolution of redox (Eh) and acidity/alkalinity (pH) etc.*	*Chemical conditioning and buffering processes*
Sulphate attack	*Silting/pore closure*	
	Geochemical changes	
Application to WMA C: *Relevant to the performance assessment in the influence of the FEP to release and transport of waste from tanks and ancillary equipment.*		
Potentially deleterious FEP*: Uncertainty in the current state and future evolution of the chemical safety functions of the waste, grout, tank, and base mat is considered in the sensitivity and uncertainty analysis.*		

Biological/biochemical processes and conditions (in wastes and EBS)	2.1.10
Definition: FEPs related to the biological/biochemical processes that affect the wastes, containers, seals and other engineered features, and the overall biological/biochemical evolution of near field with time. This includes the effects of biological/biochemical influences on wastes, containers and repository components by the surrounding geology.	
Comment:	

Key Concepts, examples, and related FEPs

Microbial growth and poisoning

Microbially/biologically mediated processes

Effect of organic material

Microbial/biological effects of evolution of redox (Eh) and acidity/alkalinity (pH), etc.

Effect of organic materials

Change in microbial caused by change in temperature

Application to WMA C: *Relevant to the performance assessment in the influence of the FEP to release and transport of waste from tanks and ancillary equipment.*

Potentially deleterious FEP*: Uncertainty in the current state and future evolution of the chemical safety functions of the waste, grout, tank, and base mat is considered in the sensitivity and uncertainty analysis.*

Thermal processes and conditions (in wastes and EBS)	2.1.11

Definition: FEPs related to the thermal processes that affect the wastes, containers, seals and other engineered features, and the overall thermal evolution of the near field with time. This includes the effects of heat on wastes, containers and repository components from the surrounding geology.

Comment:

Key Concepts, examples, and related FEPs

Temperature evolution

Differential elastic response

Non-elastic response

Fracture aperture changes caused by the temperature change

Change in microbial activity

Radiogenic, chemical and biological heat production from the wastes

Chemical heat production from engineered features, e.g. concrete hydration

Change in chemical reaction rates e.g. corrosion

Temperature dependence of physical/chemical/ biological/hydraulic processes, e.g. corrosion and re-saturation

Fluid pressure, density viscosity changes

Induced chemical changes caused by the temperature change

Application to WMA C: *Applicable in the performance assessment, but heat generated in residual waste for expected retrievals is negligible.*

Potentially deleterious FEP*: Potential heat generation in tanks that retain substantial amounts of unretrievable waste, leading to effects on flow through the waste and EBS.*

Gas sources and effects (in wastes and EBS)	2.1.12

Definition: FEPs within and around the wastes, containers and engineered features resulting in the generation of gases and their subsequent effects on the repository system.

Comment: *Gas production may result from degradation and corrosion of various waste, container and engineered feature materials, as well as radiation effects. The effects of gas production may change local chemical and hydraulic conditions, and the mechanisms for radionuclide transport, i.e. gas-induced and gas-mediated transport.*

Key Concepts, examples, and related FEPs		
Explosion	*Gas generation*	*Degradation of vault, overpacks or backfill (instigate mechanical processes)*
Pressurisation	*Corrosion*	*Chemical interaction of containers (including overpacks) with pore water*
Radiation effects	*Decomposition of organic matter (microbial)*	*Chemical interaction of waste with containers*
		Chemical interaction of backfill with containers (including overpacks)
Application to WMA C: *Relevant to the performance assessment in analyses of releases to the atmosphere.*		
Potentially deleterious FEP*: Not applicable.*		

Radiation effects (in wastes and EBS)		2.1.13
Definition: FEPs related to the effects that result from the radiation emitted from the wastes that affect the wastes, containers, seals and other engineered features, and the overall radiogenic evolution of the near field with time.		
Comment: *Examples of relevant effects are ionization, radiolytic decomposition of water (radiolysis), radiation damage to waste matrix or container materials, helium gas production due to alpha decay.*		
Key Concepts, examples, and related FEPs		
Radiolysis	*Irradiation effects on metals, concrete*	*Concrete degradation*
Decay product gas generation	*Polymer degradation (resins and high integrity containers)*	*Metallic degradation*
Application to WMA C: *Applicable in the performance assessment, but negligible.*		
Potentially deleterious FEP*: None identified..*		
Nuclear criticality		2.1.14
Definition: FEPs related to the possibility and effects of spontaneous nuclear fission chain reactions within the repository.		
Comment: *A chain reaction is the self-sustaining process of nuclear fission in which each neutron released from a fission triggers, on average, at least one other nuclear fission. Nuclear criticality requires a sufficient concentration and localized mass (critical mass) of fissile isotopes (e.g. U-235, Pu-239) and also presence of neutron moderating materials in a suitable geometry; a chain reaction is liable to be damped by the presence of neutron absorbing isotopes (e.g. Pu-240).*		
Key Concepts, examples, and related FEPs		
Radiological criticality		

Application to WMA C: *Not relevant to the tank closure performance assessment. Waste inventory screened for potential for criticality.*

Potentially deleterious FEP*: Not applicable.*

Extraneous materials	2.1.15
Definition:	
Comment:	
Key Concepts, examples, and related FEPs *None*	
Application to WMA C: *Not relevant.* ***Potentially deleterious FEP****: Not applicable.*	

GEOLOGICAL ENVIRONMENT	2.2
Definition: The features and processes of the geological environment surrounding the repository including, for example, the hydrogeological, geomechanical and geochemical features and processes, both in pre-emplacement state and as modified by the presence of the repository and other long-term changes.	
Comment: *"Geological Environment" is a sub-category in the International FEP List and is divided into individual FEPs.* *Note that FEPs 2.2.01 to 2.2.06 describe the features in the disposal system, in other words, a description of the features of the system as it is constructed, whereas FEPs 2.2.07 to 2.2.11 describe the processes or the changes in the disposal system..*	

Disturbed zone, host lithology	2.2.01
Definition: FEPs related to the host lithology zone around the repository or any other underground openings that may be mechanically disturbed during construction, and the properties and characteristics as they may evolve both before and after repository closure.	
Comment: *The disturbed zone may have different properties to the undisturbed host lithology, e.g. opening of fractures or change of hydraulic properties due to stress relief.*	
Key Concepts, examples, and related FEPs *Fracture formed by the construction* *Change of hydraulic properties due to stress relief*	
Application to WMA C: *Relevant as the excavation zone for the tank farm.* ***Potentially deleterious FEP****: Not applicable.*	

Host lithology	2.2.02
Definition: FEPs related to the properties and characteristics of the lithology in/on which the repository is sited (excluding the zone disturbed by the construction) as they may evolve both before and after repository closure. In most cases, this FEP will be associated with the unsaturated zone.	
Comment: *Relevant properties include thermal and hydraulic conductivity, compressive and shear strength, porosity etc. In most cases, this FEP will be associated with the unsaturated zone (See FEP 2.2.03).*	
Key Concepts, examples, and related FEPs	
Thermal and hydraulic conductivity *Porosity* *Description of the host lithology*	
Compressive and shear strength	
Application to WMA C: *Relevant. Here host lithology is considered the H2 sand in which the facility resides.*	
Potentially deleterious FEP*: Uncertainties in the lithology and its properties could lead to mischaracterization of the vadose zone safety functions.*	

Lithological units, other	2.2.03
Definition: FEPs related to the properties and characteristics of the lithology other than the host lithology as they may evolve both before and after repository closure.	
Comment: *These lithological units are those that make up the region in which the repository is located. These units are identified in the geological investigations of the region. Each geological unit is characterized according to its geometry and its general physical properties and characteristics. Details concerning inhomogeneity and uncertainty associated with each unit are included in the characterization. In most cases, this FEP will be associated with the saturated zone (See FEP 2.2.02).*	
Key Concepts, examples, and related FEPs	
Non-uniform stratigraphy *Heterogeneity* *Description of the lithology units*	
Application to WMA C: *Relevant. Here "other lithological units" are those below WMA C (i.e. not the "host" lithology).*	
Potentially deleterious FEP*: Uncertainties in the lithology and its properties could lead to mischaracterization of the vadose zone and saturated zone safety functions.*	

Discontinuities, large scale (in geosphere)	2.2.04
Definition: FEPs related to the properties and characteristics of discontinuities in and between the saturated and unsaturated zones, including faults, shear zones, intrusive dykes and interfaces between different rock types.	
Comment:	

Key Concepts, examples, and related FEPs
Fault *Shear zones* *Interfaces between different rock types*
Intrusive dykes
Application to WMA C: *None identified.*
Potentially deleterious FEP*: Not applicable.*

Contaminant transport path characteristics (in geosphere)	2.2.05
Definition: FEPs related to the properties and characteristics of smaller discontinuities and features within saturated and unsaturated zones that are expected to be the main paths for contaminant transport through the geosphere, as they may evolve both before and after repository closure.	
Comment: *Groundwater flow and contaminant transport through rocks may occur in a variety of systems depending on the rock characteristics. Porous flow is predominantly through pores in the medium or through the interstitial spaces between small grains of materials. Fracture flow is predominantly along fractures in the rock which represent the only connected open spaces. Changes in the contaminant transport path characteristics due to the repository construction or its chemical influence etc. are included.*	
Key Concepts, examples, and related FEPs	
Fracture flow *Fracture-matrix interaction* *Porous flow*	
Application to WMA C: *Relevant and considered in sensitivity and uncertainty analysis using alternative conceptual models.*	
Potentially deleterious FEP*: Not applicable.*	

Mechanical processes and conditions (in geosphere)	2.2.06
Definition: FEPs related to the mechanical processes that affect the saturated and unsaturated zones, and the overall evolution of conditions with time. This includes the effects of changes in condition, e.g. rock stress, due to the excavation, construction and long-term presence of the repository.	
Comment:	
Key Concepts, examples, and related FEPs	
Subsidence *Upliftment*	
Application to WMA C: *Not relevant.*	
Potentially deleterious FEP*: None identified.*	

Hydraulic/hydrogeological processes and conditions (in geosphere)		2.2.07
Definition: FEPs related to the hydraulic and hydrogeological processes that affect the saturated and unsaturated zones, and the overall evolution of conditions with time. This includes the effects of changes in condition, e.g. hydraulic head, due to the excavation, construction and long-term presence of the repository.		
Comment: *The hydrogeological regime is the characterization of the composition and movement of water through the relevant geological formations in the repository region and the factors that control this. This requires knowledge of the recharge and discharge zones, the groundwater flow systems, saturation, and other factors that may drive the hydrogeology, such as density effects due to salinity gradients or temperature gradients. Changes of the hydrogeological regime due to the construction and/or presence of the repository are included.*		
Key Concepts, examples, and related FEPs		
Saline intrusion	*Groundwater discharge to surface water, Soil, Estuary, Seas, Wells*	*Saturated/unsaturated conditions*
Darcy flow	*Channelling and preferential flow pathways*	*Flow between two aquifers*
Non-Darcy flow	*Aquifer(groundwater) discharge/recharge (e.g. well)*	*Infiltration*
Fracture flow		*Flow direction*
Application to WMA C: *Relevant and considered in sensitivity and uncertainty analysis.*		
Potentially deleterious FEP*: None identified.*		

Chemical/geochemical processes and conditions (in geosphere)		2.2.08
Definition: FEPs related to the chemical and geochemical processes that affect the saturated and unsaturated zones, and the overall evolution of conditions with time. This includes the effects of changes in condition, e.g. Eh, pH, due to the excavation, construction and long-term presence of the repository.		
Comment: *The hydrochemical regime refers to the groundwater chemistry in the geological formations in the repository region, and the factors that control this. This requires knowledge of the groundwater chemistry including speciation, solubility, complexants, redox (reduction/oxidation) conditions, rock mineral composition and weathering processes, salinity and chemical gradients. Changes of the hydrochemical regime due to the construction and/or presence of the repository are included.*		
Key Concepts, examples, and related FEPs		
pH change	*pH effects of cement on the environment, soil, etc*	*Effect of non-radioactive solute plume*
Redox potential changes	*Mineralization changes*	
Application to WMA C: *Relevant.*		
Potentially deleterious FEP*: Potential effects of past leaks on the H2 sand below the tank farm.*		

Biological/biochemical processes and conditions (in geosphere)	**2.2.09**
Definition: FEPs related to the biological and biochemical processes that affect the saturated and unsaturated zones, and the overall evolution of conditions with time. This includes the effects of changes in condition, e.g. microbe populations, due to the construction and long-term presence of the repository.	
Comment:	
Key Concepts, examples, and related FEPs	
Generating of chelating agents *Influences on redox potential* *Microbiology-enhanced mobility*	
Influences on pH *Change in microbe population*	
Application to WMA C: *Relevant primarily in the potential effect on sorption coefficients in the geosphere.*	
Potentially deleterious FEP*: None identified.*	

Thermal processes and conditions (in geosphere)	**2.2.10**
Definition: FEPs related to the thermal processes that affect the saturated and unsaturated zones, and the overall evolution of conditions with time. This includes the effects of changes in condition, e.g. temperature, due to the construction and long-term presence of the repository.	
Comment: *Geothermal regime refers to sources of geological heat, the distribution of heat by conduction and transport (convection) in fluids, and the resulting thermal field or gradient. Changes of the geothermal regime due to the construction and/or presence of the repository are included*	
Key Concepts, examples, and related FEPs	
Bio-heat *Chemical reactions* *Change in temperature*	
Application to WMA C: *Not relevant except if future tank retrievals leave behind more waste than anticipated, with associated heat generation.*	
Potentially deleterious FEP*: Not applicable.*	

Gas sources and effects (in geosphere)	2.2.11
Definition: FEPs related to natural gas sources and production of gas within the geosphere and also the effect of natural and repository produced gas on the geosphere, including the transport of bulk gases and the overall evolution of conditions with time.	
Comment: *Gas movement in the geosphere will be determined by many factors including the rate of production, gas permeability and solubility, and the hydrostatic pressure regime.*	
Examples	
Natural gas intrusion	

Application to WMA C: *Not relevant.*

Potentially deleterious FEP*: Not applicable.*

Undetected features (in geosphere)	2.2.12
Definition: FEPs related to natural or man-made features within the geology that may not be detected during the site investigation.	
Comment: *Examples of possible undetected features are fracture zones, brine pockets or old mine workings. Some physical features of the repository environment may remain undetected during site surveys and even during pilot tunnel excavations. The nature of the geological environment will indicate the likelihood that certain types of undetected features may be present and the site investigation may be able to place bounds on the maximum size or minimum proximity to such features.*	
Key Concepts, examples, and related FEPs	
Boreholes (drillings) *Mine shafts or mine galleries*	*Faults, shear zones, Breccia pipes, Lava tubes, Intrusive dykes* □ *Gas or brine pockets*
Application to WMA C: *Potentially relevant, but none identified.* ***Potentially deleterious FEP****: Potential presence of undetected major undetected feature in the vadose zone such as a clastic dike is considered as a sensitivity case.*	

Geological resources	2.2.13
Definition: FEPs related to natural resources within the geosphere, particularly those that might encourage investigation or excavation at or near the repository site.	
Comment: *Geological resources could include oil and gas, solid minerals, water, and geothermal resources. For a near-surface repository, quarrying of near-surface deposits, e.g. sand, gravel or clay, may be of interest*	
Key Concepts, examples, and related FEPs	
Oil and gas *Sand, gravel, clay*	*Solid minerals* *Water*
Application to WMA C: *Relevant, only for potential use of water resources.* ***Potentially deleterious FEP****: None identified. Water resources included in the analysis.*	

SURFACE ENVIRONMENT	2.3
Definition: The features and processes within the surface environment, including near-surface aquifers and unconsolidated sediments but excluding human activities and behaviour, see 1.4 and 2.4..	
Comment: *Surface Environment" is a sub-category in the International FEP List and is divided into individual FEPs* *Note that FEPs 2.3.01 to 2.3.06 describe the features in the disposal system, in other words, a description of the features of the system as it is constructed, whereas FEPs 2.3.07 to 2.3.11 describe the processes or the changes in the disposal system.*	

Topography and morphology	**2.3.01**
Definition: FEPs related to the relief and shape of the surface environment and its evolution.	
Comment: *This FEP refers to local land form and land form changes with implications for the surface environment, e.g. plains, hills, valleys, and effects of river and glacial erosion thereon. In the long term, such changes may occur as a response to geological changes, see 1.3.*	
Key Concepts, examples, and related FEPs *Land forms* *Hills* *Valleys* *Plains*	
Application to WMA C: *Relevant, the closure cover changes the local topography.* ***Potentially deleterious FEP****: None identified.*	

Soil and sediment	**2.3.02**
Definition: FEPs related to the characteristics of the soils and sediments and their evolution.	
Comment: *Different soil and sediment types, e.g. characterized by particle-size distribution and organic content, will have different properties with respect erosion/deposition and contaminant sorption etc.*	
Key Concepts, examples, and related FEPs *Soil and sediment development* *Soil conversion*	
Application to WMA C: *Potentially relevant. Potential movement of sand dunes onsite. However, dune migration to the site would require regional changes in air currents.* ***Potentially deleterious FEP****: May cause changes in the recharge safety function considered in sensitivity and uncertainty analysis.*	

Aquifers and water-bearing features, near surface	2.3.03
Definition: FEPs related to the characteristics of aquifers and water-bearing features within a few metres of the land surface and their evolution.	
Comment: *Aquifers are water-bearing features geological units or near-surface deposits that yield significant amounts of water to wells or springs. The presence of aquifers and other water-bearing features will be determined by the geological, hydrological and climatic factors.*	
Key Concepts, examples, and related FEPs *Weathered aquifer* *Fractured aquifer* *Description of aquifers in repository region* *Sandy aquifer*	
Application to WMA C: *Relevant.* ***Potentially deleterious FEP****: Uncertainties in aquifer properties may lead to mischaracterization of the aquifer safety function.*	

Lakes, rivers, streams and springs	2.3.04
Definition: FEPs related to the characteristics of terrestrial surface water bodies and their evolution.	
Comment: *Streams, rivers and lakes often act as boundaries on the hydrogeological system. They usually represent a significant source of dilution for materials (including) radionuclides entering these systems, but in hot dry environments, where evaporation dominates, concentration is possible.*	
Key Concepts, examples, and related FEPs *Description of lakes, rivers, streams and springs in the repository region*	
Application to WMA C: *Not relevant owing to the DOE Order 435.1 assessment point. Discharges to the Columbia River are excluded from the analysis. However, the Columbia exerts an indirect influence on the system through its influence on the aquifer gradient.* ***Potentially deleterious FEP****: Not applicable*	

Coastal features	2.3.05
Definition: FEPs related to the characteristics of coasts and the near shore, and their evolution. Coastal features include headlands, bays, beaches, spits, cliffs and estuaries.	
Comment: *The processes operating on these features, e.g. active erosion, deposition, longshore transport, determine the development of the system and may represent a significant mechanism for dilution or accumulation of materials (including radionuclides) entering the system.*	

Key Concepts, examples, and related FEPs		
Description of the coastal features in the repository region	*Coastal surge*	*Temperature change*
Headlands, Bays, Beaches, Spits	*Storm*	*Recharge*
Cliffs, Estuaries	*tsunami*	*Bed-load processes*
Coastal erosion	*Groundwater discharge to estuary, shore*	*Flooding*
Saline intrusion	*Bioturbation*	*Plant/animal uptake/metabolism*
Salinity changes	*Tidal currents*	*Sand dune encroachment*
Sedimentation	*Sea spray*	*Coastal currents*
Resuspension	*Behaviour of coastal waters and marine sediment*	*Description of coastal features in vicinity of repository*
Volatilisation	*Estuarine changes*	*Beach development*
Application to WMA C: *Not relevant.*		
Potentially deleterious FEP*: Not applicable.*		

Marine features	2.3.06
Definition: FEPs related to the characteristics of seas and oceans, including the seabed, and their evolution. Marine features include oceans, ocean trenches, shallow seas, and inland seas.	
Comment: *Processes operating on these features such as erosion, deposition, thermal stratification and salinity gradients, determine the development of the system and may represent a significant mechanism for dilution or accumulation of materials (including radionuclides) entering the system.*	

Key Concepts, examples, and related FEPs		
Ocean trenches, shallow seas	*Marine sediment transport and deposition*	*Vertical mixing and isolation*
inland seas, Oceans	*Groundwater discharge towards sea*	*Salinity changes*
Sedimentation	*Sea spray*	*Plant/animal uptake/metabolism*
Resuspension	*Sediment transport*	*Bed-load processes*
Volatilisation	*Sea currents*	*Description of marine features in vicinity of repository*
Tidal currents	*Temperature change*	*Recharge*
Marine currents		
Application to WMA C: *Not relevant.*		
Potentially deleterious FEP*: Not applicable.*		

Atmosphere	2.3.07
Definition: FEPs related to the characteristics of the atmosphere, including capacity for transport, and their evolution.	
Comment:	
Key Concepts, examples, and related FEPs	
Physical transport of gases	*Chemical and photochemical reactions*	*Aerosols and dust in the atmosphere*
Application to WMA C: *Relevant to the performance objectives in Order 435.1. Effects of atmospheric FEPs are also relevant in a stylized way through the infiltration rate.*	
Potentially deleterious FEP*: None identified.*	

Vegetation	2.3.08
Definition: FEPs related to the characteristics of terrestrial and aquatic vegetation both as individual plants and in mass, and their evolution.	
Comment:	
Key Concepts, examples, and related FEPs	
Chemical changes caused by plants	*Description of the vegetation in vicinity of repository*

Application to WMA C: *Relevant to the estimation of recharge.*

Potentially deleterious FEP*: Potential changes to vegetation may affect cover infiltration safety function (considered in sensitivity and uncertainty analysis).*

Animal populations		2.3.09
Definition: FEPs related to the characteristics of the terrestrial and aquatic animals both as individual animals and as populations, and their evolution.		
Comment:		
Key Concepts, examples, and related FEPs		
Animal diets	*External contamination of animals*	*Description of the animal population in vicinity of repository*
Application to WMA C: *Relevant. The effects of native animal populations are embedded in the assumptions regarding cover performance and general infiltration rates. Historic recharge data considers very long time frames with varying climate.*		
Potentially deleterious FEP*: None identified.*		

Meteorology		2.3.10
Definition: FEPs related to the characteristics of weather and climate, and their evolution.		
Comment: *Meteorology is characterized by precipitation, temperature, pressure and wind speed and direction. The variability in meteorology should be included so that extreme events such as drought, flooding, storms and snow melt are identified.*		
Key Concepts, examples, and related FEPs		
Rainfall	*Climate fluctuation*	*Hurricanes*
Snowfall	*Dew-freezing cycles*	*High rainfall / Flooding*
Flooding related to high precipitation	*Wet-dry cycles*	*Temperature*
Storms related to strong winds	*Seasonality*	*Tsunamis*
Application to WMA C: *Relevant to the estimation of recharge.*		
Potentially deleterious FEP*: Potential changes to climate may affect infiltration safety function are considered in sensitivity and uncertainty analysis.*		

Hydrological regime and water balance (near-surface)	2.3.11
Definition: FEPs related to near-surface hydrology at a catchment scale and also soil water balance, and their evolution.	

Comment: *The hydrological regime is a description of the movement of water through the surface and near-surface environment. It includes the movement of materials associated with the water such as sediments and particulate. Extremes such as drought, flooding, storms and snowmelt may be relevant.*		
Key Concepts, examples, and related FEPs		
Surface run-off to marines/estuaries	*Groundwater discharge to surface water, soils, estuaries/marines*	*Change in lake or reservoir levels*
River flow to marines/estuaries	*Water discharge/recharge processes that effecting radionuclide content*	*Alkali flats*
Evaporation	*Stream silting*	*Stream and river flow changes*
Evapotranspiration		*River meander*
Infiltration		*Stream flow*
Application to WMA C: *Relevant to the estimation of recharge.*		
Potentially deleterious FEP*: Potential changes in surface conditions may affect infiltration safety function are considered in sensitivity and uncertainty analysis.*		

Erosion and deposition	2.3.12
Definition: FEPs related to all the erosional and depositional processes that operate in the surface environment, and their evolution.	
Comment: *Relevant processes may include fluvial and glacial erosion and deposition, denudation, eolian erosion and deposition. These processes will be controlled by factors such as the climate, vegetation, topography and geomorphology.*	

Key Concepts, examples, and related FEPs		
Deposition	*Coastal erosion due to rise and fall of lea level (Greenhouse effect)*	*Erosion by wave action, landslides or rockfalls*
Wind erosion related to storms	*Landsliding (instigate mechanical processes)*	*Agriculture erosion*
Erosion related to flooding	*Erosion (instigate mechanical processes)*	*Erosion of cover*
Erosion related to glaciation		*Weathering*
Application to WMA C: *Relevant to the estimation of recharge.*		
Potentially deleterious FEP*: Potential changes in surface conditions may affect infiltration safety function are considered in sensitivity and uncertainty analysis.*		

Ecological/biological/microbial systems	2.3.13
Definition: FEPs related to living organisms and relations between populations of animals, plants and their evolution.	

Comment: *Characteristics of the ecological system include the vegetation regime, and natural cycles such as forest fires or flash floods that influence the development of the ecology. The plant and animal populations occupying the surface environment are an intrinsic component of its ecology. The wide range of processes that define the ecological system regulates their behaviour and population dynamics. Human activities have significantly altered the natural ecology of most environments.*
Key Concepts, examples, and related FEPs
Ecological and biological features *Chemical changes caused by micro-organisms* *Chemical changes caused by plants*
Application to WMA C: *Relevant to the estimation of recharge.*
Potentially deleterious FEP*: Potential changes in ecology may affect infiltration safety function are considered in sensitivity and uncertainty analysis.*

Animal/Plant intrusion	2.3.14
Definition: Animal and plant intrusion leading to vault or trench disruption.	
Comment:	
Key Concepts, examples, and related FEPs	
Seeds *Root intrusion (instigate mechanical processes)* *Animal intrusion (instigate mechanical processes)*	
Burrowing animals *Bio-intrusion by plants and animals*	
Application to WMA C: *Not relevant. Precluded by depth of disposal. Considered in barrier design and testing.*	
Potentially deleterious FEP*: Not applicable.*	

HUMAN BEHAVIOUR	2.4
Definition: The habits and characteristics of the individuals or populations, e.g. critical groups, to whom exposures are calculated, not including intrusive or other activities which will have an impact on the performance of the engineered or geological barriers, see 1.4.	
Comment: *"Human Behaviour (passive)" is a sub-category in the International FEP List and is divided into individual FEPs.*	

Human characteristics (physiology, metabolism)	2.4.01
Definition: FEPs related to characteristics, e.g. physiology, metabolism, of individual humans.	
Comment: *Physiology refers to body and organ form and function. Metabolism refers to the chemical and biochemical reactions, which occur within an organism, or part of an organism, in connection with the production and use of energy.*	

Key Concepts, examples, and related FEPs
Physiological and metabolism description of humans that will be the subject of the assessment
Application to WMA C: *Relevant to dose factors. Addressed in DOE orders and standards (DOE-STD-1196-2011)*
Potentially deleterious FEP*: Not applicable.*

Adults, children, infants and other variations	2.4.02
Definition: FEPs related to considerations of variability, in individual humans, of physiology, metabolism and habits.	
Comment: *Children and infants, although similar to adults, often have characteristic differences, e.g. metabolism, respiratory rates, habits (e.g. pica, ingestion of soil) which may lead to different exposure characteristics.*	
Key Concepts, examples, and related FEPs	
None	
Application to WMA C: *Relevant to dose factors. Addressed in DOE orders and standards (DOE-STD-1196-2011)*	
Potentially deleterious FEP*: Not applicable.*	

Diet and fluid intake	2.4.03
Definition: FEPs related to intake of food and water by individual humans and the compositions and origin of intake.	
Comment:*. The human diet refers to the range of food products consumed by humans.*	
Key Concepts, examples, and related FEPs	
Diet	*Description of the human diet and assumptions regarding quantities/volume*
Application to WMA C: *Relevant to exposure factors for Order 435.1 all pathways analysis.*	
Potentially deleterious FEP*: Not applicable.*	

Habits (non-diet-related behaviour)	2.4.04
Definition: FEPs related to non-diet related behaviour of individual humans, including time spent in various environments, pursuit of activities and uses of materials.	

Comment: *The human habits refer to the time spent in different environments in pursuit of different activities and other uses of materials. Agricultural practices and human factors such as culture, religion, economics and technology will influence the diet and habits. Smoking, ploughing, fishing, and swimming are examples of behaviour that might give rise to particular modes of exposure to environmental contaminants.*

Key Concepts, examples, and related FEPs

Human habits	*Location of shielding factors*	*Bathing*
Resource usage	*Impoundment of water*	*Description of human habits and behaviour*
Storage of products	*Fishing/fish farming*	*Air filtration*
Ventilation		

Application to WMA C: *Relevant to exposure factors for Order 435.1 all pathways analysis.*

Potentially deleterious FEP*: Not applicable.*

Community characteristics	2.4.05

Definition: FEPs related to characteristics, behaviour and lifestyle of groups of humans that might be considered as target groups in an assessment.

Comment: *Relevant characteristics might be the size of a group and degree of self-sufficiency in food stuffs/diet. For example, hunter/gathering describes a subsistence lifestyle employed by nomadic or semi-nomadic groups who roam relatively large areas of land hunting wild game and/or fish, and gathering native fruits, berries, roots and nuts, to obtain their dietary requirements.*

Key Concepts, examples, and related FEPs

Demographic changes	*General human society description*

Application to WMA C: *Addressed in Order 435.1 guidance.*

Potentially deleterious FEP*: Not applicable.*

Food and water processing and preparation	2.4.06

Definition: FEPs related to treatment of foodstuffs and water between raw origin and consumption.

Comment: *Once a crop is harvested or an animal slaughtered it may be subject to a variety of storage, processing and preparational activities prior to human or livestock consumption. These may change the radionuclide distribution and/or content of the product. For example, radioactive decay during storage, chemical processing, washing losses and cooking losses during food preparation.*

Water sources may be treated prior to human or livestock consumption, e.g. chemical treatment and/or filtration.

Key Concepts, examples, and related FEPs
Water filtration *Food processing*
Application to WMA C: *Relevant to exposure factors for Order 435.1 all pathways analysis.*
Potentially deleterious FEP*: Not applicable.*

Dwellings	2.4.07
Definition: FEPs related to houses or other structures or shelter in which humans spend time.	
Comment: *Dwellings are the structures which humans live in. The materials used in their construction and their location may be significant factors for determining potential radionuclide exposure pathways.*	
Key Concepts, examples, and related FEPs	
Construction of buildings, houses *Ventilation* *Location and shielding factors*	
Site occupation	
Application to WMA C: *Relevant to exposure factors for Order 435.1 all pathways analysis.*	
Potentially deleterious FEP*: Not applicable.*	

Wild and natural land and water use	2.4.08
Definition: FEPs related to use of natural or semi-natural tracts of land and water such as forest, bush and lakes.	
Comment: *Special foodstuffs and resources may be gathered from natural land and water, which may lead to significant modes of exposure.*	
Key Concepts, examples, and related FEPs	
Natural and semi-natural environments	
Application to WMA C: *Relevant to exposure factors for Order 435.1 all pathways analysis.*	
Potentially deleterious FEP*: Not applicable.*	

Rural and agricultural land and water use (incl. fisheries)	2.4.09
Definition: FEPs related to use of permanently or sporadically agriculturally managed land and managed fisheries.	

Comment: *An important set of processes are those related to agricultural practices, their effects on land form, hydrology and natural ecology, and also their impact in determining uptake through food chains and other exposure paths.*		
Key Concepts, examples, and related FEPs		
Use of land for agriculture	*Land use change*	*Fishing/ fish farming in estuaries/marines*
Ploughing	*Fertilization*	
Application to WMA C: *Relevant to exposure factors for Order 435.1 all pathways analysis.*		
Potentially deleterious FEP*: Not applicable.*		

Urban and industrial land and water use		2.4.10
Definition: FEPs related to urban and industrial developments, including transport, and their effects on hydrology and potential contaminant pathways.		
Comment: *Human populations are concentrated in urban areas in modern societies. Significant areas of land may be devoted to industrial activities. Water resources may be diverted over considerable distances to serve urban and/or industrial requirements.*		
Key Concepts, examples, and related FEPs		
Water works	*Water extraction through wells*	*De-salination of water*
Urban and industrial environments	*Water extraction for irrigation*	*Human water extraction*
Application to WMA C: *Not relevant to analyses conducted for exposures under Order 435.1 all pathways analysis. Subsistence farmer scenario is more conservative.*		
Potentially deleterious FEP*: Not applicable.*		

Leisure and other uses of environment		2.4.11
Definition: FEPs related to leisure activities, the effects on the surface environment and implications for contaminant exposure pathways.		
Comment: *Significant areas of land, water, and coastal areas may be devoted to leisure activities e.g., water bodies for recreational uses, mountains/wilderness areas for hiking and camping activities.*		
Key Concepts, examples, and related FEPs		
Recreational land use	*Impoundment of water for bathing*	*Beach development*
Application to WMA C: *Not relevant to analyses conducted for exposures under Order 435.1 all pathways analysis. Subsistence farmer scenario is more conservative.*		
Potentially deleterious FEP*: Not applicable.*		

RADIONUCLIDE/CONTAMINANT FACTORS	3
Definition: FEPs that take place in the disposal system domain that directly affect the release and migration of radionuclides and other contaminants, or directly affect the dose to members of a critical group from given concentrations of radiotoxic and chemotoxic species in environmental media.	
Comment: *"Disposal System Domain: Radionuclide Factors" is a category in the International FEP List and is divided into sub-categories..*	

CONTAMINANT CHARACTERISTICS	3.1
Definition: The characteristics of the radiotoxic and chemotoxic species that might be considered in a post-closure safety assessment.	
Comment: *"Contaminant Characteristics" is a sub-category in the International FEP List and is divided into individual FEPs.*	

Radioactive decay and in-growth	3.1.01
Definition: Radioactivity is the spontaneous disintegration of an unstable atomic nucleus resulting in the emission of sub-atomic particles. Radioactive isotopes are known as radionuclides. Where a parent radionuclide decays to a daughter radionuclide so that the population of the daughter radionuclide increases this is known as in-growth.	
Comment: *In post-closure assessment models, radioactive decay chains are often simplified, e.g. by neglecting the shorter-lived radionuclides in transport calculations, or adding dose contributions from shorter-lived radionuclides to dose factors for the longer-lived parent in dose calculations*	
Key Concepts, examples, and related FEPs	
Production of aqueous progeny *Radon emanation*	
Application to WMA C: *Relevant.*	
Potentially deleterious FEP*: Not applicable.*	

Chemical/organic toxin stability	3.1.02
Definition: FEPs related to chemical stability of chemotoxic species.	
Comment:	
Key Concepts, examples, and related FEPs	
None	

Application to WMA C: *Not relevant in this performance assessment, which is focused only on radiological exposures.* ***Potentially deleterious FEP****: Not applicable.*

Inorganic solids/solutes	3.1.03
Definition: FEPs related to the characteristics of inorganic solids/solutes that may be considered.	
Comment:	
Key Concepts, examples, and related FEPs *Source terms content*	
Application to WMA C: *Relevant.* ***Potentially deleterious FEP****: None identified.*	

Volatiles and potential for volatility	3.1.04
Definition: FEPs related to the characteristics of radiotoxic and chemotoxic species that are volatile or have the potential for volatility in repository or environmental conditions.	
Comment: *Some radionuclides may be isotopes of gaseous elements (e.g. Kr isotopes) or may form volatile compounds. Gaseous radionuclides or species may arise from chemical or biochemical reactions, e.g. metal corrosion to yield hydrogen gas and microbial degradation of organic material to yield methane and carbon dioxide.*	
Key Concepts, examples, and related FEPs *None*	
Application to WMA C: *Relevant. Addressed in atmospheric release and radon release analyses.* ***Potentially deleterious FEP****: Not applicable.*	

Organics and potential for organic forms	3.1.05
Definition: FEPs related to the characteristics of radiotoxic and chemotoxic species that are organic or have the potential to form organics in repository or environmental conditions.	
Comment:	

Key Concepts, examples, and related FEPs   *Source term content*
Application to WMA C: *Relevant, but concentrations of organic species in residual waste are low and their effects have been screened out.*   ***Potentially deleterious FEP****: Not applicable.*

Noble gases	3.1.06
Definition: FEPs related to the characteristics of noble gases.	
Comment: *Radon and thoron are special cases, see FEP 3.3.08.*	
Key Concepts, examples, and related FEPs *None*	
Application to WMA C: *Not relevant.* ***Potentially deleterious FEP****: Not applicable.*	

CONTAMINANT RELEASE/MIGRATION FACTORS	3.2
Definition: The processes that directly affect the release and/or migration of radionuclides in the disposal system domain.	
Comment: *"Release/Migration Factors" is a sub-category in the International FEP List and is divided into individual FEPs.*	

Dissolution, precipitation and crystallisation, contaminant	3.2.01
Definition: FEPs related to the dissolution, precipitation and crystallisation of radiotoxic and chemotoxic species under repository or environmental conditions.	
Comment: *Dissolution is the process by which constituents of a solid dissolve into solution. Precipitation and crystallisation are processes by which solids are formed out of liquids. Precipitation occurs when chemical species in solution react to produce a solid that does not remain in solution. Crystallisation is the process of producing pure crystals of an element, molecule or mineral from a fluid or solution undergoing a cooling process.*	

Key Concepts, examples, and related FEPs	
Chemical reactions caused by dissolution and precipitation of radionuclides	*Caused by chemical interaction of backfill with pore water*
Change in mineralization	*Caused by chemical interaction of non-radioactive waste with radioactive waste*
Caused by chemical interaction of vault material with pore water	*Caused by a change in temperature*
Application to WMA C: *Relevant.*	
Potentially deleterious FEP*: Potential rapid waste dissolution may affect the safety function of the waste dissolution (considered in sensitivity and uncertainty analysis).*	

Speciation and solubility, contaminant		3.2.02
Definition: FEPs related to the chemical speciation and solubility of radiotoxic and chemotoxic species in repository or environmental conditions.		
Comment: *The solubility of a substance in aqueous solution is an expression of the degree to which it dissolves. Factors such as temperature and pressure affect solubility, as do the pH and redox conditions. These factors affect the chemical form and speciation of the substance. Thus different species of the same element may have different solubilities in a particular solution. Porewater and groundwater speciation and solubility are very important factors affecting the behaviour and transport of radionuclides*		
Key Concepts, examples, and related FEPs		
Species equilibrium change caused by change in temperature	*Solubility change caused by change in temperature* *Solubility*	*Solubility change caused by chemical interaction between waste and pore water*
Application to WMA C: *Relevant to chemical behaviour of contaminants in residual waste.*		
Potentially deleterious FEP*: Uncertainties in chemical behaviour may affect the chemical safety functions.*		

Sorption/desorption processes, contaminant	3.2.03
Definition: FEPs related to sorption/desorption of radiotoxic and chemotoxic species in repository or environmental conditions.	
Comment: *Sorption describes the physico-chemical interaction of dissolved species with a solid phase. Desorption is the opposite effect. Sorption processes are very important for determining the transport of radionuclides in groundwater. Sorption is often described by a simple partition constant (K_d) which is the ratio of solid phase radionuclide concentration to that in solution. This assumes that sorption is reversible, reaches equilibrium rapidly, is independent of variations in water chemistry or mineralogy along the flow path, the solid-water ratio, or concentrations of other species. More sophisticated approaches involve the use of sorption isotherms.*	

Key Concepts, examples, and related FEPs		
Sorption *Chemical reactions caused by adsorption or desoption* *Anion exclusion effects*	*Effect of sorption* *Caused by chemical interaction of waste with pore water*	*Caused by chemical interaction of non-radioactive waste with radioactive waste* *Sorption change caused by change in temperature*
Application to WMA C: *Relevant to chemical behaviour of contaminants in residual waste.* ***Potentially deleterious FEP****: Uncertainties in chemical behaviour may affect the chemical safety functions (different release assumptions are considered in the sensitivity and uncertainty analysis).*		

Colloids, contaminant interactions and transport with		3.2.04
Definition: FEPs related to the transport of colloids and interaction of radiotoxic and chemotoxic species with colloids in repository or environmental conditions.		
Comment: *Colloids are particles in the nanometre to micrometre size range which can form stable suspensions in a liquid phase. Metastable solid phases are unstable thermodynamically but exist due to the very slow kinetics of their alteration into more stable products. Colloids are present in groundwater and may also be produced during degradation of the wastes or engineered barrier materials.* *Colloids may influence radionuclide transport in a variety of ways: retarding transport by sorption of aqueous radionuclide species and subsequent filtration; or, enhancing transport by sorption and transport with flowing groundwater*		
Key Concepts, examples, and related FEPs		
Colloid formation *Caused by chemical interaction of waste with pore water*	*Caused by chemical interaction of backfill with pore water* *Colloid transport*	*Caused by chemical interaction of non-radioactive waste with radioactive waste*
Application to WMA C: *Potentially relevant to transport behaviour of contaminants, but considered unlikely to play a role in this environment (DOE-ORP-2008-01, page 22-12).* ***Potentially deleterious FEP****: Not applicable.*		

Chemical/complexing agents, effects on contaminant speciation/transport	3.2.05
Definition: FEPs related to the modification of speciation or transport of radiotoxic and chemotoxic species in repository or environmental conditions due to association with chemical and complexing agents.	

Comment: *This FEP refers to any chemical agents that are present in the repository system and the effects that they may have on the release and migration of radionuclides from the repository environment. Chemical agents may be present in the wastes or in repository materials or introduced, e.g. from spillage during repository construction and operation, e.g. oil, hydraulic fluids, organic solvents. Chemical agents may be used during construction and operation, e.g. in drilling fluids, as additives to cements and grouts etc.*
Key Concepts, examples, and related FEPs *Effects of chelating agents* *Caused by chemical interaction of waste with pore water* *Caused by chemical interaction of backfill with pore water* *Caused by chemical interaction of non-radioactive waste with radioactive waste* *Microbial*
Application to WMA C: *Potentially relevant to chemical safety functions, but of minimal effect owing to low concentrations of organic material in residual waste.* ***Potentially deleterious FEP****: Potential for decrease in chemical safety functions.*

Microbial/biological/plant-mediated processes, contaminant	3.2.06
Definition: FEPs related to the modification of speciation or phase change due to microbial/biological/plant activity.	
Comment: *Microbial activity may facilitate chemical transformations of various kinds.*	
Key Concepts, examples, and related FEPs *Microbial-enhanced mobility*	
Application to WMA C: *Potentially relevant to chemical safety functions, but of minimal effect owing to low concentrations of organic material providing negligible energy source for microbes.* ***Potentially deleterious FEP****: Potential for decrease in chemical safety functions. Uncertainties in sorption are addressed in sensitivity and uncertainty analyses.*	

Water-mediated transport of contaminants	3.2.07
Definition: FEPs related to transport of radiotoxic and chemotoxic species in groundwater and surface water in aqueous phase and as sediments in surface water bodies.	
Comment: *Water-mediated transport of radionuclides includes all processes leading to transport of radionuclides in water. Radionuclides may travel in water as aqueous solutes (including dissolved gases), associated with colloids (see FEP 3.2.04) or, if flow conditions permit, with larger particulates/sediments.*	

Key Concepts, examples, and related FEPs

Multiphase transport processes

Surface water aqueous transport

Transport by surface run-off

Transport in water bodies

Percolation

Capillary rise

Groundwater transport

Infiltration

Dual flow systems

Advection, i.e. movement with the bulk movement of the fluid (in fractures, failed joints and matrix)

Molecular diffusion, i.e. random movement of individual atoms or molecules within the fluid

Dispersion, i.e. the spread of spatial distribution with time due to differential advection

Matrix diffusion, i.e. the diffusion or micro-advection of solute/colloids etc. into non-flowing pores

Transport of colloids

Percolation, i.e. movement of the fluid under gravity

Transport processes between surface water and porous media

Isotopic dilution.

Mass dilution

Discharge of radionuclides to sea

Fracture-matrix interaction

Discharge of radionuclides to foreshore

Transport of suspended sediment

Application to WMA C: *Relevant and addressed in the performance assessment.*

Potentially deleterious FEP*: Not applicable.*

Solid-mediated transport of contaminants	3.2.08

Definition: FEPs related to transport of radiotoxic and chemotoxic species in solid phase, for example large-scale movements of sediments, landslide, solifluction and volcanic activity.

Comment:

Key Concepts, examples, and related FEPs

Resuspension/deposition

Land slides

Rock falls

Rain splash

Transport by suspended sediments (sedimentation)

Erosion

Solid material release

Solid phase transport by water

Wet Deposition

Washout

Application to WMA C: *Not relevant owing to depth of disposal and facility stability.*

Potentially deleterious FEP*: Not applicable.*

Gas-mediated transport of contaminants			3.2.09
Definition: FEPs related to transport of radiotoxic and chemotoxic species in gas or vapour phase or as fine particulate or aerosol in gas or vapour.			
Comment: *Radioactive gases may be generated from the wastes, e.g. C-14-labelled carbon dioxide or methane. Radioactive aerosols or particulates may be transported along with non-radioactive gases, or gases may expel contaminated groundwater ahead of them*			
Key Concepts, examples, and related FEPs			
Gas mediated water flow	*Gas phase processes*	*Barometric pumping*	
Gaseous release	*Diffusion*	*Overpressurization*	
Atmospheric gas transport	*Atmospheric aerosol transport*		
Application to WMA C: *Relevant and addressed in the performance assessment.*			
Potentially deleterious FEP*: None identified.*			

Atmospheric transport of contaminants		3.2.10
Definition: FEPs related to transport of radiotoxic and chemotoxic species in the air as gas, vapour, fine particulate or aerosol.		
Comment: *Radionuclides may enter the atmosphere from the surface environment as a result of a variety of processes including transpiration, suspension of radioactive dusts and particulates or as aerosols. The atmospheric system may represent a significant source of dilution for these radionuclides. It may also provide exposure pathways e.g. inhalation, immersion.*		
Key Concepts, examples, and related FEPs		
Sea spray	*Aerosol transport due to waves, wind*	
Application to WMA C: *Relevant and addressed in the performance assessment.*		
Potentially deleterious FEP*: None identified.*		

Animal, plant and microbe mediated transport of contaminants	3.2.11
Definition: FEPs related to transport of radiotoxic and chemotoxic species as a result of animal, plant and microbial activity.	
Comment: *Burrowing animals, deep rooting species and movement of contaminated microbes are included*	

Key Concepts, examples, and related FEPs		
Discharge of radionuclides to soil layer (biotic intrusion)	*Transport mediated by flora and fauna*	*Bioturbation*
Animal/Plant intrusion	*Uptake and desorption*	*Intake and emission by animals*
Application to WMA C: *Not relevant owing to depth of disposal and facility design except the potential for microbially mediated transport. Microbes have a potential effect on chemical safety functions (changes in sorption) but these are expected to be small owing to small concentrations of energy sources for microbes in the vadose zone.*		
Potentially deleterious FEP*: Potential changes to chemical safety functions.*		

Human-action-mediated transport of contaminants		3.2.12
Definition: FEPs related to transport of radiotoxic and chemotoxic species as a direct result of human actions.		
Comment:*. Human-action-mediated transport of contaminants includes processes such as drilling into or excavation of the repository, the dredging of contaminated sediments from lakes, rivers and estuaries and placing them on land. Earthworks and dam construction may result in the significant movement of solid material from one part of the biosphere to another. Ploughing results in the mixing of the top layer of agricultural soil, usually on an annual basis.*		
Key Concepts, examples, and related FEPs		
Dredging of sediments	*Ploughing*	*Water abstraction*
Application to WMA C: *Relevant to intrusion analyses and evaluation of all pathways exposure analysis.*		
Potentially deleterious FEP*: None identified.*		

Foodchains, uptake of contaminants in		3.2.13
Definition: FEPs related to incorporation of radiotoxic and chemotoxic species into plant or animal species that are part of the possible eventual food chain to humans.		
Comment: *Plants may become contaminated either as a result of direct deposition of radionuclides onto their surfaces or indirectly as a result of uptake from contaminated soils or water via the roots. Animals may become contaminated with radionuclides as a result of ingesting contaminated plants, or directly as a result of ingesting contaminated soils, sediments and water sources, or via inhalation of contaminated particulates, aerosols or gases.*		
Key Concepts, examples, and related FEPs		
Plant/animal uptake in a marine/estuarine	*Crops and natural and semi-natural flora and fauna*	*Internal transfer of radionuclides within animals*
External contamination of animals		
Application to WMA C: *Relevant to post-intrusion analyses and evaluation of all pathways exposure analysis.*		
Potentially deleterious FEP*: None identified.*		

EXPOSURE FACTORS	**3.3**
Definition: Processes and conditions that directly affect the dose to members of the critical group, from given concentrations of radionuclides in environmental media.	
Comment: *Exposure Factors" is a sub-category in the International FEP List and is divided into individual FEPs.*	

Drinking water, foodstuffs and drugs, contaminant concentrations in	3.3.01
Definition: FEPs related to the presence of radiotoxic and chemotoxic species in drinking water, foodstuffs or drugs that may be consumed by human.	
Comment:	
Key Concepts, examples, and related FEPs	
Internal transfer of radionuclides within animals *Crops and natural and semi-natural flora and fauna*	
Application to WMA C: *Relevant to and considered in exposure scenarios*	
Potentially deleterious FEP*: None identified.*	

Environmental media, contaminant concentrations in	3.3.02
Definition: FEPs related to the presence of radiotoxic and chemotoxic species in environmental media other than drinking water, foodstuffs or drugs.	
Comment:*. The comparison of calculated contaminant concentrations in environmental media with naturally-occurring concentrations of similar species or species of similar toxic potential, may provide alternative or additional criteria for assessment less dependent on assumptions of human behaviour.*	
Key Concepts, examples, and related FEPs	
None	
Application to WMA C: *Relevant to and considered in exposure scenarios*	
Potentially deleterious FEP*: None identified.*	

Non-food products, contaminant concentrations in	3.3.03
Definition: FEPs related to the presence of radiotoxic and chemotoxic species in human manufactured materials or environmental materials that have special uses, e.g. clothing, building materials, peat.	

Comment: *Contaminants may be concentrated in non-food products to which humans are exposed. For example, building materials, natural fibres or animal skins used in clothing, and the use of peat for fuel.*
Key Concepts, examples, and related FEPs *None*
Application to WMA C: *Not relevant to Order 435.1 exposure scenarios* ***Potentially deleterious FEP****: Not applicable.*

Exposure modes	3.3.04
Definition: FEPs related to the exposure of man (or other organisms) to radiotoxic and chemotoxic species.	
Comment:	
Key Concepts, examples, and related FEPs *Direct radiation from airborne plumes of radioactive materials* *Injection through wounds* *Cutaneous absorption of some species.* *External exposure through water or sediment* *Dermal exposure* *Immersion in contaminated water bodies* *Ingestion (internal exposure) from drinking or eating contaminated water or foodstuffs* *Inhalation (internal exposure) from inhaling gaseous or particulate radioactive materials* *External exposure as a result of direct irradiation from radionuclides deposited on, or present on, the ground, buildings or other objects.*	
Application to WMA C: *Relevant to and considered in exposure scenarios* ***Potentially deleterious FEP****: None identified.*	

Dosimetry	3.3.05
Definition: FEPs related to the dependence between radiation or chemotoxic effect and amount and distribution of radiation or chemical agent in organs of the body.	
Comment: *Dosimetry involves the estimation of radiation dose to individual organs, tissues, or the whole body, as a result of exposure to radionuclides. The radiation dose will depend on: the form of exposure, e.g. ingestion or inhalation of radionuclides leading to internal exposure or proximity to concentrations of radionuclides leading to external exposure; the metabolism of the radioelement and physico-chemical form if inhaled or ingested, which will determine the extent to which the radionuclide may be taken up and retained in body tissues; and the energy and type of radioactive emissions of the radionuclide which will affect the distribution of energy within tissues of the body.*	

Key Concepts, examples, and related FEPs *None*
Application to WMA C: *Relevant to and considered in exposure scenarios* ***Potentially deleterious FEP****: None identified.*

Radiological toxicity/effects	3.3.06
Definition: FEPs related to the effect of radiation on man or other organisms.	
Comment: *Radiation effects are classified as somatic (occurring in the exposed individual), genetic (occurring in the offspring of the exposed individual), stochastic (the probability of the effect is a function of dose received), non-stochastic (the severity of the effect is a function of dose received and no effect may be observed below some threshold).*	
Key Concepts, examples, and related FEPs *None*	
Application to WMA C: *Not relevant to dose and concentration endpoints in the Order 435.1 analysis.* ***Potentially deleterious FEP****: Not applicable.*	

Non-radiological toxicity/effects	3.3.07
Definition: FEPs related to the effects of chemotoxic species on man or other organisms.	
Comment:	
Key Concepts, examples, and related FEPs *None*	
Application to WMA C: *Not relevant to radiological endpoints in the Order 435.1 performance assessment. Will be addressed in complementary analyses.(Groundwater protection criteria???) – may need to include some non-rads????* ***Potentially deleterious FEP****: Not applicable.*	

Radon and radon daughter exposure	**3.3.08**
Definition: FEPs related to exposure to radon and radon daughters.	

Comment: *Radon and radon daughter exposure is considered separately to exposure to other radionuclides because the behaviour of radon and its daughter, and the modes of exposure, are different to other radionuclides.* *Radon (Rn-222) is the immediate daughter of radium (Ra-226). It is a noble gas with a half-life of about 4 days and decays through a series of very short-lived radionuclides (radon daughters), with half-lives of 27 minutes or less, to a lead isotope (Pb-210) with a half-life of 21 years. The principal mode of exposure is through the inhalation of radon daughters attached to dust particles, which may deposit in the respiratory system.*
Key Concepts, examples, and related FEPs *Radon emanation*
Application to WMA C: *Relevant to the performance assessment. Evaluated as radon flux endpoint in the Order 435.1 analysis.* ***Potentially deleterious FEP****: None identified.*

H.6 REFERENCES

AECL-MISC-295, 1996, "Preliminary Safety Analysis Report (PSAR) for the Intrusion Resistant Underground Structure (IRUS)," Rev. 4, Atomic Energy of Canada, Chalk River, Ontario, Canada.

BHI-01573, 2001, "Groundwater/Vadose Zone Integration Project – The Application of Feature, Event, and Process Methodology at the Hanford Site," Rev. 0, Bechtel Hanford, Inc., Richland, Washington.

DOE/EIS-0391, 2012, "Final Tank Closure and Waste Management Environmental Impact Statement for the Hanford Site, Richland, Washington," U.S. Department of Energy, Washington, D.C.

DOE O 435.1, 2001, Radioactive Waste Management, U.S. Department of Energy, Washington, D.C.

DOE O 458.1, 2013, Radiation Protection of the Public and the Environment, U.S. Department of Energy, Office of Health, Safety and Security, Washington, D.C.

DOE P 454.1, 2011, Use of Institutional Controls, U.S. Department of Energy, Washington, D.C.

FCRD-USED-2011-000297, 2011, "Features, Events and Processes for the Disposal of Low Level Radioactive Waste – FY 2011 Status Report," Rev. 0, U.S. Department of Energy, Fuel Cycle Research and Development, Savannah River Site, Aiken, South Carolina.

IAEA-ISAM-1, 2004, "Safety Assessment Methodologies for Near Surface Disposal Facilities, Results of a co-ordinated research project, Volume 1: Review and enhancement of safety assessment approaches and tools," International Atomic Energy Agency, Vienna, Austria.

NEA Report 6923, 2012, "Methods of Safety Assessment of Geological Disposal Facilities for Radioactive Waste, Outcomes of the NEA MeSA Initiative," Nuclear Energy Agency/Organisation for Economic Co-operation and Development, Paris, France.

NUREG/CR-1667 (SAND80-1429), 1982, "Risk Methodology for Geologic Disposal of Radioactive Waste: Scenario Selection Procedure," Sandia National Laboratories for U.S. Nuclear Regulatory Commission, Washington, D.C.

Phifer, M., 2011, "2002 LLW Repository PCSC – FEP Consideration," Savannah River National Laboratory, Aiken, South Carolina.

SAND93-7100, 1993, "Preliminary Identification of Potentially Disruptive Scenarios at the Greater Confinement Disposal Facility, Area 5 of the Nevada Test Site," Sandia National Laboratories, Albuquerque, New Mexico.

SAND94-0482, 1994, "Scenario Development for the Waste Isolation Pilot Plant: Building Confidence in the Assessment," Sandia National Laboratories, Albuquerque, New Mexico.

SKB Technical Report 95-22, 1995, "The Use of Interaction Matrices for Identification, Structuring, and Ranking of FEPs in a Repository System," Swedish Nuclear Fuel and Waste Management Company, Stockholm, Sweden.

SKB Technical Report TR-10-45, 2010, "FEP report for the safety assessment SR-Site," Swedish Nuclear Fuel and Waste Management Company, Stockholm, Sweden.

SKI Report 95:26, 1995, "Systems Analysis, Scenario Construction and Consequence Analysis Definition for SITE-94," Swedish Nuclear Power Inspectorate, Stockholm, Sweden.

SKI Technical Report 93:27, 1993, "SITE-94 Scenario Development FEP Audit List Preparation: Methodology and Presentation," Swedish Nuclear Power Inspectorate, Stockholm, Sweden.

Virsek, S., T. Zagar, and M. W. Kozak, 2014, "Natural and Engineering Barriers – the Safety Concept Basis for LILW Repository in Vrbina, Krško," 23rd International Conference Nuclear Energy for New Europe, Portoroz, Slovenia.

Wakasugi, K., K. Ishiguro, T. Ebashi, H. Ueda, T. Koyama, H. Shiratsuchi, S. Yashio, and H. Kawamura, 2012, "A methodology for scenario development based on understanding of long-term evolution of geological disposal systems," Journal of Nuclear Science and Technology, Volume 49, No. 7, pp. 673–688.

WCH-520, 2013, "Performance Assessment for the Environmental Restoration Disposal Facility, Hanford Site, Washington," Rev. 1, Washington Closure Hanford, Richland, Washington.

WMP-22922, 2004, "Prototype Hanford Features, Events, and Processes (HFEP) Graphical User Interface," Rev. 0, Fluor Hanford, Inc., Richland, Washington.

This page intentionally left blank.

APPENDIX I

RESULTS OF FLOW-FIELDS DEVELOPED IN THE VADOSE ZONE FOR THE PURPOSE OF UNCERTAINTY ANALYSIS

This page intentionally left blank.

TABLE OF CONTENTS

APPENDIX I – RESULTS OF FLOW-FIELDS DEVELOPED IN THE VADOSE ZONE FOR THE PURPOSE OF UNCERTAINTY ANALYSIS I-1

LIST OF FIGURES

Figure I-1. Results for H1 Unit for Base Case Recharge Rates for Five Hydraulic Properties in Vadose Zone. I-3

Figure I-2. Results for H2 Unit for Base Case Recharge Rates for Five Hydraulic Properties in Vadose Zone. I-6

Figure I-3. Results for H3 Unit for Base Case Recharge Rates for Five Hydraulic Properties in Vadose Zone. I-9

This page intentionally left blank.

APPENDIX I

RESULTS OF FLOW-FIELDS DEVELOPED IN THE VADOSE ZONE FOR THE PURPOSE OF UNCERTAINTY ANALYSIS

The purpose of this appendix is to present information on the uncertainty range in vertical Darcy flux and volumetric moisture content in order to illustrate the range and magnitude of vertical pore water velocities over the full range of uncertainty in recharge rates. Development of vadose zone flow field and propagation of uncertainty is discussed in detail in Section 8.1.4.

The flow fields are abstracted from the three-dimensional Subsurface Transport Over Multiple Phases (STOMP)©[1] modeling results as a way to efficiently evaluate the effect of uncertainty in the vadose zone flow using the GoldSim©[2]-based system model. The flow fields are developed for five different vadose zone hydraulic properties to represent the range of vertical linear pore water velocities in the vadose zone under base case recharge conditions (Figures 8-14, 8-15, and 8-16). In order to derive the vertical pore water velocity for other recharge conditions, regression equations are developed that are used to scale the vertical Darcy flux and volumetric moisture content estimates for each of the five hydraulic properties using base case recharge rates. The regression equations for scaling vertical Darcy flux underneath 100-series tanks are presented in Table 8-10 and that for the 200-series tanks is presented in Table 8-11 for H1, H2, and H3 units. The scaling of the volumetric moisture content is simpler and presented in Table 8-12. Note that these scaling multipliers are dimensionless and are applied to values calculated under base recharge conditions, as abstracted from three-dimensional STOMP© model results for each of the five hydraulic properties.

The results are presented by taking the regression equations shown in Tables 8-10 and 8-12 (for 100-series tanks) and performing the calculations over the minimum and maximum recharge rates over the post-closure time period to illustrate the uncertainty range in vertical average linear pore water velocities. The results from 200-series tanks are not presented as they lead to similar uncertainty range as the 100-series tanks. Since the recharge rates are estimated for two time periods, an early post-closure time period (first 500 years while the surface cover is intact) and late post-closure time period (for the remaining time period with degraded surface cover), the uncertainties in recharge rates are different for these two time periods. As presented in Table 8-3, for the early post-closure time period, the minimum recharge rate within the WMA C area is 0.1 mm/yr and the maximum is 0.9 mm/yr with the base case recharge rate being 0.5 mm/yr. For the late post-closure time period, the minimum recharge rate is 0.5 mm/yr and the maximum is 5.2 mm/yr while the base case recharge rate is 3.5 mm/yr. The minimum and maximum recharge rates are applied in the regression equations to calculate the scaling of vertical Darcy flux and volumetric moisture content relative to those based on the base case recharge rates. From this, the vertical average linear pore water velocities are estimated at a given time by dividing the vertical Darcy flux with the volumetric moisture content value for each unit (H1, H2, and H3). Although the vertical Darcy flux and volumetric moisture content

[1] Subsurface Transport Over Multiple Phases (STOMP)© is copyrighted by Battelle Memorial Institute, 1996.
[2] GoldSim© simulation software is copyrighted by GoldSim Technology Group LLC of Issaquah, Washington (see http://www.goldsim.com).

for H2 and H3 are different, the scaling multipliers are the same as noted in Tables 8-10 and 8-12.

Results for each of the three units is presented below for the representative node within that unit to illustrate the uncertainty. For each unit, the time histories of vertical Darcy flux, volumetric moisture content, and vertical linear pore water velocity under base case recharge conditions are presented for each of the five hydraulic properties noted as 5th percentile, 25th percentile, 50th percentile, 75th percentile, and 95th percentile (see Section 8.1.4 for additional details). Next, the scaling multiplier calculated for vertical Darcy flux is presented based on the regression equations for the minimum and maximum recharge rate cases for each of the five hydraulic properties (percentile cases). After that, the resulting vertical linear pore water velocities are presented for each of the five hydraulic properties evaluated under minimum and maximum recharge rates. The scaling multipliers and resulting vertical velocity values do not change at late times and, therefore, the results are only presented up to 1,000 years following closure.

The variation in volumetric moisture content is not appreciable for the various recharge cases within the early post-closure time period and vary marginally after that; the scaling of volumetric moisture content is either 0.93 (for minimum recharge case) or 1.3 (for maximum recharge case) for the post-closure time period. These results are not presented separately.

Results for H1 unit are presented in Figure I-1, while those for H2 and H3 units are presented in Figures I-2 and I-3. Figure I-1c shows the range in vertical linear pore water velocity for the H1 unit under base case recharge conditions. It represents the uncertainty range that could result from the choice of hydraulic properties alone. Figure I-1d shows the range in scaling multiplier for each of the five hydraulic properties over the minimum and maximum recharge rates while Figure 1e presents the corresponding range in vertical linear pore water velocities, which affects transport of contaminants via advection. The uncertainty range (spread) in the vertical linear pore water velocities is the largest for the 95th percentile hydraulic property (factor of 6.5) and minimum for the 25th percentile hydraulic property (factor of 2). For other hydraulic properties the range varies by factor of 3 to 3.3.

For H2 and H3 units the result are similar. The uncertainty range (spread) in the vertical linear pore water velocities is the largest for the 95th percentile hydraulic property (factor of 6.4) and minimum for the 25th percentile hydraulic property (factor of 2.5). For other hydraulic properties the range varies by factor of 3 to 4.1.

These results indicate that for realizations where 95th percentile hydraulic property is selected during uncertainty analysis, greater variance in travel times can be expected compared to other hydraulic properties (under similar recharge rate range).

Figure I-1. Results for H1 Unit for Base Case Recharge Rates for Five Hydraulic Properties in Vadose Zone. (1 of 3 sheets)

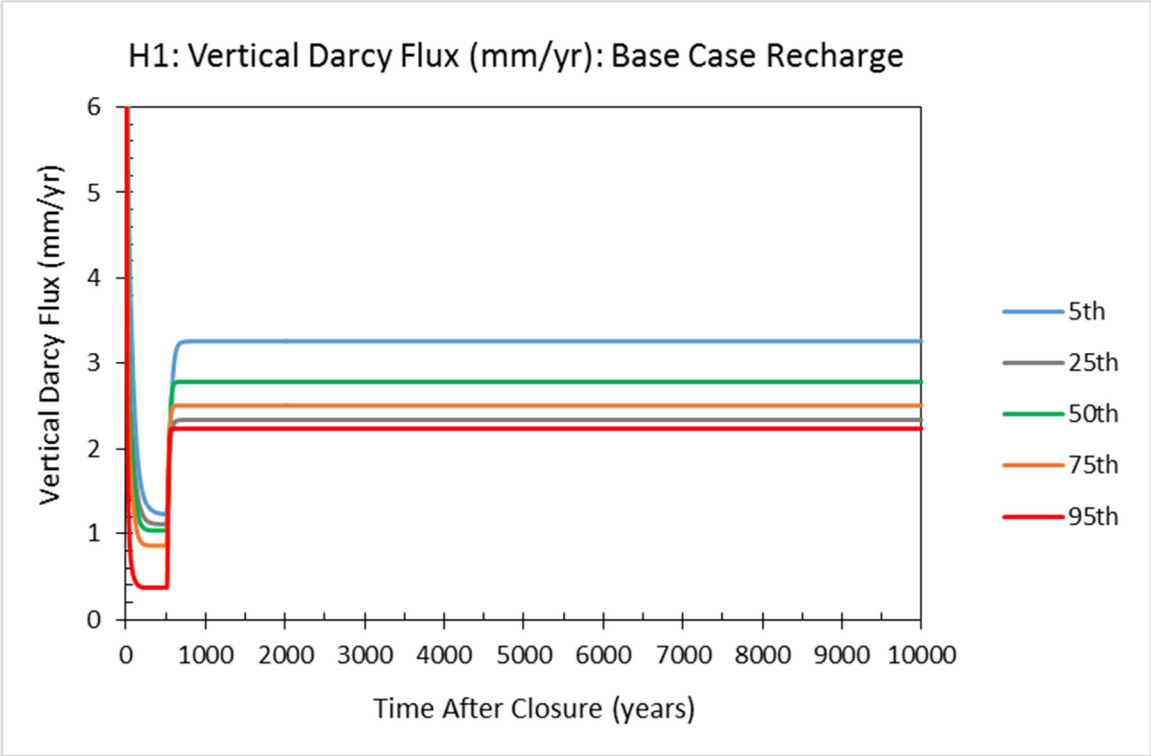

(a)

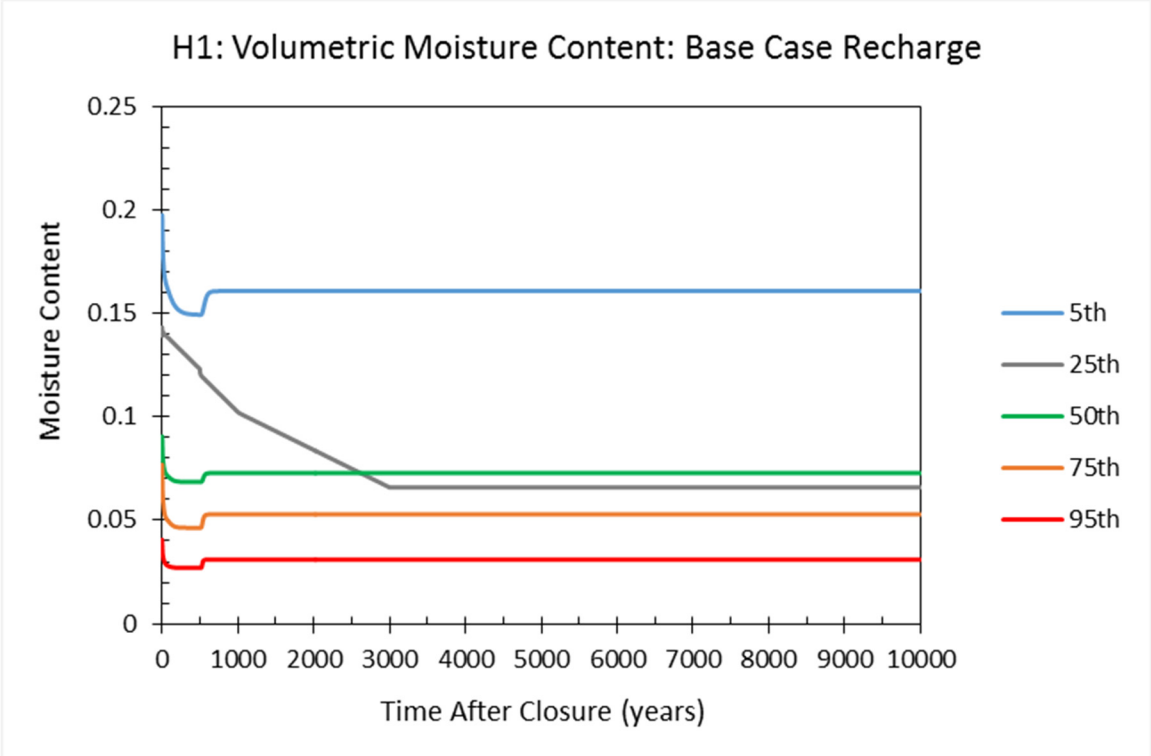

(b)

Figure I-1. Results for H1 Unit for Base Case Recharge Rates for Five Hydraulic Properties in Vadose Zone. (2 of 3 sheets)

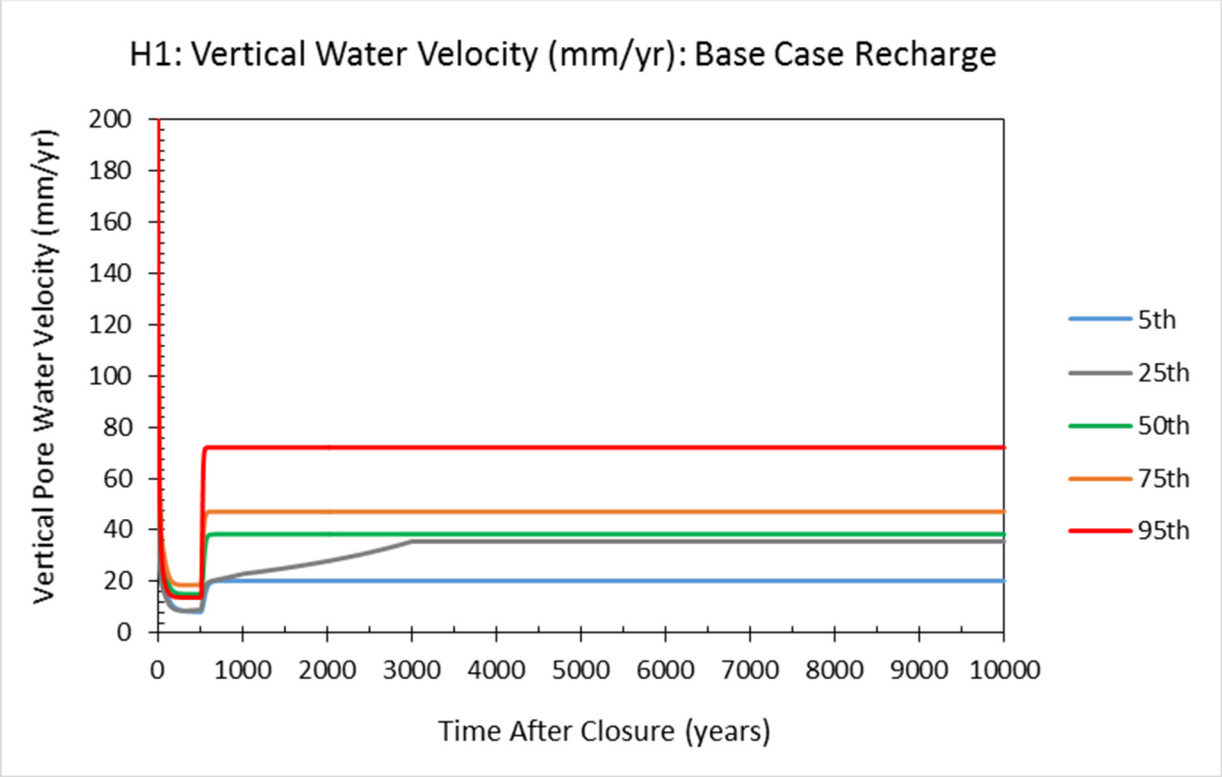

(c)

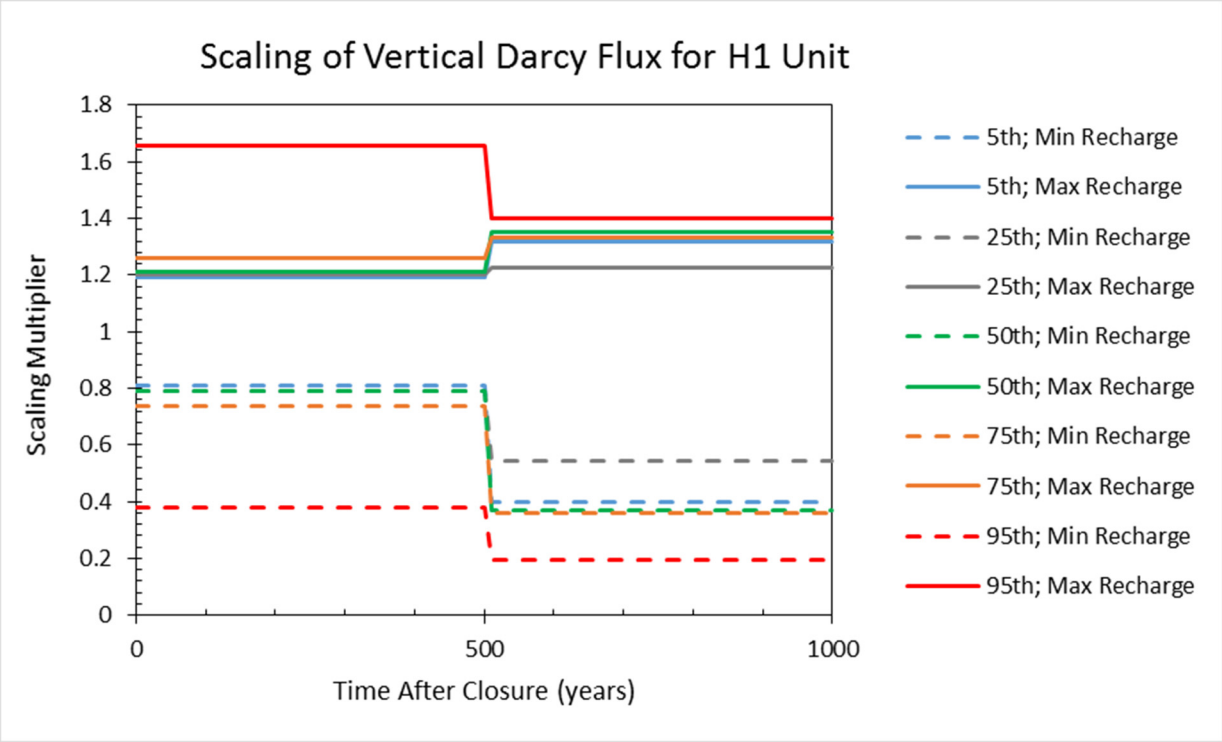

(d)

Figure I-1. Results for H1 Unit for Base Case Recharge Rates for Five Hydraulic Properties in Vadose Zone. (3 of 3 sheets)

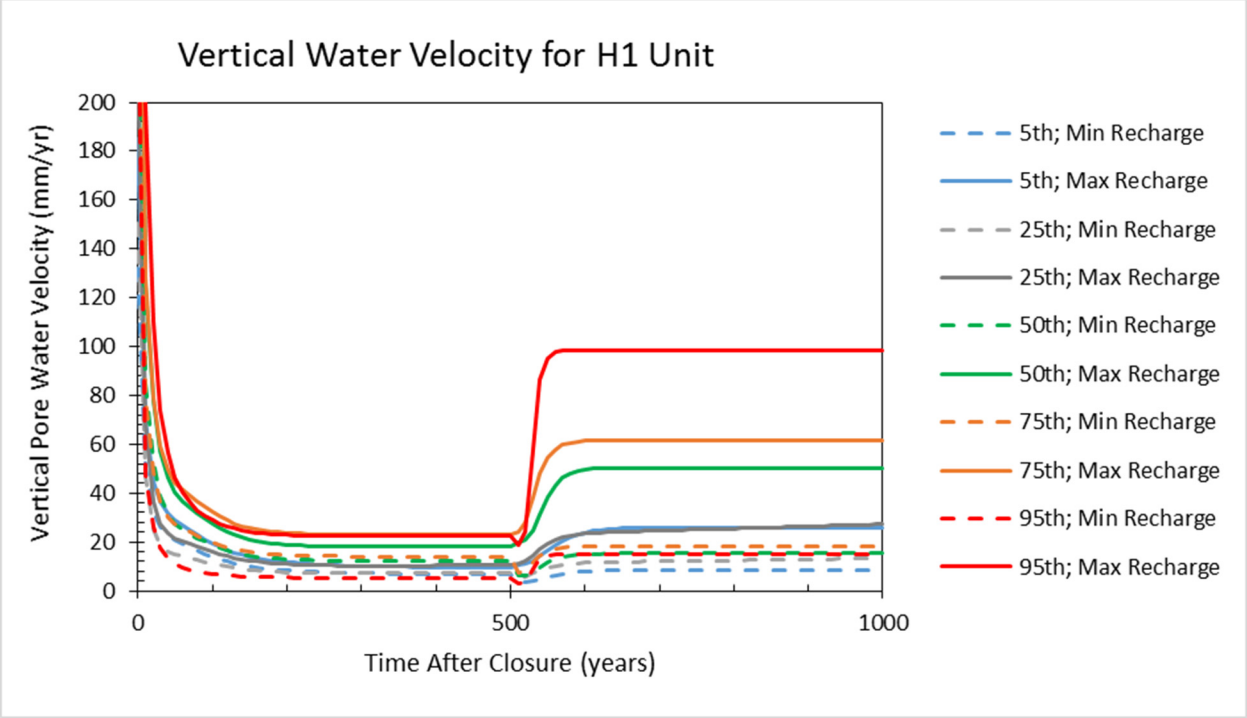

(e)

Figure I-2. Results for H2 Unit for Base Case Recharge Rates for Five Hydraulic Properties in Vadose Zone. (1 of 3 sheets)

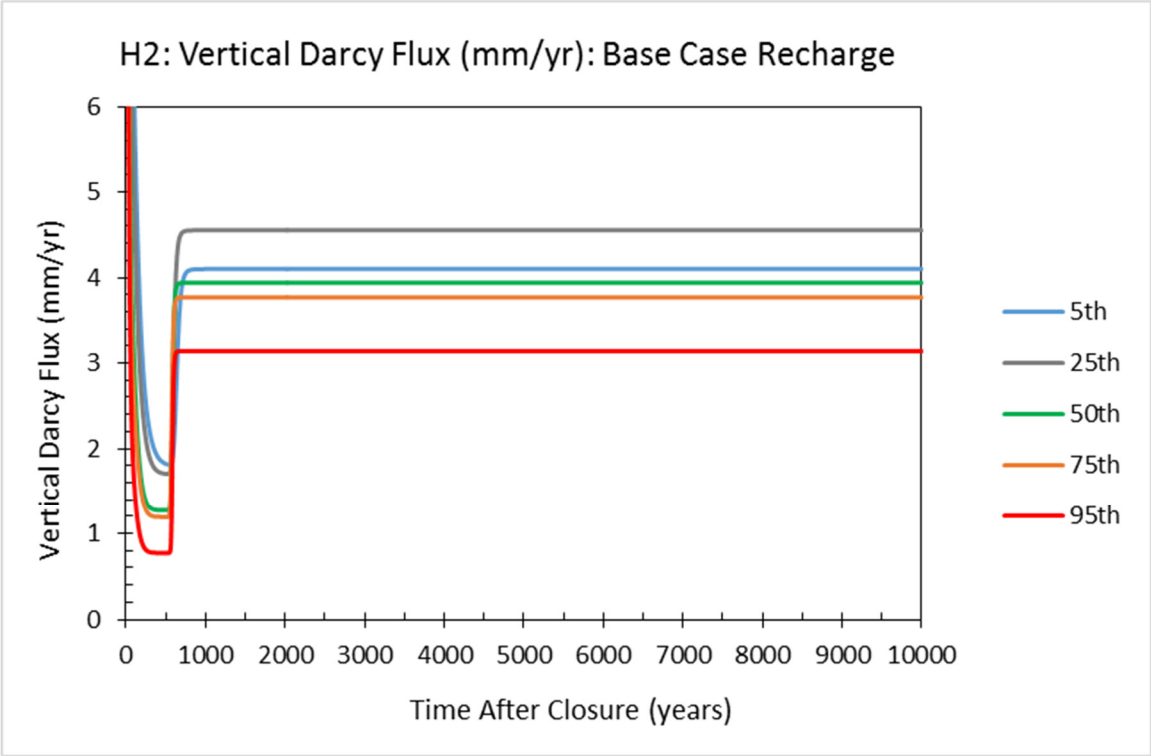

(a)

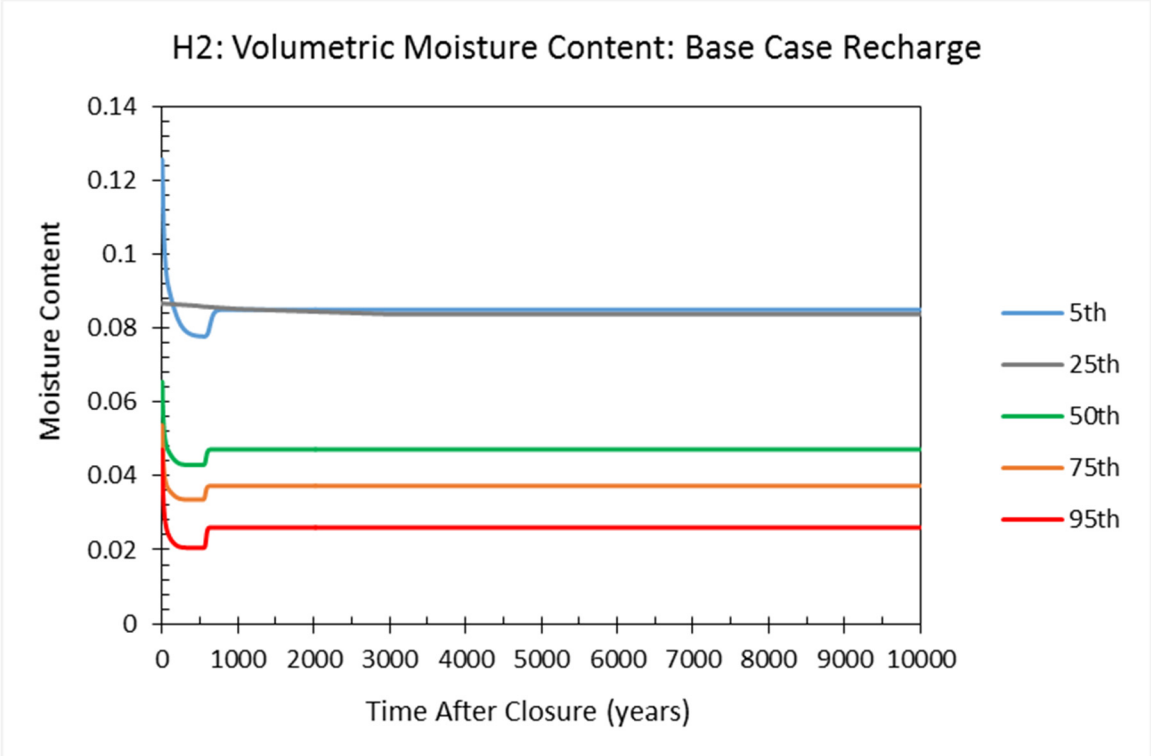

(b)

Figure I-2. Results for H2 Unit for Base Case Recharge Rates for Five Hydraulic Properties in Vadose Zone. (2 of 3 sheets)

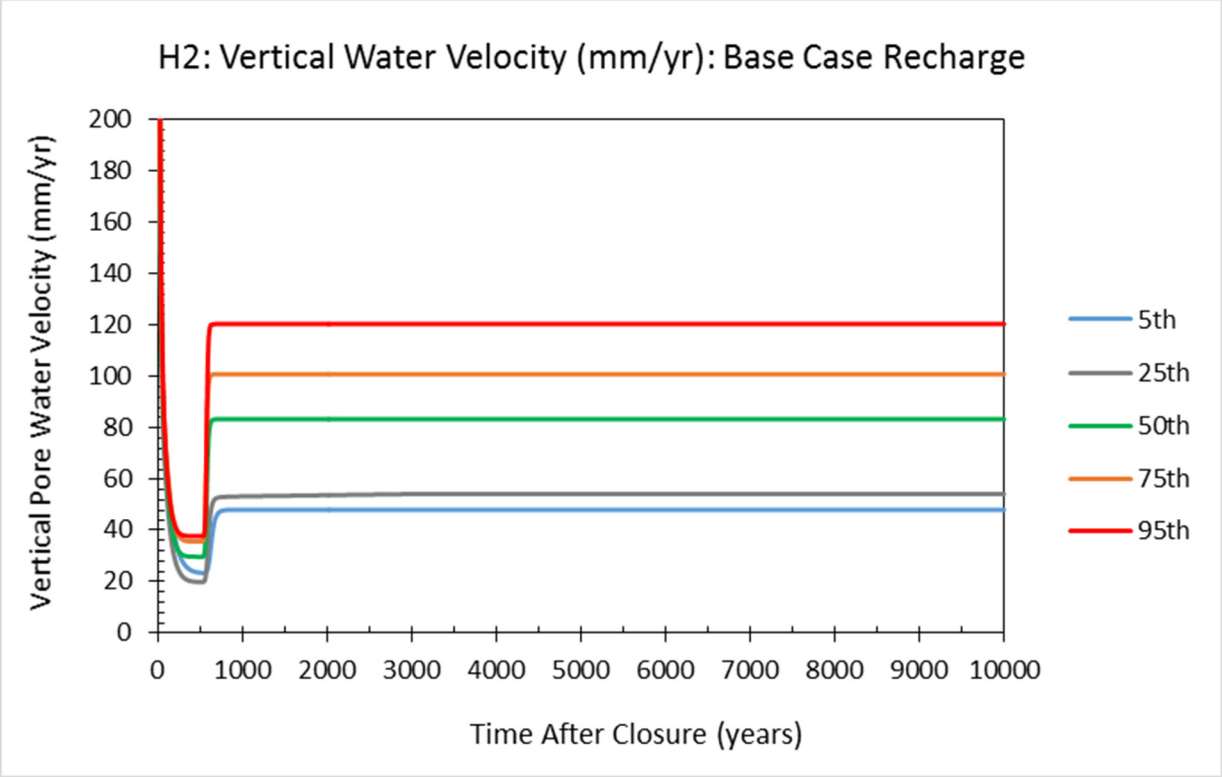

(c)

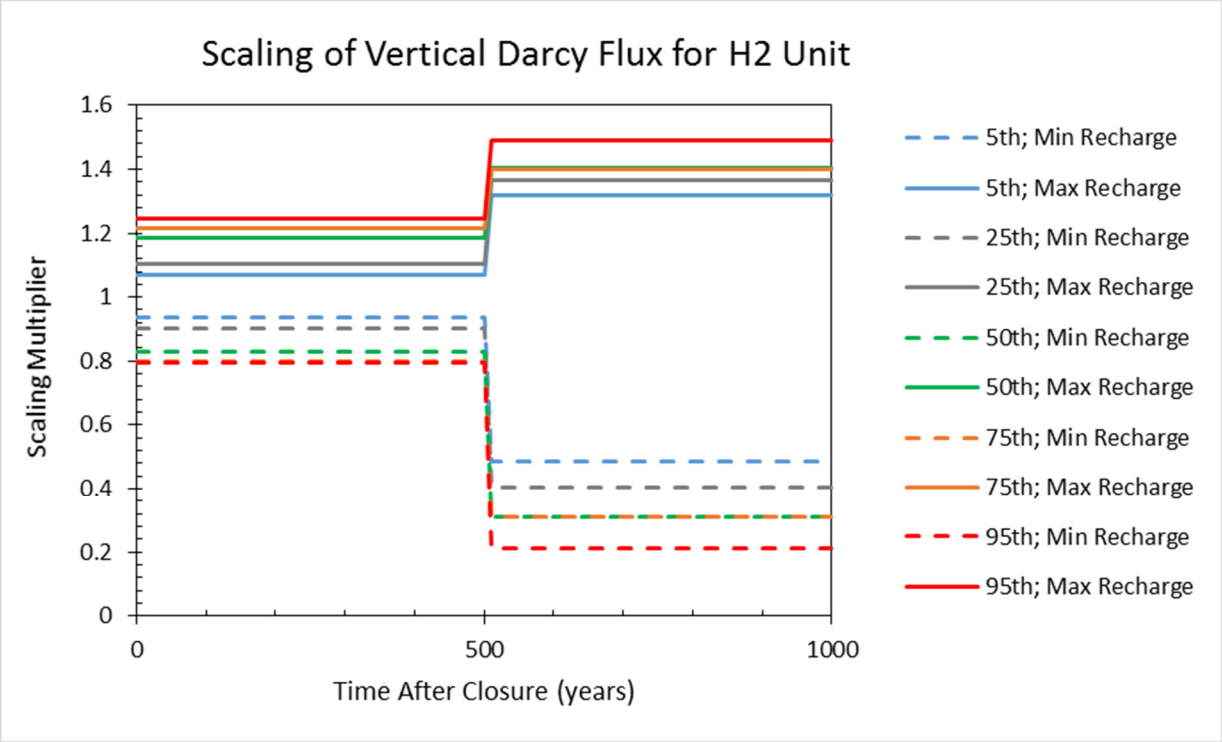

(d)

Figure I-2. Results for H2 Unit for Base Case Recharge Rates for Five Hydraulic Properties in Vadose Zone. (3 of 3 sheets)

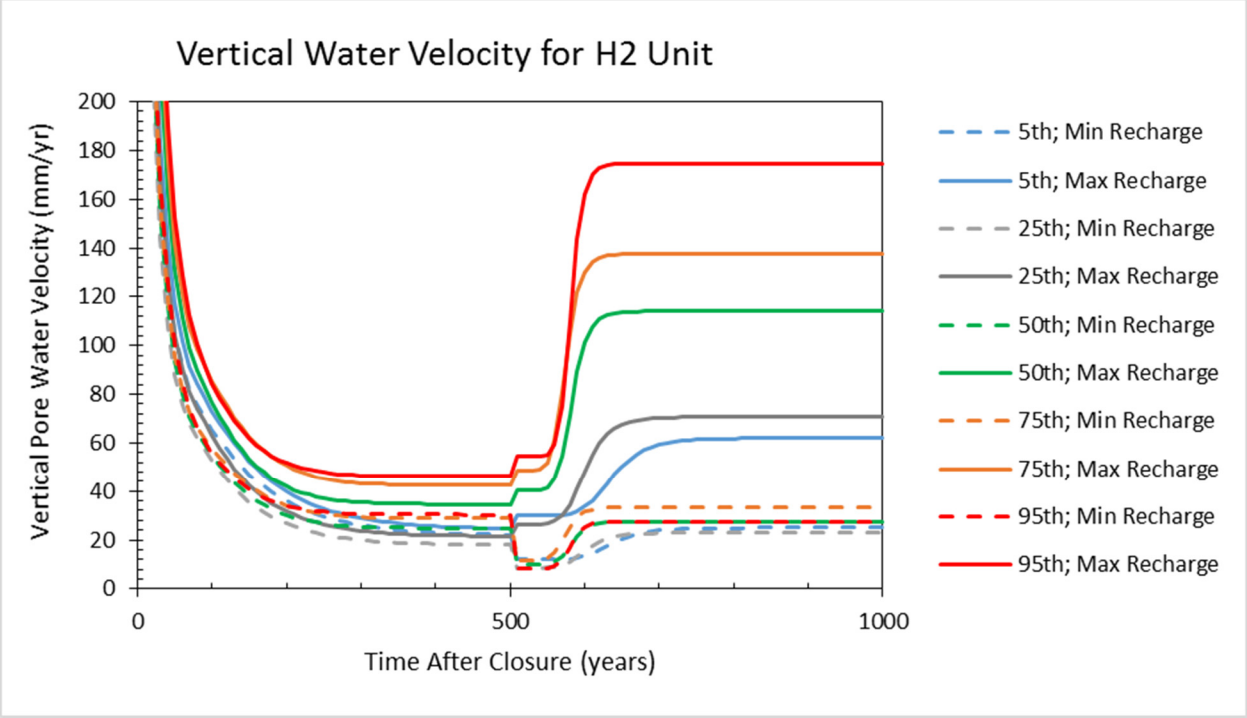

(e)

Figure I-3. Results for H3 Unit for Base Case Recharge Rates for Five Hydraulic Properties in Vadose Zone. (1 of 3 sheets)

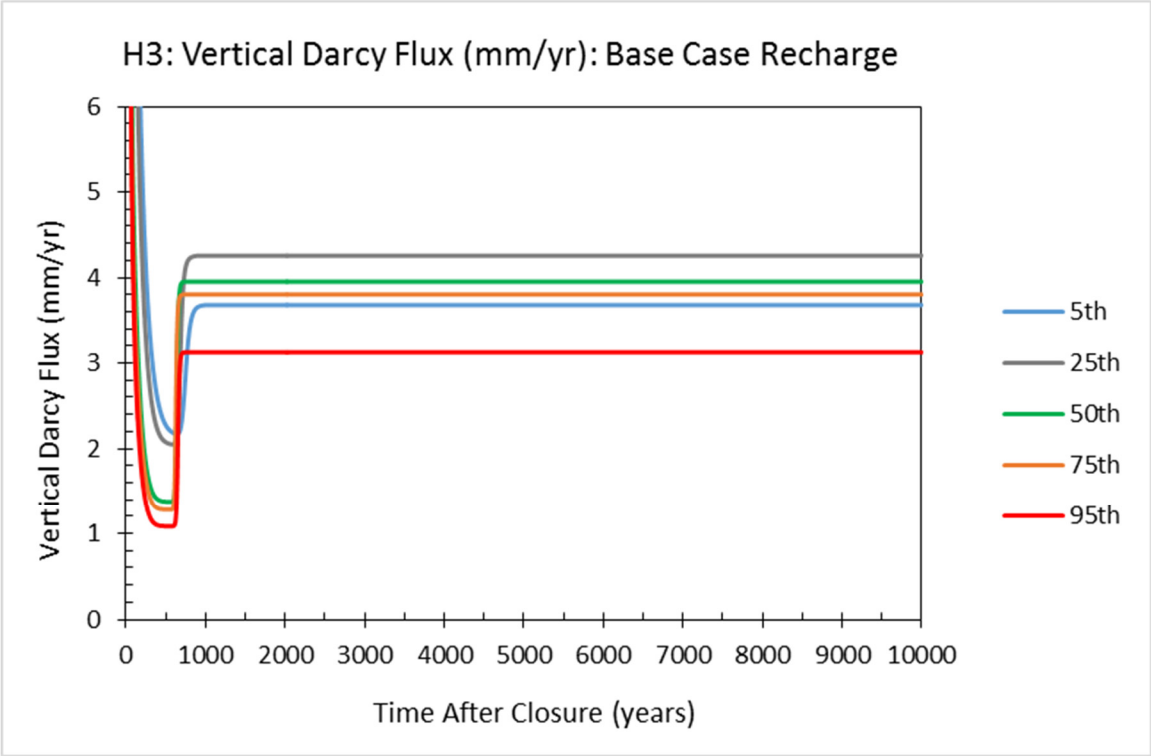

(a)

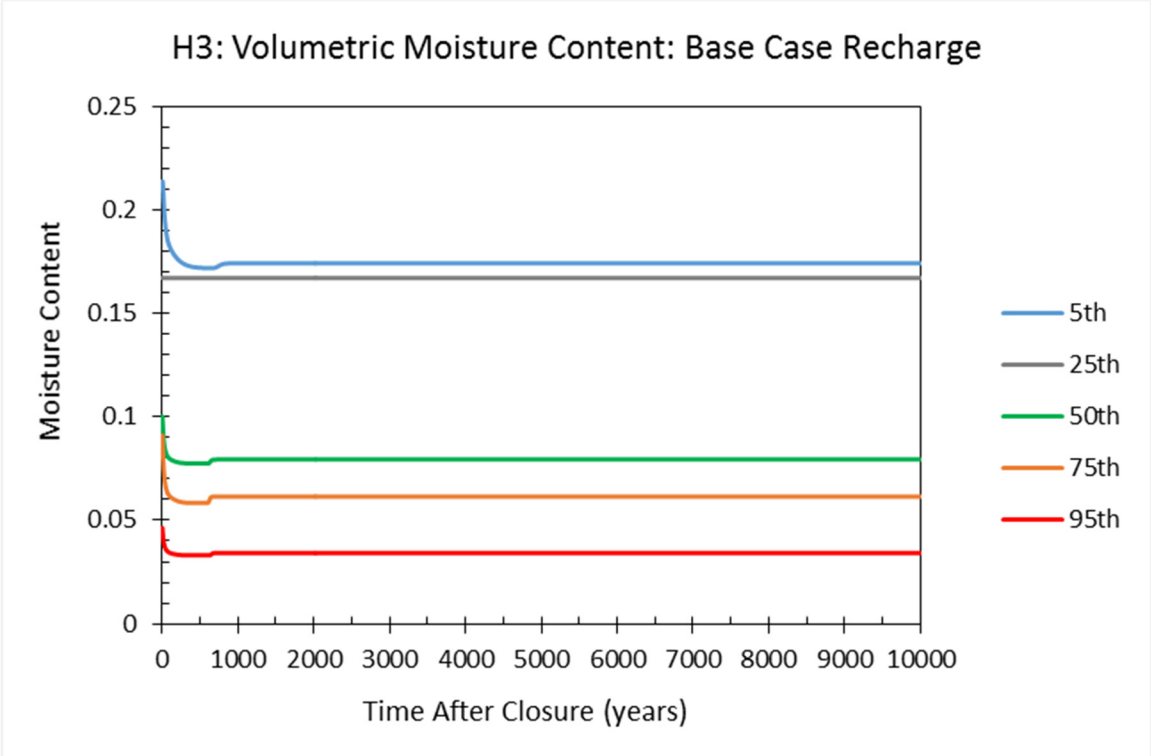

(b)

Figure I-3. Results for H3 Unit for Base Case Recharge Rates for Five Hydraulic Properties in Vadose Zone. (2 of 3 sheets)

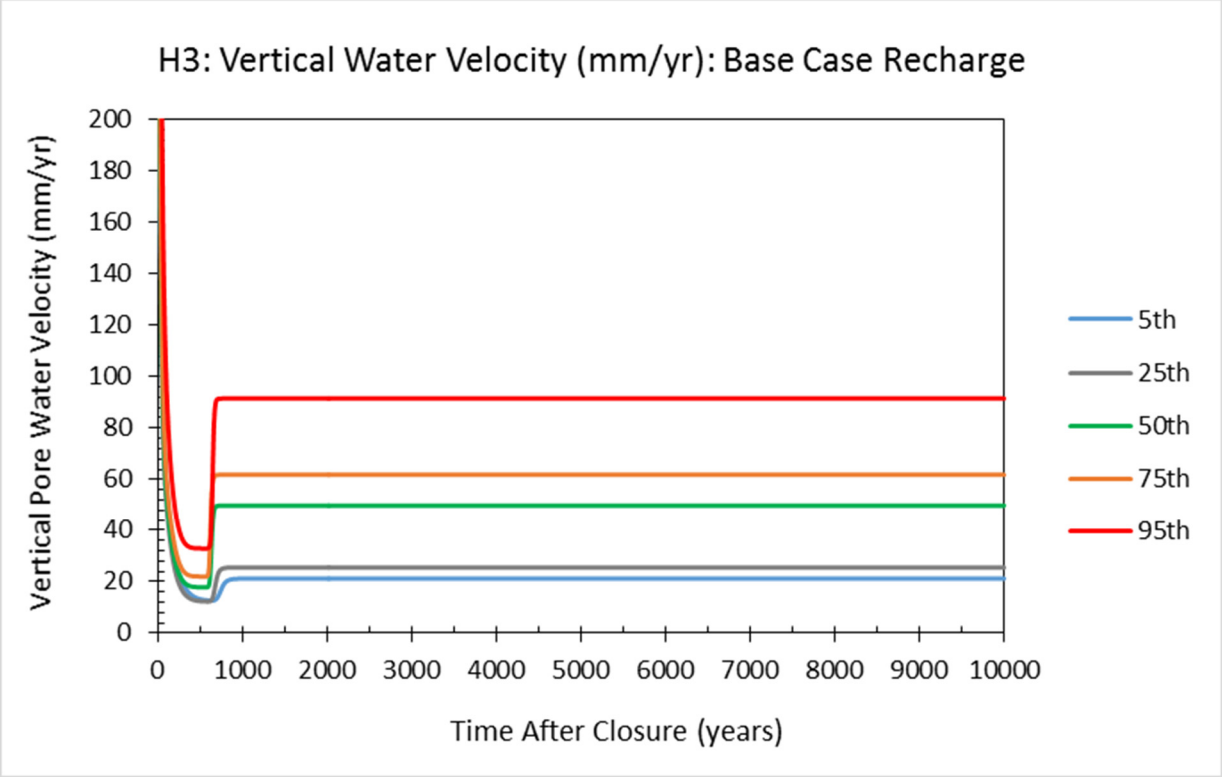

(c)

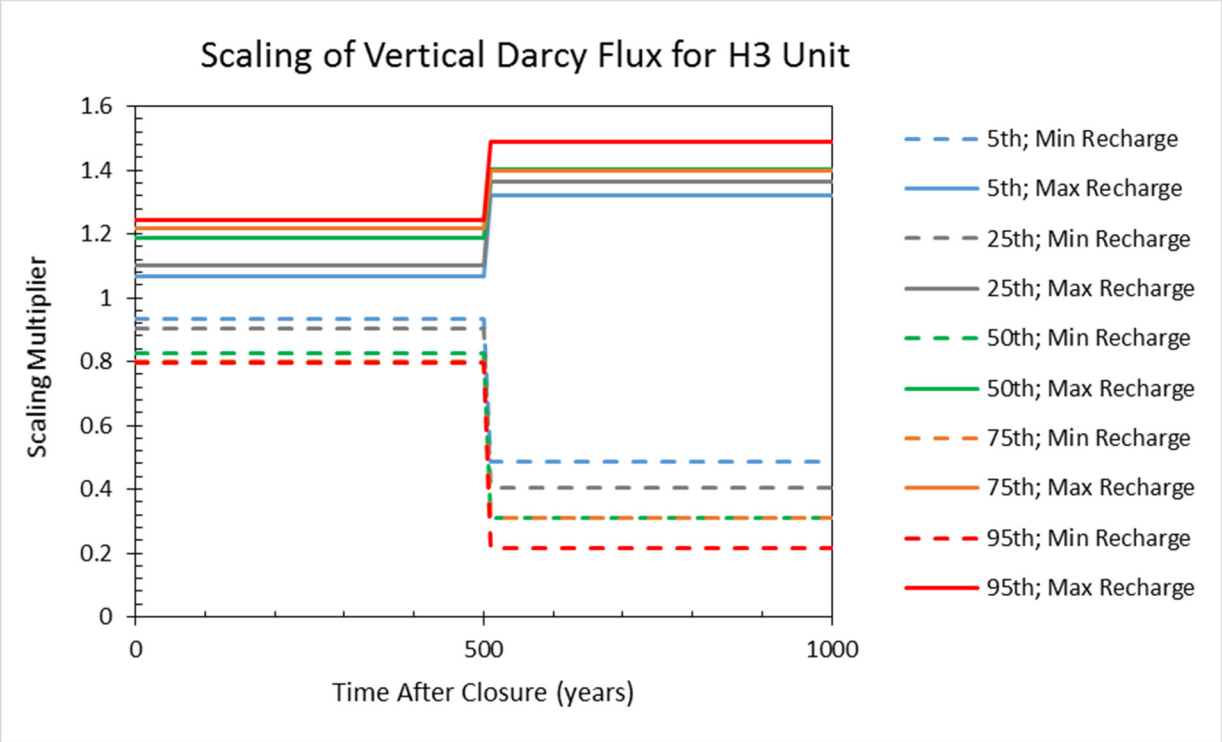

(d)

Figure I-3. Results for H3 Unit for Base Case Recharge Rates for Five Hydraulic Properties in Vadose Zone. (3 of 3 sheets)

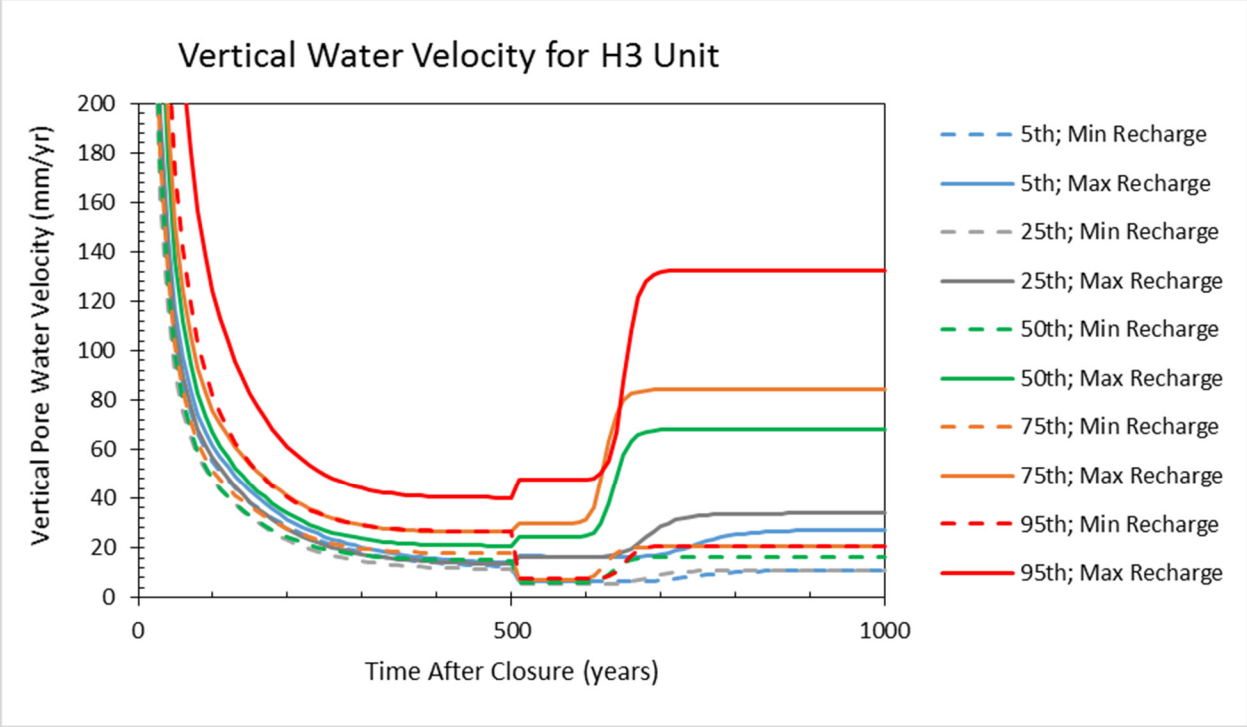

(e)

This page intentionally left blank.